McDONALD INSTITUTE MONOGRAPHS

Temple people

Bioarchaeology, resilience and culture in prehistoric Malta

By Simon Stoddart, Ronika K. Power, Jess E. Thompson, Bernardette Mercieca-Spiteri, Rowan McLaughlin, Eóin W. Parkinson, Anthony Pace & Caroline Malone

Volume 3 of Fragility and Sustainability – Studies on Early Malta, the ERC-funded *FRAGSUS Project*

Temple people

McDONALD INSTITUTE MONOGRAPHS

Temple people

Bioarchaeology, resilience and culture in prehistoric Malta

By Simon Stoddart, Ronika K. Power,
Jess E. Thompson, Bernardette Mercieca-Spiteri,
Rowan McLaughlin, Eóin W. Parkinson,
Anthony Pace & Caroline Malone

With contributions by
Bruno Ariano, Robert Barratt, Sara Boyle, Dan Bradley, Laura T. Buck, Jacinta Carruthers, Joel D. Irish, Catherine Kneale, Emma Lightfoot, John S. Magnussen, Caroline Malone, Sarah Massingham, Valeria Mattiangeli, Rowan McLaughlin, John Meneely, Bernardette Mercieca-Spiteri, Argyro Nafplioti, Tamsin C. O'Connell, Anthony Pace, Margery Pardey, Eóin W. Parkinson, Ronika K. Power, Paula Reimer, John Robb, Jaap Saers, Jay T. Stock, Simon Stoddart, Jess E. Thompson, Alessandra Varalli, Nicholas Vella & Hannah Vogel

Volume 3 of Fragility and Sustainability – Studies on Early Malta, the ERC-funded *FRAGSUS Project*

This project has received funding from the European Research Council (ERC) under the European Union's Seventh Framework Programme (FP7-2007-2013) (Grant agreement No. 323727).

Published by:
McDonald Institute for Archaeological Research
University of Cambridge
Downing Street
Cambridge, UK
CB2 3ER
(0)(1223) 339327
eaj31@cam.ac.uk
www.mcdonald.cam.ac.uk

ISBN: 978-1-913344-08-5

Cover design by Dora Kemp, Caroline Malone and Ben Plumridge.
Typesetting and layout by Ben Plumridge.

On the cover: *Stick figures from the Circle.*

Edited for the Institute by Matthew Davies (*Series Editor*).

Contents

Contributors

Bruno Ariano
Smurfit Institute of Genetics, School of Genetics and Microbiology, Trinity College Dublin, Dublin 2, D02 VF25, Ireland
Email: arianob@tcd.ie

Robert Peter Barratt
School of Natural and Built Environment, Queen's University Belfast, UK
Email: rbarratt01@qub.ac.uk

Sara Boyle (now Stewart)
Ordnance Survey Northern Ireland, Land and Property Services, Lanyon Plaza, 7 Lanyon Place, Town Parks, Belfast, Northern Ireland.

Laura T. Buck
Research Centre for Evolutionary Anthropology and Palaeoecology, Liverpool John Moores University, United Kingdom / Cambridge Biotomography Centre, University of Cambridge, Cambridge, United Kingdom
Email: l.buck@ljmu.ac.uk

Dan Bradley
Smurfit Institute of Genetics, School of Genetics and Microbiology, Trinity College Dublin
Dublin 2, D02 VF25, Ireland
Email: DBRADLEY@tcd.ie

Jacinta Carruthers
Department of History and Archaeology, Macquarie University, Sydney, Australia
Email: jacinta.carruthers@mq.edu.au

Joel D. Irish
School of Biological and Environmental Sciences, Research Centre for Evolutionary Anthropology and Palaeoecology, Liverpool John Moores University, Liverpool, United Kingdom
Email: J.D.Irish@ljmu.ac.uk

Catherine J. Kneale
McDonald Institute for Archaeological Research, Department of Archaeology, University of Cambridge, Cambridge, United Kingdom
Email: cjk37@cam.ac.uk

Emma Lightfoot
c/o McDonald Institute for Archaeological Research, Department of Archaeology, University of Cambridge, Cambridge, United Kingdom.

John S. Magnussen
Department of Clinical Medicine, Faculty of Medicine Health and Human Sciences, Macquarie University, Sydney,Australia
Email: john.magnussen@mq.edu.au

Caroline Malone
School of Natural and Built Environment, Queen's University Belfast
Email: c.malone@qub.ac.uk
& caroline.stoddart@cantab.net

Sarah Massingham
Department of History and Archaeology, Macquarie University, Sydney, Australia
Email: sarah.massingham@hdr.mq.edu.au

Valeria Mattiangeli
Smurfit Institute of Genetics, School of Genetics and Microbiology, Trinity College Dublin, Dublin 2, D02 VF25, Ireland
Email: mattianv@tcd.ie

Rowan McLaughlin
School of Natural and Built Environment, Queen's University Belfast, UK.
Email: r.mclaughlin@qub.ac.uk

John Meneely
School of Natural and Built Environment, Queen's University Belfast, UK
Email: j.meneely@qub.ac.uk

Bernardette Mercieca-Spiteri
National Inventory, Research and Archaeology Unit, Superintendence of Cultural Heritage, Valletta Malta
Email: bernardette.mercieca@gov.mt

Argyro Nafplioti
Ancient DNA Lab, Institute of Molecular Biology and Biotechnology (IMBB), FORTH, Heraklion, Greece / formerly McDonald Institute for Archaeological research, Department of Archaeology, University of Cambridge, Cambridge, United Kingdom.
Email: argyro.nafplioti@googlemail.com

Tamsin C. O'Connell
McDonald Institute for Archaeological Research, Department of Archaeology, University of Cambridge, Cambridge, United Kingdom
Email: tco21@cam.ac.uk

Eóin W. Parkinson
Department of Classics & Archaeology, University of Malta, Msida, Malta
Email: ewparkinson24@gmail.com

Anthony Pace
Former Superintendent of Cultural Heritage Malta, Malta
Email: anthonypace@cantab.net

Margery Pardey
Department of Clinical Medicine, Faculty of Medicine Health and Human Sciences, Macquarie University, Sydney, Australia
Email: margery.pardey@mq.edu.au

Ronika K. Power
Department of History and Archaeology, Macquarie University, Sydney, Australia/ formerly McDonald Institute for Archaeological Research, Department of Archaeology, University of Cambridge, Cambridge, United Kingdom
Email: ronika.power@mq.edu.au

Paula J. Reimer
School of Natural and Built Environment, Queen's University Belfast, UK
Email: p.j.reimer@qub.ac.uk

John Robb
McDonald Institute for Archaeological Research, Department of Archaeology, University of Cambridge, Cambridge, United Kingdom
Email: jer39@cam.ac.uk

Jaap Saers
McDonald Institute for Archaeological Research, Department of Archaeology, University of Cambridge, Cambridge, United Kingdom
Email: jpps2@cam.ac.uk

Jay T. Stock
Department of Anthropology, University of Western Ontario, London, Canada / Department of Archaeology, Max Planck Institute for the Science of Human History, Jena, Germany
Email: jay.stock@uwo.ca

Simon Stoddart
McDonald Institute for Archaeological Research, Department of Archaeology, University of Cambridge, Cambridge, United Kingdom
Email: ss16@cam.ac.uk

Jess E. Thompson
McDonald Institute for Archaeological Research, Department of Archaeology, University of Cambridge, Cambridge, United Kingdom
Email: jet71@cam.ac.uk

Alessandra Varalli
Department of Humanities, Universitat Pompeu Fabra, Barcelona
Email: alessandravaralli@gmail.com

Nicholas Vella
Department of Archaeology and Classics, University of Malta, Msida, Malta
Email: nicholas.vella@um.edu.mt

Hannah Vogel
Department of History and Archaeology, Macquarie University, Sydney, Australia
Email: hannah.vogel@hdr.mq.edu.au

Figures

Tables

In memoriam George Mann

Caroline Malone

The re-discovery of the Xagħra Brochtorff Circle (1987–94) and the retrieval of prehistoric burials from the site represents the material that is the subject of this volume. Here we reassess and delve deeper into the detail of the excavated remains of a large prehistoric population and other prehistoric burials known from Malta and Gozo. The original Xagħra fieldwork was intense, hot and hard, and it took place mostly at the height of summer, during university vacations. Such work was not for the faint-hearted; early morning routines and 6-day weeks, crowded communal conditions – these were the standard experience for the young team of students and professional archaeologists who participated. It was an exciting learning experience for the 'young ones'. For two much older men, retired from their careers, to choose to participate in this frenetic and noisy environment was unexpected, but enormously significant and supportive to what was then a major and pioneering undertaking. These gentlemen, Dr George Mann (a retired ENT consultant from Addenbrookes Hospital in Cambridge with a Masters in biological anthropology), and Kenneth Stoddart (just retired from a life of city commuting and business), brought maturity, wisdom, humour, compassion and humanity, as well as a vital breath of civilization to each annual season of work. We dedicated the 2009 volume to the memory of Kenneth Stoddart. This volume appropriately is dedicated to the memory of George Mann.

Dr George Edgar Mann (1923–2019) participated in the Gozo Project between 1990 and the completion of osteological study in 1996. Initially George, fresh from a post-retirement study of bioanthropology at Cambridge, came to assist Corinne Duhig who prepared the initial rock-cut tomb report. Professionally he had been a specialist consultant in otolaryngology at Addenbrookes Hospital in Cambridge, and had done his retirement MPhil dissertation on bony exostoses in the outer meatus of the ear, caused by swim-

Figure 0.1. *George and Sheila Mann at work in the kitchen of the dig house, systematically recording a skeleton 1994.*

Figure 0.2. *George Mann at work on the roof-top of the dig house in Gozo in 1994.*

ming in cold water. The Gozo assemblage demanded a rapid revision of his knowledge of the post cranial skeleton, but soon up to speed, George then came every year to participate in each field season and post-excavation study season. He worked tirelessly with his wife Sheila, processing the excavated bones, separating out the animal bones for study by Geraldine Barber, and identifying the human remains himself with his team. He cheerfully accepted the spartan and crowded living conditions where he spent much time at the kitchen table or on the roof of rented holiday flats, sorting endless sacks of bone fragments into coherent identified catalogues. He measured, studied and quantified as he went and ensured every fragment was recorded. Towards the end of the fieldwork, some osteological material was transported to Britain, and George continued to log, measure, examine and interpret the human material in preparation for the 2009 report. His systematic and painstaking recording work of the entire assemblage was of great importance, as the following pages reveal. Even with the ERC *FRAGSUS Project* resources, which provided funding at a level unimagined in the earlier excavation years, it has been possible only to re-examine a sample of the vast osteological archive. George managed to ensure that we have the fundamental knowledge of the scope of the assemblage, and this is listed in the first report (see Malone *et al.* 2009d) and it forms the base for ongoing research of these remarkable ancient people and the Xagħra site. The record was written by hand, and the hundreds of sheets of record remain in the archives of the National Museum of Archaeology, ready for future studies, and whilst the original digital database of those handwritten records becomes ever more antiquated, George's immense work remains a vital archive even as technology advances. All the teams, past and present, are delighted to dedicate this volume to George's memory and his tremendous contribution to Maltese and osteological scholarship.

Figure 0.3. *Sheila Mann cleaning bones for George in the dig house 1994.*

Another key contributor to the work of the original Gozo Project was Ann Monsarrat, who lived on Gozo, and supported the project and its team with generosity and warmth over the many years of work and study.

In memoriam Ann Monsarrat

Anthony Pace

Ann Monsarrat (1937–2020) made her home on Gozo, where she moved in 1968 with her husband Nicholas, the author of many novels about Malta and the sea. Gozo was a special place for Ann, a home with people that she truly loved, respected and admired. Ann was a remarkable person. She was welcomed and felt at home in the small village of San Lawrenz, where she lived for more than four decades. Her house was forever busy with people dropping in and sharing news, experiences, aspirations, the changing fortunes of Malta and Gozo and, of course, the difficulties of writing and the literary world. But beyond these and many other conversations, Ann was particularly interested in landscape – Gozo's in particular – where archaeology, history and legends carved meaning out of a small island full of hills, valleys, majestic cliffs and skylines marked by parish church cupolas rising above quiet village houses.

FRAGSUS owes a great deal to Ann. For, unbeknown to her, several good friends – all archaeologists – whom she supported and entertained annually during the excavation of the Xagħra Brochtorff Circle between 1987 and 1994, came together again to deliver another important project. Ann would have certainly been happy and excited with the results of *FRAGSUS*. A career journalist and a distinguished author in her own right, with works such as *And the Bride wore; Thackeray: An Uneasy Victorian*; *Gozo: island of oblivion, a graphic literary itinerary*, Ann was particularly interested in the archaeology of Malta and Gozo. She was always keen to follow research developments and new discoveries, and was eager to see young scholars, budding archaeologists, photographers, historians, artists, writers, journalists, and so many others making headway in areas that she understood to be important in promoting Maltese cultural identity. Ann was in fact a formidable advocate of Maltese arts, culture and cultural heritage. Her work on the governing board of Saint James Cavalier Centre for Creativity in Valletta, and her continuous presence in Gozitan cultural circles, as well as her various contributions to numerous publication projects reflected an enthusiasm and positiveness which was contagious and encouraging. Ann's enthusiasm shone every time she visited the Xagħra Brochtorff Circle excavations, during our long walks along the ta' Ċenċ promontory, during visits to the Cittadella, or when listening to the sounds rumbling from the depths of blocked shafts at the legendary clock-maker's salt-works on the north coast of Gozo. These were real places with real stories, some illustrated in prints, others silently waiting to be teased out from

Figure 0.4. *Anne Monsarrat (with kind permission of her family).*

stone monuments, field terraces and beautiful natural spots. Perhaps these were places whose biographies could best be understood by visiting and experiencing them in person.

One of the last places Ann and I visited together was the archaeological site at Ras il-Wardija on Gozo's western coast. The site is not an easy one to interpret, but from a spot rising several metres above the surrounding area, we shared an almost bird's-eye view of Dwejra with the distant Azur Window below us, and we chatted about the meaning of the site and its links to the sea: seascapes, ancient mariners, people lost at sea, shipwrecks; and also of builders who constructed beautiful places and made beautiful art, making the Maltese Islands their home for at least seven thousand years.

In these pages, the *FRAGSUS* team pays tribute to Ann Monsarrat.

Acknowledgements

The *FRAGSUS Project* 2013–18 is indebted to numerous individuals and institutions and acknowledges support throughout the course of a long and energetic project. In particular, we thank the European Research Council which awarded an Advanced Research Grant (Advanced Grant no. 323727) to Caroline Malone, as the Principal Investigator of the Project and the extended team in late 2012, enabling the project to take place between May 2013 and April 2018. Without this funding and the trust placed in us by the ERC and the grant assessors, this project could never have taken place. We express our gratitude for this opportunity to expand knowledge of Malta and indeed much else connected with prehistoric societies and their world in the early Mediterranaean. The research team also wants to record our indebtedness to the administrators of the grant within our own institutions, since this work required detailed and dedicated attention. In particular we thank Rory Jordan in the Research Support Office (Queen's University Belfast – QUB), Laura Cousens (Cambridge University – UoC), Glen Farrugia and Cora Magri (University of Malta – UM), the Curatorial, Finance and Designs & Exhibitions Departments in Heritage Malta (HM) and Stephen Borg at the Superintendence of Cultural Heritage (SCH).

All participants thank our Maltese colleagues for their hospitable and enthusiastic support of the research, from the CEO of Heritage Malta, the Minister for Culture Dr Owen Bonnici, and the Malta High Commissioner, his excellency Norman Hamilton and the British High Commissioner, his Excellency Stuart Gill, Dr Anthony Pace, Former Superintendent of Cultural Heritage and his deputy, Nathaniel Cutajar and their staff (Christian Mifsud, Mevrick Spiteri, Bernardette Mercieca-Spiteri) for enabling permits for the many sites explored during the research programme. We thank too the University of Malta and the staff of the Department of Archaeology and Classics, who enabled facilities, storage, meeting and research venues, student assistants, and logistics. In particular, we thank Chris Gemmell, Dr Maxine Anastasi, Prof. Nicholas Vella, Prof. Anthony Bonanno, and Dr Reuben Grima. The staff of Heritage Malta were instrumental in enabling access to sites, stores, and expertise. We especially thank Sharon Sultana in the National Museum of Archaeology, Ruby Cutajar when she was in the National Museum of Archaeology, Katya Stroud, Joanne Mallia, Dr Josef Caruana in Malta and Dr George Azzopardi, Daphne Sant Caruana, Nicolene Sagona and John Cremona in Gozo.

In Britain, the team thank the staff of the McDonald Institute, particularly Emma Jarman, and the Department of Archaeology for facilities and support and the Cambridge Biotomography Centre for access and use of facilities. At Queen's University Belfast, we thank the team in the 14CHRONO Lab under the direction of Prof. Paula Reimer for the swift and effective processing of AMS dates and isotopic analysis and, in particular, Stephen Hoper, Michelle Thompson, Jim McDonald, and Dr Ron Reimer who made this possible. We also thank John Meneeley for his exceptional work on scanning sites and processing data to provide images for ongoing research. At Trinity College Dublin, we thank Prof. Dan Bradley and his staff for supporting the aDNA study, which was funded separately from the ERC work, through the Wellcome Trust, and for the opportunity to add this important aspect of research to the study of Malta. We must also extend our thanks to all the participants, past and present who undertook the fieldwork at the Xagħra Brochtorff Circle in the 1980s–90s and to those who worked tirelessly to record the vast assemblage over the following years. For recent assistance we thank Chiara Marabelli who assisted in processing and cleaning human remains for study as part of the new bone team.

For the preparation of this volume, we thank Dr Rob Barratt, Dr Rowan McLaughlin, Dr Eóin Parkinson, Dr Jess E. Thompson and Olivia Shelton for assisting in the editing and assembly of this very substantial work. Prof. Simon Stoddart was the overall editor who undertook the major editing of the volume (including the index and glossary), the design of the opening and closing chapters and was in the grant application defined as responsible for the Human Population work group and the Landscape group in Cambridge. Prof. Caroline Malone undertook the preliminary assembly of the text, the checking and setting of tables and images, as well as much proofing and editing. We thank Emma Jarman in the McDonald Institute for her important role in coordinating the submission of material, and Dr James Barrett and Prof. Cyprian Broodbank (when James left Cambridge) for their oversight of the McDonald Monograph series. We thank Dr Matt Davies, the new Deputy Director and Editor of the Monograph Series, for guiding the volume into its final stages. In particular, we thank Ben Plumridge who undertook the task of production. Ben 'cut his teeth' in publication in 2007–9 when he was the principal assistant in the preparation of the 2009 *Mortuary Customs in Prehistoric Malta* (the original site report and the forerunner of the three companion volumes from *FRAGSUS*), making the work of the late Dora Kemp, his McDonald predecessor, as production editor so much easier. The archaeology of the island of Malta has thus continued to benefit from his support after his appointment as Production Editor of the McDonald series by Simon Stoddart when he was acting Deputy Director.

To all those involved, we thank you.

Preface

Caroline Malone and Simon Stoddart

This volume is the third in the *FRAGSUS Project* series. Volume 1: *Temple Landscapes* (edited by Charles French, Chris O. Hunt, Reuben Grima, Rowan McLaughlin, Simon Stoddart & Caroline Malone, 2020) focuses on the changing landscapes of early Malta, and provides the background for the following two volumes. Volume 2: *Temple Places* (edited by Caroline Malone, Reuben Grima, Rowan McLaughlin, Eóin W. Parkinson, Simon Stoddart & Nicholas Vella, 2020), reports on the archaeological studies of six sites through an examination of their chronological sequence, material culture and economic role in the Neolithic world of Malta. These discoveries set the scene against which Volume 3: *Temple People* (edited by Simon Stoddart, Ronika K. Power, Jess E. Thompson, Bernardette Mercieca-Spiteri, Rowan McLaughlin, Eóin W. Parkinson, Anthony Pace and Caroline Malone, 2022) are reassessed. This volume also has an additional role since it follows on more directly from the 2009 publication: *Mortuary Customs in Prehistoric Malta* (edited by Caroline Malone, Simon Stoddart, Anthony Bonanno & David Trump, 2009). That volume revealed one of the largest prehistoric burial assemblages yet discovered in the Mediterranean, amounting to some 220,000 bones, with a rich assemblage of animal bone, figurative sculpture, symbolic artefacts and architectural remains. The new volume concentrates on the human remains, taking their evidence to a new level. In the light of better understanding of the changing environment and resources of a small island world, the early people of Malta emerge as a remarkable community telling an important tale of prehistoric resilience and survival.

Chapter 1

Introduction: people of early Malta and the Circle

Caroline Malone, Simon Stoddart, Jess E. Thompson & Nicholas Vella

1.1. Introduction

This work is the third in a three-volume series that was planned from the outset of the *FRAGSUS Project* ('Fragility and sustainability in restricted island environments: Adaptation, cultural change and collapse in prehistory'), with the aim of addressing a number of key research questions about early Malta, its people, archaeology, environment, and landscape change. Volume 1 (French *et al*. 2020) examines the environment and landscape, Volume 2 (Malone *et al*. 2020) records the archaeological excavations that were undertaken during the project, and the present volume, Volume 3, revisits the Circle[1] on Gozo in a detailed re-assessment that builds on research published in 2009 (Malone *et al*. 2009d).

The award of an Advanced Research Grant (no. 323727) from the European Research Council (ERC) enabled an ambitious project that brought together both interdisciplinary approaches and a range of international scholars to focus on interrelated questions. The substantial funding revolutionized the manner of investigation by enabling the employment of numerous post-doctoral researchers to support specific scientific work. The funding enabled effective fieldwork, extended seasons of data collection, and importantly, the follow-up analysis. The outcome of this programme of remarkable, energetic work is recorded here and is a tribute to a small and skilled team of international researchers from three continents and eight nations who brought a variety of approaches and debates to the material.

1.2. The origins of work at the Circle: funerary archaeology in Malta

The study of ancient human remains and burials in Malta had, until the 1980s, not been a major subject of research or interest in comparison with the remarkable prehistoric megalithic temple structures. This was in spite of the recognition of many small rock-cut tombs (Zammit 1928) and the magnificent Ħal Saflieni Hypogeum that was discovered in the first years of the 20th century (Zammit 1910) where the main analysis was on the few recovered human skulls and crania (Zammit *et al.* 1912; Zammit 1912a). Bodies, bones and pathology had not been of much interest to anthropologists, other than for estimating burial population numbers (and their 'racial' characteristics) (Bradley 1912). The study of human bones to further understanding of their life course and the rituals of their interment was to be an interest for future scholars.

There was much excitement starting in the 1920s, and continuing into the post-war period, about the potential for the presence of Neanderthals in Malta, based on the interpretation of the morphology of teeth found by Despott (1918, 1923) allegedly at Għar Dalam (Keith 1924). However, Mangion (1962) showed that the morphology of these teeth was also present in modern populations. Although Malta was connected to Sicily until *c*. 12500 BC (Furlani *et al.* 2013), there is still no convincing evidence of a Palaeolithic presence in Malta in spite of claims to the contrary.

Themistocles Zammit, himself a medic, concentrated on other key scientific issues such as chronology, rather than the potential of the human remains. This is seen effectively in his important article on rock-cut tombs (Zammit 1928) where he saw distinct differences not only between the later Punic and the prehistoric tombs, but also within the prehistoric examples on the basis of differences in pottery. In this article, he reported on three tombs discovered at Buqana (Attard), Xagħra and Nadur Benjemma (alternative spelling: Binġemma) respectively. In the first, he noted that the bones were richly covered with red ochre:

> 'the workmen reported that they had broken into a grave in which human bones were lying in what they described as fresh blood.

> On inspecting the site, I found fragments of old human bones mixed with potsherds in a muddy pool deeply stained with red ochre.' (Zammit 1928, 481).

At the second location in Xagħra, on the same plateau as the main deposits studied in the rest of this volume, he noted articulation as well as disarticulation:

> 'Broken bones of at least four human skeletons were obtained, in addition to tiny fragments, mixed with stones and a sandy soil.' (Zammit 1928, 482)

At the final location of Nadur Benjemma, he was rather dismissive of the potential of the human remains, no doubt because they presented a challenge not often faced by the medical profession.

> 'Fragments of bones were found, but so minute that their examination could lead to no practical conclusion.' (Zammit 1928, 483).

These observations by the designated father of Maltese archaeology may explain why few intact tomb groups or skeletons were retained for study, when we now know that disarticulation was a major feature of the prehistoric ritual. Skulls were the main focus of interest (Zammit 1930, 121). Many tombs were emptied and barely reported to the museum authorities, although, as the Museum Annual Reports reveal, the Museum staff continued to record tomb discoveries almost every year until the present, reaching a total of some 480 tombs (Pace 2011).

Napoleone Tagliaferro (1843–1915), another scientist and rector of the University, was one of the few scholars who took a more positive view of the potential of human remains, but he remained frustrated by the disorder that we now know to have been the creative fruit of ritual process. This becomes clear in his comments on the discoveries at Ħal Saflieni:

> 'The mode of burial remained, however, doubtful, as there were no sufficient data to decide whether the hypogeum was a real burying place or an ossuary or both.' (Tagliaferro 1911, 147)

After initial disappointment that the human remains were not Palaeolithic, inferred from the presence of pottery, he was more positive and detailed in his description of the human remains in the cave at Bur Mgħez (Tagliaferro 1911; 1912), perhaps because there was a greater degree of articulation. In the tradition of the day, he also included in his description the fact that they were dolichocephalous (long-headed).

The Oxford anthropological expedition from December 1920 until January 1921, headed by Leonard Halford Dudley Buxton, the leading expert of his time on the nasal index, deserving of an obituary in *Nature* on his early death at 49, concentrated on the study of one hundred living females from Gozo, with the assistance of Miss Moss, Miss Russell and Miss Jenkinson. More broadly he was very keen to achieve what we might now call a representative stratified sample, excluding foreigners to produce meaningful statistics of the real Maltese population. In their more limited study of the restricted material from prehistoric times, Buxton noted the potential demographic interest of the human remains from Ħal Saflieni:

> 'It has been suggested that the large number of bones found in the Hypogaeum is evidence of a large population in Neolithic times' (Buxton 1922, 172).

Later in the report, Buxton goes on to discuss the difficulties of working with these bones and states that Bradley had already undertaken the then popular examination of crania.

> 'The Ħal Saflieni bones (whose antiquity we have already discussed) are in very bad condition; few long bones are complete. After sorting through several tons of fragments, measurements were taken on such bones as were sufficiently well preserved. A number of astragali were brought to England for more detailed examination later. The Ħal Saflieni crania, which had previously been examined by Bradley, were remeasured.' (Buxton 1922, 174).

The information on the results of these analyses for prehistoric times is limited, but he did note some details, particularly related to the physiology of respiration, specifically that:

> 'The basi-nasal length appears to be the same form Neolithic times onwards.' (Buxton 1922, 178)

and

> 'The upper facial height in Ħal Saflieni (Malta Local Neolithic) material is similar to that of the Romano-Maltese.' (Buxton 1922, 179)

and

> 'Turning to the respiratory apparatus proper, the nasal breadth of the Neolithic people is rather narrower than that of the Romano-Maltese, but only six Neolithic crania were available for measurement.' (Buxton 1922, 180).

Of great interest to the current report is the fact that he made a relatively detailed study of the 224 teeth he recovered from Ħal Saflieni, noting specifics such as 19 cases of caries (including the complete destruction of roots in 2 cases), perhaps slightly higher than the Circle populations (§4.5) although 'less' than modern populations, and canines with 'marked edge to edge bite' which might conceivably be the wear noted in the Circle populations. Much of this information was summarized in a useful table (Buxton 1922, 181–2).

He summarized his findings as follows:

> '… the general characters of the Maltese skulls at our disposal, the physical type conveniently termed "Malta first race" is associated culturally with the Malta Local Neolithic. Skulls of this type are long, narrow, and slightly built. They have low orbits, narrow zygomatic arches, and a jaw which, though often not absolutely large, has a low ascending ramus, a shallow sigmoid, and considerable breadth in the antero-posterior diameter. They appear to be representatives of the Mediterranean race.' (Buxton 1922: 182).

Later in his report, as part of the longitudinal study of Malta, he concludes in a section entitled 'Racial problems',

> 'The megalith builders, who may be conveniently termed "Malta's first race" (culturally "Local Neolithic"), are certainly akin to the early, and, indeed, present inhabitants of North Africa and to those of Sicily, Corsica, Sardinia, and Spain, and belong to what is usually known as the Mediterranean race, differing from many skulls of this type in having a shorter nasal aperture, and therefore a bigger nasal index.' (Buxton 1922, 189).

Later he remarks on the distinction from the so-called 'Malta's second race', which, in his opinion, cannot have come from 'anywhere but the Eastern Mediterranean ….' but had 'no affinities with the Carthiginians.' This change he nevertheless associated with the Phoenician period (Buxton 1922, 190). These outdated perspectives on the attribution of 'race' are typical of the research focus of the period.

Buxton was the most prominent and systematic of the relatively few scholars in the first half of the 20th century who employed biological anthropology methods, even though Zammit recorded skeletal information in the Museum Reports on Punic and Roman tombs, and some suggestions were raised by the active fieldworkers (Zammit 1930; Ashby *et al.* 1913). Others, namely Ugolini and Mayr, worked to collate and systematize knowledge (Pessina and Vella 2012; Mayr 1901) which linked Malta's early cultures with wider Mediterranean development, even though there was disagreement on where and how cultures emerged and 'diffused'. There were several reasonably well-recorded excavations between *c*. 1900 and 1930, but the great Hypogeum had largely missed any systematic work, with the consequence that human remains were little considered. Post World War II, John Evans' monumental study in the mid-late 1950s included the salvage of the Xemxija Tombs complex (Evans 1971, 112–6). There the human remains were collected and subjected to an initial study by Pike (1971, 236–8) and Rodgers (1971, 238–9). For many decades, the whereabouts of the assemblage was unknown, until located, together with other Malta related archives, in the Institute of Archaeology, University of London following the death of Evans in 2011. The human and animal bones had evidently been retained for further analysis which had not materialized (they have now been returned to the National Museum of Malta). Unfortunately, many field details of the context of this deposit have been lost. This rediscovery has nevertheless enabled additional study within this volume (Chapter 12).

Joseph L. Pace from the Anatomy department of the University of Malta summarized much of the available prehistoric information in an exhibition in the 1970s (Pace 1972) and worked on medieval material from St. Gregory's church at Zeitun (Ramaswamy & Pace 1979a; 1979b) and from the excavation of Ħal Millieri (Pace & Ramaswany 1990). David Trump, as curator of the Museum for five years, recorded tomb locations and grave goods from 1958–63, but his most significant contribution was in chronology building at the site of Skorba (Volume 2, Chapter 7), which opened a much wider debate about time, early colonization and cultural sequence (Volume 2, Chapters 1 & 2). Both Trump and Evans contributed to the ongoing systematization of material culture (Evans 1971; Trump 1966), but, in spite of their efforts, funerary archaeology remained a minor aspect of their relatively brief but intensive forays into Maltese

Figure 1.1. *Ġgantija's World Heritage status inscribed at the Visitor Centre (Photo reproduced by permission of Rene Rossignaud, Quality Assured Malta).*

prehistory. In short, the approach to tackle the complexity of funerary archaeology, was, as in much of the central Mediterranean, focused largely on artefact collection. By the 1960s, the National Museum of Archaeology displayed a reconstructed Żebbuġ-style rock-cut tomb, whilst a number of Punic burials in interesting containers and coffins were displayed in the Gozo Museum of Archaeology (Casa Bondi). By the 1980s, the megalithic monuments and the Hypogeum had become the principal focus of concern, especially their eroding and unstable state, and growing threats from rapid urban expansion and air pollution to their setting and integrity. The successful inscription of the temple monuments as a group and the Hypogeum as UNESCO World Heritage Sites was accomplished in 1980 (Fig. 1.1), and this action strengthened new interest and established the importance of the Neolithic in the heritage management of Malta. The inscription of the Hypogeum, in particular, revived questions about prehistoric burial ritual and the nature of the ancient Maltese people, making the work of the Cambridge Gozo Project particularly relevant in the late 1980s.

The imagined body was more favoured than the real body. Indeed, Zammit and Singer had written a remarkable paper on this subject already in the 1920s (Zammit & Singer 1924). One notable thrust of more speculative scholarship about prehistoric Malta by the late 1970s and early 1980s was focused on interpretations of megalithic architecture and temples, ancient imagery and notions of a Mother Goddess cult derived from Old (Balkan) Europe. Marija Gimbutas had pioneered, rather successfully, study of figurative art in Neolithic cultures in the Balkans (Gimbutas 1974; 1989; 1991). But as her ideas fermented and her feminist ideology expanded, the interpretations as applied to Malta (and probably elsewhere too) became extravagant debates, related to few observable facts. The Mother Goddess and her realm ruled absolutely across much of the scholarship, shading sensible and fact-led observation entirely, and was (and still is, see Rountree 2002, 38–40) revered by a large and enthusiastic following. Ironically it was this debate around prehistoric Mother Goddesses that indirectly gave birth to the Cambridge Gozo Project (1987–1994). In 1985, Anthony Bonanno organized a conference at the University of Malta around the theme of 'The Mother Goddess in the Mediterranean' (Bonanno 1986). The meeting attracted leading scholars including Colin

Renfrew and Marija Gimbutas. The latter expounded her extravagant theories on goddesses to such an extent and with such evident lack of archaeological detail, that Colin Renfrew determined it appropriate to suggest that new research in the field rather than the library might be timely. And thus, following an invitation to scholars in Cambridge for a programme of fieldwork, a new team and a new era of fieldwork on the prehistory of Malta were born, comprising David and Bridget Trump, Caroline Malone and Simon Stoddart, in collaboration with Anthony Bonanno and Patrick Schembri in the University of Malta and Tancred Gouder in the Museum. The goals, as set out below, were to explore the environment, landscape, settlement and burial aspects of prehistory in a modern and scientifically informed way. The invitation was broad and enabled the team to select almost anywhere as a focus of investigation (see below).

The moment for new work was timely, since Anthony Bonanno had just launched a new archaeology degree pathway at the University of Malta, giving a generation of enthusiastic young scholars the opportunity to participate in practical and scientifically focused field archaeology. For more than two decades, little teaching or research in the field of prehistoric archaeology had taken place in Malta, leaving a lack of expertise. Immediately following Independence, the main active 'research' project was undertaken at the site of Tas-Silġ by an Italian team, invited to excavate as a diplomatic concession to Malta's nearest neighbour in the central Mediterranean in 1963, just as relations were being severed with Great Britain (Vella & Anastasi 2019, 553). That work was focused initially on the Punic period, although in later years earlier prehistory emerged at the site in an exciting manner (Cazzella & Recchia 2012; 2015; Recchia & Cazzella 2011, Recchia 2004–5; Vella & Anastasi 2019). Under the later Labour administration of the new Republic of Malta (1971–87), cultural heritage was disregarded to the extent that field archaeology and international research collaboration had been almost extinguished and most Maltese scholars of archaeology studied abroad in Italy or Britain. Francis Mallia and Tancred Gouder performed miracles in keeping the Museums Department afloat in spite of the lack of resources.

When the Cambridge Gozo Project started, Malta's prehistory, perhaps the most iconic period of the islands' past, was almost entirely envisaged through the megalithic temples, the Hypogeum, pottery forms and figurative art which were presented through museum display and tourist material. In contrast, there was little interest in bioarchaeology or the nature of the early populations of Malta. Until the 1987–94 project, no prehistoric tomb in Malta had been excavated with the goal of recording human remains in context through a bone-by-bone analysis, dating and scientific study. This was not a unique situation, since few sites across the central Mediterranean could boast a systematic approach to the recovery of human remains from funerary sites (Borgognini Tarli 1992). The duration of the Cambridge Gozo Project and its immediate aftermath coincided with a changed view of the ancient cultural heritage, that was epitomized by new colourful and accessible books from the Midsea publishing house, notably those by David Trump (2002) and Anthony Bonanno (2005).

1.3. Dating early Malta and changing approaches to the past: scientific questions and approaches

The development of absolute dating and its adoption by David Trump at Skorba following his work on the temple site (1959–63) represented a major impetus to the study of Maltese prehistory (Trump 1966). The establishment of the antiquity of the Temple Culture and the early date of likely colonization of the Maltese Islands was particularly important in the growing understanding of the spread of farming and Neolithic culture in southern Europe. However, just as Malta's past emerged, access to examine it was reduced from 1964 onwards. Instead new debates and methods, led by Colin Renfrew in particular, focused on the scientific recognition of materials that connected Malta with the wider Mediterranean. Obsidian distributions and indicative chronological developments, for example, were proposed to demonstrate the indigenous nature of the Temple Culture, together with many other cultural developments in the central and western Mediterranean. Renfrew showed that the Temple Culture had nothing to do with the diffusion of Mycenaean culture that had dominated interpretative models and academic debate of cultural development for decades (Vella and Gilkes 2001). Instead, Maltese and European megaliths were explained through independent invention. David Trump had always championed that notion and recognized the absolute distinctiveness of early Malta against comparable phenomena in Sardinia, France and Spain (Trump 1981). Throughout the period after 1963, he presented a synthesis of Malta's archaeology (Trump 1976; 1999; 2002; 2004) supported more generally by his work in Sardinia (Trump 1983; 1990). But with the lack of ongoing activities, the field of interpretation lay wide open to ideas from far away.

1.4. Research goals of the Cambridge Gozo Project

The goals of the Cambridge Gozo Project were to address various questions about the prehistoric world of the Temple Culture that had hitherto escaped

Figure 1.2. *a) Preliminary sketch of the entry to the Circle by Charles de Brocktorff,* c. *1822; b) preliminary sketch of John Otto Bayer's excavations within the Circle by Charles de Brocktorff; c) aerial view of the Circle after excavations in 2017 (Photo courtesy of Tile Films drone team).*

much study. Landscape and settlement archaeology were a priority, given the severe lack of known sites to counter the rich Temple Culture monuments (Volume 1, Introduction), Burial, too, was highlighted as a theme to explore alongside the emergence and decline of the Temple Culture and its chronology. A choice was presented to the three principal project fieldworkers (Malone, Stoddart, Trump), that simply invited suggestions for sites which might be examined. Gozo was rapidly identified as the lesser known of the islands, and in need of research at every level. The choice of Gozo immediately led to the request for an investigation of a recently exposed domestic structure half-sectioned by building works at Għajjnsielem, identified by Joseph Attard-Tabone (Malone *et al.* 1988; 2009d, Volume 1, Introduction).

But more was required if the many questions emerging were to be addressed effectively. The mysterious site of the Circle, portrayed in the mid-1820s de Brocktorff images (Evans 1971, Plate 29.3,4; Grima 2004) revealed a potentially deeply stratified site, albeit probably empty and badly damaged (Fig. 1.2). So, the choice was made to re-examine the unparalleled curious site as part of the Cambridge Gozo Project. Various stone circles were known (Ashby, 1911 BSR Archive: ta_XXVIII_001; Fig. 1.3a), including another on Gozo, but the one that survived and had been investigated was the Circle. The de Brocktorff images were crucial in reidentification, because they allowed a topographical fix of the site against surviving landmarks both on the skyline (towards Malta), in the neighbourhood of the site (the surviving farmhouse) and on the horizon in a sketch of Ġgantija. One of these images showed a large crater containing megalithic elements, buried several metres below ground level, emerging from the centre of the circle. Although one of the figures portrayed in the image appeared to be holding a skull, it was not clear what material was being extracted from the site and no reliable records survived from the original site clearance (Attard Tabone 1999; Ashley *et al.*, 2016). The team determined, however, that it was definitely worth investigation. The size and the depth of the site required assessment, and before any works began, a programme of geophysical survey (resistivity, magnetometer and geo-radar) were employed to try and establish the nature and scale of the site (Malone *et al.* 2009b), to identify the best location to commence excavation.

Whilst the original goals of the Project were to range across landscape, economy and funerary archaeology, the scale of the Circle soon eclipsed aspirations of multiple lines of investigation, except for some field survey. Instead, the team refocused on funerary archaeology and the data that could be extracted from the funerary site to inform on wider

Figure 1.3 *(above). a) L-Mrejsbiet stone circle on Gozo (ta_XXVIII_001); b) Borġ l-Gharib stone structure on Gozo (ta_XXVII_098); c) L-Mrejsbiet megalithic structure on Gozo (ta_XXVII_100) (all from the Thomas Ashby Archive, All Rights Reserved, The British School at Rome).*

aspects of the Temple Culture. Environmental concerns were addressed through study of molluscs, microfauna, geology, human diet and disease, whilst the socio-cultural aspects were investigated through funerary practices, artefacts, art and symbolism. The outcomes of this work are recorded in the 2009 monograph (Malone *et al.* 2009d).

1.5. Excavation of the Circle

The excavation strategy focused initially on determining the extent of the cavity revealed by the geophysical survey. This had shown reasonably clearly the edges of the outer parts of what later became evident as an extensive collapsed cave system. The plots were tested in 1987 with a series of narrow trial trenches across the key areas. The trenches (Figs 1.4, 1.6), mainly cut through ploughsoil that was up to half a metre deep in places, revealed a complex of vine trenches aligned over the entire field. They had been excavated through soil and deep into the underlying bedrock. (Mikiel Bartolo, pictured in Figure 1.5, related that his father the tenant on the land had dug them in the first decades of the 20th century). The heavily worked soil of both the ploughsoil and vine-trenches contained mixed modern and prehistoric pottery and occasional bone fragments. The field was known to have been reclaimed by local farmers soon after the original excavations in the 1820s, and refilled with rubble, some of which soon became apparent in the excavation trenches.

Figure 1.4 *(above). The 'Circle' field before excavation in 1987 (Photo David Dunlop).*

Figure 1.5 *(left). Mikiel Bartolo, the elderly tenant of the field, in 1987 (Photo David Dunlop).*

Figure 1.6. *First trenches in 1987–88. a) Trenches in 1987, looking south; b) semi-aerial view looking north east; c) evidence of modern vine trenches in the excavations; d) expanded trenches in 1988 revealing the edges of the large cave cavity (brown). (Photos Caroline Malone).*

The annual excavation programme initially began with a June season in 1987, but from 1988 September was chosen to take advantage of university vacations. The years 1987–1990 were 4–5 weeks in length, increased to 6 in 1991, the fifth year of work, which at that stage was intended as the final year of fieldwork before a programme of writing up. However, not only were intact burial deposits revealed for the first time over an extensive area of the base of the opened caves, but the 1991 season also produced important artefacts (the twin seated figurine and the cache of stick figures) (Stoddart *et al*. 1993; Malone *et al*. 2009a, 289–305). Discussions with

Figure 1.7. *Excavation of rock-cut tomb. a.) Location of the tomb; b) the tomb shaft under excavation; c) the excavated shaft revealing the partly blocked entry to the west chamber (broken roof behind) and sealing slab over east chamber in foreground; d) the sealed east chamber entrance; e) interior of west chamber under excavation in 1988; f & g)* in situ *human remains in west chamber. (Photos Simon Stoddart & Caroline Malone).*

Figure 1.8. *Site in 1989–90. a) East Cave cavity under excavation showing remaining cave roof* in situ*; b) general view of opened site in 1989. (Photos Cambridge Gozo Project).*

the Museums Department and University staff determined that 1992 would be a season of post-excavation work, recording and field survey, followed by a final two-year excavation programme to resolve the opened parts of the site to a satisfactory level. The last two seasons were extended from July to September, typically 8–9 weeks in length, through the hottest weather and the most trying conditions for excavators.

The initial work in 1987 was split between two excavation sites, the Għajnsielem Road 'house' (Malone *et al.* 1988; 2009b) and the preparatory explorations of the Circle. Year 2, in 1988, saw focus almost entirely placed on the Circle, with some work on the landscape survey also undertaken (Volume 1, Chapter 6). That second year was directed to the careful clearance of the vine trenches and clarification of the site edges and areas of major early 19th century disturbance.

Fortuitously, clearance of two vine trenches in the SE corner of the site revealed a cavity beneath (Fig. 1.7). Between the two vine trenches, a curious red-stained circular deposit was recorded and carefully excavated to reveal a cylindrical shaft about a metre deep that divided at its base into two small openings. One was largely loose and broken, but the other was sealed by a circular slab, made to fit exactly across the opening, and concreted into position by millennia of calcrete formation. A small but distinctive carved stone 'statue menhir' was found fallen at the base of the shaft, probably once a grave marker on the ground surface (Malone *et al.* 2009a, Fig. 10.46). This was the 'Żebbuġ' rock-cut tomb (Malone *et al.* 1995) and presented the first opportunity for the project, and indeed in the Maltese Islands, to explore what appeared to be an intact burial context. Two oval chambers, each about 2 m in diameter, but barely more than a metre high formed the paired tomb, entered by a central vertical shaft (Malone *et al.* 2009f). The chambers, East and West, were significantly different, since the latter had been re-opened for the insertion of later burials with Ġgantija pottery and dates associated. Immediately facing the team was the question of a suitable field recording system that could extract the osteological material that lay below. There was no methodology that promoted the precise recording of dense commingled burial deposits. An approach was developed that ensured 3-dimensional spatial recording and precision (§1.6)

The Circle also comprised the major subterranean cave system which had been opened up by Bayer, the edges of which were clear in the geophysical plots. The West Cave (as represented in de Brocktorff's 1820s image) had been fully exposed, whilst the East Cave was still intact beneath a fallen rock roof. The roof of that cave had evidently collapsed in later prehistory, but was shown later to have always been unstable, since large worked megaliths from another site (perhaps Santa Verna, see Volume 2, Chapter 4) were used to prop up the fragile and thin rock roof in Neolithic times. Beneath the rock fall, various megalithic structures survived together with burials comprising both disarticulated and articulated remains, the latter especially in the deeper recesses of the cave. Only limited areas of the East Cave were explored by the Project, whilst the West Cave offered opportunity to salvage already damaged and disturbed areas.

Once open, the main (West) cave of the site was evidently the area revealed in the de Brocktorff image, showing a deep cavity with megalithic elements. As noted above, it had been indiscriminately refilled with rubble, rubbish and soil around 1830 (since according to letters written by Richard Colt Hoare on his travels in Gozo, he could find no trace of the site (Attard-Tabone 1999; 2010). The removal of the fill was extremely arduous and difficult, since it was not known what lay underneath, or what depth it extended to. Excavation methods were almost all by hand, other than an annual visit by a crane or JCB machine to remove especially large rocks and to remodel spoil dumps. A simple winch and pulley system lifted hand-filled buckets from the increasing depths of the site (at least 4 m); wheelbarrows and sheer human strength undertook the majority of clearance work, and it was slow, hot and quite hazardous. The directors took a strict line on site safety, whilst also ensuring all archaeological features and skeletal material was recorded in detail.

In essence, it took 4 months (over 4 years) to remove the nearly 4.5 m depth of deposit in places of heavily consolidated material. The teams initially comprised UK and international university student volunteers, some professional volunteers from the major archaeological units in the UK, and a growing number of Maltese students from the new degree course in Archaeology learning the field skills of archaeology for the first time. They were trained and organized by the direction team: David Trump, Caroline Malone, Simon Stoddart and Simon Mason, assisted by Anthony Bonanno. Logistics were supported by Bridget Trump and Kenneth Stoddart, whilst experts (Corinne Duhig, Sue Yealland, George and Sheila Mann, Cristina Sampedro and Mick Wysocki) recorded the human remains. Carol Brown undertook conservation over several years, consolidating artefacts and bones. By the final years of the project, a good number of local volunteers had become proficient fieldworkers, and indeed, the practical experience proved to be instrumental in directing many to permanent roles in heritage, museums and university teaching in Malta, Britain and beyond. For details, see the full team reported in the 2009 volume.

1.6. Development of methodologies and progress of excavation (1987–94)

In the 1980s, computerization of catalogues and the development of software to plot densities and distributions became possible, using portable personal computers and laptops in Archaeology for the first time in the field. GIS was in its infancy, but the field directors predicted the future opportunities and began to employ techniques in the recording system, especially for the osteological archaeological data, that would be applicable in the future. There was no ready access to digital recording technology at the time of excavation so conventional photography, instant photography (Polaroid) or video were the means to capture imagery, whilst traditional survey using theodolite and dumpy level was employed to ensure the spatial record until the final year of work in 1994 when an EDM was used.

1.6.1. The rock-cut tomb methodology

The removal of the upper disturbed deposits of the Circle in the first year of work revealed largely random

Figure 1.9. *Site in 1990–92. a) Site clearance of backfill and 19th-century rubble from West Cave; b) rubble and backfill from the 19th-century excavations removed to reveal earlier surfaces and deposits; c) field recording of the site in 1992 following removal of rubble and remaining cave roof fragments.*

bone deposits, and by the second year, the discovery of the intact deposits in the rock-cut tomb demanded a standardized and effective recording system. The excavation teams were comprised mainly of students of varied levels of experience, so there was a need for a fool-proof method to record the human remains, alongside the more standardized archaeological recording of context features and finds. Fresh from completing a PhD dissertation of central Mediterranean prehistoric artefacts and burials which invariably had little detailed contextual record, Malone developed a protocol for recording commingled burials and bones. This was based on piece-plotting of material within 3-dimensionally measured areas (1 m square areas in the case of the Circle) recorded as 'spits' or levels in each stratigraphic context, in this case about 10 cm depth. The method replicated that typically used for lithic scatters and Palaeolithic cave sites, and enabled refitting of fragments across levels and parts of the grid as well as accurate GIS realization in the present project, that has allowed deeper understanding of the taphonomy and placement of skeletal material. Another influence on method and interpretation was study of the Huron Younge site in Michigan by Stoddart,

Figure 1.10. *a) Excavation of 'Display Area' 783 in 1993; b) view of cleared West Cave and 783 together with Deep Zone and 951 at end of season 1994; c) the 'Shrine' area showing David Trump (in blue) excavating around the base of the screen slabs, with revealed primary burials under excavation in foreground. (Photos Cambridge Gozo Project).*

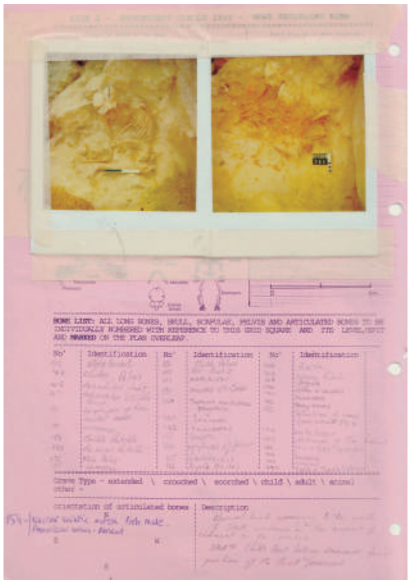

a.i

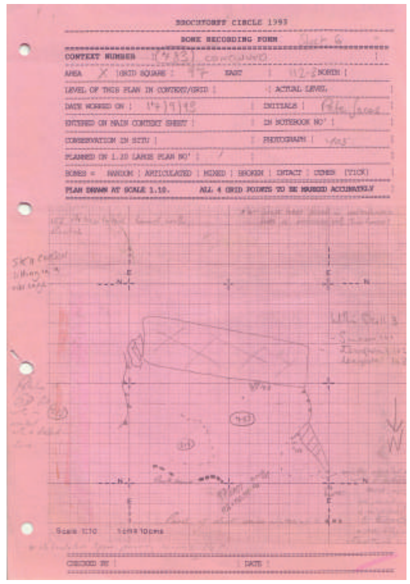

a.ii

a.iii

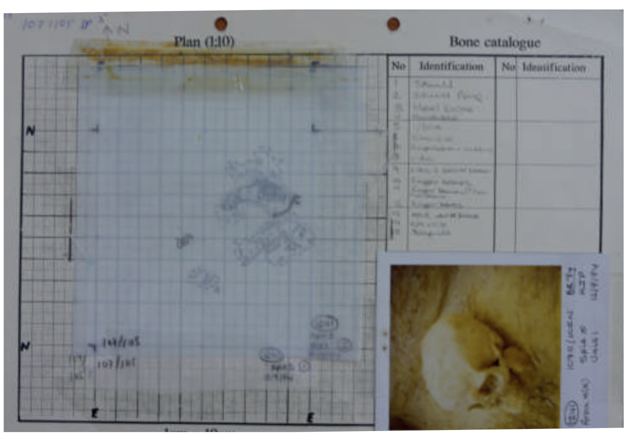

b

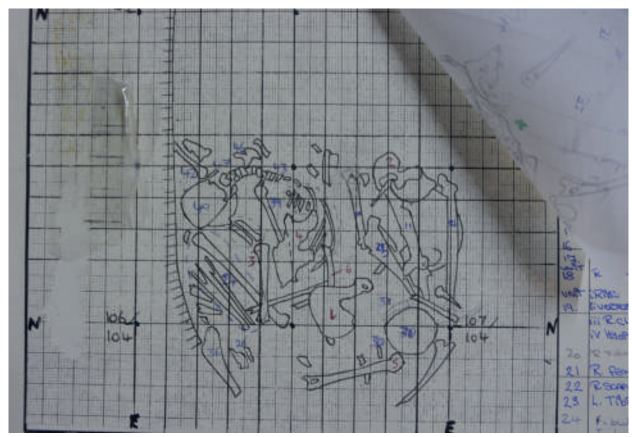

c

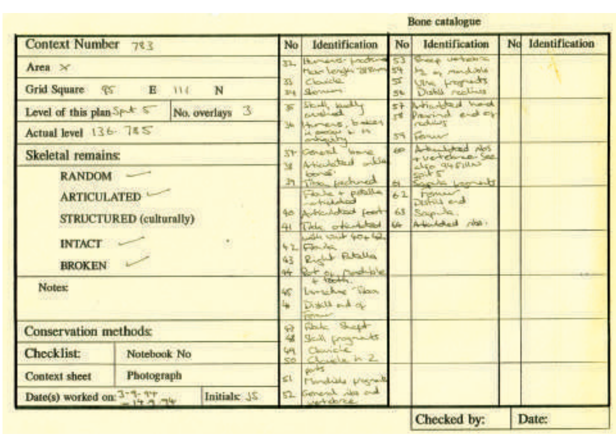

d.i

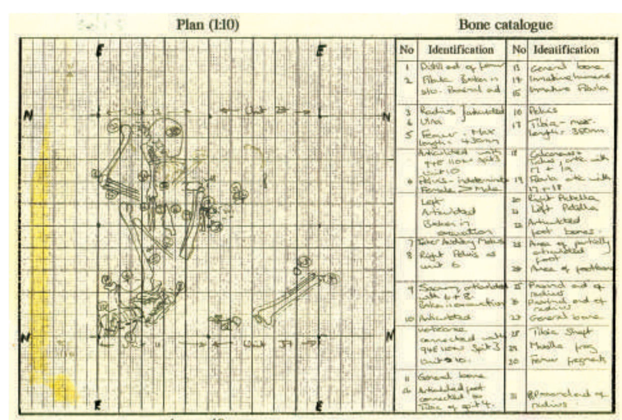

d.ii

Figure 1.11. *a.i-iii) Page from notebook showing recording methods for a 'spit' in a context (783) metre square with overlays for individual bone plotting (grid 112E/112–113N); b) Context (1241) recording sheet (grid 107E/105N); c) detailed recording of numbered bones in Context (1241), showing transparent overlay (grid 106E/104N); d.i-ii) Context 783 recording sheet showing lists of bones and related spatial plot.*

where ritual process had similarly led to distinctive disarticulation (*for more details see* Malone *et al.* 2018).

The recording system was practised and tested in the very restricted space of the West chamber, where the oval-shaped tomb was divided across the diameter with a permanent tape reference line. Material culture (bones and artefacts) were then measured and drawn/plotted at scale on grid paper in relation to the reference line, layer by layer and context by context. A graph paper notebook was employed to plot the material spatially at a scale of 1:10, with each level or spit recorded separately. Initially the bones at the surface were infrequent and badly decayed where they had been vulnerable to rock fall, soil creep, rodent activity and humidity. But as the upper layers were cleaned away, better preservation was soon encountered, and so plentiful were the dense and commingled bone deposits that it was clear that individual skeletons were unlikely to be easily identified. So, to ensure that bones in groups and as individual fragments, together with decayed material, loose teeth, beads and small objects were recorded precisely, the recording process sub-divided the tomb floor into measured squares/zones. These enabled very fragile bones to be bagged with an individual code separately packed into marked paper bags for later cleaning and study. Photography was attempted, but the conditions proved difficult for effective photographs in low light and insufficient space (Fig. 1.7 f & g). In addition, all the soil extracted from the tomb was systematically sieved over a wheelbarrow immediately set beside the tomb entrance which captured small bones, teeth, beads and objects. Soon after commencing the West chamber excavation, the East chamber was also opened, and found to be more intact, but containing a smaller assemblage of osteological material. The last elements were lifted in 1989, when the final layers of the tomb were excavated.

1.6.2. Methodology for the main caves and deposits

The rock-cut tomb provided a testing ground for the development of the recording methodology, which was then adapted and streamlined for dealing with the larger, deep cave site. The entire site was surveyed and laid out in a 1 m square grid, and systematically planned and levelled as the excavations proceeded. Intact deposits of significant burial material were not encountered until removal of at least 3–4 m of overburden in the East and West Caves, but did occur in surface pits and crevices, where the recording approach was also applied. This is related in detail in the site report (Malone *et al.* 2009b). The damage and disturbance caused by the 19th-century exploration by Otto Bayer and the crude backfilling which followed his work had exposed, damaged and destroyed an unknown quantity of features and burials, but fortuitously the work had stopped soon after 1824, and the site was backfilled, as recorded by Attard-Tabone (1999) in the years following. The upper levels of fill removed by the Cambridge Gozo Project in the early years of fieldwork (1987–90) demanded enormous physical effort, and at the time, there was little notion of discovering intact levels beneath (see below).

The mass of bone material from the site comprised some 220,000 bones/fragments/teeth, representing perhaps as many as 800–1000 individuals, depending on which element is counted and how they were combined (Stoddart *et al.* 2009a, 319–21). The exact number of individuals buried was not, and probably cannot be, firmly established (given the previous history of damage, the still incomplete removal of burial deposit remaining *in situ*, and the difficulties of estimating the *original* number of burials in the absence of pair-matching long bones). The data show a complex process of multiple burial/deposition episodes involving constant removal, replacement, reorganization and ritual activity in the movement of skeletal elements around the site. From 1989 onwards, once the rich osteological nature of the site was identified, a succession of excellent bioanthropologists/medics assisted on the site, providing vital guidance and insight into the questions that might be posed in subsequent research. They compiled reports and guided the development of the methods described below and also processed and recorded the material (the Project is indebted to Sue Yealland†, Corinne Duhig, George Mann†, Sheila Mann, Cristina Sampedro, Mick Wysocki, Caroline Barker for leading this work).

1.7. The research methodologies of the Cambridge Gozo Project (1987–94)

As described above, the recording system was based on the Harris Matrix system (Harris 1979) employed widely across British commercial archaeology, which accompanies single context recording by identifying and recording individual deposits, features, structures through the allocation of separate numbers to each component. This enables a stratigraphic hierarchy that can be readily computerized. The 2009 volume demonstrates this approach in graphic form. Instead of the notebooks employed in the rock-cut tomb, the extended site and its numerous excavators demanded a streamlined system to enable mass recording. With the gridded site set out, the skeletal remains in each metre square were separately recorded on a pre-printed form that enabled piece plotting and numbering of each fragment and group of bones. The recording

Figure 1.12. *Clearance of the Circle in 1989. a) Megalithic screen structure emerging from rubble overburden; b) removal of precarious cave roof fragments after recording; c) general view of excavations in 1992; d) semi-aerial view of site in 1993 at start of excavation season, showing the east and west caves with remnant dislodged megaliths from the 19th-century backfilling* in situ *around the cavity. (Photos Cambridge Gozo Project).*

enabled each bone group to be accurately located in 3 dimensions, supported graphically by scaled plans and Polaroid photographs that instantly captured the image of the bones and could be annotated and attached to the drawn plan, and listed as numbered items for each square and level.

The bones were then lifted and placed in numbered bags or boxes that recorded the bone number, square, level, date and excavator. Some contexts such as (783) covered over 12 m^2, so effective precision recording was particularly important for larger commingled burial areas. Such deposits varied from *c.* 20 to 80 cm depth and required successive sheets/plans to record a single metre quadrant. Such deeper stratigraphic deposits of similar sediment were excavated by spit to record otherwise unrecognized stratigraphy. The

Figure 1.13. *Bone recording in the field. a) Recording 783; b) planning bones and structures, showing Andrew Townsend; c) sampled metre squares in the deep east cave. (Photos Cambridge Gozo Project).*

drawn record was later traced onto amalgamated plans, layer by layer (e.g. Figures 8.60 and 8.61 in Stoddart *et al.* 2009c), which revealed the density of burial material in certain areas of the site. This work exposed the changing pattern of bone distribution as the burial niches and spaces and access to them evolved over some centuries. On completion of excavation of each context, the combined levels provided a view of the burial material spread over areas covering, in the case of Context (783), as much as 12 square metres and over a depth of nearly 50 cm. Such bone plotting and recording seems to be surprisingly rare in our subsequent review of prehistoric burial sites where commingled bone was encountered. The data have subsequently enabled a GIS exercise that has plotted and analysed the arrangement of skeletal remains (Chapters 3 & 12).

Figure 1.14. *Amalgamated bone plan for (783) (s = stone).*

In reviewing the methodology of the 1980s–90s from the vantage point of the present, many things might have been done differently and better. But then with restricted funding and access to Polaroids rather than digital photography, the conventional methods nevertheless proved effective. Investment in an overhead photographic rig could have been very useful, which today would be replaced by digital scanning technology. But well over 6000 photographic colour and black and white images of the entire excavation were made, which provide a substantial record. A permanent cover over the site could have enabled longer seasons of work by professional archaeologists, and a much larger budget could also have enabled different excavation approaches. But the record has been proven to be accurate and adequate, and the data has been readily extracted, enabling the present re-assessment to be undertaken. During fieldwork, the process of cleaning, recording and lifting bones became a useful training tool for students new to field archaeology. With little prior experience, they could grasp the simplicity of the grid, the spit and the scale drawing at 1:10 on grid paper. Individual elements could be referenced across the entire, extensive site, through the survey grid, and it worked because it was simple to use, with few risks of data loss. The systematic process also enabled supervisory control whilst also giving some degree of autonomy to the excavator.

The significance of the method and the reason for revisiting it here, is that two decades later we were able to identify individual bones or teeth which contain significant pathology or features because the recording system worked effectively. A substantial proportion of the material is thus capable of precise 3D location and association with other skeletal and cultural material, and individual bones associated with particular contexts and artefacts can be accurately dated (Malone *et al.* 2019). At the level of detail now demanded from the osteological material, we were also able to turn the static plan drawings, layer by layer, into a complex and accurate GIS to display and interrogate the burial complex. By plotting each significant bone in position, a full digital reconstruction has become possible including the implementation of virtual reality suitable for both research and museum display (Malone *et al.* 2018; Thompson *et al.* 2020; Chapter 3), supplemented by digital scans of the remnant cave site by John Meneely, and the extensive photographic record.

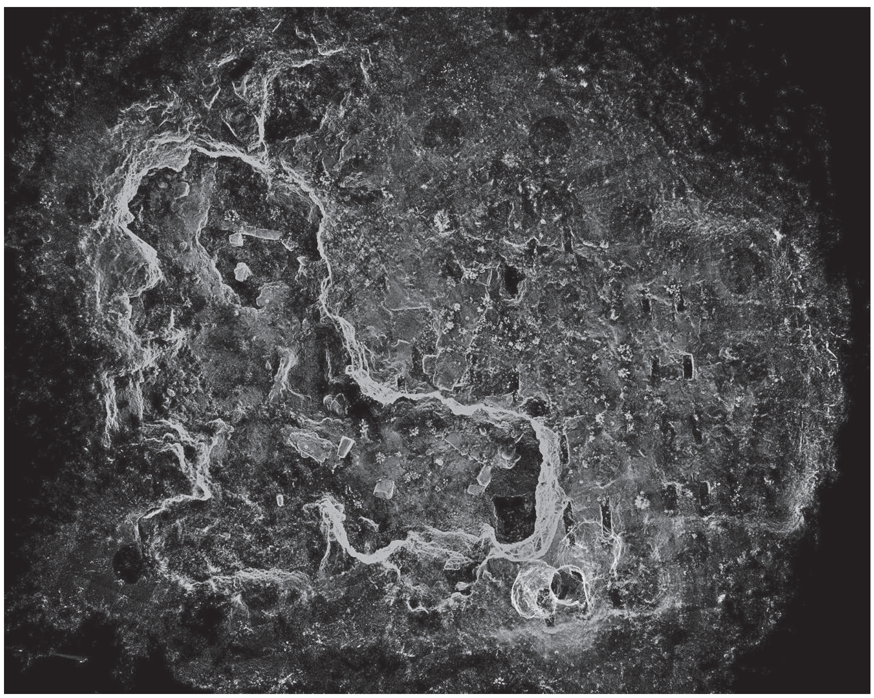

Figure 1.15. *Digital scan of the Circle cavity in 2015 (John Meneely).*

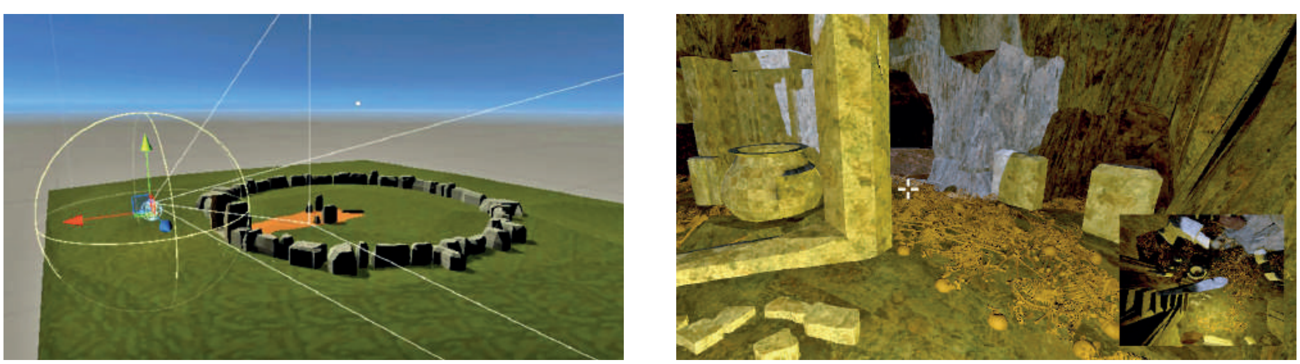

Figure 1.16. *Virtual reality study of the Circle caves (Robert Barratt).*

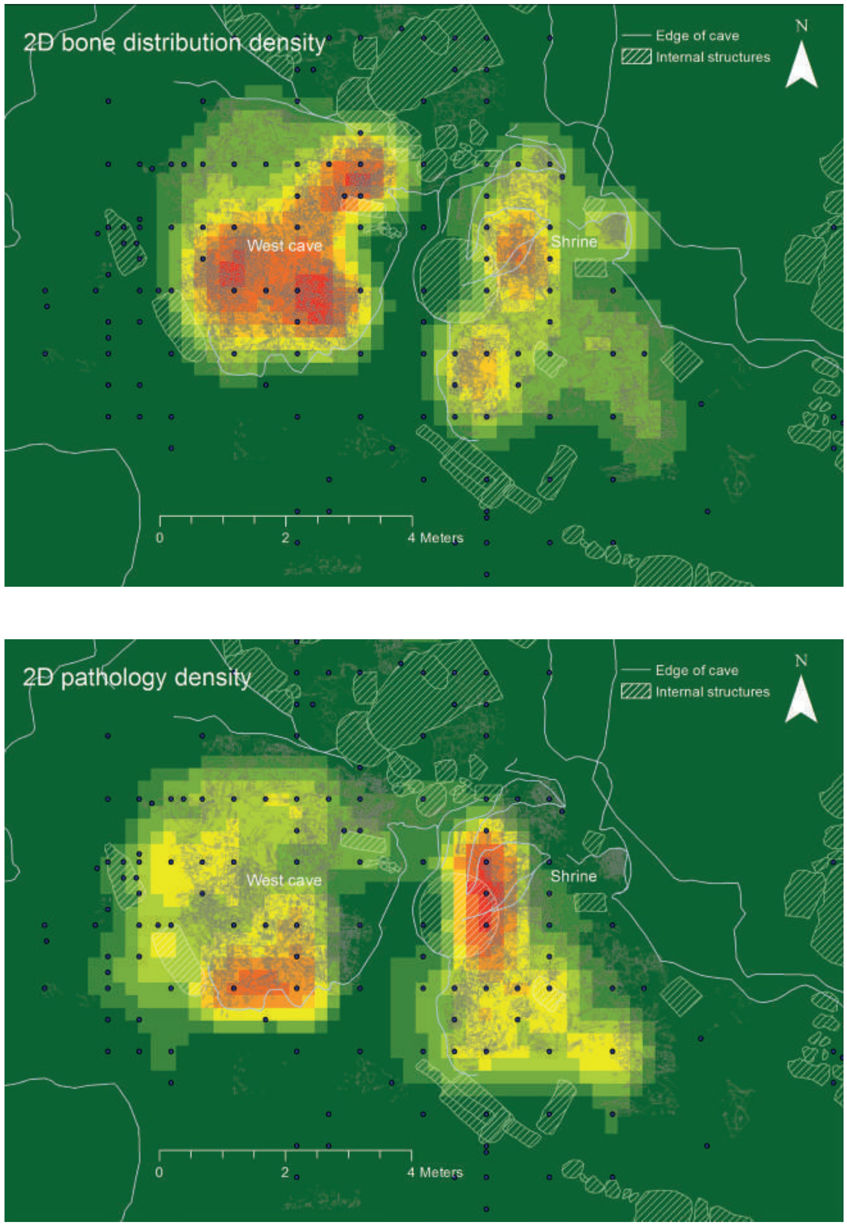

Figure 1.17. *GIS study of the excavated bones in (783) (Eóin Parkinson).*

1.7.1. Methodologies for bioarchaeological analysis

The Circle produced an astonishing quantity of bone, mostly highly fragmented, but all the bone was carefully excavated and retained for study, while the larger and more recognisable elements were recorded in detail. The next stage of work involved drying the damp material, and carefully brushing the chalky dusty deposit from it. Much of this work was undertaken within hours or days after excavation. For some contexts, lifted towards the end of a season, this had to wait until later. Some bone was heavily concreted with limey deposits, harder than the bone itself, and these posed a problem for cleaning. Most, though, were prepared for the ongoing study. Where crania or entire long bones were lifted, some conservation treatment was sometimes required to stabilize or glue elements in place, but intervention was rare, since the aim was to retain un-treated bone for future chemical/isotopic analysis. Storage of the material was in the original paper bags within purpose made cardboard boxes.

The recording process was undertaken only by experienced biological anthropologists and involved a laborious sorting through each bag/context and listing all elements, making relevant measurements, checking for pathologies and special features and the information was recorded on purpose made sheets. This was the lengthiest process of the entire project and it proved impossible to complete it all within the field and post-excavation study seasons in Malta. Fortuitously, an opportunity to transport unstudied and particularly significant contexts presented itself. This was in part thanks to a generous invitation from the British High Commission to a cocktail party to celebrate the final voyage of the Royal Yacht *Britannia*, which was harboured in Valletta in September 1995. An introduction made by Ann Monsarratt† (1937–2020) (a keen supporter of the project over many years) between Simon Stoddart and the Chief Engineer of the ship enabled a conversation that resulted in the offer to transport the large bone consignment to Portsmouth (Fig. 1.18). It was readily accepted and paperwork prepared for the export of the material. Additional boxes were transported to Bristol University where the Cambridge Gozo Project was then based. A small team of keen post-graduates assisted in the final preparation and recording of the material, which by the late autumn of 1995 was joined by the Britannia consignment. Caroline Barker, Cristina Sampedro, George Mann and Gary Burgess variously worked on the material and data-log. In 1996 the Project moved to Cambridge, where the McDonald Institute kindly provided a basement lab for continuing research on the project. The database required formatting, and David Redhouse at Cambridge developed a relational Access database.

The hundreds of recording sheets were logged over many months, funded on small and rather irregular grants. Indeed, the entire Cambridge Gozo Project was funded on what today would be impossibly small grants and relied on unpaid volunteer assistance. Eventually the mammoth task was completed in late 1998, just as the demands of the editorship of the *Antiquity* journal by the lead researchers (Malone and Stoddart) delayed opportunity to concentrate on writing and completion. On relinquishing the editorship in 2003, research again focused on the analysis and interpretation of the database. Time was pressing, money was very scarce, and the database was exported to Excel, to enable information to be extracted more easily. Simon Stoddart undertook that work and brought the complete data list to publication in the 2009 volume. But that work of archaeological reporting, in the first instance, could not explore as deeply into the complex patterns and significance of the remarkable osteological assemblage. Indeed, the volume in 2009 was over 500 pages, and its publication relied entirely on the acquisition of a number of small publication grants. It was not practical to plan to publish in even greater detail at that stage. Significant funding, much more time, and a dedicated team of scholars would be needed, and there was no opportunity in the early 2000s to find that. Applications had been made to key funding bodies in Britain to support particular aspects of the population study. Surprisingly, these applications were turned down, usually on the pretext that 'osteological and population study was not original or cutting-edge science…'!

Figure 1.18. *Collecting the bones transported in the Royal Yacht* Britannia *in 1995, showing senior crew, Toby Parker, Simon Stoddart, Louise Loe and Karen Barker.*

Fortunately, since then, attitudes have changed, however it was not British- or Maltese-based funding that enabled further study, but instead, European Research Council funding on a much greater scale than could have been provided by other sources. As these collective *FRAGSUS Project* volumes report, a number of probing and difficult, yet simple, questions arose over the decade of writing up the Cambridge Gozo Project. The story of the prehistoric population remains a key element in all the questions – who were these enigmatic and creative early people of Malta? What was the role of the population in changing the landscape and exploiting resources? How did they respond to unpredictable food supplies? What was the role of ritual and symbolism in their lives? Were they fit, healthy and well nourished? Why was half the population dead before they reached maturity? These and many other questions then laid the base for Caroline Malone's application to the European Research Council.

1.8. Recent work

Since the completion of the first phase of the work at the Circle, another key site of the same Tarxien phase has been discovered in Malta, the Kerċem burial site also on Gozo (Pace 2011, 277), where the proportion of intact skeletons (three) to considerable quantities of structured, yet commingled, human remains appears to be similar, placed in an extended chamber. Full assessment is widely anticipated. Unlike the Circle, little symbolic material was identified, and it appears to be a continuation of the much more modest 'individual' tomb tradition of particular families, rather than an extended community (Chapter 14). The opportunity to reassess the Xemxija Tomb assemblage in terms of chronological, isotopic and taphonomic aspects has also advanced research. Thompson *et al.* (2018), as one of a number of significant published contributions, has noted dermestid beetle burrowing in bone that could explain funerary practices, such as wrapping bodies in animal skins prior to deposition. New dates have also been achieved for this significant site.

1.9. Reflection

Over the last two decades, much has changed in the approaches to field archaeology and recording. In the 1990s, a video camera seemed exceptionally modern, and a small primitive computer with a tiny screen of green letters/numbers against a black ground, the height of sophistication. Indeed, sponsorship via Olivetti was extended early in the project and equipment loaned from a local dealer to enable continuous data logging and reporting. The computers were useful for data entry in dbaseIII to make lists of material and allow simple reports to be prepared. Photography was undertaken using high quality 35 mm film in conventional cameras, supplemented by expensive Polaroid instant print film for site shots requiring immediate annotation.

Today, such approaches seem antiquated when every aspect of modern fieldwork is a digital process, tied into survey, statistical graphics, photos, spreadsheets and much more. Indeed, the evolution of the Cambridge Gozo Project into the *FRAGSUS Project* is intimately related to the changing technologies and capacities available to scholars, on their own desks. The capacity to collect, process and then interpret through statistical examination, the sheer volume of archaeological information is one of the transformative aspects of current work. *FRAGSUS* has recorded incredible quantities of information, at every level of detail. In the hands of a skilled researcher, using Bayesian modelling, for example, patterns and trends invisible to the uninitiated, become clear. This volume, as in Volumes 1 and 2 (French *et al.* 2020; Malone *et al.* 2020) is the outcome of numerous varied bioarchaeological studies. Whether it is individual bones, entire population structure, aDNA, chronology, isotopic study of carbon or nitrogen elements in the diet, understanding becomes clear through the use of effective mathematic interrogation. It is a far cry from the initial work of over 30 years ago, when such precision was not even dreamt of!

1.10. Impact of the project work, past and present

The Cambridge Gozo Project study of the prehistoric population represents one of the most thoroughly studied assemblages in Europe, for its date and context. However, the *FRAGSUS Project* contribution, including a battery of new, accurate AMS dates, isotopic analyses, aDNA, assessment of disease and pathology, the population becomes clearer and ever more interesting. What are missing now are the comparative data from other sites in the Mediterranean region to provide a wider context. For Malta, the Xagħra people remain the principal informants of a lost world that otherwise could have emerged a century ago, when Ħal Saflieni was discovered. We understand that new work is proposed on the remaining crania from the Museum collection and other residual bones. We wait to see what this work brings.

Meanwhile, it is interesting to step back and review how the Xagħra people and the bioarchaeological studies of their remains has impacted local identity, as well as Maltese and wider European scholarship on understanding of prehistoric Malta and its Temple Culture. Such projects build up a momentum of their own – forming intellectual teams who remain in touch for the remainder of their careers, and who impact in turn on their associates, students and institutions as well. Here we make a brief analysis of that impact.

For these reasons, it is worth tracing the historiography of the Circle (Fig. 1.19). The first period, prior to 1986, has been reported in the 2009 volume and by the rediscoverer, Joe Attard Tabone. It covers the original discovery of the Circle, its early part clearance and its reabsorption back into the agricultural landscape. A new phase started in 1986 when the Circle was visited by the Cambridge Gozo Project team leading to four cycles of intense activity that have led up to the present day. The first phase was associated with the scientific excavation of the Circle (1988–96) and produced a burst of output that culminated in travelling exhibitions around Europe. The second phase (1997–2004) comprised numerous articles and lectures on death that digested the importance of the sheer quantity of data and their significance. Up to this point more than one hundred outputs and a data structure report had already been created (*pace* Pace 2004, 189). The third phase (2005–08) culminated in the publication of the Circle and coincided with a first serious injection of funding into related studies

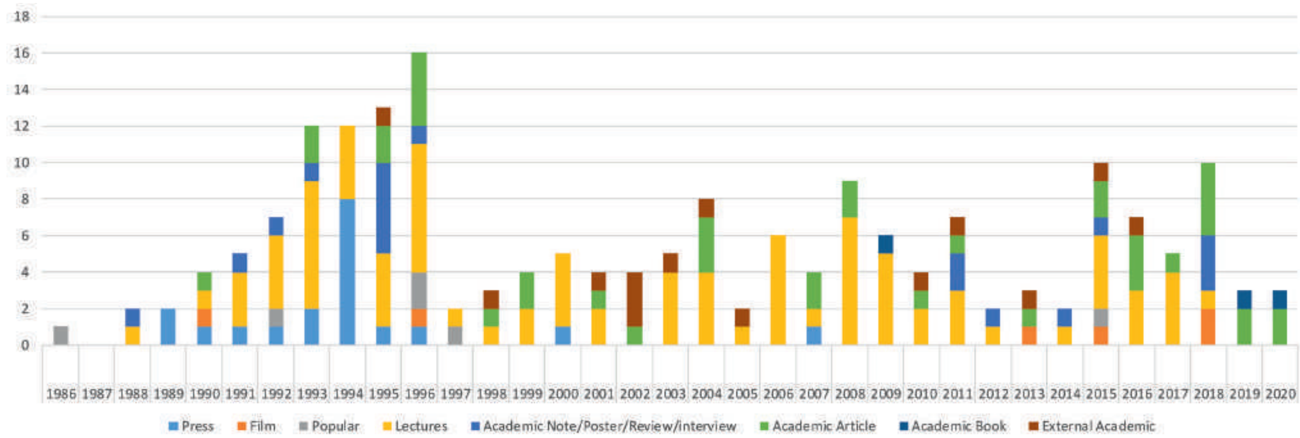

Figure 1.19. *Graph showing the output arising from the Circle research.*

by the Templeton Foundation, with further support from Leverhulme. The fourth phase (2013–present) was initiated by a British Academy grant to rejuvenate the stores of human remains and the creation of the site visitor centre, leading onto the *FRAGSUS Project.* At the present time, it is estimated that a further one hundred outputs have been generated (once the full press impact has been added) and the Circle shows every sign of being one of those sites which will be a mine for generating new interpretations and ideas into future decades and even centuries.

It is worth relating how the important data extracted from the Circle equally stimulated and generated new ideas on the theme of death over the three decades since the richness of the deposits was first grasped. The 1990 contribution to *World Archaeology* (Bonanno *et al.* 1990) drafted by Simon Stoddart, inspired by the ethnographic work of Boissevain, posited the presence of intense intra-group and personal rivalry rather than hierarchy (Renfrew 1973) as the social configuration of the populations who were buried in the Circle. This social configuration was linked to monuments, including the funerary monuments, noting the increase in complexity and the accretional size of such monuments over time.

The 1993 contribution to the *Cambridge Archaeological Journal* (Stoddart *et al.* 1993) pointed to the potential relationship between the relative physical isolation of the Maltese Islands (compared with other Mediterranean islands) and cyclical cultural isolation, and how these trends might be paralleled in the rituals of life and death in the Maltese monuments. The authors were struck by the difference between the exchange products in the Żebbuġ rock tomb within the Circle and those found in the Tarxien phases of the Circle, the first securely dated material from the Maltese Islands. The Żebbuġ tomb contained a cache of large local and smaller imported greenstone axes. The Tarxien phases of the Circle had relatively few and smaller sized imports accompanied by a substantial emphasis on the elaboration of local materials. The proposed model was that navigation to the outside world was increasingly in the hands of relatively few skilled navigators who extracted material and symbolic power for themselves, through knowledge of external lands (cf. Helms 1988), and used that power to support increasingly rich, structured and celestially/geographically orientated ritual in both the temples and mortuary complexes. The liturgical art of the Circle was substantially created from local materials deployed to great effect in support of the richness of the ritual. For the first time, Ħal Saflieni and the newly excavated Circle were placed within the same hypogeum category, since by this stage the extent of the burials had been proven. The 1993 article in the *Scientific American* (Malone *et al.* 1993) addressed the funerary ritual, as well as the liturgical art, more explicitly for the first time, and raised questions about why such an elaborate ritualization should have come to an end. In the same year, the fact that a natural biological community appeared to have been buried in the Circle was emphasized for the first time in a contribution to the *History of Humankind* (Trump *et al.* 1993).

The 1995 article in the *Proceedings of the Prehistoric Society* (Malone *et al.* 1995) provided the first systematic and comprehensive account of funerary practice based on human remains. The rock-cut tomb was originally considered to be Żebbuġ in date. The early date thus suggested, at the time, the precocious development of collective burial in the Maltese Islands compared with neighbouring areas, but a greater quantity of more recent dates and reconsideration of the old dates seem to suggest that the human depositions were principally Ġgantija in phase and that the Żebbuġ and Ġgantija phases were very closely related, so this initial interpretation needs to be revised, bringing collective burial back into line with the rest of the southern central Mediterranean. What endures as a valid interpretation is that the two chambers of this tomb continued to be used over a reasonably long period of time, where the prehistoric inhabitants removed some more substantial bones and pushed others to the back of the chamber, at least in one case leaving the most recent inhumation relatively intact in a central position. What was also noted at the time was the contrast between the size of the imported axes in this chambered tomb and the whittling down in size and piercing of so–called 'axe amulets' in the later phases of the Circle, and in other Tarxien deposits within the islands, suggesting that such imports were a differently treated resource in the later phases of Temple period ritual, including mortuary dimensions. Skeates (1995), in an article published in the same volume, also pointed to the fact that Malta was at the end of an exchange system where imported greenstones were reduced in size and perforated, and thus sacralized, reinforcing the exotic power of these exchange products, as suggested in Stoddart *et al.* (1993).

During this period, increasing attention was drawn to the diversity of the burial patterns (Malone & Stoddart 1995a) that were very different from the articulated deposits supposedly present in most cemeteries, ancient and modern. It was also noted that the Maltese government had chosen the symbols of identity recovered from the Circle as the leitmotifs of modern Maltese identity coinciding with the exhibition in Malta House in Piccadilly and accompanying lectures at the Society of Antiquaries (Malone & Stoddart 1995b; 1995c). Further publication described in detail the extraordinary prehistoric art discovered from within the Circle (Malone & Stoddart 1995d; 1996a; 1996b) and the spatial layout of the monument (Malone & Stoddart 1996c). It is significant that these publications occurred in the inaugural publication of the Malta archaeological society (Malone & Stoddart 1996b) as well as the second edition of the Magazine of the Fondazzjoni Patrimonju Malti (Malone & Stoddart 1995d).

Further work was presented shortly afterwards that focused on refinements of the funerary ritual and the art. Duhig (1996) gave her considered and definitive account of the funerary ritual of the rock-cut tomb and Stoddart *et al.* 1999 placed this within the greater complexity and diversity of the subsequent Tarxien period. The former article gave the first provisional statistics not just for the rock-cut tomb but for other Tarxien areas of the site. The latter article drew attention to other cases of structured, disarticulated human remains from Greece and North America. The analysis stressed the scale of the human remains, the necessary length of the post excavation process, and, in spite of the provisional nature of the discussion, the extraordinary diversity of practice. The cultural practice was also carefully mediated by the consideration of natural processes. Furthermore, some considerable detail of the spatial pattern of the human remains was given, providing a structure which continues to hold broadly true, although more recently, and in this volume, given statistical detail and further levels of variation. The article concluded by indicating the wealth of information available in Malta for comparing different dimensions of life and death, rarely available in early societies. In the same year 1999, further work (Stoddart 1999) introduced the idea of sensory perceptions of death, particularly sound, and placed the Circle in the broader context of the few other contemporary funerary sites identified in the Evans (1971) survey: Xemxija, Bur Mgħeż and Busbisija. A contrast was explicitly made between the focal points of Ħal Saflieni and the Circle and these smaller funerary deposits.

Robb (2001) investigated the issue of the elaborate ritualization of Malta, of which funerary activity is but one part. For the purposes of this volume, the key matter is a shared concept of 'ritual hierarchy' and just as Stoddart *et al.* (1993) cited Helms (1988), so did Robb, so despite the differences debated elsewhere (Malone & Stoddart 2004; other volumes), there is a point of convergence in the belief that ritual knowledge and differential access to materials from outside the islands endowed some members of society with increased power. In fact, Stoddart (2002) investigated the nature of that ritual power through a focus on the clustering of ritual objects found in the Circle. These finds were inserted into a wide-ranging cosmological landscape that was as much vertical as horizontal, and where the funerary landscape resided in the lowest tier, and since this tier was often physically enclosed below ground, where resonant sound would have had a profound effect. The article also raised the question of whether the whole community could have been buried in the Circle, and that this might in itself be another indicator of differential access to power. It also added action to the repeated burial ceremony, envisaging the funerary procession travelling from Ġgantija through the uprights of the enclosure, across the threshold above distinctive ancestors into the inner parts of the complex. Another ritual theme, nested cycles of life, was taken further (Stoddart 2004), inspired by his duties of teaching at Cambridge in the same subject. This approach suggested that the redolent ritual objects contained within them symbolic representations and that the short-term cycles of life were nested within longer term kinship lineages.

Malone & Stoddart (2004), in part in response to Robb (2001), pointed out that the main foci of ritualization (including funerary) in the Maltese Islands, of both monumental and portable form, were constructed substantially out of local materials. Quantitative data were employed from funerary contexts, the only ones then currently available, to assess the degree of interaction in two key periods. As a general trend, when corrected for length of time and numbers of participants, the foundation phases had larger objects and greater quantity, whereas the peak of ritualization had smaller sacralized objects, spread over a longer period. The 1993 *Scientific American* article was republished in 2005 in a collected edition (Malone *et al.* 2005). This gave the opportunity to comment on debates that had arisen in the interim. A series of questions were posed about the level of knowledge of the outside world and the degree to which this was in the hands of a few. Some of these questions are best answered in the other two volumes, but there is also a relevance vested in the level of participation in mortuary ritual and the degree to which local materials were prominently used to develop that ritual.

An important development was the funding by Templeton to look at the spirituality of prehistoric Malta. The main focus was on the temples (buildings we now designate club houses) and their art. Death rituals thus formed a relatively small part of the Templeton funded project, but two outcomes of the conference did deal with such matters. Stoddart (2007) applied some broad statistics to the evidence: a) to show how a potentially small living population might have contributed to the buried population; to illustrate the flow of bones through the site with a ternary diagram of crania, long bones and residual bones; to point out that men were deeply placed within the funerary stratigraphy. Many of these ideas anticipated deeper treatment in the final publication (Malone *et al.* 2009d). In the same conference publication, a number of the ideas of deep access originally outlined for funerary monuments, were given a quantitative computerized dimension (Anderson & Stoddart 2007).

As part of a Leverhulme funded project 'Changing Beliefs of the Human Body' (2005–2010) (PI: John Robb), one paper (Malone & Stoddart 2008) was prepared on this theme, which traced the interrelationship between the depiction, disposal and direction of the body across the various periods of prehistory. Much of the article focused on the size and context of art, showing that smaller mobiliary art was prominent in funerary ritual. It also introduced the idea of shrouds over some of the bodies, because of the presence of buttons in the parts of the funerary deposit and their probable attachment to such covers. As part of a festschrift to honour Ruth Whitehouse, Malone (2008) systematically categorized the same corpus of figurative art within a cosmological setting that expanded on Stoddart (2002) and Stoddart & Malone (2008).

A major watershed was marked by the publication of the Circle, charting the principal results of the Cambridge Gozo Project work as a detailed site report (Malone *et al.* 2009d). This volume assembled the full range of funerary data from the Circle with a comprehensive study of the stratigraphy, spatial layout, material culture and human remains. The volume concluded with a thematic account of mortuary ritual within the context of wider issues of the Maltese Islands and posed a number of questions which led to the *FRAGSUS Project.*

A number of publications continued to take analysis of the funerary ritual further in the wake of the comprehensive publication and ahead of the *FRAGSUS Project* results. Stoddart & Malone (2010) dwelt on the definition of hypogea and its particular significance historically in the Maltese Islands. The originality lay in trying to trace some of the trends of anatomically intact individuals predominantly placed on their right side in a flexed or contracted position, perhaps originally accompanied by an offering bowl, and sometimes shrouded. A further contribution looked at the cave concept in all its dimensions (Stoddart & Malone 2013), exploring materialized metaphors of history, materials, construction, physical constraint and stratigraphy.

Further articles have since investigated the implications of who contributed to the buried population (Stoddart & Malone 2015), considered the conditions of death in the light of ethnographic comparison (Stoddart 2015) and set the mortuary ritual in a broader context of religion (Malone & Stoddart 2011) and the full figurine corpus (Malone & Stoddart 2016) found in Malta. More recent articles have summarized the *FRAGSUS* experience (Malone *et al.* 2018) with a strong biographical element, starting in Michigan and ending in Malta, or reported on the wider ritual setting (Barratt *et al.* 2018; Stoddart *et al.* 2020), specific details of chronology (Malone *et al.* 2019), funerary taphonomy (Thompson *et al.* 2018; Thompson 2020) and spatial organization (Thompson *et al.* 2020). Knowledge of the Circle has had a major impact on the study of death in prehistoric Malta, and this will continue to have an effect long after the demise of the current generation of scholars.

This volume builds on these achievements by delving deeper into particular elements of the osteological sample, most notably the teeth (further detailed in §4.1). Very substantial improvements have been made to the chronology of the burial practices and the inferences that can be made from the chemistry of the human remains, especially from the perspective of diet, mobility and genetics. It is, however, on the teeth and long bones that most effort has been directed, drawing out new cultural patterns and understanding of the biology of the prehistoric inhabitants of Gozo. A more detailed investigation was also made on palaeopathology of the human remains, building on the groundwork already undertaken by George Mann to whom this volume is dedicated. From these studies, we have a deeper sense of the health and lifestyle of these communities. The broader patterns of age and sex profiles are still broadly those of the 2009 volume which also hinted at many of the greater details that will be found here. As will be frequently noted much remains to be done, drawing on the questions raised about the biological and cultural connections of these populations, as well as the state of their health and welfare. The volume ends with two chapters that situate the discoveries from the Circle within broader patterns of understanding of the funerary practices within the Maltese Islands, giving the latest interpretations of the evidence.

Note

1. We use this shortened nomenclature throughout this volume to refer to what has variously been known as the Gozo Stone Circle, the Xagħra Circle, the Xagħra hypogeum and the Brochtorff Circle (hence the BR code on all artefacts, since this was the nomenclature employed during the 1980s and 1990s excavation). Later in this chapter (§1.4) we illustrate one of the other Xagħra and Gozo Circles, photographed by Thomas Ashby, which no longer appears to be extant, and has no known associated artefacts or bones).

Chapter 2

New approaches to the bioarchaeology of complex multiple interments

Bernardette Mercieca-Spiteri, Ronika K. Power, Jess E. Thompson, Eóin W. Parkinson, Jay T. Stock, Tamsin C. O'Connell & Simon Stoddart

2.1. Introduction

This chapter presents the approaches and methods used for the recent scientific study of the human remains assemblage from the Circle underground burial complex. This study formed part of the ERC-funded *FRAGSUS Project* ('Fragility and Sustainability in restricted island environments'). We describe here the aims of the *FRAGSUS Project* and the questions addressed specifically by the Population History Workgroup, in order to contribute to the Project's wider research agenda. This chapter first outlines the complex multiple interments from the prehistoric burial caves of the Circle, and the challenges posed by the modes of deposition at the site and the density of human remains within the deposits, for subsequent post-excavation bioarchaeological analyses. We then detail the approaches and methods employed in the study of the human remains assemblage between 2013–2020, which will be expanded on in the following chapters within this volume.

2.2. The research questions of the *FRAGSUS* Population History Workgroup

The Population History Workgroup represents one of the key study areas in the *FRAGSUS Project.* The other four areas of focus were Environmental Reconstruction (Volume 1), Chronology, Archaeology (Volume 2), and Landscape History (Volume 1). As described elsewhere (Volume 1, Introduction; Volume 2, Chapter 1; This volume, Chapter 1), scientific techniques applied in an interdisciplinary manner aim to explore and present a detailed understanding of the prehistoric environment on the Maltese Islands, addressing how environmental changes impacted on the islands' early inhabitants. Through interdisciplinary work, archaeologists and scientists have together sought to identify any noticeable influences on the prehistoric population caused by settlement, land-use and a variety of other factors.

More specifically, the Population History Workgroup aimed to explore five questions that built on the preliminary results presented in the first publication of the Circle's human remains (Stoddart *et al.* 2009a):

(1) Are there particular pathological conditions in the Circle human remains assemblage which could shed more light on the health and lifestyle of the prehistoric population?

(2) Do the human remains reveal signs that this population experienced episodes of stress, perhaps caused by a change in the climate or available subsistence resources?

(3) Is there bioarchaeological evidence for particular occupational, cultural or technological practices which identify specific lifestyles or social groups within the population?

(4) Will further stable isotopic analysis of the human remains coming from numerous contexts support initial results by Richards *et al.* (2001) and Lai *et al.* (2009) that the diet of the Circle burial population consisted mainly of terrestrial food sources?

(5) Is there morphological or biochemical evidence for the burial population's ancestral origins? Specifically, was the population genetically diverse during the late Neolithic?

2.2.1. The complex multiple interments at the Circle

Through an assessment of the range of Maltese funerary sites with assemblages of human remains, it becomes clear that the prehistoric period is poorly represented when compared with the later Punic-Roman period (Chapters 1, 14 & 15). The Ħal Saflieni Hypogeum

Figure 2.1. *The site under excavation (Photo Cambridge Gozo Project).*

(Paola, Malta) is among the most notable of the Maltese Neolithic funerary sites, but was excavated in the first quarter of the 20th century, when very few human remains were retained or preserved (Evans 1971, 44–5). Zammit (1928) the final excavator, dismissed human remains as uninformative at a time when bioanthropology was in its infancy. Other Neolithic funerary sites include the still largely unexplored Santa Luċija Hypogeum (Magro-Conti 1997; Museum Annual Report 1973) and the human remains from the more recently excavated rock-cut chamber tombs from Kerċem in Gozo (excavated 2009 and 2010, see *Times of Malta* 2009), and currently under study (B. Mercieca-Spiteri, pers. comm). Between 1987 and 1994, the prehistoric human remains assemblage at the Circle in Gozo was discovered, partially excavated (Fig. 2.1), studied for the purpose of the first excavation report (Stoddart *et al.* 2009a; this volume, Chapter 1), and retained at the National Museum of Archaeology (Valletta) for future scientific research (Stoddart *et al.* 2009a, 315–340).

Only in the past few years has there been growing incentive among local osteologists and archaeologists to study human remains spanning the histories of Malta and Gozo. This is partly a result of the growing number of funerary features, mainly from the Roman Classical period, which have been unearthed from the intense construction development across the islands. It is also a result of trained personnel in place to assemble and study Malta's osteoarchaeological material. It is reassuring that ongoing research will contribute to comparative cross-period population studies and future discoveries in the coming years.[1]

The assemblage of Neolithic human remains from the Circle is probably the largest assemblage of prehistoric human remains in the southern Mediterranean, and its size makes comparative approaches possible even within its own data. The 2009 publication estimated that around 220,000 human bone fragments were unearthed by the end of the final excavation season in 1994 (Stoddart *et al.* 2009a, 315), and (depending on various MNI formulae) that a provisional estimate of 1001 corpses (when age is considered (Stoddart *et al.* 2009a, 321)) were deposited in the underground caves during the Tarxien period. This collection of human remains merits not only comparison across its own stratigraphic sequence (as already achieved in outline in the 2009 publication), but also eventual comparison with other Maltese assemblages from the period, which are now under study. Most notably, the Kerċem remains discovered in 2008 will offer valuable comparative material to the Circle assemblage, as one of the only other excavated prehistoric funerary sites on Gozo. In particular, they will enable an assessment about the degree to which prehistoric individuals were formally buried in rock-cut tombs and hypogea (an issue also explored in Chapter 12), and how ritual action was distributed across the landscape.

As already described (Stoddart *et al.* 2009a; Thompson *et al.* 2020), the Circle assemblage contains a good, *natural* representation of the Neolithic population demographic, since individuals of all ages, from foetuses to older adults (Chapter 8) have been identified in the assemblage. Additionally, where biological sex can be determined, there is an almost equal representation of male and female individuals. The assemblage indicated that the individuals deposited at the Circle experienced a range of pathological conditions as well as other occupational and anthropological skeletal markers. These were noted in the 2009 publication and will be further detailed below (Chapters 4, 5, 6, 8). As our knowledge has accumulated, our views have fluctuated about the broader, representative character of the buried population (Stoddart & Malone 2015). The data currently suggest that the Circle was not merely a depositional space for selected individuals forming an in-group, but rather was used for the members of a whole, small, Neolithic community in Xagħra (Gozo). The current hypothesis is that the scenography of the Circle was a substantially self-contained locale belonging to one of a series of very small communities engaged in the funerary rites of the long-lived Maltese Neolithic, and a locale which arguably practised democratic theatre rather than executed the materialized memory of an elite democracy. Each small community on Gozo probably had a similar funerary locale, varying in the degree of investment in monumental scenery (Chapters 11 & 12). Nevertheless, as already discussed (Stoddart & Malone 2015), there is a reasonable assumption that not all the dead of the prehistoric community have yet been discovered, either at the Circle or in the wider surrounding islandscape. Recent discoveries at Triq il-Qacca about 50 m from the main Circle deposits show how the data set is likely to expand as the built environment extends into the Gozitan landscape (Arena 2020), so that our current interpretations are likely to be modified by further research.

As detailed below (Chapter 3) the extensive dating programme has established that the earliest funerary activity at the Circle started *c.* 3700 BC (the end of Żebbuġ phase/commencement of the Ġgantija phase (Volume 2, Chapter 2) during the infancy of the megalithic temple building around the islands. The dates have been revised through additional estimates and new calibration methods, and the late 5th millennium start-date originally proposed is now revised (Malone *et al.* 2009e). The first funerary activity comprised deposition inside a rock-cut tomb and similar structures, now incorporated within the cave system (South Niche). The rock-cut tomb consisted of a vertical cylinder cut in the rock (a shaft) that opened into two separate burial chambers (Malone *et al.* 1995; Malone *et al.* 2009f). These burial chambers continued in use and were probably periodically cleared of remains over the centuries. From the current chronological assessment, the formerly Żebbuġ burial activity (mid-4th millennium BC) is now considered mainly of the Ġgantija phase in the second half of the *c.* 4th millennium BC. Later, during the Tarxien Phase from *c.* 2800 cal. BC until *c.* 2400 cal. BC, the focus of burial shifted to the large underground complex (the modified natural cave system with its insertion of architectural elements) and in this larger space intense communal deposition and funerary practices were carried out.

The primary depositional practice typically consisted of laying out the corpse on its right side and in a flexed position (Stoddart & Malone 2010). This practice was revealed during excavation through the rare preservation of articulated and undisturbed skeletons (Figs. 2.1, 2.2, 2.3). Archaeologists also recorded partially articulated skeletons (Fig. 2.2), including complete limbs or complete torsos but with other skeletal elements missing (Stoddart *et al.* 2009a, 329–30; Chapter 12). This pattern suggested that funerary practices during the Tarxien Phase also included secondary treatment to the decomposing corpse or skeletonized remains, involving the movement of body parts to other areas at the Circle (described in greater detail in the 2009 publication, and Chapter 12). Other areas of the cave complex included heaps of disarticulated elements which implied that bones were also often moved when skeletonized or in the final stages of decomposition (Stoddart *et al.* 2009a, 319–25).

The movement and rearrangement of remains is also evident in the earlier rock-cut tomb where disarticulated bones were recorded as stacked around the sides of the burial chambers (Fig. 2.3). This may have resulted from a process of clearing space within the chambers for other corpses; a form of ossuary management. It is abundantly clear that the practice became more complex and incorporated more stages over time (discussed further in Chapter 12). Additionally, such extended post-depositional practices were not just motivated by the practicalities of making room for more interments, but were also socially embedded ritual events which would have been central to the processes of grieving and managing the transformation of the dead (Stoddart *et al.* 1999; Malone *et al.* 2018; Chapter 12).

Figure 2.2. *Skeletons* in situ *showing partial articulation (Photo Cambridge Gozo Project).*

Figure 2.3. *Disarticulated bone* in situ *(Photo Cambridge Gozo Project).*

2.3. Methods employed by the *FRAGSUS* Population History Workgroup

Unless one was involved in the original excavation itself, one cannot grasp fully the quantities of bone and teeth in a large assemblage until the moment one starts opening up the boxes of bones and unpacking the remains on the laboratory table. The Circle assemblage was no exception. The human remains excavated from the Circle by the Cambridge Gozo Project team had last been examined during the excavation and post-excavation sessions in the 1980s–90s. Following excavation, all remains were packed in plastic or paper bags and placed in medium sized and then larger boxes for storage at the National Museum of Archaeology in Valletta, Malta. The ToTL (Time of their Lives) Project, another ERC-funded project, immediately preceded the *FRAGSUS* research and made a brief examination of the store to obtain radiocarbon dating samples. This was a highly targeted search for articulated remains by Dani Hoffmann, Frances Healey and Simon Stoddart in 2013, designed to provide the chronological framework for a Bayesian analysis of the Circle (Malone *et al.* 2019; Whittle 2018)

The initial publication of this assemblage as part of the excavation report (Stoddart *et al.* 2009a) prepared the *FRAGSUS* Population History group for the huge undertaking of the tasks at hand. Nonetheless, since none of the group members had worked on the original excavation, it was only during the first days of research that they realized the marvellous preservation and extent of the assemblage. Since most of the assemblage was commingled and rarely in anatomical association, it was only when the bags of bones and teeth were laid out for examination that the full realization of the large quantities of individuals deposited at the site became clear. Because the excavated contexts mainly consisted of disarticulated remains, most bags contained fragmented elements from individuals of all ages. The contents of the bags were identified by labels noting their archaeological context, grid reference, and in some instances the individual bone number assigned during excavation (Fig. 2.4). The more complete skeletons were stored in individual boxes; these articulated remains had been collected separately by the excavators, so further identification and analysis alongside a detailed excavation record was available (Malone *et al.* 2009b).

The initial stage of study involved the development of numerous methods which would address the research aims outlined above, whilst acknowledging the highly fragmented nature and large number of bones to study within the available timeframe (Fig. 2.4).

Figure 2.4. *Commingled bones with original label (Photo Ronika K. Power).*

The approaches took into account the experience of the researchers in careful discussion with the custodians of the assemblage (Heritage Malta/National Museum of Archaeology and the Superintendence of Cultural Heritage). Given the complexity of the assemblage and its archaeological record, it was essential that a transparent and meticulously organized system was devised to hand on to future managers and researchers. Time constraints for the personnel were fundamental since one specialist researcher (Power) had specific years of allocated ERC funding, before taking up a teaching position and another was not full time on the project (Mercieca-Spiteri). The senior specialist (Stock) had an oversight role whilst other assistants were recruited through the duration of the project, including two PhD Students (Parkinson and Thompson) and an intern placement (Marabelli). Within these parameters, the team developed a highly ambitious programme that aimed to assess the full assemblage in a series of five intensive museum study campaigns between 2014 and 2017, each approximately eight weeks long, that would isolate samples for further analysis. This work, mainly covering phases 1 and 2 (see below) was carried out by Power and Mercieca-Spiteri. They were assisted by volunteers and other specialists as required. During the project, further archaeometric analyses were carried out in various institutions in the United Kingdom and Republic of Ireland, whilst data processing continued throughout the project in Malta, the UK, Australia and Ireland.

These campaigns identified remains for detailed study, namely elements exhibiting indicators of stress, extreme pathology, behaviourally related changes of skeletal or dental morphology, remains that could inform about diet, environment and possible geographical provenance as detailed further (Chapters 4, 5, 6, 8, 9, 10, 11). Table 2.1 presents the various studies implemented on the isolated skeletal elements, as well as their outcomes.

2.4. The first phase: isolation and archiving

The lengthiest process of analysis was the first phase. First, the boxes had to be inventoried and stored systematically to enable rapid retrieval from the museum storage, and shelf references provided precise inventoried storage locations. Each box was numbered and linked to the inventory. The contexts contained within all boxes and their location in the NMA storage facilities were digitally inventoried to enable their easier location in current and future research. Only one box was opened at a time to prevent the misallocation of material, and each bag was studied individually. When opened, the remains were spread out on a clean surface for examination, retaining its original labels of stratigraphic provenance (Fig. 2.5). Although extensively cleaned following excavation, many of the bones were observed to be covered in chalky dust resulting from the adhering soil matrices. Some human remains were more substantially embedded within concreted soil matrix and required additional cleaning with a dry toothbrush. This was especially the case where identification of pathological lesions, such as eburnation, had been noted.

As shown in Table 2.1 above, the identified remains which were isolated for further study included:

(1) teeth both loose (exfoliated post-deposition) and still in occlusion in mandibles or maxillae; maxillae without dentition but presenting pathology; and all mandibles (intact or fragmentary) without *in situ* dentition (Fig. 2.6);

Table 2.1. *Studies carried out on the Circle assemblage.*

Skeletal elements	Studies implemented			
	Extreme pathology	**Skeletal morphology**	**Modification *in vivo***	**^{14}C, isotopes, aDNA**
Isolated teeth	✓	✓	✓	✓
Mandibles with or without teeth	✓	✓	✓	✓
Maxillae with teeth and/or pathology	✓	✓	✓	✓
Cranial elements	✓	✓	✓	✓
Non-cranial elements	✓	✓	✓	
Outcomes	Identification of individual or population stress, health, diet and congenital variation throughout Circle use-life	Estimation of ancestral affinities, provenances and population diversity	Evidence of behavioural, cultural and technological practices	Chronology, palaeodiet, lifetime mobility, and ancestry

Figure 2.5. *Population History Workgroup examining bone and cleaning (Photo Bernardette Mercieca-Spiteri).*

Figure 2.6. *Population History Workgroup isolating teeth (Photo Ronika K. Power).*

(2) bones identified to be of special interest because of extreme pathology, evidence of behavioural or cultural change and congenital variation.

During the process of isolation, the researchers also extracted some remaining faunal fragments and cultural material including pottery, which were isolated and passed to other specialists.

Once isolated, the special interest bones and teeth were placed in laboratory quality self-seal bags and labelled clearly with the provenance recorded on their original excavation label. The details of the isolated remains were entered into a digital database (the inventory) and the special interest bones and teeth were photographed with a scale. During this stage of isolation researchers also re-bagged and re-labelled, where necessary, those bags which had begun to disintegrate after 20 years in storage.

Once the digital archive was created for the isolated bone or tooth, the element in its labelled bag was placed in a designated depository. This archive of isolated remains was categorized and curated according to either dentition, pathology or other type of interest. In addition, the archive was organized according to archaeological context, forming an easily accessible library. The inventory system tracked both the quantities of isolated samples, as well as the isolation categories (Table 2.2). In total this project isolated over 11,500 teeth, 1,500 mandibular fragments and 600 maxillary fragments. In addition, over 2,800 other bones of special interest were isolated, alongside more than 700 faunal bones and other cultural material such as pottery.

Table 2.2. *Isolated bone elements.*

Types of isolated elements	Number of isolated elements
Teeth (loose and *in situ* in the mandible/ maxillae)	11,706
Mandibular fragments	1,554
Maxillary fragments	628
Special interest bone fragments	2,819
Faunal bones and other cultural material	700
Total isolated elements	17,407

2.5. The second phase: analyses of the isolated elements

Following the isolation process (phase 1), the analyses of the isolated elements (phase 2) commenced. A series of specifically designed databases were used for each of the analyses carried out. As described by Power *et al.* (Chapters 4, 5 & 6), an analytical workflow was developed that facilitated sequential data collection for dental pathology, modification and anthropology. Teeth of all types and articulation states (in occlusion or exfoliated *postmortem*) were examined individually within their context batches. The quantity and strength of expression for each analytical modality was recorded for each batch in a Microsoft Excel spreadsheet. Once analysis was complete, each batch was marked and curated in the *FRAGSUS Project* archive. For further details pertaining to the methodologies of individual analytical modalities, please see the relevant chapters of this volume, as indicated above.

Studies of the other elements of special interest took place alongside the dental and taphonomic research workflow. Within project parameters, a sub-sample of elements were identified for inclusion in the current volume owing to their novelty or significance, or potential to serve as examples for broader biological or cultural patterns observed within the burial population. Detailed pathological descriptions were carried out in collaboration between Power, Mercieca-Spiteri and Thompson in alignment with disciplinary scientific reporting protocols. These processes are further specified in Chapter 8.

During this phase of study, a group of elements were selected for radiological analysis at the Cambridge Biotomography Centre, University of Cambridge, following approval for transport and non-destructive examination by Heritage Malta and the Superintendence of Cultural Heritage in July 2015 and July 2017. With the aid of Laura T. Buck, Jaap Saers and Jay Stock from the Department of Archaeology, the CT-scans recorded data which confirmed previous observations and analysis (Figs 2.7, 2.8) and revealed new information (Chapters 4, 5 and 8).

A series of teeth from the isolation archive were selected for radiocarbon dating and isotopic analyses. The approach to this study required consultations with and formal applications to Heritage Malta and the Superintendence of Cultural Heritage in order to adhere to stringent requirements for best practice in ethical approaches to destructive analyses of archaeological human remains. In alignment with ethical strategies to ensure limited destruction of samples wherever possible, one tooth (for example, the right permanent mandibular second molar) was subject to multiple destructive analyses to reduce the likelihood of duplication of single individuals amongst the analytical sample, minimize possibilities of so-called palaeodietary isotopic 'weaning signatures' in early-erupting permanent teeth, and minimize the overall invasive impact on the burial population (Fig. 2.9). Since the chronology of the assemblage extended over

Figure 2.7. *Population History Workgroup CT scanning (Photo Bernardette Mercieca-Spiteri).*

Figure 2.8. *Population History Workgroup CT scanning (Photo Bernardette Mercieca-Spiteri).*

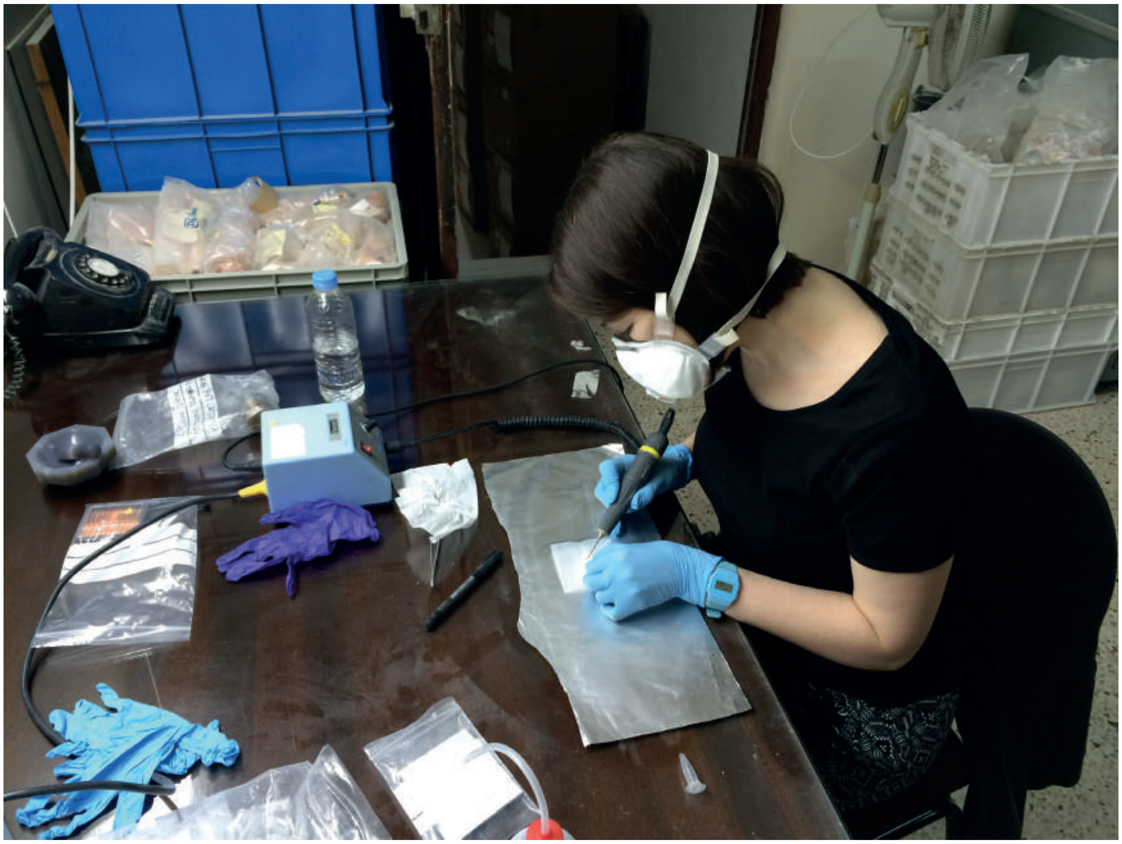

Figure 2.9. *Population History Workgroup sampling (Photo Bernardette Mercieca-Spiteri).*

centuries, it was important that samples from across the entire use-life of the site were selected for analysis, so that the isotopic mapping (of both diet and geographical provenance) was representative. The original excavators (Malone and Stoddart) and the coordinating scientific manager of the project (McLaughlin) identified the key contexts to ensure that the spatial and stratigraphic questions were properly addressed. As mentioned above, since the assemblage mainly comprised disarticulated and commingled remains, the ethical approach for the selection criteria focused on identifying suitable tooth samples for both radiocarbon dating and isotopic analyses. For some contexts or individuals, selecting a single tooth was not always possible, and therefore other teeth were chosen. Only a few contexts proved impossible to sample because they contained no suitable teeth. The condition of the teeth was also assessed during the selection process, and if the tooth appeared damaged through chemical abrasion from environmental factors during burial and taphonomic processes, it was considered unsuitable.

The sampling strategy for all *FRAGSUS Project* analytical protocols involving human remains from the Circle was co-ordinated and executed by Power and Mercieca-Spiteri with the formal permission of Heritage Malta and the Superintendence of Cultural Heritage. Once sample selection for the chronometric and isotopic testing was complete, the teeth were analysed for pathology, modification and population affinities using the methodologies described in Power *et al.* (Chapters 4, 5, & 6), and finally photographed. Any visible adhering calculus was removed from teeth to be subjected to destructive sampling and curated for future testing. Once these processes were complete, the dating and isotope sampling of the teeth was carried out. Following destructive analyses, often remnants of the tooth remained and these were packed and returned to the Circle assemblage in the NMA for further future testing if necessary. The sampling processes were carried out between 2015 and 2018 at the National Museum of Archaeology in Valletta, the University of Cambridge, Trinity College Dublin, and Queen's University in Belfast. Radiocarbon dating and isotopic analyses of collagen were carried out at Queen's University in Belfast, and isotopic analysis of tooth enamel was implemented at the University of Cambridge. These studies are detailed further in Chapters 9 and 10. A pilot study was also carried out on the assemblage for aDNA preservation. The selection criteria for this study was the preservation (preferably on intact crania) of the petrous portion of the temporal bone, since this element reports the highest success rate because of its density, and is least likely to be contaminated as it is located intra-cranially. This study was subject to the same stringent formal application process from Heritage Malta and the Superintendence of Cultural Heritage for ethical approaches to destructive analyses of ancient human remains from archaeological contexts, as described for the radiocarbon and isotopic protocols identified above. Following permission from Heritage Malta and the Superintendence of Cultural Heritage, this work was carried out at Trinity College Dublin and is reported in Chapter 11, Ariano (2021) and Ariano *et al*. (2022).

2.6. The third phase: data analysis and interpretation

The data generated by this programme of work were stored in various databases that could be related to the original excavation archives via stratigraphic context and position within the site. Together with the large number of radiocarbon dates, these databases enabled diachronic analyses of trends in health, activities, and diet across the Circle's main phase of use in the Tarxien period. In some special cases, the size of the dataset presented an opportunity for the development of new statistical tools for visualization, especially certain dental pathologies which could be mapped in terms of the position on the dental arcade where pathologies presented themselves most frequently in the population (Chapter 4). This epidemiological approach to bioarchaeology is only possible with such an exceptionally large sample, such as the remains from the Circle.

2.7. Other studies

During the work phases mentioned above, other studies were carried out on the Circle human remains assemblage. These included two doctoral projects funded by the Arts and Humanities Research Council pursued by researchers from the University of Cambridge (Parkinson and Thompson), whose studies are published within this volume (Chapters 7 & 12, respectively). Their project aims and methodologies are described below.

2.7.1. Funerary taphonomic analysis

Over recent decades, the application of taphonomic analysis has become more common in bioarchaeology, particularly because of its utility to aid in analyses of complex, commingled assemblages (for example Smith and Brickley 2009; Osterholtz *et al.* 2014; Knüsel and Robb 2016). Building upon the French tradition of archaeothanatology which explicitly links the treatment of the dead with cultural and ritual practices (Duday 2009), a sociological understanding of death and dying as significant events which transform both the deceased and society has emerged (Kellehear 2007). Funerary taphonomy provides a methodology to analyse skeletal and funerary assemblages holistically, linking the pattern of preservation and condition of human skeletal remains to their depositional environment and cultural practices (Knüsel and Robb 2016).

Taphonomic analysis has previously been applied to human remains from the Circle, principally to examine the representation of skeletal elements in the rock-cut tomb (Duhig in Malone *et al.* 1995; Duhig 1996). This work investigated both the depositional modes employed in the rock-cut tomb and cave complex (Duhig in Malone *et al.* 1995; Duhig 1996; Stoddart *et al.* 2009a) and the redistribution of human remains throughout the Circle (Stoddart *et al.* 2009a). Building upon this earlier research, a more extensive range of taphonomic methods were applied in this study, including analysis of element completeness, preservation, fragment size, fracture morphology, and cortical modifications. A sample of human remains from 16 archaeological contexts within both the rock-cut tomb and cave complex were selected for analysis. Contexts were chosen (by reference to the 2009 publication) spanning the full use-life of the site, allowing for the investigation of funerary practices over the long term, and seeking to test the provisional conclusions in the earlier publications. To infer patterns of deposition, emphasis was placed on skeletal element representation, comparing the results from the Circle with a range of sites with known funerary practices. Finally, these results are compared with those from the Xemxija Tombs, another late Neolithic burial site on Malta to which taphonomic analysis has been applied (Thompson *et al.* 2018). The methods and results of taphonomic analysis are discussed further in Chapter 12 and presented in full in Thompson (2020).

2.7.2. Metric analysis of the long bones: long bone cross-sectional geometry and body size

When the Population History group began to evaluate the available human material, a further initiative was developed to include the study of the limb bones in order to estimate body size and infer habitual behaviour of the Neolithic population buried at the Circle. Similar studies for other populations and periods (for example Stock and Macintosh 2016) have been carried out, and the opportunity of a doctoral study (Parkinson 2019) took place during the ongoing work of *FRAGSUS* (Chapter 7).

Metric analysis of humeri, femora and tibiae was undertaken to investigate temporal trends in body size and habitual behaviour; however, the fragmentary and commingled nature of the Circle collection presented considerable methodological challenges. Accurate estimations of metric data from fragmented long bones were achieved using 3D laser surface scanning, which allowed for the application of methods in 3D digital reconstruction and superimposition (Benazzi *et al.* 2009; Senck *et al.* 2015). Fragmented long bones were digitally reconstructed and superimposed using RapidForm XOR and individual bone fragments were aligned and positioned according to anatomical landmarks and fracture congruence. Given the size and complexities of the late Neolithic assemblage, the sampling strategy was directed towards specific areas and some contexts from the site (contexts (960), (1206) and (1268), from the 'Shrine' area, and context (1241) from the East Cave) since these contained higher frequencies of humeri, femora and tibiae. In addition, all contexts from the earlier rock-cut tomb were sampled. Further discussion and results are presented in Chapter 7.

2.7.3. GIS digitizing

A Geographical Information System (GIS) study was carried out using the database and records of the 1987–1994 excavation archive to investigate the spatial relationships between the commingled human remains, finds and structural features within the caves (§3.1.4.2.). During the archaeological excavations the site was excavated on a one-metre grid, and skeletal elements were recorded as 'units' within individual spits within each 1x1 metre (Malone *et al.* 2009b). These grid/spits were recorded on an individual context sheet (Fig. 1.11), which included a drawn plan, with numbered and listed skeletal units, context number, date of excavation and 3D coordinates. These records were digitized with the drawn plans and all available contextual information entered into the database. Digitization of the archive records was undertaken in ArcGIS 10.6.1 and spatial analysis was conducted in QGIS 2.18.3. To enhance the visual and spatial effect, the data was imported into ArcScene 10.2 allowing the human remains to be viewed in 3D space.

2.8. Challenges and concluding thoughts

The following chapters in this volume will tackle the details of these numerous studies and their results, but it is already very evident that the Circle human remains assemblage is an abundant source of scientific data. The early context and large size make it one of the most precious assemblages in the Maltese Islands, if not in the Mediterranean.

The site itself (the Circle) should also not be forgotten, as is it is inscribed as a UNESCO World Heritage Site, and still houses further human remains within as-yet unexplored areas. Its fragile nature calls for continued curation by Heritage Malta in communication with the Superintendence of Cultural Heritage to find solutions to protect it further. In addition, the new discoveries continue to emerge as a result of the constant surveillance by the Superintendence of Cultural Heritage (e.g. Arena 2020) in Xagħra and other parts of the Maltese Archipelago, offering opportunities to understand better the landscape and the prehistoric and historic context locally. With new discoveries and investigations come also new funerary assemblages, often of a complex nature, which require study and conservation. The tools acquired from projects such as *FRAGSUS* are already aiding in assisting the development of excavations and analyses of newly discovered prehistoric funerary sites. The data produced will create further insight into the ancient past of the Maltese Islands and the central Mediterranean region.

Note

1. For instance: Project Title: *The Sentinels of Ħal Saflieni, Malta: Science Facts versus Science Fiction*. This project is a Union Académique Internationale-funded collaboration between Principal Investigators from Heritage Malta (Sharon Sultana, National Museum of Archaeology), the Superintendence of Cultural Heritage Malta (Bernardette Mercieca-Spiteri), and Macquarie University, Sydney (Ronika K. Power), and Co-Investigators from the Universities of Cambridge, Western Ontario and Queens University Belfast. It will carry out the first-ever interdisciplinary analyses of the surviving fragmentary human skeletal remains excavated from the Ħal Saflieni Hypogeum UNESCO World Heritage. The project commenced in 2019, but has been on hold since 2020 until the time of writing because of the COVID-19 pandemic.

Chapter 3

The chronology, structure and stratigraphy of the Circle

Eóin W. Parkinson, Rowan McLaughlin, Robert Barratt, Sara Boyle, John Meneely, Ronika K. Power, Bernardette Mercieca-Spiteri, Jess E. Thompson, Simon Stoddart & Caroline Malone

3.1. Introduction

Archaeological deposits of commingled bone act as powerful records of past human activity and can provide important insights into ancient communities. Typically, theories and methods within the fields of funerary archaeology and bioanthropology focus on intact, articulated skeletons. Such methods do not reflect the vastly varied depositional circumstances reflected in the archaeological record, especially throughout later prehistory, in which dense deposits of commingled material are frequently encountered. These deposits usually derive from collective funerary practices, from subsequent grave clearance or mass burials, and consist of a matrix sparsely intermixed with cultural material and dense deposits of disarticulated bone. Such bone deposits can prove to be mobile and subject to both intentional and unintentional movement over time as human and natural processes impact on the original place of disposal.

The varied and complex archaeological deposits of the Circle have great potential for analysing the process and nature of disposal, both intentional and natural. A detailed report on the stratigraphic layers of the site has been published (Stoddart *et al.* 2009c), but as discussed in Chapter 2, many technical and digital tools now commonplace were not available two decades ago. This study presents a reassessment of parts of the excavation archive through the application of Geographical Information Systems (GIS), while a programme of AMS radiocarbon dating enables a refinement of the Circle's chronology, structure and stratigraphy. The published in-depth descriptions of the rock-cut tomb (Malone *et al.* 1995; 2009f) and Tarxien phase burial complex (Stoddart *et al.* 2009c) provide the background for this study. This chapter focuses on areas of the site that have been well preserved and excavated in detail, and where optimal recording of skeletal remains and cultural material provided the necessary information for new GIS analysis, namely the so-called 'Shrine' and 'Display' areas. The chronology-building owes much to the extensive programme of new radiocarbon dating undertaken by both the *FRAGSUS* ERC project and the ToTL ERC-funded project, which together with the previous programme of dating, have achieved a total of 117 radiocarbon dates for the Circle.

3.1.1. Archaeological and environmental context

The Circle is a large multi-phase late Neolithic site situated on the Xagħra plateau, Gozo (Fig. 3.1). The site forms part of a larger ritual landscape that comprises the nearby megalithic sites of Ġgantija and Santa Verna, numerous rock-cut tombs and caves, and other megalithic structures (Evans 1971; Grima *et al.* 2009; Chapter 14). Known in the Maltese language as Iċ-Ċirku tax-Xagħra (MAR 1987), the Circle is known by several names (§1, note 1), but has been commonly referred to in the literature as the Brochtorff Circle (Bonanno 1986; Trump 1972; MAR 1989), Brochtorff Circle at Xagħra (Malone *et al*. 2009d), Xagħra Stone Circle (Pace 1997), Gozo Stone Circle (Attard-Tabone 1999), and more recently the Xagħra hypogeum (Stoddart 2015; Thompson *et al*. 2020). In the case of the latter, the term 'hypogeum' is useful in emphasizing the important parallels between the Circle and the Ħal Saflieni hypogeum, although the Circle is of natural (albeit altered) rather than wholly human-made origin and comprises a superficial cave complex. This contrasts with the typical understanding of a hypogeum as an anthropogenically altered subterranean burial place. In the rest of this volume, 'the Circle' will designate the megalithic enclosure at Xagħra, even though at least one other Circle, most probably from the Xagħra plateau has been mentioned historically.

Excavations between 1987–1994 uncovered the large Temple period burial cave complex enclosed within a stone circle (Malone *et al*. 2009d; Fig. 3.2) and an earlier double chambered rock-cut tomb dated to

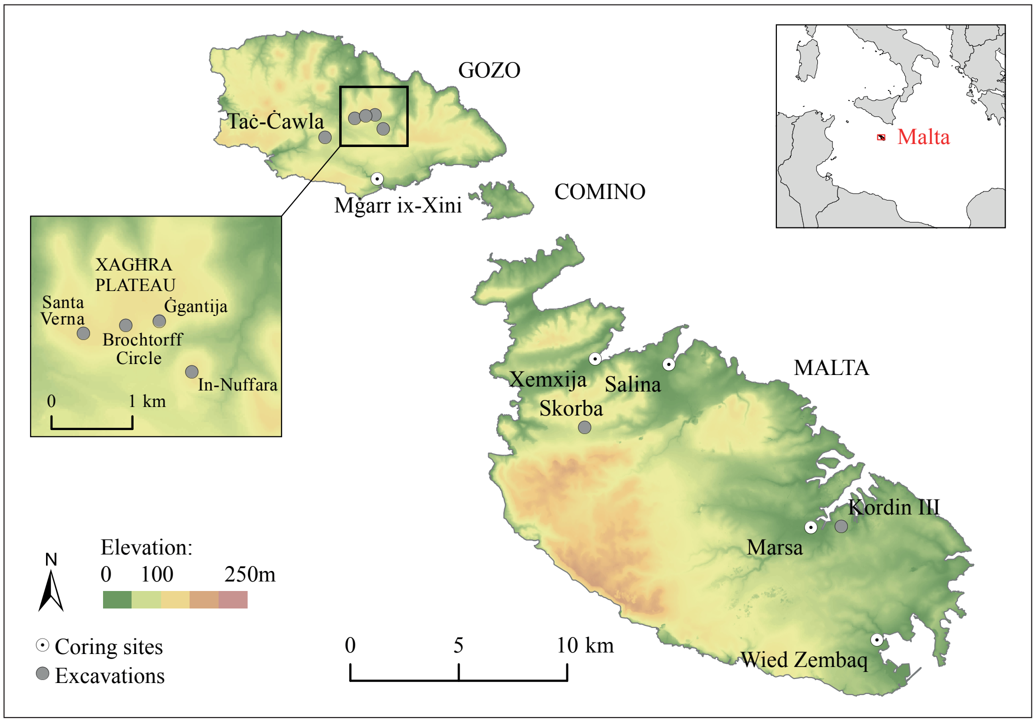

Figure 3.1. *Location map of the Circle on the Xagħra plateau, Gozo.*

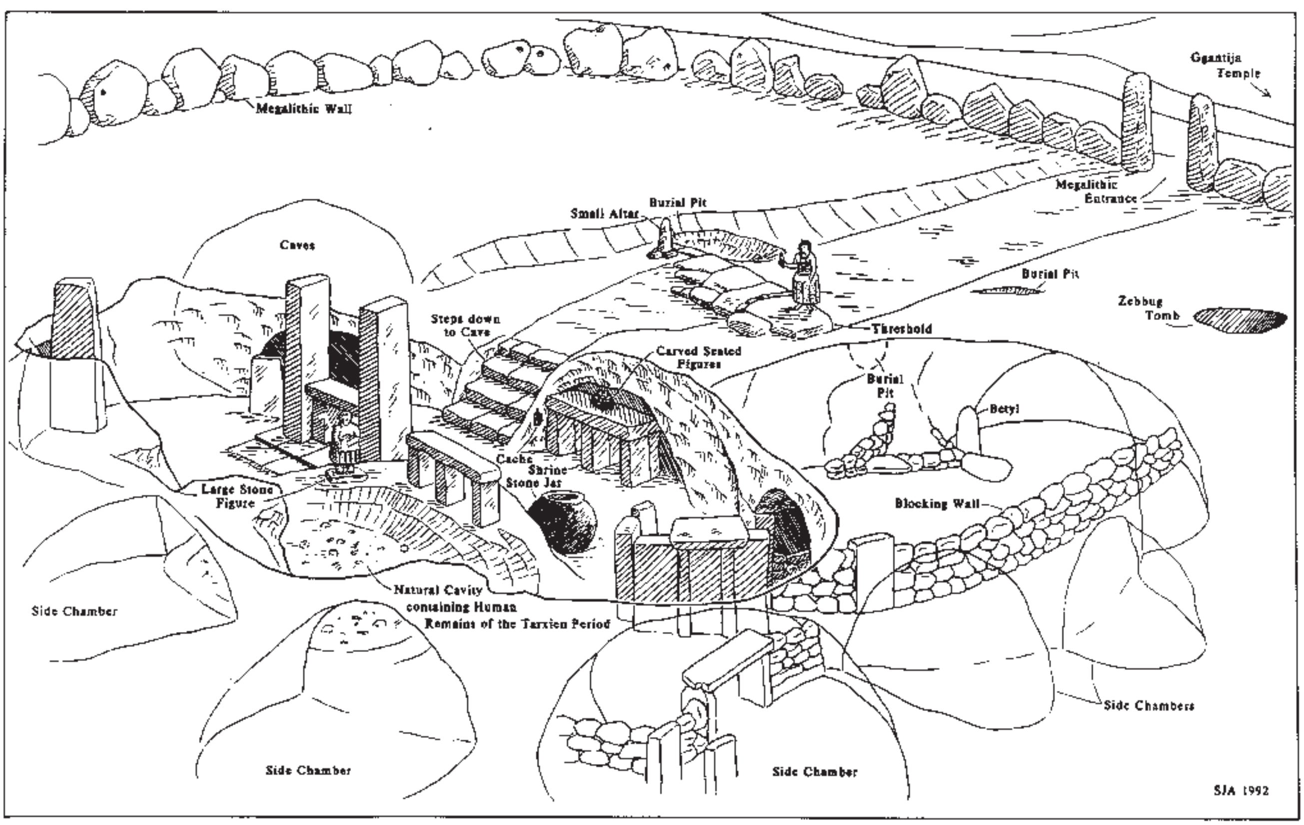

Figure 3.2. *3D reconstruction of the Circle marking the main areas.*

the mid-4th millennium BC (Malone *et al.* 1995; Malone *et al.* 2019b), in addition to evidence for later occupation during the Early Bronze Age Tarxien Cemetery phase (Cutajar *et al.* 2009). During the Tarxien phase (*c*. 2800–2400 cal. BC) (Chapter 2, Volume 2, Table 2.3), the network of caves was the setting of a complex set of funerary rites, where human remains (often following decomposition) were deliberately disarticulated and dispersed around the site in a structured and ritualized manner (Malone & Stoddart 2009; Thompson *et al.* 2020; Chapter 12).

The main structure at the Circle comprises a large adapted natural Coralline limestone cave system consisting (on current knowledge) of three principal chambers, the adjoining East and West Caves (Fig. 3.3) and a South Cave. The 1987–1994 excavations discovered partly excavated areas in the West Cave dating to the early 19th century and intact buried deposits in the East Cave. Following almost 5 years of rubble removal to reveal the (then unknown) extent of the site, work later focused on selected areas of exposed burial deposit within discrete niches and zones. These areas represent only a part of the original cave system, with much remaining only partially explored. Chambers, crevices and passages adjoining the southern, western and northern borders of the West Cave extend to unexplored cavities on the west and north sides of the excavation area. The southernmost extent of the cave system beyond the present boundary line of the enclosing wall is currently exposed in the basement of an adjoining farmhouse containing apiaries. Depressions in the ground surface to the north of the West Cave suggest substantial roof collapse (comparable to that of the East Cave, Fig. 1.8) that indicate the cave system extended well beyond the northernmost limit of excavation. The incomplete work makes accurate reconstructions of the site a challenge, and much detail remains to be learnt regarding its full original extent.

The earliest use of the site appears to be in the early to mid-4th millennium BC, with Żebbuġ activity in the form of rock-cut tombs. These were probably associated with an extensive landscape of individual

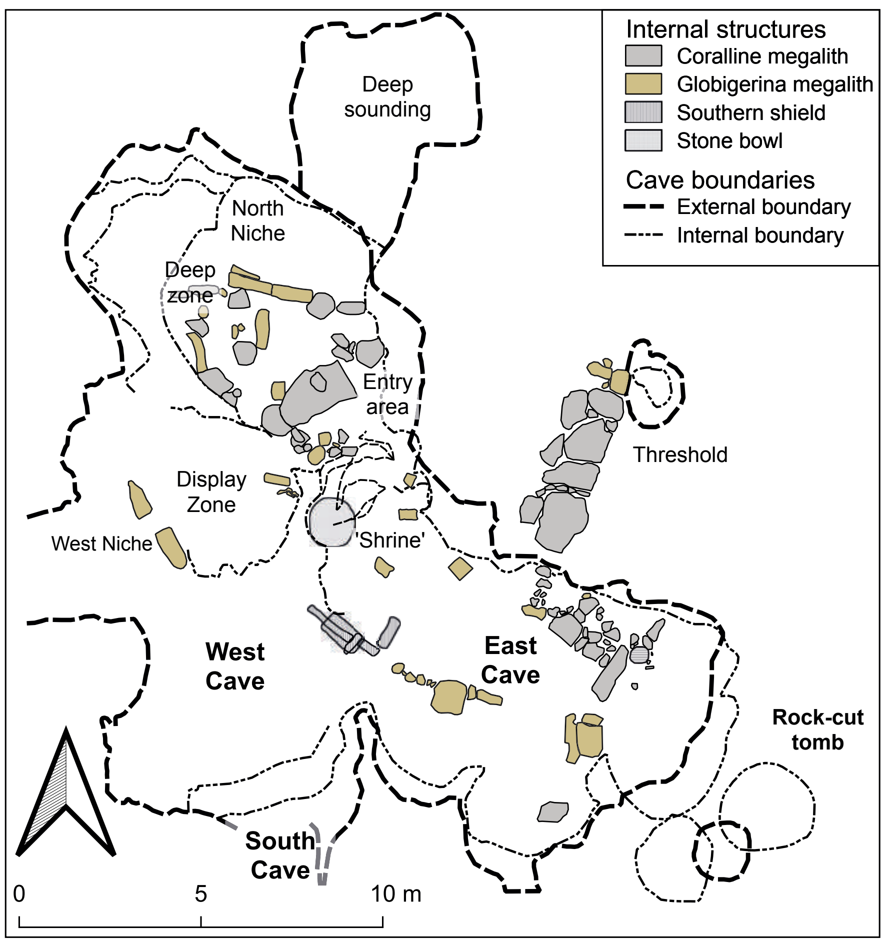

Figure 3.3. *Plan of the principal areas within the Circle.*

and small groups of tombs across the Xagħra plateau (Table 4.1). From a small number of individual tombs, the cave system was expanded, leading to a series of adjoining structures. The caves themselves were used initially as quasi- rock-cut tombs, utilizing small niches in the caves, and then through expansion were combined with the intentionally enlarged caves (e.g. the niche in East Cave, Malone *et al.* 2009f, 103). The Circle's continuously remodelled burial deposits thus seem to have extended throughout the Żebbuġ, Ġgantija and Tarxien phases. Later, the addition of megalithic structures and rock-cut features such as steps and pits were added, creating parallels with contemporary above-ground architecture and funerary hypogea elsewhere on the Islands (Malone 2007; Stoddart & Malone 2013).

Prior to the 1987–94 excavations, the site was concealed beneath a modern field bounded by a distinctive circular rubble wall containing megaliths (presumably a vestige of the stone circle that once surrounded the site at ground level) (Fig. 1.17a). The excavations required the clearance of substantial roof collapse, especially in the East Cave. There is evidence that parts of the weakened Coralline cave roof collapsed whilst the site was still in use, long after large megaliths had been placed to prop up the roof (Fig. 1.12). Antiquarian interventions and looting following explorations by Col. Otto Bayer in 1824 caused considerable damage and left the site open and exposed (Attard-Tabone 1999). The uppermost archaeological layers of the site were disturbed by modern agricultural activity, particularly though the cutting of regular vine trenches into the surface of the bedrock (Figs 1.6–8 for examples under excavation). These taphonomic processes caused further disturbance to the already complicated stratigraphy and highly commingled and fragmented burial deposits within the site.

The partial excavation of the cave system poses challenges to interpreting the chronology and development of the site as a whole. When these data are combined with a re-consideration of *in situ* structures and the excavation archives, it facilitates a re-evaluation of particular areas of the site, specifically in terms of burial and depositional activity, site composition and the distribution of material culture. The discussions on site formation processes presented here relate to the development of the burial deposits *en masse*, and are therefore general observations made on a context or site-wide scale, aimed towards understanding the overall site chronology and composition. The detailed taphonomic analysis of the human remains investigating the subtleties of funerary rites and practices are discussed elsewhere (Thompson 2020; Thompson *et al.* 2020; Chapter 12).

3.1.2. Digital organization of the excavation data

Archaeological excavation aims to preserve a site in archive form, the classic *preservation by record*, allowing subsequent interrogation and reinterpretation of the data. Like any large, highly stratified archaeological excavation, the Circle continues to present challenges in that the amount of archive is formidable, but there are also new opportunities for developing methods that allow the site and its rich archaeological complexity to be explored afresh. Since excavation concluded in 1994, work on its archives has been almost continuous, culminating in the full publication of the site (Malone *et al.* 2009d), and leading either directly or indirectly to other research projects (Templeton & ToTL), student dissertations (e.g. Barratt 2016; Meegan 2017; Parkinson 2019; Thompson 2020), and the current *FRAGSUS Project* programme of work. During this time, there have been a number of developments in computer technology, 3D-survey and digital reconstruction that allow the site to be studied in ways that ways that, although anticipated (Chalmers & Stoddart 1996; Stoddart & Chalmers 1996), were not available at the current level of sophistication during the excavation. Prompted by the opportunity to contextualize further the re-evaluation of the human bone and tooth assemblage from the site (Chapters 4–9), in this section we review some of these new and emerging methods and their application at the Circle.

A co-ordinating strand to this new phase of work has been the development of an 'intra-site GIS' system. GIS stands for 'Geographical Information System', but in many ways, this is simply a continuation of the work on-site. Accurate records made during the excavation, including use of stratigraphic recording (context sheets), and registers of contexts, finds, drawings and other archive materials, mean that geographical information is embedded at a fundamental level within a large proportion of the excavation data, and the application of computerized GIS to this is therefore a simple step.

However, there are two peculiarities to the Circle that complicate matters. The first issue is the sheer number of human remains, which poses practical difficulties, as it is costly in terms of time to enter data about each bone. The second issue is the more general interpretative difficulty caused by the complexity of the site. The long use of the cave complex, its stratigraphic complexity, antiquarian excavations, and the complicating effects of the cave roof collapse all heighten the importance of interpretative reconstruction when communicating broad descriptions of the site and its significance. The 2009 publication used drawn reconstructions depicting overlays of human remains and hypothetical views of the cave complex. Below, we introduce a number of alternative approaches derived from digital 3D models and explore their usefulness as tools for interpretation and for extracting new information about the site.

3.1.3. The implementation of appropriate field methods

The field methods were inspired by two experiences. The first was a seminar on mortuary analysis under the guidance of John O'Shea at the University of Michigan in the early 1980s (Malone *et al.* 2018). In this seminar, Simon Stoddart was assigned the Younge site, a Huron mortuary site with commingled remains, whose analysis prepared the Anglo-Maltese team for the complexity that soon faced them. The second was the experience of working in the Gubbio valley, where spatial analysis had been one of the goals of both the field survey and site analysis of the Bronze Age midden of Monte Ingino (Malone & Stoddart 1994) and the Neolithic site of San Marco (Malone *et al*. 1992), implemented with the guidance of James McVicar and Olivetti sponsorship (continued with the sponsorship of the Maltese Olivetti agent, Charles Micallef).

The upper levels of the Circle were excavated without much need for such sophistication, since Otto Bayer had damaged or removed any intact spatially significant deposits. Some discrete deposits were located in the rock-cut tomb chambers and one shallow burial pit. The former excavated in 1988–9 was recorded on graph paper in a field notebook and bagged and numbered by groups of bones. Over the next two years, 1990–1, the scale and promise of the future task was rapidly realized, as the immense overburden of intact Tarxien Cemetery and disturbed Bayer deposit was removed. This period culminated in the uncovering of the iconic figurative art on 25 September by Andrew Townsend in the final moments of the 1991 season (Stoddart 2002), within what was clearly a sea of bones at the lower cave level. The intervening year of 1992 allowed the excavators to develop firstly the pink sheets for 1993 and then the more sophisticated yellow sheets with overlays for 1994, to record accurately, numerically and systematically the swathes of bone across the site within metre squares, arranged by spits within the observed natural stratigraphy. These records (Fig. 1.11) have provided the core of the GIS data, contributing a palimpsest of plotted human remains. Those human remains not plotted individually were similarly bagged by context, grid square and spit, and form part of the more comprehensive bone database that has also been plotted spatially. This was substantially a pre-digital age. Polaroid cameras and traditional photographic film provided a complementary record, but the main record was pen/pencil and gridded card. The grid was originally laid out by theodolite, although checked with an early EDM towards the very end of the project. A development of the Bonn Harris matrix programme was deployed for the checking and display of stratigraphy, but the human remains were details concentrated within a smaller number of contexts within that framework.

3.1.4. Intra-site GIS

3.1.4.1. Background

The immense promise and richness of the data was both anticipated ahead of and during excavation and after its completion. Collaboration with Alan Chalmers of the Department of Computing at the University of Bristol led to the development of INSITE, a platform for the visualization of archaeological

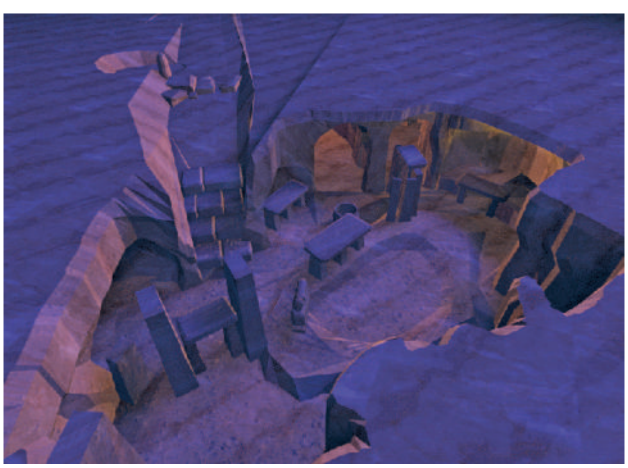

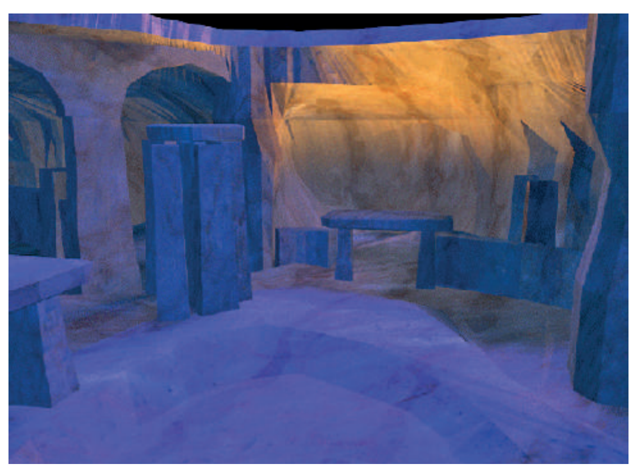

Figure 3.4. *3D reconstructions of the Circle developed by the INSITE project of the University of Bristol.*

sites (Chalmers *et al.* 1995). From this work, which produced a 3D model of the Circle, only a few images (Fig. 3.4) and not the data themselves survived the departure of the post-doctoral researcher engaged in the project. Various attempts were subsequently made at Cambridge to raise money from the AHRB to fund a GIS programme, and a graduate student was successfully funded by the British Academy to undertake the GIS of the deposits, but the selected PhD student was unable to continue for financial reasons. So, as early as 1996–7, a project design for implementing a GIS of the Circle had already been initiated (Tommony 1997) that included a number of techniques which were sophisticated at that time (Monte Carlo, etc.). A more modest scheme of computerizing the humans remains database was, though, achieved thanks to the invaluable support of the McDonald Institute. However, such was the enormity of the task and the reluctance of any funding body, prior to the European Research Council to support the funding of the 3D framework, that it has taken some 25 years to demonstrate the full promise of the original concept implemented in the fieldwork and recording.

3.1.4.2. Methods

As discussed above, the method of excavation and documentation at the cave complex was conducive to a GIS application, and at an early stage of the ERC project, Sara Boyle kindly re-designed and implemented the GIS framework, after discussion with Simon Stoddart. As explained above, the lower part of the site was excavated to a 1-metre square grid whereby skeletal elements were recorded as units within individual spits, although in some cases, groups of associated skeletal elements, either culturally structured or articulated, were recorded as units. During the excavation, each spit was recorded on a skeletal recording paper sheet, which included a drawn plan, with numbered units, context number, level, date of excavation and location on the site grid. These sheets were used as the source of raw data for the site GIS. Firstly, all contextual information was entered into a flat-file database and each skeletal recording sheet was given a unique code, comprising of a combination of the context number, southwest grid reference, spit number and unit identifier. Then, a scan of each sheet's drawing was imported into ArcGIS 10.2 and georeferenced to the site grid. Next came the laborious process of drawing a polygon round each numbered skeletal unit and saving this to a 'shapefile' in the GIS. Each digitized bone polygon was associated with an 'attribute table', a database of associated values containing in this instance a z-value (i.e. level), contextual attributes and bone identification code. Some of this information was added from the flat-file database by joining it to the attribute table. This enabled the GIS to be interrogated using structured query language (SQL), for example, all the skulls in the cave complex could be mapped very readily by constraining the dataset using a 'definition query'. As a final step, both the combined human remains shape files were imported into ArcScene 10.2 and could be viewed in 3D space. To enhance the 3D visual and spatial effect, each human bone shape was extruded by 0.05 cm vertically.

The site finds register was also imported in the GIS accompanied by the 3D co-ordinates associated with each object. The cave boundaries and internal structures were incorporated using published excavation plans (Stoddart *et al.* 2009c) and other site drawings, some of which were already in AutoCAD format and could be read directly in the GIS. For certain spatial analyses, the polygon shapefiles were converted to single points using the centroid of each bone. 'Heat maps', i.e. two-dimensional rasterized visualizations of a Gaussian kernel density estimator with a radius of 0.5 m, were conducted in ArcGIS and QGIS 2.18 to examine spatial and temporal trends in burial density across the site and, in greater detail, the Shrine and Display Zones.

Despite the high recovery rates of human remains from the archaeological deposits, their differential recording presents a limitation. Whilst larger skeletal elements were consistently recorded, smaller elements, particularly those of the extremities and dentition, were less well documented in the process of excavation, providing several challenges in attempting spatial analysis of the post-depositional processes. However, the background human database records this evidence to the nearest metre square in all areas where the larger bones were mapped.

3.1.4.3. Conclusions

The reevaluation and study of excavation archives and legacy data is now an emerging field in archaeology (Katsianis *et al.* 2014; McFarlane *et al.* 2010). Similarly, the use of GIS in analysing distributions and patterns in post-depositional processes across assemblages of human remains has proved useful in both archaeological (Geiling & Marín-Arroyo 2015; Herrmann 2002; Herrmann *et al.* 2014; Lillios *et al.* 2014) and forensic (Manheine *et al.* 2006) case studies. In the context of the Circle, the re-evaluation of the site archive has already proved extremely useful in understanding how the site functioned as a space for burial, and indeed clarifying certain stratigraphic details, the importance of which has been highlighted by the current dating programme (Chapter 2, Vol. 2; Malone *et al.* 2019).

3.1.5. 3D modelling and reconstruction

3.1.5.1. The Visibility Mapping tool

Work in the field of 3D simulation has produced new archaeological data regarding lines of sight within the Circle (Fig. 3.5). The Visibility Mapping tool created in Unity3D identifies points and areas of high visibility, using a custom-written C# script. Previous work by Anderson and Stoddart (2007) introduced a similar technique on eight temples and the Ħal Saflieni hypogeum, identifying the presence of low visibility areas which may have been used during ritual practices to create 'epiphany' moments by revealing something or someone hidden beyond sight. The Visibility Mapping script extends Anderson and Stoddart's results to the Circle, emphasizing the manipulation of space and lighting and the structural similarities between temples and hypogea. The results and interpretation of the visibility analysis are discussed eslewhere (Thompson *et al*. 2020) and below.

The Visibility Mapping scripts uses a horizontal plane intersecting the digital model within which a number of points are selected along a grid of adjustable size. A Ray is cast from each point to all other points in the grid and a value is assigned to the current point based on the number of Rays that do not encounter a solid surface. This *visibility* value (α) is given by:

$$\alpha = \frac{hit}{tot}$$

where *hit* is the number of times the ray encounters a solid surface and *tot* is the total number of possible Rays from the point. A point with a high visibility value is not obscured by solid objects, while a low value indicates an area hidden from sight. All point values are exported as a CSV file and imported into ArcMap using inverse distance weighting (IDW) interpolation. The result is a raster surface, a grid of pixels where each pixel's value corresponded to the calculated visibility (α) of that point in space.

3.1.5.2. 3D laser scan

In total, 14 sites were surveyed in 3D for the *FRAGSUS Project,* collecting a total of 47.2 billion coordinates. A FARO Focus 3D laser scanner was used at all locations. This equipment uses a spinning laser to capture up to 1 million measurements per second. By collecting multiple 3D scans around a site and then registering (joining) these individual scans, a complete three–dimensional picture of the site is generated with millimetre accuracy.

As well as recording individual x, y, z coordinates, 3D laser scanners also record the return strength of the

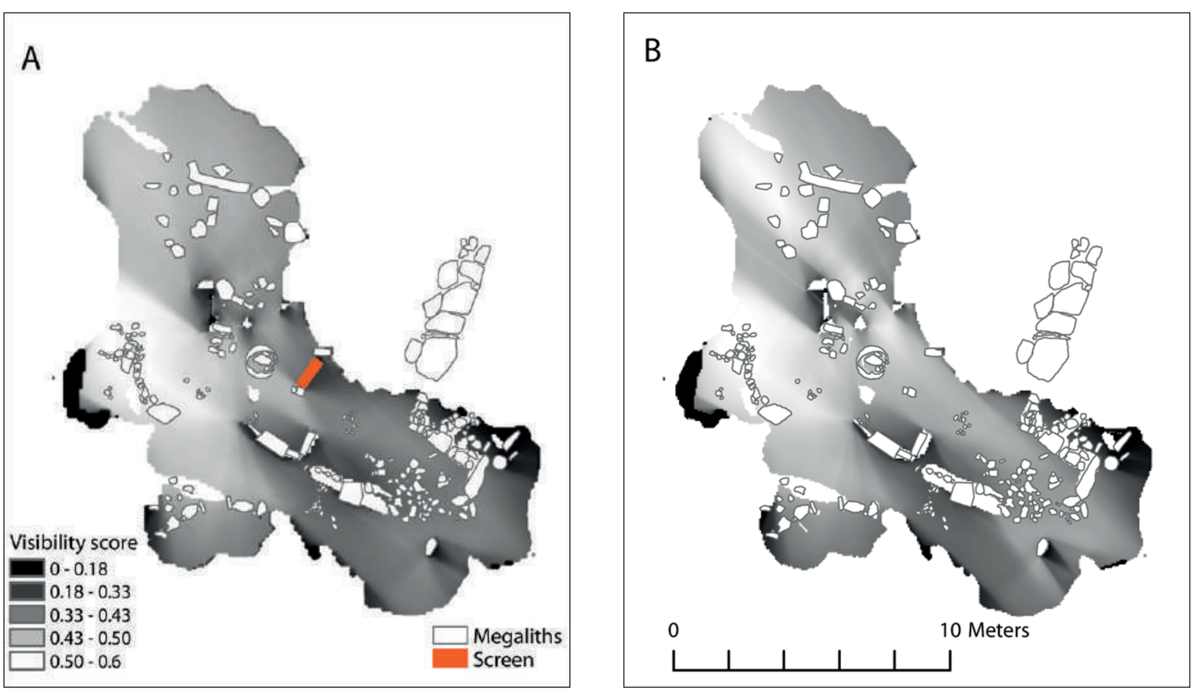

Figure 3.5. *Output from the Visibility Mapping tool for the Circle showing how visibility within the site changed with a) the inclusion of a megalithic screen in the Shrine zone and b) the absence of a megalithic screen (R. Barratt).*

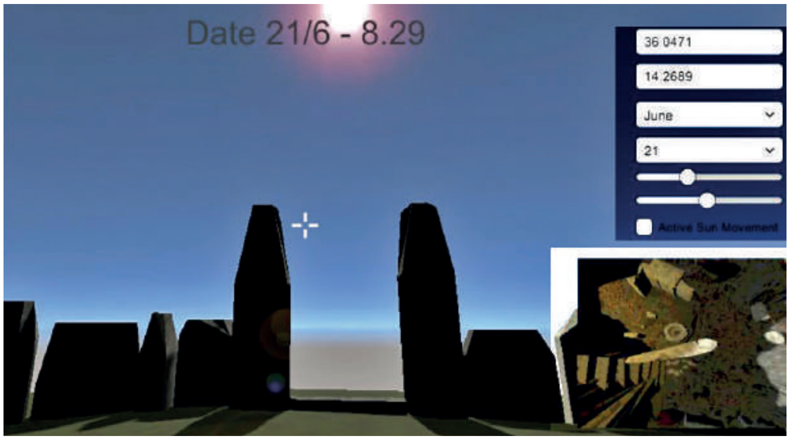

Figure 3.6. *Use of computer model for celestial alignments: Astronomical analysis of the Circle, using custom software. The SunPositionScript is used to calculate the position of the sun at specific dates and times, suggesting an alignment with the summer solstice through the entrance megaliths (R. Barratt).*

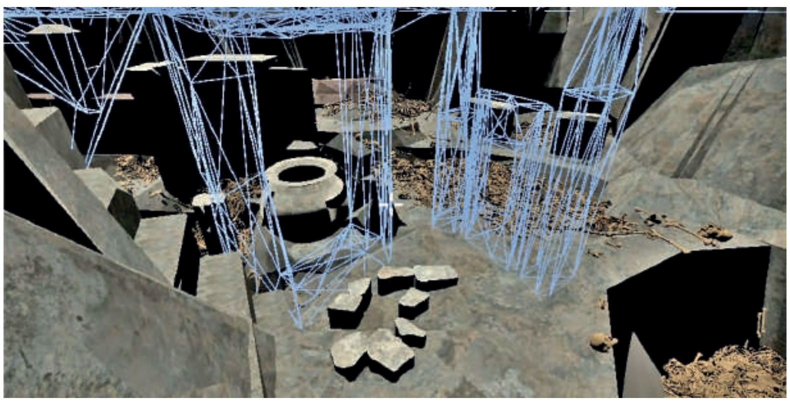

Figure 3.7. *Elements of the wire frame for a 3D reconstruction. An untextured render of the Circle model, showing the virtual geometry that forms the reconstruction. Extant elements were recreated digitally based on the excavation reports, while hypothetical portions were added to demonstrate their plausible location based on the physical constraints of the environment (R. Barratt).*

reflected laser light form the surface for each point. This is known as a reflectance or intensity value (i) and can be valuable additional information for discerning material differences. When the measurement phase of the scan is complete the scanner then captures a colour image of the surveyed scene. The R, G, B values from this image are then attached to corresponding measured point. Therefore, each measured point contains seven bits of information X, Y, Z, I, R, G, B.

The vast amounts of data collected by these systems are known as 'point clouds' and can be analysed using their own generic software or easily exported into more traditional CAD or GIS software packages for further analysis or into Augmented or Virtual reality packages for visualization.

3.1.5.3. Interpretative reconstruction

An interpretative model was created for the Circle with the intention of organizing the digital data into a 3D environment, by determining the feasibility of architectural elements and exploring issues of spatial arrangement, including celestial alignments (Fig. 3.6). The aim was to create a virtual replica of the site as it was during prehistory, for the presentation to the general public.

The general process has been described in Barratt (2016) but is reported here in brief. To create the virtual reconstruction of the site, a base model of the Circle was made based on the material evidence uncovered during excavation. As well as the report and associated monograph, photographs, plans, drawings and notes were used to identify *in situ* remains that required digitizing. The base model provided the wireframe (Fig. 3.7) for the reconstruction and was created in Sketchup through basic geometry design.

Features that are no longer surviving, such as the standing stones at the entrance visualized by Charles de Brocktorff (Fig. 3.8), required further research and experimentation. Several plausible models were created for each missing element, and each was evaluated based on the surrounding archaeological contexts. The use of 3D Reconstruction for the reinterpretation of archaeological sites has been well documented (Barceló *et al.* 2000; Levy & Dawson 2006; Reilly & Rahtz 1992). The modelling process implicitly stimulates interpretation, as it forces archaeologists to render explicit the physical relationship between archaeological elements which may be overlooked in 2D (for example, Lulof *et al.* 2013).

The reconstruction process therefore helped identify architectural queries that were originally overlooked

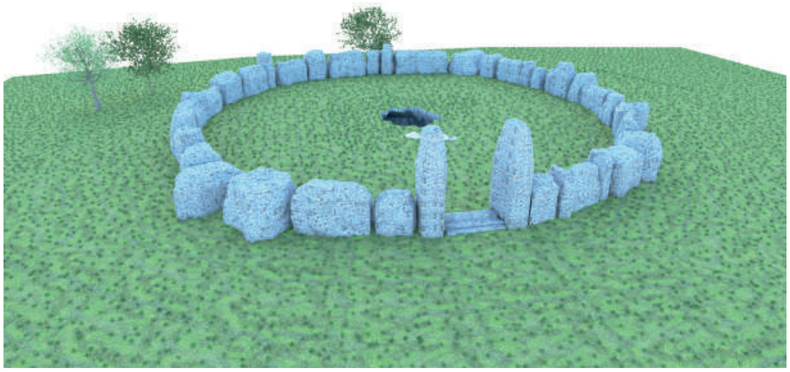

Figure 3.8. *Reconstruction of external view of the Circle (R. Barratt).*

(Barratt 2016). For example, the position of steps leading to the cave from aboveground required much experimentation to model. While original drawings in Malone & Stoddart (2009, 375) showed protruding stairs leading to the centre of the anteroom, these do not fit between the wall and entrance threshold. The most likely scenario seems to be in-cut steps adjacent to the cave wall (Fig. 3.9). Another observation obtained from the model is the height of the collapsed roof, which appears to be mostly flat and low rather than rounded and high as suggested in drawings from Malone & Stoddart (2009, 375). This arrangement would also account for the overall instability and the need for megalithic supports.

The finished 3D model has been used for the presentation of the site for the public. Several short video clips of renders were included in the *FRAGSUS* exhibition at the National Museum of Valletta. The model was also imported into the gaming engine Unity3D, through which navigation tools were written to allow exploration of the site from a more realistic first-person perspective. The model has even been modified to allow the use of a VR headset, and it has featured in Queen's University events, such as the NI Science Festival.

These new digital navigation tools have helped the public visualize the hypogeum despite physical

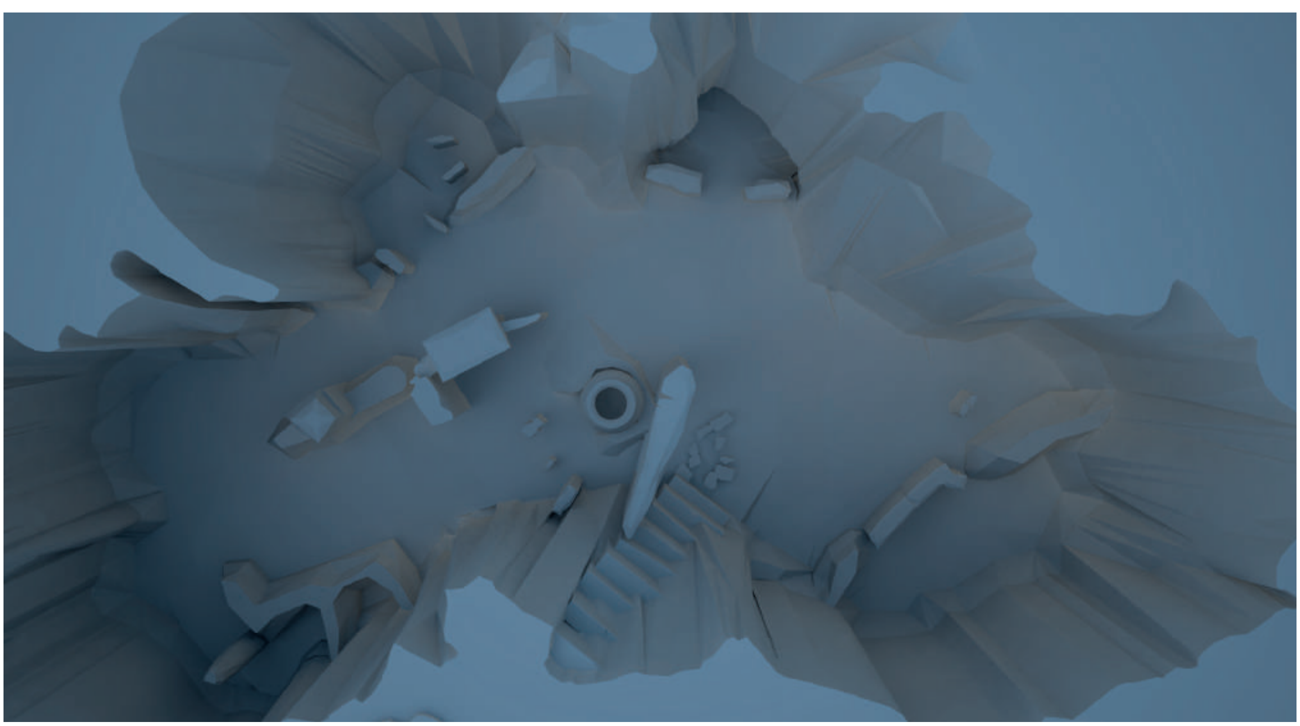

Figure 3.9. *Reconstruction of the steps into the Circle (R. Barratt).*

Figure 3.10. *Reconstruction showing low roof of inner parts of the Circle (R. Barratt).*

restrictions, providing a realistic view of the past 'as it was'. Today, the site is open with good illumination, but in the past the site would have been very dark with limited movement since the most likely reconstruction has a very low roof (Fig. 3.10). The interpretative 3D reconstruction of the Circle helps present an accurate view of history in an engaging medium.

3.2. Time: dating and chronological modelling

Two new extensive programmes of radiocarbon dating were undertaken on the human remains from Xagħra between 2013 and 2016 by the ERC-funded *Time of Their Lives* (ToTL) and *FRAGSUS* research projects (Malone *et al.* 2019). Malone *et al.* (2009e) originally acquired 21 radiocarbon dates for the site, although four are now excluded from the present analysis because of low collagen levels and other methodological issues that fall short of protocols now required by modern standards (see Malone *et al.* 2019). Of the 42 bone and tooth samples submitted as part of the ToTL project, 13 failed (31.9%). Of the 88 bone and tooth samples submitted for radiocarbon dating by *FRAGSUS,* 14 dates (15.9%) failed; the higher success rate was a result of the almost exclusive selection of molar teeth, which preserved collagen better than bone. There are now 117 'good' dates from the site in total, the full details of which appear in Appendix Table A2.1. This large new body of radiocarbon dates makes the Circle one of the most comprehensively dated prehistoric sites in the central Mediterranean and enables a detailed understanding of the changing intensity of human activity which took place at the site, as well as allowing for longitudinal perspectives on the bioarchaeology. It also allows the burial deposits to be analysed and discussed spatio-temporally (§3.4).

Two complementary chronological approaches were employed here to understand the chronology of the Circle: Bayesian modelling of the radiocarbon data as constrained by stratigraphic information, and Kernel Density Estimation (McLaughlin 2019; Chapter 2, Volume 2 for methodological details). The latter method is a frequentist technique that operates under the assumption that the radiocarbon dates associated with burial and anthropogenic activity at the site are the result of a series of quasi-random events. The distribution of these events through time contains information about the overall tempo of past human activity and is particularly useful for highlighting episodes of intensive use.

The Kernel Density Estimation (KDE) models (Fig. 3.11) and the Bayesian phase model of Malone *et al.* (2019) suggest that burial activity in the rock-cut tomb occurred mainly between 3500 and 3200 cal. BC, likely spanning the Żebbuġ, Mġarr and early Ġgantija periods (Volume 2, Chapter 2). The KDE model of the dates, which assumes a Gaussian distribution through time for this activity, indicates that it commenced around *c.* 3700 cal. BC. This is consistent with the frequent finds of Żebbuġ pottery across the site. The 95% confidence limit of Bayesian model also extends back to *3640–3500 cal. BC*, in the Żebbuġ phase. This absolute chronology stands in contrast to the results of the first radiocarbon dating programme, which dated the rock-cut tomb to the late 5th to early 4th millennium BC (Malone *et al.* 2009e). These conclusions were reached using a smaller number of samples now deemed problematic. Given the large quantity of Żebbuġ pottery from the site, especially in certain contexts, and a radiocarbon date from the south burial niche in the East Cave, it nonetheless seems likely that there was earlier burial activity, perhaps as early as 4200 cal. BC (Appendix Table A2.1). This depends on only one date, that whilst not problematic in terms of collagen preservation or laboratory protocol, still seems anomalously early given the *FRAGSUS Project's* refinements of the dates of Żebbuġ settlement at the nearby sites of Santa Verna and Taċ-Ċawla (Volume 2, Chapter 2). We attempted to investigate other potential cases of residual Żebbuġ burials by seeking new radiocarbon dates from contexts rich in that pottery type, but all proved to be Tarxien period in date upon analysis. The ubiquity of Żebbuġ pottery is therefore not easy to explain and warrants further work.

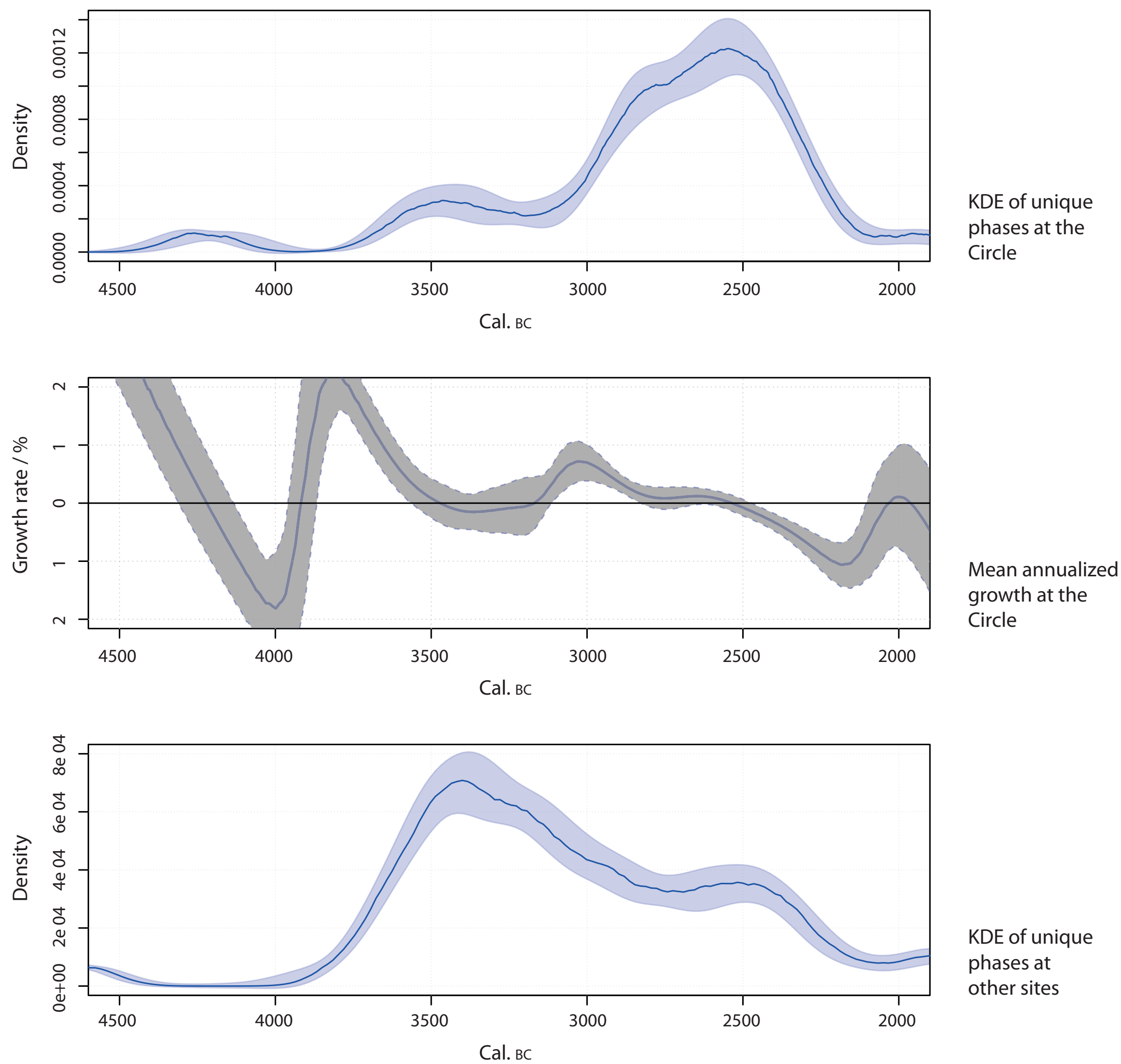

Figure. 3.11. *(top) Kernel Density Estimation (KDE) models of radiocarbon-dated burials at the Circle; (middle) a growth model derived from it; (bottom) a KDE indicating the pattern from other dated sites in Malta (Volume 2, Chapter 2). The bandwidth of the KDEs is 100 years, and phases are defined as 30-year generations (R. Mclaughlin).*

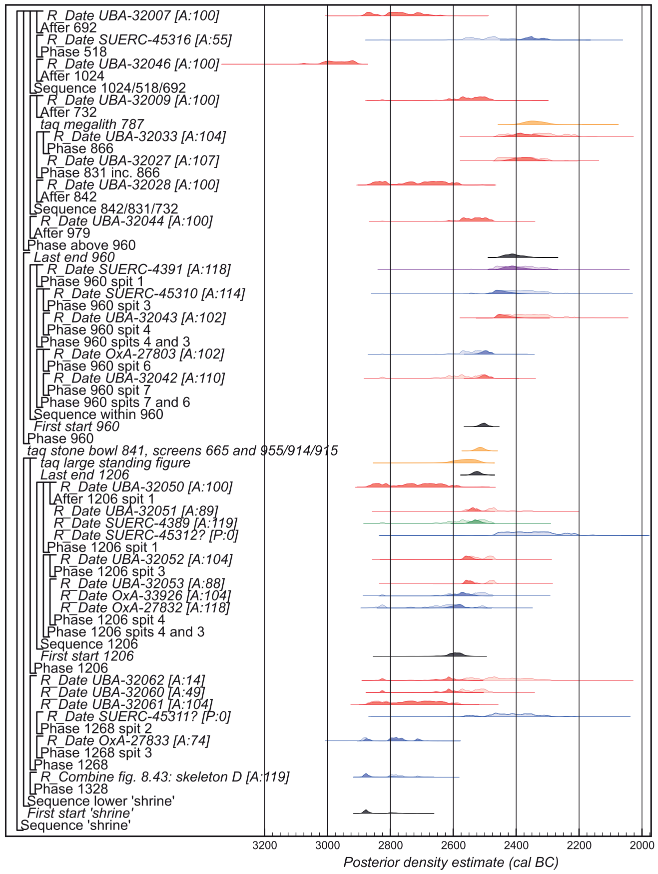

Figure 3.12. *Bayesian model of the chronology of selected contexts and events (after Malone* et al. *2019).*

The KDE models reveal a sharp increase in activity at the Circle at the onset of the 3rd millennium BC, representing the establishment of the cave system as a major burial complex during the earlier part of the Tarxien phase. The growth rate of the KDE at this point is 0.7±0.3% per annum, which would be remarkable (although not unprecedented) if representative of natural population growth, but in this context probably represents the rate at which the site developed as a burial space. The Bayesian phase model (Fig. 3.12) has refined the starting date for this main phase of activity to *2975–2900 cal. BC*. This is followed by a gradual increase in depositional activity, growing at moderate exponential rate of no more than 0.25% per year, with a slight acceleration occurring at 2600 cal. BC. The most developed point was reached at 2500 cal. BC, which, going by the radiocarbon dates from other sites, was a time of a resurgence or stabilization of activity across the Maltese Islands (Fig. 3.12 and Volume 2, Chapter 2). From this date however, the KDE model tilts into a decline, eventually reaching a stage where the deposition of human remains stopped altogether. According to the Bayesian phase model of Malone *et al.* (2019), this occurred around *2375–2255 cal. BC*. In addition to highlighting when the Circle was most intensively used, the ebb and flow of the site's use as visualized in the KDE models are significant since they correspond to periods of structural remodelling apparent within the cave system which is evidence in both our interpretation of the stratigraphy and the GIS analysis discussed below.

3.3. Rock-cut tomb: structure and stratigraphy

The rock-cut tomb was uncovered in 1988 and its location was exposed during the excavation of agricultural vine trenches which had penetrated and damaged the roofs of both chambers (Fig. 3.13). The tomb consists of two chambers orientated east-west and both entered from a central vertical shaft with a diameter of 1.4 m and 1.15 m depth from the surface (Fig. 3.14). On discovery, the East chamber was sealed by a rounded stone slab across the entrance cavity, whilst the West chamber had undergone enlargement and damage in antiquity. The oval form and domed roof of each chamber remained largely intact. The original morphology of the rock-cut

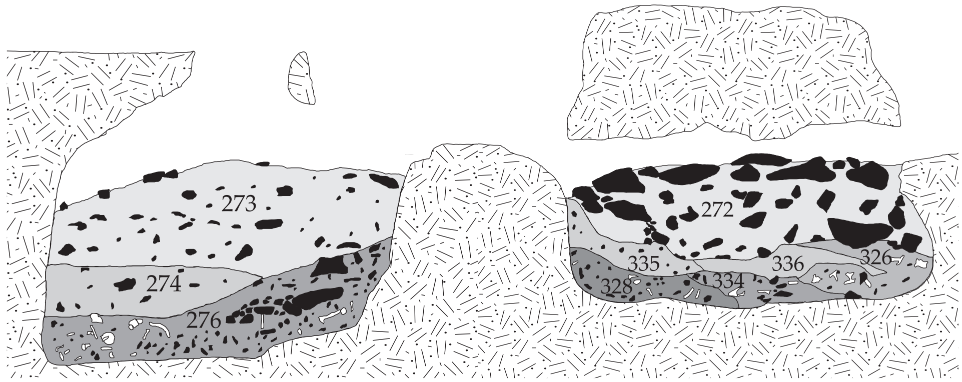

Figure 3.13. *Section of the rock-cut tomb (after Malone* et al. *2009f).*

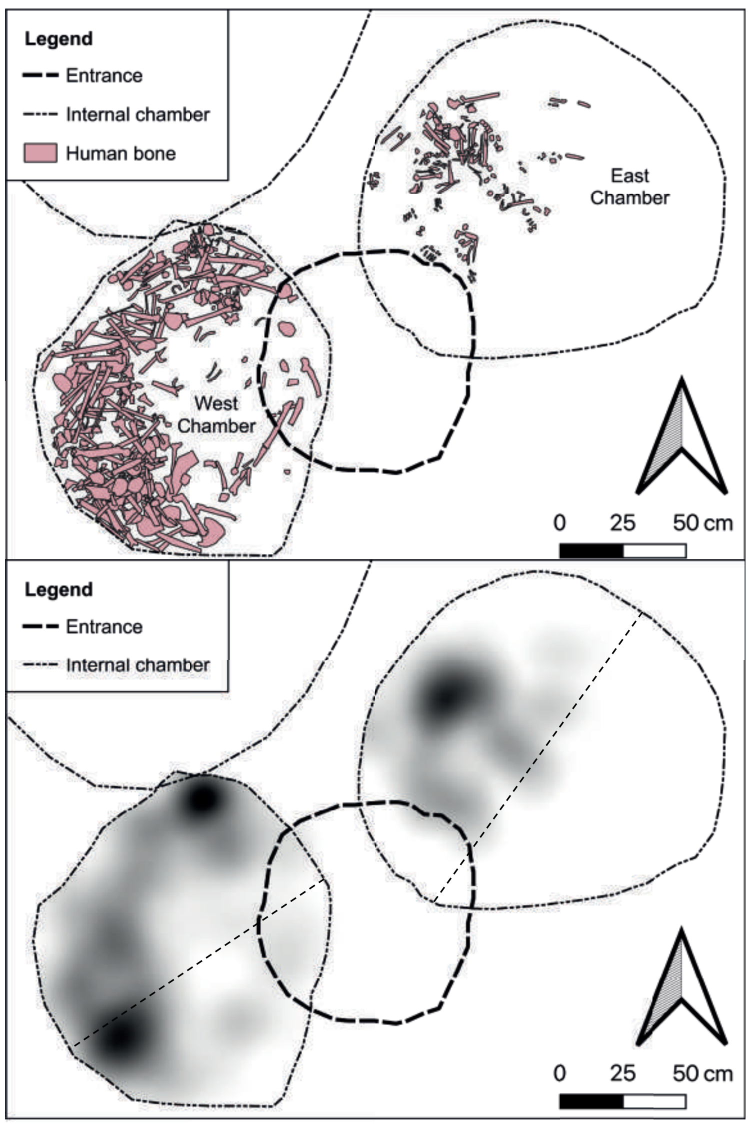

Figure 3.14. *Plan of the rock-cut tomb showing the distribution of human bone (top) and the density of depositional activity (bottom) (E.Parkinson).*

tomb conforms to the *a forno* (oven-shaped) type, typical of Sardinia, Sicily, and southern and central Italy (Hayden 2007). The rock-cut tomb from the Circle is now a well-cited example of the southernmost extension of the rock-cut tomb burial tradition in the central Mediterranean (e.g. Bocquet-Appel 2002; Guillaine 2015; Hayden 2007; Leighton 1999).

The West chamber contained three distinctive layers (Fig. 3.13). The basal layer was an ochre- rich burial deposit, Context (276), dense with human bone and pottery, mainly from the Żebbuġ but also the Ġgantija phases, and other artefacts. The human remains and artefacts were clustered around the western 'back' wall of the chamber, as reflected in the density analysis of the excavated bone (Fig. 3.14), indicative of having been pushed to the furthest point from the entrance to make room for subsequent burials. A chalky layer, Context (274), sealed the main burial deposit and contained a small number of artefacts and fragments of bone. This sealing deposit was covered by Context (273), an almost sterile layer of loose red-brown soil possibly derived from soil seep through the vine trenches. The West chamber contained a partially articulated skeleton deposited close to the entrance that was interpreted as a later 'Ġgantija insertion' (Malone *et al.* 2009f) (§3.2 above), but in light of the refined chronology instead demonstrates the protracted use of the chamber. A small anthropomorphic stela was discovered in the rubble fill surrounding the entrance to the West chamber (Malone *et al.* 1995; 2009f), similar in style to the stela found at the type-site of the Żebbuġ phase at ta' Trapna on Malta (Baldacchino & Evans 1954).

The East chamber consisted of three stratigraphic layers at its base, which were interpreted by the excavators as dumps representing clearance for new burials. The chamber contained a partially articulated skeleton which to the north, a large marine shell (Fig. 3.14) and large pot containing ochre towards the entrance (Appendix Figs. A1.5 & A1.6) along with a series of dump deposits containing very fragmented and disarticulated human bone, bone pendants, beads, axe pendants and perforated shells. The distribution of finds and burials were more dispersed in the East chamber than the West (Fig. 3.14). The burial deposits were finally sealed with a white chalky deposit and then a brown-red fine soil, covered by mixed modern soils that had penetrated through the large vine trench dug into the roof of the tomb.

Initial osteological analysis estimated that the rock-cut tomb contained a minimum of 65 individuals, comprising 54 adults and 11 non-adults (Malone *et al.* 1995; Malone *et al.* 2009f) based on the patella. Revised taphonomic analysis of the main burial contexts from the East and West chambers of the rock-cut tomb are reported elsewhere, although the MNI is not re-evaluated as only a sub-sample of the assemblage was analysed (Thompson 2019; Chapter 12). Given the site's status in the wider region as an early occurrence of a 'Copper Age' rock-cut tomb (although given the revised chronology the site is now less outlying in this regard) valuable comparisons can be drawn with similar tombs elsewhere. Although mostly undated, in Sicily rock-cut tombs are known from the San Cono-Piano Notaro and the Conca d'Oro cultures. These varied in location, size and form, but generally were single chambered tombs or pits typically containing one or two individuals. At Trancina (Tiné 1960-1; 1962) and the rather similar cemeteries of Scintilia and Piano Vento, numbers ranged from 1–3, and occasionally up to 5 individuals deposited within a tomb (Castellana 1995; Guillì 2014). However, so few burials sites in Sicily have been recorded in detail that we still have only a partial understanding of funerary ritual in the Copper Age there. The collective funerary tradition evident across the Maltese Islands during the late Neolithic has been suggested as 'an early participant in the practice of intensive collective burial in an intentionally prepared burial chamber' (Malone *et al.* 1995, 343). In light of the revised chronology presented here, the rock-cut tomb from the Circle and others across Malta conform to the wider pattern of emerging funerary complexity that had developed throughout the central Mediterranean by the late 4th millennium BC (Bailo Modesti & Salerno 1995, 1998; Conti *et al.* 1997; Dolfini 2015; Leonini and Sarti 2006). The dating of the Żebbuġ presence in the Circle does, however, remain a matter that deserves further investigation.

3.4. Temple Period burial complex

From 3000 cal. BC onwards, the activities on the site are represented by burial deposits in the large adapted Coralline limestone cave system adjacent to the rock-cut tomb. The nature of the modified cave system as a communal burial space has resulted in an extremely complex structure and stratigraphy because of the extent of the site, the various niches and spaces utilized for disposal, and the density of the deposits which built up throughout centuries of use and clearance. The Tarxien phase stratigraphy is described by Stoddart *et al.* (2009c), and the archaeological sequence and overall geological structure of the cave system are summarized by Stoddart *et al.* (2009b, 79–81). The overall structure of the site is depicted in Figure 3.3 and described below, first summarizing the ground level features, and then discussing the subterranean archaeological features of the principal chambers exposed in the East and West Caves and explored during the 1987–1994 excavations.

3.4.1. Structure

3.4.1.1. Ground level features and overall cave structure

The Temple period saw the construction of an encircling megalithic stone circle within which various rock-cut features, crevices, pits and built megalithic structures transformed the space into a progressively modified and culturally constructed 'hypogeum'. The encircling megalithic stone circle consisted of interlocking recumbent and upright stones, forming a space some 40 m in diameter, and was entered from the east side, through two upright megaliths (Stoddart *et al.* 2009c, 109–205). Although little survives of the stone circle today, three megaliths are clearly visible from within the Circle and many others can be seen externally, embedded within the enclosing field boundary. The structure was recorded several times in the 18th and 19th centuries, including by Jean-Pierre Houël and Charles de Brocktorff (Attard-Tabone 1999; Grima 2004). To date, no comprehensive archaeological clearance and survey has been undertaken on the field boundary, and more megaliths may remain *in situ* buried beneath the rubble walls. About 15 m from the entrance uprights, a threshold of several large Coralline slabs orientated north-northeast to south-southwest, approximately 4.6 m wide × 1.7 m deep, incorporated stone altars to either side. This suggests a substantial formalized building (a type of gatehouse perhaps), that formed an entry point to the caves, but only remnants of this structure survived later agricultural activity (Fig. 3.3; Stoddart *et al.* 2009c, 111–2, Figure 8.6). Excavations around the threshold also revealed a sequence of floors and cut features, whilst at the southern and northern ends of the threshold, three Tarxien phase funerary pits were identified and excavated: the northern threshold pit, East Cave central pit and East Cave southern pit.

The northern threshold pit utilized a natural fissure in the bedrock covered by a layer of Coralline pebbles. These sealed a series of intact deposits that consisted of structured, commingled but carefully arranged skeletal elements and body parts, in turn overlying a fully articulated male skeleton (Stoddart *et al.* 2009c, 116–8; Chapter 12). The central pit, located at the southern end of the threshold, contained commingled bone deposits and three partially articulated non-adult skeletons, truncated as a result of the roof collapse (Stoddart *et al.* 2009c, 121–2). The southernmost pit was cut into the roof of the East Cave, but had collapsed towards the end of the Tarxien phase as the cave roof deteriorated (Stoddart *et al.* 2009c, 121–3).

The caves were entered through an opening where the thin rock roof presumably had a natural break, although the extent of this remains unclear. A surviving feature that confirms the entry point is two remaining Globigerina stone steps that adhere to the cave wall above the Northeast niche and led to the main part of the excavated site (Figures 8.6 and 8.25a in Stoddart *et al.* 2009c). The explored areas of the site currently comprise the West and East Caves, arranged in an 'L' formation (Fig. 3.3), whilst the nature of the adjoining areas on the north and west sides remain unknown. A further cavern to the north is indicated by a circular depression in the surface, and was exposed vertically in the northernmost wall of the West Cave in 1994 (Figs 8.17 and 8.20 in Stoddart *et al.* 2009c). This northern cave was partially explored through limited excavation of superficial deposits at ground surface and a deep sondage which revealed 3 m depth of cave roof collapse and cultural deposits (Stoddart *et al.* 2009c, 126). The southern limits of the West Cave had been disturbed in the 19th-century and in part formed the South Cave. Now sealed by earlier backfill, the South Cave likely connects to the cellars beneath the farmhouse outside the current site boundary and may have once formed a southern entrance route into the complex during the late Neolithic.

3.4.1.2. West Cave

Excavations in the West Cave focused on the areas exposed after Bayer's 19th-century rubble backfill had been removed and was confined to areas considered safe to work in, given the unstable cave walls and old rubble collapse that enveloped the entire site. The excavation of the West Cave was necessarily partial, especially since an unknown quantity of archaeological deposit had been removed in the past. As a result, any interpretations of the structures remain speculative, and we must rely on the data provided by the detailed study areas.

In the northern part of the West Cave, a Northern burial niche (Context 845) was formed by a recumbent megalith (877) and stone wall (869) around a natural depression in the bedrock, creating a circular burial space similar to the Display area (below). An open space referred to as the 'Entry' zone was encountered on the northeast corner of the West Cave, at the base of the surface steps (Fig. 3.3), and these facilitated access to the internal areas of the site. The layout of the West Cave seems to have focused around a central 'Shrine' area, situated 5–8 m from the entrance on the east side of the cave (Figs. 3.2 & 3.3). The Shrine area was enclosed by a discontinuous screen of re-used stone slabs and uprights. Access to the area was likely through a porthole doorway, down a series of shallow rock-cut steps that led to an artificially levelled area in the bedrock containing a large re-used stone bowl. The Shrine area is significant in containing one of the few instances of a clear and deep stratigraphic sequence of intact archaeology which was excavated to the bedrock (Fig. 1.20). This consisted of extensive burial deposits (in particular Contexts (1328), (1268), (1206) and (960); see Stoddart *et al.* 2009c, 140–60) (§3.4.2.1). This secluded area appears to have had a dual ceremonial and funerary function and was continuously remodelled throughout the site's use. On excavation, fine artistic objects (the cache of handheld figures and the seated double figurine) were found secreted against former stone cupboards/shelves within the Shrine. Adjacent to the Shrine area is context (783), described as the 'Display' zone. This was a naturally demarcated oblong shaped depression in the soft bedrock which was utilized for primary deposition, after which the remains of the dead were extensively rearranged. Computational modelling shows a marked contrast between the high visibility of this area and the more concealed and secluded Shrine area (Stoddart *et al.* 2020; Thompson *et al.* 2020; Fig. 3.10), illustrating a duality in the role of light and dark within the hypogeum. Density modelling of the human remains reveals a noticeable path through the burial deposits, providing access to the currently unexplored parts of the West Cave. This highlights the changing function of areas within the site and how spaces packed with human remains were encountered by the living (Fig. 3.20; §3.4.2.2).

A partly excavated area northwest of the Display Zone leading to the West Cave also contained a collapsed niche. The area immediately to the north comprises deeply set megalithic structures that were probably supported by the 'Deep Zone' deposits. This was the approximate location of a prominent trilithon structure that was documented in watercolour paintings by Charles de Brocktorff in 1828 (Fig. 1.2); hence the deposits were significantly damaged by Col. Otto Bayer's explorations and the subsequent backfill activities (Stoddart *et al.* 2009c, Figure 8.24 for a plan of the rubble). This Deep area of the site was only partially explored during the 1987–1994 excavations, but an auger test indicated a further 2 m of unexcavated deposit, implying a total depth of more than 5 m from ground surface. In contrast to the sequence at Ħal Saflieni, where the lowest level represented the latest construction, the Circle appears to present a conventional stratigraphy with earlier material in the lowest levels of the site.

3.4.1.3. East Cave

Entry to the East Cave is located immediately south of the Shrine area through the 'Intermediate' zone (Fig. 3.3). The East Cave roof collapsed around 2400 cal. BC towards the end of site's use, but, prior to this, efforts were made to prop up the roof with a large supporting pillar (megalith 533) at the junction between the East and West Caves which combined with parts of the screen structure around the Shrine. The supporting megalith [553] created two arched entrances (north and south) (Appendix Figs. A1.64 & A1.65), and led into an area of torba floor and megalithic structures. In the far eastern corner, a cylindrical stone (the 'Betyl') was combined with a series of remnant stone shelves, walls and niches. These appear to have contained special deposits and disarticulated body parts (Stoddart *et al.* 2009c, 164, Figure 8.65, 175). The southern entrance to the East Cave led into the Central area, demarcated by a stone wall that encompassed a distinctive tapering Globigerina megalith [552] running east-west across the space.

The excavations in the East Cave did not reach bedrock, and instead defined the surface structures. An auger test through context (1312) indicated a remaining 0.65–1 m of underlying deposit (Stoddart *et al.* 2009c, 167). The partial excavation of the East Cave inevitably limits understanding of the area in terms of its foundation date, but a small *sondage* in the southeast corner demonstrates that the area likely held an exclusively funerary function (see Stoddart *et al.* 2009c, 169–73).

3.4.1.4. Southwest area and Southern Cave

The southwest area of the site had been badly disturbed during earlier antiquarian explorations, with excavated deposits in this part of the site consisting of modern fills (Stoddart *et al.* 2009c, 178–9, 193). Beneath the fills, modest megalithic structures formed a walled compartment marked by two Globigerina door jamb megaliths [744 and 745] in the area south of the Display Zone. This walled compartment led, in turn, to a second set of parallel Globigerina door jambs [507 and 791] through which was an area blocked by rubble and cave collapse. It is impossible to say where this routeway led, however, these compartments and doorways clearly facilitated access to other parts of the subterranean complex, and possibly linked the West Cave to the area now occupied by the modern apiaries in the South Cave (§3.4.1.1). Despite the challenges in reconstructing this area and, indeed, most of the exposed site, the arrangement of the megalithic structures into distinctive compartments and routes emphasizes the importance of the creation of delineated spaces and defined lines of movement within the hypogeum-style cave complex.

3.4.2. Stratigraphy

An important component of the current programme of research on the Circle has been the digitization of the site archive using Geographical Information Systems (GIS) (§3.1.4). The intra-site GIS database records the precise location of all human remains and small finds which were plotted on excavation plans and allows us to undertake enhanced spatial analysis of the burial deposits, augmenting the stratigraphic and spatial details originally presented by Stoddart *et al.* (2009b).

The GIS analysis focuses on two key areas of the site – the Shrine and the Display zone (Fig. 3.3) – and uses kernel density maps generated in QGIS 3.10 to examine the relative frequency of deposits within these areas. These two excavated areas present the best opportunity to explore and reconsider spatial and temporal trends in the activities that led to the formation of the burial deposits. Naturally, some assumptions must be made about these processes, especially in a cave system where gravity, soil creep, rock fall, animal activity and water ingress, together with human intervention, affected the position of the buried remains. The dynamic nature of commingled burial deposits is such that they cannot be considered as monolithic entities, as smaller skeletal elements are prone to movement around and between the archaeological layers. Taphonomic analysis of sub-samples from contexts in these areas indicate that the human remains deposited within the Shrine and Display Zone consisted largely of disturbed and rearranged primary deposits (Thompson *et al.* 2020; Chapter 12). This reveals that the deposits were formed as the result of episodic and successive deposition over a long period of time, rather than as a result of rapidly accumulated 'dump' deposits. Although GIS analysis alone cannot capture all the subtleties of the many taphonomic processes that occurred on site, the following analysis reveals considerable potential for the method.

3.4.2.1. The Shrine

The Shrine, described above, contained architectural elements (rock-cut steps, stone bowl and enclosing megalithic screen; Fig. 3.3), and deposits of human remains forming a discrete and delineated space in use for several centuries and episodically remodelled during the 3rd millennium BC (Figs. 3.15–3.17). The excavation of the Shrine area and *in situ* conservation of its megalithic structures resulted in only partial removal of the deposit, so our understanding of its chronology is incomplete. That said, the GIS density analysis has identified a fluctuating pattern of contraction and expansion of depositional activity, an

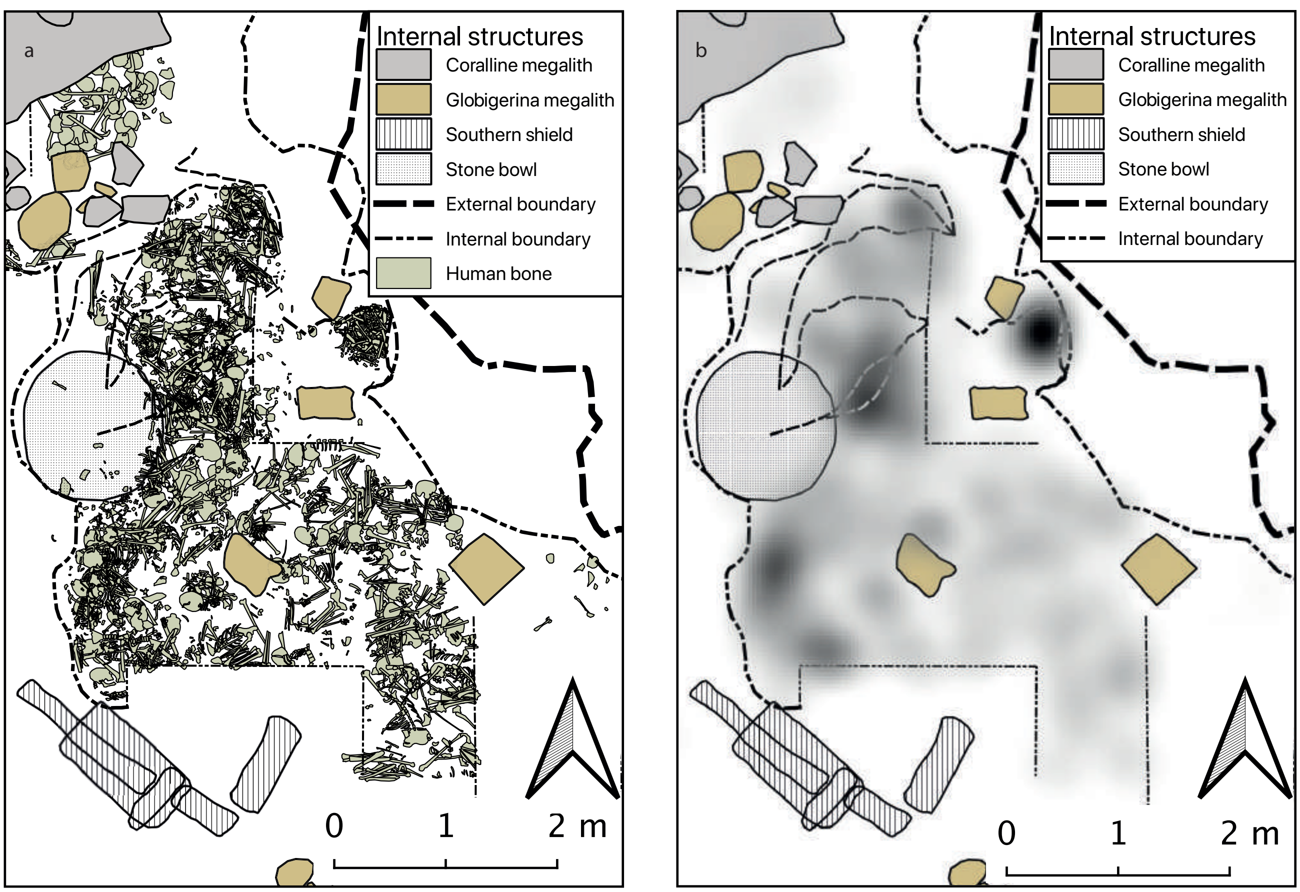

Figure 3.15. *GIS digitized human bone (a) and overall density of human bone (b) in the Shrine. Density shown by hotspots.*

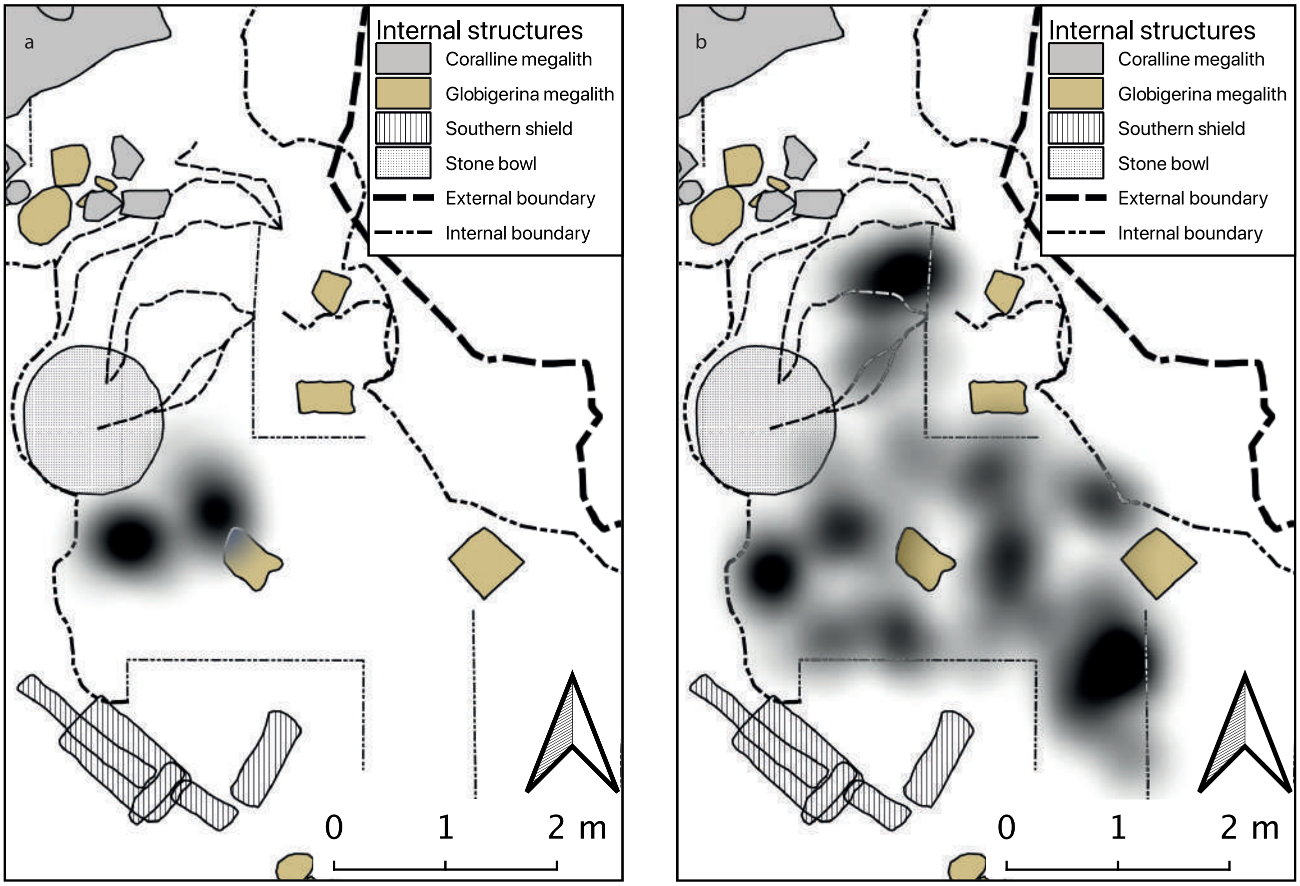

Figure 3.16. *Density of burial activity in context (1328) (a) and (1268) (b). Density shown by hotspots.*

observation that allows us to understand better the construction and restructuring events in this part of the site (Fig. 3.18).

Deposition in the Shrine area was initiated by four foundational burials (context (1328); Fig. 3.16a) within a cut feature in the natural bedrock (cut [1314]) during the early Tarxien phase, around *2890–2860 cal.* BC at 68% probability according to the chronological model of Malone *et al.* (2019). The short rock-cut feature [1314] filled by (1328) extends to the edge of the chalky ridge that supported the large stone bowl, indicating that the human remains were deposited prior to the insertion of this later structural element. Aside from commencing the Shrine stratigraphic sequence, the human remains comprising the foundational deposits in context (1328) initiated a stacked sequence of later interments (Stoddart *et al.* 2009c, 142, Figure 8.42) that continued into the base of the following deposit, context (1268), with two articulated burials overlying Individual D in context (1328).

Context (1268) is characterized by an expansion of consistent burial activity across the entire surface of bedrock (Fig. 3.16b) that occurred probably in the 29th century BC. Stoddart *et al.* (2009c, 142–5) suggested that the initial construction of the megalithic internal screen was contemporary with either the subsequent accumulation of Contexts (1268) or (1206), noting that the remodelling events had to have followed the placement of the final stacked burials towards the base of (1268). This uncertainty highlighted the difficulty in establishing the chronology of remodelling events because it was not possible to explore beneath the *in situ* megaliths. Areas of dense burial activity in the northern and southern limits of Context (1268) suggest that the Shrine transformed into an area of active funerary deposition, but the density analysis also indicates that the stone bowl was set into position before human remains gradually accumulated around its base (Fig. 3.16b). Regarding the megalithic screen itself, a cut feature that was created for the placement of megalith [955] (cut (1327); Stoddart *et al.* 2009c, 154) suggests that the structure was put in place following the accumulation of Context (1268). When integrated with the previously published stratigraphic details, the GIS density analysis

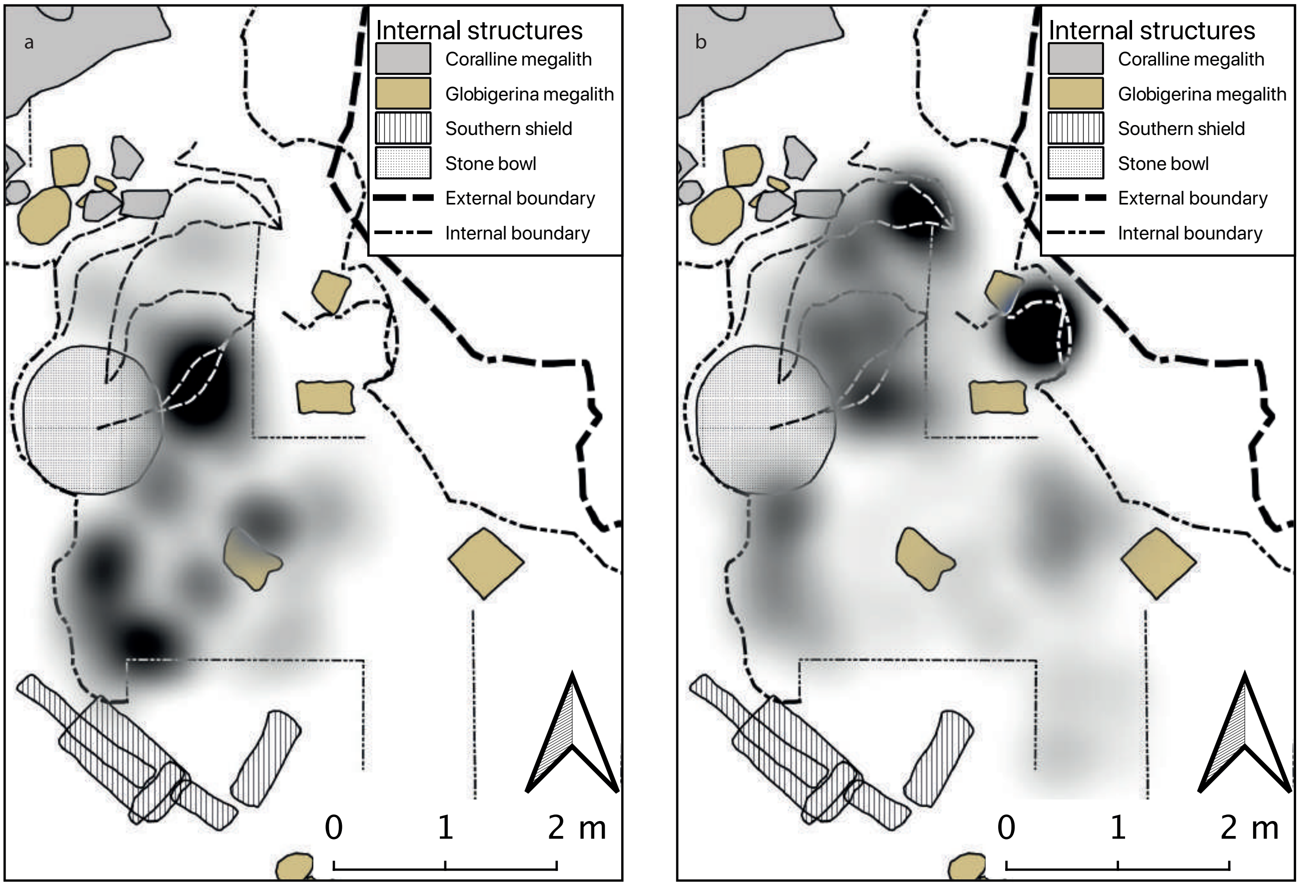

Figure 3.17. *Density of burial activity in context (1206) (a) and (960) (b). Density shown by hotspots.*

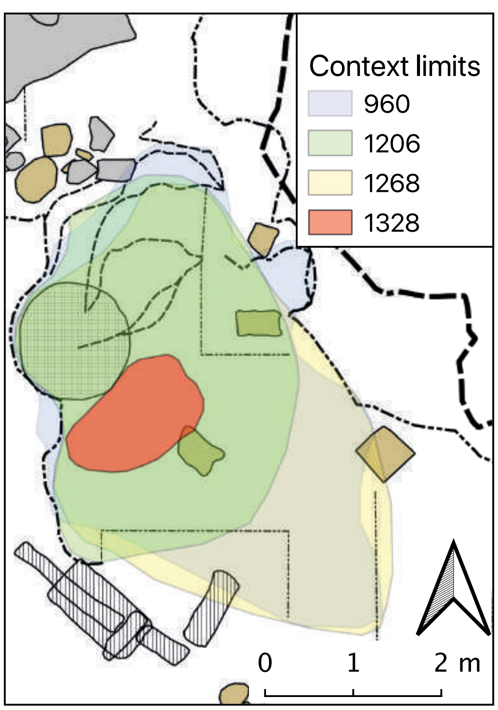

indicates that context (1268) post-dates the placement of the large stone bowl, but pre-dates the placement of megalith [955], and by extension the megalithic screen as a whole. The spatial distribution of the succeeding mortuary deposits, Contexts (1206) and (960), provide further chronological and stratigraphic constraints for deposit (1268), confirming that it pre-dates the erection of the megalithic screen which initiated the demarcation of space within the Shrine area.

As activity at the Circle continued throughout the Tarxien phase, a distinctive phase of burial activity occurred in the western half of the Shrine area, represented by Context (1206) and dating to the centuries leading up to 2500 cal. BC, at the very acme of activity at the site (Fig. 3.17a). This concentration of human remains was previously interpreted as an intentional

Figure 3.18. *Limits of the principal contexts of the Shrine, displaying the expansion and contraction of burial activity in the Shrine sequence.*

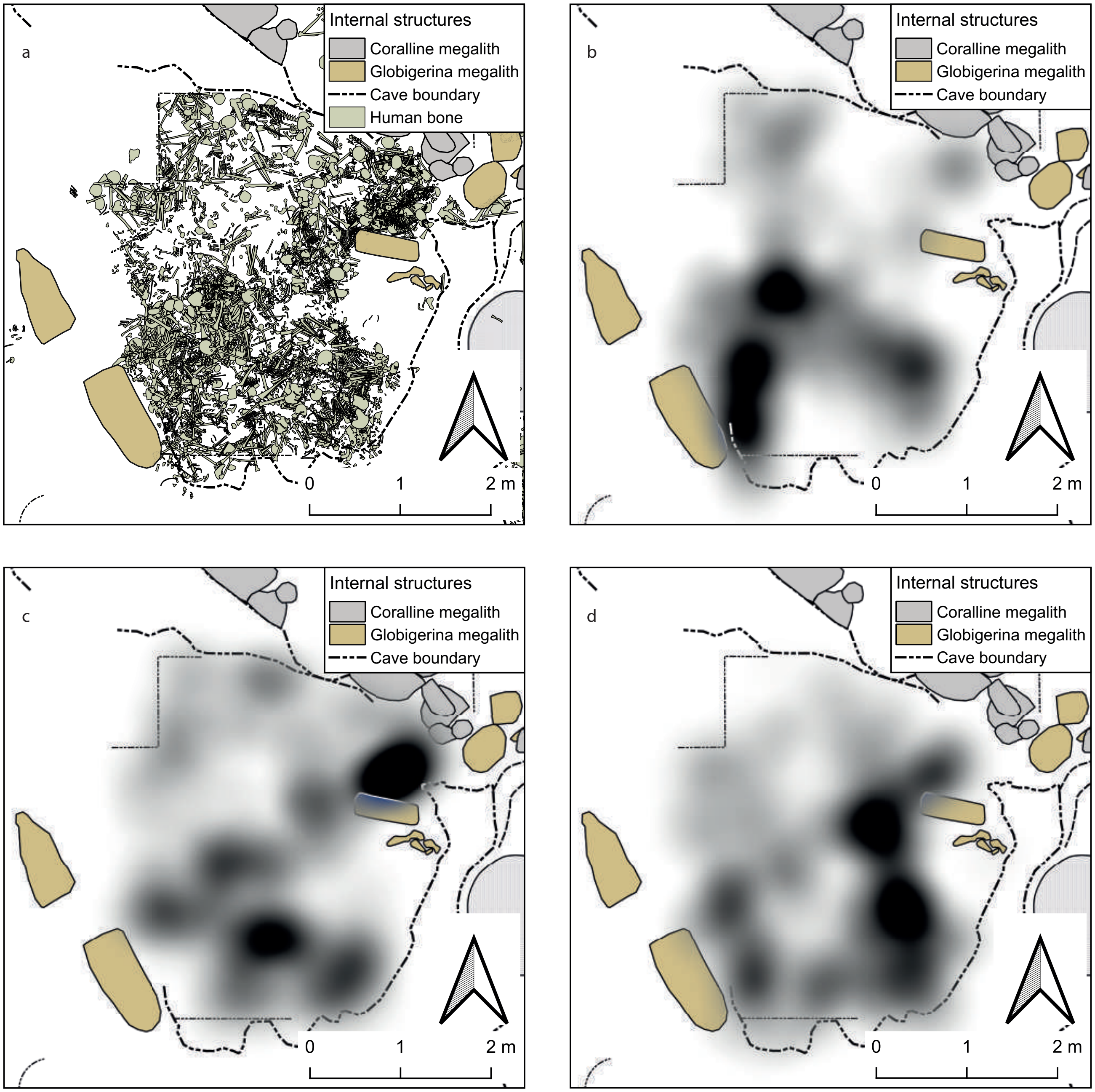

Figure 3.19. *Burial deposit 783 (a) and burial density of lower 783 (b) in the Display Zone; burial density of middle (c) and upper (d) 783 in the Display Zone. Density shown by hotspots.*

focus of burial around the large stone bowl (Malone 2007; Stoddart *et al.* 2009c, 145). However, considering the eastern extent of the deposit, it seems the distribution of bones respects an area delimited by an internal eastern screen (megaliths [955] and [951]). Whilst it is still clear that there was a concentration of burial around the stone bowl, denoted by the occurrence of partially articulated burials directly facing it, the overall distribution of burial activity within (1206) strongly suggests that the eastern internal screen was in place prior to the accumulation of this deposit. This places the construction of the internal screen before the accumulation of Context (1206) and likely associated with context (1268) in the 29th century BC.

The final phase of deposition in the Shrine area was the accumulation of a 'blanket' deposit, Context (960), at the end of the Tarxien phase (*2530–2475 to 2460–2350 cal.* BC at 95% probability; Malone *et al.* 2019)

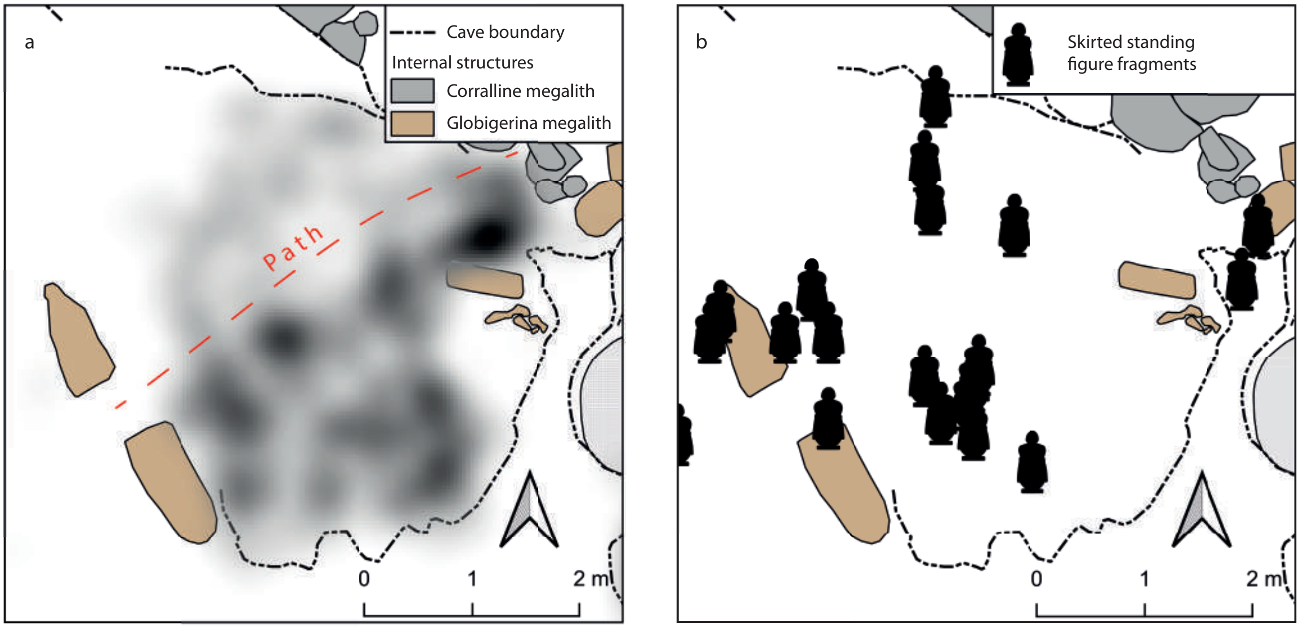

Figure 3.20. *a) Location of the path through the Display Zone; (b) distribution of the fragmented standing figure. Density shown by hotspots.*

during which deposits rapidly built up around the extant megalithic structures over a period of 50–100 years (Fig. 3.17b). The expanded depositional activity prompted a second major remodelling event of the eastern internal screen. The density analysis shows remodelling by identifying a sparse linear distribution between the uprights of the internal screen on the east side (megaliths 955 and 914), representing a cut feature [1113] (Appendix Fig. A1.25) created for the placement of an adjoining megalithic shield between the two uprights. Given the relatively short chronological span of Contexts (1206) and (960) it is likely that rapid accumulation of (960) engulfed the structural elements and prompted the need for further restructuring of the Shrine area. The intensification of both building and ritual activity in the final use-phase of the site could be considered as evidence of the classic narrative of late Tarxien peak and collapse (Evans 1959; Malone & Stoddart 2014; Stoddart *et al.* 1993). However, there was a similar peak in activity during the mid-3rd millennium, as illustrated by the Kernel Density Models (§3.2).

3.4.2.2. The Display Zone

The Display Zone (Figs. 3.3 & 3.19a) was an important component of the burial complex containing a substantial deposit of human remains, particularly Context (783) (see Stoddart *et al.* 2009c, 161–3 for full discussion). This deposit is contemporary with peak activity at the site; the Bayesian estimate of its chronology is *2585–2515 to 2420–2305 cal.* BC (Malone *et al.* 2019). The deposit was excavated in three main levels, each of about 20 cm depth. The levels were arbitrary divisions, but they have a useful heuristic value for investigating the formation of the complex deposit of commingled bone.

The basal level of (783), at a maximum depth of 50–60 cm, was initially characterized by an irregular coverage of human remains deposited across the bedrock (Fig. 3.19b). The density analysis of the base of (783) illustrates a concentration of articulated and partially articulated skeletal remains in the southwest area (Fig. 3.19a; Stoddart *et al.* 2009c, 161). A distinctive diagonal passageway or path between the burials ran through the rock basin (Stoddart *et al.* 2009c, 193) showing the pattern of corpse placement from the outset of deposition in (783). The pathway is most evident in the middle level of (783) (Fig. 3.19c), when a continuation of dense and little-disturbed burials accumulated in the southeast portion of the area. The pathway was evidently generated by continued and repeated linear navigation through the Display Zone, between the entrance to the area and the West niche, and the path may have accelerated the disturbance of burials in the northern parts of this area. A destroyed megalithic structure along the eastern border of the Display Zone is also evident in the density models (Fig. 3.19) and revealed as a large void in the density analysis. Stoddart *et al.* (2009c, 161) observed that the path through the Display Zone was not maintained during the later stages of use, which is apparent in density maps of upper (783) (Fig. 3.19d), although remnants of the path remained visible.

The GIS database also allowed integration of the small finds distribution with the burial density maps. This includes the plotting of fragments of a medium-sized stone skirted figure, the distribution of which confirms that it was probably located on the western border of the Display zone, near the end of the path through (783) (Fig. 3.20b). Computational analysis of visibility within the hypogeum (Barratt *et al.* 2020; Fig. 3.5) confirms that the Display Zone was a highly visible part of the complex. The figure's placement in this highly visible and much-frequented space lends insight to its possible function and significance.

3.5. Discussion and conclusions

The megalithic elements within the Circle's caves replicate to some extent those that were employed architecturally in Ħal Saflieni and the contemporary temple sites. These structures appear to form defined enclosures and routeways within the caves, which evidently proscribed movement between the different burial areas and the Shrine in particular. The stone structures have been published as two-dimensional plans (Stoddart *et al.* 2009c) where the impression might be one of open airy space, without a cave roof. In reality, the subterranean spaces were restricted and movement between areas clearly demarcated and controlled, as confirmed by a visit to the site. The effect of the limited space is emphasized by our computer models, and they serve to highlight the effect of the original restrictive and probably intentionally controlled passage through the cramped and closed conditions of the caves (Fig. 3.10). By the final century or so of Neolithic funerary activity, the site was dense with burial deposits that impeded passage around and through the caves. We can infer that funerary events involved navigation around and over, and in the decomposing, skeletonized and already-fragmented human remains, unless efforts had been made in advance to clear particular grave spaces.

The Display Zone (783) formed a large homogenous deposit within a naturally confined rock basin, and with few megalithic elements within the deposit, it cannot demonstrate clear evidence for the chronological development of placed architectural features. Our GIS analysis suggests that the path through the Display Zone was created and maintained throughout most of the active period of use. The area was evidently very significant in the burial ritual of the later episodes of the site, and it could be seen as both a place of embodiment and as transitional zone in ritual terms. In particular, the area was marked by a medium size standing skirted stone figure. Evidently, the statue was intentionally smashed in the final moments of the site, since a concentrated distribution of fragments were retrieved in superficial burial deposits around the western border of the Display Zone (cf Malone *et al*. 2009a, 283–9). Their location suggests a likely original location (Fig. 3.20) adjacent to the Shrine to the east, and in full view of the stone bowl set against the east edge of (783). The density analysis indicates that the standing figurine may have stood prominently and visibly at the end of the path through the Display Zone. What its role was within the funerary interactions and rituals in the space remain unclear, but evidently it had an active and tactile role in performative liturgical activities.

It is important to note that the interpretations of the formation processes of the Shrine sequence presented here are based on the partially excavated eastern internal screen (megaliths [955] and [914]). There is still much that remains unclear in terms of the construction sequence of the megalithic structures remaining *in situ*, and our reconstruction of the remodelling of the megalithic internal screens is provisional. Whilst two major remodelling phases have been identified here, only further excavation might refine the subtleties of these events, and identify further possible remodelling, assuming the deposits are sufficiently intact and informative. Nevertheless, the spatial distribution of the funerary deposits and their temporal development provide a convincing proxy for establishing the chronological sequence of the evolution of the Shrine area.

The combination of GIS analysis with radiocarbon dating and a study of stratigraphy enables a clear result to emerge. The internal history of the Circle and the density of activities performed in it was moderated and limited by the space available in the cave system. This space changed over time because even a modestly sized population still produces, over centuries, an exponentially increasing number of skeletal 'ancestors'. At the Circle, where these ancestral remains were laid to rest, ideas about how the internal space of the cave could and should be used were continually updated to meet both practical demands and the changing mortuary customs of the community. The most dynamic period of funerary activity at the Circle was around 2500 cal. BC, which followed four centuries of sustained growth and would have applied unprecedented pressure upon the limited space available. The final 150 years of the Circle's burial use was apparently less intense than what had gone before, and those years witnessed not only the collapse of the East Cave roof and its likely closure, but also the gradual demographic and economic erosion of the unique Temple

Culture. Through modelling the density of burials across space and time we can now detect a slow trend of decline and diminution. The protracted decline over a century or two, rather than a rapid 'collapse' of the Temple Culture is informative and fits neatly with the complementary data examined by the *FRAGSUS Project* as well as the trends revealed by the skeletal remains indicating a decline in health and diet. These trends towards a decline are discussed in the following chapters, and they resonate with other perspectives emerging from the archaeology and palaeoenvironmental studies by *FRAGSUS* of the Maltese Islands. The relationship between the natural environment, soils, the interventions of the human community and a changing climate over several centuries is becoming a little clearer and potentially explains the demise of the Temple Culture itself.

Acknowledgements

This chapter was collectively written with specialist attention to the individual sections as follows: 3.1.2. Rowan McLaughlin and Simon Stoddart; 3.1.3. Simon Stoddart and Caroline Malone; 3.1.4.1. Simon Stoddart; 3.1.4.2. Eóin Parkinson, Rowan McLaughlin and Sara Boyle; 3.1.4.3. Rowan McLaughlin and Eóin Parkinson; 3.1.5.1. Robert Barratt; 3.1.5.2. John Meneely; 3.1.5.3. Robert Barratt; and 3.2. Rowan McLaughlin.

Chapter 4

Dental pathology in the Circle: oral health, activity and intervention in Neolithic Malta

Ronika K. Power, Bernardette Mercieca-Spiteri, Rowan McLaughlin, Jess E. Thompson, Jacinta Carruthers, Sarah Massingham, Laura T. Buck, Jaap Saers, Margery Pardey, Jay Stock & John Magnussen

4.1. Introduction

The current work builds on the original observations established in Malone *et al.* (2009d), with particular reference to the chapter co-authored by Stoddart, Barber, Duhig, Mann, O'Connell, Lai, Redhouse and Malone on the osteological inventory, introductory analyses, and isotopic pilot study of the human and animal remains of the Circle. These primary engagements with such a challenging dataset are admirable, not least because of the innate challenges and complexities of approaching an assemblage represented by an estimated 220,000 human bones – the majority of which were disarticulated, highly fragmented and commingled – but also because of the stratigraphic complexities of their depositional environment, as well as the requisite synthesis of reports from the many and varied specialists who contributed over the course of eight years of excavation. Stoddart *et al.* (2009a) provided invaluable initial insights into local Maltese and regional Mediterranean prehistoric population profiles and mortuary behaviour via their presentation of osseous representation by element (including fragments and exfoliated teeth); preliminary observations of general pathologies and 'dental attrition' (Stoddart *et al.* 2009a, 315, 318); and (re)distribution patterns of elements across the site. This data collection, in conjunction with relative and absolute dating activities, facilitated a broad overview of the individuals represented within the Circle and their experiences of health, disease, trauma, nutrition, congenital and occupational variation and social inclusion. As a result, we have far greater understanding of the role of the space as not only an interment site for over 1000 individuals encompassing all biological sexes and ages across the life course, as well as the manner by which engagement continued between communities of the living and dead.

One of the many challenges faced by those responsible for the excavation and analysis of such a vast and complex assemblage includes decisions surrounding the dedication of resources and prioritization of activities within temporal and pecuniary project parameters. Indeed, the analytical possibilities presented by the Circle assemblage are seemingly infinite, far exceeding the capacities of person-hours and budgets assembled by the invested researchers, even over decades. The need for further archaeometric analyses has been clearly identified and articulated by Stoddart *et al.* (2009a, 329), including aDNA and additional isotopic and chronometric work. European Research Council (ERC) funding has finally enabled such endeavours through the support of the *FRAGSUS Project* and its subgroup, the Population History Workgroup, as seen in Chapters 11 (aDNA), 3 (Chronology), 7 (activity markers) and 12 (taphonomic processes). Notwithstanding their substantial contributions to advancing our knowledge of Maltese and Mediterranean prehistory, it must be noted that all works presented here represent further sub-sample studies of the overall assemblage rather than comprehensive documentation of the Neolithic population who employed the Circle for funeral and interment rites and practices. The nature and scope of the assemblage may determine that 'comprehensive' knowledge might only be possible after synthesizing several scholars' lifetime works, including those of the current authors.

As detailed in Chapter 2, the team undertaking osteological analyses faced similar sampling strategy decisions as other archaeometric colleagues in order to produce novel work within the parameters of the *FRAGSUS Project.* Mercieca-Spiteri has detailed this strategy for the Population History Workgroup both here and elsewhere (Mercieca-Spiteri 2016). It suffices to say here that in order to achieve qualitative population insights into this complex assemblage in our limited time, and to support parallel investigations into scientific dating, palaeodiet and geographical affinity, our activities focused on analyses of the dentition from those contexts determined by the excavators to be of greatest cultural and temporal significance.

A focus on dentition facilitates a multifaceted approach towards understanding aspects of population health, disease, nutrition, habitual behaviour (potentially including so-called 'occupationally' related changes) and identity markers while restricting analytical engagement to a single category of element. Over and above their physical resilience in various depositional environments, the value of teeth as veritable encyclopaedic repositories of life history information has been highlighted elsewhere (Hillson 2005, 1, 6; Langsjoen 1998, 393; Larsen & Kelley 1991, 1; Roberts & Manchester 2005, 63; White *et al.* 2012, 101); it has long been the belief of this group of authors that teeth are the 'diamonds of the archaeological record'. As such, the overarching theme of this work is devoted to reporting our observations on the pathology, modification, non-metric, biochemical, chronometric and genetic characteristics of the Neolithic population associated with the Circle. Commencing in this chapter with reportage on dental pathology, each of the preceding enterprises will be addressed within the discrete chapters that follow. Notwithstanding this demarcation by analytical modalities, the reader is encouraged to keep in mind that all activities were carried out in a carefully choreographed sequence of studies. We focused on the integrities of both inventory and workflow to ensure maximum cohesion and mutual illumination between and across all studies, and to minimize impact through sampling for isotopic, aDNA and radiocarbon analyses.

The first forays into the dental health and anthropology of the Circle population were made by Stoddart and colleagues in their overview of the assemblage within Malone *et al.* (2009d). In that case, dental analyses were restricted to general characterizations and observations on a context-by-context basis alongside similar notes for the (dis)articulation, fragmentation, distribution, and pathological statuses of the overall skeletal material for each discrete stratigraphic unit or grouping. Commentary included observations on eruption status (for the purposes of establishing age), as well the presence (or relative absence) of enamel hypoplasia, carious lesions, *antemortem* tooth loss, periodontal disease (including calculus, alveolar resorption), infectious disease (including abscesses and sinusitis), 'parafunctional' and general tooth wear and/or crowding, developmental and congenital variations (including impaction), and temporomandibular joint disease. These observations were made on both the amassed exfoliated (or 'loose') teeth and, where possible, the complete dentition of individuals where intact crania, mandibles, or even fragmentary arcades were extant. Although their work is of excellent quality, deeply considered, and eminently useful as stand-alone analyses, the authors acknowledge that it represents an initial overview, and they called for more detailed studies on numerous occasions (Stoddart *et al.* 2009a, 315, 318, 329, 339). In the current volume, we seek to undertake precisely such detailed studies, and acknowledge our predecessors for the excellent foundation they established for the work presented here.

4.2. Dental pathology

Of all the skeletal regions studied by bioarchaeologists, it may be argued that the dentition facilitates the greatest range and depth of insights into population size, composition, health, diet, diversity and behaviours (Hillson 2005, 1, 6; Langsjoen 1998, 393; Larsen & Kelley 1991, 1; Roberts & Manchester 2005, 63; White *et al.* 2012, 101). It is for these reasons that much bioarchaeological and bioanthropological research into the physical effects of the subsistence and mobility changes accompanying the Neolithic transition across the world has been focused on teeth (Eshed *et al.* 2006; Lubell *et al.* 1994; Mahoney 2006; Molnar 2008; Pinhasi *et al.* 2008). Human dentition provides the most accurate systemic proxy of the biological impact of behavioural and cultural change – if the eyes are the windows to the souls of the living, then perhaps teeth are windows to the lifestyles of the ancient dead.

The broad aim of this chapter is to provide precisely those insights into the lifestyles of the Neolithic inhabitants of Gozo, and to explore their biological responses to the massive cultural and behavioural demands they faced in their restricted island environment. The highly fragmented and predominantly disarticulated nature of the Circle assemblage precludes many of the traditional approaches to whole-body analyses of the burial population. With this in mind, we focus on the dentition as a single category of element that provides the greatest consistency, most numerous scientific analytical capabilities, maximum systemic insights and best possibility for comparative studies across contemporaneous regional populations. The current chapter presents results of our analyses of the dental pathologies observed for the study sample derived from the Circle assemblage, while subsequent chapters will present our findings for dental modification, non-metric traits, and biochemical, chronometric and genetic analyses.

Table 4.1. *Materials included in dental studies, including provenance and representation.*

Context	Location	Date	N teeth isolated	Σ teeth studied	% Context
595	East Cave	Early	123	123	100
833	West Cave: north niche	Early	18	2	11
951	West Cave: north niche	Early	2306	751	33
698	East Cave: southern pit	Early	13	3	23
1209	West Cave: shrine	Middle	4	4	100
1241	East Cave	Middle	170	170	100
433	East Cave: central	Late	35	6	17
436	East Cave: central	Late	32	32	100
715	East Cave	Late	56	54	96
738	East Cave	Late	17	15	88
790	Intermediate zone	Late	11	11	100
1206	West Cave: shrine	Late	642	508	79
960	West Cave: shrine	Latest	870	405	47
783	West Cave: display	Latest	2900	976	34
		Total	7197	3060	43

4.3. Materials

As discussed in Chapter 2, a total of 11,706 teeth were isolated from their associated highly fragmented, commingled and predominantly disarticulated skeletal remains and inventoried according to context by the *FRAGSUS* Population History Workgroup across five laboratory seasons at the National Museum of Archaeology (NMA), Valletta, between November 2014 and May 2017. Of these, a total of 3060 teeth (26.1% of the isolated sample) of all types were studied for the purposes of interrogating the experience of dental pathology, anthropology and modification among the population/s represented within the Circle. As noted previously and detailed in Table 4.1, the studied teeth are only a subsample of the overall assemblage, representing a proportion (or complete in the cases of contexts (436), (595), (790), (1209) and (1241)) of 14 selected contexts as excavated thus far. It is critical to note that the site was not excavated in totality, and further remains are preserved *in situ* to allow for work to continue at the hands of future generations of archaeologists. The examined contexts were determined by the excavators to be of greatest cultural and temporal significance to the overarching research questions, and thus included in whole or part here.

4.4. Methods

For the dental pathology study, teeth of all types and articulation states (exfoliated *postmortem* or in occlusion) were examined individually within their context batches (Fig. 4.1). The number and strength of expression for each pathology category was recorded for each batch in a Microsoft Excel spreadsheet to form a searchable digital database. Each batch was marked once analysis was complete and curated thereafter within the NMA as part of the *FRAGSUS* Research Archive.

In terms of naming conventions, we follow the notation system developed by the *Fédération Dentaire Internationale* (FDI; FDI 1971; International Organization for Standardization [ISO] 3950, ISO 1984, 1995; Alt & Türp 1998b). Anterior tooth surfaces are referred to as: incisal or occlusal (the biting or chewing surfaces; incisal is more specifically for the anterior teeth); and labial (the lip surface of the anterior teeth); lingual (the tongue surface of all teeth) or buccal (the cheek surfaces of the posterior teeth). Directions are referred to as mesial (towards the midline) and distal (away from the midline). Our general macroscopic osteological analytical techniques are based on standard criteria described in Buikstra and Ubelaker (1994: specific references indicated alongside analyses, below). All surfaces were examined macroscopically and under magnification using a 10x hand lens.

Every tooth was examined for the presence/absence of enamel hypoplasia; carious lesions (where present, caries was further scrutinized for location and severity); hypercementosis; crown and root fractures (where present, crown and root fractures were further scrutinized for precise location and tooth type); extreme wear (where present, extreme wear was further scrutinized for precise crown location and tooth type) and dental modification. Special notes were made for the

Figure 4.1. *A typical assortment of* postmortem *exfoliated loose human teeth from the Circle excavations, under analysis as part of the ERC-funded* FRAGSUS Project *in the National Museum of Archaeology, Valletta, Malta. (Photo Ronika. K. Power.)*

occurrence of juvenile wear and pathology, according to tooth type. Developing crowns were counted among the tooth totals for each batch, however they were not eligible for inclusion in analyses of wear, caries or fractures. This study has an explicit focus on disorders of the teeth, and it does not include pathologies of the jaws. Although it is acknowledged that several such pathologies are inextricably linked to dental health, including *antemortem* tooth loss, abscesses, granulomata, and the various expressions of periodontal disease, because of the high rates of *postmortem* tooth exfoliation, fragmentation of the maxillae and mandibles, and prevailing research parameters, it was decided that the current study should maintain an exclusive focus on teeth. The only exceptions are made for standalone case studies concerning the identification of therapeutic intervention and a developmental defect in two separate mandibular fragments, as reported in §4.5.7.1 and §4.5.7.3.8 respectively, below. Pathology is plotted by context following Malone *et al.* (2009d) and follows the radiocarbon sequence remodelled as part of the current phase of research (Chapter 3). Within the study sample, selected items were identified as worthy of further examination via radiographic analyses.[1]

4.5. Results: overview

Of the 3060 teeth under study, there were 866 observations of dental pathology. As shown in Table 4.2, the contexts with the highest raw incidence of pathology observations amongst the sample were found to be (783) (Σ=259), (951) (Σ=230), and (1206) (Σ=130). It must be noted that these data refer to the number of observations of the described pathologies, rather than the number of individual teeth displaying pathology. When considering those contexts with greater than 10 teeth within the sample, those with the highest prevalence (or proportion) of pathology observations were (595) (49.6%), (436) (37.5%), (951) (30.6%), closely followed by a tight cluster of Late contexts including (960) (27.6%), (783) (26.5%) and (1206) (25.6%).

In total, the pathology observed with the greatest frequency was enamel hypoplasia (Σ=209), followed by dental caries (Σ=189), dental modification (Σ=172), crown fractures (Σ=169), extreme wear (Σ=74), hypercementosis (Σ=47), and root fractures (Σ=6), respectively (Fig. 4.2). Each category of dental pathology is discussed in detail below, with the exception of dental modification, which is the subject of Chapter 5.

4.5.1. Enamel hypoplasia

Teeth were examined for evidence of defects in the tooth crown surface. These defects include grooves (or lines) and/or pits (hypoplasia), and/or opacities (hypocalcification; Hillson 2005, 168; Schulz *et al.* 1998, 294–5). Such defects are thought to be caused by deficiencies in enamel thickness because of elevated cortisone levels resulting from nutritional, environmental, psychological or pathological stress or physical trauma during the secretion phase of amelogenesis (Goodman & Rose 1990, 33; Hillson 2000, 250; Lorentz *et al.* 2019; McFadden & Oxenham 2020; Ortner 2003, 594ff.; Rose *et al.* 1985; Schulz *et al.* 1998, 298ff., 307), and disturbances to maturation, respectively (Hillson 2005, 168), during

Table 4.2. *Pathology summary by context and chronology (EH = Enamel Hypoplasia; X = Fractures; Mod. = Modification; Hyper. = Hypercementosis).*

Context	Location	Date	Σ teeth studied	EH	Caries	Crown X	Root X	Extreme wear	Mod.	Hyper.
595	East Cave	Early	123	8	21	10	1	7	13	1
833	West Cave: north niche	Early	2	1	1	0	0	0	0	1
951	West Cave: north niche	Early	751	21	65	73	1	26	15	29
698	East Cave: southern pit	Early	3	0	1	0	0	0	0	0
1209	West Cave: shrine	Middle	4	0	0	0	0	0	0	0
1241	East Cave	Middle	170	4	20	11	0	4	6	3
433	East Cave: central	Late	6	0	0	0	0	0	0	0
436	East Cave: central	Late	32	11	0	0	0	0	1	0
715	East Cave	Late	54	1	1	3	0	1	1	0
738	East Cave	Late	15	0	1	0	0	0	1	0
790	Intermediate zone	Late	11	0	0	0	0	0	1	0
1206	West Cave: shrine	Late	508	57	22	14	0	5	28	4
960	West Cave: shrine	Latest	405	26	19	21	0	13	31	2
783	West Cave: display	Latest	976	80	38	37	4	18	75	7
		Total	3060	209	189	169	6	74	172	47

the first seven years of life (Armelagos *et al.* 2009; Cares Henriquez & Oxenham 2020; Lewis 2007, 105; Ortner 2003: 595). As such, these defects provide reliable indications of the incidence of childhood stress as enamel is a fixed substance and does not remodel throughout the life course like other bodily tissues, including bone. Where observed on deciduous teeth, enamel defects can indicate pre-natal stress, and therefore provide insights into maternal gestational health (Lewis 2007).

A total of 209 teeth were observed to present enamel hypoplasia, equating to 6.8% of the total sample. Keeping in mind that the sample is generally comprised of isolated teeth rather than intact dentition, it is pertinent to state that this result (and indeed all that follow) should be viewed as an absolute *maximum* prevalence rate within the population. It is possible that some of the exfoliated teeth observed with these defects originated from one individual. Although it is still a reliable indicator of population stress, this result should therefore be considered as an *element incidence rate*, as opposed to a *population prevalence rate* in the statistical sense.

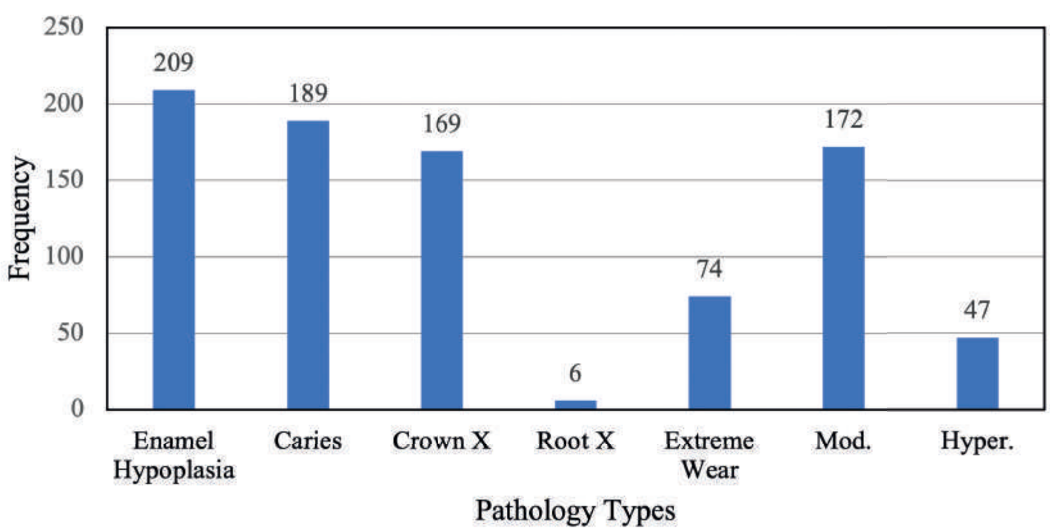

Figure 4.2. *Frequency distribution of dental pathology observations in the Circle sample (n=3060) (X = Fractures; Mod. = Modification; Hyper. = Hypercementosis).*

Notwithstanding these caveats, the data present some compelling patterns. Taken as a general indicator of population health, 6.8% is a relatively low enamel hypoplasia incidence rate over the entire occupation sequence of the Circle. When the data are distributed according to date, however, it is clear that the groups deposited within the Circle experienced particularly stressful episodes during specific occupational phases on Gozo. As seen in Figure 4.3, when condensed into cultural/temporal sequences, incidence rates of enamel hypoplasia are very low both in the Early period (Σ=30; 0.98% of total sample; 3.41% of total timeframe) and Middle period (Σ=4; 0.13% total sample; 2.29% of total timeframe). We then see a substantial increase in enamel hypoplasia in the Late period (Σ=175; 5.72% total sample; 8.71% of total timeframe), suggesting that those individuals living and dying in the final phase of the Circle use-life were subject to greater nutritional, environmental, psychological or pathological stress or physical trauma during their childhood, infancy or gestation than their predecessors. The comparative experience of these factors is strongly apparent when expressed proportionally amongst all observations of enamel hypoplasia within the sample, as seen in Figure 4.4. Here we see that of all incidences of hypoplasia, the Early period accounts for 14.35%, the Middle period for only 1.91%, and the Late period for 83.7% of affected elements (cf Stoddart *et al.* 2009a, 325–9).

The data may be more closely scrutinized to reveal the incidence of enamel hypoplasia on deciduous

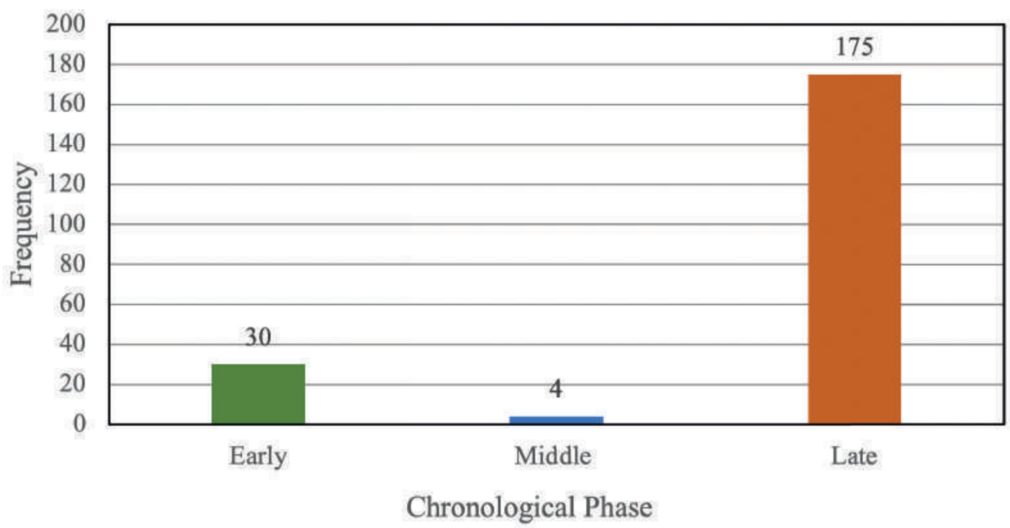

Figure 4.3. *Frequency distribution of enamel hypoplasia observations by chronological phases in the Circle sample (Σ=209).*

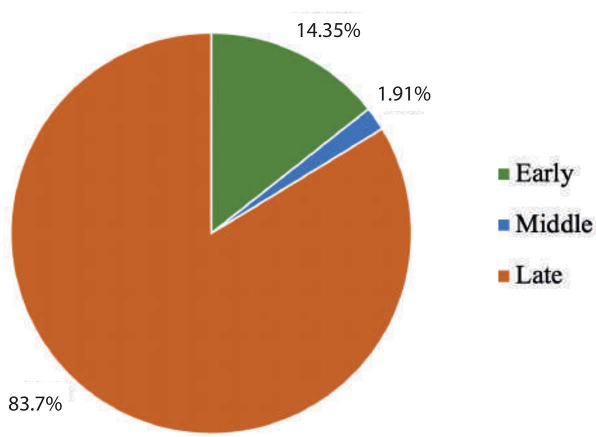

Figure 4.4. *Frequency distribution of enamel hypoplasia observations by proportion across chronological phases in the Circle sample (Σ=209).*

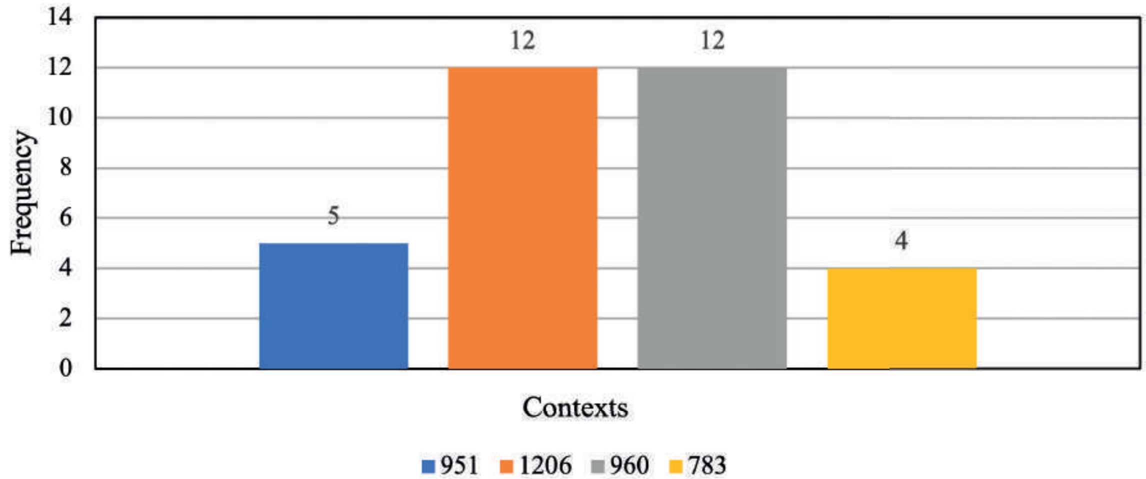

Figure 4.5. *Frequency distribution of enamel hypoplasia observations in deciduous dentition in the Circle sample (Σ=33).*

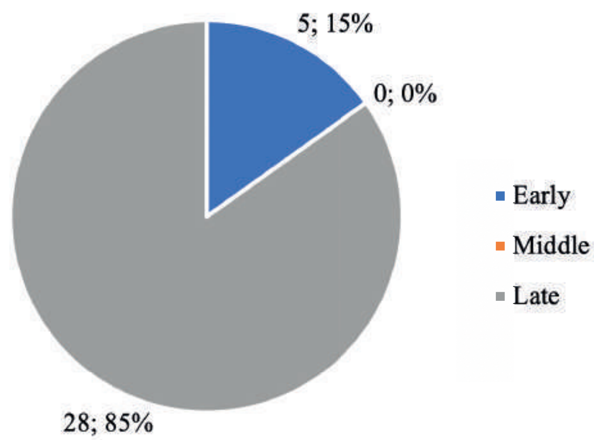

Figure 4.6. *Frequency distribution of enamel hypoplasia observations in deciduous teeth by proportion across chronological phases in the Circle sample (Σ=33).*

dentition. As previously mentioned, the appearance of enamel defects on deciduous teeth provides reliable indicators of maternal ill-health or poor nutrition during pregnancy. Further to this, other contributing factors might indicate that affected individuals were born in months of low sunlight (vitamin D) with an accompanying retinol (vitamin A) deficiency (Lewis 2007; Skinner 1986; Skinner & Goodman 1992). These combined factors can result in thinning of the alveolar bone in the foetus, thus making the area more susceptible to birth trauma, potentially leading to localized ameloblastic death (Skinner & Newell 2003). Considering the general availability of sunlight across the Maltese archipelago regardless of season, in addition to providing insights into maternal health and nutrition, these data may also allow us to construct seasonal habitation practices, including extended periods of shelter during winter months inside one of Gozo's many cave systems.

Irrespective of habitation patterns, there is little doubt that maternal health and nutrition are the preeminent determining factors for the appearance of enamel defects in deciduous teeth. This phenomenon is clearly present amongst the Circle assemblage, as shown in Figure 4.5. We observed a total of 33 deciduous teeth with hypoplastic defects amongst the sample, originating from 4 contexts: (951) (Σ=5); (1206) (Σ=12); (960) (Σ=12); and (783) (Σ=4). These data align closely with that for the overall assemblage, insofar as there is a clear pattern of an increased experience of non-specific stress over time, with 15.15% (Σ=5) of the total deciduous hypoplastic sample originating from the Early period, none from the Middle period, and 84.85% (Σ=28) dating to the Late phase of the Circle inhumations (Fig. 4.6). It appears that the non-specific stress/es experienced by this population were of sufficient severity as to impact on expectant mothers and their children, and in this case, the children represented within this dataset did not survive to adulthood.

4.5.2. Fluorosis

It is pertinent to address the possibility that the population may have presented signs of fluorosis in the dentition, considering the high endemic levels of fluoride in Gozo because of the geological substrate (Murray *et al.* 1991). This phenomenon will be discussed in more detail, below, in association with the possibility of its beneficial effects in protecting the teeth against decay; however, it is also possible that an excess of fluoride (beyond 0.5 ppm; Hillson 2005, 169) may have deleterious effects on enamel formation. Where present, fluorosis can manifest in the teeth as hypocalcifications, pit- or plane-form hypoplastic defects, and/or yellow or brown discolourations, with an overall predilection for the molars rather than incisors (Hillson 2000, 266; 2005, 169; Schulz *et al.* 1998, 300). The possibility that such defects may be present amongst the Circle assemblage was raised by Stoddart *et al.* (2009a, 324, 328), who suggested that the pitting of the teeth observed in Context (1268) may be evidence of fluorosis, citing ethnographic data as a flag for investigation of the possibility for archaeological expressions (Camilleri 1998; Galea 1971, 1997; Mangion & Olivieri-Munroe 1968; Vella & Borg 1989; Zahra & Vassallo 2011).

At this stage, the hypoplastic defects observed on the present sample of the Circle population generally appear to be that of the classic enamel hypoplasia described in §4.5.1, above, with no observations of hypocalcifications or yellow-brown discolourations of adult dentition. However, there were five observations of discolouration on deciduous teeth, all emanating from Context (960). Each tooth was examined closely to determine whether the aetiology of discolouration should be attributed to *in vivo* or *postmortem* factors. In all cases the teeth were well-preserved and showed no evidence for taphonomic or diagenetic alteration. As such, the observed discolourations were determined to have taken place within the lived experiences of these individuals. As described above, considering that deciduous teeth are primarily a reflection of maternal health and nutrition, these examples certainly raise the question of over-exposure through drinking water during pregnancy and deserve more detailed investigation. It is, however, important to note that four out of the five discoloured deciduous teeth within the current sample were central or lateral incisors, and only one was a molar. According to the arguments raised above, differential diagnosis for the discolouration of the anterior deciduous teeth should also include ameloblastic death following birth trauma.

4.5.3. Carious lesions

Carious lesions (also known as dental caries or tooth decay) are areas of demineralized enamel, dentine and cement, caused by progressively increased localized organic acid levels following the metabolism of dietary sugars by bacteria residing in dental plaque (Caselitz 1998: 203; Hillson 2008, 111, 2005, 290–1). In archaeological contexts, cariogenic foods may be those containing natural simple sugars, such as fruits, vegetables and honey or complex sugars such as carbohydrates, especially those found in cereals. Although the latter group are generally considered to be less cariogenic, it has been argued that processes such as cooking grains or grinding them into fine powders can increase their cariogenicity (Caffell & Holst 2012; Moynihan 2003). By nature, proteins and fats do not appear to have an inherent involvement in the development of carious lesions (Hillson 2005, 291), however they may inadvertently be causal factors if they become lodged interproximally (between the teeth), leading to localized decay. Further to this, nutritional, environmental, psychological or genetic factors interfering with amelogenesis, such as those described for enamel hypoplasia, above, can also impact on enamel quality (Caselitz 1998, 204, 222; Hillson 2000, 265, 2008, 112, 2000: 250). Individuals with poor enamel quality can be more vulnerable to dental caries across the life course (Ortner 2003, 590).

Despite the apparent absence of any material evidence for preventative mechanical intervention in dental hygiene (such as miswack sticks, a twig of the *salvadora persica* tree; Forshaw 2009, 423; cf Al-Otaibi *et al.* 2003; however, see §4.5.6.7, below for evidence of pressure erosion at the cementum enamel junction), or the characteristic interproximal grooving thought to be created by the use of plant material such as grass stalks as toothpicks (Alt & Pichler 1998; Frayer 1991; Hlusko 2003), the Circle population represented by this sample has relatively low overall caries rates. As seen in Table 4.1, of the 3,060 teeth examined, only 189 (6.18%) were observed to present carious lesions. Of these, there were 20 observations of obliterative caries (where the lesion has obliterated the entire crown, leaving only a root stump; 0.68% total sample; 10.99% of total caries; these are Hillson's 'gross gross' caries, 2005, 294). Although this is a relatively low overall result for a Neolithic assemblage, the data take on a different shape and meaning when distributed chronologically. For greater statistical robusticity, the caries data may be considered according to only those contexts where more than 100 teeth were examined, as displayed in Table 4.3 and Figures 4.7–4.8. Here, we can see that the

Table 4.3. *Summary of observations of frequency and reported locations of carious lesions for contexts with greater than 100 teeth in the sample (CeBL = Cervical Bucco-Lingual; CeI = Cervical Interproximal; CeL = Cervical Labial; CrI = Crown Interproximal; Obl. = Obliterative).*

Context	Location	Date	Σ teeth studied	Σ caries	Occlusal	CeBL	CeI	CeL	Root	CrI	Complex	Obl.
595	East Cave	Early	123	21	0	5	11	1	0	0	4	0
951	West Cave: north niche	Early	751	65	15	10	21	1	0	1	13	4
1241	East Cave	Middle	170	20	1	3	10	0	0	0	0	6
1206	West Cave: shrine	Late	508	22	3	6	4	0	0	0	4	5
960	West Cave: shrine	Latest	405	19	0	8	7	0	0	0	3	1
783	West Cave: display	Latest	976	35	4	6	11	0	3	1	6	4
		Total	2933	182	23	38	64	2	3	2	30	20

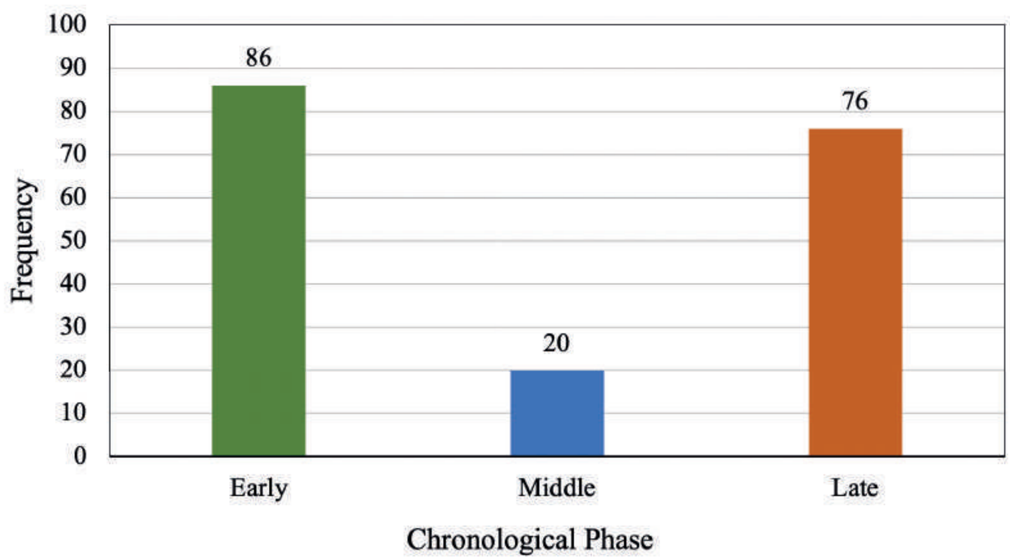

Figure 4.7. *Frequency distribution of carious lesion observations by chronological phases in the Circle sample (Σ=182).*

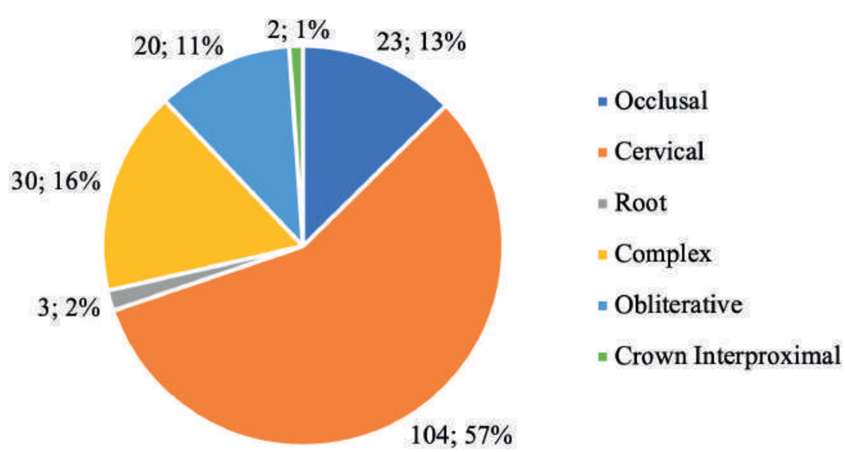

Figure 4.8. *Frequency distribution of carious lesion observations by type and proportion in the Circle sample (Σ=182).*

frequency of caries is highest in the earliest periods of the use-life of the Circle, with contexts (595) and (951) accounting for 47.25% (Σ=86) of all caries observed in the sample. There appears to be a reduction in the experience of tooth decay during the Middle phase of interments, as Context (1241) represents only 10.99% (Σ=20) of all caries. This is followed by a resurgence in cariogenic activity in the population associated with the Latest phase of activity: here, contexts (1206), (960) and (783) cumulatively feature 41.76% (Σ=76) of caries in the sample.

As highlighted above, previous work by Stoddart *et al.* (2009a; cf Murray *et al.* 1991) raised the possibility that local endemic high fluoride levels may have afforded some level of protection to the dentition in terms of strengthening enamel against the rigours of decay normally associated with contemporaneous prehistoric populations (Hillson 2000, 266). Alongside the relatively soft geological substrate of limestone as both an accidental and incidental dietary inclusion in food preparation, this chemical boon may be the strong point of difference for the inhabitants of Neolithic Gozo in terms of their experience of dental caries compared with others across the Mediterranean basin. Additional anecdotal evidence serving to support these serendipitous dental protection factors for the Circle burial population includes relatively frequent observations of retained mamelons on permanent dentition (Fig. 4.9a-b). Mamelons are small mounds or protuberances present on the incisal edge of any of the unworn, newly erupted maxillary or mandibular incisors (Chegini-Farahini *et al.* 2000; van Beek 1983, 129; White 2012, 106, 565, 585). They are usually three in number, following the three developmental lobes of the incisal crown (van Beek 1983: 49; White 2005: 17). Mamelons usually do not persist on adult dentition as they quickly erode to form the characteristic flat incisal edge after masticatory use (van Beek 1983, 45, 52; White 2005,: 17, 2012, 106, 585). However, they were often observed on teeth that had been in use in the mouth for some time, as evidenced either by the eruption of the neighbouring *in situ* permanent dentition within intact arcades or via observations of complete root development and/or apical closure on exfoliated elements.

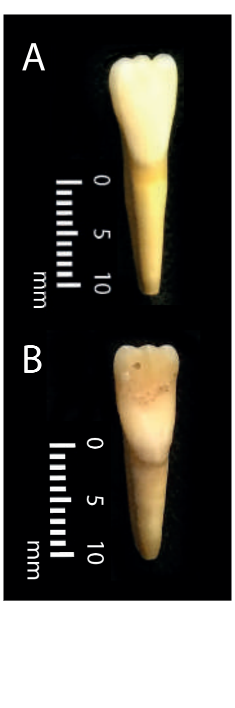

Figure 4.9. *Examples of permanent mandibular incisors presenting mamelons from Context (783) of the Circle sample. a) labial aspect of tooth from 96E/112N; b) lingual aspect of tooth from 96E/111N. Scale bar: 1 cm. (Ronika K. Power).*

Hypotheses of endemic crown strength and protection may be further tested by exploring the distribution of caries across the various locations of the dental arcade. Teeth are comprised of various surfaces, each of which has cariogenic potential, including the cutting or chewing surfaces (occlusal); the smooth surfaces of the crown, which may be in contact with neighbouring teeth from mesiodistal aspects (interproximal) or the cheek or lips (buccolingual); and the root, which may become vulnerable to cariogenesis following lesion extension from the crown, or because of exposure to oral bacteria following recession of the gingiva and alveolar bone in advanced periodontal disease (Ortner 2003, 590). While all these regions are vulnerable to dental caries, each has a particular potential which, in association with specific bacterial colonization and dietary patterns, can produce differential patterns of disease in archaeological populations (Keyes 1968; Ortner 2003).

When considering the distribution of locations of carious lesions, it is clear that the cervical region (the ‘neck’ or ‘cervix’ of the tooth, the point at which the enamel meets the dentine of the root) was most vulnerable to cariogenic activity. As presented in Table 4.3 and Figure 4.8, cervical caries account for 57.14% (Σ=104) of all caries within the sample. This is more than 4.5 times the incidence of occlusal caries (12.64% of caries; Σ=23), and almost 35 times the incidence of root caries (1.65%; Σ=3). Complex caries (those that traverse more than one location on the tooth, for example, as observed on one right maxillary first permanent molar from Context (960) that presented a cervical interproximal mesial carious lesion, which extended superiorly to become a coronal occlusal carious lesion) and obliterative caries were also observed, respectively representing 16.48% (Σ=30) and 10.99% (Σ=20) of all cariogenic teeth. It is important to note that the latter two categories would have originated in the occlusal, coronal, cervical or root zones. Moreover, it was also observed that singular teeth could feature more than one type of carious lesion. As such, the total caries location data as presented here for the former categories, should be considered as a minimum.

Interpreting the prevalence of cervical caries within the sample should be viewed in the context of preceding comments regarding the possible natural protection afforded by endemic high fluoride in the local area. Although the enamel of the crown would be fortified by elevated fluoride, the dentine of the roots does not enjoy the same benefits and is therefore vulnerable to the deleterious effects of bacterial activity associated with adhering oral plaque. As such, the prevalence of cervical caries can provide a proxy of the true quality (or indeed, poverty) of dental hygiene as experienced by the Neolithic Maltese.

Over and above considerations of the locations of caries, the question of dental hygiene may be interrogated further by considering the interfaces at which caries occurred in the sample across the dental arcade. Excluding the categories of complex, obliterative and root caries, for which an original pathological interface cannot be determined, the highest proportion of caries occurred at the interproximal surfaces (or, approximal or interstitial – the points at which neighbouring teeth in the same arcade (i.e. mandible or maxilla) come into contact Hillson 2000, 257; 2005, 214), these representing 36.26% (Σ=66) of all carious lesions. Alternatively, caries across buccolingual/labial surfaces were observed for 21.98% (Σ=40) of the carious sample. Observations of interproximal caries date back to early hominins (Caselitz 1998, 204; Grine *et al.* 1990; Hillson 2008, 128) and continue throughout human evolution and history. Research by Brothwell (1959), Corbett and Moore (1976) and Hardwick (1960; cf Mant & Roberts 2015) has demonstrated an increase in interproximal dental caries over time, and a steep increase in the incidence and prevalence of caries and indeed all dental pathology following the transition to terrestrial plant-based subsistence strategies across cultures (Caselitz 1998, 205, 209, 222; Hillson 2000, 260, 2008, 122, 128; Larsen & Kelley 1991, 2; cf Kelley, Levesque & Weidl 1991; Larsen, Shavit & Griffin 1991; as seen in regional cultural contemporaries, i.e. Boz 2005; Formicola 1987; Larsen *et al.* 2015 and Larsen *et al.* 2019; however, see also Cohen & Crane-Kramer 2007; Eshed *et al.* 2006 and Willis & Oxenham 2013 for discussion of the regional, dietary and technological specificity of these claims), while societies that had higher proportions of protein and fats in the diet generally demonstrate lower caries rates (Hillson 2000, 260, 263, 2008, 115).

Although the 'Neolithization' phenomenon must be considered for the Circle assemblage, the specific prevalence of interproximal caries among the sample may be further explained by mechanical mechanisms. In the absence of robust oral hygiene, dietary fibres lodged between the teeth following a meal can act as a breeding ground for cariogenic oral bacteria (Hillson 2005, 293), and this may especially be the case for meat fibres (for the prevalence of both plants and animal proteins in the diet of the Circle population sample (Chapter 10). Equally, the recession of the gingiva and underlying alveolar process in association with periodontal disease can inadvertently enlarge the interdental space, creating 'food traps' which can also play host to bacteria and plaque that are protected from the cleaning action of the lips, cheeks and tongue (Hillson 2008, 120; 2005: 291).

4.5.4. Hypercementosis

In contrast to dental enamel, radicular cementum remodels throughout life as a natural physiological sequela to secondary eruption (Shoor *et al.* 2014). Hypercementosis is an abnormal thickening of non-neoplastic cementum around the apices of tooth roots (Hillson 2005, 195; Ortner 2003, 607). The aetiology of this condition is not precisely known, and may be attributed to various causes, including ageing, pronounced wear, heritability, chronic inflammation secondary to pulpal or periodontal disease or caries, Paget's Disease, acromegaly, gigantism, thyroid goitre, vitamin A deficiency, supra-eruption in association with antagonist tooth loss, trauma, repair of root fracture or transplantation of teeth, rheumatic fever and arthritis (Hillson 2005: 195; Raghavan & Singh 2015; Shoor *et al.* 2014; Zhou *et al.* 2012). Hypercementosis may involve singular or multiple teeth, or may be generalized in presentation across the dentition, with a slight prevalence for predilection in the mandibular arcade (Raghavan & Singh 2015).

A total of 47 teeth in the sample were observed to present hypercementosis; this equates to 1.54% of all examined teeth. Overall, the incidence of hypercementosis is very low across the examined portion of the assemblage. The highest observed frequency was in Context (951), where 29 teeth (0.95% total teeth; 3.86% total context) presented this condition. Only six other contexts presented cases of hypercementosis, none of a magnitude greater than single figures, including (595) (Σ=1); (833) (Σ=1); (1241) (Σ=3); (1206) (Σ=4); (960) (Σ=2); (783) (Σ=7) (Fig. 4.10). When considered from a chronological perspective, the incidence of hypercementosis is greatest among the earliest interments at the Circle, with combined contexts dating to the Early period accounting for 65.96% (Σ=31) of all observations of the condition within the sample (Table 4.2; Fig. 4.11). Incidences of hypercementosis were far fewer in the Middle period (Σ=3; 6.38% of all hypercementosis); however, there appeared to be an increase in the condition during the Late use phase of the Circle (Σ=13; 27.66% of all hypercementosis).

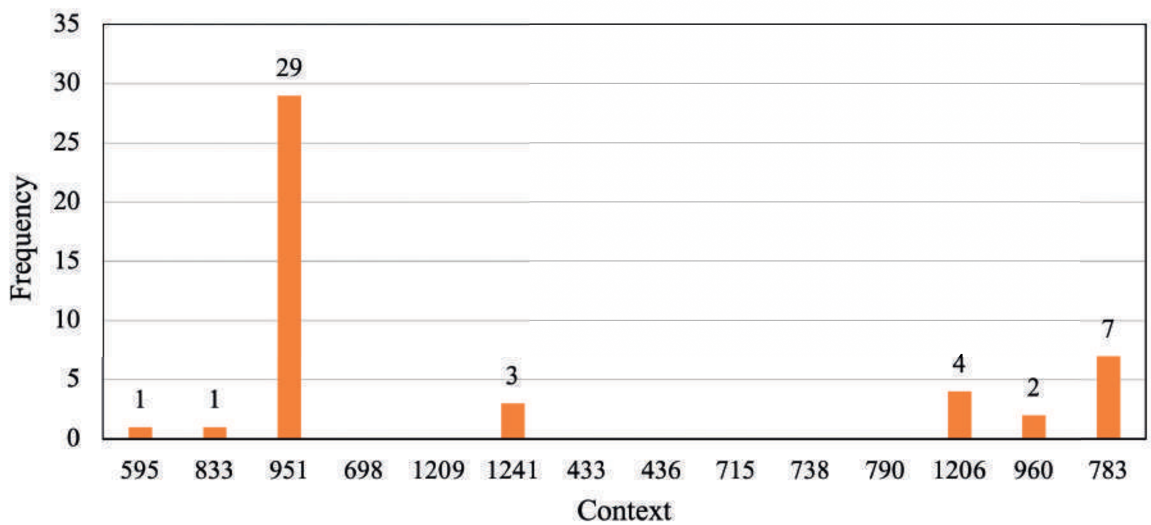

Figure 4.10. *Frequency distribution of hypercementosis observations by contexts in the Circle sample (Σ=47).*

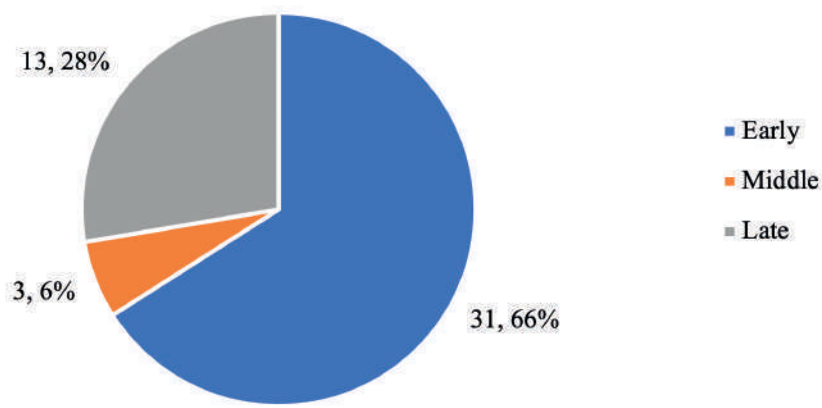

Figure 4.11. *Frequency distribution of hypercementosis observations by chronology in the Circle sample (Σ=47).*

4.5.5. Fractures: crown and root

The teeth were examined for fractures of the crown and root. Crown fractures are commonly reported in the clinical literature; however they have not received a great deal of attention in archaeological studies, certainly far less than some of the other categories of dental pathology as reported here. Comprehensive standards for recording crown fractures are absent from key instructive texts, such as Buikstra and Ubelaker (1994) and Mitchell and Brickley (2018). As such, the present study developed its own methodology for recording and reporting these lesions.

In archaeological assemblages, it is important to be able to distinguish damage done to teeth in life (*antemortem*) from that which can take place under various transformation processes after death, burial and even during excavation and recovery (*postmortem*). To determine the status of each observed fracture, each tooth was examined under a hand-lens of 10x magnification. In this study, a crown fracture is defined as any break or crack across any surface of a tooth which involved sufficient damage to remove a portion of enamel *in vivo*. Crown fracture margins and surfaces demonstrating any degree of smoothing, rounding, polishing and colour consistency were determined to be *antemortem* – these surface modifications would have taken place owing to the continued use of the tooth/teeth in the mouth following the related insult (Hillson 2000, 258; Langsjoen 1998, 410; Ortner 2003, 603). Root fractures, on the other hand, are defined by this study as any observable break, dysplasia or truncation not otherwise associated with congenital variation (such as flexion, dilaceration or dwarfism) or other pathological processes (such as hypercementosis). Root fracture margins presenting as smooth, even in texture and colour, and/or with observable secondary/tertiary dentine deposition were determined to be *antemortem* in nature. Crown and root margins and surfaces presenting as rough, irregular, powdery and inconsistent in colour were classified as *postmortem* and not included in the dataset. The recording of teeth presenting *antemortem* crown fractures included tooth type (following FDI notation) and the precise cusp location/s on which the fracture/s were observed for each tooth (following White *et al.* 2012, 105, Fig. 5.3), including observations of multiple locations on singular teeth. Likewise, for root fractures, tooth types and insult locations were recorded in detail. Results for crown and root fractures are reported separately, below.

4.5.5.1. Crown fractures

A total of 169 crown fractures were observed, representing 5.52% of the total studied sample (*Table 4.2*). In terms of chronological distribution, the majority of crown fractures were observed in the Early use-phase of the Circle, with 83 observations (2.71% of all teeth studied; 9.44% of total timeframe; 49.11% of all crown fractures) pertaining to this period (Fig. 4.12). Within this phase, the highest prevalence of incidences was attributed to Context (951), with 73 crown fractures (9.72% of total context; 43.20% of all crown fractures) emanating from this zone. Incidences during the Middle use-phase are far fewer, with only 11 observations (0.36% of all teeth; 6.32% of total timeframe; 6.51% of all crown fractures) from these contexts. A dramatic spike in crown fracture incidence took place in the Late use-phase, with 75 observations (2.45% of all teeth studied; 3.73% of total timeframe; 44.38% of all crown fractures) amongst teeth analysed from these contexts.

Clinical studies reveal that crown fractures can occur across the dental arcade for a variety of reasons, including mastication, accidental falls, interpersonal violence, using the mouth as a 'third hand' and using the teeth as tools (Bastone *et al*. 2000; Castro *et al*. 2005; Fennis *et al.* 2002; cf Lukacs 2007; for classifications of dental trauma, Andreasen 1981; Ellis & Davey 1970; Garcia-Godoy 1981; Pugliesi da Costa Feliciano & de França Caldas Jr. 2006; WHO 1978). Our study aligns with the clinical data in terms of distribution across the mouth, with crown fractures observed on the majority of tooth types, with the exception of the central maxillary and mandibular incisors (Fig. 4.13). It must be noted here, however, that there may be some cross-over between observations of crown fractures and 'chipping' on these anterior tooth types; dental modification is discussed in more detail in Chapter 5. Figure 4.13 indicates that the greatest frequency of adult crown fractures is observed on the right first maxillary permanent premolar (FDI 14) and left first permanent mandibular molar (FDI 36), sharing

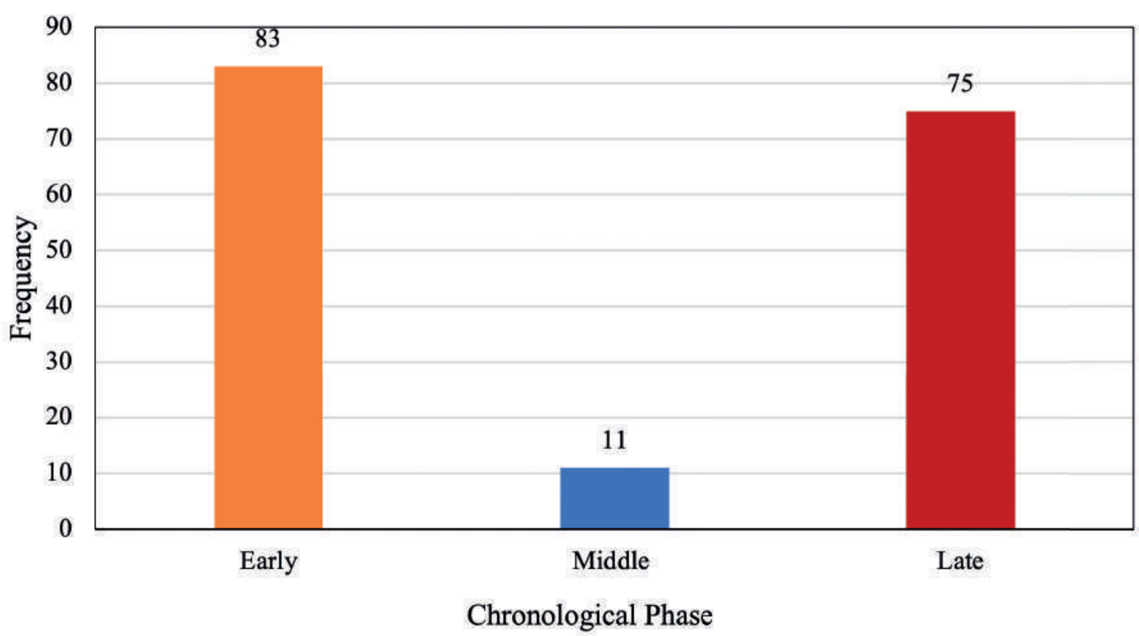

Figure 4.12. *Frequency distribution of crown fracture observations by chronology in the Circle sample (Σ=169).*

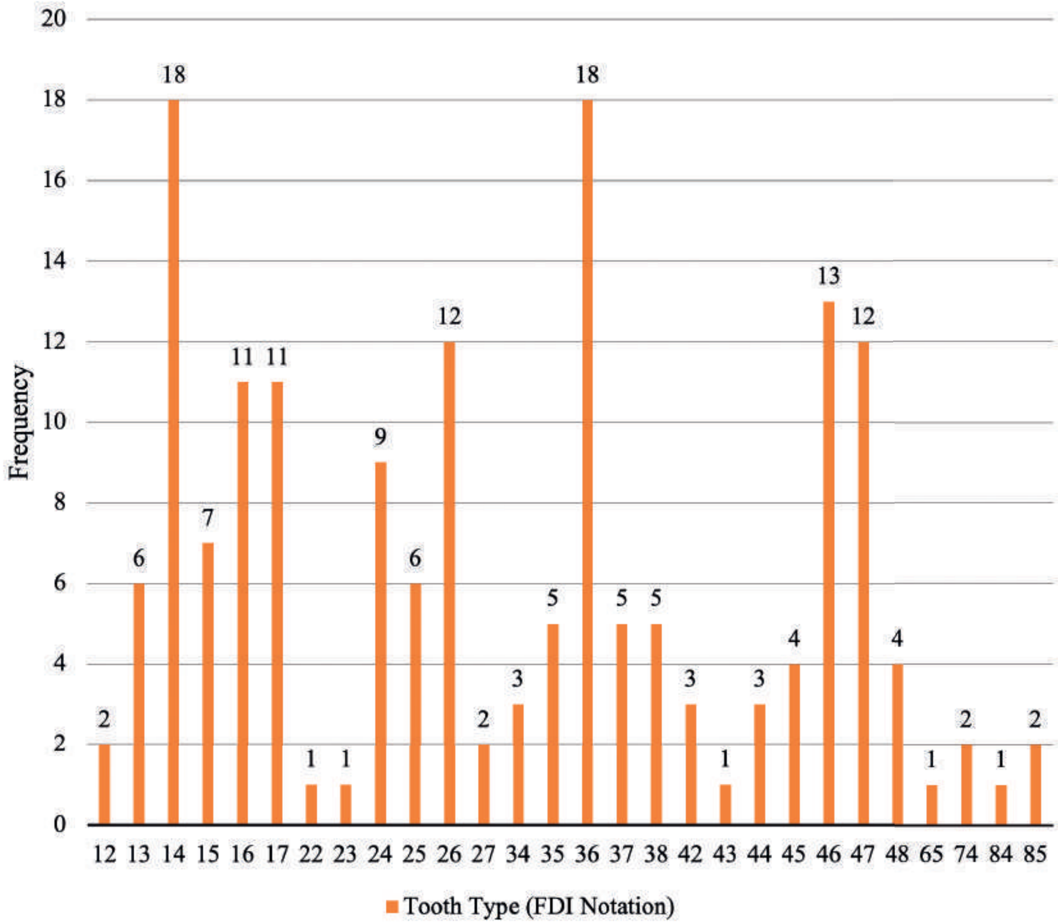

Figure 4.13. *Frequency distribution of crown fracture observations by tooth type in the Circle sample (follows FDI notations) (Σ=168).*

an incidence of 18 observations each (10.71% of all crown fractures independently; 21.43% of all crown fractures combined). Other tooth types also featuring substantial incidences of crown fractures include the right first permanent mandibular molar (FDI 46; Σ=13; 7.74% of all crown fractures), right second permanent mandibular molar (FDI 47; Σ=12; 7.14% of all crown fractures); left first permanent maxillary molar (FDI 26; Σ=12; 7.14% of all crown fractures); and the right first (FDI 16) and second (FDI 17) permanent maxillary molars (Σ=11 observations each; each accounting for 6.55% of all crown fractures).

The dynamics of this pathology as experienced across the mouth can be seen in Figure 4.14, where the predominance of the right side of the mouth and the maxillary arcade is primarily associated with adult crown fractures by a narrow margin. The pathology is observed on the right side of the adult mouth on 95 occasions (56.55% of all crown fractures), *versus* 67 observations on the left (39.88% of all crown fractures); while 86 observations are attributed to adult maxillary teeth (51.19% of all crown fractures), *versus* 76 observations across the mandibular arcade (45.24% of all crown fractures). Statistically, the observation that this pathology occurs more frequently on the right is quite significant ($\chi^2 = 4.8$, p=0.03) whereas there is no significant difference between the occurrence rate on the maxilla *versus* the mandible ($\chi^2 = 0.61$, p=0.43).

The data may be further scrutinized according to locations of fractures across the specific cusps or surfaces of affected tooth types on either side of the mouth. It is important to note here that the total number of fractured cusps is greater than the number of affected teeth, as 25 teeth had fractures to multiple cusps. As seen in Figure 4.15, the highest frequencies of fractures were observed on the premolars, with right buccal (Σ=22), left buccal (Σ=19) and right lingual (Σ=13) being most frequently fractured, followed by the incisal edge of anterior teeth (Σ=12), right entoconid (Σ=12) and right hypoconid (Σ=11) cusps

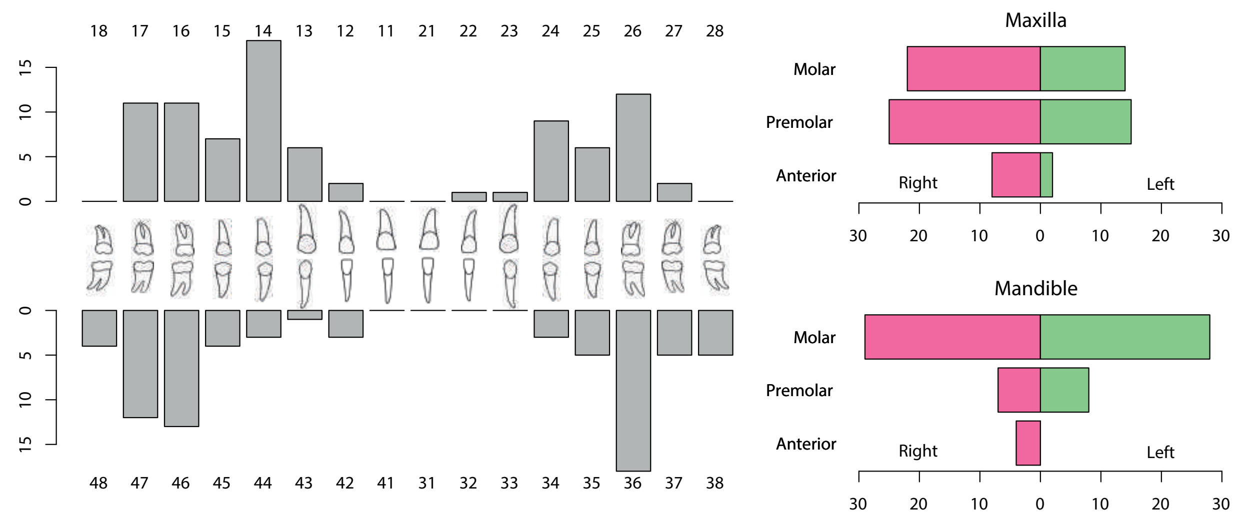

Figure 4.14. *Dynamic schema of crown fracture observations by tooth type and arcade side in the Circle sample (follows FDI notations). (Rowan McLaughlin).*

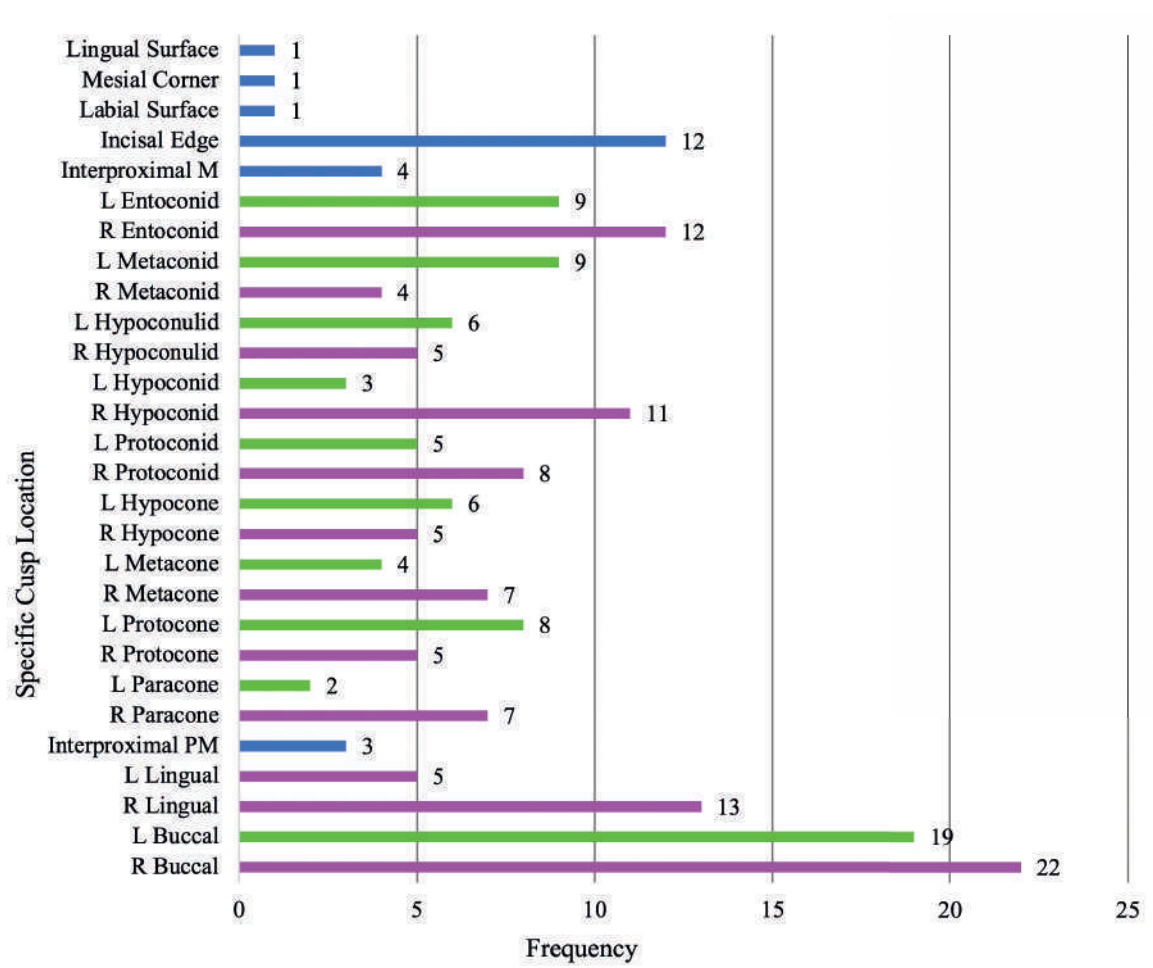

Figure 4.15. *Frequency distribution of crown fracture observations across specific cusp locations in the Circle sample (L = left; R = right; M = molar; PM = premolar).*

presenting the highest incidences. Other incidences are fewer than ten per cusp or surface.

Combining the above two approaches, we have devised a novel way to visualize these data by creating a dynamic schema which illustrates crown fracture observations by specific cusp locations by quadrant, side and surface, shown in Figure 4.16. Using principles derived from Geographical Information Systems (GIS), the 'cartography' of this pathology was mapped using Kernel Density methods. To achieve this, a generic diagram of the dental arcade (Buikstra & Ubelaker 1994, Attachment 14a) was recorded in a GIS along with the position and frequency of the fracture observations. A two-dimensional Kernel Density surface was derived from the co-ordinates of each case of crown fracture, forming a 'heat map' indicating the position along the arcade the where the pathology presented most frequently. Kernel bandwidth was optimized through trial-and-error to convey the maximum amount of information without misrepresenting the limited spatial resolution of the data. This visualization clearly demonstrates that fracture dynamics are focused in the posterior aspects of both maxillary and mandibular arcades, with the most affected tooth and surface being the buccal cusp of the right permanent maxillary first premolar, followed by the buccal cusp of the left permanent maxillary first premolar, and predominantly the lingual cusps of the right and left permanent upper and lower first and second molars.

This may be further summarized by grouping the distribution of fractures more generally by cusps or surfaces of affected tooth types without further separation according to side. When viewed this way, as in Figures 4.17 and 4.18, it is clear that the buccal cusps (cheek-side), particularly of the first premolars, are the most susceptible to fractures, with 41 observations being only slightly less than twice the number of the next-most frequent fracture site of the entoconid (distolingual cusp; Σ=21) of the mandibular molars. We then return to the lingual (tongue-side cusps) premolar cusps with the next-highest frequency of 18 fractures, followed by 14 observations on the hypoconid (distobuccal cusp) of the mandibular molars. The remaining observations across both maxillary and mandibular molars are very tightly grouped together; while observations for the anterior teeth do not exceed single figures, with the exception of the incisal edge, which was the location of 12 crown fractures within the sample.

In modern clinical studies, molars are the most common teeth to present cusp fractures (more common than premolars; Fennis *et al.* 2002); and maxillary molars are more likely to present fractures of buccal cusps, while mandibular molars are more likely to

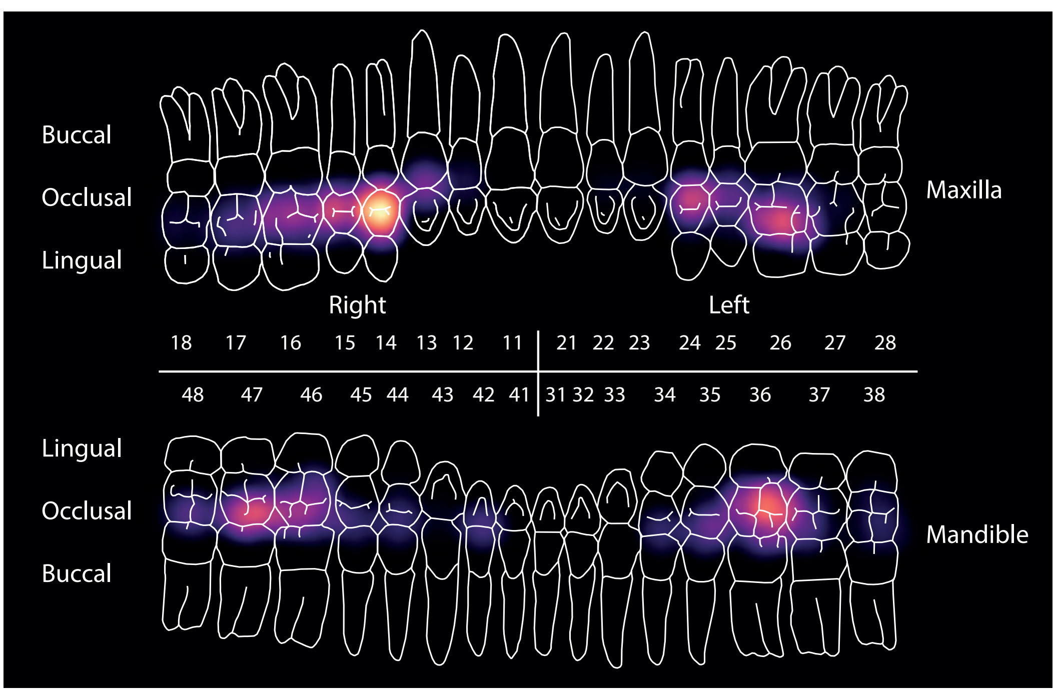

Figure 4.16. *Dynamic schema of crown fracture observations across specific cusp locations by quadrant, side and surface in the Circle sample (line drawing and layout after Buikstra & Ubelaker 1994: Chapter 5, Attachment 14a). (Rowan McLaughlin).*

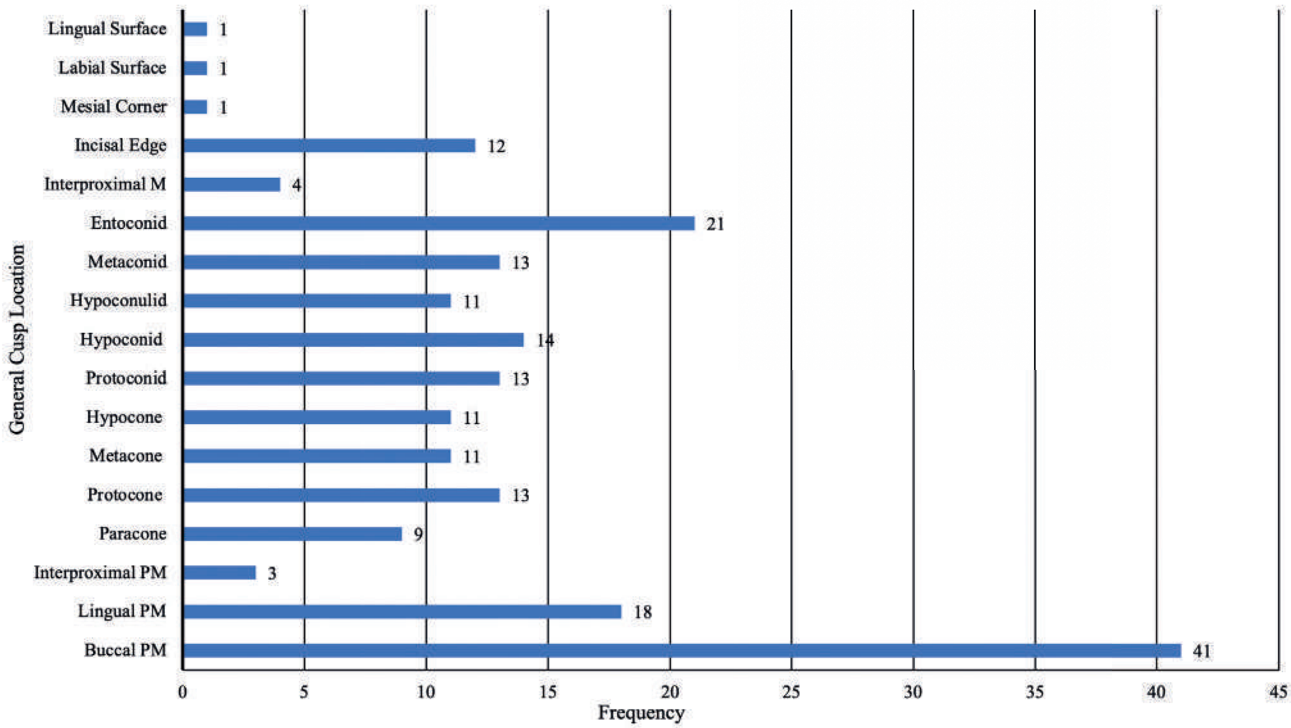

Figure 4.17. *Frequency distribution of crown fracture observations across general cusp locations in the Circle sample (M = molar; PM = premolar) (Σ=168).*

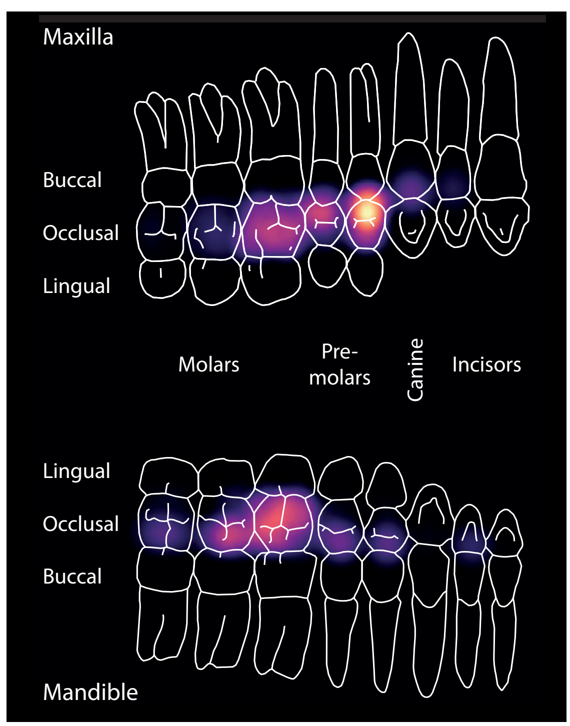

Figure 4.18. *Dynamic schema of crown fracture observations across general cusp locations by tooth type and surface in the Circle sample (line drawing and layout after Buikstra & Ubelaker 1994: Chapter 5, Attachment 14a). (Rowan McLaughlin).*

present fractures of lingual cusps. Hillson (2005, 314) also notes that the maxillary incisors are reportedly common locations for crown fractures. Although our study sample also presents a high proportion of observed fractures among the mandibular and maxillary molars (particularly the first molars), maxillary first premolars were those most susceptible to trauma amongst the Circle sample (Figs 4.15–4.18).

When considering the possible aetiologies of this pathology amongst the sample, the clinical literature suggests that trauma from parafunctional forces, excursive interferences or injury of the face or mouth would be the most likely causes for a prehistoric population, as those associated with restorative procedures, and thermal expansion and contraction of restorative materials, are irrelevant (Lubisich *et al.* 2010; cf Abou-Rass 1983; Bader *et al.* 2004; Luebke 1984; Pavone 1985; Ratcliff *et al.* 2001; Rosen 1982; cf Alexandersen 1967). Naturally, the combination of any of the previously mentioned variables increase the possibility of a coronal fracture (Ratcliff *et al.* 2001). Interestingly, clinical studies also report that coronal fractures occur more frequently in those individuals that suffer from bruxism – that is, excessive clenching or grinding of the teeth (Pavone 1985).

Although there would have been a variety of causes of crown fractures across the prehistoric Maltese population, the data presented above suggest that a combination of parafunctional forces, excursive interference and excessive grinding in mastication may have been responsible for the patterns of dental trauma described for the Circle study sample. The predominant expression of the pathology on the right side is consistent with interpretations both of right-handedness and the use of the mouth as a 'third hand' or tool (Alt & Pichler 1998: 399; Burnett 2017, 255; Molnar 2011; Pacey 2012; Volpato 2012). We propose that affected individuals in the sample were using the teeth in habitual activities outside of their most common usage, causing them to fracture in a patterned distribution (Stoddart *et al.* 2009a, 325). These activities were perhaps associated with food processing and/or consumption (for example, cracking, breaking and/or chewing hard foods); and/or processing materials other than food in association with cultural practices. The role of parafunctional activities in dental modification within the study sample will be explored further (Chapter 5).

Other factors must be considered when exploring the aetiology of crown fractures in archaeological samples. Hypoplastic enamel defects can weaken tooth crowns, thus making them more susceptible to fractures in both *ante-* and *postmortem* contexts (Hillson 2005, 286). In this study sample, there were no direct co-occurrences of enamel hypoplasia and *antemortem* fractures. Inferred from the prevalence of enamel hypoplasia, as discussed below, we would expect to have found approximately 12 cases of this co-occurrence, so this observation can be deemed to be highly significant ($\chi^2 = 12$, p=0.005) and provides evidence that people with hypoplastic defects may have avoided activities that led to crown fracture. At the very least, it appears that the aetiologies of crown fractures observed within the sample should be attributed to factors other than pathological enamel weakness. As discussed in §4.5.2, above, hypotheses regarding the beneficial effects of endemic Gozitan fluoride levels would also support this argument.

Fractures can also be associated with carious lesions, insofar as even a small crack can provide a pathway for bacteria to enter the pulp chamber (Hillson 2005, 310; Ortner 2003, 602). Apart from the case study presented in detail in §4.5.7.1, below, the relationship between these pathologies is observed within this sample, with the co-occurrence of *antemortem* crown fractures and carious lesions noted for at least 10 teeth: a left permanent mandibular second premolar (FDI 35) in Context (595); a possible right permanent maxillary third molar (FDI 18?) in Context (1206); a left permanent mandibular second molar (FDI 37) and right permanent maxillary first molar (FDI 16) in Context (783); a left permanent mandibular third molar (FDI 38) plus another 5 separate unidentifiable teeth in Context (951). These data should be seen as a minimum representation of this dynamic relationship within the Circle assemblage as it is possible that *antemortem* crown fractures may have been associated with some of the 30 obliterative carious lesions observed within the sample. Even so, the number of cases of this co-occurrence closely matches the number we would expect (11) given the prevalence rates.

Similar caveats may also extend to considerations of the links between *antemortem* crown fractures and extreme wear, which were observed to co-occur on at least 19 occasions. Even so, this is an unexpectedly high number of cases and one that is statistically significant ($\chi^2 = 9.8$, p=0.002). The cases are: a right permanent maxillary canine (FDI 13), a left permanent maxillary first premolar (FDI 25), and three left permanent maxillary first molars (FDI 26) from Context (951); a possible right permanent maxillary third molar (FDI 18?) in Context (1206) (incidentally, this tooth, also mentioned above, simultaneously features an *antemortem* crown fracture, extreme wear and a complex carious lesion); a right permanent maxillary first premolar (FDI 14), two right permanent maxillary first molars (FDI 16), and a right permanent maxillary second molar (FDI 17) from Context (1241); a right permanent maxillary first premolar (FDI 14) from Context (715); a right permanent maxillary first molar (FDI 16); a possible right permanent mandibular first molar (FDI 46?), and a left permanent maxillary first premolar (FDI 24) from Context (960); a right permanent maxillary first premolar (FDI 14), a left permanent maxillary first molar (FDI 26), a left permanent mandibular first molar (FDI 36; incidentally, this tooth simultaneously features an *antemortem* crown fracture, extreme wear and carious lesions), a right permanent maxillary first molar (FDI 18; incidentally, this tooth simultaneously features an *antemortem* crown fracture, extreme wear and a complex carious lesion), and a right permanent mandibular third molar (FDI 48) from Context (783). Once again, it is possible that there may have been further examples of related *antemortem* crown fractures and extreme wear within the study sample, with the actions of the latter potentially obfuscating incidences of the former.

Crown fractures were also observed on a small number of deciduous teeth within the sample. In total, six teeth presented this pathology, including one deciduous maxillary left second molar (FDI 65); two deciduous mandibular left first molars (FDI 74); one deciduous mandibular right first molar (FDI 84); and two deciduous mandibular right second molars (FDI 85). In the first instance (FDI 65; Context (951) [Early]), the fracture was observed to traverse multiple areas, being traced across the interproximal, buccodistal and distolingual cusps and surfaces. The first of the two affected deciduous mandibular left first molars (FDI 74; one Context (960) [Late], one Context (1206) [Late]) presented a fractured hypoconid; while the second was observed on the hypoconulid. The deciduous right mandibular first molar (FDI 84; Context (783) [Late]) featured a fractured distobuccal cusp; while the two deciduous right second molars (FDI 85; both attributed to Context (951) [Late]) presented interproximal and buccal cusp fractures, respectively. It is difficult to attribute much significance to the distribution of these fractures amongst the affected deciduous teeth considering the sample size is so small – all affected teeth derive from the distal portions of their respective arcades, and the incidences are distributed exactly evenly on both sides of the mouth. It is, however, significant to note that deciduous teeth are featured at all in this category of dental pathology, with the nature of the insults appearing to indicate that at least some children in this assemblage were participating in similar activities involving the dentition as adults. Furthermore, it is noteworthy that five out of the six incidences (83%) of deciduous crown fractures derived from contexts associated with the Late use-phase of the Circle (Fig. 4.12).

4.5.5.2. Root fractures

As with crown fractures, modern clinical studies reveal that *antemortem* root fractures can occur across the dental arcade for a variety of reasons, including excessive, heavy masticatory stress, accidental falls and interpersonal violence (Andreasen *et al*. 2012). A total of six incidences of *antemortem* root fractures were observed. This is an extremely low prevalence rate amongst the examined component of the Circle population, accounting for only 0.20% of the sample (Table 4.2). Among this handful of occurrences, two root fractures were observed in contexts associated with the Early use-phase of the Circle (0.03% total sample; 0.23% total timeframe; 33.33% total root fractures); and four root fractures were observed in Late use-phase areas (0.13% total sample; 0.20% total timeframe; 66.66% total root fractures).

The earliest example of a root fracture within the sample is observed on a child's tooth: a deciduous right maxillary first molar (FDI 53) from Context (595). This tooth presents two fractures: the first on the lingual aspect of the tooth root, extending from the superior half of the root to the apex; the second on the distal interproximal aspect, extending from the superior third of the root to the apex. Secondary dentine deposition is observed on both fracture faces. The second early example of a root fracture precipitates from Context (951) and is that of a right permanent maxillary first premolar (FDI 14). This fracture was observed on the lingual aspect, extending across two-thirds of the root to the apex. The remaining four examples of *antemortem* root fractures were all observed amongst Context (783). The first of these, a right permanent maxillary lateral incisor (FDI 12), presented a fracture on the distal aspect of the root at the approximate midpoint, which extended to the apex. The remaining three teeth all presented fractured apices, these being a right permanent maxillary first premolar (FDI 14), a left permanent maxillary second molar (FDI 27), and a left permanent mandibular central incisor (FDI 31). As the dataset of *antemortem* root fractures is extremely small, it is difficult to draw conclusions from these observations. It is nonetheless worth mentioning that five of the six cases (83.33%) of *antemortem* root fractures pertain to maxillary teeth. It is also noteworthy that a deciduous tooth is amongst the affected teeth. Although it is difficult to determine the aetiology of this insult, it is important to observe that at least some children were involved in activities that directly or indirectly placed them at risk of oral trauma, even in the earliest cultural phases associated with the Circle population.

4.5.5.3. Complicated vertical crown and root fractures

On a few occasions, fractures were observed amongst the Circle study sample that traversed the entire vertical length of individual teeth, involving the enamel, dentin, cementum and pulp chamber, effectively bisecting the affected elements (Dhawan *et al.* 2014;

cf Castro *et al.* 2005; Khasnis *et al.* 2014; Meister *et al.* 1980; Moule & Kahler 1999). These insults were determined to be *antemortem* fractures – as opposed to vertical extreme wear (described in §4.5.6.5, below) – because of the sharp and often irregular fracture margin traversing all extant surfaces of the affected tooth, accompanied by visible and palpable evidence for smoothing and/or polishing of the exposed fracture surface following retention and continued use of the tooth in the mouth *in vivo*.

The first five examples of this unusual form of dental pathology all derive from Context (783), commencing with a left (?) mandibular permanent second (?) molar (FDI 37?; Fig. 4.19a-c). The tooth is preserved in section from the crown to the apices, most likely of the buccal aspect, and features a large carious lesion occupying almost the complete internal crown space. It is possible that this lesion was caused by compromising the pulp chamber following the fracture, providing a pathway for bacteria and subsequent infection. All extant fracture surfaces are smooth, indicating that the insult took place some time before death, allowing for continued use in the mouth.

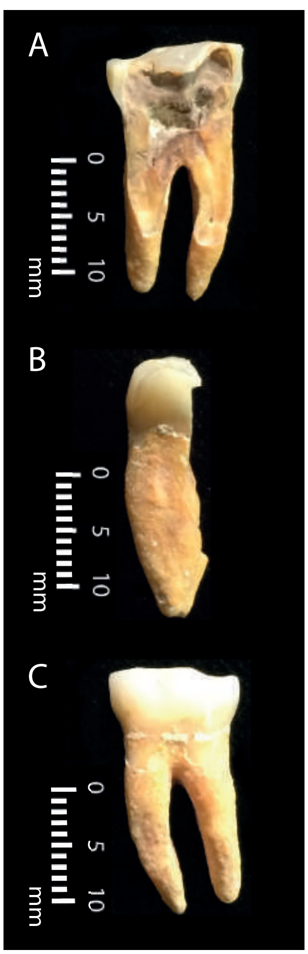

Figure 4.19. *Complicated vertical crown and root fracture of a left (?) mandibular permanent second (?) molar in a) lingual, b) distal, and c) buccal views, from Context (783) of the Circle sample. Scale bar: 1 cm. (Ronika K. Power).*

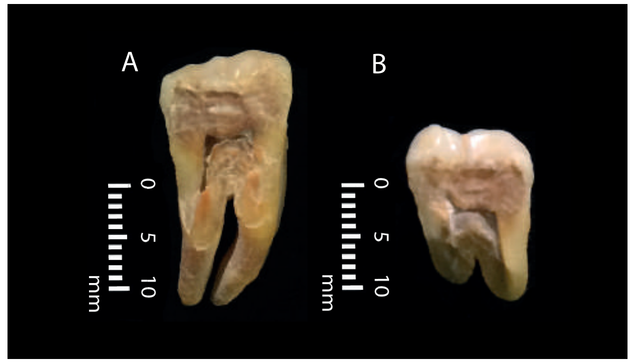

Figure 4.20. *a) Complicated vertical crown and root fracture of a right (?) mandibular permanent third (?) molar from Context (783) of the Circle sample; b) complicated vertical crown and root fracture of a right (?) mandibular permanent second (?) molar from Context (783) of the Circle sample. Scale bar: 1 cm. (Ronika K. Power).*

The second example of this phenomenon is also observed on the possible buccal aspect of a right (?) mandibular possible third permanent molar (FDI 48?; Fig. 4.20a). The fracture extends from the extant occlusal surface through to the root apices, comprising approximately two-thirds of the tooth length. All extant fracture surfaces and margins are smoothed and polished, indicating an *antemortem* insult with retention and continued masticatory use.

The third example of complicated vertical fracture also pertains to a right (?) mandibular permanent second (?) molar (FDI 47?; Fig. 4.20b). In this case, the buccal (?) aspect of the tooth also appears to be retained, however here only the fractured 'flake' is extant, comprised of the fractured portion of the crown and root, estimated to be approximately half of the tooth length. Here, we also observe smoothing and polishing of the extant fracture surfaces, indicating continued use of the tooth *in vivo* following the destructive event. For this example, it is important to note that the smoothing and polishing of the fracture 'flake' suggests that elements experiencing fractures of this nature may have retained the fragmented elements in the mouth for some time, with the respective fragments abrading each other at the fracture interface, causing the smoothing and polishing observed on all examples presented here.

The fourth example is also a right (?) mandibular permanent second (?) molar (FDI 47?; Fig. 4.21a-c). The extant fragment is comprised of the lingual aspect of the crown and approximately two-thirds of the roots at the maximum length on the mesial portion. All extant surfaces exhibit evidence for continued

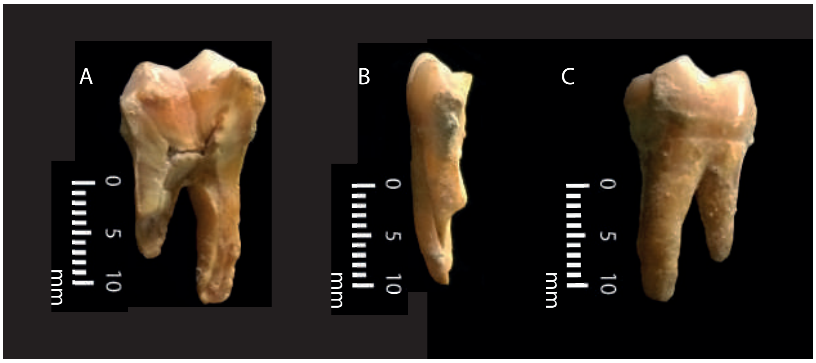

Figure 4.21. *Complicated vertical crown and root fracture of a right (?) mandibular permanent second (?) molar, showing a) buccal; b) distal; and c) lingual views, from Context (783) of the Circle. (Ronika K. Power).*

masticatory use by way of smoothing and polishing of all fracture surfaces.

The fifth example of this pathology is observed on a right (?) maxillary permanent second (?) premolar (FDI 15?; Fig. 4.22a-c). Only a portion of the heavily worn lingual cusp and a fraction of the root is retained. Here again, the fracture traverses from the occlusal surface through to the root, and the extant fragment represents approximately two-thirds of the tooth length. The majority of fracture surfaces have been smoothed and polished, again suggesting continued use in the mouth *in vivo*, however in this case there does appear to be some *postmortem* damage on one aspect of the fracture margin it, is paler in colour and chalkier in texture than the surrounding enamel and dentine. There appears to be some widening of the pulp chamber, particularly in the crown region, indicating that this tooth may also have been subject to *antemortem* infectious activity. The sixth example of a complicated vertical fracture was observed on the buccal aspect of a right mandibular permanent second premolar (FDI 45) – this example is particularly valuable for two reasons; firstly, because the tooth in question remains *in situ* in the jaw (Fig. 4.23), secondly because this is the only example in this pathology category derived from Context (960) – as mentioned above, all preceding examples derive from Context (783). The fracture extends from the occlusal surface of the tooth, through the crown and terminates at approximately two-thirds of the length of the tooth root. In this case, we can see that the terminal point of the fracture is immediately superior to the alveolar margin, the border of which appears to be intact and slightly receded indicating minor periodontal disease. The fracture surfaces and margins across the tooth

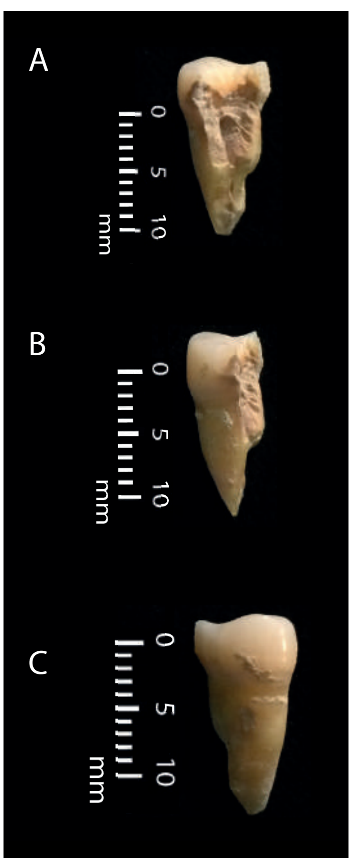

Figure 4.22. *Complicated vertical crown and root fracture of a right (?) maxillary permanent second (?) premolar, showing a) buccal; b) distal; and c) lingual views, from Context (783) of the Circle sample. Scale bar: 1 cm. (Photo Ronika K. Power).*

Figure 4.23. *Complicated vertical crown and root fracture of a right mandibular permanent second premolar from Context (960) of the Circle sample. Scale bar: 1 cm. (Photo Ronika K. Power).*

appear smooth and regular, however they are less polished than others presenting this pathology, suggesting that the insult may have happened in a relatively short time period before death, allowing a limited time for abrasion associated with continued use in the mouth. Although the pulp chamber has been compromised, there is no macroscopic evidence of an infectious reaction on any of the immediately adjacent dental tissues, or on the corresponding alveolus. Finally, it is critical to observe the highly localized nature of this insult; despite the significant force and accompanying loss of architecture demonstrated by this fracture, there is no evidence of trauma on the neighbouring dentition.

4.5.6. Extreme wear

Studies of tooth wear have long been of interest in archaeology and anthropology, particularly in light of their utility as a methodology to approach age estimation for certain geographically and temporally situated populations, and also as a means to explore and reconstruct palaeodiet (Hillson 2000, 254). Further refinements of palaeodemographic profiles of this population beyond those initially offered by Stoddart *et al.* (2009a, 315, 318–9, 320–1) are outside the scope of this study. Even if attempted, it is likely that current age-estimation methodologies based on wear studies as presented in standard texts (for example, Buikstra & Ubelaker 1994, 49ff.; Mitchell & Brickley 2018, 27; White 2005, 365ff.;) would require substantial recalibration owing to the generally low rates of attrition and abrasion observed in this population, most likely because of their fluoride-enhanced strong enamel alongside a soft local geological substrate which, when incidentally included in the diet as a by-product of food production does not enact the catastrophic wear observed on contemporaneous neighbouring regional populations for which silica (sand) is the prevailing inorganic particulate, such as Egypt (Forshaw 2009, 421, 422; Hillson 2008,: 124; Miller 2008,: 55–6).

For the present study, we were most interested in exploring incidences of extreme dental wear as these data, alongside that of all other mentioned above categories of dental pathology, might provide greatest insight into not only population health and diet, but the role of the mouth in habitual sociocultural practices. As such, only 'extreme wear' was recorded for our analyses – that is, wear that presents as the attrition of one or more cusps of the posterior teeth with accompanying dentine exposure, or substantial blunting and accompanying dentine exposure of the anterior teeth, through to complete destruction of crown architecture resulting in functional root stumps – aligning with Categories 5, 6, 7 or 8 of Buikstra and Ubelaker's (1994, Fig. 25) surface wear scoring system.

Following these parameters, the study sample was examined for the presence of extreme wear. Where observed, the individual tooth type was recorded for each affected element, alongside a detailed description of the wear location (by affected individual cusps or surfaces), orientation and extent. Where observed, the co-occurrence of extreme wear alongside other pathologies was also recorded, as detailed above. According to this methodology, a total of 74 teeth (2.42% total sample) were observed to exhibit extreme wear (Table 4.2). Overall, this is a very low incidence rate, especially considering the temporal context over which this sample extends. Comparative culturally Neolithic samples exhibit far greater incidence and prevalence rates of extreme wear than that experienced by the Circle population (Eshed *et al.* 2006; Molnar 2008; Rose & Ungar 1998). The data may be further scrutinized according to chronological incidence; when viewed in this manner, the saddle-shaped distribution observed for other dental pathologies within the sample is once again apparent (Fig. 4.24). We see 33 incidences (1.08% total sample; 3.75% total timeframe) of extreme wear in contexts associated with the Early use-phases of the Circle; followed by a sharp decline to only four incidences (0.13% total sample; 2.30% total timeframe) in the Middle use-phase; then a steep incline to 37 incidences in the Late use-phase of Circle burial activity. Within the affected sample, the distribution of extreme wear is almost equal between the Early and Late use-phases, with each presenting 44.59% and 50.00% of all observations, respectively (Fig. 4.25).

To understand better masticatory dynamics, we may examine the data for the differential experience of extreme wear across the adult dental arcade. When viewed from this perspective, the highest incidence of extreme wear is observed on the right permanent maxillary lateral incisor (FDI 12), accounting for eight examples (10.81% total extreme wear; Fig. 4.26). The second highest incidence is attributed to the left permanent maxillary first molar (FDI 26), with six examples (8.10% total extreme wear); followed by the right permanent maxillary canine (FDI 13) and right permanent maxillary first molar (FDI 16), each with five observations (6.75% total extreme wear). The right permanent maxillary central incisor (FDI 11), right permanent maxillary first premolar (FDI 14), and left permanent maxillary central incisor (FDI 21) each featured four examples (5.41% total extreme wear). All remaining observations across tooth types were of three incidences or fewer.

The dynamic experience of extreme wear across the mouth can be seen in Figure 4.27. Here, the predominance of the right side of the mouth and the maxillary arcade is clear. The pathology is observed

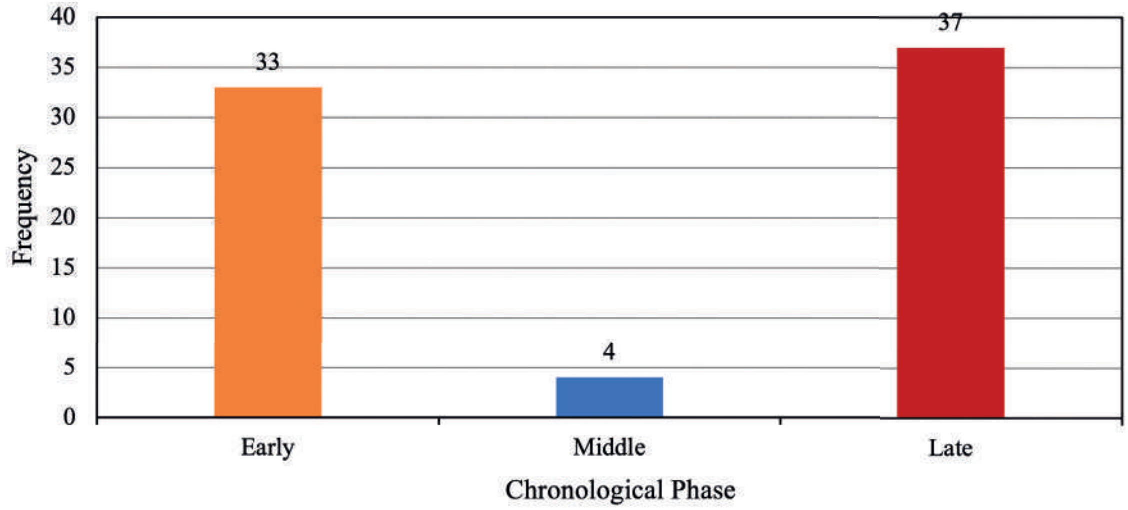

Figure 4.24. *Frequency distribution of extreme wear observations by chronological phases in the Circle sample (Σ=74).*

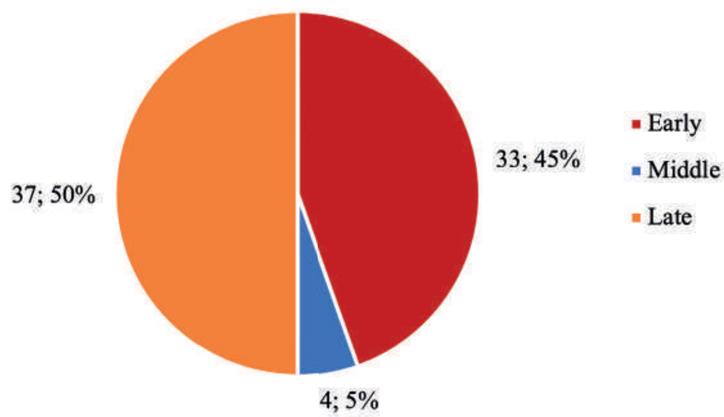

Figure 4.25. *Frequency distribution of extreme wear observations by proportion across chronological phases in the Circle sample (Σ=74).*

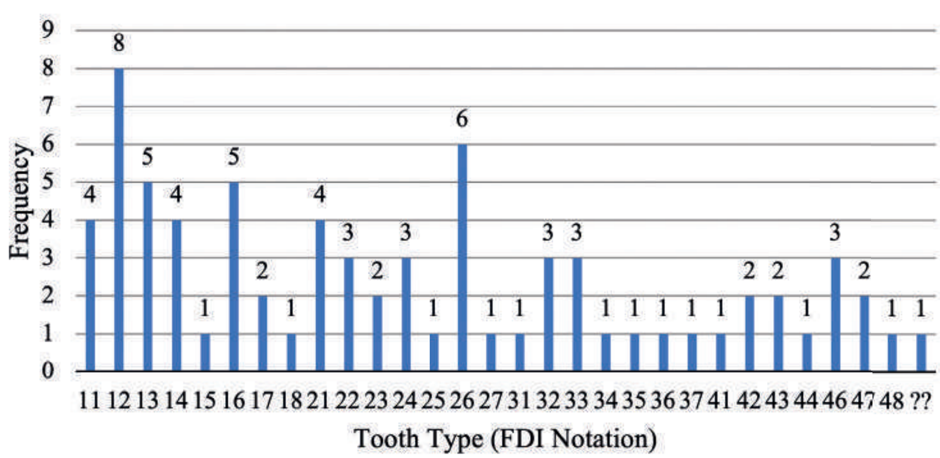

Figure 4.26. *Frequency distribution of extreme wear observations by tooth type in the Circle sample (follows FDI notations) (Σ=74).*

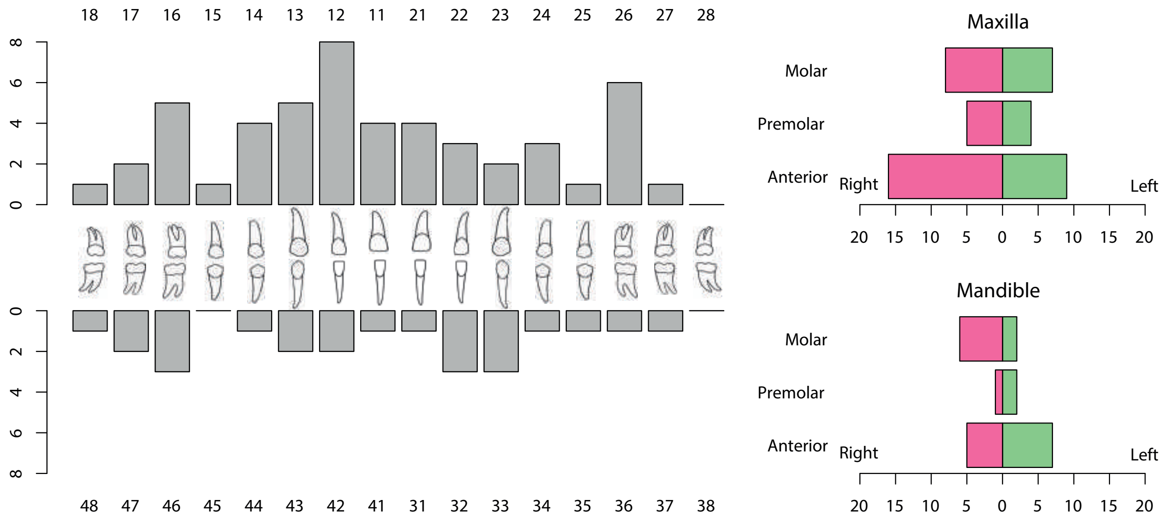

Figure 4.27. *Dynamic schema of extreme wear observations by tooth type and arcade side in the Circle sample (follows FDI notations). (Rowan McLaughlin).*

on the right side of the adult mouth on 42 occasions (56.76% total extreme wear), *versus* 31 observations on the left (41.89% total extreme wear); while 50 observations are attributed to adult maxillary teeth (67.57% total extreme wear), *versus* 23 observations across the mandibular arcade (31.08% total extreme wear). The latter of these observations is statistically significant ($\chi^2 = 10$, p=0.002).

4.5.6.1. Wear location and orientation

To understand better the aetiology of these patterns, the dataset may be further interrogated to explore the general locations and orientations of extreme wear across the Circle study sample. As displayed in Figure 4.28, it is clear that there are variable impetuses for the pronounced attrition observed on these individuals, expressed across various surfaces or locations

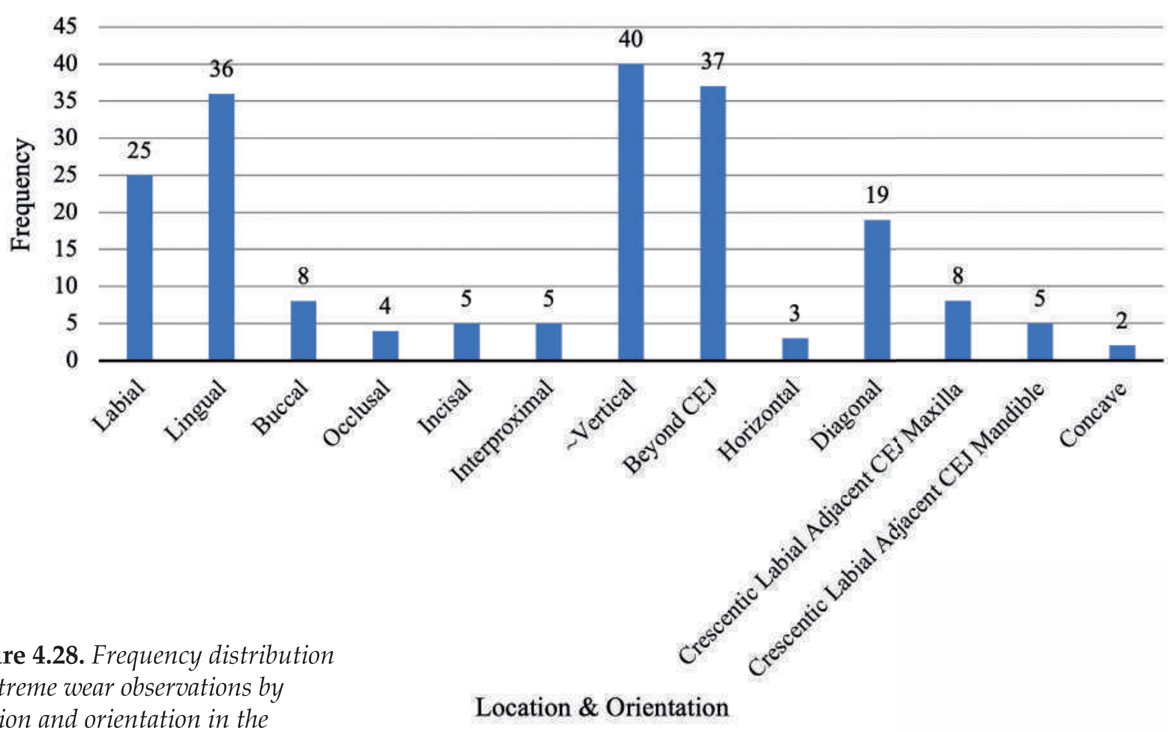

Figure 4.28. *Frequency distribution of extreme wear observations by location and orientation in the Circle sample (Σ=74).*

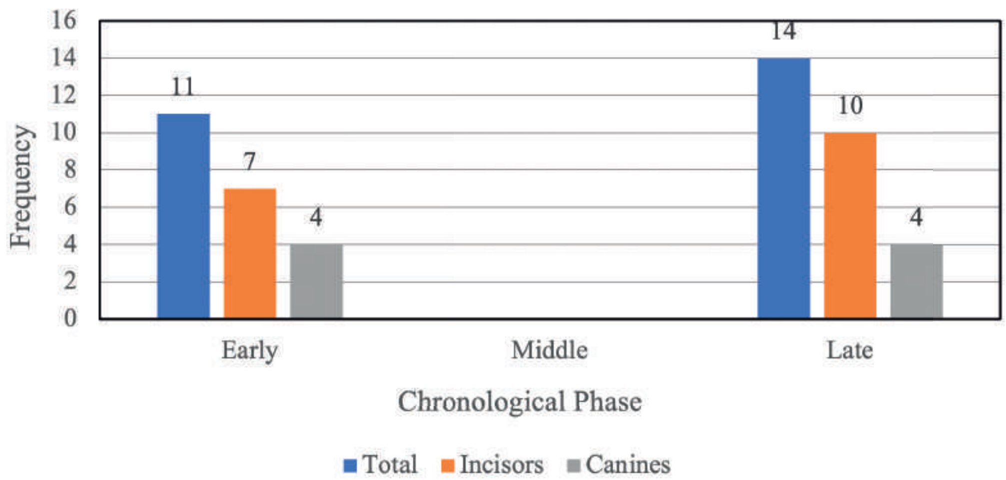

Figure 4.29. *Frequency distribution of labial extreme wear observations by chronological phases and tooth categories in the Circle sample.*

(including labial [Σ=25], lingual [Σ=36], buccal [Σ=8], occlusal [Σ=4], incisal [Σ=5], interproximal [Σ=5], beyond the cementum enamel junction [Σ=37], crescentic labial wear superior/inferior to the cementum enamel junction [Σ=11 and 2, respectively]), and orientations (including approximately vertical [Σ=40], horizontal [Σ=3], diagonal [Σ=19], concave [Σ=2]). It should be noted that the histogram observations amount to more than the affected sample number (Σ=74); this is because every tooth presents a complex wear profile of more than one affected surface and orientation. The sample mean for number of observations pertaining to affected surfaces and orientations for each tooth is $\bar{x}$ 2.70; the minimum number of observations on a single tooth is 2; the maximum is six, for a right permanent maxillary lateral incisor (FDI 12) from the earliest excavated context thus far (595), which displays an approximately diagonal wear platform that is distally inclined on the incisive edge, an approximately vertical wear platform on the lingual surface from the extant incisive edge to the cingulum, and an approximately vertical wear platform on the labial surface which extends from the extant crown beyond the cementum enamel junction onto the tooth root. For greater insights into the experience of extreme wear, the data are characterized according to the predominant locations and orientations below.

4.5.6.2. Labial extreme wear

Observations of labial wear are restricted to the lip-surface of the anterior teeth, of which there were 25 examples among the dataset (0.82% total sample; 33.78% total extreme wear). As presented in Figure 4.29, a total of 11 examples were identified in the sub-sample dating to the Early use-phase of the Circle (0.36% total sample; 1.25% total timeframe; 14.86% total extreme wear), comprising seven incisors and four canines. There were no examples of labial extreme wear amongst the Middle use-phase subset of the study sample. The highest incidence of labial extreme wear was attributed to the Late use-phase component of the sample, with 14 incidences overall (0.45% total sample; 0.70% total timeframe; 18.91% extreme wear).

4.5.6.3. Lingual extreme wear

Lingual wear may be experienced anywhere on the tongue-surface of the teeth across the maxillary and mandibular arcades. This more inclusive definition may be one of the factors contributing to the higher incidence among the study sample. A total of 36 examples of lingual wear were observed (1.18% total sample; 48.65% total extreme wear). Figure 4.30 reveals that the experience of extreme lingual wear was similar between the Early and Late use-phases of the Circle, with a total of 16 examples emerging from each of these timeframes. For the Early use-phase, this represents 0.52% of the total sample; 1.82% of the total timeframe; and 21.62% of total extreme wear. In this Early period, extreme lingual wear was observed on six incisors, three canines, one premolar and six molars. For the Late use-phase, the 16 examples amount to 0.52% of the total sample; 0.79% of the total timeframe; and 21.62% of extreme wear. For the Middle use-phase sample subset, there were only four observations of lingual extreme wear (0.13% total sample; 2.30% total timeframe; 5.41% total extreme wear), pertaining to one premolar and three molars.

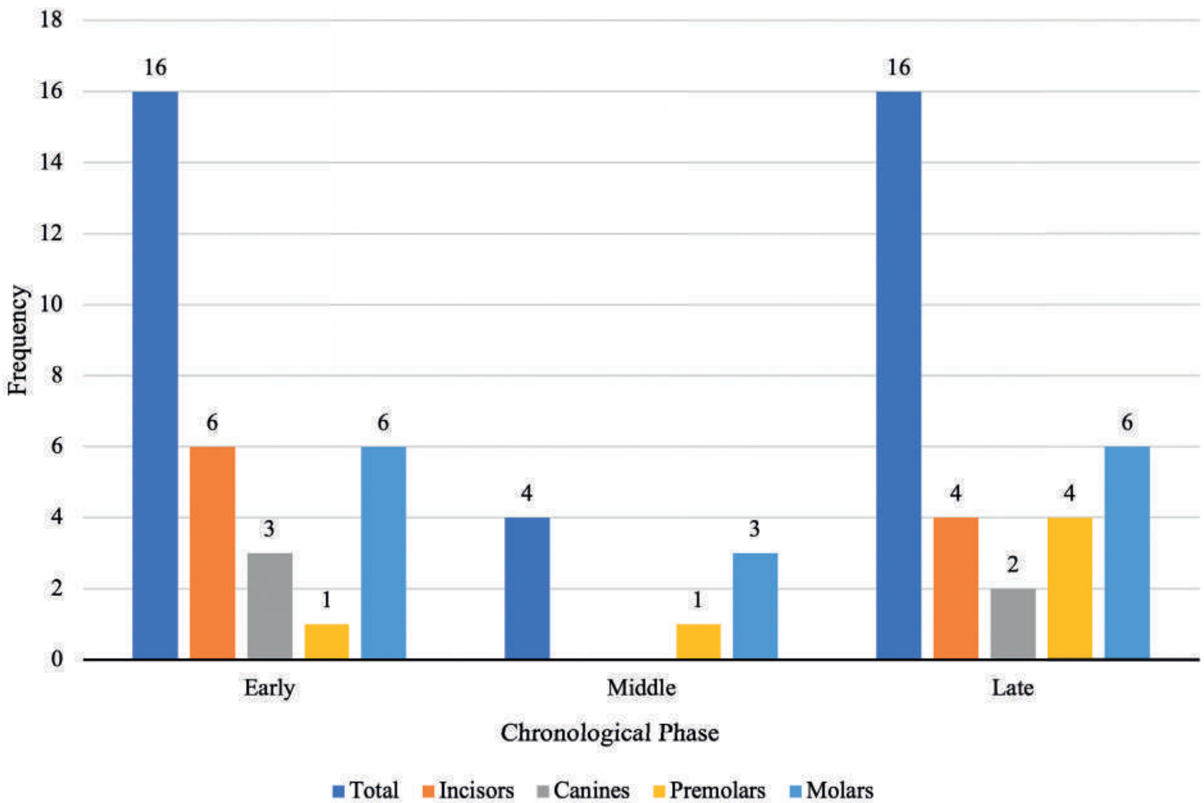

Figure 4.30. *Frequency distribution of lingual extreme wear observations by chronological phases and tooth categories in the Circle sample.*

4.5.6.4. Diagonal extreme wear

For the purposes of this study, diagonal extreme wear is classified as any wear fulfilling the established definition of extreme wear occurring across a diagonal wear platform on any tooth surface across the arcade. In total, there were 19 teeth presenting this wear type within the study sample (0.62% total sample; 25.68% total extreme wear). As seen in Figure 4.31, as with the expression of lingual extreme wear, the representation of this phenomenon was similar across the Early and Late use-phase subsets of the Circle sample, with each period presenting nine examples. For the Early use-phase, this equates to 0.29% of the total sample; 1.02% of the total timeframe; and 12.16% of total extreme wear, expressed across one incisor, one canine, three premolars and four molars. For the Late use-phase, the nine observations amount to 0.29% of the total sample; 0.45% of the total timeframe; and 12.16% of total extreme wear, in this case presented on four incisors, one premolar and four molars. For the Middle use-phase, there was only one observation of diagonal extreme wear on a molar (0.03% total sample; 0.57% total timeframe; 1.35% total extreme wear).

4.5.6.5. Approximately vertical extreme wear

An unusual form of wear was observed amongst the Circle study sample, in the form of an approximately vertical platform on any tooth surface within the mouth, separate to the labial or lingual wear described in §4.5.6.2 and §4.5.6.3, above. To be classified as extreme wear it also needed to fulfil the criteria established in §4.5.6. A total of 40 examples of approximately vertical extreme wear were observed amongst the study sample, establishing this form of wear as the most common amongst the extreme wear manifestations (Fig. 4.32; 1.31% total sample; 54.05% total extreme wear). The highest frequency of approximately vertical extreme wear was observed within the Early use-phase, with 21 occurrences amongst this material (0.69% total sample; 2.39% total timeframe; 28.38% total extreme wear). Teeth presenting this wear-type in this period included 12 incisors, six canines and three molars. In alignment with trends seen across the study sample, the incidence of approximately vertical extreme wear appears to have diminished in the population associated with the Middle use-phase Circle deposits, with only three examples observed within this sample subset (0.10% total sample; 1.72% total timeframe; 4.05% total extreme wear), including one premolar and two molars. The sample trend continues to be reflected amongst this wear-type, as we again witness a rise in incidence in the Late use-phase sample. This amounts to 16 examples of approximately vertical extreme wear (0.52% total sample; 0.78% total timeframe; 21.62% total extreme wear), expressed on two incisors, four canines, three premolars and seven molars.

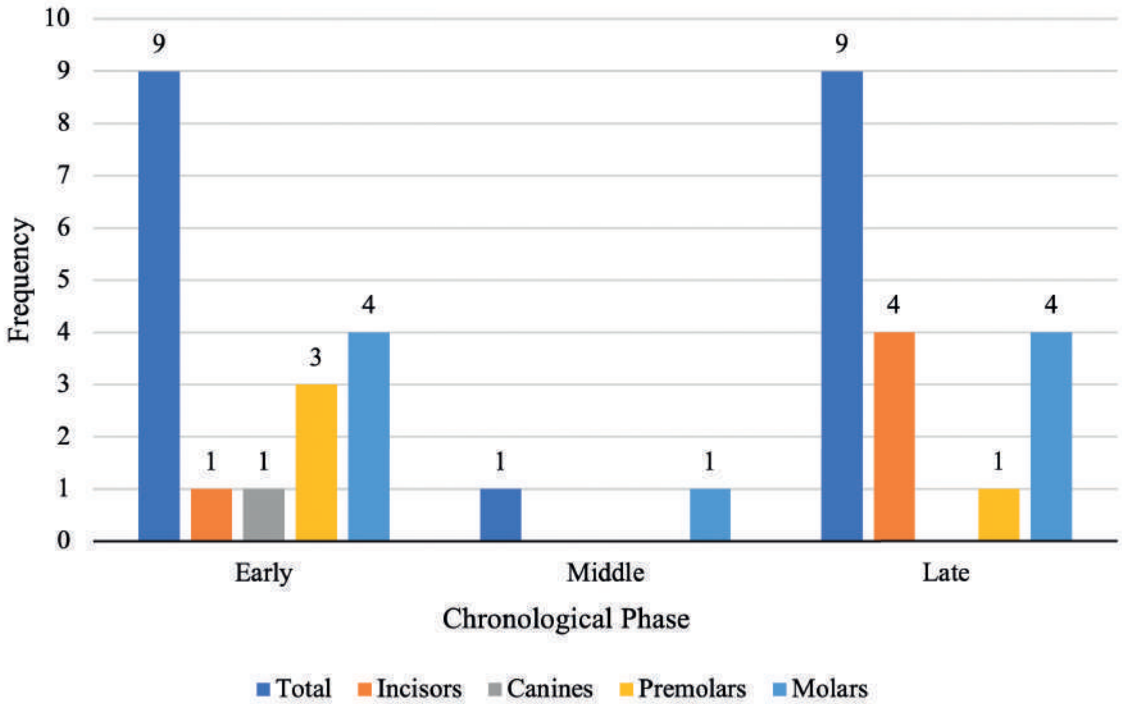

Figure 4.31. *Frequency distribution of extreme diagonal wear observations by chronological phases and tooth categories in the Circle sample.*

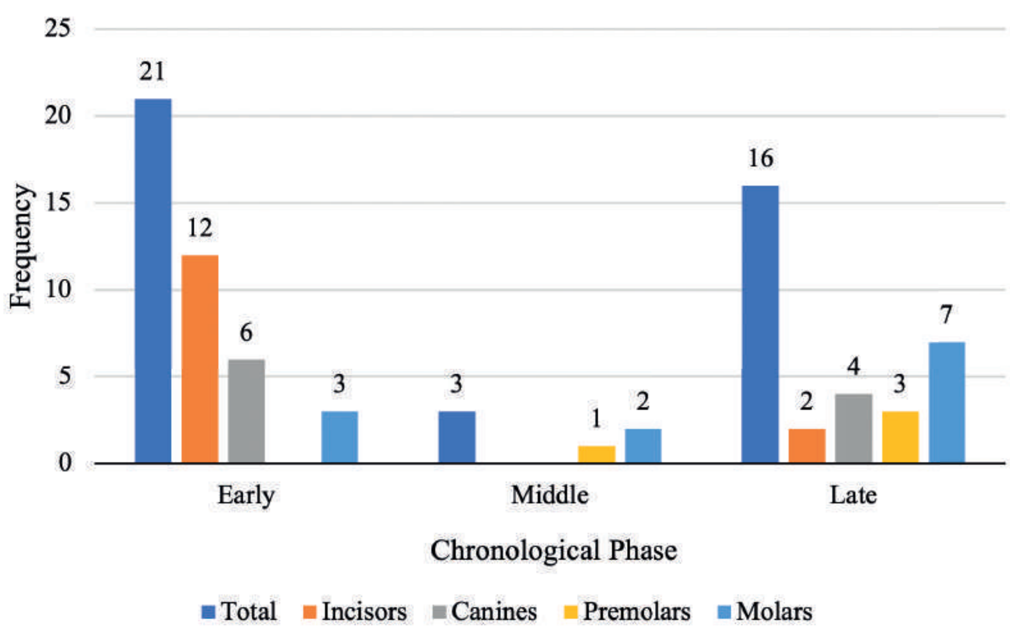

Figure 4.32. *Frequency distribution of extreme approximately vertical wear observations by chronological phases and tooth categories in the Circle sample.*

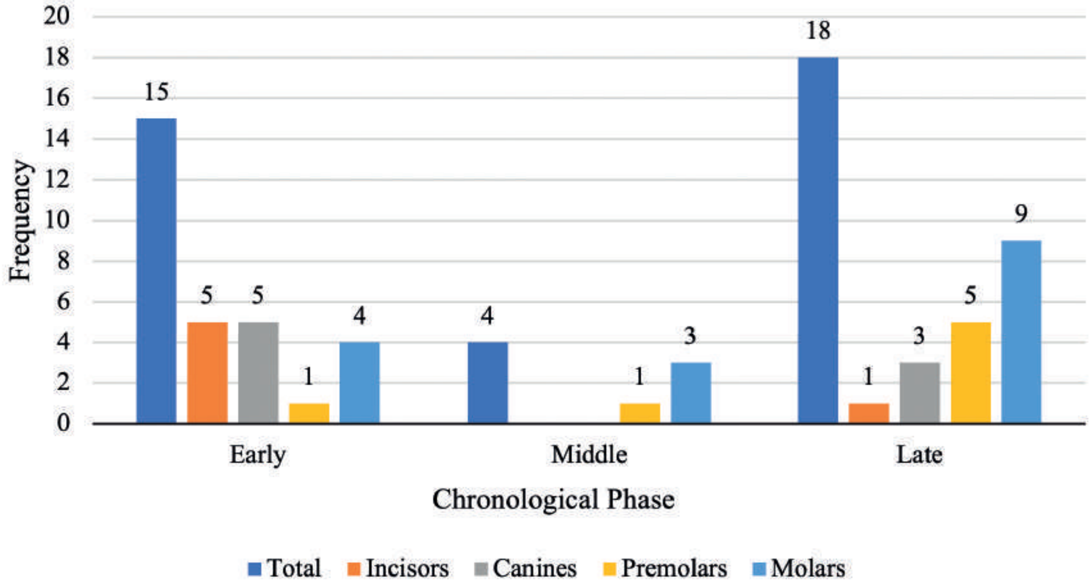

Figure 4.33. *Frequency distribution of extreme wear beyond the cementum enamel junction observations by chronological phases and tooth categories in the Circle sample.*

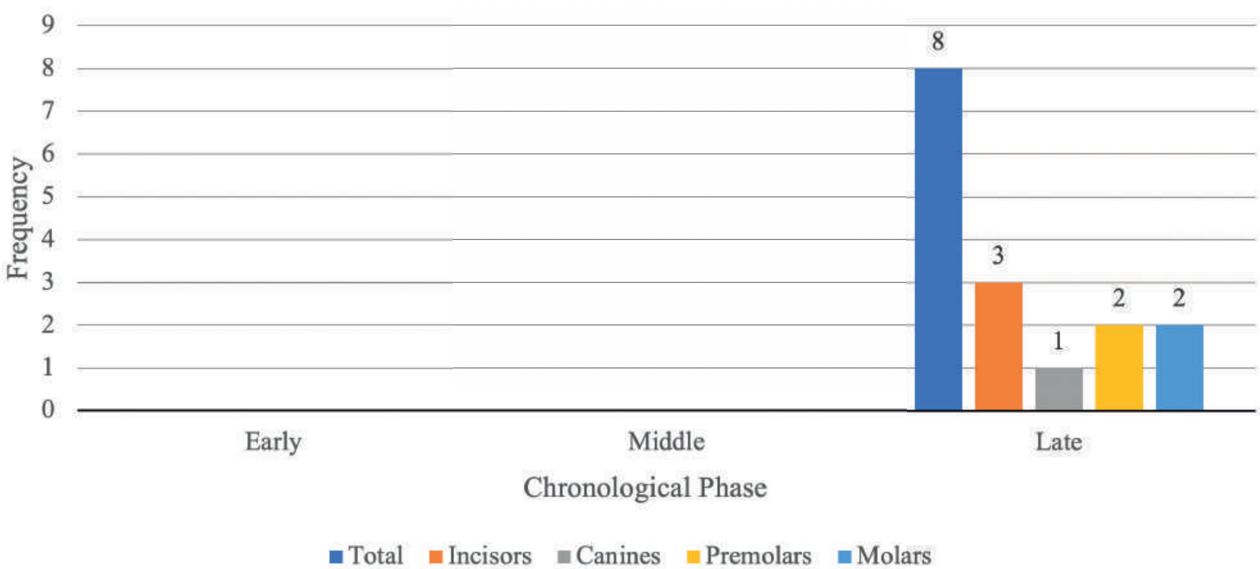

Figure 4.34. *Frequency distribution of maxillary labial crescentic wear adjacent to the cementum enamel junction observations by chronological phases and tooth categories in the Circle sample.*

4.5.6.6. Wear extending beyond the cementum enamel junction

Another wear category emerging from the Circle population was attrition extending from the tooth crown, across the cementum enamel junction and onto the tooth root. Here again, this wear phenomenon could be observed on any tooth type, surface or orientation, and needed to align with the extreme wear criteria established in §4.5.6, above. There were 37 examples of extreme wear extending beyond the cementum enamel junction within the study sample (Figure 4.33; 1.21% total sample; 50% total extreme wear), only marginally fewer than the approximately vertical wear category described in §4.5.6.5, above. In this case, the majority of the examples precipitate from the Late use-phase population of the Circle, with 18 teeth presenting this wear phenomenon (0.59% total sample; 0.90% total timeframe; 24.32% total extreme wear), including one

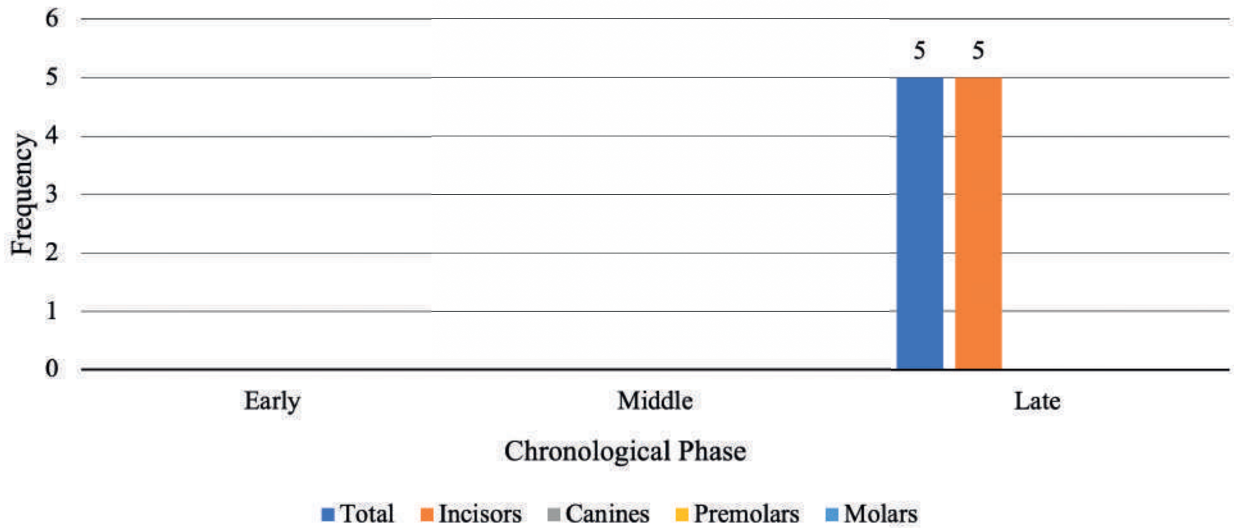

Figure 4.35. *Frequency distribution of mandibular labial crescentic wear adjacent to the cementum enamel junction observations by chronological phases and tooth categories in the Circle sample.*

incisor, three canines, five premolars and nine molars. The Early use-phase sample featured only slightly fewer examples, with 15 incidences of extreme wear extending beyond the cementum enamel junction (0.49% total sample; 1.71% total timeframe; 20.27% total extreme wear), observed on five incisors, five canines, one premolar and four molars. There were only four examples of this wear category in the Middle use-phase material (0.13% total sample; 2.30% total timeframe; 5.41% total extreme wear).

4.5.6.7. Crescentic labial wear at cementum enamel junction

An enigmatic wear signature was observed on a small number of teeth, presented here owing to the significance of their potential aetiology. The wear presents as a discreet crescent-shaped erosion, adjacent to the cementum enamel junction of maxillary (Σ=8) and mandibular teeth (Σ=5; Figs 4.34 & 4.35) on either the labial or buccal surfaces. In both arcades, the wear was either restricted to the enamel or extended onto the tooth root. It is critical to note here that all 13 examples of crescentic wear exclusively pertain to the Late use-phase of the Circle sub-sample, from contexts (1206), (960) and (783). In terms of the distribution of this wear phenomena across the mouth, the maxillary incidences were observed on three incisors, one canine, two premolars and two molars (Fig. 4.34). For the mandible, all five incidences feature on incisors (Fig. 4.35). It is also important to note that five of the teeth presenting this wear phenomenon were observed in occlusion in an intact maxillary arcade (hence, from a single individual; Fig. 4.36a-b), with the insult aligning

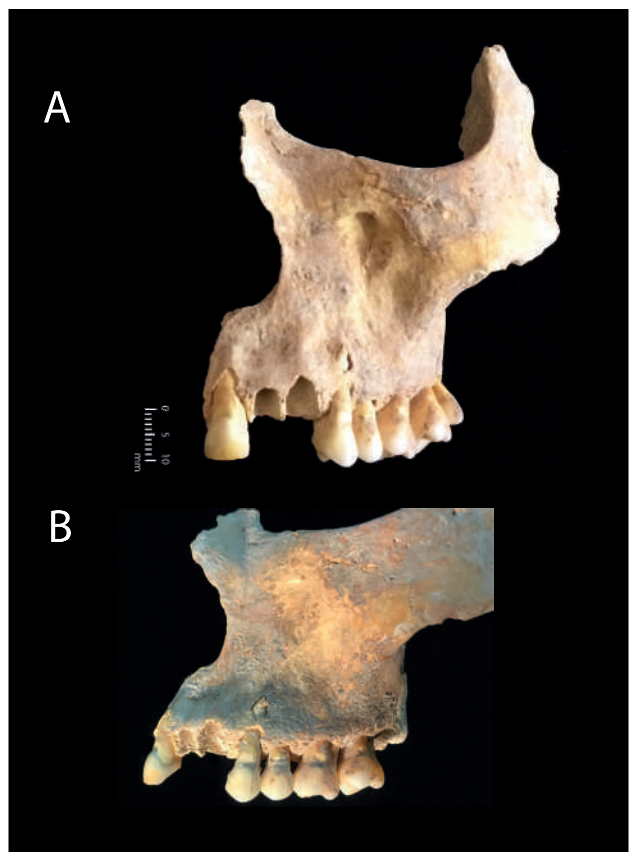

Figure 4.36. *Intact adult left maxillary arcade featuring a)* in situ *dentition, presenting b) labial/buccal crescentic wear adjacent to the cementum enamel junction from Context (960) of the Circle sample. Scale bar: 1 cm. (Photo Ronika K. Power).*

across the retained teeth (right maxillary permanent lateral incisor (FDI 12), left maxillary permanent central incisor (FDI 21), first premolar (FDI 24), first molar (FDI 26) and second molar (FDI 27); observed in Context (960). On another occasion, a left maxillary permanent canine (FDI 23) exhibited dental modification (chipping of the occlusal edge) and a carious lesion on the root superior to the crescentic-wear type described here (observed in Context (783)).

It is proposed that these particular observations may be attributed to abrasion, a mode of wear that occurs when the dentition come into contact with objects other than their neighbouring or opposing teeth, such as pipes, labrets and cleaning implements such as picks, sticks or brushes (Alt & Pichler 1998, Table 1, 404; Hillson 2000, 257). The crescent-shaped wear observed adjacent to the cementum enamel junction bears striking resemblance to the abrasion patterns described for modern teeth, associated with the overzealous use of toothbrushes (Pindborg 1970). In the absence of further analyses (especially scanning electron microscopy) it is not possible to determine precisely what implement(s) may have produced these wear patterns. It is nonetheless suggested that these phenomena were caused by the persistent and vigorous application of an object to the labial and/or buccal surfaces of the affected teeth, possibly in an attempt to practice a rudimentary form of oral hygiene. The use of vegetal matter such as miswack sticks, a twig of the salvadora persica tree, has been described in both archaeological and ethnographic populations for the purposes of teeth-cleaning (Alt & Pichler 1998, 404; Forshaw 2009, 423; cf Al-Otaibi *et al.* 2003).

From an archaeological perspective, the challenge of definitive identification of the use of such implements involves a complex of context, identification and preservation bias. Personal hygiene items such as miswack sticks do not appear to have been deliberately included amongst the funerary assemblages of individuals across cultures; and perhaps even if they were they would be difficult to identify as 'artefacts' by most field archaeologists as their appearance does not differ from any other humble twig and would require specialist archaeobotanical analysis. Moreover, even if they hypothetically were included and identifiable, as organic material they are unlikely to be preserved in many burial environments, therefore remaining archaeologically invisible.

From an ethnographic perspective, the use of vegetal matter for teeth-cleaning is noted in modern Malta. Dalli (2016) writes that migrants from Africa, the Arabian Peninsula, India and central and southeast Asia commonly use miswack sticks in their countries of origin; however, in the absence of the miswack tree in Malta, some were using twigs from the extremely common yet highly toxic oleander tree instead, with disastrous results. Dalli reports that oleander is one of the most poisonous plants in Malta, and even incidental ingestion as a result of tooth-brushing or picking can lead to a variety of symptoms, ranging from moderate to severe or even fatal. The movement of people, materials, objects and ideas into and out of the Maltese archipelago has long been a subject of discussion (for example, Malone & Stoddart 2004; Barone *et al.* 2015; Maniscalco 1989; Tanasi 2014), and the current volume contributes new data to this discourse via dental anthropology and isotopic analyses (Chapters 6 & 10), while Volume 2, Chapter 11 contributed new evidence on chert. Although these particular wear patterns are uncommon and enigmatic amongst the Circle study sample, they must nonetheless be considered as another piece of potential evidence that places Neolithic Malta within a wide regional network.

4.5.6.8. Wear location by individual cusp: specific

To explore further the dynamics of extreme wear, the study sample was assessed to determine the specific location of extreme wear across the cusps and surfaces of the adult arcade. As seen in Figure 4.37, the labial aspect of anterior teeth was the most frequently observed site for extreme wear within the sample, with 25 examples. This is followed by the lingual surface of the permanent anterior teeth, which presented 16 examples of extreme wear. The predominance of wear dynamics towards the front of the mouth is further indicated by seven examples of extreme wear on the incisal/occlusal surface of the anterior teeth, alongside the protocone of the right maxillary permanent molars which also presented seven examples. The remaining citable examples include the buccal aspect of the left premolars (Σ=6); the protocone of the left maxillary permanent molars (Σ=5); and the hypocone of the right maxillary permanent molars (Σ=4). All remaining incidences feature ≤3 examples. Here again, it is important to note that the number of affected surfaces is greater than the number of affected elements, as 20 teeth within the study sample featured extreme wear on more than one cusp or surface.

When these observations are visualized as a dynamic schema showing extreme wear by specific cusp locations across quadrants, sides and surfaces (Fig. 4.38), the focal areas of pathology are easily discernible. This visualization reveals that the experience of extreme wear was relatively evenly distributed across the labial and lingual aspects of the bilateral maxillary anterior teeth (permanent central and lateral incisors and canines; FDI 11–13, 21–22), the labial aspects of the mandibular anterior teeth (particularly the permanent

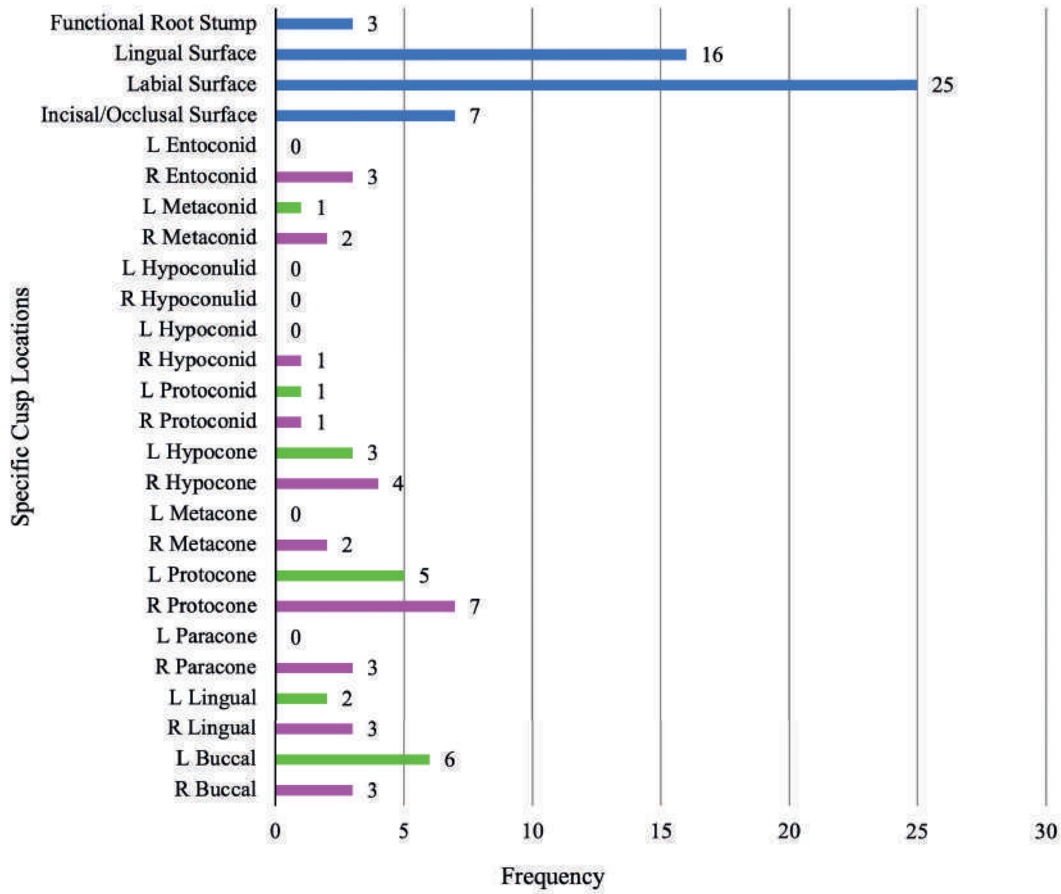

Figure 4.37. *Frequency distribution of extreme wear observations across specific cusp locations in the Circle sample (L = left; R = right).*

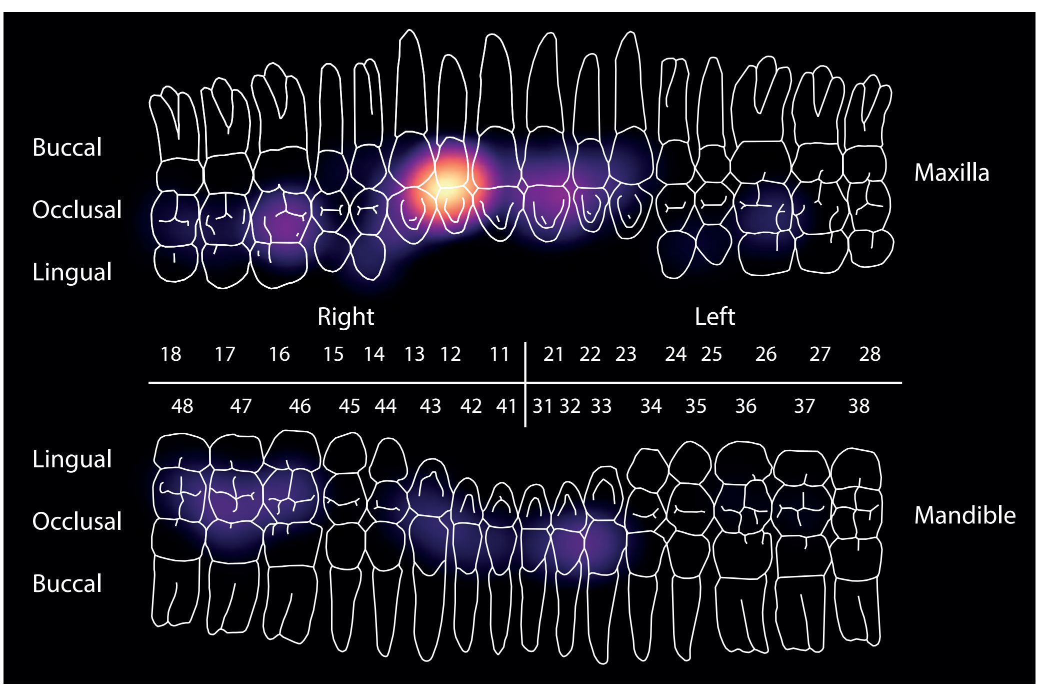

Figure 4.38. *Dynamic schema of extreme wear observations across specific cusp locations by tooth type and surface in the Circle sample (line drawing and layout after Buikstra & Ubelaker 1994: Chapter 5, Attachment 14a). (Rowan McLaughlin).*

left lateral incisor and canine; FDI 32–33), the occlusal surfaces of the right permanent maxillary first molar (FDI 16) and right permanent mandibular first and second molars (FDI 46–47). The portion of the mouth presenting the most intense experience of extreme wear is the right permanent maxillary anterior complex of the labial, incisal and lingual aspects of the right central and lateral incisors and canine (FDI 11–13). With the exception of a slight flare of extreme wear on the occlusal surface of the left permanent maxillary first molar (FDI 26), note the relative absence of this pathology on the left upper and lower distal dentition.

4.5.6.9. Wear location by individual cusp: general

The extreme wear data may also be presented in more general terms by cusps or surfaces of affected tooth types without further separation according to side, as seen in Figures 4.39 and 4.40. Here, similar results emerge, with the labial, incisal and lingual surfaces of the permanent maxillary anterior teeth remaining as the predominant areas of attrition and/or abrasion, presenting 25 and 16 examples, respectively. When viewed this way, it is important to note the relative absence of extreme wear to the permanent mandibular central incisor, and to the lingual aspects of all mandibular anterior teeth (central and lateral incisors and canine). The protocone of the permanent maxillary molars was the next most common site (Σ=12); followed by the buccal surface of the permanent premolars (Σ=9); the incisal/occlusal surfaces of the permanent anterior teeth (Σ=7); the hypocone of the permanent maxillary molars; and the lingual aspect of the permanent premolars (Σ=5). All remaining incidences amounted to three or fewer examples.

The extreme wear patterns observed for the occlusal surfaces of upper and lower bilateral permanent first molars are consistent for those generally observed in both clinical and archaeological populations (Hillson 2005: 218). As might be expected, the earliest erupting teeth are those most likely to experience wear, considering their prolonged use in mastication and/or other parafunctional activities. The first permanent molars of both mandibular and maxillary arcades are generally used as a bellwether for the expected expression of wear within individual mouths and more broadly across a population, so much so that attrition indices have been developed to standardize wear expression as a proportion of that observed on the first permanent molar (Hinton 1981, 1982; Lunt 1978; Molnar 1971; Murphy 1959a, 1959b). From this perspective, the extreme wear patterns described for the Circle study sample are worthy of further attention.

As described for crown fractures (§4.5.5.1 above), the predominant expression of extreme wear on the right maxillary anterior teeth complex is consistent with interpretations both of right-handedness and the use of the mouth as a third-hand or tool across the study sample (Molnar 2011; Pacey 2012; Volpato 2012).

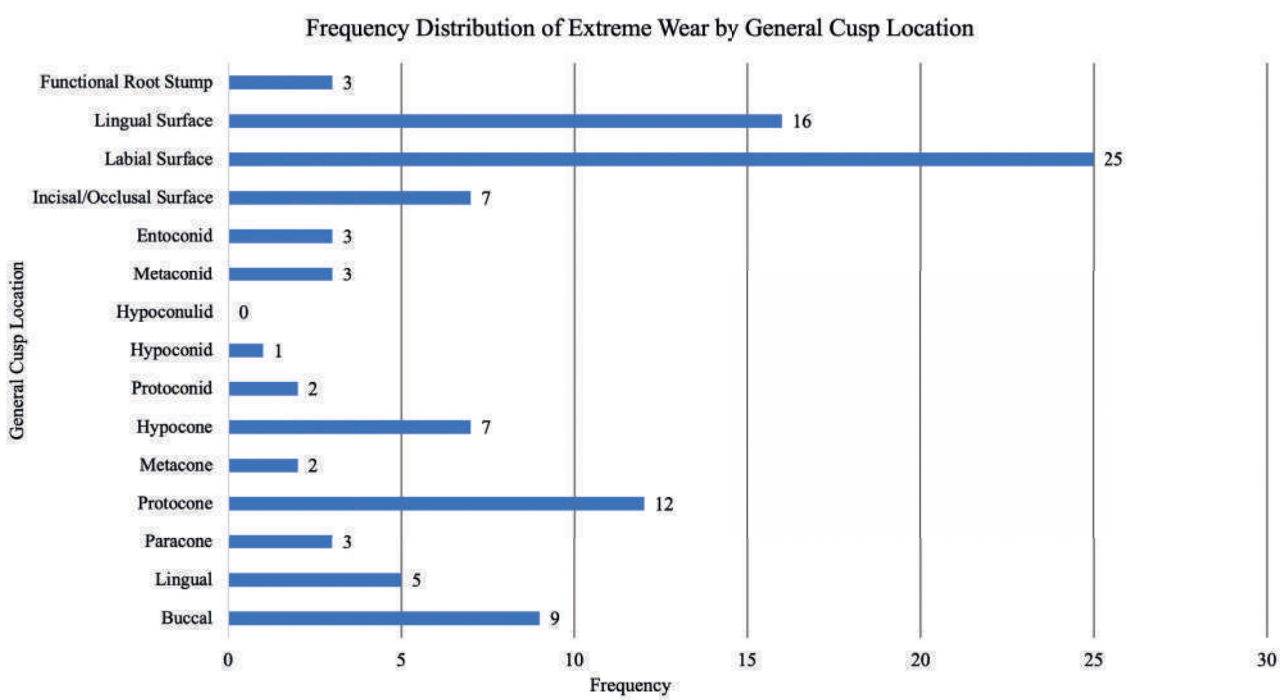

Figure 4.39. *Frequency distribution of extreme wear observations across general cusp locations in the Circle sample.*

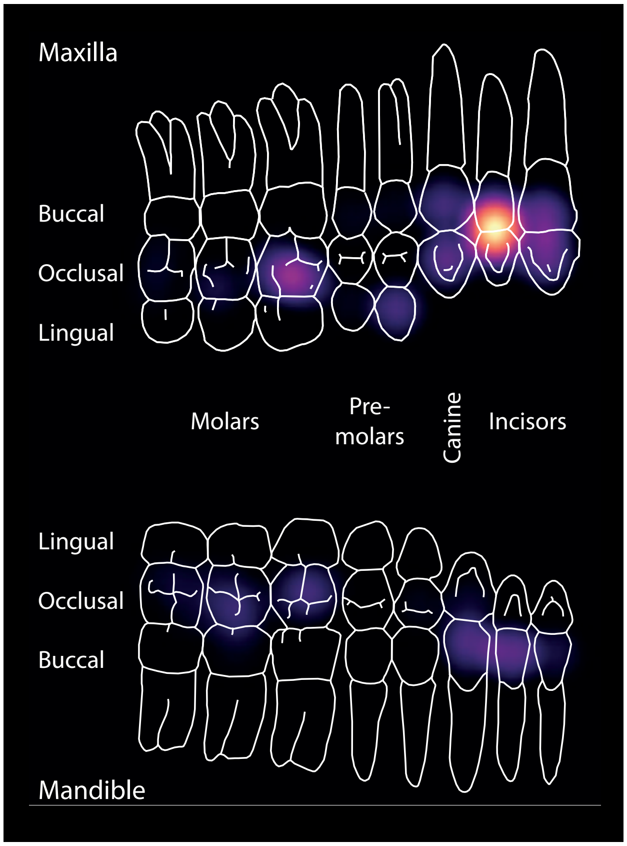

Figure 4.40. *Dynamic schema of extreme wear observations across general cusp locations by tooth type and surface in the Circle sample (line drawing and layout after Buikstra & Ubelaker 1994: Chapter 5, Attachment 14a). (Rowan McLaughlin).*

Supporting the interpretations offered for crown fractures, we further propose that affected individuals in the sample were using their teeth in habitual activities outside of their most common usage, causing them to wear in a similarly patterned distribution (Stoddart *et al.* 2009a, 325). As discussed above, these activities were perhaps associated with food processing and/or consumption, and/or processing materials other than food in association with cultural practices. Particularly considering the pattern of observations across the sample, the role of parafunctional activities in dental modification will be explored further in Chapter 5.

4.5.6.10. Gross crown loss

On 10 occasions amongst the sample, teeth were worn to the point that only fractions of the crown were extant; three of these examples present only functional roots stumps. Four teeth were observed to have approximately half of their crowns eroded by the processes of extreme wear. Amongst the earlier use-phases of the Circle in Context (951), a left permanent maxillary central incisor (FDI 21), was observed to present almost vertical concave erosion on the lingual surface from incisal margin to cingulum, leaving approximately half of the crown extant. In the Later use-phase of Context (960), another left permanent maxillary central incisor (FDI 21) presented approximately diagonal wear on the lingual surface from the incisal edge to a point just inferior to the cementum enamel junction, leaving approximately half the crown extant. Labial wear was also observed on this tooth in the area immediately superior to the cementum enamel junction, forming a slight concavity in the dentine (§4.5.6.7, above). In the latest use-phase of the Circle, two teeth recovered from Context (783) were observed to retain only half-crowns; the first was a right permanent maxillary central incisor (FDI 12) presenting an approximately horizontal wear platform across the incisal surface; the second was a left permanent maxillary central incisor (FDI 21), on which an approximately diagonal, mesially inclined, wear platform was observed across the incisal margin, leaving approximately half of the crown extant. Pronounced labial wear was also observed on this tooth, having smoothed and removed almost all extant enamel; with additional lingual wear also appearing to have eroded all enamel to a point beyond the cingulum, just inferior to the cementum enamel junction.

Three of the teeth within the sample were observed to be worn to the extent that only one-third of the crown remained. Two of these teeth were identified within the Early use-phase of Context (951): the first being a right permanent central maxillary incisor (FDI 11), the second was a right permanent maxillary lateral incisor (FDI 12). For both teeth, not only did the tooth crowns display the loss of approximately two-thirds of their height, they also presented labial wear that extended vertically across the extant surface beyond the cementum enamel junction onto the root. The other tooth within this wear category was observed in the Late use-phase Context (783): another right permanent maxillary lateral incisor (FDI 12). This tooth exhibited approximately diagonal wear which was inclined towards the lingual aspect and eroded approximately two-thirds of the crown.

As noted above for *antemortem* crown fractures, there is the possibility of cross-over between the aetiologies and quantifications of extreme wear cases such as those described here and dental modification. Indeed, alterations to the labial and incisal profiles particularly of the anterior dentition may be attributed to active and/or passive processes with identical physical and aesthetic affect(s). It is also possible that modifications to the teeth caused by habitual behaviour (so-called 'passive' modifications; Alt & Pichler 1998, 388; Milner & Larsen 1991, 357; Scott 1991, 798) may have produced specific identity-markers held as significant within a cultural group. These issues will be discussed in greater detail in Chapter 5.

Functional root stumps were also observed on three occasions, in which the tooth crowns had been obliterated *in vivo* through processes associated with extreme wear, carious lesions, *antemortem* crown fractures and/or combinations of these phenomena. The root stumps in these cases were still of functional use in the mouth prior to death, evident through wear (smoothing, glossing, rounding) of the extant occlusal surfaces. The earliest incidence was identified in the remains pertaining to Context (951), one of the Early use-phases of the Circle. This tooth was a right permanent maxillary lateral incisor (FDI 12), the crown of which was obliterated beyond the cementum enamel junction. The remaining two incidences within this wear category precipitate from one of the Late use-phases of the Circle, Context (1206), and were identified to belong to the same individual. The teeth were a left permanent mandibular second molar (FDI 37) and a right permanent mandibular first molar (FDI 46), both of which exhibited steeply inclined approximately vertical lingual wear platforms, extending from the most superior extant portion of their functional root stumps (inferior to the cementum enamel junction) to approximately half of the extant roots.

4.5.6.11. Co-occurrence of extreme wear and other pathologies

The mouth is a site of dynamic forces and processes, and as such any observed pathologies must be considered in concert with one another. The present study has already highlighted the co-occurrence of extreme wear and *antemortem* crown fractures for at least 19 teeth within the sample (§4.5.5.1, above). Extreme wear is also often associated with carious lesions, as exposure of the pulp chamber creates a vulnerability for the entry of bacteria (Hillson 2005, 293). Considering the relatively low overall incidence of both extreme wear and carious lesions within the sample, it is somewhat expected that we will also observe few examples where the two phenomena co-occur. Notwithstanding this awareness, it is surprising to encounter only three teeth featuring both extreme wear and a carious lesion. The first example is a right permanent maxillary second premolar (FDI 15) from the Late use-phase Context (960), which exhibits a vertical wear platform on the buccal aspect extending from the crown to beyond the cementum enamel junction. The remaining two examples feature three cooccurring pathological phenomena: extreme wear, carious lesions and *antemortem* fractures. The first is a possible right permanent maxillary first molar (FDI 18?) from the Late use-phase Context (1206), which features a distal steeply inclined diagonal-vertical wear platform across the hypocone-metacone, extending from the *antemortem* fracture margins to beyond the cementum enamel junction for the hypocone and a complex carious lesion extending across cervical interproximal buccal zones. The second is a left permanent mandibular first molar (FDI 36), which presents a carious lesion as well as an approximately vertical wear platform across the metaconid-protoconid, extending from the *antemortem* crown fracture margins to beyond the cementum enamel junction onto the tooth root. From a statistical perspective, by considering general prevalence of other pathologies, the low co-occurrence of extreme wear and caries is not significant (expected cases 5, $\chi^2 = 0.5$, p=0.5) whereas the co-occurrences with crown fracture, as discussed above (§4.5.5.1), is significant.

4.5.6.12. Deciduous wear/modification

Although they may not strictly align with the definition of extreme wear presented for adult dentition in §4.5.6, it is important to note that seven deciduous teeth within the study sample presented evidence for distinctive wear – significantly, all of them derived from Context (783), which dates to the latest of the Late use-phase contexts from the Circle *c.* 2350 cal. BC (Σ=7; 0.23% total sample; 0.35% total timeframe). It is also noteworthy that five of the seven deciduous teeth under discussion were canines; four of these were maxillary and one from the mandibular arcade. Some of the incidences of wear described here may also be considered as candidates for possible dental modification; this will be integrated into further discussions in Chapter 5.

There were two examples of wear observed on right deciduous maxillary dentition; in both cases, deciduous canines (FDI 53), and in both cases, the insults were observed to be steeply sloping diagonal wear in a superodistal orientation. There were three examples of wear observed on left deciduous maxillary dentition; a left central incisor (FDI 61) presenting steeply sloping diagonal wear in a superodistal orientation; and two left canines (FDI 63) one presenting a heavily worn cusp with the wear platform extending slightly onto the labial surface; the other also featured steeply sloping diagonal wear in a superodistal orientation. The remaining two examples of deciduous wear were observed on left mandibular dentition; the first, a lateral incisor (FDI 72) presenting chipping of the incisal margin on the distal third, with the facet extending onto the labial surface; the second, on a canine (FDI 73) featuring a crescent-shaped facet on the distal aspect of the occlusal surface. For the latter example, it should be noted that three teeth identified as belonging to the same individual also presented hypoplastic defects (FDI 53, 63, 74).

4.5.7. Additional observations: case studies

Population-based reporting is deservedly the focus of bioarchaeological analyses, however it remains important to present case studies to bring sharp focus to the lived experiences of 'real people' in the studies of archaeological assemblages. It is particularly important to do so in populations such as the Circle, where many might assume that the levels of fragmentation and commingling would render such testimonies inaccessible. With this in mind, we approach the categories of therapeutic intervention, dental calculus, eruption or alignment variation, and congenital variation by way of case studies to attest to their presence amongst the study sample.

4.5.7.1. Therapeutic intervention

Although they were not recovered from any of the contexts included in the study sample, an individual identified amongst the remains excavated from Context (897) is important to feature here. A fragment of an adult left mandible (Fig. 4.41a & b) was initially examined macroscopically in the National Museum of Archaeology, Valetta, and was later subject to further analysis via micro-CT-scanning. The CT-scans were captured by L.T. Buck in the Cambridge Biotomography Centre, according to the procedure outlined in §4.4, above.

Both macroscopic and radiological analyses confirm that the element has been subjected to *postmortem* breakage at both its anterior and posterior aspects. The anterior fragmentation margin is located just beyond the symphyseal line on the lateral aspect of the right side of the mental trigone. The mental spines remain intact on the lingual surface. The posterior fragmentation margin is situated on the distal aspect of the left corpus; here, the fracture transects the element at the base of the ascending ramus so that the superior portion of the element (including the coronoid process, mandibular notch and mandibular condyle) are absent. An additional *postmortem* break has fractured the gonial angle, which is also absent. The only retained teeth are the first and second left permanent mandibular molars (FDI 36 and 37).

The mental trigone is present and is observed to be quite gracile and without lateral bossing/flaring (Buikstra & Ubelaker 1994, 20, Fig. 4). The mandibular corpus is also gracile in terms of both thickness (maximum width 10.0 mm) and height (maximum 26.5 mm) and tends towards a parabolic shape. What remains of the oblique line at the base of the ascending ramus appears to be extending from the corpus at an

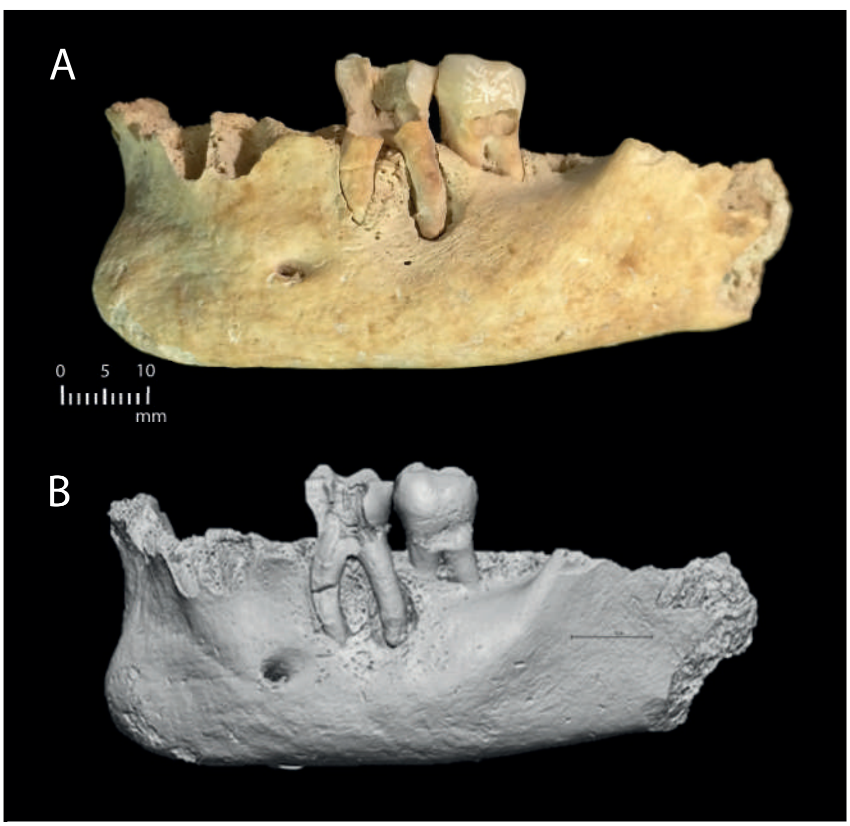

Figure 4.41. *a) Fragment of adult left mandibular corpus and retained first and second left permanent mandibular molars (FDI 36 and 37) from Context (897) of the Circle sample; b) 3D render of Context (897) mandibular corpus fragment. Scale bar: 1 cm. (Photo Ronika K. Power; radiological images captured by L.T. Buck, Cambridge Biotomography Centre; processed by J. Magnussen & M. Pardey, Macquarie Medical Imaging).*

angle exceeding 90° and there does not appear to be any bossing or flaring at the gonial angle. The retained teeth are fully erupted and the occlusal wear indicates that they were in use in the mouth. As a result of the obliteration of the buccal wall of the alveolus of the first molar, caused by associated infectious processes (described below), the apices of the root are observed to be closed on the first permanent left molar and are also determined as closed on the left permanent second molar via x-ray. Although the third left permanent molar is not retained, the alveolus is intact and appears to have sustained an adult tooth. Furthermore, a patent interproximal contact facet is observed on the distal aspect of the neighbouring second left permanent mandibular molar, indicating that the third molar had fully erupted. In consideration of all these factors, it is suggested that this fragment is derived from an adult, possible female individual.

The retained teeth present mild occlusal wear. The wear platform is focused on the superior aspect of the crowns of both teeth, and takes an approximately horizontal aspect, running mesiodistally along the central fissure. Crown morphology is generally well-preserved for both teeth, although very small amounts of dentine exposure are noted on the hypoconulid and entoconulid of the first molar (FDI 36), not exceeding 1.1 mm Ø.

There are slight extant calculus deposits on both retained teeth. For the left first permanent mandibular molar (FDI 36), the calculus deposit is located on the lingual aspect at the cementum enamel junction and traverses from the mesial margin through to the distal interproximal space, with the highest concentration observed in the distal region. There is a very small calculus deposit observed on the left second permanent mandibular molar (FDI 37), again located at the cementum enamel junction on the most distolingual aspect of the tooth.

Where intact, it is observed that there is some resorption of the alveolar process in the region of the first to third left permanent mandibular molars. The alveolar process appears to have resorbed by approximately 30%, exposing the superior portion of the roots of the retained teeth. Diffuse microporosity (<1.0 mm Ø) is observed around the extant margins of the alveolar process of the retained teeth, as well as that of the third left mandibular permanent molar. These observations are consistent with periodontal disease.

Severe carious lesions are observed on both retained teeth (Fig. 4.42a & b). Although the lesion

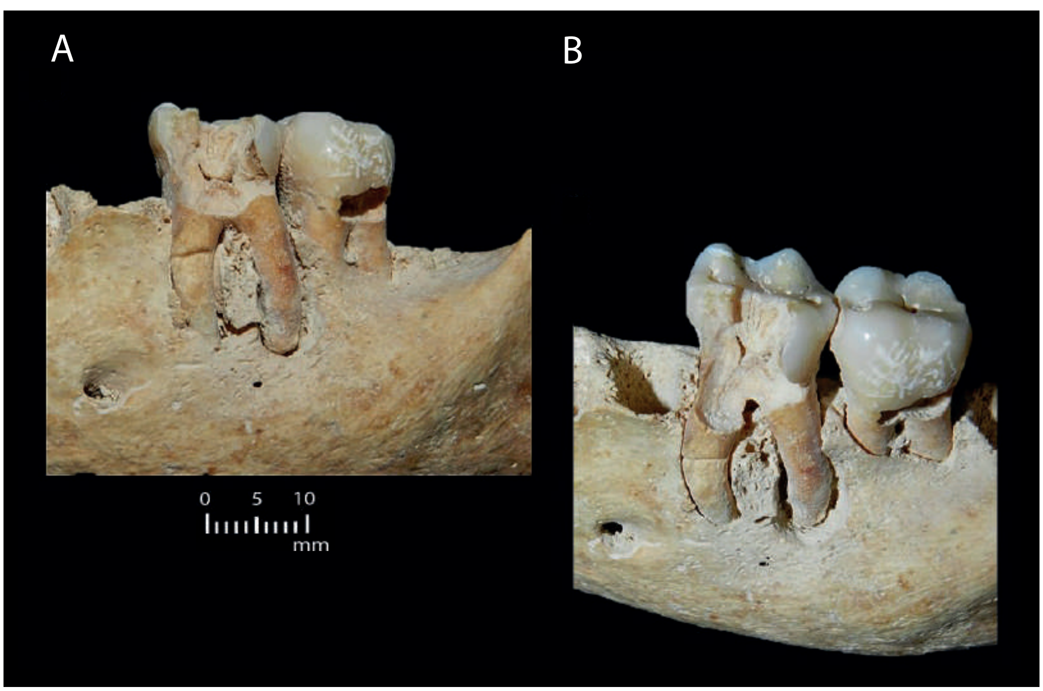

Figure 4.42. *a) Context (897) mandibular corpus fragment, showing detail of carious lesions on both retained first and second left permanent mandibular molars (FDI 36 and 37), and of lesion on buccal aspect of mesial root of the first left permanent mandibular molar (FDI 36); b) Context (897) mandibular corpus fragment, showing detail of pathological changes to alveolus of retained first left permanent mandibular molar (FDI 36). Scale bar: 1 cm. (Photos Ronika K. Power).*

on the first left permanent mandibular molar (FDI 36) appears to have obliterated almost the entire buccal aspect of the crown, close examination reveals that this lesion has a complex aetiology. The protoconid and hypoconid were lost *in vivo* because of singular or multiple *antemortem* fracturing events, as indicated by the steep, almost-vertical fracture platforms, accompanied by smoothing and rounding of the fracture margins, suggesting continued use in the mouth subsequent to the insult/s (Hillson 2000, 258). It is suggested that the *antemortem* crown fracture/s took place after the crown architecture was compromised by a gross carious lesion. The extant maximum dimensions of the tooth are mesiodistal Ø: 10.6 mm; buccolingual Ø: 10.3 mm; maximum crown height: 6.3 mm on the distolingual cusp. The shape of the lesion is irregular and it features sharp and distinct margins and smooth walls. The maximum width of the lesion is 8.5 mm; maximum length is 10.3 mm; maximum depth is 4.4 mm. The lesion has destroyed the entire protoconid and approximately half of the hypoconid of the first molar, with the destruction extending well beyond the cementum enamel junction onto the root on the buccal aspect of the tooth. The mesioinferior margin of the lesion appears to correspond with the level of the alveolar process, as it extends to encompass approximately 25–30% of the mesial tooth root. The distoinferior aspect of the lesion is slightly higher, as it appears to sit above the extant alveolar process and encompasses approximately 15% of the tooth root inferior to the cementum enamel junction. The central aspect of the lesion features a perforation of the pulp chamber, with a maximum width of 2.2 mm, maximum height 2.8 mm. The pulp horns are clearly observed in cross-section, as are the superior aspects of both the mesial and distal root canals.

This massive carious lesion is associated with the pathological change observed in the alveolus of the left first permanent mandibular molar (FDI 36; Fig. 4.42a & b). Here, erosive processes have removed the buccal wall, exposing both the mesial and distal roots, although the interradicular septum was still viable. Alveolar resorption is more extensive surrounding the distal root, creating an abscess with smooth, porous walls and rounded margins (Figs 4.41a & b, 4.42a & b). The abscess is approximately ovoid in shape, with a maximum width of 6.1 mm and maximum length of 9.7 mm, terminating immediately inferior to the apex of the buccal root. The interradicular septum appears porous and is broken at its base because of *post-mortem* damage. An area of marked porosity and slight discolouration skirts around the inferior aspect of the abscess (5.9 mm maximum length, inferior to the mesial alveolar apex; Munsell white 5Y 8/1), possibly indicative of new bone deposition which has subsequently been removed by post-depositional movement and/or exuberant cleaning. This hypothesis is supported by the appearance of a small extant deposit of new bone (1.5 mm in width, 3.2 mm in length) which sits proud of the cortex on the inferomesial margin of the fenestration of the mesial root alveolus. The sharp and ragged margins of this deposit indicate that it has been subject to *postmortem* damage. It is proposed that this abscess and the associated reactive bone lesion was both chronic and active at the time of death.

The maximum dimensions of the second left permanent maxillary molar are mesiodistal Ø: 9.8 mm; buccolingual Ø: 9.4 mm; maximum crown height: 6.4 mm on the mesiolingual cusp. The carious lesion on the second left permanent mandibular molar is located in the cervical region of the tooth (Fig. 4.42a & b). The lesion is approximately ovoid in shape and features sharp and distinct margins and smooth walls. There are occasional chips in the lesion margins, caused by *post-mortem* damage. The lesion commences at the level of the cementum enamel junction approximately 1.4 mm distal to the mesial aspect of the tooth, and extends a maximum length of 6.9 mm to traverse the entire length of the cementum enamel junction to the most distal aspect of the tooth. The maximum width of the lesion is 3.1 mm; and the maximum depth is 2.52 mm.

A much smaller lesion is observed on the occlusal surface of the second left permanent mandibular molar. The lesion presents as an approximately ovoid perforation, of 0.9 mm maximum width, located on the occlusal aspect of the entoconid cusp, immediately distolingual to the intersection of the molar fissures.

A lesion is observed on the buccal aspect of the mesial root of the first left mandibular permanent molar (Fig. 4.43a to d). The centre of the lesion is located 3.1 mm inferior to the most-inferior margin of the massive carious lesion described for this tooth, above. The lesion presents as a straight, slightly diagonal line which traverses the exposed tooth root in an inferiorly inclined direction from its most mesial to distal aspects, with a maximum width of 3.5 mm and maximum length of 0.6 mm (Fig. 4.43a to d). In section, the lesion presents a sharp, V-shaped intrusion of approximately 0.7 mm into the dentine at an angle of 40° from the base, with flat and smooth medial and lateral walls. The superior lesion margin presents a relatively smooth, angulated surface as it sharply declines inferiorly into the V-shaped intrusion. The anterior lesion margin is more irregular in organization, and it features a slight promontory of dentine at its most-mesial aspect which extends across the central lesion space. It is suggested that this lesion was initially *antemortem* sharp-force trauma, with reparative dentine deposited on its most

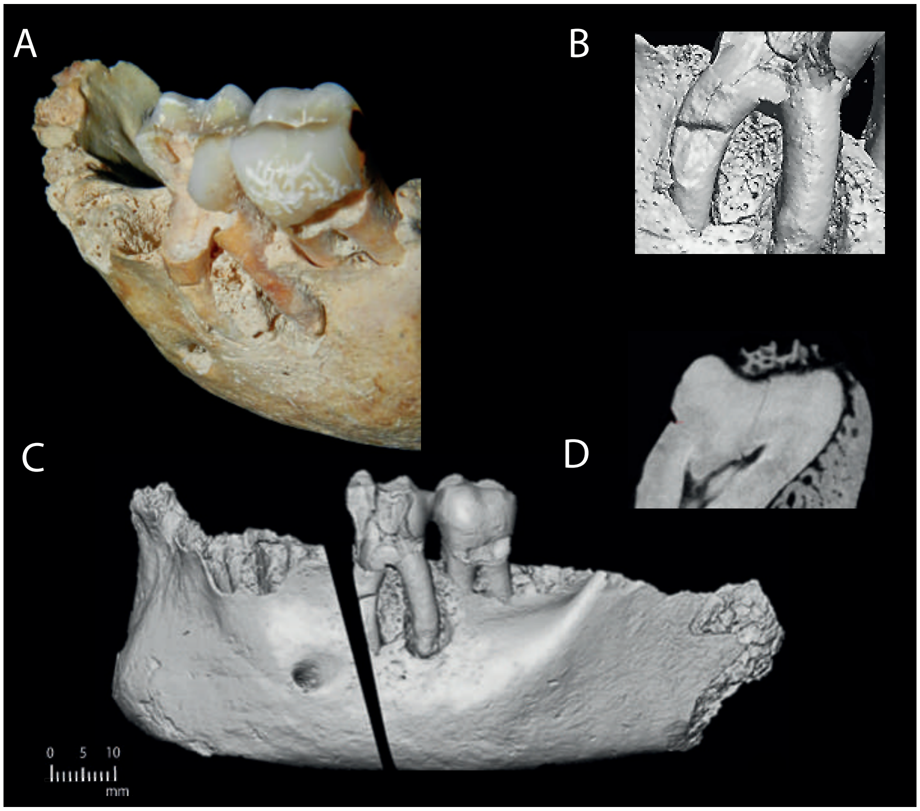

Figure 4.43. *a) Context (897) mandibular corpus fragment; b) 3D render; c) cross-section location (black plane); and d) cross-section detail of lesion on buccal aspect of mesial root of the first left permanent mandibular molar (FDI 36). (Photo Ronika K. Power; radiological images captured by L.T. Buck, Cambridge Biotomography Centre; processed by J. Magnussen & M. Pardey, Macquarie Medical Imaging).*

superior and anterior margins during a subsequent *antemortem* healing phase (Hillson 2000, 257).

It is proposed that this lesion represents deliberate therapeutic intervention to relieve the infectious and inflammatory processes within the alveolus associated with the massive carious lesion on the crown, a form of proto-dental surgery. We suggest that the sharp-force trauma lesion observed on the buccal aspect of the mesial root of the first left mandibular permanent molar (FDI 36) occurred in the process of incising the gum to lance and drain pus from the active abscess to relieve pain and pressure (Leek 1967, 704). The instrument employed for this purpose was most likely a microlithic blade, as objects with similar edge-profiles to that described for the insult, above, have been found at contemporaneous Gozitan sites. Manufactured from chert and obsidian, these objects would have been strong and sharp enough to perforate and lacerate the gingiva and dentine in a similar manner to the way they were used in the butchering of animals, for which evidence also proliferates across Neolithic Gozo (Volume 2, Chapter 9).

This is a highly significant finding, as the global corpus for prehistoric proto-surgical intervention for dental pathologies is very small (Langsjoen 1998, 411; Leigh 1937, 294), with only six known examples from Late Upper Palaeolithic to Neolithic Europe and Asia, including Riparo Villabruna, Italy (14,160–13,830 cal. BP; Oxilia *et al.* 2015); Riparo Fredian, Italy (13,040–12,600 cal. BP; Oxilia *et al.* 2017); Mehrgarh, Pakistan (7500–9000 cal. BP; Coppa *et al.* 2006); Lonche, Slovenia (6655–6400 cal. BP; Bernardini *et al.* 2012); Gaione Catena, Italy (estimated 5000–4000 BC; Mantini *et al.* 2007); and Hulberg, Denmark (estimated 2000–3000 BC; Bennike & Fredebo 1985). The Circle example described here has been radiocarbon dated to 2575–2500 cal. BC, within the Tarxien phase of the Maltese Late Neolithic (Chapter 3). Detailed comparisons between the modes, types and dates of reported prehistoric proto-surgical interventions and that described for the Circle mandible will be put forward in Power *et al.* (forthcoming), as well as comprehensive discussions of its findspot and context. It is poignant that this burial population, widely celebrated for the cultural and technological innovations that manifest the Ġgantija Temples, also contained individuals who were at the forefront of medical innovation, too.

4.5.7.2. Dental calculus

The mouth is an ecosystem, hosting myriad microscopic organisms including bacteria, viruses, yeasts and protozoa (Caselitz 1998, 203–4; Hillson 2005, 286). While there are many sites and surfaces within the mouth that provide habitats for these organisms to establish and flourish, the surfaces of the teeth are particularly desirable sites for colonization as their constituent cells are fixed and do not shed, allowing the micro-organisms to establish large communities (Caselitz 1998, 203–4; Hillson 2005, 286). In the case of pathological processes such as carious lesions, resident micro-organisms – particularly bacteria – seize upon this as an opportunity to colonize newly created space. These bacteria, most commonly including *Streptococcus*, *Actinomyces*, *Lactobacillus* and *Neisseria*, attach to each other and the tooth surface via production of a polysaccharide adhesive that is produced from human dietary sugars (Caselitz 1998, 204; Hillson 2005, 287). This adhesive, in combination with salivary proteins and gingival crevice fluid, forms a matrix in which the oral bacteria become embedded (Hillson 2005, 287; Roberts & Manchester 2005, 71). If not removed by the natural cleaning actions of the lips, tongue, other teeth and saliva, or mechanical cleaning actions such as brushing or picking (§4.5.6.7, above, for possible examples within the Circle study sample), this matrix will consolidate as dental plaque (Hillson 2000, 258).

The speed at which dental plaque accumulates is thought to be determined by the composition of the diet, with the fastest rates attributed to those consuming high levels of protein and/or carbohydrates (Roberts & Manchester 2005, 71). Over time, dental plaque can become mineralized because of its immersion in the combined wash of plaque fluid and saliva, which contain high levels of calcium phosphate (Hillson 2005, 288). This process usually commences directly adjacent to the tooth, at the deepest layers of the plaque deposit. Through the process of mineralization, the resident bacterial colonies die, and their fossilized structures are retained in the mineralized plaque deposits referred to as dental calculus (Hillson 1998, 258, 2005, 289). Calculus formation can be supragingival (above the gum) or subgingival (below the gum; Roberts & Manchester 2005, 72), with a predilection for locations closest to the salivary glands. Thus, calculus is most commonly (though not exclusively) observed on the lingual aspects of the mandibular anterior teeth adjacent to the sublingual and submaxillary ducts, and the buccal aspects of the maxillary molars adjacent to the parotid ducts (Hillson 2005: 288; Roberts & Manchester 2005, 72).

Studies of dental calculus incidence and prevalence have been fundamental to bioarchaeological praxes since the emergence of the discipline (Brothwell 1981; Dobney & Brothwell 1987; Roberts & Manchester 2005, 72). Such studies can provide wide-ranging insights regarding population density, health and diet; however, inconsistent recording and reporting standards which prioritize the reporting of total affected teeth or individuals (incidence) rather than the percentage of affected teeth or individuals (prevalence), limits the extent to which valuable comparative studies between populations can occur (Roberts & Manchester 2005, 72). More recent scientific developments have taken calculus analyses to the world stage, incorporating scanning electron microscope (SEM) studies of food debris and phytoliths (Cristiani *et al.* 2018; Dobney & Brothwell 1986; 1988; Radini 2016), X-Ray Diffraction (XRD) spectroscopy for trace element analyses (Klepinger *et al.* 1977) as well as studies at the molecular level to examine proteomic evidence for diet (Charlton *et al.* 2019; Hendy *et al.* 2018), disease (Mackie *et al.* 2017; Warriner *et al.* 2014), as well as aDNA and the human microbiome (Adler *et al.* 2013; Kawano *et al.* 1995; Warriner *et al.* 2015; Weyrich *et al.* 2015).

The Circle sample would undoubtedly benefit from such scientific analyses but, unfortunately, they were not possible within the parameters of the current project. Moreover, the idiosyncrasies of the Circle sample preclude precisely the kind of rigour required for accurate and comparable analyses, as lamented by Roberts and Manchester (2005: 72). The vigorous and inexorable *postmortem* interventions imposed upon the remains as a by-product of the Temple Period funerary behaviour (Malone *et al.* 2009d; Malone *et al.* 2019; Stoddart *et al.* 2009a; Thompson *et al.* 2018; Thompson *et al.* 2020; cf Chapter 12) has had significant impact on the retention of calculus, causing it to be frequently dislodged and separated from the dentition. Although the true extent to which this has impacted on the burial population is impossible to determine, we are nevertheless able to see its evidence among the dentition, manifest as obvious and otherwise inexplicable discontinuities in calculus deposition across arcades, or as shadows on the enamel where former deposits are no longer extant. In alignment with the methodology developed to approach general pathology in the sample – that is, to report extreme observations as a first means to characterize the outermost boundary of the lived experiences of the burial population (Chapters 2 & 8) – we have applied a consistent approach with reporting observations of extreme calculus deposition in the present study. We hope to expand upon this in future work to achieve better population-based resolution of this phenomenon amongst this challenging assemblage.

The first example of extreme calculus from the Circle study sample is observed on a right permanent maxillary third molar (FDI 18) derived from Context (951) (Fig. 4.44a to d). In this case, a calculus collar has formed around the entire distal surface architecture of the crown, closely resembling Brothwell's (1981, Fig. 6.14b; cf Buikstra & Ubelaker 1994, 56) 'large amount' categorization. The calculus collar extends superoposteriorly away from the crown, over and beyond the cementum enamel junction in a manner which must have overlain the gingiva *in vivo*. The calculus is smooth and regular in surface texture and deep beige (7.5YR 8/2) in colour.

A further instance of extreme calculus deposition within the study sample is noted on a fragment of right mandibular corpus and ascending ramus, observed within the assemblage of Context (951) (Fig. 4.44a to *d*). The fragment retains two permanent teeth, the first and second mandibular molars (FDI 46, 47). The adjacent third molar (FDI 48) has been lost *antemortem* – only recently before the time of death – as evidenced by the active remodelling taking place in the alveolar space. The hallmarks of infectious and inflammatory processes are evident in this specimen, as the alveolar process and oblique line have significantly retracted and laterally rolled away. The alveolar process surrounding (or adjacent to) the extant teeth has significantly receded, exposing approximately half of the tooth roots. Additionally, a large cervical carious lesion is observed on the interproximal aspect of the second mandibular molar, traversing the root and crown and penetrating deeply into the coronal space. An extreme calculus deposit is observed across the occlusal and buccal surfaces of the first and second molars, exceeding the 'large amount' characterization as presented by Brothwell (1981, Fig. 6.14b). The deposit has obscured almost the entire occlusal surfaces, with only the tips of the protoconid and hypoconid of both teeth emerging from the matrix. In section, the deposit appears to be of approximately regular thickness across the occlusal surface, only tapering as it crosses the lingual cusps and diminishes in descent across the lingual crown surface. On the buccal aspect, the calculus collar extends inferiorly to cover the cementum enamel junction, and gradually projects laterally, forming a trapezoidal shape in cross-section. Here again, the calculus is smooth and regular in surface texture and deep beige (10YR 9/4) in colour. Unfortunately, *antemortem* tooth loss (in the case of the second

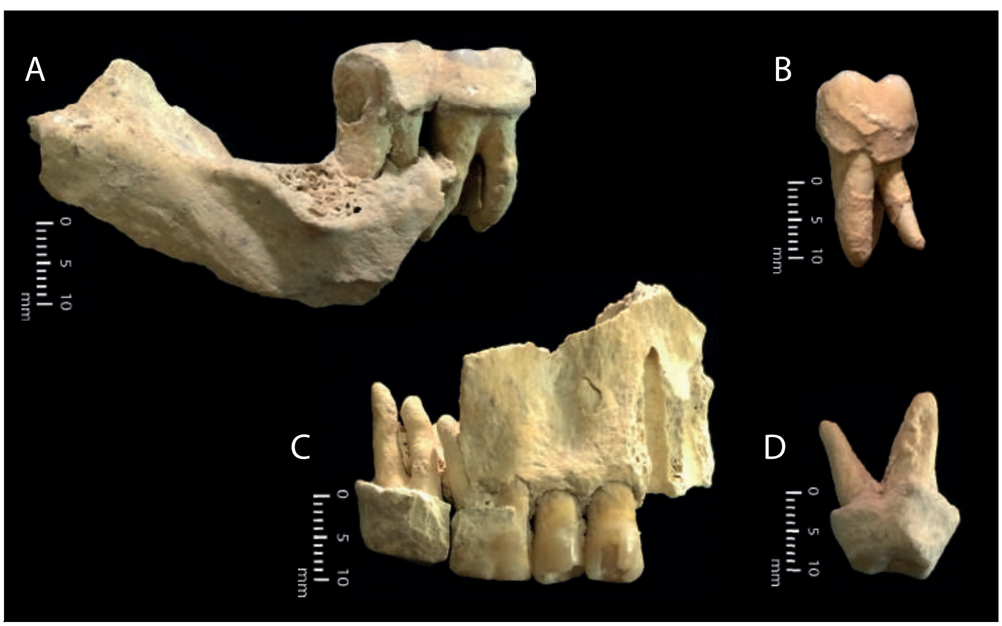

Figure 4.44. *a) Example of extreme calculus deposition on first and second mandibular molars (FDI 46, 47)* in situ *within a fragment of right mandibular corpus and ascending ramus, from Context (951) of the Circle sample; b) example of extreme calculus deposition on a right permanent maxillary third molar (FDI 18) from Context (951) of the Circle sample; c–d) example of extreme calculus deposition observed on the buccal aspect of the first molar, and buccal, distal and lingual aspects of the second molars,* in situ*/refitted within a fragment of adult right maxilla, from Context (783) of the Circle sample. Scale bar: 1 cm. (Photos Ronika K. Power).*

molar) and *postmortem* fragmentation (in the case of the first molar), make it impossible to determine the full extent of this deposit at the peak of its occupancy *in vivo*. When viewed in conjunction with the evidence for infectious and inflammatory processes associated with the *antemortem* tooth loss of the third molar and the cervical caries of the second molar, it is possible that this extreme calculus deposit was formed as a result of chronic selective disengagement of this side of the mouth in mastication and other oral activities as a result of extreme pain and/or discomfort (Lewis 2018).

The final example of extreme calculus deposition is attributed to a fragment of adult right maxilla derived from Context (783) (Fig. 4.44a to d). The fragment is comprised of a small portion of alveolar process extending from the anterior *postmortem* fragmentation margin just mesial to the alveolus of the permanent lateral incisor, to the posterior margin which transects the alveolus for the permanent first molar. Only small portions of the anterior and posterior walls of the maxillary sinus are extant – fragmentation has exposed and truncated the antrum. The retained teeth include the permanent first and second premolars as well as the first and second permanent molars (FDI 14–17). Although fragmented, the alveoli for the permanent canine and lateral incisor (FDI 12, 13) are patent and there is no indication of infectious or inflammatory activity at the time of death, hence it is suggested that these teeth were lost *postmortem*. *Antemortem* fractures are observed on the buccal aspects of both the first and second premolars, obliterating the buccal cusps of both teeth, and in the case of the first premolar producing a fracture flake which has removed a section of enamel comprising almost one-third of the buccal crown surface. The extant portion of the extreme calculus deposit is observed to traverse the buccal aspect of the first molar, and buccal, distal and lingual aspects of the second molar. On the buccal aspect of the arcade, the extant deposit commences (in fragmentary state) as a thick linear formation at the cementum enamel junction on the mesial third of the crown. As the deposit advances distally and inferiorly, it extends its coverage to traverse the vertical height of the crown. The deposit has been subject to *postmortem* damage and is fragmented at the interproximal margin between the first and second molars. In section, we can see that the deposit on the first molar is triangular in shape, being thickest at the cementum enamel junction, and tapering off as it approaches the occlusal surface. The deposit continues distally onto the second molar, enveloping the entire crown and forming a complete collar around all coronal surfaces, with the exception of the mesial interproximal facet, visible because of *postmortem* fragmentation. When observed in section, the deposit is approximately trapezoidal in shape, and on all surfaces exposed *in vivo*, the superior aspects of the deposit appear to have extended laterally to overlie the gingiva. The deposit is smooth and regular in surface texture and pale beige to grey (approximately 2.5Y 8/2) in colour. It is important to note that the deposit extends uninterrupted across the distal interproximal surface, indicating that the permanent third molar (FDI 18) was not in occlusion at the time of death. Considering the maxilla is in such a fragmentary state, it is not possible to determine whether the third molar was lost *antemortem*, was impacted in the upper jaw, or was congenitally absent. Here again, a deposit of this extent is suggestive of chronic impeded use of the mouth in this area (Lewis 2018).

4.5.7.3. Congenital variation

The sample was also examined for any evidence of congenital variation amongst tooth crowns and roots. The possibility of identifying these relatively rare traits amongst the Circle burial population was heightened not only by the sheer size of the study sample, but also by the extensive *postmortem* fragmentation of upper and lower jaws and concomitant exfoliation and exposure of many teeth. This fascinating aspect of dental anthropology is otherwise rarely approached in archaeological studies (Alt & Türp 1998a, 95); in this way, the present study marks an important contribution to scholarship in human evolution, skeletal biology, palaeopathology and forensic odontology (Alt & Türp 1998a, 95).

In agreement with Alt & Türp (1998a), the present study defines congenital variation as morphological changes to an element during development which are beyond normal variability but do not impede normal physiological functions (cf Zwemer 1993). This might include variation in form, function or position of one or more teeth as part of a syndrome or as an independent anomaly (Alt & Türp 1998a, 96). It is important to differentiate between population-specific variations in tooth morphology that might be classified as dental non-metric traits or ontogenetic disturbances. The former are considered to be normal variation in some groups, and from this perspective can be useful to identify genetic groupings amongst archaeological populations. Such studies fall under the purview of Dental Anthropology and have been pursued for the Circle study population in Chapter 6. Congenital variation, on the other hand, is more concerned with odontogenetic disturbances including tooth shape or form; concrescence, gemination, twinning and/or fusion; size and number; tooth position and malocclusion; tooth structure; disturbances of tooth eruption; and congenital variations in bone formation and development of the skeleton affecting the teeth and jaws (after Alt & Türp 1998a, 96). Examples of congenital variation encountered in the Circle study sample are reported below.

4.5.7.3.1. Variation of crown form: 'peg' teeth
So-called 'peg' teeth are one of the best-known variations of dental morphology in bioarchaeology. They are a form of microdontia and present as an unusually small (often conical-shaped) crown accompanied by a small, thin root (Alt & Türp 1998a, 96; van Beek 1983, 56). The most common elements to present this variation are the maxillary lateral incisors and maxillary or mandibular third molars (Alt & Türp 1998a, 96, 107). Examples of this amongst the sample include 'peg' maxillary lateral incisors pertaining to Context (960) (Fig. 4.45a) and Context (783) (Fig. 4.45b to d); and 'peg' molars pertaining to Context (783) (Fig. 4.45e & f).

4.5.7.3.2. Variation of root form: accessory root(let)s
Studies of tooth roots are elusive in archaeological materials owing to their general macroscopic inaccessibility (Alt & Türp 1998a, 102; Kovacs 1967). The highly fragmented nature of the Circle assemblage therefore presents a serendipitous opportunity for expanding our knowledge of ancient radicular morphology. This is particularly important considering the compelling argument that root traits are genetically determined (Townsend *et al.* 1992). According to Alt and Türp (1998, 102), small accessory roots (or 'rootlets', or *radiculae appendiciformes*) may occur buccally or lingually on any teeth. Within the study sample, accessory roots were observed on three occasions: on two maxillary molars in Context (951) (Fig. 4.46a & b); and another maxillary molar in Context (982) (Fig. 4.46c).

Figure 4.45. *Examples of 'peg' maxillary lateral incisors within the Circle sample; a) from Context (960); b–d) from Context (783); e–f) examples of 'peg' molars from Context (783) within the Circle sample. Scale bar: 1 cm. (Photos Ronika K. Power).*

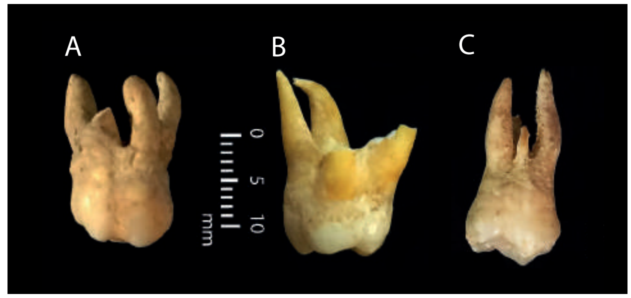

Figure 4.46. *Examples of accessory root(let)s from a–b) Context (951); and c) Context (982) from the Circle sample. Scale bar: 1 cm. (Photos Ronika K. Power).*

4.5.7.3.3. Variation of root form: dilaceration
Dilaceration is characterized by marked crescent-shaped radicular curvature but does not affect the crown (Alt & Türp 1998a, 104). These genetic curvatures are distinguished from root curvatures with exogenous aetiologies, as the latter are generally located at the apical third of the root. Examples of dilaceration within the study sample include a maxillary molar from Context (951) (Fig. 4.47a); a mandibular molar from Context (951) which also presents an interproximal cervical carious lesion and hypercementosis (Fig. 4.47b); a right maxillary third molar from Context (1268) (Fig. 4.47c); and three mandibular molars from Context (783) (Fig. 4.47d to f).

4.5.7.3.4. Variation in crown and root forms: fusion
There are several ways that teeth can become partially or wholly bound: concrescence, gemination, twinning and fusion (Alt & Türp 1998a, 106, Fig. 15). Concrescence occurs when two or more teeth are unified via fusion of the cementum, either during development ('true' concrescence; Alt & Türp 1998a, 104; Pindborg 1970; Zwemer 1993) or after eruption or completion of root formation ('acquired' concrescence; Alt & Türp 1998a, 104; Pindborg 1970). Gemination is the appearance of double crowns on a single root, formed as a result of the tooth bud or follicle attempting to divide (Alt & Türp 1998a, 104; Pindborg 1970; Zwerner 1993). Twinning (schizodontia) occurs when a tooth bud successfully divides, creating a duplicate and

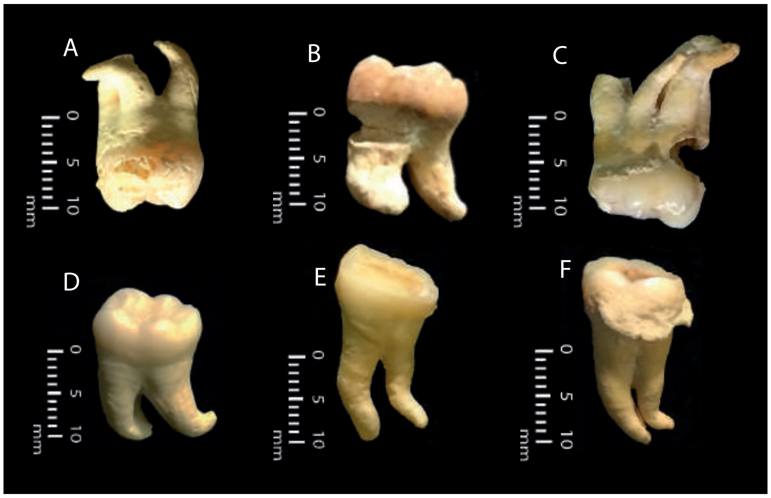

Figure 4.47. *Examples of dilaceration from Context (951), including a) maxillary molar; b) mandibular molar, also presents an interproximal cervical carious lesion and hypercementosis; c) a right maxillary third molar from Context (1268), also presents an interproximal cervical carious lesion; and Context (783), including d–f) three mandibular molars, from the Circle sample. Note that the tooth in 'f', a right permanent mandibular third molar, also presents moderate calculus deposition on the lingual aspect, particularly at the level of the cementum enamel junction. Scale bar: 1 cm. (Photos Ronika K. Power).*

supernumerary tooth in the arcade (Alt & Türp 1998a, 104; Tannenbaum & Alling 1963). Fusion (synodontia) is the binding of two or more separate teeth during development, including the enamel/coronal and/or dentin/radicular parts of teeth (Alt & Türp 1998a, 104; Pindborg 1970). Of these forms of crown and root variations, there are several examples of fusion observed within the Circle study population, including two elements from Context (960) (possibly fused mandibular premolars and first molars; Fig. 4.48a & b); an element from Context (732) (also possibly a fused mandibular premolar and first molar; Fig. 4.48c); and an element from Context (951) (possibly a maxillary premolar and first molar; Fig. 4.48d). It is difficult to determine the precursor teeth on these exfoliated elements as their morphology is extremely variable.

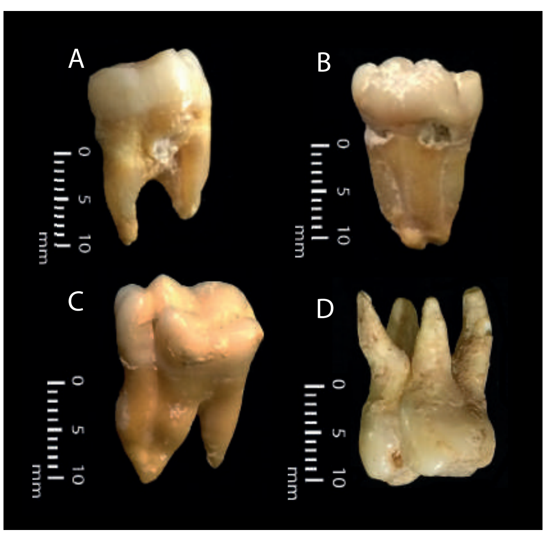

Figure 4.48. *Examples of fusion from Context (960), including a–b) fused possible mandibular premolars and first molars; from Context (732), including c) a fused possible mandibular premolar and first molar; and from Context (951), including d) a fused possible maxillary premolar and first molar, from the Circle sample. Scale bar: 1 cm. (Photos Ronika K. Power).*

4.5.7.3.5. Variation of root form: dwarfism

Tooth size is an important discriminant criterion in archaeological populations, as large-scale analyses can be helpful in determining demographic characteristics including sexual dimorphism, geographical affinity and genetic relationships (Alt & Türp 1998a: 106; Lind 1972), the latter of which is explored for the Circle study sample (Chapter 6). In terms of congenital variation in tooth size, several incidences of root dwarfism were identified amongst the population. Here again, the opportunity to observe macroscopically a substantial number of tooth roots was aided by the highly fragmented nature of this burial population. The first example pertains to a mandibular third molar from Context (951), which also presents hypercementosis (Fig. 4.49a). Dwarfed roots were also observed on three mandibular third molars from contexts (662) (Fig. 4.49b), (783) (Fig. 4.49c) and (951) (Fig. 4.49d), a maxillary third molar from Context (831) (Fig. 4.49e); and a maxillary premolar from Context (595) (Fig. 4.49f).

4.5.7.3.6. Variation in eruption or alignment

Variations of one or both of the jaws and teeth are categorized as 'dysgnathia', as opposed to 'eugnathia' which refers to a status of so-called 'normal' development (Alt & Türp 1998a, 112). Eruption pathways of teeth are generally known to follow the root orientation, which can be strongly influenced and altered by several factors, including the adjacent maxillary structures and spaces, variations in growth speed,

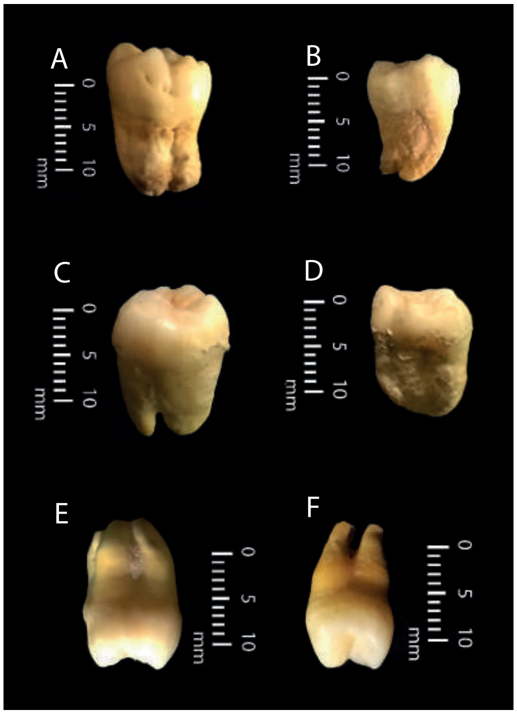

Figure 4.49. *Examples of dwarfism, featuring elements from Context (951), including a) mandibular third molar which also presents hypercementosis; three mandibular molars, from b) Context (662); c) Context (783); d) Context (951); e) a maxillary third molar from Context (831); and f) a maxillary premolar from Context (595), from the Circle sample. Scale bar: 1 cm. (Photos Ronika K. Power).*

and mechanical interference (Laptook & Silling 1983; Tripathi *et al.* 2014). It is difficult to evaluate many aspects of the dental arch relationship in this burial population, particularly malocclusion, as a result of the widespread disarticulation, fragmentation and commingling of crania and mandibles. Notwithstanding this fact, there were several examples of dysgnathic variation observed within the study sample. There is widespread interest in the incidence and prevalence of these phenomena across archaeological populations particularly because of their mixed exogenous and hereditary aetiologies (Alt & Türp 1998a, 116), so the Circle observations provide valuable additions to the global dataset. The variations within the study sample were of two expressions: atypical or ectopic eruption associated with impaction; and crowding of the anterior arcade. It is not possible to include all examples of elements within the study sample presenting evidence of dental impaction or crowding, only those demonstrating complex or unique expressions will be individually described and illustrated here.

The first example pertains to two elements examined from the same stratigraphic unit within Context (960), a fragmentary left maxilla and a fragmented yet almost-complete mandible, only missing the anterior teeth (according to the patent alveoli; Fig. 4.50a to e). Commencing with the superior element (Fig. 4.50b to d), the fragment consists of an almost-complete maxilla, fragmented on the medial aspect. The frontal process is absent, as is the medial two-thirds of the infraorbital margin and the anterior aspect of the maxillary architecture including the infraorbital foramen, nasal border, anterior nasal spine, nasoalveolar clivus and alveolar process containing the alveoli and elements of the central and lateral incisors. The maxillary sinus is fragmented and exposed. The left zygoma is intact, complete and in articulation. The retained teeth include the permanent canine, first and second premolars, and first, second and third molars (FDI 23–28), as well as a retained deciduous canine (FDI 63). The left permanent canine is observed to have erupted in an atypical manner, exiting from the alveolar process at an approximately horizontal and slightly lateral angle. The fragmentation margin transects the canine alveolus, so we are able to see macroscopically that the tooth itself is normal in formation, and has achieved complete growth as evidenced by apical closure. Observations of calculus circumnavigating the crown also confirm its presence in the mouth *in vivo*. Calculus is also observed inferior to the cementum enamel junction of all retained and occluding teeth. The aetiology of the irregular eruption is observed in the neighbouring distal tooth: a retained deciduous canine. The retained deciduous tooth has blocked the eruption pathway of the adult element, resulting in an alternative exit angle and location that remains permanent in the absence of modern orthodontic intervention. There can be no doubt that the irregular eruption profile of this tooth would have interfered with the projection of the overlying labial tissue, impacting on the physical appearance of this individual in life. Also note that the left maxillary third permanent molar is also impacted for this individual; it is mesially and laterally tilted by approximately 45°. Although there does not appear to be any active infectious process associated with the irregular eruption issues observed on the extant portion of this element, there is marked porosity and resorption of the alveolar margin associated with the retained deciduous canine, indicative of moderate periodontal disease.

Similar eruption perturbations are observed on the mandible isolated from the same stratigraphic unit (Fig. 4.50e), presenting the possibility that these elements may be attributed to the same individual.

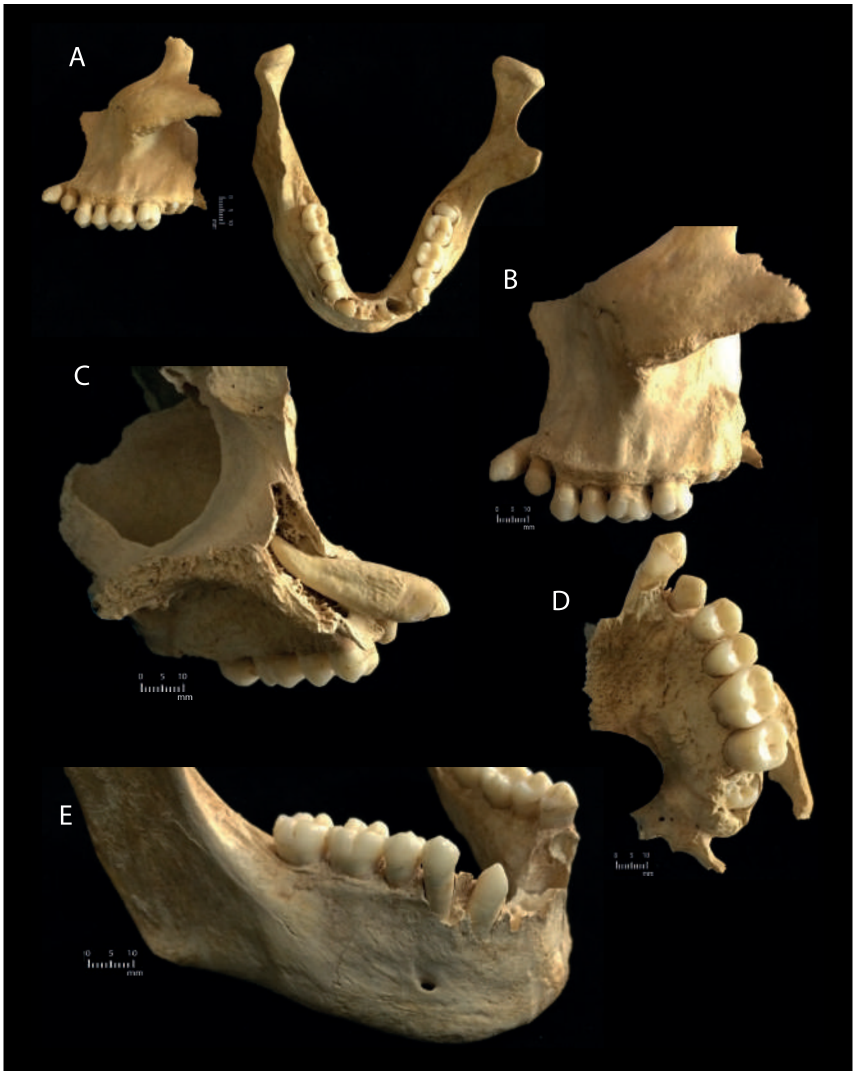

Figure 4.50. *a) Fragmentary left adult maxilla and an almost-complete mandible from Context (960) of the Circle sample; b–d) lateral, mesial and inferior (palatal) views of the left maxilla, detailing the atypical eruption of the permanent canine; e) lateral view of the right mandibular corpus, detailing the atypical eruption of the permanent canine. Scale bar: 1 cm. (Photos Ronika K. Power).*

Although fragmentary, the osseous components of the mandible are complete. The visibly retained dentition includes the left permanent canine, first and second premolars, and first and second molars (FDI 33–37); and the right first and second premolars, and first, second and third molars (FDI 44–48). The extant right mandibular permanent canine (FDI 43) is observed to be incompletely erupted, despite the appearance of other teeth in occlusion in the arcade that typically emerge later in the eruption sequence, such as the permanent second premolars and molars. The canine is situated in an irregular position, mesially tilted by approximately 35° and distally rotated in the alveolus by approximately 90°. The antimere has been subject to *postmortem* exfoliation, and the element has been fragmented at the level of the left canine alveolus, so it is not possible to determine whether this condition is bilateral. Notwithstanding these issues, and despite incomplete observation as a result of *postmortem* fragmentation, the irregular positioning and formation of the alveoli for the exfoliated anterior teeth appear to indicate crowding in this portion of the arcade. Retained deciduous dentition must also be considered as a possible aetiology for the impaction, rotation and perturbed trajectory of the extant right canine. We also observe that the left mandibular third molar (FDI 38) is impacted. The right mandibular third molar (FDI 48) is not observed macroscopically, and the apparently healthy presentation of the retromolar space provides no indication that it was subject to *antemortem* loss. Further radiographic analyses would be required to determine if this tooth is also impacted within the alveolar process, or is congenitally absent.

A fragment of anterior adult right maxilla identified within Context (783) was observed to present variation in eruption and alignment (Fig. 4.51a & b). The fragment presents partial palatine and alveolar processes, extending from the anterior fragmentation

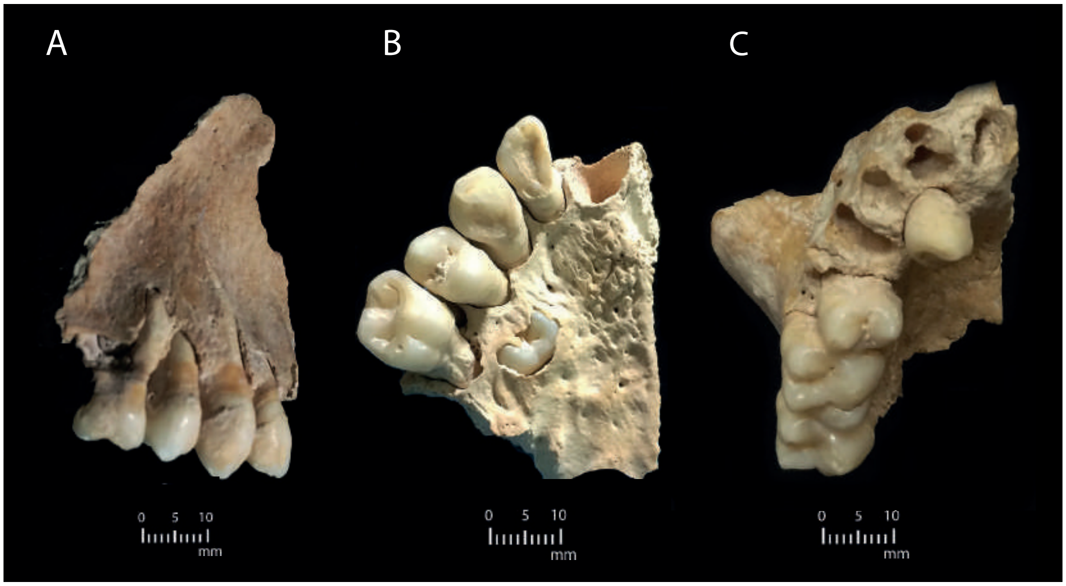

Figure 4.51. *Fragmentary right adult maxilla from Context (783) of the Circle sample, in a) lateral and b) inferior (palatal) views, detailing the retained deciduous second molar and ectopic placement of the permanent second premolar; c) fragmentary right adult maxilla from Context (1268) of the Circle sample, showing ectopic placement of the permanent canine and patent alveoli for a retained deciduous lateral incisor and deciduous canine. Scale bar: 1 cm. (Photos Ronika K. Power).*

margin at the intermaxillary suture, across to the posterior fragmentation margin distal to the retained deciduous second molar, and superiorly at the level of the nasoalveolar clivus, inferior to the infraorbital foramen. The fragmentation has exposed the maxillary sinus. The retained teeth in occlusion include the right permanent lateral incisor, canine and first premolar (FDI 12–14) and, as mentioned above, the deciduous second molar (FDI 55). The alveolus for the permanent central incisor (FDI 11) is patent and there is no indication of infectious or inflammatory activity at the time of death, hence it is suggested that this tooth was lost *postmortem*. There is also no indication of infectious or inflammatory activity at the extant distal aspect of the fragment, in the region of the alveolus of the permanent first molar. There is slight calculus deposition at the level of the cementum enamel junction on the labial/buccal aspect of all retained teeth (FDI 12–14, 55), and on the lingual aspect of the lateral incisor and canine (FDI 12–13). Concerning the retained deciduous second molar, fenestration of the alveolar process on the buccal aspect reveals that there is no resorption of at least the mesial buccal root, and it is likely that the other two roots are also intact. The retention of the deciduous second molar has blocked the eruption pathway of the permanent second premolar, leading to its ectopic placement in the medial/lingual aspect of the alveolar process, traversing into the palatine process – as observed in the roof of the mouth via fenestration caused by *postmortem* damage.

Another fragment of adult right maxilla was observed to present distinct variation in eruption and alignment, on this occasion from Context (1268) (Fig. 4.51c). Here again, the fragment consists of only partial palatine and alveolar processes, preserved from the anterior fragmentation margin at the intermaxillary suture, to the posterior fragmentation margin distal to the permanent second molar, and superiorly at the level of the nasoalveolar clivus, inferior to the infraorbital foramen. The fragmentation has exposed the maxillary sinus. The retained teeth in occlusion include the right permanent canine, second premolar and first and second molars (FDI 13, 15–17). In the absence of all other anterior teeth, the surfeit of alveoli provide insight into the dental history of this individual. The alveoli for the permanent central incisor (FDI 11) and permanent first premolar (FDI 14) are both patent and present no indication of infectious or inflammatory activity at the time of death, hence it is suggested that these teeth were lost *postmortem*. Close inspection reveals three more patent alveoli, in addition to the permanent canine, described above. Although the elements themselves are absent, the position and size of these alveoli indicate that it is likely they housed a retained deciduous lateral incisor (FDI 52) immediately anterosuperior to a permanent lateral incisor (FDI 12), and a retained deciduous canine (FDI 53) in the distal space. The retention of the deciduous lateral incisor and canine has perturbed the eruption pathway of both of their permanent successors, made particularly evident in the ectopic placement of the permanent canine, which has mesially rotated and medially drifted to erupt on the lingual aspect of the alveolar process. Despite the risk posed by the presence of so many teeth in a small space, and rudimentary (if any) dental hygiene practices, the alveoli for each of these teeth all appear to be healthy, showing no indications of infectious or inflammatory activity at the time of death. Hence, it is also suggested that these teeth were lost *postmortem*, too.

A further striking example of ectopic dental placement is observed in a fragment of adult left maxilla associated with Context (1241). The fragment articulates and refits with an also-fragmentary right maxilla identified within the same stratigraphic unit (Fig. 4.52a to f). The left maxilla is fragmented anteriorly at the frontal process, superiorly at the zygomatic process, and posteriorly in the region immediately superior to the maxillary tubercle, exposing the maxillary sinus. The retained teeth in occlusion include the permanent canine, first and second premolars, and first and second molars (FDI 23–27). There is no osseous evidence for infection or inflammation of the alveoli for the permanent central and lateral incisors, thus it is most likely that they were exfoliated *postmortem*. A slight calculus deposit is observed at the cementum enamel junction on the buccal aspects of the first maxillary molar (FDI 26), and there is slight (approximately 3–5 mm) resorption of the alveolar process indicating mild periodontal disease. The fragmentation of this element is fortuitous, insofar as it has revealed an example of eruption variation that would otherwise have not been visible macroscopically. The permanent third molar is observed in an ectopic placement; it has distally tilted slightly <90° and lies in an approximately horizontal position on the floor of

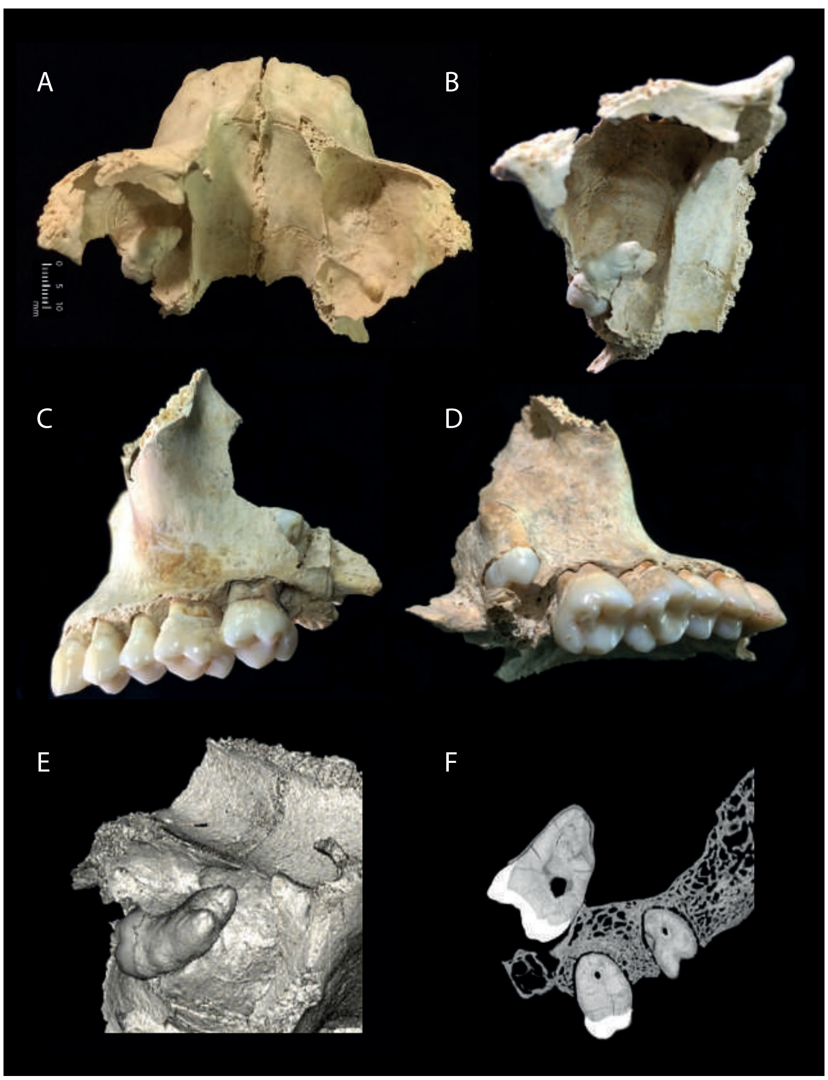

Figure 4.52. *Fragmentary refitting right and left adult maxillae from Context (1241) of the Circle sample, detailing a) the fragments in articulation, with the ectopic permanent third molar (FDI 28) observed in the posterior aspect of the left maxillary sinus; b) detailed posterosuperior view of the ectopic left permanent third molar (FDI 28); c) inferolateral view of the ectopic left permanent third molar (FDI 28), showing the mesial elements of the arcade in typical eruption and alignment position and sequence; d) inferolateral view of the right adult maxilla fragment, detailing the impacted permanent third molar superodistal to the mesial elements of the arcade which appear in typical eruption and alignment position and sequence; e) 3D render of ectopic permanent third molar (FDI 28)* in situ *in the posterior aspect of the left maxillary sinus; f) cross-section of ectopic permanent third molar (FDI 28)* in situ *in the posterior aspect of the left maxillary sinus. Scale bar: 1 cm. (Photos Ronika K. Power; radiological images captured by L.T. Buck, Cambridge Biotomography Centre; processed by J. Magnussen & M. Pardey, Macquarie Medical Imaging).*

the maxillary sinus. The tooth is observed to be fully developed to the extent of apical closure. There is no indication of infectious or inflammatory processes in the extant crypt or adjacent maxillary antrum. The impaction of this tooth does not appear to have compromised the development, eruption or alignment of any of the dentition in the left maxillary arcade.

The refitting fragmentary right maxilla mentioned above should also be described here (Fig. 4.52d). Similar to its antimere, the right maxilla is fragmented anteriorly at the nasal aperture, extending superiorly to the frontal and zygomatic processes, and posteriorly in the region immediately superior to the maxillary tubercle, exposing the maxillary sinus. The retained teeth in occlusion include the permanent canine, first and second premolars, and first and second molars (FDI 13–17). There is no osseous evidence for infection or inflammation of the alveoli for the permanent central and lateral incisors, thus they are also likely to have been exfoliated *postmortem*. Slight calculus deposits are observed at the cementum enamel junction on the buccal aspect of the first maxillary molar (FDI 16) and the interproximal aspect of the second maxillary molar (FDI 17). There is also slight (approximately 3–5 mm) resorption of the right alveolar process indicating mild periodontal disease. Here, fragmentation and fenestration has also enabled macroscopic observation of the fully developed albeit impacted permanent third molar (FDI 18). Although the tooth has medially tilted only slightly (~15°), it has still not been able to forge a pathway through the alveolar process to erupt successfully in the mouth. Fragmentation of the maxillary sinus also enables observation of the root apex penetrating the antrum floor. Here again, there is no indication of infectious or inflammatory processes in the extant crypt maxillary sinus; and the impaction does not appear to have compromised the development, eruption or alignment of any of the neighbouring dentition in the right maxillary arcade.

Additional evidence of atypical eruption and alignment amongst the Circle assemblage is observed on a fragmentary right maxilla, identified within Context (960) (Fig. 4.53). The fragment presents partial palatine and alveolar processes, extending from the anterior fragmentation margin mesial to the permanent canine, across to the posterior fragmentation margin distal to the second molar, and superiorly at the level of the nasoalveolar clivus, inferior to the infraorbital foramen. The fragmentation has exposed the maxillary sinus. The retained permanent teeth include the canine, and the first and second molars (FDI 13, 16–17). There is significant *postmortem* damage to the anterior aspect of the alveolar process, so it is not possible to determine if the permanent central and lateral incisors (FDI 11–12)

Figure 4.53. *Fragmentary right adult maxilla, detailing atypical eruption of the permanent canine (FDI 13), from Context (960) of the Circle sample. Scale bar: 1 cm. (Photo Ronika K. Power).*

were in occlusion at the time of death. The alveoli for the permanent first and second premolars are patent and there is no evidence of an osseous response suggestive of infection or inflammation; as such, these teeth may be determined to have been lost *postmortem*. On the other hand, the permanent third molar may have been lost *antemortem*; even though the element is fragmented at this level, the extant portions of both the alveolus and surrounding alveolar process present as roughened, irregular and porotic and appear to have been undergoing remodelling at the time of death. The canine (FDI 13) is only partially erupted; even though there is some *postmortem* damage to the alveolar process in this area, only the tip of the cusp appears beyond the alveolar aperture. Following the trajectory of the visible portion of the tooth, the canine is observed to be in an atypical position, presenting a mesial tilt of approximately 45°, as well as distal rotation of approximately 45°. Immediately superior to the protruding canine cusp, a roughened, irregularly shaped concavity is observed. This feature presents a clearly demarcated and raised perimeter around its extant aspects, with a pitted and porous area observed in the deeper central portion. It is proposed that this may be the remnants of a resorbing alveolus for a deciduous canine (FDI 53), the retention of which caused the impaction of the permanent canine in a similar manner as the fragment described immediately above. The remaining extant teeth appear to be in typical anatomical sequence and alignment. There is slight calculus deposition at the level of the cementum enamel junction for the first and second molars (FDI 16–17). The second molar presents a large, approximately ovoid interproximal carious lesion on the distal aspect at the cementum enamel junction. This observation agrees with the previously mentioned hypothesis that the third molar was lost *antemortem* as a sequala of an infectious insult, the distal interproximal carious lesion described for the second molar would have communicated directly with this pathological process.

Another example of variation in eruption and alignment was observed amongst the assemblage in a fragment of an adult right maxilla derived from Context (951) (Fig. 4.54a to c), which refits with another fragment of adult left maxilla derived from the same stratigraphic unit. The right fragment retains much of the palatine and alveolar processes from the level of the intermaxillary suture and alveolus of the permanent central incisor, moving distally to be truncated behind the permanent first molar, and superiorly at the level of the nasoalveolar clivus, inferior to the infraorbital foramen. The fragmentation has exposed the maxillary sinus. The retained permanent teeth include the canine, first and second premolars and first molar (FDI 13–16). It is difficult to determine with certainty whether the central and lateral incisors were lost *ante-* or *postmortem*, as there is substantial damage to the alveolar process in the anterior maxillary region. The fully erupted canine is observed to be in an atypical position, presenting a mesial tilt of approximately 45°, as well as distal rotation of approximately 45° (Fig. 4.54a & b). The tooth root follows the same tilted trajectory, as observed via fenestration of the canine jugum. There is a slight interproximal gap in the alveolar process between the canine and the first premolar, with the bone surface presenting as slightly pitted and irregular. The remaining extant teeth appear to be in typical anatomical sequence and alignment. Despite the previously mentioned *postmortem* damage, the extant portions of the alveoli for the central and lateral incisors appear to be in typical orientation and alignment, apparently unaffected by the pronounced variation observed for the position and orientation of the canine. All teeth retained in this fragment present slight calculus deposits at the level of the cementum enamel junction.

The articulating (albeit fragmentary) left maxilla also retains the majority of the palatine and alveolar processes, in this case from the level of the intermaxillary suture and alveolus of the permanent central incisor through to the maxillary tubercle at the distal aspect of the alveolar process; and superiorly essentially reflects the preservation of the opposing element. It is fragmented at the level of the nasoalveolar clivus, inferior to the infraorbital foramen, exposing the maxillary sinus. The retained permanent teeth include the second premolar, and first, second and third molars (FDI 25–28). Although there is some *postmortem* damage to the anterior aspect of the alveolar process, the extant portions of the alveoli for the absent central and lateral incisors, canine and first premolar (FDI 21–24) appear to have been patent at the time of death, and there is no evidence for infectious processes or alveolar resorption that might indicate *antemortem* loss. As such, it is suggested that all absent teeth were exfoliated *postmortem*. There is

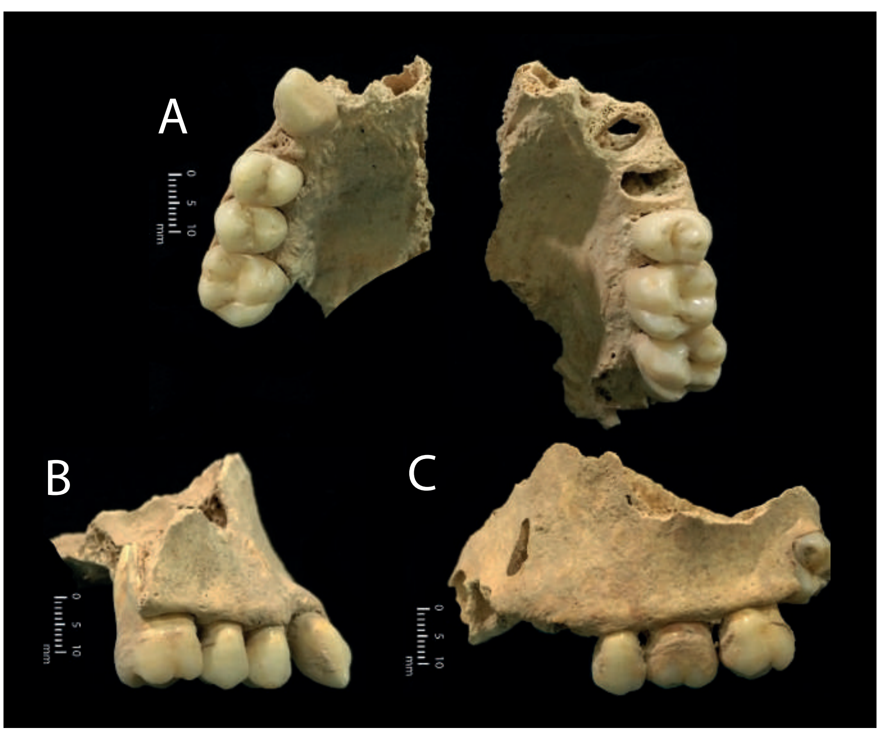

Figure 4.54. *Fragmentary refitting right and left adult maxillae from Context (951) of the Circle sample, detailing a) the fragments in approximate anatomical position, viewed inferiorly (palatal); b) the right maxilla fragment in lateral view, detailing the atypical position and eruption of the permanent canine (FDI 13); and c) the left maxilla fragment in lateral view, detailing the atypical position and impaction of the permanent molar (FDI 28). (Photos Ronika K. Power).*

slight calculus deposition at the level of the cementum enamel junction for the second premolar and first and second molars (FDI 25–27). It is important to note that this fragment also presents evidence of atypical eruption orientation and alignment; here, the permanent third molar (FDI 28) has tilted distally by approximately 45°, laterally by approximately 25°, and has distally rotated by approximately 15° (Fig. 4.54c). The atypical position and orientation has resulted in the impaction of this tooth. There are no osseous indicators for infection or inflammation surrounding the impacted tooth. Note also that this tooth presents a non-metric trait – Carabelli's cusp – an accessory cusp on the lingual surface.

4.5.7.3.7. Variation in eruption or alignment: diastemata

Diastemata (sing. 'diastema') are another dysgnathic variation, in this case referring to superfluous interproximal spacing greater than 0.5 mm persistent in the mouth after eruption of the adult dentition (Lavelle 1970). To be an authentic diastema, spaces must be determined to have a developmental aetiology as opposed to responses to *antemortem* tooth loss, hypodontia elsewhere in the arcade, the presence of a mesiodens between the left and right central incisors, and oral habits such as thumb sucking (Alt & Türp 1998a, 117; Huang & Creath 1995; Scott & Irish 2017, 159; cf Keene 1963). Diastemata are purported to indicate genetic connections within a population (Terwee 1922; cited in Alt & Türp 1998a, 117). They have been observed in individuals from all populations, although high frequencies of the trait have been reported for many Sub-Saharan African groups including the Babinga Pygmies, African San and African Masai (Scott & Irish 2017, 159). Although the relative absence of the trait in populations outside Africa may result from methodological and recording biases as opposed to genuine incidence and prevalence rates, the trait is widely accepted to be less common in other populations and is acknowledged as at least a potential indicator for African presence or admixture amongst archaeological populations (Scott & Irish 2017, 159).

Diastemata are typically observed at the anterior aspect of the arcade. Several examples within the Circle assemblage nicely illustrate this phenomenon, commencing with fragmentary articulating left and right adult maxillae identified within Context (783) (Fig. 4.55a–c). Both left and right fragments retain much of the palatine and alveolar processes from the level of the intermaxillary suture and alveolus of the permanent central incisor, moving distally to be truncated across the alveolus for the permanent third molar on the left, and behind the permanent second molar on the right. Superiorly, the fragmentation margin is traced bilaterally at the level of the nasoalveolar clivus, inferior to the infraorbital foramen. The fragmentation has exposed the maxillary sinus. The retained permanent teeth include the permanent right central incisor through to the permanent second premolar (FDI 11–15); and the permanent left lateral incisor through to the permanent second molar (FDI 22–27). Although there is some *postmortem* damage to the bilateral posterior aspects of the left and right alveolar processes, the

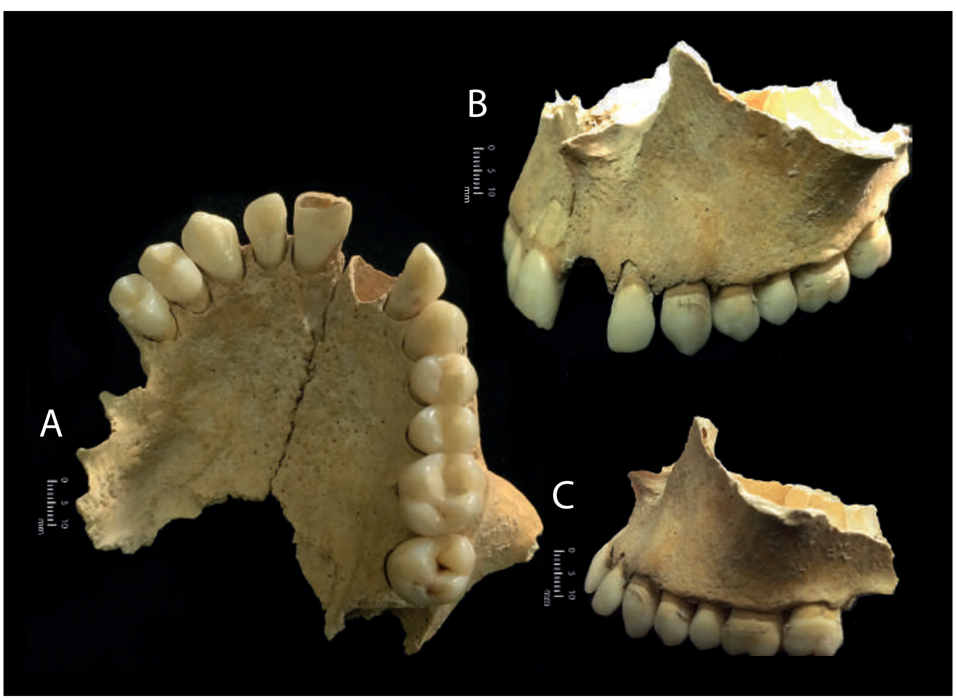

Figure 4.55. *Fragmentary articulating left and right adult maxillae from Context (783) of the Circle sample, detailing multiple diastemata as seen in a) inferolateral; b) left superolateral; and c) left lateral views. Scale bar: 1 cm. (Photos Ronika K. Power).*

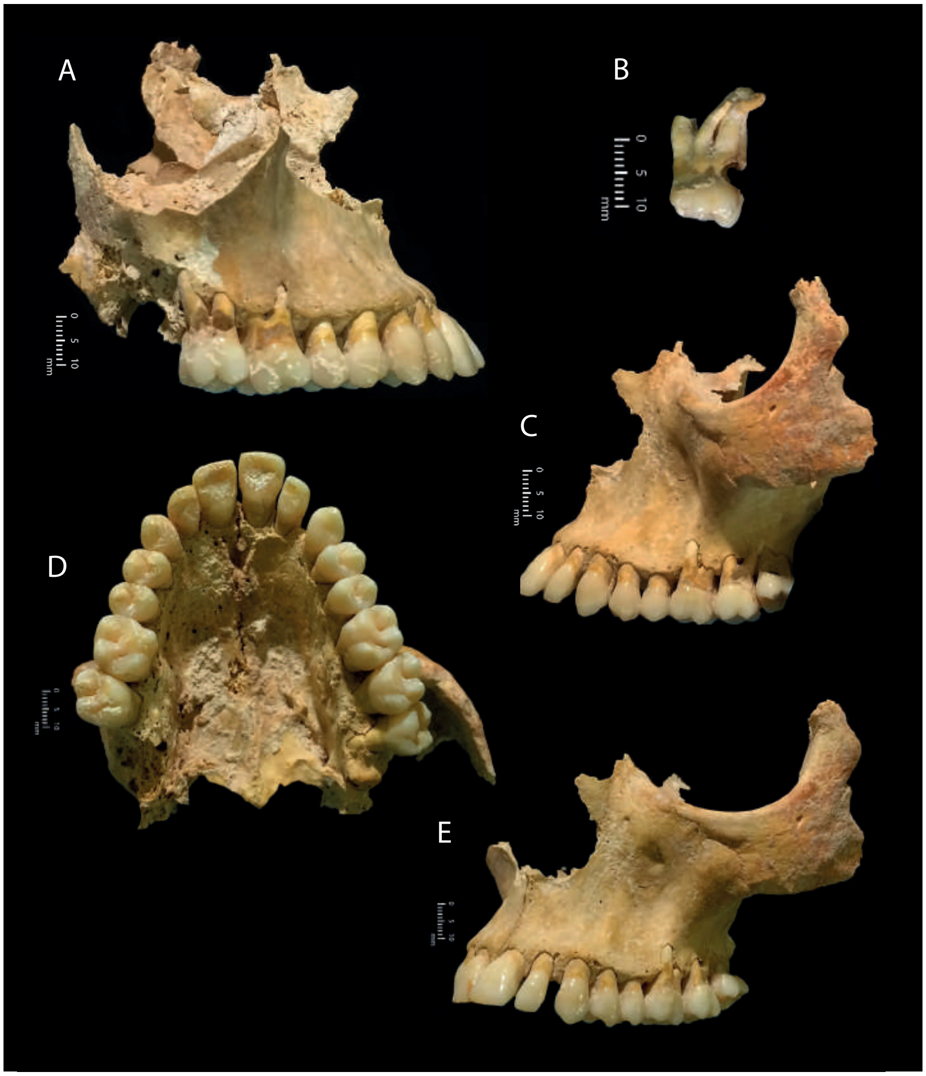

Figure 4.56. *Fragmentary articulating left and right adult maxillae from Context (1268) of the Circle sample, detailing multiple diastemata, prognathism and congenital variation as seen in a) right lateral; b) permanent third molar (FDI 18) displaying accessory root, dilaceration and a cervical carious lesion; c) left lateral; d) inferior (palatal); and e) left anterolateral views. Scale bar: 1 cm. (Photos Ronika K. Power).*

extant portions of the alveoli for the absent permanent right third molar (FDI 18) and permanent left central incisor (FDI 21), and first, second and third molars (FDI 26–28) appear to have been patent at the time of death, and there is no evidence for infectious process or alveolar resorption that might indicate *antemortem* loss. In this case, multiple diastemata are observed in the anterior arcade as patent spacing between the permanent right central and lateral incisor (FDI 11 and 12) and the permanent right lateral incisor and canine (FDI 12 and 13); as well as the permanent left lateral incisor and canine (FDI 22 and 23). It is possible that further diastemata may have persisted in the anterior arcade, however the *postmortem* exfoliation of the permanent left central incisor (FDI 21) renders further observations impossible. The anterior aspect of the arcade presents as slightly prognathic (Fig. 4.55c). Furthermore, the permanent right central incisor (FDI 11) has been subject to active focal modification in the form of a steep diagonal distally inclined incisal margin; the extant neighbouring tooth (permanent right lateral incisor (FDI 12) presents no signs of modification. Dental modification amongst the Circle burial population will be discussed in detail in Chapter 5.

Another pair of articulating, albeit fragmentary, left and right maxillae were observed to present diastemata in Context (1268) (Fig. 4.56a–e). The right fragment retains much of the palatine and alveolar processes from the level of the intermaxillary suture and alveolus of the permanent central incisor, moving distally to present slight *postmortem* damage to the alveolus for the permanent third molar and alveolar tubercle. Superiorly, the fragmentation margin runs across the level of the nasoalveolar clivus, inferior to the infraorbital foramen. The fragmentation has exposed the maxillary sinus. The retained teeth include all right permanent maxillary dentition (FDI 11–18); the permanent third molar (FDI 18) has been exfoliated because of the previously mentioned *postmortem* damage, however it is extant and curated with the remains of this individual. This tooth presents additional congenital variations in the form of an accessory root as well as dilaceration and a cervical carious lesion (Fig. 4.56b; cf §4.5.7.3.2–3, above). Each of the right molars present large, approximately ovoid-shaped buccal cervical carious lesions (FDI 16–18), extending from the cementum enamel junction to the bifurcation point of the buccal roots. In the case of the second molar (FDI 17), the lesion extends even further on to the individual buccal roots. There are indications of inflammatory processes across the right side of the arcade, with pitting and resorption evident across the buccal aspect of the alveolar process. The articulating left maxilla is almost complete and intact; only a small amount of *postmortem* damage is observed to the frontal process and the inferolateral border of the nasal aperture. The left zygoma is also in articulation, and is also almost complete and intact except for a small amount of *postmortem* damage to the temporal process. All left permanent maxillary dentition are present in occlusion (FDI 21–28). As observed for their antimeres, each of the left molars present approximately ovoid-shaped buccal cervical carious lesions (FDI 26–28), in this case distally progressing in size from 'small' on the first molar to 'large' on the third molar, although no left-sided lesions traverse the bifurcation points to compromise the buccal roots. As described for the right side, indications of inflammatory processes are observed on the left arcade, with pitting and resorption also evident across the buccal aspect of the alveolar process. A dysgnathic variation is also observed (§4.5.7.3.6, above) in the alignment profile of the left permanent third molar (FDI 28); it is tilted approximately 45° in buccal incline. In this case, multiple diastemata are observed in the anterior arcade, commencing with a mesial diastema between the permanent left and right central incisors (FDI 11 and 21), and as patent spacing between the permanent right central and lateral incisor (FDI 11 and 12) and the permanent right lateral incisor and canine (FDI 12 and 13); as well as the permanent left central and lateral incisors (FDI 21 and 22), and the left lateral incisor and canine (FDI 22 and 23). Note that the anterior aspect of the arcade presents pronounced prognathism.

A further example of diastemata within the current Circle study sample was observed on another articulating pair of fragmentary left and right maxillae identified in Context (1328) (Fig. 4.57a). Here, the right maxilla is almost complete and intact; only a small amount of *postmortem* damage is observed to the frontal process. The right zygoma is also in articulation, and is also almost complete and intact except for a small amount of *postmortem* damage to the temporal and frontal

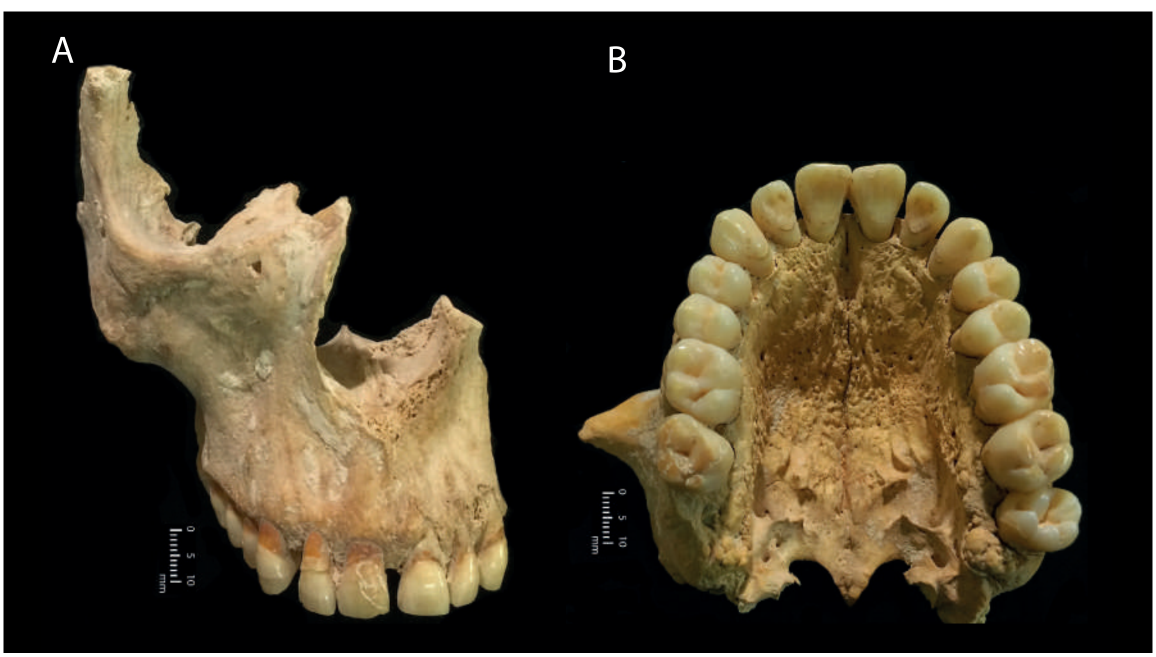

Figure 4.57. *a) Fragmentary left maxilla, articulated with right maxilla and zygoma Context (1328) of the Circle sample, detailing multiple diastemata in anterosuperior view; b) fragmentary articulating left and right adult maxillae from Context (1206) of the Circle sample, detailing multiple diastemata in inferior (palatal) view. Scale bar: 1 cm. (Photos Ronika K. Power).*

Figure 4.58. *Fragmentary splanchnocranium of adult individual from Context (1206) of the Circle sample, detailing extant diastema in a) anterior and b) right anterolateral views. Scale bar: 1 cm. (Photo Ronika K. Power).*

processes. All right permanent maxillary dentition are present in occlusion (FDI 11–18), however there are several indications of *postmortem* damage and taphonomic change to the teeth, including cracking, flaking, root etching and colour change. The left fragment has suffered substantial *postmortem* damage; only the anterior aspect of the element is intact, with the palatine and alveolar process retained from the point of the intermaxillary suture to the canine distal interdental septum. The fragmentation margin extends superiorly to be truncated approximately 3.0 mm lateral to alare. *Postmortem* damage is observed around the border of the nasal aperture and the floor of the nasal cavity. The left fragment retains the permanent central and lateral incisors and canine. There is no evidence for carious lesions on any of the extant teeth, and there does not appear to be any indication of infection or inflammation on the extant alveolar process. Once again, multiple diastemata are noted in the anterior arcade, including a mesial diastema between the permanent left and right central incisors (FDI 11 and 21), and as patent bilateral spacing between the permanent right and left lateral incisors and canines (FDI 12 and 13; FDI 22 and 23). Prognathism is also observed for this individual.

A complete and intact maxillary arcade precipitating from Context (1206) also presents multiple diastemata (Fig. 4.57b). The arcade is comprised of a pair of left and right maxillae fused along the median palatine suture. All elements of the hard palate are complete and intact; however the superior aspects of the maxillae have been subject to substantial *postmortem* damage. The fragmentation margin runs across the level of the nasoalveolar clivus, inferior to the infraorbital foramen. The fragmentation has exposed the maxillary sinus. The retained teeth include all right permanent maxillary dentition (FDI 11–18), although the third molar is impacted with the crown visible through an aperture in the alveolar process. All left permanent dentition are erupted and in occlusion (FDI 21–28), with slight impaction of the third molar (FDI 28) caused by mesial tipping of <15°. There is no evidence for carious lesions on any of the extant dentition, and although there are slight extant calculus deposits on the lingual aspects of several of the teeth inferior to the cementum enamel junction, there does not appear to be any indication of infection or inflammation on the extant alveolar process. In this case, bilateral diastemata are observed between the right and left central and lateral incisors (FDI 11 and 12; FDI 21 and 22), as well as between the right and left lateral incisors and canines (FDI 12 and 13; FDI 22 and 23).

A fragmentary splanchnocranium of an adult individual excavated from Context (1206) presents a patent diastema in the extant dental arcade (Fig. 4.58a–b). The facial skeleton consists of a partial left zygoma, fragmented at the root of the temporal process, but otherwise intact; a partial left maxilla, which is fragmented at the inferolateral aspect of the nasal aperture, and the frontal process is absent; additionally, the left maxilla retains all dentition from the left permanent canine through to the third molar (FDI 23–28), while the central and lateral incisors are absent (FDI 21–22). There does not appear to be any indication of infection or inflammation on the extant alveolar process and it is proposed that these teeth were exfoliated *postmortem*. The right maxilla is effectively intact; however, the right permanent central incisor is absent (FDI 11). As for the opposing elements, there also does not appear to be any evidence of infection or inflammation on the extant alveolar process and it is proposed that this tooth was lost *postmortem*. There is no evidence for carious lesions on any of the extant dentition, although there are slight extant calculus deposits on the buccal aspects of several of the teeth inferior to the cementum enamel junction. Like its antimere, the right zygoma is fragmented at the root of the temporal process, but is otherwise largely intact. The frontal bone is less than 50% complete, with the fragmentation margin extending from the approximate midway point of the right temporal line, running below the right frontal eminence, across the midline of the frontal squama, then descending to truncate the left aspect of the element medial to the superomedial border of the left orbit. The right orbital roof is partially retained. The right nasal bone is intact, while the left has sustained some damage around the lateral margin. The vomer, nasal conchae, sphenoid and lacrimal bones are all absent. A diastema is observed between the right lateral incisor and canine (FDI 12 and 13). Although the spacing of the interradicular septum presents on the left alveolar process appears similar to the opposing side, unfortunately the *postmortem* loss of the left lateral incisor (FDI 22), or indeed of both right and left central incisors (FDI 11 and 21), obfuscates observations as to whether there was bilateral (or multiple) presentation of this phenomenon.

The final example of diastemata observed within the study sample was observed on a pair of fragmentary articulating left and right maxillae from Context (845) (Fig. 4.59). Only small portions of the anterior aspects of these elements are represented: on both left and right sides, the palatine and alveolar process are retained from the point of the intermaxillary suture to the first premolar distal interdental septum. Superiorly, the fragmentation margin runs across the level of the nasoalveolar clivus, inferior to the infraorbital foramen. The fragmentation has exposed the maxillary sinus. The retained teeth include the right permanent central and lateral incisors, canine and first premolar (FDI 11–14), and the left permanent central and lateral incisors and canine (FDI 21–23). There is no evidence for carious lesions on any of the extant dentition, and there does not appear to be any indication of infection or inflammation on the extant alveolar process. Multiple bilateral diastemata are observed here: commencing with the mesial diastema between the central incisors (FDI 11 and 21); followed by additional spacing between the central and lateral incisors on both the right and left sides (FDI 11 and 12; 21 and 22), as well as between the left and right lateral incisors and canines (FDI 12 and 13; 22 and 23).

Figure 4.59. *Fragmentary articulating left and right adult maxillae from Context (845) of the Circle sample, detailing multiple diastema in inferior (palatal) view. Scale bar: 1 cm. (Photo Ronika K. Power).*

4.5.7.3.8. Morphological variation of the mandible

A fragment of left mandibular corpus was observed within Context (876) (Fig. 4.60a–e). This context was a layer of soil in the East Cave, where the fragment lay immediately beside another adult mandible, in stratigraphic association with five adult skulls, 374 other human bones, and a mixture of ceramic material from various phases of the late Neolithic. Beneath this layer lay a 25 cm-thick blanket-like spread of limestone roof collapse and, under this, a megalithic threshold slab that once connected the central part of the cave and its southeast corner (Stoddart *et al.* 2009c: Fig. 8.65 & 168). The archaeological context of the mandible fragment was therefore one of cave roof collapse, so its precise date cannot be read from its stratigraphic position. Unfortunately, a sample of bone tissue from the mandible failed to produce enough collagen for a radiocarbon determination, so its date can only be given as broadly ascribed to the main Tarxien phase of burial at the site, i.e. 2900–2350 cal. BC (Chapter 7). The fragment was initially examined macroscopically in the National Museum of Archaeology, Valetta,

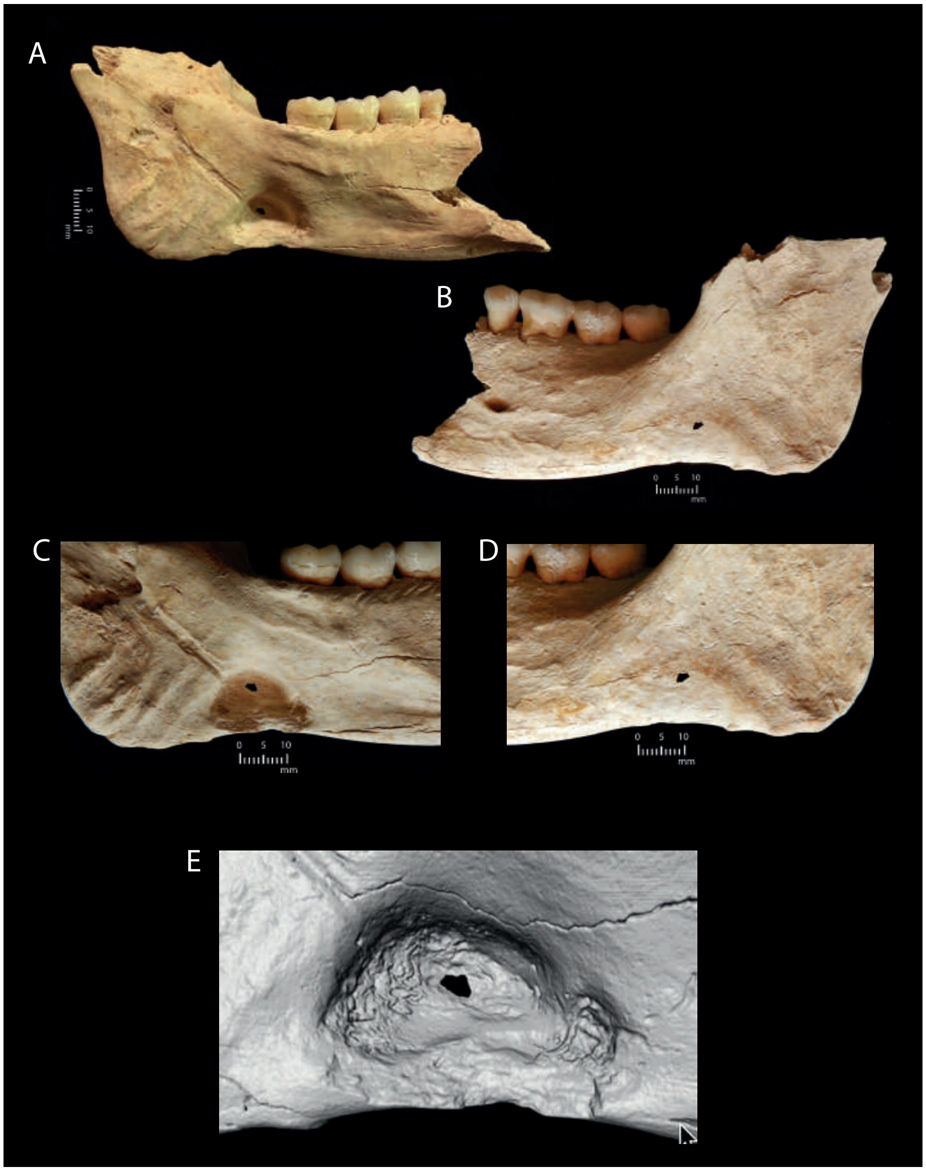

Figure 4.60. *Fragmentary left adult mandibular corpus from Context (876) of the Circle sample, shown in a) lingual view; b) buccal view; c) detailed lingual view, featuring defect; d) detailed buccal view, featuring small area of* postmortem *damage; e) detailed 3D render, featuring defect. Scale bar: 1 cm. (Photos Ronika K. Power; radiological images captured by L.T. Buck, Cambridge Biotomography Centre; processed by J. Magnussen & M. Pardey, Macquarie Medical Imaging).*

and was then subject to further analysis via micro-CT-scanning with a Nikon Metrology XT H 225 ST at the Cambridge Biotomography Centre (UK). The CT-scans were captured by L.T. Buck in the Cambridge Biotomography Centre, according to the procedure outlined in §4.4, above.

Both macroscopic and radiological analyses confirm that the element was subject to *postmortem* breakage at its anterior and superoposterior aspects. When viewed anterolaterally, the anterior fragmentation margin is located just mesial to the alveolus of the second left permanent mandibular premolar, extending inferiorly to pass just anterior to the left mental foramen, then extending inferiorly and anteriorly to terminate at the most lateral aspect of the mental trigone. When viewed anterolaterally, the superoposterior fragmentation margin is located on the superior aspect of the ascending ramus: on the anterior aspect, the coronoid process is absent, as well as the mandibular notch; on the posterior aspect, the mandibular condyle and neck are also absent. The only retained teeth are the fully erupted left permanent mandibular second premolar, and the first-to-third molars (FDI 35–38).

The gonial angle is present, and is observed to be quite robust and square, although with minimal flaring (Buikstra & Ubelaker 1994, 20, Fig. 4). The attachments for *M. masseter* are quite rugose at both lateral and medial sites. The mandibular corpus is relatively robust in terms of both thickness (maximum 17.6 mm) and height (maximum 33.1 mm). The ascending ramus appears to be extending from the corpus at an angle of approximately 90°. As such, it is suggested that this is the remnant of an adult, possible male mandible.

The retained teeth present mild occlusal wear, indicating that they were in use in the mouth. For the second premolar (FDI 35), the wear platform is focused on the mesial aspect of the buccal cusp and is slightly diagonal/inferior in orientation. The wear platform is similar across the first-to-third molars (FDI 36–38), as it is focused on the buccal aspect and presents a diagonal/inferior orientation. Crown morphology is generally well-preserved for all teeth, although very small amounts of dentine exposure are noted on the protoconid and hypoconid of the first molar (FDI 36). No carious lesions are observed on any extant dentition.

There is a small extant calculus deposit observed on the left permanent third mandibular molar (FDI 38), traversing from the most buccodistal to the most linguomesial aspects of the tooth at the cementum enamel junction. A second small calculus deposit is observed on the left permanent mandibular second premolar (FDI 35), extending from the most-linguomesial to interproximal aspect of the tooth at the cementum enamel junction. It is possible that the calculus deposits may have been more extensive across the dentition, as staining of the teeth superior to the cementum enamel junction (particularly observed on the lingual aspect of the left permanent second mandibular molar; FDI 37) suggest that calculus may once have been present but has subsequently been removed as a result of post-depositional and excavation processes.

There is some resorption of the alveolar process inferior to all retained teeth. When viewed from the lateral aspect, the alveolar process appears to have resorbed by approximately <30%, exposing the superior portion of the roots of the retained teeth. Microporosity (<1 mm Ø) is observed anterior to the second premolar on the lingual aspect of the alveolar process, and between the alveolar margins of the first and second, and second and third left mandibular permanent molars (FDI 36–38). These observations are consistent with mild periodontal disease.

A large defect is observed on the medial aspect of the element (Fig. 4.60a, c, e). This feature presents as a discrete area of bone absence, located on the posteroinferior aspect of the medial mandibular corpus. The inferior aspect of the mylohyoid line terminates in the posterosuperior aspect of the feature. The feature is approximately hemispherical-to-lozenge shaped and has smooth, rounded walls and margins comprised of compact bone. There is no evidence of woven bone deposition. The feature can best be described as though bone has been 'scooped-out' of the mandibular corpus. The maximum dimensions of the lesion are 19.2 mm width and 13.0 mm height. There is a smaller feature within the perimeter of the major feature, located at its anteroinferor-most aspect. This smaller feature is also approximately hemispherical, with smooth but billowing walls. The maximum dimensions of the smaller lesion are 2.7 mm width and 3.0 mm height. There is a small perforation in the lateral wall of the major feature, measuring approximately 2.5 mm wide and 1.5 mm high. The sharp, irregular margins of this perforation indicate that it is a result of *postmortem* damage. There appears to be further *postmortem* damage running along the most inferior aspect of the feature, characterized by a ragged, uneven fracture margin. The margins of the feature are sharply defined and there is clear preservation of the cortex.

On the buccal aspect of the fragment, just lateral to the left permanent third mandibular molar (FDI 38), there is considerable bony bossing and thickening of the oblique line, and there is also evidence of more extensive bossing towards the inferior attachment of *M. masseter*.

The trabeculae throughout the extant mandibular fragment are very well-defined without evidence of sclerosis, eliminating chronic infection or inflammation as differential diagnoses. The canal for the inferior alveolar nerve is well-demonstrated and it is filled with mixed-density material with small particles of higher-point density, most likely to be dust or depositional matrix.

Overall, the appearance of this feature aligns with extrinsic, pressure-related modelling of the bone rather than an invasive process, and there is no indication that it is a primary mandibular cystic lesion which has then eroded out through the lingual surface. The anatomical position of this change is such that it may abut the submandibular gland, with possible aetiologies including submandibular, sublingual or salivary gland enlargement: either tumour, infection or impaction with gradual glandular expansion. There is also a very fine, ridge-like impression which extends from the posterolateral aspect of this depression and extends superiorly – considering that no normal structure exists in this location, it is possible that this feature represents the impression of a vessel against the bone as it was compressed by the submandibular gland.

Finnegan and Marcisk (1980, 19–20) reviewed 260 cases in the clinical, radiological, surgical and histological literature pertaining to depressions located near the angle of the mandible, with the defect variably referred to as latent bone cysts (Fordyce 1956; Nishijima *et al.* 1969; Rushton 1946; Thoma 1955; Yoshiga *et al.* 1973); mandibular embryonic defect (Jacobs 1955); static bone defect cavity (Bernstein *et al.* 1958; Choukas & Toto 1960; Fontaine *et al*. 1966; Glahn & Rud 1962; Karmiol & Walsh 1968; Mack &

Woodward 1969; Menzel 1968; Stafne 1942); aberrant salivary gland defect (Amaral & Jacobs 1961; Araiche & Brode 1959; Hayes 1961; Richard & Ziskind 1957; Sugawara 1972); idiopathic bone cavity (Bergenholtz & Persson 1963; Boerger *et al.* 1972; Drinnan 1974 Senno *et al.* 1969); ectopic salivary gland of the mandible (Abramson 1966; Friedman 1964; Forrest 1974; Slavin 1950); and lingual mandibular bone cavity (Alvares *et al.* 1969; Ito *et al.* 1974; Olech & Arora 1961). The fundamental report in all these cases was that of Stafne (1942), and this defect has now become eponymous to him, attributed as a developmental defect of the mandible, or Stafne's so-called defect of the mandible (Abe *et al.* 1974; Harvey & Noble 1968; Oikarinen & Julku 1974; Stene & Pedersen 1977; Tolman & Stafne 1967; Uemura *et al.* 1976).

Radiological descriptions of the Stafne defect are generally characterized as round or oval, unilocular, well-circumscribed, corticated and with uniform radiolucency (Whaites 2007; cf Lukacs & Rodríguez Martin 2002; Wasterlain & Silva 2010). One of the principle diagnostic criteria is that the mandibular cavity is always open on its lingual aspect and there is no compromise of the mandibular cortical bone (Araújo *et al.* 2009). The Stafne defect bears striking resemblance to the feature described for the mandibular fragment excavated from Context (876) in terms of size, placement and character. As with the Circle individual's case, these defects are most commonly observed below the third molar or between the third molar and the angle of the mandible (66.6%; Finnegan & Marcisk 1980, 26; cf Regezi *et al.* 2000; Shafer *et al.* 1983; Soames & Southam 2005; Wasterlain & Silva 2010); on the left side (52.8%; Finnegan & Marcisk 1980: 26; occasionally bilateral (Queiroz *et al.* 2004; Shafer *et al.* 1983; Wasterlain & Silva 2010); below the mylohyoid line (100%; Finnegan & Marcisk 1980, 27); with the widest portion parallel to the inferior border of the mandible (Vodanović *et al.* 2009; Whaites 2007); and on males (70.7%; Finnegan & Marcisk 1980, 26; Wasterlain & Silva 2010: 427; in clinical studies, this attribution is even higher at 84%; Uemura *et al.* 1976). The Circle mandible's defect is much larger than the average reported for archaeological populations, with a maximum Ø of 19.2 mm (*versus* $\bar{x}$ 10.1 mm; Finnegan & Marcisk 1980, 27).

In clinical contexts, Stafne defects are generally detected incidentally on oral radiographical examinations, and only infrequently present symptoms such as low-level regional pain or swelling (Apruzzese & Longoni 1999; Harvey & Noble 1968; Quesada-Gómez *et al.* 2006; Wasterlain & Silva 2010). The aetiology of the Stafne idiopathic bone defect is unknown. In the clinical literature, only one pathology seems to be related to the defect pleomorphic adenoma, or a neoplasm of granular epithelium (Finnegan & Marcisk 1980, 27; Simpson 1965). Further considerations in terms of differential diagnosis include benign non-ossifying fibroma which, by nature, is only rarely preserved by calcification, however its presence can be detected by smoothly delineated areas of lytic destruction caused by pressure atrophy (Strouhal 1998, 278; Wasterlain & Silva 2010). It has also been postulated that they are congenital, or associated with some form of pressure resorption (Wasterlain & Silva 2010). Especially in archaeological materials, it is almost impossible to determine a causal link between these phenomena, as they could equally have independent aetiologies (Finnegan & Marcisk 1980, 27; Simpson 1965). Further options might include traumatic or hemorrhagic cysts, however these are more commonly clinically seen on individuals in the first two decades of life (Daramola *et al.* 1978; Ivy & Curtis 1937; Jacobs 1955; Jaffe & Lichtenstein 1942; Killey & Kay 1972; Leemkuil 1958). The general consensus, however, is that the Stafne defect is formed as a result of focal pressure-atrophy or resorption of the cortical bone. Variations are presented according to the structures responsible for the pressure, including hyperplasia of the submandibular, sublingual and/or parotid salivary glands (Barker 1988; de Courten *et al.* 2002; Philipsen *et al.* 2002; Wasterlain & Silva 2010; Wood & Goaz 1997); muscular, fibrous connective tissue, lymphatic or adipose tissues or blood vessels (Wasterlain & Silva 2010); the facial artery (Ariji *et al.* 1993); or intermitted gland herniation (Sandy & Williams 1981; cf Iwanaga *et al.* 2019; Liu *et al.* 2018; Mann & Tuamsak 2016).

As a result of its distinctive size, shape, character and location in the mandible as reported in both archaeological and clinical literature, the feature described for the mandible fragment from Context (876) is attributed with greatest confidence as a Stafne idiopathic bone defect. This finding identifies for the first time the presence of this trait in the Maltese osteological record, and alongside the Neolithic Portuguese individual from Tholos de Paimogo I (3090–2580 cal. BC (Sac-1556, 4250±90 BP)) is amongst the oldest examples ever published (Wasterlain & Silva 2010). The Stafne defect has been described for individuals in archaeological populations from North America, Hungary, Tenerife, Slovakia, Croatia and Portugal, (Assis *et al.* 2018; Finnegan & Marcisk 1980; Graham 1980; Harvey & Noble 1968; Jordana *et al.* 2007; Keith 1975; Lukacs & Rodríguez Martin 2002; Mann 1990; Mann & Tsaknis 1991; Mann & Shields 1992; Masnicová & Beňuš 2003; Morse 1968; Shields 2000; Vodanović *et al.* 2009, Table 1; Vodanović *et al.* 2012; Wasterlain &

Silva 2010). The case described here represents an invaluable addition to understanding the incidence of this trait amongst human populations, and provide further insights into its incidence across temporal, geographical, environmental and cultural contexts.

4.6. Discussion

4.6.1. Limitations of study

The Circle assemblage has not been fully excavated, nor has the excavated population been exhaustively analysed. We therefore underscore our awareness that any results and interpretations presented here should only be perceived as a minimum number of incidences, and not as overall statistical prevalence of a complete burial population. Notwithstanding these factors, the sheer size of the sample should ensure our data are sufficiently powered to reveal trends across the centuries. Ongoing studies by the current authors will seek to further elucidate all aspects of the lived experiences of the Neolithic community interred in this space, including their dental pathology.

Concerning chronology, a degree of uncertainty and noise are inherent in data such as these. Although the archaeological contexts can be well-dated thanks to Bayesian modelling, the situation and mobility of individual skeletal elements, particularly teeth, are not necessarily stratigraphically secure in a culturally modified depositional context such as the Circle. Despite the inherent challenges of disarticulated and commingled material, we made concerted efforts to ensure that the study sample incorporated both spatial and stratigraphic considerations from across the Circle, as it was apparent upon excavation that particular zones were favoured for use at certain times (Stoddart *et al.* 2009c). The broad trends revealed here support those observations.

In terms of methodology, we acknowledge that the majority of the sample were not examined using light microscopy, scanning electron microscopy, or micro-CT scanning, as it was beyond the temporal, logistical and pecuniary parameters of the current project. As stated in §4.4, above, every tooth was examined macroscopically, observations were enhanced using a 10x magnification hand lens, and only some elements were selected for micro-CT scans. Furthermore, this study operated under inherent methodological constraints that somewhat delimit demographic analyses. As a result of the highly fragmentary, predominantly disarticulated and commingled nature of the Circle burial population, we were unable to record sex for the majority of the study sample, and could only record age insofar as noting whether dentition were 'permanent' or 'deciduous'. As such, our capacity to apportion detailed demographic interpretations to the pathology observed within the study sample is limited. Moreover, we are aware that general disciplinary protocols do not favour the reporting of dental pathologies as a percentage of all teeth present (Hillson 2005, 295), however the nature of this assemblage makes it practically impossible to do otherwise. The insights afforded by our single element methodology have demonstrated the utility of this approach for this type of skeletal assemblage.

4.6.2. The Circle in context

At present, less than two dozen late Neolithic funerary sites are known from across Malta and Gozo (Chapters 2, 13 & 14; cf Malone *et al.* 2009d). Relatively little is known about the context and distribution of human remains at many sites because of their antiquarian date of excavation, consistent with contemporaneous global archaeological praxes. As discussed in the Introduction (Chapter 1), skeletal remains were frequently overlooked in favour of material culture and were not recorded carefully, although Tagliaferro's (1912) description of the human remains from Bur Mgħez cave provides a notable exception. As a result, the burial populations from many well-known funerary sites (including the UNESCO-inscribed Ħal Saflieni Hypogeum) remain to be studied utilizing current standards, methodologies and techniques. Skeletal remains from contemporary Maltese late Neolithic sites provide a large comparative resource for the Circle population. As yet, however, this study provides the largest analysis of dental health and pathology for late Neolithic Malta, presenting significant findings which warrant greater comparative regional studies.

Perhaps the only other published osteological analysis of Neolithic Maltese remains to date are presented within Evans' (1971) compendium of prehistoric Maltese sites. The excavation of the Xemxija Tombs 1–6 in 1955 by John Evans and his team uncovered almost 15,000 fragments of human remains distributed across the six tombs in a similarly commingled and disarticulated state as the rock-cut tomb at the Circle and Circle itself (Evans 1971, 112–6). A brief inventory of the human remains and overview of several identified cases of pathology and trauma are outlined by Pike (1971) while Rodgers (1971) presented an overview of the dentition, including dental pathology. Rodgers tabulated 728 teeth in total (including those in occlusion and loose), although it should be noted that this differs from the number currently present in the assemblage. From a total of 384 adult teeth from the Xemxija Tombs, caries was the most prevalent pathology (Σ=53 cases), hypoplasia was minimal (Σ=20), and periodontal disease and AMTL appeared to be similarly low (Rogers 1971, 238). Interestingly, what we refer to here as extreme wear was noted on seven teeth (three single-rooted teeth worn to the cervix, and four molars with buccal cusps worn to the cervix; Rodgers 1971, 238). A total of four abscesses were recorded, including three abscesses of the lower first premolar associated with crown loss (perhaps because of caries, extreme wear or fracture; Rodgers 1971, 238). Across 328 loose deciduous teeth, caries (Σ=3), wear (Σ=2) and hypoplasia (Σ=1) were observed, all with low incidence rates. Further pathologies noted included one case of an impacted third molar, one cyst affecting the central incisors, and a case of possible malocclusion of the mandibular central incisors (Rodgers 1971, 239). It is difficult to compare these results with the present study, however, because of the lack of photographic evidence presented in Evans (1971) and the minimal detail provided by Rodgers (1971), although there do appear to be some broad similarities with the Circle sample presented here. It is thus necessary to return to the remaining dentition in the preserved Xemxija Tombs assemblage to provide an updated account of the presence and incidence rates of dental pathologies, and especially to identify whether unusual pathologies observed within the Circle assemblage (i.e. crescentic wear, complicated crown and root fractures) are also present in the Xemxija Tombs burial population.

The dental pathology of the remains of the Circle can be placed within the broader trends associated with long-term cultural change and dietary transitions associated with the transition to agriculture. As the dentition included in the current study represent different temporal and cultural phases within a Neolithic population, it is not possible to study changes in dental pathology around the transition to agriculture locally. Indeed, it is probable that the islands were settled by early Neolithic farmers, and as such, there was no local transition from foraging to farming. The analyses presented here, however, can provide insight into variation in dental health within Neolithic Malta and comparative perspectives relative to early farming populations elsewhere in the Mediterranean and beyond.

Studies of assemblages associated with the adoption of agriculture in the Levant (Smith *et al.* 1984) and North America (Cook 1984; Goodman *et al.* 1980, 1984a, 1984b; Larsen 1995; Sciulli 1977, 1978) have found that enamel hypoplasia became more common following the shift in subsistence strategies. It is argued that the sources of increased stress experienced by these populations may have been because of dependence on decreased or fewer food resources, in conjunction with the increased exposure to infectious disease as a result of sedentism and population growth and density (Hillson 2005, 176). A similar increase in the frequency of enamel hypoplasia was noted among the early Neolithic (Predynastic) populations of the Nile, but subsequently frequencies dropped with the development of the Dynastic system and enhanced trade and distribution networks (Starling & Stock 2007). The frequencies of hypoplasias among the Neolithic population of Malta remain relatively low compared with agricultural populations elsewhere but increase in the final phases, suggesting an increase in developmental stress, either through reduced environmental productivity or more variable resource distribution in these later phases.

Increase in the incidence of carious lesions following the adoption of agriculture have also been noted elsewhere (Hillson 2005, 301), with caries rates reported as being as much as twice as frequent and severe in some agriculturalists as compared with some foragers (Ortner 2003, 591). As for enamel hypoplasia, this phenomenon has been attributed to the relative malnutrition experienced in the former group, which can reduce enamel quality and therefore increase vulnerability to caries, as well as elevated levels of dietary carbohydrates. These factors, in conjunction with the sources of non-specific stress mentioned above associated with agricultural subsistence strategies, appear to have led to significant decline in oral health for many populations through the Neolithic transition. Perhaps foremost amongst them is population density: caries is, after all, essentially an infectious and transmissible disease (Pindborg 1970, 256). It is important to note, however, that recent studies in Southeast Asia and the Levant have revealed that correlation between agricultural subsistence transitions and poor dental health is not universal (Eshed *et al.* 2006; Pietrusewsky & Douglas 2001; Tayles *et al.* 2000).

The cultural significance of these findings becomes even more prominent when organized according to chronological sequence, as shown in Table 4.3 and represented graphically in Figure 4.61. Broad trends in the data exist and are visualized here by plotting the occurrence rate per context of enamel hypoplasia, caries, crown fractures, extreme wear and hypercementosis are alongside dental modification (Chapter 5), nitrogen isotope values (Chapter 10) and burial density (Chapter 3). Despite the clear trends that emerge, it is noteworthy that sample prevalence rates of all pathologies are relatively low throughout the use-life of the Circle, ranging between 1.0–12.0% across the timeframe under study.

For all pathologies, with the exception of enamel hypoplasia, we see the highest sample prevalence

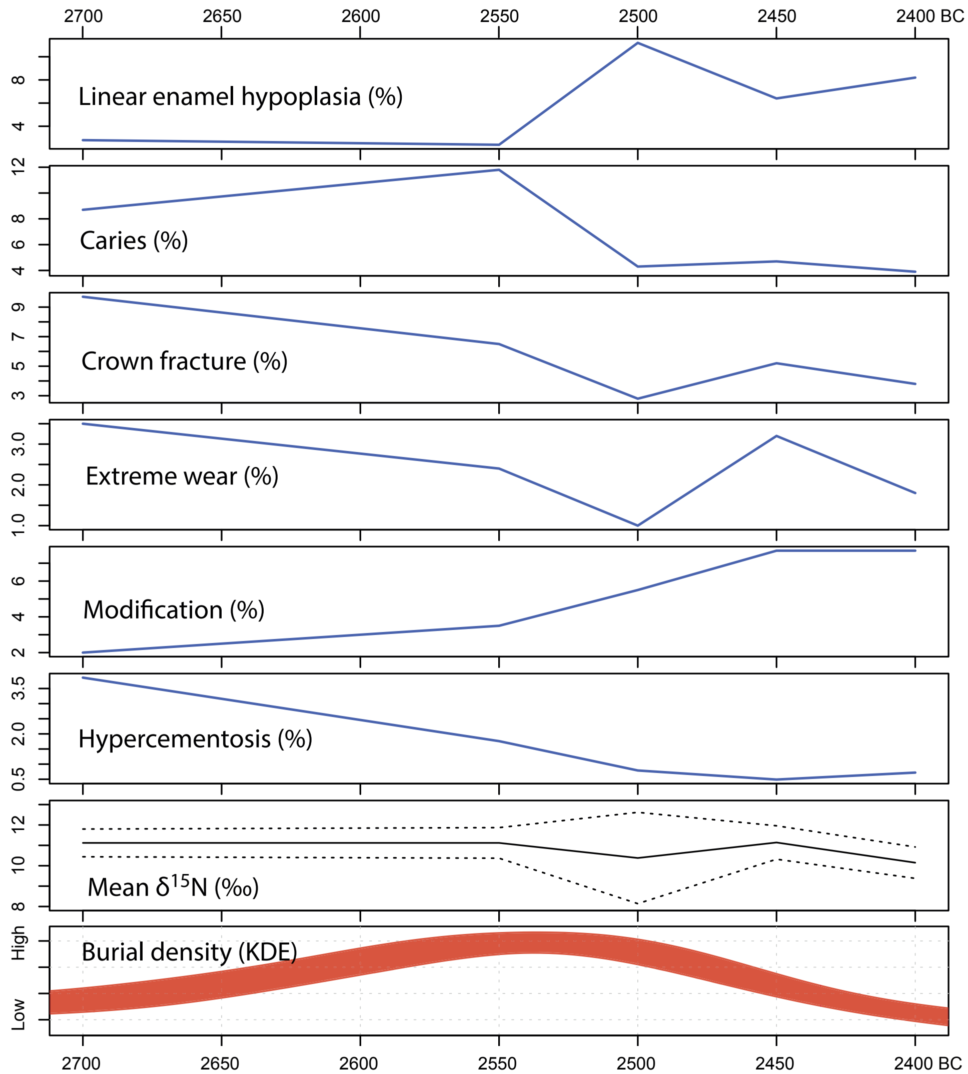

Figure 4.61. *Schematic chronological representation of dental pathology incidence within the Circle sample, also featuring dental modification, average nitrogen isotope values and burial density from ~2700–2400* BC. *(Rowan McLaughlin).*

during the earlier use phases of the Circle, around 2700 BC. This can be broadly read as indicative of a stress response by some individuals to environmental factors. It is important to note that the 'environmental' aetiology of the particular stress responses featured here (caries, crown fractures, extreme wear and hypercementosis) may be attributed to exogenous factors including high carbohydrate diets and poor dental hygiene (§4.5.3 & §4.5.4) and use of the mouth in habitual or 'occupational' behaviours such as craft or food production (§4.5.5.1 & §4.5.6), as opposed to more endogenous biological factors such as disease processes or malnutrition commonly associated with enamel hypoplasia (§4.5.1). Over and above the rudimentary hygiene levels axiomatic to Neolithic populations, these results may indicate that the mouth was an important apparatus within the prehistoric Maltese toolkit during this occupational phase, subject to its own suite of mechanical stressors alongside other parts of the body.

We see a gradual decrease in crown fractures, extreme wear and hypercementosis from around 2700 and 2550 BC, with further decline in these pathologies until 2500 BC. Conversely, caries prevalence amongst the sample appears to gradually increase from 2700 BC until 2550 BC, at which point it steeply declines until 2500 BC. At this critical chronological point, nearing the end of the Neolithic period, caries, crown fractures and extreme wear each present increased prevalence rates. This was also the point in time when burial and probably all forms of activity in the Circle was at its most intense (Chapter 3). The closing decades of the site, as activity began to fade away, saw a concomitant decline in the prevalence of these pathologies. Hypercementosis presents a different trajectory, continually declining in prevalence from 2500–2450 BC, followed by a slight upturn until 2400 BC, although as the sample size here is very small it is difficult to assess the significance of this observation.

As discussed in greater detail in Chapter 5, the prevalence of dental modification makes for an interesting comparison with dental pathologies. Rates of dental modification steadily increased throughout the use-life of the Circle, commencing at 2% around 2700 BC, and maintaining a plateau at approximately 8% after 2450 BC. Chapter 5 presents a greater level of detail regarding the separation of 'active' (cultural signifiers) and 'passive' (incidental behavioural) dental modifications. Whatever the impetus, it is apparent that dental modification increased over time, and, of all other pathologies, bears closest (albeit loose) relationship to the prevalence of enamel hypoplasia within the sample. This is an important point of consideration because of the tendency of enamel hypoplasia to serve as a proxy for more endogenous biological stress indicators. As already stated, and as seen in Figures 4.2 and 4.61, enamel hypoplasia has a very low sample prevalence rate during the Earliest-to-Middle use-phases of the Circle (approximately 2% until 2550 BC). From this point, we witness a steep increase in enamel hypoplasia, eventually occurring in one in ten of the teeth found within each stratigraphic context. In effect, the prevailing biological stressors during this period resulted in a very significant increase in the number of observations for this pathology. Crucially, this is the moment of maximum activity at the site, when other dental pathologies were reduced in frequency. Subsequently, there was a slight oscillation in the number of cases, but the average rates were nonetheless still much higher than earlier in the Circle's history.

Our interpretation of these data is that some members of the population were subject to prevailing mechanical, environmental and biological stressors during different phases of the use-life of the Circle. Observations of increasing biological stress, especially around the period 2550–2500 BC, is shadowed by a trend towards lower enrichment of dietary $\delta^{15}N$ in samples of human bone from the site (Chapter 10). This trend was itself caused by palaeodietary shifts or changes in the balance of the nitrogen cycle in how the population of the Circle grew the crops from which they drew nourishment. Combining these multiple lines of evidence, the signal of nutritional stress that can be read from the sharply increasing rates of enamel hypoplasia, and subsequent increasing rates of most other dental pathologies, all seem to indicate that although the site was at its apogee in terms of levels of activity and rates of burial, all was not well in the population itself.

This was a pivotal moment in Maltese prehistory. Much has been written on the disappearance of the 'Temple Culture' in the islands. Indeed, the possibility that there was a socioeconomic or environmental collapse of some kind was one of the key questions that motivated the *FRAGSUS Project*. The dental evidence, quite remarkably, does indeed indicate that environmental and biological stressors occurred more frequently as the site's history drew towards its conclusion.

Like many other lines of evidence considered by the *FRAGSUS Project*, the evidence for diachronic change in dental pathologies is quite slight in itself but hints at broad-scale patterns that evolved slowly. Such data ultimately reflect forces that were operating in the external world, and similar observations using palaeoecology and geoarchaeology have been made during the current research. For example, at nearby Ġgantija, around 2500 BC, the residents of the Xagħra plateau were skilfully but laboriously re-working the soil, adding midden materials in an ill-fated bid to counteract long-term trends towards aridification and lower soil fertility (Volume 1). Excavations in 2014 at Taċ-Ċawla, less than 3 km from Xagħra, suggest the end of the 'Temple Period' was a complex affair, and cannot be easily characterized by environmental collapse alone (Volume 2, Chapter 3). Pollen evidence from across Malta and Gozo suggests the scale of arable farming was reduced at the end of the 'Temple Period' and perhaps was restricted only to certain coastal locations by the Early Bronze Age (Volume 1, Chapter 3).

Our research reveals that prevalence rates of all pathologies are relatively low throughout the use-life of the Circle, ranging between 1.0–12.0% across the timeframe under study. With the exception of enamel hypoplasia, the highest sample prevalence for all pathologies is noted during the earliest use phases of the Circle, *c*. 2700 BC. We interpret this as indicative of a stress response by some individuals to environmental factors. It is important to note that the 'environmental' aetiology of the particular stress responses featured here (caries, crown fractures, extreme wear and hypercementosis) may be attributed to exogenous factors including high carbohydrate diets and poor dental hygiene, as well as use of the mouth in habitual or 'occupational' behaviours such as craft or food production. On the other hand, it appears that more endogenous biological stressors prevailed upon the later inhabitants of the Xagħra plateau. The higher rates of enamel hypoplasia observed on individuals interred within the final phase of the Circle are indicative of greater nutritional, environmental, psychological or pathological stress or physical trauma during their childhood, infancy or gestation than those in the Early and Middle phases. To extend these general biocultural insights, we provided deeper consideration for the experience of maternal health and nutrition in prehistoric Malta. Our observations of enamel hypoplasia on deciduous teeth within the study sample, 85% of which were attributed to the Late use phase of the Circle, indicates that the stressors experienced by this population were of sufficient severity as to impact on expectant mothers and their children. Although axiomatic, it is important to note that those children represented within this burial population did not survive to adulthood.

Our study explored the question posed by Stoddart *et al.* (2009a) regarding the potential for fluorosis to manifest within the population, considering the endemic high fluoride levels in Gozo because of the geological substrate. We observed no hypocalcifications or yellow-brown discolourations of adult dentition, although there were five observations of discolouration on deciduous teeth within the sample. Maternal over-exposure to fluoride through drinking water during pregnancy should certainly be considered as a differential diagnosis for these observations. It is, however, important to note that four out of the five discoloured deciduous teeth were central or lateral incisors, and only one was a molar. As such, differential diagnosis for the discolouration of the anterior deciduous teeth should also include ameloblastic death following birth trauma.

Considerations of the impact of fluoride extended to analyses of caries incidence and prevalence within the population from the Circle. Less than 10% of the study sample exhibited carious lesions, suggesting that the benefits of fluoride far outweighed the risks by protecting the teeth against decay. In conjunction with the relatively soft geological substrate of limestone as an incidental inclusion in food preparation, geochemistry provided a significant advantage for the inhabitants of Neolithic Gozo in terms of their experience of dental caries compared with contemporaneous prehistoric populations, including those of neighbouring Malta. We hypothesize that similar factors also contributed to the generally low rates of attrition and abrasion observed in this population, as reported in our discussions of extreme wear. Nevertheless, we identified some important wear dynamics amongst the Circle assemblage, including labial; lingual; diagonal; approximately vertical; wear extending beyond the cementum enamel junction; and crescentic wear at the cementum enamel junction. The first three observations (labial, lingual and diagonal extreme wear) are discussed in more detail in Chapter 5, owing to their aetiologies in cultural dental modification. The last of the litany (crescentic wear) is of distinct biocultural interest as it may represent an early attempt to practise oral hygiene, similar to the tooth-brushing recommended by dentists today.

In summary, the population represented at the Circle lived during interesting and changeable times, and factors that brought about the demise of this culture were probably rooted in the mode through which human life depended upon the landscape, the fragile balance of which was eventually pushed too far towards a state of stress.

4.7. Conclusion

This research has extended the work of Stoddart *et al.* (2009a) by presenting greater resolution to the experience of dental pathology in Neolithic Gozo. Alongside broader observations of general pathology on a context-by-context basis, Stoddart *et al.* (2009a)'s reportage included an initial overview of the eruption status, enamel hypoplasia, carious lesions, *antemortem* tooth loss, periodontal disease, infectious disease, 'parafunctional' and general tooth wear and/or crowding, developmental and congenital variations, and temporomandibular joint disease observed in the Circle burial population. Our study addressed the call for more detailed analyses to offer deeper personal, cultural and temporal experiences of dental health and disease in prehistoric Malta.

Through our focus on teeth as a single category of element, we have presented detailed analyses of enamel hypoplasia, dental caries, crown and root fractures, extreme wear and hypercementosis. Dental modification was also noted and is reported separately in Chapter 5. Through consideration of the occurrence of these pathologies over time, we characterized the evolving nature of stress as it took effect in the prehistoric human population of the Xagħra plateau. This degree of insight is virtually unparalleled for a Neolithic context, and future work will have the opportunity to further refine these findings via comparative studies of contemporary assemblages.

Beyond our single element methodology, this research devised novel approaches to the study of dental pathology in archaeologically derived human skeletal assemblages. Our recording, reporting and graphical representations of crown and root fractures are rare within osteoarchaeology and, we hope, will encourage others to pursue such methods in future studies. Of particular note is our innovative use of

GIS principles to map the 'cartography' of crown fractures using Kernel Density methods. When also applied to our analyses of extreme wear, this methodology assisted our interpretation of the biocultural importance of the mouth in Neolithic Maltese communities, as it appears to have been used for a range of activities beyond ordinary mastication. Importantly, this observation extends to deciduous dentition, too, providing welcome insights into the inclusion of children in cultural activities in prehistoric Gozo. The predominant expression of the pathology on the right side is consistent with interpretations both of right-handedness and the use of the mouth as a 'third hand' or tool – both matters that will be explored further in Chapters 5 and 7.

While aligning with the disciplinary habitus of population-based reporting, our biocultural focus necessitates the inclusion of individual case studies to illuminate the lived experiences of 'real people' amongst archaeological assemblages. We have assumed this as a particularly important objective for an assemblage such as the Circle, where many might assume that the levels of fragmentation and commingling would render such testimonies inaccessible. This approach enabled us to present examples of extreme dental calculus, as well the fascinating manifestations of dental congenital variation amongst the burial population, including 'peg' teeth, accessory rootlets, dilaceration, fusion and dwarfism, variation in eruption or alignment and diastemata. These congenital phenomena are rarely addressed in archaeological studies, and as such this research is an important contribution to scholarship in human evolution, skeletal biology, palaeopathology and forensic odontology.

Moreover, our biocultural approach has facilitated the identification of two globally significant case studies. The first of these is the description of proto-surgical therapeutic intervention on an adult mandible, radiocarbon dated to 2575–2500 cal. BC, within the Tarxien phase of the Maltese Late Neolithic. This mandible fragment displays evidence for complex dental pathology, including an *antemortem* crown fracture, associated with a massive carious lesion, leading to an abscess in the mandibular corpus. A sharp-force trauma lesion observed on the root of the first molar is argued to be a consequence of an incision in the gum to lance and drain pus from the active abscess in order to relieve pain and pressure. This is a highly significant finding, as there are currently only six known examples for prehistoric proto-surgical intervention from Late Upper Palaeolithic to Neolithic Europe and Asia. The second significant case study is the identification of a morphological variation of the mandible, a so-called 'Stafne's defect', on a fragment of adult mandible radiocarbon dated to the main Tarxien phase of burial at the site, *c.* 2900–2350 cal. BC. This is the first time this trait has been identified in the Maltese osteological record and is amongst the oldest examples ever published. As such, this research represents a significant addition to understanding the incidence of this trait amongst human populations across temporal, geographical, environmental and cultural contexts.

Our work within the *FRAGSUS Project* extended the first studies of human dentition from the Circle by Stoddart *et al.* (2009a); however, by no means should this research be considered complete. There are still a vast range of opportunities for further analyses of this extremely important population to extend our understanding of life and death in Neolithic Malta. Future study could include complete analyses of the partial contexts studied here, as well as additional analyses of contexts not yet explored. Our findings would benefit from complementary analyses of the pathologies of the jaws, including *antemortem* tooth loss, abscesses, granulomata, and the various expressions of periodontal disease, which were beyond the scope of the present study. Opportunities for additional macroscopic analyses includes more detailed considerations of enamel hypoplasia. This may involve recording affected individual tooth types, as well as the specific type/s of defect present (i.e. grooves, pits, opacities; Buikstra & Ubelaker 1994, 56) and the metrics of these defects in order to acquire a more refined understanding the kinds of stress experienced by this population (i.e. systemic metabolic stress, hereditary anomalies or localized trauma; Buikstra & Ubelaker 1994, 56) and the age at which they were most vulnerable to perturbations in development (Goodman & Rose 1990). Similarly, opportunities to extend the study of dental caries include detailed recording of individual tooth types for all incidences.

We also envisage ways in which cutting-edge archaeometric techniques might enhance the research presented here. Such opportunities may involve wider microscopic analyses to better understand the incidence, variation and aetiologies of crown and root fractures and extreme wear, including standard light microscopy through to scanning electron microscopy. Population-based radiological studies would improve the initial insights into tooth crown and root morphological variations as offered here; X-Ray analyses for *in situ* dentition would complement and extend the findings presented for exfoliated elements. Radiological analyses would also enhance our understanding of other congenital and dysgnathic phenomena such as impaction, agenesis and ectopic eruption. Scientific studies of dental calculus are of profound interest, including genomic and metagenomic studies to determine caries pathogenicity (Peterson *et al.* 2011); scanning electron microscope (SEM) studies of food debris and phytoliths (Cristiani *et al.* 2018; Dobney & Brothwell 1986; 1988; Radini 2016), X-Ray Diffraction (XRD) spectroscopy for trace element analyses (Klepinger *et al.* 1977); and molecular analyses to examine proteomic evidence for diet (Charlton *et al.* 2019; Hendy *et al.* 2018), disease (Mackie *et al.* 2017; Warriner *et al.* 2014), as well as aDNA and the human microbiome (Adler *et al.* 2013; Kawano *et al.* 1995; Warriner *et al.* 2015; Weyrich *et al.* 2015).

This research has demonstrated the utility of our approach to focus on dentition as a single category of element. In a highly fragmented, commingled skeletal assemblage such as the Circle, it has provided the greatest consistency, most numerous scientific analytical capabilities, maximum systemic insights and best possibility for comparative studies across contemporaneous regional populations. Considering that many contemporary populations, in whole or in part, feature similar levels of posthumous engagement with the dead, we hope that our study provides a methodology that unites these logistically challenging assemblages and facilitates sharing their remarkable biocultural testimonies with the world. As we have shown here, and in the chapters that follow, a focus on dentition facilitates a multifaceted approach towards understanding aspects of population health, disease, nutrition, affinity and mobility, habitual behaviour, lifestyle and identity markers. This research has reinforced our belief that teeth truly are the 'diamonds of the archaeological record' and is testament to Hillson's (2005, 6) advice that, 'As a class of archaeological finds, [teeth] usually repay the amount of effort put into study'.

Note

1. These analyses were carried out in two tranches with the approval of Heritage Malta and the Superintendence of Cultural Heritage, Malta, the first in July 2015 and the second in July 2017. Transport was carried out by Bernardette Mercieca-Spiteri, Officer of the Superintendence of Cultural Heritage, Malta, with the agreement of Heritage Malta. On both occasions, radiographic analyses (micro-CT scans) were carried out by Jay Stock, Laura T. Buck and Jaap Saers at the Cambridge Biotomography Centre, University of Cambridge, UK, with a Nikon Metrology XT H 225 ST. Scans were created with voxel sizes ranging from 0.06 to 0.12μm3 (to two decimal places) as appropriate for the region of interest and the overall size of the specimen. Further processing of individual files was carried out by Jaap Saers in the Department of Biological Anthropology, University of Cambridge, UK. Radiological examination and description of the micro-CT-scans was carried out by John Magnussen, Ronika K. Power and Jess E. Thompson, using 3D Slicer (BWH, slicer.org), RaDiant DICOM Viewer (Medixant, radiantviewer.com) and AW Server (GE Medical Systems, Milwaukee, USA) software at Macquarie Medical Imaging, Macquarie University Hospital, Sydney, Australia. Radiological images were processed for publication by John Magnussen and Margery Pardey at Macquarie Medical Imaging.

Chapter 5

Dental modification in the Circle: shaping bodies, shaping culture in Neolithic Malta

Ronika K. Power, Bernardette Mercieca-Spiteri, Jess E. Thompson, Rowan McLaughlin, Jacinta Carruthers, Laura T. Buck, Jaap Saers, Margery Pardey, Jay Stock & John Magnussen

5.1. Introduction

The modification of human teeth is a subject of great curiosity and enquiry across bioarchaeology, anthropology and ethnography for many reasons, not the least of which includes its expression in apparently disparate cultures across time and geographical space. Substantial efforts have been devoted to categorizing the myriad variations of shape and style; demographic incidence; technology and intention of intervention ('passive' or 'active'; Alt & Pichler 1998, 388; Bocquentin *et al.* 2013, 386; Larsen & Kelley 1991, 4; Mayes *et al.* 2017, 285; Milner & Larsen 1991); and, where undertaken as an act of deliberate physical manipulation, the aetiology and impetus for such dramatic, irreversible and potentially dangerous change. While individual-level variation in dental modification may provide powerful indicators of individual identity, at a broader societal level, there is ample cross-cultural evidence that, in many societies, intentional dental modifications play an important role in the expression and mediation of social identities (De Groote & Humphrey 2016; Knudson & Stojanowski 2008).

Comprehensive reviews of the practice, incidence and cross-cultural attestations of dental modification have been carried out by Scott & Turner (1988), Milner & Larsen (1991), Alt & Pichler (1998), and Mower (1999). More recent work by van der Reijden (2014) has focused on attempts to standardize the terminology and categorization of dental modification phenomena, as called for by many practitioners in the field (González *et al.* 2010). The variation in previous works has unwittingly obfuscated understanding of the true incidence and prevalence rates of specific modification types, thus limiting our ability to harness observations as signifiers of possible connection and communication amongst and between cultures.

The current study presents the first dedicated enquiry into the nature and scope of dental modification in any skeletal population from the Maltese archipelago, and thus hopes to contribute to broader research into the phenomenon across the Mediterranean, particularly for the prehistoric period. It must be noted, however, that modified teeth were first observed in the Circle assemblage by Stoddart *et al.* (2009a), with reports of 'parafunctional wear' (pp. 318, 325) as well as the use of the teeth as a 'third hand' (p. 329). These comments delineate the extent of reporting into this matter to-date, and were followed by a recommendation that 'the teeth need to be investigated further in order to take this idea forward' (Stoddart *et al.* 2009a, 329). It is from this platform that the present work emerges, and seeks to offer the first detailed, quantitative investigation into this fascinating aspect of human behaviour for Neolithic Malta.

The broad aim of this chapter is to introduce the Neolithic population of the Xagħra plateau to the wider discourse of dental modification. It seeks to report the nature and scope of this phenomenon amongst contemporary prehistoric central Mediterranean populations, and to look towards a wider network of activity and identity markers across broader Mediterranean, African and European cultural contexts. Despite the significant challenges presented by the highly fragmented, commingled and predominantly disarticulated nature of the Circle assemblage, the present study seeks to demonstrate the importance and value of including Neolithic populations from such contexts into scholarly accounts of these intriguing phenomena. The very nature of assemblages like Xagħra precludes traditional approaches to whole-body analyses; however, aspects of funerary behaviour should not exclude these populations from their rightful inclusion in considerations of broader cultural dynamics. Despite long-standing disciplinary traditions of recording and reporting intact arcades, we argue that our shift in focus to teeth as a single category of element provides: i) the greatest consistency, ii) most numerous scientific analytical capabilities, iii) maximum systemic insights, and iv) best possibility for comparative studies across contemporaneous regional populations. This chapter will consider the background to dental modification in human behaviour and the history of its study in biological anthropology. For context, we will offer a brief review of the incidence of these phenomena across Africa and Europe. We will then present the findings of our analyses of dental modification within the Circle burial population and discuss their significance for Maltese prehistory.

It must be remembered that this group of people most likely contained the individuals responsible for constructing amongst the oldest free-standing stone structures in the world, the megalithic temples of Ġgantija, located 400 m away from the Circle. The members of this population were therefore globally significant innovators in design, architecture, technology, materials extraction and craftwork, all requiring a combination of substantial intellectual and physical activity. As reported in Chapters 4, 7 and 8, the body offers a powerful means to access the activities and lived experiences reflected within its hard tissues. By considering the ways the people of Xagħra applied intellectual and/or physical activities to shape their teeth, we are situating this important Neolithic Maltese community within the wider local and regional cultural dynamics that were also shaping the rapidly changing world around them.

5.2. Background

'Active' dental modification is a highly visible and geographically widespread form of body modification, while 'passive' dental modification is an almost ubiquitous phenomenon. As a result of the exceptional preservation of teeth, it is also the most likely form of body modification to preserve in the archaeological record and is increasingly noted to have been practised amongst diverse prehistoric populations (Burnett & Irish 2017b, 2; Geller 2006; López Olivares 1997; van der Reijden 2014, 7). As humans communicate predominantly through movements of the mouth during speech and other non-verbal interpersonal forms of expression, these gestures involve regularly displaying and observing the dentition (van der Reijden 2014, 7). Recognizing this, cultural groups spanning much of the globe have exploited the orofacial complex as a key site for conveying messages about identity, ethnicity, status and even emotion (Anderson *et al.* 2005; Burnett 2017. 252; De Groot & Humphrey 2017, 26; Langsjoen 1998, 410; Larsen 2017, xvi; Linne 1940; Mower 1999, 47; van Reenen 1978a; van der Reijden 2014, 7; Watson & García 2017, 298). For this reason, the majority of dental modification observations recorded for archaeological populations pertains to the anterior dentition of the maxillary incisors and canines, referred to by Larsen as 'the social six' (Larsen 2017, xvi), considering their capacity to provide important social cues and signals. Cases of active dental modification have been recorded in the ethnographic and ethnohistoric literature from a staggering number of regions, including cultures in Australia, Africa, Asia, North, central and South America and, in several places, these practices appear to have significant time depth (Burnett & Irish 2017a; Campbell 1925; De Groote & Humphrey 2016; Ikehara-Quebral *et al.* 2017; Jones 1992, 2001; Langsjoen 1998, 41; Lee 2017; Milner & Larsen 1991; Ortner 2003, 603; Pardoe & Durband 2017; Pietrusewsky *et al.* 2017; Tayles 1996). Despite its widespread distribution, the styles and patterns of dental modification often follow highly localized forms, resulting in marked regional characteristics (Alt & Pichler 1998, 405). The archaeological evidence similarly reflects this historic and contemporary diversity, in terms of the form or style of dental modification, the means by which tooth shape is altered, and the motivations for such practices.

The importance of distinguishing between dentition altered through usual mastication, and through non-alimentary practices such as intentional shaping and using the teeth as tools (parafunctional wear), has been recognized within biological anthropology for several decades. An early dental modification recording system categorized modifications arising from the following processes: i) dietary wear; ii) implemental wear (commonly referred to as 'use of teeth as tools'); iii) incidental cultural practices; and iv) intentional cultural practices (Scott 1997). Alt & Pichler (1998) later refined these to distinguish between 'active' (intentional) and 'passive' modifications (encompassing those caused by diet, habitual practices and parafunctional wear). Importantly, they noted that passive changes to the dentition develop through repetitive action, accruing over a greater timeframe than active modifications (Alt & Pichler 1998, 388). Active modifications are carried out purposefully to fulfil specific aesthetic, cultural or ritual aims. Therapeutic or palliative interventions are excluded from these categories; although these were defined as active modifications by Alt & Pichler (1998, 388), we classify these as preventative procedures unrelated to symbolic socio-cultural practices.

Teeth can be intentionally altered through chiselling, drilling, extraction (ablation or avulsion), filing, inlaying, polishing, repositioning, scoring and staining

(Burnett & Irish 2017b, 1; Langsjoen 1998, 410; Milner 2017, 318; Ortner 2003, 603; Roberts & Manchester 2005, 81). These interventions involve a range of tools across cultures, but typically a hammer and chisel, stone or metal file, knife, stone axe and/or hardwood stick are required (Aseffa *et al.* 2016; Fastlicht 1976; Headland 1977; Kanner 1928; van Reenen 1978a, 1978b; van Rippen 1917). Ethnographic observations of sub-Saharan African groups describe the subject laying with their head in the operator's lap, biting on a stick between their molars while the operator chipped their anterior teeth using a knife or a chisel, pounded by a hammer stone (Irish 2017, 40; van der Reijden 2014, 22). Depending on the desired effect, a file could then be used to smooth the margins (Irish 2017, 41).

Other modifications include attaching prostheses such as dentures and decorative caps or grills (Milner & Larsen 1991; Alt & Pichler 1998; Peter *et al.* 2013). In her recent review of active (cultural) dental modification, van der Reijden (2014, 16) argues that chipping should be considered an outcome of passive modification, while germectomy (Barzangi *et al.* 2013; Bataringaya *et al.* 2005; Garve *et al.* 2016; van der Reijden 2014) is often sought as a treatment for infant illness (cf Pindborg 1969). Distinguishing between modification processes, means, and other dental pathologies can be challenging (Burnett 2017, 251; Burnett & Irish 2017b, 4; Milner 2017, 318; Milner & Larsen 1991; Molnar 1972). In general, active modifications are primarily found on the anterior dentition and are symmetrical in pattern, while habitual changes are more likely to appear on the anterior dentition but may also be observed for the distal arcade (Alt & Pichler 1998, 399; Langsjoen 1998, 410; cf. Chapter 4). Furthermore, intentional reduction of crown height may be confused with extensive attrition because of parafunctional wear (van der Reijden 2014, 18). Additionally, dental avulsion and *antemortem* tooth loss may be indistinguishable if alveolar bone resorption is advanced, although several scholars (Milner & Larsen 1991, 363) recommend the following criteria for identifying avulsion: lack of surrounding dental pathology; symmetry in the pattern of tooth loss; and repetition of this pattern amongst multiple individuals in the skeletal assemblage (Buikstra 1987; Lee 2017, 97; Milner & Larsen 1991, 363; Newton & Domett 2017, 161–162; Pietrusewsky *et al.* 2017, 107; however see Spencer & Gillen 1927; van der Reijden 2014, 21; van Rippen 1918a, 1918b). The same methodology is also useful in evaluating various other forms of dental modification.

5.2.1. 'Active' versus 'passive' modifications

There are myriad different reasons as to why past populations practised or experienced dental modification (Burnett & Irish 2017b, 2). Cross-cultural reviews of active dental modification (Benedix 1998; Burnett & Irish 2017b, 2; Mower 1999; Pinchi *et al.* 2015) reveal a plethora of intentions behind this practice, including: cosmetic enhancements; ensuring feeding if lockjaw arises as a result of tetanus; tradition; initiations or rites of passage, especially into adulthood or parenthood; mourning; improving linguistic pronunciation; intimidating enemies; signalling tribal or ethnic identity or affiliation; punishment; pain endurance; to practise folk medicine; and/or to mimic or differentiate appearance from totemic animals (Artaria 2017; Bolhofner 2017; De Groote & Humphrey 2017; Erlandsson & Bäckman 1999; Geller 2004, 2006; Irish 2017; Mower 1999; Noman *et al.* 2015; Pardoe & Durband 2017; Pietrusewsky *et al.* 2017; Watson & García 2017; van der Reiden 2014; Scott & Turner 1997; Milner & Larsen 1991; Van Rippen 1918a; Shaw 1931; Singer 1953; Campbell 1925). Alt & Pichler (1998) have summarized these intentions as being of either therapeutic or non-therapeutic motivations; and Stojanowksi *et al.* (2016) have characterized the latter as 'culturally mediated dental modification'. Intentionally altering the shape of teeth induces significant pain and carries the risk of future complications from infection and tooth loss. Amongst practising cultures, dental modification is frequently endured and persists with some longevity, illustrating the cultural significance of this form of body modification (Alt & Pichler 1998, 407). Dental modification is noted as early as the Upper Palaeolithic in Maghreb (20,160–12,000 cal. BP), with the majority of preserved maxillae from the Iberomaurusian period presenting avulsion of at least one incisor (De Groote & Humphrey 2016, 2017; Humphrey & Bocaege 2008). While there is variation in the avulsion pattern throughout this period, it appears to have been carried out almost universally regardless of sex and, in cases of multiple extraction, at different times in most individuals' lives (De Groote & Humphrey 2016). Yet, considering the staggering range of potential motivations noted across numerous studies, the specific reasons for dental modification observed in the archaeological record are difficult to identify with certainty.

Passive dental modification is a universal occurrence but highly variable according to environment and subsistence base, as well as individually specific occupations, habits and idiosyncrasies. Unintentional shape changes can be caused by dietary and non-dietary chewing. Non-dietary tooth wear is often a result of the use of teeth as tools, for example to split materials such as bone, shell, plants and fibres (Buikstra & Ubelaker 1994; Cybulski 1974; Lukacs & Pastor 1988; Schulz 1977); to process fibres or scrape hides (Langsjoen 1998, 410; Roberts & Manchester 2005, 81); to edge flaked stone tools (Buikstra & Ubelaker 1994; Turner & Cadien 1969); or as a 'third hand' to hold material static in the teeth to allow manipulation (Alt & Pichler 1998, 394; Merbs 1983; Roberts & Manchester 2005, 81). Further means of passive modification include holding or carrying objects with the teeth; wearing jewellery such as lower lip labrets and discs; bruxism; trauma and/or violence (Alt & Pichler 1998; Milner & Larsen 1991; Molnar 1972). The repetitive use of toothpicks to remove food trapped in the interproximal spaces is typically the most common form of passive dental modification and also appears to be the oldest, noted in numerous Pleistocene populations (Boaz & Howell 1977; Bermudez de Castro *et al.* 1997; Frayer & Russell 1987; Ungar *et al.* 2001; Sun *et al.* 2014; cf Ubelaker *et al.* 1969; Buikstra & Ubelaker 1994).

5.2.2. History of study in biological anthropology

Records of dental modification provided from late 19th and early 20th century travellers have been of interest to social and biological anthropologists since they were produced (Livingstone 1861, 185, 348; Milner 2017, 318; cf Galton 1853; Hamy 1882; Schweinfurth 1874; Serpa Pinto 1881; Werner 1906; Starr 1909; van Rippen 1918a, 1918b, 1918c; Guthe 1934; Tozzer 1941). From the 1960s, there is an evident increase in bioarchaeological research on the topic, some describing the phenomenon as 'dental transfigurement' (Turner 2000), or more negatively as a form of 'dental mutilation', a pejorative term which has regularly been criticized (Burnett & Irish 2017b, 2; Geller 2006; Jones 2001; Mower 1999; Turner 2000). Within biological anthropology, much work until recently has been restricted to the description and analysis of regional trends, according to the availability of skeletal remains from archaeological excavations and ethnological collections. This has led to particularly rich literature on dental modifications amongst Indigenous and prehistoric North American, Mesoamerican and South American populations (Blakely & Beck 1984; Fastlicht 1976; Kirk 2006; Scherer 2018; Schulz 1977; Tiesler *et al.* 2017; Turner II 2000, 2004; Turner II & Cadien 1969; Turner II & Machado 1983; Ubelaker 1984; Williams & White 2006).

The primary focus of much research has been to develop classification systems encompassing ever-greater numbers of modification styles. These have often been regional in focus, with catalogues compiled for African (Almeida 1953, 1957; Starr 1909; von Jhering 1882; Wasterlain *et al.* 2016) and South American and Mesoamerican styles (Fastlicht 1948; Romero 1986; Rubín de la Borbolla 1940; Saville 1913). The relevance of these classificatory efforts beyond the intended region is unfortunately limited, because of their localized nature. Despite this, Romero's (1986) catalogue, recognized until recently as the largest and most sophisticated coding system, is often referred to as the general standard for active dental modifications. However, it has been noted that errors have been introduced into the classification systems over time through transcription errors and misinterpretations of drawings and/or descriptions (van der Reijden 2014, 38).

Perhaps as a result of the extensive (but often difficult to access) literature on this topic, there is little standardization in terms of recording dental modifications. Buikstra and Ubelaker (1994, 58) recommend thoroughly describing all altered dentition, noting the affected surface(s), the nature of modification and any introduced foreign materials, and providing codes for filing; drilling (with or without inlays); dental restorations or applications; wear associated with artefact use or production; and tooth evulsion or ablation. Recently, the most comprehensive recording system for intentional modifications has been collated, uniting all forms in the current literature and introducing several recently identified types (van der Reijden 2014). This global classification system comprises almost 300 styles, making a series of recommendations for recording and coding. In particular, van der Reijden (2014, 15, 36) emphasizes that shaped teeth often exhibit multiple forms of modification, each of which should be coded separately. Passive modifications have been researched by Bonfiglioli (2002) and, although not fully published, her criteria for scoring chipping, interproximal grooves and notches are presented in a recent work (Bonfiglioli *et al.* 2004). A recent brief review of AIDMs (activity induced dental modifications; including notching, grooving, labial and occlusal striations); LSAMAT (lingual surface attrition of the maxillary anterior teeth; Turner & Machado 1983); wear facets and polishing; interproximal striations; and chipping, highlights the need for both standardized terminology and recording methods (Molnar 2011).

Beyond the limitations of many existing corpora of dental modification styles, and the variation in recording standards, there are opportunities for the development of this field in alignment with the aims of social bioarchaeology. Milner and Larsen (1991, 373) were early to note the interpretative difficulties concerning the cultural significance of intentional modifications and the causes of unintentional modifications. These difficulties largely remain; while there are many available ethnographic studies, establishing the means by which modifications were achieved amongst a given population (whether active or passive) often relies upon a combination of contextual data and inference. Greater attention is needed to consider the dynamic use of the mouth in non-alimentary activities, combining archaeological and biochemical evidence for subsistence and craft practices. Furthermore, the age at which individuals underwent intentional dental modification, and the length of time it may have taken to shape teeth, are pertinent for advancing our understanding of both the social and individual experience of this phenomenon (van der Reijden 2014, 91). Although this is difficult to assess in many cases, recent work by De Groote and Humphrey (2016, 2017) accounts for stages of alveolar remodelling to identify typical ages at which dental avulsion was implemented during the Late Stone Age in Northwest Africa.

Increasingly, scholarship is considering the socio-cultural implications of such visible and visceral practices, establishing the relationship between age, sex, diet, mobility, and group identity amongst individuals displaying modified dentition (Artaria 2017; Bolhofner 2017; De Groote & Humphrey 2017; Erlandsson & Bäckman 1999; Geller 2004, 2006; Irish 2017; Milner & Larsen 1991; Mower 1999; Noman *et al.* 2015; Scott & Burgett Jolie 2008; Scott & Turner 1997; Pardoe & Durband 2017; Pietrusewsky *et al.* 2017; van der Reiden 2014; Watson & García 2017). Interestingly, where it is possible to scrutinize the demographic profile of individuals with intentionally and/or incidentally modified dentition, there is often little engagement with the relationship of this phenomenon to gender identity (for example, Blakely & Beck 1984; Bonfiglioli *et al.* 2004; Sperduti *et al.* 2018; Williams & White 2006), even and especially where incidences do not fit the culturally expected pattern (for example, Sperduti *et al.* 2018, 237), there are clear regional differences (Waters-Rist *et al.* 2010), or significant diachronic changes (Humphrey & Boceage 2008; Stojanowski *et al.* 2014). Future studies of dental modification must seek to move beyond biological markers of sex and age to examine the significance of such practices within their cultural framework of meaning.

5.2.3. Dental modification in prehistoric Africa and Europe

Intentional dental modification by way of ablation is noted as early as the Late Stone Age in the Maghreb (Northwest Africa) and endured through to the Neolithic (Bonfiglioli *et al.* 2004; De Groote & Humphrey 2016, 2017; Humphrey & Bocaege 2008). Skeletal remains from the Iberomaurusian period (21,160–*c.* 12,000 cal. BP), indicate that nearly all adults underwent ablation of at least one maxillary incisor (Briggs 1955; De Groote & Humphrey 2016; Humphrey & Bocaege 2008). The earliest evidence derives from Taza (Eastern Algeria), between 16,100 and 13,800 cal. BP (Meier *et al.* 2003), although it is possible that earlier material remains to be dated. The extraction of both maxillary central incisors has been deemed 'characteristic' of this period although, interestingly, individuals presenting only one ablated incisor were not always younger in age (De Groote & Humphrey 2016, 56; Humphrey & Bocaege 2008, 115). Analysing only dental arcades presenting alveolar remodelling in individuals with >1 ablated tooth, De Groote & Humphrey (2016) found that most individuals presented at least one phase difference between remodelling alveoli; this suggests that ablation was practised sequentially and was not strongly correlated with chronological age. At Taforalt necropolis (Morocco), 44 adults with complete maxillae and/or mandibles displayed incisor ablation, while enamel chipping and notches were noted predominantly on male adults, suggesting sex-specific dietary aspects or task distribution (Bonfiglioli *et al.* 2004). Across the region, avulsion declined during the subsequent Capsian period, present on just over half of the sampled individuals (62%), although it was markedly more common in females who had often undergone the removal of all eight incisors (Humphrey & Bocaege 2008, 116). Avulsion was increasingly uncommon during the Neolithic (27% of the sample), with significant regional variation, in contrast to the initial cultural homogeneity of this practice (Humphrey & Bocaege 2008).

Incisor avulsion amongst groups around the Sahara from 9500 cal. BP suggests the region was at least partially settled by populations moving from Northwest Africa, further supported by phenotypic and cultural evidence (Sereno *et al.* 2008; Stojanowski *et al.* 2014, 86). At Gobero, in the central Niger, amongst Early Holocene remains (9500–8200 cal. BP), 21% of the sample (four adults) presented avulsion of at least one central incisor with no apparent jaw or side preference (Stojanowski *et al.* 2014, 84). Of burials dating to the Middle Holocene (6500–4500 cal. BP), 16% of the sample (five adults) displayed avulsion of between two to six incisors (Stojanowski *et al.* 2014, 84–6). The practice extended to include lateral incisors and appears to have been restricted to male individuals, two of which also displayed intentional filing (Stojanowski *et al.* 2014). Nearby, in Libya, a male adult deposited in levels pre-dating 7800–7500 cal. BP presented occlusal grooves on all seven preserved teeth alongside wear facets on the mandibular dentition, likely a result of clenching fibres between the teeth while weaving mats, ropes and baskets (Minozzi *et al.* 2003). Further prehistoric evidence suggests that dental modification was not practised in West Africa until the 3rd millennium BC (Finucane *et al.* 2008). At Karkarichinkat Nord (Mali), four individuals of unknown sex displayed shaping of the maxillary incisors and canines, probably through filing, to create pointed teeth (Finucane *et al.* 2008). Dental modification persisted throughout Sub-Saharan

Africa into the historical period (Finucane *et al.* 2008) and is still practised by some cultures, albeit to a diminished degree (Alt & Pichler 1998; Friedling 2017; Friedling & Morris 2005, 2007; Irish 2017; Jones 1992; Milner 2017; Willis *et al.* 2008).

Outside Africa, early evidence for dental avulsion is recorded at several Natufian sites in the Levant (Crognier & Dupouy-Madre 1974; Eshed *et al.* 2006; McCown 1939). There is far greater evidence for AIDMs, frequently in the form of occlusal grooves as well as severe attrition, interproximal grooves and LSAMAT across individuals dating from the Natufian to the late Chalcolithic (Bocquentin *et al.* 2013; Eshed *et al.* 2006; Irvine *et al.* 2014; Molleson 1994, 2005). Chipping and severe attrition of the anterior dentition are likely attributed to a combination of both masticatory and habitual activities (Irvine *et al.* 2014, 27), especially when individuals present advanced AMTL (*antemortem* tooth loss) of the posterior dentition (Eshed *et al.* 2006, 153). Inferred habitual activities include abrasion of the incisors as a result of use of a bow drill or application of a gritty substance to stain the teeth (Bocquentin *et al.* 2013), processing animal skins (Eshed *et al.* 2006), holding objects such as staves in the mouth while making baskets or nets (Eshed *et al.* 2006), and processing materials including lithics and fibres (Irvine *et al.* 2014).

Heading westwards into Europe and the Mediterranean, there is relatively minimal evidence for intentional dental modification during prehistory (Burnett & Irish 2017b, 6; for later examples, see Alexandersen & Lunnerup 2017; Arcini 2005, 2011; Kjellström 2014). The clearest indication for a cultural practice of dental modification comes from Neolithic Central and Southern Italy (*c.* 6500–3200 BC), where only women displayed avulsion primarily of the maxillary incisors and/or canines (Robb 1997). Allowing for the limitations of the analysed skeletal sample, Robb (1997) estimates that between 25–50% of Neolithic women would have undergone selective and intentional tooth removal, perhaps optionally as a cosmetic treatment or according to specific life experiences or rituals, such as mourning. There is even rarer evidence for incisor avulsion in Neolithic Britain, with several cases reported from cave sites in Lancashire and Wales (Jackson 1915) and Ty Isaf chambered tomb in Wales (Wysocki & Whittle 2000, 592). At the latter site, *antemortem* tooth loss of the anterior dentition is an unusual pattern and is suggested to be a result of either avulsion, trauma or parafunctional wear (Wysocki & Whittle 2000).

In contrast, skeletal remains from Neolithic and Copper Age sites across Europe display an impressive range of passive modifications associated with habitual practices or parafunctional wear. At numerous Eastern, Central and Northern European sites, AIDMs including incisal notches, labial grooves and chipping are regularly observed and often present local or site-specific patterns in terms of their distribution in the dental arcade and relationship to sex. A study of 76 individuals from a range of early to late Neolithic sites in the western Lake Baikal region (Siberia), found that occlusal grooves were commonly encountered in 17-36% of individuals at each site and their prevalence increased with age (Waters-Rist *et al.* 2010, 272–3). Grooves were often orientated in linguo-labial direction, likely representing the processing of plant fibres and animal sinews for a variety of purposes, including sewing string, baskets, nets, snares, and sinew or cordage for fastening composite tools (Waters-Rist *et al.* 2010). The importance of fishing amongst indigenous populations in the region particularly suggests these activities involved the manufacture of fishing nets and baskets. Dental modifications did not show a strong preference according to arcade or side, but variation was found between riverine and lakeshore sites, as well as diachronically (with greater variation in late Neolithic-Bronze Age sites and increased thickness in grooves over time), and in terms of the prevalence according to sex at each site (Waters-Rist *et al.* 2010, 275). This reveals the extent to which dental modifications are intertwined with diet, ecology, material culture production, and the distribution of tasks and activities according to sex and/or gender.

Incisal notches amongst a Neolithic Polish assemblage present sex-specific differences in terms of orientation and morphology, with males apparently clenching a thicker material or holding objects in their teeth while females processed thinner fibres or sinews (Lorkiewicz 2011). In Slovakia and the Czech Republic, incisal notches were again mostly observed on female individuals, and craft processing appears to have first involved the lateral incisors and progressed to the central incisors throughout life (Frayer 2004). Alt & Pichler (1998, 394–7) present a mandible of a single Neolithic individual from Wandersleben (Germany) displaying occlusal grooves on their heavily worn central incisors; these grooves track a hemispherical 'path' and are suggested to indicate fibre or sinew processing. A middle Neolithic hunter-gatherer-fisher population in Sweden displayed occlusal wear facets, labial striations, interproximal grooves, chipping and excessive attrition, with slight differences observed in their distribution between male and female individuals (Molnar 2008). Overall, Molnar (2008, 428) found that males used their teeth more intensely for habitual purposes, displaying a high proportion of occlusal facets, attrition and interproximal grooves, while females mostly presented labial striae, possibly by holding meat in the mouth in order to cut it. Finally, in Britain, at Ty

Table 5.1. *Materials included in dental studies, including provenance and representation.*

Context	Location	Date	N teeth isolated	Σ teeth studied	% Context
595	East Cave	Early	123	123	100
833	West Cave: north niche	Early	18	2	11
951	West Cave: north niche	Early	2306	751	33
698	East Cave: southern pit	Early	13	3	23
1209	West Cave: shrine	Middle	4	4	100
1241	East Cave	Middle	170	170	100
433	East Cave: central	Late	35	6	17
436	East Cave: central	Late	32	32	100
715	East Cave	Late	56	54	96
738	East Cave	Late	17	15	88
790	Intermediate zone	Late	11	11	100
1206	West Cave: shrine	Late	642	508	79
960	West Cave: shrine	Latest	870	405	47
783	West Cave: display	Latest	2900	976	34
		Total	7197	3060	43

Isaf, one maxillary central incisor displayed an incisal notch as a result of parafunctional wear (Wysocki & Whittle 2000, 592).

In Southern Europe, the most comprehensive study of passive dental modifications derives from a large Eneolithic–Bronze Age cemetery in Southwest Italy (Sperduti *et al.* 2018). At Gricignano d'Aversa, 117 individuals with >1 incisor preserved were analysed for the presence of AIDMs. Incisal notches and striations on the maxillary incisors were commonly observed on 36 individuals, all >15 years old and predominantly female adults (Sperduti *et al.* 2018). As with contemporary archaeological and further ethnographic evidence, this is attributed largely to fibre processing. The presence of preserved textiles in the calculus of two adult females with AIDMs strengthens this interpretation (Sperduti *et al.* 2018). Although later prehistoric skeletal remains from the central Mediterranean often present analytical challenges because of frequent commingling, fragmentation and poor preservation (Robb 2007, 222), teeth are often the best-preserved skeletal elements and offer a wealth of insights into diet, health, habitual and cultural practices. There is evidently scope for a more widespread and comprehensive investigation of both active and passive dental modifications in this region. It is clear that the Circle population has a great deal to contribute to this discourse.

5.3. Materials

As discussed by Mercieca-Spiteri *et al.* (Chapter 2), a total of 11,706 teeth were isolated from their associated highly fragmented, commingled and predominantly disarticulated skeletal remains and inventoried according to context by the *FRAGSUS* Population History Workgroup across five laboratory seasons at the National Museum of Archaeology (NMA), Valletta, between November 2014 and May 2017. Of these, a total of 3,060 teeth (26.1% of isolated sample) of all types were studied for the purposes of interrogating the experience of dental pathology, anthropology and modification among the population/s represented within the Circle. Any observations for dental modification were recorded as part of these analyses. As noted previously and detailed in Table 5.1, the studied teeth are only a subsample of the overall assemblage, representing a proportion (or, complete in the cases of contexts (436), (595), (790), (1209) and (1241)) of 14 selected contexts as excavated thus far. Further to this, it is critical to note that the site was not completely excavated, and it is known that further remains are preserved at the site to allow for work to continue at the hands of future generations of archaeologists. As previously mentioned, in accordance with the temporal and pecuniary parameters of the project, the contexts examined here were determined by the excavators to be of greatest cultural and temporal significance to the overarching research questions, and thus included in whole or part here.

5.4. Methods

For the Circle dental modification study, anterior teeth (maxillary and mandibular central and lateral incisors and canines) of all articulation states (exfoliated and loose *postmortem* or in occlusion) were examined individually within their context batches. The individual tooth type, as well as the modification location, type and severity was recorded for each batch in a Microsoft Excel spreadsheet to form a searchable digital database/inventory. Each batch was marked once analysis was completed and curated within the NMA as part of the *FRAGSUS* Research Archive.

In terms of naming conventions, we follow the notation system developed by the *Fédération Dentaire Internationale* (FDI; FDI 1971; International Organization for Standardization [ISO] 3950, ISO 1984, 1995; Alt & Türp 1998b). Anterior tooth surfaces are referred to as: incisal or occlusal (the biting or chewing surfaces; incisal is more specifically for the anterior teeth); and labial (the lip surface of the anterior teeth) or lingual (the tongue surface of all teeth). Directions are referred to as mesial (towards the midline) and distal (away from the midline). Our formal and technical classifications follow the taxonomy of van der Reijden (2014), which builds on the foundational works of Romero (1958, 1960, 1965, 1970, 1986). Our general macroscopic osteological analytical techniques are based on standard criteria described in Buikstra and Ubelaker (1994: specific references indicated alongside analyses, below). All surfaces were examined macroscopically and under magnification using a 10x hand lens.

In alignment with the methodologies recommended by Buikstra and Ubelaker (1994), Bonfiglioli (2002), Molnar (2011) and van der Rijden (2014), every tooth was examined for the presence/absence of modifications including chipping, chiselling, drilling, extraction (ablation or avulsion), inlaying, polishing, repositioning, scoring and staining, notching, and/or a change of occlusal profile (discreet wear/filing in various directions/orientations). Where present, modifications were further scrutinized for location across the crown and root, and severity (dentine exposure). Observations of relative age (permanent or deciduous) were recorded for every affected tooth, and special notes were made for the occurrence of modification of juvenile teeth; where observed, modifications were recorded in the same manner as adults. Unfortunately, because of the highly fragmented and commingled nature of the assemblage, it was not possible to undertake comprehensive sex assessment as part of this study. In all cases, only *in vivo* modifications were recorded, these were distinguished from *postmortem* phenomena via the identification of *antemortem* wear (appearing as sheen) on extant surfaces, confirming their use in the mouth subsequent to modification (Hillson 2000, 258; Langsjoen 1998, 410; Ortner 2003, 603). Each instance of modification was recorded, resulting in some observations of more than one modification type on a single tooth. In alignment with the recommendations made by Milner and Larsen (1991, 369), we ensured that the frequency and distribution of damaged teeth were recorded in detail, forming the basis of the results presented and discussed below. We also recorded the size of chips and fractures, as well as their location and distribution for every affected tooth. Analysis of these particular data is ongoing and will be the subject of further publications. Coincidentally, certain types of extreme wear reported in Chapter 4 should also be considered alongside the dental modification data for anterior teeth within the study sample. The categories of extreme wear relevant to the current analysis include labial and lingual extreme wear and gross crown loss of the anterior teeth. Within the study sample, selected items were identified as worthy of further examination via radiographic analyses.[1]

5.5. Results: overview

Amongst the 3060 teeth in the study sample, 172 were observed to feature some form of dental modification (Table 5.2; note that the number of modifications is greater than the number of teeth as some teeth featured more than one modification). At 5.62%, this indicates that a relatively low proportion of the examined population were engaged in activities that actively or passively modified their teeth. When organized according to chronological distribution, the Late contexts are observed to feature the highest incidences of dental modification by some measure (Fig. 5.1). With 138 observations (80.23% total modification; 6.86% of 'Late' total study sample), the Late use phase of the Circle featured six times the number of observations of dental modification for the Early use phase (Σ=28; 16.28% total modification; 3.19% of 'Early' total study sample) and 23 times the number of observations for the Middle use phase (Σ=6; 3.49% total modification; 3.45% of 'Middle' total study sample). The individual contexts with the highest raw incidences of dental modification amongst the dataset were (783) (Σ=75); (960) (Σ=31); (1206) (Σ=8); (951) (Σ=15); and (595) (Σ=13). When expressed as prevalence rates within the full study sample of each context, the distribution is (783) (7.68%); (960) (7.65%); (1206) (5.51%); (951) (1.99%); and (595) (10.56%). According to the latter distribution, while the Late contexts had the highest overall incidence of dental modification, the prevalence rate was highest amongst Context (595), the earliest of the study sample.

Also noteworthy are the observations of certain types of 'extreme wear', described in Chapter 4 of this volume. The nature and location of such extreme attrition on the anterior teeth of both adult and non-adult members of the Xagħra population are suggestive of

Table 5.2. *Dental modification of anterior teeth summary by context and chronology (Σ teeth mod. = Σ teeth modified; >1 mod. = Σ teeth presenting >1 modification).*

Context	Location	Date	Σ teeth studied	Σ teeth mod.	% teeth mod.	Incisal notch	Chipping	Undulating	Diagonal	>1 mod.	Σ deciduous
595	East Cave	Early	123	13	10.57	5	6	2	2	2	2
833	West Cave: north niche	Early	2	0	0	0	0	0	0	0	0
951	West Cave: north niche	Early	751	15	2.00	5	3	6	1	0	0
698	East Cave: southern pit	Early	3	0	0	0	0	0	0	0	0
1209	West Cave: shrine	Middle	4	0	0	0	0	0	0	0	0
1241	East Cave	Middle	170	6	3.53	1	4	1	3	1	1
433	East Cave central	Late	6	0	0	0	0	0	0	0	0
436	East Cave central	Late	32	1	3.13	0	1	0	0	0	0
715	East Cave	Late	54	1	1.85	0	0	0	1	0	0
738	East Cave	Late	15	1	6.67	1	0	0	0	0	0
790	Intermediate zone	Late	11	1	9.09	1	0	0	0	0	0
1206	West Cave: shrine	Late	508	28	5.51	15	11	1	2	1	3
960	West Cave: shrine	Latest	405	31	7.65	16	16	3	1	4	6
783	West Cave: display	Latest	976	75	7.68	27	49	1	5	11	6
		Total	3060	172	5.62	71	90	14	15	20	18

an aetiology beyond 'ordinary' mastication, perhaps associated with food processing (for example, cracking, breaking and/or chewing hard foods); and/or processing materials other than food in association with cultural practices. As such, they must be included in considerations of both 'active' and 'passive' dental modification and are thus also presented here. Table 5.3 presents the data for extreme wear of anterior teeth by context, chronology and tooth surfaces, and also features the incidences of extreme wear to anterior

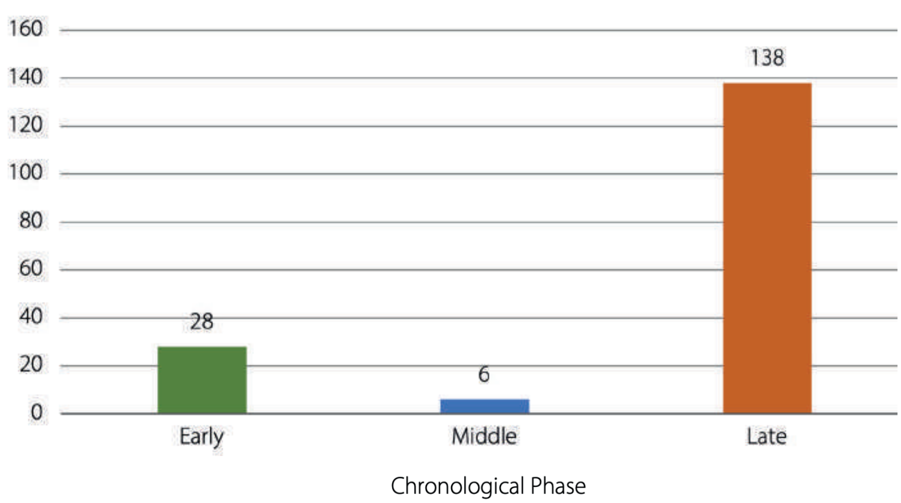

Figure 5.1. *Frequency distribution of dental modification observations by chronological phases in the Circle sample (Σ=172).*

Table 5.3. *Extreme wear of anterior teeth summary by context, chronology and tooth surface observations.*

Context	Location	Date	Σ teeth studied	Labial xWear	Lingual xWear
595	East Cave	Early	123	7	2
833	West Cave: north niche	Early	2	0	0
951	West Cave: north niche	Early	751	4	7
698	East Cave: southern pit	Early	3	0	0
1209	West Cave: shrine	Middle	4	0	0
1241	East Cave	Middle	170	0	0
433	East Cave central	Late	6	0	0
436	East Cave central	Late	32	0	0
715	East Cave	Late	54	0	0
738	East Cave	Late	15	0	0
790	Intermediate zone	Late	11	0	0
1206	West Cave: shrine	Late	508	2	0
960	West Cave: shrine	Latest	405	4	3
783	West Cave: display	Latest	976	8	3
		Total	3060	25	15

deciduous teeth amongst the study sample. Observations include extreme labial and lingual wear, and alongside individual descriptions of deciduous dental modification and extreme wear to the anterior teeth, these phenomena are presented in more detail in §5.5.1, below.

As enumerated in Figure 5.2, adult teeth were most often observed to be modified, with 154 teeth identified with these phenomena amongst the study sample (89.53% total modified teeth). Modified deciduous teeth were far fewer in number, but are present in the dataset nonetheless. A total of 18 modified deciduous teeth were observed amongst the current study sample (10.47% total modified teeth). The distribution of adult modified teeth is schematically presented in Figure 5.3. Here, we see that the maxillary dentition features substantially more examples of modification, with 110 teeth accounting for 71.43% of total adult observations, compared to 44 modified mandibular teeth (28.57% total adult modified teeth). There also appears to be a slight bias towards modifications by side, with 87 examples observed on the left side (56.50% total adult

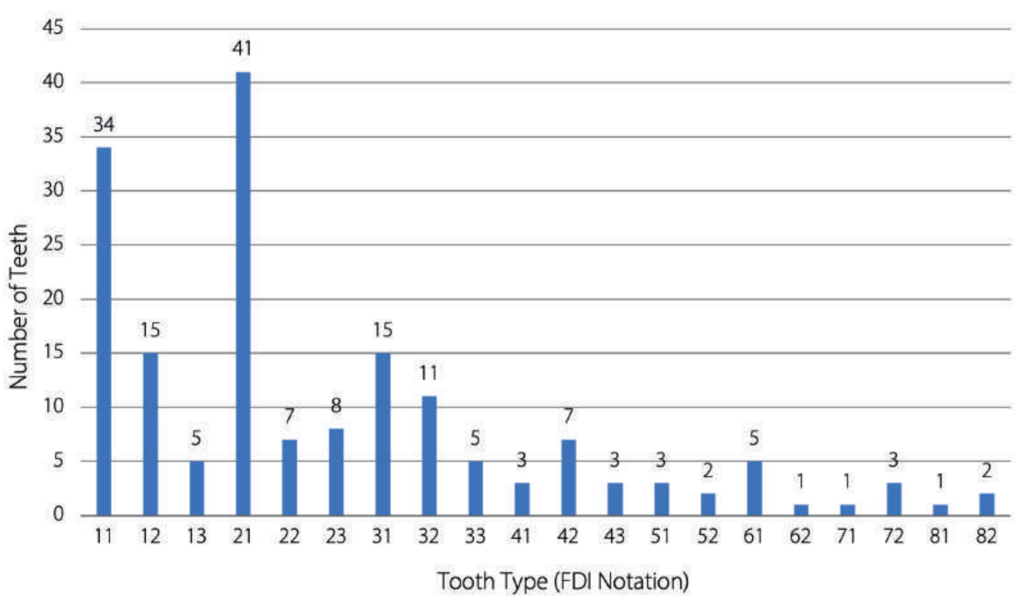

Figure 5.2. *Frequency distribution of tooth types featuring dental modification in the Circle sample (Σ=172).*

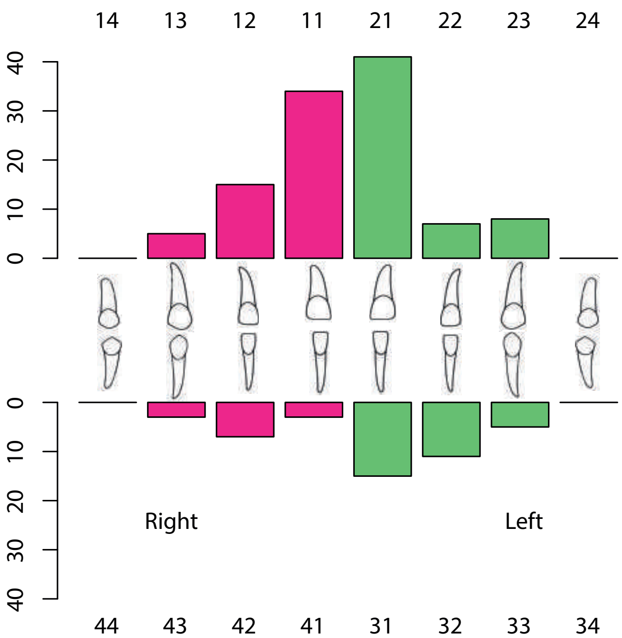

Figure 5.3. *Dynamic schema of dental modification observations by permanent anterior tooth type and arcade side in the Circle sample (follows FDI notations). (Rowan McLaughlin).*

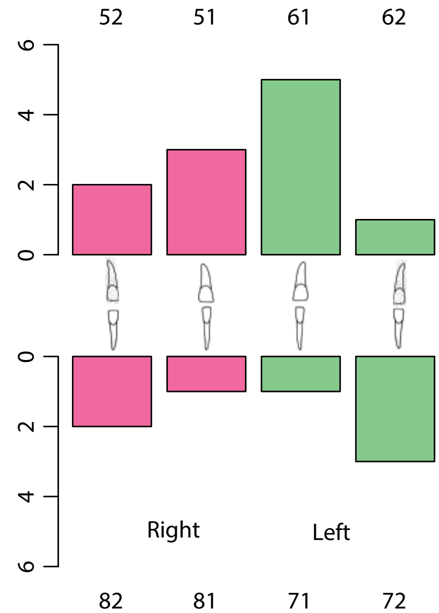

Figure 5.4. *Dynamic schema of dental modification observations by deciduous anterior tooth type and arcade side in the Circle sample (follows FDI notations). (Rowan McLaughlin).*

modified teeth) and 67 examples identified on the right (43.50% total adult modified teeth). The distribution of deciduous modified teeth is schematically presented in Figure 5.4. Although the overall numbers are far fewer than for the adult dentition, we see a similar pattern emerge in terms of distribution across the mouth. Here again, there are more observations of modified teeth on the maxilla (Σ=11; 61.11% total deciduous modified teeth) than on the mandible (Σ=7; 38.89% total deciduous modified teeth; and more observations of modification on the left side of the mouth (Σ=10; 55.56% total deciduous modified teeth) than on the right (Σ=8; 44.44% total deciduous modified teeth).

The data may be further examined to determine the individual tooth types most frequently affected by modification practices. The left permanent maxillary central incisor (FDI 21) was the most commonly involved tooth, with 41 observations amongst the study sample accounting for almost a quarter of all modified teeth (23.83%). This was followed by 34 examples of right permanent maxillary central incisor engagement (19.77% total modified teeth); while 15 observations were recorded for both the right permanent maxillary lateral incisor (FDI 12) and left permanent mandibular central incisor (FDI 31; each 8.72% total modified teeth). There were 11 examples of modified left permanent mandibular lateral incisors (FDI 32; 6.39% total modified teeth), while all other affected anterior tooth types presented fewer than 10 modifications each.

Although the numbers of modified teeth for any single deciduous tooth type do not exceed single figures, the relative rarity of this phenomenon for non-adults in archaeological data demands that all examples are highlighted (Frayer 2004, 94; Irvine *et al.* 2014, 25). Extending the patterns already described above, the most frequently modified tooth type is the same for the affected children and adults of the Circle sample population. Left deciduous maxillary central incisors were the most commonly modified teeth, with five observations amongst the sample (FDI 61; 27.78% total deciduous modified teeth; 2.90% total modified teeth). Further to this, there were three examples each of right deciduous maxillary central incisors (FDI 51) and left deciduous mandibular lateral incisors (FDI 72; each 16.67% total deciduous modified teeth; 1.74% total modified teeth); two examples each of right deciduous maxillary lateral incisors (FDI 52) and left deciduous mandibular lateral incisors (FDI 82; each 11.11% total deciduous modified teeth; 1.16% total modified teeth); and one example each of left deciduous maxillary lateral incisor (FDI 62), left deciduous mandibular central incisor (FDI 71) and right deciduous mandibular central incisor (FDI 81; each 5.56% total deciduous modified teeth; 0.60% total modified teeth).

5.5.1. Modification types

Dental modification observations were classified according to particular types, including chipping, incisal notches, labial extreme wear, diagonal profiling, lingual extreme wear and undulations. When combined, there were 230 individual observations of these phenomena on anterior adult and deciduous teeth amongst the study sample. These are expressed proportionately in Figure 5.5, and presented in more detail, below. Incidences of gross crown loss of the anterior teeth are also reported.

5.5.1.1. Chipping

'Chipping' refers to any form of enamel removal in discrete portions or 'chunks' by either deliberate ('active') or incidental ('passive') means. Chipping often has a 'disorganized' appearance, and can present as a sequence of micro-insults, resulting in stepped, rough or jagged margins. This form of modification can occur across the incisal margin of the anterior teeth, although it is frequently observed on either mesial or distal corners. van der Reijden (2014, 16) recommends a distinction between 'chipping' and 'chiselling' as respectively incidental and intentional phenomena. Chipping of the anterior teeth is one of the most commonly reported forms of dental modification across archaeological populations (Alt & Pichler 1998, 398), and it can now be reported that the phenomenon extends to Neolithic Malta. A selection of examples from amongst the dataset are presented in Figure 5.6a to k. In this figure, it is apparent that there are a variety of forms of chipping amongst the Circle population, with some clearly identifiable as incidental or parafunctional wear. Others, however, closely resemble forms described by van den Reijden as intentional (2014, Table 4.5; B1.1; B1.3; B1.4; B4.3; B4.4; C2.3). As seen in Figure 5.5, chipping was the most commonly observed dental modification amongst the study sample, with 90 recorded incidences accounting for 39.13% of all modifications. When plotted by chronological distribution (Fig. 5.7), the highest frequencies of chipping modification were observed among the Late contexts of the dataset. A total of 77 chipped teeth were identified in this phase (85.56% total chipping), representing 8.5 times more observations than for the Early use-phase contexts (Σ=9; 10.00% total chipping) and slightly less than 20 times more observations than for the Middle use-phase (Σ=4; 4.44% total chipping). As seen in Table 5.2, incidences of chipping within individual contexts in descending order are: (783) (Σ=49); (960) (Σ=16); (1206) (Σ=11); (595) (Σ=5); (1241) (Σ=4); (951) (Σ=3); and (436) (Σ=1). Expressed as a proportion of the chipped teeth sample, the distribution is (783) (54.44%); (960) (17.78%); (1206) (12.22%); (595) (6.67%); (1241) (4.44%); (951) (3.33%); and (436) (1.11%). Across both distributions, Context (783) has the highest raw and proportional incidences of chipping modifications within the Xagħra study sample.

Figure 5.8 reveals that the majority of chipping modifications amongst the Xagħra study sample were observed on adult dentition, with 81 observations (90.00% total chipping) as opposed to nine on deciduous teeth (10.00% total chipping). Within the adult category, maxillary teeth were more likely to be chipped, with 57 observations pertaining to upper permanent anterior teeth (70.37% total adult chipping;

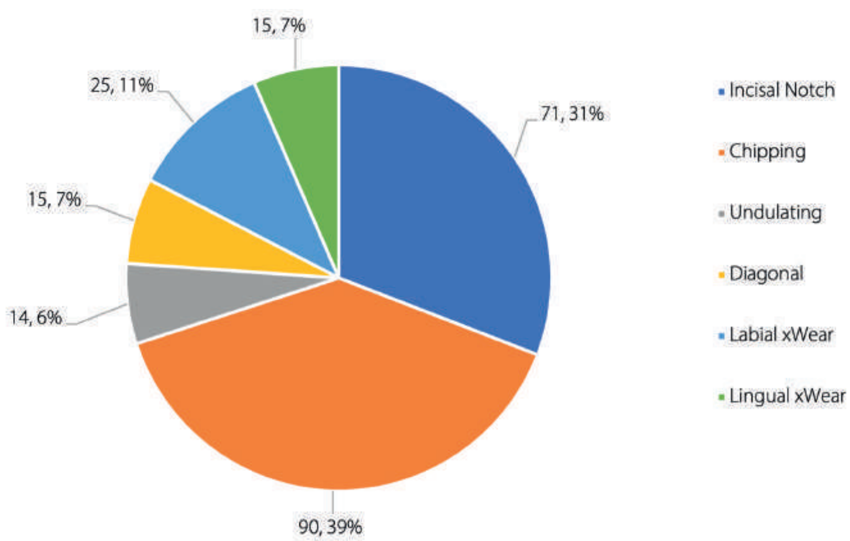

Figure 5.5. *Frequency distribution of dental modification types in the Circle sample (Labial xWear = Labial Extreme Wear; Lingual xWear = Lingual Extreme Wear) (Σ=230).*

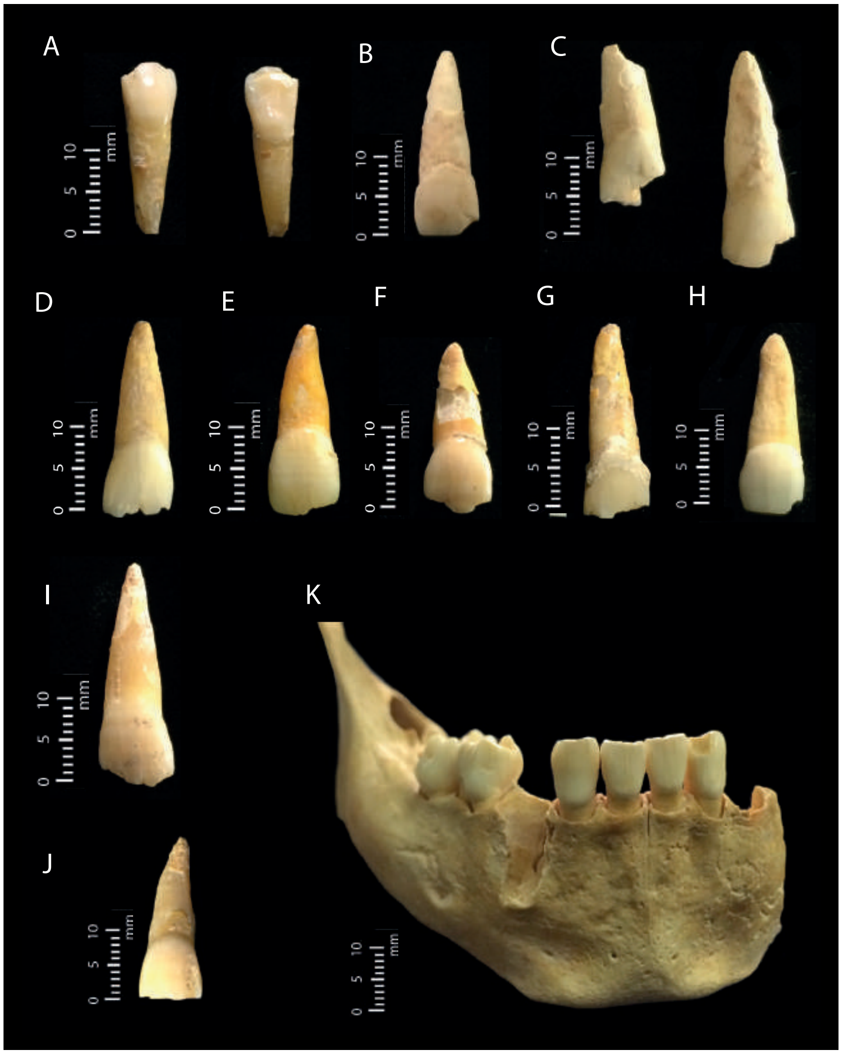

Figure 5.6. *Examples of chipping modifications in the Circle sample. a) labial and lingual aspects, Context (951) 96E/115N; b) Context (951) E3 No. 34; c) Context (951) 96E/ 114N; d) Context (960) 99E/111N Spit 3, Unit 1; e) Context (783) 95E/110N; f) Context (783) 95E/113N (deciduous); g) (783) 94E/111N; h) (783) 95E/112N; i) Context (783) 96E/113N; j) Context (783) 96E/112N Spit 1, No. 13; k) Context (783) 97E/112N Sk. 9 (deciduous). Scale bar: 1 cm. (Photos Ronika K. Power).*

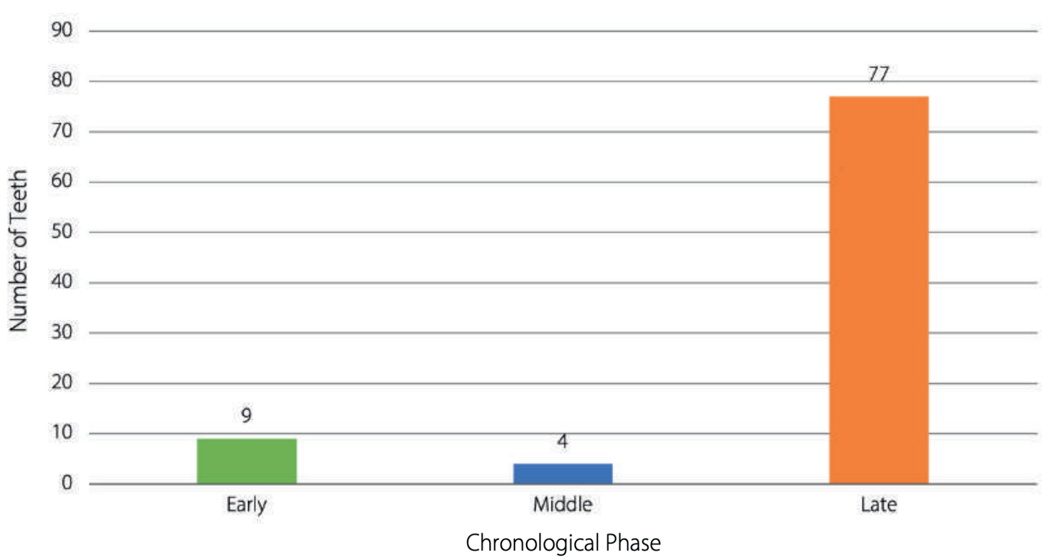

Figure 5.7. *Frequency distribution of chipping modifications by chronology in the Circle sample (Σ=90).*

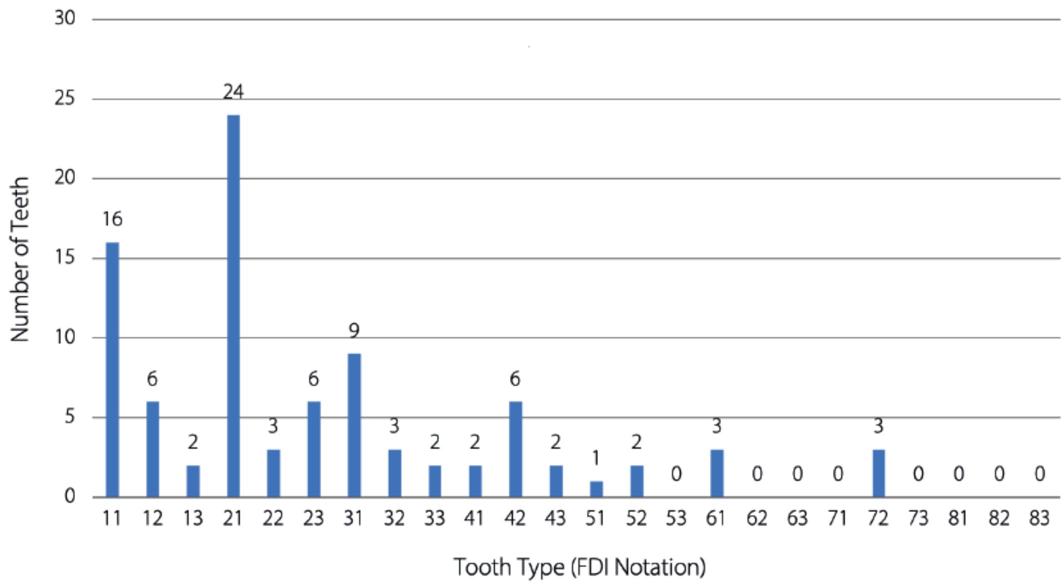

Figure 5.8. *Frequency distribution of chipping by tooth types in the Circle sample (tooth type follows FDI notation) (Σ=90).*

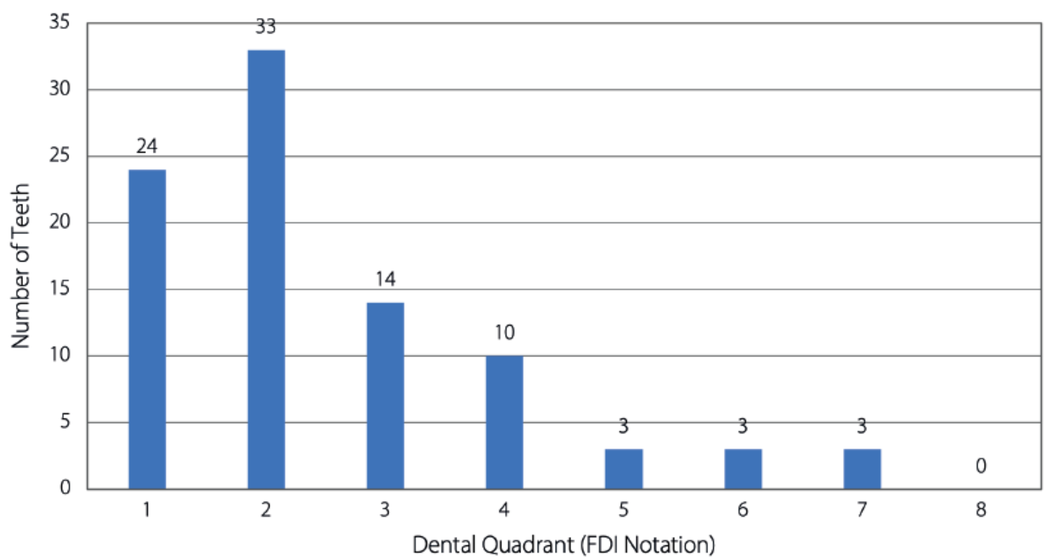

Figure 5.9. *Frequency distribution of chipping by quadrants in the Circle sample (quadrants follow FDI notation) (Σ=90).*

63.33% total chipping) as opposed to 24 on the lower anterior arcade (42.11% total adult chipping; 26.67% total chipping). Among the affected deciduous dentition, maxillary teeth were observed to be chipped twice as frequently, with six examples (66.67% of deciduous chipping; 6.67% total chipping) *versus* only three on mandibular teeth (33.33% of deciduous chipping; 3.33% total chipping).

When considered in terms of distribution by quadrants (Fig. 5.9), the left permanent maxillary anterior dentition account for the highest number of chipping observations with 33 teeth presenting this phenomenon (36.67% total chipping; 40.74% total adult chipping). The right permanent maxillary anterior teeth featured the second highest number of affected teeth with 24 observations (26.67% total chipping; 29.63% total adult chipping), followed by the left permanent mandibular (Σ=14; 15.56% total chipping; 17.28% total adult chipping) and right permanent mandibular arcades (Σ=10; 11.11% total chipping; 12.35% total adult chipping). The nine deciduous teeth presenting chipping were evenly distributed across three quadrants, with the upper right and left and lower left each featuring 3 affected teeth (each 3.33% total chipping; each 33.33% total deciduous chipping). There were no observations for the deciduous mandibular right quadrant.

The most commonly chipped individual type of anterior tooth amongst the sample was the left permanent maxillary central incisor, with 24 teeth presenting this form of modification (FDI 21; 26.67% total chipping; 29.63% total adult chipping). This was followed by the right permanent maxillary central incisor, which was observed to be chipped on 16 occasions (FDI 11; 17.78% total chipping; 19.75% total adult chipping). All remaining affected adult dentition presented less than ten observations per tooth type. In terms of deciduous dentition, the affected teeth are clustered tightly in numbers, with chipping observed on three left deciduous maxillary central incisors (FDI 61) and three left deciduous mandibular lateral incisors (FDI 72; each 33.33% total deciduous chipping; 3.33% total chipping), followed by two right deciduous maxillary lateral incisors (FDI 52; each 22.22% total deciduous chipping; 2.22% total chipping) and one right deciduous maxillary central incisor (FDI 51; 11.11% total deciduous chipping; 1.11% total chipping).

5.5.1.2. Incisal notches

'Incisal notches' may be variably referred to as 'incising' or 'grooving' (Burnett & Irish 2017b, 3; Langsjoen 1998, 410; van der Reijden 2014, 16). Incisal notches involve the removal of enamel from the incisive margins of the anterior teeth, however in this case the affected area is quite discrete or contained, with smooth and well-demarcated margins. They may present as either tightly shaped notches or grooves, or be more expansive in their gauge. The latter form of incisal notches can take on a 'swallow-tail' appearance (Irish 2017, Fig. 3.2e). Incisal notches may also be caused by either deliberate ('active') or incidental ('passive') means and are a common mode of dental modification across cultures. In the selection presented from the Circle sample (Fig. 5.10a–j), incisal notches

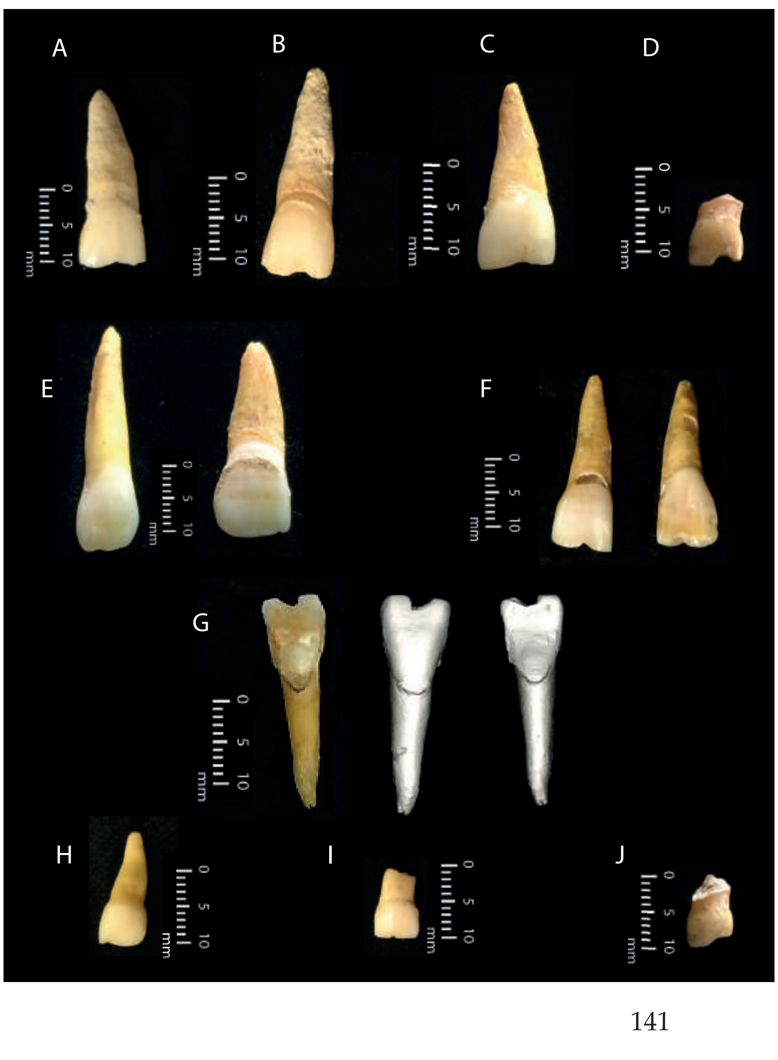

Figure 5.10. *Examples of incisal notch modifications in the Circle sample. a) Context (960) 99E/111N Spit 3, Unit 12; b) Context (783) 96E/110N Quad X; c) Context (783) 95E/112N; d) Context (783) 94E/113N Quad X (deciduous); e) Context (783) 94E/113N Quad X; f) labial and lingual aspects, Context (595) 100E/104N Quad H; g) lingual aspect (photo), labial and lingual aspects (3D render), Context (783) 95E/111N (?) Spit 1; h) Context (783) 95E/113N (deciduous); i) Context (783) 95E/111N Spit 1 (deciduous); j) Context (783) 94E/112N Quad X (deciduous). Scale bar: 1 cm. (Photos Ronika K. Power; radiological images captured by L. Buck, Cambridge Biotomography Centre; processed by J. Magnussen & M. Pardey, Macquarie Medical Imaging).*

feature across the incisal edge in a linguo-labial direction but are more commonly observed within the central portion rather than on the mesial or distal corners, with the direction of the groove indicating the direction of the pulling force (Langsjoen 1998, 410). As for chipping, Figure 5.10a–j reveals a variety of forms of notching amongst the Circle burial population. Although some are readily identified as incidental or parafunctional wear; others align with forms described by van der Reijden as intentional (2014, Table 4.5; Types A6.4; A8.1). They were the second most common dental modification amongst the Circle study sample (Fig. 5.5), observed on 71 teeth and representing slightly less than one-third of all modifications (30.87%).

Considered from a chronological perspective (Figure 5.11), the majority of incisal notch modifications precipitated from Late contexts of the Circle. In total, 60 teeth were attributed to the final phase of interments (85.7% total notches). This is substantially more than was observed for the Early contexts (Σ=10; 14.08% total notches); and the Middle use-phase had only one example of an incisal notch modification (1.14% total notches). Table 5.2 reveals the intensity of the Late

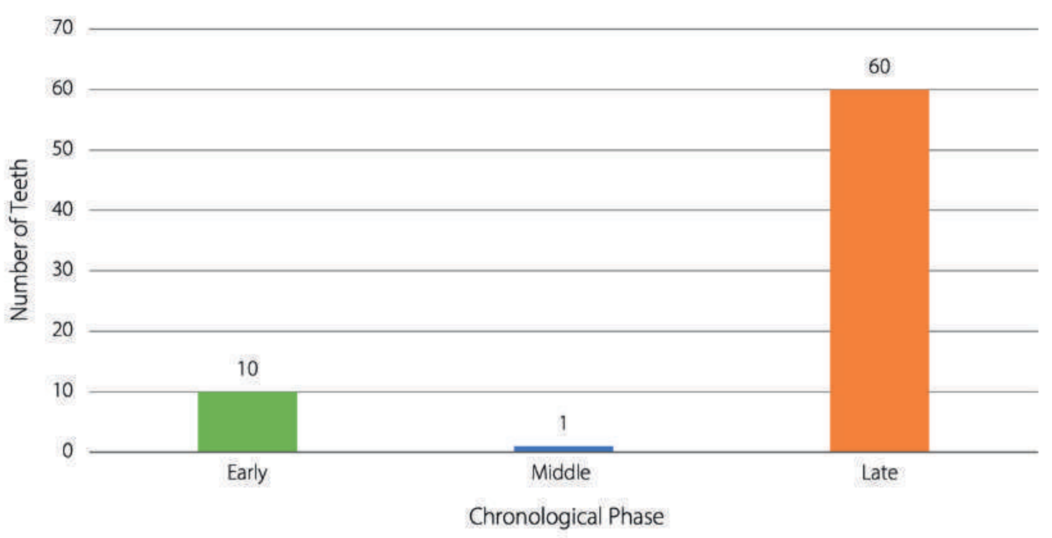

Figure 5.11. *Frequency distribution of incisal notch modifications by chronology in the Circle sample (Σ=71).*

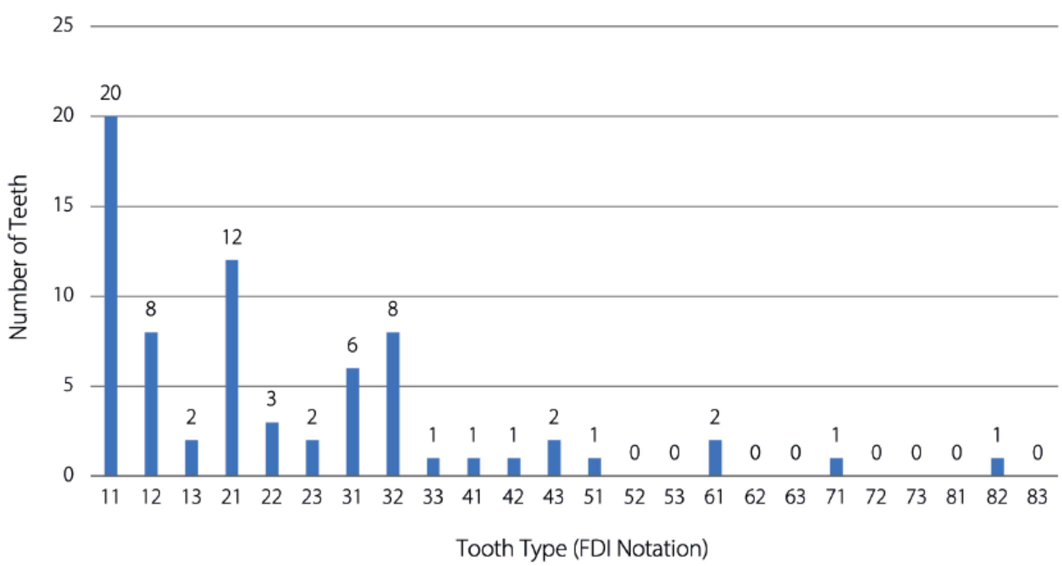

Figure 5.12. *Frequency distribution of incisal notches by tooth types in the Circle sample (tooth type follows FDI notation) (Σ=71).*

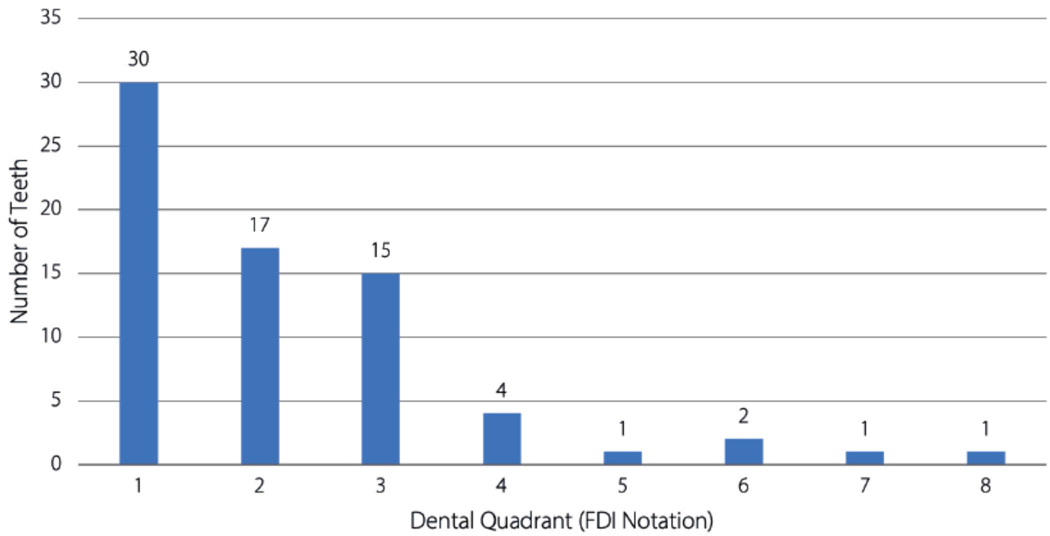

Figure 5.13. *Frequency distribution of incisal notches by quadrants in the Circle sample (quadrants follow FDI notation) (Σ=71).*

use-phase incidence of incisal notches, with the data listed in descending order as: (783) (Σ=27); (960) (Σ=16); (1206) (Σ=15); (595) and (951) (each Σ=5); and (1241), (738) and (790) (each Σ=1). Viewed proportionately for all notched teeth, the results are: (783) (38.02%); (960) (22.54%); (1206) (21.13%); (595) and (951) (7.04%); and (1241), (738) and (790) (1.41%). In both incidence and proportion, Context (783) features the highest representation of incisal notches across this sample of the burial population.

When analysed according to tooth types (Fig. 5.12), we see that 66 adult teeth presented incisal notch modifications (92.96% total notches), alongside five examples of deciduous teeth (7.04% total notches). Within the affected adult teeth, 47 maxillary teeth presented incisal notches (71.21% total adult notches; 66.20% total notches) compared with 19 instances on mandibular teeth (28.79% total adult notches; 26.76% total notches). The data are more balanced among the deciduous group, with three examples observed on maxillary teeth (60.00% total deciduous notches; 4.23% total notches) and two on mandibular dentition (40.00% total deciduous notches; 2.82% total notches).

To interrogate further the representation of incisal notches, we may consider their appearance across the oral quadrants (Fig. 5.13). In this case, the distribution follows FDI notation order: the right permanent maxillary anterior dentition features 30 examples of incisal notches (45.45% total adult notches; 42.25% total notches), which is just under twice the amount of notched left permanent maxillary teeth (Σ=17; 25.76% total adult notches; 23.94% total notches). The left permanent mandibular teeth featured 15 examples of incisal notches (22.73% total adult notches; 21.13% total notches), which is substantially greater than the four observations attributed to right permanent mandibular dentition (6.06% total adult notches; 5.63% total notches). The five deciduous teeth presenting incisal notches were almost evenly distributed across the oral quadrants, with the right deciduous maxillary arcade featuring 2 examples (40% total deciduous notches; 2.82% total notches), and one example on each of the right maxillary and left and right mandibular quadrants (each 20.00% total deciduous notches; 1.41% total notches).

The permanent right and left maxillary central incisors (FDI 11, 21) most frequently displayed incisal notches amongst the study sample, accounting for 20 (30.30% total adult notches; 28.17% total notches; Fig. 5.12) and 12 (18.18% total adult notches; 16.90% total notches) examples respectively, or 32 collectively (48.49% total adult notches; 45.07% total notches). The remaining teeth presented less than 10 examples for each type, although it is noteworthy that the right permanent maxillary lateral incisors and left permanent mandibular lateral incisors each featured 8 notched teeth (12.12% total adult notches; 11.26% total notches). The affected deciduous teeth are tightly grouped, with two examples of notches attributed to left deciduous maxillary central incisors (FDI 61), and single examples observed for a right deciduous maxillary central incisor (FDI 51), left deciduous mandibular central incisor (FDI 71), and right deciduous mandibular lateral incisor (FDI 82).

5.5.1.3. Labial extreme wear

In addition to discussions presented in Chapter 4 of this volume, labial extreme wear is included here because of its likely aetiologies in activities beyond 'ordinary' mastication, potentially including food processing and/or processing materials other than food in association with cultural practices. For the purposes of this study, labial 'extreme wear' is defined as wear resulting in the substantial blunting and accompanying dentine exposure of the anterior teeth on the labial surface. This mode of dental modification is known in populations across the globe (Burnett & Irish 2017b, 3), and is particularly associated with the use of the mouth as a tool during the processing of animal skins (Alt & Pichler 1998, 394; Eshed *et al.* 2006; Langsjoen 1998, 410; Lous 1970; Roberts & Manchester 2005, 81). In these circumstances, the fibrous nature of the hide erodes the enamel from the labial surface of the anterior teeth, and in some cases can also compromise the gingiva. In some cultural contexts, this mode of modification is also associated with wearing labial body ornaments such as labrets (Alt & Pichler 1998, 402). Examples of this 'passive' modification phenomenon were observed amongst the Circle study sample, as seen in Figure 5.14a–j. Here, an extreme case is noted in Figure 5.14i, where the entire labial surface of an unsided permanent mandibular incisor has been eroded in coronal section, obliterating the architecture of the tooth from the incisal margin to the apex of the root, including the destruction of the pulp chamber and root canal. The level of destruction prevents identifying the tooth as either a central or lateral mandibular incisor. It is difficult to appreciate how this tooth remained viable in the mouth, considering not only the compromise and destruction of the dental nerve, but also that the level of labial attrition indicates that the anterior aspect of the alveolar margin must have also been completely abraded. This abrasive process may have happened in isolation, but it may also have occurred in concert with alveolar recession if the individual in question was suffering a co-morbidity of severe periodontal disease (Hillson 2005, 292, 305–6). In addition to these

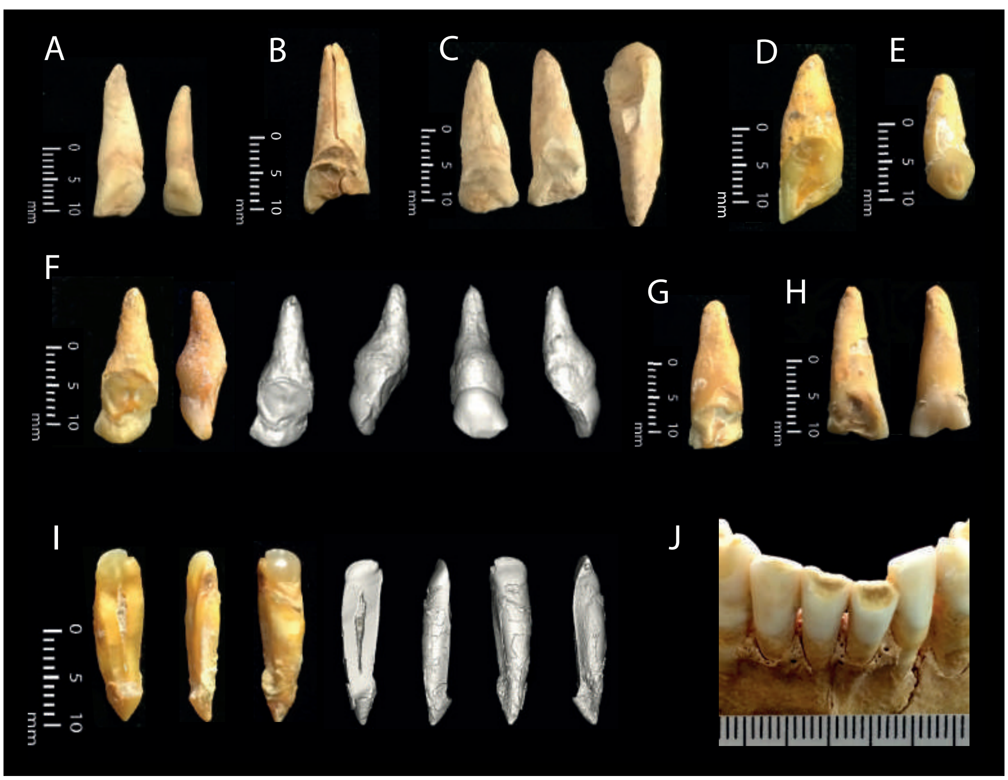

Figure 5.14. *Examples of labial extreme wear modifications in the Circle study sample. a) Context (951) 98E/116N; b) Context (951); c) Context (951) 98E/116N Area X; d) Context (783) 96E/111N; e) Context (783) 95E/110N Quad X; f) photographs and micro-CT 3D renders, Context (783) 95E/11N Quad X; g) Context (783) 96E/110N Quad X; h) labial and lingual aspects, Context (783) 96E/110N; i) photographs and micro-CT 3D renders, Context (783) 95E/112N Quad X; j) Context (783) 95E/115N Skull 1. Scale bar: 1 cm. (Photos Ronika K. Power; radiological images captured by L.T. Buck, Cambridge Biotomography Centre; processed by J. Magnussen & M. Pardey, Macquarie Medical Imaging).*

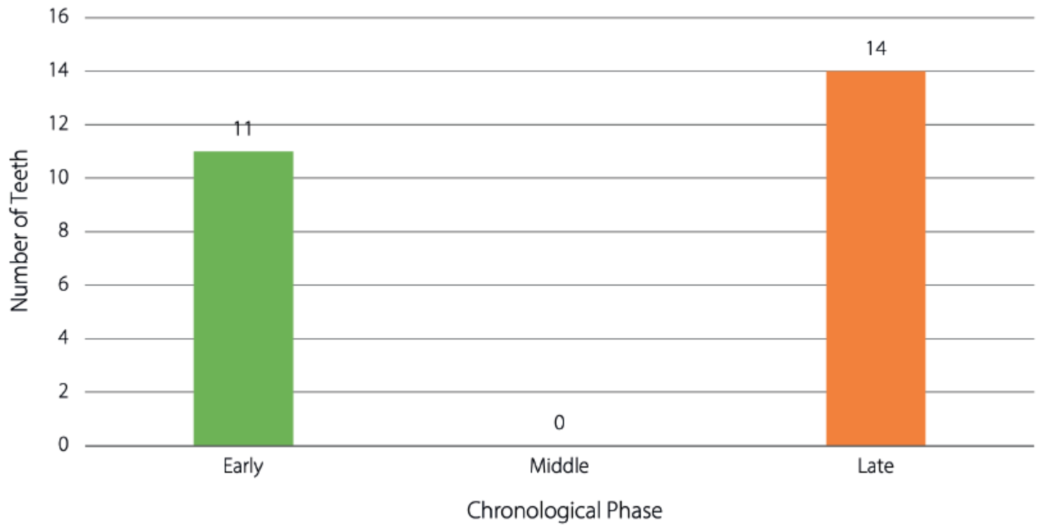

Figure 5.15. *Frequency distribution of labial extreme wear by chronology in the Circle sample (Σ=25).*

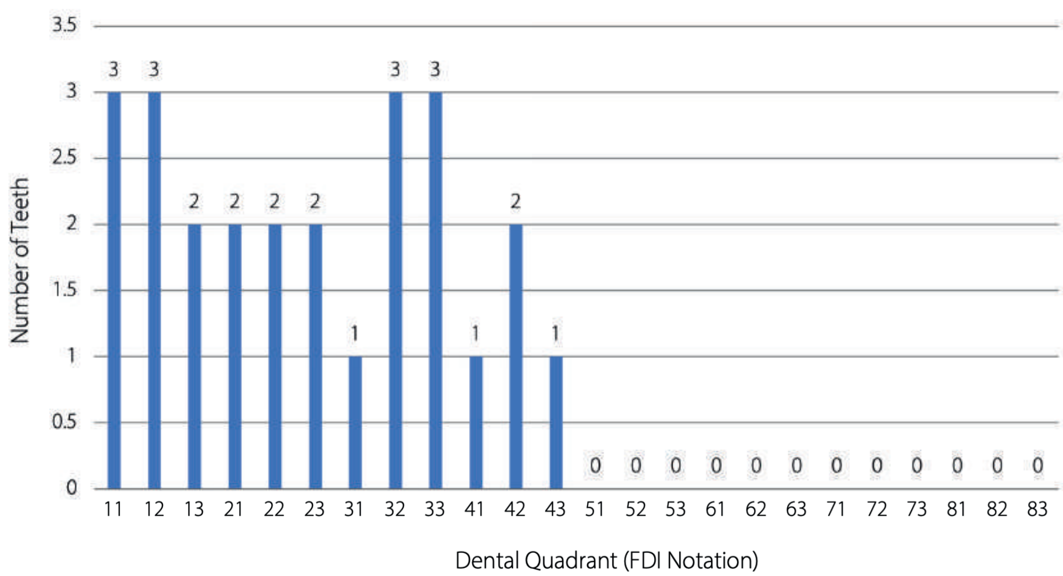

Figure 5.16. *Frequency distribution of labial extreme wear by tooth types in the Circle sample (tooth type follows FDI notation) (Σ=25).*

phenomena, we can see that this particular individual was using the mouth as a multi-purpose tool. A pronounced incisal notch is also observed on the occlusal margin (Fig. 5.14i). Whatever activities produced and maintained the incisal notch were occurring until close to the time of death, as the notch channel is embedded into both the incisal margin and abraded labial surface. This individual was not alone in their employment of their mouth as a multi-purpose tool or signifier. Several of the teeth included in these images feature more than one kind of modification, including manipulation of the incisal edges resembling van der Reijden's 'B' Types, where the modification distinctly affects one edge (2014: Table 4.5). This type of modification will be discussed regarding 'Diagonal' types in §5.5.1.5, below.

Labial extreme wear is the third most common dental modification amongst the Xagħra study sample (Fig. 5.5), observed on 25 teeth and representing 10.87% of the modified dataset. Considered from a chronological perspective, labial extreme wear has an intriguing distribution (Table 5.3 & Fig. 5.15). All recorded cases of this mode of dental modification are derived from either the Early (Σ=11; 44.00% total labial extreme wear) or Late (Σ=14; 56.00% total labial

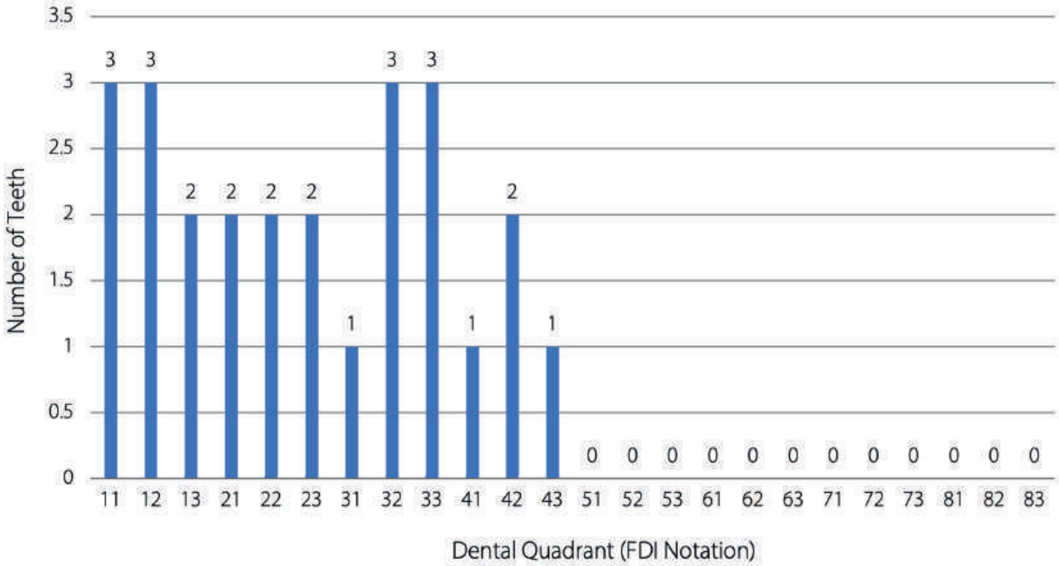

Figure 5.17. *Frequency distribution of labial extreme wear by quadrants in the Circle sample (quadrants follow FDI notation) (Σ=25).*

extreme wear) use-phases of the Circle. Of these, the Late use-phase had slightly more examples. There were no observations of labial extreme wear amongst the Middle use-phase dataset whatsoever. In terms of individual contexts, Table 5.3 also reveals that the experience of this modification was quite similar between the Early and Late use-phases, with the data tightly clustered in descending order as follows: (783) (Σ=8); (595) (Σ=7); (951) and (960) (each Σ=4); and (1206) (Σ=2). When calculated proportionately for all teeth affected with extreme labial wear, the results table as: (783) (32.00%); (595) (28.00%); (951) and (960) (each 16.00%); and (1206) (8.00%). Context (783) features the highest representation of labial extreme wear in both incidence and proportion across this sample of the burial population.

To explore the broader experience of extreme labial wear, the teeth were analysed according to individual types (Fig. 5.16). In this case, this particular form of modification is restricted to adult teeth; no deciduous dentition was observed with extreme labial wear. Amongst the 25 affected adult teeth, the maxillary dentition was slightly more frequently observed, with 14 examples recorded (56.00% total labial extreme wear) as opposed to 11 mandibular observations (44.00% total labial extreme wear). The experience of this modification was relatively even across the oral quadrants (Fig. 5.17). Although the right permanent maxillary anterior dentition presented the highest incidence of extreme labial wear (Σ=8; 32.00% total labial extreme wear), this was closely followed by the left permanent mandibular anterior dentition (Σ=7; 28.00% total labial extreme wear), the left permanent maxillary anterior teeth (Σ=6; 24.00% total labial extreme wear) and the right permanent mandibular anterior teeth (Σ=4; 16.00% total labial extreme wear). This suggests that these abrasive activities were relatively evenly experienced across both upper and lower arcades.

This observation extends to analyses of the experience of labial extreme wear across individual tooth types (Fig. 5.16). Results were very tightly clustered amongst the individual affected teeth, supporting the notion of broad impact of abrasive parafunctional activities across the upper and lower anterior arcades. The right permanent maxillary central and lateral incisors (FDI 11, 12) and left permanent mandibular lateral incisors and canines (FDI 32, 33) each presented three examples within the dataset (each 12.00% total labial extreme wear). Further to this, the right permanent maxillary canine (FDI 13), left permanent maxillary central and lateral incisors and canine (FDI 21, 22, 23), and right permanent mandibular lateral incisor (FDI 42) each featured two examples (each 8.00% total labial extreme wear). Finally, single observations were recorded for the left permanent mandibular central incisor (FDI 31), and right permanent mandibular central incisor and canine (FDI 41, 42; each 4.00% total labial extreme wear).

5.5.1.4. Lingual extreme wear

As with labial wear, lingual wear is included in discussions of both dental pathology (Chapter 4) and modification. This is because its aetiology was attributed to parafunctional activities including food and/

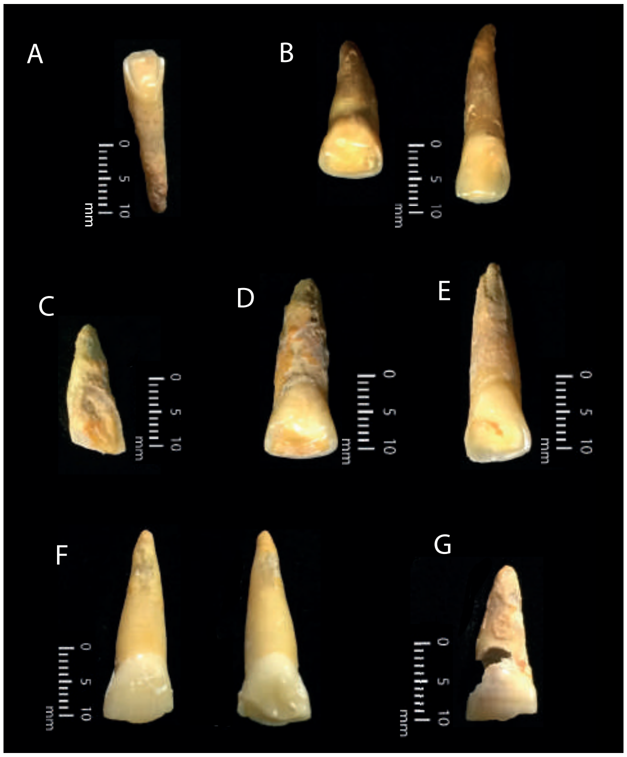

Figure 5.18. *Examples of lingual extreme wear modifications in the Circle sample: a) (951) 95E/110N; b) (783) 95E/112N Quad X; c) (783) 94E/112N; d) (783) 95E/111N Quad X; e) (783) 94E/113N. Examples of undulating profile modifications in the Circle sample: f) (783) 95E/113N labial and lingual aspects (also loss of vertical height, possibly multiple small notches); g) (783) 94E/111N Quad X (also cervical carious lesion). Scale bar: 1 cm. (Photos Ronika K. Power).*

or material processing in association with cultural practices. In this study, lingual 'extreme wear' is defined as wear that results in the substantial blunting and accompanying dentine exposure of the anterior teeth, on this occasion on the lingual surface. For consistency with the current analyses, this chapter will restrict investigations to observations of lingual wear on the anterior teeth. Considering that this mode of modification takes place inside the mouth outside of public view, it may be that it is a 'passive' modification which results from the kinds of processing activities suggested above. Examples of lingual extreme wear were observed amongst the Circle study sample, as seen in Figure 5.18a–e. Alongside diagonal profiling, lingual extreme wear was the equal-fourth most common form of dental modification amongst the dataset, each with 15 observations (6.52% total modifications).

Echoing the reported distribution for labial extreme wear, similar modifications of the lingual surface were also observed amongst only the Early and Late use-phases of the Circle study sample, with no identification of extreme lingual wear for the Middle use-phase data at all (Fig. 5.19). A total of nine examples were observed amongst the Early use phase population (60.00% total lingual extreme wear), and six within the sample for the Late interment contexts (40.00% total lingual extreme wear). As seen in Table 5.3, only four contexts presented evidence for this mode of dental modification amongst the sample. In this case, the data were also quite tightly clustered, following the highest frequency of observations in an Early use-phase context, (951) (Σ=7), equal observations in (960) and (783) (each Σ=3), and finally (595) (Σ=2). Expressed proportionately for all teeth affected with extreme lingual wear, these

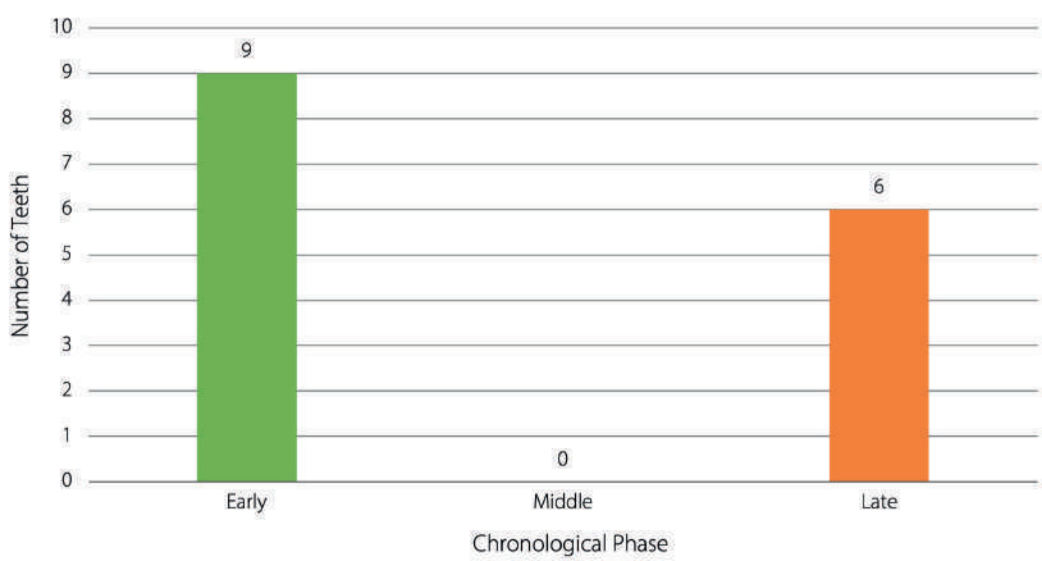

Figure 5.19. *Frequency distribution of lingual extreme wear by chronology in the Circle sample (Σ=15).*

results table as: (951) (46.67%), (960) and (783) (each 20.00%), and (595) (13.33%). On this occasion, Context (951) features the highest representation of lingual extreme wear in both incidence and proportion across this sample of the Circle population.

The data may also be evaluated according to tooth types (Fig. 5.20). As for labial extreme wear, incidences of lingual modifications were restricted to adult dentition; there were no observations of deciduous teeth with extreme lingual wear. Even amongst this small sample size, there appears to be a bias towards maxillary teeth being exposed to lingual extreme wear; there were 14 maxillary teeth to present this type of modification (93.33% total lingual extreme wear), as opposed to only one mandibular tooth (6.67% total lingual extreme wear). Naturally, this bias extends to the distribution by oral quadrants (Fig. 5.21). Here we see that the right permanent maxillary anterior arcade predominates with eight examples (53.33% total lingual extreme wear), followed closely by six observations for the left permanent maxillary anterior teeth (40.00% total lingual extreme wear). There were no observations whatsoever for the left permanent mandibular anterior dentition, and only one for the right permanent mandibular anterior arcade (6.67% total lingual extreme wear).

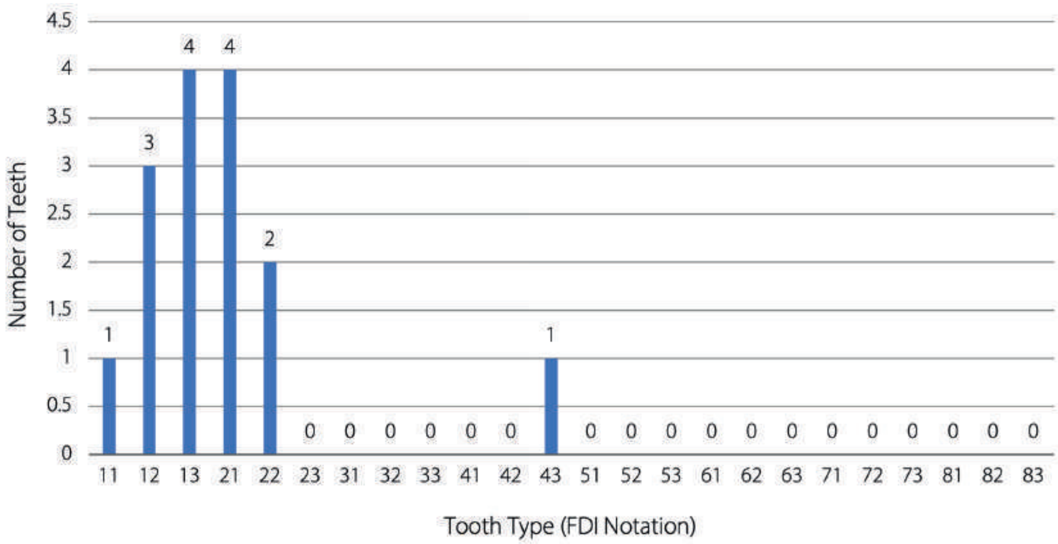

Figure 5.20. *Frequency distribution of lingual extreme wear by tooth types in the Circle sample (tooth type follows FDI notation) (Σ=15).*

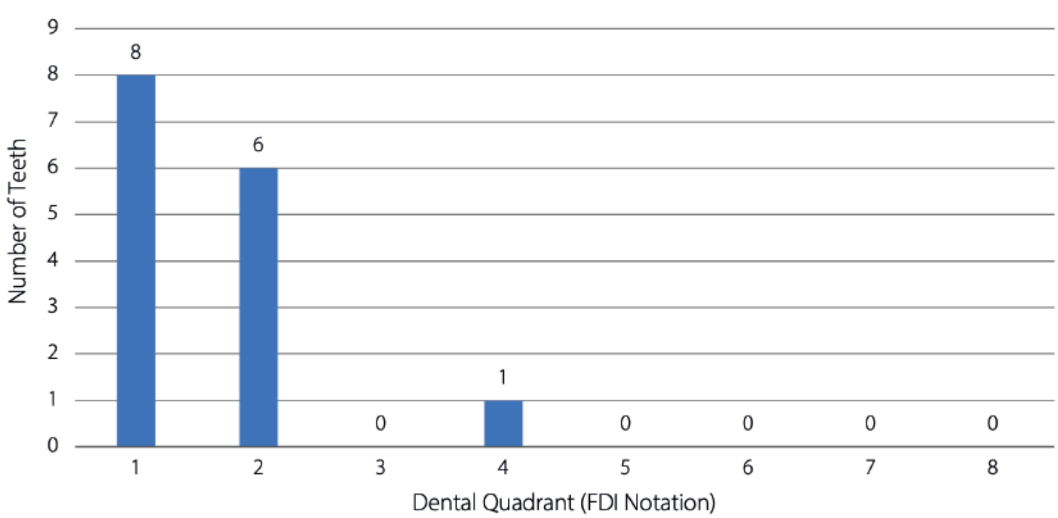

Figure 5.21. *Frequency distribution of labial extreme wear by quadrants in the Circle sample (quadrants follow FDI notation) (Σ=15).*

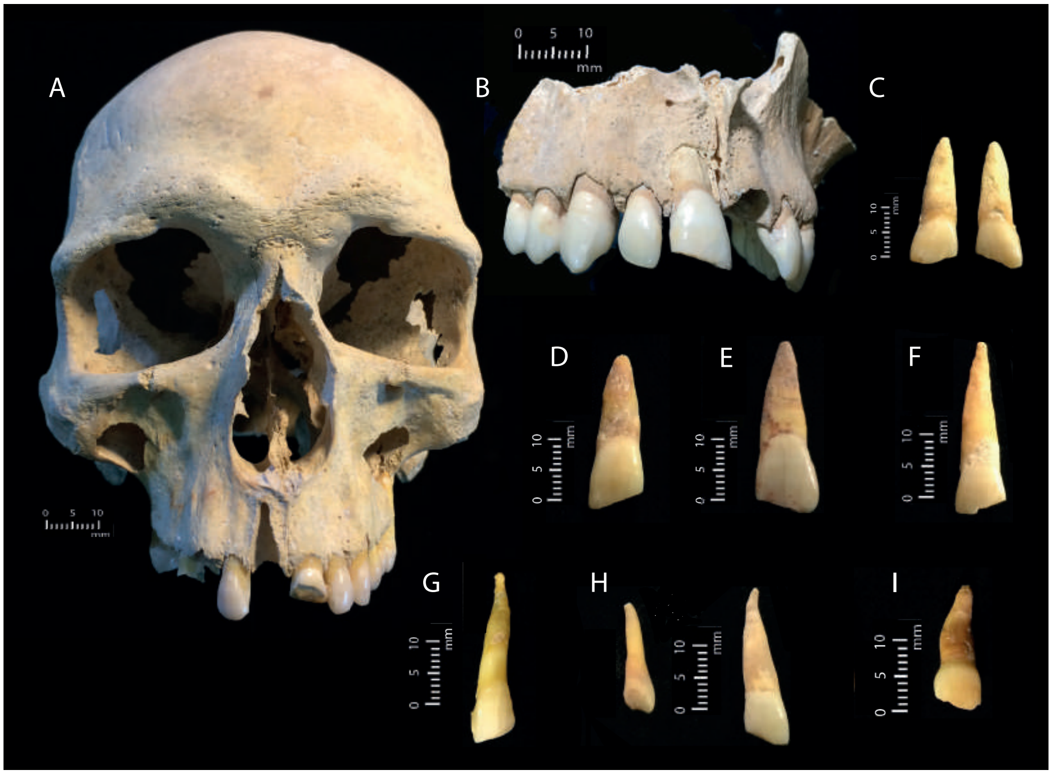

Figure 5.22. *Examples of diagonal profile modifications in the Circle sample. a) Context (1241) 105E/104N Spit 4, Unit 5; b) Context (783) 95E/113N; c) Context (783) 96E/110N; d) Context (783) 95E/111N; e) Context (960) 101E/109N Spit 5; f) Context (783); g) Context (783) 96E/110N Spit 1; h) Context (960) 100E/111N Spit 4; i) Context (783) 95E/111N Spit 1 (deciduous, also chipping and notching). Scale bar: 1 cm. (Photo Ronika K. Power).*

Only six types of permanent anterior teeth presented this phenomenon (Fig. 5.20), with the most numerous observations reported for the right permanent maxillary canine (FDI 13) and left permanent maxillary central incisor (FDI 21; each Σ=4; each 26.67% total lingual extreme wear). There were three observations of this modification for right permanent maxillary lateral incisors (FDI 12; 20.00% total lingual extreme wear); two for left permanent maxillary lateral incisors (FDI 22; 13.33% total lingual extreme wear); and one observation each for a right permanent maxillary central incisor (FDI 11) and a right permanent mandibular canine (6.67% total lingual extreme wear).

5.5.1.5. Diagonal profile

A diagonal profile modification involves the deliberate or incidental attrition of the incisal margin of the anterior teeth. The modification may be either mesially or distally inclined (maxilla) or declined (mandible), and may range between irregular to extremely sharp and smooth in character. The steepness of the modification is also variable. Despite the dramatic appearance of this form of modification, singular teeth within the arcade may be subject to alteration while the adjacent dentition show no evidence of manipulation whatsoever, as seen in examples from the Circle (Fig. 5.22a–i). One of the most striking images to emerge from this dataset soundly demonstrates this phenomenon. In Figure 5.22a we observe the cranium of an individual excavated from Context (1241) during the Middle use-phase of the Circle. The individual was determined to be an adult, based on the complete eruption and occlusion of the right and left maxillary permanent second molars (FDI 17, 27); bilaterally, the third molars appear to be either impacted or congenitally absent. The commencement of sutural obliteration also supports an adult age determination (Buikstra & Ubelaker 1994, 33ff.). The individual was subject to sex assessment based on evaluation of the cranial sexually dimorphic traits presented in Buikstra and Ubelaker (1994, 20), including nuchal crest (4/5), mastoid process (5/5), supraorbital margin (5/5) and supraorbital ridge/glabella (5/5). According to these criteria, the individual was assessed as a probable male. This individual presents a complex diagonal modification observed in occlusion on the left permanent maxillary central incisor (FDI 21). In this case, diagonal wear of the incisal edge is noted, mesially inclined from distal margin and terminating inferior to the cementum enamel junction. This individual illustrates the co-existence of modification modes, as we also observe approximately vertical labial wear extending from extant incisal margin. The labial wear comprises approximately two-thirds of the extant tooth crown, and also terminates inferior to the cementum enamel junction. Perhaps in association with both the diagonal and labial modes of attrition, the dentine has been exposed and presents a concave wear platform. Additionally, we observe that the crown height has been reduced by half, aligning with van der Reijden's N1.2 type (2014, 68). Although the neighbouring right permanent maxillary central incisor has been lost *postmortem* (FDI 11), we are able to observe that the adjacent left permanent maxillary lateral incisor (FDI 22) bears no changes to the mesial, labial or incisal surfaces or margins corresponding to the pronounced modifications described for the central incisor. Moreover, as seen in Figure 5.22a, no further modifications or extreme wear observations were recorded for any other of the extant retained dentition.

This is also the case for the arcade of an individual excavated from Context (783), for whom we were able to refit fragmentary left and right adult maxillae (Fig. 5.22.b). In this case, we observe a sharp, steeply inclined diagonal modification of the incisal edge of a right permanent maxillary central incisor (FDI 11). The modification is distally inclined from the mesial margin, comprising the inferior distal approximate third of the tooth. The tooth also displays mild chipping on the mesial margin; and this individual was also reported to feature multiple diastemata across the anterior maxillary arcade (Chapter 4). Again, note that the neighbouring right permanent maxillary lateral incisor (FDI 12) bears no evidence of the substantial abrasive processes that would have been required to produce this sharp, steeply inclined modification to the central incisor. Unfortunately, the adjacent left permanent maxillary central incisor has been lost *postmortem*; however, we observe that the extant retained maxillary dentition is in almost pristine condition, showing no further evidence of modification or extreme (or even moderate) wear.

Diagonal profiling is another commonly observed mode of dental modification across cultures, with the means of alteration being some form of abrasion or filing, of either 'active' or 'passive' impetus (Burnett & Irish 2017b, 3). The diagonal modifications observed in the Circle assemblage most closely align with van der Reijden's 'B' Types, where the modification distinctly affects one edge (2014, Table 4.5; B1.1, B1.3, B1.4); however, it is possible that some of the examples extend her criteria, as the filed edge is observed to extend across the entire incisal margin; and in some case the crown height is reduced by more than half. As mentioned above, diagonal profile modifications were the equal-fourth most frequently observed amongst the study sample, featuring 15 observations together with lingual extreme wear (Fig. 5.5; 6.52% total modifications). The chronological distribution of diagonal profiling was quite balanced amongst the population, with an equal number of observations attributed to both the Early and Middle use-phases (each Σ=3; each 20.00% total diagonal; Fig. 5.23). The highest frequencies of diagonal profiling were amongst the Late use-phase, with 9 observed within this component of the sample (60.00% total diagonal). Table 5.2 indicates that the

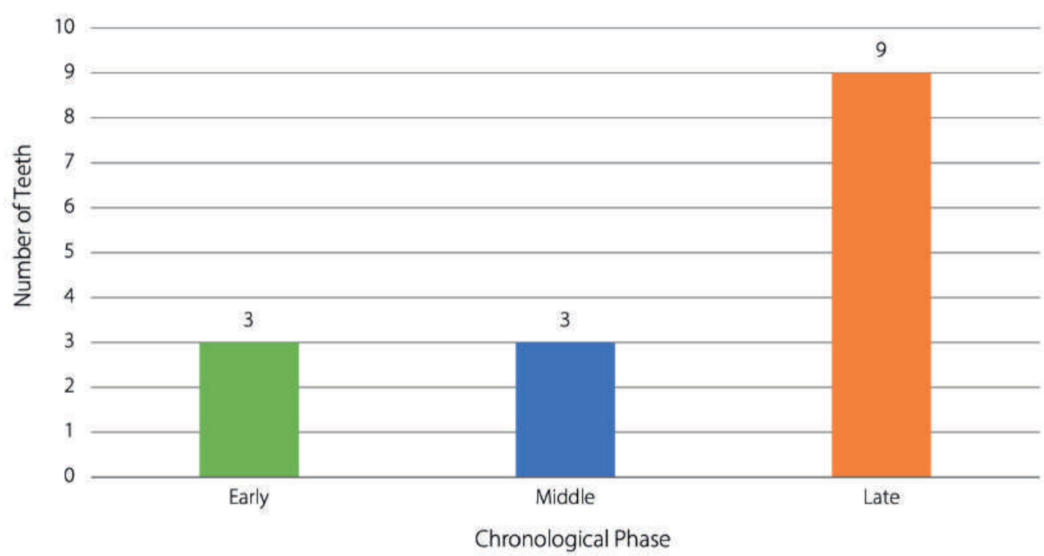

Figure 5.23. *Frequency distribution of diagonal profile modification by chronology in the Circle sample (Σ=15).*

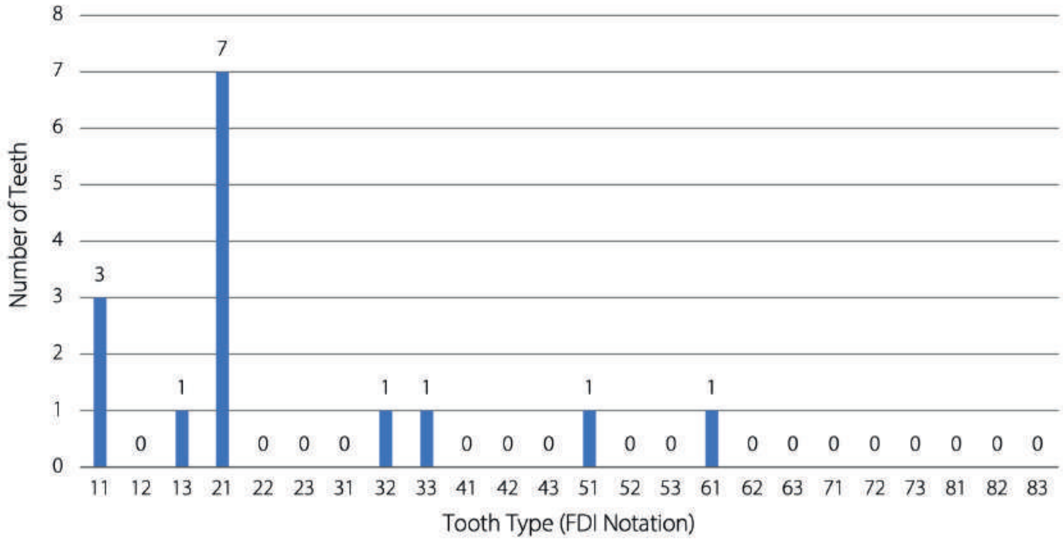

Figure 5.24. *Frequency distribution of diagonal profile modification by tooth types in the Circle sample (tooth type follows FDI notation) (Σ=15).*

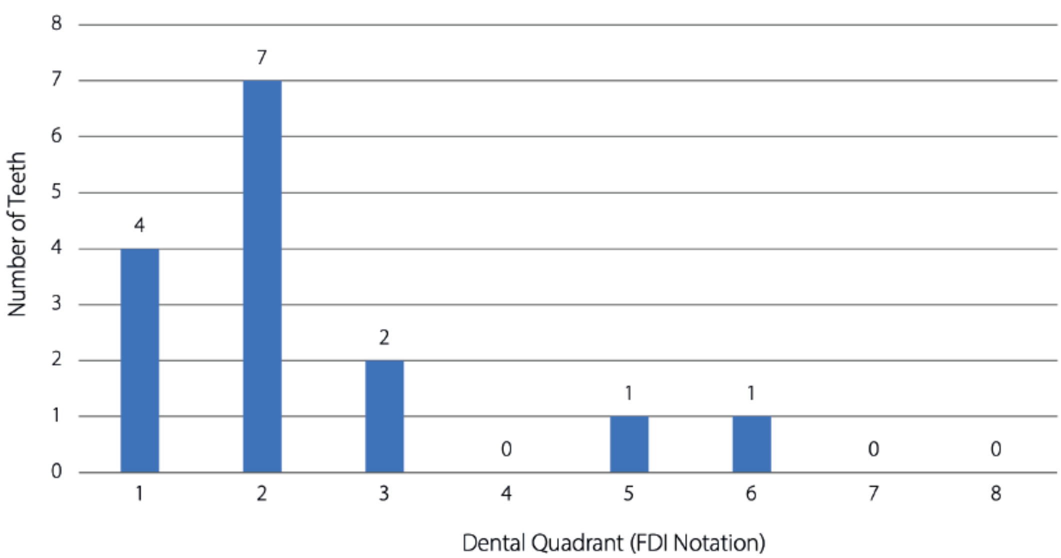

Figure 5.25. *Frequency distribution of diagonal profile modification by quadrants in the Circle sample (quadrants follow FDI notation) (Σ=15).*

majority of these precipitated from the latest of the Late use-phase contexts, (783), which featured five observations. The remaining contexts with diagonal profile modifications fall in descending order as: (1241) (Σ=3); (595) and (1206) (each Σ=2); and (951), (715) and (960) (each Σ=1). The proportions of teeth with diagonal profiling attributed to each context are: (783) (33.33%); (1241) (20.00%); (595) and (1206) (each 13.33%); and (951), (715) and (960) (each 6.67%). Here, we see that both in number of observations and proportionally (783) features the highest rates of diagonal profile modifications amongst the Circle study sample.

To understand better the expression of this mode of modification amongst the Neolithic Circle population, the data can be analysed according to tooth types (Fig. 5.24). Although both adults and non-adults appear to have been included in this form of dental manipulation, incidence was far higher amongst the adult members, with 13 observations recorded for permanent teeth (86.67% total diagonal), and two for deciduous dentition (13.33% total diagonal). There also appears to be a predilection for the maxillary teeth for this form of manipulation, with 11 observations attributed to the adult upper dentition (73.33% total diagonal; 84.62% total adult diagonal), *versus* only two for the mandibular permanent teeth. A similar pattern extends to the affected non-adult dentition, with both observations pertaining to maxillary teeth (13.33% total diagonal; 100.00% total deciduous diagonal). When considered according to distribution by oral quadrants (Fig. 5.25), the left permanent maxillary anterior teeth featured the highest number of diagonal profile modifications (Σ=7; 46.67% total diagonal; 63.64% total adult diagonal). This was followed by four observations for right permanent maxillary anterior teeth (26.67% total diagonal; 30.77% total adult diagonal); and two examples for the left permanent mandibular anterior arcade (13.33% total diagonal; 15.38% total adult diagonal). For the deciduous teeth, we observed one example of diagonal profile modification for each of the right and left maxillary anterior dentition (each 6.67% total diagonal; each 50.00% total deciduous diagonal).

A singular individual tooth type emerged as most frequently subjected to diagonal profile modification amongst the Circle study sample (Fig. 5.24). Almost half of all observations of this mode of modification were attributed to left permanent maxillary central incisors (FDI 21; Σ=7; 46.67% total diagonal; 53.85% total adult diagonal). This was more than double the next highest-frequency tooth, and greater than the sum of all other adult affected teeth. Three observations were recorded for right permanent maxillary central incisors (FDI 11; 20.00% total diagonal; 23.08% total adult diagonal); and one example each observed for a right permanent maxillary canine (FDI 13); left permanent mandibular lateral incisor (FDI 32); and a left permanent mandibular canine (FDI 33; each 6.67% total diagonal; each 7.69% total adult diagonal). As previously mentioned, both deciduous teeth displaying diagonal profile modification were attributed to the upper arcade, and both were central incisors, however one precipitated from the right (FDI 51) and one from the left (FDI 61; each 6.67% total diagonal; each 50.00% total deciduous diagonal).

5.5.1.6. Undulating profile

Undulating profile modifications are those observed to present a distinctly uneven, amorphous incisal margin across the anterior teeth. As seen on the examples displayed from the Circle study sample (Fig. 5.18f & g), the expression of this type of modification is extremely variable and its aetiology is somewhat enigmatic. Although this emerged as a distinct form of anterior tooth modification for this assemblage, it is not a widely reported phenomenon amongst other archaeological populations. As such, it is difficult to attribute it as either an 'active' or 'passive' modification, however it seems more likely to be the latter. Although undulating profile modifications were the least common of all the dental manipulations (Σ=14; 6.09% total modifications; Fig. 5.5), this is only by a margin of one, so it should be considered with equal gravity to both diagonal modifications and extreme lingual wear (each Σ=15; 6.52% total modifications).

Despite the small number of affected teeth, the chronological distribution appears to be relatively consistent across the dataset (Fig. 5.26). For undulating profile modifications, the greatest number of examples were observed amongst the Early use-phase interments (Σ=8; 57.14% total undulating teeth). There was only one example attributed to the Middle use-phase (7.14% total undulating); and a small resurgence was observed amongst the Late use-phase population sample (Σ=5;

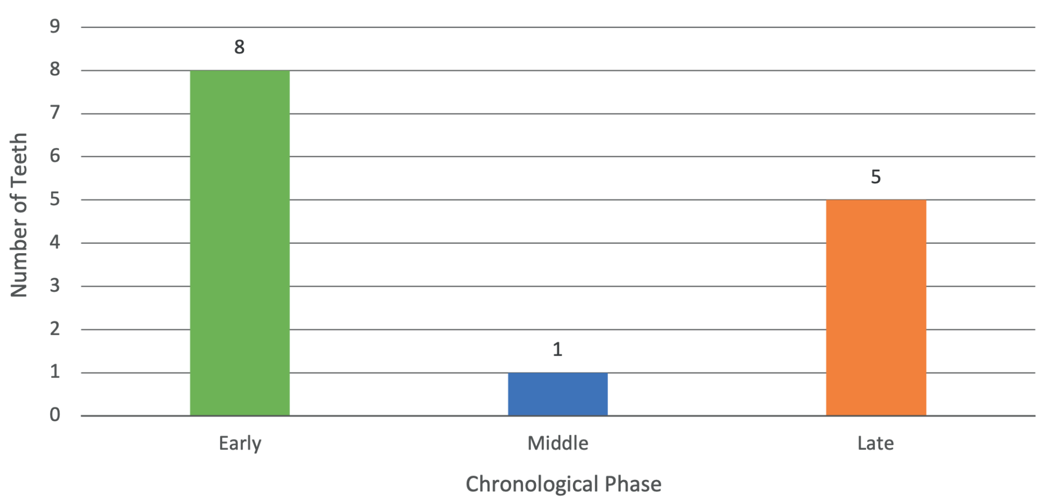

Figure 5.26. *Frequency distribution of undulating profile modification by chronology in the Circle sample (Σ=14).*

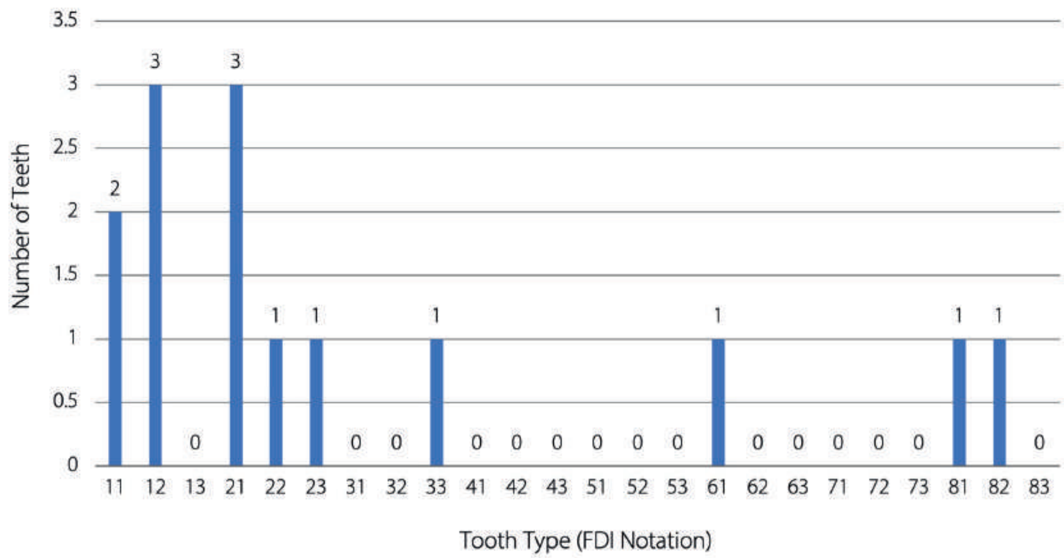

Figure 5.27. *Frequency distribution of undulating profile modification by tooth type in the Circle sample (Σ=14).*

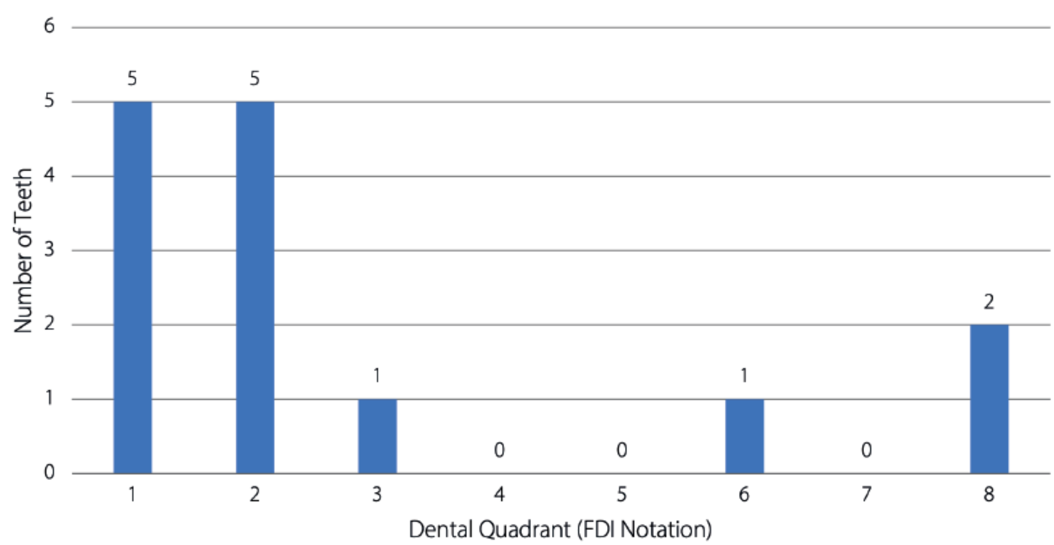

Figure 5.28. *Frequency distribution of undulating profile modification by quadrants in the Circle sample (quadrants follow FDI notation) (Σ=14).*

35.71% total undulating teeth). Table 5.3 demonstrates that although six contexts featured teeth with undulating modifications, the greatest proportion of affected teeth precipitate from Context (951), with six of the 14 teeth recorded from these Early stratigraphic units. The remaining contexts only feature scattered representations, listed in descending order as: (960) (Σ=3); (595) (Σ=2); and (1241), (1206) and (783) each feature one example (7.14% total undulating teeth). When presented as a proportion of all undulating modifications, the results emerge as: (951) (42.86%); (960) (21.43%); (595) (14.29%); (1241), (1206) and (783) (each 7.14%). Here again, both in raw incidence and proportion, Context (951) has the highest occurrence of undulating profile modifications across the study sample.

Figure 5.27 reveals the distribution of data when analysed according to tooth types. In this case, we see that there is a spread of incidences of undulating profile modifications across both adult and non-adult members of the Circle population, with 11 examples recorded for permanent teeth (78.57% total undulating teeth), and three examples for deciduous dentition (21.43% total undulating teeth). Across the sample, there is a pronounced pattern in terms of distribution across the arcade. Amongst the affected adult teeth, 10 of the 11 examples were identified on maxillary dentition (90.91% total adult undulating teeth; 71.43% total undulating teeth), and only one on a mandibular tooth (9.10% total adult undulating profile teeth; 7.14% total undulating teeth). For the deciduous dentition, this was reversed, with two of the three affected non-adult teeth recorded as mandibular (66.66% total deciduous undulating teeth; 14.29% total undulating teeth), and only one as maxillary (33.33% total deciduous undulating teeth; 7.14% total undulating teeth). These trends are reinforced when viewing the data according to oral quadrant distribution (Fig. 5.28). The adult maxillary left and right anterior quadrants are the strongest – and equal – representatives amongst the dataset, each featuring five examples of this mode of modification (each 45.45% total adult undulating teeth; each 35.71% total undulating teeth). The left permanent mandibular anterior teeth had only one example (9.10% total adult undulating profile teeth; 7.14% total undulating teeth); while the right permanent mandibular anterior quadrant had none. Amongst the deciduous sample, only two quadrants featured affected teeth, including two for the right deciduous mandibular anterior arcade (66.66% total deciduous undulating teeth; 14.29% total undulating teeth) and one for the left deciduous maxillary anterior dentition (33.33% total deciduous undulating teeth; 7.14% total undulating teeth).

Although the expression of undulating profile modifications appears to cluster when analysed according to chronological, demographic and quadrant distributions, it disperses when organized according to individual tooth types (Fig. 5.27). There is a slight grouping across the adult maxillary anterior teeth, with the right lateral incisor (FDI 12) and left central incisor (FDI 21) each presenting three examples (each 27.27% total adult undulating teeth; each 21.43% total undulating teeth); and two examples recorded for right central incisors (FDI 11; 18.18% total adult undulating teeth; 14.29% total undulating teeth). All remaining affected teeth presented only single examples across both adult and non-adult dentition, including a left permanent maxillary lateral incisor and canine (FDI 22, 23); a left permanent mandibular canine (FDI 33); a right deciduous maxillary central incisor (FDI 61), and a right deciduous mandibular central and lateral incisor (FDI 81, 82; each 7.14% total undulating teeth).

5.5.1.7. Gross crown loss

As discussed above for labial and lingual extreme wear (§5.5.1.3–4, above), there is the possibility of cross-over between the aetiologies and quantifications of extreme wear cases and dental modification. As mentioned above, especially when considering the anterior dentition, alterations to the labial and incisal profiles may be attributed to either active and/or passive processes which result in identical physical and aesthetic affect(s). It is also possible that modifications to the teeth caused by habitual behaviour may have produced specific identity-markers held as significant within a cultural group (Alt & Pichler 1998, 388; Milner & Larson 1991, 357; Scott 1991, 798; cf Chapter 4). For these reasons, the phenomenon of gross crown loss to the anterior teeth is also presented here.

On 10 occasions amongst the sample, teeth were worn to the extent that only fractions of the crown remained; three of these examples left only functional root stumps. Four teeth were observed to have approximately half of their crowns eroded by the processes of extreme wear. Amongst the earlier use-phases of the Circle, in Context (951) a left permanent maxillary central incisor (FDI 21) was observed to present almost vertical concave erosion on the lingual surface from incisal margin to cingulum, leaving approximately half of the crown extant. In the Later use-phase of Context (960), another left permanent maxillary central incisor (FDI 21) presented approximately diagonal wear on the lingual surface from the incisal edge to a point just inferior to the cementum enamel junction, leaving approximately half the crown extant. In this case, we see another example of complex dental attrition processes, as labial wear was also observed on this tooth in the area immediately superior to the cementum enamel junction, forming a slight concavity in the dentine. Two teeth recovered from Context (783), the latest use-phase of the Circle, were observed to retain only half-crowns; the first was a right permanent maxillary central incisor (FDI 12) presenting an approximately horizontal wear platform across the incisal surface; the second was a left permanent maxillary central incisor (FDI 21), on which an approximately diagonal, mesially inclined, wear platform was observed across the incisal margin, leaving approximately half of the crown extant. Pronounced labial wear was also observed on this tooth, having smoothed and removed almost all extant enamel; additional lingual wear also appears to have eroded all enamel to a point beyond the cingulum, just inferior to the cementum enamel junction.

Three of the teeth within the sample were observed to be worn to the extent that only one-third of the crown remained. Two of these teeth were identified within the Early use-phase of Context (951): the first being a right permanent central maxillary incisor (FDI 11), the second was a right permanent maxillary lateral incisor (FDI 12). For both teeth, not only did the tooth crowns display the loss of approximately two-thirds of their height, they also presented labial wear that extended vertically across the extant surface beyond the cementum enamel junction onto the root. The other tooth within this wear category was observed in the Late use-phase Context (783): another right permanent maxillary lateral incisor (FDI 12). This tooth exhibited approximately diagonal wear which was inclined towards the lingual aspect and eroded approximately two-thirds of the crown.

Functional root stumps were also observed, as reported in Chapter 4. In these cases, the tooth crowns are thought to have been obliterated *in vivo* through processes associated with extreme wear, carious lesions, *antemortem* crown fractures and/or combinations of these phenomena. The continued functional use of these root stumps in the mouth prior to death is evident through wear (smoothing, glossing, rounding) of the extant occlusal surfaces. The earliest incidence was identified on a right permanent maxillary lateral incisor (FDI 12) associated with Context (951), one of the early use-phases of the Circle. The crown of this tooth was obliterated beyond the cementum enamel junction. The remaining two incidences within this wear category are attributed to the distal dentition, and therefore not within the focus of the current analyses. For further information on these teeth, see Chapter 4.

5.6. Case studies

Although population-based reporting is the foundation of bioarchaeological analyses, it is important to present case studies to bring sharp focus to the lived experiences of 'real people' amongst archaeological assemblages. It is particularly important to do so in assemblages such as the Circle, where many might assume that the levels of fragmentation and commingling would render such testimonies inaccessible. With this in mind, two case studies are presented to shed light on the complexities of identifying intentional dental modification in past populations, and to introduce two compelling individuals to the discourse.

5.6.1. Congenital variation, cultural intervention, or both?

An intriguing example of apparent variation in eruption and alignment can be seen in the articulated cranium and mandible of an individual from Context (960) (2500–2400 cal. BC); Figures 5.29a–e; 5.30a–i. The individual was determined to be an adult, based on the complete eruption and occlusion of the right and left maxillary permanent third molars (FDI 18, 28). The left and right mandibular permanent third molars are also completely erupted and in occlusion (FDI 38, 48) and all apices are observed to be closed under radiological examination. The individual was subject to sex assessment based on evaluation of the cranial sexually dimorphic traits presented in Buikstra and Ubelaker (1994, 20), including nuchal crest (2/5), mastoid process (2/5), supraorbital margin (2/5), supraorbital ridge/glabella (3/5) and mental trigone (2/5). According to these criteria, the individual was assessed as a possible female.

Close observation of the maxillary dentition reveals that both right and left permanent lateral incisors are absent (FDI 12, 22), and the permanent canines (FDI 13, 23) appear in their place. Distal to the canines, bilateral patent spaces are observed in the maxillary alveolar process. These spaces present as pitted, slightly roughened patches of bone. When viewed from both right and left lateral aspects of the maxillae, the margins of these spaces present as roughened and irregular, appearing to retain residual evidence of vascular impressions, pitting and porosity (Fig. 5.29b–e). The bilateral aspects of the labial-buccal alveolar process also present slight focal resorption in these areas. The lingual margins appear to be slightly smoother, however they also present slight pitting and porosity. The canine pillar is absent on both left and right labial aspects of the maxilla. The remainder of the bilateral maxillary dentition is in correct anatomical sequence. Slight calculus is observed on the labial/buccal aspects of all extant dentition at the level of the cementum enamel junction, accompanied by indications of mild periodontal disease including minimal resorption of the alveolar process (approximately 3–5 mm) and slight pitting and porosity. There is no indication of mesial drift in the teeth distally adjacent to the spaces in the anterior arcade, despite the bilateral impaction of the permanent third molars; the right is mesially tilted by approximately 30°, the left by approximately 20°. There is slight distal rotation of the right maxillary permanent first premolar (~10°), however the lack of tilting or encroachment into the adjacent space suggests that this may be an ontogenetic variation. It is also important to highlight that this individual presents moderate prognathism of the maxillary arcade, which is noticeable against the overall gracility of the skull. The associated mandible articulates well with the cranium, and all posterior teeth occlude evenly with their antagonists (Fig. 5.29d & e).

The mandible presents all adult teeth in correct anatomical sequence – the right permanent lateral incisor has been lost *postmortem*. Perturbations in alignment are minimal; the left permanent second premolar presents slight mesial rotation (~15°), while the right permanent third molar is slightly impacted, being mesially tilted by approximately 45°. It is important to note here that the teeth opposing the previously mentioned bilateral spaces in the maxilla, the left and

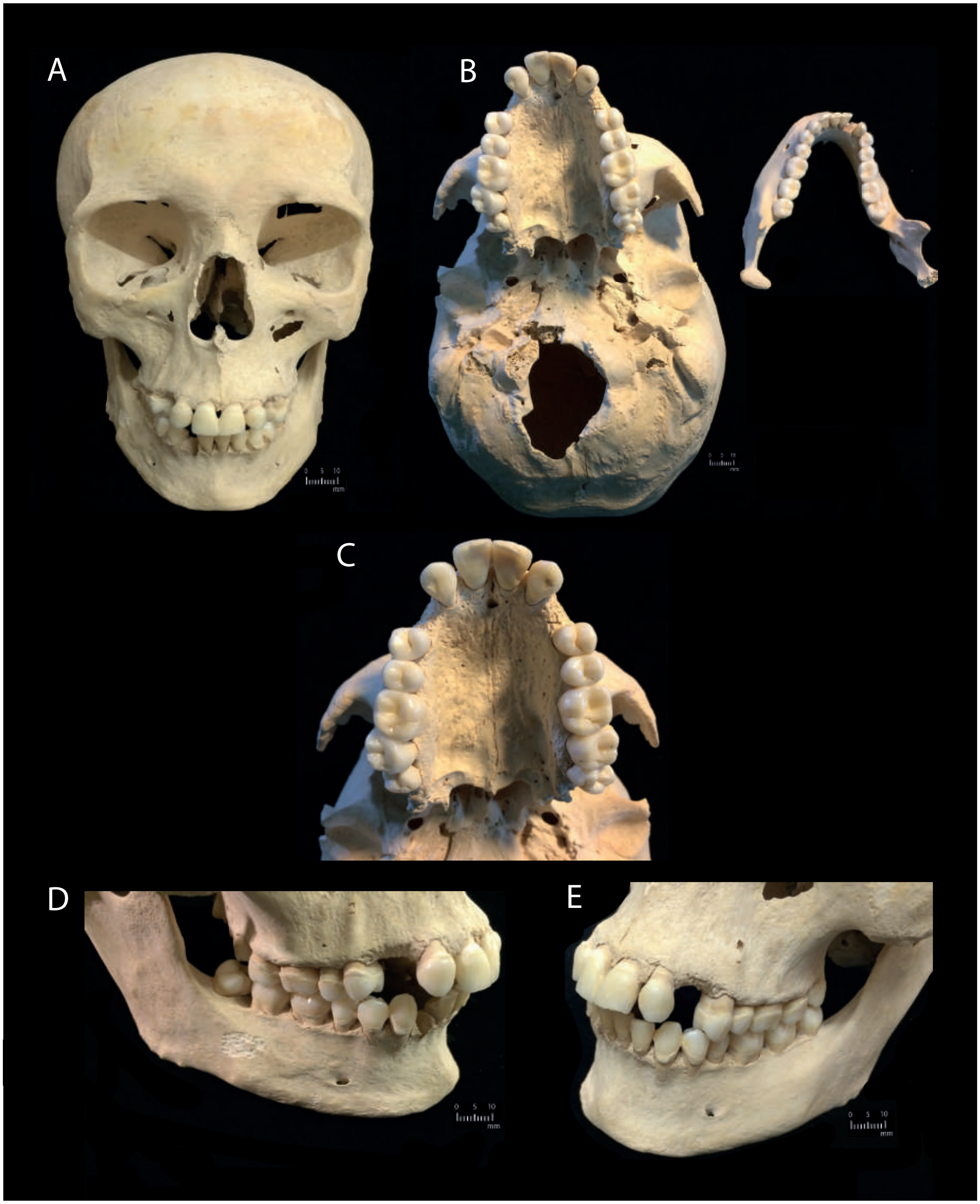

Figure 5.29. *Almost complete skull of probable female adult individual with variation of eruption and alignment from Context (960) of the Circle sample: a) articulated cranium and mandible in anterior view; b) disarticulated, inferior view of cranium and superior view of mandible; c) detailed inferior (palatal) view of maxillary dental arcade, featuring atypical positioning of the bilateral permanent canines (FDI 13, 23) and immediately distal patent alveolar spacing; d–e) detailed right and left anterolateral views of the articulated maxillae and mandible, detailing the opposing relationships of the dentition relative to the atypical positioning of the maxillary permanent canines and the distal patent alveolar spacing. Scale bar: 1 cm. (Photos Ronika K. Power).*

right permanent canines, both present evidence of wear consistent with all other extant dentition, and do not demonstrate any evidence for compensating (or 'continuous') eruption in the absence of vertical opposition (Fig. 5.30d–e; Hillson 2000, 254). Slight calculus is observed on the labial/buccal aspects of the mandibular arcade at the level of the cementum enamel junction on the left (FDI 31–36) and right (FDI 41, 43–46) sides; and also at the cementum enamel junction on the lingual aspects of the left (FDI 31–33) and right (FDI 41–43) sides.

To determine the aetiology of the phenomena described above for the anterior maxillary teeth of this individual, CT-scans were taken of both the cranium and mandible by L.T. Buck in the Cambridge Biotomography Centre, according to the procedure outlined in §5.4, above (Fig. 5.30a–c). For the cranium, these scans reveal that the maxillary central incisors appear morphologically normal, with symmetrical wear on incisal surface and no periodontal ligament space changes within the alveolus (Fig. 5.30e & f). The maxillary canines also appear normal and well-spaced as lateral teeth in relation to the central incisors, and present slight bilateral wear on the tips of the cusps. The horizontal and vertical dimensions of the alveolar process appear very well preserved, and the bilateral remnant portions of the alveolar process where the dentition are absent appears slightly rounded. The profile of the maxilla is continuous and indicative of consistent load-bearing through normal mastication and use of the mouth. As seen in Figure 5.30d–f, no residual socket is observed within the right or left alveolar processes superior to these spaces. There is no evidence of either impacted maxillary lateral incisors, or any ectopic dentition. For the mandible (Fig. 5.30g–i), the CT-scans confirm that occlusal wear is present on all crowns, suggesting good apposition across the arcade (cf De Groote & Humphrey 2016, 2017; Milner *et al.* 1991; Newton & Domett 2017). The bilateral mandibular canine cusps are both worn to the

Figure 5.30. *a–c) 3D render of cranium in anterior, right lateral and posterior views; d–f) cross-sections of maxillary alveolar process in transverse and right and left lateral views; g–i) 3D render of mandible in anterior, left lateral and posterior views. Radiological images captured by L.T. Buck, Cambridge Biotomography Centre; processed by J. Magnussen & M. Pardey, Macquarie Medical Imaging.*

extent that they present slight dentine exposure, and neither display any evidence of compensating eruption.

In combination, this evidence presents a curious case for which there may be several differential diagnoses. Firstly, there are a number of possible explanations to account for the presence of the bilateral maxillary permanent canines in the positions normally occupied by the lateral incisors. Agenesis (or congenital absence) of the maxillary permanent lateral incisors is one of the more common variations of the development and eruption of the adult dentition (Hillson 2005, 281; Lee 2017, 92; Kavadia *et al.* 2011). It is possible that the lateral incisors simply did not develop, potentially creating an opportunity for another congenital variation to manifest: canine transposition. Canine transposition is a well-described dental phenomenon involving the development and eruption of the permanent canine in either of the adjacent positions within the same quadrant; maxillary canines are the category of teeth second-most frequently presenting eruption disturbances, after the third molars. (Tripathi *et al.* 2014; cf Garib *et al.* 2010; Shapira & Kuftinec 1989). In clinical studies, tooth transposition is more frequent and variable in the maxilla, the canine presents the most common involvement, and females are most commonly affected (Tripathi *et al.* 2014; cf Budai *et al.* 2003; Mayes *et al.* 2017, 288, 289; Peck & Peck 1995; Plunket *et al.* 1998; Shapira & Kuftinec 1989). The aetiology of this phenomenon is associated with several factors, including genetics, position exchange of developing tooth buds, trauma, cyst and tumour formation, mechanical interference and early loss of incisors (Tripathi *et al.* 2014; cf Feichtinger *et al.* 1977; Peck *et al.* 1993; Peck *et al.* 1998; Shapira 1980; Shapira & Kuftinec 2001). Canine transposition can occur with or without accompanying agenesis of other dental elements, however studies have revealed co-occurrence in 40% of cases with agenesis; in 25% of cases with peg-shaped lateral incisors; and in 50% of cases with retention of deciduous teeth (Budai *et al.* 2003; Lee 2017; Tripathi *et al.* 2014).

In one clinical case, a nineteen-year-old female presented with a retained left deciduous maxillary canine (FDI 63), agenesis of the left permanent maxillary lateral incisor (FDI 22) and transposition of the left permanent maxillary canine (FDI 23) in its place (Tripathi *et al.* 2014). In this case, although the crown of the deciduous canine was still *in situ* and being used for functional occlusion and mastication in the mouth, radiographic examination revealed that the roots and the corresponding alveolus were almost entirely resorbed (Tripathi *et al.* 2014, Fig. 1). This case bears striking resemblance to that of the individual excavated from Context (960). All phenomena parallel those observed on our Neolithic Maltese individual, including the resorbed alveolus, absence of canine pillar, and pitted and porous alveolar margin in the traditional canine space. Were a living, functional deciduous tooth with resorbed root retained here within the gingiva, it is likely that it would have promoted the pitted, roughened and porous character of the alveolar margin via vascular and masticatory activity. It also accounts for the lack of mesial drift and interproximal contact facets in the neighbouring dentition, as well as the absence of compensating eruption on the opposing elements.

The above presents a convincing scenario and compelling comparative case study. However, differential diagnoses may extend further, and for this reason the possibility of autogenous transplantation must also be addressed. Autogenous transplantation (or autotransplantation) involves the transplantation of one tooth within an individual's mouth to another location elsewhere in the arcade (Clokie *et al.* 2001; Northway & Konigsberg 1980). This is opposed to allotransplantation, which involves the transplantation of a tooth from one individual's mouth to that of another individual (Nimčenko *et al.* 2013). Both of these practices are argued to have ancient origins, with medical historians arguing for attestations of the practice in ancient Egypt (Heithersay 1975; Morel *et al.* 2018; Nimčenko *et al.* 2013; Schwartz *et al.* 1985). When considering these possibilities, the former is perhaps more likely than the latter, as allotransplantation is known to have a high likelihood of rejection caused by histoincompatibility (Nimčenko *et al.* 2013). We are obliged to consider a scenario in which the maxillary lateral incisors (permanent or deciduous in the case of retention) may have been extracted or avulsed for various reasons (including but not limited to pathology, culture or ritual), and the canines extracted and transplanted into the neighbouring alveoli. After all, as discussed in §5.2.3, above, the intentional removal (variably referred to as extraction, avulsion or ablation) of the anterior teeth is known for Neolithic populations within the Mediterranean (Robb 1997), Levant (Eshed *et al.* 2006), Europe (Jackson 1915), extending into the Middle East and Africa (Humphrey & Bocaege 2008) and all the way to Taiwan (Pietrusewsky *et al.* 2017).

On one hand, there is nothing within the bilateral internal architecture of the maxillary alveolar process to indicate that there were ever alveoli (and thus, teeth) within the patent spaces normally occupied by the permanent canines. However, it is clinically noted that alveoli can be completely remodelled within less than one-year post tooth loss (Covani *et al.* 2011; Johnson 1969; Morgan 2011; Pietrokovski & Massler

1967; Schropp *et al.* 2003). Considering the evidence mentioned above including the absence of mesial drift on the neighbouring bilateral first maxillary premolars; the absence of compensating eruption on the opposing bilateral mandibular permanent canines; and the presence of occlusal wear across the arcade, including the opposing bilateral mandibular permanent canines, it is possible that there were once teeth within the maxillary alveolar spaces, or perhaps proto-prosthetic devices or spacers of some description. Early accounts of dental prostheses have been attributed to ancient Egypt in approximately 2500 BC (Harris *et al.* 1975; Junker 1929), although physical re-examination of the prostheses and recent research casts some doubt on these claims (Forshaw 2009; Leek 1972 cf. Becker 1999a, 1999b; Crubézy *et al.* 1998; Seguin *et al.* 2014). While the bilateral absence of interproximal contact facets for both the distal interproximal aspects of the maxillary permanent canines and the mesial interproximal aspects of the maxillary permanent first premolars suggests that there was no enduring *in situ* adult dentition in these spaces, one cannot absolutely rule out that there were never teeth (deciduous – exfoliated or retained, as argued above – and/or adult) or prostheses present. In parallel cases in Neolithic China, where selective avulsion or ablation of anterior teeth was practised, including lateral incisors, scholars classify any absent teeth with persistent spaces as evidence for ablation (Lee 2017, 96). The same diagnosis applies for observations of symmetrically absent teeth, as previous research across cultures revealed very little symmetry in dental agenesis and/or pathology resulting in *antemortem* tooth loss (Buikstra 1987; Lee 2017, 97; Newton & Domett 2017, 161–2; Pietrusewsky *et al.* 2017, 107; Spencer & Gillen 1927; van der Reijden 2014, 21; van Rippen 1918a, 1918b).

5.6.2. Active modification, passive alteration, or both?

Although they were not recovered from any of the contexts included in the study sample, an individual identified amongst the remains excavated from Context (845) is important to feature here (Fig. 5.31a–e). This context was a substantial burial deposit found in the northern niche of the 'West Cave' dating to between 2625–2500 cal. BC (Chapter 3), at the height of the Tarxien phase. To determine the aetiology of the phenomena described below for the anterior maxillary teeth of this individual, their remains were initially examined macroscopically in the National Museum of Archaeology, Valletta, and CT-scans were later taken by L.T. Buck in the Cambridge Biotomography Centre, and subsequently analysed at the Macquarie Medical Imaging Unit, Macquarie University Hospital, according to the procedure outlined in §5.4, above.

These are the fragmentary remains of an adult cranium, approximately 20% complete. The remains are restricted only to the splanchnocranium (facial skeleton), consisting of the inferior aspect of the frontal bone, incorporating the inferior third of the frontal squama, the glabella, the left and right supraorbital margins, zygomatic processes and partial orbital roofs; the left and right nasal bones; the left and right zygomae, bilaterally fragmented at the roots of the temporal processes; and the left and right maxillae. The left maxilla is fragmented at the posterior aspect, so that the alveolar process is absent distal to the left permanent second premolar (FDI 25); the corresponding dentition are also absent, including the permanent first, second and third molars (FDI 26, 27, 28). All remaining left permanent maxillary dentition are present and *in situ* within the alveolar process (FDI 21–25). The right maxilla is fragmented immediately distal to the permanent third molar (FDI 28), so that the maxillary tubercle is absent. All right permanent maxillary dentition is present and *in situ* within the alveolar process (FDI 11–18). The posterior walls of the left and right maxillae are fragmented and absent, so that the bilateral maxillary antra are exposed. The left and right palatines are absent. The vomer and all nasal conchae are absent. All reported damage is assessed to be *postmortem*.

Age estimation is based on overall size, robusticity, density of cortices and the eruption of the left permanent maxillary third molar (FDI 28). Furthermore, the apices of all permanent teeth are observed to be closed under radiological examination. Although this individual is highly fragmented, the extant splanchnocranium was subject to sex assessment, based on evaluation of the cranial sexually dimorphic traits presented in Buikstra and Ubelaker (1994, 20), including supraorbital margin (4/5), and supraorbital ridge/glabella (4/5). We also note the rugosity and breadth of the zygomae, and the length, breadth and robusticity of the palate (Schwartz 1995, 280). According to these criteria, the individual was assessed as a possible male. Despite the strength of expression of the extant traits, we remain conservative in our evaluation considering the absence of the majority of the cranium and further diagnostic traits.

Linear hypoplastic defects are observed on the enamel of the anterior teeth (central incisor: between 2.0 mm to 9.5 mm from cementum enamel junction [equates to 5.4–8.8 years of age; Goodman & Rose 1990, 98, Table 3]; canine: 7.2 mm from cementum enamel junction [equates to 10.5 years of age, Goodman & Rose 1990, 98, Table 3]). The observation of hypoplastic defects across these permanent teeth indicates that this individual was subject to chronic biological,

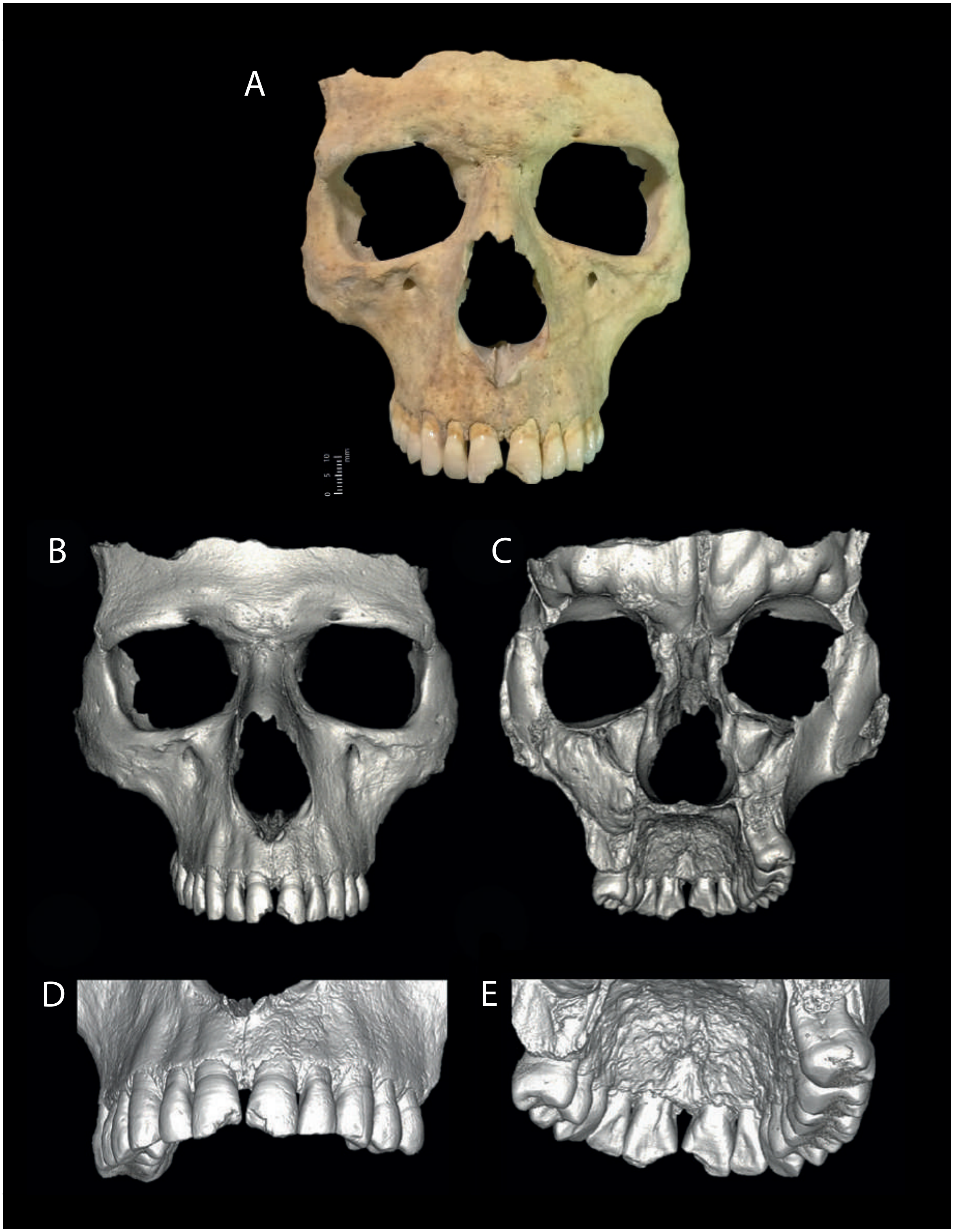

Figure 5.31. *Adult splanchnocranium featuring modification of the left and right permanent maxillary central incisors (FDI 11, 21): a) anterior view; b) 3D render anterior view; c) 3D render posterior view; d) 3D render maxillary arcade anterior close-up view; e) 3D render maxillary arcade posterior close-up view. Scale bar: 1 cm. (Photos Ronika K. Power; radiological images captured by L.T. Buck, Cambridge Biotomography Centre; processed by J. Magnussen & M. Pardey, Macquarie Medical Imaging).*

nutritional, environmental and/or psychological stress throughout childhood (Goodman 1991; Goodman & Capasso 1992; Goodman & Rose 1990, 1991; Ortner 2003; Pindborg 1970; Roberts & Manchester 2005). As a result of fragmentation, we are unable to determine if further indicators of systemic stress including *cribra orbitalia* or porotic hyperostosis were also present on the orbital roofs or cranial vaults, respectively.

The right and left permanent maxillary central incisors (FDI 11, 21) are both observed to be modified in a similar, symmetrical manner. Both teeth have approximately two-thirds of the incisal margin removed at the mesial aspect, to a height of approximately one-third of the inferior aspect of the crown. The distal aspects and corners of the extant incisal margins do not appear to have been subject to modification beyond normal masticatory processes. The extant labial and lingual surfaces of the crown also do not appear to have been modified. The alterations are determined to have taken place *in vivo*, as interpreted from pronounced smoothing, rounding, polishing and colour consistency across the extant margins, all indicating the continued use of the teeth in the mouth following modification (Hillson 2000, 258; Langsjoen 1998, 410; Ortner 2003, 603). Both teeth appear to have had the enamel removed in small chunks, as the extant surfaces are relatively uneven and do not appear to have been subject to subsequent intentional smoothing. Under magnification, the modification margin differs slightly in appearance between the right and left teeth – the right margin is slightly more stepped, while the left is slightly rounder. Furthermore, the margin on the left incisor appears to have had slightly more enamel removed on the labial aspect, resulting in a more concave appearance because of the additional exposure and attrition of dentine. We must keep in mind that these alterations were most likely carried out using lithic tools, so a degree of variation should be expected. Notwithstanding these slight differences, when viewed naturally as one would *in vivo*, the modification appears as an approximately symmetrical hemispherical negative space between the two most prominent teeth of the entire human dentition. The modifications most closely resemble van der Reijden's type B2.3 (2014, 49), having modified crown height reduced by one-quarter to one-third; crown width reduced by two-thirds; and concave edges returning to reach the incisive margin.

It is important to note that none of the remaining maxillary dentition for this individual bear any indication of modification whatsoever. A few of the incisal and/or occlusal margins feature miniature cracks and chips consistent with normal *in vivo* oral activity (but none to the extent that they would be recorded as *antemortem* fractures or chips), and/or *postmortem* damage as is consistent for this assemblage. Considering these factors, and the description presented above, it is argued that this individual was subject to intentional dental modification a substantial amount of time prior to his death and interment within the Circle.

To place this individual within an even wider context, we can consider if there is any evidence reported for similar modifications in populations elsewhere. As will be discussed in §5.7.5, below, although it is not a definitive or comprehensive methodology, the manner in which groups modified their bodies, particularly their teeth, may infer some degree of cultural contact or connection. The many caveats that must be applied to such hypotheses are addressed in detail below. Notwithstanding these precautions, we can report that a similar modification type (B2.3) has been identified by van der Reijden (2014, 49), who traces the form to Starr's (1909, 18) ethnographic work in the Congo. We acknowledge that millennia separate these observations, and we do not propose any direct connection. It is nonetheless an important addition to the discourse that this particular mode of corporeal expression observed on the African continent in the early 20th century was once performed on an individual who, by all accounts, lived and died in Neolithic Gozo.

5.7. Discussion

5.7.1. Limitations of study

Even under the most straightforward burial and depositional circumstances, it can be difficult to ascertain reliable rates of dental modification within a population because of *ante-* and *postmortem* tooth loss and dental attrition and pathology (Milner & Larsen 1991; Stojanowski *et al.* 2016). These challenges are compounded for the Circle assemblage as a result of its highly fragmented, commingled and predominantly disarticulated nature. This calls us to address a number of issues. Firstly, while the majority of published modification studies have been carried out on intact dental arcades, the nature of our assemblage necessitates that we study loose *postmortem* exfoliated teeth and/or fragmented bony jaws with *in situ* dentition. Secondly, concerning *in vivo* processes, as has been noted previously (Stoddart *et al.* 2009a, 318) and expanded upon in Chapter 4, dental attrition across the population is relatively minimal. This is perhaps because of their fluoride fortified enamel in concert with a soft local limestone substrate which, when incidentally included in the diet as a by-product of food production, does not bring about the catastrophic wear observed on contemporaneous neighbouring regional populations embattled by silica (sand) as the prevailing inorganic particulate (Forshaw 2009, 421, 422; Hillson 2008, 124; Miller 2008, 55–6). As such, the observations tabled here are thought to be genuine reflections of the lived experiences of both intentional and incidental modification processes across the life course. With these factors in mind, the systematic and detailed recording practices applied to this population offer valuable contributions towards local and global understanding of this phenomenon.

In archaeological populations, complications of dental modification have included tooth fracture or caries (Ikehara-Quebral *et al.* 2017, 201–2; Irish 2017, 39, 41; Milner 2017, 320; Tiesler *et al.* 2017). We have reported on both crown fractures and caries in Chapter 4, however on no occasion did we note a primary modification as the fracture or caries aetiology of an anterior tooth. This is demonstrated in Figures 5.10f and 5.18g, where cervical carious lesions are observed on central maxillary incisors presenting incisal notch and undulating profile modifications from contexts (595) and (783), respectively. In these cases, there were no observations of pulp chamber compromise, nor of secondary dentine deposition, suggesting that factors other than the modifications were responsible for the carious lesions. Notwithstanding this, we did not include observations of infectious or inflammatory processes in the maxillary or mandibular alveolar processes, as it was not within current project parameters, particularly because of the high incidence of *postmortem* exfoliated teeth amongst the study sample. This component of the research design is discussed further in §4.4. Future considerations of the wider lived experience of dental modification for this population would benefit from such investigations, and it is hoped that they can be included in further studies wherever they are observed *in situ* in alveoli.

For similar reasons, we are unable to offer extended commentary on the incidence of avulsion or ablation amongst the Circle assemblage, beyond the single potential example described in §5.6.1, above. As mentioned before, the primary focus of this project was on the dentition itself, rather than the hard tissues of the jaws, which would be essential for identifying *antemortem* tooth loss of any aetiology. Considering the difficulties associated with identifying avulsion or ablation in intact skulls within discrete burials (Buikstra 1987; Lee 2017, 97; Milner & Larsen 1991, 363; Newton & Domett 2017, 161–2; Pietrusewsky *et al.* 2017, 107), we anticipate that these obstacles would be amplified for this, and other, highly fragmented, commingled and predominantly disarticulated samples. Nevertheless, considering the widespread nature of ablation and/or avulsion in the deeper prehistoric periods and the general North African regional diminishment of the practice in the Neolithic (Humphrey & Bocaege 2008), we would like to incorporate these considerations into future research to understand the extent to which it did or did not manifest across the Maltese archipelago.

We also acknowledge that the majority of the sample were not examined using light microscopy, scanning electron microscopy or micro-CT data as it was beyond the temporal, logistical and pecuniary parameters of the current project. As stated in §5.4, above, every tooth was examined macroscopically, observations were enhanced using a 10x magnification hand lens, and selected specimens were chosen for micro-CT scanning.

Finally, we underscore the awareness that any results and interpretations presented here should only be perceived as a minimum number of incidences, and not as overall statistical prevalence of a complete burial population. The Circle assemblage has not been fully excavated, nor has the excavated population been exhaustively analysed. Ongoing studies by the current authors will seek to further elucidate all aspects of the pathology, anthropology, demographics, affinity and cultural engagement of the Neolithic Maltese community interred in this space, including their practices of dental modification.

5.7.2. The Circle in context

The observations reported here are of profound significance for Maltese archaeology, and indeed prehistoric archaeology across the central Mediterranean, as it presents the first detailed analyses of dental modification for the archipelago. We have reported a relatively low incidence rate of dental modification (Σ=172; 5.62% total sample) across all use-phases of the Circle, which accords with the generally low-to-moderate rates described for archaeological populations across the globe (Burnett & Irish 2017b, 5). We have described both active and passive modification types that are commonly reported across prehistoric cultures, including chipping (or chiselling), incisal notches, labial and lingual wear, diagonal and undulating profile modifications and gross crown loss, while also presenting some potentially novel augmentation types, including diagonal incisal profile modification. Acting upon these observations, we seek to address the calls for illuminating the biocultural significance of these practices – it is not enough to merely describe what we see; we must strive to incorporate all available data to understand *why* people altered or removed their teeth. Through these acts, be they intentional or unintentional, these individuals forever changed themselves and each other, making powerful statements through their bodies about who they were, what they did and where they came from (Burnett & Irish 2017, 6; Milner 2017, 321). The following sections explore these issues.

5.7.3. Demographic insights

As with all subdisciplines of human bioarcheology, the demographic distribution of dental modification is one of the primary touchpoints for biocultural research. To understand best the cultural and behavioural impetuses behind the selection of individuals for this intentional cultural practice –or their participation in the behavioural practices that incidentally caused them– and the subsequent lived experiences of affected individuals, we seek to determine if there are any observable patterns in the distribution of the modifications by age, biological sex, health or any other observable skeletal markers. In this case, our observations are somewhat limited because of the fragmented and commingled nature of the assemblage, and the fact that for the overwhelming majority of the study sample we are analysing *postmortem* exfoliated loose teeth. One of the great advantages of working with dentition is that they are amongst the most reliable indicators of age-at-death; however, in isolation and from commingled assemblages, we are reliant upon this assessment for a single tooth rather than an entire arcade. Moreover, although there are some populations for which metric dental analyses may be somewhat reliable for sex assessment (Black 1978a, 1978b; Garn *et al.* 1964, 1966, 1967, 1979; Mayhall 1992; Molleson 1993; Moss & Moss-Salentijn 1977; Owsley & Webb 1983; De Vito & Saunders 1990), such seriations have not yet been performed for the Circle assemblage. In the absence of widespread biomolecular analyses, the determination of biological sex is currently beyond our reach for this dental dataset. As such, we are as yet unable to provide any detailed insights into the sex distribution of labour or aesthetic markers based on dental modification data. Chapter 7 provides further information on other corporeal pathways to understanding demographic patterns of activity-related changes in Neolithic Malta.

Based on this research, however, we have a preliminary understanding of the relative experience of dental modification across the life course for the people interred in the Circle. Adults were by far the dominant group to feature this mode of cultural engagement, representing 89.53% (Σ=154) of affected teeth within the sample. Although the number of affected deciduous teeth is far fewer (Σ=18; 10.47% total modified teeth) their appearance within the sample is highly significant, as is the similarity to adults for the distribution of these modifications across the anterior arcade (Figs 5.3 & 5.4). Observations of either intentional or incidental modification or extreme wear on deciduous teeth are very rare in archaeological populations (Van der Reijden 2014, 7), so this represents an important finding. The presence of children in this space confirms their inclusion in the range of cultural practices that produced these corporeal interventions: either the sudden and most likely ritual and/or aesthetic interventions of intentional dental modification, or the enduring and repetitive behavioural interventions of incidental augmentation (Alt & Pichler 1998), discussed further below.

Although the nature of the assemblage precludes broader and more precise understanding of the age at which modifications took place, the observation of four types of modification (chipping, incisal notches, diagonal and undulating profiles) on deciduous anterior dentition suggests that if/when practised locally, the augmentation of anterior teeth was not exclusively reserved for pubescent or post-pubescent community members, as in other cultures (Irish 2017, 39). In terms of incidental modification, parallels may be found with the Namibian Herero and Sambyu groups, who are known to have practised modification before puberty (van Reenen 1978b; van Reenen & Briedenhann 1985). For the Sambyu people, agency for the timing of the modification lay with the children themselves, who decided when the timing of the chipping, or *mbereko*, would take place (Irish 2017, 39). This observation serves to acknowledge the role of human agency in the analyses of dental modification. Individual choices and decisions as well as purposeful or accidental variations from traditional practices also contribute to expressions of the phenomena that we witness in the Circle assemblage (Milner 2017, 326). All these factors should be considered as we build pictures of Malta's ancient past through this growing research.

The absence of deciduous dentition from two modes of dental modification (labial and lingual extreme wear) does not rule out the participation of children in the particular activities that are closely associated with these phenomena (such as the processing of hides). There are numerous possibilities which may explain this apparent absence of evidence. Firstly, the length of time engaged in the specific activities required to impact on the labial and lingual surfaces to the extent represented in Figures 5.14a–j and 5.18a–e may exceed the lifespan of the deciduous anterior teeth: from the point at which the individual is developmentally able to participate in the activity to tooth exfoliation. It is also possible that such examples might exist within the population but were not included in the current study sample. Further analyses are required to understand better the demographic distribution of these particular phenomena for the communities of Neolithic Gozo.

When we consider what archaeological and ethnographical research has put forward as possible aetiologies for the incidental or 'passive' modifications observed within the Circle population sample, our picture of life in prehistoric Gozo acquires a finer resolution. Activities including clenching fibres between the teeth while weaving mats, ropes and baskets (Minozzi *et al.* 2003); processing animal skins (Eshed *et al.* 2006; Langsjoen 1998, 410; Roberts & Manchester 2005, 81); holding objects such as staves in the mouth while making baskets or nets (Eshed *et al.* 2006); processing materials including lithics, plant fibres, bone, shell and animal sinews (Buikstra & Ubelaker 1994; Cybulski 1974; Irvine *et al.* 2014; Lukacs & Pastor 1988; Schulz 1977; Turner & Cadien 1969; Waters-Rist *et al.* 2010); and using the mouth as a 'third hand' to hold material static in the teeth to allow manipulation (Alt & Pichler 1998, 394; Merbs 1983; Roberts & Manchester 2005, 81) are all raised as prospective impetuses for the incidental dental augmentation observed on some of the children and adults in these communities. It is also possible that other activities beyond those listed here were augmenting the dentition of some of those interred in the Circle. While populations elsewhere also include activities associated with fishing as prospective activities, such as the manufacture of fishing nets and baskets, research carried out by McLaughlin *et al.* indicates that marine proteins were a marginal feature of the Neolithic Maltese subsistence strategy (Chapter 10).

Over and above considerations of the specific activities involved in incidental dental modification, we can view the identification of these markers not only as embodied teaching and learning experiences, but also as economic events within prehistoric communities. Studies undertaken by Finlay (1997) on the identification of children in lithic production are of relevance here, as they cause us to consider children as imbricated in ancient knowledge transfer and socio-economic frameworks. They learned their skills from more experienced people within a community of practice (Lave & Wenger 1991), and then served as producers themselves, creating items or services to comply with societal norms and circulate within local or regional networks – or perhaps even more broadly (Finlay 1997, 205; cf Power 2012). These considerations expand our conceptions of the producers of material culture and highly skilled craft practitioners in prehistoric Malta also to include children. Frequently, in archaeological narratives across cultures, these activities and agencies are reconstructed as andro- and adult-centric (Finlay 1997, 204; Gero 1991; Wajcman 1991).

Following this, an important point to return to is the relatively low incidence rate of dental modification (Σ=172; 5.62% total sample) across all use-phases of the Circle within the study sample. Furthermore, it is noteworthy that on at least 20 occasions within the sample (Table 5.2), more than one type of modification was observed on a singular tooth. When translated into lived experiences, these observations suggest that at any given time, only a relatively small number of adults and children were participating in some of the proposed activities (and possibly others) described above. For some, these may have been a specific task or a range of tasks and/or rituals that modified their anterior teeth in more than one way. In sum, this evidence provides insights into the proportion of individuals engaged in specialized crafts or services, or selected for ceremonial or aesthetic augmentation, at various times across the use-life of this burial space and therefore also within prehistoric Maltese communities. Assuming the equitable funerary treatment afforded to members of the population across demographic categories within the Circle (Chapter 12), there is little reason to believe that dental modification in this population was restricted to any particular status group, or resulted in any form of social differentiation within the mortuary sphere. We do, however, require further study of this and other contemporary populations to understand better if any discernible patterns exist.

5.7.4. Aetiologies

As discussed in §5.2.1, above, it can be extremely difficult and, on occasion, impossible to distinguish between intentional and incidental dental modifications (Blakely & Beck 1984; Dembo *et al.* 1949; van der Reijden 2014, 9). Abrasion from processing fibres for textile production and/or basketry can result in incisal grooves that are difficult to differentiate from intentional notching (Burnett 2017, 251; Larsen 1995; Schulz 1977). Similarly, dental chipping can result from both masticatory, parafunctional and intentional modification activities (Burnett 2017, 251; Milner & Larsen 1991). It can also be extremely challenging to identify the difference between *antemortem* tooth loss caused by carious lesions, trauma and intentional avulsion and/or ablation (Burnett 2017, 251; Cook 1981; Hrdlička 1940; Merbs 1968; Milner 2017, 319). The findings of the current study for Neolithic Malta are not immune from these ambiguities. If we align with Reichart *et al.*'s (2008) analyses of Cameroonian populations to see chipping of the mesial corners of maxillary central incisors as a common form of intentional or 'active' modification, we will likely fall foul of those who agree with studies such as Haour and Pearson (2005), who argue that similarly modified teeth in Niger are attributed to parafunctional or 'passive' modification (Burnett 2017, 252). Others may contest that deep incisal notches are the clear signature of intentional alteration (Afsin *et al.* 2013), yet be met by opposition from those who view it as *postmortem* damage (Burnett 2017, 252; Dembo *et al.* 1949; van der Reijden 2014, 40). Further consideration must be devoted to these diverging opinions in order to determine the aetiologies of the modifications reported for the Circle dentition by this research.

We accept the likelihood that many of the modifications within the Circle population sample are 'passive', unintentional or parafunctional alterations to the teeth, associated with habitual cultural activities. Certainly, as emphasized by Burnett (2017, 255), intentional or active modifications are rarely observed to encompass the entire crown and are therefore unlikely to extend to the cementum enamel junction or traverse onto the tooth root, as described and illustrated for the categories of labial and lingual wear to both maxillary and mandibular anterior teeth in §5.5.1.3 and §5.5.1.4, above, and Figures 5.14a–j and 5.18a–e. Furthermore, most deliberate modifications manipulate the enamel and/or dentine only and will infrequently compromise the pulp chamber (Burnett 2017, 255; Tiesler 2001). We propose that some of the observations of chipping and incisal notches presented in §5.5.1.1 and §5.5.1.2, above, and Figures 5.6a–k and 5.10a–j are clearly activity-related change, as indeed are some of the modifications described as diagonal and undulating profile modifications in §5.5.1.5–6, above, and Figures 5.22a–i and 5.18f and g.

Although the nature of the modification itself is of critical importance, classification of passive dental augmentation may also be addressed via analyses of distribution. While agreeing that the anterior teeth are most commonly affected, Burnett (2017, 255) asserts that the distribution of parafunctional modifications are quite random, unilateral and irregular across the 'social six', and may present a lateralization bias towards handedness. It is in these considerations of lateralization that the biocultural narrative of modification within the Circle population begins to crystallize. The results here demonstrate wear patterns that are most frequent in the left first maxillary incisors, with decreasing frequencies from the right first maxillary incisor as one moves distally in the right maxillary arcade. As reported in Chapter 4, distributions of the major forms of activity-related dental pathology across the Circle sample align with this distribution, insofar as crown fractures and extreme wear all predominate on the right side. It is proposed that this pattern is associated with parafunctional wear. Chapter 7 reports findings of sample-wide trends towards right handedness. Their research echoes global patterns of right-handed predominance in anthropological studies of fossil hominins and anatomically modern humans, usually ranging between 70–80% of populations (Steele 2000, 307, 316–7; cf Constandse-Westermann & Newell 1989; Steele & Mays 1995; Stock *et al.* 2013; Macintosh *et al.* 2014a; Trinkaus *et al.* 1994; Walker & Leakey 1993). The remainder are characterized as left-handed and ambidextrous. The predominance of right-sided dental wear and the contralateral wear on the left maxillary first incisor is consistent with the use of the dentition as tools among right-handed individuals.

However, distributions of both adult and non-adult dental modification across the Circle population sample oppose the handedness trend, as the majority of modified teeth are observed on the left side of the mouth (§5.5, above, & Figs 5.2, 5.3 & 5.4); that said, this observation is not statistically significant (χ^2 = 2.2, p=0.14). Moreover, Burnett argues that maxillary dentition is more visible than the mandibular arcade and are therefore observed to be more frequently modified across cultures (Burnett 2017, 252; Romero Molina 1952; Tiesler 2001). The Circle data emphatically agree with this, with both adult and non-adult distributions significantly favouring the maxilla as the locale for this mode of cultural display (χ^2 = 29, p<0.0001 for the adult dentition).

Additionally, active modifications are most often observed as bilateral and will be present in both antimeres (Burnett 2017, 252). It is also argued that deliberate modifications are symmetrical in both type (for example: notching, chipping) and appearance (for example: single, double; Burnett 2017, 255; cf Alt & Pichler 1998, 399; Langsjoen 1998). The depositional context of our sample prevents us from studying –and therefore presenting– many complete and intact dental arcades. We have nonetheless put forward some compelling case studies in §5.6, above, and also argue throughout this chapter for the alignment of some of the distinctive shape changes observed amongst the Circle population sample with several of van der Reijden's (2014) intentional modification classifications.

Rather than determining that *either* intentional *or* incidental dental modification took place amongst the Neolithic communities represented within the Circle, we propose that both are noted within the population.

5.7.5. Cross-cultural insights

The identification of dental modification types in archaeological assemblages are often used as proxies for connections between groups and/or cultures (De Groote & Humphrey 2017, 22; van der Reijden 2014; van Rippen 1918a), and to infer migration patterns (De Groote & Humphrey 2017, 19, 23; Hedman *et al.* 2017, 241–2; Irish 2017, 35, 44; Kusaka 2017, 150; Kusaka *et al.* 2008, 2009, 2011; Lee 2017, 99; Milner 2017, 325; Morita *et al.* 2012; van Reenen 1977, 1978a, 1978b, 1986). In §5.6, above, we presented scenarios in which the potential intentional modifications observed on an adult female and male indicate either that these individuals experienced dental interventions in Malta itself, or that they travelled to Malta having had the alterations carried out elsewhere. Such modifications are relatively rare in European and more common in African populations; however, the modification is not diagnostic alone and its presence could represent either migration or cultural influence from Central or Southern Italy, or Africa. Often the appearance of similar types of modification can be enigmatic and inexplicable, and this can be because of purposeful or accidental variations from traditional practices, individual choices and decisions, serendipity, and the innumerable possibilities for pattern combinations (Gould *et al.* 1984; Larsen 2017, xvi; van Reenen 1986). Appearances of specific modification types in various geographical settings may also be unrelated (Larsen 2017, xvi). Further to this, one must account for errors of interpretation, translation and identification between and amongst classification systems and researchers (van der Reijden 2014, 10); a consideration from which the present study is certainly not immune, despite our most stringent efforts. However, perhaps the most significant issue to contend with is that of the geographical bias inherent within the classification systems themselves. Most diagnostic hypotheses/taxonomies have been developed on modified teeth from the Americas, so they are therefore not exhaustive in terms of type, mode or expression and are generally far younger in appearance than our prehistoric context. They are nonetheless helpful in informing our evaluation of dental modification in Malta, and likewise our observations for the predominantly under-studied prehistoric Central Mediterranean region will inform global understanding of this enigmatic aspect of human behaviour.

As presented above, this study has identified dental modifications within the Circle population that resemble van der Reijden's (2014) A6.4, A8.1, B1.1, B1.3, B1.4, B2.3, B4.3, B4.4, C2.3 and N1.2 types, and may even present new forms. In terms of cultural attestations, several of these types have only previously been reported for individuals and groups from the Americas, including A8.1 ('notch' type – van der Reijden 2014, 47; after Autry 1991; Boman 1908; Gill 1985; Perino 1967; Romero 1986; Spence & Pereira 2007 Weinburger 1948; Whittlesey 1935); B4.3 ('right-angled cut-out' – van der Reijden 2014, 49; after Coe 1959; Weinburger 1948); C2.3 ('concave side edges with flattened occlusal end' type – van der Reijden 2014, 51; after Rojas *et al.* 2011); and N1.2 ('reduction in crown height' type – van der Reijden 2014, 68; after Montandon 1934; Rojas *et al.* 2011; Romero 1986; Rubín de la Borbolla 1940; Smith 1972). Other forms observed within the Circle population have further attestations across the Americas, but have also been observed on the African continent, including B1.1 ('single corner, straight edge' type – van der Reijden 2014, 48; after Romero 1986; Starr 1909; von Jhering 1882); and B4.4 ('right-angled cut-out' – van der Reijden 2014, 49; after Campbell 1944; Lignitz 1919; Novotny 2008; Starr 1909; van Reenen 1978a; van Rippen 1917). Finally, the remaining intentional modification forms observed within the Circle assemblage have direct parallels restricted to the African continent, including B1.3 ('single corner, straight edge' type – van der Reijden 2014, 48; after van Reenen 1978a); B1.4; ('single corner, straight edge' type – van der Reijden 2014, 48; after Starr 1909); and B2.3 ('concave edge, reduced crown height' type – van der Reijden 2014, 49; after Starr 1909). The only modification form within the Circle sample without cultural attribution in van der Reijden's classification was A6.4 ('one notch reaching to corners' type – van der Reijden 2014, 47), however this form is well-known throughout the literature as the 'swallow-tail' type, and has also been attributed to the African continent (Irish 2017, 36).

Considering both the temporal and geographical context of the Circle use life, the similarities with African dental modification forms is certainly worthy of further consideration because of its relative proximity and contemporaneity for the beginnings of intentional modification (Finucane *et al.* 2008). More research is required to determine Malta's position within this biocultural dynamic. Genetic data (Chapter 11) suggest the immediate ancestors of the majority of the individuals studied had similar origins, descended from a broadly 'Neolithic' group of people. These analyses attest to potential genetic influences on the relationships between the people of the Circle and mid-Holocene agricultural and hunter-gatherer populations from the Northern Mediterranean and Europe. At this stage the aDNA analyses are principally derived from three individuals and as such, provide information on only a subset of the people interred in the Circle. Despite the relatively small sample size, the genetic analyses reveal relative homogeneity. In contrast, the non-metric traits of the dentition (Chapter 6) were analysed for a larger subset of the assemblage, with comparative samples derived from the entire circum-Mediterranean region, including North Africa. Analyses of non-metric traits of the posterior dentition revealed similarities throughout the region, and to populations in Southern Europe and North Africa. Whilst it is premature to interpret these as definitive indicators of genetic distance, without further analyses of the anterior dentition, they are suggestive of broader genetic links between the populations of Neolithic Malta and others to both the North and South. When the results of dental modification are interpreted in this context, cultural or biological influences from Africa are certainly plausible and may explain the presence of patterns of dental wear in the Circle assemblage that would be considered rare or unknown in Europe.

Strontium isotope data (Chapter 9) tentatively speak to the limited degree of mobility over the life of the individuals we have studied, all of whom ranged within the limestone areas of Malta and/or southern Sicily. Thus, the dental modification evidence potentially opens a new bioarchaeological perspective on biological and/or cultural connectivity beyond Malta's shores that is not possible from as-yet limited isotopic or genomic perspectives. Such biocultural hints of outside influence in prehistoric Malta are also suggested by the material culture of the Temple Period, which saw raw materials such as obsidian circulated throughout the Central Mediterranean and several traits in pottery style and decoration shared across the region (Volume 2, Chapter 10).

A possible single case for dental avulsion amongst the sample is presented in §5.6.1, above, and it is intended that future analyses of the hard tissues of the jaws will explore the extent to which this may or may not have been an isolated case. Although the differential diagnosis for this young adult female is complex, extraction and/or avulsion must be considered as potential interventions. It is appropriate to propose that she may have been involved in the activities described by Robb (1997) for Neolithic Central and Southern Italy. As discussed in §5.2.3, above, he estimated that between 25–50% of Neolithic women from this region would have undergone selective and intentional removal of the maxillary incisors and/or canines for symbolic or ceremonial reasons. This young woman prompts us to consider the possibility that she may have lived in Italy and been subject to these cultural practices before coming to live –and ultimately die– at a young age in Malta. Alternatively, she may have been subject to these practices in Malta, presenting evidence for the movement of cultural ideas and practices as well as material culture into the archipelago (Evans 1971, 223; Malone *et al.* 2009a, 238, 242; Robb & Farr 2005; Malone & Stoddart 2004; Trump 2002; Vella 2009; cf Volume 2, Chapters 10 & 12). Of particular relevance to this discussion is the appearance of 'Thermi' pottery in Malta in the 25th century BC, which occurred around the time or not long after the burial of the young woman discussed above (Volume 2, Chapters 2 & 10). Was she a personal agent of this cultural change? To answer these questions, we may follow the methodologies established in research involving more recent populations of enslaved peoples in the New World. Here, dental modification analyses have been aided by targeted isotopic studies to determine whether the modifications were performed in individuals' country of origin or in the diaspora (Corrucini *et al.* 1987; Goodman *et al.* 2009; Price *et al.* 2006, 2012; Schroeder *et al.* 2009; 2014; cf Hedman *et al.* 2017; Kusaka 2017; Pietrusewsky *et al.* 2017, 128). Considering the role that modification plays in understanding migration patterns (Irish 2017, 44; cf Handler 1994; Handler *et al.* 1982; Ortner 1966; van Reenen 1977, 1978a, 1978b, 1985, 1986), alongside the work presented in Chapters 6, 9 and 10, further archaeometric analyses incorporating the biochemical, biomolecular and morphological characteristics of the dentition may refine insights regarding the origins and connections of dental modification practices amongst the Circle population.

In addition to further scientific analyses, extended research into the attestations of the intentional shape modifications may also shed light on the scope of cross-cultural connections at play in Neolithic Malta. Following the painstaking work of van der Reijden (2014) and many of her predecessors across continents (Almeida 1953, 1957; Fastlicht 1948; Romero 1986; Rubín de la Borbolla 1940; Saville 1913; Starr 1909; von Jhering 1882; Wasterlain *et al.* 2016), we have illustrated above that Malta needs to be considered within a dynamic web of biocultural innovation and expression – and perhaps even be located towards its centre.

5.7.6. Chronological insights

Humans have been modifying their teeth for millennia. To determine where the Circle populations sit in terms of regional and global chronological representations of modification, the most relevant issues for consideration are: i) whether the modifications were undertaken for therapeutic or non-therapeutic purposes; ii) whether avulsion or ablation was practised; and iii) whether the reported modifications were intentional or incidental. These issues are discussed in more detail, below.

Early evidence for therapeutic intervention appears to date back to at least the Neolithic (Coppa *et al.* 2006), with some claims extending as far as the Late Upper Palaeolithic (Oxilia *et al.* 2015; cf. Bennike & Fredebo 1986; Ortiz *et al.* 2016; Seidel *et al.* 2005; Turner 2004; White *et al.* 1997). In terms of the representation of therapeutic dental intervention amongst the Circle study sample, a prospective case is presented in Chapter 4. Here, a fragment of adult left mandible from Context (897), radiocarbon dated to 2575–2500 cal. BC, features a sharp-force trauma lesion to the buccal aspect of the mesial root of the first left mandibular permanent molar (FDI 36). It is argued that this observation indicates that this individual was subject to a proto-surgical procedure to relieve probable symptoms of pain and pressure resulting from the infectious and inflammatory response observed in the alveolus surrounding both mesial and distal roots, associated with a massive carious lesion on the crown. Although this case does not directly augment the crown *per se*, it is nonetheless an example of therapeutic intervention on a pathological tooth, and should thus be included amongst the small global corpus of prehistoric dental proto-surgery (Langsjoen 1998, 411; Leigh 1937, 294).

As discussed in §5.2.3, above, avulsion and ablation extend even deeper into human prehistory, with the earliest known examples attributed to the middle Iberomaurusian (~13,800–16,100 cal. BP) on an isolated skull from Taza, Morrocco (Meier *et al.* 2003). The practice is widespread at Maghrebian sites thereafter and continues through to the Neolithic (De Groote & Humphrey 2016, 2017; Humphrey & Bocaege 2008), including the Mediterranean region according to Robb's (1997) reporting of the practice as carried out on women in Central and Southern Italy (*c.* 6500–3200 BC). A possible single case for avulsion amongst the Circle sample analysed thus far is presented in §5.6.1, above, and further research is required to determine the nature and scope of the practice within this population. This is the first potential case of avulsion presented for prehistoric Malta; however, an enigmatic link in early literature proposes a connection between the 'Neolithic Maltese' (Keith 1932, 284) and the peoples of North Africa and the Fertile Crescent, who are also reported to have engaged in this practice. Considering that this individual was excavated from Context (960) (2530–2475 cal. BC, Malone *et al.* 2019), during one of the later use-phases of the Circle, it seems that avulsion was being carried out in Malta towards the end of the Temple Period in the 26th and 25th centuries BC (Chapter 3), or that individuals already bearing this type of modification were travelling to Gozo at this time. Either way, this case extends our knowledge of this practice into the 3rd millennium.

When considering the chronology of both incidental and intentional modification amongst the study sample, we argue that both were part of the cultural and lived experiences of the prehistoric communities of the Xagħra plateau. Evidence presented throughout this chapter, and Chapter 4 of this volume, indicates that parafunctional wear was observed amongst the earliest use-phases of the Circle. This research has qualified and quantified the initial observations made by Stoddart *et al.* (2009a) that 'parafunctional', 'distinctive' or 'habitual' wear was present for individuals interred from the Żebbuġ period onwards (Stoddart *et al.* 2009a, 318, 319, 323, 324, 325, 329). As presented in detail over the preceding pages, these forms of non-alimentary wear included some forms of chipping, incisal notches, lingual and labial extreme wear, and diagonal and undulating profile changes associated with a range of habitual practices most likely associated with food processing (for example, cracking, breaking or stripping hard foods); and/or processing materials other than food in association with cultural practices commencing from the earliest contexts included within this study.

The earliest known intentional non-therapeutic shape changes appear to be more recent than the practices of avulsion and ablation. As described in §5.2.3, above, examples come from across the globe, including observations from an adult male burial dating between 2570 BC and 2332 BC in Michoacán, Mexico (Kirk 2006). It is reported that the man's maxillary teeth were intentionally filed down to insert a ceremonial prosthesis, most likely of animal origin, such as the palate of a wolf or jaguar. In Africa, early examples are attributed to Karkarichinkat Nord in Mali in the 3rd millennium BC, where four individuals of unknown sex had their maxillary incisors and canines intentionally shaped to points, probably through filing (Finucane *et al.* 2008). Situated within both regional and global contexts, some of the findings reported here for the Circle population are of great significance, as they may represent amongst the earliest incidences of intentional non-therapeutic dental modification in the world. As reported above, and presented in Figures 5.6a–k, 5.10a–j and 5.22a–i, the Neolithic people of Gozo deposited within the earliest use-phases of the Circle had deliberately modified anterior dentition, featuring shapes that resemble van der Reijden's (2014) A6.4, A8.1, B1.1, B1.3, B1.4, B2.3, B4.3, B4.4, C2.3 and N1.2 types, and may even present new forms. As described in §5.5.1.5, the diagonal modifications observed in the study sample align with van der Reijden's 'B' Types, where the modification distinctly affects one edge (2014, Table 4.5; B1.1, B1.3, B1.4); however, for some of the Circle examples, the filed edge extends across the entire incisal margin; and in some case the crown height is reduced by more than half.

As discussed in greater detail in Chapter 4 of this volume, the prevalence of dental modification presents an interesting comparison with dental pathologies. Rates of dental modification steadily increased throughout the use-life of the Circle, commencing at 2% around 2700 BC, and maintaining a plateau at approximately 8% after 2450 BC (Fig. 5.32). It is apparent that dental modification increased over time, and, of all other pathologies (including enamel hypoplasia, caries, crown fractures, extreme wear and hypercementosis) bears closest (albeit loose) relationship to the prevalence of enamel hypoplasia within the sample. This is an important point of consideration because of the tendency of enamel hypoplasia to serve as a proxy for more endogenous biological stress indicators

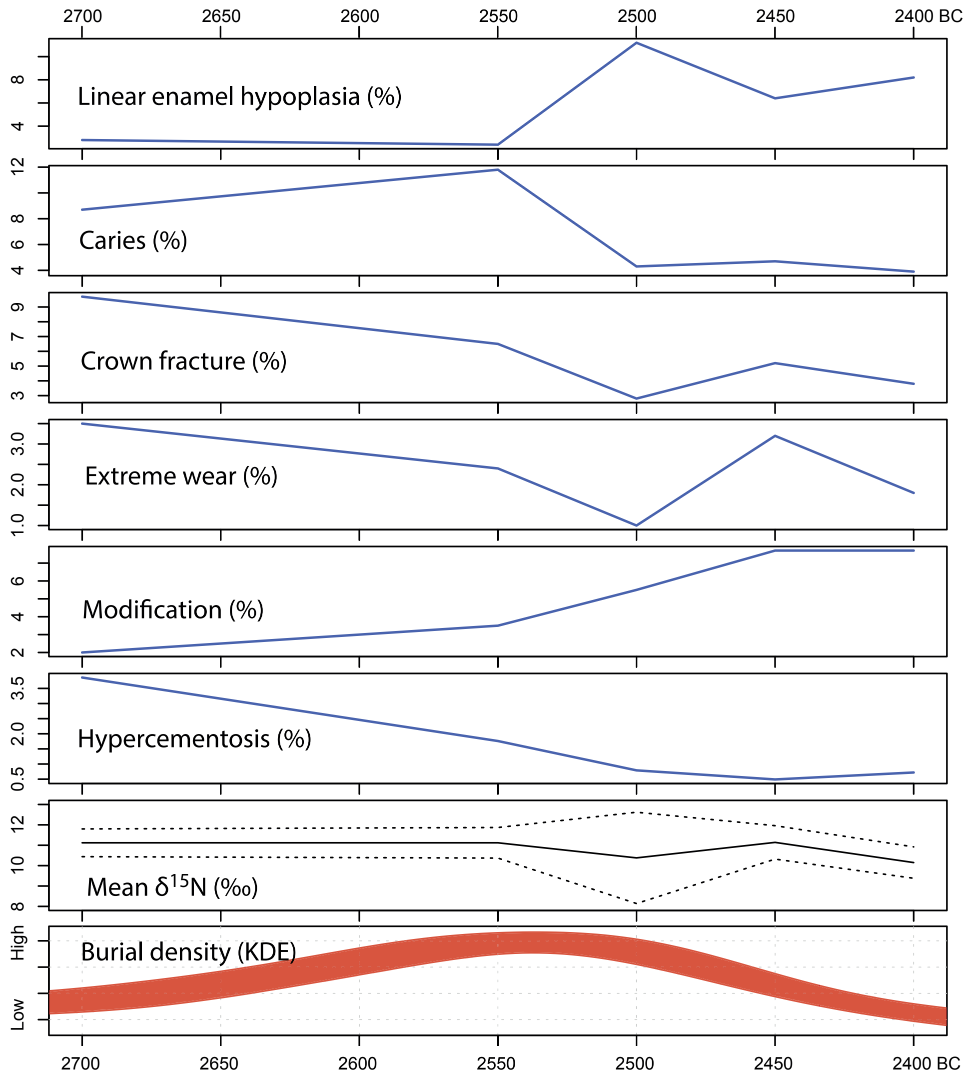

Figure 5.32. *Schematic chronological representation of dental modification incidence within the Circle sample, plotted alongside various dental pathologies, average nitrogen isotope values and burial density from ~2700-2400 BC. (Rowan McLaughlin).*

(Goodman 1991; Goodman & Capasso 1992; Goodman & Rose 1990, 1991; Ortner 2003; Pindborg 1970; Roberts & Manchester 2005). As discussed in Chapter 4, enamel hypoplasia has a very low sample prevalence rate during the Earliest-to-Middle use-phases of the Circle (approximately 2% until 2550 BC). From this point, a steep increase in enamel hypoplasia is observed, eventually occurring in one in ten of the teeth found within each stratigraphic context. In effect, the prevailing biological stressors during this period resulted in a very significant increase in the number of observations for this pathology. Crucially, this is the moment of maximum activity at the site, when other dental pathologies were reduced in frequency. Subsequently, there was a slight oscillation in the number of cases of enamel hypoplasia, but the average rates were nonetheless still much higher than earlier in the Circle's history.

Of all the recorded dental phenomena, dental modification was unique in remaining at peak incidence rates from around 2500 BC until the end of the Circle's use-life at approximately 2350 BC. All modification types recorded by this study, with the exception of lingual wear and undulating profiles, were observed to increase in incidence across the use-life of the Circle. The peak of incidence in the Late use-phase is particularly noticeable after very low rates recorded for the Middle use-phase for all modification types. Thus, a correlation exists between increased dental modification and indicators of the prevailing biological and cultural stressors present, especially enamel hypoplasia. Biological stress was therefore present during the circumstances that led to the end of the Temple Period in Neolithic Gozo. Whatever the causes of this stress, it is clear that at this time some of the adults and children within these communities were increasingly engaging in food or material culture production requiring parafunctional use of the mouth; in cultural activities designed to create intentional permanent corporeal identity markers; or in travel that brought them to Malta from elsewhere, already bearing these modifications.

5.8. Conclusion

The present study represents the first dedicated enquiry into the nature and scope of dental modification in any skeletal population from the Maltese archipelago. Observations of modified teeth were first reported in the Circle population by Stoddart *et al.* (2009a). The current research has met recommendations for further investigations into this intriguing aspect of human corporeal intervention for prehistoric Malta, and it introduces the experiences of those living in Neolithic Gozo into the wider discourse of dental modification across the Mediterranean and the world. Notwithstanding the numerous and important insights summarized below, as a first foray into the field we anticipate that this work will serve as a genuine introduction, and that subsequent analyses can build on our foundation to clarify and extend these primary engagements.

Overall, our reporting of the relatively low incidence and proportion of modification amongst the Circle study sample accords with studies elsewhere. These findings suggest that at any given time, only a relatively small number of people were participating in specific tasks or a range of tasks and/or rituals that modified their anterior teeth. These observations provide insights into the proportion of individuals engaged in particular specialized crafts or services, or those selected for ceremonial or aesthetic augmentation within prehistoric Maltese communities.

This research has also made important discoveries concerning *who* was undertaking these activities, or perhaps even selected for participation. In Neolithic Gozo, both adults *and* children were engaged in the range of cultural practices that produced these corporeal interventions: either the immediate and most likely ritual and/or aesthetic interventions of intentional dental modification, or the gradual and repetitive behavioural interventions of incidental practices. Adult teeth were most often observed to be modified, but deciduous teeth are present in the dataset, with examples reported for every modification type except labial and lingual extreme wear. Observations of either intentional or incidental modification or extreme wear on deciduous teeth are very rare in archaeological populations, so this represents an important finding. This research calls us to reconsider existing archaeological narratives of prehistoric Mediterranean communities and view children as key participants and contributors in ancient knowledge transfer and socio-economic frameworks.

Biocultural approaches to intentional corporeal modifications engage the body as a translator of lived experiences and actions. Our research provides tangible evidence for tactile activities, the material components of many of which are as-yet elusive in the prehistoric Maltese archaeological record as a result of the tyranny of preservation. We have described features which may be associated with food processing (for example, cracking, breaking and/or chewing hard foods); and/or processing materials other than food in association with cultural practices such as clenching fibres between the teeth while weaving mats, ropes, nets and baskets; processing animal skins; holding objects in the mouth while making baskets or nets; processing materials including lithics, plant fibres, bone, shell and animal sinews; and using the mouth as a 'third hand' to hold material between the teeth.

This research extends the findings offered in Chapter 4, by shedding light on corporeal engagement and the effects of aspects of Maltese Neolithic behaviours on the body. Amongst other results, we report consistent evidence for fibre processing in the form of incisal notches on deciduous and permanent dentition. No organic materials have yet been found preserved in late Neolithic contexts on the Maltese archipelago, yet scrutiny of the figurative and burial records provides some tantalizing glimpses into textile production techniques and uses. The most well-known figurines from the islands, the 'Sleeping Lady' from the Ħal Saflieni Hypogeum, and the seated paired figurine from the Circle, both appear to be resting upon a 'bed' comprising a frame of wooden struts overlain with straw and/or reed bundles (Malone *et al.* 2009a, 289–98). Other similar styles of figurines are known from Tarxien and Ħaġar Qim, although they depict these 'beds' less clearly (Malone *et al.* 2009a, 296–8). It is inferred that the straw and/or reed bundles, as well as the struts and bearers forming the base of the frame, were tied with cordage (Malone *et al.* 2009a, 293). These exceptional figurines might provide a rare depiction of a relatively routine furnishing, one core component of which was created through repeatedly passing fibres through and between the teeth and hands, resulting in permanent and visible wear to the anterior dentition. Further insights might be gleaned through careful analysis of depositional practices within the Circle itself. The unique cache of nine figurines referred to as the 'Shaman's Cache' was carefully placed together in a tightly grouped package, alongside a small Tarxien ochre offering pot (Malone *et al.* 2009a, 298). Such a close spatial relationship strongly suggested that they were placed within a box, bag or other organic wrapping material. If the latter, it might have been woven from small fibres, although no trace remains. Finally, it remains possible that some of the dead were interred in the Circle covered or shrouded in textiles of some kind, which, upon disintegration, allowed the remains to be accessed later and redistributed throughout the cave system. Indeed, Stoddart and Malone (2010, 24) and more recently Thompson *et al.* (2018) have suggested that some individuals were deposited in the Circle and the Xemxija tombs covered in animal hides that may still have retained head and hoof elements, providing a precedent for a packaged and wrapped form of engagement with the dead.

We have described both active and passive dental modification types that are commonly reported across prehistoric cultures, including chipping (or chiselling), incisal notches, labial and lingual wear, diagonal and undulating profile modifications and gross crown loss, while also presenting some potentially novel augmentation types, too, including diagonal incisal profile modification. We have also presented an intriguing case study of a young woman with complex presentation of her anterior teeth, for which extraction and/or avulsion must be considered amongst other potential interventions. Based on our analyses of the nature, forms and distributions of the modification types observed within the study sample, we have argued that *both* intentional and incidental dental modification took place amongst the Neolithic communities of the Xagħra plateau. Some of the findings reported here for this population are of great significance, as they may represent amongst the earliest incidences of intentional non-therapeutic dental modification in the world. Moreover, in terms of cultural connections, our findings may contribute to consolidating Neolithic Malta's important position within wide mobility networks of people and ideas across broader Mediterranean, African and European cultural contexts.

In terms of chronological distribution, we have reported that the Late contexts feature the highest incidences of dental modification by a substantial proportion. The Late use phase of the Circle featured >80% of all dental modifications observed within the study sample; more than six times the number of observations for the Early use phase and 23 times the number of observations for the Middle use phase. With the exception of lingual wear and undulating profiles, all modification types were observed to increase in incidence across the use-life of the Circle. The peak of incidence in the Late use-phase is particularly noticeable after very low rates recorded for all modification types in the Middle use-phase. When paired with observations of the loose relationship between prevalence rates of dental modification and enamel hypoplasia, this suggests that a correlation may exist between increased dental modification and the prevailing biological and cultural stressors present during the circumstances leading to the end of the Temple Period in Neolithic Gozo.

Our research has only 'scratched the surface' of the possibilities for dental modification analyses in Neolithic Malta. There is a great deal more work to be done, particularly in the pursuit of additional archaeometric multiproxy analyses. Opportunities for further study include (but are not limited to): deeper discussion of the precise location, surface and size of modification locations on individual teeth to understand modification phenomena of the Circle at an even greater resolution; associations of infectious or inflammatory processes on the maxillary and/or mandibular alveolar processes wherever affected teeth are retained *in situ* to determine if relationships exist between dental modification and pathology for this population; studies of extant dental calculus to determine if microscopic fragments of processed fibres or other materials (stone chips, *etc.*) retained in the mouth can shed further light on inferences about tasks involving the teeth (Sperduti *et al.* 2018); scanning electron microscopy of affected tooth surfaces to complement and extend our efforts to distinguish between intentional and incidental modifications (van der Reijden 2014, 19; Farrell 2013; Havill *et al.* 1997); and aDNA analyses to assist in attempts to determine if there are any associations between dental modification, biological sex distribution and geographical affinities.

This work contributes important Neolithic Maltese evidence to the global quest to examine how the body can help us understand fundamental questions about human cultures, including the structure and composition of communities, connections between groups, the production of goods and services, the nature and persistence of traditions and the movement of people and ideas across space and time (Milner 2017, 317, 327). Despite the significant challenges presented by the nature of the Circle assemblage, our contextualized study of dental modification has allowed us to approach ancient people from both biological and cultural perspectives (Larsen 2017, xvii). In this way, our research presents a truly rare opportunity to view corporeal expressions of action, agency and meaning in the prehistoric Maltese archaeological record.

Note

1. These analyses were carried out in two tranches with the approval of Heritage Malta and the Superintendence of Cultural Heritage, Malta, the first in July 2015 and the second in July 2017. Transport was carried out by Bernardette Mercieca-Spiteri, Officer of the Superintendence of Cultural Heritage, Malta, with the agreement of Heritage Malta. On both occasions, radiographic analyses (micro-CT scans) were carried out by Jay Stock, Laura T. Buck and Jaap Saers at the Cambridge Biotomography Centre, University of Cambridge, UK, with a Nikon Metrology XT H 225 ST. Scans were created with voxel sizes ranging from 0.06 to 0.12μm3 (to two decimal places) as appropriate for the region of interest and specimen size. Further processing of individual files was carried out by Jaap Saers in the Department of Biological Anthropology, University of Cambridge, UK. Radiological examination and description of the micro-CT scans was carried out by John Magnussen, Ronika K. Power and Jess E. Thompson, using 3D Slicer (BWH, slicer.org), RaDiant DICOM Viewer (Medixant, radiantviewer.com) and AW Server (GE Medical Systems, Milwaukee, USA) software at Macquarie Medical Imaging, Macquarie University Hospital, Sydney, Australia. Radiological images were processed for publication by John Magnussen and Margery Pardey at Macquarie Medical Imaging.

Chapter 6

Dental anthropology from the Circle: non-metric traits of the posterior dentition and population relationships in the Neolithic Mediterranean

Ronika K. Power, Bernardette Mercieca-Spiteri,
Jay T. Stock & Joel D. Irish

6.1. Introduction

The ubiquity of human teeth within the Circle assemblage, combined with their innate durability, provides an excellent platform to explore how the dentition can illuminate our understanding of *who* the individuals and groups were that utilized the Circle for generations, or perhaps more importantly, *how* or indeed *if* they were connected. Many have wondered whether this burial place was the preserve of certain families, kinship groups, or 'classes' of individuals, organized in some manner by status, kinship or occupation (Stoddart & Malone 2008, 27; Stoddart & Malone 2015). However, before this volume, no studies have sought to analyse biological indications of proximity or distance among the hundreds of people interred and commingled in this space for hundreds of years, nor how they related to other groups around the Mediterranean region.

Research conducted as part of this project has investigated genetic relationships between the people deposited in the Circle and mid-Holocene agricultural populations from the Northern Mediterranean and Europe (Chapter 11). These analyses were based on aDNA extracted from the remains of nine individuals and provide a preliminary and, by necessity of conservation, partial evaluation of the genetic affinities of the people of the Circle. The results show similarities between the late Neolithic populations of Malta and the Neolithic peoples of central Europe. While genetic analyses provide unparalleled insights into broader population relationships, they are by nature destructive and must be supplemented by broader non-destructive bioarchaeological analyses in order to understand variation better. With its focus on inferring genetic pathways through non-destructive statistical analyses of tooth morphology and size, the discipline of dental anthropology offers ideal means to approach the critically important questions of population affinities within the large assemblage from the Circle.

Dental anthropology provides a range of useful interpretations in archaeological research, particularly among fragmentary and commingled funerary assemblages, as discussed elsewhere in this volume (Chapters 4 & 5), because of the strength and resilience of teeth even under the most unfavourable depositional environments (Hillson 2005, 158). Additionally, once formed in childhood, the shape of teeth is unchanged throughout adult life, provided they can withstand the impacts of wear and decay through diet and disease (Hillson 2005, 257; Chapter 10). Scholars have been interested in exploring the utility of the dentition as a means to provide insights into human variation and behaviour since the early 20th century (Scott & Turner 2008, 11). The observation and quantification of non-metric traits of the dentition is a useful approach for the study of microevolutionary patterns within and between populations, including genetic drift, mutation, gene flow and, to a lesser extent, natural selection (Turner 1969, 1986a). While it is not generally possible to differentiate these processes based on dental traits alone, the study of variation is useful for biological distance estimates or affinity assessment, in which genetic relationships are estimated by similarities observed in phenetic expression within and between groups. Observed differences are the result of one or more of the four evolutionary processes listed above. In this respect, greater observed differences generally suggest a greater influence of these processes, and hence a longer period of separation or divergence between groups.

The shape and morphological characteristics of teeth are under tight genetic control during development (Alvesalo & Tigerstedt 1974; Berry 1978; Garn *et* *al.* 1965; Goose 1971; Harris & Bailit 1980; Nichol 1990; Scott & Turner 2008, 11; Townsend & Brown 1978), and can therefore provide valuable information for those wishing to trace relationships between and amongst groups of humans. As anatomical structures, the forms of teeth are primarily determined by the genotype, along with prevailing environments and behaviours (Hillson 2005, 257), for example, geographical isolation and reproductive strategies. In this way, certain dental characteristics and structures may be more common in some populations than others; equally, we may characterize groups according to the degree of observed variations (Hillson 2005, 257).

Morphological study of dentition involves the inspection of specific features of the crowns and roots of teeth. While it is beyond the scope and intention of the current work to summarize the history and vast achievements of dental anthropology as a sub-discipline (this has been achieved to great effect elsewhere; Scott & Turner 2008, 11), early investigations including those by Hrdlička (1920) and Hellman (1928) revealed that dental traits often vary in their frequency of occurrence and expression between populations. Furthermore, it was recognized that several of these discrete traits are characteristic of certain populations (for example, Carabelli's trait in Europeans; Kraus 1951), and thus not only aid in assessing biological relationships but also in estimating the amounts of genetic admixture between populations (Turner 1967). Many researchers have used suites of these dental features to describe a variety of human populations (Dahlberg 1971; Hanihara 1963; Kirveskari 1974; Moorrees 1957; Morris 1965; Pedersen 1949; Turner 1984, 1985a; Zubov 1979). Considering dental traits on a global scale, Turner (1984, 1985a) found that modern populations share enough dental similarities to support the interpretation of a recent common ancestral population, an interpretation that is supported by a wealth of other morphological and genetic evidence. Regionally, Lukacs and Walimbe (1984) demonstrated that the prehistoric people of India express variation in dental traits that are clinally distributed relative to European and Asian populations. On a local scale, similarities in non-metric traits have supported the hypothesis of common ancestry among some Southern African populations (Haeussler *et al.* 1989).

Dental non-metric traits with useful discriminatory power are found across tooth types. In the anterior dentition, incisor shovelling and winging have both demonstrated utility, while useful dental traits of the posterior dentition include maxillary and mandibular molar cusp number and size variation, mandibular molar groove pattern and deflecting wrinkle, and premolar and molar root number (Dahlberg 1963; Kirveskari 1974; Lukacs 1985; Moorrees 1957; Pedersen 1949; Turner 1984, 1985a; Turner *et al.* 1991).

The purpose of this study is to compare non-metric traits of selected subsets of the posterior dentition of the Circle assemblage to test for the frequency of traits that may represent close genetic affinities within the population and to test for broader population affinities throughout the Mediterranean region. While it is beyond the scope of the current work to present a full analysis of dental non-metric traits across the entire dentition, the present study represents the first attempt to apply these methods to the Circle population or indeed *any* Maltese skeletal assemblage. We focus here on the non-metric traits of the permanent maxillary and mandibular molars (posterior dentition) from selected contexts within the Circle and compare the resulting trait frequencies to a range of populations from the circum-Mediterranean region to investigate population affinities. This study should therefore be considered only as a baseline analysis, and we anticipate developing this branch of research to include a broader range of traits and archaeological contexts in the near future.

6.2. Materials

As discussed in Chapter 2, a total of 11,706 teeth were isolated from their associated skeletal remains and inventoried according to context by the *FRAGSUS* Population History Workgroup across five laboratory seasons at the National Museum of Archaeology (NMA), Valletta, between November 2014 and May 2017. Of these, a total of 815 teeth (7.0% of isolated sample) of adult maxillary and mandibular molar types were studied by the first author (RKP) for the purposes of quantifying the non-metric traits among the population/s represented within the Circle. The posterior dentition (molars) were analysed in order to align with the broader archaeometric sampling strategy of the Population History Workgroup which focused on analyses of the posterior teeth. As noted previously and detailed in Table 6.1, the studied teeth are only a subsample of the overall assemblage, representing a proportion of 14 selected contexts as excavated thus far across the entire use-life of the Circle, from Early to Late use-phases dating to *c.* 2900–2350 BC. Further to this, it is critical to note that the site was not completely excavated, and it is known that further remains are preserved at the site to allow for work to continue at the hands of future generations of archaeologists. As mentioned, in accordance with the temporal and pecuniary parameters of the project, the contexts examined here were determined by the excavators to be of greatest cultural and temporal significance to the

Table 6.1. *Materials included in pathology study, including provenance and representation.*

Context	Location	Date	N teeth isolated	Σ teeth studied	% Context
595	East Cave	Early	123	123	100
833	West Cave: north niche	Early	18	2	11
951	West Cave: north niche	Early	2306	751	33
698	East Cave: southern pit	Early	13	3	23
1209	West Cave: shrine	Middle	4	4	100
1241	East Cave	Middle	170	170	100
433	East Cave: central	Late	35	6	17
436	East Cave: central	Late	32	32	100
715	East Cave	Late	56	54	96
738	East Cave	Late	17	15	88
790	Intermediate zone	Late	11	11	100
1206	West Cave: shrine	Late	642	508	79
960	West Cave: shrine	Latest	870	405	47
783	West Cave: display	Latest	2900	976	34
		Total	7197	3060	43

overarching research questions, and thus included in whole or part here.

Comparative data were derived from thirteen dental assemblages from southern Europe, the Middle East, and northern Africa, all compiled and recorded by the senior author (JDI). These were used for qualitative and quantitative comparisons of non-metric traits with those recorded by the first author (RKP). These particular samples were selected based on their geographical and, in several instances, temporal proximity to the date of the Circle occupation to assess the presence (if any) and degree of genetic input to the Circle burial population. Summary data for these samples are provided in Table 6.2. Detailed descriptions are available in several prior publications (Dicke-Toupin 2012; Irish 1993, 1998a, 1998b, 2000, 2006; Irish *et al.* 2017).

6.3. Methods

6.3.1. Data collection

For the dental non-metric study, selected permanent maxillary and mandibular molars of both left and right sides and articulation states (exfoliated or in occlusion) were examined individually within their context batches. Each tooth was apportioned a unique inventory code, that comprised the sample number, find context and tooth type according to the notation convention established by the *Fédération Dentaire Internationale* (ISO 3950). Each tooth was examined and scored according to trait expressions established by the *Arizona State University Dental Anthropology System* (ASUDAS; Scott & Irish 2016 Turner *et al.* 1991), for permanent molars, including maxillary (Hypocone, Cusp 5 Metaconule, Carabelli's Trait, C2 Parastyle, Enamel Extensions, Enamel Pearls, Upper Molar Root Number, Peg-Shaped Molar, Congenital Absence) and mandibular (Anterior Fovea, Groove Pattern, Cusp Number, Distal Trigonid Crest, Protosylid, Cusp 5, Cusp 6, Cusp 7, Lower Molar Root Number and, where extant, Torsomolar Angle) traits. Radical Number and Deflecting Wrinkle traits were not recorded.

An additional trait, Buccal Fovea, was scored, though not used in the final analyses. This feature is described by van Beek (1983, 82) as the '*foramen caecum molarum*': a patent pit or hole located at the terminal aspect of the groove which runs between the lobes of the protoconid and hypoconid (or mesio- and distobuccal cusps) and was scored in this study as 0=present, 1=absent. Although this trait is not recognized by the ASUDAS, it was included within the study because of anecdotal observations of its frequency within the assemblage during the initial sorting process described in Chapter 2. We sought to quantify its incidence and prevalence rates within the selected sample to determine if it aligns with the estimated rates described by van Beek (approximately 60%; 1983, 82), or if any statistical correlations exist with the appearance of other traits.

In total, 39 traits were used for the present comparative study (refer to Table 6.3 for the full list). Tooth status and caries were also recorded for each tooth (following Turner *et al.* 1991, 26–7), along with notes describing any prevailing circumstances which may have impacted on the presence

Table 6.2. *The 13 comparative dental samples. *Institutions in which the samples are curated: MMLT = Museu Municipal Leonel Trindade - Torres Vedras; AMNH = American Museum of Natural History, New York; NHM = Natural History Museum, London; MH = Museé de l'Homme, Paris; UM = University of Minnesota, Minneapolis; NMNH = National Museum of Natural History, Washington, DC; CAM = Cambridge University, UK.*

	Sample	Geographical origin	Affiliation	Dates	n	Institution*
S. Europe/Middle East	Cova da Moura (CDM)	Estremadura, Portugal	Neolithic/Copper Age	3700–2300 BC	41	MMLT
	Greece (GRK)	Greece	Classic to Historic	475–300 BC to ~ AD 1800+	77	AMNH
	Italy (ITA)	Italy	Roman	30 BC – AD 395	35	NHM
	Italy (ITM)	Italy	Historic/Modern	AD 1800–1900s	55	NHM
	Pai Mogo I (PAI)	Estremadura, Portugal	Neolithic/Copper Age	3000–2600 BC	49	MMLT
	Palestine (PAL)	Lachish/Jericho, Palestine	Copper to Iron Age	1150–1047 BC	86	NHM
	Turkey (TRK)	Anatolia/Turkey and Cyprus	Classic to Ottoman	>300 BC to ~ AD 1300+	40	AMNH
North Africa	Bedouin (BED)	Morocco, Tunisia, Libya	Historic Arab	AD 1800–1900s	49	MH, UM
	Carthage (CAR)	Tunisia	Phoenician	751–146 BC	28	MH
	Kabyle (KAB)	Northern Algeria	Historic Berber	AD 1800–1900s	32	MH
	Lisht (LIS)	Lower Egypt	Middle Kingdom	1991–1783 BC	61	NMNH
	Shawia (SHA)	Southern Algeria	Historic Berber	AD 1800–1900s	26	MH
	Tarkhan (TAR)	Lower Egypt	Early Dynastic	~3000–2890 BC	51	CAM

or observable expression of each trait (for example, fractures, extreme wear, calculus, pathology including caries and enamel hypoplasia, eruption status, taphonomy/diagenesis, congenital variation). An inter-observer error study was carried out in 2016 at the NMA, based on traits scored by the first author and assessed by the senior author.

In addition to the above, all teeth (both left and right) examined for non-metric traits were also subject to metric analysis by Power. Following Hillson (2005, 261ff., Fig. 4.1), measurements were recorded in millimeters to 0.01 for the maximum mesiodistal (length between most mesial and distal points of the crown, often characterized by interproximal contact facets between the teeth; Hillson 2005, 260) and buccolingual (approximate right-angle to the mesiodistal line, length between the lip/cheek and tongue surfaces of the tooth; Hillson 2005, 260) diameters of both the crown and cementum enamel junctions using digital Mitutoyo calipers as standard Vernier for exfoliated teeth; needle-point for teeth still in occlusion. Data were recorded for all teeth in a Microsoft Excel spreadsheet to form a searchable digital database/inventory. The sample bags containing each tooth were marked once analysis was completed and curated within the NMA as part of the *FRAGSUS* Research Archive.

6.3.2. Quantitative analyses

All analyses were conducted by the senior author (JDI). First, the rank-scale ASUDAS traits were dichotomized into categories of present or absent, based on their appraised morphological thresholds (Nichol 1990; Scott 1973) following standard procedure (Irish 1993; Turner 1985b, 1987). Dichotomization simplifies tabulation of the trait frequencies for presentation and is necessary before these data can be compared using available distance statistics, including the mean measure of divergence (MMD) as used here (Berry & Berry 1967; Green & Suchey 1976; Harris & Sjøvold 2004; Irish 2010; Sjøvold 1973, 1977).

Next, the MMD was used to estimate among-sample phenetic affinities by calculating a dissimilarity measure between each sample pair; i.e., high values indicate divergence and *vice versa*. Beyond holding several advantages over other distance measures (Irish 2010) the MMD works well with pooled sample data, to address missing data common among archaeological remains and, importantly, the use of composite individuals for this study as necessitated by the commingled state of all human remains. However, it is important to edit these data prior to final quantitative analyses. Specifically, those traits that have little (i.e., invariant across samples) or no contributory information should be deleted (Harris & Sjøvold 2004). Those traits that are invariant can be recognized qualitatively, whereas traits that are the least, or conversely the most, likely to influence the inter-sample variation may be quantitatively identified; to do so, principal components analysis (PCA) was used in the present analysis (Irish 2016; Irish & Guatelli-Steinberg 2003). The MMD distances should also be based on as many traits as possible, though none should be highly inter-correlated – which could render inaccurate inter-sample results (Sjøvold 1977). To identify traits of this kind, the rank-scale data were submitted to Kendall's tau-*b* correlation coefficient.

Table 6.3. *Frequencies of the 39 dental traits by ASUDAS grade for the Circle sample and total present (%). *Grade frequencies in bold indicate those considered 'present' and, when totalled, equal the % Present in the final column for each trait. See text for details.*

			Grade*									%
Trait	**Presence**	**n**	**0**	**1**	**2**	**3**	**3.5**	**4**	**5**	**6**	**7**	**Present**
Hypocone UM1	Grade=3+	133	0.000	0.000	0.038	0.278	0.000	**0.662**	**0.023**			**96.3**
Hypocone UM2	Grade=3+	98	0.112	0.153	0.173	**0.255**	**0.051**	**0.245**	0.010			**56.1**
Hypocone UM3	Grade=3+	67	0.239	0.358	0.134	**0.179**	**0.060**	**0.030**	**0.000**			**26.9**
Cusp 5 Metaconule UM1	Grade=2+	129	0.868	0.100	0.023	0.008		0.000	0.000			**3.1**
Cusp 5 Metaconule UM2	Grade=2+	100	0.710	0.130	**0.060**	**0.050**		0.030	0.020			**16.0**
Cusp 5 Metaconule UM3	Grade=2+	68	0.456	0.103	**0.103**	**0.161**		0.103	0.073			**44.0**
Carabelli's Trait UM1	Grade=5+	126	0.460	0.127	0.071	0.103		0.071	**0.095**	**0.048**	**0.024**	**16.7**
Carabeli's Trait UM2	Grade=5+	98	0.888	0.051	0.010	0.010		0.010	**0.030**	**0.000**	**0.000**	**3.0**
Carabelli's Trait UM3	Grade=5+	68	0.882	0.029	0.000	0.029		0.000	**0.044**	**0.000**	**0.015**	**5.9**
C2 Parastyle UM1	Grade=2+	128	1.000	0.000	**0.000**	**0.000**		0.000	0.000			**0.0**
C2 Parastyle UM2	Grade=2+	102	1.000	0.000	**0.000**	**0.000**		0.000	0.000			**0.0**
C2 Parastyle UM3	Grade=2+	68	1.000	0.000	**0.000**	0.000		0.000	0.000			**0.0**
Enamel Extensions UM1	Grade=2+	121	0.992	0.008	**0.000**	**0.000**						**0.0**
Enamel Extensions UM2	Grade=2+	97	0.918	0.062	0.021	0.000						**2.1**
Enamel Extensions UM3	Grade=2+	66	0.924	0.061	**0.015**	**0.000**						**1.5**
Root Number UM1	Grade=3+	70	0.000	0.000	0.043	**0.957**						**95.7**
Root Number UM2	Grade=3+	62	0.000	0.097	0.113	**0.774**		0.016				**79.0**
Root Number UM3	Grade=3+	50	0.000	0.420	0.280	**0.300**						**30.0**
Congenital Absence UM3	Grade=1	69	1.000	**0.000**								**0.0**
Anterior Fovea LM1	Grade=2+	190	0.279	0.232	**0.242**	**0.174**		0.073				48.9
Groove Pattern LM2	Grade=Y	156	**0.417**	0.288	0.295							**41.7**
Groove Pattern LM3	Grade=Y	101	**0.485**	0.079	0.436							**48.5**
Cusp Number LM1	Grade=6	212	0.000	0.000	0.005	0.000		0.024	0.892	**0.080**		**8.0**
Cusp Number LM2	Grade=5+	160	0.000	0.000	0.000	0.000		0.719	**0.275**	**0.006**		**28.1**
Cusp Number LM3	Grade=5+	113	0.000	0.000	0.000	0.053		0.336	**0.504**	**0.097**	**0.009**	**61.0**
Distal Trigonid Crest LM1	Grade=1	205	0.995	**0.005**								**0.5**
Distal Trigonid Crest LM2	Grade=1	156	1.000	**0.000**								**0.0**
Distal Trigonid Crest LM3	Grade=1	112	0.991	**0.009**								**0.9**
Protostylid LM1	Grade=3+	210	0.971	0.014	0.010	**0.000**		**0.000**	**0.000**	**0.005**	**0.000**	**0.5**
Protostylid LM2	Grade=3+	160	0.963	0.025	0.006	**0.000**		0.006	0.000	0.000	**0.000**	**0.0**
Protostylid LM3	Grade=3+	112	0.714	0.125	0.071	**0.000**		**0.036**	**0.027**	**0.000**	**0.027**	**9.0**
Cusp 7 LM1	Grade=2+	210	0.962	0.005	0.019	**0.000**	**0.000**	**0.014**				**1.4**
Cusp 7 LM2	Grade=2+	163	0.994	0.000	0.000	**0.006**	**0.000**	**0.000**				**0.6**
Cusp 7 LM3	Grade=2+	113	0.965	0.000	0.000	**0.018**	**0.000**	**0.018**				**3.6**
Root Number LM1	Grade=3+	100		0.000	1.000	**0.000**						**0.0**
Root Number LM2	Grade=2+	84		0.083	**0.893**	**0.000**		0.024				**91.7**
Root number LM3	Grade=2+	62		0.355	**0.581**	**0.065**						**64.6**
Torsomolar Angle LM3	Grade=1	44	0.901	**0.091**								**9.0**
Congenital Absence LM3	Grade=1	118	1.000	**0.000**								**0.0**

The MMD formula used here contains the Freeman and Tukey angular transformation to correct for low (<0.05) or high (>0.95) trait frequencies and small sample sizes (n>10) (Green & Suchey 1976; Sjøvold 1973, 1977). To determine whether two samples differ significantly, the resultant MMD value is compared with its standard deviation (SD). If the MMD >2xSD, then the null hypothesis of P1=P2 (P=sample population) is rejected at the 0.025 level. The MMD and standard deviation formulae, rationale for significance, and other details can be found elsewhere (Irish 2010; Sjøvold 1977). To visualize the MMD distance values among samples (i.e., the matrix), interval-level multi-dimensional scaling (MDS) (Kruskal & Wish 1978) in SPSS 24.0 Procedure Alscal was used to create 3D spatial representations of the sample variation to aid interpretation.

Finally, the correlation between MMD and geographical distances in kilometres between Xagħra and each comparative sample was calculated using a simple bivariate Pearson's correlation; both distances were then used as coordinates to plot pertinent sample pair relationships in 2D. These methods help explore if the Circle sample appears more similar to an extra-regional group than expected, under the assumption that genetic (and phenetic) relatedness among populations decreases exponentially as spatial distance increases (Relethford 2004). Gene flow, the causative agent with isolation-by-distance (Wright 1943), cannot pertain directly to those samples which differ in age from those from the Circle; still, some indication of potential northern African, southern European, and/or Middle Eastern influence may be obtained to help supplement the MMD results. The Geographical Distance Matrix Generator (vers. 1.2.3) (Ersts 2014) was used to calculate the inter-sample straight line distances. The latter rarely reflect reality on land, but in this instance are most appropriate concerning across-water movement, i.e., the most direct routes from surrounding mainland regions to the island location of Malta.

6.4. Results

The frequencies for each ASUDAS grade for all 39 traits recorded in the Circle sample are provided in Table 6.3, along with the total number scored and cumulative percent considered present based on standard ASUDAS dichotomization protocol (Scott & Irish 2017; Turner *et al.* 1991). These trait percentages are then carried over to Table 6.4, to contrast with the same traits for the 13 comparative samples. The sheer amount of data makes qualitative comparisons difficult, but it can be seen that several trait percentages are comparable by region. In particular, the data from the Circle share a number of similarities with, for example, the ancient Italians (ITA), Carthage (CAR), the Kabyle Berbers (KAB), and others. Specific frequencies and phenetic distances are provided in the tables and figures below. Similarities among comparative samples are also evident in particular geographical regions.

Next, trait editing was conducted as noted. First, patently invariant traits were deleted (Table 6.4); these included Hypocone UM1 (all fixed at or near 100% across samples), Parastyle UM1 (0% across samples), and Protostylid LM1 (at or near 0%). Further, traits with minimal variation across all samples, here defined as <10% (with exception), were dropped, including Carabelli's Trait UM2 and UM3, Parastyle UM2, and Cusp 7 LM2, among others, to reduce the trait number from 39 to 29. As mentioned, highly inter-correlated traits should also be dropped prior to using the MMD, here considered to as Tau ≥|0.5| based on prior research (for example, Irish 2006, 2010). Because only molar traits were recorded,

Table 6.4. *Dental trait percentages (%) and number of individuals scored (n) for the Malta (the Circle) and comparative samples. See text for details. *Malta = the Circle; BED = Bedouin, CAR = Carthage, CDM = Cova da Moura, GRK = Greece, ITA = Italy ancient, ITM = Italy historic/modern, KAB = Kabyle, LIS = Lisht, PAI = Pai Mogo I, PAL = Palestine, SHA = Shawia, TAR = Tarkhan, TRK = Anatolia/Turkey and Cyprus (see Table 6.2 and text for details).*

Trait / presence		Malta*	BED	CAR	CDM	GRK	ITA	ITM	KAB	LIS	PAI	PAL	SHA	TAR	TRK
Hypocone UM1	%	96.30	100.00	100.00	100.00	100.00	100.00	95.74	100.00	100.00	100.00	100.00	100.00	100.00	100.00
(ASU Grade=3+)	n	133	39	19	34	57	26	47	22	40	49	67	23	45	28
Hypocone UM2	%	56.10	58.82	68.42	56.00	50.00	60.00	59.57	63.64	88.10	63.83	82.46	68.42	75.00	60.00
(ASU Grade=3+)	n	98	34	19	25	54	25	47	22	42	47	57	19	40	25
Hypocone UM3	%	26.90	30.00	25.00	13.64	44.44	41.67	44.83	29.17	35.48	44.19	37.14	30.77	57.14	46.15
(ASU Grade=3+)	n	67	20	12	22	36	12	29	24	31	43	35	13	35	13
Cusp 5 Metaconule UM1	%	3.10	8.82	8.33	8.70	5.66	5.00	23.26	11.76	15.38	17.02	21.43	10.00	0.00	4.55
(ASU Grade=2+)	n	129	34	12	23	53	20	43	17	26	47	42	20	23	22
Cusp 5 Metaconule UM2	%	16.00	3.03	10.00	8.33	4.08	8.70	13.33	16.67	5.56	9.09	10.87	10.53	9.09	9.52
(ASU Grade=2+)	n	100	33	10	24	49	23	45	18	36	44	46	19	33	21
Cusp 5 Metaconule UM3	%	44.00	25.00	30.00	19.05	22.86	20.00	28.57	10.53	23.33	23.08	25.00	30.77	33.33	0.00
(ASU Grade=2+)	n	68	20	10	21	35	10	28	19	30	39	32	13	33	12
Carabelli's Trait UM1	%	16.70	18.18	25.00	29.63	16.67	10.53	25.58	26.32	26.09	26.53	31.71	11.11	35.71	19.05
(ASU Grade=5+)	n	126	33	16	27	48	19	43	19	23	49	41	18	28	21
Carabelli's Trait UM2	%	3.00	0.00	0.00	0.00	0.00	0.00	2.17	0.00	2.78	0.00	1.79	0.00	2.63	0.00
(ASU Grade=5+)	n	98	33	17	20	48	25	46	23	36	45	56	19	38	22
Carabelli's Trait UM3	%	5.90	5.00	0.00	0.00	0.00	0.00	7.69	0.00	6.90	0.00	0.00	0.00	0.00	0.00
(ASU Grade=5+)	n	68	20	13	22	34	13	26	22	29	38	35	13	34	13

Table 6.4 *(cont.).*

Trait / presence		Malta*	BED	CAR	CDM	GRK	ITA	ITM	KAB	LIS	PAI	PAL	SHA	TAR	TRK
C2 Parastyle UM1	%	0.00	0.00	0.00	0.00	0.00	0.00	0.00	0.00	0.00	0.00	0.00	0.00	0.00	0.00
(ASU Grade=2+)	n	128	39	19	26	54	25	46	23	40	49	64	22	42	27
C2 Parastyle UM2	%	0.00	0.00	0.00	0.00	0.00	0.00	2.08	4.35	0.00	0.00	1.69	0.00	0.00	0.00
(ASU Grade=2+)	n	102	34	18	23	50	25	48	23	42	48	59	19	42	24
C2 Parastyle UM3	%	0.00	0.00	0.00	0.00	0.00	0.00	0.00	0.00	0.00	4.76	5.56	7.69	2.63	0.00
(ASU Grade=2+)	n	68	20	14	22	33	13	28	22	32	42	36	13	38	13
Enamel Extensions UM1	%	0.00	5.56	5.56	3.70	3.70	0.00	2.33	0.00	10.64	2.27	1.56	4.76	0.00	4.17
(ASU Grade=2+)	n	121	36	18	27	54	26	43	23	47	44	64	21	45	24
Enamel Extensions UM2	%	2.10	12.90	5.56	18.75	16.67	3.85	6.38	8.70	18.60	19.44	4.92	11.11	9.76	22.73
(ASU Grade=2+)	n	97	31	18	16	48	26	47	23	43	36	61	18	41	22
Enamel Extensions UM3	%	1.50	6.25	0.00	0.00	0.00	0.00	0.00	5.26	12.90	4.17	0.00	10.00	3.33	10.00
(ASU Grade=2+)	n	66	16	11	14	32	12	22	19	31	24	35	10	30	10
Upper Molar Root Number UM1	%	95.70	97.37	100.00	95.45	97.50	94.12	90.91	100.00	97.73	100.00	95.00	100.00	100.00	100.00
(ASU Grade=3+)	n	70	38	16	22	40	17	22	19	44	24	20	22	24	25
Upper Molar Root Number UM2	%	79.00	68.97	77.78	57.14	58.33	70.59	81.82	68.42	77.27	89.80	80.00	72.22	72.22	62.07
(ASU Grade=3+)	n	62	29	18	21	36	17	22	19	44	49	20	18	18	29
Upper Molar Root Number UM3	%	30.00	26.32	40.00	58.82	30.00	38.46	40.00	57.14	34.38	41.94	22.73	61.54	66.67	11.11
(ASU Grade=3+)	n	50	19	15	17	30	13	15	14	32	31	22	13	21	18
Congenital Absence UM3	%	0.00	21.05	30.43	6.90	17.65	29.03	20.00	3.45	3.64	8.33	18.75	23.08	4.08	21.88
(ASU Grade=1)	n	69	38	23	29	68	31	50	29	55	48	64	26	49	32
Anterior Fovea LM1	%	48.90	37.50	20.00	58.82	36.36	20.00	56.67	60.00	37.50	80.56	40.00	29.41	0.00	40.00
(ASU Grade=2+)	n	190	24	10	17	11	5	30	10	8	36	20	17	2	10
Groove Pattern LM2	%	41.70	46.88	38.46	32.50	43.48	22.22	27.91	27.78	37.50	52.08	34.29	36.84	30.56	5.88
(ASU Grade=Y)	n	156	32	13	40	23	18	43	18	24	48	70	19	36	17
Groove Pattern LM3	%	48.50	40.91	22.22	36.11	22.73	8.33	25.00	30.77	35.29	23.81	18.18	29.41	22.22	36.36
(ASU Grade=Y)	n	101	22	9	36	22	12	32	13	17	21	44	17	27	11
Cusp Number LM1	%	8.00	12.50	0.00	2.50	0.00	0.00	2.63	31.25	5.56	9.09	3.70	9.52	5.00	0.00
(ASU Grade=6)	n	212	32	11	40	19	13	38	16	18	44	54	21	20	19
Cusp Number LM2	%	28.10	42.86	16.67	23.68	47.62	30.00	37.14	33.33	20.83	40.43	37.04	31.58	50.00	41.18
(ASU Grade=5+)	n	160	28	12	38	21	10	35	18	24	47	54	19	28	17
Cusp Number LM3	%	61.00	62.50	44.44	70.27	60.00	60.00	63.33	50.00	44.44	66.67	51.22	58.82	76.00	80.00
(ASU Grade=5+)	n	113	24	9	37	20	10	30	14	18	21	41	17	25	10
Distal Trigonid Crest LM1	%	0.50	3.03	0.00	0.00	5.88	9.09	5.56	0.00	11.11	0.00	3.13	0.00	0.00	0.00
(ASU Grade=1)	n	205	33	9	26	17	11	36	14	9	41	32	20	16	13
Distal Trigonid Crest LM2	%	0.00	3.13	0.00	0.00	0.00	0.00	0.00	0.00	0.00	2.08	0.00	0.00	5.56	0.00
(ASU Grade=1)	n	156	32	12	40	21	16	42	18	20	48	67	20	36	17
Distal Trigonid Crest LM3	%	0.90	4.17	0.00	10.81	10.53	0.00	0.00	0.00	0.00	0.00	11.63	0.00	6.90	0.00
(ASU Grade=1)	n	112	24	9	37	19	10	33	14	17	23	43	17	29	11
Protostylid LM1	%	0.50	0.00	0.00	0.00	0.00	0.00	0.00	0.00	0.00	0.00	0.00	0.00	0.00	0.00
(ASU Grade=3+)	n	210	33	10	30	19	13	38	16	15	42	58	21	20	17
Protostylid LM2	%	0.00	0.00	0.00	2.56	9.52	0.00	0.00	0.00	0.00	2.13	2.94	0.00	0.00	0.00
(ASU Grade=3+)	n	160	29	12	39	21	17	43	18	21	47	68	22	34	16
Protostylid LM3	%	9.00	12.00	10.00	20.59	0.00	0.00	6.25	0.00	5.56	22.73	12.24	6.25	3.45	10.00
(ASU Grade=3+)	n	112	25	10	34	21	12	32	14	18	22	49	16	29	10
Cusp 7 LM1	%	1.40	5.88	7.69	0.00	5.56	11.11	2.63	5.88	0.00	6.25	0.00	4.76	3.70	0.00
(ASU Grade=2+)	n	210	34	13	39	18	18	38	17	23	48	67	21	27	19
Cusp 7 LM2	%	0.60	0.00	0.00	2.50	9.52	0.00	0.00	0.00	0.00	0.00	0.00	0.00	0.00	0.00
(ASU Grade=2+)	n	163	32	13	40	21	18	43	18	25	49	71	20	38	17
Cusp 7 LM3	%	3.60	0.00	10.00	5.13	0.00	0.00	3.03	7.14	0.00	0.00	6.12	5.88	3.57	9.09
(ASU Grade=2+)	n	113	24	10	39	21	12	33	14	20	23	49	17	28	11
Root Number LM1	%	0.00	0.00	0.00	0.00	0.00	0.00	0.00	0.00	0.00	0.00	3.03	0.00	0.00	5.26
(ASU Grade=3+)	n	100	33	11	36	22	18	25	17	29	30	33	22	33	19
Root Number LM2	%	91.70	88.89	80.00	82.50	91.30	100.00	100.00	88.89	86.21	100.00	79.55	95.45	85.00	89.47
(ASU Grade=2+)	n	84	27	10	40	23	19	38	18	29	43	44	22	40	19
Root number LM3	%	64.60	88.00	100.00	84.38	91.67	66.67	100.00	100.00	85.71	76.47	73.68	85.71	90.91	70.00
(ASU Grade=2+)	n	62	25	2	32	12	15	18	11	21	17	19	14	22	10
Torsomolar Angle LM3	%	9.01	20.00	10.00	8.82	13.04	12.50	18.52	21.43	30.77	5.56	14.29	23.53	5.56	31.25
(ASU Grade=1)	n	44	25	10	34	23	16	27	14	26	36	56	17	36	16
Congenital Absence LM3	%	0.00	12.12	23.08	7.32	10.71	9.09	23.91	27.78	11.11	24.44	14.67	16.67	8.33	25.00
(ASU Grade=0)	n	118	33	13	41	28	22	46	18	36	45	75	24	48	20

Table 6.5. *Component loadings, eigenvalues, and variance explained for 22 traits in the Malta and 13 comparative samples. Values in boldface indicate strong loadings (≥|0.5|). *Denotes the 12 traits used in the MMD comparison, as detailed in text.*

Trait	Comp 1	Comp 2	Comp 3
Hypocone UM2	.491	.368	.010
Cusp 5 UM1*	.226	**.542**	**.716**
Cusp 5 UM2	-.437	.400	.122
Carabelli's Trait UM1*	.118	**.707**	-.311
C2 Parastyle UM3	.041	.447	.007
Enamel Extensions UM1*	**.850**	-.124	.107
Enamel Extensions UM2*	**.696**	-.018	-.212
Enamel Extensions UM3*	**.804**	-.097	-.060
Root Number UM1*	.352	.088	**-.615**
Root Number UM2*	-.113	**.585**	**.513**
Root Number UM3	-.264	.313	-.445
Congenital Absence UM3	-.055	-.486	.329
Anterior Fovea LM1*	.056	**.509**	.427
Groove Pattern LM2	-.099	.381	.039
Cusp Number LM2	-.137	-.095	-.192
Distal Trigonid Crest LM1*	.208	-.453	**.531**
Protostylid LM3*	.160	**.609**	.030
Cusp 7 LM1	-.489	-.358	.089
Root Number LM2*	-.293	-.210	**.546**
Root number LM3	.095	.149	-.159
Torsomolar Angle LM3*	**.752**	-.345	.260
Congenital Absence LM3	.242	.240	.264
Eigenvalue	3.620	3.358	2.604
% of Variance	16.454	15.264	11.836
Cumulative %	16.454	31.719	43.555

inter-correlation was particularly problematic, relative to the field concept (Scott & Irish 2017; Turner *et al.* 1991). In this case, the 10 traits deleted because of minimal variation were also all highly correlated with many other molar traits (i.e., ranging from two to 13 total trait pairs). However, seven additional traits that are not invariant also had to be deleted on this basis (i.e., Tau ≥|0.5|), including Hypocone UM3, Cusp Number LM1 and LM3, Cusp 7 LM3, and others, which further reduced the trait number to 22. Lastly, percentages of these traits were submitted to PCA in order to identify those which contribute little to among-sample variation (Table 6.5). The first three components were used for this purpose, as they contribute much, though certainly not all, of the total variance. Based on those loadings considered to be strong (i.e., ≥|0.5|) in the table, 12 of the remaining 22 traits were retained for the MMD analysis: Cusp 5 UM1, Carabelli's UM1, Enamel Extensions UM1–UM3, Root Number UM1–UM2, Anterior Fovea LM1, Distal Trigonid Crest LM1, Protostylid LM3, Root Number LM2, and Torsomolar Angle LM3. Again, detailed descriptions of these highly hereditary traits can be found elsewhere (Scott & Irish 2017; Turner *et al.* 1991).

The resulting MMD distances (and geographical distances, see below) between the Circle and the comparative samples are listed in Table 6.6. The full MMD distance matrix is not provided because: 1) relatedness among the comparative samples is not critical, given the focus of this chapter, and 2) these distances are available elsewhere—based on a full suite of 36 non-metric traits throughout the dentition (Dicke-Toupin 2012; Irish 1993, 1998a, 1998b, 2000, 2006; Irish *et al.* 2017). Based just on these 12 molar traits, it is evident that, with some exceptions (i.e., Egyptian Lisht (LIS), Portuguese Pai Mogo (PAI), and to a lesser extent, Greece (GRK)), the Circle sample does not differ significantly from most comparative samples. It is particularly close phenetically to the comparative samples from Carthage (CAR), Kabyle (KAB), ancient Italy (ITA), and Palestine (PAL), which may suggest evidence for more genetic input from these regions. This relatedness is visualized in the MDS plot of the full MMD matrix (Fig. 6.1). For example, except for Portuguese Pai Mogo (PAI) (Irish *et al.* 2017 for rationale), much sample homogeneity is evident, including the Circle. Moreover, this homogeneity may show some regional bias but overall it appears that, Mediterranean-wide, genetic contact among all populations was common.

Table 6.6. *Pairwise distances between Malta (the Circle) and the 13 comparative samples based on MMD for 12 dental traits and kilometers (KM). [1]Underlined MMD distances indicate significant difference at the 0.025 alpha level. [2]BED = Bedouin, CAR = Carthage, CDM = Cova da Moura, GRK = Greece, ITA = Italy ancient, ITM = Italy historic/modern, KAB = Kabyle, LIS = Lisht, PAI = Pai Mogo I, PAL = Palestine, SHA = Shawia, TAR = Tarkhan, TRK = Anatolia/Turkey and Cyprus.*

	MMD[1]	KM
BED[2]	0.03239	1571.02
CAR	0.00000	364.60
CDM	0.03906	2103.64
GRK	0.05010	730.90
ITA	0.00155	624.69
ITM	0.01268	624.69
KAB	0.00000	790.00
LIS	0.09864	1739.79
PAI	0.08825	2104.81
PAL	0.00119	1963.46
SHA	0.01595	644.41
TAR	0.04242	1743.07
TRK	0.05117	1704.51

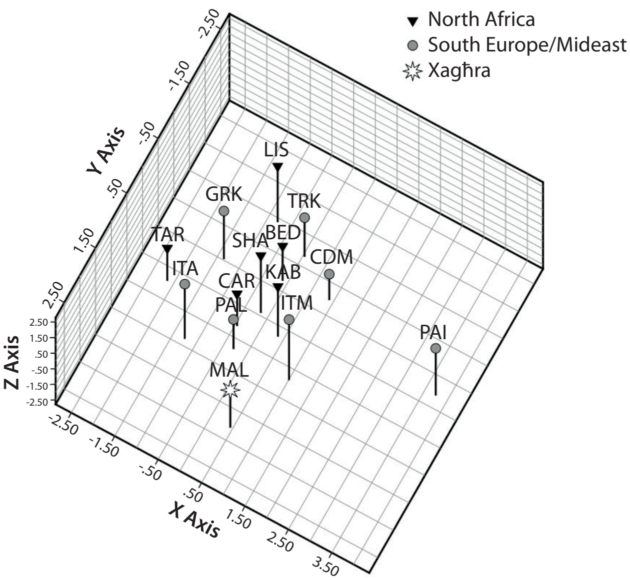

Figure 6.1. *Three-dimensional MDS of 12-trait MMD distances between the Circle and the 13 comparative samples. The three-letter sample abbreviations are defined in Tables 6.2, 6.4 and 6.6 (see text for details).*

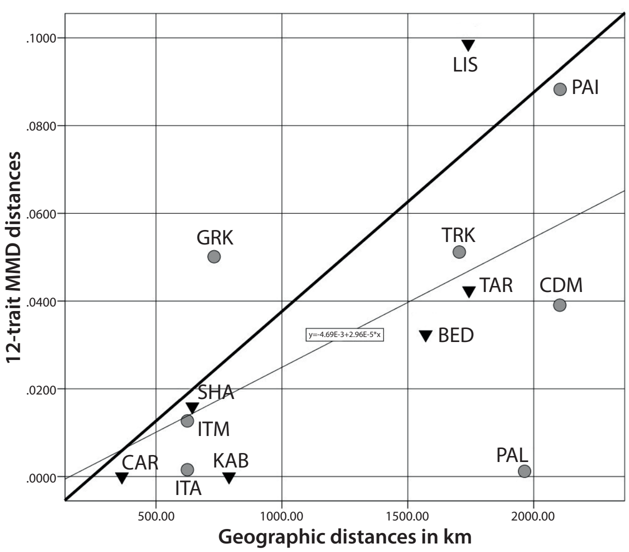

Figure 6.2. *Two-dimensional scatterplot of the Circle sample relative to the 13 comparative samples based on geographical (x-axis) vs. phenetic (y-axis) distances. The thick black linear equation reference line with slope (b) of 1 and y-intercept (a) of 0 provided (i.e., y=0+1x, where y=a+bx) is provided to illustrate where the other samples would be if a 1:1 correspondence existed between the distances. The actual regression coefficient is also provided as the line of best fit (thin black line) through the data cloud (with equation provided; r2 = 0.348). See text for details.*

Lastly, the data from the Circle were plotted against the rest of the samples using pairwise geographical and MMD distances as co-ordinates on the x- and y-axes in Figure 6.2. A linear equation reference line (thick black) with a slope (b) of 1 and y-intercept (a) of 0 is provided (i.e., y=0+1x, where y=a+bx) to simply illustrate where the other samples would be located if a 1:1 correspondence existed between spatial and phenetic distances. The actual sample locations identify those which are phenetically closer to the Circle than expected (i.e., below the reference line), and vice versa (above the line), relative to the geographical separation.

For comparison purposes, the true regression coefficient is also provided as the line of best fit (thin black) through the data cloud of comparative samples. Assuming that phenetic affinity is a function of spatial separation, a coefficient of determination was calculated via the linear regression procedure in SPSS 24.0 ($r^2 = 0.348$, $r = 0.590$, $p = 0.034$). Thus, 35% of the variability in MMD distances is associated with or explained by variability in the geographical distances.

6.5. Discussion and conclusions

This chapter has reported on the analysis of 39 non-metric traits of the posterior dentition (maxillary and mandibular molars) derived from selected archaeological contexts of the Circle. While the results provide interesting evidence for broad genetic affinities throughout the Mediterranean region, it is important to identify a number of limitations of the current analysis. Firstly, with over 11,000 isolated teeth in the Circle assemblage that provide a potential wealth of data on the population affinities and lifestyle of the Neolithic peoples of Malta, this analysis represents only the first step in consideration of the broader population affinities reflected in the dental morphology. We focused on the posterior dentition because of the wealth of observable non-metric traits with discriminatory power.

That said, the analyses presented here can be refined by the inclusion of data representing non-metric trait frequencies of the incisors, canines, and premolars. By focusing on the molars, and because of the absence of some traits (such as the Deflecting Wrinkle and Radical Number) among all populations, the discriminatory power of analyses was limited. Furthermore, the commingled nature of the site means that we were unable to analyse the complete dentition of intact individuals; although these data are available, articulated and undisturbed individuals represent only a small percentage of the total depositional population in the Circle (estimated at 2% in Malone & Stoddart 2009, 365–6). Recent research, however, has demonstrated that even among such assemblages, dental non-metric traits provide useful data on regional population affinities (Irish *et al.* 2017). Additional complexities arise because our sampling strategy did not, by necessity, provide comprehensive coverage of the site, which is compounded by the likelihood of some tooth movement through stratigraphy related to diachronic cultural and natural commingling processes following *postmortem* exfoliation (Chapter 3 & Chapter 12).

With these caveats in mind, the results provide preliminary evidence of the population affinities of the Neolithic people interred in the Circle. In general, the populations of the northern, eastern and southern Mediterranean share a range of dental characteristics that suggest broad patterns of prehistoric gene flow throughout the region. The non-metric traits of the posterior dentition of the Maltese, however, show somewhat stronger affinities to the Ancient Italian, Carthaginian, and more distantly Kabyle Berber and Palestinian populations. While we cannot interpret this as direct evidence for ancestor-descendent relationships, the results suggest that Neolithic Malta was connected by population movements throughout the Mediterranean, albeit somewhat isolated as a genetic pool. One might predict, because of its relative distance, either a strong signature of genetic isolation, or particular affinities with only individual regions, such as Italy, within the Mediterranean. The observation of affinities with populations of the north, south and more distant eastern Mediterranean regions suggest that the Neolithic Maltese population remained well-connected throughout the region. The results also suggest that future and more expansive genetic analyses should investigate links to populations in Northern Africa (see discussions on prospective cultural links to this region via dental modification analyses in Chapter 5).

These relationships can also be clarified by further dental non-metric trait analyses, as they have been demonstrated to be an excellent proxy for neutral genetic distances (Irish *et al.* 2020). Some of the patterns of variation observed in the present analyses are undoubtedly shaped by the limitations of data analysis from the posterior dentition only. Inclusion of traits from incisors, canines and pre-molars will improve the resolution of such analyses and clarify phenetic distances to the other Mediterranean populations. These results must be interpreted as a first step in this process, which nevertheless highlight both the interconnectedness of the Neolithic Maltese population within the Mediterranean cultural sphere, and the utility of dental non-metric approaches in the further exploration and understanding of these patterns of human movement and interaction in prehistory.

Chapter 7

Physical activity and body size in Temple Period Malta: biomechanical analysis of commingled and fragmentary long bones

Eóin W. Parkinson & Jay T. Stock

7.1. Introduction

The reconstruction of physical activity from the human skeleton provides archaeologists with important insights into past lifestyles and lived experiences. Whilst a range of approaches have been developed to reconstruct activity in archaeological skeletons (Jurmain *et al.* 2012; Larsen 2015; Meyer *et al.* 2011), the application of skeletal biomechanics offers an objective means of quantifying and exploring habitual behaviour in past populations that has benefits over other approaches which rely on activity-related pathology or analysis of muscle attachment sites (Waldron & Rogers 1991; Wallace *et al.* 2017; Wilczak *et al.* 2017). Skeletal biomechanics applies mechanical principles to bone tissue in order to understand its form and function, and has been most widely employed to understand structural adaptation of long bones diaphyses. This particular method models the long bones as structural beams in order to quantify their cross-sectional geometric (henceforth CSG) properties related to bone strength and bending rigidity (Huiskes 1982; Ruff & Hayes 1983a,1983b), thus making it possible for bioarchaeologists to estimate the degree of mechanical strain associated with habitual activity during life.

Although skeletal morphology is influenced by a wide range of genetic, environmental, hormonal and age related factors (Kini & Nandeesh 2012), experimental studies have demonstrated that bone tissue adapts and remodels in response to *in vivo* mechanical loading (Biewener *et al.* 1983; Lanyon 1984; Lanyon & Baggott 1976; Lanyon *et al.* 1982; Simkin *et al.* 1989), and in a manner consistent with particular patterns of known and inferred habitual behaviour (Macintosh & Stock 2019; Shaw & Stock 2009a, 2009b; Stock & Pfeiffer 2001; Ruff 2019). This process, referred to as 'bone functional adaptation' (Ruff *et al.* 2006a), enables bioarchaeologists to reconstruct broad patterns of behaviour from the human skeleton and has been successfully applied to a variety of archaeological contexts to examine changes in subsistence strategy (Marchi *et al.* 2011), social change (Sparacello *et al.* 2011), patterns of mobility behaviour (Sládek *et al.* 2006b, 2006a), economy and trade (Pomeroy 2013) or genetic and cultural discontinuity (Stock & Macintosh 2016). The analysis of the Xagħra assemblage, presented in this chapter, forms a discrete part of a much larger study that explored spatial and temporal trends in body size and post-cranial robusticity across the longue durée of central Mediterranean prehistory (Parkinson 2019).

A useful by-product of CSG analysis is the acquisition of osteometric data related to body mass and long bone lengths which can be converted into estimates of stature, thus enabling an exploration of body size. The relationship between body size, skeletal growth, physiological stress and life history has been used by bioarchaeologists and economic historians to understand social and economic circumstances in modern (Stock & Migliano 2009; Tyrrell *et al.* 2016) and archaeological populations (Formicola & Holt 2007; Macintosh *et al.* 2016; Niskanen *et al.* 2018). Population history has also been shown to have an important role in understanding body size in archaeological populations, in acknowledgement of the genetic control over final adult height (Cox *et al.* 2019; Martiniano *et al.*, 2017). Estimates of stature heritability have been reported to be as high as 80-90% (Silventoinen *et al.*, 2003), however, final adult stature has also been shown to be influenced by non-genetic factors, such as developmental stress and growth impairment, as well as adaptive life history traits (for reviews see Wells & Stock 2011, 2020). The analysis of estimated stature and body mass at Xagħra therefore provides a means of investigating these themes, which are complementary to palaeopathological analysis presented elsewhere (Chapter 4, Chapter 8).

Another important element of this study was overcoming the considerable methodological challenges that were encountered during the analysis of the highly commingled and fragmented Xagħra assemblage. The acquisition of reliable and accurate osteometric data is one of the fundamental challenges of working with fragmentary and commingled human bone, and therefore this chapter also introduces the various approaches used in the analysis. The application of 3D surface scanning technology particularly aided in the reconstruction and estimation of bone dimensions that were necessary for the acquisition of CSG properties.

Few studies have attempted to analyse long bone CSG properties from commingled and fragmentary skeletal material because of the difficulties of acquiring the necessary osteometric data. Stock & Willmore (2003) investigated broad patterns of habitual activity through the application of skeletal biomechanics in a large fragmented and commingled Iroquoian burial assemblage, successfully illustrating the validity of such studies. Palaeoanthropological studies have also demonstrated the wealth of information that can be extracted from small samples of fragmented fossil hominin remains (Ruff 2008b; Trinkaus & Ruff 1999; Xing *et al.* 2018), providing a strong methodological framework on which to build. In particular, recent analysis of a large commingled and fragmented assemblage of *Homo naledi* remains (see Marchi *et al.* 2017) has also addressed many of the issues faced in this research.

7.2. Materials

7.2.1. Sampling strategy

The main period of use at the Circle was during the Tarxien phase (*c.* 2800–2400 cal. BC; Chapter 3), when the site was the setting of an elaborate set of funerary rites, whereby human remains underwent complex and varied processes of disarticulation and dispersal (Malone & Stoddart 2009; Chapter 12 in this volume). The natural cave system was elaborated with megalithic architecture and periodically restructured throughout the Tarxien period, where burial deposits functioned as structural deposits (§3.4.2). The combination of these site formation processes with the funeral rituals performed on site resulted in the formation a large commingled and highly fragmentary skeletal assemblage.

The large size and complexity of the Xagħra assemblage therefore required a targeted sampling strategy aimed at contexts containing high frequencies of long bones as reported in the original study by Malone *et al.* (2009d). Sampling was initially targeted at both the earlier rock-cut tomb (*c.* 3500–3200 cal. BC) and the main Tarxien phase burial complex (*c.* 2975–2250 cal. BC), although material from the rock-cut tomb was eventually excluded from the final analysis owing its small sample size and extreme level of fragmentation. Furthermore, extensive concretion obscured much of the cortical surface of the long bones from the rock-cut tomb, limiting the potential to retrieve accurate CSG properties. Sampling of the Tarxien phase deposits was directed towards three articulated individuals from contexts (799), (960) and (1241), in addition to three large commingled mortuary deposits, Contexts (783), (1206) and (1268). Contexts (1206) and (1268) from the 'Shrine' area were specifically targeted for their high frequencies of humeri, femora and tibiae, and because they presented the clearest record of a stratified sequence within the site that spanned the Tarxien phase (Stoddart *et al.* 2009c). The nature of the Xagħra assemblage was such that complete skeletons could not be reconstructed, eliminating the potential to explore sex-based or whole-body trends in skeletal robusticity, and restricting the analysis to an exploration of broad patterns in body size and physical activity.

7.2.2. Comparative sample

Comparative data for Copper Age central Italy from Parkinson (2019) were included in the analysis in order to place the Maltese data within a broader central Mediterranean regional context. The comparative sample consists of 32 individuals from Ponte San Pietro (Latium) and Fontenoce-Recanati (Marche) dated to the Italian early Copper Age (3600–3300 cal. BC) (Dolfini 2010; Silvestrini *et al.* 2004). Both sites are associated with the Rinaldone burial tradition (Cazzella & Moscoloni 2012; Dolfini 2006b, 2006a), and are traditionally considered as agro-pastoralists that navigated the mountainous and hilly terrain of the central Italian Apennines (Cocchi Genick 2009; Manfredini *et al.* 2009; Skeates 1997). The comparative central Italian sample consists almost entirely of fully articulated skeletons, thus enabling a more detailed exploration of patterns across the skeleton. One major benefit of this comparison is the ability of the more detailed results from central Italy to help tease out underlying trends in the Xagħra sample.

7.3. Methods

7.3.1. Long bone cross-sectional geometry

Long bone solid CSG properties were captured at the mid-shaft (50% of bone length) of the femur and tibia, and at the mid-distal (35% of bone length) point of the humeral diaphysis thereby avoiding the morphology of the deltoid muscle attachment (Ruff 2019). Given the relationship between endosteal (internal) and periosteal (external) contours, capturing both internal and external cross-sectional properties is preferred (Larsen 2015; Ruff & Hayes 1983a). However, solid CSG properties based on external contours alone have

Table 7.1. *Cross-sectional geometric properties used in the study.*

Property	Definition	Biomechanical relevance
TA	Total cross-sectional area	Correlate of compressive strength
J	Polar Second Moments of Area (SMA)	Sum of $I_{max}+I_{min}$, correlate of torsional strength and average bending rigidity
I_x/I_y	Cross-sectional shape ratio	Distribution of bone about the anterior-posterior and medio-lateral axes, indicator of cross-sectional shape and direction of mechanical loading
I_{max}/I_{min}	Cross-sectional shape ratio	Distribution of bone about maximum and minimum axes, indicator of cross-sectional shape

been shown to correlate strongly with true cross-sections and likely reflect the most mechanically relevant bone tissue (Davies *et al.* 2012; Macintosh *et al.* 2013; Stock & Shaw 2007). The solid cross-sectional properties used in this study are total cross-sectional area (*TA*), a correlate of compressional strength, the Polar Second Moments Area (*J*), a correlate of bending and torsional rigidity, and the cross-sectional shape ratios I_{max}/I_{min} and I_x/I_y, which give an indication of cross-sectional shape and the direction of mechanical loading (Table 7.1). Solid CSG properties were derived from 3D laser surface scans of individual bones captured with a NextEngine object scanner using AsciiiSection v.3.2 (Davies *et al.* 2012). All 3D scans were processed in Rapidform XOR and aligned to standard anatomical axes defined by Ruff (2002). As body size itself constitutes a mechanical force, CSG properties must be body size standardized using a combination of bone length and body mass (Ruff 2000, 2019). Body mass estimations were derived from femoral head diameter using regression equations developed for European Holocene populations (Ruff *et al.* 2012), whereas knee breadth was used to estimate body mass from isolated tibiae (Squyres & Ruff 2015). The bones of the upper limb have also been shown to scale with body mass, and therefore humeral CSG properties must also be standardized for the influence of body size (Pomeroy *et al.* 2018; Ruff 2002; Ruff *et al.* 1993). Upper limb CSG properties are typically standardized using body mass estimates derived from associated femora, however, the commingling of the Maltese sample makes this impossible. Instead, CSG properties for isolated humeri were standardized using powers of bone length, as recommended by Ruff (2019). The recommended power of bone length for standardizing *TA* is maximum length$^{\wedge 3}$, whilst the recommended powers for Second Moments of Area (*I* and *J*) are maximum length$^{\wedge 5.33}$ (Ruff *et al.* 1993).

7.3.2. Approaches to fragmented material

A series of adapted and original approaches were used to overcome the methodological challenges that were posed by the fragmented and commingled Xagħra assemblage. The use of 3D scanning to acquire long bone CSG properties in this study was particularly useful in enabling the application of digital reconstruction techniques to overcome some of the methodological challenges of working with fragmented skeletal material. Specific to this study was the need for estimates of complete bone length and femoral head diameter from fragmentary long bones. Maximum bone length is not only required to establish accurate, standardized cross-section locations along the diaphysis, such as the femoral and tibial mid-shaft (50% of bone length) and mid-distal humerus (35% of bone length from the distal end) (Ruff & Hayes 1983a), but it is also a vital component in size standardization of CSG properties (Ruff *et al.* 1993).

Ruff (2008a, 2019; §7.3.1) recommends the use of estimated bone lengths when working with fragmented and isolated skeletal elements, and estimated bone lengths are widely used in the analysis of fragmentary fossil hominin material (Day & Molleson 1976; Haeusler & McHenry 2004; Korey 1990; Ruff 2008b; Trinkaus & Ruff 1989, 1996; Trinkaus *et al.* 1998). Slight misplacement of cross-section location within 5% of bone length has been shown to have little effect on CSG properties of the femur and humerus (Ruff 2008b; Sládek *et al.* 2010), enabling biomechanical analysis of these elements with confidence. However, CSG properties of the tibia have been shown to be most sensitive to cross-section misplacement because of the irregular and angular morphology of the tibial medial and lateral surfaces (Sládek *et al.* 2010). For this reason, extra care was taken to screen CSG data from tibiae, and only elements that were more than approximately 75% complete were selected for analysis.

7.3.2.1. Estimation of maximum bone length: 3D reconstruction and superimposition

Estimation of maximum bone length was achieved primarily through 3D digital reconstruction and 3D superimposition. Forensic anthropologists have developed a range of methods to estimate complete maximum bone length from fragmented long bones for the purposes of stature estimation (Jacobs 1992; Simmons *et al.* 1990; Steele 1970; Steele & McKern 1969; Wright & Vasquez 2003), but available methods are problematic in that they are often exclusively developed for the lower limb and often calculate stature directly rather than provide an estimate of bone length. Considerable doubt has also been placed over the accuracy and repeatability of current methods for estimating complete length from fragmented long bones, which are population specific and often rely on highly variable anatomical landmarks (Bidmos 2009).

A major benefit of the 3D scanning approach, however, is the opportunity to manipulate skeletal elements digitally in virtual space, enabling the use of techniques in 3D digital reconstruction and 3D superimposition (Fig. 7.1). Both 3D digital reconstruction and 3D superimposition provide accurate estimates of complete long bone length, which have advantages over traditional visual approaches (Sylvester *et al.* 2008). Long bone reconstruction was performed in Rapidform XOR using the Interactive Alignment function, where individual fragments were aligned and positioned according to anatomical landmarks, estimated anatomical axes and fracture congruence (Benazzi *et al.* 2014; Grine *et al.* 2010; Gunz *et al.* 2009; Senck *et al.* 2015). Once reconstructed, the individual 3D scanned meshes of each fragment were fused to form a single mesh using Rapidform's Combine tool (Fig. 7.1). As with any analysis involving fragmentary skeletal material, digital reconstruction relies on careful documentation during the initial data collection stage and reference to, whenever possible, excavation notes. 3D digital reconstruction also offsets the need to undertake restoration and reconstruction of the physical skeletal element, which often requires the use of adhesives that can lead to serious long-term conservation issues (Caffell *et al.* 2001; Johnson 1994).

Figure 7.1. *Examples of digitally reconstructed humeri: a) 3D superimposed humerus; b) 3D digitally reconstructed humerus (E. Parkinson).*

3D digital superimposition was undertaken to estimate complete bone length for incomplete fragmented long bones, such as those without epiphyses. Similar to visual pair matching, which is used widely in forensic (Adams & Byrd 2006; Adams & Konigsberg 2004) and palaeoanthropological (Marchi *et al.* 2017; Trinkaus *et al.* 1998) research, this approach compares the diaphyseal contours and anatomical landmarks of a fragmented skeletal element with a complete element from a reference collection. The combination of the incomplete and complete elements can then be used to make a reliable estimation of complete bone length (Fig. 7.1). Traditional visual comparison methods are more subjective, in that they rely on comparison between two bones positioned next to one-another, whilst 3D digital superimposition allows for clearer and more accurate comparisons to be made *in silico*, thus limiting subjectivity. In a test of this approach, Karell *et al.* (2016) showed that manual 3D superimposition outperformed automated matches and traditional visual comparison methods in 100% of comparisons. The application of 3D digital superimposition has also been effectively employed in analysis of very fragmented fossil hominin material (Xing *et al.* 2018). 3D superimposition was performed in Rapidform XOR by importing a 3D mesh of a complete bone of similar size and morphology, on the basis of approximate length estimations made during initial data collection. Incomplete bones were then positioned and orientated over the complete reference bone, on the basis of a comparable morphology, using the Interactive Alignment and Datum Match functions in Rapidform XOR. Whilst this approach requires experience in handling 3D data, as well as access to specialist software and 3D scanning equipment, 3D superimposition achieves reliable estimations of complete bone length and can be replicated using open-source software alternatives (Fig. 7.1). In the case of fragmentary elements belonging to articulated individuals (i.e., two humeri from the same individual, the left missing a distal epiphysis and the right missing a proximal epiphysis), both sides were scanned and used to create 'hypothetical' reconstructions whereby the individual models where mirrored and superimposed on to the corresponding skeletal element.

7.3.2.2. Estimating femoral head diameter: shape fitting

Femoral head diameter was required for the estimation of body mass (*i.e.*, Ruff *et al.* 1997) and the standardization of CSG properties. Whilst the femur is one of the best surviving elements in archaeological contexts

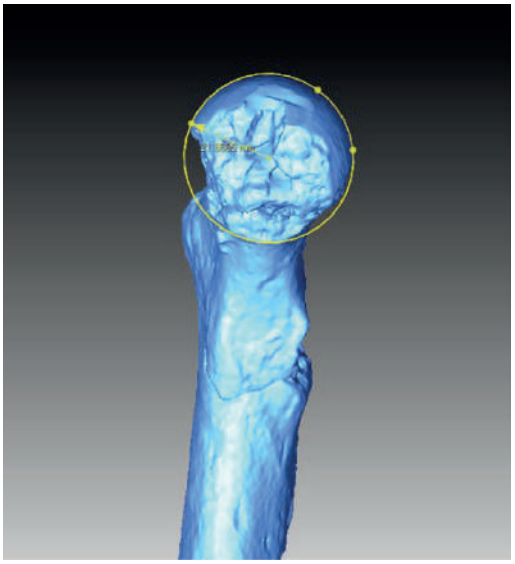

Figure 7.2. *Example of shape fitting method applied to fragmented femoral head. The femoral head is modelled as a sphere and the curvature of the surviving surface is then extrapolated to achieve an estimated diameter (E. Parkinson).*

(Stojanowski *et al.* 2002; Waldron 1987), long bone epiphyses are often damaged in commingled assemblages (Adams & Byrd 2006). In these cases, shape fitting can be used to estimate the diameter of fragmented femoral heads. By modelling the femoral head as a sphere and extrapolating the curvature of the surviving surface with the Measure Radius tool in Rapidform XOR, it was possible to estimate the complete diameter (Fig. 7.2). The estimated radius was then multiplied by two to achieve an estimated femoral head diameter. Whilst this approach does assume perfect sphericity of the femoral head, clinical and experimental research has shown that the femoral head can be confidently modelled as a sphere (Cereatti *et al.* 2010; Hammond & Charnley 1967; Kim 1989) or partial sphere (Parkinson 2014; Ruff 1990, 2002; Rafferty & Ruff 1994). Similar approaches applied to fossil hominin acetabula have proved an effective means of estimating femoral head size in palaeoanthropological literature (Berger *et al.* 2010; Hammond *et al.* 2013; MacLatchy & Bossert 1996; Plavcan *et al.* 2014a, 2014b).

7.3.3. Statistical approach

Independent *t*-tests were used to compare CSG properties between the Xagħra and central Italian Early Copper Age groups and between the left and right humeri from the Xagħra assemblage. Box-and-whisker plots are used here to visualize the data, with the box component depicting the first and third quartiles and the whiskers representing the maximum and minimum values, with the exception of outliers which are plotted as separate points. The threshold for statistical significance was set was p<0.05 for all analysis and statistical tests were conducted in SPSS 25.

7.4. Results

7.4.1. Upper and lower limb CSG properties

Descriptive statistics and results of the independent *t*-tests comparing solid CSG properties of the humerus, tibia and femur of Xagħra and Italian Copper Age groups are displayed in Table 7.2 and Table 7.3. Box-and-whisker plots comparing the solid CSG properties of the humerus, femur and tibia between the Xagħra and central Italian groups are displayed in Figure 7.3, Figure 7.4 and Figure 7.5 respectively. The results show a significant difference in both *TA* (p<0.001) and *J* (p=0.002) in the humerus between the two groups (Table 7.2), where the Xagħra group has lower average values (Fig. 7.3; Table 7.3). The comparison of humeral cross-sectional shape also shows a significant difference between groups (p=0.004), with the Xagħra group having more elliptically shaped humeral cross-sections, as indicated by average greater I_x/I_y values (Table 7.2). A consideration of the standard deviations (Table 7.3) and box-and-whisker plots (Fig. 7.3), which reflect the degree of variability within a sample, shows constrained variation in both measures of upper limb robusticity and cross-sectional shape among the Xagħra group. The results for the lower limb, however, show a considerably different pattern to that observed in the upper limb in that no statistical difference was observed between both groups in any of the comparisons in CSG properties of the femur and tibia (Table 7.3). The descriptive

Table 7.2. *Summary statistics and results of independent t-test comparing cross-sectional properties of upper limb (humerus) between Xagħra and Copper Age Italy.* [a]*Sample contains individuals that have determined biological sex, but are included as a pooled-sex sample here.* [b]*Significant difference,* p = <0.05.

Cross-sectional property	*N*	Mean	St.D.	*t*-test *p* [b]
Humerus TA (35%)				
Xagħra	32	808.56	121.76	<0.001[b]
Copper Age central Italy[a]	61	917.92	143.99	
Humerus *J* (35%)				
Xagħra	32	5114.34	1388.71	*0.002[b]
Copper Age central Italy[a]	61	6335.67	1908.11	
Humerus I_x/I_y (35%)				
Xagħra	32	1.19	0.13	*0.004[b]
Copper Age central Italy[a]	61	1.09	0.16	

Table 7.3. *Summary statistics and results of independent t-test comparing cross-sectional properties of lower limb (femur and tibia) between Xagħra and Copper Age Italy. [a]Sample contains individuals that have determined biological sex, but are included as a pooled-sex sample here. [b]Significant difference,* p = *<0.05.*

Cross-sectional property	*N*	Mean	St.D.	*t*-test *p* [b]
Femur TA (50%)				
Xagħra	31	882.84	108.56	0.658
Copper Age central Italy[a]	32	871.84	87.06	
Femur I_{max}/I_{min} (50%)				
Xagħra	31	1.31	0.18	0.893
Copper Age central Italy[a]	32	1.31	0.17	
Femur *J* (50%)				
Xagħra	31	4097.77	958.26	0.508
Copper Age central Italy[a]	32	3947.53	827.85	
Tibia TA (50%)				
Xagħra	27	713.15	106.45	0.866
Copper Age central Italy[a]	32	717.5	90.29	
Tibia *J* (50%)				
Xagħra	27	4419.78	939.48	0.552
Copper Age central Italy[a]	32	4264.19	1039.61	
Tibia I_{max}/I_{min} (50%)				
Xagħra	27	2.29	0.51	0.269
Copper Age central Italy[a]	32	2.42	0.44	

statistics (Table 7.3) and box-and-whisker plots (Figs 7.4 & 7.5) for the lower limb also display remarkable consistency in CSG properties of the femur between the central Italian and Xagħra groups. In particular, both Xagħra and the central Italian group have identical femoral I_{max}/I_{min} values of 1.31. However, all CSG properties in the tibia, except *TA*, are numerically greater at Xagħra, and the Xagħra group generally exhibits greater variation in CSG properties of the lower limb (Table 7.3).

Table 7.4. *Descriptive statistics for CSG properties of the humerus (35%) by side and results of independent samples t-test comparing left and right CSG properties of humerus from Xagħra. [a]Significant difference, p = <0.05.*

Cross-sectional property	Left (*N*=11)		Right (*N*=21)		
	Mean	**St.D.**	**Mean**	**St.D.**	***t*-test *p*** [a]
J	220.19	57.03	249.82	92.97	0.363
TA	786.98	107.44	824.79	161.11	0.507
I_{max}/I_{min}	1.27	0.16	1.26	0.09	0.818
I_x/I_y	1.2	0.17	1.18	0.13	0.628

Although it is not possible to examine upper limb bilateral asymmetry within single individuals from Xagħra, comparisons between the left and right humeri were made on a group-wide basis in order to explore broad patterns in hand preference. Summary statistics and results of the independent *t*-tests comparing differences between the CSG properties of the left and right humeri within the Xagħra group are presented in Table 7.4. Figure 7.6 and Figure 7.7 display box-and-whisker plots for the CSG properties of the left and right humerus for the Xagħra sample. No significant difference between the any of the CSG properties of the left and right humeri were observed, although interesting numeric differences are apparent (Table 7.4). In TA and *J*, right humeri display considerably more variation (Fig. 7.6), whereas the shape ratios (I_{max}/I_{min} and I_x/I_y) show a slightly different pattern. In particular, I_{max}/I_{min} in right humeri exhibits extremely limited variability (Table 7.4; Fig. 7.7). These results suggest different patterns of mechanical loading and habitual behaviour between the left and right upper limb and indicate preference for the right side, at least on a sample wide basis.

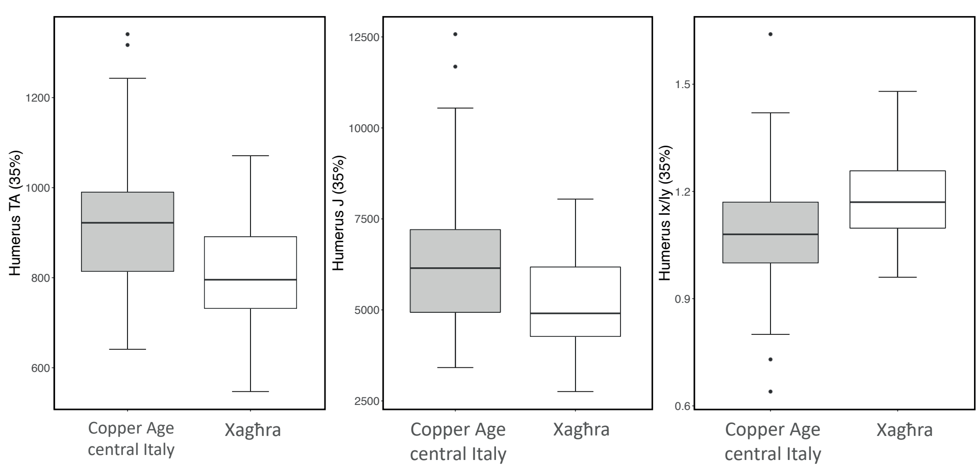

Figure 7.3. *Comparison of solid CSG properties of the humerus between Xagħra and central Italy.*

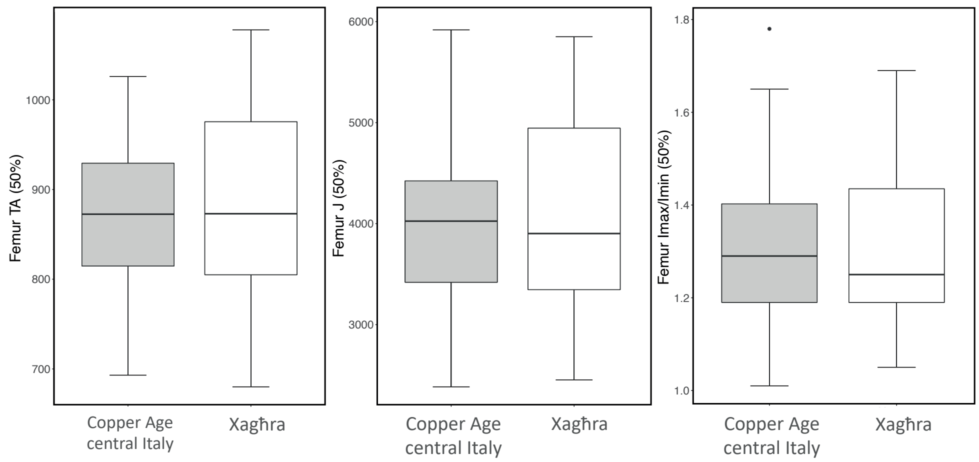

Figure 7.4. *Comparison of solid CSG properties of the femur between Xagħra and central Italy.*

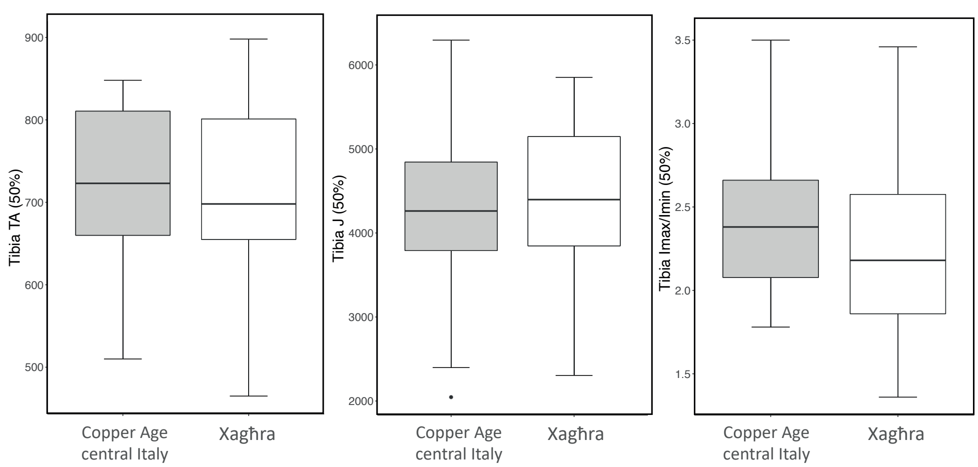

Figure 7.5. *Comparison of solid CSG properties of the tibia between Xagħra and central Italy.*

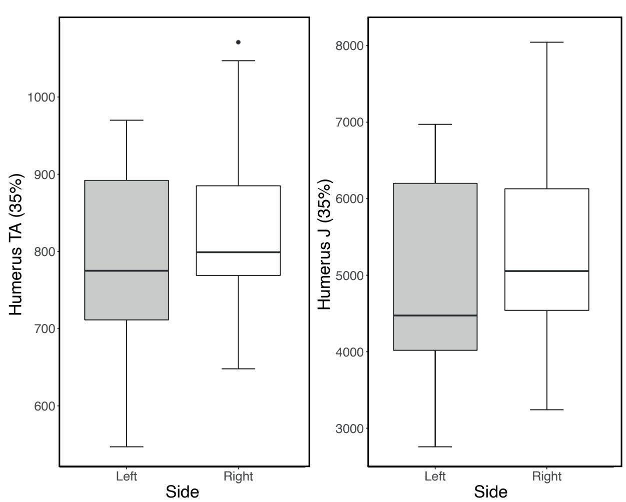

Figure 7.6. *Side differences in TA (left) and J (right) of the humerus at Xagħra.*

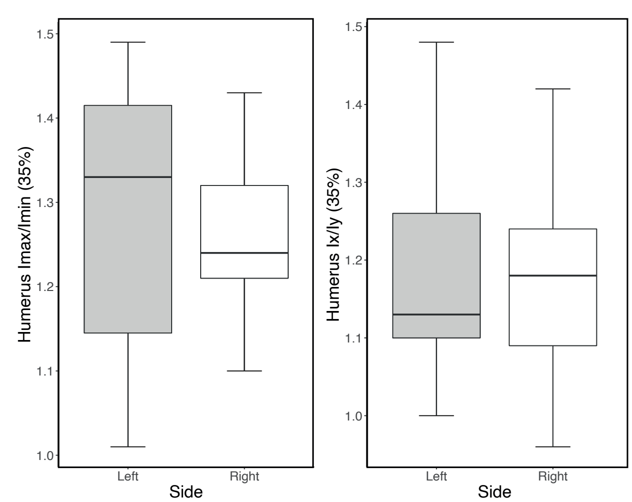

Figure 7.7. *Side differences in cross-sectional shape of the humerus (left, I_{max}/I_{min} and right I_x/I_y) at Xagħra.*

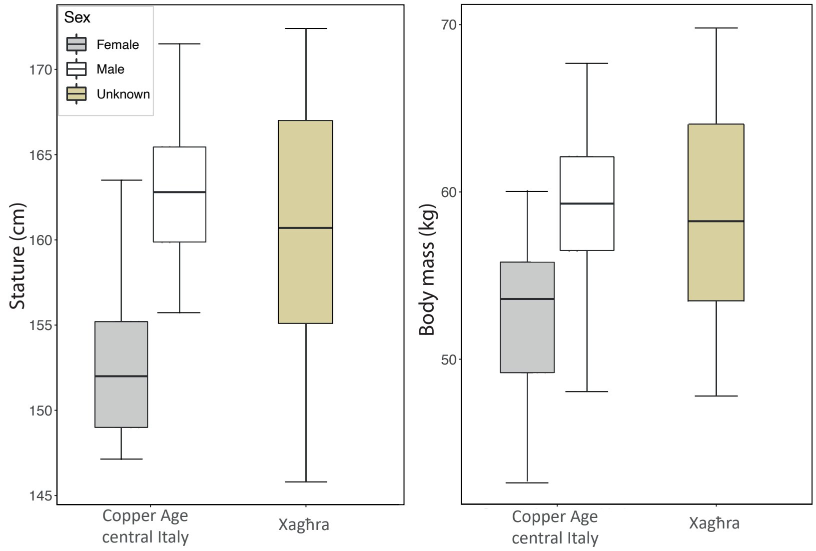

Figure 7.8. *Comparisons of estimated stature (cm) and body mass (kg) between Xagħra and central Italy.*

7.4.2. Body size

Table 7.5 contains descriptive statistics and independent *t*-test comparisons of estimated stature (cm) and body mass (kg) between the Xagħra and central Italian groups. Box-and-whisker plots showing body size variables for the Xagħra (pooled-sex) and central Italian (by sex) groups are displayed in Figure 7.8. Whilst no significant difference in either stature or body mass is observed, the summary statistics and box-plots indicate that the Xagħra group exhibits greater overall body size. Although the analysis presented here only offers one comparison, the results follow a broader central Mediterranean trend were late Neolithic Malta exhibits larger body size than contemporary and near-contemporary groups (Parkinson 2019). The greater range of variation in body size variables at Xagħra is reflective of this group being a pooled-sex sample, where males and females cannot be identified because of commingling. This is highlighted by the clear body size differences between males and females in the central Italian group, where males have a numerically greater average body size than females.

Table 7.5. *Descriptive statistics and results of independent t-tests comparing body mass and stature. [a]Significant difference, p = <0.05.*

	Estimated stature (cm)			Estimated body mass (kg)			
Group	***N***	**Mean**	**St.d.**	***N***	**Mean**	**St.d.**	***t*-test *p*** [a]
Late Neolithic Malta	22	160.72	7.71	28	58.63	6.76	0.159
Copper Age central Italy	25	158.34	6.85	30	56.19	6.27	0.268

7.5. Discussion

The results of the biomechanical analysis of the humerus, femur and tibia indicate that the late Neolithic population of the Maltese Islands had gracile upper limbs, but that the mechanical profiles of the lower limb were similar to Copper Age populations in central Italy. The results also demonstrate preferential use of the right hand within the Xagħra sample, alongside limited variability in CSG properties of the upper limb in stark contrast to the greater variation observed the lower limb. The data are interpreted here as reflecting evidence for reduced levels of physically demanding manual activity in late Neolithic Malta, relative to near-contemporary groups, in contrast to adaptations in the lower limb to heightened levels of terrestrial logistical mobility around the rugged terrain of Gozo. A further interesting feature of the Xagħra assemblage was the constrained variation of upper limb CSG properties.

Increased I_x/I_y values in humeri indicate an elliptical cross-section shape in the antero-posterior plane and are usually interpreted as evidence for repetitive unidirectional habitual (Ruff 2019; Stock & Pfeiffer 2004) and food processing among early agricultural societies (Larsen 2015; Stock *et al.* 2011). Large numbers of querns are known from late Neolithic Malta (Malone *et al*. 2009a, 264; Trump 1966), and it has been suggested that agriculture intensified during the Tarxien phase under a more controlled system, of which the megalithic Temples formed a focus (Stoddart *et al.* 1993; Trump 1980; Volume 2, Chapter 13). More recent palaeoeconomic models for late Neolithic Malta have added nuance to this view, suggesting that landscape management practices were increasingly employed during the Tarxien phase to offset the diminution of soil cover and aridification (Volume 2, Chapter 5), causing potential dietary changes (Chapter 10). Furthermore, the proliferation of stone masonry on the Maltese Islands during the Tarxien phase (Trump 2002) could also be argued as a plausible explanation for the high I_x/I_y values among the late Neolithic Maltese sample. Experimental studies have shown that such activities would have involved vigorous and repetitive unidirectional manual activity (Caruso 2016; Larocca 2016).

However, the decreased humeral robusticity and rigidity (*TA* & *J*) of the Maltese sample is also important to consider, and an alternative interpretation for the patterning in the data may also be driven by the upper limb gracility of the Maltese sample. Pronounced anterior ridges along the distal humeral diaphysis are an artefact of gracility that may result in a more triangular or elliptical cross-section shape. When viewed alongside the decreased TA and *J* values, this shape suggests that the results for all three CSG properties could be related and reflective of decreased levels of mechanically demanding manual behaviour in late Neolithic Malta. The evidence for decreased mechanical loading in the upper limb is somewhat supported by the lack of activity-related pathology, specifically degenerative joint disease, on the major joints of the limbs (§8.4.3). However, incidences of pathology in the upper extremities (bones of the hands) are indicative that intensive manual activities were part of the lived experience of late Neolithic Malta (§8.4.2), but that such behaviours could have involved repetitive and strenuous fine-motor skills, rather than significant mechanical loading of the upper appendicular skeleton.

Although analysis of humeral asymmetry was not possible with the Xagħra assemblage, comparisons between the left and right humeri from the site showed that right humeri exhibited greater robusticity, allowing for a broad exploration of handedness in late Neolithic Malta. Comparisons of shape ratios did not, however, reveal any differences between the left and right sides. When interpreting these broad results, it is important to consider the full spectrum of potential behaviours in late Neolithic Malta and analysis of the dentition from Xagħra also shows evidence for the use of the mouth as a 'third hand', likely as part of a variety of craft-working or food processing activities (§5.8). Recorded instances of enamel trauma and wear at Xagħra occur most frequently on the right maxillary premolars and left mandibular molars. Such a distinctive diagonal pattern of dental trauma and wear is consistent with repeated clamping and gripping of abrasive materials extending from the right side of the mouth. The biomechanical evidence for preferential use of the right hand among the Xagħra group, although typical for modern (McManus 2009; Raymond & Pontier 2004) and prehistoric populations (Sladék *et al*. 2018), seems to be conducive with the model of habitual activity evidenced through dental wear.

The results of the comparative analysis showed that both the Xagħra central Italian Copper Age groups have similarly robust lower limbs. These results are surprising, given that the Xagħra sample might have been expected to exhibit evidence for decreased terrestrial mobility because of their geographically restricted island context – the Maltese Islands have a combined area of 316 km^2, of which Gozo is only 67 km^2 (Schembri *et al.* 2009). Reduced lower limb loading and terrestrial mobility has been observed in Island groups from the Andaman Islands (Stock & Pfeiffer 2001), but in contrast the Xagħra group show lower limb CSG properties that are comparable with those of the Italian Copper Age. A recent comparison between the central Italian Copper Age sample used in this study and a coeval Copper Age sample from the Po Plain, northern Italy, demonstrated increased lower limb robusticity in the central Italian sample, interpreted as reflecting logistical mobility around the hilly terrain of central Italy (Parkinson *et al.* 2018). The influence of terrain and landscape context on lower limb CSG properties has been well studied in Neolithic Liguria, northern Italy, where high levels of lower limb robusticity and greater bending rigidities were also attributed to an adaptation to rugged terrain and high levels of mobility associated with pastoralism (Marchi *et al.* 2006, 2011; Marchi 2008; Sparacello & Marchi 2008). In these studies, the Neolithic Ligurian population displayed levels of lower limb robusticity closer to highly terrestrially mobile Late Upper Palaeolithic or Mesolithic groups (Marchi 2008; Marchi *et al.* 2011), with similar results seen in 'Ötzi' the Alpine Iceman (Ruff 2006b) and Neolithic groups from mountainous regions of southern France (Lambert *et al.* 2013). In spite of their restricted geographical context, the Xagħra population exhibits evidence for undertaking similarly intensive mobility behaviours to central Italian Copper Age groups. The results therefore seem to suggest that the late Neolithic population of Gozo were engaging extensively with their physical landscape, evidently navigating the harsh and irregular terrain of the island. However, the unique and restricted landscape setting of the Maltese case study may also have future implications for how we define, discuss and interpret mobility behaviour in studies of CSG properties in archaeological populations.

The contrasting variability between the CSG properties of upper and lower limb for the Xagħra sample is also interesting. Understanding the precise relationship between the upper and lower limb at Xagħra is difficult in the absence of a larger sample of articulated individuals, although the results do hint at an opposing relationship between patterns physical manual activity and mobility behaviour. The constrained variation in CSG properties of the humerus within the Xagħra sample, when compared to the Italian Copper Age sample, offers useful insights into the division of labour in late Neolithic Malta. Comparison with the humeral CSG properties of the central Italian sample (Fig. 7.3) illustrates how increased variation – at least within that particular archaeological context – can be driven by sexual dimorphism. Considering the Xagħra sample as a commingled assemblage, composed of a mixture of males, females and adult age categories, the limited variation may suggest there was no sex-based division of manual labour during the Tarxien phase. Various social models have been put-forth for late Neolithic Malta that suggest the megalithic temples formed part of structured or hierarchical chiefdom system (Renfrew 1973; see also Cazzella & Recchia 2015, *contra* Bonanno *et al.* 1990 who suggest internal rivalry). The data from the upper limb, with its relative homogeneity, perhaps suggests a more inclusive and heterarchical society and division of labour. Ultimately, attempting to interpret sex-based differences using only CSG values is problematic, however, since post-cranial robusticity has been shown to be heavily influenced by physiological differences between men and women (Macintosh *et al.* 2017, 2019). Examination of sexual dimorphism in the upper limb therefore requires analysis of bilateral asymmetry, which is independent of the physiological factors affecting post-cranial robusticity, although such analysis is simply not possible with the Xagħra commingled assemblage.

The analysis of body size, which revealed a larger average body mass for late Neolithic Malta relative to near-contemporary groups, also has implications for discussions on skeletal growth, stress and development. The averages for body mass (58.6 kg) and stature (160.72 cm) in late Neolithic Malta are at the higher end of ranges obtained from Neolithic and contemporary Copper Age groups in the central Mediterranean (Parkinson 2019) and wider Europe (Macintosh 2016; Niinasken *et al*. 2018), suggesting that the physiological factors affecting skeletal growth and development were less prevalent in Temple Period Malta. In this respect, the higher body size of the Xagħra assemblage lies in apparent contrast to evidence of skeletal stress suggested before (Stoddart *et al*. 2009a) and strengthened in this volume. In particular, the analysis of dental pathology (Chapter 4) and palaeodiet (Chapter 10) shows increasingly marked incidences of linear enamel hypoplasia, decreasing incidences of caries and fluctuating ^{13}N throughout the duration of the Tarxien phase, indicative of developmental stress and changes in diet in the final years of the Temple Period. When viewed together, the evidence therefore appears to present an interesting case whereby the late Neolithic population of Xagħra were clearly faced with increased stress and a changing dietary regimen, but not to the extent that there was a major impact on normal skeletal growth and development. The increased average body size from Xagħra is further surprising given the small island context of the site, where smaller body size might be expected (Foster 1964). Insular dwarfism has been documented in modern human populations (Berger *et al.* 2008; Diamond 2004), although socio-economic factors and life histories have also been shown to affect this phenomenon (Stock & Migliano 2009). When considered alongside the broader archaeological, environmental and palaeoeconomical data for the period (Volume 2, Chapter 12), the Tarxien phase appears to have been a time of considerable changes in diet, behaviour and agricultural practices that suggest the late Neolithic population of the Maltese Islands was grappling with the ever changing environmental instability of their island world.

7.6. Conclusion

Few studies have attempted to analyse long bone cross-sectional geometry in large commingled and fragmented burial assemblages because of the methodological issues they pose, however the results presented here show that meaningful insights into past lifestyles and lived experiences can be gained from such challenging material. This is especially true in cases, such as at Xagħra, where CSG properties and body size data are viewed and interpreted alongside studies exploring diet, health and pathology. The gracile upper limbs of the Xagħra group, when compared with the central Italian group, indicate that levels of manual activity in late Neolithic Malta were perhaps less intensive than in contemporary Copper Age societies in the central Mediterranean. By contrast, the surprising evidence for robust lower limbs among the Xagħra group has shown that despite their geographically restricted island context, the late Neolithic inhabitants of Gozo were actively mobile and engaging with their rugged and hilly natural landscape. The broad patterns of side bias in the upper limb also correspond with side biases in identified dental wear elsewhere in the volume, which when integrated provide exciting glimpses into the lived experience of late Neolithic Malta. The results from the analysis of stature and body mass indicate that average body size among the Xagħra group was greater than that of contemporary groups in the central Mediterranean, suggesting that the physiological factors affecting stature and body mass were perhaps less prevalent in late Neolithic Malta. Interestingly, the body size data presented here shows some contrasts with the palaeodietary and palaeopathological data for Xagħra reported elsewhere, highlighting the complex interplay between skeletal indicators of developmental stress and life history.

Despite the interpretive limitations imposed by the commingling at Xagħra, the broad insights into habitual behaviour derived from the biomechanical analysis presented in this chapter were augmented by the analysis of dentition and palaeopathology presented in Chapters 5 and 8, underscoring the effectiveness of multi-method research programmes in bioarchaeology. However, one particular limitation of this study was that it only considered adult long bones. The evidence from dental wear (Chapter 5) demonstrates that adolescents undertook similar habitual tasks to adults, suggesting a broader division of labour in late Neolithic Malta that integrated younger members of society. It is worth noting, however, that the activity induced bone growth reflected in long bone CSG properties appears to correspond to mechanical loading during adolescence (Haapasalo *et al.* 1996; Kontulainen *et al.* 2002; Pearson & Lieberman 2004). The emphasis on particular contexts also imposes further constraints on the inferences that can be drawn on the data collected here, however; the main contexts that were analysed (from the Shrine, Chapter 3) do offer a representative sample for the entire duration of the Tarxien phase.

The discussions in this chapter also highlight the impact that recent developments in archaeological science have had on the study of complex commingled assemblages, enabling minimal and efficient sampling procedures that provide maximum results. For this study, the application of 3D laser scanning aided the acquisition of osteometric data that would have otherwise been impossible since it enabled a flexible approach whereby study materials could be revisited *in silico*, allowing methodologies to be constantly refined, developed and reapplied.

Acknowledgements

The authors would like to thank Sharon Sultana at the National Museum of Archaeology, Valletta, and Heritage Malta for granting access to the Xagħra assemblage, and to the Superintendence for Cultural Heritage for Malta for permitting this research. We would also like to thank Jacopo Moggi-Cecchi (Università degli Studi di Firenze) and Monica Zavattaro (Museo di Storia Naturale di Firenze, Sezione di Antropologia ed Etnologia) for enabling access to the comparative material from Ponte San Pietro at such short notice, and to Elsa Pacciani (former Soprintendenza per i Beni Archeologici della Toscana, Sezione Antropologia), Mara Silvestrini (Soprintendenza per i Beni Archeologici delle Marche) and Gaia Pignocchi for facilitating access to comparative material from Fontenoce-Recanati. Finally, we would like to thank our *FRAGSUS* colleagues for their help, support and insight over the years. This research was funded by the University of Cambridge *Arts & Humanities Research Council* Doctoral Training Partnership and the University of Cambridge's Smuts Memorial Fund.

Chapter 8

General pathology in the Circle: biocultural insights into population health, trauma and care in Neolithic Malta

Ronika K. Power, Bernardette Mercieca-Spiteri, Jess E. Thompson, Rowan McLaughlin, Jacinta Carruthers, Hannah Vogel, Laura T. Buck, Jaap Saers, Margery Pardey, Jay T. Stock & John S. Magnussen

8.1. Introduction

As with other components of this volume, this chapter builds on the original observations established in Malone *et al.* (2009d), with particular reference to the co-authored paper by Stoddart, Barber, Duhig, Mann, O'Connell, Lai, Redhouse and Malone on the osteological inventory, introductory analyses, and isotopic pilot study of the human and animal remains of the Circle. The primary report (Stoddart *et al.* 2009a) provided invaluable initial insights into local Maltese and regional Mediterranean prehistoric population profiles and mortuary behaviour via their presentation of osseous representation by element (including fragments and exfoliated teeth); preliminary observations of general pathologies and 'dental attrition' (Stoddart *et al.* 2009a, 315, 318); and (re)distribution patterns of elements across the site.

The 2009 volume records the people and processes responsible for extracting data from one of the most analytically challenging assemblages of human bones within the region for the Neolithic period. The challenge of the assemblage lies not only in its scale – an estimated minimum of 220,000 human elements – but also in its disarticulated, highly fragmented and commingled nature (Fig. 8.1). The seemingly unfathomable nature of this challenge is brought to bear when considering that almost 41,000 fragments (~19.0%) were in such a deteriorated state that they could not be identified to a skeletal element (Stoddart *et al.* 2009a, 317). Nevertheless, from 1988–1995, under the direction of Caroline Malone and Simon Stoddart, a devoted and resilient team comprised of Caroline Barker, Gary Burgess, Andrew Clarke, Corinne Duhig, George Mann and Cristina Sampedro undertook the painstaking process of attempting to identify each fragment to element, part of element and side. Further pathology observations were undertaken by George Mann, an Ear, Nose and Throat physician with further qualifications in biological anthropology, to whom this volume is dedicated. These activities resulted in a baseline profile of the Circle burial population, including key demographic indicators of age and sex (p.320–1), and other population descriptors such as stature (p.325). This data collection, in conjunction with relative and absolute dating activities, facilitated a broad overview of the individuals represented within the Circle and their experiences of health, disease, trauma, nutrition, congenital and behavioural variation and social inclusion. As a result, we have far greater understanding of the role of the space as an interment site for more than 1000 individuals of all biological sexes and ages across the life course, in which engagement continued between communities of the living and dead.

The greater focus of the initial report from Stoddart *et al.* (2009a) was to relay the demography, general taphonomic character and organization, and incidental osteological observations for each major context and chronological phase within the Circle. The original analysts commented on the general 'good health' of the population, noting the relative absence of osteological markers for chronic disease (Stoddart *et al.* 2009a, 318). When viewed through the perspective of the 'Osteological Paradox' (Wood *et al.* 1992; cf McFadden & Oxenham 2020), it is clear that the implied inference was that the causes of death for the majority of the initial Circle tudy sample appear to be of an acute nature, perhaps including those respiratory or gastrointestinal illnesses that modern medicine has since brought into submission for the Western world (Stoddart *et al.* 2009a, 321; cf Roberts & Manchester 2005). With the exception of occasional observations of localized periostitis, sinusitis, osteomyelitis and chronic

Figure 8.1. *A typical bag of disarticulated, fragmented and commingled human remains from the Xagħra Brochtorff Circle Cambridge Gozo Project excavations, under analysis as part of the ERC-funded FRAGSUS Project in the National Museum of Archaeology, Valletta, Malta. (Photo Ronika. K. Power).*

ear infections, mastoiditis and meningitis (p.325, 329), pathognomonic evidence for chronic infectious disease processes such as tuberculosis are absent from the initial Circle study sample, in contrast to contemporaneous populations elsewhere (for example, Canci *et al.* 1996; Formicola *et al.* 1987).

Stoddart *et al.* (2009a) attribute the most numerous pathological osseous changes to degenerative joint disease, mostly in the spine, hands and feet (overall attribution: 38% of pathology; Stoddart *et al.* 2009a, 318, 322, 323, 324, 325), and very occasionally elsewhere in the body, such as the shoulder (Stoddart *et al.* 2009a, 319), clavicle (Stoddart *et al.* 2009a, 323), temporomandibular joint (Stoddart *et al.* 2009a, 323, 328), tibia, fibula and patella (Stoddart *et al.* 2009a, 324). Higher incidences of degenerative joint disease are particularly noted in Context (1268) (Stoddart *et al.* 2009a, 328). Healed fractures are mentioned (but not described) on two ribs (Context 1241/6; Stoddart *et al.* 2009a, 324), a humerus (Context (1268); Stoddart *et al.* 2009a, 325), and an overall total of 40 observations are reported for the Tarxien deposits, including insults to the manual and pedal elements, teeth, clavicle, arm, leg, knee and nose (Stoddart *et al.* 2009a, 329). Neoplastic disease is also mentioned, as are congenital variations such as sutural ossicles (Stoddart *et al.* 2009a, 325), and developmental disturbances such as spina bifida (especially in Context (783); Stoddart *et al.* 2009a, 328). The authors make particular note of the relatively low occurrence of indicators of nutritional, environmental or psychological stress, such as *cribra orbitalia*, porotic hyperostosis or enamel hypoplasia (Stoddart *et al.* 2009a, 318, 322, 325, 329). Furthermore, other forms of dental pathology, including carious lesions and dental calculus (Stoddart *et al.* 2009a, 318, 322, 323, 324; overall attribution: 23% of pathology, Stoddart *et al.* 2009a, 325), presented low overall incidence rates.

Within the parameters of the *FRAGSUS Project*, significant advancements have been made to further characterize the experience of dental pathology amongst a sample of the Circle burial population. These findings are reported in Chapter 4 of this volume. The current chapter makes similar advancements in the description of other osseous pathologies, presenting an updated and detailed account of severe conditions and traumas experienced by individuals within the study sample.

8.2. Materials

All available human skeletal material pertaining to the 1987–1994 Circle excavations curated by Heritage Malta within the National Museum of Archaeology was subject to examination for this component of the study. As mentioned above, this amounts to approximately 220,000 human bone fragments which, although varying in size and preservation, are mostly in advanced stages of fragmentation. Analysis of >19,000 fragments from 16 contexts across the rock-cut tomb and cave complex, accounting for approximately 8.6% of the total assemblage, found that mean fragment size was between 21–50 mm in each context and most elements were between 25–49% complete (Chapter 12; cf Thompson 2020). Such high fragmentation is attributed to the process of successive deposition of human remains, resulting in deep deposits which were frequently disturbed. However, bone preservation was qualitatively fair-to-good across many contexts, as conditions within the limestone cave environment were largely favourable. Bone surface preservation varied more strongly between contexts because of a complex interplay of factors including depositional methods, flow of water, duration of use, soil ecology and extent of post-depositional disturbance.

8.3. Methods

The 2009 report established a framework of close investigation of 'significant intact individuals' (Stoddart *et al.* 2009a, 321ff.) to shape inferences regarding the Circle burial population. In an assemblage such as this, our colleagues were right to draw upon the osteobiographies of individuals who, for various reasons, were subject to less *postmortem* disturbance than the majority of those interred in the Circle. From these profiles, we were able to gain great insight into the lived experiences of the Neolithic inhabitants of Gozo. Notwithstanding these achievements, it was not the mandate of the 2009 volume to present any of the reported pathologies in the form of complete scientific description including differential diagnoses. The current study seeks to bring further clarity to the known spectrum of health and disease for the Circle population by continuing the original focus on case studies of so-called 'extreme pathology', and to present them according to scientific recording and reporting convention (§8.5, below). We also present a methodological case study of how careful observation, description and contextual recording of pathological lesions can serve to reunite fragmentary individuals posthumously in commingled skeletal assemblages (§8.6, below).

As detailed in Chapter 2, the team undertaking the osteological analyses faced similar sampling strategy decisions as other archaeometric colleagues in order to produce novel work within the temporal and pecuniary parameters of the *FRAGSUS Project.* Mercieca-Spiteri has detailed this strategy for the Population History Workgroup both here and elsewhere (Mercieca-Spiteri 2016). In order to achieve meaningful population insights into this complex assemblage in our limited time, and to support parallel investigations into scientific dating, palaeodiet and geographical affinity, our activities focused on analyses of 'extreme' skeletal pathology determined by the investigators to be of greatest cultural and temporal significance.

The team developed a highly ambitious programme that aimed to examine the whole available collection (*c.* 220,000 fragmentary elements) in a series of five intensive seasons in the stores of the National Museum of Archaeology (henceforth, NMA), Valletta, with a two-stage mandate to 1) isolate; and 2) examine the remains requiring further study. These remains included all exfoliated dentition and all maxillae and mandibular elements, and all other elements of special interest, including those presenting 'extreme' pathology, such as healed or unhealed fractures, osteoarthritis to an expression of eburnation, activity- and/or entheseal changes to an expression of dysplasia, and periostitis. The logic here is that extreme presentations of pathology thereby also infer that lesser expressions were present amongst the assemblage. This was pertinent for various reasons, particularly that the expression of spinal degenerative joint disease was so prevalent in the assemblage that dedicated study of this pathology alone would have consumed the entire workgroup's resources for the duration of the project. Although unconventional, our approach was deemed to be the most efficient and effective way of characterizing the lived experiences of this population in light of the significant challenges posed by the disarticulated, highly fragmented and commingled nature of the assemblage.

Considering the size of the assemblage, the logistical scale of the *FRAGSUS* sorting, storage and analytical enterprise was immense. The managerial and archival processes required to ensure that every isolated tooth and bone fragment was traceable not only to its archaeological context but also to its curatorial context within the NMA are described in more detail in Chapter 2.

It is important to note that observations of pathology were significantly inhibited in some contexts because of adhering burial matrix (including dirt, mud and ochre); concretion and mineralization of the burial matrix; and severe taphonomic/diagenetic change (cf Stoddart *et al.* 2009a, 318). Once items of special interest were isolated, they were placed in laboratory-quality self-seal bags and clearly labelled with all available archaeological data transcribed from their original label, which continued to be curated with the remaining skeletal material from the find context. All archaeological and curatorial data of the isolated remains were entered into a Microsoft Excel spreadsheet to form a searchable digital database/inventory. All elements of special interest were photographed with a scale, and all photographs were curated using the Google Photos platform. Once a digital archive was created for every isolated element, the element was placed in a designated depository according to its category of study within the *FRAGSUS Project*, either dentition or pathology. Additionally, the depositories were also organized according to context reference to make them searchable and easily accessible for the research team.

The methodology and results of the dental pathology, modification and anthropology studies are presented in Chapters 4, 5 and 6 of this volume, respectively. Gross morphological analyses undertaken for this chapter took place in the NMA over the final two seasons of work in December 2016–February 2017, and April–June 2017, alongside all dental and taphonomic research, and the execution of the Population History Workgroup destructive sampling strategy for isotopic, chronometric and genetic research. For the present study, a sub-sample of elements were selected according to their novelty or significance within the assemblage, or their capacity to serve as case studies for particular biological or cultural phenomena. Pathological descriptions for each element (or fragment) were the collaborative effort of Power, Mercieca-Spiteri and Thompson. Our approach included the recording of inventory numbers; element identification; anatomical side; element preservation assessment; anatomical location of insult; lesion measurement/s; lesion preservation; lesion type; healing status; and description. Our general osteological analytical techniques are based on standard criteria described in Buikstra and Ubelaker (1994: specific references indicated alongside analyses, below). All surfaces were examined macroscopically and under magnification using a 10x hand lens. Within the study sample, selected items were identified as worthy of further examination via radiographic analyses. Eligibility included those of sufficient scientific interest that were also suitable for transport from Malta from a preservation perspective, and of a compatible size with the radiographic equipment.[1]

The results of these analyses are presented below. As with all endeavours pertaining to this site, it must be noted that the work presented here is a further strategic sub-sample of the overall assemblage achieved during the parameters of the *FRAGSUS Project*, rather than comprehensive documentation of the Neolithic population who employed the Circle for funeral and interment rites and practices from 2900–2350 BC. 'Comprehensive' knowledge of the complete preserved archaeological nature and scope of the Circle assemblage will require not only exhaustive excavation of the site, but also the synthesis of several scholars' lifetime of works, including those of the current authors.

8.4. Results: overview

The *FRAGSUS* Population History Workgroup identified 2,819 fragments of human remains of special interest from the Circle study sample (Fig. 8.2). This is slightly lower than the 2,891 reported pathological observations in Stoddart *et al.* (2009a, 325), however it must be noted that the 2009 data included dental pathology whereas the results presented here do not. In the earlier reports, dental disease and 'habitual activities' predominated within the sample, accounting for 1,218 observations or 42.1% (Stoddart *et al.* 2009a, 325), leaving 1,673 observations restricted to skeletal pathology. As mentioned above, the *FRAGSUS*

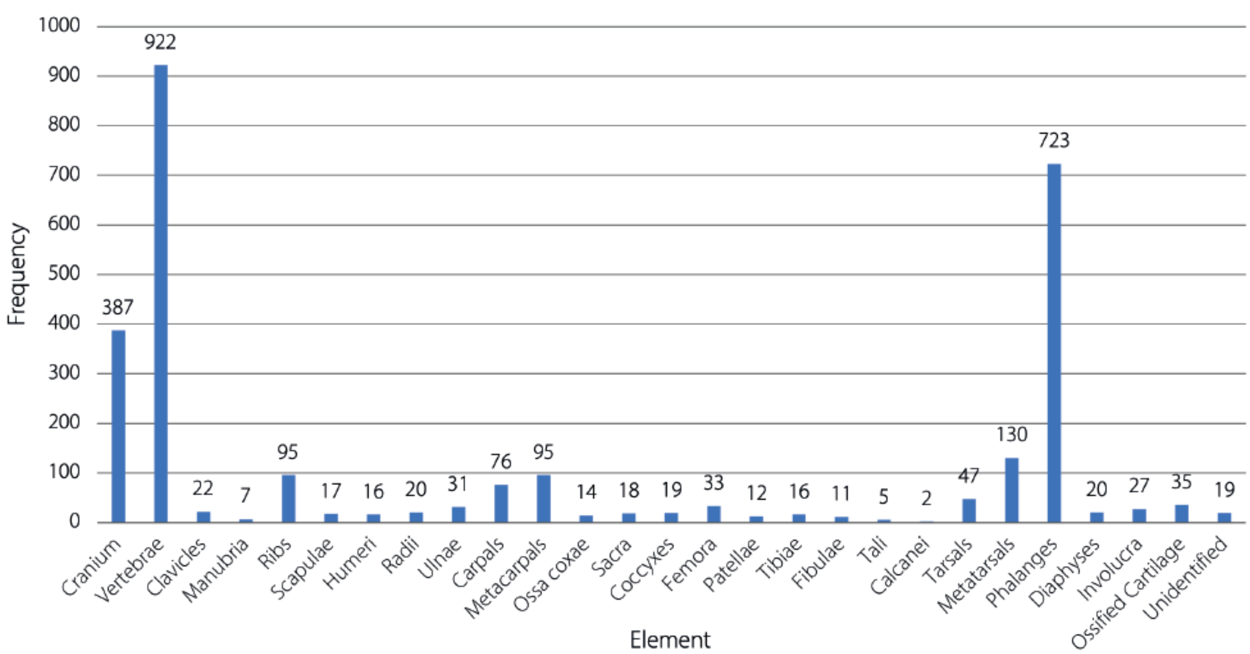

Figure 8.2. *Frequency distribution of human remains of special interest from the Circle (Σ=2819).*

observations of dental pathology and modification are recorded and reported separately (Chapters 4 & 5).

The current identification of 2,819 elements/fragments of special interest therefore represents a raw increase of 1,146 observations across the study sample, or 168.5% increase expressed proportionately. It is important to note that even though the current analyses were subject to tight temporal and pecuniary parameters, they took place under relatively controlled laboratory circumstances, which were far more conducive to systematic observations as opposed to the field conditions experienced by Stoddart *et al.* (2009a). Notwithstanding these logistical differences, the consonance between the respective findings is reassuring.

8.4.1. Spinal pathologies

As seen in Figure 8.2, the spinal column presented the most substantial observations of pathology, with 922 vertebral fragments isolated, accounting for 32.7% of all pathological observations. The majority of these observations were associated with osteoarthritis, including the remodelling and dysplasia of superior and inferior articular processes and facets of vertebrae of all regions (cervical, thoracic and lumbar), with a tendency towards unilateral presentation (i.e. one-sided, suggestive of bodily lateralization). Observations of spondylosis; osteophytosis; fractures; vertebral depression (a.k.a. 'codfish' vertebrae); scoliosis and Schmorl's nodes also featured amongst the assemblage (Fig. 8.3a-i). The majority of the preceding observations are indicative of quotidian, extraordinary, chronic stress and physiological loading of the spine, leading to degenerative change (Rogers 2000, 166), and can be exacerbated by other factors including age, malnutrition and genetic predisposition. The lived experiences of these stressors are described and considered in more detail via a small selection of case studies presented in §8.5.3, below. Further discussions of activity-related changes observed within the assemblage are presented by Parkinson and Stock in Chapter 7.

8.4.2. Extreme extremities

Another prevailing trend within the assemblage was the observation of severe osteoarthritis, enthesopathies, osteophytosis, dysplasia, fractures and *myositis ossificans traumatica* in the bones of the hands and feet. Figure 8.2 demonstrates that the manual and pedal phalanges (Σ=723; 25.6%), carpals (Σ=76; 2.7%), metacarpals (Σ=95; 3.4%); tarsals (Σ=47; 1.7%) and metatarsals (v=130; 4.6%) collectively account for 1,071 (or 38.0%) fragments of special interest within the sample. As with spinal pathologies, the observed manual and pedal pathologies indicate extreme, chronic stress and physiological loading of the extremities; however, these elements also present substantial evidence for single-event insults, such as trauma. A selection of images pertaining to manual and pedal pathology are presented in Figure 8.4a-m.

8.4.3. Notable absences

As always in bioarchaeology, what we *don't* see is as compelling and revealing as what we *do* see. In this case, the almost complete absence of extreme degenerative joint disease and so-called occupationally related change in the major weight- and stress-bearing joints of the shoulder, elbow, hip and knee is astonishing. This is not an artefact of fragmentation, as every observable joint surface was closely examined. Notwithstanding this fact, it is acknowledged that diaphyseal preservation is generally better than that of epiphyses and metaphyses, owing to their more robust structure. In tandem with the pathologies described above, this observation provides critical information regarding the type, frequency and severity of habitual physical behaviour/s carried out by those individuals represented within this assemblage. This is investigated further with biomechanical analyses carried out by Parkinson and Stock in Chapter 7.

Also of note is the relative absence of skeletal indicators of chronic or systemic nutritional, environmental, psychological or pathological stress, including porotic hyperostosis and *cribra orbitalia* (Goodman 1984; Goodman & Armelagos 1989; Goodman *et al.* 1988; Larsen 2015; McFadden & Oxenham 2020). Again, this is not an artefact of fragmentation or taphonomy, as every extant cortical surface was closely examined. Although there were some observations of enamel hypoplasia, these were generally not as severe, nor as frequent as might be expected for an ostensibly geographically isolated and environmentally constrained population of this period (Chapter 4). These observations suggest that, generally speaking, the majority of individuals appear to have had adequate access to subsistence strategies that addressed both their qualitative and quantitative dietary requirements and were only under acute stress for a restricted amount of time. Further commentary on Neolithic Maltese palaeodietary reconstructions is undertaken by McLaughlin *et al.* in Chapter 10; and individual case studies of potential nutritional deficiencies amongst the sample are presented in §8.5–8.6 and §8.7.6, below.

Observations regarding systemic stress also provide a human biocultural framework in which to situate environmental findings reported by colleagues in other *FRAGSUS* Workgroups. For example, Fenech *et al.* (Volume 1, Chapter 4) have identified specimens of *Bulinus* freshwater snails in core samples, including Xemxija 1, Marsa Core 2 and in the Salina Deep Core. This species is indicative of a variety of perennial

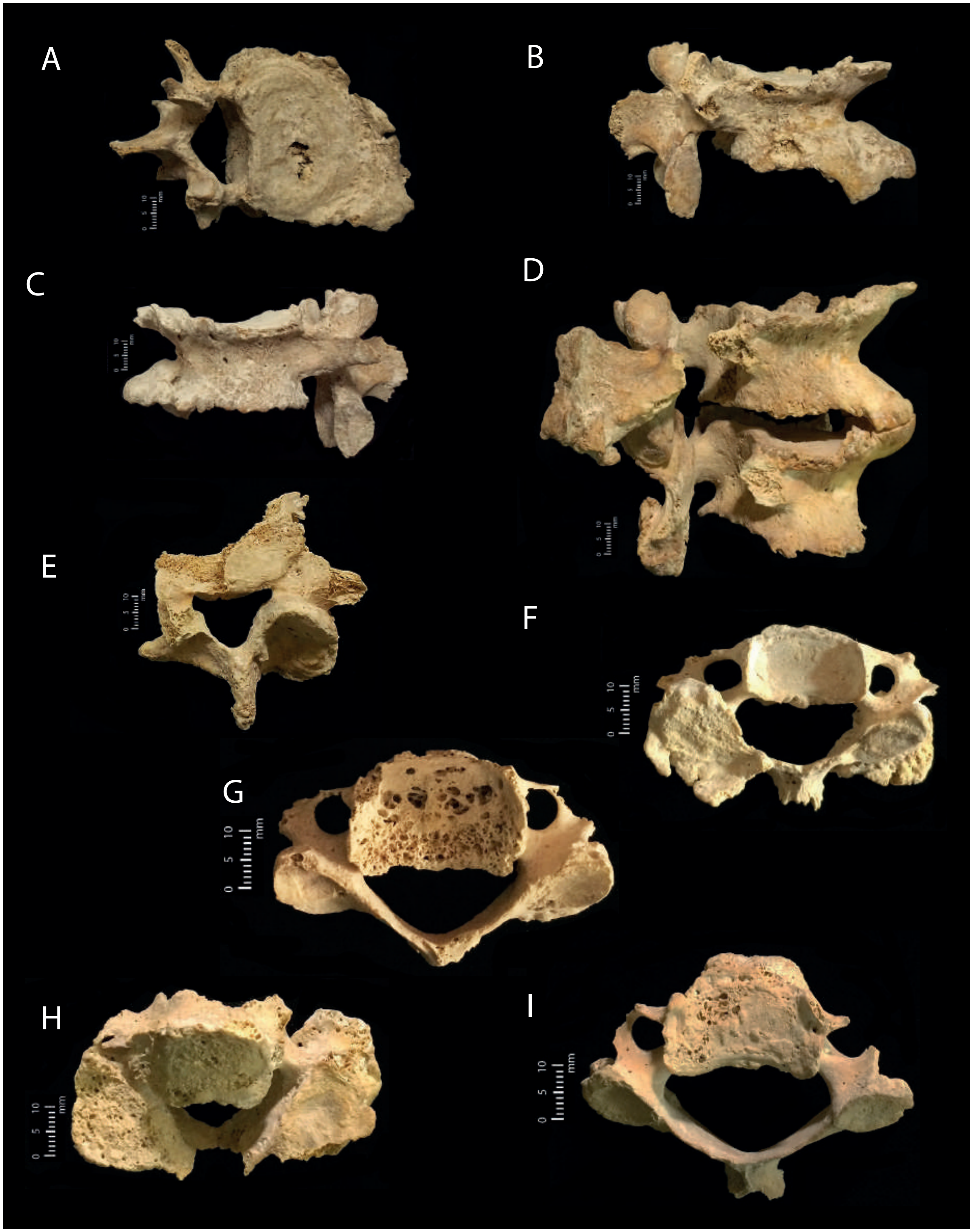

Figure 8.3. *A representative selection of vertebrae presenting extreme pathology including osteophytosis and degenerative joint disease from various contexts of the Circle sample: a–c) Context (1268) 99E/111N Spit 2, Unit 4; d) Context (1268) 99E/111N Spit 2, Unit 12; e) Context (1206) 100E/110N, Spit 4, Unit 2; f) Context (960) 98E/109N Spit 3; g) Context (1024) 98E/113N Spit 1; h) Context (783) 96E/110N; i) Context (783) 96E/110N Spit 1, No. 84. Scale bar: 1 cm. (Photos Ronika K. Power).*

Figure 8.4. *A representative selection of metacarpals, metatarsals and manual and pedal phalanges presenting extreme pathology including healed and* perimortem *fractures, myositis ossificans traumatica and degenerative joint disease from across various contexts of the Circle sample: a) Context (595) 100E/104N No. 320; b) Context (697); c) Context (1268) 101E/109N Spit 2; d) Context (1268) 100E/109N Spit 2, Unit 9; e) Context (1268) 99E/110N Spit 2, Unit 5; f) Context (1206) 100E/110N Spit 1, No. 1; g) Context (783) 96E/113N; h) Context (783) 95E/113N; i) Context (783) 94E/112N; j) Context (783) 95E/112N; k) Context (783) 94E/113N; l) Context (783) 96E/111N Spit 1; m) Context (783) 96E/110N Spit 1, No. 38. Scale bar: 1 cm. (Photos Ronika K. Power).*

flowing and standing water bodies, where it lives on the banks among vegetation and on stony beaches (Giusti *et al.* 1995; IUCN 2017). It was found in deposits pre-dating the end of the Temple Period in Xemxija 1 and in the upper half of the Salina Deep Core. In Marsa Core 2 it was last found in deposits dated to the Late Bronze Age/Early Phoenician Period. This species is extinct from the Maltese Islands today, which is of interest from a public health perspective, as it is an intermediate host for the schistosomiasis (bilharzia) parasite. This debilitating disease has been traced back to the Neolithic period in Chad and in Egypt, where it is likened to the '*Aaa*' disease (King & Bertsch 2015; cf Anastasiou *et al.* 2014; Kloos & David 2002). It is therefore possible that within the Maltese Islands *Bulinus truncatus* also acted as an intermediate host for the parasites causing the disease (trematode worms of the genus *Schistosoma*), which could have negatively affected the local human and animal populations.

Humans and animals contract schistosomiasis when wading in warm freshwater, for such activities as bathing, swimming, crop irrigation, fishing, fowling or foraging, and coming into contact with the intermediate forms of the bilharzia parasite, cercariae, when they leave the *Bulinus* snail in free-swimming form (Nunn 1996, 68). The cercariae burrow into human or animal skin, from where they continue their life cycle and grow into adult worms, variably taking up residence in either the blood vessels of the bladder and kidneys (*S. haematobium*) or intestines (*S. intercalatum*) depending upon their species. Once established, they mate, reproduce, and their eggs are excreted in either the urine or the faeces, again depending on genus (Anastasiou *et al.* 2014). Although people across the ancient world may not have explicitly understood the cause of schistosomiasis, they would have been able to identify its symptoms. In the case of *S. haematobium*, bilharzia infestation leads to haematuria (blood in the urine), and ancient Assyrian medical texts dating to ~4000 BC describe diseases causing such symptoms (Adamson 1976); while more recently (and famously) Napoleon's troops reported that Egypt was the 'land of menstruating men' (Nunn 1996, 69). Considering both the life–cycle of the parasite and the pathogenesis of infestation, positive identification of schistosomes in bioarchaeological studies is either restricted to observations of the effects of the worms and/or their calcified eggs in preserved soft tissue via radiological analyses, such as in mummified Egyptian human remains (Sandison & Tapp 1998, 39–40); the worms themselves are dissolved by autolysis within twenty-four hours of the death of the host (Ghalioungui 1987). Alternatively, the eggs may be preserved in sediment excavated from the thoracic cavities of skeletonized human remains and later identified under light microscopy (Anastasiou *et al.* 2014); or the preserved human tissue samples may be subjected to schistosome circulating anodic antigen (Deedler *et al.* 1990; Miller *et al.* 1993; Nunn 1996).

Untreated, schistosomiasis brings a significant morbidity burden to affected populations, with sequelae including anaemia, lassitude, loss of appetite, kidney failure, bladder cancer, immunocompromise and, in up to 60% of cases, death (Anastasiou *et al.* 2014; Hicks 1983; Fenech *et al.* 2020; Nunn 1996, 69). Chronic infestations can lead to liver dysfunction, which in itself can produce gynaecomastia (breast glandular tissue development in males; Nunn 1996). In other cultural contexts, including ancient Egypt, scholars have argued that chronic schistosomiasis amongst the population may explain the representations of plump-breasted men in visual culture, including representations of the so-called heretic pharaoh Akhenaten (Ghaliounghui 1973; Nunn 1996, 69). In light of Fenech *et al.*'s recent discoveries, perhaps similar considerations should also now be included in the long-standing debates surrounding the gender-fluid figurative art of Neolithic Malta? In the absence of current definitive identification of schistosome eggs, larvae or adult worms in reliable Maltese funerary contexts, we are unable to claim unequivocally that this parasite also imposed its notorious morbidity and mortality burden on the Neolithic population of Gozo. However, it seems unlikely that the Gozitans would have been able to avoid what many other contemporary regional populations suffered. Such a claim would need to justify a lack of engagement with freshwater sources at a time when we already have evidence for human manipulation of water sources for the purposes of proto–irrigation, such as at the nearby sites of Santa Verna and Ġgantija (Volume 1, Chapter 3, & Volume 2, Chapter 9). Despite the relatively low levels of biological stress reported for the Circle population, we are again called to reflect on the implications of the 'Osteological Paradox', and the necessity for further integrated archaeometric and palaeopathological research to articulate the nuances of traditional systemic stress indicators such as *cribra orbitalia*, porotic hyperostosis and enamel hypoplasia (McFadden & Oxenham 2020; Oxenham & Cavill 2010; Rivera & Lahr 2017; Temple & Goodman 2014).

8.4.4. Persons of interest

Although the current research was not focused on demographic analyses, it is nonetheless important to report observed evidence for age across the life course (Fig. 8.5a-g), including several cases of *hyperostosis frontalis interna* (§8.5.2 & §8.7.4, below), extreme pubic symphysis degeneration (x3; Fig. 8.5b-d) and ossified cartilage (Fig. 8.5e-g; Boylston *et al.* 2000, 51), indicating that some individuals lived to an advanced age in Neolithic Gozo. At the opposite end of the life-course, our team also examined the remains of many foetuses and perinates (Fig. 8.5a). The inclusion of individuals of all ages and stages of life is a significant point of discussion for the Population History Workgroup and is expanded upon by Thompson *et al.* in Chapter 12 of this volume and in §8.7.3, below.

8.4.5. Taphonomic considerations

Thompson *et al.* (Chapter 12; cf Thompson *et al.* 2018; 2020; Thompson 2020) explored some of the taphonomic phenomena observed while sorting the assemblage, including the extensive fragmentation of most elements, alongside the preservation of small and/or delicate elements such as auditory ossicles; hyoids;

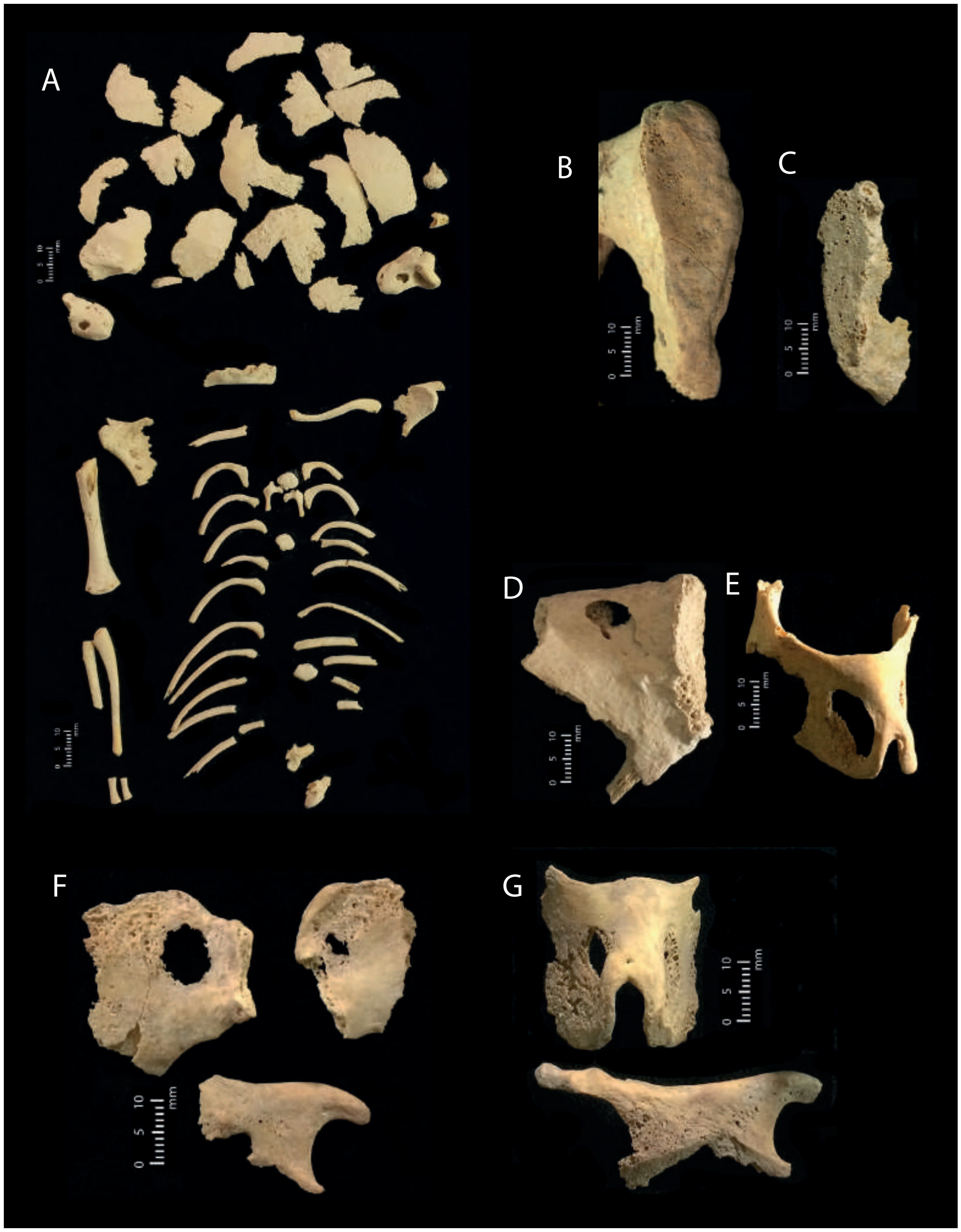

Figure 8.5. *A selection of indicators that the Circle was used as an interment space for individuals across the life course: a) from the partially articulated skeleton of a 24–26 week-old foetus from Context (831); to the markers of advanced age, including: b–d) eroded and eburnated pubic symphyseal fragments from Contexts (845), (1206) and (960), respectively; and f–g) ossified cartilage from Contexts (960), (960) and (783), respectively. Scale bar: 1 cm. (Photos Ronika K. Power).*

ossified cricoid and thyroid cartilage; vomers; styloid processes (of basicrania), phalanges, patellae, carpals and tarsals (especially pisiforms), sesamoids and foetal and neonatal bones. This may seem paradoxical but can be explained by the complex interaction between fair preservation conditions within the natural limestone geology and a long history of successive deposition incorporating substantial rearrangement of remains. Altogether, the burial deposits were likely quite turbulent, leading to the fragmentation of most of the larger skeletal elements, as well as the destruction of an unquantifiable number of bones. However, as described in Chapter 12, while small bones are present and therefore indicate the largely primary nature of deposition, proportionately they are considerably under-represented across the full assemblage. It appears that the combination of natural taphonomic degradation and compaction because of sediment pressure particularly undermined the survival and preservation of less robust elements with a high proportion of trabecular bone. Movement and tumbling within deposits may have provided spaces for small and fragile elements to shift and therefore preserve.

8.5. Results: case studies

The remainder of this chapter is devoted to the presentation of case studies of skeletal changes or variations, providing insights into the spectrum of health issues experienced by the living Neolithic Maltese community before their eventual demise and deposition in the Circle. Considering the highly fragmented, disarticulated and commingled nature of the assemblage, the case studies are presented as individual extant elements grouped by bodily zonation – trauma of the cranium and mandible; other cranial pathology; and post-cranial pathology. The intention of this approach is to draw forth a small number of key reflections from the lived experiences of Gozo's ancient inhabitants and bring life to the extraordinary (and mundane) achievements represented (or invisible) in the Maltese prehistoric archaeological record. At all times, we must hold at the forefront of our minds that the temples, terraces and all manner of technological and artistic endeavours were made *by* real people, *for* real people. As such, the case studies presented below build into bigger conversations regarding the lived experiences of poor health, ageing and interpersonal violence across centuries, reinforcing the impact that considerations of the 'bioarchaeology of care' have on our reconstructions of past populations (§8.7.3, below; Tilley 2013, 2015, 2017; Tilley & Cameron 2014; Tilley & Oxenham 2011). Notwithstanding these important facts, what is presented here represents only a sub-sample of the extant pathological bone from the Circle, and the overall incidence and prevalence of all forms of skeletal pathology is relatively low across the assemblage.

In terms of data presentation, many excellent resources provide direction and frameworks for the reporting of pathology in bioarchaeology (for example, Roberts & Manchester 2005, 96ff.) and some offer further specialty in recording and description of trauma in fragmented assemblages (for example, Judd 2000, 2002a, 2002b). In agreement with Roberts and Connell (2004, 34; cf Buikstra & Ubelaker 1994; Lovell 2000; Ortner 2003), our own direction seeks to abide by the fundamental elements for recording skeletal pathology, namely unambiguous terminology; precise identification of the position of lesions in affected elements; and a descriptive summary of the morphology of the observed variation. The description is offered prior to any differential diagnoses, so that others may be resourced to evaluate each case as they see fit. Following the foundational intentions of Buikstra and Ubelaker (1994, 105) regarding palaeopathological analyses, our Workgroup goal is always to encourage further discussion, collaboration and scholarship.

8.5.1. Trauma: cranium and mandible

A selection of case studies featuring trauma to the cranium and mandible are presented below. Where available, radiological observations supplement macroscopic descriptions. Note that 'diameter' is expressed as: Ø; and 'no data' is expressed as: n/d.

8.5.1.1. FB0002: Mandible

Context:	(951)
Grid Ref.:	-
Year of Excavation:	BR93
Other Details:	Skull No. 15, E. Layer 2

Element identification and preservation:

Adult mandible, based on eruption and occlusion of right permanent mandibular third molar (FDI 48). Sex assessment is indeterminate because of element dysplasia. The element is ~90% complete and fragmented at both left and right ascending rami. Retained dentition includes the left permanent mandibular first and second premolars (FDI 34–35) and first and second molars (FDI 36–37); and the right permanent mandibular first, second and third molars (FDI 46–48). All absent dentition has been exfoliated *postmortem*. Extant element is in excellent condition. All damage is assessed as *postmortem*.

Macroscopic observations:

A complete fracture is observed comprising the left mandibular corpus and ascending ramus (Figs 8.6a-c, 8.7a-g). When viewed from the lateral aspect the fracture is located along the oblique line (Figs 8.6b, 8.7c); from the lingual aspect it is located immediately distal to the tooth-row, posterior to the retro-molar space and truncating the base of the left mylohyoid line (Fig. 8.6c, 8.7d). The fracture is not reduced; the element is dysplastic; the inferior border of the left mandibular corpus is laterally displaced at the level of the left ramus, which is offset in a lateral direction (Fig. 8.6a-c, 8.7c-g). There is a slight superior displacement of the ascending ramus. At the fracture site, the inferior

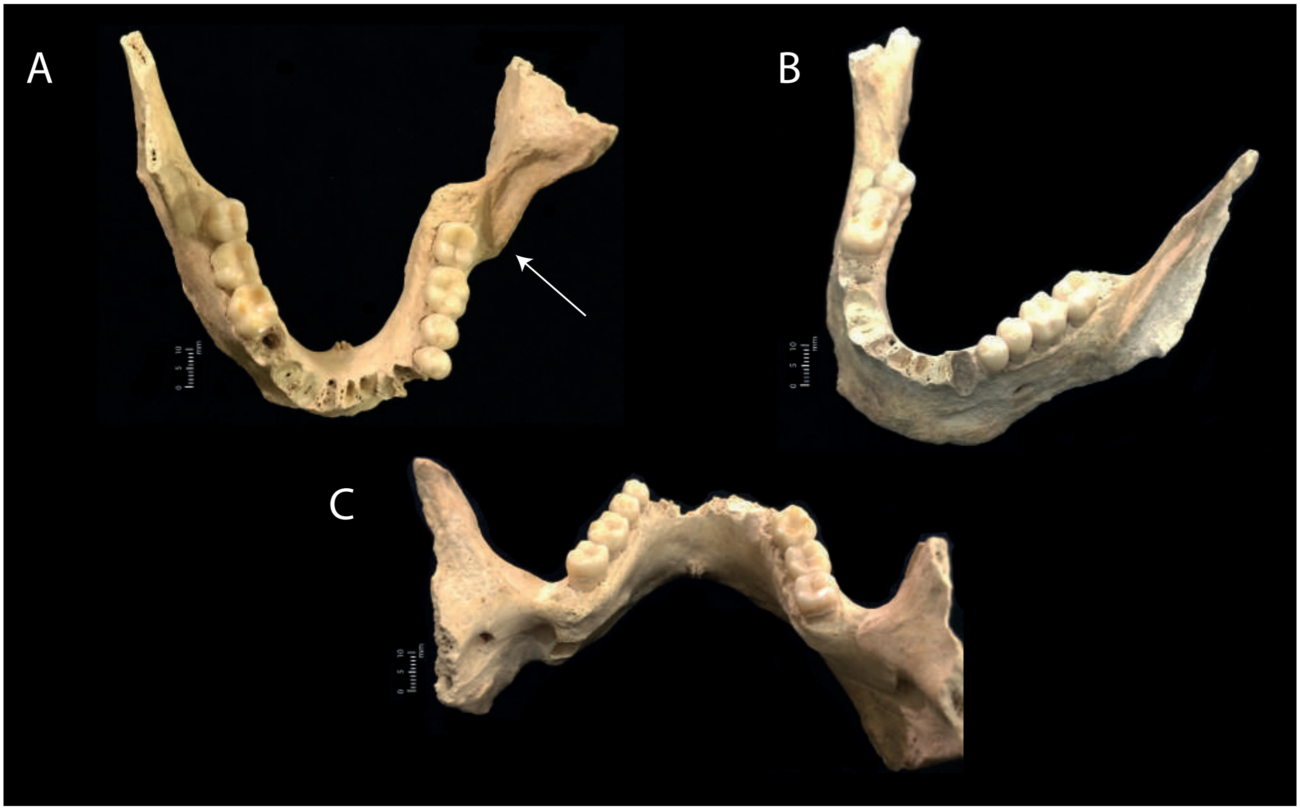

Figure 8.6. *A selection of photographic images pertaining to an adult mandible of indeterminate biological sex (FB0002) from Context (951) of the Circle sample, detailing healed fracture of the left mandibular corpus and ascending ramus, including: a) superior view; b) left supero-lateral view; c) supero-posterior view. Scale bar: 1 cm. (Photos Ronika K. Power).*

aspect of the left ramus is thicker than the opposing side. The left permanent mandibular third molar (FDI 38) is absent and there are no visible indications of peri-mortem tooth-loss or impaction. A small, smooth-walled cavity is observed in the lingual aspect of the corpus at the fracture line.

The left lateral aspect of the corpus is observed to be dysplastic (Figs 8.6a-c, 8.7c-d). The dysplasia presents as a slight elevation of the intermediate component of the left corpus in comparison with the opposing side. In this case, the intermediate component is comprised of the section of the mandibular corpus from the left tubercle of the mental trigone to the fracture margin described above, distal to the left retromolar space. This segment is approximately 51.8 mm in length.

The dysplasia is noted both at the inferior border of the mandibular corpus as well as in the alignment of the left dental arcade (Figs 8.6a-c, 8.7d-g); here, the intermediate segment of the mandibular corpus is superiorly and laterally displaced. When viewed inferiorly, the lingual aspect of the left dental arcade presents pronounced asymmetry, with the intermediate segment described above appearing to be displaced towards the midline. When the element is viewed anteriorly, the point at which the dysplasia commences is located just anterior to the left tubercle of the mental trigone, approximately 12.8 mm infero-lateral to the mental symphysis.

Radiological observations:
The mandible presents a significantly laterally and anteriorly displaced posterior fragment on the left side. Complete healing is evident across the fracture line, as is reestablishment of the cortical surface and trabeculae throughout the fracture site (Fig. 8.7e-g). No scarring is observed to indicate osteomyelitis was suffered *in vivo*, as the effects would have continued into the adjacent cortical bone on the lingual aspect of the mandible, and rarefaction of the trabeculae would be observed. The lingual surface at the posterior aspect of the anterior component of the fracture segment is less well-organized, which would be the expected location of the mesial margin of the third molar – appearing

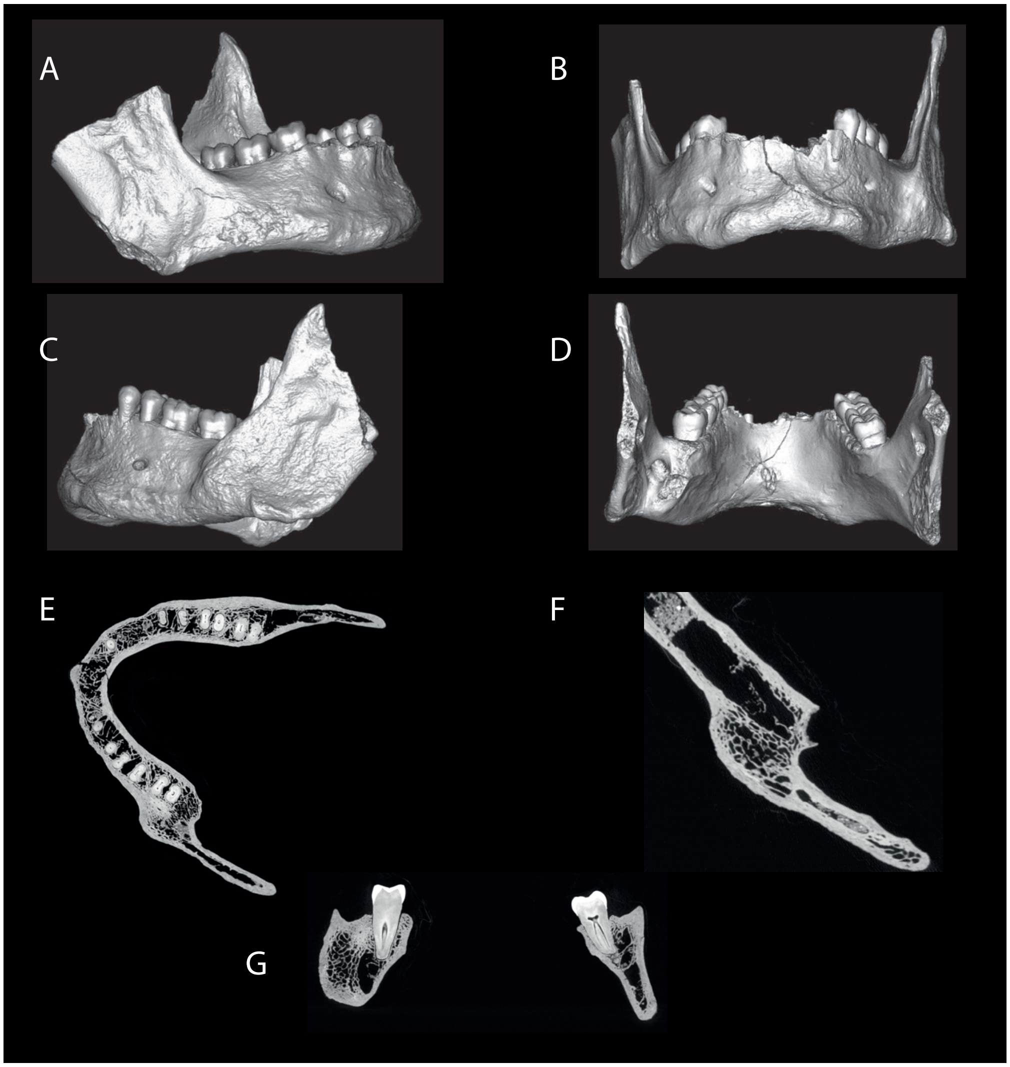

Figure 8.7. *A selection of radiological images pertaining to an adult mandible of indeterminate biological sex (FB0002) from Context (951) of the Circle sample, detailing healed fracture of the left mandibular corpus and ascending ramus, including: a) 3D render right lateral view; b) 3D render anterior view; c) 3D render left lateral view; d) 3D render posterior view; e) transverse cross-section detailing healed fracture; f) transverse cross-section close-up of left aspect of mandible, detailing healed fracture; g) sagittal cross-section detailing left and right mandibular corpora and permanent second molars* in situ *(FDI 37, 47), featuring healed fracture on left aspect. (Radiological images captured by L. Buck, Cambridge Biotomography Centre; processed by J. Magnussen & M. Pardey, Macquarie Medical Imaging).*

quite sharp and irregular (Figs 8.6c, 8.7d-f). Considering the inferior position of the feature in relation to the remainder of the arcade, it is possible that this was a cyst associated with an unerupted third molar. If this is the case, it would indicate that the individual was at least 14–16 years of age at the time of insult (White & Folkens 2005, 366–7). In clinical cases, fractures such as these present as a result of direct impact either onto the mental eminence, or lateral impact onto the corpus (Dreizin *et al*. 2016). It is common to see two points of fracture associated with these injuries, especially in the mandibular condyles (Dreizin *et al.* 2016); however, the element is fragmented and thus further pathological evidence may be absent.

The canal for the inferior alveolar nerve is filled with matrix. The fracture line has traversed the canal but has also partially overlapped as the affected segments resolved in a dysplastic position. It is possible that the dysplasia observed at the anterior aspect of the mandible is associated with the disuse and misuse of the element in association with the major fracture insult and subsequent healing.

In terms of the dentition, the occlusal surfaces present slightly more wear on the ipsilateral than contralateral side, almost to the extent of dentine exposure on the left permanent mandibular first molar (FDI 36). A root remnant is observed in the retromolar space deep within the trabeculae of the right arcade.

Lesion type and healing status: Trauma; Healed.
Lesion preservation: Excellent.
Differential diagnosis: Blunt-force trauma.

8.5.1.2. FB0014: Nasal Bone

Context:	(468)
Grid Ref:	99E/113N
Year of Excavation:	BR93
Other Details:	n/d

Element identification and preservation:
Fragmentary remains of an adult cranium, featuring partial frontal, left and right nasal and right temporal bones. Age estimation is based on size, robusticity, density of cortices and the commencement of sutural obliteration as observed in extant right coronal, sphenofrontal and sphenotemporal sutures. Sex assessment is possible male, based on evaluation of the extant sexually dimorphic traits presented in Buikstra and Ubelaker (1994, 20), including supraorbital margin (4/5) and supraorbital ridge/glabella (4/5). There is no extant dentition. The extant elements are assessed as representing ~30% of a complete cranium and are in very good condition. All damage is assessed as *postmortem*.

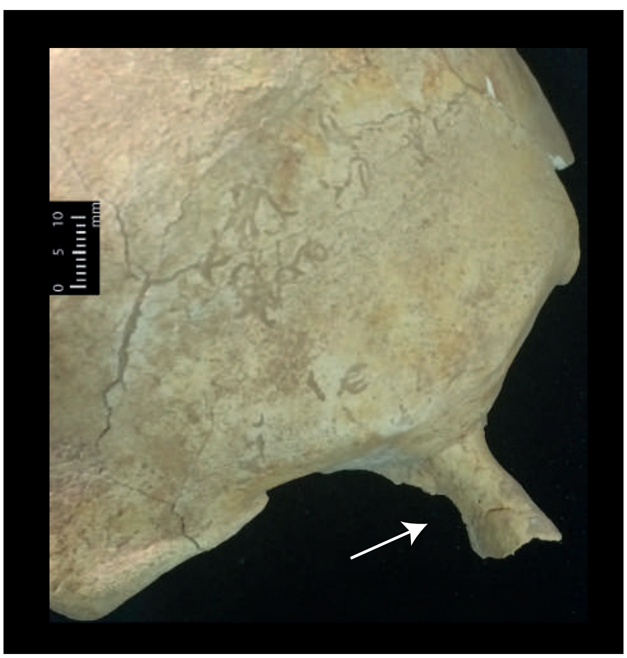

Figure 8.8. *Fragmentary remains of adult possible male cranium (FB0014) from Context (468) of the Circle, featuring healed fracture of the right nasal bone. Scale bar: 1 cm. (Photos Ronika K. Power).*

Macroscopic observations:
A healed fracture is observed on the ectocranial surface of the antero-medial aspect of the right nasal bone (Fig. 8.8). The nasal bone is fragmented at the most distal and lateral aspects. The feature presents as a canal-shaped trough; the inferior aspect of the fracture margin has smooth, rounded contours and slightly overlies the superior aspect of the fracture indicative of slight superior displacement. The superior aspect of the fracture margin is continuous with the surrounding cortical bone with no clearly defined margin. The character of the cortical bone within and across this feature is continuous with the surrounding elements. The maximum dimensions of the feature are 6.51 mm length and 0.5 mm width. The most superior aspect of the feature is located 2.0 mm inferior to the right nasal foramen; the most inferior aspect of the feature is located approximately at 14.2 mm inferior to nasion and meeting the internasal suture.

Lesion type and healing status: Trauma; Healed.
Lesion preservation: Excellent.
Differential diagnosis: Trauma.

8.5.2. Other cranial pathology
A selection of case studies featuring general cranial pathology is presented below. Where available, radiological observations supplement macroscopic descriptions.

8.5.2.1. FB0005: Frontal bone

Context:	(783)
Grid Ref.:	94E/111N
Year of Excavation:	BR94
Other Details:	Spit 4, Unit 8

Element identification and preservation:
Adult cranium, based on eruption and occlusion of left permanent maxillary third molar and fusion of the spheno-occipital synchondrosis. Sex assessment is possible male, based on evaluation of the sexually dimorphic traits presented in Buikstra and Ubelaker (1994, 20), including nuchal crest (5/5), mastoid process (4/5), supraorbital margin (4/5), and supraorbital ridge/glabella (4/5). The cranium is ~95% complete; there are small areas of *postmortem* damage to the palatine process of the left maxilla. Dentition exfoliated *postmortem*

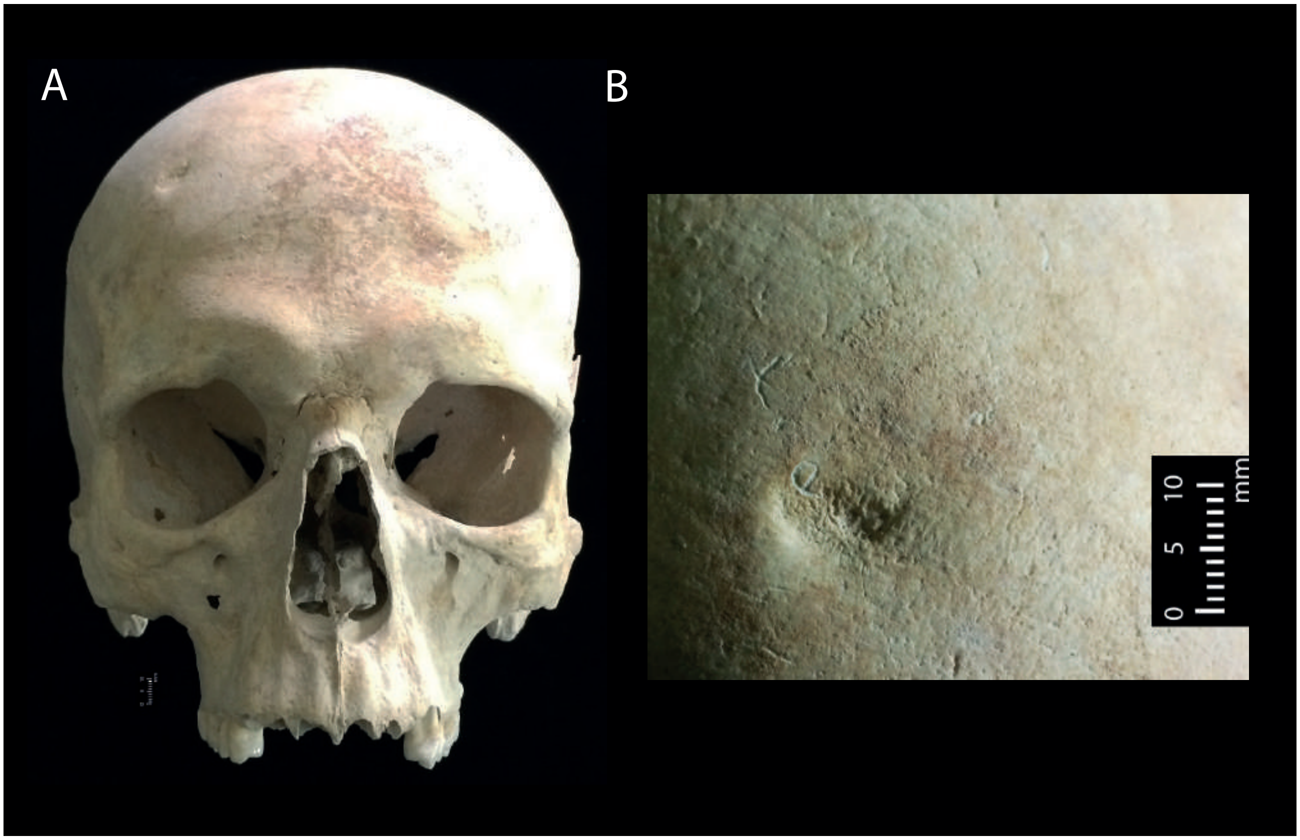

Figure 8.9. *a) Adult possible male cranium (FB0005) from Context (783) of the Circle; b) detailing focal depression on ectocranial surface of the right antero-lateral aspect of the frontal squama. Scale bar: 1 cm. (Photos Ronika K. Power).*

includes the right and left permanent maxillary central and lateral incisors and canine (FDI 11–13; 21–23), and the right permanent maxillary third molar (FDI 18). Extant element is in excellent condition. All damage is assessed as *postmortem*.

Macroscopic observations:
A focal depression is observed on the ectocranial surface of the right antero-lateral aspect of the frontal squama (Fig. 8.9a-b). The feature presents as an approximately crescent-shaped depression with smooth, rounded margins. The cortical bone within this feature presents a pitted surface when compared with the surrounding bone; the character of this pitting is smooth and is not suggestive of an active lesion. The maximum dimensions of the feature are 8.1 mm width and 5.6 mm length. The most inferior aspect of the feature is located 46.2 mm supero-lateral to the right supraorbital notch.

Lesion type and healing status: Erosive; Healed.
Lesion preservation: Excellent.
Differential diagnosis: Infection, Neoplasm.

8.5.2.2. FB0006: Frontal bone

Context:	(1238)
Grid Ref:	98E/114N
Year of Excavation:	BR94
Other Details:	Spit 1, Unit 4

Element identification and preservation:
Fragmentary remains of adult cranium, featuring partial frontal and left and right parietal bones. Age estimation is based on size, robusticity, density of cortices and the commencement of sutural obliteration as observed in extant left coronal and anterior sagittal sutures. Sex assessment is possible male, based on evaluation of the extant sexually dimorphic traits presented in Buikstra and Ubelaker (1994, 20), including supraorbital margin (5/5) and supraorbital ridge/glabella (5/5). Despite the strength of expression of these two extant traits, we remain conservative in our expression considering the absence of the majority of the cranium. There is no extant dentition. The extant elements are assessed as representing ~20% of a complete cranium. The elements are in very good condition. All damage is assessed as *postmortem*.

Macroscopic observations:
Two focal depressions are observed on the ectocranial surface of the left supero-lateral aspect of the left frontal squama (Fig. 8.10a-c). The most anterior aspect of the first of these two features is located 54.0 mm supero-lateral to the left supraorbital notch. The second depression, described below, is located 9.4 mm postero-lateral to the first depression.

The first depression presents as an approximately oval-shaped concavity with smooth, rounded margins. The cortical bone within this feature presents as a pitted and rugged surface when compared with the surrounding bone, with pronounced rugosity observed on the most superior and left lateral aspects of the feature. The character of this pitting is smooth and is not suggestive of an active lesion. The maximum dimensions of the feature are 9.4 mm width and 15.2 mm length.

The most anterior aspect of the second of these two features is located 66.0 mm supero-lateral to the left supraorbital notch. The first depression, described above, is located 9.4 mm supero-medial to the second depression. The second depression presents as an approximately trapezoidal-shaped concavity with smooth, rounded margins. The cortical bone within and across this feature is continuous in character with the surrounding bone. The maximum dimensions of the feature are 10.7 mm width and 14.0 mm length.

Radiological observations:
From a radiological point of view, the anterior lesion is more irregular at its base, while the other is smoother in nature (Fig. 8.10a-b). All bony changes for both lesions are isolated to the outer table (Fig. 8.10c). The more anterior lesion extends three-quarters through the outer table, but does not enter the diploic space. Critically, the diploic space architecture is observed to be normal in character and organization and is not involved in any pathological process. Differential diagnoses for these lesions should include scalp infection, potentially caused by organisms related to contaminated wounds, such as *Staphylococcus aureus* and *Streptococcus pyogenes* (Group A *Streptococcus*). These are the most important and common bacterial causes of skin and soft tissue infections (SSTIs) worldwide. *S. pyogenes* causes well-known infections in the superficial keratin layer (impetigo), the superficial epidermis (erysipelas), the subcutaneous tissue (cellulitis), the fascia (necrotizing fasciitis), or muscle (myositis and myonecrosis; Stevens & Bryant 2016; Bessen 2009). *S. pyogenes* infections have been reported for the scalp (Mastro *et al.* 1990). This type of bacterial infection has particularly high rates of infection in summer months (Ferrieri *et al.* 1972) and is often clinically observed in individuals

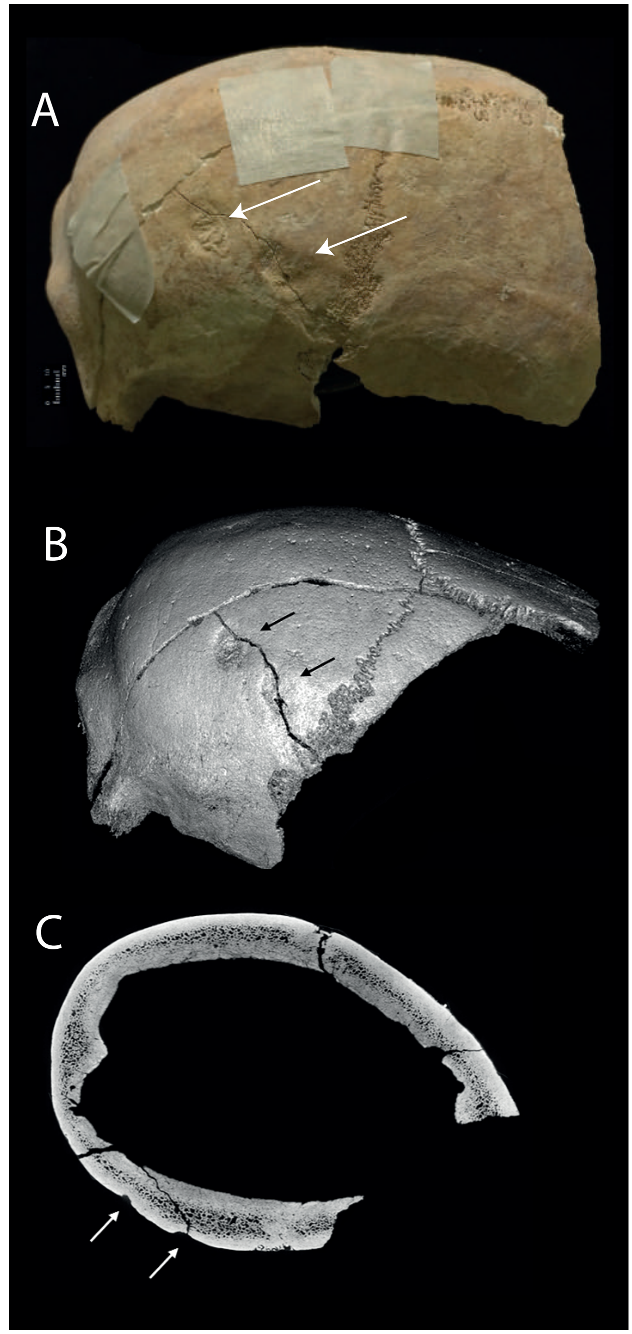

Figure 8.10. *a) Fragmentary remains of adult possible male cranium (FB0006) from Context (1238) of the Circle, featuring two focal depressions on the ectocranial surface of the left supero-lateral aspect of the frontal squama; b) 3D render of fragmentary remains; c) cross-section from CT data of fragmentary remains, showing that both focal depressions do not extend deeper than the outer table. Scale bar: 1 cm (photograph only). (Photos Ronika. K. Power; radiological images captured by L. Buck, Cambridge Biotomography Centre; processed by J. Magnussen & M. Pardey, Macquarie Medical Imaging).*

whose occupation or recreational activities result in cutaneous cuts or abrasions (Adams 2002; Fehrs *et al.* 1987; Wasserzug *et al.* 2009).

Similarly, *S. aureus* causes significant global health burdens owing to its virulence, highly contagious nature, ease of transmission and tendency to recur (Creech *et al.* 2016). This is particularly as a result of its capacity to persist in the environment for long intervals (Knox *et al.* 2012; Miller *et al.* 2015), placing those who live, work and socialize in close quarters, such as households, at high risk (Knox *et al.* 2012; Miller *et al.* 2015). In clinical studies, up to 70% of patients diagnosed with *S. aureus* infections will experience recurrent infections within one year (Kaplan *et al.* 2014; Miller *et al.* 2015) however, the role of antimicrobial resistance must be kept in mind when referring to modern contexts. It is considered the most prevalent pathogen associated with skin and soft tissue infections (Creech *et al.* 2016) *S. aureus* has a predilection for the scalp, face and shoulders, but any bodily region may be affected (Creech *et al.* 2016). Although these infections are usually superficial, they have significant morbidity implications for sufferers and communities, including pain, scarring and the various social, economic and psychological implications of chronic ill health (Creech *et al.* 2016).

Further differential diagnoses should include neoplastic disease, such as scalp tumours including squamous cell carcinoma (SCC) or basal cell carcinoma (BCC). These are the most common non-melanoma skin cancers that affect the head and neck (Dundar *et al.* 2017; Mendenhall *et al.* 2007). The prevailing aetiologies for SCC and BCCs are genetic factors and sun exposure (Sewell *et al.* 2003; Buzzell 1996), the latter of which is plentiful in Malta at any time of human occupation. Consideration should be weighted towards the bacterial infections described above, as non-melanoma skin cancers are likely to compromise the outer table and involve diploë (Dundar *et al.* 2017), which is not observed in this case.

Lesion type and healing status: Erosive; Healed.
Lesion preservation: Excellent.
Differential diagnosis: Infection, Neoplasm.

8.5.2.3. FB0016: Parietal, occipital and other cranial fragments

Context:	(951)
Grid Ref:	96E/114N
Year of Excavation:	BR94
Other Details:	Area X, Spit 1, Skull 9

Element identification and preservation:
A group of assorted cranial fragments, including a fragmented right parietal, occipital and other non-diagnostic cranial fragments. The elements all appear to be derived from an adult individual/s, according to their size, architectural character and cranial suture development (Buikstra & Ubelaker 1994, 32ff.; White & Folkens 2005, 369ff.; White *et al.* 2012, 389ff.). Unfortunately, these elements are too fragmentary to retain key anatomical landmarks for sex assessment according to diagnostic criteria (Buikstra & Ubelaker 1994, 15ff.;

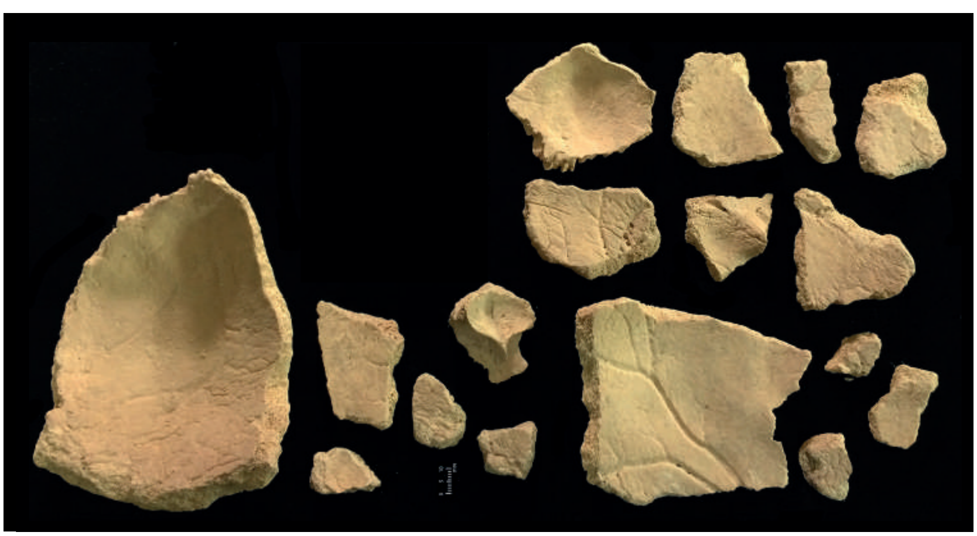

Figure 8.11. *Assorted adult cranial fragments (FB0016) from Context (951) of the Circle, including right parietal, occipital and non-diagnostic pieces. The fragments all exhibit abnormal endocranial focal impressions, classified as hypervascularity. Scale bar: 1 cm. (Photos Ronika. K. Power).*

White & Folkens 2005, 385ff.; White *et al.* 2012, 408ff.). Although these fragments present a similar colour, character, expression of pathology, taphonomic change and there is no duplication of the fragments, it is not possible to state with absolute certainty that they may all be attributed to the same individual. The extant elements are in fair condition. All damage is assessed to be *postmortem*.

Macroscopic observations:
These assorted cranial fragments are observed to have abnormal endocranial impressions (Fig. 8.11). These endocranial impressions can be classified as hypervascularity; the impressions consist of diffuse vascular networks of shallow tunnel-like etching emitting from the meningeal grooves. In section, it is noted that the character of the cortical ectocranial and endocranial portions of the cranial fragments are hardly distinguishable and not easily differentiated from the diploë.

Porotic hyperostosis is observed across the ectocranial surface of at least one cranial fragment. Extant portions of the lesion are observed on a possibly left anterior parietal fragment, extending superiorly and medially from the superior temporal line to encompass all the extant area of the parietal squama.

The porosity consists of a range of holes ranging from very small (<1.0 mm Ø) to large in size (>1.0 mm Ø) that are tightly spaced and, in some cases, do coalesce. The cortical bone appears thickened in some areas of the lesion. The lesion exhibits mixed activity phases, presenting both healed and active states, suggesting it was chronic at the time of death.

Lesion types: Mixed (Lytic; Proliferative); Chronic (Active; Healing).
Lesion preservation: Good; Incomplete because of *postmortem* damage.
Differential diagnosis: Infectious; Metabolic; Endocrine.

8.5.2.4. FB0017: Parietal, occipital, temporal and other cranial fragments

Context:	(951)
Grid Ref:	n/d
Year of Excavation:	BR1994
Other Details:	n/d

Element identification and preservation:
A group of assorted cranial fragments, including a fragmented parietal, occipital, right temporal and other non-diagnostic cranial fragments. The elements all appear to be derived from an adult individual/s, according to their size, architectural character and cranial suture development (Buikstra & Ubelaker 1994, 32ff.; White & Folkens 2005, 369ff.; White *et al.* 2012, 389ff.). Although reliable sexually dimorphic criteria exist for sex assessment of human crania (Buikstra & Ubelaker 1994, 15ff.; White & Folkens 2005, 385ff.; White *et al.* 2012, 408ff.), these elements are too fragmentary to retain key anatomical landmarks for analyses. One fragment of right temporal presents an extant mastoid process, but it is of indeterminate character and should be approached with caution for sex assessment in isolation. Although these fragments present a similar colour, character, expression of pathology, taphonomic change, and there is no duplication of the fragments, it is not possible to state with absolute certainty that they may all be attributed to the same individual. The extant elements are in fair condition. All damage is assessed to be *postmortem*.

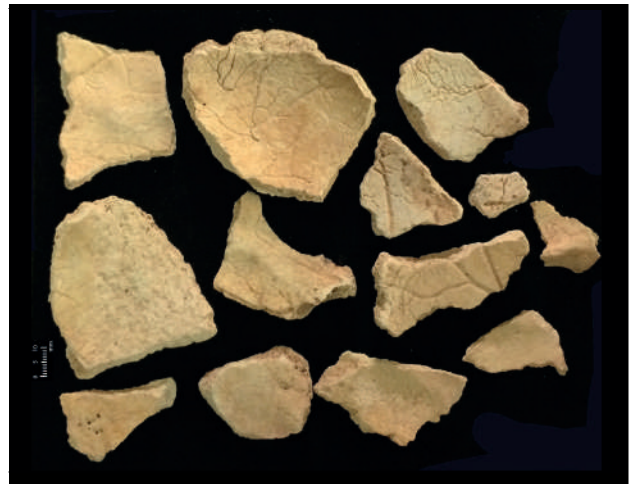

Figure 8.12. *Assorted adult cranial fragments (FB0017) from Context (951) of the Circle, including parietal, occipital, right temporal and non-diagnostic pieces. The fragments all exhibit abnormal endocranial focal impressions, classified as hypervascularity. Scale bar: 1 cm. (Photos Ronika. K. Power).*

Macroscopic observations:
The fragmented parietal and the other non-diagnostic cranial fragments are observed to have abnormal endocranial impressions (Fig. 8.12). These endocranial impressions can be classified as hypervascularity; the impressions are observed to consist of diffuse vascular networks of shallow tunnel-like etching emitting from the meningeal grooves.

Lesion type: Lytic.
Lesion preservation: Good; Incomplete because of *postmortem* damage.
Differential diagnosis: Infectious; Metabolic; Endocrine.

8.5.2.5. FB0018: Parietal fragment

Context:	(951)
Grid Ref:	98E/116N
Year of Excavation:	BR94
Other Details:	n/d

Element identification and preservation:
An isolated right parietal fragment, likely from an adult individual, according to its size and architectural character (Buikstra & Ubelaker 1994, 32ff.; White & Folkens 2005, 369ff.; White *et al.* 2012, 389ff.). Although reliable sexually dimorphic criteria exist for sex assessment of human crania (Buikstra & Ubelaker 1994, 15ff.; White & Folkens 2005, 385ff.; White *et al.* 2012, 408ff.), this element is too fragmentary to retain key anatomical landmarks for analyses. The extant element is in fair condition. All damage is assessed to be *postmortem*.

Macroscopic observations:
The right parietal fragment is observed to have abnormal endocranial impressions located on the cortical bone of the central area of the fragment; the impressions emit from the terminal aspects of the meningeal grooves (Fig. 8.13). These impressions can be classified as hypervascularity consisting of localized vascular networks of shallow channel-like etching and including diffuse micro- and macroporosity amongst the impressions. The margins are smooth, rounded and well-demarcated. The remaining surrounding endocranial surface is uneven and flaky because of taphonomic change.

Figure 8.13. *Adult right parietal fragment (FB0018) from Context (951) of the Circle. The fragment exhibits abnormal endocranial focal impressions, classified as hypervascularity. Scale bar: 1 cm. (Photos Ronika. K. Power).*

Lesion type: Lytic
Lesion preservation: Good; Incomplete because of *postmortem* damage.
Differential diagnosis: Infectious; Metabolic; Endocrine.

8.5.2.6. FB0019: Parietal fragments

Context:	(951)
Grid Ref:	98E/116.5-117N
Year of Excavation:	BR94
Other Details:	Area X

Element identification and preservation:
Two left parietal fragments. The element/s appears to be derived from an adult individual/s, according to their size and architectural character (Buikstra & Ubelaker 1994, 32ff.; White & Folkens 2005, 369ff.; White *et al.* 2012, 389ff.). Although reliable sexually dimorphic criteria exist for sex assessment of human crania (Buikstra & Ubelaker 1994, 15ff.; White & Folkens 2005, 385ff.; White *et al.* 2012, 408ff.), these fragments are too fragmentary to retain key anatomical landmarks for analyses. The extant fragments are in fair condition. All damage is assessed to be *postmortem*.

Macroscopic observations:
The fragments are observed to have abnormal endocranial impressions (Fig. 8.14a). These endocranial impressions can be classified as mild hypervascularity; the impressions are observed to consist of localized vascular networks of shallow channel-like etching emitting from the meningeal grooves.

Lesion type: Lytic.
Lesion preservation: Good; Incomplete because of *postmortem* damage.
Differential diagnosis: Infectious; Metabolic; Endocrine.

8.5.2.7. FB0020: Parietal fragments

Context:	(951)
Grid Ref:	96E/114N
Year of Excavation:	BR94
Other Details:	Area X, Spit 1, Mixed Bone

Element identification and preservation:
Two right parietal fragments. The element/s appears to be derived from an adult individual/s, according to their size and architectural character (Buikstra &

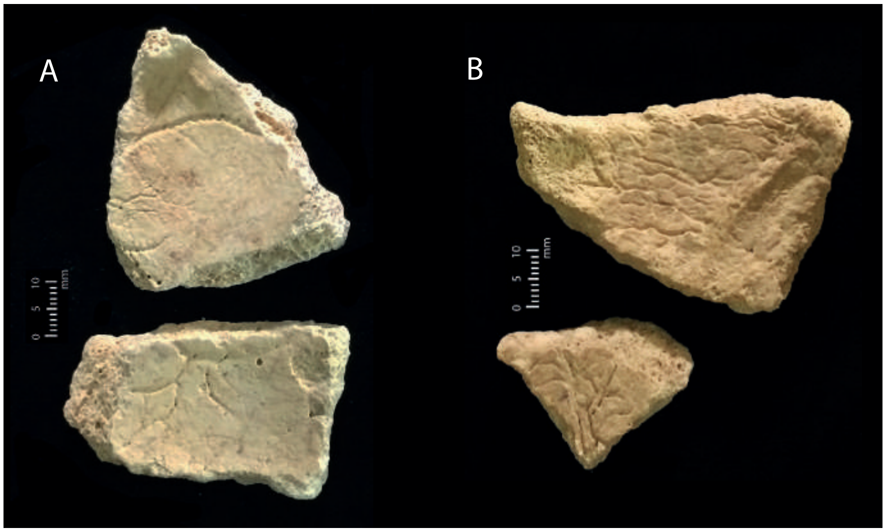

Figure 8.14. *a) Adult left parietal fragments (FB0019) from Context (951) of the Circle. The fragments exhibit abnormal endocranial focal impressions, classified as hypervascularity; b) Adult right parietal fragments (FB0020) from Context (951) of the Circle. The fragments exhibit abnormal endocranial focal impressions, classified as hypervascularity. Scale bar: 1 cm. (Photos Ronika. K. Power).*

Ubelaker 1994: 32ff.; White & Folkens 2005, 369ff.; White *et al.* 2012, 389ff.). Although reliable sexually dimorphic criteria exist for sex assessment of human crania (Buikstra & Ubelaker 1994, 15ff.; White & Folkens 2005, 385ff.; White *et al.* 2012, 408ff.), these fragments are too fragmentary to retain key anatomical landmarks for analyses. The extant fragments are in fair condition. All damage is assessed to be *postmortem*.

Macroscopic observations:
These fragments are observed to have abnormal endocranial impressions (Fig. 8.14b). The endocranial impressions can be classified as hypervascularity consisting of diffuse vascular networks of shallow channel-like etching. The margins are characterized to be smooth, rounded and well-demarcated. The remaining surrounding endocranial surface is uneven and flaky because of taphonomic change.

Lesion type: Lytic.
Lesion preservation: Good. Incomplete because of *postmortem* damage.
Differential diagnosis: Infectious; Metabolic; Endocrine.

8.5.2.8. FB0021: Frontal and parietal fragments

Context:	(518)
Grid Ref:	97E/113N
Year of Excavation:	BR94
Other Details:	Bone 2

Element identification and preservation:
A group of assorted cranial fragments, including a fragmented left parietal and frontal bones which refit. The elements all appear to be derived from an adult individual, according to their size, architectural character and cranial suture development (Buikstra & Ubelaker 1994, 32ff.; White & Folkens 2005, 369ff.; White *et al.* 2012, 389ff.). Although reliable sexually dimorphic criteria exist for sex assessment of human crania (Buikstra & Ubelaker 1994, 15ff.; White & Folkens 2005, 385ff.; White *et al.* 2012, 408ff.), these elements are too fragmentary to retain key anatomical landmarks for analyses. The extant elements are in fair condition. All damage is assessed to be *postmortem*.

Macroscopic observations:
The refitted left parietal fragments and frontal fragments are observed to have abnormal endocranial impressions and lesions (Fig. 8.15). The parietal fragment is observed to have an abnormal endocranial long and deep lesion running inferior and adjacent to the left endocranial aspect of the coronal suture. The extant portion of the lesion, measuring 1.78 mm deep, maximum 34.32 mm length and 4.11 mm width, is observed to cut through the endocranial cortical bone and part of the diploë. A part of the margin of the inferior aspect of the lesion is sharp; the exposed diploë at the base of the lesion is billowed. Although fragmented, the lesion seems to continue on the supero-lateral aspect of the parietal. Additional lesions, although narrower, are observed posterior to the long and deep lesion mentioned earlier. The characteristics are similar in nature to the long lesion.

Macroporosity (≥1.0 mm Ø) extends across a maximum area of 3.3 mm Ø, and is observed on the parietal to the posterior aspect of the long lesion described earlier. The margins of these circular lesions are smooth and rounded.

Focal macroporosity (≥1.0 mm Ø) and irregular channel-like lesions are observed on the frontal bone adjacent to the left coronal suture just anterior and

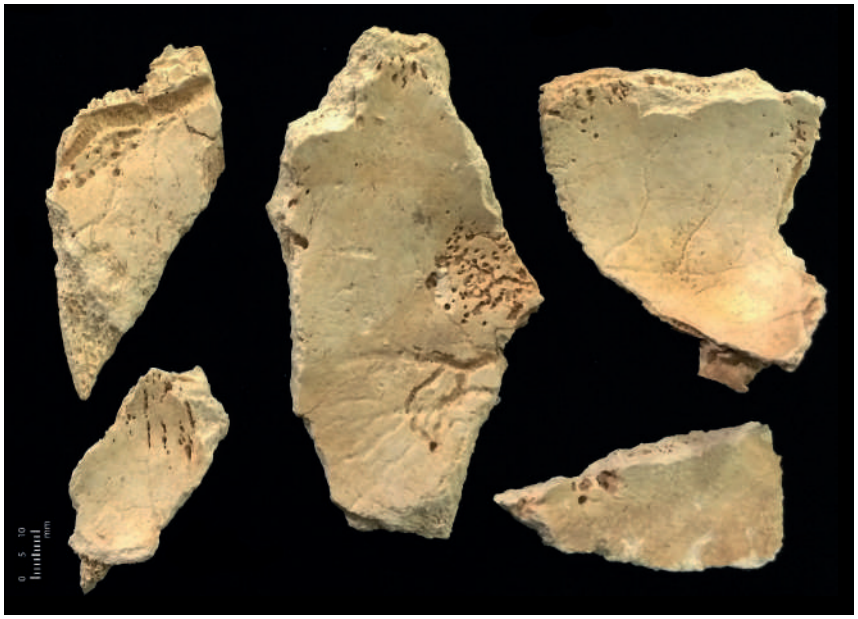

Figure 8.15. *Assorted adult cranial fragments (FB0021) from Context (518) of the Circle, including left parietal and frontal bones which refit. The fragments all exhibit abnormal endocranial focal impressions, classified as hypervascularity. Scale bar: 1 cm. (Photos Ronika. K. Power).*

superior to the long lesion observed on the parietal fragment and described earlier. The lesion occupies an area approximately 22.4 mm x 35.1 mm. The margins of these lesions are smooth and rounded; however, *postmortem* damage is also observed in this area. The macroporosity ranges in size with a maximum of 4.0 mm and minimum of 1.0 mm Ø.

Lesion type: Lytic.
Lesion preservation: Good; Incomplete because of *postmortem* damage.
Differential diagnosis: Infectious; Metabolic; Endocrine.

8.5.2.9. FB0022: Parietal and other cranial fragments

Context:	(838)
Grid Ref:	95.6E/119N
Year of Excavation:	BR93
Other Details:	Skull 7

Element identification and preservation:
A group of assorted cranial fragments, including a fragmented parietal bone/s and other non-diagnostic cranial fragments. The elements all appear to be derived from an adult individual/s, according to their size, architectural character and cranial suture development (Buikstra & Ubelaker 1994, 32ff.; White & Folkens 2005, 369ff.; White *et al.* 2012, 389ff.). Although reliable sexually dimorphic criteria exist for sex assessment of human crania (Buikstra & Ubelaker 1994, 15ff.; White & Folkens 2005, 385ff.; White *et al.* 2012, 408ff.), these elements are too fragmentary to retain key anatomical landmarks for analyses. Although these fragments present a similar colour, character, expression of pathology, taphonomic change and there is no duplication of the fragments, it is not possible to state with certainty that they may all be attributed to the same individual. The extant elements are in fair condition. All damage is assessed to be *postmortem*.

Macroscopic observations:
The cranial fragments are observed to have abnormal endocranial impressions located on the cortical bone (Fig. 8.16). These endocranial impressions can be classified as hypervascularity consisting of diffuse vascular networks of shallow channel-like etching emitting from the meningeal grooves; one parietal fragment presents these impressions within the sagittal sinus. The margins are characterized to be smooth, rounded and well-demarcated. The remaining surrounding endocranial surface is uneven and flaky because of taphonomic change.

Lesion type: Lytic.
Lesion preservation: Good; Incomplete because of *postmortem* damage.
Differential diagnosis: Infectious; Metabolic; Endocrine.

Figure 8.16. *Assorted adult cranial fragments (FB0022) from Context (838) of the Circle, including parietal and non-diagnostic pieces. The fragments all exhibit abnormal endocranial focal impressions, classified as hypervascularity. Scale bar: 1 cm. (Photos Ronika. K. Power).*

8.5.2.10. FB0023: Frontal fragment

Context:	(1268)
Grid Ref:	98/110
Year of Excavation:	BR94
Other Details:	Unit 3 Spit 2

Element identification and preservation:
Fragment of adult frontal bone, consisting of the frontonasal suture, glabella, left supraorbital margin and a portion of the left frontal squama. *Postmortem* damage has fragmented and exposed the frontal sinus. The element appears to be derived from an adult individual, according to its size, architectural character and the pathology described below (Buikstra & Ubelaker 1994, 32ff.; White & Folkens 2005, 369ff.; White *et al.* 2012, 389ff.). Sex assessment is possible female, based on evaluation of the cranial sexually dimorphic traits presented in Buikstra and Ubelaker (1994, 20), including supraorbital margin (2/5), and supraorbital ridge/glabella (2/5). The extant element is in fair condition and represents ~10% of a complete cranium. All damage is assessed to be *postmortem*.

Macroscopic observations:
Proliferation of bone is observed on the endocranial surface of a fragment of frontal bone (Fig. 8.17). The lesion presents as a billowing mass of dense cortical bone either side of the frontal crest. The element is fragmentary, so the full extent of the lesion is not preserved. The extant portion of the lesion occupies the entire endocranial surface area extending approximately 73.5 mm superiorly from the endocranial aspect of nasion; approximately 24.8 mm to the right of the frontal crest (maximum extant portion); approximately 54.3 mm to the left of the frontal crest (intact); and is approximately 3.5 mm in height compared to the surrounding cortical surface. The greatest concentration of osseous deposition is observed immediately bilateral to the frontal crest. Small islands of bone deposition are observed at the lesion periphery on the left side, with maximum dimensions of 7.8 mm length by 4.4 mm width by 1.0 mm height. In some areas, the margins of the lesions are observed to sit proud of the endocranial cortex, but in other areas, and particularly in fragmented section, the proliferation merges with the underlying bone. No cranial sutures are retained on this fragment, so it is not possible to comment on the level of sutural fusion.

Cribra orbitalia is observed on the left orbital roof, occupying the complete anterior aspect. The maximum dimensions of the extant lesion are 23.4 mm length by 11.6 mm width. The lesion presents as capillary-like impressions, aligning with Stuart-Macadam's Type 1 lesion category (1991, 109, Figures 9.3a & b). The right orbital roof is fragmented and absent.

Radiological observations:
The lesion is observed as a proliferation of the diploic space within the frontal fossa, with extension into the

endocranial cavity and very little overlying cortical bone. The lesion presents a lobulated appearance. In places, the hypertrophic activity is observed to fold over itself in a wave-like organization – as illustrated by cross-section images (Fig. 8.17d). Multiple areas are observed where trabeculae extend up to the cortical surface. In this case, the proliferation is restricted to the trabecular component of the bone rather than the cortex – this is an exostosis similar to palatine and mandibular tori. The lesion does not present characteristic features of cortical osteoma or other hypertrophic expansions of diploic space into the cranial cavity, so these are excluded from differential diagnoses. The lesion does, however, exhibit characteristic features of *hyperostosis calvaria interna*, more specifically *hyperostosis frontalis interna* (Cvetković *et al.* 2018; Hershkovitz *et al.* 1999).

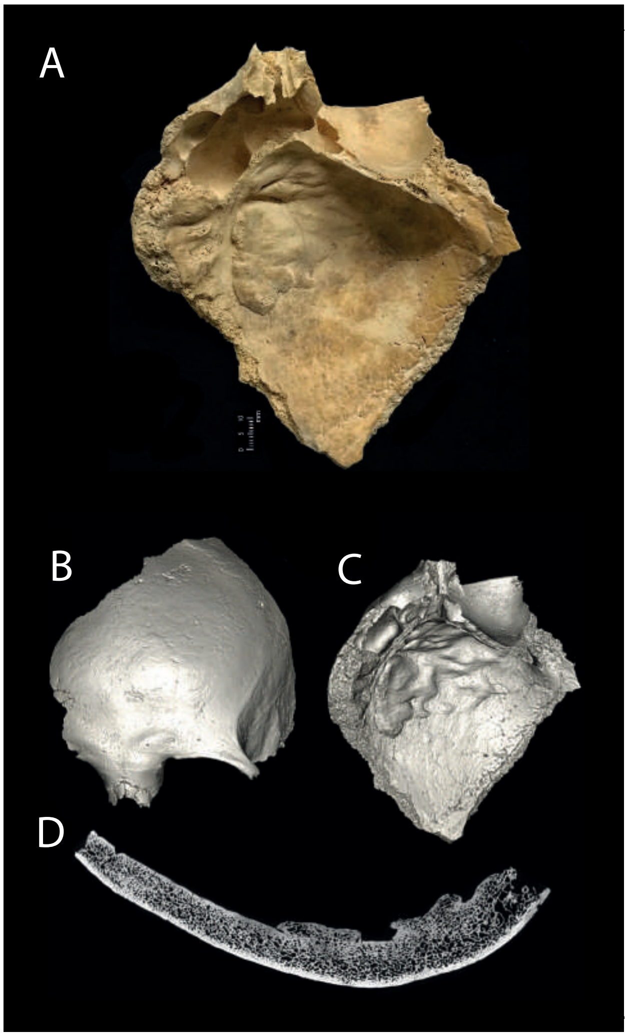

Figure 8.17. *A selection of photographic and radiological images pertaining to a fragment of adult possible female frontal bone (FB0023) from Context (1268) of the Circle sample, detailing a proliferative endocranial lesion within the frontal fossa, including: a) endocranial view; b) 3D render anterior view; c) 3D render endocranial view; d) cross-section from CT data. Scale bar: 1 cm (photograph only). (Photo Ronika. K. Power; radiological images captured by L. Buck, Cambridge Biotomography Centre; processed by J. Magnussen & M. Pardey, Macquarie Medical Imaging).*

Lesion type: Proliferative.
Lesion preservation: Excellent; Incomplete because of *postmortem* damage.
Differential diagnosis: Metabolic; Endocrine.

8.5.2.11. FB0024: Frontal fragment

Context:	(1268)
Grid Ref:	99/110
Year of Excavation:	BR94
Other Details:	Spit 3, Unit 3

Element identification and preservation:
Fragment of adult frontal bone, partial left and right nasal bones, partial frontal processes of left and right maxillae, partial right zygoma, and partial right greater wing of sphenoid. The extant frontal retains the frontonasal suture, glabella, left and right supraorbital margins and the majority of the frontal squama. *Postmortem* damage has fragmented and exposed the inferior aspect of the frontal sinus. The element appears to be derived from an adult individual, according to its size, architectural character and the pathology described below (Buikstra & Ubelaker 1994, 32ff.; White & Folkens 2005, 369ff.; White *et al.* 2012, 389ff.). Sex assessment is possible female, based on evaluation of the cranial sexually dimorphic traits presented in Buikstra and Ubelaker (1994, 20), including supraorbital margin (2/5), and supraorbital ridge/glabella (2/5). The extant element is in fair condition and represents ~15% of a complete cranium. All damage is assessed to be *postmortem*.

Macroscopic observations:
A small, discrete area of bone proliferation is observed on the endocranial aspect of a fragment of frontal bone (Fig. 8.18a-c). The lesion presents as a clearly demarcated, billowing concentration of dense cortical bone on the right side of the frontal crest, lateral to its approximate apex. Although the element is fragmentary, the lesion is observed to be intact. The maximum dimensions of the lesion are 12.4 mm length by 9.1 mm width by 1.9 mm height. The lesion appears to be continuous with the underlying endocranial cortex, with the exception of the most infero-lateral aspect on

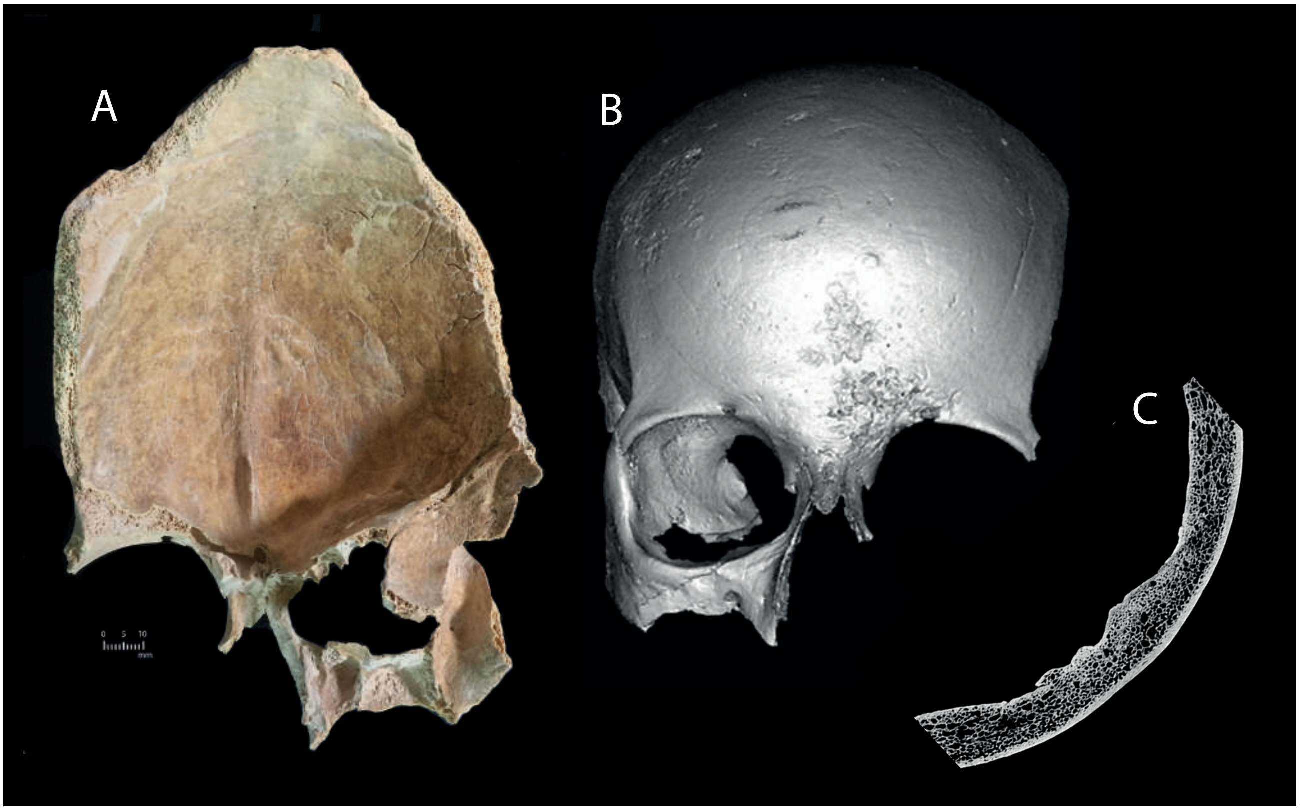

Figure 8.18. *A selection of photographic and radiological images pertaining to a fragmentary adult possible female cranium (FB0024), with extant portions of adult frontal bone, partial left and right nasal bones, partial frontal processes of left and right maxillae, partial right zygoma, and partial right greater wing of sphenoid from Context (1268) of the Circle sample, detailing a proliferative endocranial lesion within the frontal fossa, including: a) endocranial view; b) 3D rendered anterior view; c) cross-section from CT data. Scale bar: 1 cm (photograph only). (Photo Ronika. K. Power; radiological images captured by L. Buck, Cambridge Biotomography Centre; processed by J. Magnussen & M. Pardey, Macquarie Medical Imaging).*

the right side, which is observed to sit proud of the cortex. Note that a button osteoma is also observed on the ectocranial surface of the frontal bone, located approximately 43.3 mm supero-lateral to nasion on the left side (immediately lateral to the nasion-bregma subtense [FRF]; Howells 1973, 181). The lesion presents as a slightly domed, circular focal deposition of dense bone, approximately 3.5 mm Ø, 0.3 mm in height. The margins of the lesion are clearly demarcated and discontinuous with the cortical surface.

Cribra orbitalia is also observed in both orbital roofs. The left orbital roof is fragmented and only partially preserved, but the right orbital roof is intact. The *cribra orbitalia* observed in the right orbital roof, occupies the antero-lateral quadrant. The maximum dimensions of the lesion are 19.4 mm length by approximately 10.1 mm width. The lesions present as larger foramina with a tendency to cluster together and link into a trabecular structure, interspersed with capillary-like impressions, aligning with Stuart-Macadam's Type 4 lesion category (1991, 109, Figs. 9.3a & b). The lesion appears to have been active at the time of death.

Radiological observations:

The lesion is observed as a proliferation of the diploic space within the frontal fossa, with trabeculae extending into the cranial cavity and featuring very little overlying cortical bone. Here again, we see folding hypertrophic activity in places, as previously observed for FB0023 (§8.5.2.10, above), although less advanced in this case (Fig. 8.18c). The lesion is situated at the superior aspect of the frontal crest, calling for consideration as possible calcification associated with the superior sagittal sinus. It is, however, distinctly separate from the anterior aspect of the superior sagittal sinus, thus excluding this option. Further considerations should include falcine or parafalcine calcification, and calcified meningioma of the frontal bone. Meningiomas are primary central nervous system tumours that arise from arachnoidal cap cells of the leptomeninges (arachnoid and pia mater; Oya *et al.* 2011; Sanson & Cornu 2000; Wiemels *et al.* 2010). They may be discounted on this occasion, however, as the extension of trabeculae does not resemble characteristic neoplastic involvement of the diploë. Rather, this appears to be another – albeit minor – case of *hyperostosis calvaria interna*, more specifically *hyperostosis frontalis interna* (Cvetković *et al.* 2018; Hershkovitz *et al.* 1999).

Lesion type: Proliferative.
Lesion preservation: Excellent; Incomplete because of *postmortem* damage.
Differential diagnosis: Metabolic; Endocrine.

8.5.2.12. FB0025: Frontal and parietal fragments

Context:	(960)
Grid Ref:	99/112
Year of Excavation:	BR94
Other Details:	Spit 4, Unit 10

Element identification and preservation:
Fragmentary adult frontal bone, consisting of the frontonasal suture, glabella, left and right supraorbital margins and a portion of the frontal squama. These fragments refit with additional fragments of the supero-medial aspects of the left and right parietal squamae. The elements appear to be derived from an adult individual, according to their size, architectural character, sutural development and the pathology described below (Buikstra & Ubelaker 1994, 32ff.; White & Folkens 2005, 369ff.; White *et al.* 2012, 389ff.). Sex assessment is possible male, based on evaluation of the cranial sexually dimorphic traits presented in Buikstra and Ubelaker (1994, 20), including supraorbital margin (4/5), and supraorbital ridge/glabella (4/5). The extant element is in fair condition and represents ~15% of a complete cranium. All damage is assessed to be *postmortem*.

Macroscopic observations:
Six refitting fragments of frontal and left and right parietal bones were examined. The largest two fragments of frontal and parietal and one small fragment of frontal exhibit pronounced, generalized, diffuse bone proliferation on the endocranial aspects (Fig. 8.19a-c). The two fragments of parietal bone exhibit general thickening of the diploë in the areas immediately bilateral to the sagittal suture (and sulcus), and across the left sagittal squama. These two fragments are continuous in character with the previously mentioned fragments, but do not refit directly. The lesion observed on the two fragments of frontal and parietal and one small fragment of frontal present as extensive, billowing, massive bone proliferation, occupying the entire frontal fossa, bilateral to the frontal crest, extending superiorly past the sagittal sulcus towards the endocranial aspects of bregma and the sagittal suture, traversing onto the frontal angle of the

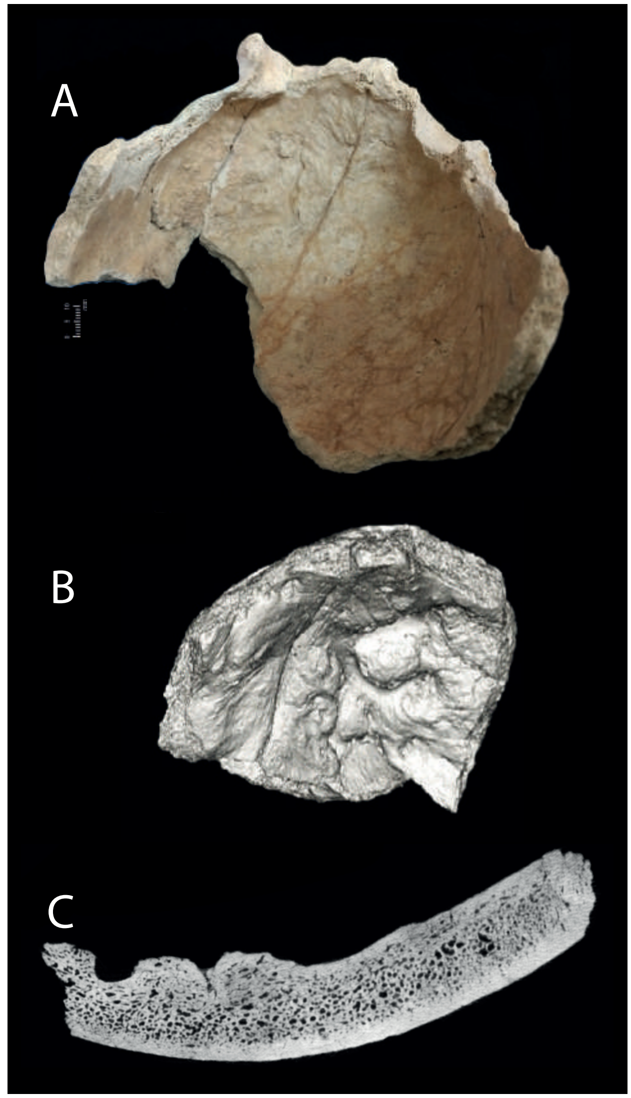

Figure 8.19. *A selection of photographic and radiological images pertaining to a fragmentary adult possible male cranium (FB0025), with extant portions of adult frontal bone from Context (960) of the Circle sample, detailing a proliferative endocranial lesion within the frontal fossa, including: a) endocranial view; b) 3D render endocranial view; c) cross-section from CT data. Scale bar: 1 cm (photograph only). (Photo Ronika. K. Power; radiological images captured by L. Buck, Cambridge Biotomography Centre; processed by J. Magnussen & M. Pardey, Macquarie Medical Imaging).*

left parietal bone on the extant portion of the fragment. As a result of osseous proliferation, the frontal crest has been enveloped and now appears as a cleavage. As a result of fragmentation, the full extent of the lesion is not known. Arachnoid fovea are observed around the extant peripheral aspects of the lesion. When observed macroscopically, in both intact and fragmented portions of the lesion, the lesion appears to be continuous with the underlying endocranial cortex.

The two fragments of parietal bone are observed to be generally thickened in character. In section, the diploë is well-organized and the endo- and ectocranial cortices are clearly demarcated. A lesion is observed to traverse the entire extant supraorbital ridge-glabella complex on both left and right aspects of the frontal bone. The lesion presents as capillary-like impressions, interspersed with microporosity (<1.0 mm Ø). The lesion is most severe at the highest point of the supraorbital ridges, which are extremely robust on this individual. On the left side, the lesion is observed to extend inferiorly into the antero-medial aspect of the orbital roof. The lesion appears to have been healing at the time of death.

Radiological observations:
Once again, the endocranial lesion is observed as a proliferation of the diploic space within the frontal fossa, with trabeculae extending into the cranial cavity in an undulating organization and featuring very little overlying cortical bone. As reported for FB0023 and FB0024 (§8.5.2.10 & §8.5.2.11, above), we see folding hypertrophic osseous activity in places (Fig. 8.19c). The lesion presents sharply demarcated margins with no associated demineralization. This appears to be another case of *hyperostosis calvaria interna*, more specifically *hyperostosis frontalis interna* (Cvetković *et al.* 2018; Hershkovitz *et al.* 1999).

Lesion types: Proliferative; Lytic.
Lesion preservation: Good; Incomplete because of *postmortem* damage.
Differential diagnosis: Metabolic; Endocrine; Infectious.

8.5.2.13. FB0026: Frontal and parietal fragments

Context:	(979)
Grid Ref:	101/109
Year of Excavation:	BR93
Other Details:	Quad XA/H

Element identification and preservation:
Fragment of adult frontal and right parietal bones, consisting of glabella, left and supraorbital margins and orbital roofs and portions of the left and right frontal squama; however, there is significant *postmortem* damage to the right aspect of the frontal squama. A small portion of the supero-medial aspect of the right parietal squama is retained and continuous with the frontal fragment. Additional refitting parietal fragments are also retained. *Postmortem* damage has fragmented and exposed the frontal sinus. The element all appears to be derived from an adult individual, according to their size, architectural character, sutural development and the pathology described below (Buikstra & Ubelaker 1994, 32ff.; White & Folkens 2005, 369ff.; White *et al.* 2012, 389ff.). Sex assessment is possible male, based on evaluation of the cranial sexually dimorphic traits presented in Buikstra and Ubelaker (1994, 20), including supraorbital margin (4/5), and supraorbital ridge/glabella (4/5). The extant element is in fair condition and represents ~10% of a complete cranium. All damage is assessed to be *postmortem*.

Macroscopic observations:
Fragment of frontal and right parietal bones. Small, discrete areas of bone proliferation are observed on the endocranial aspect of a fragment of frontal and parietal bones. The lesion presents as four clearly demarcated, billowing concentrations of dense cortical bone islands bilateral to the apex of the frontal crest, plus plate-like lamellar osseous deposits bilateral to and overlying the frontal crest (Fig. 8.20a-d). There is also a lamellar osseous deposit on the right aspect of the frontal squama, approximately 22.5 mm supero-lateral to the apex of the frontal crest. Although the element is fragmentary, the extant lesion is observed to be intact, although its full extent is not known. The billowing cortical bone islands range in size from 4.5 mm length by 2.3 mm width by 0.7 mm height to 7.1 mm length by 6.6 mm width by 3.7 mm height. These aspects of the lesion are observed to be both continuous and discontinuous with the underlying endocranial cortex; the singular billowing deposit on the right aspect of the frontal fossa is continuous with the endocranial surface, while the three billowing deposits on the left aspect of the frontal fossa are continuous with the endocranial surface on the medial side, yet sit proud of the endocranial surface on the lateral side. The plate-like lamellar osseous deposits merge with the endocranial surface in their lateral and inferior aspects, yet sit proud of the cortex on their superior and medial aspects.

Capillary-like vascular impressions surround the billowing bone island deposits and traverse the plate-like lamellar deposits. These vascular impressions extend the entire extant length of the sagittal sulcus on this fragment, as well as the sagittal sulcus and its immediately bilateral area on refitted fragments. Note that all cranial sutures on all fragments of this cranium are observed to be obliterated on both endo- and ectocranial surfaces.

Cribra orbitalia is observed on the left and right orbital roofs, occupying the antero-lateral quadrants. The maximum dimensions of the lesion are 20.8 mm length by 13.4 mm width on the left orbital roof and 17.4 mm length by 9.8 mm width on the right orbital roof. In both orbits, the lesion presents as capillary-like impressions, aligning with Stuart-Macadam's Type 1 lesion category (1991, 109, Figs. 9.3a & b).

A button osteoma is observed on the posterior aspect of the right parietal bone, approximately 37.0 mm lateral to lambda. The lesion presents as a slightly domed, irregularly shaped focal deposition of dense bone, approx. 10.0 mm in maximum Ø, 0.9 mm in height. The margins of the lesion are diffuse and continuous with the cortical surface.

Radiological observations:
Here again, we observe an endocranial lesion characterized by proliferation of the diploic space within the frontal fossa. Trabeculae extend into the cranial cavity as large lobulated ridges with very little overlying cortical bone. Vascular channels traverse through the trabeculae. As reported for FB0023, FB0024 and FB0025 (§8.5.2.10–12, above), we see folding hypertrophic osseous activity in places (Fig. 8.20c-d). The lesion presents sharply demarcated margins and there is no associated demineralization observed. This appears to be another case of *hyperostosis calvaria interna*, more

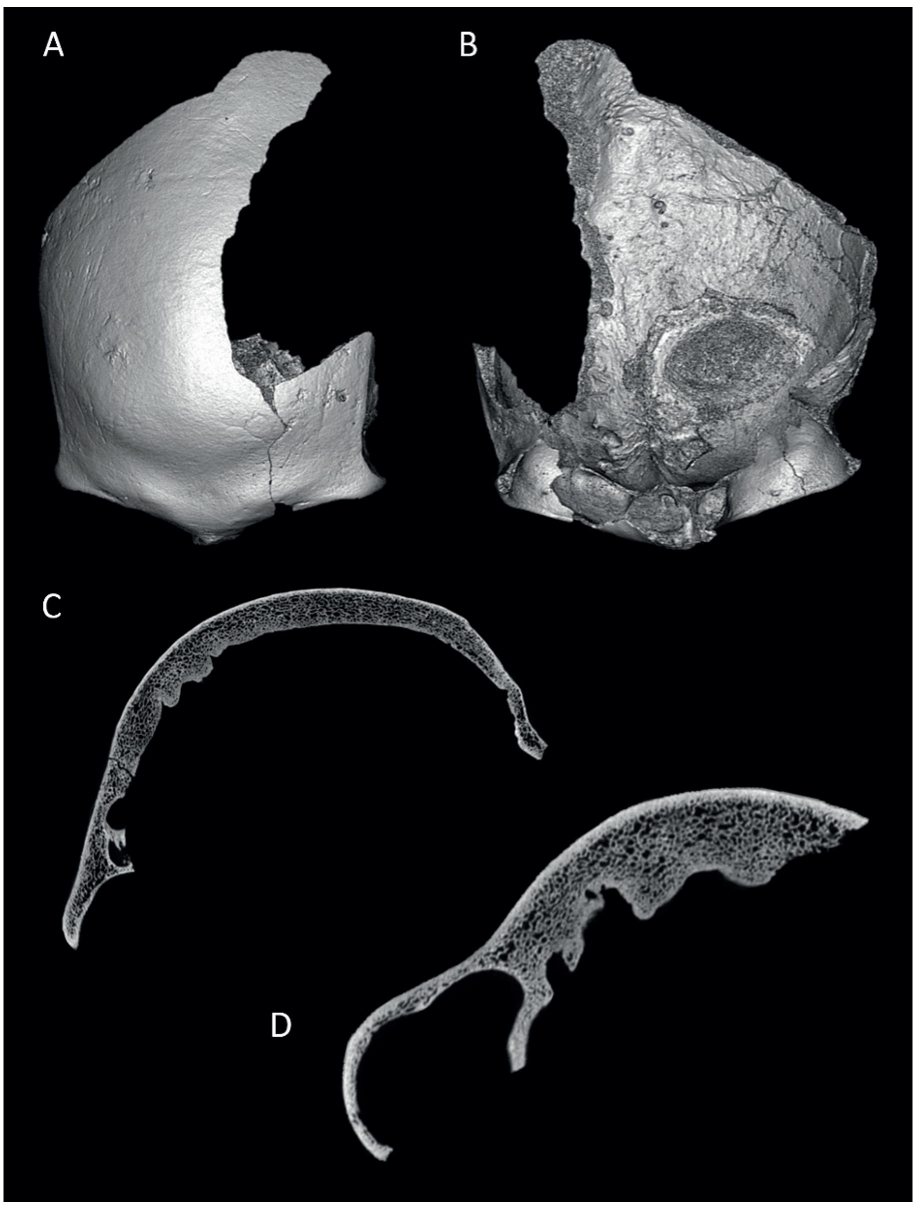

Figure 8.20. *A selection of radiological images pertaining to a fragmentary adult possible male cranium (FB0026), with extant portions of frontal and right parietal bones from Context (979) of the Circle sample, detailing a proliferative endocranial lesion within the frontal fossa, including: a) 3D render anterior view; b) 3D render endocranial view; c–d) cross-sections. Radiological images captured by L. Buck, Cambridge Biotomography Centre; processed by J. Magnussen & M. Pardey, Macquarie Medical Imaging.*

specifically *hyperostosis frontalis interna* (Cvetković *et al.* 2018; Hershkovitz *et al.* 1999).

Lesion types: Proliferative; Lytic.
Lesion preservation: Excellent; Incomplete because of *postmortem* damage.
Differential diagnoses: 1) Metabolic; Endocrine; 2) Neoplastic.

8.5.3. Post-cranial pathology
A selection of case studies featuring post-cranial pathology are presented below, including observations of vertebrae, humeri, ulnae, and a femur, tibia and fibula. Where available, radiological observations supplement macroscopic descriptions.

8.5.3.1. FB0031: Second cervical vertebra

Context:	(951)
Grid Ref:	n/d
Year of Excavation:	BR93
Other Details:	E3, No.37

Element identification and preservation:
Fragment of an adult second cervical vertebra (axis), consisting of the body, dens/odontoid process and a small portion of the left and right superior articular facets. Age estimation is based on the degree of fusion (Scheuer & Black 2000, 180ff.) and the extreme pathology described below. At present, there are no methods of sex assessment for isolated and fragmented vertebrae. The fragment represents ~30% of a complete second cervical vertebra. The extant element is in very good condition. All damage is assessed as *postmortem*.

Macroscopic observations:
When viewed both anteriorly and posteriorly, the dens is observed to be postero-laterally shifted on its axis towards the right side by approximately 10° (Fig. 8.21). When viewed anteriorly, the articular facet for the first cervical vertebra (atlas) is also observed to be postero-laterally displaced to the right side, again by approximately 10°. No fracture lines are observed with the naked eye.

Substantial osseous change is observed on the extant portion of the right superior articular facet (Fig. 8.21b); here, macroporosity of <2.0 mm Ø indicates the presence of subchondral cysts. In addition, ≥7 deep channels of striations traverse the extant facet face are observed, occupying a space of less than 2 cm^2. Eburnation is observed on the most lateral and superior aspects of the striations. Joint contour change is

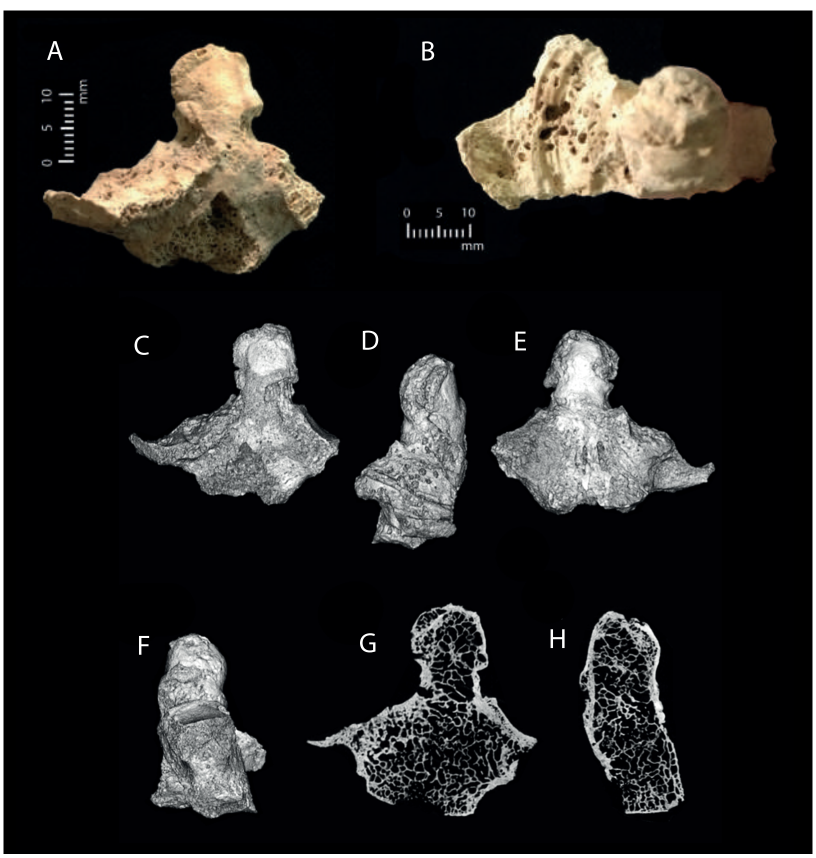

Figure 8.21. *A selection of photographic and radiological images pertaining to a fragmentary adult second cervical vertebra (axis) (FB0031) from Context (951) of the Circle sample, exhibiting severe degenerative joint disease and dysplasia: a) anterior view; b) superior view, displaying joint contour change and eburnation on right superior articular facet; c) 3D render anterior view; d) 3D render right lateral view; e) 3D render posterior view; f) 3D render left lateral view; g) coronal cross-section from CT data; h) sagittal cross-section. Scale bar: 1 cm (photographs only). (Photos Ronika K. Power; radiological images captured by L. Buck, Cambridge Biotomography Centre; processed by J. Magnussen & M. Pardey, Macquarie Medical Imaging).*

also apparent, with the extant medial and lateral borders of the facet appearing spread and diffused, and the postero-medial border of the facet extended in a medial direction, intruding into the vertebral foramen. No eburnation is observed on the dens articular facet for the first cervical vertebra and no osseous change is observed on the extant portion of the left superior articular facet. The osseous changes observed on the right superior articular facet are consistent with degenerative joint disease.

Radiological observations:
Observed subchondral cysts and morphological and joint contour changes to the right superior articular facet are consistent with advanced cervical osteoarthritis (Fig. 8.21g-h). Despite the described displacement of the dens, there is no radiological indication that a fracture was sustained by this element. In clinical cases, it is rare to see individuals aged 50+ without atlantoaxial joint contour change (Zapletal *et al*. 1995). The bony irregularity described for the odontoid process is most likely related to age and activity-related degenerative change.

Lesion type and healing status: Mixed; Dysplastic; Active.
Lesion preservation: Excellent.
Differential diagnosis: Degenerative Joint Disease; Activity-related change.

8.5.3.2. FB0029: Twelfth thoracic vertebra

Context:	(1024)
Grid Ref:	98/113
Year of Excavation:	BR93
Other Details:	n/d

Element identification and preservation:
Fragment of an adult twelfth thoracic vertebra, consisting of the vertebral body, neural arch and superior and inferior articular facets. The element has been evaluated to numerical order according to the position and orientation of the superior and inferior articular

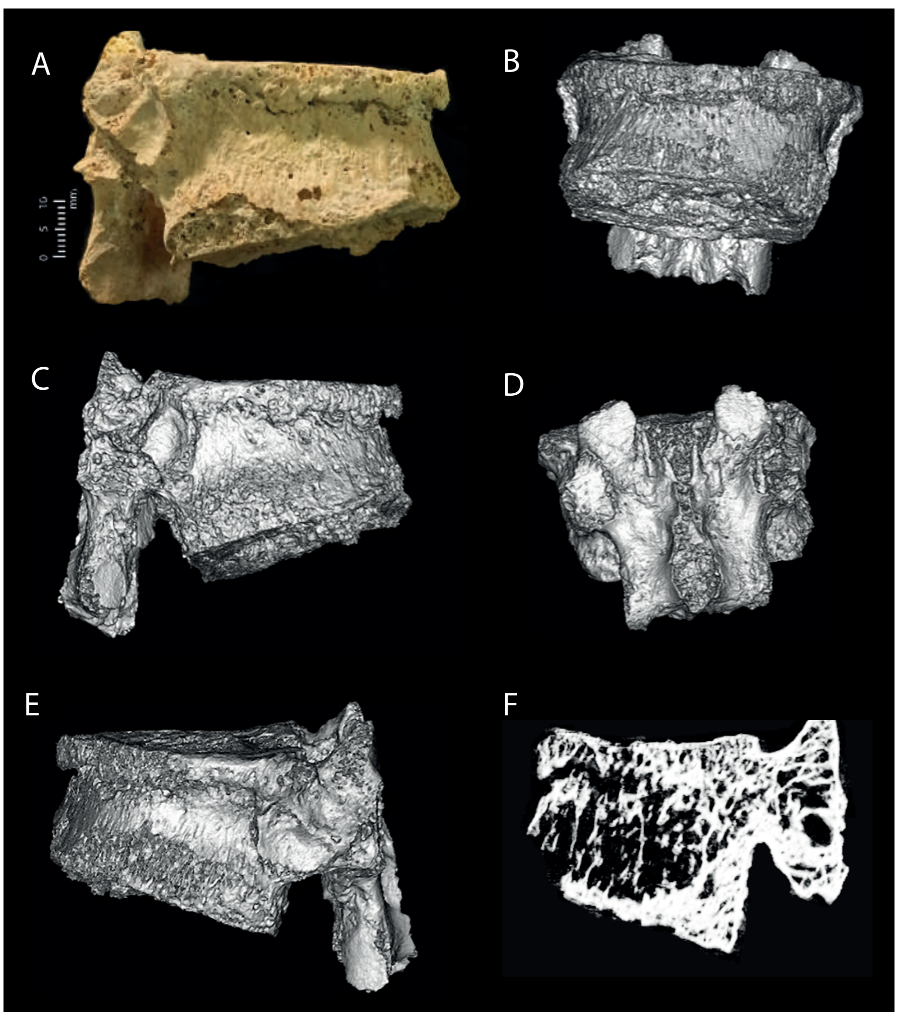

Figure 8.22. *A selection of photographic and radiological images pertaining to a fragmentary adult twelfth thoracic vertebra (FB0029) from Context (1024) of the Circle sample, exhibiting a compression fracture, intervertebral osteochondrosis and a Schmorl's Node: a) right lateral view; b) 3D render anterior view; c) 3D render right lateral view; d) 3D render posterior view; e) 3D render left lateral view; f) sagittal cross-section from CT data detailing fracture extending from anterior vertebral body through to the pedicle and pars interarticularis. Scale bar: 1 cm (photograph only). (Photo Ronika K. Power; radiological images captured by L. Buck, Cambridge Biotomography Centre; processed by J. Magnussen & M. Pardey, Macquarie Medical Imaging).*

facets and the costal articular facet. Age estimation is based on the degree of fusion of the overall element as well as the appearance and fusion of the superior and inferior annular rings (Scheuer & Black 2000: 183ff; esp. 211.). At present, there are no methods of sex assessment for isolated and fragmented vertebrae. The fragment represents ~30% of a complete second cervical vertebra. The extant element is in very good condition. All damage is assessed as *postmortem*.

Macroscopic observations:
The vertebral body exhibits a compression fracture on the anterior superior aspect (Fig. 8.22). The fracture is observed to be a clearly demarcated, approximately horizontal line that extends across the anterior and left and right lateral aspects of the vertebral body, approximately 6.5 mm immediately inferior to the superior border, terminating approximately 10.0 mm anterior to the costal articular facets on both left and right sides. The compression has resulted in the anterior aspect of the vertebral body assuming a wedge-shaped presentation: the height at the posterior aspect of the body is approximately 29.0 mm; while at the anterior aspect the body height is approximately 20.0 mm. Vertebral body fractures are commonly attributed to a vertical force-induced hyperflexion injury (Crawford-Adams 1983; Roberts & Manchester 2005, 105), which may include falling or jumping from a height and landing on the feet. This category of trauma is referred to as a compression fracture. Although compression fractures may occur as a result of vertical force injuries to healthy bone, differential diagnoses should also consider the possibility of underlying osteoporosis making the bone weak and susceptible to trauma (Brickley 2002; Brickley & Ives 2008; Roberts & Manchester 2005, 105).

There is a small amount of osseous change on the anterior superior aspect of the vertebral body, within the perimeter of the annular ring. This change presents as macroporosity (>1.0 mm Ø), cortical erosion and disorganization, which is slightly compromised by *postmortem* damage and diagenesis. It is likely that the changes described here are associated with degeneration of the cartilaginous joint surface of the intervertebral space (Roberts & Manchester 2005, 140). This type of degenerative disc disease is variably known as spondylosis and/or intervertebral osteochondrosis, presenting as porosity, pitting and disorganization of the vertebral body superior and/or inferior surfaces, sometimes accompanied by the formation of new bone (Rodgers 2000).

The inferior aspect of the vertebral body also presents osseous change, presenting as rough, irregular hypertrophy across the anterior third of the body, and also surrounding a convex feature on the posterior third of the body, which resembles a Schmorl's node. This change appears to be *antemortem* in nature and is thus not associated with the *perimortem* compression fracture described for this element, above. Schmorl's nodes are also associated with degenerative disc disease, whereby the herniating disc contents induce pressure erosion on the vertebral body surfaces (Roberts & Manchester 2005, 140; Rodgers 2000, 168). The specific aetiology of Schmorl's nodes is idiopathic (Park *et al.* 2015; Saluja *et al.* 1986), with associations ranging from trauma, infection, osteoporosis and neoplastic disease (Park *et al.* 2015; Resnick & Niwayama 1988). It should be noted that this element was identified within the same context as FB0030 (§8.5.3.3, below).

Radiological observations:
Anterior wedge compression fracture of the vertebral body, with 39% anterior height loss. The fracture line is visible through the vertebral body into the pedicle and *pars interarticularis*. There is significant disruption of the anterior body cortex, which is observed to have folded down upon itself as a result of the insult. Some trabeculae are observed to overlap posteriorly because of impaction, and a band of sclerosis above and below the fracture line in the posterior vertebral body indicates that the insult occurred moderately if not significantly *premortem*. This fracture has occurred alongside pre-existing severe osteoporosis; generalized demineralization and cortical bone loss is observed across the entire vertebral body, demonstrating osteopenia. An inferior endplate disc intrusion (Schmorl's node) is also observed.

Lesion types and healing status: Trauma; Mixed; Active.
Lesion preservation: Excellent; Incomplete because of fragmentation.
Differential diagnosis: Trauma; Metabolic; Degenerative Joint Disease.

8.5.3.3. FB0030: Lumbar vertebra

Context:	(1024)
Grid Ref:	98/113
Year of Excavation:	BR93
Other Details:	n/d

Element identification and preservation:
Fragment of an adult lumbar vertebral body of unknown order (possibly fourth or fifth – assessed according to the position and orientation of the extant superior articular facet); only the body, left pedicle and a portion of the left superior articular facet are extant. Age estimation is based on the degree of fusion of the overall element as well as the appearance and fusion

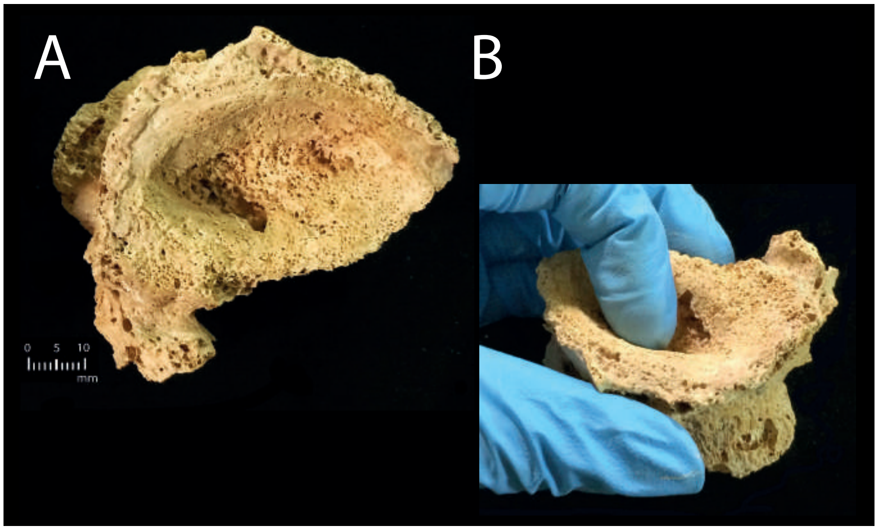

Figure 8.23. *Fragment of adult lumbar vertebral body of unknown order (FB0030) from Context (1024) of the Circle sample, exhibiting a central compression fracture: a) superior view; b) left supero-lateral view, detailing depth of central depression. Scale bar: 1 cm. (Photos Ronika K. Power).*

of the superior and inferior annular rings (Scheuer & Black 2000, 183ff; esp. 211.). At present, there are no methods of sex assessment for isolated and fragmented vertebrae. The fragment represents ~50% of a complete lumbar vertebra. The extant element is in very good condition. All damage is assessed as *postmortem*.

Macroscopic observations:
The extant portion of the vertebral body exhibits a compression fracture towards its central portion on the superior aspect on the coronal plane, creating a concave depression (Fig. 8.23a-b). On the anterior aspect of the body, the extant portion of this depression commences immediately posterior to the annular ring, and then steeply declines at an angle >45°; the depth of the compression fracture is approximately 13.6 mm. The fracture margin is discernible on the anterior aspect of the lesion, with the stark discontinuity of cortical bone presenting as an approximately straight line, adjacent to the exposed underlying trabeculae. At the antero-lateral aspects of the lesion, the fracture margin presents as V-shaped tears in the cortical bone, overlying the exposed trabeculae. *Postmortem* damage on the posterior and inferior aspects obfuscates the full extent of the lesion, so further observations are not possible.

As discussed above, vertebral body compression fractures are commonly attributed to a vertical force-induced hyperflexion injury (Roberts & Manchester 2005, 105). Although compression fractures may occur as a result of vertical force injuries to healthy bone, differential diagnoses should consider the possibility of underlying osteoporosis making the bone weak and susceptible to trauma (Brickley 2002; Brickley & Ives 2008; Roberts & Manchester 2005, 105). Marginal osteophytes are also observed on the left supero-antero-lateral aspects of the vertebral body.

It should be noted that this element was identified within the same context as FB0029 (§8.5.3.2, above). Considering these elements present similar forms of insult, it is possible that they may originate from the same individual. For further discussions of how pathology may assist in attempts to posthumously reunite individuals in highly fragmented and commingled assemblages, see §8.6, below.

Lesion type and healing status: Trauma; Healed.
Lesion preservation: Excellent; Incomplete because of *postmortem* damage.
Differential diagnosis: Trauma; Metabolic; Activity-related change.

8.5.3.4. FB0027: First lumbar vertebra

Context:	(1206)
Grid Ref:	99/111
Year of Excavation:	BR94
Other Details:	Unit 18

Element identification and preservation:
Fragmentary adult possible first lumbar vertebra. The position is estimated from the narrowness of the superior and inferior articular facets, and length and orientation of the spinous process in relation to the lamina. Approximately one-third of the vertebral body is extant on the left side, with the fragmentation margin observed to transect the body on the sagittal plane, exposing the trabecular bone. The remaining two-thirds of the vertebral body on the right side are not extant. The pedicle and right transverse process are also absent, and only the base of the right superior articular facet is extant. The apex of the left superior articular facet is also damaged, and the left transverse

process is broken and absent. Age estimation is based on the degree of fusion of the overall element as well as the appearance and fusions of the superior and inferior annular rings (Scheuer & Black 2000, 183ff; esp 211.). At present, there are no methods of sex assessment for isolated and fragmented vertebrae. The fragment represents ~65% of a complete lumbar vertebra. The extant element is in very good condition. All observed damage is attributed to *postmortem* processes.

Macroscopic observations:
The extant portion of the vertebral body exhibits a healed compression fracture towards its central portion on the superior aspect, creating a concave depression (Fig. 8.24a-e). The innermost extant portion of this depression is located approximately 17.1 mm posterior to the most anterior aspect of the vertebral body, and approximately 15.0 mm medial to the most lateral extant aspect of the vertebral body, and approximately 8.2 mm deep to the most lateral-superior extant aspect of the vertebral body. On the extant portion of the superior aspect of the vertebral body, a ridge of irregular, rough, disorganized bone of approximately 5.1 mm width and approximately 2.6 mm height is observed directly superior to the fracture margin, extending from the fragmentation margin in a curvilinear, postero-lateral direction across the surface to terminate at the supero-lateral margin of the vertebral body.

As discussed above, vertebral body compression fractures are commonly attributed to a vertical force-induced hyperflexion injury (Roberts & Manchester 2005, 105). Although compression fractures may occur as a result of vertical force injuries to healthy bone, differential diagnoses should consider the possibility of underlying osteoporosis making the bone weak and susceptible to trauma (Brickley 2002; Brickley & Ives 2008; Roberts & Manchester 2005, 105).

Many of the underlying trabeculae are damaged because of *postmortem* processes, so further observations are not possible. Eburnation is observed on the extant portion of the left superior and left and right inferior articular facets. On the left superior articular facet, a thin strip of eburnation is observed on the most antero-superior aspect of the extant facet border. As

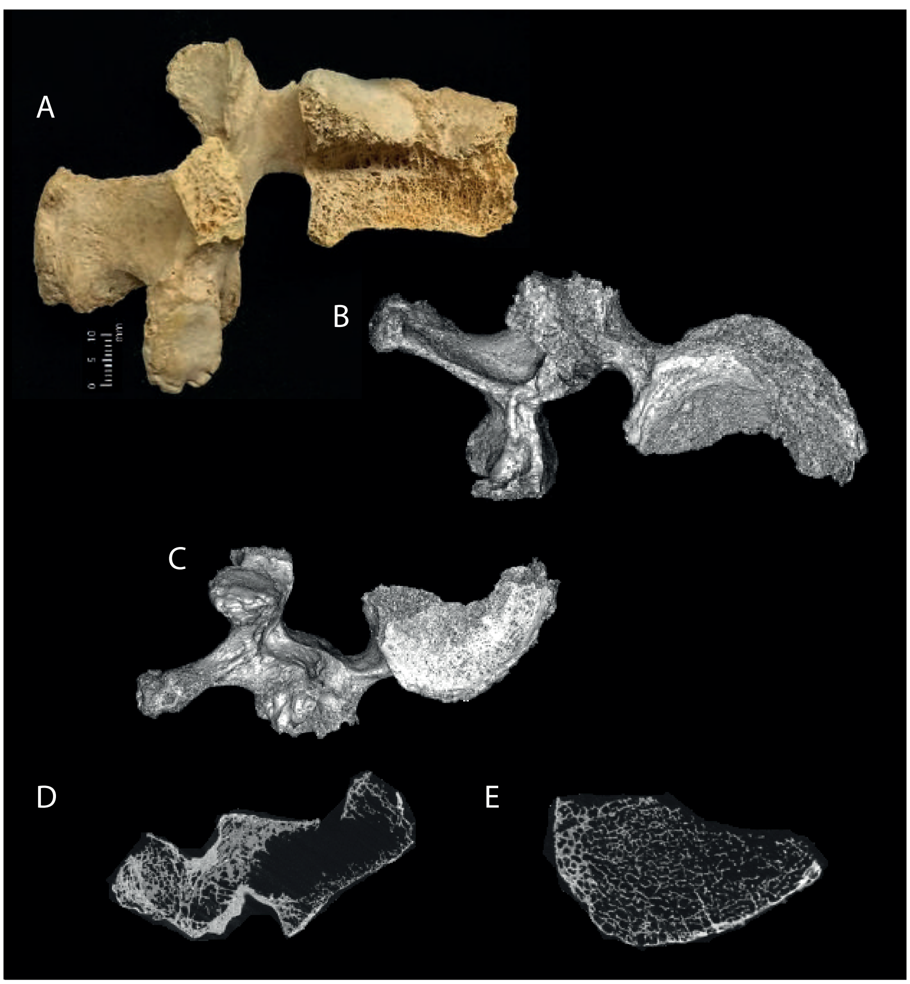

Figure 8.24. *A selection of photographic and radiological images of a fragment of adult possible first lumbar vertebra (FB0027) from Context (1026) of the Circle sample, exhibiting a central compression fracture: a) right lateral view; b) 3D render superior view; c) 3D render inferior view; d) sagittal cross-section from CT data detailing depth of central depression; e) transverse cross-section detailing osteopenia indicative of osteoporosis. Scale bar: 1 cm (photograph only). (Photos Ronika K. Power; radiological images captured by L. Buck, Cambridge Biotomography Centre; processed by J. Magnussen & M. Pardey, Macquarie Medical Imaging).*

a result of fragmentation, the full extent of the lesion is not known. The dimensions of the extant portion of the lesion are 5.2 mm length by 1.1 mm width. The lesion comprises a focal, narrow strip of dense, highly reflective bone. On the left inferior articular facet, tiny eburnation points are observed along the most postero-superior aspects of the facet border, extending across a length of approximately 11.3 mm. On the right inferior articular facet, eburnation is observed on the most postero-superior aspect of the facet in an approximate crescent-shaped lesion with maximum dimensions of approximately 11.5 mm length by 4.5 mm width; and tiny eburnation points are observed along the anterior aspect of the facet border, extending across a length of approximately 14.0 mm. In all aspects, the lesion is characterized as a discrete area of dense, highly reflective bone.

Radiological observations:
Significant vertebral endplate crush fracture. There has been an estimated 35% anterior height loss, and 56% central height loss (Fig. 8.24d). This is typical expression of central endplate collapse as opposed to a vertebral body compression fracture associated with purely traumatic origins. Here again, we observe characteristic signs of severe osteopenia indicative of osteoporosis – general demineralization and diminution of trabeculae (Fig. 8.24e). The vertebral body lost structural integrity and with axial loading the intervertebral disc has intruded into the end plate. Of the extant facet joints, there is evidence of moderate hypertrophic change in this individual, indicative of degenerative joint disease.

Lesion types and healing status: Trauma; Healed; Mixed; Active.
Lesion preservation: Excellent; Incomplete because of *postmortem* damage.
Differential diagnosis: Trauma; Degenerative Joint Disease; Metabolic.

8.5.3.5. FB0028: Lumbar vertebra

Context:	(951)
Grid Ref:	n/d
Year of Excavation:	BR94
Other Details:	Misc. A4

Element identification and preservation:
The element consists of a fragmented lumbar vertebral body of unknown order; only the body is extant. The body itself is incomplete, being fragmented anterior to the bilateral pedical bases and the anterior wall of the vertebral foramen. Age estimation is based on the degree of fusion of the overall element as well as the appearance and fusion of the superior and inferior annular rings (Scheuer & Black 2000, 183ff; esp 211). At present, there are no methods of sex assessment for isolated and fragmented vertebrae. The fragment represents ~45% of a complete lumbar vertebra. The extant element is in very good condition. All damage is assessed as *postmortem*.

Macroscopic observations:
The extant portion of the vertebral body exhibits a compression fracture towards its central portion on the superior aspect on the sagittal plane, creating a

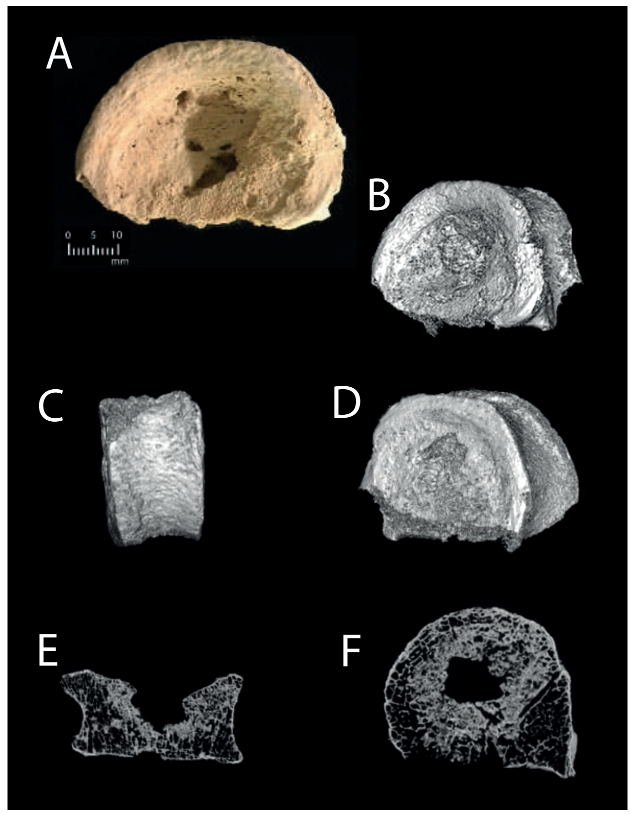

Figure 8.25. *A selection of photographic and radiological images of a fragment of adult lumbar vertebral body of unknown order (FB0028) from Context (951) of the Circle sample, exhibiting a central compression fracture: a) superior view; b) 3D render right supero-lateral view; c) 3D render anterior view; d) 3D render left infero-lateral view; e) coronal cross-section from CT data detailing depth of central depression; f) transverse cross-section detailing osteopenia indicative of osteoporosis. Scale bar: 1 cm (photograph only). (Photos Ronika K. Power; radiological images captured by L. Buck, Cambridge Biotomography Centre; processed by J. Magnussen & M. Pardey, Macquarie Medical Imaging).*

concave depression (Fig. 8.25a-f). On the anterior aspect of the body, the extant portion of this depression commences immediately posterior to the annular ring, and then steeply declines at an angle >45°; the true depth of the compression fracture is unable to be determined because of *postmortem* damage. One aspect of the fracture margin is extant on the right anterior superior aspect of the vertebral body, with a sharp discontinuity between the cortical surfaces on either side of the margin, while the cortical surfaces are still intact. *Postmortem* damage on the posterior and central aspects obfuscates the full extent of the lesion, so further observations are not possible.

As discussed above, vertebral body compression fractures are commonly attributed to a vertical force-induced hyperflexion injury (Roberts & Manchester 2005, 105). Although compression fractures may occur as a result of vertical force injuries to healthy bone, differential diagnoses should consider the possibility of underlying osteoporosis making the bone weak and susceptible to trauma (Brickley 2002; Brickley & Ives 2008; Roberts & Manchester 2005, 105).

Radiological observations:
Another vertebral endplate crush fracture. There has been significant disc intrusion through the endplate; the element has lost approximately 30% height overall with bowing of the endplate, and 72% height centrally at the site of disc intrusion (Fig. 8.25e-f). The margins are observed to be quite sclerotic; implying this insult occurred a long time before death. The insult has once again occurred because of pre-existing moderate trabecular loss, demonstrating osteopenia, characteristic of osteoporosis. Although the insult appears to be more extreme than those described for FB0027 and FB0029 (§8.5.3.4 & §8.5.3.2, above), the underlying osteopenic condition appears to be slightly less severe (Fig. 8.25f).

Lesion type and healing status: Trauma; Healed.
Lesion preservation: Excellent; Incomplete because of *postmortem* damage.
Differential diagnosis: Trauma; Metabolic.

8.5.3.6. FB0032: Lumbar vertebra

Context:	(662)
Grid Ref:	98-99/107
Year of Excavation:	BR91
Other Details:	Quad X

Element identification and preservation:
Fragment of an adult lumbar vertebra of unknown order (possibly fourth or fifth – assessed from the position and orientation of the extant superior articular facet); only the body, right pedicle and a portion of the left superior articular facet and lamina are extant. Age estimation is based on the degree of fusion of the overall element as well as the appearance and fusions of the superior and inferior annular rings (Scheuer & Black 2000, 183ff; esp. 211). At present, there are no methods of sex assessment for isolated and fragmented vertebrae. The fragment represents ~30% of a complete second cervical vertebra. The extant element is in very good condition. All damage is assessed as *postmortem*.

Macroscopic observations:
The extant portion of the vertebral body exhibits a compression fracture on the left supero-lateral aspect on the sagittal plane, creating a concave depressio*n* (Fig. 8.26). On the anterior aspect of the body, the extant portion of this depression commences immediately posterior to the annular ring, and then steeply declines at an angle of >45°; the maximum extant depth of the compression fracture is approximately 3.6 mm, however the full extent of the lesion is obfuscated as a result of *postmortem* damage. The fracture margin is discernible on the anterior aspect of the lesion, with the compression of the superior border of the body creating a ridge approximately 5.0 mm thick, which traverses the entire anterior aspect of the body. The compression has resulted in the anterior aspect of the vertebral body assuming a wedge-shaped presentation: the height at the posterior aspect of the body is approximately 26.5 mm; while at the anterior aspect the body height is approximately 19.5 mm. All bone surrounding the fracture site is intact and continuous, there is no evidence of new bone deposition, so the insult is determined to have occurred *antemortem* and is

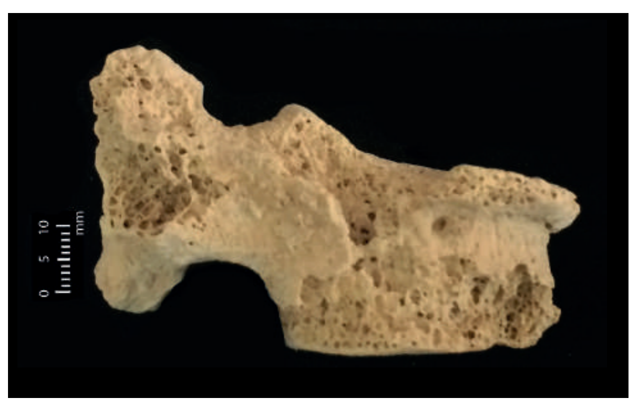

Figure 8.26. *Fragment of adult lumbar vertebral body of unknown order (FB0032) from Context (662) of the Circle sample, exhibiting an anterior compression fracture; right lateral view. Scale bar: 1 cm. (Photo Ronika K. Power).*

fully healed. *Postmortem* damage on the posterior and inferior aspects obfuscates the full extent of the lesion, so further observations are not possible.

As discussed above, vertebral body compression fractures are commonly attributed to a vertical force-induced hyperflexion injury (Roberts & Manchester 2005, 105). Although compression fractures may occur as a result of vertical force injuries to healthy bone, differential diagnoses should consider the possibility of underlying osteoporosis making the bone weak and susceptible to trauma (Brickley 2002; Brickley & Ives 2008; Roberts & Manchester 2005, 105). Marginal osteophytes are observed on the right infero-lateral aspects of the vertebral body – the full extent of osteophyte development is obfuscated as a result of *postmortem* damage.

Lesion types and healing status: Trauma; Healed; Proliferative.
Lesion preservation: Excellent, Incomplete because of *postmortem* damage.
Differential diagnosis: Trauma; Metabolic; Activity-related change.

8.5.3.7. FB0007: Humerus

Context:	(951)
Grid Ref:	n/d
Year of Excavation:	BR94
Other Details:	B1–13

Element identification and preservation:
Fragment of a right adult humerus. At the distal aspect, the element is fragmented inferior to the deltoid tuberosity so that approximately half of the diaphysis is retained. At the proximal aspect, the element is fragmented at the approximate surgical neck so that the supero-medial features are absent, including the humeral head. Proximally and anteriorly the fragmentation line is medial to the lesser tubercle running inferiorly to the approximate surgical neck. Posteriorly, only part of the trabecular bone is retained in the region of the head and surgical neck. The fragmentation described here pertains to *postmortem* damage, however it is important to note that the extant element was severely dysplastic *in vivo*, as discussed further, below. It is thus difficult to attribute the extant features to typical anatomical landmarks. As a result of the *postmortem* fragmentation, it is likely that some observations of pathology are obfuscated. Adult age estimation is based on the extant size of the element as well as the relative thickness of the diaphyseal cortex. At present, there are no reliable methods of sex assessment for isolated humeri. Although Bass (1995, 156) reports on several methods based on metric analyses including the head vertical and transverse diameters (Dittrick 1979; Dittrick & Suchey 1986; Dwight 1905; Krogman 1962; Stewart 1979); length and epicondylar width (Thieme 1957; Rodgers 1999); and a single variable complex (France 1983), there is still little confidence in these methods as reliable stand-alone indicators of sexual dimorphism without further studies. A further non-metric approach to sex assessment of the adult humerus is that proposed by Trotter (1934) whereby the septal aperture (or supratrochlear foramen) occurs slightly more frequently in females than males. In any case, the element under study is too fragmentary and dysplastic to submit to any of these modes of analysis. The fragment represents ~55% of a complete humerus. The extant element is in good condition. All damage is assessed as *postmortem*.

Macroscopic observations:
A complex non-reduced healed fracture is observed on the proximal metaphysis and proximal half of the diaphysis of the right humerus (Fig. 8.27a-h). The lesion is located at the approximate surgical neck. The element is severely dysplastic as a result of the fracture complex which includes at least one complete oblique displaced fracture and one metaphyseal compression/crush fracture. When viewed anteriorly, the extant proximal third of the humeral metaphysis has been infero-laterally displaced (Fig. 8.27a), possibly associated with a complete oblique displaced fracture. When viewed medially, the humeral head is posteriorly and inferiorly displaced (Fig. 8.27b), possibly associated with a metaphyseal compression/crush fracture.

From posterior and lateral views, bony callus is observed to envelop the lateral aspect of the diaphysis (Fig. 8.27c-d), with the extant portion emanating from a point 12.3 mm superior to the most superior aspect of the deltoid tuberosity and extending 39.9 mm in a supero-lateral direction. When viewed anteriorly (Fig. 8.27a), bony callus is also observed to extend from the diaphysis to meet the displaced complete fracture fragment approximately 38.9 mm inferior to the superior aspect of the greater tubercle. The anterior portion of bony callus emanates approximately 8.8 mm directly anterior to the most superior aspect of the deltoid tuberosity. Posteriorly the bony callus is 39.0 mm in length and has a maximum width of 30.1 mm. The maximum antero-posterior width of the callus is 25.7 mm.

The surface of the bony callus is observed to be smooth and even in some areas, while undulating, billowing and/or porous in others. The undulating areas are characterized by peaks and troughs of new bone deposition with diffuse circular and oval pitting.

Figure 8.27. *A selection of photographic and radiological images pertaining to a fragmentary adult right humerus (FB0007) from Context (951) of the Circle sample, detailing a complex non-reduced healed fracture of the proximal metaphysis and diaphysis in the region of the surgical neck, including: a) anterior view; b) medial view; c) posterior view; d) lateral view; e) coronal cross-section from CT data; f–h) transverse cross-sections of varying heights moving superiorly to inferiorly through the bony callus. Scale bar: 1 cm (photographs only). (Photos Ronika K. Power; radiological images captured by L. Buck, Cambridge Biotomography Centre; processed by J. Magnussen & M. Pardey, Macquarie Medical Imaging).*

The pits range from 0.6–4.6 mm Ø, meaning that both macroporosity and microporosity are observed; the pits are generally well-defined with smooth margins. The extent and character of the extant callus and the associated porosity suggests that the element may have been subject to infectious processes such as osteomyelitis which were no longer active at the time of death of the individual. As a result of the *post-mortem* fragmentation, it is impossible to assess reliably the overall healing status of the complex fracture of this element.

Postmortem fragmentation enables components of the fracture complex to be observed in cross-section. As a result, a possible third complete transverse fracture is observed for the diaphysis approximately 56.4 mm supero-medial to the most superior point of the deltoid tuberosity. New bone deposition is observed on the margin of this transverse fracture, indicating that it had not unified with any associated superior bone fragments within the fracture complex.

Roberts and Manchester report that humerus fractures are not common in archaeological populations (2005, 105), so the evidence presented here is particularly valuable to the palaeopathological discourse. Clinical reports provide indications that proximal humerus fractures are most often observed in elderly women with osteoporosis who have suffered a falling accident (Crawford-Adams 1983; cf Buhr & Cooke 1959; Roberts & Manchester 2005, 95). In the absence of any other diagnostic elements or biomolecular analyses, however, the demographic profile of this individual remains unknown.

Radiological observations:

A great deal of osseous remodelling is observed radiologically for the proximal aspect of the humerus (Fig. 8.27e-h). The diaphyseal cortex appears demineralized and denuded, indicative of disuse atrophy. The new bone deposition is not of a high density or quality, but rather it is comprised of several thin layers with a porotic appearance. There is a discernible margin between the original cortex and the new bone. The features observed here nonetheless indicate that the cortex was being re-established with some ongoing biomechanical stress and weightbearing at the time of death – although the poor quality and density of the remodelled bone and underlying cortex are suggestive of prolonged disuse atrophy. It is apparent that this individual has survived for a long time after the initial insult, indicative of a level of care administered to them within their community while recuperating from this very serious injury.

The fractures described above are most likely because of a combination of impaction, rotation and comminution – potentially associated with a falling accident, direct trauma, and/or rotational injuries (especially forced external rotation), in isolation or combination. Areas of irregular dysplastic bone could be *myositis ossificans traumatica*, or partially resorptive change associated with comminuted fragments being resorbed into surrounding tissue; it is not possible to distinguish between them radiologically.

Lesion type and healing status: Trauma; Healing.
Lesion preservation: Good; Incomplete because of *postmortem* damage.
Differential diagnosis: Trauma.

8.5.3.8. FB0015: Humerus

Context:	(951)
Grid Ref:	n/d
Year of Excavation:	BR93
Other Details:	G1, No.42

Element identification and preservation:
Right adult humerus, fragmented proximally and distally *postmortem*. The proximal fragmentation margin is located at the approximate mid-shaft of the diaphysis, inferior to the deltoid tuberosity. The proximal fragments of this element are not retained. At the distal aspect, the element is fragmented in an approximately diagonal manner across the metaphysis. The fragmentation margins are sharp and linear, indicative of excavation trauma. From an anterior perspective, the fragmentation line transects the lateral epicondyle, radial fossa, coronoid fossa and medial epicondyle. The distal fragment is retained. Adult age estimation is based on the size of the extant element, the relative thickness of the diaphyseal cortex and the complete fusion of the distal epiphysis (Scheuer & Black 2000, 274). As discussed above, there are currently no reliable methods of sex assessment for isolated humeri. The fragment represents ~55% of a complete humerus and is in excellent condition. All damage is assessed as *postmortem*.

Figure 8.28. *Fragment of adult right humerus (FB0015) from Context (951) of the Circle sample, exhibiting dysplasia of the of the mid-diaphysis; anterior view. Scale bar: 1 cm. (Photo Ronika K. Power).*

Macroscopic observations:
The mid-shaft of the diaphysis is dysplastic (Fig. 8.28). When viewed anteriorly, the extant supero-lateral aspect of the fragmented diaphysis is observed to be misshapen, bowing laterally relative to the infero-lateral aspect of the element. The most infero-lateral point of this misshapen area may be placed at approximately 36.4 mm from the most superior extant point of the lateral aspect of the diaphysis. The character of the cortical surface of this area is even and smooth and generally continuous with the surrounding bone surface, except for the most inferior aspect which is more rugose.

When viewed anteriorly, the medial aspect of the diaphysis communicates with the previously mentioned dysplasia by reflecting slight misalignment through bowing parallel to the lateral aspect of the element at this level. Inferior to this described dysplasia, the diaphysis descends inferiorly in a normal manner. When viewed laterally it is possible that the distal aspect of the element may curve anteriorly.

The dysplasia is attributed to a healed fracture with associated displacement of muscle attachments subsequent to healing; the continuous and even character of the cortical surface in the region of the feature is suggestive of this being a historic insult. As discussed above, humerus fractures are infrequently observed in archaeological populations and as such this example is of particular interest for understanding lived experiences of trauma and care within Neolithic Maltese populations.

Lesion type and healing status: Trauma; Healed.
Lesion preservation: Excellent; Incomplete because of *postmortem* damage.
Differential diagnosis: Trauma; Congenital variation; Activity-related change.

8.5.3.9. FB0008: Ulna

Context:	(354)
Grid Ref:	n/d
Year of Excavation:	BR89
Other Details:	Area 3, Unit 75

Element identification and preservation:
Right adult ulna, fragmented distally *postmortem*. The fragmentation margin is located in the distal quarter of the diaphysis, transecting the superior aspect of the pronator ridge. The distal fragment is not retained. There is a slight amount of *postmortem* damage observed on the infero-medial aspect of the olecranon, on the medial margin of the trochlear notch, extending onto the coronoid process. Adult age estimation is based on the size of the extant element, the relative thickness of the diaphyseal cortex and the complete fusion of the proximal epiphysis (Scheuer & Black 2000, 298ff.). Although Purkait (2001) devised

Figure 8.29. *A selection of photographic and radiological images pertaining to a fragmentary adult right ulna (FB0008) from Context (354) of the Circle sample, detailing a healed fracture of the distal diaphysis, including: a) antero-medial view; b) 3D render posterior view; c) 3D render postero-lateral view; d) 3D render anterior view; e) coronal cross-section from CT data; f–g) transverse cross-sections moving superiorly to inferiorly through the bony callus, detailing fracture dynamics. Scale bar: 1 cm (photograph only). (Photos Ronika K. Power; radiological images captured by L. Buck, Cambridge Biotomography Centre; processed by J. Magnussen & M. Pardey, Macquarie Medical Imaging).*

a discriminant function for metric sex assessment of ulnae, it is not widely applied as it is yet to be comprehensively tested beyond the population on which it was based. As such, there are currently no reliable methods of sex assessment for isolated ulnae (Bass 1995, 175; White & Folkens 2005). The fragment represents ~90% of a complete ulna and is in very good condition. All damage is assessed as *postmortem*.

Macroscopic observations:
A healed fracture is observed on the distal third of the diaphysis of the right ulna (Fig. 8.29a-g). The element is slightly dysplastic as a result of the fracture which has healed completely. When viewed anteriorly, the healed fracture margin runs from a point along the interosseous crest 147.5 mm inferior to the most inferior point of the radial notch; the fracture margin then diverts infero-medially 14.9 mm superior to the most superior point of the pronator ridge.

Bony callus is observed to envelop the entire circumference of the diaphysis in the location of the fracture; when viewed anteriorly the maximum callus length is 31.8 mm and maximum width is 19.1 mm. The extant surface of the bony callus across this feature is continuous in character with the surrounding bone. When viewed medially an oval-shaped area of *postmortem* damage is observed in the bony callus 25.9 mm supero-posterior to the pronator ridge.

Forearm and wrist (radius and ulna) fractures have been observed in both archaeological and modern populations across cultures (Buhr & Cooke 1959; Judd 2000; Roberts & Manchester 2005). It is likely that this fracture was caused by an acute and direct insult to the forearm *in vivo* (Roberts & Manchester 2005, 90), either as a result of intentional interpersonal violence (such as defending a blow to the head) or accidental injury, such as a falling accident or misadventure involving animals (Judd 2004; Jurmain 1999).

Radiological observations:
A completely healed transverse fracture is observed in the distal third of the ulna diaphysis with minor residual angulation and discontinuity of the underlying native cortex (Fig. 8.29e-g). Periosteal new bone has bridged the defect and has been exuberant in activity. The fracture is completely healed but malaligned. Malalignment is approximately 15°; and the offset at the fracture site is approximately 34% (Fig. 8.29*e*). There is no evidence of sequestrum or involucrum, and no evidence of infection. The periosteal new bone is trabeculated, indicating that this is a very old fracture, which occurred many years before death (Fig. 8.29f-*g*). Transverse fractures of the distal ulnar diaphysis are commonly associated with self-defence – so-called 'parry' or 'nightstick' fractures, named from injuries sustained by modern individuals' holding up the forearm in front of the face to defend themselves when struck with a police baton, or any direct trauma to the forearm (Ali *et al.* 2019; Cai *et al.* 2013; Court-Brown & Caesar 2006; Cybulski 2014; Du Toit & Gräbe 1979; Glencross & Boz 2014; Hooper 1974; Klaus 2014; Knüsel & Smith 2014, 10; Ortner 2003; Redfern 2015; Roberts & Manchester 2005; however, cf Judd 2008). Falls and twisting injuries more commonly result in spiral fractures (Mackay *et al.* 2000), which lead to a greater extent of periosteal and cortical remodelling than observed for this individual.

Lesion type and healing status: Trauma; Healed
Lesion preservation: Excellent.
Differential diagnosis: Trauma; Congenital variation; Activity-related change.

8.5.3.10. FB0009: Ulna

Context:	(951)
Grid Ref:	n/d
Year of Excavation:	BR93
Other Details:	H1, No.6

Element identification and preservation:
Left adult ulna, fragmented and complete. The element is fragmented distal to the midpoint of the diaphysis. The fragmentation margins are clean and sharp, and both retained proximal and distal fragments perfectly refit. Adult age estimation is based on the size of the extant element, the relative thickness of the diaphyseal cortex and the complete fusion of the proximal epiphysis (Scheuer & Black 2000, 298ff.). As previously mentioned, there are currently no reliable methods of sex assessment for isolated ulnae (Bass 1995, 175). The extant element is in excellent condition. All damage is assessed as *postmortem*.

Macroscopic observations:
A healed fracture is observed on the distal quarter of the diaphysis of the left ulna (Fig. 8.30a-f). The element is slightly dysplastic; it is observed that the distal quarter of the diaphysis is misaligned in a lateral direction by 10°. This dysplasia is also clearly observed from a posterior aspect. The extant surface area surrounding the fracture is continuous in character with the surrounding bone and the fracture margin is not visible. When viewed anteriorly the most infero-lateral aspect of the healed fracture is located 21.4 mm superior to the most infero-lateral aspect of the radial articulation.

It is likely that this fracture was caused by an acute and direct insult to the forearm *in vivo* (Roberts

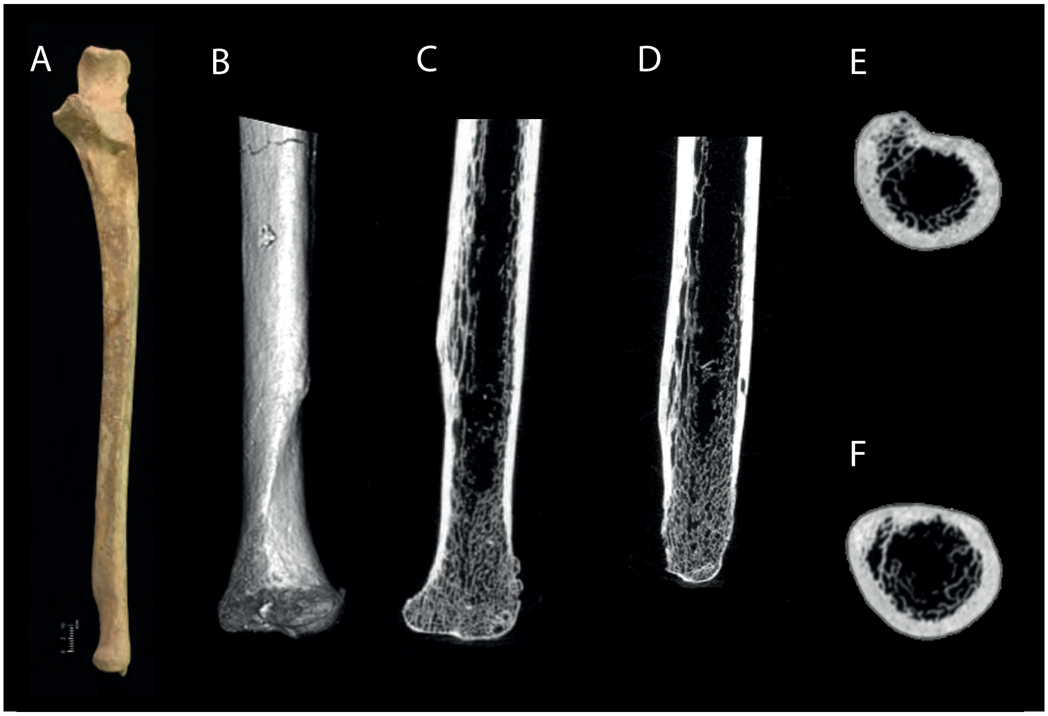

Figure 8.30. *A selection of photographic and radiological images pertaining to an adult left ulna (FB0009) from Context (951) of the Circle sample, detailing a healed fracture of the distal diaphysis, including: a) anterior view; b) 3D render, lateral view; c–d) coronal cross-sections from CT data, detailing cortical dysplasia and deeper internal margin of medullary wall; e–f) transverse cross-sections moving superiorly to inferiorly through the diaphysis, internal margin of medullary wall. Scale bar: 1 cm (photograph only). (Photo Ronika K. Power; radiological images captured by L. Buck, Cambridge Biotomography Centre; processed by J. Magnussen & M. Pardey, Macquarie Medical Imaging).*

& Manchester 2005, 90), either as a result of intentional interpersonal violence or accidental injury (Judd 2004; Jurmain 1999). It is suggested that this fracture occurred many years *antemortem*, as there are no observable fracture or callus margins. The cortex surrounding the dysplastic area is smooth and continuous.

Radiological observations:
Slight dysplasia is observed in the distal ulnar diaphysis. Although the element appears relatively underwhelming in cross section, we nonetheless note a bulge in the cortex at the site of dysplasia with focal cortical thinning (Fig. 8.30c-d). Small vascular channels are observed to pierce the cortex, although this is normal. In cross-section, a thin internal margin is observed to delineate a narrower internal wall of the medullary cavity, possibly indicating an original margin displaced by a fracture (Fig. 8.30c-f). In the absence of periosteal reaction, the extensive cortical remodelling suggests this is a long-standing abnormality. See comments above regarding possible causes of this abnormality (FB0008; §8.5.3.9). This represents a long-term healed and slightly remodelled fracture.

Lesion type and healing status: Trauma; Healed.
Lesion preservation: Excellent.
Differential diagnosis: Trauma; Congenital variation; Activity-related change.

8.5.3.11. FB0010: Ulna

Context:	(960)
Grid Ref:	99E/113N
Year of Excavation:	BR94
Other Details:	Spit 3, No.7–8

Element identification and preservation:
Left adult ulna, fragmented distally *postmortem*. The fragmentation margin is located in the distal quarter of the diaphysis, immediately superior to the ulnar head. The distal fragment is not retained. There is a slight amount of *postmortem* damage observed on the proximal aspect of the olecranon. Adult age estimation is based on the size of the extant element, the relative thickness of the diaphyseal cortex and the complete fusion of the proximal epiphysis (Scheuer & Black 2000, 298ff.). As mentioned above, there are currently

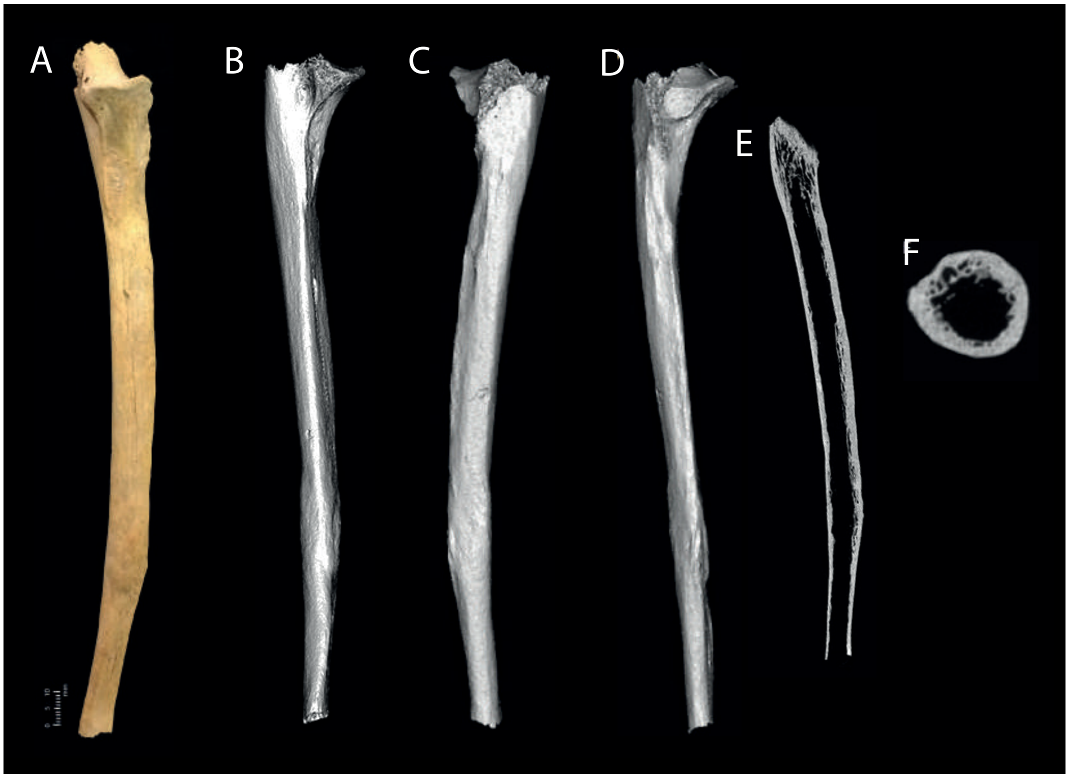

Figure 8.31. *A selection of photographic and radiological images pertaining to a fragmented adult left ulna (FB00010) from Context (960) of the Circle sample, detailing a healed fracture of the distal diaphysis, including: a) anterior view; b) 3D render medial view; c) 3D render posterior view; d) 3D render lateral view; e) coronal cross-section from CT data detailing dysplasia; f) transverse cross-section detailing cortical thinning and altered trabeculation. Scale bar: 1 cm (photograph only). (Photo Ronika K. Power; radiological images captured by L. Buck, Cambridge Biotomography Centre; processed by J. Magnussen & M. Pardey, Macquarie Medical Imaging).*

no reliable methods of sex assessment for isolated ulnae (Bass 1995, 175). The fragment represents ~95% of a complete ulna. The extant element is in excellent condition. All damage is assessed as *postmortem*.

Macroscopic observations:
A healed fracture is observed on the distal quarter of the diaphysis of the left ulna (Fig. 8.31a-f). The element is slightly dysplastic; it is observed that the distal quarter of the diaphysis is misaligned in a lateral direction at the approximate most superior point of the pronator ridge. This dysplasia is also clearly observed from a posterior aspect.

From an anterior view, bony callus is observed with the extant portion emanating from a point 10.4 mm superior to the most superior aspect of the pronator ridge and extending superiorly 21.2 mm with a maximum width of 7.8 mm. The surface of the bony callus is observed to be smooth and even in most areas, while slightly billowing in others. The extant surface area surrounding the fracture is continuous in character where the surrounding bone and the fracture margin are not visible.

Here again, it is likely that this fracture was caused by an acute and direct insult to the forearm *in vivo* (Roberts & Manchester 2005, 90), either as a result of intentional interpersonal violence or accidental injury (Judd 2004; Jurmain 1999). It is also suggested that this fracture occurred many years *antemortem*, as there are no observable fracture or callus margins. The cortex surrounding the dysplastic area is smooth and continuous.

Radiological observations:
A completely healed transverse fracture is observed on the distal ulna diaphysis. The element is dysplastic distal to the fracture site; the diaphysis is diverted 22° from the proximal aspect (Fig. 8.31e). At the fracture site, cortical irregularity and loss of cortical thickness is noted, as well as altered trabeculation (Fig. 8.31f). On the convex side of the curvature there is overall cortical thinning and remodelling at the site of prior

injury. See comments above regarding possible causes of this fracture (FB0008; §8.5.3.9).

Lesion type and healing status: Trauma; Healed.
Lesion preservation: Excellent.
Differential diagnosis: Trauma; Congenital variation; Activity-related change.

8.5.3.12. FB0011: Ulna

Context:	(951)
Grid Ref:	98E/116.5–117N
Year of Excavation:	BR94
Other Details:	Area X

Element identification and preservation:
Right adult ulna, fragmented *postmortem*. The fragmentation margin is located in the distal quarter of the diaphysis, in the region of the pronator ridge. The styloid process is fragmented and absent. The proximal aspect of the element is not retained. Adult age estimation is based on the size of the extant element, the relative thickness of the diaphyseal cortex and the complete fusion of the distal epiphysis (Scheuer & Black 2000, 298ff.). As mentioned before, there are currently no reliable methods of sex assessment for isolated ulnae (Bass 1995, 175). The fragment represents ~15% of a complete ulna. The extant element is in excellent condition. All damage is assessed as *postmortem*.

Macroscopic observations:
A complete healed fracture is observed on the distal quarter of the diaphysis of the right ulna (Fig. 8.32a-g). When viewed from a lateral aspect, the distal portion of the element is displaced posteriorly and superiorly to the proximal portion. The element is slightly dysplastic; it is observed that the distal third of the diaphysis is misaligned in a lateral direction by approximately 5°.

Bony callus is observed to envelop the circumference of the diaphysis. When viewed anteriorly, the extant portion of callus emanates from a point 36.5 mm superior to the most inferior aspect of the radial articulation, extending superiorly 14.6 mm with a maximum width of 13.4 mm. When viewed laterally the maximum callus length is 18.0 mm with a maximum width of 16.5 mm. The surface of the bony callus is smooth and even in most areas, while slightly billowing in others. The extant surface area of the bony callus is continuous in character with the surrounding bone, and the fracture margin is not visible.

Figure 8.32. *A selection of photographic and radiological images pertaining to a fragmented adult right ulna (FB00011) from Context (951) of the Circle sample, detailing a healed fracture of the distal diaphysis, including: a) antero-lateral view; b) 3D render lateral view; c) 3D render posterior view; d) 3D render medial view; e) sagittal cross-section from CT data, detailing impaction and overlap of cortices and bony callus; f) coronal cross-section, detailing fracture site and bony callus; g) transverse cross-section, detailing bony callus and trabecular reorganization. Scale bar: 1 cm (photograph only). (Photo Ronika K. Power; radiological images captured by L. Buck, Cambridge Biotomography Centre; processed by J. Magnussen & M. Pardey, Macquarie Medical Imaging).*

Once again, it is likely that this fracture was caused by an acute and direct insult to the forearm *in vivo* (Roberts & Manchester 2005, 90), either as a result of intentional interpersonal violence or accidental injury (Judd 2004; Jurmain 1999).

Radiological observations:
Observed radiologically, the fracture plane appears to be simple and transverse (Fig. 8.32e-g). The extant element presents relatively minor angulation because of the fracture, with only small amounts of impaction and overlap between cortices (Fig. 8.32e-f). Extensive, healthy bony remodelling is observed, indicating that the injury is completely healed. The extant cortex looks dense and consistent at both proximal and distal aspects, with no evidence of complicating factors including disuse or infection (Fig. 8.32g). The insult is located in the classical position for so-called 'nightstick' fractures, presenting the possibility that this fracture may have been sustained in an act of self-defence. See comments above for further description (FB0008; §8.5.3.9).

Lesion type and healing status: Trauma; Healed.
Lesion preservation: Excellent.
Differential diagnosis: Trauma.

8.5.3.13. FB0012: Ulna

Context:	(799)
Grid Ref:	107E/114N
Year of Excavation:	BR93
Other Details:	Layer 37, Complete Skeleton

Element identification and preservation:
Complete left adult ulna. Adult age estimation is based on the size of the extant element and the complete fusion of both proximal and distal epiphyses (Scheuer & Black 2000, 298ff.). As mentioned before, there are currently no reliable methods of sex assessment for isolated ulnae (Bass 1995, 175). The element is in excellent condition.

Macroscopic observations:
A complete healed fracture is observed at the root of the styloid process (Fig. 8.33). The fractured styloid process fragment is absent. When viewed inferiorly the fracture margin is observed to be irregular with disorganized pitting. The pits are approximately ≤0.5 mm Ø. New bone deposition is observed at the disto-lateral aspect of the ulna, extending superiorly from the fracture margin with the most superior point approximately 13.6 mm superior to the fracture margin. The surface of the new bone deposition is characterized as even. Here again, it is likely that this fracture was caused by an acute and direct insult to the wrist *in vivo* (Roberts & Manchester 2005, 90), either as a result of intentional interpersonal violence or accidental injury, such as a fall onto an open hand (Judd 2004; Jurmain 1999).

Entheseal change is observed on the superior point of the pronator ridge. This entheseal change is characterized by marked bone deposition of approximately 6.9 mm in length and 3.7 mm in width. When viewed from a medial aspect the superior point of this deposition is 49.0 mm superior to the radial articulation. The surface of this deposition is in general smooth

Figure 8.33. *Complete adult left ulna (FB0012) from Context (799) of the Circle sample, exhibiting healed fracture of the styloid process; medial view. Scale bar: 1 cm. (Photo Ronika K. Power).*

with rounded margins. The cortical bone within and across this feature is continuous with the surrounding elements. It is possible that the activity related change is associated with the trauma described above.

Lesion type and healing status: Trauma; Healed; Proliferative.
Lesion preservation: Excellent.
Differential diagnosis: Trauma; Activity-related change; Congenital variation.

8.5.3.14. FB0013: Ulna

Context:	(997)
Grid Ref:	94-94.4E/112–114N
Year of Excavation:	BR93
Other Details:	Area X

Element identification and preservation:
Right adult ulna, fragmented *postmortem*. The fragmentation margin is located in the distal quarter of the diaphysis, in the region of the pronator ridge. The proximal aspect of the element is not retained. Adult age estimation is based on the size of the extant element, the relative thickness of the diaphyseal cortex and the complete fusion of the distal epiphysis (Scheuer & Black 2000, 298ff.). As mentioned before, there are currently no reliable methods of sex assessment for isolated ulnae (Bass 1995, 175). The fragment represents ~20% of a complete ulna and is in excellent condition. All damage is assessed as *postmortem*.

Figure 8.34. *Fragmentary adult right ulna (FB0013) from Context (997) of the Circle sample, exhibiting healed fracture of the styloid process; antero-lateral view. Scale bar 1 cm. (Photo Ronika K. Power).*

Macroscopic observations:
A complete healed fracture is observed at the root of the styloid process of the right ulna (Fig. 8.34). The ulna is fragmented, only the distal third is extant. The fractured styloid process fragment is absent. When viewed inferiorly the fracture margin is observed to be quite even, smooth and continuous with the surrounding bone. New bone deposition is observed at the disto-medial aspect of the ulna, extending superiorly from the fracture margin with the most superior point being approximately 10.2 mm superior to the fracture margin. The surface of the new bone deposition is characterized as even.

As with the other example, it is likely that this fracture was caused by an acute and direct insult to the wrist *in vivo* (Roberts & Manchester 2005: 90), either as a result of intentional interpersonal violence or accidental injury, such as a fall onto an open hand (Judd 2004; Jurmain 1999).

Lesion type and healing status: Trauma; Healed.
Lesion preservation: Excellent.
Differential diagnosis: Trauma; Activity-related change; Congenital variation.

8.5.3.15. FB0001: Femur

Context:	(1241)
Grid Ref:	106E/104N
Year of Excavation:	BR94
Other Details:	Area H [E], Spit 5, Bone No.11

Element identification and preservation:
Intact left adult femur. Slight *postmortem* damage is observed around the inferior and posterior aspects of the femoral head, and the antero-medial aspects of the cortical surface of the medial epicondyle. Adult age estimation is based on the size of the extant element and the complete fusion of both proximal and distal epiphyses (Scheuer & Black 2000, 375ff.). Although metric sex estimation methods for femora have been employed by biological anthropologists for more than a century, they should be used with caution considering they were developed on temporally and geographically distinct populations exclusive of the central Mediterranean (Black 1978; Di Bennardo & Taylor 1979; Dittrick 1979; Isçan & Miller-Shaivitz 1986; Krogman 1962; Pearson 1917; Reichs 1986; Spruiell 1984; Stewart 1979; Thieme 1957; White & Folkens 2005). In any case, it is not possible to apply metric analysis to this element as it is both fragmentary (femoral head) and dysplastic in all the required regions, because of the pathology described below. The femur is approximately 95% complete and the element is in excellent condition. All damage is assessed as *postmortem*.

Macroscopic observations:
A complete transverse fracture is observed on the approximate proximal third of the femoral diaphysis (Fig. 8.35a-f). The fracture is not reduced and the element is severely dysplastic; the proximal third of the femoral diaphysis has been anteriorly displaced to overlie the posterior aspect of the fracture margin. The most inferior point of the healed lesion (callus) on the anterior aspect of the element is situated at approximately 160.6 mm inferior to the most superior point of the greater trochanter; the most superior point of the callus on the posterior aspect of the element is situated at approximately 117.3 mm inferior to the most superior point of the greater trochanter. The extent to which the anterior and posterior components of the fractured diaphysis overlie each other is approximately 42.5 mm.

The fracture has completely healed. The misalignment is characterized by slight medial rotation of the distal two-thirds of the diaphysis, and lateral and posterior displacement of the proximal third of the diaphysis. The healed fracture is enveloped by a bony callus on both posterior and anterior aspects.

On the anterior aspect a gap is observed between the most inferior point of the callus and the anterior diaphyseal surface (Fig. 8.35a). There is evidence of displaced muscle attachment on the posterior aspect of the element (Fig. 8.35c); the *linea aspera* is observed to be significantly laterally displaced, commencing lateral to the lesser trochanter on the most postero-lateral aspect of the diaphysis, it then descends distally for approximately 73.5 mm before traversing medially and then inferiorly to assume a sigmoid presentation across both medial and lateral aspects of the callus. The *linea aspera* assumes its normal presentation immediately inferior to the terminal point of the callus at approximately the distal third of the diaphysis.

Figure 8.35. *Photographic and radiological images pertaining to an adult left femur (FB0001) from Context (1241) of the Circle sample, detailing a complete non-reduced healed transverse fracture with severe dysplasia and diaphyseal discontinuity, including: a) anterior view; b) medial view; c) posterior view; d) lateral view; e) sagittal cross-sections detailing diaphyseal discontinuity, medullary cavity malalignment and bony callus; f) transverse cross-section from CT data detailing diaphyseal discontinuity, medullary cavity malalignment and bony callus. Scale bar: 1 cm (photographs only). (Photos Ronika K. Power; radiological images captured by L. Buck, Cambridge Biotomography Centre; processed by J. Magnussen & M. Pardey, Macquarie Medical Imaging).*

Eburnation is observed on the postero-medial aspect of the medial femoral condyle articular surface. The maximum dimensions of the lesion are: 15.5 mm length by 8.3 mm width. Microporosity (<1.0 mm Ø) is noted within the lesion. The lesion most likely developed because of the dysplasia of the element associated with the trauma described above and corresponding misalignment of the knee joint surfaces. This lesion suggests that the element was used for weight-bearing after the fracture was healed.

A bony ridge is observed on the antero-lateral aspect of the left proximal femur (8.35b & d). On the anterior aspect the ridge starts at 25.0 mm distal to the top of greater trochanter and extends diagonally 18.9 mm to the lateral aspect of the femur. It then turns at approximately 110° to extend horizontally, turning around the lateral aspect of the femur for approximately 29.5 mm (using a tape measure because of the curvature of the feature). The lateral-most aspect of the feature is located 40.5 mm distal to the top of the greater trochanter; the terminal point of the feature is located 43.7 mm diagonal and supero-lateral to the lesser trochanter. The feature is most likely developed as a result of the dysplasia of the element associated with the trauma described above and corresponding misalignment of the proximal joint surface and other muscle attachment areas. This lesion further indicates that the element was used for weight-bearing following healing of the fracture.

Radiological observations:
A complete fracture is observed at the approximate proximal one-third point of the left femoral diaphysis. The fracture margin is observed to be relatively straight (Fig. 8.35e), presenting as a transverse line suggestive of a direct lateral impact injury of great force. Injuries of this kind are often clinically associated with significant falls or direct impact injuries (Bucholz & Jones 1991). At the fracture site, the new bone is thick and regular. There are no signs of irregularity or lamellation suggestive of infection.

There is significant overlap, angulation and impaction at the fracture margins. The central points of the medullary cavities of the proximal and distal femoral components are 32.0 mm displaced (Fig. 8.35e-f). Considering the diameter of the diaphysis at the fracture point is only 27.0 mm, this is a significant displacement. The distance between the closest adjacent cortices is 7.0 mm; this gap has been successfully bridged by new bone deposition and restored in healing. The medullary cavities are observed to be patent in both proximal and distal components of the fractured element. The distal aspect of the diaphysis is angulated at the fracture margin by 40° (Fig. 8.35e).

The femoral head presents some *postmortem* damage on its antero-inferior and posterior aspects. The extant trabeculae are all well-preserved and organized. There is no evidence for subchondral cysts, and no osteophytes are observed at the supero-lateral margins. The extant portion of the femoral head maintains a regular joint contour. The absence of all indicators of degenerative joint disease, morphological change or disuse atrophy suggest that this joint functioned effectively and bore weight in the time subsequent to the fracture incident and prior to the time of death.

There is mild bony irregularity or osteophytosis in the region of the greater trochanter, leading to further bony crests and significant entheseal changes along the superior half of the *linea aspera*. The *linea aspera* is distorted proximally as it approaches the fracture site; distally it appears very wide (Fig. 8.35c). These changes are consistent with periosteal new bone deposition within the adjacent musculature alongside remodelling – *myositis ossificans traumatica.* At the distal aspect of the element, marginal osteophytes are observed on the medial and lateral aspects of medial condyle; on the condylar notch; and on the lateral condyle. The medial condyle presents a slightly irregular contour. Widespread subchondral sclerosis is observed at the lateral margin of the lateral condyle, however there are no subchondral cysts.

The severity of this injury prompts consideration of trauma management in this prehistoric context. Significant blood loss is associated with profound proximal femoral fractures such as this – an individual can lose a quarter to one-third of their total blood volume from this category of injury (Buchloz & Jones 1991; American College of Surgeons 2012). At the very least, the individual who sustained this injury would have been in shock, experiencing tachycardia and hypotension (Buchloz & Jones 1991; American College of Surgeons 2012), yet they survived without any modern clinical intervention. Moreover, they completely recovered from the injury without localized complication or infection and went on to effectively use the affected limb for a long time after healing was complete and before their ultimate demise. This individual's case represents a significant finding in the (pre)history of therapeutic practices, including the dimensions of acute care, convalescence and rehabilitation.

Lesion types and healing status: Trauma; Healed; Proliferative; Active.
Lesion preservation: Excellent.
Differential diagnoses: Trauma; Degenerative Joint Disease; Activity-related change.

8.5.3.16. FB0003: Tibia, fibula

Context:	(783)
Grid Ref:	95E/110N
Year of Excavation:	BR91
Other Details:	n/d

Element identification and preservation:
The distal aspects of a right adult tibia and fibula are observed to be fused and fragmented. For the tibia, only the medial malleolus, distal articular surface and antero-lateral aspect of the metaphysis are extant; the fragmentation margin diagonally transects the metaphysis exposing the trabecular and cortical bone in section. For the fibula, only the distal quarter of the diaphysis is extant; the proximal fragmentation margin is at the approximate peak of the triangular subcutaneous area, while the distal margin is at the approximate metaphyseal line. The proximal fragments of both elements are not retained. Adult age estimation is based on the size of the extant elements, the relative thicknesses of the diaphyseal cortices and the complete fusion of the distal tibial epiphyses (Scheuer & Black 2000, 399ff.). Although metric sex estimation methods for tibiae are often employed by biological anthropologists, they should also be used with caution considering they were developed on temporally and geographically distinct populations (Bass 1995; Holland 1991; Isçan & Miller-Shaivitz 1984a, 1984b; Isçan *et al.* 1994; Kieser *et al.* 1992; Singh *et al.* 1975). Regardless, it is not possible to apply metric analysis to this element because of its highly fragmentary and incomplete state. Both elements are approximately 10% complete. The extant elements are in good condition. All damage is assessed to be *postmortem*.

Macroscopic observations:
The right tibial metaphysis and fibula diaphysis are fused distally at their respective interosseous borders (Fig. 8.36a-d) by a bony bridge between the elements which is consistent in appearance with the surrounding cortical bone. For the tibia, the most distal fusion point starts at approximately 4.10 mm superior to the inferior articular surface, at approximately the fibular notch. It is not possible to describe the precise anatomical location of the fusion for the fibula, as the distal aspect is fragmented as a result of *postmortem* damage. The length of the fused position of these elements is 64.0 mm, measure from the most distal to most proximal points. The distal aspect of the fibula diaphysis is observed to be dysplastic; the extant proximal aspect

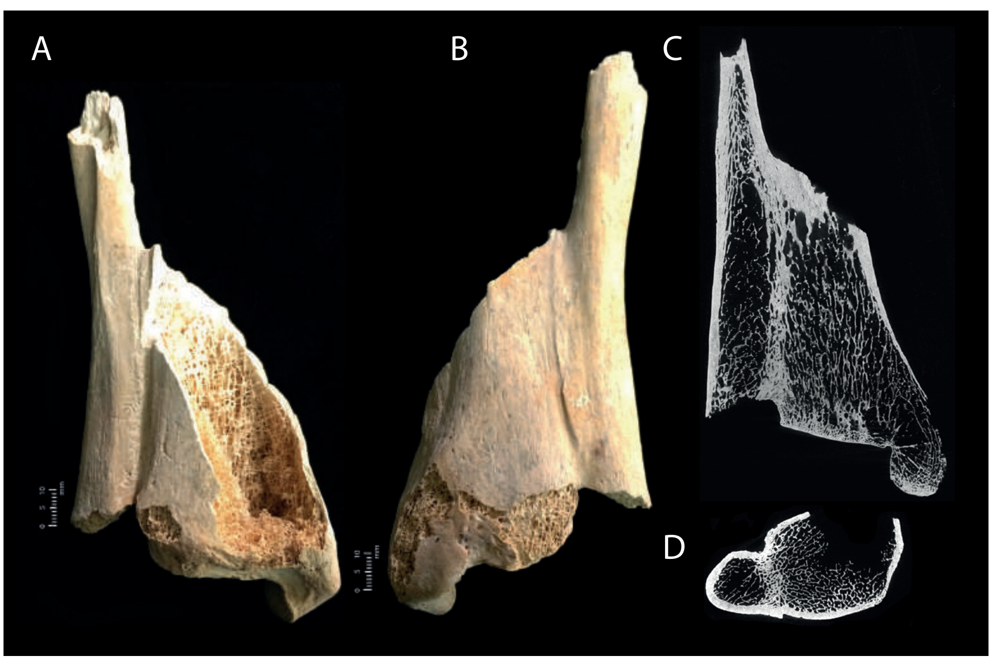

Figure 8.36. *Photographic and radiological images pertaining to fragmentary adult right tibia and fibula (FB0003) from Context (783) of the Circle sample, detailing complete fusion of the distal diaphysis and metaphyses at the interosseous border, including: a) anterior view; b) posterior view; c) coronal cross-section from CT data detailing the complete extent of fusion; d) transverse cross-section at the fusion site detailing the commonality of trabeculae. Scale bar: 1 cm (photographs only). (Photos Ronika K. Power; radiological images captured by L. Buck, Cambridge Biotomography Centre; processed by J. Magnussen & M. Pardey, Macquarie Medical Imaging).*

of the fibula diaphysis is diverted from the anatomical midline and fused portion by approximately 10°.

Radiological observations:
The fragmentary distal aspects of the right adult tibia and fibula are completely fused across the distal tibiofibular syndesmosis. The medial malleolus appears to have been healthy at the time of death, and the tibial plafond is preserved. The most distal aspect of the fibula is absent. A thick corticated margin is observed between the two elements, which extends for a substantial segment. Furthermore, there is a commonality of trabeculae between the elements with only a slight remnant of cortex in the intermediate space. This is classified as tibiofibula coalition, or tibiofibular synostosis, a condition only rarely described in orthopaedic literature (Sureka *et al.* 2012). This can be either a congenital or acquired condition; in the case of the latter, trauma such as ankle fracture or eversion ankle sprain is the most common aetiology, particularly in the case of distal joint involvement (Fu *et al.* 2003; Munjal *et al.* 2004; O'Dwyer 1991; Vitale & Fallat 1990). Sureka *et al.* (2012) report that tibiofibular synostosis may also be secondary to iatrogenic causes or pre-existing conditions including so-called 'kissing' osteochondroma, *fibrodysplasia ossificans progressiva*, subperiosteal haemorrhage (a sequela of scurvy or haemophilia) and fluorosis (Bostman 1993; Fu *et al.* 2003; Lee *et al.* 2010). Although iatrogenic causes may be ruled out for this prehistoric individual, it is likely that the structural changes described here may be attributed to a traumatic incident many years prior to the time of death, considering the almost-common medullary cavity, smooth remodelled cortices with no periosteal thickening or irregularity. In considering how this may have affected the lived experience of the afflicted individual, clinical cases of distal tibiofibular syndesmosis report relatively rigid, stable joints with minimal loss of mobility and no pain directly associated with the coalition *per se* (Sureka *et al.* 2012).

Lesion type and healing status: Proliferative; Healed.
Lesion preservation: Excellent.
Differential diagnosis: Trauma; Congenital; Activity-related change; Metabolic.

8.6. Methodology case study: periosteal lesions in Context (960)

Periosteal lesions were rarely observed across the full assemblage of excavated remains; however, a concentration of elements within Context (960) demonstrated this pathology. Context (960) is dated to *c*. 2530–2475 cal. BC, late within the site's use, although some remains were residual and dated to as early as 2850 cal. BC (Malone *et al*. 2019). The previous summary of pathological observations within the assemblage noted, but did not quantify, observations of 'extra cortical new bone' (Stoddart *et al.* 2009a, 325). Within Context (960), two adjacent 1x1 m grid squares contained 12 elements presenting periosteal lesions of varied expression and severity. These elements are represented by 44 fragments deriving from non-adult and adult individuals. The assemblage excavated from Context (960) contained nearly 12,000 fragments of human bone and only one articulated skeleton (Stoddart *et al.* 2009a, 149); this discrete deposit of pathological elements is therefore exceptional. These elements are described below, according to grid square. Interestingly, element distribution corresponds with biological age, with only adult elements presenting periosteal lesions in one 1 × 1 m grid square, and only non-adult elements presenting periosteal lesions in the adjacent grid square. Below, radiological observations supplement macroscopic descriptions of the lesions on these elements in all cases. This integrated approach enhances differential diagnosis and represents a greater level of attention than is typically paid to fragmented remains, providing the opportunity to assess the potential of this methodology to re-unite remains from discrete individuals in fragmentary and commingled contexts. Differential diagnosis of periosteal lesions on singular elements is not recommended (Weston 2008, 57). We therefore discuss varied possible pathogeneses in the case of each element, before assessing the potential relationship between the adult and non-adult elements, respectively.

8.6.1. Context (960) adult remains

8.6.1.1. FB0033: Radius

Context:	(960)
Grid Ref:	99/112
Year of Excavation:	BR94
Other Details:	Unit 2, Spit 4

Element identification and preservation:
Left adult radius refitted from two fragments presenting a diagonal and stepped *postmortem* fracture at the distal point of the proximal third of the diaphysis. These fragments are observed to conjoin well. The proximal and distal metaphyses and the radial tubercle are fragmented *postmortem* and these portions are not retained. Several small patches of red ochre are observed on the extant portion of the diaphysis. Adult age estimation is based on the size of the extant element and the relative thickness of the diaphyseal cortex (Scheuer & Black 2000, 289ff.). Bass (1995, 168) reports that several attempts have been made to establish metric sex determination

for the radius, however they have not been successful in characterizing dimorphism from a single isolated bone, much less for a fragmentary element (cf White 2012, 415). Additional studies show that ossification timing of particular epiphyses of the distal humerus and proximal radius can successfully determine biological sex in 70% of cases (Garn *et al.* 1996, 106). However, considering the fragmentary and disarticulated nature of this element and individual, we are unable to access either of these criteria. The extant portion of the element represents ~90% of a complete radius and the fragments are in good condition. All damage is assessed as *postmortem*.

Macroscopic observations:
Periosteal new bone deposition is observed in four focal areas: the radial tubercle, the proximal aspect of the interosseous crest, the lateral aspect of the middle third of the diaphysis and on the extant portion of the distal metaphysis (Fig. 8.37a-d). In all cases where the lesion can be viewed in cross-section from fragmentation margins, no changes to the underlying cortex are observed. There are no indications of fracture, cloaca, or sequestra on the extant portion of the element.

The extant portion of the radial tubercle is enveloped by periosteal new bone, although the medial and most elevated aspect of the radial tubercle has been eroded because of *postmortem* damage which obfuscates further observations of pathology. On the anterior aspect, the lesion commences approximately 16.9 mm from the proximal fragmentation margin, continuing for 22.6 mm. The lesion commences approximately 13.9 mm from the proximal fragmentation margin on the medial aspect and extends for 25.4 mm. On the posterior aspect, the lesion commences approximately 11.7 mm from the proximal fragmentation margin and continues for 18.8 mm. Using a flexible paper tape measure, the maximum width of the lesion is 29.0 mm medio-laterally across the centre of the radial tubercle. The maximum length of the lesion along the medial aspect of the radial tubercle is 25.4 mm. The lesion exhibits mixed activity phases, presenting lamellar bone interspersed with microporosity (<1.0 mm Ø) on the anterior and posterior aspects and woven bone with capillary impressions and microporosity alongside the fragmentation margins on the radial tubercle. The centre of the extant lesion can be viewed in cross-section at the fragmentation margin and the periosteal woven bone is observed to sit proud of the underlying cortex. In relation to the surrounding cortex, the lesion differs in colour and presents increased porosity. The margins of the lesion are diffuse, less dense and more porous.

On the proximal aspect of the interosseous crest, periosteal woven bone extends across the fragmentation margin of the two diaphyseal fragments which are observed to re-fit. On the medial aspect, the lesion commences approximately 50.3 mm from the proximal fragmentation margin and extends for 48.6 mm. The maximum width of the lesion is 6.8 mm, taken 5.0 mm proximal to the fragmentation margin of the diaphyseal fragments using a flexible paper tape. On the peripheral margins of the lesion, bony plaque deposits and microporosity are observed. In some areas, the plaque-like deposits assume a striated position because of their location overlying the interosseous crest. In the central portion of the lesion, rugose plaque deposits are interspersed with microporosity. Some *postmortem* damage to the centre of the lesion may obfuscate further observations of pathology. The lesion differs in colour to the surrounding cortex; the plaque-like deposits are denser and more rugose. At the centre of the lesion, the periosteal new bone is observed to sit proud of the underlying cortex.

On the lateral aspect of the middle third of the diaphysis, the lesion commences approximately 6.4 mm from the proximal fragmentation margin and continues for 19.7 mm. The maximum width, taken antero-posteriorly across the centre of the lesion measures 6.0 mm. The lesion exhibits mixed activity phases. In the distal two thirds of the lesion, well-healed and diffuse plaque-like bone is interspersed with microporosity. In the proximal third, the lesion appears to be slightly more active; it is more rugose, and there is more separation and definition between the periosteal new bone and the cortex. A small amount of *postmortem* damage is observed on the proximal aspect of the lesion. The lesion is a slightly different colour to the surrounding cortex, although the margins are diffuse.

On the extant portion of the distal metaphysis, periosteal new bone is observed on the anterior surface, the distal aspect of the interosseous crest and medial aspect of the posterior surface. On the anterior surface, the extant portion of the lesion occupies an approximately triangular shape, extending from the most lateral inferior border to the interosseous crest. The midpoint of the lesion on the anterior surface is located approximately 29.3 mm superior to the distal fragmentation margin on the sagittal plane. On the medial aspect, the extant portion of the lesion extends 34.0 mm proximal to the distal fragmentation margin. On the postero-medial aspect, the extant portion of the lesion is also observed to occupy an approximately triangular shape; the midpoint of the lesion is located 17.4 mm proximal to the distal fragmentation margin on the sagittal plane. The maximum length of the lesion is 34.3 mm on the medial aspect. The maximum width of the lesion is approximately 33.0 mm, taken 4.0 mm proximal to the distal fragmentation margin using a flexible paper tape. The lesion presents mixed activity phases. The peripheral

Figure 8.37. *Photographic images pertaining to fragmented adult left radius (FB0033) from Context (960) of the Circle sample, depicting refitted fragments and periosteal lesions in the regions of the radial tubercle, proximal aspect of the interosseous crest and distal metaphysis, including: a) anterior view; b) medial view; c) 3D rendered lateral view; d) posterior view. Scale bar: 1 cm. (Photos Jess E. Thompson; radiological images captured by L. Buck, Cambridge Biotomography Centre; processed by J. Magnussen & M. Pardey, Macquarie Medical Imaging).*

margins on the anterior and posterior surfaces present smooth plaque-like deposits interspersed with diffuse microporosity. Within the central portion of the lesion, both micro- and macroporosity (≥1.0 mm Ø) are observed. Clusters of microporosity are observed on the antero-lateral aspect with pores occasionally coalescing and partial capillary impressions truncated by the fragmentation margin. On the antero-medial aspect, single and coalescing macropores are present. On the medial aspect, the distal three-quarters of the lesion presents a more rugose topography of woven bone interspersed with microporosity. The proximal quarter of the lesion presents a smooth plaque-like deposit of bone. On the posterior aspect, the central portion of the lesion presents woven bone and microporosity. The margins of the extant portion of the lesion on the anterior and posterior aspect are diffuse and not well-demarcated; they do not differ in colour to the surrounding cortex although they are denser. On the medial and posterior aspect, the lesion is observed to differ in colour.

Radiological observations:
A minor area of periosteal new bone deposition is observed on the extant portion of the radial tubercle. Mid-diaphysis, in the area of the refitted fragmentation margins, cortical bone loss is observed, although this may be attributed to *postmortem* taphonomic damage. The distal diaphysis and distal metaphysis present a thick layer of periosteal new bone deposition which is radiolucent and very well-remodelled. This lesion is well-organized and exhibits dense bone with regular and smooth margins, indicating a long and chronic process which may have been halted in the process of remodelling.

There is no evidence of fracture or typical sequelae (i.e. cloaca, sequestra) on the extant radius, suggesting the lesions are unlikely to be the result of traumatic fracture or infectious processes such as osteomyelitis. The lesions on the interosseous surface and on the distal metaphysis present diffuse margins and are therefore not characteristic of subperiosteal haematomata (Ortner 2003, 84). Periosteal new bone forms in response to damage to the periosteum, including even relatively minor tearing and stretching (Richardson 2001). The lesions on the extant element are observed on attachment sites for the *Mm. biceps brachii*, *flexor pollicis longus*, and *pronator quadratus*. These muscles are involved in flexion and pronation of the forearm, thumb flexion, and gripping with the hand (Parkin & Logan 2007, 138). Repetitive activity-related microtrauma may have resulted in chronic periosteal inflammation. This phenomenon is commonly reported amongst athletes as a result of overuse and overloading of the forearm, and may co-occur with stress fractures (Meese & Sebastianelli 1996; Meijer *et al.* 2017).

Lesion type and healing status: Mixed; Mixed.
Lesion preservation: Excellent.
Differential diagnosis: Activity-related change.

8.6.1.2. FB0034: Ulna

Context:	(960)
Grid Ref:	99/112
Year of Excavation:	BR94
Other Details:	Unit 21, Spit 4

Element identification and preservation:
Left adult ulna refitted from two fragments presenting a transverse *postmortem* fracture across the pronator ridge. These fragments are observed to conjoin well. The distal metaphysis and epiphysis are absent as a result of further fragmentation immediately superior to the distal metaphysis. Slight areas of *postmortem* damage are observed on the anterior-most aspects of the olecranon and the coronoid process, the radial notch, infero-medial to the margin of the trochlear notch, and on the postero-medial aspect of the olecranon. Diffuse flecks and patches of red ochre are observed across the extant portion of the diaphysis. Adult age estimation is based on the size of the extant element, the relative thickness of the diaphyseal cortex and the complete fusion of the proximal epiphysis (Scheuer & Black 2000, 298ff.). As mentioned before, although Purkait (2001) devised a discriminant function for metric sex assessment of ulnae, this method is not widely applied (Bass 1995, 175; White & Folkens 2005). Furthermore, it is not possible to apply metric analysis to this element because of its fragmentary and incomplete state. The fragment represents ~95% of a complete ulna and is in good condition. All damage is assessed as *postmortem*.

Macroscopic observations:
The periosteal new bone extends across the extant anterior and lateral aspects of the proximal metaphysis, although *postmortem* damage may obfuscate further observations of pathology (Fig. 8.38a-d). On the anterior surface, the lesion commences on the inferior aspect of

Figure 8.38. *Photographic images pertaining to fragmented adult left ulna (FB0034) from Context (960) of the Circle sample, depicting refitted fragments and periosteal lesions in the regions of the proximal metaphysis and the distal third of the diaphysis, traversing the fragmentation margin, including: a) anterior view; b) medial view; c) lateral view; d) posterior view. Scale bar: 1 cm. (Photos Jess E. Thompson).*

the coronoid process and extends for approximately 51.0 mm, measured with a flexible paper tape. On the lateral aspect, the lesion commences approximately 18.9 mm from the proximal epiphysis and continues for approximately 59.5 mm. The maximum length of the lesion is 59.5 mm on the lateral aspect. The maximum width of the lesion is 34.0 mm taken medio-laterally from the centre of the ulnar tuberosity with a flexible paper tape. The lesion exhibits mixed activity phases. A plaque-like deposit of woven bone is observed on the ulnar tuberosity, interspersed with microporosity and small bony nodules. Well-healed smooth deposits of bone are observed inferior to the coronoid process. On the antero-lateral aspect, the lesion exhibits woven bone incorporating both micro- and macroporosity. Infero-medial to the trochlear notch, a depression is observed, measuring 12.1 mm proximal to distal and 3.6 mm superior to inferior. Woven bone continuous with the surrounding lesion is observed within this depression and, alongside microporosity, four macropores are present. The lesion is denser, more porous and lighter in colour than the surrounding cortex.

On the distal third of the diaphysis, periosteal woven bone is observed on the interosseous crest extending across the fragmentation margin of the two diaphyseal fragments which are observed to re-fit (Fig. 8.38a & c). On the distal fragment, the lesion continues across the anterior surface to the pronator ridge. The distal fragmentation margin truncates the lesion and some *postmortem* damage to the woven bone is observed, obfuscating full observation of pathology. The lesion commences on the lateral aspect of the proximal fragment, 9.5 mm superior to the re-fit fragmentation margin and extends for 39.2 mm. On the anterior aspect, the lesion commences on the distal fragment, 8.1 mm distal to the conjoined fragmentation margin and extends over the extant portion of the diaphysis for 39.3 mm. The maximum length of the lesion is 39.3 mm on the anterior aspect. The maximum width of the lesion, using a flexible paper tape, is 10.0 mm taken medio-laterally along the distal aspect of the pronator ridge. The plaque-like deposits of bone assume a striated organization along the interosseous crest and pronator ridge, interspersed with microporosity. In relation to the surrounding cortex, the lesion is more porous and differs in colour. In cross-section, when viewed from the fragmentation margins, the periosteal woven bone sits proud of the underlying cortex. There are no indications of fracture, cloaca, or sequestra on the extant portion of the element.

Radiological observations:
On the lateral margin of the proximal diaphysis, the periosteal lesions are in the process of healing and appear long-standing. The lesion presents mixed activity phases: components of the lesion exhibit spiculated and active presentation, while other components appear to be in a more advanced stage of remodelling. The underlying cortex is observed to be in poor condition, presenting a diffuse, poorly demarcated lesion characterized by small radiolucent holes, which worsens in areas where the overlying lesion is irregular in expression. This appearance is referred to as 'moth-eaten' in radiological descriptions, describing a true permeative process of bone (Brant & Helms 2012). In the region of the mid-diaphysis, the bone is observed to present healthy tissue with thick and well-preserved cortices. Toward the distal diaphysis, there is further periosteal new bone deposition and the underlying cortex is thin, pockmarked and trabeculated.

There is no evidence of fracture or typical sequelae (i.e. cloaca, sequestra) on the extant ulna, suggesting the lesions are unlikely to be a result of traumatic fracture or infectious processes such as osteomyelitis. The lesions present diffuse margins and are not characteristic of subperiosteal haematomata (Ortner 2003, 84). As mentioned before, periosteal new bone forms in response to damage to the periosteum, including even relatively minor tearing and stretching (Richardson 2001). Notably, lesions are present on articular and interosseous surfaces, in this case on attachment sites for the *Mm. supinator*, *brachialis, pronator quadratus, extensor carpi ulnaris* and *flexor digitorum profundus*. These muscles are involved in elbow flexion, forearm pronation and supination, wrist flexion and extension, and finger flexion (Parkin & Logan 2007, 138, 140). Thus, chronic periosteal inflammation in this case may be a result of repetitive activity-related microtrauma. Activity-related ulnar periostitis is reported amongst athletes as a result of overuse and overloading of the forearm muscles (e.g. Grossfeld *et al.* 1998; Meese & Sebastianelli 1996).

Lesion type and healing status: Mixed; Mixed.
Lesion preservation: Excellent.
Differential diagnosis: Activity-related change.

8.6.1.3. FB0035: Femur

Context:	(960)
Grid Ref:	99/112
Year of Excavation:	BR94
Other Details:	Unit 16, Spit 4

Element identification and preservation:
Fragmentary and incomplete left adult femur. Many fragments are very small and most represent the distal epiphysis. The two largest fragments comprise the majority of the diaphysis and are observed to refit

along a transverse *postmortem* fracture which transects the *linea aspera* at the approximate mid-point. The proximal diaphysis is fragmented diagonally superior to the spiral line, and the distal diaphysis is fragmented irregularly across the popliteal surface. Small areas of *postmortem* damage are present on the postero-lateral margin of the *linea aspera*, and on the antero-medial aspect of the proximal third of the diaphysis. Longitudinal cortical cracks and root etching are observed on the proximal third of the diaphysis, eroding areas of the cortical surface and the periosteal lesions. Diffuse flecks and patches of red ochre are observed across the extant portion of the diaphysis. Adult age estimation is based on the size of the extant element (Scheuer & Black 2000, 375ff.). Although metric sex estimation methods for femora have been employed by biological anthropologists for more than a century (references in §8.5.3.15, above) it is not possible to apply metric analysis to this element as it is both fragmentary and incomplete. The femur is ~75% complete and the extant portions of the element are in fair condition. All damage is assessed as *postmortem*.

Macroscopic observations:
Periosteal new bone is observed on the anterior aspect of the proximal diaphysis and on the anterior and lateral aspects of the distal diaphysis (Fig. 8.39a-c). All lesions are affected by *postmortem* taphonomic damage and the fragmentation of the proximal and distal diaphysis truncates the lesions, obfuscating full observation of pathology. There are no indications of fracture, cloaca, or sequestra on the extant portions of the element.

On all aspects, the lesion is observed adjacent to the proximal fragmentation margin. From the proximal fragmentation margin on the anterior aspect of the extant proximal diaphysis, the lesion extends for approximately 162.6 mm. On the posterior aspect, the lesion extends for approximately 210.0 mm, traversing the two re-fitted diaphyseal fragments. On the lateral aspect, the lesion extends for 170.8 mm, again traversing the re-fitted fragments. On the medial aspect, the lesion extends for approximately 144.6 mm. The maximum length of the extant portion of the lesion is 210.0 mm on the posterior aspect along the *linea aspera*. The maximum width of the lesion is 75.0 mm, taken antero-posteriorly along the pectineal line using a flexible paper tape. The lesion exhibits mixed activity phases. On the antero-medial aspect, the peripheral margins of the extant portion of the lesion present well-healed lamellar bone interspersed with diffuse microporosity. On the antero-lateral aspect, islands of periosteal woven bone have been

Figure 8.39. *Photographic and radiological images pertaining to fragmented adult left femur (FB0035) from Context (960) of the Circle sample, depicting refitted fragments and periosteal lesions on the proximal and distal thirds of the diaphysis, including: a) anterior view; b) lateral view; c) posterior view; d) transverse cross-section from CT data at the proximal diaphysis demonstrating cortical demineralization and separation between the cortex and periosteal lesion on the lateral aspect of the linea aspera; e) transverse cross-section at mid-diaphysis demonstrating cortical irregularity and radiolucent holes (so-called 'moth-eaten' appearance); f) transverse cross-section at the proximal aspect of the distal third of the diaphysis demonstrating cortical demineralization and radiolucent holes (so-called 'moth-eaten' appearance). Scale bar: 1 cm (photographs only). (Photos Jess E. Thompson; radiological images captured by L. Buck, Cambridge Biotomography Centre; processed by J. Magnussen & M. Pardey, Macquarie Medical Imaging).*

eroded by *postmortem* damage. On the extant portion of the lesion, plaque-like deposits of woven bone are interspersed with microporosity. On the posterior aspect, periosteal woven bone envelops the pectineal line, spiral line, gluteal tuberosity and *linea aspera*, exhibiting extensive microporosity. Extending distally, the medial lip of the *linea aspera* presents woven bone with extensive microporosity, while the lateral lip presents well-healed bone with diffuse microporosity. The margins of the lesion are diffuse and not well-demarcated on the antero-medial aspect, although the posterior margins of the lesion are marked by rugosity. The lesion differs in colour to the surrounding cortex and exhibits less dense and more porous bone. When viewed from the fragmentation margins, the periosteal woven bone sits proud of the underlying cortex and no cortical change is observed.

On the anterior aspect of the distal diaphysis, the lesion commences approximately 45.8 mm superior to the distal fragmentation margin. On the lateral aspect, the lesion commences approximately 109.5 mm superior to the distal fragmentation margin. The maximum length of the extant portion of the lesion is 109.5 mm on the lateral aspect. The maximum width of the lesion is 58.0 mm, taken 5.0 mm proximal to the distal fragmentation margin using a flexible paper tape. The extant portion of the lesion exhibits well-healed lamellar bone and microporosity. The margins are diffuse and not well demarcated, differing in colour to the surrounding cortex and demonstrating increased porosity. When viewed from the fragmentation margin, the periosteal new bone is observed to sit proud of the underlying cortex and cortical thickness has decreased, measuring 0.8 mm on the anterior aspect and 1.1 mm on the lateral aspect. The area usually occupied by dense cortical bone now presents focal micro- to macroporosity and cancellous proliferation, an apparent extension of trabecular bone within the medullary cavity. When held in the hand, the extant element feels very light as compared to the weight of 'normal' bone.

Radiological observations:
The proximal fragment presents slightly more extant cortex than the refitted fragment of the middle and distal diaphysis. However, the cortex is observed to be in poor condition, presenting an eroded and poorly demarcated lesion characterized by small radiolucent holes (Fig. 8.39d-f). Such cortical change is unlikely to be the result of diagenetic processes; the outermost portion of the cortex is better preserved than the endosteal aspect, most likely a result of demineralization because of pathological processes. Focal periosteal new bone is present around the *linea aspera*, tracking its full length on the extant portion of the element. A partial boundary is observed between the cortex and the lesion, and the underlying cortex exhibits increased porosity and is relatively irregular in appearance. The cortex is markedly thin and demineralized across the extant portion of the element, compared with the expected cortical thickness of an adult femoral mid-diaphysis. Bone density loss across the element demonstrates osteopenia and may signal osteoporosis.

Both the proximal and distal lesions are truncated by *postmortem* fragmentation, indicating that periosteal new bone deposition extended onto the metaphyseal surfaces and was more widespread across the element than is observable. Given that the proximal and distal metaphyses and epiphyses are absent because of fragmentation and cannot be assessed, fracture must be considered in the differential diagnosis. While it is not possible to ascertain whether this element was fractured *in vivo*, the evidence for extensive minor periosteal reaction and cortical resorption may be related and important factors to consider in the differential diagnosis. Sequelae and long-term effects of femoral fractures which may stimulate periosteal reaction and/or cortical bone loss include osteomyelitis, localized disuse osteoporosis or osteopenia, and reflex sympathetic dystrophy. Typical infectious indicators are not observed on the extant element and the cortex has been compromised as a result of demineralization rather than erosive processes associated with infection. The diffuse nature of the lesions and the extensive cortical change may instead support a systemic pathogenesis (Ortner 2003). Osteoporosis and traumatic fracture, especially of the hip, have a complex relationship. Reduced mobility secondary to fracture may lead to localized osteoporosis (Bartl *et al.* 2007, 111–3; Kiratli 2003), while generalized osteoporosis or osteopenia increases the likelihood of bone fracture following trauma as a result of significant reduction in bone density (Ortner 2003, 410ff.; Warriner *et al.* 2011). Reflex sympathetic dystrophy (or complex regional pain syndrome) is occasionally experienced following fracture, sprain, venous or nerve damage, and may also result in osteoporosis, amongst other complications (Borchers and Gershwin 2014, 246). Additionally, the involvement of the *linea aspera* may indicate the co-occurrence of activity-related microtrauma and/or altered biomechanics.

Lesion type and healing status: Mixed; Mixed.
Lesion preservation: Moderate.
Differential diagnosis: Activity-Related Change; Metabolic; Trauma.

8.6.1.4. FB0036: Tibia

Context:	(960)
Grid Ref:	99/112
Year of Excavation:	BR94
Other Details:	Units 2 & 33, Spit 4

Element identification and preservation:
Fragmentary and incomplete right adult tibia represented by five fragments, four of which are observed to refit. The refitted portion of the element represents the approximate mid-point of the diaphysis and extends to the distal diaphysis, which is fragmented superiorly to the distal metaphysis. The fragments present diffuse root etching and focal areas of erosion on the lesions and adjacent to the fragmentation margins. Small flecks and patches of red ochre are observed on many fragments. Adult age estimation is based on the size of the extant element and the relative thicknesses of the diaphyseal cortex (Scheuer & Black 2000, 399ff.). Although metric sex estimation methods for tibiae are often employed by biological anthropologists (Bass 1995; Holland 1991; Isçan & Miller-Shaivitz 1984a, 1984b; Isçan *et al.* 1994; Kieser *et al.* 1992; Singh *et al.* 1975), it is not possible to apply metric analysis to this element because of its highly fragmentary and incomplete state. The element is ~35% complete and the extant portions of the element are in fair condition. All damage is assessed to be *postmortem*.

Macroscopic observations:
Periosteal new bone is observed on all extant fragments; fragmentation truncates the lesions and thus obfuscates a full observation of pathology. When viewed from the fragmentation margins, the periosteal lesions sit proud of the underlying cortex and no cortical change is observed. On the extant portions of the element, there are no indications of fracture, cloacae or sequestra.

On the anterior aspect, the extant portion of the lesion extends across four fragments which are observed to re-fit (Fig. 8.40a – only three fragments are visible in this view). The lesion extends across the full length of the fragments for 243.3 mm. The maximum width of the extant portion of the lesion is approximately 29.0 mm, using a flexible paper tape. The lesion demonstrates mixed activity phases. The proximal three-quarters present well-healed smooth deposits of bone with diffuse microporosity. The distal quarter exhibits rugose plaque-like deposits of bone with microporosity, although *postmortem* taphonomic damage obfuscates a full observation of the lesion. With respect to the surrounding cortex, the lesion demonstrates increased porosity and the distal quarter differs in colour.

On the lateral aspect of the distal third of the diaphysis, periosteal new bone deposition traverses the length of the extant fragment (Fig. 8.40b). The lesion is truncated both proximally and distally and has been partially eroded by *postmortem* root damage, obfuscating a full observation of pathology. The maximum length of the extant portion of the lesion is 126.6 mm along the interosseous surface. The maximum width of the lesion is 26.0 mm, using a flexible paper tape. The lesion exhibits mixed activity phases. The peripheral

Figure 8.40. *Photographic and radiological images pertaining to fragmented adult right tibia (FB0036) from Context (960) of the Circle sample, depicting periosteal lesions on the refitted fragments of the proximal diaphysis and on the distal third of the diaphysis, including: a) anterior view of refitted fragments of proximal diaphysis; b) lateral view of distal third of diaphysis; c) transverse cross-section from CT data toward distal fragmentation margin of distal diaphysis, demonstrating irregular cortex with periosteal lesion partly separated from underlying cortex. Some sediment is observed within the medullary cavity. Scale bar: 1 cm (photographs only). (Photos Jess E. Thompson; radiological images captured by L. Buck, Cambridge Biotomography Centre; processed by J. Magnussen & M. Pardey, Macquarie Medical Imaging).*

margins of the proximal aspect of the lesion present well-healed deposits of bone with microporosity and capillary impressions. The remainder of the lesion exhibits successive layers of plaque-like deposits of bone interspersed with micro- and macroporosity. The organization of the periosteal new bone varies across the lesion; striated plaque deposits overlie the interosseous surface while angular plaque deposits interspersed with capillary impressions are present on the antero-lateral aspect. The lesion differs in colour to the surrounding cortex and demonstrates increased rugosity and porosity.

Radiological observations:
The largest available fragment of the extant tibia, representing the distal diaphysis, displays widespread periosteal new bone for the full length of the fragment. The lesion is deposited in discrete zones and extends from the anterior aspect to the interosseous surface. The cortex presents slightly diffuse radiolucent holes, and it is trabeculated and thinner than expected (Fig. 8.40c). Radiologically, the margins of the lesion are clearer, and it is apparent that there are further extensions of the lesion onto the interosseous surface, where they may have been truncated by *postmortem* taphonomic damage. The lesion is observed to sit proud of the cortex in several areas, at the proximal and distal aspects of the extant fragment. The character of the periosteal new bone is not lamellated nor is any cortical thickness change evident as would be expected in association with chronic infectious processes.

All lesions are truncated because of *postmortem* fragmentation and, given that much of the element cannot be assessed, trauma and fracture must be considered in the differential diagnosis. Subperiosteal haematomata are commonly observed on the tibia secondary to trauma or scurvy, but exhibit microporotic ossification of the periosteum, as opposed to the diffuse nature of the lesions on the extant portion of this element (Ortner 2003, 88). Further potential aetiologies include chronic venous insufficiency, hypertrophic osteoarthropathy, and microtrauma because of tibial stress syndrome, commonly known as 'shin splints'. Chronic venous insufficiency (CVI) is microporosity by damage or weakness in the valves and/or venous walls of lower leg veins, resulting in increased blood pressure and stasis in the lower legs as blood is unable to flow upward to the heart. Periosteal reaction may form in response to chronic soft tissue inflammation because of CVI, and has been observed clinically at ulcer sites, at a distance from ulcer sites, or not in association with ulceration (Gensburg *et al.* 1988, 1280; Nicholls 2005). Periosteal new bone in CVI cases is noted to be thick and undulating, resembling lesions seen in cases of hypertrophic osteoarthropathy (Gensburg *et al.* 1988, 1280).

Hypertrophic osteoarthropathy (HOA) refers to either a primary or secondary syndrome; the primary form of the disease is pachydermoperiostosis and genetic in origin, while the secondary form arises in response to varied conditions including those of pulmonary, endocrine, gastrointestinal, haematological and inflammatory origin (Ortner 2003, 354). HOA is typically identified through clubbing and arthritis of the digits alongside symmetrical periosteal bone deposition on long bones (Ortner 2003, 354). Lesions are typically separated from the cortex by a fibrous layer in the early stages and may gradually progress to involve cortical and endosteal resorption as the lesion thickens (Ortner 2003, 354–6; Pineda *et al.* 1987). The largest fragment of the extant tibia is damaged by fragmentation and erosion, yet the extant portion of the lesion on the distal diaphysis exhibits a slightly coagulated and ropey appearance. This may be consistent with the early stages of HOA or HOA secondary to lung cancer (Pineda *et al.* 1987, 778). However, it is impossible to ascertain whether other long bones and/or the digits were affected, as would expected, or whether articular surfaces are involved, which would rule out HOA (Ortner 2003, 354). Tibial stress syndrome encompasses stress injuries and pain because of overloading and improper bone remodelling which may present as tibial periostitis and/or stress fractures (Couture & Karlson 2002; Gaeta *et al.* 2008; Mubarak *et al.* 1982), deep posterior compartment syndrome, or a shin splint. The lesion on the anterior aspect of the extant tibia appears to be in a more advanced stage of healing, suggesting it represents an earlier insult, and it is therefore possible that the distal diaphyseal lesion is unrelated and of differing aetiology.

Lesion type and healing status: Mixed; Mixed.
Lesion preservation: Excellent.
Differential diagnosis: Activity-Related Change; Trauma; Other.

8.6.1.5. FB0037: Fibula

Context:	(960)
Grid Ref:	99/112
Year of Excavation:	BR94
Other Details:	Unit 2, Spit 4

Element identification and preservation:
Fragmentary and incomplete left adult fibula represented by two fragments presenting a transverse and stepped fragmentation margin across the distal third of the diaphysis. The fragments are observed to

conjoin well. The distal diaphysis is fragmented in a stepped profile while a curved fragmentation margin transects the distal-most portion of the middle third of the diaphysis. Small areas of root etching are diffuse across the extant portion of the element, as well as focal erosion and minor longitudinal cracks emanating from the refitted fragmentation margins. Some red ochre flecks are observed on the middle third of diaphysis. Adult age estimation is based on the size of the extant element and the relative thickness of the cortex (White *et al.* 2012, 315). There are no current morphological or metric sex assessment methods engaged for isolated, fragmentary fibulae. The element is ~35% complete and the extant portions of the element are in fair condition. All damage is observed to be *postmortem*.

Macroscopic observations:
Periosteal woven bone encircles the extant portion of the element, traversing the re-fitted fragments (Fig. 8.41a-d). The lesion is truncated both proximally and distally and, combined with some *postmortem* erosion, this obfuscates full observation of pathology. On the anterior aspect, the lesion extends the length of the extant fragments, measuring 148.2 mm. The lesion is continuous across the medial surface, extending a maximum length of 190.2 mm. On the posterior aspect, the lesion extends the full length of the extant fragments for 168.2 mm. On the lateral aspect, the extant portion of the lesion extends for 81.8 mm from the proximal fragmentation margin. The maximum length of the extant portion of the lesion is 190.2 mm. The maximum width is 45.0 mm,

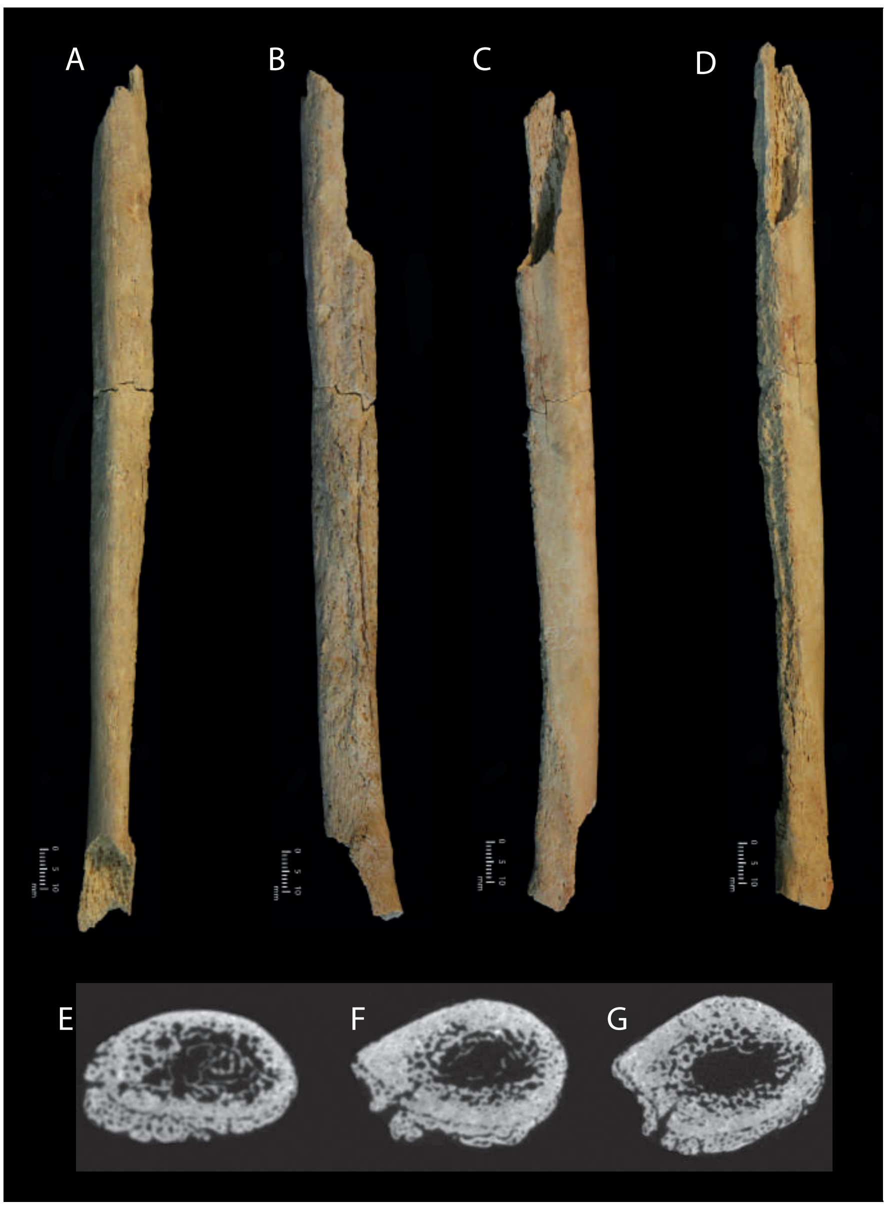

Figure 8.41. *Photographic and radiological images pertaining to fragmented adult left fibula (FB0037) from Context (960) of the Circle sample, depicting periosteal lesions traversing the refitted fragments, including: a) anterior view; b) medial view; c) lateral view; d) posterior view; e) transverse cross-section from CT data at mid-diaphysis showing globulated character of lesion, partially separated from underlying cortex which is slightly pockmarked; f) transverse cross-section at mid-point of extant element showing layered character of the lesion with vascularization on the medial surface; g) transverse cross-section at distal aspect of extant element, showing continued vascularization within the lesion and pockmarked cortex. Scale bar: 1 cm (photographs only). Photos Jess E. Thompson. (radiological images captured by L. Buck, Cambridge Biotomography Centre; processed by J. Magnussen & M. Pardey, Macquarie Medical Imaging.)*

taken inferior to the proximal fragmentation margin using a flexible paper tape.

The lesion exhibits mixed activity phases. The anterior and medial aspects of the lesion present a rugose topography of periosteal woven bone of mixed organization. Islands and layers of successive periosteal bone deposition contain bony nodules and billowing flows interspersed with extensive microporosity of single and coalescing pores, as well as diffuse microporosity. A vascular channel of 84.7 mm length is observed on the medial aspect, bordered by raised lamellar margins created by successive, chronic deposition of new periosteal bone. Sinuous impressions across the entire surface of the lesion indicate hypervascularity. The postero-medial aspect presents more recent osteoblastic activity, presenting as periosteal woven bone interspersed with microporosity. Here, islands of woven bone are observed but they are less rugose with finer microporosity. The antero-lateral and posterior margins of the lesion exhibit smooth deposits of well-healed bone with diffuse microporosity. On the lateral aspect, periosteal woven bone extends across the triangular subcutaneous area interspersed with micro- and microporosity. In this area, the lesion margins are sharply defined and directly correspond to the superior and lateral borders of the triangular subcutaneous area. Elsewhere, the margins of the extant portion of the lesion are diffuse and not well demarcated. The lesion is more rugose and porous than the surrounding cortex and is observed to differ in colour. When viewed from the fragmentation margin, the woven bone sits proud of the underlying cortex and no cortical change is observed. There are no indications of fracture, cloaca, or sequestra on the extant portion of the element.

Radiological observations:
The lesion is markedly more prolific on the anterior and medial surfaces on the extant portion of the element, where the new bone is dense and compact. Some separation is evident between the cortex and the periosteal new bone, and vascularity is observed within the lesion on the medial aspect (Fig. 8.41e-g). The character of the periosteal new bone is not as well-organized as the underlying cortex and presents an almost globular appearance. The underlying cortex appears pockmarked across almost the full extent of the extant fragment; approximately <10% of the extant element presents unaffected cortex, largely on the lateral surface. The new bone continues across the extant portion of the diaphysis on the lateral and posterior aspects. On the lateral surface, the cortex is in good condition and appears to be unaffected.

The lesion is truncated because of *postmortem* fragmentation, indicating that it extended onto at least the proximal metaphysis and distal diaphysis and was more widespread than is observable. Given that much of the element cannot be assessed, trauma and fracture must be considered in the differential diagnosis. The lesion is diffuse, extensive and associated with cortical change, suggesting a systemic process (Ortner 2003). Dense periosteal new bone formation on the fibula has been reported in cases of melorheostosis, hypertrophic osteoarthropathy (HOA) and chronic venous insufficiency (CVI) (Fennell & Trinkaus 1997; Gensburg *et al.* 1988; Kelley & Lytle 1995; Lester 1967; Martinez-Lavin *et al.* 1994; Yap *et al.* 2017). Melorheostosis is a rare condition which typically affects one, and occasionally several, bones of the lower limb, presenting dense and nodular new bone in a characteristic 'dripping candle wax' formation (Ortner 2003, 499 ff). Melorheostosis can be discounted in this case, as the lesion presents a layered, ropey and plaque-like expression. As mentioned before, HOA presents as symmetrical diaphyseal lesions on long bones, often alongside clubbing of the digits (Ortner 2003, 354). The location and expression of the lesion on the extant fibula resembles reported cases of HOA, although it cannot be ascertained whether the contralateral element or further long bones and/or digits were affected. As a result of the similar expression of periostitis because of HOA and CVI, CVI remains a possible aetiology in this case (Gensburg *et al.* 1988, 1280).

Lesion type and healing status: Mixed; Mixed.
Lesion preservation: Excellent.
Differential diagnosis: Trauma; Other.

8.6.1.6. FB0038: Fibula

Context:	(960)
Grid Ref:	99/112
Year of Excavation:	BR94
Other Details:	Unit 1, Spit 4

Element identification and preservation:
Fragment of right adult fibula which comprises the proximal metaphysis and approximately half of the proximal third of the diaphysis. A stepped fragmentation margin transects the fibular neck and an irregular fragmentation margin truncates the diaphysis. Minor areas of focal erosion are observed on the margins of the lesion. Adult age estimation is based on the size of the extant element and the relative thickness of the cortex (White *et al.* 2012, 315). As mentioned before, there are no current morphological or metric sex assessment methods engaged for isolated, fragmentary fibulae. The element is ~15% complete and the extant portion of the element is in fair condition. All damage is observed to be *postmortem*.

Figure 8.42. *Photographic and radiological images pertaining to fragmented adult right fibula (FB0038) from Context (960) of the Circle sample, depicting periosteal lesions traversing the refitted fragments of the proximal metaphysis and diaphysis, including: a) anterior view; b) medial view; c) lateral view; d) posterior view; e) transverse cross-section from CT data at proximal metaphysis showing sediment adhesion and pockmarked cortex; f) transverse cross-section toward the distal aspect of the extant element showing periosteal deposition on the medial aspect, perpendicular to the cortex. Scale bar: 1 cm (photographs only). Photos Jess E. Thompson; (radiological images captured by L. Buck, Cambridge Biotomography Centre; processed by J. Magnussen & M. Pardey, Macquarie Medical Imaging).*

Macroscopic observations:
Periosteal woven bone is observed on the extant portion of the element, although fragmentation of the proximal metaphysis and the diaphysis obfuscate full observation of pathology (Fig. 8.42a-d). On the anterior aspect, the lesion extends the full extent of the extant portion of the element along the interosseous crest, measuring 64.8 mm. From the proximal fragmentation margin, the lesion extends for 17.3 mm on the lateral aspect, 46.1 mm on the posterior aspect, and 11.4 mm on the medial aspect. The maximum length of the extant portion of the lesion is 64.8 mm along the interosseous crest; the maximum width measures 42.0 mm, encompassing the circumference of proximal metaphysis, inferior to the proximal fragmentation margin.

The lesion surrounds the metaphysis and exhibits mixed stages of activity. Woven bone exhibiting microporosity is present on the anterior and antero-lateral aspects. On the anterior aspect, the woven bone forms sheet-like deposits, while it is organized in approximately parallel lines of varying thickness along the interosseous crest, some of which coalesce towards the distal aspect of the extant portion of the diaphysis to become ropey and sit perpendicular to the cortex; these linear features extend onto the lateral aspect in two areas. Smooth plaque-like deposits of well-healed bone are present from the postero-lateral aspect to the medio-lateral aspect, interspersed with microporosity. On the antero-medial aspect, spicules are observed extending from the plaque deposit. The margins of the extant portion of the lesion are diffuse and not well-demarcated. With respect to the surrounding cortex, the woven bone is more rugose and porous and differs in colour. When viewed from the fragmentation margin, the woven bone sits proud of the underlying cortex and no cortical change is observed. There are no indications of fracture, cloaca, or sequestra.

Radiological observations:
Sediment is observed within the medullary cavity, particularly in the region of the proximal metaphysis, and therefore much trabecular bone has not been preserved. Some co-occurrence is observed with sediment adhesion and erosion of adjacent cortices, suggesting demineralization because of taphonomic processes (Fig. 8.42e). The cortex, particularly in the region of the proximal diaphysis, is irregular and pockmarked. Toward the distal end of the extant fragment, where sediment has not penetrated the element, the cortices underlying the periosteal lesions are observed to be slightly thicker and better preserved (Fig. 8.42f). Adjacent to the distal fragmentation margin, periosteal new

bone is observed on the anterior aspect and the underlying cortex is irregular. On the posterior aspect, the cortex is more regular and well-preserved, indicating that the lesions represent zonal deposits of new bone. The lesions are more apparent on the extant portion of the diaphysis than the metaphysis.

The lesion is truncated because of *postmortem* fragmentation, indicating that it extended further on the proximal metaphysis and diaphysis and was more widespread than is observable. As much of the element cannot be assessed, trauma and fracture must be considered in the differential diagnosis. The lesion occupies multiple surfaces and therefore does not represent a subperiosteal haematoma or ulcer (Ortner 2003, 84, 207). Although the extant portion of the lesion is damaged because of *postmortem* taphonomic processes, the expression of the periosteal new bone is ropey as opposed to nodular and therefore does not resemble that seen in cases of melorheostosis (Ortner 2003, 499 ff.). As outlined above, HOA and CVI are potential differential diagnoses. The character of the lesion on the extant fragment may be consistent with HOA, although we would expect the lesion to be more prolific on the mid-diaphysis, which is absent. Moreover, it cannot be ascertained whether the contralateral element or further long bones and/or digits were also affected. As a result of the similar expression of periostitis because of HOA and CVI, CVI again remains a possible aetiology in this case (Gensburg *et al.* 1988, 1280).

Lesion type and healing status: Mixed; Mixed.
Lesion preservation: Excellent.
Differential diagnosis: Trauma; Other.

8.6.1.7. Summary

Surprisingly, given their discrete depositional context, the adult elements described above exhibit periosteal lesions of widely varying expression. This presents a challenge to differential diagnosis. Research by Weston (2008, 2009) demonstrates that the morphology of periosteal lesions does not strongly correlate with their aetiology, but rather relates more closely to healing status and chronicity. Only some general conclusions can be made based on lesion type; for example, thick periosteal new bone deposits often indicate a chronic condition or osteomyelitis (Weston 2008, 55). Knowledge of the individual's age, sex, and health status (especially co-morbidities) are of key importance for differential diagnoses (Weston 2008, 56). Unfortunately, beyond broad adult age range, these factors cannot be addressed here, and caution must be exercised in attempts to identify aetiology/ies.

Nevertheless, through reference to bioarchaeological, clinical and palaeopathological literature, it is possible to exclude some potential aetiologies for each element. Significantly, there is no repetition of elements in this sample, as even the fibula fragments represent different sides and zones. The left ulna and radius present focal deposits of minor periosteal reaction on several muscle attachment sites; the character of the lesions, mixed healing stages, and muscles involved are similar across both elements. Furthermore, they are both observed to be of similar size and morphology (Fig. 8.43) and were excavated from the same level within this grid square. This may suggest that they originate from the same individual, who repetitively placed their left forearm under excessive strain. The

Figure 8.43. *Fragmented adult left radius (FB0033) and ulna (FB0034) from Context (960) of the Circle sample, both from grid square 99E/112N. While excavated in a disarticulated state, these elements are both of similar condition, size and morphology. Periosteal lesions are observed on contiguous muscle attachment sites on both elements, suggesting they precipitate from the same individual. Scale bar: 1 cm. (Photo Jess E. Thompson).*

lower limb elements provide different insights. The femoral fragment is likely osteoporotic, a factor which may relate to the aetiology of the periosteal lesions. Osteoporosis is not indicated in the lower leg elements, for which a small range of diagnoses are considered. Lesions on the extant portion of the right tibia, however, may represent multiple aetiologies and/or insults, and are distinct from those on the fibula fragments. In addition to the complexities of differential diagnosis when presented with disarticulated fragments, it is difficult to distinguish between prospective aetiologies for the lower leg elements. Many clinical reports highlight extreme cases and do not deal with dry bone specimens, while radiography is unlikely to register the early stages of periosteal bone formation (Weston 2012, 495). Altogether, we suggest that these elements originate from at least five individuals and demonstrate a range of pathological processes.

The high proportion of adult elements displaying periosteal lesions in this area is exceptional because of both their close spatial association and the relative under-representation of this category of lesions in all other contexts within the Circle. Context (960) is dated toward the end of the Circle's use, a period when declining environmental conditions and changing agricultural practices may have signaled restricted dietary diversity (§8.7.6). These elements may precipitate from individuals who lived through phases or cycles of resource instability and experienced heightened psychological, nutritional, metabolic and physical stress as a result.

8.6.2. Context (960) non-adult remains

8.6.2.1. FB0039: Frontal fragments

Context:	(960)
Grid Ref:	99/111
Year of Excavation:	BR94
Other Details:	Unit 1, Spit 3

Element identification and preservation:
Fragmentary non-adult frontal bone represented by three fragments which are observed to refit (Fig. 8.44a). The fragments comprise the left orbit, the frontonasal suture, the medial aspect of the right orbit, the left frontal eminence, and the left and medial portions of the frontal squama. On the supero-medial aspect of the frontal squama, an ovoid-shaped area of *postmortem* damage fully penetrating the cortex is observed. The margins of the defect are broader on the ectocranial surface, and they are rough, clean and differ in colour to the ecto- and endo-cranial surfaces. Minimal sediment is observed within the diploë. This damage therefore likely occurred during excavation. Taphonomic erosion and root etching interrupt the lesion in numerous locations. Although standards exist for estimating age based on measurements of the frontal bone (Young 1957; cf Scheuer & Black 2000, 108), it is not possible to apply metric analysis to this element because of its highly fragmentary and incomplete state. The metopic suture is in the process of closure and is only retained immediately superior to the frontonasal suture, suggesting the individual was in the range of 2–4 years of age at the time of death (Scheuer & Black 2000, 108). The extant element is in fair condition and represents ~60% of a complete frontal. All damage is assessed to be *postmortem*.

Macroscopic observations:
Periosteal lesions are observed on the ecto- and endocranial surfaces and within the left orbit and extant medial portion of the right orbit (Fig. 8.44b-e). *Postmortem* fragmentation truncates the lesion on all aspects; sediment has adhered to spicules in some areas, and root etching has interrupted the lesion. Full observation of pathology is therefore obfuscated. When viewed from the fragmentation margins, the lesions are observed to sit proud of the underlying cortex. Potential cortical involvement is only observed on a small area within the right and left supra-orbital margins. Since the lesion is truncated by fragmentation, its relationship to the surrounding cortex cannot be defined. There are no indications of fracture, cloaca or sequestra on the extant portion of the element.

On the ectocranial surface, the maximum length of the lesion is approximately 112.0 mm, measured with a flexible paper tape from the lateral border of the coronal suture to the most medial extent of the element; the maximum width of the lesion is approximately 130 mm on the sagittal plane. On the endocranial surface, the maximum length of the lesion is approximately 106.0 mm, from the most lateral border of the coronal suture to the medial extent of the element; the maximum width of the lesion is approximately 125.0 mm on the sagittal plane. On the infraorbital surface, the maximum length of the lesion is 38 mm along the centre of the orbit on the coronal plane; the maximum width of the lesion is approximately 40.0 mm along the centre of the orbit on the sagittal plane.

The lesion presents mixed activity phases. On the ectocranial surface, approximately 90% of the superior aspect of the frontal squama exhibits compact bone with hypervascular activity. Extensive branching capillary impressions are observed posterior to left frontal eminence and along the sagittal midline, interspersed with diffuse microporosity. Focal microporosity with grooved exit channels is observed on the supero-medial aspect of both the right and left

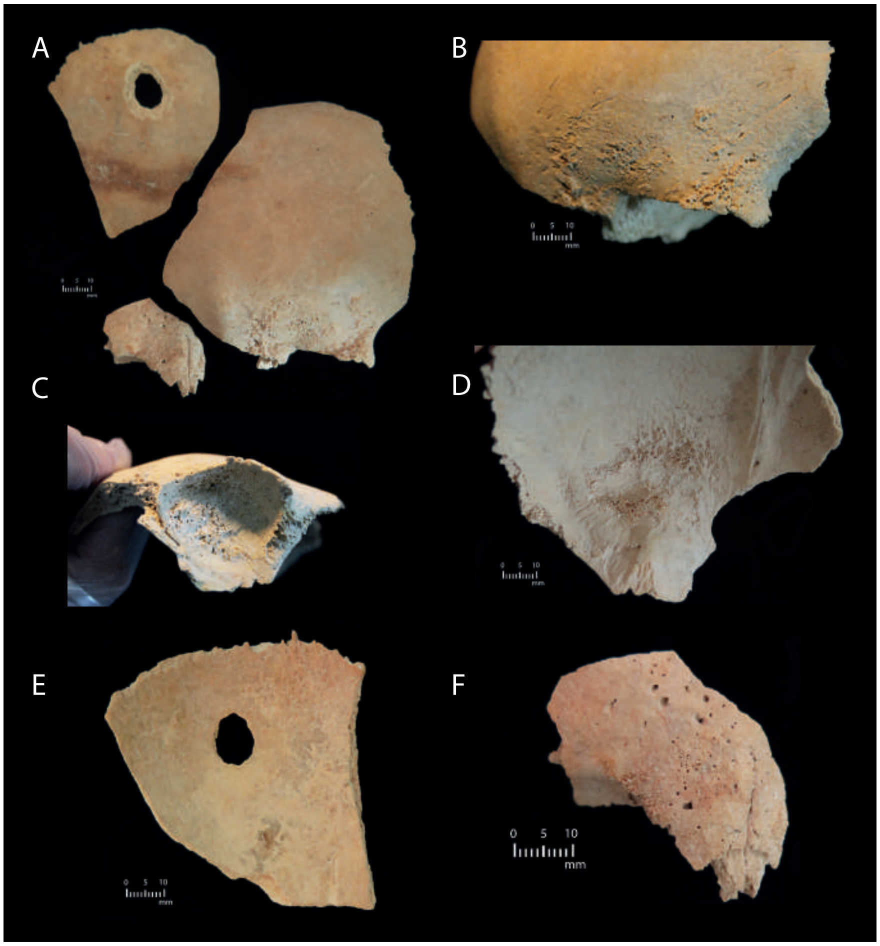

Figure 8.44. *Photographic images pertaining to fragmented non-adult frontal (FB0039) from Context (960) displaying extensive periosteal lesions, including: a) three re-fitting fragments of frontal bone; b) woven bone, capillary impressions and exit channels surrounding the left supraorbital margin on the ectocranial aspect; c) inferior view of left orbital roof presenting woven bone, macroporosity and extending spicules on the lateral aspect of the supraorbital margin; d) endocranial aspect of the frontal, displaying island of woven bone in the left frontal fossa; e) endocranial aspect of the central fragment of the frontal squama, presenting plaques of periosteal new bone; f) ectocranial aspect of the glabella and the extant portion of the right supraorbital margin displaying finely woven bone and macroporosity. Scale bar: 1 cm. (Photos Jess E. Thompson).*

supra-orbital margins, and on the lateral aspect of the left supra-orbital margin (Fig. 8.44b). Additionally, macroporosity with grooved exit channels is observed in this region. The margins of at least five micropores appear to have been eroded and enlarged *postmortem* because of taphonomic activity. A small area on the left frontal eminence differs in colour compared to the surrounding lesion; it is more yellow, glossy, and is most likely the original cortical surface. Extensive periosteal woven bone is observed in the glabella region and on the left supra-orbital margin. Perhaps as a result of *postmortem* truncation which may have eroded surrounding new bone, the woven bone appears to cluster in islands across this area. On the medial aspect of the left supra-orbital margin, supero-lateral to the metopic suture, and on the supero-lateral aspect of the right supra-orbital margin, these islands present as arrangements of fine, interconnected spicules perpendicular to the cortex, interspersed with micro- and macroporosity. The spicules on the left supra-orbital margin communicate with the lesion on the orbital roof. These islands are interspersed with micro- and macroporosity and bordered by capillary impressions. On the supero-lateral aspects of the left supra-orbital margins, the woven bone is extremely prolific and presents a more rugose topography of plates of bone organized perpendicular to the cortical surface, interspersed with micro- and macroporosity. On the left supraorbital margin, these plates of bone extend out from the margins, changing the anatomical profile of these features. The most supero-lateral aspects of the lesion in this region assume a more plaque-like deposit of woven bone and fine microporosity.

Extensive deposits of woven bone extend across the entire surface of the left orbital roof (Fig. 8.44c). The organization of woven bone is variable and interspersed with microporosity. The woven bone assumes a rugose topography within the anterior and medial aspects of the orbital roof, presenting as tall, perpendicular interconnected spicules assuming a trabecular-like organization. At the most medial aspect of the orbital roof, extensive osseous proliferation has produced sizeable, nodular projections, compromising the orbital space. On the postero-lateral aspect of the orbital roof, fine linear deposits of new bone overlie the cortex, often coalescing to form successive sheet-like plaques resulting in raised platforms that compromise the orbital space. Postero-medial to this is a border of finely woven bone which assumes a trabecular-like organization. Posterior to this, an area of compact bone with diffuse capillary impressions is observed across the orbital wall, interrupted by a deposit of finely woven bone, bordered by capillary impressions at the most inferior extant margin.

On the endocranial surface, mixed activity phases are observed. In the region of the superior aspect of the frontal crest, branching capillary impressions are observed within the compact bone. Diffuse microporosity is observed on the inferior aspect of the frontal crest, bordered laterally by woven bone. Extensive woven bone deposits are observed on the endocranial aspects of the extant portions of the right orbital roof, the left orbital roof, and in the area immediately extending from and infero-medial to the midcoronal suture landmark, although these lesions are truncated by *postmortem* fragmentation. Extensive proliferation of woven bone is observed on the superficial and anterior endocranial aspects of the left orbital roof. A plaque-like deposit of finely woven bone is observed on the medial aspect of the left orbital roof superficial to the horizontal portion. This lesion exhibits increased rugosity as it extends laterally and superiorly onto the left frontal fossa, where the lesion projects from the cortical surface into the cerebral space (Fig. 8.44d). Here, the lesion presents as focal areas of interconnecting perpendicular spicules and plates of new bone, which in some places exhibit trabecular organization. *Postmortem* damage has compromised complete observations of this lesion. Deposits of fine woven bone, interspersed with capillary impressions, border the lesion on all sides. The maximum length of this lesion is 18.3 mm (medial-lateral) and the maximum width is 13.4 mm (anterior-posterior). On the supero-medial aspect, the lesion is interrupted by circular granular depressions approximately 2–3 mm Ø.

Extending supero-laterally from the frontal crest on both extant right and left sides, capillary impressions are observed within plaque-like deposits of bone, occasionally interspersed with small islands of finely woven bone. These capillary impressions extend to lesions adjacent to the coronal suture on both sides. On the left side, a plaque-like deposit of disorganized and rugose woven bone is present, exhibiting microporosity and capillary impressions; its maximum length is 28.3 mm (medial-lateral), and maximum width is 32.8 mm (superior to inferior). On the right side, the lesion presents similarly as a plaque of disorganized, rugose woven bone, although the extant portion of the lesion is smaller as it is truncated because of *postmortem* fragmentation. It occupies a maximum length of 28.6 mm (medial to lateral) and a maximum width of 30.3 mm (superior to inferior) (Fig. 8.44*e*). The character, healing stage and organization of the woven bone and hypervascularity suggests the lesions adjacent to the left and right coronal suture pre-date the lesion in the left frontal fossa. Furthermore, it is likely that the lesion occupied other elements of the calvarium, because of its close relationship to cranial sutures on the extant portion of the frontal.

Radiological observations:
On the largest fragment, encompassing the left orbit, left frontal eminence and lateral aspect of the frontal squama, the outer table appears irregular in the area of the supra-orbital margin (Figs 8.44f & 8.45a-b). The periosteal new bone deposition is pronounced toward the floor of the anterior cranial fossa and, here, the outer table is more well-defined and radiolucent than the inner table. Elsewhere, the cortices and diploë are in good condition on this fragment. The greatest degree of spiculation is observed closest to, and involving, the frontal sinus (Fig. 8.45c). At the cross-section of the frontal sinus, the cortices change from smooth and well-defined margins to develop a diffuse, poorly demarcated lesion characterized by small radiolucent holes. The diploë and trabecular bone are eroded and there appear to be multiple layers and pockmarks throughout the inner and outer tables of the sinus alongside pronounced spiculation. The outer table of the supra-orbital margin is markedly thin and the cortical bone has been stripped away as a result of pathological processes. The central frontal fragment with extant nasal bones also features some diffuse radiolucent holes on the outer table, however there are no spiculations and there is no obvious periosteal new bone formation in this area. On this fragment, the trabeculae are in good condition and well-preserved. There are small spicules on the medial margin of the left orbit, but the underlying cortex is well-preserved.

Pathogenically, the lesion on the extant frontal is widespread but not generalized. The inner and outer tables and diploë are mostly well-preserved and intact except where they directly underlie prolific lesions. Therefore, haematopoietic disorders, specifically haemolytic anaemia and beta thalassaemia (commonly found in central Mediterranean populations), can be discounted, as these conditions are characterized by hyperplasia as a result of expansion of the erythropoietic marrow (Lewis 2018, 200; Ortner 2003, 364–5). In this element, localized trabecular erosion with overall preservation of the bone architecture strongly indicates a metabolic or inflammatory process. A localized intra-cranial infection in the regions of greatest spiculation – the cone of the orbit, sinus and/or ethmoid – may be considered. Intra-cranial infections such as sinusitis rarely develop suppurative complications, including meningitis and subdural empyema (Farmer & Wise 1973; Skelton *et al.* 1992). Childhood meningitis commonly develops following a bacterial infection, such as gastroenteritis, measles, mumps, *otitis media*, pneumonia, syphilis, tuberculosis, typhoid fever, and whooping cough (Lewis 2018, 144). Lesions involving the meninges on this element present as plaque-like deposits with capillary impressions and micropores, suggesting healing was underway at the time of death. Characteristic granulations associated with tubercular meningitis are absent (Lewis 2018, 144; Ortner 2003, 94). The proliferative lesions are reminiscent of metastasizing secondary bone tumours such as neuroblastoma; however, no osteoclastic activity is observed, and the new bone does not exhibit a radiating appearance (Ortner 2003, 536–7). Infantile cortical hyperostosis (ICH) occasionally reoccurs past infancy and has been reported in children of 2–4 years of age (Swerdloff *et al.* 1970). The condition sometimes involves the skull, provoking the deposition of pitted layered new bone, although most often affects the mandible, clavicle and long bones (Lewis 2018, 145; Lewis & Gowland 2009; Neuhauser 1970). The lesions on the extant frontal are distinct, presenting a more spiculated and hypervascular character without increased cortical thickening or involvement of the cortex.

Figure 8.45. *Radiological images pertaining to fragmented non-adult frontal (FB0039) from Context (960) displaying extensive periosteal lesions, including: a) sagittal cross-section from CT data displaying periosteal new bone in infraorbital surface, the endocranial aspect of the pars orbitalis and the frontal squama, and thinning of the outer table on the supraorbital margin; b) sagittal cross-section from CT data through the glabella displaying woven bone in the orbital vault and on the supraorbital margin; c) orthogonal plane cross-section from CT data displaying spicules of new bone within the left frontal sinus. (Radiological images captured by L.T. Buck, Cambridge Biotomography Centre; processed by J. Magnussen & M. Pardey, Macquarie Medical Imaging).*

The concentrations of reactive, woven and spiculated new bone on the supra-orbital margin, orbital roof and anterior cranial fossa are disorganized and were active at the time of death. These lesions are characteristic of subperiosteal and subdural haematomata, representing ossification following localized bleeding. In infants and children, such cranial lesions form part of the typical signature of trauma and abuse, alongside postcranial fractures of the ribs and long bones (Caffey 1946, 1974). No evidence of traumatic fracture is present on the extant frontal bone, and further periosteal reaction on the ecto- and endocranial surfaces of the frontal squama do not accord with a traumatic origin. As such, systemic metabolic disorders are the strongest candidates in this case. Vitamin C (scurvy) and vitamin D (rickets) deficiencies both stimulate periosteal new bone formation on the cranium in non-adult individuals (Brickley & Ives 2008; Lewis 2018, 211, 214; Ortner 2003, 386, 394). Rachitic features include osteopenia, bone thinning, frontal bossing, delayed fontanelle closure, and woven bone deposition which may eventually replace the inner and outer table (Brickley & Ives 2008, 103 ff.). On the extant frontal, the anterior fontanelle is observed to be closed (although this does not rule out the possibility that its closure was delayed), and there are no indications of osteopenia. Woven bone is zonally deposited on the ectocranial aspect of the frontal squama, and may indicate a phase of healing rickets with the commencement of osteoid mineralization. Scorbutic features include bilateral microporosity on the cranium and orbits and new bone formation in the orbits following haemorrhage because of weakened blood vessel walls (Brickley & Ives 2008, 57ff.; Lewis 2018, 214). Snoddy *et al.* (2018, 887) deem subperiosteal new bone and porosity on the endocranial surface suggestive markers of scurvy, while bilateral haemorrhage in the orbital roof is diagnostic. On the extant portion of the frontal bone assessed here, it is not possible to ascertain whether lesions are bilateral, although the proliferative new bone observed on the extant medial aspect of the right orbit and supra-orbital margin provides a strong association. The proliferative lesion in the region of the anterior cranial fossa is consistent with subdural haematoma. The plaque-like lesions occupying the frontal squama may suggest this individual experienced chronic episodes of vitamin C deficiency, as they appear to be in a healing state. Diffuse capillary impressions and porotic lesions present across much of the frontal squama indicate an inflammatory response to extravasated blood (Snoddy *et al.* 2018, 878; Stark 2014, 19). The lesions on the extant frontal are therefore most consistent with scurvy but are not diagnostic in isolation.

Lesion type and healing status: Proliferative; Active.
Lesion preservation: Good.
Differential diagnosis: Metabolic.

8.6.2.2. FB0040: Frontal fragment

Context:	(960)
Grid Ref:	99/111
Year of Excavation:	BR94
Other Details:	Unit 1, Spit 3

Element identification and preservation:
Fragment of right non-adult frontal bone comprising the lateral three quarters of the orbit and right sphenofrontal suture. Although this fragment does not re-fit to the extant portion of frontal described in §8.6.2.1 above, the location and expression of the lesion corresponds to that seen on, and surrounding, the left orbit of fragment FB0039. Additionally, this fragment is consistent in size and morphology with the extant portion of the frontal. A quadrangular-shaped area of *postmortem* taphonomic erosion is observed on the supero-lateral aspect of the supraorbital margin and interrupts the lesion. Further *postmortem* erosion and sediment is observed adhering to the spicules on all aspects of the lesion. Although standards exist for estimating age based on measurements of the frontal bone (Young 1957; cf Scheuer & Black 2000, 108), it is not possible to apply metric analysis to this element because of its fragmentary and incomplete state. Given that this fragment is similar in size and morphology to the element described above, we can assign it to a similar age range (2–4 years of age). The extant element is in fair condition and represents ~10% of a complete frontal. All damage is assessed to be *postmortem*.

Macroscopic observations:
Periosteal new bone deposition is observed on the ecto- and endocranial surface and within the extant portion of the right orbit (Fig. 8.46a-c). *Postmortem* fragmentation truncates the lesion on all aspects, and full observation of pathology is therefore obfuscated. When viewed from the fragmentation margins, the lesion is observed to sit proud of the underlying cortex. Since the lesion is truncated by fragmentation, its relationship to the surrounding cortex cannot be defined. There are no indications of fracture, cloaca or sequestra on the extant portion of the element.

The lesion traverses the full extent of the extant portion of the element on all aspects. On the ectocranial surface, the maximum length of the lesion is 42.2 mm; the maximum width is 26.7 mm. On the endocranial surface, the maximum length of the lesion is 44.0 mm (measured with a flexible paper tape); the maximum width is 29.0 mm. On the infraorbital surface, the maximum length of the lesion is 27.6 mm; the maximum width is 27.0 mm (measured with a flexible paper tape. Mixed activity phases are observed. On the ectocranial surface, the superior and supero-medial margins of the lesion exhibit compact bone interspersed with capillary impressions (Fig. 8.46a). Capillary impressions including microporosity are extensive adjacent to the border of the medial fragmentation margin. The lateral and inferior portion of the lesion exhibits extensive periosteal woven bone. The supero-lateral aspect exhibits microporosity; here, the woven bone presents a diverse organization of narrow spicules which lie both parallel, and at an approximate 45° angle to, the original cortex. The infero-lateral aspect of the lesion is truncated because of the quadrangular area of *postmortem* erosion. Bordering the erosion, on the infero-medial aspect, a more rugose topography of extensive woven bone is observed. In the central portion, interconnecting plates of bone arranged perpendicular to the cortex and interspersed with macroporosity are observed. The medial aspect of this area displays a cluster of finer spicules arranged in trabecular-like organization interspersed with extensive microporosity. Adjacent to this, on the supero-medial aspect of the supra-orbital margin, discolouration is observed with respect to the surrounding lesion and may represent truncation of the lesion subsequent to post-excavation cleaning.

On the endocranial surface, sediment adhesion suggests that stages of *postmortem* taphonomic erosion and other processes have interrupted the lesion, truncating its original expression (Fig. 8.46b). The superior, lateral and inferior margins of the lesion present compact bone interspersed with capillary impressions, some of which are truncated by the fragmentation margins. Within the centre of the lesion, woven bone presents an arrangement of fine spicules perpendicular to the cortex arranged in trabecular-like organization, interspersed with microporosity. The woven bone is

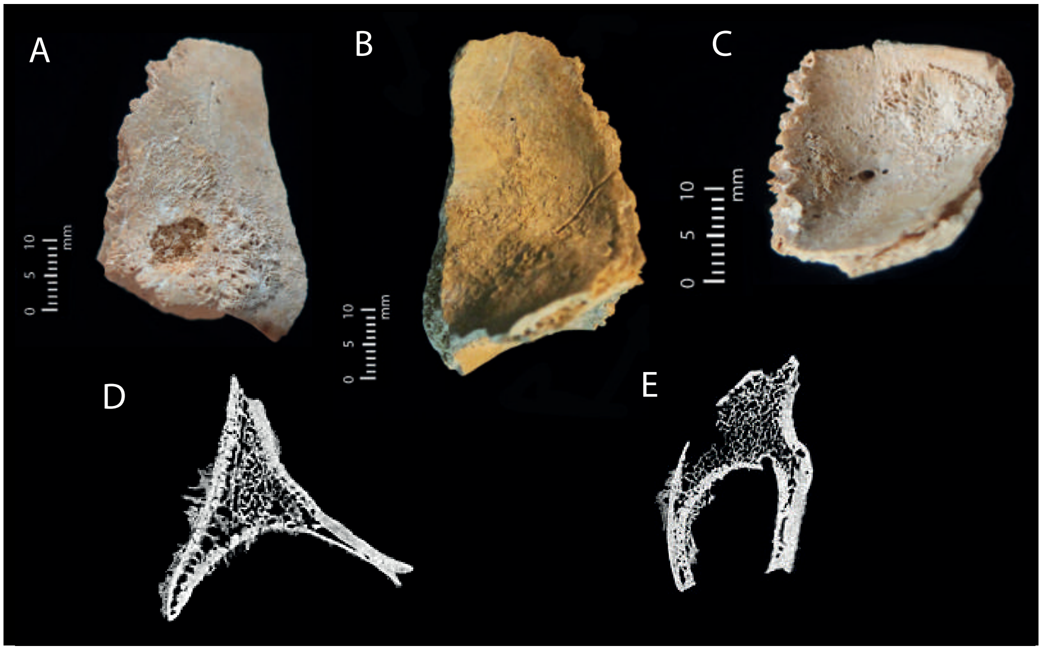

Figure 8.46. *Photographic and radiological images pertaining to fragment of non-adult frontal (FB0040) from Context (960) displaying extensive periosteal lesions, including: a) antero-lateral view of the ectocranial surface, with woven bone superior to the supraorbital margin and truncated by* postmortem *taphonomic erosion; b) endocranial view displaying woven bone and capillary impressions; c) inferior view of right orbital roof presenting islands of woven bone; d) sagittal cross-section from CT data through the mid-point of the orbit displaying spiculated new bone on the supraorbital margin, infraorbital surface and pars orbitalis; e) sagittal cross-section through the lateral aspect of the orbit, displaying woven bone on the supraorbital margin and infraorbital surface. Scale bar: 1 cm (photographs only). (Photos Jess E. Thompson; radiological images captured by L. Buck, Cambridge Biotomography Centre; processed by J. Magnussen & M. Pardey, Macquarie Medical Imaging).*

interrupted with small granular impressions on the infero-medial border.

On the infraorbital surface, the anterior border of the lesion along the supra-orbital margin presents compact bone. The antero-medial quadrant of the orbital roof exhibits woven bone interspersed with microporosity. The spicular organization varies; spicules overlying the cortex project anteriorly to the supra-orbital margin, while others are arranged at a sharply acute angle to the cortex. The postero-lateral quadrant of the orbital roof exhibits woven bone; fine spicules are arranged at an angle to the cortex, projecting medially, and interspersed with microporosity. Within the centre of the lesion, three distinct pores are observed. The posterior half of the lesion presents compact bone interspersed with capillary margins and microporosity.

Radiological observations:
The periosteal new bone is observed to be thicker than the cortex in most areas. Compared with the larger portion of the frontal, described above, there is more extant proliferative new bone formation on the ectocranial surface (Fig. 8.46d). On the lateral aspect of the extant portion of the right frontal, the cortices are in fair condition, but are observed to deteriorate progressively and are increasingly thinned approaching the medial aspect (Fig. 8.46d & e). The trabeculae are in fair condition. Given the similar expression and location of the lesion on this fragment when compared with the left orbital roof and supra-orbital margin, described above, it is highly probable that these fragments originate from the same individual and represent the same pathogenic process. As mentioned before, such proliferative lesions in the orbital roof indicate subperiosteal haematoma, usually attributed to trauma or scurvy (Brickley 2018; Brickley & Ives 2008, 58; Caffey 1974). As outlined above, reactive new bone formation along the supra-orbital margin is not consistent with trauma. The developmental stage, morphology, and lesion character on the extant right frontal are strongly compatible with the re-fitted fragments described above, and all were excavated from the same level and unit. Therefore, we argue that these fragments

all originate from the same young child. As such, the orbital lesions indicate bilateral orbital haemorrhage, diagnostic of scurvy (Brickley & Ives 2008, 57; Snoddy *et al.* 2018, 887; Thompson *et al*. 2021).

Lesion type and healing status: Proliferative; Active.
Lesion preservation: Good.
Differential diagnosis: Metabolic.

8.6.2.3. FB0041: Zygoma

Context:	(960)
Grid Ref:	99/111
Year of Excavation:	BR94
Other Details:	Unit 1, Spit 3

Element identification and preservation:
Left zygoma with frontal process fragmented. *Postmortem* damage is observed on the infraorbital margin. The maximum length of the zygoma, measured from the maxillary process to the temporal process using digital callipers, is 34.3 mm. Postnatal age estimation through metric analyses for the zygoma is not provided; however, the element is observed to present adult proportions, with a serrated temporal process, characteristic of individuals at least 2–3 years of age (Scheuer & Black 2000, 124). The extant element is in fair condition and is ~95% complete. All damage is assessed to be *postmortem*.

Macroscopic observations:
Periosteal new bone deposition is observed on the anterior, posterior and superior aspects of the element, extending across the full extent of each surface (Fig. 8.47a-c). The maximum length of the lesion from the maxillary process to the temporal process on the anterior aspect is 34.2 mm. the maximum width of the lesion on the midpoint of the sagittal plane is 16.2 mm. On the posterior aspect, the maximum length of the lesion from the maxillary process to the temporal process is 34.4 mm; the maximum width of the lesion is 15.5 mm. On the infraorbital surface, the maximum length of the lesion is 21.5 mm and the width of the lesion is 9.6 mm.

The lesion presents mixed activity phases. On the anterior surface, the proximal half of the lesion presents woven bone arranged in plate-like formations, perpendicular to the cortex, interspersed with diffuse micro- and macroporosity (Fig. 8.47a). Capillary impressions are observed on the medial and lateral margins of the element. The distal half of the lesion presents well-healed bone with microporosity; the inferior border exhibits capillary impressions and one macropore. On the posterior surface, spicules

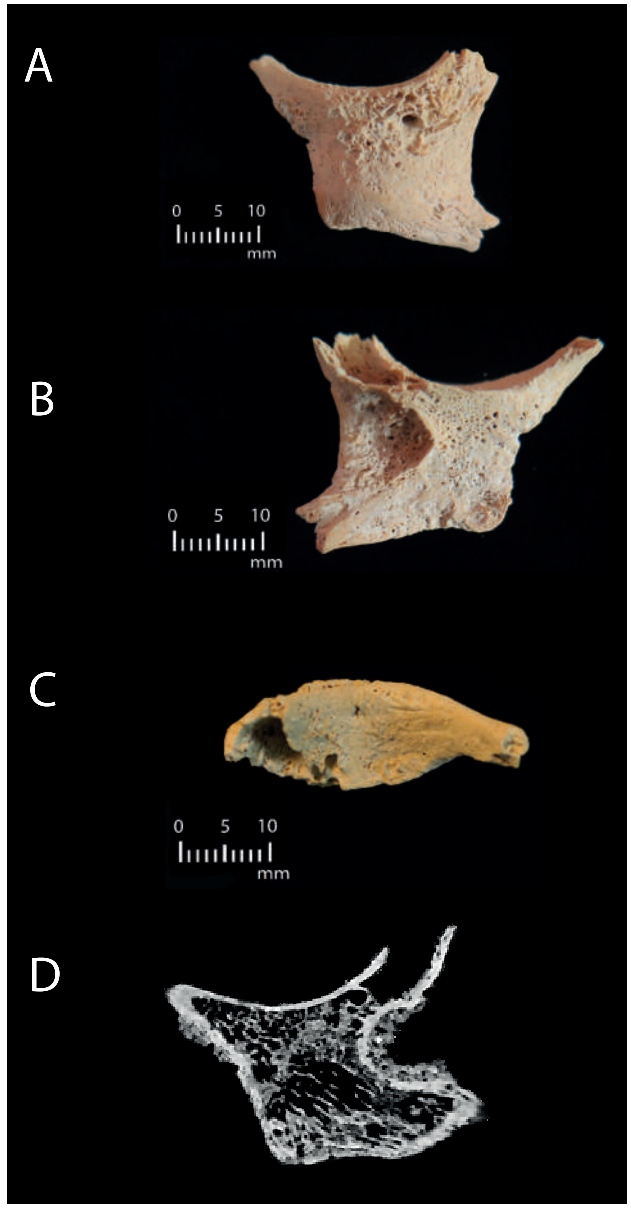

Figure 8.47. *Photographic and radiological images pertaining to non-adult left zygoma (FB0041) from Context (960) displaying extensive periosteal lesions, including: a) anterior view with woven bone concentrated on the proximal half of the element; b) posterior view presenting diffuse microporosity and woven bone; c) superior view displaying woven bone and microporosity on infraorbital surface, interrupted by excavation toolmarks; d) coronal cross-section from CT data presenting discontinuous cortex and periosteal new bone on the medial, lateral and inferior aspects. Scale bar: 1 cm (photographs only). (Photos Jess E. Thompson; radiological images captured by L. Buck, Cambridge Biotomography Centre; processed by J. Magnussen & M. Pardey, Macquarie Medical Imaging).*

perpendicular to the cortex are observed on the lateral portion interspersed with more diffuse woven bone deposition and micro- and macroporosity (Fig. 8.47b). On the medial and inferior aspect, smooth deposits of bone exhibit extensive microporosity. The infraorbital surface presents woven bone, becoming perpendicular in organization, interspersed with microporosity although some taphonomic damage, including excavation cutmarks, interrupts the lesion (Fig. 8.47c). Within the centre of the lesion, well-healed bone presenting microporosity is observed. The margins of the lesion cannot be defined and its relationship to the original cortex cannot be described. There are no indications of fracture, cloaca, or sequestra.

Radiological observations:
Considerable demineralization of the cortices is evident. The outer cortex underlying the lesion is both discontinuous and porotic (Fig. 8.47d). The trabeculae are relatively well-preserved, and the margins of nutrient foramina and vascular channels remain intact, indicating a minimal degree of internal bone loss. The new bone deposition is neither lamellated nor particularly spiculated on any aspects of the element, rather it is markedly disorganized and thick. The lesion does not resemble the typical lamellar new bone observed in cases of traumatic fracture.

Periosteal lesions on the zygoma are relatively uncommon, reported in association with tuberculosis (Meng & Wu 1942; Ortner 2003, 250), iron-deficiency anaemia (Ortner 203, 373), and scurvy (Buckley *et al.* 2014; Ortner *et al.* 1999, 2001; Snoddy *et al.* 2017). Tuberculous lesions on the cranium are most often observed in non-adult individuals (Lewis 2004, 150) and may involve the zygoma, especially the orbital margin (Ortner 2003, 250). Lesions are typically focal and destructive, however, in contrast to the extensive woven bone observed on this element. Ortner (2003, 373) presents a severe case of porotic hyperostosis and marrow hyperplasia indicating iron-deficiency anaemia in a young child; the zygomae exhibited porous lesions, expansion of the diploë and destruction of the outer table. Beta thalassaemia can cause more extensive changes, as trabecular expansion, cortical thinning and delayed sinus development lead to altered facial features, including 'bulging' zygomae (Lewis 2018, 200; Ortner 2003, 365). On the extant element, however, the trabeculae are well-preserved with no indication of enlargement, and porosity is mostly focussed on the internal aspect.

Scorbutic lesions on the zygoma are typically located on the internal/posterior aspect and the lateral orbital margin (Ortner *et al.* 2001, 346; Snoddy *et al.* 2018, 879). These locations are associated with *Mm. masseter*, *temporalis* and *orbicularis occuli* as well as branches of the masseteric, superficial temporal, zygomaticoorbital and zygomaticofacial arteries, all implicated in facial movement and expression (Snoddy *et al.* 2018, 879). The extant element presents extensive woven bone and porosity on the posterior surface, while the infraorbital and anterior surfaces exhibit islands of spiculated woven bone, suggestive of subperiosteal haematomas. The *Mm. zygomaticus minor* and *major* attach to the anterior aspect of the zygomae, essential for movement of the mouth. Brown and Ortner (2011, 200) present a case of scurvy in a Medieval two-year-old child, observing unilateral porosity inferior to the zygomaticofacial foramen. The lesions on the anterior aspect of the extant element appear to be rare in the presentation of scurvy. Snoddy *et al.* (2018, 888) note that porosity and subperiosteal new bone on the zygoma is suggestive of scurvy when observed bilaterally. Unfortunately, the contralateral zygoma is unavailable for assessment. However, the expression and location of the lesions are most consistent with a scorbutic aetiology.

Lesion type and healing status: Mixed; Mixed.
Lesion preservation: Excellent.
Differential diagnosis: Metabolic.

8.6.2.4. FB0042: Mandible fragments

Context:	(960)
Grid Ref:	99/111
Year of Excavation:	BR94
Other Details:	Unit 1, Spit 3

Element identification and preservation:
Two non-adult mandible fragments are observed to refit. The largest fragment comprises the right ramus, with right coronoid process almost complete and right mandibular condyle fragmented along the neck, and most of the mandibular corpus. The corpus is fragmented on the posterior aspect of the alveolus of the second left deciduous molar. The smaller fragment is observed to refit along the superior aspect of the corpus, completing the alveolus containing the second left deciduous molar, although the inferior portion of the mandibular corpus is fragmented and absent. The left coronoid process is almost complete, while the left mandibular condyle is fragmented along the neck. Focal areas of *postmortem* erosion are observed on the element, while a small triangular area of fragmentation on the lingual aspect of the right mandibular corpus exposes the crypt containing the developing germ of the right first permanent molar. The mandibular symphysis is fused. Mandibular dental eruption indicates

an age at death of 2 years (±8 months) because of the eruption of the deciduous right first molar (FDI 84), incomplete root development of the deciduous left second molar (FDI 74), and developing crown of the permanent right first molar (FDI 46; Ubelaker 1989). The extant portion of the element is in good condition and is ~90% complete. All damage is assessed to be *postmortem*.

Macroscopic observations:
Periosteal new bone deposition is observed on all aspects of the element. *Postmortem* fragmentation in the alveolus posterior to the second left deciduous molar obfuscates full observation of pathology. When viewed from the fragmentation margins, the lesions are observed to sit proud of the underlying cortex and no cortical change is discerned. All lesions differ in colour to the surrounding cortex, but present diffuse margins which are not well demarcated. There are no indications of fracture, cloaca or sequestra.

The lesion envelops the anterior and lateral aspects of the mandibular corpus, encompassing approximately 90% of the right ramus. The lesion commences approximately 6.9 mm from the superior-most projection of the right mandibular condyle and extends anteriorly for 20.5 mm to the coronoid process and 27.0 mm inferiorly to the gonial angle, where a small localized area of *postmortem* erosion truncates the lesion. From its most posterior extent on the right gonial angle, the lesion envelops the mandibular corpus for a maximum length of approximately 111.0 mm (measured with a flexible paper tape) and is truncated by the fragmentation margin (Fig. 8.48a & b). The maximum height of the lesion on the posterior border of the right ramus is 32.1 mm. The lesion demonstrates mixed activity phases. On the right ramus, capillary impressions are observed on the superior margins, on the condyle and coronoid process. Woven bone is observed on the margins of the lesion, interspersed with micro- and macroporosity. Postero-inferior to the oblique line, woven bone is arranged in conjoined spicules and plates perpendicular to the cortical surface, assuming a trabecular-like appearance, bordered inferiorly by fine capillary impressions on the gonial angle. *Postmortem* damage has removed portions of the new bone in this area. Macroporosity is observed on the posterior border of the oblique line. A small area of plaque-like bone is present in the centre of the ramus, interspersed with fine capillary impressions.

On the lingual aspect, periosteal new bone is observed in two focal areas: adjacent to the fragmentation margin associated with the crypt of the developing germ of the first permanent right mandibular molar (FDI 46), and on the right ramus extending to the submandibular fossa (Fig. 8.48c). The first lesion is truncated by the previously mentioned fragmentation margin, but is observed to commence within the posterior aspect of the left submandibular fossa 6.5 mm proximal to the fragmentation margin. The extant portion of the lesion encompasses a maximum length of 6.5 mm and a maximum height of 2.5 mm. The lesion presents mixed activity phases. The peripheral margins exhibit well-healed plaque deposits of bone interspersed with capillary impressions, while the centre exhibits extensive woven bone deposition with focal micro- and macroporosity. The margins of the lesion are diffuse and not well-demarcated. The second lesion commences 5.2 mm inferior to the fragmentation margin on the right coronoid process, extending 20.7 mm posteriorly to the mandibular condyle and inferiorly for 28.2 mm to the gonial angle. From the most posterior extent of the lesion on the gonial angle, its maximum length is 30.7 mm to the submandibular fossa. On the coronal plane, the maximum height of the lesion is 28.0 mm on the right ramus. The lesion demonstrates mixed activity phases. The superior and posterior margins of the lesion present compact bone with increased micro- and macroporosity. The central portion of the lesion, within and surrounding the mylohyoid groove, demonstrate periosteal woven bone. Capillary impressions surround the mylohyoid groove, particularly on the superior aspect, and extensive micro- and macroporosity is observed within the mylohyoid groove. Some islands of woven bone are observed posterior and inferior to the mylohyoid groove, interrupted by compact bone. Increased porosity is demonstrated across the lesion. On the inferior aspect of the right mandibular corpus, periosteal new bone deposition is observed anterior to the previously mentioned fragmentation margin, encompassing a maximum length of 4.2 mm and a maximum width of 2.8 mm. The extant portion of the lesion exhibits periosteal woven bone interspersed with microporosity; its margins are distinct from the surrounding cortex and the bone is observed to be more rugose and porous.

Woven bone interspersed with microporosity extends across the right side of the mandibular corpus on the distal half and on the left mandibular corpus. *Postmortem* erosion has damaged the lesion, however, and the margins are not well demarcated. A small island of woven bone is observed in the fossa between the right mental foramen and mental eminence, presenting microporosity. Extensive microporosity is present on the mental eminence, interspersed with patches of woven bone deposition and capillary impressions on the inferior border (Fig. 8.48b). Well-healed plaque deposits of bone are observed posterior to this, interspersed with microporosity. Across the

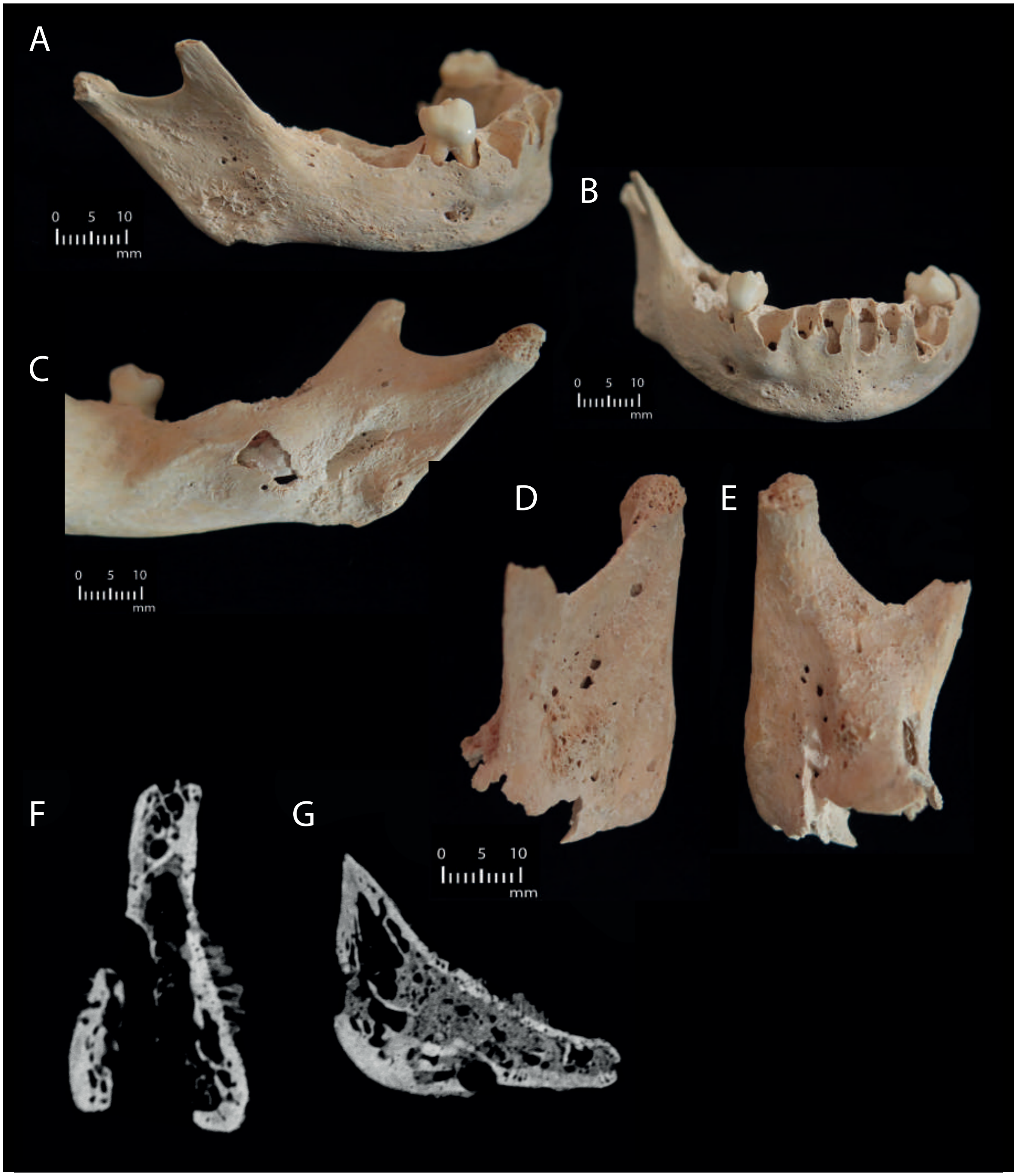

Figure 8.48. *Photographic and radiological images pertaining to fragmented non-adult mandible (FB0042) from Context (960) displaying focal periosteal lesions, including: a) lateral view of right ramus and corpus with woven bone concentrated on the ramus; b) anterior view presenting microporosity and finely woven bone on the mental eminence; c) medial view of right ramus with woven bone surrounding crypt containing developing right first permanent molar (FDI 46) and finely woven bone surrounding the mylohyoid groove; d) antero-lateral view of fragmented left ramus displaying woven bone and macro- and microporosity; e) medial view of fragmented left ramus with finely woven bone on anterior border of mylohyoid groove; f) transverse cross-section from CT data through left ramus vertical short axis displaying spicules on lateral aspect; g) sagittal cross-section through right ramus displaying spicules on medial aspect. Scale bar: 1 cm (photographs only). (Photos Jess E. Thompson; radiological images captured by L.T. Buck, Cambridge Biotomography Centre; processed by J. Magnussen & M. Pardey, Macquarie Medical Imaging).*

entire anterior surface of the mandible, the lesion demonstrates hypervascularity although the margins are diffuse and not well-demarcated. A small island of woven bone deposition is observed in the fossa between the right mental foramen and the mental eminence, presenting microporosity bordered by fine capillary impressions. Further capillary impressions and plaque-like bone deposition extend inferiorly and posteriorly along the corpus. Four micropores are observed inferior to the left mental foramen. Well-healed plaque deposits of bone are observed posterior to this, interspersed with microporosity.

On the lateral aspect of the left ramus, periosteal new bone deposition commences 7.2 mm inferior to the fragmentation margin on the coronoid process, extending 19.1 mm posteriorly and 20.3 mm inferiorl*y* (Fig. 8.48d). The maximum height of the lesion on the coronal plane is 27.1 mm; the maximum width of the lesion is 20.8 mm. The lesion exhibits mixed activity phases. The posterior margins of the lesion exhibit well-healed lamellar bone interspersed with micro- and macroporosity and capillary impressions. Well-healed bone extends into the centre of the lesion with macroporosity on the oblique line. Islands of woven bone are observed on the anterior aspect inferior to the mandibular notch, on the most inferior aspect of the coronoid process and posterior to the oblique line. In the latter location, bony nodules are observed on the superior aspect and, inferior to this, clusters of spicules and conjoined bony plates are present at a perpendicular angle to the cortex, interspersed with microporosity. On the posterior aspect, the lesion commences 28.7 mm inferior to the mandibular condyle and extends for 8.1 mm. The maximum width of the lesion is 3.4 mm. The lesion presents smooth deposits of bone surrounding focal macroporosity.

On the medial aspect, the extant portion of the lesion commences inferior to the margins of *postmortem* erosion on the left condyle, extending inferiorly for 36.5 mm and anteriorly for 22.7 mm (Fig. 8.48e). The maximum height of the lesion is 36.7 mm on the posterior border and the maximum width of the lesion is 15.6 mm on the inferior aspect of the mandibular notch. The lesion presents mixed activity phases. Inferior to the mandibular condyle, small granular and capillary impressions are observed. Inferior to the mandibular notch, woven bone is interspersed with microporosity, continuing inferiorly onto the anterior and posterior border of the mylohyoid groove. Macroporosity is observed within the mylohyoid groove. On the anterior border of the mylohyoid groove, clusters of bony spicules and plates sit perpendicular to the cortex. Woven bone is observed on the margins of the lesion, interspersed with capillary impressions and micro- and macroporosity.

Radiological observations:
On the largest fragment, the cortices are smooth and well-defined on the lingual and buccal aspect of the mandibular corpus, particularly around the sagittal midline, representing healthy tissue. Some small spiculations are preserved on the anterior aspect of the mandibular corpus, superficial to the alveoli containing the developing permanent canines, presenting a bilateral expression on the labial aspect of the corpus. No lesions are observed on the lingual aspect. The mandible retains a 'normal' appearance until just posterior to the crypt containing the developing right first permanent molar, after which the lesion progressively worsen*s* (Fig. 8.48f). On the right ramus, the degree of bone loss on the buccal surface around the area of the developing right first permanent molar is extensive. At the angle of the mandible on the right side, small areas of periosteal new bone are observed. Similarly, periosteal new bone is observed on the left mandibular angle, although the lesion is more widespread, especially on the buccal surface (Fig. 8.48g). On the left mandibular ramus, the cortices present diffuse poorly demarcated radiolucent holes and the trabeculae are observed to be pockmarked. Lesions are located close to the alveoli on the buccal aspect of the posterior teeth and are expressed bilaterally. No periosteal new bone is observed within the crypts.

As Lewis (2018, 3) notes, distinguishing new bone formation as a result of the normal growth process from infectious or traumatic new bone deposition is challenging. Focal areas of micro- and macro-porosity on the extant mandible may usually be attributed to growth, however, their association with finely woven new bone across much of the element, as well as the bilateral expression of the reactive new bone is suggestive of pathological processes. There is no evidence of fracture; the element is re-fitted along a *postmortem* fracture margin and a small portion of the lingual surface of the corpus is absent. Such extensive porosity and new bone deposition likely has either an infectious, neoplastic or metabolic origin.

As mentioned before, infantile cortical hyperostosis (ICH) has been reported past infancy, in children of 2–4 years of age (Swerdloff *et al.* 1970). The condition most often affects the mandible and clavicle and is characterized by extensive periosteal new bone formation (Lewis 2018, 145). In the early stages of inflammation, cortical hyperostosis is pronounced, while later remodelling is evident through widening of the medullary cavity (Lewis 2018, 145). On the extant element, the cortex is of expected thickness and only demonstrates irregularity in the region of the periosteal lesions, and no expansion of the medullary space is observed. Such observations, alongside dental eruption in the expected sequence, also rule out beta thalassaemia (Lewis 2018, 200; Ortner 2003, 365). Primary or secondary tuberculosis may involve mandibular lesions, including osteomyelitis (Imamura *et al.* 2004) and lytic destruction in the region of the mandibular angle alongside new bone formation (Gupta & Singh 2007). Actinomycosis, a rare bacterial infection, can present similarly; *Actinomyces* bacteria commonly line the oral cavity and may provoke localized infection secondary to tissue damage, for example following injury, trauma or periodontal disease (Ortner 2003, 319). Inflammatory reactions on the mandible include periosteal new bone deposition, hypervascularity, and numerous focal lytic lesions alongside some cortical and trabecular erosion (Ortner 2003, 319-20). On the extant element, new bone deposition is observed, including on the mandibular angle, but there is minimal cortical erosion and no lytic foci are present. Leukemia, cancers of the myeloid and lymphoid hematopoetic cells, peaks in children from 2–5 years of age, presenting as periosteal new bone formation and extensive lytic pitting (Lewis 2018, 206). Rothschild *et al.* (1997) present a case of childhood leukemia in which periosteal new bone was observed on the external aspect of the mandibular ramus alongside lytic pitting on the cranium, scapula, long bones, pelvis and pedal elements. On the extant mandible, porosity is less frequent than woven new bone deposition and no lytic pitting is observed.

Therefore, a metabolic disorder is most likely. The concentrations of woven subperiosteal new bone bilaterally on the ascending ramus, between the mental foramen and mental eminence, and in the region of the mylohyoid groove were active at the time of death and are characteristic of subperiosteal haematomata. Scorbutic lesions on the mandible include extensive microporosity (Brickley & Ives 2008, 57; Ortner *et al.* 2001), new bone on the coronoid process, ramus, alveoli and mylohyoid line (Lewis 2018, 217; Ortner *et al.* 2001; Snoddy *et al.* 2018), and *antemortem* tooth loss (Lewis 2018, 217). The coronoid processes are fragmented on the extant mandible and cannot be assessed, however new bone is observed on the lateral and medial aspect of the rami, as well as on the mandibular corpus. There is no evidence of periodontal disease or alveolar resorption, indicative of *antemortem* tooth loss. Bilateral deposits of subperiosteal new bone on the rami are diagnostic of scurvy (Snoddy *et al.* 2018, 890). Significantly, the lesions on this element accord with attachment sites for the *Mm. mentalis*, *masseter*, and *medial* and *lateral pterygoid*, which are involved in movement of the lower lip, mastication and speech (Parkin & Logan 2007, 40, 42), indicating micro-trauma associated with these essential facial movements.

Lesion type and healing status: Mixed; Mixed.
Lesion preservation: Excellent.
Differential diagnosis: Metabolic.

8.6.2.5. FB0043: Rib fragment

Context:	(960)
Grid Ref:	99/111
Year of Excavation:	BR94
Other Details:	Unit 1, Spit 3

Element identification and preservation:
Fragment of left middle-lower order rib shaft. The head and the neck of the rib are fragmented and absent. A *postmortem* transverse fracture truncates the shaft of the rib at the approximate mid-point. Regression equations exist for age estimation according to the length of individual ribs in prenatal individuals (Fazekas & Kosa 1978; cf Scheuer & Black 2000, 243). Amongst infants and children however, the major factor affecting rib morphology is increased torsion in rib shafts as the ventral aspect of the thorax descends (Scheuer & Black 2000, 241). Although incomplete, the morphology of the extant portion of the rib shaft demonstrates torsion and may indicate that this individual was between the ages of at least 1–3 at the time of death (Scheuer & Black 2000, 241). The extant portion of the element is in good condition and represents ~50% of a complete rib. All damage is assessed to be *postmortem*.

Macroscopic observations:
Periosteal new bone deposition is observed almost circumferentially on the extant portion of the body of the rib, involving the external and pleural surfaces (Fig. 8.49a-b). The lesion is truncated medially and laterally, obfuscating full observation of pathology. There are no indications of fracture, cloaca, or sequestra on the extant portion of the element.

On the external aspect, the lesion commences 24.5 mm from the anterior fragmentation margin and extends for 67.0 mm. The lesion demonstrates mixed activity phases. On the pleural aspect, the extant portion of the lesion commences adjacent to the anterior fragmentation margin and extends for 77.0 mm (measured with a flexible paper tape). On the external aspect, partially healed plaque-like deposits of bone are observed, interspersed with diffuse capillary impressions (Fig. 8.49a). The margins of the extant portion of the lesion are diffuse and not well demarcated.

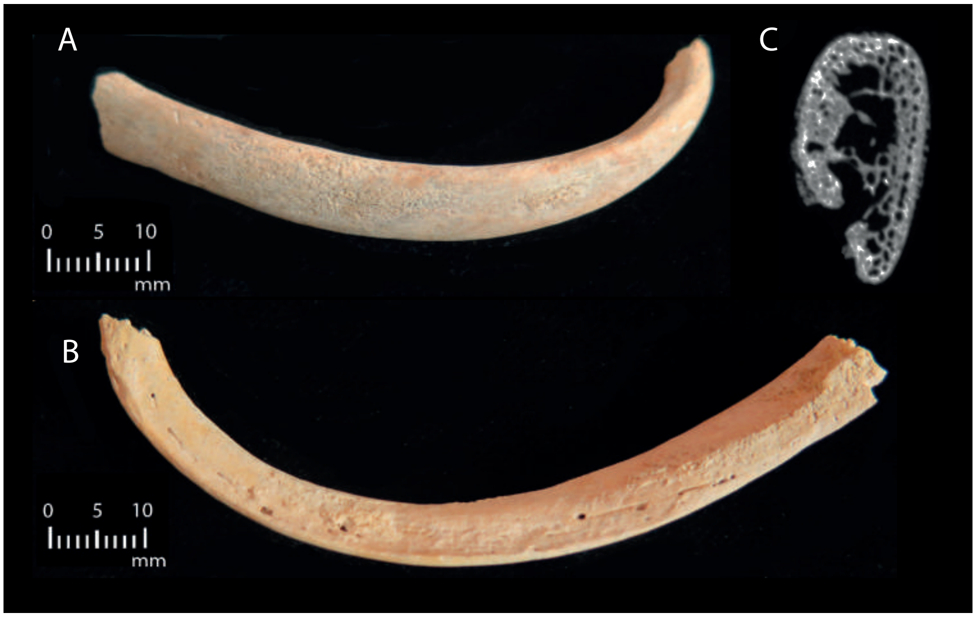

Figure 8.49. *Photographic and radiological images pertaining to fragmented non-adult left rib (FB0043) from Context (960) displaying focal periosteal lesions, including: a) posterior/external view displaying finely woven bone with capillary impressions; b) inferior view of pleural surface displaying focal lesions of woven bone; c) sagittal cross-section from CT data through distal aspect of extant portion of rib, displaying fine spiculation on superior, external and pleural aspects. Scale bar: 1 cm (photographs only). (Photos Jess E. Thompson; radiological images captured by L. Buck, Cambridge Biotomography Centre; processed by J. Magnussen & M. Pardey, Macquarie Medical Imaging).*

The lesion is taller than the surrounding cortex and is observed to differ in colour. When viewed from the lateral fragmentation margin, the lesion merges with the original cortex. On the pleural surface, the most medial and lateral portions of the extant lesion present clusters of bony spicules and plates, sitting perpendicular to the cortex in trabecular-like organization (Fig. 8.49b). The lesion is more severe on the anterior aspect. In the central aspect of the extant pleural surface, mild and partially healed periosteal new bone deposition is observed, interspersed with capillary impressions. Micro- and macroporosity is present along the costal groove on the extant portion of the element.

Radiological observations:
At the mid-point of the extant portion of the rib, fine periosteal lesions are observed on the external surface. Towards the medial aspect, periosteal new bone is also observed on the pleural surface, and patchy new bone deposition extends almost circumferentially. Towards the lateral end of the extant fragment, there are thicker spiculated lesions with separation evident in parts between the periosteum and the new bone, indicating subperiosteal haematoma (Fig. 8.49c). There are more widespread but subtle changes throughout much of the shaft toward the distal aspect.

There is no evidence of fracture on the extant portion of the element, suggesting the observed lesions are not associated with trauma. As Lewis (2018, 3) notes, distinguishing new bone formation as a result of the normal growth process from infectious or traumatic new bone deposition is challenging. The extant element presents focal lesions incorporating capillary impressions on the external aspect and diffuse finely woven new bone on the pleural aspect, suggestive of pathological processes. Lesions on the pleural rib surface suggest inflammation of the pleura, typically associated with respiratory infections, such as tuberculosis. Tuberculous rib lesions commonly affect the middle ribs, incorporating lytic foci, enlargement of the costochrondral joint and minimal periosteal new bone on the pleural surface (Ortner 2003, 246). Unfortunately, the sternal end of the rib is absent and cannot be assessed; however, lesions on the extant fragment are not observed to be lytic. The external lesions appear to be in a more advanced stage of the healing process, while the pleural lesions are more active, suggesting a chronic process. Subperiosteal new bone deposition on the ribs is occasionally noted in cases of non-adult scurvy (Buckley *et al.* 2014; Snoddy *et al.* 2017), and may be observed alongside fracture and/or enlargement of the costochrondral junction (the 'scorbutic rosary') (Brickley & Ives 2008, 57). The external rib surface is associated with *Mm. serratus anterior* and *pectoralis major* (Snoddy *et al.* 2018, 880). Therefore, subperiosteal new bone on the external surface of the extant rib may be a result of micro-trauma associated with movements involving these muscles, while the pleural lesions indicate subperiosteal haemorrhage because of expansion and contraction of the lungs. These features are deemed suggestive of scurvy but should be observed bilaterally alongside further characteristic lesions (Snoddy *et al.* 2018, 891; Thompson *et al*. 2021).

Lesion type and healing status: Mixed; Mixed.
Lesion preservation: Excellent.
Differential diagnosis: Metabolic.

8.6.2.6. FB0044: Rib fragment

Context:	(960)
Grid Ref:	99/111
Year of Excavation:	BR94
Other Details:	Spit 3

Element identification and preservation:
Fragment of right lower order rib shaft. The head of the rib is fragmented and absent. A transverse fragmentation margin truncates the shaft of the rib at the approximate mid-point and *postmortem* taphonomic erosion is observed in several locations. As mentioned before, regression equations exist for age estimation according to the length of individual ribs in prenatal individuals (Fazekas & Kosa 1978; cf Scheuer & Black 2000, 243). Amongst infants and children however, the major factor affecting rib morphology is increased torsion in rib shafts as the ventral aspect of the thorax descends (Scheuer & Black 2000, 241). Although incomplete, the morphology of the extant portion of the rib shaft demonstrates torsion and may indicate that this individual was between the ages of at least 1–3 years old at the time of death (Scheuer & Black 2000, 241). The extant portion of the element is in fair condition and represents ~50% of a complete rib. All damage is assessed to be *postmortem*.

Macroscopic observations:
Periosteal new bone deposition is observed on the superior, pleural and posterior aspects of the extant portion of the body of the rib (Fig. 8.50a-c). *Postmortem* fragmentation truncates the lesion both medially and laterally, and *postmortem* taphonomic erosion has removed some of the periosteal new bone on the anterior surface. These factors obfuscate a full observation of pathology. There are no indications of fracture, cloaca, or sequestra on the extant portion of the element.

On the superior aspect, the lesion commences 16.9 mm from the anterior fragmentation margin and extends for 45.0 mm. On the pleural aspect, the lesion commences 16.5 mm from the anterior fragmentation margin and extends for 67.0 mm (measured with a flexible paper tape). On the posterior aspect, two lesions are observed. The most medial lesion commences adjacent to the medial fragmentation margin and extends for 28.0 mm. The second lesion commences approximately 42.0 mm from the medial fragmentation margin and extends for 18.4 mm. The maximum length of the extant portion of the lesion is 67.0 mm on the pleural aspect. Where apparent, the lesion is continuous across the pleural, cranial edge and external surfaces of the element.

The lesion exhibits mixed stages of activity. On the cranial edge, the lesion is interrupted by *postmortem* taphonomic erosion and small areas of sediment adhesion, although small spicules extend superiorly from the proximal lesion on the posterior aspect (Fig. 8.50a). The lesions are more rugose and porous than the surrounding cortex and are observed to differ in colour. On the pleural surface, the extant posterior portion of the lesion presents rugose deposits of periosteal woven bone interspersed with microporosity; spicules are observed on the neck of the rib on the superior and inferior aspects, perpendicular to the cortical surface (Fig. 8.50b). Moving anteriorly, the lesion exhibits fine woven bone deposition, interspersed with capillary impressions. Macroporosity is observed along the costal groove on the extant portion of the element. The margins of the extant portion of the lesion are diffuse and not well-demarcated. On the posterior aspect of the rib body, two lesions comprising healing plaque deposits of bone are observed (Fig. 8.50c). The most medial lesion exhibits microporosity on the peripheral margins and diffuse microporosity in the centre, along the angle of the rib. The second lesion exhibits extensive microporosity with both single and coalescing foramina.

Radiological observations:
The lesions on the extant portion of the rib present a similar expression radiologically as the rib described above. Circumferential spiculation is evident and is observed to be more widespread than the left rib although subtler in expression (Fig. 8.50d).

Once again, the absence of any fracture on the extant portion of the element suggests that the observed lesions are not associated with traumatic fracture. In non-adult material, it is difficult to distinguish new bone formation as a result of the normal growth process from infectious or traumatic new bone deposition (Lewis 2018, 3). The extant element presents diffuse lesions incorporating woven bone and microporosity on the pleural and external surfaces and cranial edge, suggestive of pathological processes. Lesions on the pleural rib surface suggest inflammation of the pleura, typically associated with respiratory infections, such as tuberculosis. Tuberculous rib lesions commonly affect the middle ribs, incorporating lytic foci, enlargement of the costochrondral joint and minimal periosteal new bone on the pleural surface (Ortner 2003, 246). Unfortunately, the sternal end of the rib is absent and cannot be assessed; however, lesions on the extant fragment are not observed to be lytic. The external lesions appear to be slightly more advanced in healing, while the pleural lesions are more active, suggesting a chronic process. As mentioned before, subperiosteal new bone deposition on the ribs is occasionally noted in cases of non-adult scurvy (Buckley *et al.* 2014; Snoddy *et al.* 2017), and may be observed alongside fracture and/or enlargement of the costochrondral junction (the 'scorbutic rosary') (Brickley & Ives 2008, 57). The external rib surface is associated with *Mm. serratus anterior* and *pectoralis major* (Snoddy *et al.* 2018, 880). Therefore, subperiosteal new bone on the external surface of the extant rib may be a result of micro-trauma associated with movements involving these muscles, while the pleural lesions indicate subperiosteal haemorrhage because of expansion and contraction of the lungs associated with respiration. These features are deemed suggestive of scurvy, but should be observed bilaterally alongside further characteristic lesions (Snoddy *et al.* 2018, 891). Both this rib and the rib described above (§8.6.2.5) were excavated from the same level and are observed to be of similar size, morphology and developmental stage. The presentation and location of the lesions on both elements are strongly consistent with one another, suggesting they may derive from the same individual and demonstrate bilateral rib lesions attributable to scurvy.

Lesion type and healing status: Mixed; Mixed.
Lesion preservation: Excellent.
Differential diagnosis: Metabolic.

8.6.2.7. FB0045: Ulna fragment

Context:	(960)
Grid Ref:	99/111
Year of Excavation:	BR94
Other Details:	Unit 1, Spit 3

Element identification and preservation:
Fragment of non-adult ulna, representing the distal half of the diaphysis. *Postmortem* fragmentation truncates the element at the approximate midpoint of the diaphysis, while the distal metaphysis is eroded as a result of *postmortem* taphonomic processes. As a result of the severity of the lesion, no anatomical landmarks are visible and the element cannot be confidently assigned to side. Small areas of *postmortem* taphonomic erosion are observed on the fragment. Standards exist for age estimation based on ulnar length (Maresh 1970; cf Scheuer & Black 2000, 207). However, metric analyses cannot be applied because of the incomplete state of the element. The extant portion of the element is in fair condition and represents ~40% of a complete ulna. All damage is assessed to be *postmortem*.

Macroscopic observations:
Periosteal new bone deposition envelops the diaphysis for the extent of the fragment, obscuring anatomical features (notably the interosseous crest and pronator ridge) and no traces of the original cortex can be discerned (Fig. 8.51a-c). The new bone comprises perpendicular spicules which, in some areas, are bridged and appear 'frosted' and dense. The lesion is truncated by fragmentation, severe *postmortem* taphonomic erosion and sediment adhesion, obfuscating full observation of pathology. There are no indications of fracture, cloaca, or sequestra on the extant portion of the element.

The maximum length of the extant portion of the lesion is 55.5 mm. The maximum width of the lesion is approximately 28.0 mm encircling the diaphysis at the midpoint of the fragment, measured with a flexible paper tape. The lesion comprises woven bone tightly organized in trabecular-like formation. When viewed from the fragmentation margin, the lesion is observed to sit proud of the underlying cortex, extending approximately 0.9 mm in height. Post-depositional taphonomic processes have eroded most of the trabeculae, with only some trabeculae preserved at the area of the distal metaphysis. As such, the degree of trabecular involvement cannot be characterized. No lesion margins can be identified for this fragment.

Radiological observations:
No healthy cortex remains on the extant portion of this element; it is completely comprised of radiating spicules (Fig. 8.51d-f). There is marked cortical thickening alongside demineralization and a pockmarked appearance to the cortical bone. As a result of taphonomic erosion of the distal metaphysis, the element cannot be assessed for diagnostic radiological features, including Pelkan spurs, metaphyseal white lines ('white line of Frankel') and the Trümmerfeld zone. Within the medullary cavity, few trabeculae are retained; this is most likely an artefact of *postmortem* damage as some trabecular bone is preserved in the region of the distal diaphysis. On the distal third of the diaphysis, segments of periosteal new bone appear

Figure 8.50. *Photographic and radiological images pertaining to fragmented non-adult right rib (FB0044) from Context (960) displaying focal periosteal lesions, including: a) superior view of cranial edge displaying finely woven bone and spiculations; b) anterior view of pleural surface displaying rugose deposits of woven bone; c) posterior/ external view displaying finely woven bone with capillary impressions; d) sagittal cross-section from CT data through mid-point of extant portion of rib, displaying almost circumferential fine spiculations. Scale bar: 1 cm (photographs only). (Photos Jess E. Thompson; radiological images captured by L. Buck, Cambridge Biotomography Centre; processed by J. Magnussen & M. Pardey, Macquarie Medical Imaging).*

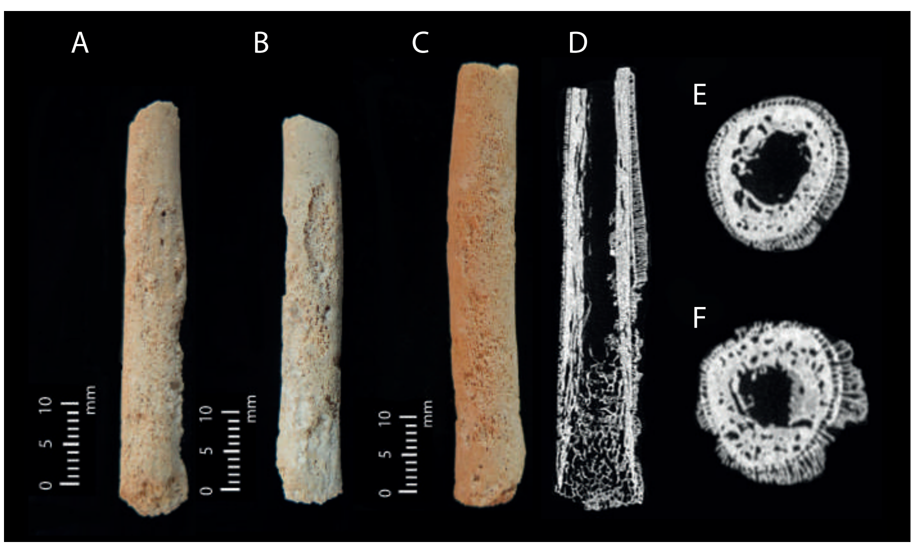

Figure 8.51. *Photographic and radiological images pertaining to fragmented non-adult ulna (FB0045) from Context (960) displaying circumferential periosteal new bone; all anatomical features are obscured: a)* postmortem *taphonomic erosion has removed the lesion in small areas, revealing the depth of new bone; b) microporosity underlying areas of erosion; c) spicules which are occasionally bridged or 'frosted' are evident; d) sagittal cross-section from CT data revealing extensive spiculation overlying cortex, and some separation between the cortex and lesion is evident; e) transverse cross-section at proximal aspect of extant element; f) transverse cross-section at mid-point of extant portion of element. Scale bar: 1 cm (photographs only). (Photos Jess E. Thompson; radiological images captured by L. Buck, Cambridge Biotomography Centre; processed by J. Magnussen & M. Pardey, Macquarie Medical Imaging).*

elevated from the underlying cortex, indicative of subperiosteal haematoma (Fig. 8.51e-f).

Such extensive bony change because of infection would lead to sequestra, cloaca, and/or significant cortical bone loss. Additionally, beta thalassaemia can be discounted because of the typical proportions of the medullary space and the evidence for osteoblastic activity (Lewis 2018, 2000; Ortner 2003, 365). Therefore, a metabolic disorder is the most likely differential diagnosis. Widespread and porous subperiosteal new bone deposition on long bone diaphyses and/or metaphyses are diagnostic of scurvy when observed alongside lesions on the cranium (Brickley & Ives 2008, 57; Snoddy *et al.* 2018, 891–2). Although this element appears to have been disarticulated when excavated, it was assigned the same unit number as the frontal fragments described above (FB0039 & FB0040; §8.6.2.1–2) and is observed to be of a similar developmental stage. It is therefore possible that these elements originate from the same individual, but this cannot be verified without further bimolecular analyses. Snoddy *et al.* (2018, 892) further note that periosteal lesions on the long bones are expected to be bilateral. As the contralateral ulna is absent, this cannot be ascertained. However, while microporosity and finely woven bone ought to be exhibited bilaterally, subperiosteal haemorrhage occurs as a result of trauma and is therefore unlikely to be symmetrical in location (Stark 2014, 19). On the extant portion of the ulna, new bone deposition covers the regions of several muscle attachment sites, including *Mm. flexor digitorum profundus, pronator quadratus, extensor carpi ulnaris,* and *extensor pollicis longus.*

The extent of proliferative, spiculated new bone on the extant element exceeds cases of subperiosteal new bone deposition on the long bones of scorbutic non-adults presented in the bioarchaeological literature (e.g. Brown & Ortner 2011; Buckley *et al.* 2014; Geber & Murphy 2012; Ortner *et al.* 2001; Snoddy *et al.* 2017). Klaus (2014) presents two cases of non-adult scurvy with more diffuse long bone lesions: woven bone and porosity on the upper limb bones of a 16–21 month old child, and cortical thickening alongside woven periosteal new bone on the ulna, femora and tibiae of a 1–1.5 year old child. On the latter individual, the ulna and tibia exhibit a very fine layer of woven bone which is clearly separated from the underlying cortex (Klaus 2014, 41). The extant ulna presents a distinctive case of long bone diaphyseal periosteal reaction alongside cortical thickening which, given its severity of expression, may indicate a chronic process.

Lesion type and healing status: Proliferative; Active.
Lesion preservation: Moderate.
Differential diagnosis: Metabolic.

8.6.2.8. Summary

All non-adult elements described above (except for FB0044, for which this information is lacking) were assigned the same unit number upon excavation, indicating their close spatial association. Mandibular dental eruption provides the narrowest estimated age range, of 2 years ±8 months, while all other elements are consistent with an estimated age of 2–4 years. In addition to their restricted depositional context and similar developmental stages, the extant elements present periosteal lesions which are remarkably consistent in both macroscopic and radiological presentations. Islands or extensive regions of thick, woven new bone extruding perpendicular to, and sitting on top of, the cortex, are observed on all elements. Additionally, hypervascularity and porosity are common and minimal cortical erosion is observed. The radiological presentation of the lesions on the left rib fragment (FB0043, §8.6.2.5), when viewed in cross-section were observed to be similar to all other non-adult elements, but especially the ulna fragment (FB0045, §8.6.2.7). It is therefore possible that these elements originate from one young child, but this cannot be definitively verified without further biomolecular analyses.

Differential diagnosis of individual elements is challenging, especially as periosteal lesions are frequently regarded to be of non-specific aetiology (although see Weston 2009 for critique). However, such proliferative lesions within non-adults are striking and sufficiently characteristic to aid differential diagnosis. For each element, traumatic fractures were not evident, and several pathological processes were considered. The expression and location of the lesions consistently indicated a metabolic disorder. Considered in isolation, the fragmented frontal bone might accord with an alternative aetiology of intra-cranial infection. However, the widespread periosteal new bone deposition and the likely bilateral nature of the orbital lesions indicates a severe progression that would not have been survivable in a prehistoric context in the absence of modern antibiotics. Furthermore, such an advanced infectious process would be expected to present cloaca or sequestra.

As the fragmented right frontal is consistent with the larger frontal bone fragments, a bilateral expression of orbital and supra-orbital lesions is observed. The zygoma further presents proliferative lesions, and bilateral lesion sites are observed on the mandible. Both ribs presented healing posterior/external surface lesions, with woven new bone on the pleural surface. The involvement of the external rib surface and lack of lytic lesions is not consistent with a diagnosis of pulmonary infection. The fragmented ulna presents the most severe proliferative new bone within this sample, alongside subperiosteal haematoma, marking a rarely observed case of diaphyseal scorbutic lesions. Overall, when considered together, the distribution of lesions across these elements is diagnostic of scurvy, possibly co-morbid with vitamin D deficiency (rickets) and iron-deficiency anaemia (Brickley 2000; Brickley & Ives 2008, 57ff.; Ortner *et al.* 2001; Snoddy *et al.* 2018). This finding is significant as it may represent one of the earliest descriptions of scurvy for the central Mediterranean region.

Scurvy often occurs alongside other micro-nutrient deficiencies, resulting in a complicated disease presentation as each affects the pathophysiology of the other. Significantly, the biology of vitamin C, D and iron absorption and function are strongly linked. Extensive bleeding caused by the weakening of blood vessel walls in chronic scurvy can exacerbate or lead to iron-deficiency anaemia, which in turn may inhibit intestinal absorption of minerals such as vitamin D, potentially leading to rickets (Fain 2005; Brickley & Ives 2008, 113). Scurvy and rickets can lead to similar osseous changes, with characteristic and diagnostic features of each disease observed in similar locations (such as long bone metaphyses and costochrondral rib junctions). When scurvy and rickets co-occur, their presentation depends on the order in which they developed, healing status, and severity, with one disease usually dominating the other (Schattman *et al.* 2016). Clinical and bioarchaeological research has found that scurvy usually dominates in infants, with the skeletal features of rickets masked and requiring radiological and/or microscopic imaging to identify more confidently (Bromer & Harvey 1948; Schattman *et al.* 2016).

In addition to lesions preserved on suggestive and diagnostic locations for scurvy on the extant elements, described above, we have also presented lesions attributed to scurvy in locations which have received less attention in the palaeopathological literature. Of particular note are the bilateral proliferative lesions on the supero-lateral aspect of the supra-orbital margin, bilateral woven bone and porosity on the anterior margin of the mylohyoid groove and within the mandibular foramen, and circumferential spiculations on the ulna diaphysis. Similar mandibular lesions have been observed previously (Brickley 2000, 187; Brickley & Ives 2006, 166; Brown & Ortner 2011, 200), and lesions on the medial or internal aspect of the ramus are diagnostic when bilateral (Snoddy *et al.* 2018, 890). However, these cases do not demonstrate subperiosteal new bone extending as far inferiorly on the mylohyoid groove as the present example. These lesion sites provide greater insight into the pathogenesis of scurvy, as well as revealing the process experienced by this individual. This child experienced a severe and chronic case of vitamin C deficiency, resulting in more advanced proliferative lesions – especially on the zygoma and ulna – than many presented in the bioarchaeological literature. As a result, our research brings together pathognomic scorbutic lesions with those which indicate specific individual circumstances, demonstrating the extent to which periosteal lesions may develop in chronic cases.

Vitamin C, or ascorbic acid, is essential for collagen and osteoid formation because of its role in amino acid hydroxylation (Hodges *et al.* 1971). It is therefore critical for normal bone growth, as well as for blood formation and the metabolism of iron and folate (Lipschitz *et al.* 1971; Popovich *et al.* 2009). Furthermore, the role of ascorbic acid as a co-factor in 15 enzymes means that chronic dietary deficiency can lead to the failure of multiple physiological systems and, if untreated, is fatal (Padayatty & Levine 2016). Humans are unable to synthesize ascorbic acid and must consume vitamin C rich foods, in particular fresh produce, especially citrus fruits and dark green vegetables, as protein-rich foods such as milk, fish and meat contain lower levels of vitamin C; critically, however, the nutritional content of fresh produce is reduced when foods are cooked (Fain 2005, 124). Vitamin D is mostly synthesized through exposure of the skin to UVB rays in sunlight, with natural dietary sources limited to eggs and oily fish (Brickley & Ives 2006,83; Holick 2003).

Human breastmilk is high in vitamin C (Grewar 1965) but breastfeeding increases the daily metabolic requirements of vitamin C to an estimated 120 mg, almost double the amount required prior to pregnancy (NIH 2020). In contrast, breastmilk is low in vitamin D, and breastfeeding individuals must maintain healthy levels of vitamin D through exposure to sunlight (Pettifor 2004). If this child was breastfed by an individual who was deficient, and perhaps malnourished, they would have received insufficient nutrition in turn (Fain 2005, 126; Hirschmann & Raugi 1999, 899). Alternatively, weaning may have precipitated nutritional deficiency in this young child (Brickley & Ives 2008, 45). The process of weaning is often related to micro-nutrient deficiencies and weaning diets must be carefully considered (Davies & Hare 2004; Mosha *et al.* 2000; Tontisirin *et al.* 2002, 246) as nutritional status during the early years of life is strongly correlated with long–term health (Barker *et al.* 2002; Gluckman & Hanson 2006; Heijmans *et al.* 2008; Hoffman *et al.* 2017; Mandy & Nyirenda 2018; McFadden & Oxenham 2020; Roberts & Manchester 2005; Temple 2019). If appropriate animal–based dairy products were lacking or introduced too early, or dietary diversity was low because of resource scarcity, for example on a seasonal basis (Cheung *et al.* 2003; Ianotti & Lesorogol 2014), this would have adversely affected the diet and health of vulnerable individuals. Importantly, it has been shown that cereal phytates can bind to calcium, reducing the overall intake of calcium, and this in turn affects vitamin D synthesis (Pettifor 2004). In Neolithic Malta, it is possible that infants and children were weaned onto diets either lacking in dairy or containing non–fermented dairy products, especially given the high rates of lactose intolerance which persist in the contemporary Maltese population (Burger *et al.* 2007; Storhaug *et al.* 2017). The potential for periodic resource scarcity cannot be excluded, and it is probable that weaning diets were cereal–rich, limiting the synthesis of vitamin D. In §8.7.6, we place this individual in chronological context to further evaluate the circumstances which lead to insufficient nutritional intake in this young child.

The current recommended daily amount of vitamin C for 1–3-year olds is 15 mg (NIH 2020). In non-adults, when the bodily pool of vitamin C is <300 mg, scorbutic symptoms are expected to commence at any time between 29–90 days (Brickley & Ives 2008, 45) and 6–10 months after the onset of dietary deficiency (Jaffe 1972). These include a suite of behavioural and soft tissue changes: failure to gain weight, loss of appetite, fatigue, irritability, depression, weakness, gingival bleeding and swollen gums (leading to periodontal disease and *antemortem* tooth loss), pinpoint bleeding in the skin (petechiae) and/or bruising (purpura) (Fain 2005; Hirschmann & Raugi 1999; Hodges *et al.* 1971). Chronic bleeding in response to muscular trauma, in subperiosteal and joint spaces, is especially painful and can result in restricted mobility (Hirschmann & Raugi 1999, 902). Such severe joint and muscle pain may be alleviated by the child assuming a 'frog position', lying on their back with limbs semi-flexed and externally rotated (Popovich *et al.* 2009). The deposition of periosteal new bone usually indicates that some vitamin C has been reintroduced to the diet, facilitating osteoblastic activity. We hypothesize that this individual may have experienced chronic, recurrent vitamin C deficiency or a consistently low dietary intake to provoke such extensive proliferative new bone deposition. Rickets, if present, may have been a late onset, possibly as the child became too ill to move independently and therefore spent less time outside.

This methodological case study provides an ambitious and rare example of detailed pathological analysis of fragmentary and disarticulated elements. The level of attention demonstrated here is uncommon in complex, commingled assemblages such as these, as the ability to carry out differential diagnosis is limited when discrete individuals cannot be recognized. Palaeopathological analysis is typically employed to characterize health on a population-wide scale, or to illustrate significant singular case studies. Rarely have pathological lesions provided the opportunity to unite the remains of disarticulated individuals (González-Reimers *et al.* 2015; Ortner 2003, 210). The approach employed herein supports appeals for the integration of macroscopic analyses and radiological imaging (Stark 2014) to aid differential diagnosis and, crucially, bring palaeopathological studies into alignment with the clinical literature. Radiological observation of these periosteal lesions reveals surprising variation in their character and architecture, a finding which may also be clinically significant, as they are typically not subject to radiological imaging in contemporary contexts. Although requiring significant investment of time and resources, this work highlights the utility and value of pathological analyses of highly fragmented and disarticulated assemblages. The benefits, exemplified here, include the potential for posthumous reunification of individuals, increased accuracy of differential diagnoses, and greater insights into the lived experiences of health and disease in communities such as those inhabiting the prehistoric Xagħra plateau (Thompson *et al.* 2021).

8.7. Discussion

8.7.1. Limitations of study

To echo our statements at the outset of this research, we underscore the awareness that the results and interpretations presented here should only be perceived as a minimum number of incidences, and not as overall statistical prevalence of a complete burial population. The Circle assemblage has not been fully excavated, nor has the excavated population been exhaustively analysed. For example, the six examples of vertebral pathology presented in §8.5.3.1–6 represent only 0.7% of the 922 isolated elements (or fragments thereof) from the curated burial population. Our objective here was to bring further clarity to the known spectrum of health and disease for the Circle population by focusing on case studies of 'extreme pathology', an approach first applied to this population by Stoddart *et al.* (2009a). Ongoing scientific studies by the current authors will seek to further elucidate all aspects of the pathology, anthropology, demographics, affinity and cultural engagement of the Neolithic community interred in this space.

We were fortunate to have received permission to subject some of the remains included in the case studies to radiological analyses via micro-CT. Undoubtedly, further scanning would have enhanced the pathological descriptions and differential diagnoses of those elements that were subject to macroscopic analysis alone; however, the temporal, pecuniary and logistical parameters of the current project could not permit comprehensive inclusion for this component of the study. It is hoped that future extensions of the project will facilitate further radiological studies, ideally with local facilities and experts in Malta.

8.7.2. The Circle in context

As described in §4.6.2, less than two dozen late Neolithic funerary sites are known from across Malta and Gozo (Chapters 13 & 14; cf Malone *et al.* 2009d). Of these others, only the human skeletal remains from the Xemxija tombs have previously been subjected to osteological analysis and published (Pike 1971; Rodgers 1971). Although several publications refer to the human remains identified within the Ħal Saflieni Hypogeum (Zammit 1910, 1926a; Zammit *et al.* 1912), commentary pertains to cranial morphology and metrics, as was the prevailing focus of the emerging field of biological anthropology. Indeed, in alignment with contemporary archaeological praxes across the region, the disciplinary focus on architecture and material culture combined with the fragmentary and poorly preserved nature of many skeletal remains, precluded their analysis. This study therefore presents the largest and most fine-grained investigation of skeletal pathology from late Neolithic Maltese sites to date.

The excavation of Xemxija tombs 1–6 brought to light almost 15,000 fragments of human bone from similarly commingled and disarticulated contexts as the Circle rock-cut tomb and cave complex (Evans 1971, 112–6). An inventory and brief overview of the human skeletal and dental remains was provided (Pike 1971; Rodgers 1971), although their treatment was not exhaustive, and the descriptions are not supplemented by figures of the few elements discussed in detail. Pike (1971, 236) noted the presence of non-adult individuals of all age ranges but commented on the under-representation of older adults because of a lack of age-related osseous change. At least one old adult (50+ years) was recently identified through a fragment of right pubic symphysis displaying age-related degeneration (Thompson 2020, 138). However, the fragmented nature of the assemblage impedes identification of further older individuals.

As discussed above (§8.4.4), individuals of advanced age have primarily been identified at the Circle through well-preserved ossified cartilage, pubic symphyseal degeneration, rare observations of *hyperostosis frontalis interna* (§8.5.2.8–11) and potentially age- or diet-related osteoporosis (§8.7.6). In the Xemxija tombs, there were low incidences of skeletal pathology: one well-healed (non-reduced) clavicle fracture; one well-healed (non-reduced) tibia fracture; one healed non-reduced tibia fracture exhibiting misalignment with overlapping of the fractured segments by 1.2–1.9 cm, associated with possible infectious change; two healed fifth metatarsal fractures, one with callus; one tibia fragment presenting endosteal thickening perhaps because of haematoma; one talus with osteomyelitis and cloacae indicating local infection (Pike 1971, 236–7). These elements complement and extend the case studies offered above from the Circle, and further the evidence for the treatment and short-term care of injured individuals in Neolithic Malta, aligning with the 'bioarchaeology of care' approach, described below.

There has been a relatively long history of research documenting human pathological indicators of health associated with the transition from foraging to agriculture. The publication of the foundational volume '*Palaepathology at the Origins of Agriculture*' by Cohen & Armelagos (1984) provided the first systematic and global documentation of the impact of this dietary and cultural transition on human health. Multiple chapters in this volume provided evidence for a widespread deterioration in palaeopathological indicators of health across this transition, an interpretation that was later challenged by the publication of the 'Osteological Paradox' (Wood *et al.* 1992) which raised a range of reasons why it is difficult to interpret population frequencies of skeletal pathology in a straightforward manner. Despite the controversy over interpretation of palaeopathological data in Neolithic populations, the early observations of widespread increases in the frequency of lesions associated with infectious and metabolic diseases, as well as indicators of systemic stress such as enamel hypoplasia, have been broadly supported by more recent studies (Cohen 2009). The past few decades have seen quite significant changes in our understanding of the Neolithic. Among these are the acknowledgement that social and dietary changes occurred over a considerable timespan and were regionally variable. As a result, the implications of the Neolithic lifestyle on human health are also variable and locally contingent (Stock & Pinhasi 2011). Recent research has also demonstrated that there were strong selective pressures on human populations following the adoption of agriculture which have shaped genetic variation within our species (Richerson *et al.* 2010). Recently it has been proposed that agricultural societies also shift their energetic ecology and life-history strategies, resulting in a greater investment in immune function and reproduction at the expense of somatic growth (Wells & Stock 2020).

These perspectives on human ecology and health in the Neolithic have emphasized the importance of understanding regional variation and local impacts of the Neolithic upon populations, as well as subtler analyses of how human impact on the environment changed and shaped health throughout the Neolithic as farming practices and land usage changed, and environmental impacts of human activity compounded (Stephens *et al.* 2019). The observations of pathology in the Neolithic populations of the Circle provide a unique opportunity to interpret the patterns of health and disease in an island Neolithic population. As resources are known to be limited in island environments, it also provides an opportunity to consider how local ecology, population dynamics and activities impacted human pathology during this period.

8.7.3. The bioarchaeology of care

The interpretative lens for the case studies detailed above aligns with the 'bioarchaeology of care'. The bioarchaeology of care is a conceptual framework which seeks to promote understanding of the lived experiences of disease, disability and physical impairment in the past. It applies social theoretical concepts to bioarchaeological evidence to study the indicators of health-related caregiving practice and psycho-social, emotionally supportive care (Tilley 2013, 2015; Tilley & Oxenham 2011; for the *Index of Care*, cf Tilley & Cameron 2014; Tilley 2017). The framework was developed to examine the broader implications of health-related care provision in past populations via case study-based research, including caregiving across the life course, emic attitudes towards illness, impairment and disability, and the role of animals as both recipients of and agents for care provisions (Powell *et al.* 2017). The bioarchaeology of care is founded on a combination of elements drawn from a range of sub-disciplines, such as post-processualism, social, cognitive and mortuary archaeologies, and palaeopathology (Tilley 2017, 12). Additional influence is drawn from other disciplines relevant to caregiving including nursing, clinical medicine, philosophy, sociology and psychology (Tilley 2017, 12). Originally focused on skeletal remains, the bioarchaeology of care has recently been repositioned to also incorporate naturally and artificially mummified human remains (Nystrom & Tilley 2019).

The first principle of the bioarchaeology of care is that the research of disease, disability and care in the past is 'quintessentially bioarchaeological' (Tilley 2017, 15; cf Buikstra & Beck 2006). Although the evidence-base of the bioarcheology of care is bioanthropological, it cannot be analysed without continuous reference to what is known regarding the associated socioeconomic, material, geographical, chronological and cultural contexts (Tilley 2017, 15). It argues that although some symptoms of pathology may be biologically evident, or even pathognomonic, health, disease and disability were perceived, addressed and understood very differently across cultures (Tilley 2015, 3). Moreover, the bioarchaeology of care advocates for the uniqueness of any lived experience, maintaining that 'everybody experiences disease in their own way, disability for one person may not be a dis-ability (or not the same disability) for another' (Tilley 2015, 3; cf Shakespeare 1999, 99).

The second principle is that agency is central to all features of health-related caregiving (Tilley 2017, 15). According to Tilley, any 'human remains bearing evidence of caregiving literally embodies the collective agency of those involved in providing care' (2015, 128). This agency should be contextualized temporally and geographically to the period in which care was provided. Human remains displaying evidence of pathology requiring care can be seen as both actor and artefact. Traditional palaeopathological study typically views remains as only 'artefact'; however, the person receiving care is also an actor or agent. Palaeopathology's tendency to concentrate on 'fossilised disease' (Cross 1999, 23) in the form of observable bodily variations risks objectifying the remains of sick and/or physically impaired individuals as purely material resources. Assumptions of dependency, exclusion, marginalization or disadvantage based solely on observed bodily variation risks misrepresenting and dehumanizing the lived experiences of people from the past (Cross 1999, 8).

The bioarchaeology of care rallies against the reconstruction of individuals receiving care as passive or deficient. To do so negates their agency in the 'negotiation of, contribution to, and cooperation with their care [as] integral to its design and its outcomes' (Tilley 2017, 15). The passivity and concomitant medicalized study of physical impairments, bodily difference and disability as a pathological 'deficit' is a key feature of much archaeological, palaeopathological and osteoarchaeological research. These fields have emerged from the so-called 'medical model', the origins of which may be traced to the Industrial Revolution (*circa* 1760–1840), developing alongside the professionalization and standardization of modern Western medicine (Byrnes & Muller 2017, 2; Davis 2013; Siebers 2008). The medical model pathologizes physical and mental impairments, and any other deviation from an idealized bodily 'norm', conceptualized by western medicine as functional limitations (Byrnes & Muller 2017, 2). The expression 'medical model' is used by many disability studies scholars as a synonym for the biased view of disease and disability that attributes an individual's biological 'deficits' to inadequate health practices, genetics or incidents (such as traumatic accidents) (Vehmas *et al.* 2009, 2; cf Pfeiffer 2001, 30). The first wave of disability scholarship, and indeed the activist origins of the field, strongly reject medicalization, believing it to perpetuate modern dominance hierarchies of medical practices and experts (Vehmas *et al.* 2009, 2).

Palaeopathology has perhaps inadvertently played a role in the continuation of the medical model within historical and archaeological research. The study of disease in past populations originally developed as an interdisciplinary pursuit by historians, doctors, archaeologists and biologists, often with little examination of socio-cultural contexts (Živanović 1982, 2). While palaeopathology relies heavily upon the medicalized examination of human remains, this should not automatically result in the dominance of the medical model as it is problematic in a number of ways. Firstly, it supports a dualistic notion of health; namely, that healthy and unhealthy exist as binary opposites, rather than acknowledging that people move between these states throughout the life course, and may never be entirely one or the other. 'Health' is most often experienced as a spectrum rather than a binary status. Secondly, the dualism of health treats biological and psychological problems separately when they are in fact inextricably linked (Appleby 2015; Cole & Dendukuri 2003; Roberts & Manchester 2005; Taylor 1995). Thirdly, especially applied to past populations, the medical model can be deterministic. By interpreting bodily differences as 'deficits', the medical model suggests that a particular person's 'problem' – a disease/impairment *etcetera* – indicates that person could not have been an equal; they are assumed to be inherently disadvantaged. Additionally, the medical model risks implying that a person with a potential illness or disability was solely a passive recipient of treatment (or lack thereof). In this way, the medical model, and its application in palaeopathology is inclined towards disablist narratives as it defines health in terms of a 'modern' able-bodied norm. While acknowledging biological imperatives of health, it is important to recognize that perceptions of 'healthy' and 'functioning', and understandings of the aetiologies of disease, congenital variation and the implications of disease or trauma, were variable in past societies, as they remain in the present.

Bioarchaeology now routinely incorporates social theories to increase the biocultural and sociocultural investigation of multiple categories of evidence and more critically (re)interpret past embodied experiences and interpretations of corporeality and corporeal difference (Byrnes & Muller 2017, 3). The bioarchaeology of care offers a means to record, interpret and report palaeopathological analyses in an embodied and human-centred way (Boutin 2016; Byrnes & Muller 2017; Tilley 2014). When archaeologically derived remains indicate that a person experienced acute or chronic, congenital or acquired, resolved or unresolved disease during their lifetime (Tilley 2017, 11), it is justifiable to infer that this person received some degree of health-related care to manage the impacts of disease, and survive to their ultimate age of death. Considerations of the characteristics of caregiving, and even the willingness to give care, offers a range of opportunities for scholars to 'reflect not only the motivations and commitment of the carers themselves, but also the values, traditions, experience, knowledge, beliefs, skills, resources, politics, economy and organization of the society in which care occurs' (Tilley 2017, 12; cf Hofrichter 2003; Pol & Thomas 2001). The bioarchaeology of care offers a means of analysis that overcomes many of the issues that arise from the medical model and its dominance in palaeopathology, facilitating insights into the lived experiences of individuals in our archaeological narratives that have been hitherto inaccessible or ignored.

From this perspective, the individuals encountered through our studies of the Circle population contribute a great deal to the global discourse surrounding the bioarchaeology of care. Particularly considering the severe fractures described for a mandible (FB0002, Context (951); §8.5.1.1, above), humerus (FB0007, Context (951); §8.5.3.7, above) and femur (FB0001, Context (1241); §8.5.3.15), it is clear that the individuals who sustained these injuries would have required significant and enduring care from other members of their communities. Initially, care would have been required to survive the biological shock associated with such serious physical trauma (Britt *et al.* 1996; Eastridge *et al.* 2019; Hardaway 2006; Kahl *et al.* 2013). In clinical studies, after brain injury, shock is the second leading cause of death after trauma (Siegel 1995). Assistance would have also been required in the procurement, preparation and consumption of food and drink, as well as securing other basic human needs (such as safe shelter and warmth) while incapacitated (Pittman & Zeigler 2007). Further to this, affected individuals would have required varying levels of support and care during recuperation and rehabilitation, as they healed from their injuries and learned to integrate the associated changes in mobility and/or function. It is important to acknowledge that the cases presented here precipitate from the earliest and middle use-phases of the Circle (from approximately 2900–2500 BC), making these findings even more significant. The survival of these individuals beyond the initial trauma and resumed effective use of their affected elements is evidence for many combined months of successful care extended to them by their communities, without which in a prehistoric context would almost certainly have resulted in the loss of their lives.

8.7.4. Hyperostosis frontalis interna

Above, we have demonstrated the presence of *Hyperostosis frontalis interna* (HFI) in four individuals from the Circle, two possible females and two possible males deriving from Contexts (1268), (960) and (979), dated from the Early to the Late use-phase of the site (FB0023, FB0024, FB0025 and FB0026; §8.5.2.10–13, above). *Hyperostosis frontalis interna* describes the growth of thick, irregular and undulating nodules on the endocranial surface of the frontal bone (Ortner 2003, 416). It is distinct from *hyperostosis calvaria diffusa* (HCD) or *hyperostosis cranii interna* (HCI) because of discrete involvement of the frontal bone; whereas HCI is often observed in association with severe HFI, HCD is determined to be a separate phenomenon (Hershkovitz *et al.* 1999; Talarico *et al.* 2008). HFI is usually observed bilaterally and spares the midline, resembling a butterfly in appearance (Mann & Hunt 2012, 57; She & Szakacs 2004). The nodular lesions are contained within the region bordered by the superior sagittal sinus and the middle meningeal artery and these features, as well as sutures, are not involved (May *et al.* 2011b). Although appearing macroscopically as dense lamellar bone, histological and radiological analysis reveal that the inner table is remodelled with cancellous bone and the diploic space is preserved (Bracanovic *et al.* 2016; Cvetković *et al.* 2019; Hershkovitz *et al.* 1999, 310; Ortner 2003, 416). As a result, the frontal bone is noticeably thickened but the ectocranial surface retains a normal appearance. HFI is categorized morphologically based on its extent and appearance into four types (Types A-D) (Hershkovitz *et al.* 1999); more recently, a fifth type has been introduced following recognition of the involvement of the *falx cerebri* in cadavers (Raikos *et al.* 2011). However, analysis of the microstructure of HFI only identified significant differences between two types, moderate (Types A-C) and severe (Type D) (Bracanovic *et al.* 2016).

This pathology was first reported in the 18th century as part of the triad defining Morgagni's syndrome, alongside virilism (the development of male secondary sexual characteristics in women, such as hirsutism) and obesity (Morgagni 1719). This syndrome, combining metabolic and endocrine disorders, is sometimes linked with neuropsychiatric symptoms and termed Morgagni-Stewart-Morel syndrome (Morel 1929; Stewart 1928). HFI has also been reported in Troell-Junet syndrome, other characteristics of which include acromegaly, toxic goitre, and diabetes mellitus (Moore 1953). Several studies have found that HFI is not strongly correlated with these syndromes and it is widely accepted to be an independent and benign phenomenon (Dann 1951; Gershon-Cohen *et al.* 1955; Hershkovitz *et al.* 1999; Schneeberg *et al.* 1947; Smith & Hemphill 1956). However, the increased bone thickness and endocranial outgrowths consistent with HFI can cause compression of the brain tissue and, in exceptional cases, cerebral atrophy leading to cognitive impairment, neuropsychiatric symptoms, frontal headaches and epilepsy (Attanasio *et al.* 2013; Hasegawa *et al.* 1983). A recent study does not support an association between HFI and reduction in cranial vault size (Cvetković *et al.* 2019), although profuse cases of HFI may affect the soft tissues and thereby precipitate behavioural changes (Chaljub *et al.* 1999; Talarico *et al.* 2008).

HFI is idiopathic but given its common occurrence in post-menopausal individuals and low prevalence in males and young females, it is most likely related to endocrine imbalance and hormone dysregulation. The ratio of androgen, oestrogen and IGF-1 (insulin-like growth factor) are commonly cited as central to its pathogenesis (Hershkovitz *et al.* 1999; May *et al.* 2010; Talarico *et al.* 2008; Western & Bekvalac 2017), although the role of parathyroid hormones, calcium metabolism, neuropeptides, leptin and dietary phytoestrogens are also questioned (Raikos *et al.* 2011; Talarico *et al.* 2008). The extent to which HFI is a genetic or hereditary condition is debated (Hershkovitz *et al.* 1999, 323), although at least two cases of HFI in individuals with potential biological affiliation have been reported (Glab *et al.* 2006; Hajdu *et al.* 2009). When present in male individuals, HFI co-occurs with hormonal irregularities disrupting the androgen/oestrogen ratio (Belcastro *et al.* 2011; May *et al.* 2010; Ramchandren & Liebeskind 2007; Yamakawa *et al.* 2006). Menopause seems key to the pathogenesis of HFI, marking a decline in oestrogen production and, post-menopause, the conversion of androgens into oestrogen via aromatization; further, the age of onset of menopause appears to be genetically determined and usually occurs in the mid-40s to mid-50s (Lamberts *et al.* 1997). Hershkovitz *et al.* (1999, 322-3) note that the correlation between HFI progression and age may vary in ancient populations because of differing ages at menarche and menopause. The increase in HFI prevalence in modern populations indicates that environment and lifestyle are also critical factors, namely where the risk of diabetes and obesity are heightened, and where exposure to oestrogen is increased during the lifespan (Hershkovitz *et al.* 1999; May *et al.* 2011a; Western & Bekvalac 2017). However, a lower average life expectancy may explain the under-representation of HFI in pre-modern populations.

The prevalence of HFI is debated, with estimates ranging from 5–12% of the population (Moore 1955; Jaffe 1972), to 5% of males and 25% of females affected (Hershkovitz *et al.* 1999). The demographic most consistently presenting HFI are post-menopausal individuals, at rates of 40–60% (Gershon-Cohen *et al.* 1955). The prevalence and extent of HFI increases with age in female individuals (although plateaus past 50 years of age; Western & Bekvelac 2017), while only the likelihood of HFI increases with age in males, as its expression is typically limited to the minor Type A and B forms (Cvetković *et al.* 2019; Hershkovitz *et al.* 1999; May *et al.* 2011b). It therefore provides an exceptional opportunity to explore the presence of older individuals in past populations and can be a strong diagnostic tool for sex and age determination (Cvetković *et al.* 2019; Hershkovitz *et al.* 1999; Moore 1955; May *et al.* 2011b). When HFI is minor in expression, age and sex cannot be predicted; however, severe HFI in an isolated cranium or skull likely signifies an older female individual (Cvetković *et al.* 2019; May *et al.* 2011b). Here, we seek to be inclusive in our terminology and distinguish the prevalence of HFI in biological females from its links with the menopause, recognizing that menstruation (and its cessation) and does not directly map onto either past or present understandings of gender (Chrisler *et al.* 2016; Farikullah *et al.* 2012).

In a sample of 2,019 archaeological skeletal remains, Hershkovitz *et al.* (1999) did not find any evidence of HFI, and it is a relatively rare finding in archaeological assemblages (Flohr & Witzel 2011; Shahin *et al.* 2014; Szeniczey *et al.* 2019). Nevertheless, it has been reported in *H. erectus* and *H. neanderthalensis* remains and is evidently not a modern phenomenon (Antón 1997; Garralda *et al.* 2014). There are few contemporary later prehistoric cases for this pathology. Outside of Europe, HFI has been reported in several ancient Egyptians, including a young adult male from Tarkhan dated to 2890–2650 BC (Shahin *et al.* 2014), two males and a female from the 2300 mastaba group of the Western Cemetery at Giza (*c.* 2630–2350 BC) and one female from Naga-ed-Deir (*c.* 2200-–1800 BC; Watrous *et al.* 1993). To date, four cases of HFI within Neolithic Europe have been presented. At Les Boileau hypogeum (France), where successive deposition was practised over several centuries from the early to mid-3rd millennium BC, two individuals (from a minimum of 294) presented mild cases of HFI, both identified as females >50 years of age (Devriendt *et al.* 2004). When published, these cases were potentially the first incidences of this pathology reported in Neolithic Europe. We have only been able to locate two other cases. From the La Varde passage grave (Guernsey) likely dating between the 4th–3rd millennium BC, one fragmented probable frontal bone presented either mild HFI or osteoma (Cataroche & Gowland 2015, 30). In Sumburgh (Shetland), a cist containing at least 20 individuals dating from 3510–2660 cal. BC, presented evidence of a frontal bone with HFI although no age or sex determination was given for this individual (Walsh *et al.* 2011, 13).

Our findings of HFI from the Circle assemblage are significant insofar as they are the first to be reported for Malta, and supplement existing early cases for Neolithic Europe. Moreover, as a group of four cases, they equal in number all published evidence for this phenomenon to date for prehistoric Europe, therefore representing a significant addition to knowledge of this category of cranial lesions for the region and period. However, the real significance of these cases arises through considerations of their demographic and cultural meaning. As mentioned before, HFI is most strongly associated with increased age, and thus presents an excellent opportunity to consider the presence of older individuals in archaeological assemblages. There are widespread assumptions regarding low life expectancies in preindustrial societies (Appleby 2015; Cave & Oxenham 2016; Cox 2000), despite the fact that ethnographic research on the mortality profiles of modern hunter-gatherers and forager-horticulturalists from across the Americas, Australia, Africa, Europe and Island South East Asia indicates that the modal age of adult death is approximately 70, with survivorship variability applicable to either side of that estimate (Gurven & Kaplan 2007, 322; Walter & DeWitt 2017; cf Laslett 1991). This research has been supported as a feasible platform from which to infer demographic profiles of archaeological populations (Cave & Oxenham 2016; Hoppa 2002; Milner *et al.* 1989; Paine 1989; Weiss 1973; White 2014).

These observations from the Circle suggest that some members of the Neolithic communities of Gozo lived to a relatively advanced age. Our diagnoses of HFI are supported and extended by the observations tabled in §8.4.4, above, regarding further evidence for individuals of advanced age, including public symphysis degeneration and ossified cartilage (Fig. 8.5a-g). We have also reported other conditions for which age may be a contributing factor, such as osteoporosis (§8.5.3.2–7, §8.6.1.3, & §8.7.6). These discoveries call for a consideration of the bioarchaeology of caregiving across the life course for Neolithic Malta, particularly as shared with, offered and experienced by community members of advanced age.

In agreement with Appleby (2010, 2011, 2015; cf Fahlander 2013), we argue that discussions of old age in past populations have been neglected within archaeological discourse. Despite the deserved focus apportioned to infants and children in archaeological narratives (Bacvarov 2008; Baxter 2005; Lillehammer 1989, 2000, 2010; Moore & Scott 1997; Power 2012, 2016; Schwartzman 2006; Scott 1999; Sofaer-Derevenski 2000), those at the other end of the life course have, for the most part, remained invisible to critical discussions of age and identity. However, as stated by Appleby, if we do not explore the 'actions, intentions and meanings associated with the oldest members of prehistoric communities, we risk significantly misunderstanding those communities' (2011, 146; cf Appleby 2010, 2015). This observation becomes particularly poignant when we consider the role of elders in certain cultures and pre-literate societies as leaders, caretakers and repositories of cultural and social knowledge (Goody 1976; Hazan 1994; Simmons 1945; Sokolovsky 1983; Press & McCool 1972).

The *status quo* of old age in archaeology perhaps reflects a modern Western lens through which the elderly are often viewed, where they are removed from socioeconomic significance through forced retirement, isolated through placement in nursing homes, and regarded as mentally and physically vulnerable and burdensome (Anderson 1972; Appleby 2011, 2015; Cumming & Henry 1961; Smith *et al.* 2017; Townsend 1981). It is often also attributed to the difficulties in assigning an accurate chronological age to older individuals by osteological assessment (Buckberry 2015; Cave & Oxenham 2016; Cox 2000; Hoppa & Vaupel 2002; Mays 2015; Ross & Oxenham 2015; Smith *et al.* 2017). In contrast to the relatively stable rate at which the younger members of the population grow (notwithstanding genetic and environmental variation), the rate at which humans senesce is profoundly variable. This is not only because of similar genetic and environmental influences faced by the younger members of the community, but amplified by other factors including lifestyle, health and disease and significant life events (Aykroyd *et al.* 1999; Buckberry 2015; Cox 2000; Kemkes-Grottenthaler 2002; Márquez Grant 2015; Mays 2015; Roksandic & Armstrong 2011; Tayles & Halcrow 2015). As such, the accuracy with which skeletal age determination can be effectively attributed diminishes following the fusion of the medial clavicular epiphysis between 20–30 years of age (White & Folkens 2005, 195, 372). The reliability of skeletal ageing methods beyond this physiological milestone, such as cranial suture closure, are considered controversial, at best (Appleby 2011; Aykroyd *et al.* 1999; Cox 2000; Molleson *et al.* 1993; White & Folkens 2005).

However, to reduce the concept of age to purely chronological or biological factors is to misunderstand and underestimate grossly the importance of the social aspects of the ageing process in both individual and community identity dynamics. Such considerations have been promoted by Arber and Ginn (1995) as a threefold division of age which encompasses contextualized considerations of chronological, biological and social processes of ageing, an approach which has also been embraced in some archaeological analyses (Appleby 2010, 2011, 2015; Gowland 2002, 2007, 2015, 2016; Sofaer 2006, 2011). Particularly important for prehistoric populations, this approach acknowledges that there is no universal relationship between chronological age, social identity and physiological status (Appleby 2011; Cox 2000; Ginn & Arber 1995), and that understanding of identities later in life should be culturally situated (La Fontaine 1986; Riley 1984; Thompson 1990).

We understand that an 'archaeology of age' for Neolithic Malta is beyond the scope of the current project, considering that its prerequisite negotiations of complex interrelated characteristics includes biological sex, gender, health, kinship, social status, geographical affinity and power amongst myriad other factors (Appleby 2011; Arber & Ginn 1995; Bury 1995; Lock 1993; McMullin 1995), and may prescribe, proscribe or permit various social roles (Appleby 2011; Blaikie 1999; Hazan 1994; Neugarten & Hagestad 1977). What we offer here, however, is an initial attestation of the presence of individuals of advanced age within the Circle from which further study may proceed. As discussed by Thompson *et al.* in Chapter 12 of this volume, the identification of individuals from across the life course in this highly significant cultural space implies a rich picture of inclusion and integration within the lived communities of Neolithic Malta, too.

8.7.5. Endocranial lesions

Our analyses of palaepathological lesions from the Circle assemblage revealed numerous examples of endocranial lesions in crania representing a multitude of individuals, demonstrating relatively widespread prevalence within the population. The endocranium is separated from the brain by the meninges, comprising the outer dura mater (pachymeninges), covering the arachnoid and pia mater (leptomeninges). The dura mater is a highly vascularized fibrous tissue which forms the endocranial periosteum and provides blood supply to the cranial bones (Lewis 2004, 84). In children, the dura adheres strongly to the sutures; this lessens throughout the process of cranial suture closure but the dura again firmly attaches to the endocranium in older adults (Weller *et al.* 2018). Inflammation and/or haemorrhage of the meninges can stimulate an osseous response on the endocranial surface in the form of 'diffuse or isolated layers of new bone on the original cortical surface, expanding around meningeal vessels, as "hair-on-end" extensions of the diploë, or as "capillary" impressions extending into the inner lamina of the cranium' (Lewis 2004, 82; cf Roberts & Manchester 2005, 178–9). As has been commented upon (Hershkovitz *et al.* 2002, 201; Lewis 2004, 83), research into the variation, expression and aetiology of endocranial lesions has been limited. Such lesions have previously been referred to as *cribra cranii* (Koganei 1912; Henschen 1961) or *cribra cranii interna* (Møller-Christensen 1961) and were often observed in association with *cribra orbitalia* and porotic hyperostosis. Analyses of their location, form, and comorbidities in adults (Gomez *et al.* 2018; Hershkovitz *et al.* 2002; Janovic *et al.* 2015) and non-adults (Lewis 2004; Mensforth *et al.* 1978; Schultz 1993) have suggested a range of possible aetiologies including anaemia, meningitis, neoplasia, epidural or subdural haemorrhage, trauma, tuberculosis, venous drainage disorders, vascular malformations, vitamin deficiencies, and non-specific inflammation.

As reported by Lewis (2004), the first description of endocranial lesions was carried out by Koganei (1912), who observed endocranial lesions more frequently in adults than non-adults. Subsequent research has found endocranial lesions in association with porotic hyperostosis (Henschen 1961; Møller-Christensen 1961), intrathoracic infections such as tuberculosis and pneumonia (Hershkovitz *et al.* 2002), non-specific inflammation (Mensforth *et al.* 1978), and vascular malformation (Janovic *et al.* 2015). Endocranial lesions as a result of trauma or chronic Vitamin A, C or D deficiencies are more typically found in non-adults (Brickley & Ives 2006, 2008; Caffey 1974; Ortner & Ericksen 1997). Ortner (2003, 84) distinguishes between 'endocranial meningeal reactions' produced following haemorrhage, inflammation and tumorous processes. Haematomata overlie the inner table, and progress from small branching impressions to porotic new bone deposition which eventually remodels; inflammatory and tumorous processes involve the inner table and may penetrate the diploë, but while inflammation can produce plate-like new bone, neoplasms stimulate remarkably dense and proliferative new bone deposition (Ortner 2003, 84).

Comprehensive study of the distribution and expression of endocranial lesions has so far only been attempted in non-adult remains from Medieval and post-Medieval sites in England (Lewis 2004). In 528 individuals from neonatal to 17 years of age, Lewis (2004) distinguished between four types of endocranial lesions: (1) pitted; (2) fibrous; (3) capillary formations; (4) hair-on-end formations (these may become 'frosted' or thickened as they remodel). It was further noted that the lytic and granular endocranial lesions pathognomic of tuberculous meningitis represent a fifth type, which was rarely observed in the collections studied (Lewis 2004, 91). In contrast to their distribution in adults, in non-adult individuals endocranial lesions were most often found on the occipital, followed by the parietal and frontal, and often followed regions of venous drainage (Lewis 2004). Through analysis of their expression and relationship to age, it was found that porous and fibrous endocranial lesions in individuals younger than 6 months of age were most likely not pathological but rather the result of new bone production from the osteogenic dura (Lewis 2004, 94). Capillary and vascular impressions were often found on multiple cranial elements in the same individual and are suggested to represent healed lesions, supporting Schultz's (1993) earlier findings in adult individuals. Finally, hair-on-end lesions, whether spiculated or frosted, were deemed most likely to be secondary to infection (Lewis 2004, 95). Although developed for non-adult skeletons, Lewis' classification of endocranial lesions is largely applicable to adult individuals, with the caveat that aetiologies and differential diagnoses may not be directly comparable.

The relationship between endocranial lesions and meningeal and vascular anatomy, as well as their expression (for example, osteoblastic new bone formation, osteoclastic erosive lesions, or a combination of the two), is critical for differential diagnosis. In their study of the Hamann-Todd collection, Hershkovitz *et al.* (2002) defined a distinct form of endocranial lesion characterized by snaking canal-like erosions of the inner table with occasional marginal pitting, which they termed *serpens endocrania symmetrica* (SES). These lesions were distinct from tuberculous granular lesions, or 'sharply demarcated erosive defects' (SDED). SES were often bilateral, multifocal and located on the frontal, parietal and occipital bones, typically in the region of the sinuses or bosses (Hershkovitz *et al.* 2002, 204–5). They were observed in 32 adults, most of whom died as a result of tuberculosis (78.1%) and often also presented HOA, although myocarditis, syphilis, pneumonia, and gastric carcinoma were also reported. Therefore, SES is primarily argued to indicate intracranial infection, but may occasionally be congenital or age-related (Hershkovitz *et al.* 2002, 210).

There are two main types of endocranial lesions described within the Circle study sample; the first type is characterized as capillary impressions extending into the inner lamina extending from or surrounding meningeal vessels (see cases described in §8.5.2.3–9); the second type is characterized as the exuberant proliferation of the diploë within the frontal fossa, identified as *hyperostosis frontalis interna* (see cases described in §8.5.2.10–13, and contextualized in §8.7.4, above). The previously mentioned vagaries associated with attributing aetiologies of the first type of endocranial lesion are compounded in the Circle burial population because of the high levels of fragmentation and commingling – we are unable to understand these osseous responses in relation to any of the required biocultural frameworks of age, biological sex or broader health statuses of any of the affected individuals. Although the preceding text presents many differential diagnoses which have been apportioned to these types of hypervascular lesions, in the absence of further osteological evidence we are restricted to describing these observed in the Circle as non-specific infectious or inflammatory meningeal responses (Mensforth *et al.* 1978; Ortner 2003), the severity of which enabled the affected individuals to survive long enough to produce an osseous response.

Notwithstanding this wide diagnostic bracket, the parentheses tighten when we consider lesion distribution according to chronology. Five of the seven cases identified amongst the sample precipitate from Context (951), one of the earliest use phases of the burial space. The remaining two derive from contexts (518), one of the final burial deposits dating to around 2350 BC, and (838), an undated Tarxien phase deposit to the north of the site. The former case presents more as macroporosity than hypervascularity. Considering that the cases presented above in §8.5.2.3–9 feature a substantial amount of element repetition it is likely that the cranial fragments are representative of ≥5 individuals, all of whom experienced some form of meningeal illness in Neolithic Malta, which (according to Schultz 1993, 2001) they survived. At least one individual also featured porotic hyperostosis on the ectocranial surface (also reported by Henschen 1961 and Møller-Christensen 1961), indicating that they had been subject to chronic nutritional, environmental or psychological stress. For such a cluster to be identified within one context of the Circle and be relatively absent elsewhere, we must consider the possibility of some form of infectious disease being present in Neolithic Gozo, such as meningitis (Patterson 1993). Meningitis is usually a result of a bacterial or viral infection, some of which are mildly to moderately contagious, but may also derive from non-infectious comorbidities such as neoplastic disease (Roberts & Manchester 2005). There is much debate about whether meningitis would have been survivable in pre-industrial populations prior to the development of antibiotics, however, according to Roberts (2000), this would depend on the virulence of the organism, which may have been lower in past populations. If these lesions are attributed to some form of infectious disease, we may then consider broader biocultural questions such as the vector from which the infection arose in an otherwise ostensibly isolated island environment; the population density required to support and/or transmit infection; the seasonality of infection (meningitis, for example, is most commonly observed clinically in winter and spring (Patterson 1993); and the care required to nurse affected individuals through the worst of the infection back to health.

8.7.6. Nutrition

The statement 'you are what you eat' is axiomatic for the human condition. Nutrition is one of the most important factors to influence our health and well-being, applying equally to prehistoric and contemporary populations. Numerous archaeometric approaches explore this universal concept for individuals and groups from the past, including isotopic analyses (Chapter 10), zooarchaeology (Volume 2, Chapter 9), palaeobotany (Volume 1, Chapter 3; Volume 2, Chapter 9), dental calculus analyses and coprology, to name only a few. However, equally important for nutrition (albeit less frequently discussed) is that 'you are what you *don't* eat', too. This consideration is extremely important in palaeopathology, as many of the most commonly diagnosed conditions including *cribra orbitalia*, porotic hyperostosis and enamel hypoplasia all include nutritional deficiencies amongst their differential diagnoses (Aufderheide & Rodríguez-Martín 1998; Ortner 2003; Roberts & Manchester 2005). Diet has critical bearing on many other factors that influence the lived experiences of past individuals, including but not limited to stature and body composition, fertility, immunity (Roberts & Manchester 2005; Steckel 1995) and dental health (Cook 1984; Goodman *et al.* 1980, 1984a, 1984b; Hillson 2005; Larsen 1995; Ortner 2003; Sciulli 1977, 1978; Smith *et al.* 1984; cf Chapter 4). Considerations of nutritional status are particularly important for many Neolithic cultures across the world in light of the transition to agricultural subsistence strategies and increasingly sedentary lifestyles that characterize this phase. The Maltese Islands are no exception to these developments; thus, any discussions of population health, behaviour and culture should include reference to food.

As stated in §8.4.3, above, observations by both the current study and Stoddart *et al.* (2009a) indicate that the previously mentioned characteristic indicators of nutritional and environmental stress, including *cribra orbitalia*, porotic hyperostosis and enamel hypoplasia, have very low incidence and prevalence rates within the Circle burial population. Power *et al.* reported in Chapter 4 specifically on enamel hypoplasia, revealing that although enamel hypoplasia was noted at a generally low rate throughout the use-life of the Circle, it had highest population incidence in the Late use phase of interments. This observation of increasing biological and/or nutritional stress around 2550–2500 BC aligns with a trend observed in isotopic analyses towards lower enrichment of dietary $\delta^{15}N$ in samples of human bone from the site (Chapter 10). This trend was itself caused by palaeodietary shifts or changes in the balance of the nitrogen cycle in agricultural practices across the Xagħra plateau. Apart from the indicators outlined above, we may consider how these subsistence challenges might have physically manifest in other ways within the prehistoric population.

Extending the present study's biocultural focus, our research strategy embraces the inclusion of individual case studies to illuminate the lived experiences of 'real people' amongst archaeological assemblages, above and beyond requisite population-based reporting. As such, several of the pathologies described for the individuals above are relevant to discussions of compromised nutritional status in Neolithic Gozo. We presented several cases of vertebral crush fractures (§8.5.3.2–6), a proximal humerus fracture (§8.5.3.7), and a femoral fragment (§8.6.1.3) all of which demonstrated characteristic signs of severe osteopenia indicative of osteoporosis under radiological examination, including generalized demineralization and cortical bone loss. It is noteworthy that these elements precipitate from contexts that span from Early to Late interment phases of the site. There have been several investigations of osteoporosis in archaeological populations across Europe and more broadly (for example, Agarwal 2016; Agarwal & Grynpas 1996, 2009; Agarwal & Stout 2003; Beauchesne & Agarwal 2014; Mays 1996, 1999, 2016; Mays *et al.* 2006; Sansilbano-Collilieux *et al.* 1994; Spinek *et al.* 2016; Turner-Walker & Mays 2001; cf Brickley 2002; Brickley & Ives 2008). As noted in §8.7.4, above, osteoporosis is most commonly associated with age-related changes, particularly in biological females, because of physiological stressors imposed by short birth intervals, prolonged lactation and hormonal changes following the menopause (Ortner 2003; Turner-Walker & Mays 2001, 265), but it is also experienced by some biological males (Lorkiewicz *et al.* 2019). However, nutritional factors must be considered when attributing aetiologies to these cases, especially dietary deficiency of calcium (Brickley 2000; Martin *et al.* 1985, 1987; Ortner 2003; Roberts & Manchester 2005, 242ff.; Stini 1995). As the most abundant mineral in the body, calcium is essential for the healthy formation, growth and maintenance of bones and teeth. Calcium is available in dairy foods and certain vegetables (including broccoli, cabbage, beans and leafy green vegetables), and modern studies recommend an intake of between 230–1000 mg per day (Stini 1995).

While milk-producing animals were certainly present in Neolithic Gozo, and the archaeozoological evidence is consistent with their use as such, (Volume 2, Chapter 9), we cannot be certain of the extent to which all community members were able to access their products regularly. Similarly, further research is required to determine if the vegetal matter and crops grown and consumed on the prehistoric Xagħra plateau had sufficient bioavailable calcium. Another source of calcium is fish consumed whole with bones (Stini 1995), however isotopic analyses reveal that marine protein was not a major component of the Neolithic Maltese diet (Chapter 10). Over and above dietary deprivation, other factors may compromise the body's ability to absorb calcium, including dietary deficiency of vitamin D – essential for the absorption of calcium and phosphorous – or a high-protein diet, which may increase calcium excretion (Breslau *et al.* 1988; Orwall 1991; Stini 1990; Yuen *et al.* 1984). The latter is potentially supported by the enriched Nitrogen-15 results from the site, consistent with a high-protein diet, although environmental factors could also be driving this signal (Chapter 9). Coincidentally, studies have shown that fluoride may provide some protection against osteoporosis (Boivin *et al.* 1993; Stini 1995), which would theoretically stand the prehistoric Gozitan community in good stead considering the high endemic fluoride levels, cited by Stoddart *et al.* (2009a) and Power *et al.* in Chapter 4. However, for some individuals, this geological boon did not appear to deliver such benefits.

Regardless of the aetiology, the biocultural implications of osteoporosis for individuals and communities past and present can be profound. As we have seen in the Circle population, vertebral crush and compression fractures significantly alter the architecture of individual vertebral bodies, and therefore the physiology of the spine (Foldes *et al.* 1995; Frigo & Lang 1995; Mays 1996; Roberts & Wakely 1992). Depending on the number and severity of fractures sustained, an individual may develop a pronounced kyphosis (so-called 'Dowager's hump'; Aufderheide & Rodríguez-Martín 1998). In addition to compromised mobility, kyphosis may reduce the volume and efficacy of the pulmonary and abdominal cavities and lead to serious (and even fatal) respiratory and/or digestive complications (Shane 1998; Stini 1995). Although not yet noted within the Circle assemblage, osteoporosis is a well-known cause of other fractures within the body, especially those of the femoral neck, *ossa coxae* (pelvis) and radius (Aufderheide & Rodríguez-Martín 1998; Brickley 2000; Dequeker *et al.* 1997; Ortner 2003; Roberts & Manchester 2005; Stini 1995). Considering the present study's call for greater focus on the identification and inclusion of more senior members of ancient populations, these discussions offer another opportunity to highlight their significance within bioarchaeologies of care. After all, in both the past and the present, it is this group for whom osteoporosis poses the greatest risk (Aufderheide & Rodríguez-Martín 1998; Roberts & Manchester 2005; Stini 1995; Woolf & St John Dixon 1988). Our current under-representation of this important demographic group undermines our understanding of the incidence and prevalence of this disease and its effects on morbidity and mortality in past populations.

Our methodological case study, presented in §8.6.2, above, enables us to consider dietary deficiency at the opposite end of the life course via a rare and compelling diagnosis of scurvy on a non-adult individual of approximately 2–4 years of age. This child experienced severe and chronic vitamin C deficiency. Considering the young age of this individual, we must consider whether their condition is indicative of their own direct dietary insufficiency, perhaps associated with a lack of dietary diversity or seasonal/cyclical famine (Brickley 2000); or whether we are witnessing the complications of weaning, such as the lack of availability of appropriate foods or digestive maladaptation (Brickley & Ives 2008, 45); or if the diagnosis represents malnourishment of the mother or wet nurse if the child was still breastfeeding. In any case, our findings indicate that at least one individual suffered considerably as a result of this specific form of malnutrition. In our summary above (§8.6.2), the osteological evidence is paired with clinical accounts of the lived experience of scurvy, producing evocative imagery of how this disease might have been experienced by this individual – harrowing for anyone, but especially for such a small child. Aligning with the principles of the bioarchaeology of care, we also must consider how this illness and eventual death may have impacted the community surrounding this very sick, very young individual (Thompson *et al*. 2021).

The chronology of this case aligns with the declining phase of the 'Temple Culture' in the Maltese Islands. Considering the unique nature of these lesions within the assemblage, it would be inappropriate to extrapolate the experience of this individual to a population level. Notwithstanding this, we note the wide acknowledgement that studies of mortality and morbidity during infancy and childhood provide the most accurate barometer by which the overall health of past populations may be measured (Adler & Ostrove 1999; Hewlett 1991; Lewis 2007; Lewis & Gowland 2007; Murray & Frenk 2002; Perry 2005; Power 2007, 2012; Saunders & Barrans 1999; Schutkowski & Power 2010). By occupying the most sensitive and dependent phase of the human lifecycle (Roth 1992), children and infants readily reflect a population's ambient living conditions and local socio-ecology (Saunders *et al.* 1995; Saunders & Barrans 1999). From this perspective, this small child is a sentinel for the final years of the temple building period, offering a biological translation of the lived experience of the prevailing natural and cultural environments – at least for some members of the population. Though much remains to be understood about synchronic and diachronic nutrition and dietary diversity in prehistoric Malta, this case provides the impetus for further interdisciplinary studies to explore the corporeality of cultural change across the archipelago.

8.7.7. Interpersonal violence

Our case studies include reports of healed fractures to the head and face (nasal bone, FB0014, §8.5.1.2; mandible, FB0002, §8.5.1.1) as well as the upper limb, including two humeri (FB0007, §8.5.3.7; FB0015, §8.5.3.8), and five ulnae (FB0008-FB0012, §8.5.3.9–13). Reports of interpersonal violence (IPV), including domestic violence, frequently cite injuries to these regions of the body, although male victims may experience more upper limb trauma compared with females (Redfern 2015, 19). Differential diagnosis of the mechanisms responsible for the fractures observed on these elements (i.e. accidental or intentional) is complex even in undisturbed burials, becoming more so in a disarticulated depositional context such as the Circle. Post-cranial elements associated with the fractured cranial bone and mandible are unobservable, as are further upper limb elements. As such, patterns of trauma and injury recidivism across discrete individuals cannot be traced within this burial population. Another consequence of this mode of funerary behaviour, in the absence of further biomolecular analyses, is our inability to determine the sex of the individuals from whom these elements derived. Only the nasal bone (FB0014) displaying traumatic fractures precipitated from a cranium with extant sexually-dimorphic characteristics and was assessed as a possible male. All the cases discussed here present a minimum incidence rate of trauma to isolated elements, impeding biocultural interpretations which account for factors such as age and sex.

The head and face are easy and common targets in violent encounters, at a convenient height for a raised arm, and with the potential to harm a victim's self-esteem through disfigurement (Brink *et al.* 1998; Rangel Goulart *et al.* 2014). Nasal bones are the most frequently fractured facial element, usually followed by the mandible, and a major cause of fractures in both regions is assault (Brickley & Smith 2006; Hershkovitz *et al.* 1996; King *et al.* 2004; Ogundare *et al.* 2003; Shepherd *et al.* 1990; Yabe *et al.* 2012). As a result of right-handed dominance, fractures resulting from IPV are expected to be found on the left side, as observed on the mandible FB0002 (§8.5.1.1; Lovell 1997, 156; Novak 2000, 96). In the case of FB0014 (§8.5.1.2), the insult is observed on the right nasal bone. This, however, does not exclude the possibility of an assault with the left hand. It must also be remembered that the nose is the most prominent facial feature, and nasal bones are particularly fragile, increasing the potential for accidental injuries to the nose. Alternative aetiologies for nasal and mandibular fractures observed in clinical studies include falls either of significant force or from a height and sporting injuries (Hwang *et al.* 2017; King *et al.* 2004). Violent combat or duelling may be sporting and recreational, but can also be symbolic, ritualized, or otherwise socially sanctioned, as noted in numerous cultures, although Hershkovitz *et al.* (1996) demonstrate that regular combat is expected to produce a suite of lesions, including robust muscular attachments, as well as numerous rib and hand fractures.

The humerus fractures presented above may have arisen from accidental falls or direct trauma; as discussed in §8.5.3.7, fractures of the surgical neck of the humerus are often seen in osteoporotic women, while mid-diaphyseal humerus fractures (such as FB0015, §8.5.3.8) may be caused by overuse and weight-bearing straining the *M. Biceps brachii* and rotator cuff muscles (Brukner 1998, 416–8). Transverse fractures to the distal third of the ulna diaphysis, without involvement of the radius, are usually diagnosed as 'parry' or 'nightstick' fractures, although this eponym dictates that the injury was sustained as a result of fending off a blow (Judd 2008; Lovell 1997, 165). Clinical assessment reveals that ulna fractures are rarely caused by alternative mechanisms, although stress fractures must be considered in the differential diagnosis (Brukner 1998, 419–21; Richards & Nicole Deal 2014). Ulnar stress fractures as a result of repetitive muscular strain and athletic activity present well-aligned segments, smooth periosteal fusiform swelling and often occur at the junction of the mid-to-distal diaphysis (Judd 2008; Morris & Blickenstaff 1967). Parry fractures, in contrast, are located more distally, displacement of ≤10° may be observed and up to 50% of the fractured segment may be horizontally apposed (Judd 2008; Richards & Corley 1996). Notwithstanding the absence of ipsilateral radii, we observed at least four possible parry fractures in the current study of the Circle burial population (FB0008-FB0011, §8.5.3.9–12). Ulnar styloid fractures (such as FB0012 and FB0013, §8.5.3.13–14) are often caused by a fall onto an outstretched hand or sudden force applied to the wrist (for example, object thrown with momentum at wrist; Jurmain 1999). While the common differential diagnosis of many arm fractures is an accidental trip or fall, routine pushing is a recognized form of domestic abuse. For this reason, falls as a result of accidental injury (for example, sustained while quarrying, erecting large limestone megaliths in the Neolithic Maltese context, or walking over slippery or uneven surfaces) or violence are difficult to distinguish in the archaeological record.

Redfern (2015, 20) provides an important cautionary note for the interpretation of violent trauma in archaeological assemblages: IPV is not always the cause of blunt force trauma or facial fractures and there is no cross-cultural pattern of injuries which signify such altercations. It is also important to remember that traumatic insults more commonly result in soft tissue as opposed to skeletal injuries (Shepherd *et al.* 1990). Nevertheless, where sufficient data are present, patterns of injury in past populations are informative of a host of social phenomena, including inter- and intra-group relations, structural inequality, scales of violence, occupational and habitual activities, gendered behaviour, and even medical knowledge and care (Judd 2002b; Knüsel & Smith 2014; Redfern 2015).

Research on European Neolithic skeletal assemblages, until more recently, has tended to focus on cranial trauma as an indicator of close-range violence. Ante- and peri-mortem cranial trauma, often depressed fractures caused by blunt force, is usually evident in <15% of the assessed skeletal sample (Lorkiewicz 2012; Papathanasiou 2012; Robb 2007, 39; Schulting & Wysocki 2005; Silva *et al.* 2012). These figures indicate minimal (cf Stoddart *et al.* 2019, 329), but regular interpersonal conflict, often seemingly without lethal intent. The apparent absence of cranial trauma in the present sample from the Circle is therefore noteworthy, prompting us to consider whether violent encounters really were infrequent during the late Neolithic in Gozo, whether injuries were more often limited to the soft tissue, or if alternative means of resolving or de-escalating conflict were commonly practised. Alternatively, individuals who transgressed may have been deposited at other burial sites or by other – less enduring – means. Importantly, however, the bioarchaeological evidence corresponds with a similar paucity of weaponry in the lithic culture of the islands. The obsidian arrowhead from Santa Verna (Volume 2, Chapter 4), for example, counts as one of a very small number of such items known.

In contrast, post-cranial trauma is generally less prevalent (Lorkiewicz 2012; Papathanasiou 2012; Silva *et al.* 2012; Smith 2014). However, peri-mortem trauma from projectile weapons - often indicated by arrowheads still embedded in bone – demonstrates that attacks were sometimes planned and carried out over a greater distance (Beyneix 2012; Lahr *et al.* 2016; Pernter *et al.* 2007; Silva & Marques 2010; Smith 2014, 115; Vegas *et al.* 2012). The picture across much of Neolithic Europe is of occasional to regular incidences of interpersonal conflict as well as collective violence, perhaps equivalent to inter-group raids and feuding, which – especially in central Europe – could result in mass graves containing entire executed families or villages (Loison 1998; Meyer *et al.* 2015, 2018; Teschler-Nicola *et al.* 1999; Wahl & Trautmann 2012). In nearby Italy, conflict was usually small-scale, but may have been greater in the more densely settled lowland villages and appears to have decreased during the Copper Age (Robb 1997, 2007, 259). There are two potential mass burial sites in Italy, at Diga di Occhito (Puglia) and Grotta Pavolella (Calabria), yet the circumstances of these individuals' deaths remain to be known (Carancini & Guerzani 1987; Tunzi Sisto 1999; cf Robb 2007, 259).

Overall, ulna fractures are relatively rare in both large archaeological and clinical studies (Judd 2008, 1665), occasionally a single example is present (Lorkiewicz 2012; Smith 2014), although five possible parry fractures to right ulnae were reported at late Neolithic San Juan ante Portam Latinam (Spain) (Vegas *et al.* 2012, 288). The presence of several distal ulna fractures within the Circle sample is significant, especially given the low overall prevalence of long bone fractures. These examples of cranial and post-cranial fractures present a picture of exceptionally low incidences of conflict and violence which resulted in skeletal trauma in late Neolithic Malta. All fractures are healed; in each case, this would have taken at least several months, during which time the individuals' capacity to participate in expected routine tasks which would have been hindered, attesting to post-traumatic treatment (Lovell 1997, 144–5). While violence may increase as a consequence of economic hardship (Papathanasiou *et al.* 2000; Torres-Rouff & Junqueira 2006), there is so far minimal evidence to indicate that this was the case in the declining environment of the Maltese archipelago in the late 3rd millennium BC. Nonetheless, it is important to acknowledge that violence was part of the lived experience of some individuals interred within the Circle – as recipients or perpetrators. These cases offer a sobering indication that for some members of Gozo's prehistoric communities, island life was far from idyllic.

8.8. Conclusion

The report by Stoddart *et al.* (2009a) offered extensive observations of pathology for the excavated portion of the Circle burial population. These observations included the frequency and severity of spinal degenerative joint disease across the cervical, thoracic and lumbar regions. Cited diagnostic criteria included joint contour change, porosity and subchondral cysts, extension of joint margins and eburnation, as well as other indicators of chronic activity-related changes such as osteophytosis and Schmorl's nodes. Similarly, observations were made regarding the presence of osteoarthritis and entheseal changes across the manual and pedal elements, also indicative of chronic activity-related change, plus an observation of temporomandibular joint disease. Notations were made regarding the presence of healed fractures on ribs, a humerus, metatarsals, manual and pedal phalanges, clavicle, an 'arm', 'leg', 'knee', 'nose' (Stoddart *et al.* 2009a, 329) and unnamed elements. Further notes pertained to observations of sinusitis, osteomyelitis, neoplasia, periostitis, myositis, cholesteatoma (chronic ear infection) and meningitis. Congenital variations were also reported, including notes on *spina bifida occulta*. As with our own findings, Stoddart *et al.* (2009a) reported that the overall presentation of skeletal pathology is very low across the Circle, including low site-wide representations of the classic indicators of nutritional, environmental or psychological stress, such as *cribra orbitalia*, porotic hyperostosis or enamel hypoplasia.

The present study has employed several analytical approaches to build upon this foundational reporting on general pathology in the Circle. Our inclusion of radiological analyses for select pathological elements significantly enhanced our capacity to develop more comprehensive differential diagnoses than that possible through macroscopic observations alone. Further to this, the extensive radiocarbon dating programme described by Parkinson *et al.* in Chapter 3 of this volume provides a sturdy chronological platform from which the experiences of health, disease and trauma may be viewed for the Neolithic people interred within this burial space. Moreover, our commitment to representing the lived experiences of these individuals and communities through the interpretative lens of the bioarchaeology of care has facilitated an opportunity to engage more deeply with individual case studies as opposed to the broader population-based reporting presented in the 2009 volume.

Our research argues that the therapeutic accomplishments of the Neolithic Circle population are amongst the most significant discoveries for the bioarchaeology of care in prehistoric Europe, and perhaps the world. The examples presented above for the stabilization, treatment, rehabilitation and recovery of life-threatening fractures (even in modern clinical contexts) testify to the efficacy of therapeutic intervention practices in prehistoric Malta. The case of therapeutic dental intervention presented by Power *et al.* in Chapter 4 extends and secures this claim.

Considerations of care must also extend to our studies of certain forms of nutritional deficiencies and potentially infectious illnesses across the Neolithic Xagħra plateau. Foremost amongst these is the case of scurvy described for a 2–4-year-old child within the Late use phase of the Circle. The case is significant for a number of reasons: i) it is the earliest attestation of scurvy for Malta and is amongst the earliest for the central Mediterranean region; ii) non-adult scurvy is extremely rare in known global archaeological assemblages; iii) the case is a sentinel for the prevailing natural and cultural environments of the final years of the temple culture; and iv) perhaps most importantly, it provides further insight into the capacity for care within these ancient communities. Considering the length of time required for osseous responses to manifest, the extensive skeletal lesions described for this case are powerful biological evidence for the substantial efforts invested to try and keep this very young child alive. Despite the ultimate failure of their efforts, care for this child persisted after their death, as evidenced by their inclusion in this communal burial space and the continued engagement with their remains for many years afterwards. Similar testimonies emerge from our descriptions of endocranial lesions for a small number of adult individuals amongst the population, indicative of non-specific infection or inflammation, possibly meningitis. Here again, any determination of aetiology is equaled in significance by Schultz's (1993) argument that these kinds of capillary and vascular impressions represent *healed* lesions in adult individuals – thus, they are echoes of survival and care.

Despite these evocative biocultural narratives of the presence of the most favourable aspects of the human condition in Neolithic Gozo, it is important to note that our research suggests that some of our species' less-favourable qualities were also present. The patterning of certain healed fractures within the burial population, particularly those of the distal ulna, urge us to consider that some individuals were subject to interpersonal violence within their lived experiences on the Xagħra plateau. Therefore, it is axiomatic that perpetrators of violence lived amongst these communities, too. While differential diagnoses for these injuries must include accidental falls or impacts, the location and transverse nature of the fracture dynamics are strongly indicative of blows to the forearm sustained during self-defence. Although there is no evidence at this stage to indicate that interpersonal violence was widespread amongst the prehistoric Maltese population, especially compared with some other prehistoric communities, these case studies provide a strong indication that it did occur, at least occasionally. Although unsettling, it is important to report these findings, as they attest to the entire spectrum of human behaviour as it was undoubtedly expressed and experienced in past populations.

Similarly, we have aligned with contemporary voices in bioarchaeology to call for greater granularity regarding the entire spectrum of demographic experience in past populations, particularly concerning indicators of advanced age. Our findings of four cases of *hyperostosis frontalis interna* within the Circle burial population greatly enhance our understanding of this rarely noted condition for archaeological assemblages of human remains, as they equal the total number of published cases for prehistoric Europe and are the first described for the Maltese Islands. In combination with our descriptions of well-preserved ossified cartilage, pubic symphyseal degeneration and potentially age- or diet-related osteoporosis among the sample, this study has made substantial contributions to clearer characterization of the latter phase of the life course for some individuals in Neolithic Malta. In so doing, we have extended the discourse surrounding demography and culture in these ancient communities, thereby inviting further considerations of social inclusion, integration and knowledge exchange through an 'archaeology of age' across the archipelago.

Within a burial population of this size and complexity, there are myriad opportunities for further study to extend on the findings tabled here. Several of the phenomena described by Stoddart *et al.* were beyond the scope of our temporal and pecuniary research parameters to address within the current project, such as further analyses of the nature and significance of mastoiditis and chronic ear infections within the population, and dedicated comprehensive studies of the spinal, manual and pedal pathology observed by both Stoddart *et al.* (2009a) and the current authors. Perhaps the greatest opportunity for better understanding of population health for Neolithic Malta lies in a comprehensive analysis of non-adult pathology, considering the innate biological imperative for children to reflect ambient living conditions and local socio-ecologies. From methodological perspectives, additional detailed studies of particular contexts associated with key chronological phases would serve to illuminate the spectrum of health, disease and trauma in prehistoric Gozo beyond the singular or 'extreme' analyses carried out thus far. Moreover, the present study attests to the profound utility of partnering radiological analyses with any macroscopic palaeopathological project. A more comprehensive micro-CT-scanning regime would enhance our insights of the incidence, prevalence and experience of those conditions which are significantly aided in differential diagnoses through radiological techniques. Similarly, histomorphometric analyses would greatly benefit our understanding of osteoporosis amongst the burial population.

Over and above palaeopathological analyses, additional opportunities exist for osteological studies to further characterize the relationships and affinities of those interred within the Circle. Such studies might address our observations of non-metric trait representations in discrete contexts, such as the vastus notch of patella, parietal emissary foramina and mandibular tori. We also observed a significant amount of cranial and postcranial morphological variation within the population, which would benefit from multiproxy analyses including CT/surface scanning, 3D geometric morphometrics and isotopic analysis.

Our research has demonstrated the benefits of biocultural approaches to archaeological assemblages of human remains. While building on population-level observations regarding the health, disease and trauma of those interred within the Circle, our biocultural focus necessitated that we consider them as individual people, with as much intellectual energy dedicated to understanding the experience and meaning of their lives as that devoted to diagnosing their pathologies. Our analyses have stepped beyond the 'medical model' that predominates in palaeopathological analyses which risks implying that those suffering illness or disability were passive in the processes of treatment, rehabilitation and recovery. By focusing on individual case studies contextualized within their cultural framework, this research has restored agency to both those receiving and giving care. Our research has argued that human remains displaying evidence of pathology are much more than 'artefacts' – they are the agents of their own lived experiences, and further are the literal embodiment of the collective agency of all involved in care provision within their communities (Tilley 2015). The ethical and interpretative benefits of this approach are clear. We have assumed this as a particularly important objective for a mixed collective funerary ritual assemblage such as the Circle, where many might expect that the levels of fragmentation and commingling would render such individual testimonies inaccessible. Considering that the cultural impetus behind this form of funerary behaviour appears to encourage the individual to reflect the collective, and the collective to reflect the individual, our approach is more than beneficial – it is appropriate.

Note

1. These analyses were carried out in two tranches with the approval of Heritage Malta and the Superintendence of Cultural Heritage, Malta, the first in July 2015 and the second in July 2017. Transport was carried out by Bernardette Mercieca-Spiteri, Officer of the Superintendence of Cultural Heritage, Malta, with the agreement of Heritage Malta. On both occasions, radiographic analyses (micro-CT scans) were carried out by Jay Stock, Laura Buck and Jaap Saers at the Cambridge Biotomography Centre, University of Cambridge, UK, with a Nikon Metrology XT H 225 ST. Scans were created with voxel sizes ranging from 0.06 to 0.12μm3 (to two decimal places) as appropriate for the region of interest and specimen size. Further processing of individual files was carried out by Jaap Saers in the Department of Biological Anthropology, University of Cambridge, UK. Radiological examination and description of the micro-CT scans was carried out by John Magnussen, Ronika K. Power and Jess E. Thompson, using 3D Slicer (BWH, slicer.org), RaDiant DICOM Viewer (Medixant, radiantviewer.com) and AW Server (GE Medical Systems, Milwaukee, USA) software at Macquarie Medical Imaging, Macquarie University Hospital, Sydney, Australia. Radiological images were processed for publication by John Magnussen and Margery Pardey at Macquarie Medical Imaging.

Chapter 9

An isotopic study of provenance and residential mobility at the Circle and the Xemxija tombs

Argyro Nafplioti, Rowan McLaughlin, Emma Lightfoot, Ronika K. Power, Bernardette Mercieca-Spiteri, Catherine J. Kneale, Tamsin C. O'Connell, Simon Stoddart & Caroline Malone

9.1. Introduction

The island context of Malta and the relative isolation of its prehistoric population presents an opportunity to test ideas about the origins and ancestral provenance of the changing communities throughout the Neolithic. As part of a multi-pronged approach, the *FRAGSUS Project* has employed various methods that can explore the possible origins, through aDNA, through bioanthropological characteristics and by isotopic analysis. In this volume, the application of multi-isotope (strontium, oxygen, carbon and nitrogen) ratio analysis of the remains of the people themselves, demonstrates the potential of these methods to reveal direct information about past people's lifeways. The *FRAGSUS Project* has explored carbon and nitrogen isotopes which link to dietary practices (Chapter 10) as well as those relating to provenance and residential mobility in this chapter. The samples studied are from the Neolithic burial contexts at the Circle and Xemxija, and this chapter represents the first isotopic investigation aiming to identify the geographical origins of these communities in the Maltese Islands. It focuses on provenance, migration and residential mobility in relation to the early settlers and presents and discusses the results of oxygen ($^{18}O/^{16}O$) and strontium ($^{87}Sr/^{86}Sr$) isotope ratio analyses of human teeth from the two sites. These results may enable the reconstruction of geographical origins and the tracking of residential change of the analysed individuals. The work specifically addresses hypotheses for contact and mobility within the Maltese Islands, as well as between Malta and the rest of the Mediterranean, as also supported by bioanthropological and material culture data.

The complementary bioanthropological studies by the *FRAGSUS* Population History Workgroup indicates that some physical characteristics in dentition and skull shape/structure of a group of late Neolithic individuals in the Circle suggest an African origin (Chapter 6). If (some of) these people are first generation immigrants, analysis of strontium and oxygen isotope ratios of their teeth can potentially confirm this. Until now, there had been no strong indication of a southern origin for the prehistoric populations, but this omission is perhaps typical of more traditional scholarship of the Mediterranean. It is quite clear that Neolithic communities in the region had access to seacraft of some kind, undertook voyages of colonization, and over millennia, managed to populate most of the habitable islands and regions of the Mediterranean by 3000 BC (Dawson 2014). Malta's almost central location in the Mediterranean offered ample opportunity for peoples from all directions of the sea to arrive and settle on Malta. The questions about those origins, however, have rarely been posed with any supporting evidence, until now.

9.2. Background

9.2.1. Neolithic transition and population/settlement history in the Maltese Islands

Current evidence points to a Neolithic colonization of the islands from early in the 6th millennium BC (Volume 2, Chapter 2). The islands cover a total surface area of only 316 km^2. It seems likely that the Neolithic was the earliest period when a viable permanent occupation of the islands based on agriculture, became possible (Schembri *et al.* 2009, 17). These newcomers are generally considered to be the first settlers, while any visitation by earlier hunter-gatherers most likely was sporadic and short-lived, owing to insufficient local biomass in the restricted island space (Malone 1997–99). To date there is no material evidence for Mesolithic foragers on the island, and the distance, even if it had been somewhat shorter than the present, was nevertheless a long and risky voyage of perhaps 60–80 km of open water (Volume 1, Chapter 6). Whilst settlement before farming communities arrived is unknown, it is possible that Mesolithic scouting expeditions could have landed on the islands, perhaps for brief hunting activities, and traces of charcoal in the sediment cores (Volume 1) might suggest burning of the landscape to clear brushwood or herd animals.

9.3. Materials and methods

Oxygen and strontium form two independent isotopic systems, which reflect local geology and environmental conditions, respectively. As oxygen and strontium isotopes in teeth are fixed in enamel biogenic apatite at the time of formation and enamel undergoes little remodelling thereafter, the isotope ratio values recorded reflect childhood provenance and provide complementary evidence for the latter, for mobility and relocation (Hillson 2002; Hoppe *et al*. 2003; Price *et al*. 2002: White *et al*. 1998). The combined application of these two independent isotope systems enhances their potential for identifying newcomers and tracking past residential mobility compared with that of either system applied in isolation (Evans *et al*. 2019; Killgrove & Montgomery 2016; Knipper *et al*. 2017; Knudson & Price 2007; Mitchell & Millard 2009; Nafplioti *et al*. 2021).

9.3.1. Principles of oxygen isotope ratio analysis

$^{18}O/^{16}O$ reflects the regional climatic conditions (i.e. temperature, humidity, distance from the sea and elevation) and passes to the tissues of humans and animals primarily from the imbibed meteoric water, i.e. water from precipitation (rain or snow), and to a lesser extent from water in food and water in air with predictable metabolic fractionation. $^{18}O/^{16}O$ of meteoric precipitation has been demonstrated to decrease with falling temperature, distance from the sea, and high altitudes. Also, $^{18}O/^{16}O$ values are negatively correlated with humidity levels (Yurtsever & Gat 1981, Darling *et al.* 1996).

Oxygen isotopes in the body of humans and other mammals are subject to several stages of metabolic fractionation from imbibed water to body fluids and from the latter to skeletal bioapatite. This fractionation is now adequately understood and predictable, so that approximate $^{18}O/^{16}O$ values for the imbibed meteoric water can be calculated and used to characterize the regional ecological context and probable geographical origins for the individuals analysed. Despite the difference between the oxygen isotope composition of the structural carbonate and phosphate components of bone or enamel bioapatite, oxygen of both the structural carbonate and phosphate of biogenic apatite has been demonstrated for modern mammals to be in equilibrium with body water (D'Angela & Longinelli 1990; Daux *et al.* 2008; Iacumin *et al.* 1996a; Kohn *et al.* 1996; Levinson *et al.* 1987; Longinelli 1984). Also, there is a known quantitative relationship between the oxygen isotopic compositions of the two components of skeletal bioapatite (Bryant *et al.* 1996; Iacumin *et al.* 1996).

$^{18}O/^{16}O$ in dental enamel reflects the $^{18}O/^{16}O$ in imbibed water and water in foods consumed by the individual during childhood, when teeth are formed (Hillson 2002), with some enrichment in ^{18}O owing to metabolic fractionation, discussed above. Moreover, enamel of teeth formed during the first few years of the life of the individuals, i.e. the 1st and 2nd incisors, the canine and 1st molar, when the individuals were most probably still breastfeeding, are enriched in ^{18}O ($\delta^{18}O$ values raised by *c*. 1‰) compared with teeth formed following cessation of the breastfeeding (Wright & Schwarcz 1998). This is known as the 'breastfeeding effect' where the oxygen isotope signal of enamel mineralized during breastfeeding is raised by up to 1‰ over that of later forming teeth, reflecting the fact that nursing infants are feeding at a higher trophic level than their mothers (Jay *et al.* 2008; Hoppe *et al.* 2003; Hillson 2002; Montgomery 2002; White *et al.* 2000; Wright & Schwarcz 1998).

Determination of the local biologically available $^{18}O/^{16}O$ is not as straightforward as for $^{87}Sr/^{86}Sr$ (§9.3.2), because of the difficulty in determining the various water sources used by the population tested and the possibility that exact values for prehistoric $^{18}O/^{16}O$ and their patterning were different from $^{18}O/^{16}O$ in modern precipitation. Moreover, there is evidence for inter-species variation in $^{18}O/^{16}O$ values largely linked to physiology and dietary differences (Bentley & Knipper 2005; Kohn 1996; White *et al.* 2004).

Because of the overlap in human oxygen values from different locations across the continents, it is not possible to establish an individual's geographical origin on the basis of oxygen isotope analysis alone (Lightfoot & O'Connell 2016). Instead, the efficiency of oxygen isotopes for tracing the provenance of human skeletal remains is reinforced when combined with strontium and/or other isotope ratios such as lead or sulphur, which serve as proxies not of the local environment, but the local geological context (Muldner *et al*. 2011; Redfern *et al*. 2016; Turner *et al*. 2009).

9.3.2. Principles of strontium isotope ratio analysis

In nature, strontium occurs in the form of four isotopes, ^{87}Sr, ^{88}Sr, ^{86}Sr and ^{84}Sr. Strontium isotope ^{87}Sr is radiogenic and is the product of the radioactive decay of rubidium isotope ^{87}Rb with a half-life of approximately 4.7×10^{10} years, while the other three strontium isotopes are all non-radiogenic (Faure 1986). Therefore,

$^{87}Sr/^{86}Sr$ in any local geology depends on the relative abundance of rubidium and strontium at the time the rocks crystallized, and the age of the rocks.

The strontium isotope ratio ($^{87}Sr/^{86}Sr$) passes from bedrock into the soil and groundwater and hence into the food chain, reaching, without any fractionation (Graustein 1989), human tissues from the food and water consumed (Bentley 2006). $^{87}Sr/^{86}Sr$ in human tissues therefore largely reflects local geology (Graustein 1989). Because tooth enamel is a cell-free tissue that forms during early childhood and does not remodel thereafter (Hillson 2002), it is possible to identify migrants who moved between geologically and isotopically different regions by comparing ratios measured in human enamel samples and the local biologically available $^{87}Sr/^{86}Sr$ at the site where the respective individuals were buried (Price *et al*. 2002, Bentley 2006). In theory, therefore, significant differences in the ratios measured in the tooth enamel of an individual and the local biologically available $^{87}Sr/^{86}Sr$ where he/she was buried, indicate that he/she spent his/her childhood at a location geologically and isotopically different from his/her residence prior to death (Sealy *et al.* 1991).

9.3.3. The geological context

The geology of the Maltese Islands is dominated by sedimentary rocks in five limestone formations of different ages (Schembri *et al.* 2009, 17). $^{87}Sr/^{86}Sr$ signatures of marine limestones through time are reported by Elderfield (1986). However, although the differential weathering of minerals within the rocks, and the mixing of various sources of sediment within the soil and in the groundwater result in a range of $^{87}Sr/^{86}Sr$ values for the local soils (Jorgensen *et al.* 1999), the local bioavailable $^{87}Sr/^{86}Sr$ cannot simply be equated to $^{87}Sr/^{86}Sr$ in bedrock geology (Faure 1986; Price *et al.* 2002). The local bioavailable $^{87}Sr/^{86}Sr$ is normally determined from archaeological and/or modern animal skeletal tissues that provide an average of the bioavailable $^{87}Sr/^{86}Sr$ signatures of the feeding territories that these animals occupied in life (Nafplioti *et al.* 2021; Nafplioti 2011; Price *et al.* 2002), or from modern plant and water signatures (Evans *et al.* 2009; Evans *et al.* 2010). In relation to the latter, however, there are potential pitfalls linked to contamination by atmospheric pollution and fertilizers (Bentley 2006), which need to be taken into consideration.

9.3.4. Samples

A total of 181 teeth from both project sites were sampled for oxygen, and 29 selected teeth were also sampled for corresponding $^{87}Sr/^{86}Sr$ values. These isotope ratio analyses were performed on enamel, while for one individual (XEM9130.11.37) only $^{87}Sr/^{86}Sr$ was measured in both the enamel and dentine components of the same tooth. All the measured isotope ratio values are reported in Appendix Table A2.2, and graphically represented in Figures 9.1, 9.2, 9.3, 9.4.

The teeth sampled had previously been studied macroscopically by the Population History Workgroup. The majority of teeth had been recovered as loose teeth, with only 19 of the 181 teeth extracted from their position in the maxillary or mandibular dental arcade; hence it was not possible to determine

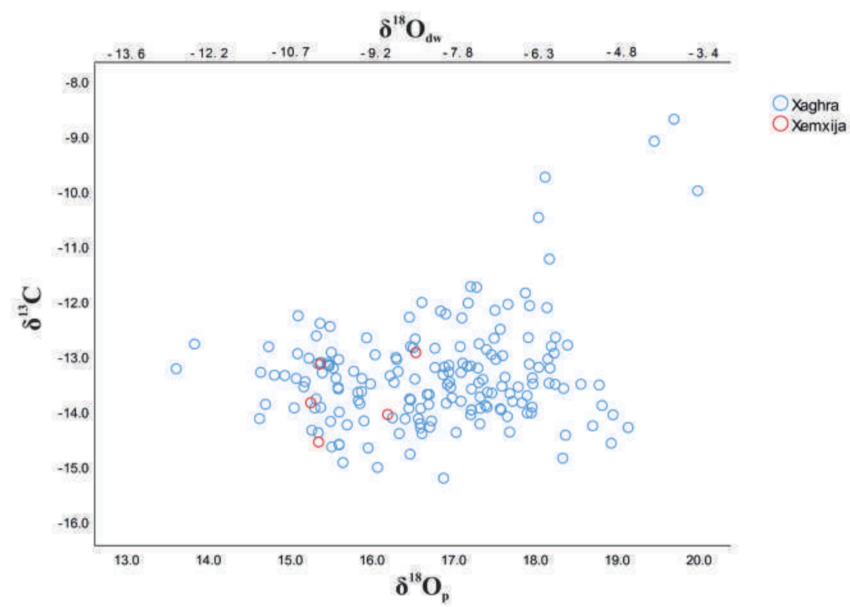

Figure 9.1. *Biplot of oxygen (phosphate and calculated drinking water values) and carbon isotope ratios.*

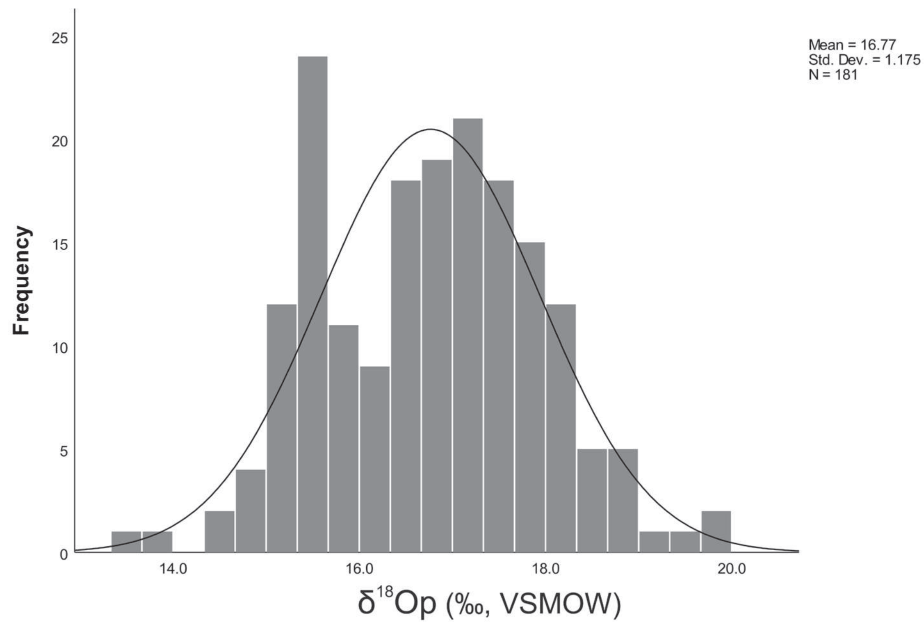

Figure 9.2. *Histogram of enamel δ^{18}Op values indicating a bimodal distribution, with normal distribution curve for comparison.*

whether they belonged to male or female individuals or their precise age-at-death.

For the purposes of $^{18}O/^{16}O$ analysis, we aimed for the second (M2). In the few (27) cases where the M2 could not be sampled, it was substituted by the third molar (M3) in twenty-six cases and the first molar (M1) in one case, respectively. Because the M2 and M3 enamel is known to form largely between the age of 6 and 10, and between 13 and 17, respectively (Scheuer & Black 2000; Ubelaker 1989), the measured oxygen isotope signatures are not expected to be affected by the consumption of breastmilk (Hillson 1996; Hoppe *et al*. 2003; Jay *et al*. 2008; Montgomery 2002), which we discussed above as the 'breastfeeding effect'. Conversely, the M1 $^{18}O/^{16}O$ signatures, can potentially be affected by breastfeeding as M1 enamel forms roughly between the age of 3 and 5.

9.3.5. Sample preparation and analytical procedures

All samples were prepared and analysed at the University of Cambridge, using the facilities of the McDonald Institute for Archaeological Research, the Godwin Laboratory and the Department of Earth Science, as appropriate.

9.3.5.1. Oxygen isotope ratio analysis

$^{18}O/^{16}O$ was measured in the structural carbonate of enamel or bone bioapatite, because it is an easier, faster and less expensive method than measuring $^{18}O/^{16}O$ in the phosphate component of bioapatite, while it simultaneously recovers $^{13}C/^{12}C$ values as well (Bentley & Knipper 2005; Bryant *et al*. 1996). Moreover, the isotope compositions of oxygen in the structural carbonate and phosphate components of bone or enamel bioapatite are related in a quantitative manner and $^{18}O/^{16}O$ carbonate values can easily be converted to the corresponding $^{18}O/^{16}O$ phosphate values (Bryant *et al.* 1996; Iacumin *et al.* 1996).

Following abrasion of the external crown enamel surface using a dremel tool, enamel powder of approximately 8–12 mg was drilled out from the entire crown height avoiding any adhering dentine. Enamel powders were then treated for bioapatite extraction following Balasse & colleagues (2002). After soaking samples in 2–3% aq. sodium hypochlorite (24 h at 4°C) to remove organic matter, the samples were rinsed five times in distilled water and mixed with 0.1 M acetic acid (0.1 ml/mg) for four hours at room temperature to remove exogenous carbonate. Following five rinses, the samples were placed in the freezer at -20°C for 1 hour, and then at -80°C for an additional 30 minutes before being freeze dried for 90 minutes. The dried samples were then transferred into suitable tubes and placed into a VG SIRA mass spectrometer, where each sample was reacted with 100% ortho phosphoric acid at 70 °C. Liberated CO_2 was then trapped and transferred to the mass spectrometer for the isotopic analysis. Results are reported with reference to the international standard VPDB calibrated through the NBS19 standard (Coplen 1995; Hoefs 1997) and the long-term analytical precision is better than ±0.08‰ for $^{13}C/^{12}C$ and better than ±0.10‰ for $^{18}O/^{16}O$.

9.3.5.2. Strontium isotope ratio analysis
The analytical protocol, including procedures of sample extraction and sample preparation prior to analysis, are already published in earlier papers by Nafplioti (Nafplioti 2008, 2009). Strontium isotope values for this project were measured to the sixth decimal digit by a VG Sector 54 Thermal Ionization Mass Spectrometer. A total of 37 analyses of NBS 987 during the two year period around these analyses gave a long term mean value of 0.710265 +/- 0.000009 (1 sigma). Also, strontium blank for the Sr spectrometry method was 68pg and negligible for the Sr concentration of these samples.

9.4. Results

Oxygen and strontium isotope data from the 181 individuals from the Maltese Islands tested are displayed in Appendix Table A2.2 and in Figures 9.1 to 9.5. Full details of these results, including cross-references to other analyses published in this volume, are given below. Oxygen isotope ratio analysis of enamel carbonate yielded values which are reported in standard delta (δ) notation relative to the VPDB international standard and are expressed in units per mil (‰), i.e. $\delta^{18}O = 1000 \times [(^{18}O/^{16}O\ \text{sample})/(^{18}O/^{16}O_{VPDB}) - 1]$ (Table 9.2).

In order to facilitate comparison of the human $\delta^{18}O_c$ values to local precipitation data from the region and further explore provenance for the respective individuals, we converted the carbonate oxygen VPDB data to carbonate oxygen VSMOW values using the equation below:

$\delta^{18}O_{VSMOW} = (1.0309 \times \delta^{18}O_{VPDB}) + 30.9$ (Friedman & O'Neil 1977; Henton *et al*. 2010, 439)

and calculated the corresponding $\delta^{18}O$ values for drinking water ($\delta^{18}O_{dw}$). Converting the human phosphate $\delta^{18}O$ to $\delta^{18}O$ water signatures allows comparability to data from modern precipitation. To this end we used the equation formulated by Daux *et al.* (2008) modified following Iacumin and colleagues (1996) to reflect the correlation between $\delta^{18}O$ values measured in the structural carbonate and phosphate components of bioapatite, respectively, as follows:

If $\delta^{18}O_{mw} = 1.54\ (\pm 0.09) \times \delta^{18}O_p - 33.72\ (\pm 1.51)$ (2)
Daux *et al.* (2008)
and
$\delta^{18}O_p = 0.98 \times \delta^{18}O_c - 8.5$ (Iacumin *et al.* 1996a)
Then
$\delta^{18}O_{mw} = 1.51 \times \delta^{18}O_c - 46.81$

The results of the above calculations are given in Appendix Table A2.2.

Although we acknowledge that the use of the above conversions used to generate Op values expressed in delta notation in relation to the VSMOW international standard introduces some degree of uncertainty, associated errors are shown to be minimal (Lightfoot & O'Connell 2016). Similarly, the benefits of converting the human phosphate $\delta^{18}O$ to $\delta^{18}O$ drinking water signatures, so that it allows comparability to data from modern precipitation, outweigh any concerns with the choice of appropriate published equation or with error propagation (Chenery *et al*. 2010; Chenery *et al*. 2012; Daux *et al*. 2008; Levinson *et al*. 1987; Longinelli 1984; Luz & Kolodny 1985; Pollard *et al*. 2011; Pryor *et al*. 2014).

The $\delta^{18}Op$ signatures from the individuals in this study follow a rather broad distribution, from 13.6‰ to 20.0 ‰ (mean 16.8 ±2.4‰, 2σ) with corresponding drinking water values between -12.7‰ and -3.4‰ (mean -8.1 ±3.4‰, 2 σ) (Appendix Table A2.2; Fig. 9.1*)*. The results of the descriptive statistics applied to the $\delta^{18}Op$ data suggest a significant deviation from a normal distribution (Kolmogorov-Smirov Test: $p=0.012$) (Table 9.2); the data rather follow a bimodal distribution. Of the individuals tested, two (FRAG468.783.47, FRAG306.1206.47) are clear statistical outliers. These gave unusually low values for $\delta^{18}Op$ and corresponding $\delta^{18}O_{dw}$ ($\delta^{18}Op$=13.6‰ and $\delta^{18}O_{dw}$=-12.7‰; $\delta^{18}Op$ = 13.83‰, $\delta^{18}O_{dw}$=-12.4‰), which fall further than 3σ from the mean (Fig. 9.2). An additional four samples (BR1, BR2, BR4, FRAG1081268.37), which gave high Op and corresponding $\delta^{18}O_{dw}$ values, also fall further than 2σ from the mean towards the right tail of the distribution curve ($\delta^{18}Op$=19.1‰ and $\delta^{18}Odw$=-4.7‰; $\delta^{18}Op$=19.5‰ and $\delta^{18}O_{dw}$=-4.2; $\delta^{18}Op$=19.7‰ and $\delta^{18}O_{dw}$=-3.8‰; $\delta^{18}Op$=20.0‰ and $\delta^{18}O_{dw}$=-3.4‰) and are also treated as outliers (Fig. 9.2). However, when the 1.5IQR method, which is more robust to outliers, is used, none of the individuals tested can be identified as an outlier based on their $\delta^{18}Op$ tooth data or their corresponding $\delta^{18}Odw$ values.

Strontium isotope ratios measured from a selected 29 individuals from the two sites range between 0.70875 and 0.70920 (mean: 0.70920, 0.00010, σ) (Appendix Table A2.2; Fig. 9.3). Variation (σ=0.00010) is relatively low compared to other prehistoric human skeletal assemblages from the Mediterranean (e.g. Nafplioti 2008, 2009a, 2012, 2022; Nafplioti *et al*. 2021; Tafuri *et al*. 2015). Even if the two mortuary sites, the Circle and the Xemxija, are considered separately, intra-group variation is the same (σ=0.00010) for either of the two sites. Moreover, the $^{87}Sr/^{86}Sr$ signatures are normally distributed (Kolmogorov-Smirov=0.200) (Appendix Table A2.2, Fig. 9.4).

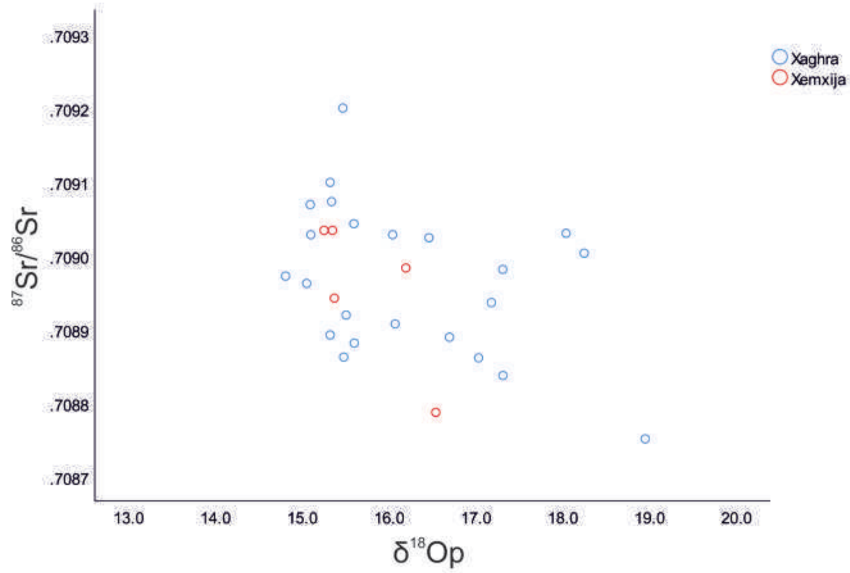

Figure 9.3. *Biplot of enamel δ^{18}Op and ^{87}Sr/^{86}Sr values.*

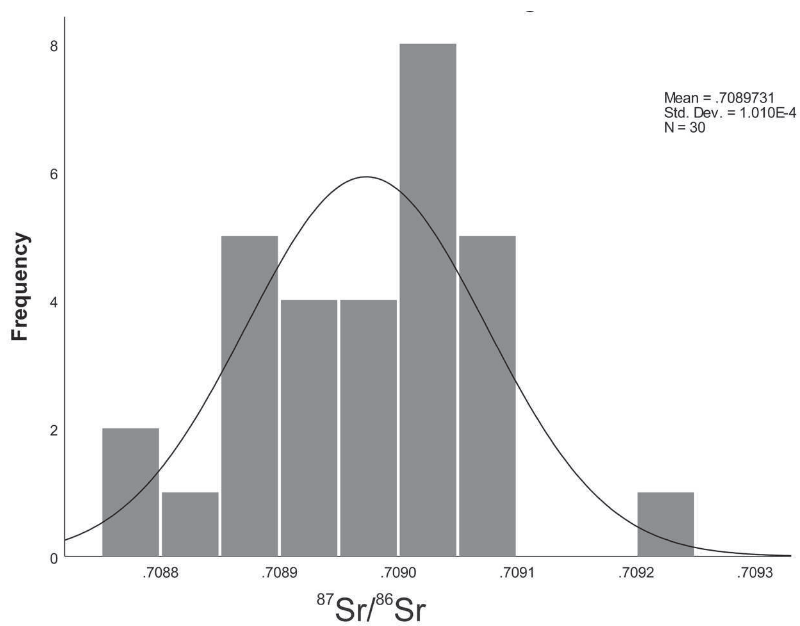

Figure 9.4. *Histogram of enamel strontium isotope ratios.*

9.5. Discussion

9.5.1. Variation in oxygen isotope ratio values

The human enamel δ^{18}Op signatures in Figure 9.1 follow a broad data distribution (13.6‰ to 20.0 ‰ (mean 16.8 ±2.4‰, 2σ). Albeit not statistically justified, values at the tails of the distribution (Fig. 9.2) may indicate non-locals on the Maltese Islands. Nonetheless, it is not clear where exactly in the distribution one should safely draw the boundaries for the local population. Moreover, because of the lack of empirical data on the range of oxygen isotope ratio variation for populations local to the Maltese Islands consuming the same drinking water sources, as we have for instance for Great Britain, where the local ^{87}Sr/^{86}Sr signatures were used to determine corresponding local δ^{18}Op values (Eckardt *et al.* 2009, Hughes *et al.* 2014), we were not able to determine local δ^{18}Op ranges for humans in this context. Instead, we used published oxygen data on modern precipitation (Lykoudis & Argyriou 2007) to extrapolate what might be acceptable drinking water $\delta^{18}O$ values for the Neolithic inhabitants of the Maltese Islands. Based on these data, $\delta^{18}O_{mw}$ values around -5‰ can provisionally be used to identify individuals who were born and raised locally on the islands.

Moreover, Lightfoot and O'Connell (2016) have shown that the range of $\delta^{18}O$ values within most archaeological populations can be greater than 3‰. Such a range is higher than the range of the oxygen data from either the Circle or Xemxija, so in principle these data could be compatible with local provenance. Most variation in human enamel $\delta^{18}O$ values has been shown to be linked largely to physiological factors and the use of more than one sources of water with different oxygen isotope values (Lightfoot & O'Connell 2016). Acknowledging that part of the variation of the human $\delta^{18}Op$ values is normal and links to biological processes, the broad range of the human $\delta^{18}Op$ signatures most probably reflects different water sources used by the individuals analysed. Use of different water sources is corroborated by contemporary evidence for freshwater availability through springs and wells on the Maltese Islands (Jones & Hunt 1994: Ruffell *et al*. 2018, 187–8). To some extent, variation in the human oxygen isotope signatures may also reflect climatic fluctuations and variable annual rainfall during the occupation of the two sites (Schembri *et al.* 2009, 18), as also suggested by the corresponding $\delta^{13}C$ values for some of the individuals (Appendix Table A2.2; Fig. 9.1). Nevertheless, the Temple Period climate did not have appreciably higher precipitation than the present day, based on current estimates of past climate (Hunt 2015; Carroll *et al.* 2012). Conversely, human $\delta^{18}Op$ values (19.5‰, 19.7‰ & 20.0‰), which fall 3σ higher than the mean, with corresponding very high $\delta^{13}C$ values, are compatible with hotter climatic conditions extant during the early childhood of the individuals in question. Based on these values we may infer that these individuals represent nonlocals on the Maltese Islands, originating from comparatively warmer and more arid environments. In fact, modern precipitation $\delta^{18}O$ data (Lykoudis & Argiriou 2007, 17) from the neighbouring coasts of Sicily, Tunisia and Libya, situated approximately 90 km, 300 km and 350 km respectively away from the Maltese Islands, are compatible with this scenario.

Finally, by cross-referencing our results with the radiocarbon-dated teeth (detailed in Volume 3, Chapter 3) we can investigate whether there was any temporal trend apparent in the human $\delta^{18}O$ results. Although the mean value does not change with time (Fig. 9.5), indicating a stable climate, the variability in $\delta^{18}Op$ values does change. Allowing for unequal sample sizes between the periods tested, this variability is highest during the early phase of the Tarxien burials at the

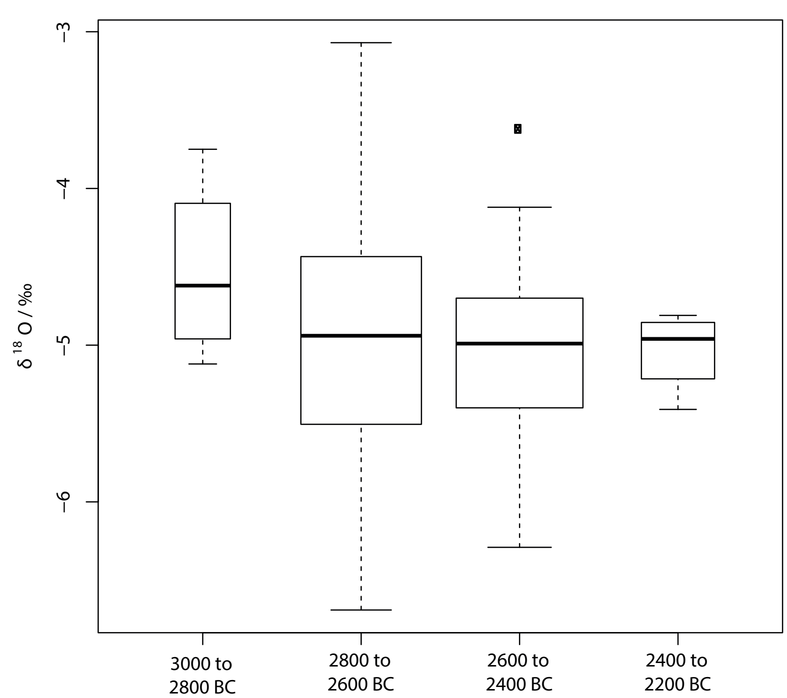

Figure 9.5. *Boxplot of average enamel δ18O values for four categories of context stratified in time, showing reducing variability in the results.*

Circle and gets progressively lower as time goes on. This pattern is therefore consistent with comparatively fewer nonlocal individuals being incorporated into the site with time, provided the variability in δ^{18}Op values reflects different origins.

9.5.2. Variation in ^{87}Sr/^{86}Sr values

Constraining the 'local range' for the Maltese population further with the help of the ^{87}Sr/^{86}Sr is not possible. The human enamel ^{87}Sr/^{86}Sr signatures measured show little variation and are normally distributed, hence data variation is suggestive of people who were born and raised locally and subsisted on more or less the same locally grown or locally procured foods. The data suggest that there was no differential access to food resources of any kind, and the people were not appreciably mobile (Wright 2005). Moreover, despite the lack of data on the bioavailable ^{87}Sr/^{86}Sr at the two sites under investigation, the ^{87}Sr/^{86}Sr signatures recorded from the human community from Malta are very close to the seawater constant of 0.7092; they are thus compatible with the local limestone geology, with the proximity of the sites to the sea and the seaspray effect on coastal sites. However, establishing that their ^{87}Sr/^{86}Sr signatures are compatible with an origin from the Maltese Islands, does not altogether exclude the possibility that at least some of the individuals tested, for example those with very high enamel δ^{18}Op values, came from places of similar geology to the geology of the Maltese Islands (see also Nafplioti 2021 for relevant discussion), hence similar ^{87}Sr/^{86}Sr bioavailable signatures, such as southern Sicily, or coastal Tunisia and/or Libya.

9.6. Conclusion

Patterning of the human enamel oxygen isotope ratio signatures suggests use of different water sources and, possibly, more than one provenance for the prehistoric inhabitants of the Maltese Islands. Use of different water sources by these people is in tune with contemporary evidence for freshwater consumption from the numerous springs and wells on the two islands. In addition, connections with other, somewhat hotter, parts of the world are hinted at. Although the corresponding strontium isotope ratio data do not support this, they do not altogether reject residential mobility and potential arrivals from sites/regions of similar limestone geology either. In fact, based on the combined oxygen and strontium isotope data from some of these individuals, there are a number of potential provenance sites amongst north African locales that have limestone geology and annual temperatures higher than Malta. This resonates with other lines of evidence of outward connectivity, as seen in the material culture of the Temple Period (Volume 2, Chapter 10) and observations on skeletal and dental anthropology made elsewhere in this volume. These results serve to illustrate how much of a 'melting pot' prehistoric sites actually were, since whilst local roots remain predominantly important, it seems that the community/ies deposited in the Circle probably also accommodated visitors and new settlers from far and wide since at least the Temple Period, if not before. The recent publication of isotopic results for 1st millennium BC Sicily (Reinberger *et al.* 2021) shows both the difficulty of interpretation of sub-regional provenance (i.e. locations within the southern central Mediterranean) without more extensive sampling particularly for oxygen values, and yet the capacity to detect some exotic provenances (suggested to be Greek mercenaries on the basis of strontium values in 1st millennium BC Sicily). The Malta data are strongly compatible with the local strontium values of Sicily and offer no evidence for outliers, but the broader range of oxygen values is more challenging to interpret geographically.

Chapter 10

An isotopic study of palaeodiet at the Circle and the Xemxija tombs

Rowan McLaughlin, Ronika K. Power, Bernardette Mercieca-Spiteri, Eóin W. Parkinson, Emma Lightfoot, Alessandra Varalli, Jess E. Thompson, Catherine J. Kneale, Tamsin C. O'Connell, Paula J. Reimer, Simon Stoddart & Caroline Malone

10.1. Introduction

A key aim of the *FRAGSUS Project* was to improve understanding of the subsistence patterns and changes of the ancient residents of the Maltese Islands. As detailed in the introduction of Volume 1, food supply and dietary health were identified as important aspects of the sustainability of the prehistoric community. The goal has been to elucidate the relationship between the remarkable prehistoric cultures of the Maltese Islands and the landscape upon which human life depended, especially over two millennia of unstable environmental conditions. It is the notion of time that is particularly significant in this study, and the *FRAGSUS Project* has focused particular interest on dietary changes associated with the degradation of the island's soils, which was a natural process, but one likely accelerated with the pressures of intensifying agricultural practices (Volume 1, Chapters 2 and 3). In this chapter, we present an analysis of the palaeodietary inferences that can be drawn from stable isotopic analysis of human and animal tissue.

10.2. Background: previous work

Richards *et al.* (2001) measured carbon and nitrogen isotopic values in collagen samples from two individuals from the rock-cut tomb at the Circle, and five from the cave system. They concluded that there was no significant input of marine protein, nor any detectable dietary differences between the two time periods, and that 'Neolithic'-style agriculture was the subsistence base for the population. Lai, O'Connell and Tykot, reporting on their results in Stoddart *et al.* (2009a), expanded upon this initial study with carbon and nitrogen isotopic analyses of 24 individuals made in tandem with AMS radiocarbon dates, and four additional measurements of $\delta^{13}C_{coll}$, $\delta^{15}N_{coll}$, $\delta^{13}C_{apa}$ and $\delta^{18}O$ from bioapatite, of which the latter is a climatic and demographic proxy (discussed in Chapter 9). Their results confirmed the findings of Richards *et al.* (2001), and highlighted the rather substantial dietary differences between individuals from the site. They also detected a trend of decreasing collagen carbon isotopic values over time, although the significance of this trend could not be assessed given the relatively small number of samples. The lack of comparative faunal data to provide a baseline for the human isotope measurements hampered the ability of these earlier studies to quantify the relative importance of meat in the diet, and to exclude fully the possibility of some limited amount of fish.

10.3. Food sources in prehistoric Malta

Recent excavations by the *FRAGSUS Project* at prehistoric sites in Malta have unearthed a wealth of new archaeobotanical and faunal data. These consisted of assemblages constituting the traditional Neolithic 'package': wheat, barley, lentil and pea, and cattle, ovicaprines (sheep and goat, largely indistinguishable from each other) and pigs. Barley and wheat seemed to have been the most important food crops and ovicaprines were by far the most commonplace animal (see Volume 2, Chapter 9) and their slaughter patterns are consistent with a dairy economy.

Fish bones were only encountered sporadically in the faunal remains from prehistoric Malta, although shellfish (particularly limpets) are very commonplace, albeit in low numbers. This suggests that they were a regular part of the diet, but had limited significance in terms of their calorific value. The lack of fish bones on the archaeological sites, which seems surprising for an archipelago such as Malta, does not exclude

Table 10.1. *Comparative terrestrial faunal isotope data from the Maltese Islands.*

Code	$\delta^{13}C_{coll}$	$\delta^{15}N_{coll}$	C:N ratio	Site	Species	Island	Period	Reference
UBA-37689	-20.8	5.8	3.20	Santa Verna	*Bos*	Gozo	Skorba	This study
UBA-37665	-20.6	6.7	3.24	Kordin III	*Ovis*	Malta	Mġarr	This study
UBA-37669	-20.5	6.9	3.23	Kordin III	*Ovis*	Malta	Mġarr	This study
UBA-29833	-20.6	11.1	3.23	Taċ-Ċawla	Ovicaprine	Gozo	Ġgantija	This study
UBA-37681	-20.5	8.5	3.22	Taċ-Ċawla	*Bos*	Gozo	Ġgantija	This study
UBA-29835	-21	6.7	3.22	Taċ-Ċawla	*Bos*	Gozo	Tarxien	This study
UBA-29836	-20.1	7.1	3.22	Taċ-Ċawla	*Sus*	Gozo	Tarxien	This study
UBA-31711	-19.5	6.8	3.23	Taċ-Ċawla	*Sus*	Gozo	Tarxien	This study
UBA-37683	-21.1	6.9	3.23	Taċ-Ċawla	*Ovis*	Gozo	Tarxien	This study
OxA-27687	-20.6	6.7	3.3	The Circle (Context 714)	Ovicaprine	Gozo	Tarxien	Malone *et al.* 2009d
UBA-10385	-21.7	4.23	3.1	The Circle (Context 1206)	*Bos*	Gozo	Tarxien	Malone *et al.* 2009d

Table 10.2. *Comparative stable isotope measurements from ancient fish bone collagen from the Mediterranean region.*

Species	Site	$\delta^{15}N_{coll}$ (‰)	$\delta^{13}C_{coll}$ (‰)	Period	Reference
Sparus sp.	Santa Maira (Spain)	8.6	-15.2	Mesolithic	Salazar-Garcia *et al.* 2014
Mugil sp.	Santa Maira (Spain)	8.5	-15.2	Mesolithic	Salazar-Garcia *et al.* 2014
Sparidae (n=5)	Pompei (Italy)	6.7 ± 1.1	-14.6 ± 0.6	Roman period	Craig *et al.* 2013
Epinephelus marginatus	Cova des Riuets (Formentera)	10.1	-10.5	Bronze Age	Garcia-Guixé *et al.* 2010
Pagellus erythrinus	Cova des Riuets (Formentera)	8.2	-11	Bronze age	Garcia-Guixé *et al.* 2010
Sphyraena sphyraena	Cova des Riuets (Formentera)	9.4	-12.4	Bronze age	Garcia-Guixé *et al.* 2010

the possibility that they were an important part of the diet. Fish could have been consumed differently from terrestrial animals and their bones do have different taphonomic properties; together, these factors could render them less visible in the archaeological record. Therefore, a key objective of the stable isotope study was to clarify the stable isotope results and allow for an independent check on whether marine protein featured prominently in the diets of those buried at the Circle.

Measurements of carbon and nitrogen isotope ratios from animal bones, taken in tandem with the *FRAGSUS Project*'s programme of radiocarbon dating, provide a baseline for interpreting the results from human tissue (Tables 10.1 and 10.2).

10.3.1. Tooth enamel samples

Enamel surfaces were first cleaned by ablation prior to sampling. Approximately 6 to 10 mg of enamel were sampled by drilling enamel powder using a hand-held drill with a diamond-tipped drill bit. Sampling was performed in a vertical line along the crown. Enamel powder was pre-treated following Balasse (2002); samples were treated with 2–3% aqueous sodium hypochlorite (0.1 ml/mg) for 24 hrs at 4°C and then rinsed. They were then treated with 0.1M acetic acid (0.1 ml/mg) for four hours at room temperature, rinsed again and freeze-dried. Four modern horse dental standards were treated and analysed in the same manner to provide a control. The samples were analysed using an automated gas bench interfaced with a Thermo Finnigan MAT253 isotope-ratio mass spectrometer at the University of Cambridge. Carbon and oxygen isotopic ratios were measured on the delta scale against the international standard VPDB scales. Analytical error for this instrument has been recorded as less than 0.10‰ for oxygen and 0.08‰ for carbon.

10.3.2. Bone collagen

The samples of collagen in the current study were extracted from the roots of human molar teeth using the method described by Reimer *et al.* (2015). All samples were also ^{14}C dated using AMS (Chapter 3); the isotope results discussed here were obtained on a separate line using IRMS at the 14CHRONO centre at Queen's University Belfast. Results are reported as delta values relative to the VPDB (carbon) and AIR (nitrogen) scales. IRMS machine uncertainties are sig$\delta^{13}C$=0.22, sig$\delta^{15}N$=0.15.

10.4. Data analysis

The data were first analysed using standard tools in the R environment for statistical computing, which was used to calculate summary statistics for various groupings of the data, and to project the data into their principal components. To study trends in palaeodiet with time, linear regression models were applied using palaeodietary isotope results and their associated radiocarbon dates (Chapter 3). However, because of the radiocarbon history of the atmosphere, radiocarbon measurements have a complex probability structure once they have been 'calibrated' into calendar time and cannot be reduced to a reliable point estimate for inclusion in a linear model. To circumvent this natural limitation of the radiocarbon technique, we incorporated radiocarbon uncertainty by bootstrapping 500 individual linear regression models, each built from repeated 'Monte Carlo' samples drawn from the probability density functions of each radiocarbon date. The IntCal13 (Reimer *et al.* 2013) calibration dataset was used to calculate these using ***rowcal*** (McLaughlin 2019). The resulting set of 500 linear models were used to estimate a plausible range of correlation coefficients and R-squared values, using the mean and standard deviation of these statistics for each model. In this way we could assess the significance of any temporal trend apparent in the data. This is a new method for extracting information from paired radiocarbon / stable isotope samples developed for this project.

We also explored a Bayesian mixing model as a first step towards interpreting these results in the context of what is known about the isotopic content of dietary sources, and how these are routed through the food web. This approach depends on prior information about both the isotopic content of the foods people were eating, and how it was metabolized by their bodies. This exercise can only be considered preliminary, as data for dietary sources are still scant. We now have a reasonably good set of data for prehistoric Maltese terrestrial animals, measured as part of this study, although their results were rather variable. Unfortunately, few direct measurements of terrestrial plants and marine animals have been made (although see below, promising studies have emerged around lipid residue characterization in prehistoric pottery (Debone Spiteri and Craig, 2011)). The lack of suitable material from our excavations undertaken by *FRAGSUS* and at the Circle, namely the small size and sparse quantity of the charred seeds, meant priority was given to securing an AMS date in preference to stable isotope measurements. Without a direct AMS date, any stable isotope measurements of charred seeds would not be a reliable indicator of conditions in prehistoric Malta because we could not be sure about their chronology. This situation is a result of the poor stratigraphic integrity of seeds in the rather loose soil profiles and the large amount of intrusive material that results. Indeed, we have detected significant quantities of this material in the sites excavated by the *FRAGSUS Project* in Malta and Gozo (see Volume 2, Chapter 9).

For the purposes of modelling food sources, we considered a 'concentration-independent' estimate of dietary protein, where the quantity of protein in the bulk of the source food is not considered during the mixture modelling process. This was done using the Bayesian mixing model simmr 0.4.5 (Parnell 2021), which was used to infer the proportions of food sources represented by the stable isotope data. Offsets for the enrichment of source isotopes took the values of 0.8±0.5‰ for ^{13}C and 4±1.0‰ for ^{15}N (cf Knipper *et al.* 2020; Styring *et al.* 2017 Hedges & Reynard 2007). For the central Mediterranean, the relatively small number of published source values for marine foods inevitably limits the scope of this exercise, as the bones of fish and marine mammals tend to be rare and poorly preserved on prehistoric sites. A review of the available literature illustrates how variable the isotope values from fish were, so for the purposes of this preliminary assessment a figure of 8.4±2.1‰ $\delta^{15}N_{coll}$ and -13.5±2.1‰ $\delta^{13}C_{coll}$ was used for fish (based on Table 10.3), 7±1.5 $\delta^{15}N_{coll}$ and -20.6±0.6‰ $\delta^{13}C_{coll}$ for terrestrial herbivores (this study), and 4.5±2.5‰ $\delta^{15}N_{coll}$ and -23.5±2‰ $\delta^{13}C_{coll}$ for terrestrial plants (based on averaging results from Knipper *et al.* 2020 & Vaiglova *et al.* 2014). The potentially complicating factor of C_4 pathway plants does not apply in Malta in the Temple Period (see Volume 2, Chapter 9).

10.5. Results

The average (mean, standard deviation) results for each site are shown in Table 10.3. Full details of each sample are given in Appendix Tables A2.3 & A2.4 and visualized in Figure 10.1.

Table 10.3. *Summary results for each site. A full list detailing the results from each sample appears in Appendix Tables A2.3 & A2.4. *Note that not all isotope measurements were made for each element – see Appendix Table A2.3. Also note that at the Circle the minimum number of individuals in the isotope study is less than this figure.*

Site	N elements*	Mean $\delta^{13}C_{coll}$ (‰)	S.d.	Mean $\delta^{15}N_{coll}$l (‰)	S.d.	Mean $\delta^{13}C_{apa}$ (‰)	S.d.
The Circle rock-cut tomb	18	-19.3	0.29	10.4	1.59	-12.5	0.88
The Circle main cave system	206	-19.3	0.36	10.7	0.98	-13.2	2.29
Xemxija	5	-19.3	0.23	10.3	0.26	-13.7	0.67

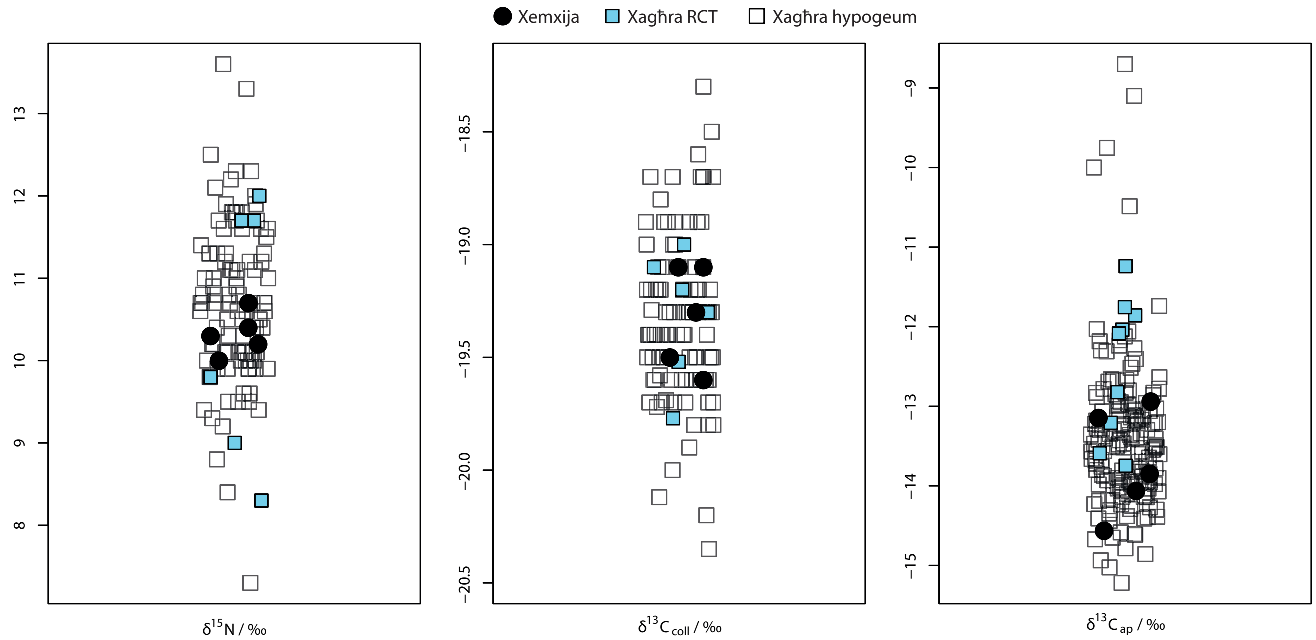

Figure 10.1. *Stripcharts indicating the range and distribution of carbon and nitrogen isotopes in collagen from tooth dentine, and tooth enamel bioapatite carbon isotopic values at the Circle and Xemxija. The x-axis is random jitter allowing the variance of the data to be visualized.*

In Figure 10.2 the results from collagen samples are visualized and compared with faunal samples from the Maltese Islands, and other human populations in the wider central Mediterranean region. The results indicate that both the Circle and the Xemxija individuals are consistently more enriched in nitrogen-15 compared with individuals from peninsular Italy, or indeed from neighbouring Sicily. One individual, identified as UB-10375 from Context (714) could be read as a recent immigrant to Malta as their diet is atypical, or a simply a statistical outlier as their isotopic measurements were made during earlier work with less refined laboratory protocols.

The offsets between the $\delta^{15}N_{coll}$ and $\delta^{13}C_{coll}$ animal mean values and the means of the three human groups show that the diet was consistent between the

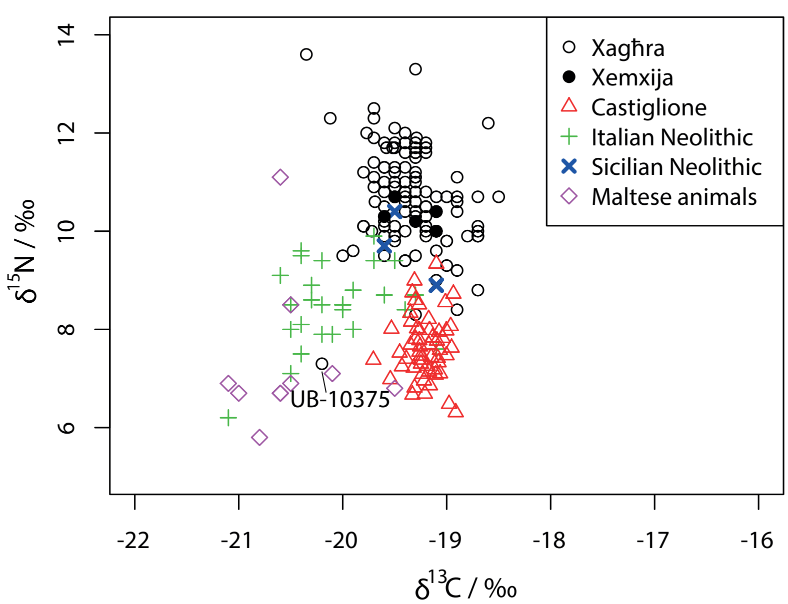

Figure 10.2. *Biplot of bone collagen carbon and nitrogen isotopic values from Circle and Xemxija, plotted with comparative data for the Neolithic of peninsular Italy and prehistoric Sicily, and Castiglione, an early Bronze Age site in southern Sicily (Varalli* et al. *2014).*

Table 10.4 *Offsets between the $\delta^{15}N_{coll}$ and $\delta^{13}C_{coll}$ human and animal values.*

Site	$\Delta^{13}C_{human-animal}$ (‰)	$\Delta^{15}N_{human-animal}$ (‰)
Circle (rock-cut tomb)	1.3	3.4
Circle main cave / hypogeum	1.3	3.7
Xemxija	1.3	3.3

rock-cut tomb and the main Tarxien phase burials, and also between Xagħra and Xemxija. These offsets (Table 10.4) are consistent with a mixed diet based on terrestrial animals and plant protein. The importance of animals in particular is suggested by the degree that the offsets fall with the established range of values that indicate a step to higher trophic levels (Minagawa and Wada 1984; Schoeninger & DeNiro 1984; Bocherens & Drucker 2003).

To investigate this in more detail, the results of our preliminary attempt at Bayesian mixture modelling of source foods are shown in Figure 10.3. The results clearly indicate a small but significant contribution from marine protein, as well as the likelihood that animal foods were the dominant sources of protein in the palaeodiet at Xagħra. The same pattern holds for the individuals from Xemxija and indeed for the earlier rock-cut tomb at Xagħra, although with less certainty because of the smaller sample size.

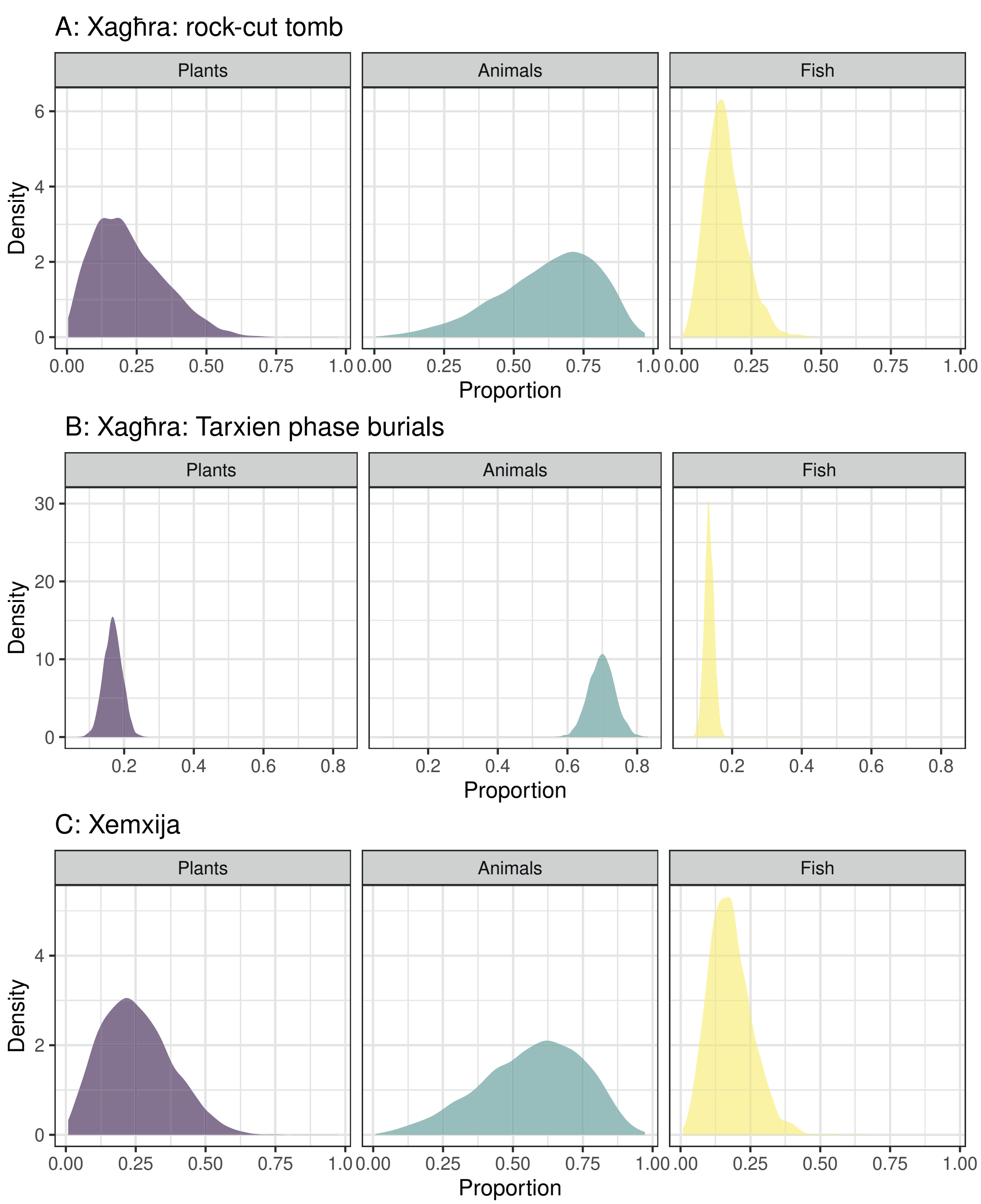

Figure 10.3. *Modelled contribution of terrestrial plants, terrestrial animals and marine fish to the palaeodiet at the Tarxien phase burials at Xagħra calculated using Bayesian mixing model.*

Table 10.5. *Number of samples of human bone from well-sampled contexts subjected to isotopic analysis.*

Context	Number ($\delta^{15}N_{coll}$ and $\delta^{13}C_{coll}$)	Number ($\delta^{13}C_{apa}$)
783	16	36
951	5	41
960	6	9
1206	8	19
1241	6	5
1268	6	9

The large number of samples from certain contexts (Table 10.5) provides an opportunity to test whether some parts of the site contained human remains with palaeodietary signatures that differed significantly from the average results from across the site. In the event, however, the readings are remarkably homogenous, aside from statistical noise caused by the smaller sample size in certain contexts (Fig. 10.4). One possible exception is ^{15}N values from Context (783), which tend to be lower than average, which probably reflects a chronological pattern, as discussed below.

Time-dependent changes in nitrogen isotope values can be caused by palaeoenvironmental changes, especially soil development and aridity, so a detailed look at this variable is called for. Turning first to faunal remains, using the bootstrapping method detailed above (§10.4) to develop the data into a time-series, there is an apparent spike in the ^{15}N enrichment around 3300 cal. BC (Ġgantija period), apparent in samples of both sheep/goat and, to a lesser degree, cattle from Taċ-Ċawla. Although more samples would be required to confirm this pattern, it suggests that there was an episode of aridity that drove ^{15}N enrichment of herbivore remains to very high levels. An alternative explanation

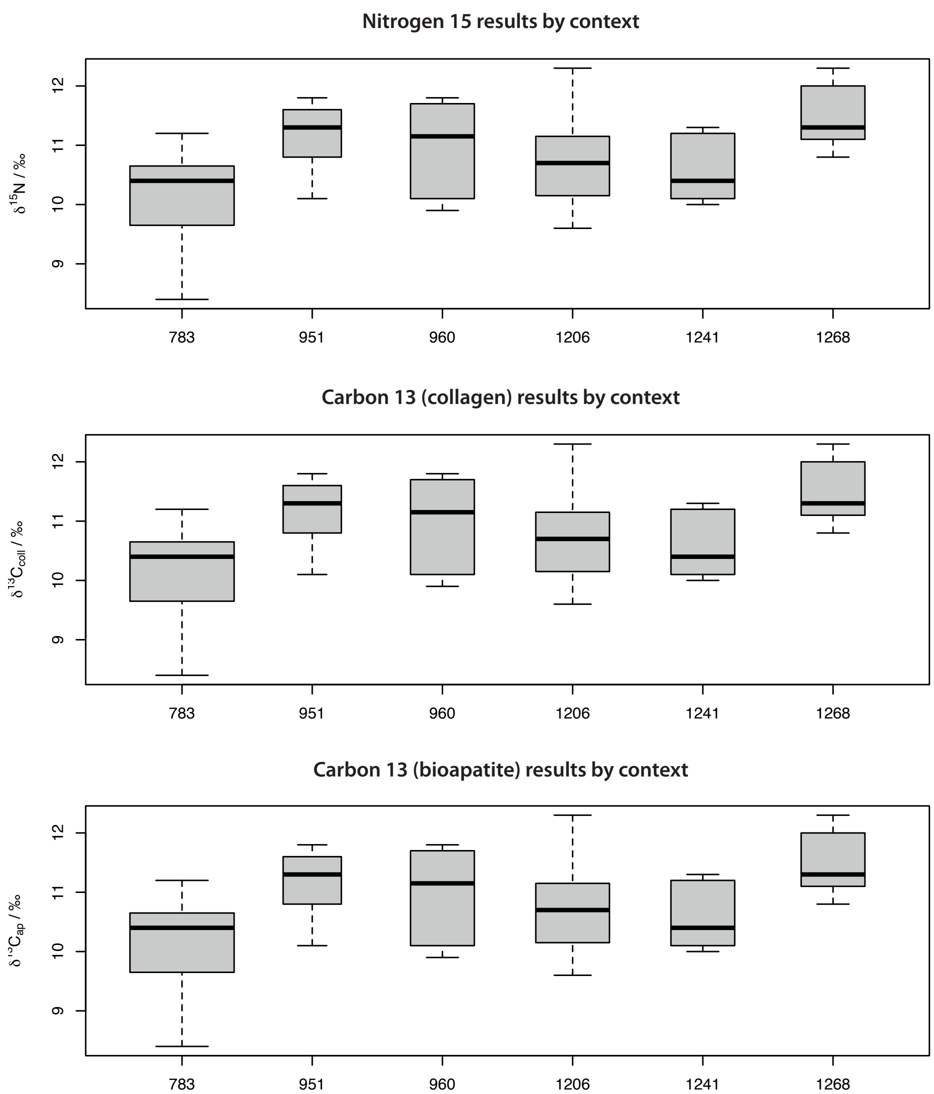

Figure 10.4. *Boxplots of the main isotopic results by context (width of the boxes is proportional to the sample size).*

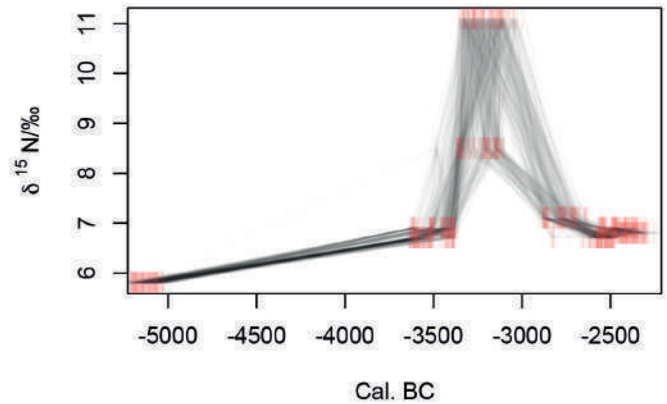

Figure 10.5. *Nitrogen isotopic values of animal bone collagen, plotted as a time series using multiple bootstraps of the radiocarbon dates to represent chronological uncertainty. The spike around 3300* BC *during the Ġgantija period is very noticeable and may imply either heavily manuring or an episode of extreme aridity although further work will be needed to assess the significance of this.*

is manuring (Bogaard *et al.* 2013), although this seems unlikely, as we would then expect to also find the signal in human remains from the period. In the event, however, the results the burials of this period from the rock-cut tomb are not significantly different from the later Tarxien-period individuals from the cave complex.

There is a slight but significant trend towards less enrichment of nitrogen-15 during that intensive phase of Tarxien-period mortuary activity. Using a linear regression model we can estimate that the average $\delta^{15}N_{coll}$ value fell from around 11‰ to 10‰ over between 2900 and 2400 cal. BC. The regression is statistically significant ($p<0.0005$) and explains between 11% and 16% of the variability, with the confidence envelope caused by the inherent uncertainties of the radiocarbon dating process (Figure 10.6).

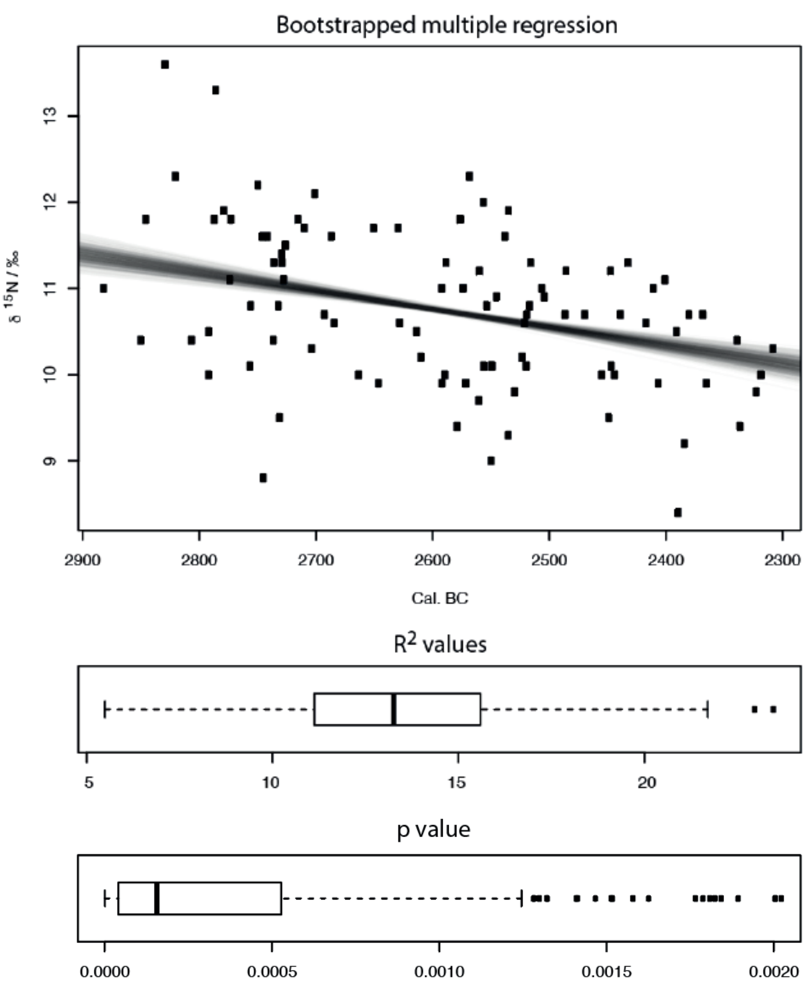

Figure 10.6. *Multiple regression modelling the dependence of nitrogen isotope ratios on time. The results indicate a significant linear trend of decreasing enrichment explaining approximately 13% of the variability in the data (R^2 values).*

10.6. Discussion and conclusion

It is clear that there is a palaeodietary signal that is distinct to the Maltese Islands. Within Malta, our study has found little difference between sites and time periods, aside from the subtle trend in nitrogen isotope ratios discussed above. One important finding is that the results from the Xemxija tombs are very similar to those from the Circle. Until this study, any generalizations about prehistoric human diet in the Maltese Islands have, to date, been made using results from the Circle alone. When we consider the dietary sources and their offsets, the highly elevated $\delta^{15}N$ values for the Ġgantija period skew any potential inference. The similarity of the Ġgantija period individuals from the rock-cut tomb to the main cave system would suggest that whatever was causing the elevation of $\delta^{15}N$ in animal bones at this time did not affect humans; perhaps because animals did not feature prominently in the human diet and were foddered on separate crops to humans.

The human-animal offsets and the results of the source mixing modelling suggest that animal protein was more important than plant protein during the Temple Period in Malta. We cannot at present make a distinction between meat and dairy in this regard, other than point to zooarchaeological evidence of slaughter patterns consistent with a dairy economy (see Volume 2, Chapter 9). Future modelling work can avail of the additional information provided by our $\delta^{13}C_{apa}$ data, especially if a more extensive database for food sources can be assembled, in attempts to understand other components in the total diet, such as carbohydrate intake, which may present a more balanced picture of the relative importance of plants and animals. However, it remains that meat and/or dairy was of critical importance in Malta during the Temple Period, and this reiterates the fundamental relationship between people and domesticated animals that was key to sustaining island life. Dairy products have been reported from the early levels of Skorba by lipid analysis (Debono Spiteri *et al.* 2011; 2016) and an extension of such research combined with proteomic analysis would be invaluable in providing another line of evidence for dairy intake into the diet of prehistoric Malta. Could this factor have given rise to occasional occurrences of obesity (seen in the prehistoric art)? If some individuals had access to relatively high levels of dairy after impoverishment of diet in their early life course (§8.6.2.8), this could have led to the corpulence for which the artistic record is so famous.

It is also clear that throughout the Temple Period, marine food was much less important to these island residents than the foods grown and raised on the island. However, given the results of the Bayesian isotopic mixing modelling, the sea cannot be completely excluded as a secondary source of nourishment. This finding aligns with the archaeological data discussed in Volume 2, Chapter 9. *FRAGSUS Project* excavations at Taċ-Ċawla and Santa Verna produced a very small number of fish bones, but shellfish remains were ubiquitous in archaeological strata across the island, and the bones of marine birds are also quite numerous, several of which were modified into simple artefacts (see McCormick and Hamilton-Dyer in Volume 2, Chapter 9). The question of whether marine foods were eaten regularly, in small quantities, or whether they provided a major base of subsistence at during times of the year when other resources were scarce, must be left for future research.

Comparing the different strands of our analysis, aside from two outliers, the offset between $\delta^{13}C_{apa}$ and $\delta^{13}C_{col}$ for paired measurements was seemingly random, normally distributed around a mean value of -6‰. Outliers UBA-32038 and UBA-32039, both from Context (951) have significantly lower $\delta^{13}C_{apa}$ relative to their $\delta^{13}C_{col}$ values (-9‰ and -8‰ respectively), although this offset is not as extreme as the -10‰ measured during previous work for the samples BR2 and BR4 by Lai, O'Connell and Tykot (2009). Therefore, it seems the proxies are telling us different things, although no clear chronological or context-dependent pattern is forthcoming from either sets of data, the results are difficult to interpret beyond the exclusion of marine diet.

Compared with other regions, the nitrogen-15 results are most intriguing. These set Malta apart from peninsular Italy, and even neighbouring Sicily, reflecting the more arid climate and poorer soil development. The trend detected at the Circle in nitrogen-15 could reflect changing dietary practices, such as a gradual decline of the importance of meat and milk in the diet, or environmental factors. The latter interpretation is slightly at odds with geoarchaeological work undertaken by the *FRAGSUS Project* on Gozo, which suggests that a gradual aridification trend operated throughout the period considered here (Volume 1, Chapter 5).

More research will be needed to resolve the ultimate cause of this interesting pattern, and this should primarily focus on measurement of animal bone samples. This may prove challenging as, during the current phase of work, we attempted analysis of a further 22 animal bones from the archaeological sites excavated by the project, but all failed because of low collagen preservation (see Volume 2, Chapter 2). Despite these uncertainties and gaps that remain in our knowledge, the results discussed here nonetheless reveal a dynamic relationship between environment, agriculture and diet that was no doubt central to the lived experience of the individuals whose remains we study.

Chapter 11

aDNA: an investigation of uniparental genetic heritage in Neolithic Malta

Bruno Ariano, Valeria Mattiangeli, Rowan McLaughlin, Ronika K. Power, Jay T. Stock, Bernardette Mercieca-Spiteri, Simon Stoddart, Caroline Malone & Dan Bradley

11.1. Introduction

11.1.1. The genome and ancient DNA

Modern genetic studies and the use of the biological component offer considerable potential in the study of past individuals and populations. The genome refers to the full genetic component of an organism which is passed through generation from parents to offspring. The key components of this structure are molecules called nucleotide base which are codified in four different letters: A(adenine), T(thymine), G(guanine) and C(cytosine). These molecules are bonded together within the DNA (Deoxyribonucleic acid) structure. The way these bases are ordered in a genome is, with the exception of monozygotic twins, unique to each individual; for example, two unrelated individuals differ for 3 million nucleotides over approximately 3 billion that compose a human genome. The study of DNA can help to estimate how different people are related, past and present. Using modern biological techniques, DNA can be extracted intact from living persons without losing information. However, when dealing with samples that date far back into the past, dead cells cannot preserve the integrity of the genetic information, and therefore old/ancient DNA is difficult to reassemble. Nevertheless, the ancient DNA (aDNA) field has an important role in dealing and using this type of information to study the history and evolution of ancient organisms. In recent years, thanks to the advancement of a new generation of DNA sequencing techniques, aDNA studies have revolutionized most of the previous concepts about genetics and history and shed light on the origin of different species.

11.1.2. Ancient DNA

The field of aDNA emerged in 1984 when Russ Higuchi and colleagues (Higuchi *et al*. 1984) extracted a fragment of DNA from a dry tissue of a quagga, an historical relative of the horse family. Soon after, Pääbo (1985) reported the first aDNA extraction from an ancient mummy. aDNA became even more prolific, giving the opportunity to analyse a multitude of material, such as bones (Hagelberg *et al*. 1989), hair (Gilbert *et al*. 2004) and even parchment (Teasdale *et al*. 2015).

Many hundreds of ancient genomes from different periods and parts of the world have been screened with high resolution, making it possible in particular, to shed light on human migrations (Mathieson *et al*. 2015) and on animal domestication (Daly *et al*. 2018; Zeder *et al*. 2006). Despite this recent progress, there are still some challenges that arise when dealing with ancient DNA samples.

Due to spontaneous damage that occurs after death, the DNA in ancient samples is usually present in short fragments with a size range between 50 to 70 nucleotides. With smaller and more numerous fragments, it is more difficult to assemble the DNA molecule in its original form. Moreover, due to the lack of a repair system in dead cells, spontaneous mutations in nucleotide base pairs accumulate. A study published by Skoglund *et al*. (2014) showed that the amount of a particular type of DNA mutations, deamination, in a sample is proportional to its age. If not taken in consideration, these damages can lead to erroneous interpretation of DNA results during population and evolutionary genetic analyses. In recent years, the deamination problem has been partially solved thanks to particular software that can target and quantify these specific patterns of postmortem damages (Jónsson *et al*. 2013).

A third problem that emerges when working with ancient samples is the low quantity of endogenous DNA present. These values can be as low as 0.1% (Stoneking & Krause 2011), posing a problem from bacterial and human genome contamination. For this reason, it is important that the extraction of DNA from ancient samples is carried out in special cleanroom facilities, where particular procedures are adopted to keep the bacterial and human contamination levels as low as possible (MacHugh *et al.* 2000). Once the DNA has been extracted, two common approaches are used for obtaining the sequence data, shotgun genome sequencing and targeted capture.

The first method consists of fragmenting and sequencing the available genome of a sample. This technique has been extensively used for modern DNA analysis and can also be applied to ancient genomes as long as the samples are of good quality. The main advantage of this method is the opportunity to cover every position in a genome and study mutations that are still unknown or present in low frequency in a comparator population.

The targeted capture method, on the other hand, usually focuses on a predefined set of high frequency variants (referred as SNPs) that are enriched using a custom-built probe. This technique has the advantage of obtaining more data compared with the WGS approach, especially when dealing with samples with low DNA quantity. With more than 1.2 million SNPs covered (Mathieson *et al.* 2015), this technique has become frequently used for ancient DNA analysis. However, the main drawback of this approach resides in the limited number of analyses that can be performed using these variant positions. For example, the majority of rare mutations that are important for Mendelian diseases are not covered by the capture method and therefore cannot be directly studied.

11.1.3. Background: the genetic context of the Mesolithic in Europe

The Mesolithic period dates from the end of the Epipalaeolithic period, around 12,000 years ago, and it was heralded by rapidly rising temperatures accompanied by the establishment of a Holocene forest biome across Europe. These conditions contrasted with the preceding tundra and glacial conditions (Clark *et al.* 2009). During the Mesolithic, human populations were scattered in groups around Europe, living in small groups, and following a typical hunter-gatherer (HG) existence. Different published studies have investigated the genetic background of these populations, dividing them into three main groups. On the western side of Europe, individuals from Spain, Hungary and Luxembourg have been reported as genetically similar, and for this reason they have been identified as the Western Hunter-Gatherer (WHG) group. Also included in this group are individuals from eastern Europe that displayed a similar pattern of genetic affinity (González-Fortes *et al.* 2017; Jones *et al.* 2017). On the eastern side of Europe, two Mesolithic individuals from Russia were found to have some marked genetic distinctions from the WHG group (Haak *et al.* 2015). These individuals, who lived approximately 8000 years ago, are now considered part of a genetically distinct cluster identified as Eastern Hunter-Gatherer (EHG). This group can be considered a mix between WHG populations and Upper Palaeolithic individuals from Siberia (Mal'ta and Afontova Gora) (Raghavan *et al.* 2014; Fu *et al.* 2016). The influence of this group on other populations has been detected in hunter-gatherer individuals from Sweden and the Balkans (Gonzales Fortes *et al.* 2017; Lazaridis *et al.* 2014; Lazaridis 2018) and in populations from the steppe during the Bronze Age period (Haak *et al.* 2015).

A third genetic cluster is formed by two individuals found in western Georgia that are now identified as members of a Caucasus Hunter Gatherer (CHG) group. This population diverged from the WHG group long before the Last Glacial Maximum, approximately between 40 and 50 thousand years ago. It is a population that had a strong influence in both Mesolithic and Neolithic populations from Iran, and its influence is still present in the genomes of modern populations from Southern Caucasus (Jones *et al.* 2015).

11.1.4 The genetic impact of the agricultural revolution

The adoption of agriculture was a turning point in human history which occurred in different parts of Eurasia and the Middle East between 12,000 and 7000 BC. In the Levant and Southern Anatolia between 11,000 and 9600 BC, local hunter-gatherer populations began to adopt a farming and sedentary lifestyle, accompanied by animal and plant domestication. With the help of aDNA studies it was discovered in 2016 that the origin of Near Eastern farming had two genetically distinct roots, one residing in Anatolia and the other in Iran (Broushaki *et al.* 2016). Between *c.* 6,600 and 6,500 BC Iranian farmers spread genetically towards eastern Eurasia whilst the Anatolian farming communities became well-established in north-western Anatolia and had begun to move into Europe via Greece and the Balkans (Lazaridis 2018; Lazaridis *et al*. 2014). The arrival of farmers in Europe represented a genetic replacement with limited admixture from the local hunter-gatherer populations. This admixture became evident in 2009, when aDNA showed a genetic discontinuity between these two populations in Europe during the Neolithic period (Malstrom *et al.* 2009). More recent studies have emphasized this observation, giving a better view of the phenomenon. From the lower part of the Danube, the Anatolian farming culture reached the Hungarian plain by 5500 BC and gave birth to different farming groups

(Starčevo, Körös and Criş). Some centuries later, from the same region, another cultural movement started to spread into north-west Europe with a new form of decorated pottery called the Linearbandkeramik (LBK) (Cunliffe 2015). A second culturally different wave of Neolithicization moved from the Adriatic Balkans through to the Mediterranean coast where it is associated with the pottery of the Impressed and Cardial traditions pottery style. The Impressed Ware culture was more closely associated with regions across Italy towards the Ligurian coast, whilst a variant of this pottery group, the Cardial Ware culture, arrived in Provence and extended towards the Atlantic and Portugal (Price 2000). It is important however, to point that these cultures were different, even though they were all close genetically to the same Anatolian Neolithic source (Olalde *et al*. 2015, Mathieson *et al.* 2018). The earliest Neolithic settlements in Italy, which date from about 6200 BC, are located along the lowland coastal areas of south-east Italy (the Apulian Salento peninsula and Tavoliere) (Malone 2003; Natali & Forgia 2018). Very high densities (*c*. one site per 3 km^2) of ditched settlements across the area signal a major population increase (Whitehouse 2013). Adoption of the Neolithic economy then rapidly spread westward into Calabria (Morter & Robb 2010) and Sicily (Leighton 1999; Natali & Forgia 2018), reaching Malta by at least 5800 BC, based on environmental evidence (see Volume 1, Chapters 3 & 4), with clear archaeological traces present in the archipelago by 5500 BC (see Volume 2, Chapter 2*).*

11.1.5. Arrival in Malta

The evidence supplied by archaeology, particularly the affinities between Għar Dalam and early Neolithic Impressed Wares of Southern Italy, strongly suggest that the source population of the Neolithic expansion into the Maltese Islands were located in Southern Italy and Sicily (see Volume 2, Chapter 10). Theories of an earlier colonization of Malta have been debated, but since hunter-gatherer populations require a large space for foraging, it seems unlikely that Malta would have been a viable long-term home before the advent of agriculture (Malone 1997–8). From the first evidence of human settlement, the early Maltese society evolved through different cultural phases: Għar Dalam, Grey Skorba, Red Skorba and finally Żebbuġ, signalling the start of the Temple Period and an increasingly distinctive island culture. In this last phase, the use of rock-cut tombs, containing collective burials and distinctive pottery defined the island culture (Malone *et al.* 1995).

Subsequent cultural phases (the Temple Period) witnessed an unprecedented development in Maltese society, culminating in the Tarxien phase between 2800 and 2400 BC (Volume 2, Chapter 2). During the Tarxien phase, collective burial in the elaborate Circle cave

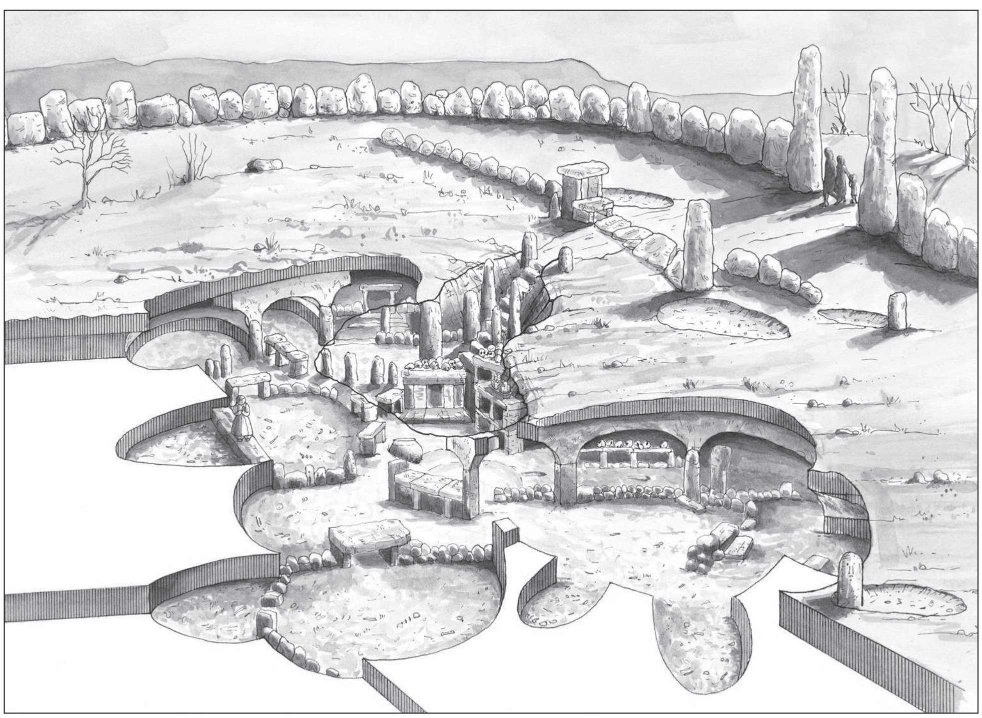

Figure 11.1. *Reconstruction of the Circle (Malone* et al. *2009d).*

complex on Gozo (Fig. 11.1) and at the Ħal Saflieni Hypogeum in Malta represent exceptional mortuary sites. The Circle excavations unearthed the individuals analysed for this study in the early 1990s (Malone *et al.* 2009d) and are the subject of additional study in this volume. The ancient DNA work we report here was undertaken in collaboration with the *FRAGSUS Project* (2013–2018) as part of a programme of environmental and archaeological research, including an extensive re-assessment of the Circle, applying additional radiocarbon dating and stable isotope studies. The overall aim of this research has been to understand better the cultural, economic and environmental dynamics of prehistoric Malta (Malone *et al.* 2019; Ariano *et al*. 2022).

11.2. Research questions

Since ancient times the Mediterranean Sea has represented one of the most important routes for migration in southern Europe. For example, during the late Neolithic period there is proof of both a cultural and a direct genetic connection between Portuguese and Greek Neolithic populations (Hofmanova *et al.* 2016). Despite this evidence, the prehistoric population history of South Europe remains under-explored in terms of genetic studies. In contrast, most aDNA publications have focused on the history of Central and Northern European populations, with little attention paid to southern Europe. The reason for this absence is because of the particularly warm climate conditions that tend to accelerate the degradation process of aDNA samples. Importantly, the Maltese work we are reporting here is the genetic analysis of one of the most southerly archipelagos of the Mediterranean. Specifically, we obtained uniparental genetic data (mitochrondrial DNA and Y-chromosome haplotypes) from 3 ancient individuals that lived in Malta during the transition between the Neolithic and Bronze Age periods. Thanks to this data we addressed the question of whether the Maltese were genetically more similar to Neolithic or to Bronze Age populations in Eurasia.

11.3. Methods

11.3.1. aDNA data collection and mitochondrial analysis
For this project we used data submitted by Ariano *et al*. (2022) from 3 petrous bones from the Circle. Reads obtained for each sample were aligned to the human reference genome (hg19/GRCh37). Both private and Haplogroup defining mutations were taken from the software **Haplofind** (Vianello *et al.* 2013) output. For each individual, these mutations were then used to measure the number of mismatches with the consensus *fasta* sequence. The contamination rate was calculated as the ratio of the number of mismatches over the total count of positions in the consensus sequence. When the mismatches included deaminated bases, these were counted as an upper limit value of contamination. Fastq files were aligned to the human Revised Cambridge Reference Sequence, (rCRS, NC_012920.1) using the tool **mpileup** from the software **samtools** (Li *et al.* 2009). Only SNP calls with a base quality above 30 (parameter -Q30) were then retained for further analyses. The genome coverage of each sample was calculated using the tool **qualimap** (Okonechnikov *et al.* 2016). A consensus mitochondrial Fasta sequence was first obtained for each sample using **bcftools** software (Li *et al.* 2011) (parameter -c) and then given to the software Haplofind (Vianello *et al.* 2013) for the haplogroup assignment (Table 11.2). From this analysis, we considered as valid only the haplogroups that were at the most terminal part of a branch and had an assignment score of at least 0.9 and where the assignment did not derive from a transition SNP.

11.3.2. Contamination
There are two common ways of checking for sample contamination in ancient DNA samples; the first method consists of checking for the presence of molecular damage at the 5′ and 3′ end of aligned reads. The second method is used also in modern DNA analyses and involves checking for the haploid state of the mitochondrial and X-chromosome DNA in male individuals. Given that all our samples were already treated for *postmortem* damages, we concentrated upon this last method for our contamination analyses.

11.3.3. Y-chromosome haplogroup determination
Samples that were identified as male were evaluated for Y-chromosome haplogroup lineage. This task was executed using the software Yleaf v2 (Ralf *et al*. 2018) and the ISOGG (International Society of Genetic Genealogy) 2019 database as reference (https://isogg.org/tree/ISOGG_YDNA_SNP_Index.html). SNPs annotated with the '~' label were excluded from this analysis (Table 11.3).

11.3.4. Collection of publicly available data
To contextualize our haplogroup results with other published ancient samples, we downloaded a well curated dataset of ancient DNA metadata from AmtDB (Ehler *et al*. 2018). We then used this resource to compare the geographical distribution of all sample haplogroups (both mitochondrial and Y-chromosome), focusing in particular on Neolithic, and Bronze Age periods. The samples were finally filtered for latitude and longitude thus restricting our analysis to Eurasia.

11.4. Results

11.4.1. Mitochondrial contamination and history

A common method for estimating DNA contamination of a sample is to check the rate of heterozygous sites present in the mitochondrial DNA. The contamination percentages of our high coverage samples, not considering sites that can derive from transition, range from values of 0.3% to 0.78% (Table 11.1). These values can be considered as acceptable for a no-contamination hypothesis. Once assured about the quality of our samples, we used the software **Haplofind** to investigate mitochondrial haplogroups, with the following results (Table 11.2):

- MLT5 belongs to the haplogroup K1a which is a subgroup of the major branch K. This branch has already been described in individuals that come from Anatolia during the Pottery and pre-Pottery Neolithic period (Mathieson *et al.* 2015).

- The individual MLT6 belongs to the haplogroup V which, although low in frequency, has been found in populations from central Europe associated with LBK, Únětice and Pitted ware culture, and from Neolithic populations in Portugal (Haak *et al.* 2015).

- MLT9 belongs to the haplogroup H4a1, which is a derived branch of haplogroup H. This major group evolved first in the Near East during the Neolithic period and afterward spread into western Europe (Torroni *et al.* 1998). It appears in fact to be frequent in France during Middle Neolithic period and Iberia during the Epi-Cardial Neolithic period.

By inspecting the distribution of ancient haplogroups, it appears that the Maltese belonged to mitochondrial branches that were particularly widespread during the Neolithic period. Interestingly, samples that matched the Maltese haplogroups during the Bronze Age period (details in Fig. 11.2) tended to come from central Europe and the Iberian Peninsula and belonged to the Bell Beaker culture.

11.4.2. Y-chromosome contamination and lineages

The results from Y chromosome screening indicate that two of our samples (MLT5 and MLT9) were male. We then used SNP information from the ISOGG database to define haplogroups and we found that the two individuals each belonged to one of two common European Neolithic haplogroup branches. MLT5 belongs to haplogroup H2. This haplogroup is rarely found in modern European populations and its earliest evidence dates back to a pre–pottery sample

Table 11.1. *Results from the contamination analysis. No sample shows significant traces of contamination, both excluding and including Transition sites (MD).*

Sample ID	Mean coverage	Site contamination %	Site contamination no-MD %
MLT5	128.26	1.422	0.533
MLT6	106.8	1.548	0.787
MLT9	184.87	0.563	0.340

Table 11.2. *Haplogroup assignment from Haplofind. The assignment score gives a probability of a sequence to be part of an haplogroup. The Haploscore gives an assignment score taking into account the previous major haplogroup from the same branch.*

Sample ID	Mitochondrial coverage	Haplo-group	Haplo-score	Assignment score
MLT5	128.26	K1a	0.8	0.96
MLT6	106.8	V	1	0.98
MLT9	184.87	H4a1	1	0.99

Table 11.3. *Sex assignment for each sample. When a sample did not reach a sufficient confidence interval it is indicated as 'Not Assigned'. For male individuals also the Haplogroup is assigned using the ISOGG database as reference.*

Sample ID	Only ChrY	Ratio ChrY/ChrY+ChrX	SE	95% CI	Sex assignment	Haplogroup
MLT5	208312	0.1162	0.0002	0.115-0.116	Male	H2
MLT6	43469	0.0178	0.0001	0.017-0.018	Not assigned	-
MLT9	177879	0.1224	0.0003	0.121-0.122	Male	G2a2a1a3

Table 11.4. *Values associated with contamination level using the X chromosome in male individuals.*

Sample ID	Contamination %	SE	P-value
MLT5	0.6	0.0014	6.789e-11
MLT9	1.1	0.0017	1.128e-08

in the Levant between 7300–6750 BC (Lazaridis *et al.* 2016). In more recent times this haplogroup was found in an Anatolian farmer and a European Neolithic sample belonging to the Starcevo culture. MLT9 has the haplogroup G2a2a1a3, one of the subclades of the major branch G commonly present in Europe during the Neolithic period (Broushaki *et al.* 2016). From examination of the incidence these haplogroups in ancient Eurasia, their prevalence during the Neolithic period compared with later times is clear (details in Fig. 11.3). There is a trend for matches to follow a more southern distribution. In the post-Neolithic comparison, only two H2 matches were found, in an Early Bronze Age sample from Bulgaria. Haplogroup G2a2a1a3 was interestingly found in 3 samples from Neolithic-Copper Age in Spain and Portugal. Other close subclades are common among Early European farmers and rarely feature in the Bronze period sample where they are mostly replaced by haplogroups R1a and R1b (Haak *et al.* 2015).

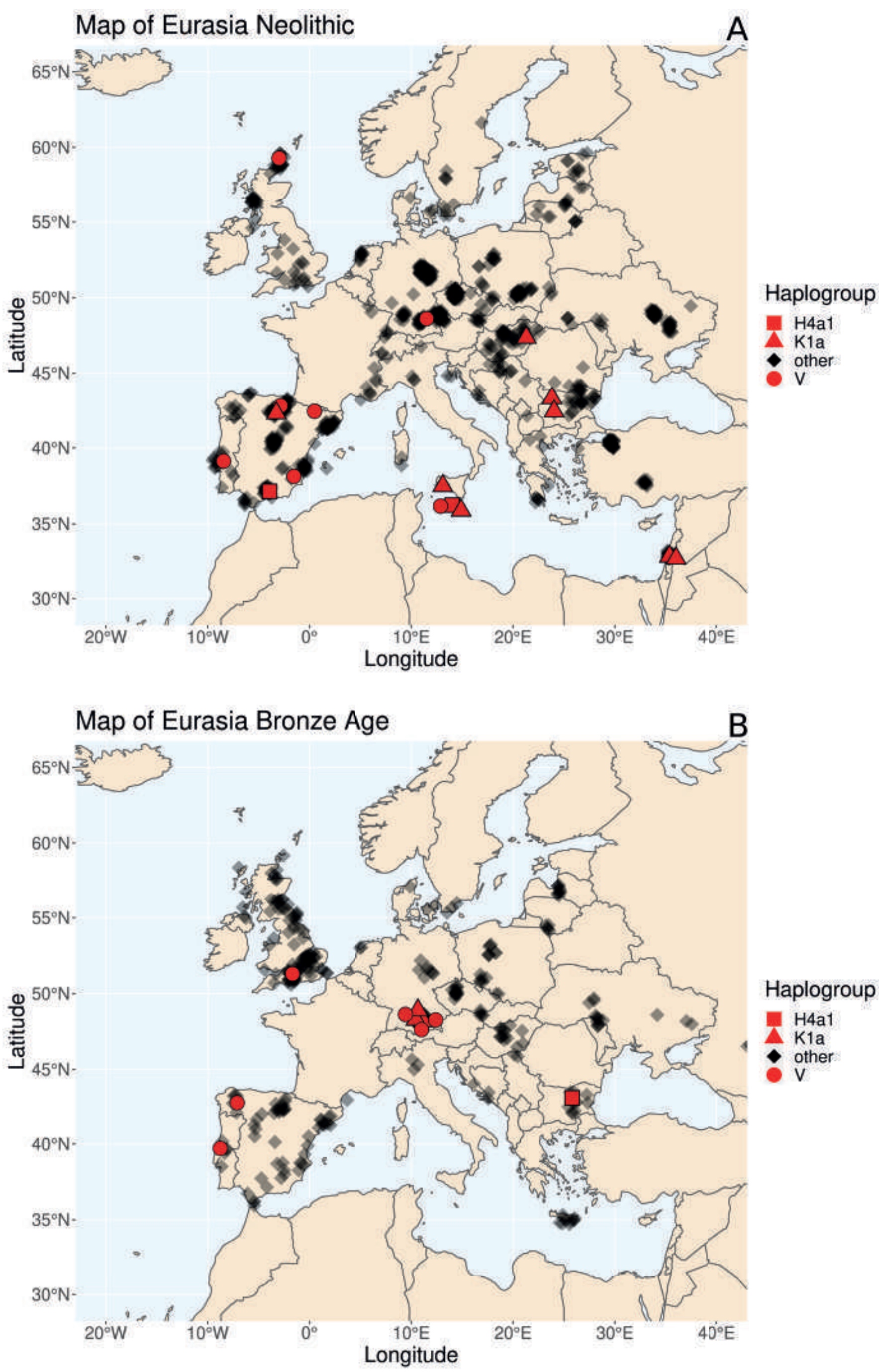

Figure 11.2. *Distribution of ancient mitochondrial haplogroups in Eurasia. Each point is a sample with the shape representing the haplogroup to which it belongs. A red colour indicates a match with one of the Maltese haplogroups encountered in this work, dark grey points show the geographical distribution of unmatched samples. Panel A: distribution of haplogroups during the Neolithic. Panel B: distribution of haplogroups in Bronze and Iron Age samples.*

11.5. Discussion

Mitochondrial DNA and Y-chromosome sequences from Neolithic Maltese individuals from the Temple Period (3rd millennium cal. BC) were analysed. Y chromosome haplogroup information showed that MLT5 and MLT9 are both part of Neolithic haplogroups common during the Neolithic period. Interestingly the MLT9 haplogroup was also found in samples from Copper Age Iberia pointing to a possible connection with the Cardial culture. These haplogroups almost disappeared during the Bronze Age and Iron Age periods with the only three matches found in Bronze Age individuals from Eastern Europe and Central Asia. Mitochondrial haplogroups results mirrored these findings with samples that matched the Maltese mostly as Neolithic farmers and Bell Beaker samples from Western Europe. Both these results point to a Western European Neolithic or Bell Beaker ancestry of our ancient Maltese and we believe further analysis

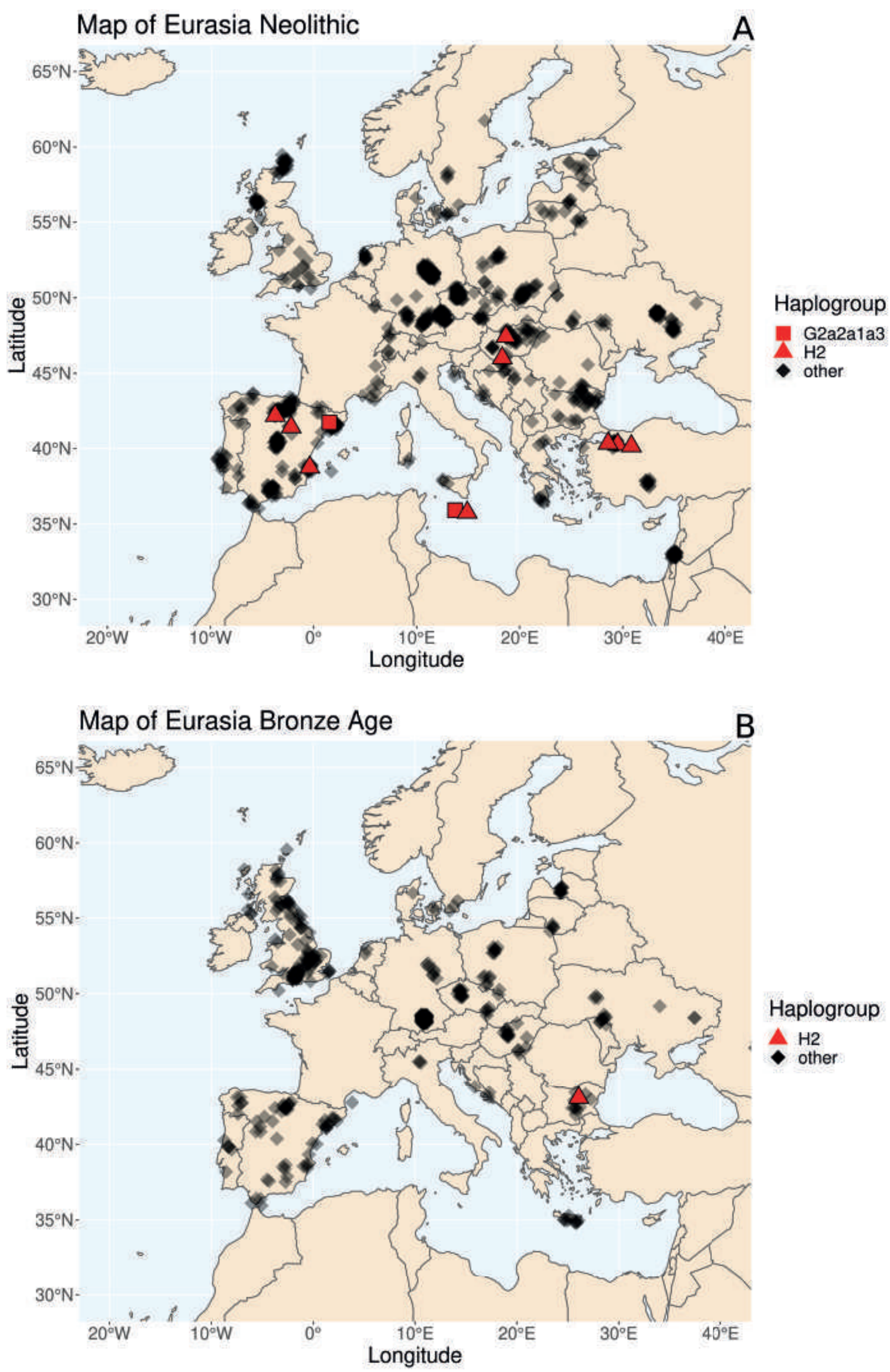

Figure 11.3. *Distribution of ancient Y haplogroups in Eurasia. Each point is a sample with the shape representing haplogroup. A red symbol indicates a match with one of the Maltese haplogroups encountered in this work. Panel A: distribution of haplogroups during Neolithic. Panel B: distribution of haplogroups in Bronze Age samples.*

of autosomal markers will clarify and refine estimates of their ancestry.

11.6. Conclusion

The populations of the Maltese islands, located in the south of the Mediterranean Sea, were shaped by a succession of different cultures during the Neolithic period. The first group settled on the islands just after 6000 BC, probably as an Early Neolithic population. After an initial oscillation between growth and decline (see Volume 1, Chapter 2) an apogee of culture and population density was reached during Temple Period, especially in the Tarxien phase between *c*. 2800 and 2400 BC, which saw the construction of unparalleled sophisticated megalithic structures. Then this culture seemingly collapsed, and a number of questions have vexed scholars of early Malta ever sense: who were these ancient inhabits of Malta, and which ancient population did they resemble the most? To answer these questions, we offer here a first assessment of Maltese ancient DNA data using three individuals that lived during the Tarxien phase of the Temple Period.

11.6.1. The Neolithic routes

The culture of Neolithic farming spread from northwest Anatolia into western Europe following two main routes. One route was associated with the Linearbandkeramik culture (LBK) and followed the Danube valley and spread northwest towards northern Europe. The other route was associated with Impressa-Cardial pottery culture and followed a westward Mediterranean route reaching the Atlantic in France and Iberia. Malta's early settlers were likely part of this latter route with their uniparental markers resembling other southern European Neolithic samples most strongly.

11.6.2. The eastern influence

By the 2nd millennium BC, the Bronze Age period populations from the steppe migrated from eastern to western Europe, displacing preceding local cultures (Olalde *et al*. 2018). Exotic pottery coming from eastern Europe, even before the Bronze Age period, could suggest a connection between the Maltese and other populations (for example, Thermi, Bell Beakers and the potential Balkan Cetina style). No genetic evidence in our samples implies contact with eastern populations.

11.7. Future perspectives

The field of ancient DNA study is in continuous development, especially as the financial cost of sequencing analysis reduces. Although haploid lineage markers can give hints about ancestry, using autosomal markers will help us to answer more important questions about migration and admixture. Therefore, our first next step will be to deepen our investigations by using methods to detect admixture, kinship and population structure from autosomal markers.

Chapter 12

Reconstructing deathways at the Circle and the Xemxija tombs through funerary taphonomy

Jess. E. Thompson, Ronika K. Power, Bernardette Mercieca-Spiteri, Rowan McLaughlin, John Robb, Simon Stoddart & Caroline Malone

12.1. Introduction

What is death? These three innocuous words ask us to reflect on a concept we can be certain that we'll never truly understand until we experience it, and by then it will be too late to share what we find out. But death is a thought worth ruminating on. In a modern Western context, most of us are quite comfortable with the idea that death constitutes but a single moment, founded upon a biological inevitability. Our hearts will stop beating, yes, but what if that is not (or does not have to be) the end? Neurological and genetic activity can continue after cardiac arrest (Norton *et al.* 2017; Pozhitkov *et al.* 2017), revealing the extended process of cellular death. These findings are relatively recent, yet cultural practices across the world have long acknowledged the slow transformation of death, by holding space for the continued presence of the dead in the world of the living. This chapter deals with this apparently simple question in the case of Malta from the 4th–3rd millennia BC.

Understanding how death was perceived in the past is largely accessible only through social practices. The preparation of the dead body, its place and mode of deposition, associated material culture, and commemorative markers, all provide compelling details about the relationship between the living and the dead, and how it was negotiated temporally. These practices encompass 'deathways': meaningful ways of transforming the state of the dead physically, socially and ontologically (Kellehear 2007; Robb 2013). There are several important points to acknowledge about deathways. The ever-changing condition of the dead body might be understood to reflect the individual's tenuous or altered position. Funerary practices typically respond to such changes by directly interacting with the dead body, reflecting a series of beliefs about death, dying, and the means through which these processes were achieved. Moreover, amongst all cultures, there are multiple pathways for the treatment of the dead. Varied deathways might account for factors such as the place or means of death, social position, age, or gender identity.

Funerary practices transition the dead body through a series of stages to the appropriate end point, be that a coffin buried in a cemetery or a communal cliff-side tomb, but reconstruction of these actions involves working backwards from the preserved remains. This reconstruction is the domain of funerary taphonomy, which recognizes the potential to access parts of past ritual actions and beliefs by characterizing the ways that the human remains have altered since death (Knüsel & Robb 2016). Taphonomy has long been a central aspect of palaeontological and zooarchaeological analyses but has emerged as an important step in osteoarchaeological studies from the 1980s. More recently, its value in defining funerary practices has been realized. A standard suite of methods is now recognized for classifying the condition, preservation, modification, and representation of human remains, most of which post-date the original excavation and initial post-excavation analysis of the Circle remains.

Taphonomic methods are particularly well-suited to the analysis of commingled assemblages which have often been formed, modified and affected by diverse agents (e.g. Adams & Konigsberg 2004; Moutafi & Voutsaki 2016; Osterholtz *et al.* 2014). Recent taphonomic research has particularly focused on complex prehistoric collective deposits, often noting multiple funerary practices within single burial spaces (e.g. Alt *et al.* 2016; Beckett 2011; Crozier 2018; Geber *et al.* 2017; Lorentz 2016; Smith & Brickley 2009). Previous research on funerary practices at the Circle sought to address the processes of disarticulation and commingling through modelling the movement of remains across the site (Stoddart *et al*. 1999; Stoddart *et al.* 2009a, 320). Initial taphonomic observations indicated that skeletal remains were not exposed to the elements nor accessible to local fauna, and no cutmarks were identified (Duhig in Malone *et al.* 1995: 340; Duhig 1996; Stoddart *et al.* 2009a, 320). It was therefore clear that the disarticulated and commingled deposits were formed through human action. However, questions remained as to the timing and nature of post-depositional manipulation, and the role of secondary depositional practices and redistribution of the assemblage. The increasingly formalized methodology of funerary taphonomy now provides the opportunity to re-examine the Circle material and, for the first time, to compare the site with another contemporary skeletal assemblage, the Xemxija tombs. Within the broader aims of the *FRAGSUS Project,* this research contributes to a greater understanding of the site's use, establishing the temporal nature of depositional practices and assessing change in funerary practices over time.

This chapter presents the results of the first large-scale taphonomic analysis of human remains from Neolithic Malta by investigating the range, sequence and role of funerary practices. The aims and methods of funerary taphonomy are first discussed, before outlining the methodology applied to the skeletal remains from the Circle and the Xemxija tombs. These methods aimed to define the variety of ways the dead were treated and deposited, as well as the means and timing of disarticulation to produce an understanding of the typical funerary programme. An overview of the sample size and results from each site is then presented. The range of taphonomic modifications identified on this material, and analysis of skeletal element representation, is combined with an examination of *in situ* articulation (see Thompson 2020 for full results). These results build upon the initial analyses (Duhig in Malone *et al.* 1995; Duhig 1996; Stoddart *et al.* 1999; Stoddart *et al.* 2009a), and provide a detailed account of the taphonomic condition of human remains from both sites to develop a model of deathways during the 4th–3rd millennia BC in the Maltese Islands.

12.2. Funerary taphonomy

A wide range of cultural beliefs structure interactions with the dead during funerary rituals, including concepts of the afterlife, taboo, pollution, personhood, and bodily ontologies (e.g. Bloch & Parry 1982; Douglas 1966; Fowler 2004; Harris & Robb 2012; Huntington & Metcalf 1979). Death and dying are socially and culturally contingent processes, involving ontological transformation of the deceased, renegotiation of their role in society, and reorganization of the social structure (Bloch & Parry 1982; Kellehear 2007; Robb 2013). Such transformations are often achieved through engaging with the dead by handling their remains, and these actions may be discerned through archaeothanatological and taphonomic analysis (Duday 2006, 2009; Knüsel & Robb 2016).

Funerary taphonomy provides a methodology to characterize burial assemblages holistically, analysing the relationship between the condition of human remains, their depositional environment, and cultural practices (Duday 2009, 7–13; Knüsel & Robb 2016: 656; Osterholtz, Baustian & Martin 2014). As such, it may be described as a middle range theory, building up from the skeletal data to broad interpretations of cultural beliefs and behaviours (Knüsel & Robb 2016, 656; Robb 2016, 684). Patterns of skeletal element representation are used to link modes of deposition to the burial environment and cultural behaviour, identifying whether deposition was primary or secondary, and whether cultural practices of bone curation or removal can be identified. Crucially, funerary taphonomy requires understanding of the relationship between the multiple factors which can affect human remains before, during, and after burial or deposition, as well as distinguishing between numerous agents which can modify human remains (Duday 2009; Lyman 2004; Ubelaker 1997).

Collective deposition, especially common in Neolithic Europe during the 4th to 3rd millennia BC, is often thought to demonstrate widespread and enduring beliefs about communal identity and the ancestors (e.g. Alt *et al.* 2016; Kuijt 2002; Li 2000; Stoddart & Malone 2015). However, the means by which burial assemblages became commingled and disarticulated is frequently overlooked. As cross-cultural analyses of deathways reveal, interactions with the dead are important for understanding *how* dying is perceived and managed, and its relationship with concepts of descent, kinship, personhood and identity. The process and timing of collective deposition, as well as the range of funerary practices represented within sites, provides crucial detail for addressing the social dynamics of burial. Taphonomic analysis often illustrates the multitude of funerary practices present both within and between sites of the same period, situating local adaptations within broader cultural trends. For example, considerable research on deathways in early Neolithic Britain and Ireland has identified a typical practice of selective deposition in monumental tombs, often followed by the rearrangement of remains. There is also evidence for excarnation and direct processing of remains (including defleshing and disarticulation), cremation, and selective deposition in non-funerary sites and natural locales (Beckett 2011; Crozier 2018; Geber *et al.* 2017; Smith & Brickley 2009). Similarly, detailed synthesis of the Neolithic Italian burial record

Table 12.1. *Total number of fragments analysed from the Xemxija tombs and contexts at the Circle. The Tarxien period is divided into early (2900–2700 BC), middle (2700–2500 BC), late (2500–2400 BC) and latest (<2400 BC) phases.*

Context	Location	Phase	NISP	No. analysed	% analysed
276	Rock-cut tomb: West chamber	Ġgantija	~7000	1033	14.8%
326	Rock-cut tomb: East chamber	Ġgantija	~3500	1050	30%
354	North bone pit	Early	1565	232	14.8%
436	East Cave: Central bone pit	Late	383	235	61.4%
595	East Cave: Southwest niche	Early	3333	2414	72%
656	East Cave: Southwest niche	Early	241	401	100%
734	East Cave: Southwest niche	Early	82	54	65%
743	East Cave: Central bone pit	Late	145	120	82.8%
783	West Cave: Display Zone	Latest Tarxien	53,139	4953	9.3%
799	North bone pit	Early	4468	2066	46.2%
951	West Cave: Deep Zone	Early	12,796	1923	15%
960	West Cave: 'Shrine'	Latest Tarxien	11,547	2953	25.6%
1024	West Cave: 'Shrine'	Middle	145	194	100%
1144	West Cave: Deep Zone	Middle/Late	1619	151	9.3%
1206	West Cave: 'Shrine'	Late	6783	765	11.3%
1307	West Cave: Deep Zone	Early	465	278	59.8%
Xemxija tombs		Early–Middle	14,760	14,760	100%

has established that, while discussion of primary inhumations in villages and caves tends to dominate the literature, most individuals' remains were actually disturbed and scattered across settlement sites (Robb 1994, 2007a, 2007b). Distinctive practices or locations of burial reveal alternative deathways, including exposure (perhaps for socially stigmatized individuals), mass burial (likely the result of warfare or epidemics), and the selective curation and deposition of skulls (Robb 2007a, 57–61). The reconstruction of funerary rites in Neolithic Malta can therefore address the sequence, variety, and temporality of deathways.

12.3. Materials and sampling strategy

The sample included in this study represents the full assemblage from the Xemxija tombs and samples from 16 contexts from the Circle. At Xemxija, six rock-cut tombs excavated in 1955 (Evans 1971, 112–6) yielded a large quantity of human remains but, unfortunately, no contextual record survives from the excavation. In 2001, a further tomb connected to tomb 6 was accidentally discovered and cleared before intervention by the Museums Department (Pace 2004, 164); it is uncertain whether any human remains were encountered in this tomb. The published notes from the 1955 excavations describe two fills: an upper brown clay and a lower deposit of white lime stained with red ochre (Evans 1971, 113). Three fills were recorded from tombs 3 and 5, which had a red ochre-stained soil beneath the lime layer. Human remains were found in the lowest levels of each tomb, whilst multi-period pottery was found in the upper fills. Exceptionally, tomb 4 lacked ceramics. Rare personal ornaments from tomb 5 included five *Spondylus* shell v-perforated buttons, two shell beads, three shell pendants and two miniature greenstone axe pendants (Evans 1971, 114–5). The lack of spatial record of the human remains was further complicated by their post-excavation curation, as the remains from each tomb were aggregated, presumably after the initial study (Pike 1971). As a result, detailed assessment of the depositional practices within each tomb is not possible, and the aggregation of the assemblage suppresses the minimum number of individuals (MNI) identifiable from the site

In contrast to Xemxija, the Circle assemblage provided the opportunity to explore funerary practices across diverse burial spaces and contexts, supplemented by records of *in situ* skeletal remains. Contexts were chosen for analysis based on several criteria, including those which: (1) were selected for radiocarbon dating and isotopic analyses; (2) spanned the full duration of the site's use; (3) contained both articulated and disarticulated remains, and (4) were associated with excellent excavation records. Where possible, contexts containing more than 1000 identified specimens (NISP) were sampled to a threshold of at least 10% in an effort to ensure the taphonomic results were representative of the full context. The sample size for this study is detailed in Table 12.1 and the spatial

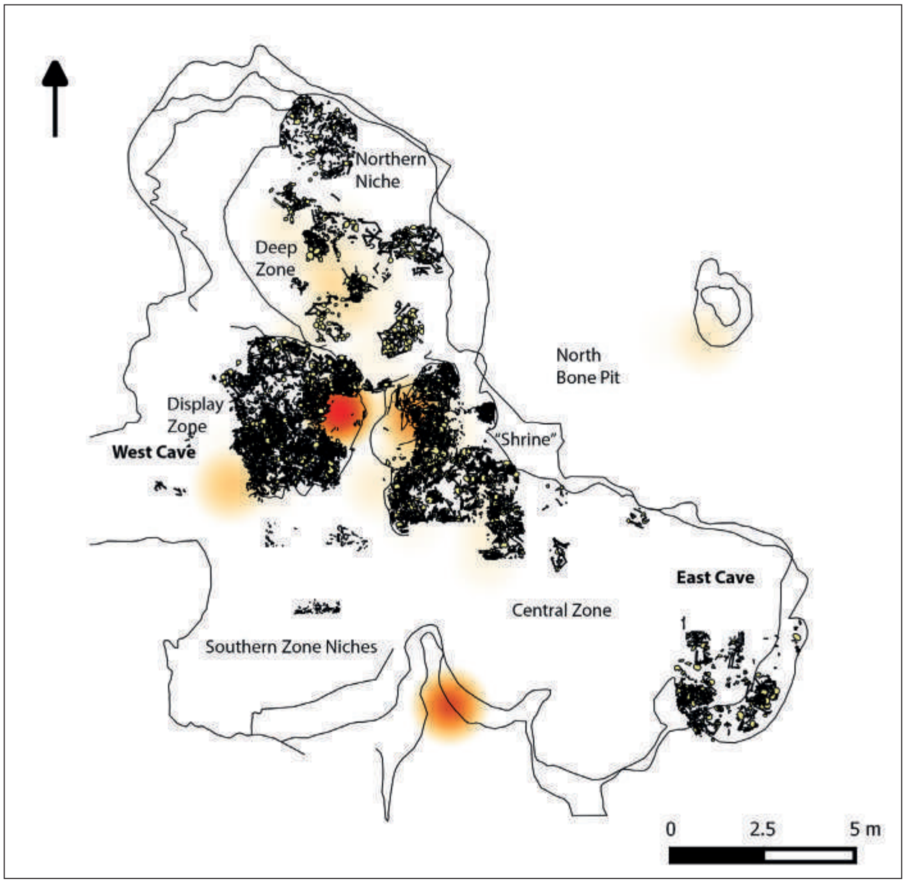

Figure 12.1. *Heatmap illustrating the location of remains analysed from the Circle. Map by Rowan McLaughlin.*

distribution is visualized in Figure 12.1. In two cases, the sample falls just short of the target: the total assemblage from Context (1144) could not be located, and there was insufficient time for further study of Context (783). Some of the largest bone-bearing deposits have been sampled to a high level: nearly 50% of Context (799) in the North Bone Pit, and 72% of Context (595) in the Southwest niche. A further three large contexts were partially analysed: Context (783) almost to 10%, Context (951) to 15%, and more than 25% of (960).

12.4. Methods

All bone fragments were examined macroscopically and with a 10x hand lens. Where possible, surface modifications were further examined under an optical microscope. Skeletal remains were divided into identifiable and unidentifiable fragments (usually smaller than 100 mm). Unidentifiable fragments were sorted into categories (cranial bones, long bones and miscellaneous bones), then sorted by size and preservation level, and counted. Fragments smaller than 5 mm were not included. Following this process, each fragment (or group of unidentifiable fragments) was entered into an Access database, alongside results for the variables detailed in Table 12.2. The full assemblage from each site or context was then quantified, calculating the minimum number of elements (MNE) and minimum number of individuals (MNI) in each sample, to analyse skeletal element representation (SER).

Element completeness and preservation were recorded using the Anatomical Preservation Index (API) and Qualitative Bone Index (QBI), following Bello (2005). The API classifies specimens according to whether they represent 0%, 1–24%, 25–49%, 50–74%, 75–99% or 100% of the original element, while QBI denotes the extent of cortical surface preservation, using the same indices. The maximum length of each identifiable element was measured to the nearest millimetre, while unidentifiable fragments were measured in size categories (0–20 mm, 21–30 mm, 31–40 mm and so on) following Knüsel and Outram (2004). Fragment size provides a means of assessing post-depositional processing and can be examined alongside element representation to discern whether taphonomic factors have biased the representation of skeletal elements. To ensure minimal double counting of elements when calculating MNE and MNI, fragments were recorded to the zone they represented of the original element largely using the method described by Buikstra &

Table 12.2. *Description of taphonomic variables recorded in this study.*

Category	Description	Reference
Anatomical Preservation Index (API)	The percentage of the complete element represented by each fragment.	Bello 2005.
Qualitative Bone Index (QBI)	The percentage of the cortical surface preserved well.	Bello 2005.
Fragment size	Identifiable fragments are measured to maximum length in mm. Unidentifiable fragments are grouped in size classes.	Knüsel & Outram 2004.
Zones present	Each element is divided into zones and the zones represented by each fragment are recorded when >50% complete. Long bones have 5 zones (proximal and distal epiphyses and the diaphysis is divided into thirds). Mandibles and elements of the axial skeleton, shoulder and pelvic girdles have subdivided into 5 zones represented by their main features which are usually diagnostic when fragmented. Small bones of the hands and feet have 1–3 zones. A complete cranium has 15 zones.	Buikstra & Ubelaker 1994; Knüsel & Outram 2004.
Fragmentation morphology (FFI)	The fracture freshness index (FFI) records angle, outline and texture on a scale of 0–2 (where 0 is consistent with bone breakage soon after death and 2 is consistent with dry bone fracture). Different types of breaks may be evident on one fragment, and in this case the earliest break is recorded.	Outram 2001.
Abrasion and erosion	Surface abrasion or erosion, such as that because of root damage (recorded on a scale of 0–5).	McKinley 2004a.
Weathering	Damage consistent with exposure to the elements, usually in the form of splitting and flaking of the bone surface (recorded on a scale of 0–5), although other post-depositional practices may result in similar modifications.	Behrensmeyer 1978.
Discolouration	Cortical staining or adhesions are described, including their colour, size and location.	Dupras & Schultz 2014.
Animal damage	The result of either rodent, carnivore or insect damage to bone surfaces.	Haglund 1997a, 1997b; Huchet *et al.* 2013.
Burning	The colour, location and extent of burning is recorded when present.	McKinley 2004b.
Cutmarks	The number, location and morphology of cutmarks is recorded when present.	Greenfield 2006.

Ubelaker (1994, 8). Although more comprehensive zonation methods exist (e.g. Knüsel & Outram 2004; Mack *et al.* 2016), time constraints necessitated the use of a less extensive method. Therefore, zones were only recorded as present when they were >50% complete. To investigate whether long bones were broken while fresh (shortly after death) or dry, the Fracture Freshness Index (FFI) was implemented, recording the fracture angle, outline and texture (Outram 2001). Surface modifications, including weathering, abrasion, erosion, discolouration, burning, animal damage and cutmarks were recorded following standard protocol, detailed below. Statistical analyses were carried out in IBM SPSS 25.

Remains from the Circle were quantified on a context-by-context basis; however, because of the aggregation of the assemblage, the Xemxija tombs remains were treated as one deposit. The MNE was calculated for each skeletal element or region (e.g. cervical vertebrae), including only specimens 50% or more complete, and utilizing the best-preserved zone. From this, MNI was calculated separately for adults and non-adults. The highest number for each age category was summed to produce the MNI for each site or context. Skeletal element representation was then calculated, providing a measure of the proportion of specific elements (MNE) with reference to the estimated MNI, expressing the relative composition of elements within a sample. For each skeletal element, the MNE is divided by the expected number if all elements of the total estimated population (MNI) were present, using the formula for the Bone Representation Index (BRI) devised by Dodson and Wexlar (1979):

BRI= (MNE)/(number of elements in complete skeleton x MNI) x 100

For example, there are 10 metacarpals in each body, and if 19 metacarpals are present in a context containing 20 individuals, the MNE of 19 is divided by 200 (BRI=9.5%).

This method provides a useful tool for both intra- and inter-site analyses. Simulation modelling of successive interment in a collective tomb, including parameters for the rate of decay of different types of bone, has revealed distinctive patterns in element representation according to varied funerary practices (Beckett & Robb 2006; Robb 2016). Primary depositions, if left undisturbed, are only subject to natural processes of degradation which typically affect less robust bones (especially the sternum and *ossa coxae*). Primary deposition is therefore usually indicated through the high representation of nearly all skeletal elements except those high in trabecular bone (Bello & Andrews 2006). Thus, a lack of small and fragile bones is not always indicative of secondary deposition. Secondary deposition, in contrast, may be distinguished through an uneven representation of elements. The curation of specific elements such as skulls or long bones might be evident through their over-representation (Robb 2016, 690). Repeated removal of bones from primary deposition spaces is indicated through the over-representation of small, fragile bones which may either be overlooked or deemed culturally insignificant (Robb 2016, 690). The process of successive deposition—commonly represented in Neolithic tombs—shares some characteristics with secondary deposition, such as the dearth of small bones and high level of *in situ* decay, and the two can therefore be difficult to distinguish (Robb 2016, 689–90). Successive deposition often leads to high fragmentation, which can suppress the representation of elements with respect to the MNI (Robb 2016, 687).

Altogether, assessing taphonomic characteristics such as bone completeness, size, preservation, surface modifications, and the relative presence of skeletal elements facilitates a holistic interpretation of assemblage formation which accounts for the influence of environmental and cultural factors. Analyses of diverse funerary assemblages, alongside ethnohistoric and ethnographic accounts of mortuary practices, have produced indicators for the taphonomic profiles of several core funerary practices. Exposure of the dead, resulting in defleshing and perhaps excarnation through animal scavenging, is expected to produce disarticulated skeletal remains, exhibiting weathering and gnawing (e.g. Carr & Knüsel 1997, 170). Uneven element representation will result from this process, with scattered small bones remaining in the location where excarnation took place, and predominantly larger elements removed to the final burial place (e.g. Smith 2006; Whittle & Wysocki 1998). Other forms of secondary deposition might involve direct dismemberment and defleshing, leaving tool marks at joint or muscle attachment sites (e.g. Bello *et al.* 2016; Robb *et al.* 2015; Wallduck & Bello 2016) and/or percussion pits caused by striking bone with a hard material (Crozier 2016, 2018; White 1992, 140). Again, minimal articulations would be expected to remain, and element representation would be unpredictable. Conversely, rearranging and redistributing remains in spaces used for successive depositions, as is often seen in prehistoric tombs, can result in a mixed profile of complete and partial articulation alongside disarticulated remains, and direct evidence for intervention with fleshed or decomposing remains is often, but not always, minimal (e.g. Beckett 2011). Such wide-ranging studies provide a series of expectations with which taphonomic results can be compared to interpret funerary practices.

12.5. Results

12.5.1. Taphonomic analysis

The full results for the Xemxija tombs and the Circle (with contexts grouped according to location) are summarized in Table 12.3. The percentage of each sample with fragments <5 cm, affected by high fragmentation, low preservation, weathering, abrasion/erosion, animal damage, burning and cutmarks is presented. The mean score (and standard deviation) for bone completeness, preservation, fragmentation morphology, weathering and abrasion/erosion is also given (calculated in SPSS).

Fragment size is consistently low across all samples analysed, with 66.8–84.2% of each sample represented by fragments <5 cm in maximum length. The Xemxija tombs are at the lowest end of this range, with 66.8% of skeletal remains measuring <5 cm in maximum length, indicating a highly disturbed deposit. As expected, a similar range of scores is observed for element completeness, with 68–87.9% of each sample comprising elements <50% complete. According to the mean API, three areas presented slightly higher levels of element completeness: the Display Zone, the 'Shrine' and the Southwest niche. Cortical bone preservation is more varied, revealing the influence of diverse agents. The poorest levels of preservation are seen in the Circle rock-cut tomb (94.5% of the fragments analysed were <1/2 well-preserved), according with previous accounts for the friability of the bone, alongside sediment concretion and ochre staining (Duhig in Malone *et al.* 1995, 337). The best bone preservation is evident in the 'Shrine' sequence (with only 18.3% of the sample <1/2 well-preserved).

The majority of long bone breakage occurred to dry bone, with mean FFI scores between 5.96–6. Only 12 fragments displayed evidence of fresh bone breakage (scoring 0–3 on the FFI scale), including six long bones from the Xemxija tombs and six from the Circle cave complex, in the Deep Zone, Southwest niche and 'Shrine'. Therefore, although most bones

Table 12.3. *Overall taphonomic results for the Xemxija tombs and the Circle (according to spatial location). Abbreviation: SD= Standard Deviation.*

Taphonomic feature	**Xemxija tombs 1–6**	**Circle rock-cut tombs** (276), (326)	**North bone pit** (354), (799)	**Display Zone** (783)	**Deep Zone** (951), (1144), (1307)	**'Shrine'** (960), (1024), (1206)	**Central pit** (436), (743)	**Southwest niche** (595), (656), (734)
<5 cm in size	66.8%	84.2%	77.1%	81.1%	76.1%	81.2%	83.7%	79.1%
Mean fragment size	3.87 (SD 2.635)	3.61 (SD 2.754)	3.36 (SD 3.08)	2.74 (SD 2.325)	2.83 (SD 2.27)	2.78 (SD 2.738)	2.85 (SD 2.20)	2.95 (SD 2.745)
<1/2 complete	74.4%	78.2%	84.8%	71.7%	87.8%	68.6%	81.4%	68%
Mean API	1.89 (SD 1.451)	1.66 (SD 1.245)	1.51 (SD 1.178)	1.93 (SD 1.407)	1.43 (SD 1.094)	2.03 (SD 1.463)	1.45 (SD 1.08)	1.91 (SD 1.438)
<1/2 well preserved	66.3%	94.5%	76.5%	12.6%	41%	18.3%	85.3%	33.6%
Mean QBI	1.87 (SD 1.63)	0.28 (SD 0.589)	1.01 (SD 1.472)	3.35 (SD 1.070)	2.24 (SD 1.310)	3.36 (SD 1.068)	0.99 (SD 1.18)	2.82 (SD 1.503)
Mean FFI	5.96 (SD 0.293)	5.99 (SD 0.125)	5.97 (SD 0.179)	5.99 (SD 0.054)	5.8 (SD 0.926)	5.97 (SD 0.359)	6.0 (SD 0.0)	5.97 (SD 0.26)
Abrasion/ erosion	15.3%	10.3%	7.4%	11.4%	6.4%	8.9%	7.6%	24.4%
Mean abrasion/ erosion	0.30 (SD 0.819)	0.15 (SD 0.5)	0.08 (SD 0.288)	0.12 (SD 0.352)	0.08 (SD 0.356)	0.09 (SD 0.303)	0.08 (SD 0.26)	0.33 (SD 0.684)
Weathering	9.1%	16.6%	0.3%	2.8%	13.3%	2.2%	3.9%	4.7%
Mean weathering	0.15 (SD 0.533)	0.43 (SD 1.078)	0.0 (SD 0.055)	0.04 (SD 0.273)	0.22 (SD 0.583)	0.03 (SD 0.241)	0.04 (SD 0.19)	0.06 (SD 0.303)
Insect damage	0.3%	0.1%	0.9%	0	0	0	0	0
Gnawing	0.9%	0	0	0	0	0	0	0
Burning	0.2%	0.9%	0	0.02%	0	0.1%	0	0
Cutmarks	0	0	0	0	0	0	0	0
Total analysed	**14760**	**2083**	**2298**	**4953**	**2384**	**3912**	**355**	**2869**

were fragmented, breakage rarely occurred during the *perimortem* interval after death, suggesting that the destructive process of successive deposition is largely responsible for fragmentation. Evidence of abrasion and erosion was highest in the Southwest niche (24.4%), followed by the Xemxija tombs (15.3%), and lowest in the Deep Zone (6.4%). The most extensive abrasion and erosion—to the complete extant surface of the bone—was recorded in the Xemxija tombs, the Circle rock-cut tomb, the Southwest niche and the Deep Zone. These modifications may be attributed to several processes, including the erosive action of plant roots, as well as abrasion through tumbling and perhaps even trampling of remains.

Weathering was most prevalent in areas with poor preservation and/or high fragmentation: the Circle rock-cut tomb (16.6%), followed by the Deep Zone (13.3%), and Xemxija tombs (9.1%) (Fig. 12.2). This suggests that both natural and cultural processes are responsible for cortical cracking, flaking and splitting, including extensive rearrangement of remains, successive deposition, compaction as a result of overlying deposits, cyclical inundation and drying, and tumbling. Indeed, these modifications can be caused by a range of factors in addition to surface exposure, including alkalinity (a factor relevant because of the limestone geology of the Maltese Islands), humidity, moisture, and sediment pressure (Fernández-Jalvo & Andrews 2016, 201). Additionally, at the Xemxija tombs, it is unknown whether tomb shafts were blocked when not in use; it is therefore possible that any remains placed near to the tomb entrance were exposed to processes of weathering. However, given the indicators for the circulation of bone, including the removal of selected elements from the Xemxija tombs, and the redistribution of crania and long bones in the Circle, rare instances of secondary deposition following exposure cannot be entirely ruled out.

Animal damage was observed on a small number of remains. Insect damage, in the form of rounded pits and bores mostly between 1–4 mm in diameter, was identified in the Xemxija tombs (Fig. 12.3a, c-f), Circle rock-cut tomb West chamber (Fig. 12.3b) and North bone pit. Through comparison with marks of similar morphology on both human and faunal bone, these modifications are attributed to dermestid beetles (Thompson *et al.* 2018). Dermestids consume

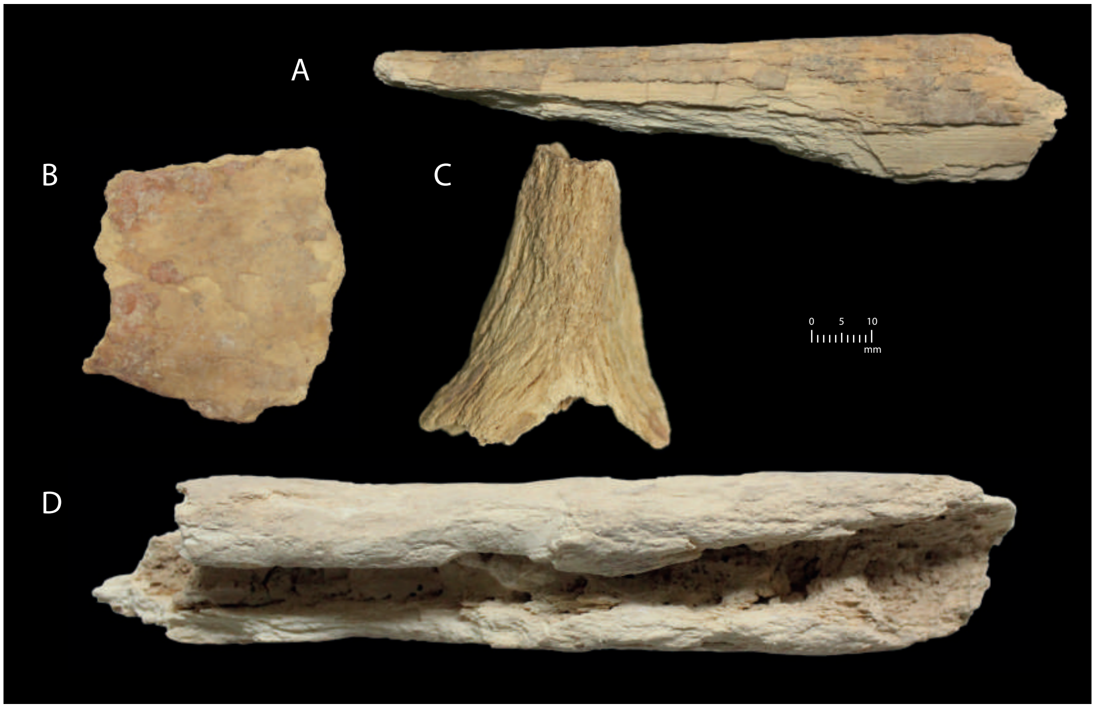

Figure 12.2. *Cortical thinning, splintering and delamination indicating weathering on: a) a long bone fragment from Context (951); b) a cranial fragment and c) a distal humerus fragment from the Xemxija tombs; d) a femur fragment from Context (951) in the Deep zone of the Circle cave complex. Scale bar: 1 cm. (Photos Jess E. Thompson).*

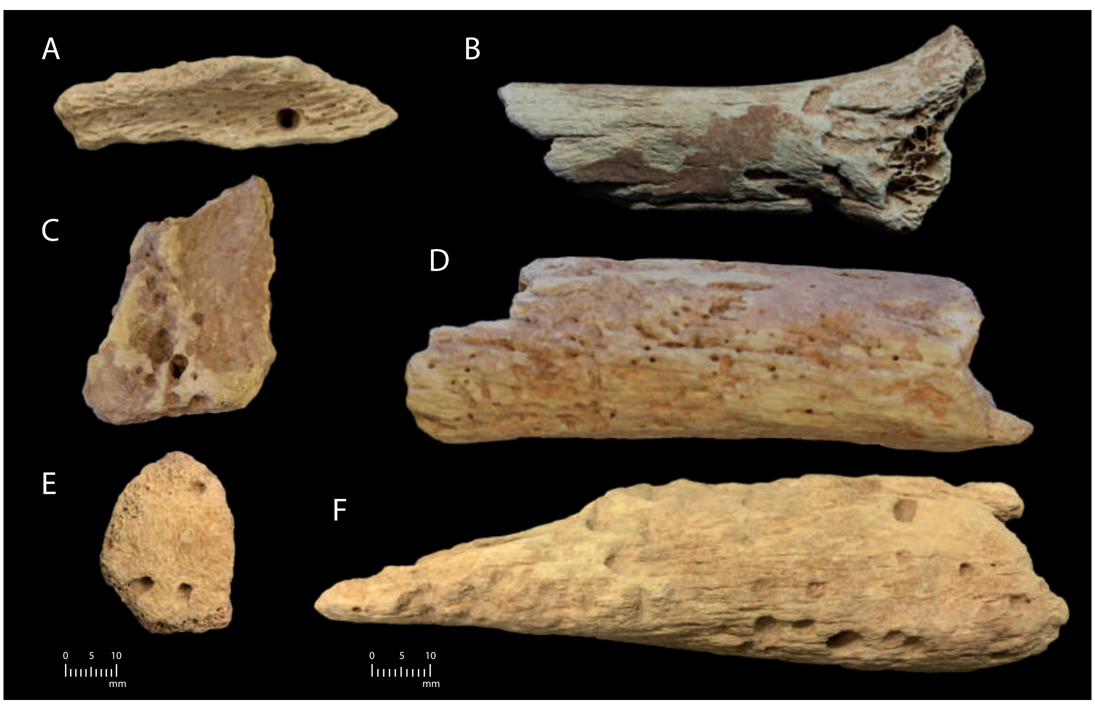

Figure 12.3. *Insect modifications to a range of elements from the Xemxija tombs (a, c–f) and Circle rock-cut tomb (b) in the form of pits, bores and furrows: a) long bone fragment; b) distal humerus fragment; c) cranial fragment; d) long bone fragment; e) parietal fragment; f) femoral fragment. Scale bar: 1 cm. (Photos Jess E. Thompson).*

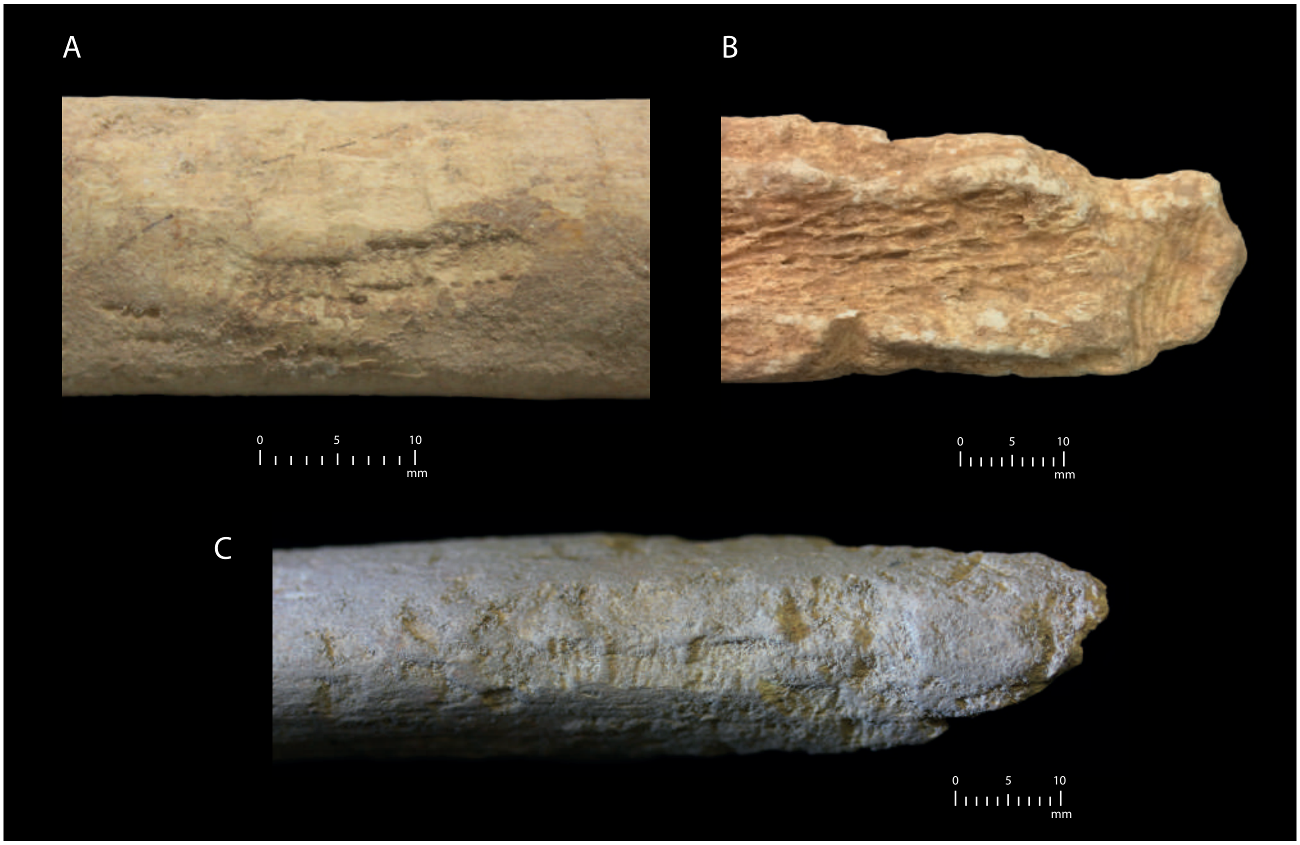

Figure 12.4. *Rodent gnawing to elements from the Xemxija tombs: a) humerus fragment; b) femur fragment; c) tibia fragment. Scale bar: 1 cm. (Photos Jess E. Thompson).*

desiccated tissues and will bore pupation chambers into bone when there is no softer surrounding substrate (Archer & Elgar 1998; Charabidze *et al.* 2014; Martin & West 1995). Nineteen species of dermestids have been recorded on the Maltese Islands (Háva 2003; Háva & Mifsud 2006), including those which have been directly observed on human remains: *Dermestes maculatus* De Geer, *Dermestes frischii* Kugelan and *Dermestes undulatus* Brahm (Charabidze *et al.* 2014). The presence of dermestid bores and pits on a small number of bones at both sites is revealing of funerary practices. On the Xemxija tombs remains, pupation chambers were observed on fragmentation margins, while bores were present on the long bones of an articulated male adult deposited in the North bone pit. In both cases, therefore, dermestids appear to have been present in the burial environment. However, dermestids would not have been an endemic species within the tombs. As such, they must have been transported during the burial process, perhaps in organic materials such as hide, which could have been used to wrap corpses (Stoddart & Malone 2010, 24; Fontenot *et al.* 2015; Thompson *et al.* 2018).

Rodent gnawing (n=14) was only present on remains from the Xemxija tombs (Fig. 12.4).[1] Gnaw marks occurred in sets of parallel linear grooves with flat bases, characteristic of rodent incisors (Fernández-Jalvo & Andrews 2016, 31). Gnawing was typically on crests or ridges of long bone (although in one case was present on the endosteal surface of a fragmented bone). The internal aspect of the marks was consistent with the cortical surface, indicating gnawing occurred in antiquity. The limited number of observations may be attributed to the poor preservation of most remains, which has often obfuscated observation of the complete cortical surface. While it is possible that some remains were exposed prior to deposition, there is no secure evidence that the tomb entrances were blocked, and rodents and scavengers were likely able to access the tomb contents on occasion.

Burning was evident on a small number of remains in the Xemxija tombs, the Circle rock-cut tomb (Fig. 12.5), Display Zone and 'Shrine'. Further evidence of burning was recorded in eight contexts in the Circle (Ronika K. Power pers. comm.), but not included in this study.[2] Burning was not observed to

Figure 12.5. *Burning on endocranial surface of fragments from Context (326) in the East chamber of the Circle Rock-cut tomb. Scale bar: 1 cm. (Photos Jess E. Thompson).*

penetrate the cortex on any specimens and is consistent with incomplete charring. Simulation modelling of the Circle cave complex has demonstrated that it would have largely been experienced as a dark space; during the summer solstice, sunlight would have illuminated the entrance pillars, casting a corridor of shadow leading through to the burial space (Barratt *et al.* 2018). This suggests that fire would have enabled visibility in the underground burial space and, if used, open flames from lamps or torches could have scorched nearby bones.

At both the Xemxija tombs and Circle, the limestone geology and general lack of animal damage have contributed to largely fair preservation of bone, including even highly fragmented remains. The extent of bone fragmentation is largely consistent across both sites, demonstrating the destructive effects of successive deposition. However, the above summary reveals some distinctions between both assemblages. The preservation and condition of bone is highly varied, reflecting differing treatment of remains across contexts and burial spaces. In terms of bone surface preservation, more fragments from the Circle were either fully degraded or fully preserved. Within the Xemxija tombs assemblage, the greater destruction of bone surfaces, alongside incidences of dermestid boring and rodent gnawing indicates more varied pre- and post-depositional histories at this site.

12.5.2. Skeletal element representation

As discussed above, skeletal element representation (SER) can be used to identify some key modes of deposition following expectations regarding the relative presence of elements (Table 12.4). When remains are only disturbed by natural taphonomic factors, it is expected that small bones and those with a high proportion of trabecular bone will be under-represented relative to other elements, and there will be variations in the presence of more robust elements. Although in these cases, more robust elements would be expected to represent close to 100% of the MNI, this depends upon local environmental conditions. Furthermore, simulation modelling has shown that similar patterns of bone attrition may be expected in primary inhumations, disturbed primary inhumations, and secondary burial spaces (Robb 2016).

As such, very different forms of funerary treatment may be almost indistinguishable through element representation alone and taphonomic modifications must also be considered. Deviations from this baseline, which indicate cultural intervention, can be identified through the significant over-representation of selected elements (Robb 2016, 690). This may take the form of 'residual' assemblages, in which small bones are present at similar levels to robust elements, suggesting the selective removal of larger bones to other locations. Conversely, when selected robust elements are present in higher numbers relative to other elements, this indicates their preferential curation; this pattern is typically seen with crania.

SER profiles from both the Xemxija tombs and Circle are explored below according to the main patterns they present: residuality, secondary deposition, and successive deposition. These analyses were constructed from MNE, MNI and BRI calculations from each context analysed (Appendix Tables A2.5–A2.22). Residual assemblages denote primary deposition followed by selective bone removals, resulting in the over-representation of small bones. Secondary deposition is demonstrated through the over-representation of specific, usually more robust bones, particularly crania and long bones. Lastly, SER profiles reflecting the presence of most elements, but with an overall low and uneven representation, most likely reflect the effects of successive deposition. When inferring funerary practices through element representation, however, the combination of processes which have affected the preservation of remains at both sites must be kept in mind.

Residuality is only strongly demonstrated in the Xemxija tombs assemblage (Fig. 12.6). There is a weaker signal of residuality in the Circle rock-cut tombs and in the main deposit in the Southwest niche, Context (595). Both contexts analysed from the Circle rock-cut tomb present an over-representation of some small bones, but there is no corresponding lack of robust bones to suggest their removal. Similarly, (595) presents a mixed profile whereby both small bones and robust bones are well-represented and may demonstrate both primary and secondary practices). In the Xemxija

Table 12.4. *Examples of typical funerary practices and their expected skeletal part representation (collated from Duday 2009 & Robb 2016).*

Funerary practice	Expected skeletal part representation	Examples
Primary deposition	Most skeletal elements expected to represent close to 100% of MNI. Natural taphonomic factors have affected element representation, including *in situ* decay of elements high in trabecular bone (especially sterna and *ossa coxae*), and small bones may not be recovered (Robb 2016, 690)	Single graves or simultaneous mass burials such as massacre and plague pits
Secondary deposition	Uneven skeletal part representation is likely, with under-representation of small bones because of movement from original place of burial (Robb 2016, 690). Two types of deposits can sometimes be distinguished: selection of bones, and residual assemblages (see below)	Ossuaries used as repositories for exhumed remains, such as charnel houses
Multiple successive inhumation	Both *in situ* decay and the biased representation of small and fragile bones is likely. Small bones often fall to base of deposit, and fragile bones may be crushed by later depositions. However, results likely to be very similar to that for secondary deposition (Robb 2016, 689)	Common in European prehistoric tombs used for collective deposition
Reduction	Reduction is related to secondary deposition, defined as the clearance of remains for successive inhumation. It is difficult to distinguish from these two modes of deposition via skeletal element representation. Since it is usually spatially discrete, evidence for reduction is best found through spatial analysis of skeletal elements (Duday 2009, 72)	Distinguished in some prehistoric collective burial spaces, and in the re-use of graves for later interments
Selection or curation	The cultural selection of specific elements for curation will result in their over-representation within a typical element representation curve for secondary deposition (Robb 2016, 690)	Curation of crania common in prehistory, alongside emphasis on long bones in some prehistoric tombs
Residual assemblages	Bones remaining from a primary deposition after most elements have been moved for secondary deposition or some have been selected for curation. This produces an uneven representation of skeletal elements and is commonly identified through the over-representation of small bones which may be missed or deemed unimportant. The result is the inverse pattern to secondary deposition or bone selection (Robb 2016, 690)	Remains from primary disturbed burials, e.g. Poulnabrone Neolithic tomb (Beckett 2011)

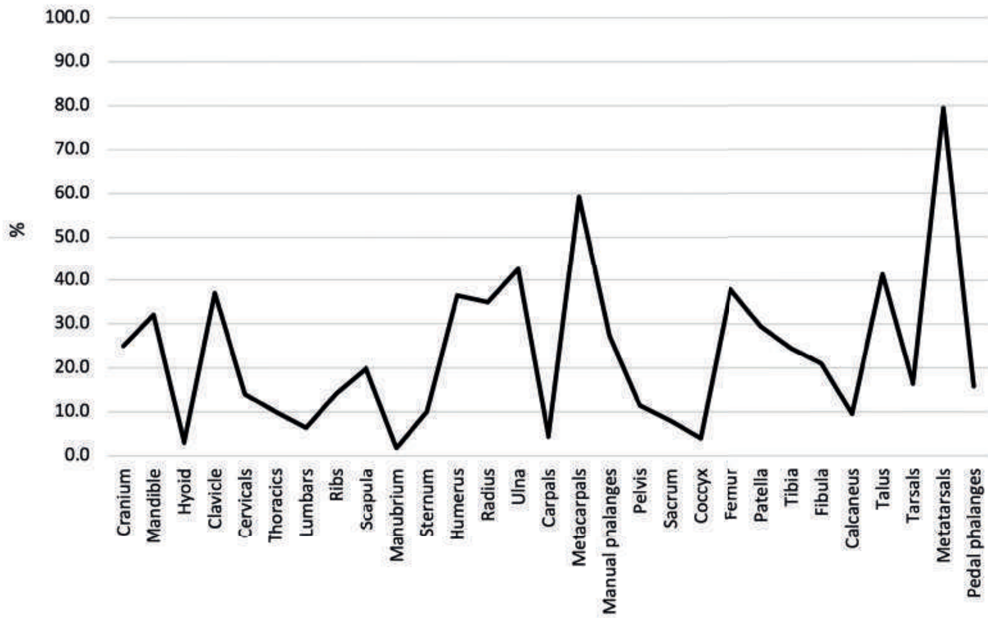

Figure 12.6. *Skeletal element representation in the Xemxija tombs indicating a residual pattern.*

tombs, crania (BRI=22.3%) and long bones (18.8–38%) are significantly under-represented. Metatarsals are the best-represented element, accounting for 70.1% of the MNI, and metacarpals are second, at 52.3%. This reflects a high degree of disturbance. The presence of small bones in the assemblage demonstrates primary interments were made, but robust elements were subsequently removed. The resulting varied profile of other skeletal elements is a result of both intrinsic and extrinsic factors, and in large part may be attributed to the nature of successive deposition. If the fragmentation of crania and long bones could be controlled for, for example through refitting, it is likely that their relative representation would increase. Furthermore, if it were possible to account for depositional practices within each tomb, it is feasible that some distinctions would emerge in each deposit.

The over-representation of specific elements is seen in numerous contexts, demonstrating secondary deposition. Cranial curation is evident in five contexts at the Circle: (354) from the upper levels of the North bone pit, (1307), (1144) and (951) in the Deep Zone, and (1024) from the 'Shrine' (Fig. 12.7). Cranial caching occurred throughout the caves, but there is a repeated emphasis on their deposition throughout the Deep Zone (cf Malone & Stoddart 2009, 367, Fig. 14.4) (Appendix Fig A1.45). Context (1307) dates to the early Tarxien phase, from 2930–2870 cal. BC (90% probability), while Context (951) may have continued in use as late as 2470 cal. BC (Malone *et al.* 2019). This area appears to have been used for re-deposition and careful clearance of remains from other areas of the cave complex over several centuries. The upper levels of the North bone pit contained largely disarticulated deposits and may likewise have been formed through the re-deposition of selected bones from the central space of the cave complex (Appendix Fig. A1.14). Radiocarbon dates indicate that at least one cranium in Context (354) pre-dates the basal deposit (799), and there is further evidence of curation in (669), from the mid-levels of the North bone pit. In all contexts in the pit except (354), an equal number of non-adult and adult crania were identified, suggesting curation was not just extended to adult remains.

Crania represent 67% of the MNI in Context (354), evidencing cranial curation alongside the apparent secondary deposition of elements including the pelvic girdle (the pelvis represents 50% of the MNI, and the sacrum 33%) and fibulae (17%). This sample is not representative of the full context, because of the high number of small fragments encountered. The original analysis further noted an equal representation of mandibles, humeri and femora, but the curation of crania is noted in the full deposit (Stoddart *et al.* 2009a, 118).

In the Deep Zone, cranial curation is evident in the samples of all the contexts analysed in this study. Only crania and mandibles are present in the sample from (1307), representing 50% of the MNI. In the full context, a high number of arm bones were noted (Stoddart *et al.* 2009a, 136), suggesting that this deposit contained the secondary deposition of both crania and long bones. In Context (1144), the mandible, hyoid, clavicle, sternum, humerus, radius, patella and talus are all absent; these elements are not just those which are prone to *in situ* degradation, therefore suggesting both natural taphonomic decay and cultural selection. Long bones account for 25% of the MNI, with similar values for elements of the axial skeleton. Surprisingly, the pelvic girdle represents 50–100% of the MNI, reflecting selective removal of long bones from primary interments, leaving behind the axial skeleton and pelvic girdle. In the upper levels, crania are over-represented in Context (951), at 86% of the MNI, with all other elements representing <40% of the MNI. Very few extremities and small bones are present. During excavation, the structured nature of secondary deposition in (951) was clear, with clusters of crania removed from associated mandibles, as well as caches of teeth observed (Stoddart *et al.* 2009a, 137).

Context (1024) covers both the 'Shrine' and Display Zone, evidencing a clear over-representation of crania. The remaining elements in this context are predominantly of the axial skeleton and pelvic girdle. Given the small number of bones encountered in this context, and its large distribution across the centre of the site, it is most likely that this represents selective deposition, primarily of disarticulated crania.

Long bones are over-represented in three contexts: (656) from the Southwest niche, and (436) and (743) from the Central pit (Fig. 12.8). In Context (656), the femur

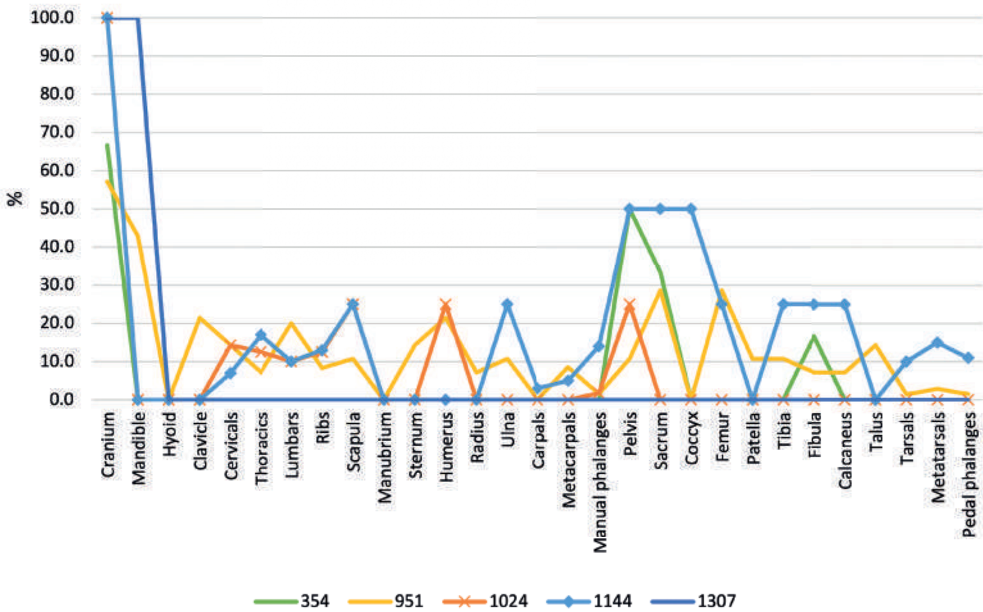

Figure 12.7. *Skeletal element representation profiles reflecting cranial curation.*

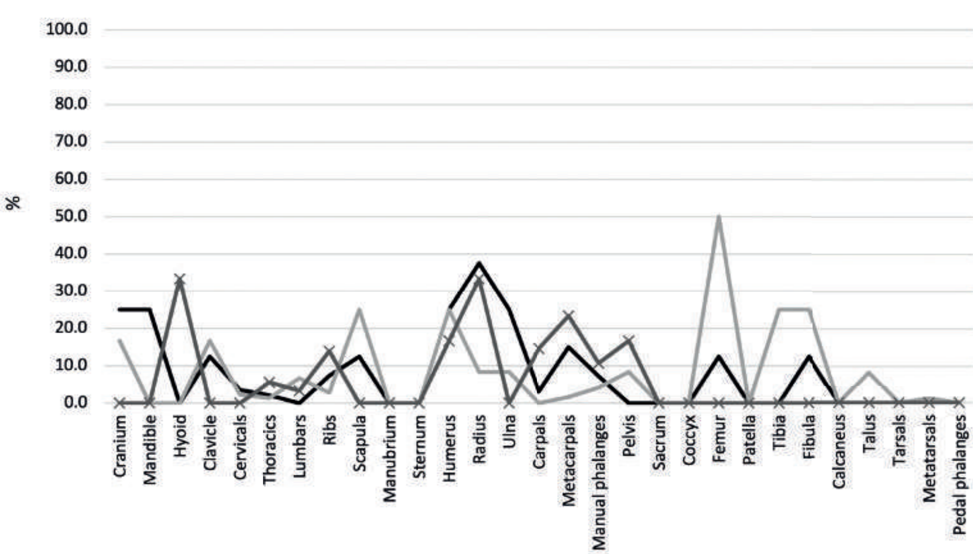

Figure 12.8. *Skeletal element representation profiles with an over-representation of long bones.*

is clearly the best-represented element (50%), followed by the tibia, fibula and humerus (25%). In the full assemblage from (656), teeth and femora produced the MNI (Stoddart *et al.* 2009a, 176), indicating the largely selective character of the deposit. Contexts (436) and (743), both in the Central Pit cut into the East Cave roof, were affected by the collapse of the cave roof, leading to slumping (Stoddart *et al.* 2009a, 118). The Central Pit reveals a depositional sequence of articulated non-adult individuals, interrupted by silting; the slumping is likely responsible for truncating the inhumations below the pelvis (Stoddart *et al.* 2009a, 121–2), accounting for the lower representation of elements of the lower limbs. The under-representation of small bones in both contexts is particularly emphasized because of the contrast with long bones, leading to the interpretation of these as secondary deposits. These results reveal the difficulties of interpreting element representation profiles without contextual data; the slumping of the deposits is responsible for the biased profile of element representation, and excavation records allow us to interpret these contexts as primarily indicating inhumation.

The remaining contexts from the Circle display notably uneven SER profiles. In most, nearly all elements are present, but they are often poorly represented. These can be broadly divided into two groups. The first group presents much lower overall element representation and includes contexts from the Circle rock-cut tomb, (595) and (734) from the Southwest niche, and (960) from the 'Shrine' (Fig. 12.9). In many of these contexts, claviculae are well-represented and there is an overlapping pattern of representation for elements of the pectoral girdle and vertebrae. Small and friable elements such as the hyoid, carpals, coccyges and phalanges are under-represented or absent. This pattern seems to correlate with density-related attrition, compounded by successive deposition. The presence of small bones indicates primary deposition, and the lack of fragile bones can be attributed to *in situ* destruction. At the base of one part of the Southwest niche, Context (734) is slightly more difficult to categorize, as elements of the pectoral and pelvic girdles are mostly absent, as well as lower leg bones. However, the presence of some vertebrae and small bones suggests primary depositions; this area may therefore have contained both disturbed primary interments and some secondary depositions.

The second group presents generally higher overall element representation, with some distinctions between each context (Fig. 12.10). In Context (799), from the base of North bone pit, (783) from the Display Zone, and (1206) from the 'Shrine', nearly all elements are present. Viewed alongside the taphonomic and contextual data, these profiles predominantly indicate primary deposition alongside alternative funerary practices. For example, (799) contains a male adult inhumation (Appendix Fig. A1.18) surrounded by secondary deposits of disarticulated remains, which are likely responsible for the over-representation of mandibles, *os coxae* and fibulae. The Display Zone is so-called because of the higher number of articulated remains encountered during excavation and its position within the site (Appendix Figs. A1.53–A1.61), suggesting this location was primarily used for inhumation (Malone & Stoddart 2009, 365). However, many individuals were disarticulated and rearranged. SER shows that

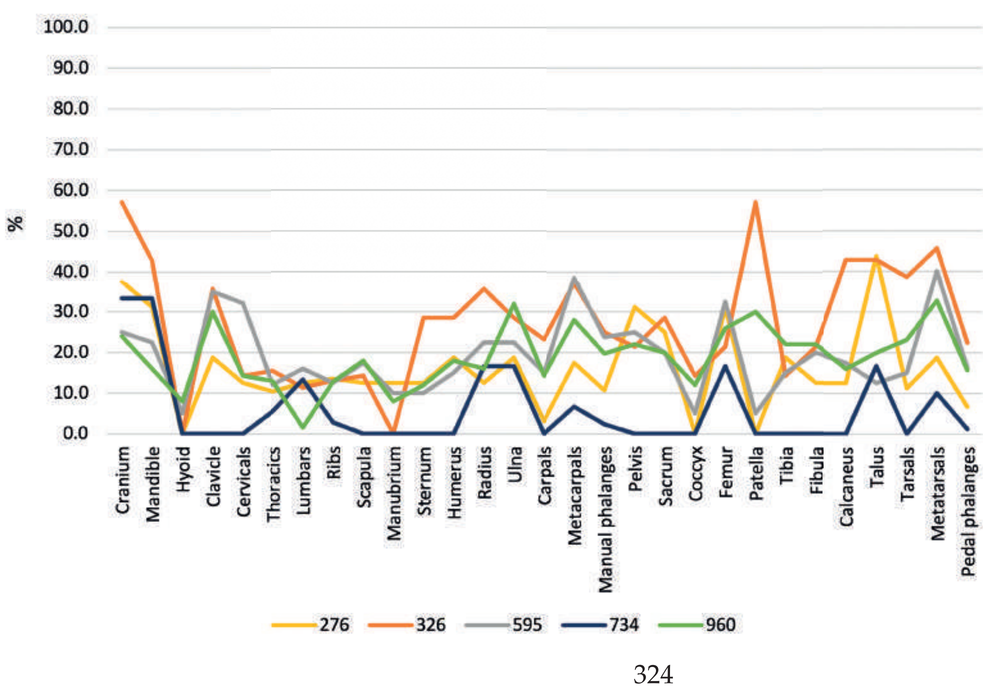

Figure 12.9. *Skeletal element representation profiles indicating primary successive deposition, with low overall element representation.*

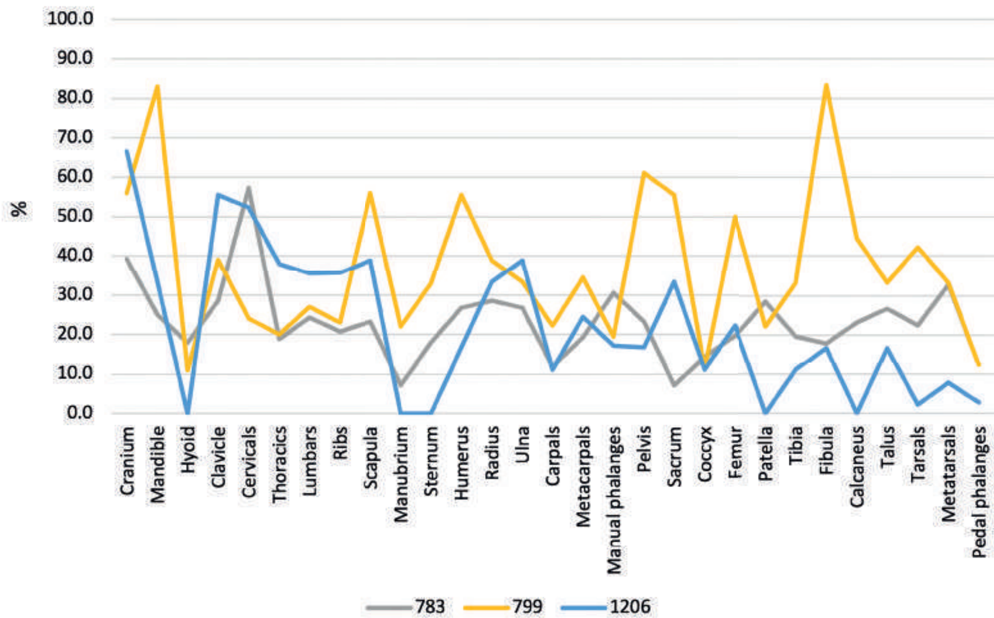

Figure 12.10. *Skeletal element representation profiles indicating primary successive deposition, with higher overall element representation.*

all bones were present in this deposit, although all elements except cervical bones represent <40% of the MNI. The low overall representation of most elements is likely a result of rearrangement and fragmentation because of overlying deposits, although it remains possible that some elements were removed from this deposit. In Context (1206), crania are the best represented element (66.7%) followed by claviculae (55.6%), and the presence of axial bones and small bones clearly indicates primary deposition. The lower limbs are less well-represented compared to the upper limbs, suggesting a patterned removal of selected elements. The successive deposition and disturbance of primary interments has therefore resulted in a mixed profile of element representation in these contexts.

In summary, secondary practices including the removal of specific bones, and their curation and deposition, are indicated through both residual element representation curves (Xemxija) and selective curation (Contexts (354), (656), (951), (1024), (1144), (1307)). However, deposits representing multiple or prolonged sequences of funerary practices are more challenging to interpret, particularly when extensive commingling has occurred. At the Circle, element representation profiles in which most bones are present but unevenly represented, correlate with successive deposition of primary, often subsequently disturbed, interments. This finding may be applicable to other commingled deposits which are lacking contextual and spatial information, suggesting that uneven SER profiles signal multiple funerary rites which have not strongly biased the representation of any specific elements.

The initial model of bone redistribution at the Circle examined the ratio of skull elements, long bones and residual bones within the largest contexts, based on the elements within each category which produced the highest MNI (Stoddart *et al.* 2009a, 320). This analysis found a core group of 5 contexts – (1268), (1206), (960), (799) and (1241) – with a similar representation of most elements, suggesting they were 'anatomically correct' in composition. However, this metric does not account for the *relative* presence of elements, as with the BRI. As the SER profiles of Contexts (1206), (960) and (799) indicate, primary deposition is demonstrated in these areas, but is not always the predominant practice, and the representation of elements varies according to a range of factors. While significant bones of each type are almost equally represented in these contexts, this pattern does not accord with the *sole* practice of primary deposition, nor with a similar repertoire of funerary practices in each context.

Analysis of skeletal element representation demonstrates a variety of funerary practices across both sites, including within discrete contexts and burial spaces. Primary deposition is noted in many areas through the presence of small and fragile bones. At the Xemxija tombs, long bones and crania are highly fragmented, which has suppressed their representation, but they are also likely to have been selectively removed from some tombs. At the Circle, bone removal is much more difficult to assess but, at the very least, remains were regularly and extensively redistributed across the cave complex, in some cases producing caches of crania and/or long bones. The proposed element representation signature for successive deposition, illustrated in

Figure 12.10, raises a significant question for analyses of collective, commingled deposits: how can multiple depositional practices, which are individually distinguishable, be recognized when they occur alongside each other? In the Display Zone, the 'Shrine' and the North bone pit, the slightly higher level of element completeness in these areas supports the interpretation for predominantly primary depositions, while the uneven representation of elements indicates mixed practices. In contrast, deposits with high levels of abrasion and erosion, including the Southwest niche, Xemxija tombs and Circle rock-cut tomb suggest greater disturbance of the remains and burial deposits.

12.5.3. In situ *articulation*

Analysis of *in situ* articulation provides crucial information regarding depositional practices. Applying the principles of archaeothanatological analysis, which distinguishes between labile and persistent joints, it is possible to interpret the timing of the disruption of anatomical connections and infer the original depositional position of a corpse (Duday 2006, 2009; Duday & Guillon 2006). Labile articulations comprise small bones or unstable joints, including the cervical vertebrae, scapulo-thoracic joint, hip, patellae, hands and distal feet (Duday & Guillon 2006, 128; Knüsel 2014, 32). These disarticulate early during decomposition and their disruption can evidence movement soon after death. Labile joints will usually, though not always, be preserved in undisturbed primary inhumations. The dislocation of elements forming a persistent joint can indicate disruption further into the *postmortem* interval, unless anthropogenic intervention is evidenced, for example through cutmarks. Persistent articulations tend to form weight-bearing joints, including the atlanto-occipital joint, humero-ulnar joint, lumbar vertebrae, the lumbo-sacral and sacro-iliac joint, tibio-femoral joint, ankle and tarsals (Duday & Guillon 2006, 128; Knüsel 2014, 32). However, depending upon a range of factors, including depositional position, environmental conditions, and whether a burial space is filled or left open, the usual sequence of joint disarticulation can vary (Mickleburgh & Wescott 2018).

In situ articulation at the Circle has been examined in deposits with excellent excavation records through cross-referencing skeletal elements studied post-excavation with their spatial location on plans. Where such cross-referencing is not available, the post-excavation analysis of non-adult remains which were stored together has inferred their discrete depositional context. Examples of both will be discussed, including (1) a study of the complete deposit from 1x1 m in (783), for which exceptionally good levels of recording were present; (2) analysis of non-adult remains in (1206) presenting varied levels of completeness, for which excavation plans reveal the close spatial location of elements.

All elements (Σ=3632) in grid square 97E/112N in (783) were analysed as the presence of bone numbers on excavation plans and storage bags allowed their cross-referencing. The excavation plans were digitized in ArcGIS by the lead author (§13.3 for detail of the intra-site GIS). The cross-referenced bone numbers, attributed to either individual bones or groups of bones, allowed analysis of the *in situ* spatial location and anatomical relationship of remains alongside taphonomic analysis. Investigating the sequence of deposition in this area, a striking pattern emerged. At the lowest levels, directly on the bedrock, an articulated non-adult skeleton was deposited, flexed on their right side with their right arm extended alongside the body, and their left arm flexed across the chest (Fig. 12.11). A chert scraper was found posterior to their pelvis and may have been deposited simultaneously (indicated by the red circle on Fig. 12.11). In the overlying levels, three partial axial skeletons in anatomical relationship were observed (Fig. 12.12). The anatomical relationship of these labile joints indicates primary deposition; the removal of skulls (from two) and limbs (from all), leaving vertebrae and ribs in connection, suggests this to be a significant residual signature. This was confirmed by analysis of element representation of the remains in this area: the pelvis represented 76% of the MNI and the scapula, 66%. Two of these axial skeletons indicate that individuals were placed on a

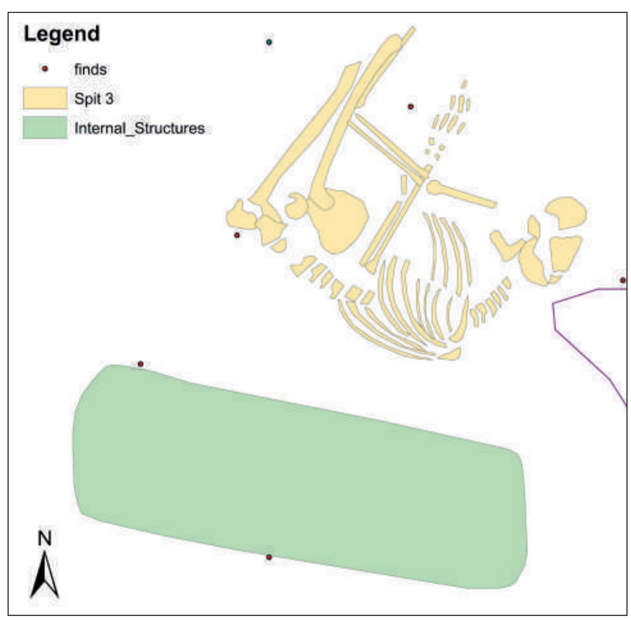

Figure 12.11. *Articulated non-adult skeleton in spit 3 at the base of (783) 97E/112N.*

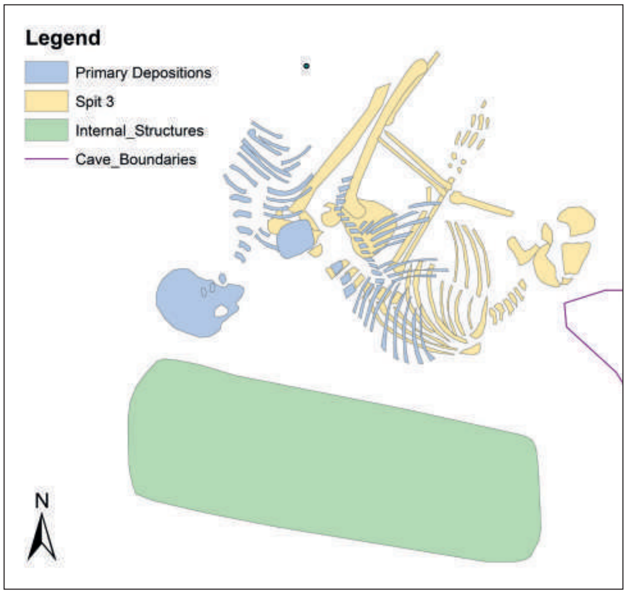

Figure 12.12. *Remains of primary inhumations evident as axial skeletons (in blue), with two in the same position as the individual in spit 3.*

similar axis as the basal inhumation. The third individual was placed on a north-south axis, with their head to the south, facing east. There are two important implications of this finding: firstly, depositional sequences were not always initiated by the interment of adults (such as in the North bone pit and the 'Shrine' area). Secondly, similar burial positions throughout depositional sequences are observed throughout the cave complex; a high number of non-adult remains in this area (at least 73%) attests to the parity of treatment across individuals of all ages (Thompson *et al.* 2020).

In Context (1206), in the lower levels of the 'Shrine', many perinatal and infant remains were encountered during excavation. Four non-adult skeletons were analysed and varying levels of completeness were observed, from a nearly complete cranium, torso and upper limbs of a perinate (Fig. 12.13), to only cervical and thoracic vertebrae, some ribs, claviculae and basicranium of an infant (Fig. 12.14). These results accord with the evidence from Context (783) for a sequential process of disarticulation; perhaps limbs were removed in stages, and skulls removed as a final step in disarticulating or 'unmaking' the dead. While

Figure 12.13. *Perinate in (1206) 98E/110N, spit 4, units 23 and 25. The skeleton is missing below the lumbar vertebrae. Scale bar: 2 cm. (Photo Jess E. Thompson).*

Figure 12.14. *Infant (1206) 99E/111N, spit 3, skeleton 19. The calvarium, facial bones, all long bones and the pelvis seem to have been removed. Scale bar: 2 cm. (Photo Jess E. Thompson).*

a residual signature of selective removals is typically indicated through the over-representation of small bones (discussed above and in Robb 2016), elements of the extremities are exceptionally prone to taphonomic degradation in very young individuals. The residual signature of a high representation of elements of the axial skeleton therefore also reveals the selective removal of remains from non-adult skeletons.

12.6. Deathways at the Circle and the Xemxija tombs

Several key variables have affected the preservation and condition of skeletal remains at both sites. Although the limestone geology of the Maltese Islands is amenable to bone preservation, its porosity also means that it is prone to inundation. Located at high elevations, it is possible that both the Xemxija tombs and the Circle occasionally experienced low levels of inundation because of surface water run-off, and this may have shifted bones, accelerated their degradation, and caused sediment concretion in some areas. Indeed, soil lenses demonstrated that this occasionally happened at the Circle, and these were evident as former puddles around the edges of the caves and in depressed zones, such as Context (783). Root etching has also undermined bone preservation, contributing to cortical degradation and occasionally causing bones to split. Deposits would also have been susceptible to tumbling; if corpses were placed on precarious deposits or at angled orientations, such positioning would have influenced the movement of bones as they progressed through decomposition (Appendix Fig. A1.61). With exceptionally deep burial deposits throughout the cave complex, bones were almost certainly trampled, especially during the later stages of the site's use. These processes, alongside the effects of successive deposition, contributed to substantial disarticulation and fragmentation.

Untangling the effects of natural processes and cultural practices on element representation, the predominance of primary interment in most contexts is demonstrated. Apart from several contexts with a clear emphasis on the re-deposition of disarticulated elements, most demonstrate the co-occurrence of both primary and secondary practices, with the balance differing in each space. Classification of the element representation profile and inferred funerary practices in each context is presented in Table 12.5. As discussed above, several contexts did not present a clear or predictable signature of depositional modes through SER, and therefore small differences in the representation of some elements alongside reference to excavation records, provides further insight into funerary practices.

Drawing together the results from both sites, a model for the typical sequence of deathways is proposed (Fig. 12.15). At both the Xemxija tombs and the Circle, non-adults are incorporated in the burial space and treated similarly to adults, although fewer

Table 12.5. *Chronological phasing of contexts and dominant funerary practices (abbreviations: P: Primary; R: Reduction, SD: Secondary Deposition, BR: Bone Removal; CC: Cranial Curation).*

Context	Location	Phase	SER profile	Inferred practices
276	Rock-cut tomb: West chamber	Ġgantija	Successive deposition	P, R, BR, CC
326	Rock-cut tomb: East chamber	Ġgantija	Successive deposition	P, R, BR
Xemxija tombs		Ġgantija, Early–Middle	Residual	P, R, SD, BR
354	North bone pit	Early	Cranial curation	SD, CC
1307	West Cave: Deep Zone	Early	Cranial curation	SD, CC
595	East Cave: Southwest niche	Early	Residual	P, R, SD, BR
656	East Cave: Southwest niche	Early	Secondary deposition	SD (especially long bones)
734	East Cave: Southwest niche	Early	Successive deposition	P, R
799	North bone pit	Early	Successive deposition	P, R, SD
951	West Cave: Deep Zone	Early	Cranial curation	P (occasional), SD, CC
1024	West Cave: 'Shrine'	Middle	Cranial curation	SD, CC
1144	West Cave: Deep Zone	Middle/Late	Cranial curation	P, SD, CC
960	West Cave: 'Shrine'	Middle/Late	Successive deposition	P, BR
436	East Cave: Central bone pit	Latest	Long bone curation	P
1206	West Cave: 'Shrine'	Late	Successive deposition	P, BR
743	East Cave: Central bone pit	Latest	Long bone curation	P
783	West Cave: Display Zone	Latest	Successive deposition	P, SD, BR, CC

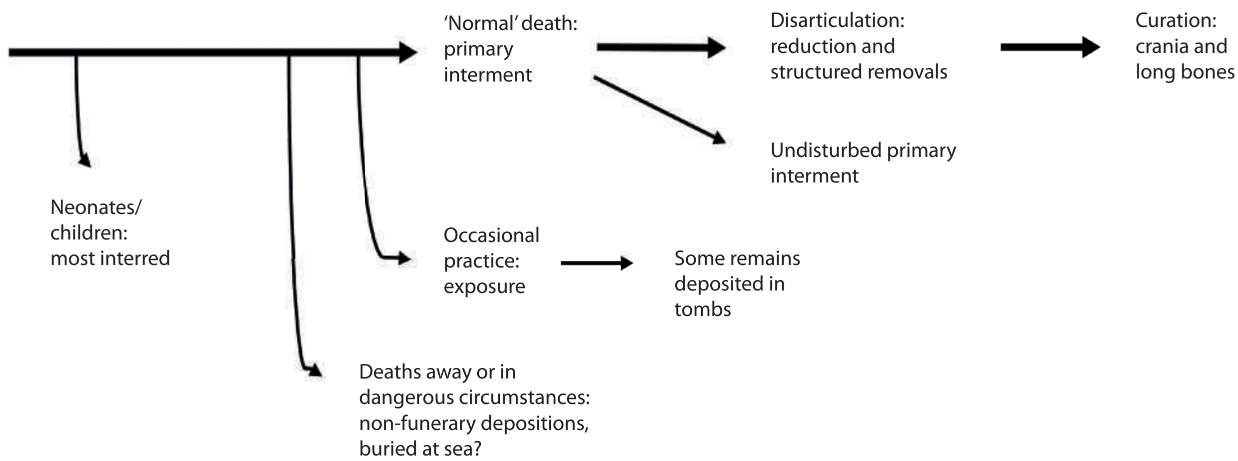

Figure 12.15. *Proposed model of deathways based on reconstructing funerary practices at the Circle and Xemxija tombs.*

non-adult remains appear to have been removed from the Xemxija tombs. At the Circle, the representation of non-adults fluctuated over time, increasing in the caves compared to the rock-cut tomb, with a slight peak during the middle Tarxien phase (Thompson *et al.* 2020). This accords with the KDE analysis of radiocarbon dates which indicate increased density of deposition around this time (§3.2 & Fig. 3.4), and also coincides with a widespread phase of cultural elaboration across the islands (Evans 1959). The greater number of non-adults buried in this phase may suggest increased fertility, demonstrating the close relationship between burial demographics and the population structure (Thompson *et al.* 2020).

The close similarities between the treatment of adults and non-adults in Neolithic Malta are especially noteworthy, contrasting the differential deathways for infants and young children across many regions of Neolithic Europe. In Neolithic Italy, non-adult remains were more likely to be disarticulated compared with adults, suggesting that younger individuals achieved a social death more quickly, and were retained within cultural memory for a shorter period of time (Robb 2007a, 62–3, 2007b, 292). At Copper Age Italian sites, neonates and infants are often under-represented (Bailo Modesti & Salerno 1998; de Marinis 2013) or lack grave goods and post-depositional treatment (Colini 1898; Muntoni 2001). Their significant under-representation is also noted at sites dating to the Copper Age in Iberia and along the Atlantic coast of Portugal (Beck 2016; Waterman & Thomas 2011), and at Neolithic sites in France (Le Roy 2017) and Britain (Smith & Brickley 2009). This demographic pattern is not solely as a result of taphonomic processes, and appears to be culturally motivated, suggesting that very young individuals were frequently understood to inhabit a marginal place in the life course, which affected their social position and personhood.

The usual funerary treatment at both sites involved primary deposition, often followed by rearrangement and curation of remains, perhaps multiple times. At Xemxija, curation occasionally involved the removal of selected bones from the burial space.[3] In contrast, at the Circle, remains appear to have circulated solely within the limits of the Circle. However, these secondary practices typically focused on the skull or cranium, and the limbs (or long bones), reducing the body to the trunk and its appendages. The extent and process of rearrangement cannot be examined at the Xemxija tombs. In comparison with the Circle rock-cut tombs, we might expect that fewer articulations would have remained in the Xemxija tombs than we see at the Circle caves, suggesting increased rearrangement of remains in small chambers. At the very least, the extent of fragmentation of the Xemxija bones supports this hypothesis.

At the Circle, the application of archaeothanatological principles has provided new details on the process by which some individuals were disarticulated. In several areas, including the Circle rock-cut tomb, the Display Zone and the 'Shrine', a paradoxical pattern of *in situ* articulation was discerned (Maureille & Sellier 1996), with the disruption of persistent joints and maintenance of more unstable articulations suggesting the disarticulation of partially fleshed remains. Several photographs of *in situ* deposits capture this phenomenon, depicting articulated extremities separated from the rest of the skeleton (Appendix Figs. A1.15, A1.21

& A1.46) and instances of articulated vertebrae, sometimes alongside ribs (Appendix Figs. A1.31, A1.56, A1.58, A1.60 & A1.70). While earlier analyses noted the manipulation of skeletonized remains (Malone *et al.* 1995; Stoddart *et al*. 1999; Stoddart *et al.* 2009a), these results reveal occasional encounters with the fleshed, and perhaps also decomposing, dead. The absence of cutmarks remains difficult to understand, though cannot be entirely attributed to poor cortical surface preservation, as bone cortices are notably better preserved at the Circle than in the Xemxija tombs. As has been noted with reference to secondary burial practices in sub-Saharan Africa, these actions require 'considerable anatomical knowledge and autopsy skill' (Insoll 2015, 161). As such, it is evident that at least certain individuals were knowledgeable about the process of decomposition, as well as anatomy, and this knowledge was used to intervene with and manipulate the remains of the dead.

Engagement with the dead after their initial deposition took a variety of forms. This stage of the *postmortem* process appears to have been flexible and dynamic, shaped by a whole series of factors, perhaps principally the timing at which remains were revisited. The length of time between deposition and post-depositional intervention influenced the stage of decomposition or disarticulation an individual would have reached. Yet, which choices were made in the sequence of disarticulation, and the timing at which these actions were carried out, are typically difficult to assess as they result in different, and sometimes overlapping, taphonomic signatures. At the Circle, careful comparison between taphonomic modifications, statistical analyses of element representation, and observation of remains *in situ* has been crucial in identifying both the evident variation in deathways, and their flexibility, with little difference noted between individuals on the basis of their age or sex.

Nevertheless, these processes indicate that progressive disarticulation was the core aim of post-depositional rites, producing deposits of bones and remains in mixed stages of disarticulation. In many cases, dense deposits of disarticulated remains were interspersed with occasional semi-articulated individuals or body parts, or with clusters of crania or long bones. These distinctions might have related to different types of death and been reserved for individuals with very specific life histories or social positions, although these qualifiers do not seem to have related to age at death or to gender identity. Overall, death was brought about over a protracted period of, perhaps repeatedly, reducing the person to ever smaller parts.

This raises the question of alternative deathways, as all societies incorporate multiple strategies for disposing of the dead. It is unlikely that the majority of the Neolithic population of the Maltese Islands was deposited in a rock-cut tomb, cave complex or hypogeum upon their death. Prehistoric population size estimates for the islands range from 4713 individuals (Grima 2008) to 11,000 (Renfrew 1973, Renfrew & Level 1979). Recent carrying capacity estimates suggest the population size could have been close to 10,000 based on the nuances of soil stability (Bennett 2020, 246). The total number of individuals accounted for from Neolithic burial sites to date is far lower than any of these carrying capacity estimates, therefore revealing potentially thousands of dead individuals missing from the archaeological record (Chapter 14 for an overview of burial sites, and Thompson 2020 for a synthesis). Recognizing that the MNI always significantly under-estimates the *original* burial population (Robb 2016) might take us to the lower end of these population size estimates. The few cases of rodent gnawing and extensive weathering at the Xemxija tombs suggests that some individuals might have occasionally been exposed, after which selected remains were placed in the tombs. As a result of the apparent infrequency of this practice, circumstances surrounding an individual's death, or relating to their social role, might have influenced this treatment. However, it is also possible that the tombs remained open during use, and the issue of equifinality makes it difficult to resolve this.

From the Neolithic Italian burial record, rare burial locations and unusual circumstances of death stand out clearly from the typical practice of interment and subsequent disarticulation within villages (Robb 2007a, 64; 2007b, 293). These include exposure, in one case in a ditch (Robb *et al.* 1991) and another in a well (Tinè 1983), and some potential cases of mass burials perhaps because of epidemics or warfare (Carancini & Guerzani 1987; Tunzi Sisto 1990). There is relatively little evidence for trauma as a result of interpersonal violence in Neolithic Malta (§8.7.7), and at present no evidence for violence on a greater scale. Nevertheless, it remains probable that there were individuals who were excluded from collective funerary spaces, perhaps if they were perceived to have died a 'bad' death or transgressed socially. Given the current lack of evidence for human remains at contemporary settlements, it is likely that any distinctive treatment took forms which did not leave a lasting archaeological trace. Exposure without subsequent retrieval and deposition of remains would be unlikely to be detected, unless a built platform was used and maintained for some time. Grima (2001) has argued for the significant cosmological role played by the sea, as a liminal space surrounding the islands; perhaps it may have been further conceptualized as a space appropriate for the transition of death, with deposition at sea occurring in exceptional cases.

12.7. Conclusion

Reconstructing the treatment of the dead at the Circle and Xemxija tombs through taphonomic analysis has revealed a greater diversity of practices than previously realized. This research provides the first reported evidence of charred bone and dermestid beetle modifications to Neolithic Maltese human remains (Thompson *et al.* 2018; Thompson 2020). The latter, importantly, demonstrate that the identification of what might be deemed natural taphonomic processes can have implications for understanding cultural practices. Crucially, primary deposition and subsequent disarticulation within underground burial spaces were practices which endured throughout the late Neolithic, from the 4th to late 3rd millennium BC. This repertoire appears to have expanded in the Tarxien phase, around 2900 cal. BC, to encompass careful selective removal of specific elements. Identified through paradoxical patterns of *in situ* articulation, these selective removals strongly suggest that some disarticulation occurred while individuals were in advanced stages of decomposition. Furthermore, this initial analysis of articulation through the intra-site GIS suggests that there were more cases of partial articulation preserved in the Circle cave complex than originally realized.

As the categorization of funerary practices within each context shows (Table 12.5), there was constant, persistent variation in the ways that the dead were treated, and also in the range of skeletal elements and processes represented within each discrete burial space. Within this variation, the prolonged and repetitive nature of these acts speaks to a lengthy process of dying, in which social interaction with the dead was gradually curtailed. The specific ways in which this was achieved were negotiated on an individual basis. Once death was final, most often signalled through complete or partial disarticulation, greater freedom in the treatment of remains may have been possible. For example, the movement and rearrangement of body parts over larger distances, the clearance of deposits from niches and into harder-to-access spaces, and the erection of megaliths into older deposits (such as the eastern stone screen, see Stoddart *et al.* 2009a, 154). The North bone pit at the Circle appears to have built up through clearance of remains from the cave complex, over a period of several generations, and incorporated fully and partially disarticulated remains, as well as curated crania (Malone *et al.* 2019). Contextual and element representation data likewise indicate that the main deposit in the Deep Zone, Context (951), was formed through clearance episodes in which remains from across the cave complex were redistributed (Stoddart *et al.* 2009a, 137).

The timing of funerary practices was likely closely related to the ongoing remembrance of the dead and their burial location. Over the short-term, perhaps from a single to several generations, commemoration would have guided the placement and positioning of successive depositions, and sequential disarticulation could have been a process of managing the gradual forgetting of the dead person. Altogether, the collective power and presence of the dead assured the living that they, too, would remain present in collective memory long after biological death. Such a prolonged ontological transformation of the dead, further sedimented through the longevity of use at many burial sites, may be almost unique in the context of Neolithic Europe.

Ethnographic and ethnohistoric documentation of collective funerary practices consistently demonstrates the significance of these rites for maintaining relationships with place and community, in ways that differ locally (e.g. Bloch 1982; Creese 2015; Lau 2015; Seeman 2011). Recent research into the maintenance of the prehistoric ecology of the Maltese Islands convincingly argues that co-operative communal labour was necessary to sustain life on the islands (Clark 2004; Barratt *et al.* 2018; McLaughlin *et al.* 2018). The products of that labour, however, produced a theatrical architecture where ritual specialists could undoubtedly show their skills and charisma. In the same way, whereas the inclusion of all age grades and genders echoes these values, highlighting 'the dialectic relationship of the person and the corporate social group' (Skeates 2010, 235), it is still worth asking why a number of significant locations in the complex gave prominence to males. Most notably, the very threshold of the site partly covered a male who was memorialized with his ancestors. On the one hand, the significance of place and materiality in prehistoric Maltese identity is apparent, supporting the case made by Robb (2001) for a deliberate construction of difference. On the other hand, the very biology of these very inhabitants suggests (a small gene pool with) a fluctuating and ultimately reduced mobility with the outside world (Ariano *et al*. 2022). As so often, the prehistoric past is proven to be more complex and ultimately richer than the first simple models suggest.

Acknowledgements

This chapter is based on the first author's PhD research, funded by the University of Cambridge *Arts & Humanities Research Council* Doctoral Training Partnership [Grant Number 1652796] and Magdalene College, Cambridge. Permission to analyse the skeletal remains from the Circle and the Xemxija tombs was granted by the Superintendence of Cultural Heritage for Malta, Heritage Malta, and University College London (UCL), for which we are extremely grateful. We extend thanks to Sharon Sultana, senior curator of the National Museum of Archaeology, Valletta, for access to the Circle assemblage, and to Dr Rachael Sparks, keeper of collections at UCL, for access to the Xemxija tombs assemblage.

Notes

1. Rodent gnawing was also identified by Ronika K. Power on one perinatal femur from Context (951) in the Deep Zone at the Circle, but this element was not included in this study.
2. Further burning was recorded in Context (68) (n=1), Context (75) (n=1), Context (113) (n=2), Context (132) (n=1), Context (329) (n=1), Context (433) (n=1), Context (920) (n=1), Context (931) (n=1), and Context (951) (n=1) (Ronika K. Power pers. comm.)
3. Some alternative hypotheses may be put forward for this, including historic looting, and differential practices across tombs. However, neither are verifiable, and the biased representation of long bones at Xemxija accords with their centrality in secondary practices at the Circle.

Chapter 13

The development of Late Neolithic burial places in Malta and Gozo: an overview

Anthony Pace

To the memory of Ann Monsarrat (1937–2020)

13.1. Introduction

The development of Maltese Late Neolithic funerary monuments as a distinguishable cultural phenomenon which, in many ways, was the other important cultural aspect that accompanied the great megalithic structures of Malta and Gozo, is made clear in the Ħal Saflieni Hypogeum and the Circle. The more conspicuous and well-known megalithic buildings have been studied for their evolution, design and construction engineering (Mayr 1901; Zammit 1910; Ceschi 1939, 1970; Evans 1971; Trump 1981, Renfrew 1973; Torpiano 2004; Clark 2004). In such studies, the Ħal Saflieni Hypogeum and the Xemxija tomb cluster, have been cited as important elements in the evolution of the Maltese megaliths: in the case of the Hypogeum, to illustrate Ceschi's theory of corbelled roofs (Ceschi 1939) and in the case of the Xemxija tombs, as the original inspiration behind the surface architecture of the archipelago (Evans 1971, 1977; Trump 1981).

However, alternative explanations have been suggested for an autonomous structural evolution of Maltese prehistoric burial places following a departure from initial central Mediterranean cultural traditions (Pace 1990). This 'parting of ways' is best represented by a distinct elaboration of burial places which occurred together with the emergence of an advanced form of megalithic architecture which has been dated to the Ġgantija and Tarxien phases (Pace 1990, 1992, 2000, 2004a, 2004b). Unlike the central Mediterranean origins of rock-cut tombs, however, the genesis of Malta's Late Neolithic buildings in the form known today, is unknown, although a much older tradition of building significant structures have been noted from much earlier phases at Skorba, which went on to become a megalithic complex that complemented ta' Ħaġrat (Trump 2002; Pace 2004b). During the Ġgantija and the Tarxien phases, Late Neolithic Malta and Gozo experienced a flowering of home-grown creativity with materialities that comprised art and architecture (Pace 1996), idiosyncratic representations of the human figure (Vella Gregory 2005), the use of landscape (Renfrew 1973, Grima 2004a), rituals, possible celestial observations (Ventura & Agius 2017, Cox 2001) and maritime activity. The manner in which burial sites were thought of, located (Fig. 13.1), embellished and architecturally developed was naturally influenced by the cultural developments of the Ġgantija and Tarxien phases. Here I revisit earlier work on the subject in order to articulate new developments in Maltese Late Neolithic funerary architecture.

13.2. Background

The study of prehistoric rock-cut cemeteries came to the fore with the reporting of the Ħal Saflieni Hypogeum (Fig.13.2) to government authorities in December 1902 (Caruana, 1903; Zammit 1910; Pace 2000). The impact of this discovery was far-reaching in raising awareness about the importance of Maltese antiquities both as cultural assets and as visitor attractions (Grima 2000). During the subsequent three decades, up to the death of Sir Temi Zammit in 1935, a number of important prehistoric burial sites were discovered and reported to the newly established Museum Department. With the exception of the Nadur (Binġemma) tomb, these discoveries were made accidentally during trenching works, quarrying, or when exposed after heavy rains. The Hypogeum also confirmed the existence of a prehistoric past, an idea that had been broached during the 19th century (Smyth 1829; Rhind 1856; Fergusson 1872), but was firmly introduced by Albert Mayr in 1901 (Mayr 1901; Stöger 2000). The discovery of Bronze Age and earlier deposits at Tarxien in 1915 (Zammit 1916) reinforced the chronological divisions in Malta's past. Pottery from Tarxien could also be correlated

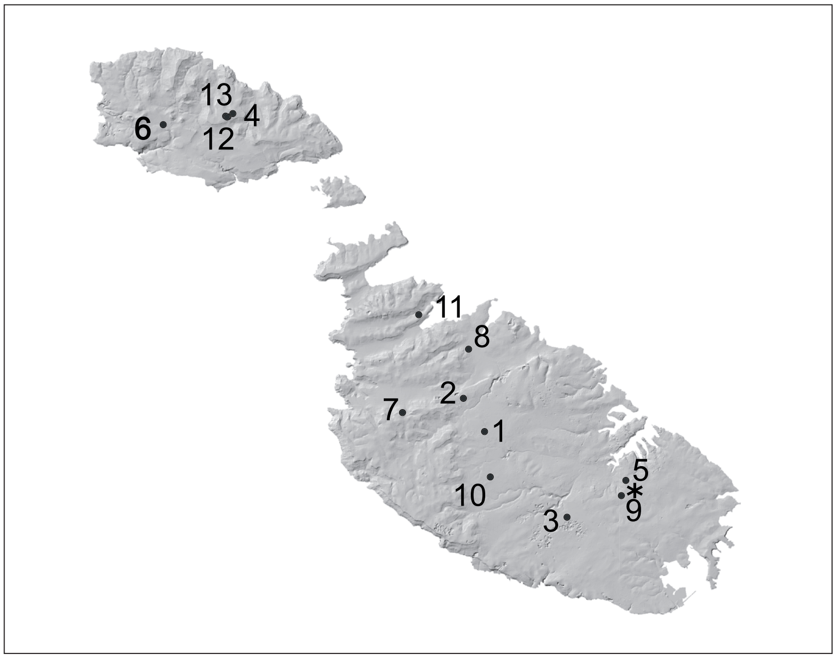

Figure 13.1. *Distribution of rock-cut burial sites referred to in this chapter: 1. Buqana (Attard); 2. Busbesija; 3. Bur Megħeż; 4. Ġgantija North Cave; 5. Ħal Saflieni Hypogeum; 6. Kerċem; 7. Nadur (Binġemma); 8. San Pawl Milqi; 9. Santa Luċija; 10. ta' Trapna (Żebbuġ); 11. Xemxija; 12. Xagħra; 13. Circle; * Tarxien Cremation Cemetery.*

with that gathered from other sites. At the time, Prof. N. Tagliaferro had examined pottery from the Hypogeum as well as the cave at Bur Megħeż (Tagliaferro 1910; 1911) (Figs.13.3 & 13.4). In his 1928 monograph on Maltese rock-tombs, Zammit could therefore distingush prehistoric burials from the later Phoenician and Roman examples. In a relatively short span of time therefore, the idea of a Maltese prehistory comprising buildings, art objects, cemeteries and human remains was firmly established.

Though exceptional, the various discoveries of the few prehistoric burial sites in Malta and Gozo present an uneven picture of their state of preservation, a factor which has an important bearing on how best to understand the monumentality of these sacred places. The first group of rock-cut cemeteries were encountered during the 'Zammit decades', with six discoveries being made between 1902 and 1928 (see Table 13.1).

The discovery of the Hypogeum (Figs. 13.2 & 13.13.) in the closing weeks of 1902 was not reported immediately to authorities, despite the extent of the underground levels of the site. Though substantial in scale, the existence of the monument was concealed while the entire area of Ħal Saflieni was being rapidly urbanized. Temi Zammit observed that this urbanization was the result of hundreds of workers moving into the area to be closer to the harbour dockyards (Zammit 1910). By the time the newly appointed Museum management committee requested Fr Magri to explore the Hypogeum (Museum Department 1904, iii), Ħal Saflieni had been covered over by houses and streets (Zammit 1910). Foundation trenches at the surface level of the site show that the construction of the houses was carefully carried out in such a way as to bridge over the subterranean voids (Pace 2000). During the first official inspection of the site, Caruana could only report on the existence of two subterranean levels, but noted that the original entrance of the site was still undiscovered and that access to the monument was through shafts in the surface (Caruana 1903). The house and street construction obliterated any remains of surface structures that may have once existed on top of the Hypogeum.

Figure 13.2. *Old view of the Ħal Saflieni Hypogeum Middle Level by R Ellis, courtesy of Heritage Malta/ National Museum of Archaeology. The photograph captures the site cleared of debris and deposits. The site was excavated by Fr M. Magri and Sir T. Zammit between 1903 and 1911 (Photo National Museum of Archaeology).*

Table 13.1. *Catalogue of known and likely late Neolithic burial sites in Malta and Gozo.*

Site	Location	Region	Site type	Phase	Level of recovery	Date of discovery	References
ta' Trapna iz-Żgħira (Żebbuġ tombs)	Malta	Żebbuġ	Rock-cut tombs (5)	Żebbuġ	Moderate	1947	Baldacchino & Evans 1954; Evans 1971, 166–9
San Pawl Milqi	Malta	Burmarrad	Rock-cut tombs (4)	Żebbuġ	Moderate	1968	Cagiano de Azevedo 1969
Near ta' Kola Windmill	Gozo	Xagħra	Rock-cut tomb?	Żebbuġ	Low	?	?
Buqana	Malta	Attard	Rock-cut tomb	Żebbuġ–Ġgantija	Limited	1910	Evans 1971, 6; Zammit 1912, 1928
Xagħra rock-cut tomb	Gozo	Xagħra	Rock-cut tomb	Ġgantija	Limited	1928	Evans 1971, 190; Zammit 1928
Xagħra Brochtorff Circle rock-cut tomb	Gozo	Xagħra	Rock-cut tomb	Ggantija	Good	1988	Malone et al. 1995; Malone et al. 2009f
Xagħra Brochtorff Circle	Gozo	Xagħra	Hypogeum	Żebbuġ–Tarxien Cemetery	Good	1989	Malone et al. 2009d
Ħal Saflieni	Malta	Paola	Hypogeum	Żebbuġ–Tarxien	Limited	*c.* 1900	Dukinfield Astley 1914; Mifsud & Mifsud 1999; Pace 2000, 2004; Tagliaferro 1910; Zammit 1925
Xemxija rock-cut tombs	Malta	St Paul's Bay	Rock-cut tombs (7)	Ġgantija–Tarxien	Moderate	1954	Evans 1971, 112–16; Pike 1971b, 1971a
Bur Mgħez	Malta	Mqabba	Natural cave	Ġgantija–Tarxien Cemetery	Moderate	1911	Evans 1971, 40; Tagliaferro 1911, 1912
North Cave	Gozo	Xagħra	Rock-cut tombs	Ġgantija	Low	1949	Evans 1971, 183
Nadur	Malta	Rabat	Rock-cut tomb	Ġgantija	Low	1926	Evans 1971, 107–8; Zammit 1928, 483
Bubisija	Malta	Mdina	Rock-cut tomb	Ġgantija	Limited	1928	Evans 1971, 28
Kerċem	Gozo	Kerċem	Rock-cut tombs	Tarxien	Good	2009	Bernardette Mercieca-Spiteri pers. comm.; Times of Malta 2009
Santa Luċija	Malta	Santa Luċija	Hypogeum	'Temple' period	Limited	?	Magro Conti 1997; Skeates 2010, 224–5
Ta' Vnezja	Malta	Mosta	Rock-cut tomb	'Temple' period	Limited	1936	Evans 1971, 28

Such a megalithic structure also marked the Circle on Gozo, which still retains a number of stones (Stoddart *et al.* 2009c, 188). Between 1990 and 1992, a series of archaeological excavations were undertaken at street level as part of the Hypogeum conservation project (Bonello 2000; Cassar 2000). The excavations revealed remains of a surface structure which included a ceremonial entrance and a ramp leading to the Upper Level (Cutajar 2000). A number of megaliths from this surface structure are still visible in the Upper Level.

In November 1910, the year that Zammit published the first report on his work at the Hypogeum, a small tomb was encountered at Buqana (Figs. 13.3 & 13.6), Attard, during trenching works. By the time Zammit arrived on site to inspect the discovery in the afternoon, most of the tomb was destroyed (Zammit 1909–12, 77). A corner of the tomb did however survive in section, enabling Zammit to make a rough sketch of what he later described as a bell-shaped 'well-tomb' (Museum Department 1910-1911, iii). The bottom of the tomb was about 1.5 m across, its depth about 1 m from the surface of the road. An interesting aspect of this discovery is the amount of Punic pottery and human bones which Zammit retrieved from the oblong

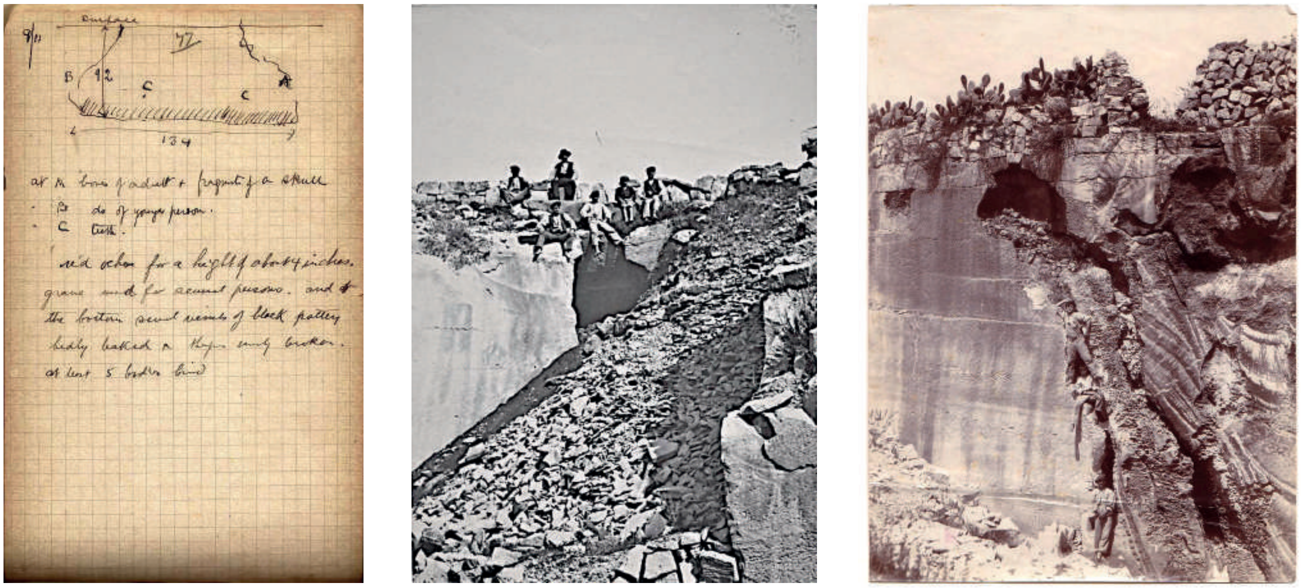

Figure 13.3. *a) Buqana tomb: a section sketch by Sir Temi Zammit who inspected the site in 1910; the tomb was damaged during trenching works and today lies buried underneath the former World War II airfield at Ta' Qali. b) Bur Megħeż cave: one of many features discovered during industrial quarrying and examined by Prof. N. Tagliaferro in 1911. The quarry in which the burial cave was discovered was later purchased by government authorities in 1920. Neighbouring quarries remained active into the 1930s. Zammit persisted in recommending the purchase of additional land to safeguard the Tagliaferro cave. c) Bur Megħeż quarry: a large cavity in the quarry face, but partly obscured by modern debris, seen in the forefront.*

shaft, suggesting that prehistoric tombs may have been disturbed and re-used. Prehistoric pottery, which John Evans later dated to the Żebbuġ, Mġarr and Ġgantija phases (Evans 1971, 6), was retrieved from a deposit of earth and red ochre from the bottom of the tomb (Museum Department 1910–1911, iii). The Buqana discovery suggests that, though uncommon, prehistoric rock-cut tombs may have been reused in later times. This is also suggested by the Nadur (Binġemma) tomb (Fig. 13.1) which Zammit came across when surveying Punic tombs.

The burial cave at Bur Megħeż (Figs. 13.1, 13.3, 13.4, 13.7) sometimes spelt Bur Meghoz, Burmghez (Farrugia 2016) or Bur Mghez (Evans 1971) was one of the most important discoveries of the early 20th century. Knowledge about the cave and its contents is limited to Prof. N. Tagliaferro's accounts (Tagliaferro 1911, 1912). The cave had been known to quarrymen for some time. They informed Prof. Tagliaferro of its presence during his examination of a fissure in the quarry known as 'tan-Naxxari'. This deep quarry still exists and is now within the security area of Malta's international airport. The present author has inspected the site. The immediate area of the cave appears to have been quarried away. The area was also damaged by enemy action during the second World War. Only a small feature, perhaps belonging to the original entrance of the burial cave, seems to have survived. Modern military structures have been built in the space once occupied by the cave. A number of features can still be seen in the quarry faces. Some of these are natural, but one in particular is a rock-cut bell-shaped feature which was truncated in section by the quarrying. It is quite possible that the site of Bur Megħeż was more extensive than the burial cave studied by Prof. Tagliaferro.

The burial cave which Tagliaferro examined was the largest of the features that survived deep quarrying at Bur Megħeż. A plan of the cave was published by John Evans (1970, Plate 12). According to Tagliaferro, the cave had two long galleries. The main gallery ran for about 19 m on an ENE axis. The second gallery, also running on an east north east axis, was linked to the first by a widened space. The two galleries showed signs of human modifications. Tagliaferro noted that, in spite of debris, the cave contained a number of articulated skeletons. Burials took place within spaces that were marked by stones. These stones and pebbles had been used to prop up or cover the deceased. The entire cave was lit and ventilated by 12 ceiling holes which served as skylights. Though very little survives of the Bur Megħeż complex, Tagliaferro's account, the plan published in Evans and remaining visible features suggest that the site was a complex and extensive one.

In June and November 1926, Zammit examined two rock-cut tombs, and in his field notebooks, he refers to similarities between the two (Zammit 1926b), a factor which helps date these burial sites. The first tomb was discovered at Xagħra on Gozo, located a few metres to the SE of the tomb close to the junction of Triq tal-Qacca and Triq Hammet (Figs. 13.1, 13.8, 13.9, 13.10). The tomb was broken into accidentally by a farmer, but there still remained enough of the structure to record. The sealing slab was still in place, though the tomb's contents had been recently removed and piled nearby (Zammit 1926b, 33-35). The farmer reported the discovery to the police because he was surprised by the red ochre-stained human bones, a prehistoric feature. The second tomb was discovered at Nadur, Binġemma. At the time, Temi Zammit was examining a number of rock-tombs that were known in the area and this particular tomb was described as of the primitive type, 'similar to the one found in Gozo' (Zammit 1926b, 55). The tomb was found without a sealing stone, but diagnostic pottery sherds were retrieved from the

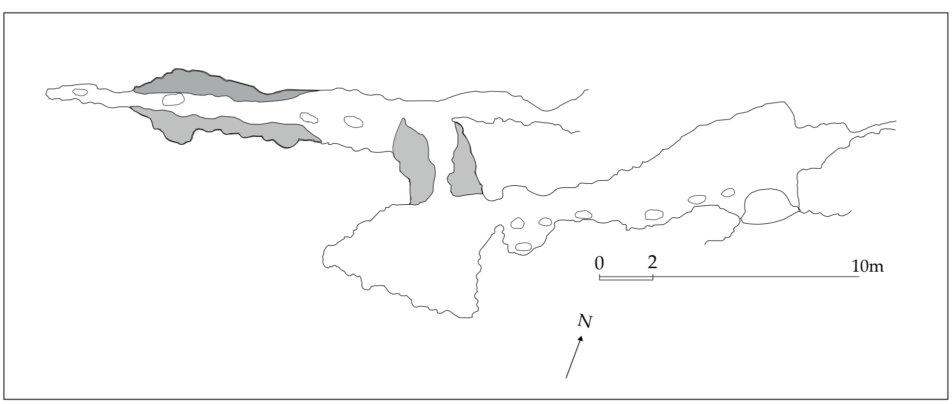

Figure 13.4. *(above) Now located near Imqabba within the precincts of Malta's international airport, the site of Bur Megħeż lies less than 4 km to the north east of Ħaġar Qim and Mnajdra. The burial place formed part of a larger site that was characterised by caves and deep rock fissures. Along with natural features of the upper level of the Ħal Saflieni Hypogeum and some areas of the Circle, Bur Megħeż was a one of the few known caves that were adapted for burial (courtesy of SIntegraM data, 2018, Developing Spatial Data Integration for the Maltese Islands, Planning Authority); (below) plan of Bur Megħeż (after Evans 1971).*

Table 13.2. *Prehistoric burial sequence based on ceramic remains identified from rock-cut tombs drawn from J D Evans' examination and classification of pottery remains.*

Burial Site	GħD	Skb	Break in Sequence?	Żb	Ġg	Tx	Break in Sequence?	TxC	Bn
Buqana				•	•				
Busbesija					•				
Bur Megħez					•	•		•	
Ġgantija North Cave					•				
Ħal Saflieni Hypogeum				•	•	•		•	
Kerċem						‡			
Nadur (Binġemma)					•				
San Pawl Milqi				•					
Santa Lucia						!			
Tarxien								•	
Ta' Trapna (Żebbuġ)				•					
Xemxija				•	•	•			
Xagħra					•				
Iċ-Ċirku tax-Xagħra				≈	≈	≈		≈	

Għar Dalam, Grey & Red Skorba (6000-5400 bc): no formal burials have been identified.

Żebbuġ (3800-3600 bc): first formal burials.

Ġgantija & Tarxien (3400-2400 bc): Rock-cut chamber tombs, caves and hypogea and megalithic complexes.

Tarxien Cemetery Cremation (2000-1700 bc): Cremation deposit at the Tarxien megalithic complex.

• Relative dating based on Evans (1971) review and sherd count.
≈ Malone *et al.* (2009) and FRAGSUS dating.
† Missione Archeologica Italiana a Malta based on Zammit/Evans/Trump sequences.
‡ Pace, A excavations (report in preparation) based on Zammit/Evans/Trump sequences.
! Mallia, F (1965) based on Zammit/Evans/Trump sequences.

debris that dated the tomb to the late Neolithic (Zammit 1928). An interesting aspect of this tomb is its location near rock-tombs of the Phoenician/Punic period. Like the Buqana tomb, the Nadur- Binġemma tomb may represent an instance of reuse of prehistoric tombs during later periods (see Table 13.2).

The last rock-cut tomb that Zammit examined was discovered in 1928 at Busbesija and was exposed during the winter rains. It was located just east of Falca Gap and Mosta in an area modified by modern road building. According to Zammit, the remains consisted of a rock-cut hollow which contained soil, pottery and remains representing five humans. The hollow was interpreted as the bottom of a rock-cut tomb that had been truncated by terrace levelling for field building (Museum Department 1928-29, iv). As shall be discussed below, an alternative interpretation is that the hollow may have been a shallow grave, as in the case of ta' Trapna and San Pawl Milqi.

After the Second World War prehistoric burials were again encountered. As in previous decades, discoveries were made mostly by accident during construction projects. The first discovery was made in 1947 in the grounds of the former Royal Navy Wireless station, now a Caritas institution, at ta' Trapna, in Haz- Żebbuġ, Malta (Figs. 13.1, 13.6). Five hollows were unearthed during foundation trenching for a new building. Unfortunately, the trenching works cut through the middle of the hollows. The burial deposits were damaged. However, the graves were examined carefully especially as they represented material which had not been encountered before. The material culture that Temi Zammit and Napoleone Tagliaferro had examined between 1902 and 1928 was all datable to the later Neolithic. The ta' Trapna cluster had earlier material which also predated that retrieved from the important sites of Tarxien and ta' Ħaġrat, which had been excavated a few decades previously. Ta' Trapna was significant for other important aspects: it was the oldest burial site, and comprising the hollow form of depositional areas, the tombs were similar to Sicilian San Cono-Piano Notaro examples (Evans 1959; Pace 1992): ta' Trapna therefore provided material affinities, if not direct links, with contemporary Sicilian developments, as had happened in previous centuries.

The next site to be unearthed was the 'Ġgantija North Cave' (Fig. 13.8). This rock-cut tomb was found in 1949 during quarrying, just a few metres to the north east of Ġgantija North Cave (Museum Department 1949–50, 218). The ceramic material in the tomb was dated by John Evans to the Ġgantija, but mostly to the Tarxien phases. 'The Ġgantija North Cave' is perhaps the only tomb known with certainty to be within close proximity of a contemporary megalithic centre. At almost 2.50 m across, the chamber of this tomb was also one of the largest of its kind.

The Xemxija tombs were excavated in 1955 by Prof. John Evans, and the first comprehensive analysis of the human remains is contained in this volume. Their excavation was included in the post-Second World War survey of Maltese prehistoric antiquities which was being carried out on behalf of the government. Apart from the Ta' Trapna, Żebbuġ burial site, the Xemxija cluster was the second prehistoric burial site comprising a number of autonomous tombs set together in a particular location. The importance of the Xemxija tomb cluster lies in a number of regards. The site consisted of rock-cut tombs whose structure had survived intact. The burial sites examined during the 'Zammit decades' were all damaged and therefore, structurally incomplete with the exception of the Binġemma tomb. The internal arrangements of Xemxija tombs 1, 2 and 5 were slightly more elaborate than the simple-chambered tombs known from Xagħra, Binġemma and the Ġgantija North Cave. The internal arrangement of the Xemxija tombs gave rise to the idea that they had originally inspired the design concept of Malta's megalithic structures (Evans 1959; Trump 2004). This interpretation was based on stylistic comparisons of the tomb plans with those of the megaliths. Alternative explanations have been proposed. Carlo Ceschi believed that Maltese megaliths followed their own trajectory after having developed from simple structures (Ceschi, 1939, 1970). An explanation favoured here is that architectural achievements of megalithic Malta and Gozo were profound and impressive enough as to influence the material aesthetics not only of tombs, but also of small models, amulets and carvings (Pace 1996). Finally, the importance of the Xemxija site also lies in its marking a pivotal change between the older central Mediterranean type of rock-cut tombs and the highly complex subterranean burials of Malta and Gozo.

In 1968 a small group of prehistoric burials was unearthed at the Punico-Roman villa of San Pawl Milqi, Burmarrad (Figs. 13.1, 13.9). The burials were unearthed in zone Z4, at a distance of about 8 m to the NE of the edge of the villa (Cagiano de Azevedo 1969a; Rossignani 1969). The zone in which these burials were unearthed has not been totally explored. Fortunately, the extensive construction of the villa during the Punic, Roman and later periods did not obliterate the prehistoric burials altogether. The Missione Archeologica Italiana a Malta who excavated the site, noted the presence of skeletons when retrieving amphorae of later periods (Rossignani 1969, 101-102). The amphorae were placed in two circular hollows with a diameter of about 2.12 m (Cagiano de Azevedo 1969a, 94). It transpired that the amphorae lay in reutilized prehistoric burial pits which still contained human remains. Burial T1 consisted of a skeleton, lying on the left side in an antenatal position on a bed of pebbles that had been carefully placed on the ground and a lump of red ochre was found near the skull. A few metres to the west of this burial, two similar hollows, T3 and T4, were uncovered which also contained human remains. Burial T4 yielded Żebbuġ phase pottery (Cagiano de Azevedo 1969a, 94). As in the case of ta' Trapna, the San Pawl Milqi burials had made use of hollows.

A prehistoric hypogeum was discovered at Santa Luċija in 1973 during the construction of a social housing project (Figs 13.1, 13.9 & 13.11). This small hypogeum lies within a kilometre's distance from the Tarxien megalithic complex and the Ħal Saflieni Hypogeum. The site was inspected by government authorities but was not surveyed, and the extent of the internal spaces of this likely hypogeum are unknown. The entrance to the Santa Luċija hypogeum was embellished with a megalithic structure, and the monument was provisionally dated to the Tarxien phase.

Though known for a number of centuries (Malone *et al.* 2009c; Attard Tabone 2010, 2011), the Circle was excavated with modern techniques between 1987 and 1994. The site is by far the most important of the Maltese prehistoric burial places in terms of artistic artefacts, figurative sculpture and numbers of the buried human remains which totalled just over 220,000 specimens (Stoddart *et al.* 2009a). In terms of architectural qualities, the site is today not as easily read as the Ħal Saflieni Hypogeum. The immediate fractured cave geology of the Circle is not as robust as that of Ħal Saflieni (which is cut out of solid Globigerina limestone). Instead, the burials were placed within a series of superficial intercommunicating caves in the Coralline limestone. These were susceptible to the odd collapse, and were evidently propped up with walls and megaliths in prehistoric times. During the 19th century, the site was partly dug up by Otto Bayer who concentrated mainly on the central area of the Circle. A contemporary watercolour painting by de Brocktorff gives a highly stylized view of the large cavity created by Bayer within what was originally a natural cave system. However, the real extent of Bayer's impact is unknown. Judging by de Brocktorff's view, an internal altar structure may have been lost although many worked megaliths were retrieved in the spoil. Bayer missed other important structures which survived to be documented in the recent excavations, and it seems that he may have not have encountered ritual artefacts. In addition, the Circle may have been quarried and certainly acted as a dump following Bayer's work.

Unlike the Ħal Saflieni Hypogeum, the Circle preserved its surface plan. A good number of megaliths and rubble walls still form a large circle. The more iconic megaliths used for the main entrance to the site as depicted in old drawings and water colours, have disappeared. With an average diameter of just over 40 m, the Circle is slightly more extensive than Ġgantija. A recent discovery (2017) of a burial deposit just 60 m to the SE of the Circle, suggests that the prehistoric burial site may have been more extensive. Indeed, the discovery combined with the rock-cut tomb encountered further downhill in 1926, suggests that much of the promontory may have accommodated a number of satellite burial monuments. The promontory on which the Circle is located has undergone several changes (Fig. 13.10) and the surrounding landscape is today covered with fields, old and modern buildings and quarries. As discussed below, the Ġgantija and Tarxien phases both saw a marked use of important locations in the landscape used for burial places.

The most recent discovery of prehistoric rock-cut tombs was at Kerċem, in 2008, where the remains of two chamber tombs dating to the Tarxien phase were unearthed during a building extension project at the back of the village's parish church. The remains of the tombs have been preserved, and during the 2008 construction work, a good amount of fill was extracted from the surviving chamber. One of the chambers, three articulated human skeletons survived in a small side chamber. Originally the tombs may have been first encountered during the construction of the church between 1846 and 1851, when the tombs were damaged, and the upper parts of the two chambers were found to have been truncated horizontally. No sign of the original entrance to the chambers survived whilst the complete form of the structure could not be determined. The twin rock-cut tombs were cut facing west, downslope from the highest point of Kerċem in a location reminiscent of the positioning of other contemporary cemeteries, especially Xemxija, the Circle and the Hypogeum which are all sited on prominent hillsides.

13.3. Central Mediterranean beginnings

The place of Malta and Gozo in Mediterranean prehistory has received continuous scholarly attention since the beginning of the 20th century. Within a few decades of Albert Mayr's monograph on Maltese prehistory, the first publications on the Ħal Saflieni Hypogeum (Zammit 1910), the Tarxien megalithic complex (Zammit 1930) and a series of studies on Maltese prehistoric antiquities revealed the uniqueness of the archipelago's antiquities. Writing in 1925, Vere Gordon Childe treated Malta on its own in his synthesis of European prehistory (Childe 1925). The megalithic architecture of the Maltese Islands and their rich repertoire of artefacts, statues and art however, could not be reconciled with the material cultural of Europe and the Mediterranean. Likewise, attempts to derive Aegean origins proved fruitless, a difference much later confirmed by radiocarbon dating. Since the second half of the 20th century, Mediterranean prehistory and history have become highly specialized subjects (Horden & Purcell 2000; Broodbank 2015; Abulafia 2011). The specific sub-regions of the sea forming the focus of particular research areas, reflecting the complexities and rich variety of material culture found discovered within them. In tandem, the 1970s also saw the emergence of specialized island studies (Evans 1977; Cherry 1981; Broodbank 2000). The recent studies have articulated explanations of insularity and the dynamics of islands lifeways in a manner which would have surprised Vere Gordon Childe.

The Maltese Islands are tied by geographical proximity to the history of Italy and Sicily, the nearest points of contact. Indeed, the first farming communities of Malta and Gozo probably derived from Sicily (Evans 1959; Bernabò Brea 1960; Trump 1962). The islanders were naturally a part of a broader Mediterranean world which they may have imagined and occasionally actually travelled. Today it is difficult to gauge the frequency, volume and extent of such travels from Malta and Gozo (Pace 1996b; Malone & Stoddart 2004; Volume 2, Chapter 11; this volume, Chapter 9). The sea would have played roles as a malevolent or harmless filter, forming a timeless bridge to neighbouring or distant lands. We are on sounder ground with regards the geographical extent of the archipelago's regional links for most of prehistory. A number of imported diagnostic materials and objects provide broad indications of sources located on mainland Italy, Sicily, the Lipari islands and Pantelleria. These

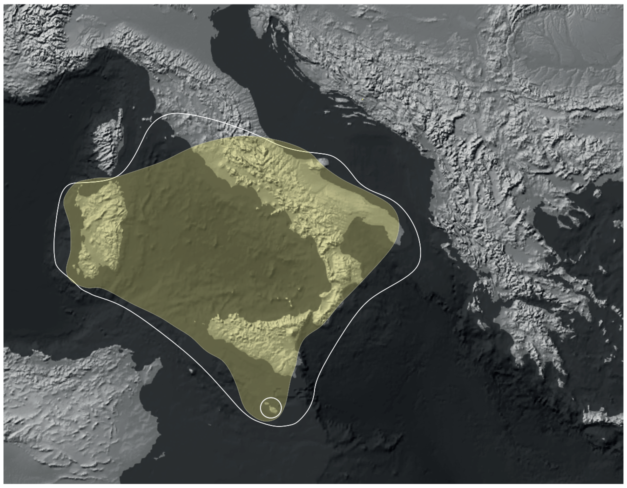

Figure 13.5. *Regional presence of rock cut tombs in the central Mediterranean (after Ruth Whitehouse, 1972. Background map courtesy of Natural Earth © 2009–2020. https://www.naturalearthdata.com/)*

materials may not have always been directly obtained from source, but may have involved several trade and exchange points along long-established routes. To a certain extent obsidian (Tykot 2011), chert (Volume 2, Chapter 11) or green stone axes (Dixon *et al.* 2009), can serve as proxies for understanding the persistence of cultural connections between the Maltese Islands and the larger landmasses over several centuries. This does not mean that the islands were dependent on neighbouring lands, since, as in many other island communities, the inhabitants of Malta and Gozo created their particular 'world view' through powerful architecture, art, cemeteries and the thoughtful use of an immediate landscape (Pace 1996b; Malone & Stoddart 1998; Grima 2004). Concepts and materials, even if imported, could be transformed and subsumed into local constructs. A very particular example of this transformation is seen in the two remarkable alabaster figurines from the Ħal Saflieni Hypogeum and the stylized alabaster head from Tarxien (Evans 1971; Pace 1996b; Vella Gregory 2005). In these examples, an imported material was transformed into a typical local concept, perhaps known only to the inhabitants of Malta and Gozo. The development of Late Neolithic burial monuments in Malta and Gozo might be explained in a similar way: a central Mediterranean phenomenon of funerary practice assumed a very particular materiality as the archipelago's communities developed their particular notions of the afterlife its representation in physical form.

The first radiocarbon dates for Malta and their subsequent calibration demanded new ways of thinking about central Mediterranean prehistoric tombs (Trump 1966; Renfrew 1973; Whitehouse 1972). Renfrew emphasized the autonomous flowering of Malta's late Neolithic megalithism, underlining the need to seek local origins to the archipelago's prehistoric antiquities (Renfrew 1973). Ruth Whitehouse set the general tone for approaching the structural development of rock-cut tombs as burial tradition focused in the central Mediterranean (Fig. 13.5). Peninsular Italy and its outlying islands emerged as the heartland of rock-cut tomb and traditions, quite independent of the Aegean. Likewise, the development of the late Neolithic architectural structures, interpreted by Ceschi (Ceschi 1939, 1970) and later by Evans (Evans 1959; Trump 1966), required similar explanation for the indigenous monumentality of Malta's prehistoric funerary sites (Pace 1992).

Whitehouse's own work on the development of rock-cut tombs refocused scholarly attention of prehistoric cemeteries, since, apart from highlighting the regional origins of rock-cut chamber tombs, she also noted that the small subterranean structures seemed to have experienced a sequence of changing rites. Earlier use of rock-chamber tombs was dated to the Neolithic, with later structures appearing in the Copper Age (Whitehouse 1972; Cazzella 1994). The earlier burials consisted mainly of single or double inhumations, whilst collective burials in rock-cut tombs appeared later during the Copper Age. The distinction between the two forms of burial rites may be explained as a change in ideology or belief systems. As in peninsular Italy, these changing burial rites did not result in structural changes of the rock-cut tombs. Indeed, the rite of collective burials may have emerged independently as a socio-religious concern. What is perhaps more significant is the development of more elaborate burial structures on some of the islands, such as the large number of rock-cut tombs with elaborate facades on Sardinia, and the complex subterranean cemeteries of Malta and Gozo (Whitehouse 1972). Given this scenario, more detailed studies of central Mediterranean prehistoric burials began to explore a variety of explanations.

A series of studies undertaken by the present author were an early exploration of the independent development of Maltese prehistoric burial sites: first, as a phenomenon which evolved independently (Pace 1990), and secondly, as a development which formed part of the broader socio-cultural flowering of late Neolithic Malta (Pace 1992). These studies were designed to explore aspects of Maltese prehistory that had not attracted the same attention as the renowned megalithic centres and the Ħal Saflieni Hypogeum had achieved. Adopting a broader perspective, the studies examined processes of how a funerary rite gave rise to a particular form of architecture over a number of generations. Sometime during the Ġgantija Phase of the 3rd millennium BC, the communities of Malta and Gozo departed from cultural norms that had long permeated central and south Italy. The islanders created burial centres which, in some cases, rivalled surface megalithic architecture in scale and embellishment. This departure was an intentional expression of autonomy, but whether it was fuelled by internal ideologies or a cultural break from trends on mainland Italy is now difficult to say. More importantly for this contribution, the development of Maltese and Gozitan burial sites formed part of unified cultural setting, in which specific social and material aesthetics, commonly shared among the archipelago's small communities, characterized funerary architecture.

Another perspective on central Mediterranean rock-cut tombs was the idea of the almost simultaneous but autonomous developments of funerary rituals in rock-cut tombs, natural caves and cavities throughout peninsular Italy and adjacent islands. Prof. Alberto Cazzella noted that two ritual traditions, one comprising single inhumations in rock-cut chambers, and another of collective burials associated with the use of natural caves, may have led to the development of hypogea at the juncture between the late and final Neolithic. This change did not see the elimination of older rites of burials, but it simply ushered in a combination of the two (Cazzella 1994). In some instances, such as Malta, funerary monumentality became more pronounced during the final Neolithic. A similar approach was adopted by Christopher Hayden who, inspired by Kroeber (1948) argued for the possibility of a simultaneous development of rock-cut tombs as a result of similar conditions in different areas within the same region (Hayden 2006). Hayden suggested that according to available dates, two independent areas within which rock-cut tombs had originated were Sardinia and the other, southern Italy, Sicily and the Maltese Islands. However, the extent to which these two areas were isolated from each other is difficult to establish. Interestingly, Hayden lists a range of features which, although different in the detail, were a common occurrence in the geo-cultural setting within which rock-cut tombs emerged. Figurines, the elaboration of the treatment of the dead, ritualization and changes in burial practices were some of these common features (Hayden 2006). Added to these, especially in the case of Malta and Gozo, there was the progressive elaboration of funerary monuments (Pace 1992) and the symbolic use of the landscape (Grima 2004, 2008).

Finally, Malta's rock-cut tombs and those of the Central Mediterranean have been amply discussed

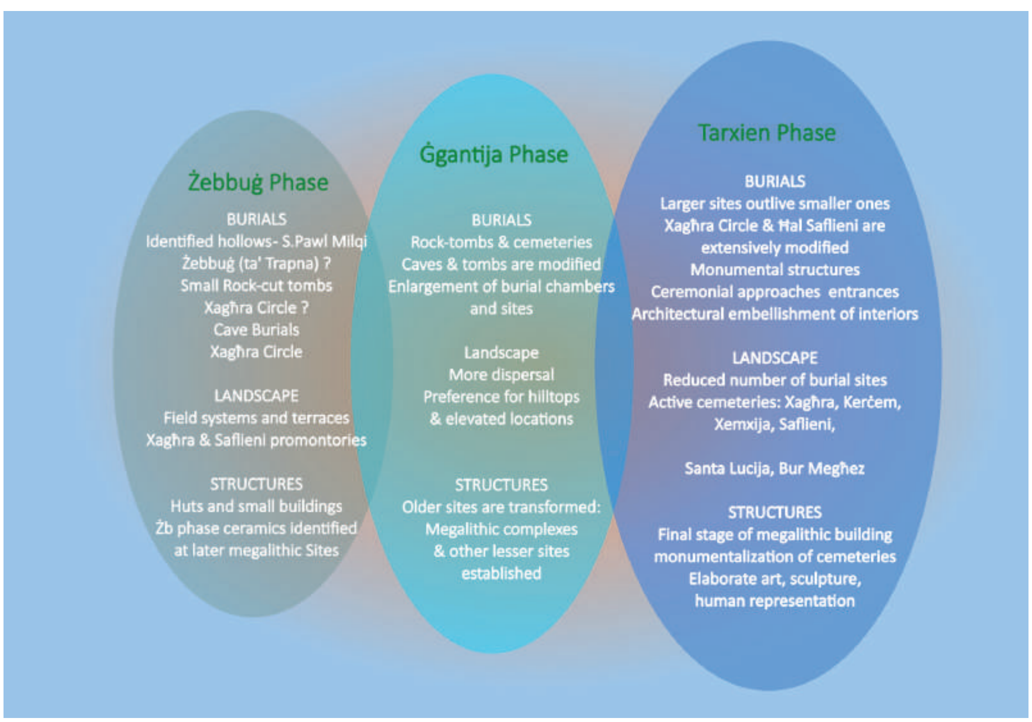

Figure 13.6. *Schematic flow chart summarising the changes in mortuary custom, landscape and settlement in the Temple Period of Malta.*

in terms of their development as a cultural phenomenon (Whitehouse 1972; Malone 2003; Skeates 2010; Dolfini 2015; Parkinson 2019; Robb 2001). The Neolithic rock tombs of the Central Mediterranean developed differently throughout the region, with more conspicuous and sophisticated developments in funerary architecture occurring on the islands (Malta, Sicily, Sardinia and Mallorca) (Whitehouse 1972; Tusa 1999; Leighton 1999). The core of communities centred around peninsular Italy suggests shared knowledge of customs during the earlier use of rock-cut tombs, yet over time, they developed particular variants of rock-cut tombs, and in the case of the Maltese Islands, subterranean cemeteries that were much larger than simple tombs and easily accessible as constructed buildings (Fig. 13.6). The underlying rite of collective burial was a cultural trait that was common to several central Mediterranean communities, but this rite was expressed differently in terms of monumentality and content. The Circle on Gozo and the Ħal Saflieni Hypoeum on Malta may be extraordinary anomalies within central Mediterranean mortuary traditions, but these monuments may also reflect broader trends that accentuated individuality in different locations. These trends clearly reflect a progressive elaboration of rituals, funerary goods (which included figurines, personal ornaments, long-range exchange materials) and the construction of elaborate funerary monuments. Such changes coincided with the beginning of the late Neolithic phase, which has been read as an indication of ideological and belief systems change.

13.4. The development of burial sites in Malta and Gozo

From the above discussion, it is difficult to discount central Mediterranean origins for Maltese prehistoric burial customs and cemeteries, whilst acknowledging that the central elements in the development of Maltese cemeteries were unique and different from other neighbouring regions. First, there is a sequential development of structures which, over a number of generations, came under the influence of the archipelago's megalithic architecture; second, the creation of large accessible subterranean structures that functioned in the same way as surface buildings; third, the cognitive use of the landscape and the occupation of prominent places for locating burial sites, and fourth, the distinct ideological shift towards collective and multiple burials. The sequential details of typical sites is described below.

13.4.1. Għar Dalam and Skorba

Burials from the Neolithic phases of Għar Dalam and Skorba (5500–5000 bc) have not been confirmed in Malta and Gozo. Some reasons for this may be that a Neolithic mode of burial may not have survived in Malta, or that human remains from this period have not been securely identified. However, the discovery of human teeth at Għar Dalam during levelling works of the cave's visitor walkway may be of interest (John J. Borg personal communication). This discovery recalls the human remains, pottery and stone artefacts noted at the upper levels of the site by Despott (1923) and Baldacchino (Museum Department 1933–4; 1934–5; 1936–7; 1937–8, 43-62; Evans 1971, 19). Unfortunately, the precise nature of the Neolithic and late Neolithic remains from Għar Dalam do not provide secure evidence of burials, although such a possibility should not be ruled out, and parts of the cave may have even served for burials. Other tantalizing archaeological data come from the Għar Dalam phase hut floor at Skorba. Three fragments of human mandible, belonging to two children, lay in the debris on this floor. Adult human skull fragments came from a refuse deposit in the same area (Trump 1966, 10). These human remains are difficult to interpret, other than their being found in what was an Għar Dalam domestic context. Absolute dating would help answer questions raised by this important discovery. One question that arises from the foregoing is whether Għar Dalam phase burials were closely associated with dwellings. An almost similar association had been noted in south–east Italy, where a burial feature was closely associated with ditch-enclosed village settlement at Fonteviva (Foggia); it consisted of a small domed circular chamber cut in the side of an enclosing village ditch, therefore in close proximity of houses. Pottery associated with a surviving burial deposit was of the Impressed ware type (Whitehouse 1972).

13.4.2. Żebbuġ

The earliest secure evidence that we have for formalized burial arrangements dates to the Żebbuġ phase (4200–3400 bc) and it is likely rock-cut tombs were introduced in the Maltese Islands at this time (Fig. 13.7). This period was contemporary to, and broadly related to the Sicilian San Cono/Piano Notaro culture, representing the transitory centuries from the late Neolithic to the earlier parts of the Copper Age (Whitehouse 1972; Tusa 1999; Leighton 1999; Malone 2003). Diagnostic Żebbuġ ceramics at the Buqana tomb (Attard), the Ħal Saflieni Hypogeum, the San Pawl Milqi burial cluster, the ta' Trapna site (Żebbuġ, Malta) and the Circle (Gozo) show that formal burials were present in several locations on the two islands. Views on this now depend on how the revised dating of the Circle rock-cut tombs are interpreted (Malone *et al.* 2019) and also on the possibility that other forms of

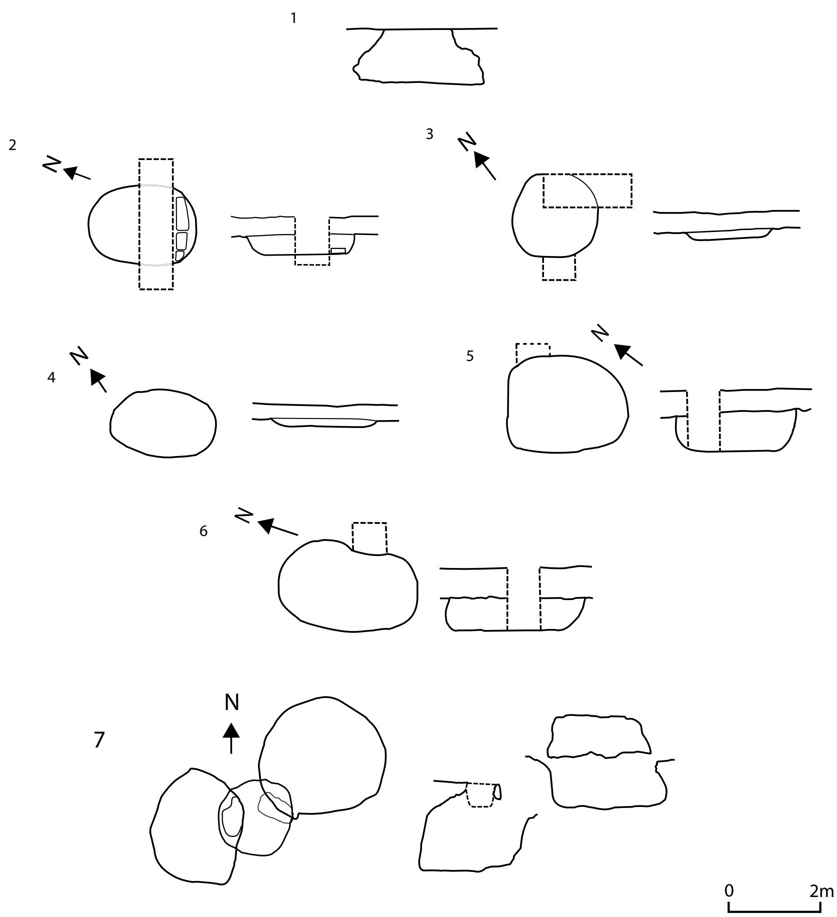

Figure 13.7. *1. Żebbuġ Phase Buqana – section only (after Zammit, T. 1909-1912); 2. – 6. Żebbuġ, ta' Trapna, plans and sections (after Baldacchino & Evans 1954); 7. Circle rock-tombs, plans and sections (after Malone* et al. *2009d).*

burial arrangements may have been used. The strongest evidence for the introduction of rock-cut tombs during the Żebbuġ phase is still that of the Xagħra tomb (Malone *et al.* 1995, 2009f). Although the earliest secure deposition in this twin-chambered rock-tomb has now been dated to the Ġgantija phase, the deposits still yielded a large quantity of Żebbuġ phase pottery. The tombs had been used over a number of generations and they represent the oldest elements of the Circle (Malone *et al.* 2019). Other areas of the upper parts and cave areas of the yielded quantities of Żebbuġ phase pottery, once again suggesting that the site had been used as early as the beginning of the late Neolithic, though the monumentalization of the Circle would take place only later, in the Tarxien phase (Malone *et al.* 2019). This interpretation complements earlier models of the evolution of funerary monuments in the Maltese Islands (Pace 1990; 1992). Similarly, residues of Żebbuġ pottery were identified from the old excavations of the Ħal Saflieni Hypogeum (Evans 1971), though the architectural embellishments of the site, like those of the Circle, date to the Tarxien phase (Pace 2000). The damaged Buqana tomb, which contained Żebbuġ pottery (Evans 1971) (Table 13.2), still provided a good idea of its original structure. From Zammit's field drawing, we know that the tomb was bell-shaped, about a metre deep with a width of about a 1.40 m and an oval opening at the top (Zammit 1909–1912, 77). The presence of Żebbuġ phase pottery at both the Ħal Saflieni Hypogeum and the Circle suggest that at the beginning of the late Neolithic, natural caves, even if modified, were used for burial purposes along with rock-cut structures.

The contemporary sites of ta' Trapna (Żebbuġ) and San Pawl Milqi offer an interesting perspective on the possibility that rock-cut hollows were also used as burial structures during the Żebbuġ phase (Pace 2006), although interpretations are tentative. At Żebbuġ, a site comprising five shallow hollows, was discovered in a small area of about 40 square metres. A similar burial site comprising three rock-cut hollows was unearthed at San Pawl Milqi (Cagiano de Azevedo 1969a). Baldacchino, the original excavator of ta' Trapna, interpreted the hollows as the surviving floors of rock-cut chamber tombs that may have been quarried away to level ground during field construction (Baldacchino & Evans 1954). Baldacchino suggested structures that were similar to Buqana. Evidence of rock-levelling for field building and other purposes is common in Malta and Gozo, and in recent years, the Superintendence of Cultural Heritage has encountered a number of such sites in various parts of the islands. The general pattern is one where ancient rock-cut features such as silos, Punic and Roman tombs, Christian catacombs and wells, were horizontally truncated to a depth that only preserved the floors of the features. Sometimes, original burial deposits survived within these remaining floors, albeit mixed with quarrying debris. Such features have been encountered at Xarolla, Zurrieq/Safi, the Rabat catacomb complexes and in the American Embassy grounds at ta' Qali, just two kilometres north of ta' Trapna. Rock-levelling and terrace building in the Maltese Islands is difficult to date, though on the basis of hand tool marks, it can be said that it generally pre-dated mechanized rock-cutting of the 20th century. Manual rock-cutting should have enabled detection of the burials and archaeological features, as happened in 1947 when the ta' Trapna site was accidentally encountered, although the excavation report does not provide strong evidence for extensive rock-cutting. Contrary to the expected disturbance associated with mechanized rock-cutting, the remains contained in the five burials at ta' Trapna were still *in situ* and contained within the hollows, sealed by field soil. The five burials shared a number of common features. Each feature consisted of a cavity which was roughly cut in Globigerina limestone. These hollows were on average about 1.80 cm in diameter and about 50 cm deep at the centre. The floors were covered with small roughly shaped stone slabs covered by a layer of marl, on top of which inhumations were placed. The burials were sealed by a 25 cm deep layer of stone chippings, which was in turn covered by field soil (Baldacchino & Evans 1954).

The three Żebbuġ burial hollows from San Pawl Milqi showed certain similarities with those of ta' Trapna. Even here, inhumations were discovered in rock-cut hollows on a site which had experienced a number of changes. But in contrast to the ta' Trapna discoveries, the San Pawl Milqi skeletons were better preserved. The site was used at the beginning of the late Neolithic and was later re-used during the Bronze Age (Borġ in-Nadur period). The remains of an archaic winepress suggest a prolonged use of the site into the Punic period. 2nd century BC tombs reflect a mixed use of the site, with the construction of the Roman villa also during the 2nd century BC. Thereafter, the complex went through successive changes, through Late Antiquity, and the Byzantine and the Arab periods. The footprint of the villa covered a number of terraces on a gentle slope, and faced north towards the ancient harbour in present-day Salina Bay and Burmarrad. The core buildings of the villa complex were constructed on the upper areas of the site. The *Missione Archeologica Italiana a Malta* excavations unearthed the remains of a corner wall at the northeast perimeter corner of the villa. These large masonry remains were interpreted as fortification walls, and within the corner of the remains lay a fill which, when excavated, contained two small 2nd century BC amphorae and Żebbuġ burials. The excavators noted a number of inhumations but excavated only one human skeleton. This was preserved in a crouched position resting on a layer of pebbles that had been carefully placed on the floor of the hollow (Cagiano de Azevedo 1969b, 115). The burials had escaped major damaging impacts, including the villa's foundation offerings. The survival of these Żebbuġ features suggest that rock-cut hollows rather than rock-cut tombs were another form of burial structure that was used at the beginning of the late Neolithic. In addition to these burial hollows, the San Pawl Milqi excavators unearthed a number of postholes and other hollows beneath the present-day church which stands on site. If prehistoric, these features raise interesting questions concerning their possible domestic function and perhaps the close association of a small village settlement with the burial hollows.

The Circle offers a tantalizing possibility of the use of rock-cut tombs as early as the Żebbuġ phase, although the radiocarbon dates now imply an early Ġgantija date. Within the Circle, two rock burial chambers were cut opposite each other and shared a common vertical shaft. These rock-tombs represent the oldest intentionally constructed structural features of the site, although there are other earlier phases a niche of the cave, subsequently reworked by Tarxien burial activity. The Circle defined as a quasi-hypogeum constructed within a series of subterranean caverns, had been modified and embellished with architectural elements, a process paralleled by developments at the Ħal Saflieni Hypogeum. The caves within the Circle yielded a large quantity of Żebbuġ pottery, indicating the early use of natural subterranean spaces in the late Neolithic (Stoddart *et al.* 2009b). The two-chambered rock-cut tomb is located close to the present entrance, just beyond the south east edge of the collapsed east cave of the Circle complex. The two chambers follow a classic *tomba a forno* structure, which are mostly intact, in spite of some roof damage during more recent vine-trenching. The chambers open from a common 1.4 m diameter vertical access shaft, and were cut roughly opposite each other on a southwest–northeast axis. The chambers were accessed through small entrance holes cut in the bottom of the common shaft. Chamber 1, to the southwest of the shaft, had a sub-circular plan with a maximum diameter of about

2.50 m and a ceiling height of just over 1.2 m. Chamber 2, was more rounded in plan also with a diameter of about 2.50 m and a ceiling height of about 1.20 m (Malone *et al.* 1995, 2009f). The earliest ceramic material found within the chambers was that of Żebbuġ phase, with some later forms of Ġgantija date. The material culture, which also includes a small 'statue menhir' from chamber 1, reflects a prolonged use of the two tombs. Radiocarbon dates, recently reviewed as part of the *FRAGSUS Project,* now place the inhumations of these chambers in the earlier part of the Ġgantija phase, reinforcing the possibility of a prolonged use of the chambers which is also reflected in the presence of Żebbuġ and Ġgantija ceramics (Malone *et al.* 2019). As reported in Volume 2, residuality is a recurring theme of the Maltese Islands, not only in pollen cores and site stratigraphy but also in funerary ritual.

13.4.3. Ġgantija

The second stage in the development of Maltese late Neolithic burial monuments took place during the Ġgantija phase (*c.* 3400–3100 BC) (Fig. 13.8). Inevitably, modern chronologies sometimes create a sense of abruptness in the way that we characterize change which instead would have happened over a number of generations. The Ġgantija phase is one such example of this. The importance of this phase lies in the more conspicuous visibility of a materiality which among other aspects, was expressed through monumentality. It was during the Ġgantija phase that megalithic structures began to assume a monumental character. The structural sequence of the buildings was first explained by Carlo Ceschi who outlined the engineering requirements and solutions that enabled the technical construction of the structures and assessed

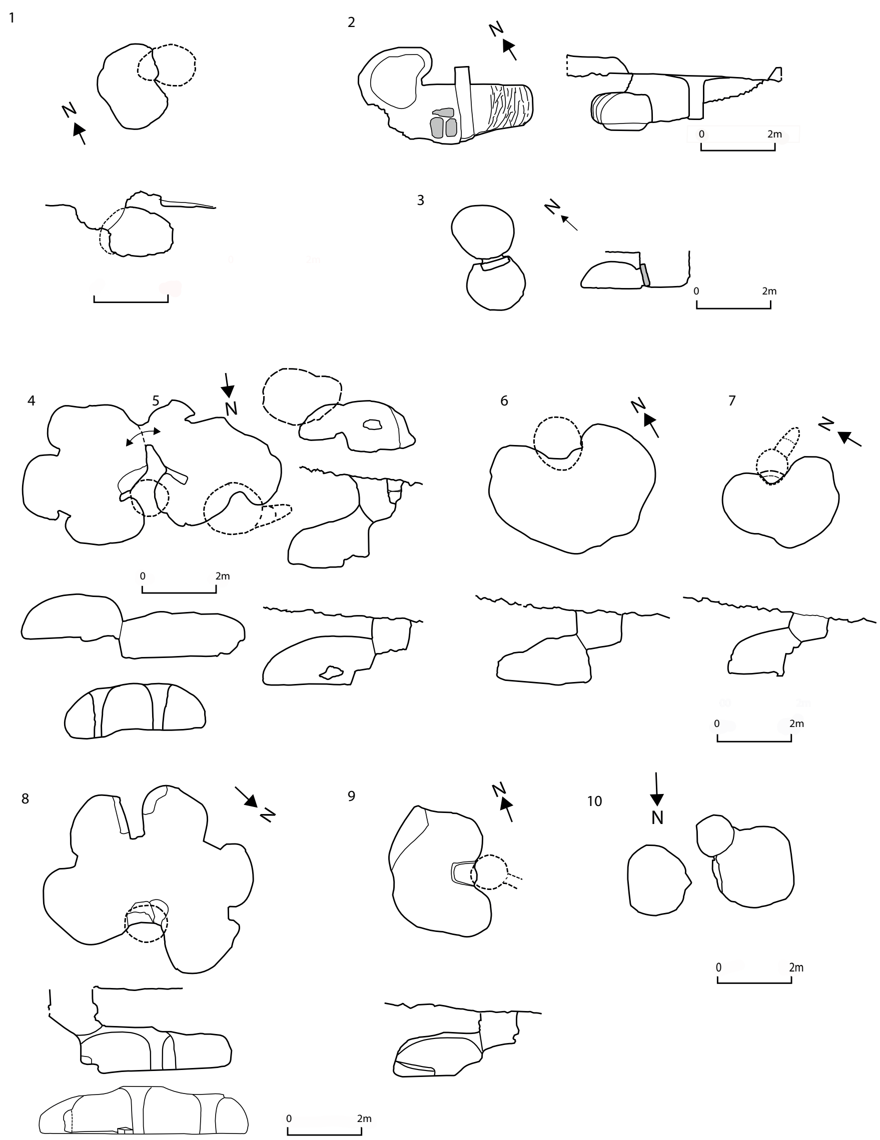

Figure 13.8. *Rock-cut tombs (Ġgantija Phase with extended use into Tarxien). 1. Binġemma/ Nadur, plan & section (after Evans 1971); 2. Ġgantija North Cave, plan & section (after Evans 1971); 3. Xagħra 1926, plan & section (after Zammit, T. 1923-26); 4 – 9. Xemxija tombs, plans and sections (after Evans 1971); 10. Kerċem, plan only (Pace & Mercieca 2008).*

the properties of the megaliths themselves (Ceschi 1939, 197). John Evans and David Trump suggested a two phased sequence for the building of the megalithic complexes, based on excavated diagnostic pottery. They suggested that the first phase of megalithic building at most of sites began during the Ġgantija phase and subsequently followed by another construction phase during Tarxien phase (Evans 1959; Trump 1981). This idea of a two-stage construction process still needs to be tested, but if considered on structural engineering grounds then some of the megalithic complexes may have been built as a single process, without the lengthy intervals suggested by ceramic and radiocarbon dating. Clearly however, the construction of the megalithic complexes was characterized by sophisticated engineering solutions and refined designs, which in time also included internal embellishments and artwork. The manner in which the skilled late Neolithic artisans engaged with the materiality of stone and formed such architectural creations has been examined by several scholars of Maltese archaeology (Pace 1996b). The phenomenon of megalithic construction and art was too significant for it not to have an impact on the ways in which the small communities of the Maltese Islands viewed their immediate world. It is against this broad context that we should consider the development of burial sites during the Ġgantija and subsequent Tarxien phase (see Fig 13.9 for changing distribution of cemeteries over the Temple Period).

During these phases, significant changes are detected in the archaeology of funerary monuments. First, the archaeology of the Ġgantija phase burial sites reflects a degree of growing complexity in form as well as variety of cemeteries. The Żebbuġ hollow cemeteries at San Pawl Milqi and ta' Trapna seem to have run the full course of their use, perhaps as a result of the more structurally defined rock-cut tombs. By this stage, the classic *tomba a forno* was well established in various locations in Malta and Gozo. Typically, they consisted of an access shaft with a small entrance at the bottom leading to the burial chamber (Fig 13.8). As in the case of the Xagħra tomb examined by Zammit (1928) and the Circle rock-cut tomb, sealing stones closed off the chambers. The Circle double chamber tomb arrangement is an exception to the classic *tomba a forno* having had a common access shaft serving two burial spaces. Individual *tomb a forno* rock-tombs were found at in-Nadur (Binġemma), Busbesija, the Ġgantija North Cave and a few metres downhill from the Circle. Another exceptional form for this period is the lone Buqana rock-tomb, which according to Zammit's description and field drawing, was bell shaped and probably access from the top (Zammit 1924-5). A similar structure was excavated by the author in the modern street level areas of the Ħal Saflieni Hypogeum (Cutajar 2000). The widely dispersed rock-cut tombs were mainly single isolated structures in the landscape. In a few cases, namely at the Circle, Xemxija and Ħal Saflieni, rock-tomb locations developed into complex cemeteries. At Xemxija, a group of six individual tombs were closely grouped forming a cemetery. At this site, however, three tombs, 1, 2 and 5, have slightly more complex interior plans which included irregular side apse-like spaces. These features, which are very pronounced in Xemxija 1 and 5, were thought to be the original inspiration of Maltese late Neolithic megalithic structures (Evans 1959; Trump 1981), though this idea has been questioned on technical structural grounds (Ceschi 1939, 1970), and an over reliance on coincidental stylistic analogies (Pace 2006). Finally, the Ġgantija phase burial cemeteries include the use of large caves. The classic sites are those of the Ħal Saflieni Hypogeum, especially the Upper level where deposits belonged for the greater part to the Ġgantija phase, the Circle and Bur Megħeż. In all cases, large caves and crevices were modified to enable multiple burials. Collective burials were encountered at the former sites, but at Bur Megħeż, formal individual inhumations were noted (Tagliaferro 1911) and a series of light shafts were cut to illuminate the cave's interiors (Evans 1971).

The second characteristic of Ġgantija phase burials is the increase in the number of cemeteries and their dispersal in the landscape (Pace 1990; 2006; Grima 2004) (see Fig. 13.10). Available information on burial site patterning in the landscape tends to be biased, the number of late Neolithic burial sites is quite small, and the extent of survival, loss or detection is unknown. As discussed above, most of the known burial sites were discovered during construction, quarrying, trenching or agricultural activities causing intense change in the Maltese landscape through destructive sprawling urbanization. Exploration through field survey remains very limited, so that detection relies on accidental discoveries, whilst reuse of rock-cut tombs during prehistory and occasional reutilization during Phoenician-Punic times (as the Nadur (Binġemma) tombs suggests), would have had a significant impact on the survival of Neolithic burial sites.

The dense but relatively small size of late Neolithic populations in Malta and Gozo, as well as an ideology of collective burial may have led to a preference for central burial places as opposed to marginal burial sites. Rudimentary dispersal patterns (Fig. 13.9) reflect how the use and location of late Neolithic burial sites were strongly influenced by two significant factors: the emergence of large central cemeteries and the construction of megalithic complexes which were themselves designed to serve as important centres. Of the five known Żebbuġ phase burial sites, only three - Buqana, Ħal Saflieni and the Circle - remained active into later phases. The Ta' Trapna and San Pawl Milqi burial hollows went out of use. The increase in number of Ġgantija phase burial sites suggests that a peak in the use of rock-cut burial sites was may have been reached at this time, although the peak may have been relatively short lived. The Ġgantija phase cemeteries reflect two levels of scale, from shorter lived rock-cut tombs to the sites which remained active into the following Tarxien phase which were significantly much larger in terms of burial space. This latter category had origins in burial cave systems, with Bur Megħeż the least elaborate of these sites, since it retained much of its natural configuration. Santa Luċija was also a partly modified subterranean cave. The Upper Level caves of the Ħal Saflieni Hypogeum were modified during the transition to the Tarxien phase, with major rock-cutting and elaborate carvings at the site taking place beyond this level. Similarly, the Circle was made up of subterranean caves that were later extensively modified with the introduction of architectural elements built of dressed Globigerina limestone.

A fourth element that emerged during the Ġgantija phase was the manner by which topography was intentionally used to locate or develop burial sites, with prominent hillsides and hill tops favoured as designated monumentalized burial places. The Xemxija tomb cluster epitomizes this phenomenon very clearly. A similar arrangement may have existed at Kerċem, though in this case, the hilltop into which tombs were cut was extensively developed into the present-day village. The Kerċem tombs were cut slightly

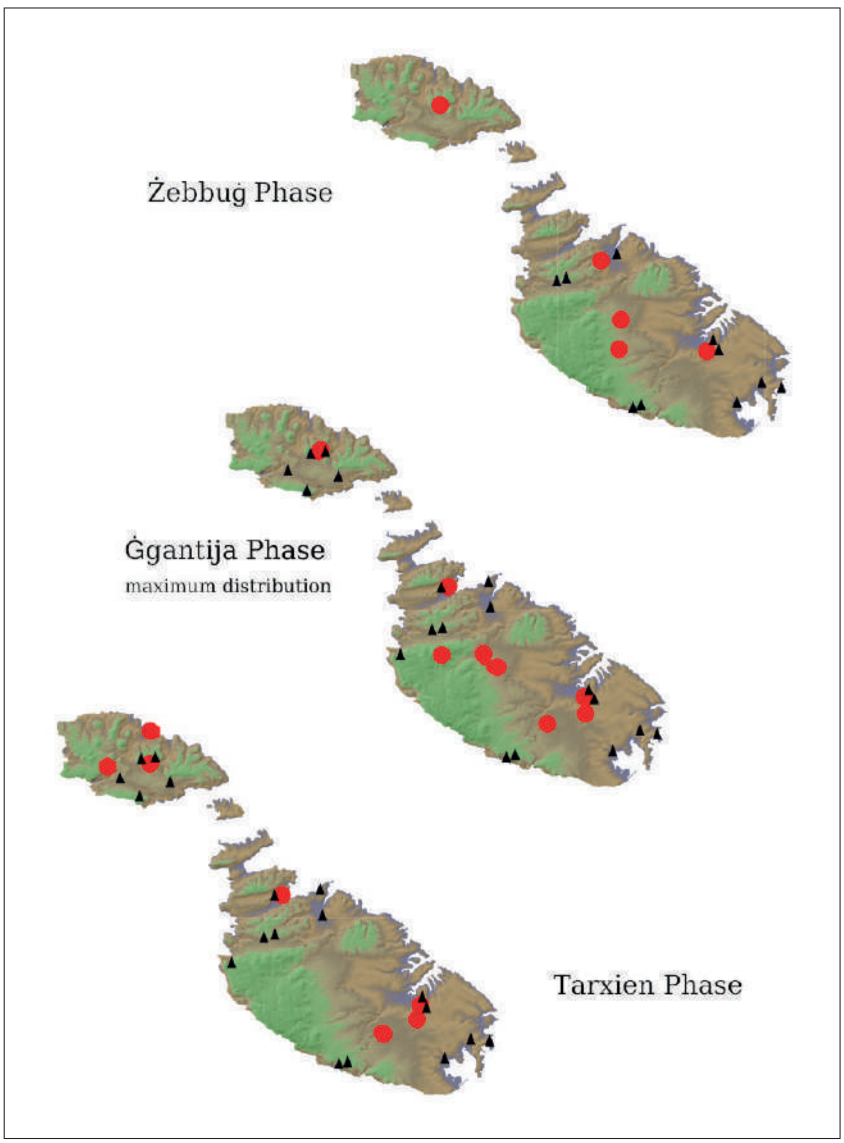

Figure 13.9. *Spatial patterning of rock-cut tombs from the Żebbuġ through to the Tarxien phases. The three maps each show the relationship between rock-cut tombs, shown in red, and the major Maltese megalithic sites, represented by black triangles, through time. The maps provide a graphic interpretation of the sequential dynamics of Late Neolithic monuments in the Maltese archipelago. The spread of tombs seems to have peaked during the Ġgantija Phase when megalithic construction became very widespread. Eventually, funerary sites becoming fewer in number. By the closing decades of the Tarxien phase the burial sites that were still active, were those with close affinities to major megalithic complexes. These burial sites were significantly larger and more complex than the early rock-cut tombs. While the megalithic complexes retained a constant geographic presence, funerary landscape patterns seemed to have contracted significantly.*

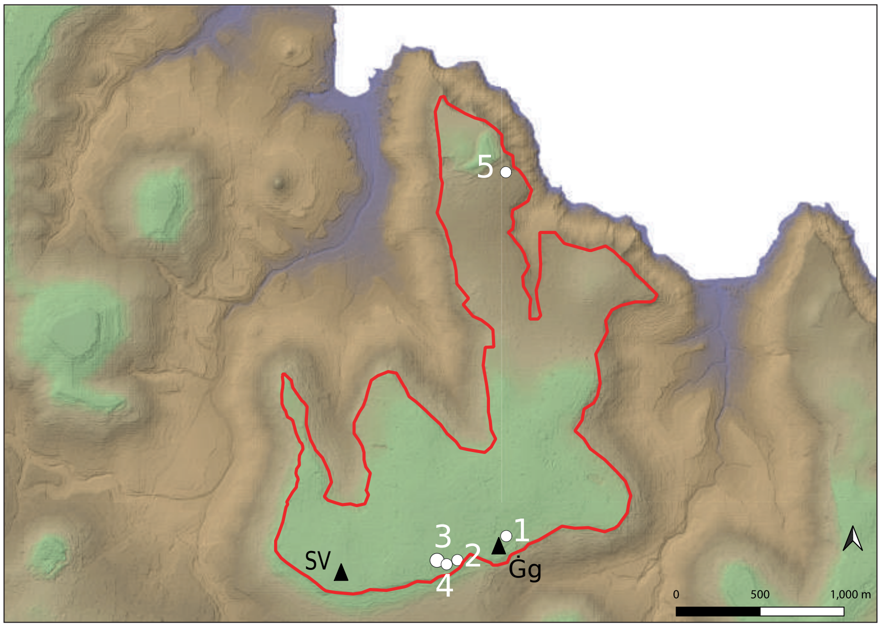

Figure 13.10. *Map of the Xagħra Plateau Gozo, showing Burial Sites: 1. Ġgantija North Cave; 2. Xagħra (1926); 3. Circle; 4. Xagħra (2012); 5. Għajn Damma (possible burial site) marked by circle. Megalithic Building: Ġg – Ġgantija; SV – Santa Verna, marked by triangle. Legal copyright and use Credit: Basemap data provided by ERDF 156 data (2013) Developing National Environmental Monitoring Infrastructure and Capacity, Malta Environment & Planning Authority.*

downslope from the top of the hill at a point which is now dominated by the village parish church. Likewise, the promontory on which the Circle was extensively used with Zammit's tomb located on the south-east slope just over 120 m from the Circle, and only 60 m downhill from the Circle, another burial deposit was recently excavated by the Superintendence of Cultural Heritage. To the north-east of the Circle numerous other caves may have also been used for burial, such as Ghar ta' Ghejzu (Fig. 13.10). The Circle may have evolved as the epicentre of a more extensive burial ground with peripheral rock-tombs and caves (cf. Grima *et al.* 2009). Hierarchical arrangements of core and ancillary burial structures on similar prominent ground seem to have developed at Ħal Saflieni, where smaller tombs and caves are known from the site's upper levels. Less than a kilometre to the south of Ħal Saflieni lies the small subterranean burial structure of Santa Luċija (Fig. 13.11). Similarly, at Bur Megħeż, a series of natural caves on the high plateau of the area now mostly occupied by the Malta International Airport and quarries, were found to contain burials. To various degrees, the phenomenon of late Neolithic monumentalized topographic features can still be experienced albeit with great difficulty because of intensive urban sprawl.

Finally, an important element which coincided with, and perhaps shaped, the second stage in the development of funerary monuments during the Ġgantija phase, was the predominant adoption of collective burial rites. This development was to a certain extent synchronized with similar changes happening elsewhere in the central Mediterranean (Whitehouse 1972). In Malta, the earliest evidence for collective burials, even if cumulative or sequential, comes from ta' Trapna and possibly from the Circle. At ta' Trapna, the remains of seven individuals were identified in burial 1, while the other hollows contained single or double inhumations (Baldacchino & Evans 1954). Collective burials may have been used at the Circle, where Żebbuġ phase pottery was discovered in various areas of the site's subterranean caves as well as in the two rock-cut tombs located within the precincts of the circle (Malone *et al.* 2009f). Here, however, detection of Żebbuġ phase collective burials is difficult because of the constant re-utilization of the area, as well as the remanagement of human remains, ossuaries and structures over several generations. At San Pawl Milqi, the excavated and partially examined Żebbuġ phase hollows contained single inhumations. However, the site has not been fully excavated (Cagiano de Azevado 1969b) and may yet provide new data.

The rite of collective burial in Late Neolithic Malta and Gozo also signalled an important change in the materiality of burial spaces. The archaeology of the Ġgantija phase, confirms a preference for larger burial places rather than several single tombs. This preference was not influenced by an advantage in economizing laborious rock-cutting efforts. Indeed, the Ġgantija phase saw a larger number of independent rock-cut tombs spreading across Malta. Collective burial may have reflected a new cultural construct of 'collectivity' to define the ultimate status of the dead, where social differences became less significant and in certain respects less conspicuous. Physically, collective burial may have created new demands for accommodating the deceased of the archipelago's small and closely related communities in a common space. Larger spaces could be created by modifying natural caves, as in the case of Ħal Saflieni upper level, Bur Megħeż cave and the Circle cave system. Collectivity on such a large scale known from late Neolithic Malta required common interiors that could be accessed repeatedly. Links between burial interiors were also important. These could be achieved by for instance a common access shaft, as in the case of the Circle rock tombs, a complex arrangement of passageways and intermediary spaces as in the case of Ħal Saflieni and the Circle, or, as in the case of Xemxija 1 and 2, the intentional linking of two neighbouring tombs by an interior access hole.

13.4.4. Tarxien

The third and final stage in the development of burial sites occurred during the Tarxien phase but has to be understood as a continuation of processes that had started previously during the Żebbuġ and Ġgantija phases. If these earlier phases were tentative precursors, the Tarxien phase marked a peak in the development of subterranean cemeteries. The overall pattern of this development is hampered by the relatively small number of known burial sites on Malta and Gozo. As already discussed, this limiting factor in our interpretation could be result of uneven discovery and survival of burial sites in the limited geographical space available on Malta and Gozo. However, the nature of the Tarxien phase burial monuments (Fig. 13.11) could also be a reflection of broader social phenomena that may have favoured rites of collectivity and, therefore, the growth of particular sites and not others. This may have resulted in the creation of a hierarchy of burial monuments, where large-scale central cemeteries led to a decrease in the use of small burial sites and individual rock-cut chamber tombs.

A number of features characterize the materiality of Tarxien phase burial monuments. Firstly, at a macro-regional level, the larger monumental cemeteries as well as those located on prominent promontories seem to be the ones that continue in use into the later decades of the Tarxien phase. On a long-term scale of almost two millennia (Żebbuġ, Ġgantija and Tarxien phases), this phenomenon is also reflected in the broad three-stage geographical pattern in which rock-cut hollows and chamber tombs were first adopted, followed by a significant dispersal of burial sites across several parts of the archipelago during the Ġgantija phase, to finally culminate in the survival of the most elaborate cemeteries of Ħal Saflieni, Bur Megħeż and the Circle.

The second important characteristic of Tarxien phase burial sites is the pattern of their location in the landscape. This patterning seems to synchronize with the construction and development of the late Neolithic megalithic complexes. Evidence for maximum dispersal of burials sites dates to the Ġgantija phase, followed by a significant decrease in dispersed burial sites in the Tarxien phase. Importantly, the two largest surviving cemeteries were both within 500 m of the two most extensive megalithic complexes with which they were paired: Ħal Saflieni and Tarxien, the Circle and Ġgantija. The development of Ħal Saflieni and the Circle as large cemeteries occurred as they were drawn into the immediate orbit of their large megalithic

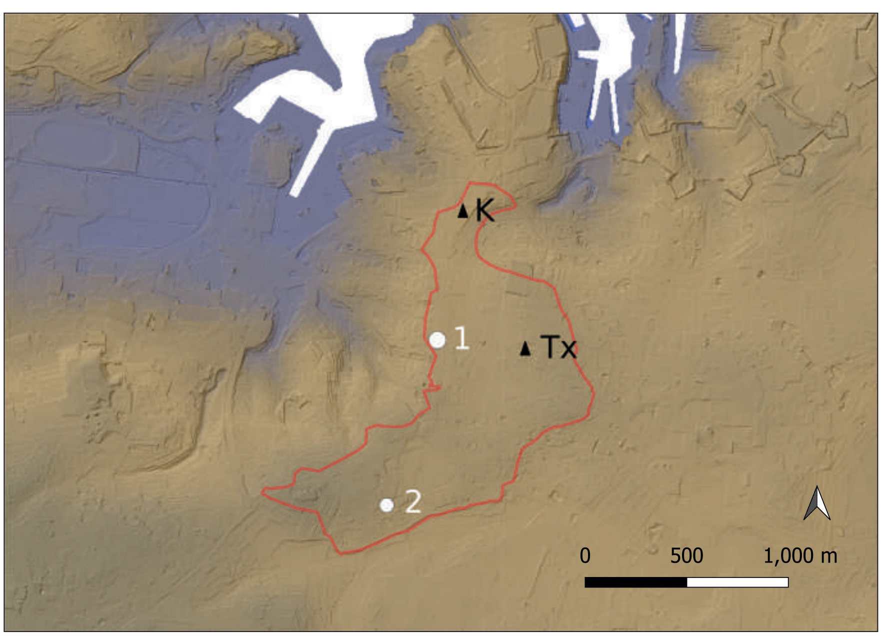

Figure 13.11. *The Tarxien, Kordin and Santa Luċija plateau. 1. Ħal Saflieni Hypogeum; 2. Santa Luċija subterranean Hypogeum. K. Kordin megalithic building; Tx. Tarxien megalithic complex. Legal copyright and use requirement: Figure Credit Basemap data provided by ERDF 156 data (2013) Developing National Environmental Monitoring Infrastructure and Capacity, Malta Environment & Planning Authority.*

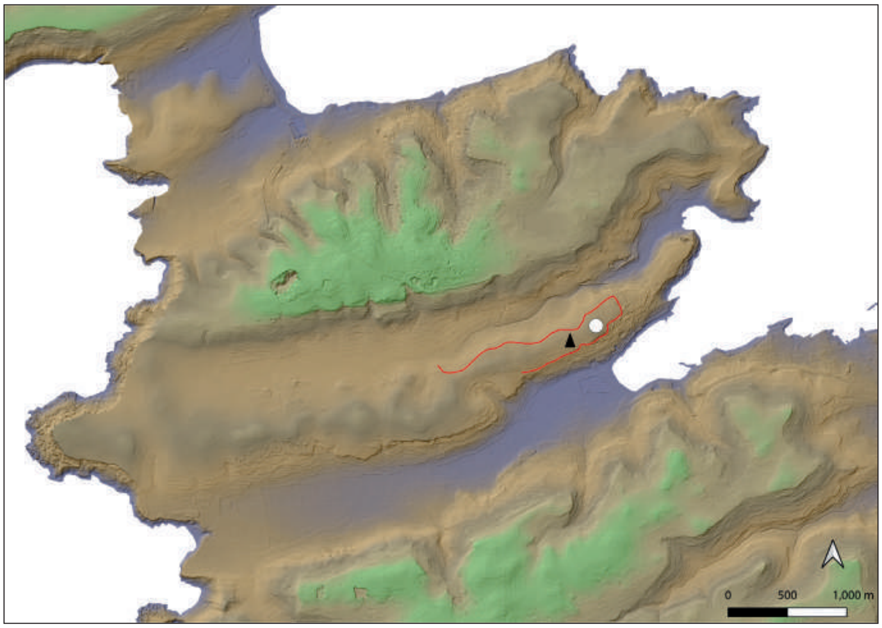

Figure 13.12. *The Xemxija promontory with the cemetery marked by a white circle and the nearby megaliths marked by a triangle. Credit: Basemap data provided by ERDF 156 data (2013) Developing National Environmental Monitoring Infrastructure and Capacity, Malta Environment & Planning Authority.*

complexes, while in contrast, less prominent or smaller buildings supported the more modest cemeteries of Xemxija (Fig. 13.12) Bur Megħeż and Kerċem. In this model, however, Ħaġar Qim and Mnajdra remain a mystery since no corresponding near neighbour burial sites has yet been identified, in spite of the extent and complexity of the two megalithic complexes.

The third important feature of Tarxien Phase burial cemeteries is the choice of natural caves. The use of caves continued alongside the use of smaller rock-cut chamber tombs. However, caves were chosen perhaps because they offered easier possibilities for creating large 'walk in' spaces. The choice of locations reflects a good geological knowledge of the characteristics of friable rock, fissures, cavities or solution holes, and how such features could be exploited to create underground spaces. Subterranean caves were preferred to hillside caves/rock shelters, perhaps because their more malleable geological composition could be easily quarried and shaped. The three well-known examples of subterranean cave cemeteries are the Ħal Saflieni Hypogeum, Bur Megħeż Cave, and the Circle. The Upper Level of Ħal Saflieni best provides a sense of how a cave system, which was first used and modified during the Ġgantija Phase (Pace 2000), retained many natural features but was transformed into a primary access level to deeper levels that were entirely cut in the live rock. The Circle reflects a similar engagement with Maltese geology, though in this case, rock collapse and surface erosion have distorted much of the site. The Bur Megħeż. site is now mostly lost to industrial quarrying and World War II military action, but it was located in a prime area of stone extraction. Surviving remains suggest that a number of natural geological features were used alongside others that were specifically rock-cut to form the site.

A fourth important characteristic of Tarxien Phase burial sites is their monumentalization. which included the use of the most conspicuous topographic locations, the use of structural elements and the adoption of internal architectural elements. The Ġgantija/Tarxien site locations are in marked contrast with many of the earlier Żebbuġ Phase burial sites which seemed to follow terraces and field systems. The burial sites of Xemxija, Busbesija (Fig. 13.12), Bur Megħeż, Nadur (Binġemma), Xagħra and Kerċem were located on high ground, that formed identifiable landmarks and accentuated the significance and sense of place of these cemeteries. The same factors characterize Ħal Saflieni (Fig. 13.11) and the Circle (Fig. 13.10). The preference for prominent as opposed to random site locations reflects a deliberate definition of space using natural settings across the archipelago. Hilltops were locations that could be used to define and name bounded places and be accorded significance, especially in relation to other settings, such as the late Neolithic megalithic complexes, settlements, pathways and other geo-cultural constructs. The interaction between burial monuments and megalithic complexes was probably a particular cultural phenomenon which defines Maltese Late Neolithic archaeology (Pace 1992, 2004).

Another aspect of burial monumentality was the adoption of the architectural canon that developed at megalithic complexes, and its influence on cemetery construction which. was more than just spatial. The structural elements, internal embellishments and spatial arrangements of the megalithic buildings influenced some of the burial sites, most conspicuously the Ħal Saflieni Hypogeum (Fig 13.13), Santa Luċija and the Circle (Fig. 13.14). Smaller structures, such as those at Xemxija and Kerċem, reflected this influence in rock-cutting techniques and evidence for deliberate enlargement.

13.5. Neolithic architecture

The emergence of Maltese late Neolithic architecture continues to be a matter of debate. Various traditional explanations around the origins of the megaliths have suggested an imported architectural concept coupled with the local development of a unique style and method of building (Fergusson 1872; Childe 1925; Ceschi 1939, 1970; Evans 1971; Trump 1981; Pace 2004). The classic explanation for an imported form of architecture referred to Aegean influences as a probable source at a time when Euro-Mediterranean archaeological chronologies were uneven and far from secure. Aegean links were doubted by Childe (1925) and later firmly discounted by radiocarbon dating (Renfrew 1973). In seeking local origins, John Evans suggested that the plans of the megalithic buildings had been derived from rock-cut tombs, particularly Xemxija Tombs 1, 2, and 5 (Evans 1959). Evans used what he believed were typological similarities between the plans of the rock-cut tombs and those of the late Neolithic megalithic buildings. However, the buildings do not exhibit the organic arrangements of any of the tombs, suggesting instead other origins may have been embedded in longer construction traditions. Carlo Ceschi argued that the design and construction of the megalithic buildings were very advanced and followed logical solutions for creating apsidal spaces along formal layouts, in which a primary axis, re-enforcing trilithon doorways, retaining walls, well-dressed megaliths and other features were combined through engineering and architectural creativity. Ceschi argued strongly that Malta's refined megalithic architecture had not been influenced by rock-cut tombs (Ceschi 1939; 1970). In considering the designs of Ħal Saflieni, Santa Luċija and the Circle, it would have been difficult for these sites to escape the strong influence imposed by megalithic construction across the archipelago.

The Tarxien Phase of Ħal Saflieni and the Circle are noteworthy for their architectural arrangements. The two sites developed from natural caves which were progressively modified, and though the engineering employed was remarkable, the organic arrangements of the burial places suggest that subterranean rock-cutting did not lend itself to the more formal arrangements for which the surface megalithic complexes are known. The structural instability of the Circle caves contributed to instances of cave-roof collapse, demonstrating that subterranean quarrying was less effective for architectural construction than building on ground surface. The large subterranean burial sites were marked by external megalithic structures and other arrangements, as well

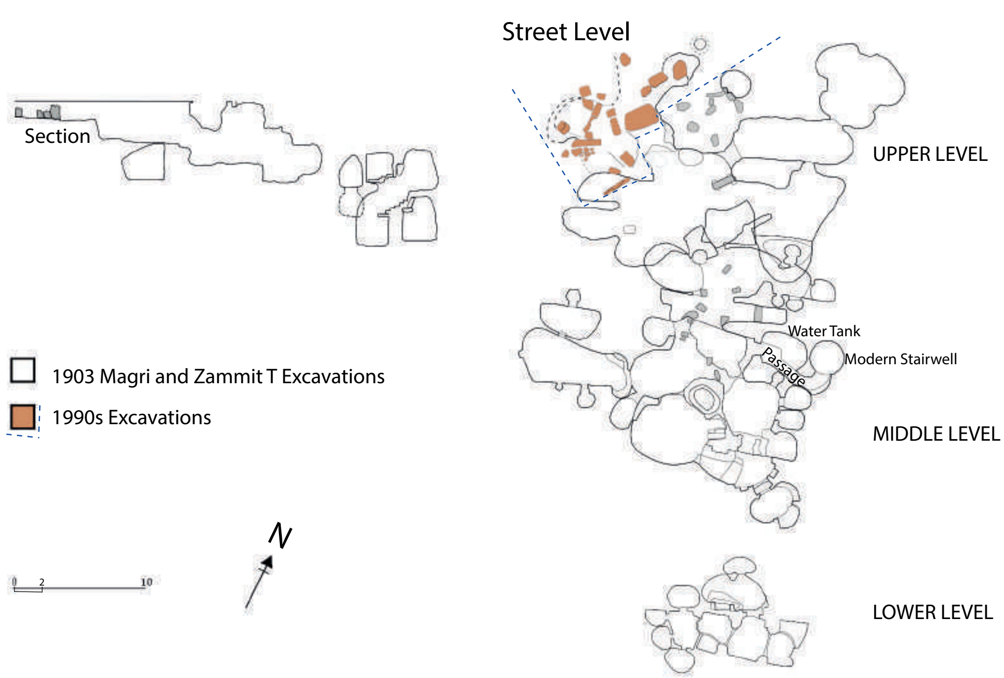

Figure 13.13. *Plan of levels 2 and 3 of the Ħal Saflieni Hypogeum.*

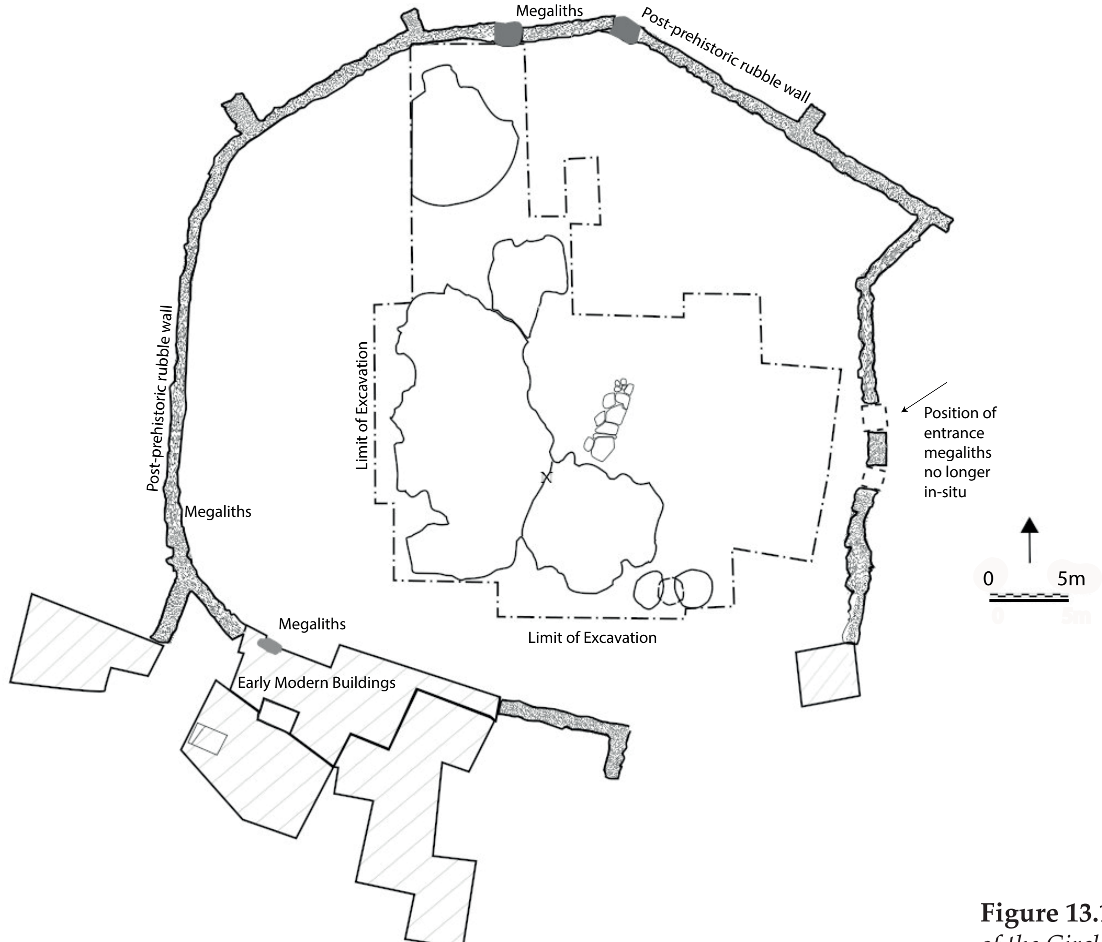

Figure 13.14. *Site plan of the Circle.*

as internal architectural features (Fig. 13.2). The best preserved external monumental remains are those of the Circle which to a large degree still preserves the extent and original form of the Circle's megalithic perimeter wall. A similar structure may have been built on top of the Ħal Saflieni Hypogeum, but this would have disappeared as a result of late 19th-century development extension of the town of Casal Paola. A similar arrangement of megaliths embellished parts of the nearby Santa Luċija hypogeum. At both the Circle and Ħal Saflieni, ceremonial passageways and entrances were also created (Bonanno *et al.* 1990; Stoddart *et al.* 1993; Pace 2000; Cutajar 2000; Malone 2000; Malone & Stoddart 2011; Chapter 13) (Fig. 13.14). Within, both sites were transformed into chambers, passageways and niches which later contained soil deposits for the interment, as well as a complex array of figurines, statues, ceramics and personal ornaments. At Ħal Saflieni (Fig. 13.13), some of the cave-like interiors were embellished with large-scale carvings of megalithic facades (Zammit 1925; Evans 1971; Pace 2000, 2004), and paintings. The introduction of architectural features and the attention that was given to their carving at Ħal Saflieni reflects the significance of imitating the buildings of the living. The emphasis on subterranean architecture was mirrored at the Circle where imported worked Globigerina megaliths formed structural compartments for the shrines and features within the rugged natural Coralline limestone caves, which unlike the geology of Ħal Saflieni, did not permit fine carving or architectural detail.

A final important aspect of the Tarxien phase funerary monuments is that the multiple functions of the tombs demanded they became more accessible. The restricted access and space of the small rock-cut tombs of the Żebbuġ and Ġgantija phases limited their functionality. Possibly the need for performing repeated rituals, the provision of a comfortable settings and greater accessibility demanded more space within a single subterranean tomb. This requirement promoted the construction of larger, more architectural proportions in the tombs, and corresponded not only to the requirements of collectivity as a shared expression of small island social relations, but also formalized the physical expression of a unifying underworld, in which the after-life could only be perceived through a familiar materiality.

13.6. Summary

Late Neolithic funerary customs in Malta and Gozo developed extraordinary rituals in which an elaboration of funerary architecture was a key element. The history of the discovery of Maltese prehistoric burial sites provides useful information on the remains themselves. In particular, this history provides good chronological frameworks into which different stages of development of the funerary monuments in the Maltese Islands may be sequenced. Other useful information, such as the Żebbuġ (ta' Trapna) burial hollows, implies they predate rock-cut *a forno tombs*. The islands initially formed part of broader central Mediterranean cultural settings, but as the small insular communities developed, their unique megalithic architecture and art emerged in response to a demanding island environment and the sea. These phenomena have often been described as inward-looking cultural traits. Set against this unique background, belief systems and ideological constructs followed very distinct forms of creativity and expressions. Among these, was a persistent expression of collective burial which may have been extended to include large numbers of a society, whose small scale would have naturally required interpersonal and kinship relations, and overt expression of social inclusion. In the Maltese context, such concerns seem to have been applied in funerary customs and remembrance, for which a particular type of monumental space was required. Funerary monuments thus culminated in the complex subterranean cemeteries of the Tarxien phase, after a long elaboration of the idea of the rock-cut tomb.

Acknowledgements

A number of colleagues have provided valuable help during the drafting of this chapter. I am indebted to the following for their suggestions, discussions and patience: Caroline Malone, Simon Stoddart, Ruth Whitehouse, Reuben Grima, Eóin Parkinson, Jeremy Bennett, Gianmarco Alberti, Sharon Sultana, Jess E. Thompson, Bernardette Mercieca, Marcia Grima and John J. Borg.

Chapter 14

Conclusion: current inferences from the study of death in prehistoric Malta

Simon Stoddart, Caroline Malone, Ronika K. Power, Rowan McLaughlin & Jess E. Thompson

14.1. The state of death in prehistoric Malta

We follow on from the review of burial monuments (Chapter 13) to present an understanding of funerary practices, perceived through the treatment of human remains. We pass from a study of the structures to a study of their bodily contents; from a landscape narrative to the agency of the people involved. Some 16 late Neolithic burial sites are known (Table 14.1), most representing rock-cut tombs, alongside three settings for large-scale collective burial: Ħal Saflieni, Santa Luċija and the Circle. Clusters of burial sites are evident on the Xagħra plateau, Gozo, where numerous excavations have focused, as well as in north, south and west Malta. Few excavations have recovered skeletal remains in any significant number. Human remains were recorded with contextual detail and recovered as fully as possible only at recently excavated sites (the Circle, the Xemxija tombs and Kerċem). Osteological analysis at these sites has allowed generally higher estimates of the number of individuals, as well as firmer interpretations of funerary practices. Importantly, these results provide some insight into burial sites which are poorly recorded, allowing us to piece together an overview of funerary practices throughout the 'Temple' Period.

The corpus of burial sites is approached chronologically. Although absolute dates are available for only a few sites, this approach emphasizes the elaboration of funerary practices from the early 4th to the late 3rd millennium BC. The minimum number of individuals (MNI) represented at each site is recorded, and depositional modes are categorized (Table 14.1). Where articulated remains are present, primary deposition of individuals soon after death is inferred (Knüsel 2014, 46). Disarticulated deposits do not exclude the possibility of initial primary deposition, especially in cases of successive burial as is represented at many Neolithic tombs (Robb 2016, 689). Disarticulation is attributed to distinct practices (Stoddart *et al*. 1999; Chapter 12), including: reduction, the clearance of remains which is not pre-planned (Duday 2009, 72), and secondary deposition, which involves the redistribution of remains from their initial burial location, and often focuses on particular skeletal elements (Knüsel 2014, 50).

Rock-cut tombs attributed to the Żebbuġ period typically contained small numbers of individuals. The highest recorded MNI is from the ta' Trapna iz-Żgħira tombs, where at least 12 individuals were deposited in 5 tombs. However, these figures are likely to under-represent the original number of individuals deposited in rock-cut tombs, owing to selective excavation methods, site disturbance, and the absence of osteological analysis. Based upon the limited evidence available, successive primary depositions, followed by reduction of the skeletal remains to the edges of the chambers, are indicated (Cagiano de Azevedo 1969a; Baldacchino & Evans 1954; Zammit 1928). Ochre formed a central part of the funerary rite in this early period; deposits were covered with bright red ochre, which adhered to the surface of the skeletal remains. It has been suggested that rock-cut tombs were used by familial or kin groups, largely based upon the small size of the chambers (generally 1.5–2 m in diameter) and low numbers of burials (Malone & Stoddart 2009, 363).

Radiocarbon dates from rock-cut tombs at the Circle and Xemxija reveal the longevity of their use (Chapter 11), and analysis has established that larger numbers of individuals were deposited in these tombs. Although their earliest use is dated to the Ġgantija period, these finds may nevertheless challenge interpretation as to the size of the community/ies utilizing earlier burial sites. We also need to undertake a more detailed dating programme of human remains from these tombs to establish definitively the onset of the burial practices.

Burial in rock-cut tombs during the Ġgantija period mostly continued on a similar scale (indicated

Table 14.1 *Known prehistoric funerary remains in the Maltese Islands (PD = Primary Deposition; R = Reduction, SD = Secondary Deposition).*

Site	Location	Region	Site type	Phase	MNI	Depositional modes
Ta' Trapna iz-Żgħira (Żebbuġ tombs)	Malta	Żebbuġ	Rock-cut tombs (5)	Żebbuġ	>12	PD, R?
San Pawl Milqi	Malta	Burmarrad	Rock-cut tombs (4)	Żebbuġ	>4	PD, SD?
Near ta' Kola Windmill	Gozo	Xagħra	Rock-cut tomb?	Żebbuġ	?	?
Buqana	Malta	Attard	Rock-cut tomb	Żebbuġ–Ġgantija	>3	Probable PD, R
Xagħra rock-cut tomb	Gozo	Xagħra	Rock-cut tomb	Ġgantija	>4	PD, R
Circle rock-cut tomb	Gozo	Xagħra	Rock-cut tomb	Ggantija	65 (11 non-adults)	PD, R
Circle	Gozo	Xagħra	Substantial burial enclosure	Żebbuġ–Tarxien	450–1001	PD, R, SD, MD
Ħal Saflieni	Malta	Paola	Substantial burial enclosure	Żebbuġ–Tarxien	*c.* 7000 (over-estimate)	PD, R, SD
Xemxija rock-cut tombs	Malta	St Paul's Bay	Rock-cut tombs (7)	Ġgantija–Tarxien	112	PD, R, SD?
Bur Megħeż	Malta	Mqabba	Natural cave	Ġgantija–Tarxien	45–100	PD, R, SD
North Cave	Gozo	Xagħra	Rock-cut tombs	Ġgantija	1	SD
Nadur	Malta	Rabat	Rock-cut tomb	Ġgantija	?	?
Bubisija	Malta	Mdina	Rock-cut tomb	Ġgantija	>5	?
Kerċem	Gozo	Kerċem	Rock-cut tombs	Tarxien	>4	PD, R
Santa Luċija	Malta	Santa Luċija	Hypogeum	'Temple' period	Many	SD
Ta' Vnezja	Malta	Mosta	Rock-cut tomb	'Temple' period	2	PD

at the North Cave, Busbisija, Nadur and the Circle), although much larger spaces began to be used. At Bur Megħeż, burials were placed in a compartment in the 18–19 m long cave system (Evans 1971, 40; Tagliaferro 1911). Tombs 1, 2 and 5 at Xemxija have an enlarged lobate form (Evans 1971, 113–4), and multiple chambers were cut into the limestone at Ħal Saflieni – each larger than a single rock-cut tomb (Zammit 1925). A single radiocarbon date from Bur Megħeż indicates Ġgantija to Tarxien use of the site, from 3150–2650 cal. BC (OxA-8165, 4305±65 BP calibrated at 2σ cited in Malone *et al.* 2009e, 342). This complex deposit contained skeletal remains in various states: articulated flexed primary inhumations, disarticulated remains, and caches of crania and long bones, often covered with megalithic slabs and ochred earth (Tagliaferro 1911, 1912). Human remains were commingled with faunal remains and material culture, including potsherds, flint and shells. There are varying estimates for the number of individuals deposited in the cave and it is unclear whether the deposit was fully excavated, but it is evident a larger number of individuals seem to have been buried than in contemporary rock-cut tombs.

Little recorded observation survives of the skeletal remains *in situ* at the Xemxija tombs, but deposits were sieved, leading to an exceptional level of recovery (Evans 1971, 113). Tomb 5 was both the largest and the only tomb to contain items of personal adornment, including shell buttons and beads, and two miniature axe-head pendants (Evans 1971, 114). The first burial deposits were likely made during the Ġgantija period at Ħal Saflieni. Zammit (1925, 36) reported that one of the chambers to the right of the entrance in the Upper Level contained a complete, articulated skeleton of a male adult in ochred soil. In the first chamber on the left, the remains of an original burial deposit were left *in situ* by Zammit. Recent excavations (1990–3) as part of conservation works, have identified further intact deposits in the Upper Level, including articulated human remains (Cutajar 2001).

Collective deposition continued to intensify in the Saflieni and Tarxien periods with the construction and use of more formal substantial burial enclosures. Some smaller sites also remained in use throughout much of this time; Tarxien material was present in the Kerċem tombs (Pace 2011; Bernardette Mercieca-Spiteri pers. comm.), and Tarxien activity is evident at the Xemxija tombs (Chapter 12). Deposition in the substantial burial enclosures was varied; primary inhumation is evident alongside the contemporary reworking of deposits, including disarticulation and redistribution. There is unfortunately little information regarding the skeletal remains from Santa Luċija. Deposits from the Middle and Lower Levels of Ħal Saflieni may date to this period but were unfortunately excavated and cleared out in 1902 by Father Magri. The Lower Level is reached by a series of steps, the last of which is raised 2 metres above the ground level (Pace 2000, 7). Thin walls extending to 2 m in height separate many of the chambers on this level, suggesting that a much deeper soil deposit—which likely contained skeletal remains—may have been contained here (Pace 2004, 41). At Kerċem, at least three successive primary interments were separated by platforms of rubble, and punctuated by episodes of reduction, in which remains were pushed to the back of the chamber (Bernardette Mercieca-Spiteri pers. comm; Times of Malta 2009; Pace 2011).

The largely disarticulated character of most deposits has often been associated either with the clearance of earlier burials to make space for new interments, or with secondary deposition following exposure (Tagliaferro 1912, 146; Trump 2002, 118; Zammit 1925). While the former is indicated at most sites, and there is some evidence for the latter at the Xemxija tombs and the Circle (Chapter 12), a more complex set of rites is indicated by recent work, which may be inferred at contemporary sites. Current interpretations of funerary practices at the Circle have drawn on element representation and taphonomy of remains from the rock-cut tomb (Duhig in Malone *et al.* 1995; Duhig 1996) and the redistribution of body parts within the hypogeum (Stoddart *et al.* 2009a; Chapter 12). In the rock-cut tomb, more individuals were deposited in the West chamber, resulting in high levels of disarticulation, but repeated episodes of disturbance were evident in the East chamber (Malone *et al.* 1995; Malone *et al.* 2009f). Element representation revealed that small bones were the highest represented elements in both chambers (Duhig in Malone *et al.* 1995, 339). Alongside some evidence for *in situ* articulation, this indicated primary interment, but both disarticulated bones in the uppermost levels and the differing numbers of long bones present suggested that secondary deposition was also practised. Within the cave system of the Circle, secondary treatment of remains was identified (Stoddart *et al.* 2009f, 320; Chapter 12 in this volume). Cranial curation of both humans and animals was evident in several areas, as was long bone curation. Residual deposits, from which these larger elements were removed, were indicated by an over-representation of small bones. Both primary deposition and secondary deposition are evident; primary deposition seems to have been carried out directly in the limestone caves and most remains were subsequently disarticulated in rites which selected specific parts of the body for curation.

This discussion reveals some key trends in funerary practices: primary deposition often predominates, but successive overlying interments and *postmortem* disarticulation have resulted in highly fragmented remains. A key question is the degree of intentionality of the disarticulation, a question that was asked in the first preliminary analysis of the Circle (Stoddart *et al.* 1999). Where inhumations survive, individuals were often placed on one side usually the right, with their lower limbs flexed (Stoddart & Malone 2010). The structured nature of disarticulated deposits at some sites also show an emphasis on particular bones, particularly the skull and long bones. Interpreting funerary behaviour has broad implications. As is evident through recent, and ongoing analyses (Chapter 12), the treatment of the dead was a complex and protracted process throughout this period on the Maltese Islands. Funerary practices indicate that it was often necessary to manipulate the remains of the dead in order to achieve their proper transformation. The modification of the body did not begin in death, however, as there is evidence for both active and passive dental modification in life (Chapter 5). This finding reveals compelling insights into understandings of the body, providing the opportunity to build on earlier interpretations (Stoddart & Malone 2008). Combined with a demographic analysis of the treatment of individuals of all ages and sexes, it is also possible to refine current models of social organization (Stoddart & Malone 2015).

This is the context in which the rest of this volume has been set, adding new details to an already detailed and unusual story of death that also contributes to our understanding of the life of these undoubtedly resilient and creative islanders: the 'Temple' people, who frequented what we prefer now to think of as club houses (Barratt *et al.* 2020), an interpretation which breaks the mould, as do many of the conclusions that follow.

14.2. The sample

The funerary evidence for Malta is still substantially based on the Circle sample. In the current volume, the sample of the Circle burial population is but a sample of a sample of a sample (compared with the 2009 analysis) and that is the first matter that must be emphasized. Only part of the site has been excavated and only part of the recovered sample has been re-analysed. Additionally, only the human remains from Xemxija and from Kerċem add in any material way quantitatively to our overall knowledge. An important break-through is that Xemxija, despite several issues relating to context and curation, is beginning to contribute to the overall picture notably in terms of diet, taphonomy and population profile. In spite of these provisos, some important questions can be addressed:

1. Are the remains left in the Circle the full product of the 'biological material culture' from the ritual process? We use the term 'biological material culture' because the burying population treated human remains of their kith and kin as manipulable material culture in a way that requires ethnographic knowledge to appreciate (Kus 1992, 170). This is an issue that has already been addressed (Malone & Stoddart 2009; Stoddart & Malone 2015), but now assessed to be more likely only part of the human remains originally involved in the ceremonies (see below). As discussed above, the Circle and Ħal Saflieni are apparently self-contained focal points of the 'biological material culture', but contemporary satellite burial places in the same immediate landscape (as discussed above, Chapter 13) have been discovered within 50 m of the Circle and close to Ħal Saflieni at Santa Luċija, suggesting treatment of other bodies in other parts of the landscape.

2. To what extent are the human remains left in the Circle a complete recovery of those originally left in antiquity? The calcareous chemistry of the Coralline limestone and the movement of water at this level on the Xagħra plateau seems to have been relatively favourable to the survival of even the smallest fragment of human bone, including foetuses, neonates and perinates. The excavation recovery of 1987–94 also seems to have been relatively complete within the excavated areas. However, the depredations of the 1820s clearly removed substantial quantities of remains, as is made clear from the descriptions that remain from the period (Attard Tabone 1999). Furthermore, the 1994 excavations ended with known deposits still in the ground, most notably in the open display area of Context (783), the disturbed area to the south, the deeper areas to the north, and the inner cave to the east. We still do not know the extent of deposits under the collapsed cave under Tarxien Cemetery deposits to the north of the site or whether the Circle contained other cavities. A new campaign of GeoRadar with modern equipment might solve this latter problem.

3. What are the core differences and similarities between the 2009 reporting of the full excavated assemblage and the current detailed analysis of a subsample of the assemblage?

In the first chapter, we posed a number of questions. We now summarize the answers to some of these questions that have been covered in more detail in the preceding chapters.

14.3. Who was buried?

The crucial question for any buried community is its level of representativeness of the once living population. Does the scale of mortuary practice in any way reflect the level and characteristics of the people who lived in the 3rd millennium BC? The large scale of the buried remains may tempt the observer to suggest a large population, but the length of time over which burial practices elapsed, and the application of simple statistics, soon recommend a level of caution in making any such interpretation. We must simultaneously ask how inclusive the burial rite was of the local community, a question that we have previously raised without definite conclusions. Some advances appear to have been made by the recent research in indicating that the apparently substantial quantities of human remains were a small, but representative, reflection of the much greater size of the community which was originally involved. This suggests both a full access of the living community to the rite of burial (already suggested by the balanced sex and age profiles) and a very much larger community than that framed by the minimum numbers of individuals. Some simulations suggest that MNI data substantially under-represent the original burial population (Robb 2016), although practical re-fitting of remains from commingled deposits can sometimes suggest quite the opposite (Knight pers. comm. 2019 from the Must Farm deposit). If we make the (likely false) assumption that we are dealing with a true reflection of the living population, then application of the Bocquet-Appel (2002) palaeodemographic formula (already applied by Bocquet-Appel to the rock-cut tomb in the Circle) suggests that the buried population, and by implication the living population, were a relatively stable and resilient, or possibly slightly declining population, particularly towards the end of the use of the site. This is supported by the fact that some of those who survived to adulthood had the capacity to survive to a substantial age (Chapter 8). The same analysis by the current investigative team established incontrovertibly that the prehistoric inhabitants took care of the members of their community, no doubt contributing to their longevity. Furthermore, inter-personal violence although present was at a relatively low level, in so far as osteological evidence permits that conclusion.

Absolute density of the population is more difficult to gauge. Modern Malta has the 9th largest density of any political community in the world (after Monaco, Macao, Singapore, Hong Kong, Gibraltar, Bahrain, the Vatican and the Maldives), but this is a product of modern globalization. There is no independent evidence, such as from settlement or land-use, that the human presence in the Maltese Islands had a similarly relatively dense occupation in prehistory compared with the rest of the central Mediterranean at the same time. Indeed, recent genetic evidence suggests that the gene pool of three sampled individuals (not the same as the size of the community) was quite small (Ariano *et al*. 2022). We consequently have a continuing debate over the degree to which the Circle contained the whole community after death. On the one hand, the buried community strikingly mirrors our expectations of the age and sex profile of a Neolithic community, including very large numbers of non-adults and and a roughly equal ratio of men and women. On the other hand, there were many other staging posts of ritual both within and without the Circle. Within the Circle, we have some tantalizing deposits in the upper levels which give indication of other intermediate resting places. Without the Circle, we have several locales such as the North Cave near Ġgantija or the new deposit close to the Circle (Chapter 13) and, further away, Kerċem on Gozo or Santa Luċija on Malta (near Ħal Saflieni) which might be relics of such an extenuated ritual process (Chapter 13). There are some hints that the complexity of the ritual with many more structured practices may have increased with time, in a way that matches what has been interpreted as increased complexity in the monumental 'club-houses' above ground.

As has been already remarked in earlier publications, this ritual was very highly structured in terms of orientation and structure, rules of dress and hairstyle, scale, periodicity, seasonality, pollution, water and fire (Malone 2007; Stoddart & Malone 2018). There is a strong argument that the life cycle was signalled through material culture. This was a very highly ordered society. Complexity appears to have been expressed in terms of prescribed rules rather than diversity. Yet, there was enormous creativity in some aspects of art. In others, there was a very clear replication of form across different scales, from the minuscule to the gigantic. This can be seen in the representation of the human form and in the making of clay and stone vessels (Stoddart & Malone 2008).

The imagined body appears to have been intentionally contrasted with the real body. The imagined body was endowed with generous quantities of flesh and usually, although not exclusively, without primary sexual characteristics. The real bodies show clear evidence of being worked hard, both from the vertebrae and from the extremities, particularly the hands, and use of the teeth as a third hand. It is thus difficult to imagine that they in any way approached the corpulence shown in their figuration. There is at least one figurine with a possible scarification on the flat chest, but that level of detail is exceptional. A notable proportion of the teeth have been reworked in a manner that can only be considered as related to identity (Chapter 5), either related to age or gender or to some other sub-group within the community. What was the agency and periodicity of this modification? At present, this is difficult to assess. Another indicator of identity is granted by the association of some bones, especially skulls, with animal remains often themselves skulls, a fact noted in the 2009 publication.

If we are to accept that the Circle was in some structured way representative of the full community, we can move on to ask questions about the diversity of that community. The physical morphology of the human community seems to suggest an ancestry from both north and south of the Maltese Islands. Isotopic information indicates a movement of people from both cooler and warmer climes but one mainly distinctive of a broadly limestone environment (Chapter 9). The limited aDNA nevertheless suggests a standard Mediterranean ancestry without any surprising outliers, although this is very much work in progress. The work on dental modification shows that a small proportion of the population had these distinctive cultural features which may have been caused by a variety of different conscious and unconscious cultural practices (Chapter 5). Research into dental morphology (Chapter 6), while indicating a close affinity with ancient Italians, Punic Carthage and Berbers, also shows a moderate degree of insularity, that is distinction from other populations.

It is tempting to seek to identify the presence of a population that can be associated with the so-called Thermi ware in the transitional phase towards the end of the Temple Period, but this is difficult to substantiate (an issue highlighted in Volume 2). On the other hand, the trends over time are remarkable, since they do suggest an increasing insularity of the population over a course of time that may run in tandem with trends of health remarked upon below and, might we hazard, trends of changing contact with the outside world.

There are some notable spatial variations. The Display Zone (783) does appear to be particularly distinctive in both chronological and spatial terms, with a disproportionate quantity of the figurines, both ceramic and bone, as well as showing some important trends of health. However, this is, itself, work in progress, work that will be much aided by the intra-site GIS that is now available for ongoing work.

14.4. When were they buried?

A major change in our knowledge of the Circle human remains is in the details of their chronological distribution (Chapter 3). This is in response to the greatly increased number of radiocarbon dates, their greater precision and the application of new statistics that include Bayesian models.

The first major change is that the rock-cut tomb on the site has been brought in line with the Ġgantija period rather than the preceding Żebbuġ. This fits well with developments in the surrounding southern central Mediterranean, but this conclusion is still dependent on a relatively small number of dated samples from the rock-cut tomb. We know from the results presented in all three volumes that residuality of material is a major issue in the Maltese Islands, and we need to gauge the date of the Żebbuġ pottery amongst what are, apparently later, directly dated human remains.

The second major change is in the dissection of greater detail in the Tarxien phase. Most notably there appears to have been change in burial density at about 2500 BC, leading to a protracted decline (Chapter 3) and the termination of burial deposition at about 2350 BC.

14.5. Can we identify changes in the health of the prehistoric populations?

The Maltese bodies demonstrated considerable resilience (Chapter 8). On the one hand there was a surprisingly low frequency of stress reflected in low incidences of *cribra orbitalia*, porotic hyperostosis, enamel hypoplasia, caries and joint disease. On the other hand, their bodies had suffered, including from severe use of the teeth, and differential wear and of their backs and hands, shown by eburnation and lipping of the joints. Curiously, their upper limbs were more gracile than their lower limbs in comparison with other Mediterranean populations (Chapter 7) and their body size was greater than their Mediterranean contemporaries. These habitual activities were sufficiently prolonged to show a preference for right handedness, similar to modern human populations. Furthermore, the trends of a combined range of measures focused on teeth indicate a general decline in health over the period 2500 until 2350 BC (Chapter 4). These subtle changes may be indicative of pressures that led the continuing biological population of prehistoric Malta to decide that the divine spirits were against them and the protected gardens around their club house temples no longer offered the millennial protection which had been so certain for their ancestors.

Health may be strongly related to diet. The latest modelling (Figure 10.3) shows a strong animal contribution to the diet, perhaps sourced through dairying, that showed less variation in the population in the Tarxien phases, with a very small contribution from marine resources (Chapter 10). In the Ġgantija phase of the Temple Period, there may have been a relatively short-lived attempt to boost the manuring of the fields close to the temples in order to reverse the deterioration of the landscape.

14.6. Contemporary body concepts and belief in Neolithic Malta

We end on a much more speculative note. Modern western humans have a well-defined belief associated with their bodies, even if some of the categories are now in the course of being reformulated, faced with the decline of religion and the more detailed investigation of science. The problem for prehistorians is that we only have direct experience of our modern framework, our own ethnography. This raises the question of how to address beliefs in the body in the past. One project supported by Leverhulme (Robb & Harris 2013), where one of us (Stoddart) had a role, looked at the broad scales of the body in history, across time, searching out patterns and trends. This section addresses the smaller scale of one prehistoric island. The sole matter that links them is the richness of spatially organized material culture from the micro to the macroscale. The intent is as much methodological as theoretical.

In part inspired by the Leverhulme project, seven fundamental questions are proposed in looking at Maltese societies. **Firstly**, is it possible to execute a somatic ethnography of the prehistoric past? Some archaeologists have returned to the issue of creative ethnography, after a reluctance in the processual era, albeit this time invested with detailed excavation records, and scientifically supported facts. Do these accounts add to or distort our interpretations? To what extent are they governed by the legacies of our own lives and histories? **Secondly**, to what extent do these prehistoric societies make a clear distinction between humans and animals in their belief systems? The separation (or not) of the human from the animal form speaks strongly of the definition of belief in the human body. **Thirdly**, how does the human form fit with a different scale of cosmological space, both at the level of landscape and at the human earthly scale? Can we see constraints on the human form, defined by the built environment? **Fourthly**, and closely connected with the third question, how does the sacred affect the appearance of the human form? And by consequence how is belief in the body linked to the sacred? **Fifthly**, how profoundly are distinctions of gender drawn in the societies concerned? Might there be any blurring of the preconceptions of male and female in the deployment of material culture, even if a third or alternative gender is not explicitly visible? **Penultimately**, we address the question most frequently investigated by archaeologists: what happened to the human body after death? **Finally**, what is the relationship between social and/or fictive kinship and the biological body? This latter is a question that the increasing sophistication of science is allowing us to address more effectively as we combine evidence from the different sources of different scale and chemistry. As **an endnote** we direct our attention to where future studies of belief in the body might be addressed.

These questions are addressed to a society which has a rich material culture that delineated the human form, provided a built environment that constrained that same form, remodelled bodies in life and preserved a burial tradition that manipulated the human body. Many prehistoric societies have a rich body of evidence in one sector, but Malta has preserved evidence in multiple, complementary sectors. As demonstrated in the other volumes, the society comprised agricultural communities, centred on the 3rd millennium BC in the restricted confines of a *c*. 300 km^2 archipelago. The geological conditions of the island and the absence of other raw materials focused the creativity of the prehistoric Maltese on fashioning elaborate material forms at different scales (see below) out of clay and limestone. The Maltese evidence survives in many forms: large above ground three dimensional structures generally designated temples, substantial underground interconnecting structures generally designated funerary hypogea, elaborate figurative sculpture and substantial quantities of human remains recently recorded with reasonable precision. If these difficult questions can be addressed to any prehistoric society, the best case can be made for the Maltese.

1. Archaeologists are increasingly deploying the technique of fictive ethnography to develop the sentient elements of reconstructions of the past. In the case of Malta, we present two contrasting accounts. The first appears in the previous publication of the Circle and is explicitly highlighted as an attempt at creative fiction to fill in the gaps behind the static material culture.

> 'The elders were dressed in their formal attire of headdresses and long skirts, clothing that had a reserved status and was only worn for festivals and ceremonies.' (the words of Caroline Malone in Malone & Stoddart 2009, 380).

These words are built out of a social anthropological study of the evidence in two regards. Firstly, the reference to elders draws on the cross-cultural evidence that senior age grades were often those entrusted with such performances and who are shown to have longevity in this volume and could easily have been women. These elders are reservoirs of memory (cf. Stoddart 2015). This makes the monuments, above and below ground, worthy of the designation *memory monuments*. The subtle reorganization of screens and the maintenance of routeways identified through the burial spaces of the Circle (**Chapter 13**) indicates that there was an intense and continued relationship between the living and the dead. Secondly, the material culture itself (see below), set within a social anthropological framework, suggests that a special timeless style was allocated to sacred events such as the funerary ceremony described here.

> *'Elle est trop maigre. Ici, nous aimons les femmes épaisses, avec des corps à bourrelets empilés, des seins à faite téter des familles entières, des ventres donnant la vie à qui mieux mieux, des postérieurs gonflés au possible.'*
>
> 'She is too thin. Here, we like well endowed women, ample rolls of flesh, breasts to suckle entire families, bellies giving life to the best, buttocks as swollen as possible' (Guilaine 2016).

These words are a much more direct observation of the bodily form deployed by the prehistoric artists of Malta. It is indeed true that the prehistoric people of Malta did project emphasis on *substantial* individuals as an artistic style. However, two questions need to be raised in the interpretation of meaning of that style. Firstly, does the representation of the human form truly represent the female sex, when primary sexual characteristics (such as breasts, pubic triangle/genitalia) are missing in most cases? Secondly, how frequently did the prehistoric inhabitants of Malta achieve these voluptuous forms? There is sufficient anatomical observation in ancient Maltese art to suggest that these accumulations of flesh had at some time been observed, but there is equally sufficient osteological evidence that the prehistoric bodies of Malta suffered from a resilient response to their fragile environment rather than from the pressures of carrying substantial stores of fat (Chapter 7). These two parallel body narratives convey the difficulty in interpreting the evidence that we have to address in building up a framework of body belief in the prehistoric past. As discussed in Chapter 8, a combination of impoverishment of diet in the early life course combined with relatively high levels of dairy in later life might have granted some members of the community a greater degree of corpulence and thus the observations recorded in the contemporary art. A notable feature of the corpulence is that it is focussed more on the lower body, so the explanation that this is a product of a specific medical condition such as gynaecomastia seems unlikely.

2. The relationship of humans to the animal world has changed over the course of human development (Robb & Harris 2013). The prehistoric society of Malta appears to have developed a clear and distinctive separation between the human and animal form where any form of merger was generally avoided. The only exception that appears to break this rule is a small hybrid figurine found in the Circle that combines what appears to be a form of snail with a human head (Malone *et al.* 2009a, 307). Equally the two classes of human and animal were generally treated differently by the prehistoric craftsmen. Humans were generally presented in the round. Animals were generally presented in bas relief (Grima 2003). We can, therefore, on these two related grounds, make the interpretation that the belief in prehistoric Malta was to place them in differently conceived categories.

3. These considerations about the relationship of humans and animals to their world raise questions of where these categories were granted access in terms of cosmological space. Through interpretation of the ethnographic literature, we can register that many ethnographic landscapes were not only horizontal, but also vertical (Stoddart 2002; Malone 2008). We may tentatively be able to allocate some of the delineations of body forms to different levels in this cosmological world: birds (alongside the celestial lights and the volcano Etna) to the sky; humans and domestic animals to the earth; monstrous animals, snails, fish, serpents and the human dead to the underworld. This is clearly a structure more difficult to prove but is compatible with the existing evidence. There is some indication that individual club houses may have also been associated with different bodily attributes which in three cases derive from the underworld: Buġibba - fish; Santa Verna – Snail; Ġgantija – snake. The fourth case of Tarxien has strong evidence for domestic animals, as well as the human form.

4. The Maltese prehistoric communities did have stylistic tropes of the body, which some of us interpret as connected to the sacred. The best evidence is focused on the head. The standardized headdress is a form of gathered hair. Long hair and well-shorn hair form a minority delineation. Many human forms are undressed, but when clothing does take place, it regularly involves the distinctive pleated skirt. This combination of gathered hair and pleated skirt is how a sacred state of the body was characterized (Stoddart & Malone 2018) and was probably connected with the long-term memories of the society.

A further characteristic of this stylized dress is that it operated at different scales. The smallest figurines which focus on the head are a mere couple of centimetres in size. These smaller objects tend to be associated with the liturgical activity of funerary ritual. Intermediate sizes preside over funerary activity and serve a similar purpose in temples. The largest statues are found in temples and form static elements in the ritualized theatre. It is a very particular characteristic of Maltese material culture that not only modelling of the body, but the modelling of pottery and stone and of the temples themselves, operated across many scales from the intimate object held in the hand, to the object of intermediate scale held on a niche, to the massive creation that presided over a club house, commensurate in size to the club houses themselves.

These scales are profoundly linked to the scale of the built environment and the degree of control over the body provided by these deliberate constructions. In prehistoric Malta, the unusually well-preserved built environment offers opportunities to study constraints on the human form in the service of ritual performance. At least two broad categories of club house exist. The first is the hierarchical temple, iconically represented by the two examples of Ġgantija. The human body was controlled by architectural space so that the majority of the participants were held outside the façade with limited visual and bodily access to the interior. By the same measure this type of temple was a hierarchical *cul de sac*, where the external eye is drawn up to its axial point, an effect that can even be theatrically staged in two or three acts. By contrast, at least two temples (Ħaġar Qim and Tas Silġ) allowed entry and access by one formal door and exit by another. This architecture suggests the transformation of the participant from one status to another, a veritable rite of passage, that operated within the theatrical scenery of the temple. The ultimate rite of passage is that of death, recorded in this volume, but in the case of the Maltese temples, such is the preservation of the built environment, we even have evidence of the setting of the rites of passage of life.

5. The traditional interpretation of Maltese figurative art has been to see the art of islands as a subset of a strong appreciation of the well-endowed feminine form. The most famous exponent of this approach was Maria Gimbutas who saw Malta as an outlier of her Old Europe (1991), a zone of matriarchal religion. She saw the aerial perspective of the temples as a scaled-up version of the bodily representations that lay within. A closer inspection of the corpulent forms reveals their ambiguity in comparisons with other types from continental Europe (Malone *et al.* 1995). In other words, the emphasis is on unsexualized corpulence rather than specific anatomical reference to the feminine form.

The presence of some fully feminine figurines shows that there was not a taboo on their representation. The male human form was never shown in the nude, but only by representation of a significant part, namely the phallus. Once these observations are quantified (Malone & Stoddart 2016), it is clear that corpulent ambiguity is the dominant theme. Gender was relatively rarely represented and seemingly downplayed in their outward belief in the body (cf. Thompson 2020).

6. The strongest evidence for belief in the body, as in many archaeological contexts, derives from death, the subject of this volume. The data from Malta are a recent development in archaeological historiography (Chapter 1) because of excavation of the Circle in the late 1980s and early 1990s. The evidence of death is very elaborate. It involves the delivery of the intact body to an enclosed area and then the later dismemberment of its individuality so that the ultimate form of the majority of the deceased was in the form of a new restructured corporate body. This was originally analysed in broad statistical terms, assessing the relative proportion of body parts in differently arranged deposits (Stoddart *et al.* 2009a). The new work has interrogated in greater detail the taphonomy (Chapter 12) and dating (Chapter 3) of the individual body parts to establish whether new details can be established within the overall flow of body parts within the underground complex. This flow of bones has been interpreted by drawing on ethnographic studies as a constant cycling of conception and deconception so that individuals join the eternity of the corporate community (Stoddart 2015). Similar patterns of cyclicity can be observed in craftsmanship production and in the meaningful symbolism of those craft products. The priest figure from Tarxien appears to have several layers of plaster. The cache of plaque figurines found in the Circle are individually in different stages of craft production. The individuals that make the seated pair from the same funerary deposit appear to represent the beginning and end of the cycle of life. In both the club houses and in the domestic sphere there appear to have been cycles of plastering that register other temporal patterns in the life of the community. In this manner, we can register a series of scales of nested time that build up from individual lives into the eternity of the community sustained by the ritual specialists, until such time as it failed to operate and was deliberately closed down in *c*. 2350 BC.

7. The final issue of belief that we wish to address is the relationship between the social genealogy (at its various temporal scales) and the biological genealogy that can be established from scientific sampling. The island context and the limestone geology of Malta gave its inhabitants a potentially distinctive chemical signature that can be further investigated through studies of birthplace temperature and ancient DNA. These multiple sources of evidence are working towards a deeper understanding of what it was to be a prehistoric Maltese islander both biologically from the inside out and socially from the outside in. At least some prehistoric Maltese demonstrate morphological traits closely associated with African populations, but this does not mean that they were socially African, since isotopes suggests a proportion of these individuals were born on the Maltese Islands. Regardless of what origins people may have had, a posthumous social inclusion into an indivisible community in death is reflected in the burials of the Circle.

It is difficult to foresee how future studies of the prehistoric body will develop. What is certain, however, is that the study of the relationship between the social and biological body will be further explored, establishing to a greater degree how much the social 'facts' mapped onto biological data where they survive. The potential for asking new questions through interdisciplinary engagements between the sciences and social sciences is enormous.

14.7. Conclusion

The overall conclusion is that the island community originally had a diverse range of origins including potentially African and northern Mediterranean ancestry. This was a highly resilient population, coping well with local island conditions and displaying a clear local identity both in terms of outward representation and bodily modification. However, towards the latter end of the use of the temples, some clear indicators of increasing insularity and decreasing health became apparent. This may have brought the so-called temple period to an end and led to the inclusion of new cultural practices and other population groups, even before the temples went completely out of use. The bodies of the populations of the early Bronze Age were unfortunately cremated, making it much more difficult to investigate the implicit contrast between these two phases of island prehistory.

14.8. Whither death studies in Malta?

This volume has presented a detailed study of the sample that was excavated until 1994, building on, deepening and sometimes reworking the generalities assembled in the 2009 publication. It can perhaps be claimed that the current sophisticated and detailed interdisciplinary work has overcome as much as is feasible the issues of the osteological paradox, that osteological data are reluctant to yield their secrets to the living. This will be a continuing process, since this extraordinary assemblage deserves work by new generations of scholars, long after the demise of the current research team.

A number of future directions are clearly indicated already by the current research, and not reported here since this is ongoing work. We opened the volume by reporting on the early interest in the crania found in Ħal Saflieni by both Bradley and Buxton. Work on the Circle population, but not reported in detail here, might suggest that some of crania have a distinctive morphology that reflect African affinities, and other sites too may reveal distinctive features. Diverse origins have not yet been picked up in the aDNA work, and further inter-related research can be expected to explore the complex ancestry of the buried population, including more developed work on the aDNA of individuals amongst those already sequenced.

Enormous advances have been made in the dating of the human remains within the Circle. These results have notably suggested that some of the earliest deposits accompanied by Żebbuġ ceramic material may be better dated in the Ġgantija chronological phase. It would be at least prudent to increase the number of dated human remains to consolidate this conclusion.

In the study of a large, even if commingled, population, there are bound to be individual pathologies, particularly those that offer information on cultural practice. There will be further work outside this volume on the cultural practice of the remedial care of an abscess in a mandible, proto-surgical therapeutic intervention on an adult mandible (Chapter 4), which shows a sophisticated bodily knowledge not yet widely recognized in pre-urban populations. Other case studies of medical detail will merit more detailed investigation in the same way (Thompson *et al.* 2021).

Another major direction will be the analysis of context, illustrating how in future research the collaboration of the original excavators with the anthropological specialists is crucial for research of this nature. Earlier in the volume we have indicated the potential that derives from the care with which these human remains were recorded *in situ*. We have given some indication of how this can be used for visualization of the ritual, but this knowledge of context will continue to be deployed to allow for an integration of chronology, spatial association and medical insights into these ancient people. This is the value of a multi-disciplinary team continuing to work together.

Another important direction is the preservation and future interrogation of the deposits that still lie *in situ* in the Circle. A substantial quantity of human remains is still underground within deeper unexplored chambers and beneath the backfill of our excavations which are fragile, and will require supervision should further fieldwork be undertaken, hopefully informed by this 2022 volume and its predecessor of 2009. All involved in this volume will be pleased to support any future investigations. A major achievement of the recent work has been to establish clearly the evidence of care (Chapter 8) by the prehistoric community towards injured or sick individuals. The human remains already curated in Valletta and those still resting in Xagħra deserve the same level of continuing care, enabled by the original excavation team, the current and future investigative teams and the curators of the museum.

References

Abe, H., N. Honma, Y. Nakamura, H. Oogiuchi & K. Kasai, 1974. So-called latent bone cyst (two cases). *Journal of the Japanese Stomatological Society* 23, 209.

Abou-Rass, M., 1983. Crack lines: The precursors of tooth fractures – their diagnosis and treatment. *Quintessence International Dental Digest* 14(4), 437–47.

Abramson, A.S., 1966. Ectopic submaxillary gland in the mandible: Report of a case. *Journal of the American Dental Association* 73(5), 1114–16.

Abulafia, D., 2011. *The Great Sea: A Human History of the Mediterranean*. London: Allen Lane.

Adams B.B., 2002. Dermatologic disorders of the athlete. *Sports Medicine* 32(5), 309–21.

Adams, B.J. & J.E. Byrd, 2006. Resolution of small-scale commingling: A case report from the Vietnam War. *Forensic Science International* 156(1), 63–9.

Adams, B.J. & L.W. Konigsberg, 2004. Estimation of the most likely number of individuals from commingled human skeletal remains. *American Journal of Physical Anthropology* 125(2), 138–51.

Adamson, P.B., 1976. Schistosomiasis in antiquity. *Medical History* 20(2), 176–88.

Adler, C.J., K. Dobney, L.S. Weyrich, J. Kaidonis, A.W. Walker, *et al*., 2013. Sequencing ancient calcified dental plaque shows changes in oral microbiota with dietary shifts of the Neolithic and Industrial revolutions. *Nature Genetics* 45, 450–5.

Adler, N.E. & J.M. Ostrove, 1999. Socioeconomic status and health: What we know and what we don't. *Annals of the New York Academy of Sciences* 896, 3–15.

Afsin, H., A.S. Cagdir, Y. Büyük & B. Karaday, 2013. Cosmetic dentistry in ancient times: V-shaped dental mutilation in skeletal remains from Corycus, Turkey. *Bulletin of the International Association for Paleodontology* 7(2), 148–56.

Agarwal, S.C., 2016. Bone morphologies and histories: Life course approaches in bioarchaeology. *American Journal of Physical Anthropology* 159(S61), 130–49.

Agarwal, S.C. & M.D. Grynpas, 1996. Bone quality and quantity in past populations. *The Anatomical Record* 246(4), 423–32.

Agarwal, S.C. & M.D. Grynpas, 2009. Measuring and interpreting age-related loss of vertebral bone mineral density in a medieval population. *American Journal of Physical Anthropology* 139(2), 244–52.

Agarwal, S. & S.D. Stout (eds.), 2003. *Bone Loss and Osteoporosis: An Anthropological Perspective.* New York (NY): Springer.

Alexandersen, V., 1967. The pathology of the jaws and temporomandibular joint, in *Diseases in Antiquity: A Survey of the Diseases, Injuries and Surgery of Early Populations*, eds. D.R. Brothwell & A.T. Sandison. Springfield (IL): Charles C. Thomas, 551–95.

Alexandersen, V. & N. Lynnerup, 2017. Dental modifications of anterior teeth in the Danish Viking Age, in *A World View of Bioculturally Modified Teeth*, eds. S.E. Burnett & J.D. Irish. Gainesville (FL): University Press of Florida, 79–91.

Ali, M., D.I. Clark & A. Tambe, 2019. Nightstick fractures, outcomes of operative and non-operative treatment. *Acta Medica (Hradec Kralove)* 62(1), 19–23.

Al-Otaibi, M., M. al-Harthy, B. Soder, A. Gustafsson & B. Angmar-Mansson, 2003. Comparative effect of chewing sticks and toothbrushing on plaque removal and gingival health. *Oral Health and Preventive Dentistry* 1(4), 301–8.

Almeida, R., 1953. Mutilações dentárias nos Negros da Lunda. *Anais do Instituto de Medicina Tropical* 10(4), 3601–39.

Almeida, R., 1957. *Mutilações Dentárias nos Negros da Lunda. Subsídios para o Estudo da Antropologia na Lunda*. Lisbon: Companhia de Diamantes de Angola (Diamang).

Alt., K.W. & S.L. Pichler, 1998a. Artificial modifications of human teeth, in *Dental Anthropology. Fundamentals, Limits and Prospects*, eds. K.W. Alt, F.W. Rösing & M. Teschler-Nicola. Vienna: Springer-Verlag, 387–415.

Alt, K.W. & J.C. Türp, 1998b. Hereditary dental anomalies, in *Dental Anthropology. Fundamentals, Limits and Prospects*, eds. K.W. Alt, F.W. Rösing & M. Teschler-Nicola. Vienna: Springer-Verlag, 95–128.

Alt, K.W. & J.C. Türp, 1998. Roll call: Thirty-two white horses on a red field. The advantages of the FDI two-digit system of designating teeth, in *Dental Anthropology. Fundamentals, Limits and Prospects*, eds. K.W. Alt, F.W. Rösing & M. Teschler-Nicola. Vienna: Springer-Verlag, 41–55.

Alt, K.W., S. Zesch, R. Garrido-Pena, C. Knipper, A. Szécsényi-Nagy, *et al*., 2016. A community in life and death: The late Neolithic megalithic tomb at Alto de Reinoso (Burgos, Spain). *PLoS ONE* 11(1), e0146176.

Alvares, O., E. Olech & L.B. Silverglade, 1969. Lingual mandibular bone cavity concomitant with a dentigerous cyst: A clinical and histologic report. *Oral Surgery, Oral Medicine, Oral Pathology* 27(2), 252–6.

Alvesalo, L. & P.M.A. Tigerstedt, 1974. Heritabilities of human tooth dimensions. *Hereditas* 77(2), 311–8.

Amaral, W.J. & D.S. Jacobs, 1961. Aberrant salivary gland defect in the mandible: Report of a case. *Oral Surgery, Oral Medicine, Oral Pathology* 14(2), 748–52.

American College of Surgeons Committee on Trauma, 2012. *Advanced Trauma Life Support* (10th edition). Chicago (IL): American College of Surgeons.

Anastasiou, E., K.O. Lorentz, G.J. Stein & P.D. Mitchell, 2014. Prehistoric schistosomiasis parasite found in the Middle East. *The Lancet Infectious Diseases* 14(7), 553–4.

Anastasi, M. & N. Vella, 2019. Malta and Gozo, in *The Oxford Handbook of Phoenician and Punic Studies*, eds. C. López-Ruiz & B.R. Doak. Oxford: Oxford University Press, 553–68.

Anderson, B.G., 1972. The process of deculturation: Its dynamics among United States aged. *Anthropological Quarterly* 45(4), 209–16.

Anderson, K.M., R.G. Behrents, T. McKinney & P.H. Buschang, 2005. Tooth shape preferences in an esthetic smile. *American Journal of Orthodontics and Dentofacial Orthopedics* 128(4), 458–65.

Anderson, M. & S. Stoddart, 2007. Mapping cult context: GIS applications in Maltese temples, in *Cult in Context*, eds. D. Barrowclough & C. Malone. Oxford: Oxbow Books, 41–4.

Andreasen, J.O., 1981. *Traumatic Injuries of the Teeth*. Copenhagen: Munksgaard.

Andreasen, J.O., S.S. Ahrensburg & G. Tsilingaridis, 2012. Root fractures: The influence of type of healing and location of fracture on tooth survival rates – an analysis of 492 cases. *Dental Traumatology* 28(5), 404–9.

Antón, S.C., 1997. Endocranial hyperostosis in Sangiran 2, Gibraltar 1, and Shanidar 5. *American Journal of Physical Anthropology* 102(1), 111–22.

Appleby, J.E.P., 2010. Why we need an archaeology of Old Age, and a suggested approach. *Norwegian Archaeological Review* 43(2), 145–68.

Appleby, J.E.P., 2011. Bodies, burials and ageing: Accessing the temporality of old age in prehistoric societies. *Oxford Journal of Archaeology* 30(3), 231–46.

Appleby, J.E.P., 2015. Ageing and the body in archaeology. *Cambridge Archaeological Journal* 28(1), 145–63.

Apruzzese, D. & S. Longoni, 1999. Stafne cyst in an anterior location. *Journal of Oral and Maxillofacial Surgery* 57(3), 333–8.

Araiche, M. & H. Brode, 1959. Aberrant salivary gland tissue in mandible. *Oral Surgery, Oral Medicine, Oral Pathology* 10(10), 727–9.

Araújo, F., T. Marques, A. Correia, A. Silva & J. Tinoco, 2009. Differential diagnosis of a salivary gland bone defect by means of computerized tomography: A case report. *Revista Odonto Ciências* 24(2), 218–20.

Arber, S. & J. Ginn, 1995. Connecting gender and ageing: A new beginning?, in *Connecting Gender and Ageing: A Sociological Approach*, eds. S. Arber & J. Ginn. Buckingham: Open University Press, 173–8.

Archer, M.S. & M.A. Elgar, 1998. Cannibalism and delayed pupation in hide beetles, Dermestes maculatus DeGeer (Coleoptera: Dermestidae). *Australian Journal of Entomology* 37(2), 158–61.

Arcini, C., 2005. The Vikings bare their filed teeth. *American Journal of Physical Anthropology* 128(4), 727–37.

Arcini, C., 2011. *The Vikings' Grim Grin*. Visby: Fornsalen Publishing.

Arena, J., 2020. Neolithic mass burial site discovered in Xagħra. *Times of Malta*, 10 August 2020. https://timesofmalta.com/articles/view/neolithic-mass-burial-site-discovered-in-xaghra.810723

Ariano, B., 2021. 'Ancient Maltese genomes and the nature of Neolithic maritime communication'. Unpublished Manuscript, Trinity College Dublin.

Ariano, B., V. Mattiangeli, E. Breslin, E.W. Parkinson, T.R. McLaughlin, *et al*. 2022. Ancient Maltese genomes and the genetic geography of Neolithic Europe. *Current Biology* 32(12), 2668–80.e6. https://doi.org/10.1016/j.cub.2022.04.069

Ariji, E., N. Fujiwara, O. Tabata, E. Nakayama, S. Kanda, *et al*., 1993. Stafne's bone cavity: Classification based on outline and content determined by computer tomography. *Oral Surgery, Oral Medicine, Oral Pathology* 76(3), 375–80.

Armelagos, G.J., A.H. Goodman, K.N. Harper & M.L. Blakey, 2009. Enamel hypoplasia and early mortality: Bioarcheological support for the Barker hypothesis. *Evolutionary Anthropology: Issues, News, and Reviews* 18(6), 261–71.

Aseffa, A., B. Sirika Wayessa & T. Burka, 2016. 'I have to resemble my ancestors through modification of midline diastema': An ethnoarchaeological study of dental modification among Karrayyu Oromo, Central Ethiopia. *Ethnoarchaeology* 8(1), 57–68.

Ashley, S., C. Malone & S. Stoddart, 2016. Foreword. Appreciation of Joseph Attard Tabone, in *A Man of Cultural Achievements - Essays in Honour of Joseph Attard Tabone*, ed. J. Sultana, San Gwann (Malta): BDL, 9–13.

Assis, S., S. Casimiro & F.A. Cardoso, 2018. Is it a cystic or a cyst-like condition? Discussing the etiology of an unusual large mandibular lesion in a Roman skeleton from Quinta da Torrinha/Quinta de Santo António (Almada, Portugal). *International Journal of Paleopathology* 22, 149–57.

Ataria, M.D., 2017. Tooth filing in Surabayan Javanese and Balinese, in *A World View of Bioculturally Modified Teeth*, eds. S.E. Burnett & J.D. Irish. Gainesville (FL): University Press of Florida, 182–92.

Attanasio, F., S. Granziera, V. Giantin & E. Manzato, 2013. Full penetrance of Morgagni-Stewart-Morel syndrome in a 75-year-old woman: Case report and review of the literature. *The Journal of Clinical Endocrinology & Metabolism* 98(2), 453–7.

Attard Tabone, J., 1999. The Gozo circle rediscovered, in *Facets of Maltese Prehistory*, eds. A. Mifsud & C. Savona Ventura. Malta: Prehistoric Society of Malta, 169–81.

Attard Tabone, J., 2010. Robert Hay in Gozo and the lost stone circle, in *60th Anniversary of the Malta Historical Society: A Commemoration*, ed. J.F. Grima. Malta: The Malta Historical Society, 73–84.

Aufderheide, A.C. & C. Rodríguez-Martín, 1998. *The Cambridge Encyclopedia of Human Palaeopathology*. Cambridge: Cambridge University Press.

Autry, A.O., 1991. An example of intentional late prehistoric dental mutilation from Middle Tennessee. *Research Notes.* Available at: https://mcclungmuseum.utk.edu/1991/08/01/dental-mutilation/

Aykroyd, R.G., D. Lucy, A.M. Pollard & C.A. Roberts, 1999. Nasty, brutish, but not necessarily short: A reconsideration of the statistical methods used to calculate age at death from adult human skeletal and dental age indicators. *American Antiquity* 64(1), 55–70.

Bacvarov, K. (ed.), 2008. *Babies Reborn: Infant/Child Burials in Pre- and Protohistory*. Oxford: Archaeopress.

Bader, J.D., D.A. Shugars & J.A. Martin, 2004. Risk indicators for posterior tooth fracture. *Journal of the American Dental Association* 135(7), 883–992.

Bailo Modesti, G. & A. Salerno, 1995. Il Gaudo d'Eboli. *Origini* 19, 327–93.

Bailo Modesti, G. & A. Salerno, 1998. *Pontecagnano II.5 La Necropoli Eneolitica*. Naples: Istituto Universitario Orientale.

Balasse, M., 2002. Reconstructing dietary and environmental history from enamel isotopic analysis: time resolution of intra-tooth sequential sampling. *International Journal of Osteoarchaeology* 12, 155–65. https://doi.org/10.1002/oa.601

Baldacchino, J.G. & J.D. Evans, 1954. Prehistoric tombs near Żebbuġ, Malta. *Papers of the British School at Rome* 22, 1–21.

Barcelò, J.A., M. Forte & D.H. Sanders, 2000. *Virtual Reality in Archaeology.* Oxford: Archaeopress.

Barker, D.J., J.G. Eriksson, T. Forsén & C. Osmond, 2002. Fetal origins of adult disease: Strength of effects and biological basis. *International Journal of Epidemiology* 31(6), 1235–9.

Barker, G.R., 1988. A radiolucency of the ascending ramus of the mandible associated with invested parotid salivary gland material and analogous with a Stafne bone cavity. *British Journal of Oral and Maxillofacial Surgery* 26(1), 81–4.

Barker, G., 2005. Agriculture, pastoralism, and Mediterranean landscapes in prehistory, in *The Archaeology of Mediterranean Prehistory*, eds. E. Blake & A.B. Knapp. Oxford: Blackwell Publishing Ltd., 46–76.

Barone, G., D. Gullì, P. Mazzoleni, S. Raneri & D. Tanasi, 2015. Archaeometric identification of Maltese imports in prehistoric Sicily: Żebbuġ phase pottery from Licata-Caduta (Agrigento). *Malta Archaeological Review* 2010–2011(10), 23–30.

Barratt, R.P., 2016. 'Interpreting and Presenting Archaeological Sites Using 3D Reconstruction: Virtual Exploration of the Xaghra Brochtorff Circle in Gozo.' MPhil, University of Cambridge. Available at: https://www.academia.edu/35713061/Interpreting_and_Presenting_Archaeological_Sites_Using_3D_Reconstruction_Virtual_Exploration_of_the_Xaghra_Brochtorff_Circle_in_Gozo

Barratt, R., C. Malone, R. McLaughlin & E. Parkinson 2020. Hypogea and the clubhouse: Neolithic Malta's houses of the living and houses of the dead, in *Houses of the Dead*, eds. A. Barclay, D. Field & J. Leary, Oxford: Oxbow, 15–38.

Barratt, R., C. Malone, T.R. McLaughlin & S. Stoddart, 2018. Celebrations in prehistoric Malta. *World Archaeology* 50(2), 271–84.

Bartl, R., B. Frisch, E. von Tresckow & C. Bartl, 2007. *Bisphosphonates in Medical Practice*. Berlin: Springer-Verlag.

Barzangi, J., L. Unell, B. Söderfeldt & K. Arnrup, 2013. Infant dental enucleation: A literature review on a traditional remedial practice in East Africa. *Acta Odontologica Scandinavica* 72(3), 168–78.

Bass, W.M., 1995. *Human Osteology: A Laboratory and Field Manual* (4th edition). Columbia (SC): Missouri Archaeological Society.

Bastone, E.B., T.J. Freer & J.R. McNamara, 2000. Epidemiology of dental trauma: A review of the literature. *Australian Dental Journal* 45(1), 2–9.

Bataringaya, A., M. Ferguson & R. Lalloo, 2005. The impact of ebinyo, a form of dental mutilation, on the malocclusion status in Uganda. *Community Dental Health* 22(3), 146–50.

Baxter, J.E., 2005. *The Archaeology of Childhood: Children, Gender and Material Culture*. Walnut Creek (CA): Altamira Press.

Beauchesne, P. & S.C. Agarwal, 2014. Age-related cortical bone maintenance and loss in an Imperial Roman population. *International Journal of Osteoarchaeology* 24(1), 15–30.

Beck, J., 2016. Part of the family: Age, identity and burial in Copper Age Iberia, in *Theoretical Approaches to Analysis and Interpretation of Commingled Human Remains*, ed. A.J. Osterholtz. Cham: Springer International, 47–73.

Becker, M.J., 1999a. Etruscan gold dental applicances: Three newly 'discovered' examples. *American Journal of Archaeology* 103(1), 103–11.

Becker, M.J., 1999b. Ancient 'dental implants': A recently proposed example from France evaluated with other spurious examples. *International Journal of Oral & Maxillofacial Implants* 14(1), 19–29.

Beckett, J.F., 2011. Interactions with the dead: A taphonomic analysis of burial practices in three megalithic tombs in County Clare, Ireland. *European Journal of Archaeology* 14(3), 394–418.

Beckett, J. & J. Robb, 2006. Neolithic burial taphonomy, ritual and interpretation in Britain and Ireland: A review, in *Social Archaeology of Funerary Remains*, eds. R. Gowland & C. Knüsel. Oxford: Oxbow Books, 57–80.

Behrensmeyer, A.K., 1978. Taphonomic and ecologic information from bone weathering. *Palaeo-biology* 4(2), 150–62.

Belcastro, M.G., A. Todero, G. Fornaciari & V. Mariotti, 2011. Hyperostosis frontalis interna (HFI) and castration: The case of the famous singer Farinelli (1705–1782). *Journal of Anatomy* 219(5), 632–7.

Bello, S., 2005. The reciprocal effects of taphonomy, funerary practices and anatomical features on the state of preservation of human remains, in *Proceedings of the 5th Conference of the BABAO*, eds. S.R. Zakrzewski & M. Clegg. Oxford: BAR International Series 1383, 1–10.

Bello, S. & P. Andrews, 2006. The intrinsic pattern of preservation of human skeletons and its influence on the interpretation of funerary behaviours, in *Social Archaeology of Funerary Remains,* eds. R. Gowland & C. Knüsel. Oxford: Oxbow Books, 1–13.

Bello, S.M., R. Wallduck, V. Dimitrijević, I. Živaljević & C.B. Stringer, 2016. Cannibalism versus funerary defleshing and disarticulation after a period of decay: comparisons of bone modifications from four prehistoric sites. *American Journal of Physical Anthropology* 161(4), 722–43.

Benazzi, S., G. Gruppioni, D.S. Strait & J.-J. Hublin, 2014. Technical note: Virtual reconstruction of KNM-ER 1813 Homo habilis cranium. *American Journal of Physical Anthropology* 153(1), 154–60.

Benazzi, S., M. Orlandi & G. Gruppioni, 2009. Technical note: Virtual reconstruction of a fragmentary clavicle. *American Journal of Physical Anthropology* 138(4), 507–14.

Benedix, D.C., 1998. *A Biocultural Analysis of Intentional Dental Modifications*. Knoxville (TN): University of Tennessee.

Bennett, J., 2020. The intensification of the agricultural landscape in the Maltese Archipelago, in *Changing Holocene Environments and Landscapes of the Maltese Islands*, eds. C. French, C.O. Hunt, M. Farrell, R. McLaughlin, S. Stoddart, & C. Malone. Cambridge: McDonald Institute for Archaeological Research, 241–53.

Bennike, P & L. Fredebo, 1985. Dental treatment in the Stone Age. *Tandlaegebladet* 89(12), 459–65.

Bentley, R.A., 2006. Strontium isotopes from the earth to the archaeological skeleton: A review. *Journal of Archaeological Method and Theory* 13, 135–87.

Bentley, R.A. & C. Knipper, 2005. Geographic patterns in biologically available strontium, carbon and oxygen isotope signatures in prehistoric SW Germany. *Archaeometry* 47, 629–44.

Bergenholtz, A. & G. Persson, 1963. Idiopathic bone cavities: A report of four cases. *Oral Surgery, Oral Medicine, Oral Pathology* 16(6), 703–12.

Berger, L.R., S.E. Churchill, B. De Klerk & R.L. Quinn, 2008. Small-bodied humans from Palau, Micronesia. *PLoS ONE* 3(3), e1780.

Berger, L.R., D.J. de Ruiter, S.E. Churchill, P. Schmid, K.J. Carlson, *et al*., 2010. *Australopithecus sediba*: A new species of *Homo*-like Australopith from South Africa. *Science* 328(5975), 195–204.

Bermudez de Castro, J.M., J.L. Arsuaga & P.-J. Perez, 1997. Interproximal grooving in the Atapuerca-SH hominid dentitions. *American Journal of Physical Anthropology* 102(3), 369–76.

Bernabò Brea, L., 1957. *Sicily Before the Greeks*. London: Thames & Hudson

Bernardini, F., C. Tuniz, A. Coppa, L. Mancini, D. Dreossi, *et al*., 2012. Beeswax as dental filling on a Neolithic human tooth. *PLoS ONE* 7(9), 1–9.

Bernstein, H.F., R.C. Lam & F.W. Pomije, 1958. Static bone cavities of the mandible: Review of the literature and report of case. *Journal of Oral Surgery* 16(1), 46–52.

Berry, A.C., 1978. Anthropological and family studies on minor variants of the dental crown, in *Development, Function and Evolution of Teeth*, eds. P.M. Butler & K.A. Joysey. London: Academic Press, 81–97.

Berry, A.C. & R.J. Berry, 1967. Epigenetic variation in the human cranium. *Journal of Anatomy* 101(Pt 2), 361–79.

Bessen, D.E., 2009. Population biology of the human restricted pathogen, Streptococcus pyogenes. *Infection, Genetics and Evolution* 9(4), 581–93.

Beyneix, A., 2012. Neolithic violence in France: An overview, in *Sticks, Stones, and Broken Bones: Neolithic Violence in a European Perspective*, eds. R.J. Schulting & L. Fibiger. Oxford: Oxford University Press, 207–22

Bidmos, M.A., 2009. Fragmentary femora: Evaluation of the accuracy of the direct and indirect methods in stature reconstruction. *Forensic Science International* 192(1–3), 131.e1-5.

Black III, T.K., 1978a. Sexual dimorphism in the tooth-crown diameters of the deciduous teeth. *American Journal of Physical Anthropology* 48(1), 77–82.

Black III, T.K., 1978b. A new method for assessing the sex of fragmentary skeletal remains. *American Journal of Physical Anthropology* 48(2), 227–32.

Blaikie, A., 1999. *Ageing and Popular Culture*. Cambridge: Cambridge University Press.

Blakely, R.L., & L. Beck, 1984. Tooth-tool use versus dental mutilation: A case study from the prehistoric southeast. *Midcontinental Journal of Archaeology* 9(2), 269–84.

Bloch, M., 1982. Death, women and power, in *Death and the Regeneration of Life*, eds. M. Bloch & J. Parry. Cambridge: Cambridge University Press, 211–30.

Bloch, M. & J. Parry, 1982. *Death and the Regeneration of Life*. Cambridge: Cambridge University Press.

Boaz, N.T. & F.C. Howell, 1977. A gracile hominid cranium Upper Member G of the Shungura Formation, Ethiopia. *American Journal of Physical Anthropology* 46(1), 93–108.

Bocquet-Appel, J.P., 2002. Paleoanthropological traces of a Neolithic demographic transition. *Current Anthropology* 43(4), 637–50.

Bocquentin, F., I. Crevecoeur & P. Semal, 2013. Artificial modification of the central upper incisors of Homo 4 (Plot XX J Burial), in *Wadi Hammeh 27, An Early Natufian Settlement at Pella in Jordan*, ed. P.C. Edwards. Leiden: Brill, 383–7.

Boerger, W.G., D.E. Waite & G.W. Carroll, 1972. Idiopathic bone cavities of the mandible: A review of the literature and report of case. *Journal of Oral Surgery* 30(7), 506–9.

Bogaard, A., R. Fraser, T.H.E. Heaton, M. Wallace, P. Vaiglova, *et al*., 2013. Crop manuring and intensive land management by Europe's first farmers. *Proceedings of the National Academy of Sciences* 110, 12589 LP – 12594. https://doi.org/10.1073/pnas.1305918110

Boivin, G., J. Dupuis & P.J. Meunier, 1993. Fluoride and osteoporosis. *World Review of Nutrition and Dietetics* 73, 81–103.

Bolhofner, K.L., 2017. Identity marker or medicinal treatment? An exploration of the practice and purpose of dental ablation in ancient Nubia, in *A World View of Bioculturally Modified Teeth*, eds. S.E. Burnett & J.D. Irish. Gainesville (FL): University Press of Florida, 48–61.

Boman, É., 1908. *Antiquités de la Région Andine de la République Argentine et du Désert d'Atacama.* Tome II. Paris: Imprimerie Nationale.

Bonanno, A. (ed.), 1986a. *Archaeology and Fertility Cult in the Ancient Mediterranean. Papers Presented at the First International Conference on Archaeology of the Ancient Mediterranean. The University of Malta 2–5 September 1985.* Amsterdam: B.R. Grüner Publishing Co.

Bonanno, A., 1986b. *An Illustrated Guide to Prehistoric Gozo.* Victoria: Gaulitana.

Bonanno, A., T. Gouder, C. Malone & S. Stoddart, 1990. Monuments in an island society: The Maltese context. *World Archaeology* 22(2), 190–205.

Bonello, M., 2000. The Ħal Saflieni Hypogeum conservation through compliant building technology, in *The Ħal Saflieni Hypogeum 4000 BC–2000 AD*, ed. A. Pace. Malta: National Museum of Archaeology, 53–8.

Bonfiglioli, B., 2002. 'Le Alterazioni Dentarie di Tipo Non Masticatorio Come Indicatore di Attività.' Unpublished PhD, University of Bologna.

Bonfiglioli, B., V. Mariotti, F. Facchini, M.G. Belcastro & S. Condemi, 2004. Masticatory and non-masticatory dental modifications in the Epipalaeolithic necropolis of Taforalt (Morocco). *International Journal of Osteoarchaeology* 14(6), 448–56.

Borgognini-Tarli, S. 1992. Aspetti antropologici e paleodemografici dal paleolitico superiore all prima età del ferro, in *Italia preistorica*, eds. A. Guidi & M. Piperno, Bari: Laterza, 238–73.

Boutin, A., 2016. Exploring the social construction of disability: An application of the bioarchaeology of personhood model to a pathological skeleton from ancient Bahrain. *International Journal of Paleopathology* 12, 17–28.

Bowen, G.J. & J. Revenaugh, 2003. Interpolating the isotopic composition of modern meteoric precipitation. *Water Resources Research* 39, 1–13.

Boylston, A., M. Holst & J. Coughlan, 2000. Physical anthropology, in *Blood Red Roses: The Archaeology of a Mass Grave from the Battle of Towton AD 1461*, eds. V. Fiorato, A. Boylston & C. Knüsel. Oxford: Oxbow Books, 45–59.

Boz, B. 2005. The oral health of Çatalhöyük Neolithic people, in *Inhabiting Çatalhöyük: Reports from the 1995–99 Seasons*, ed. I. Hodder. Cambridge: British Archaeological Institute at Ankara & McDonald Institute for Archaeological Research, 587–91.

Bracanovic, D., D. Djonic, S. Nikolic, P. Milovanovic, Z. Rakocevic, *et al*., 2016. 3D-Microarchitectural patterns of Hyperostosis frontalis interna: A micro-computed tomography study in aged women. *Journal of Anatomy* 229(5), 673–80.

Bradley, R.N., 1912. *Malta and the Mediterranean race*. London: T. Fisher.

Brant, W.E. & C. Helms, 2012. *Fundamentals of Diagnostic Radiology* (4th Edition). Philadelphia: Lippincott, Williams and Wilkins.

Breslau, N.A., L. Brinkley, K.D. Hill & C. Pak, 1988. Relationship of animal protein-rich diet to kidney stone formation and calcium metabolism. *Journal of Clinical Endocrinology & Metabolism* 66(1), 140–6.

Brickley, M., 2000. The diagnosis of metabolic disease in archaeological bone, in *Human Osteology in Archaeology and Forensic Science,* eds. M. Cox & S. Mays. London: Greenwich Medical Media, 183–98.

Brickley, M., 2002. An investigation of historical and archaeological evidence for age-related bone loss and osteoporosis. *International Journal of Osteoarchaeology* 12(5), 364–71.

Brickley, M., 2018. Cribra orbitalia and porotic hyperostosis: A biological approach to diagnosis. *American Journal of Physical Anthropology* 167(4), 896–902.

Brickley, M. & R. Ives, 2006. Skeletal manifestations of infantile scurvy. *American Journal of Physical Anthropology* 129(2), 163–72.

Brickley, M. & R. Ives, 2008. *The Bioarchaeology of Metabolic Bone Disease*. Oxford: Elsevier.

Brickley, M. & M. Smith, 2006. Culturally determined patterns of violence: Biological anthropological investigations at a historic urban cemetery. *American Anthropologist* 108(1), 163–77.

Bridges, P.S., 1991. Skeletal evidence of changes in subsistence activities between the Archaic and Mississippian time periods in northwestern Alabama, in *What Mean These Bones? Studies in Southeastern Bioarchaeology*, eds. M. Powell, P.S. Bridges & M. Mires. Tuscaloosa (AL): University of Alabama Press, 89–101.

Briggs, L.C., 1955. *The Stone Age Races of Northwest Africa*. Cambridge (MA): Peabody Museum, Harvard University.

Brink, O., A. Vesterby & J. Jensen, 1998. Pattern of injuries due to interpersonal violence. *Injury* 29(9), 705–9.

Britt, L.D., L.J. Weireter Jr., J.L. Riblet, J.A. Asensio & K. Maull, 1996. Priorities in the management of profound shock. *Surgical Clinics of North America* 76(4), 645.

Bromer, R.S. & R.M. Harvey, 1948. The roentgen diagnosis of rickets associated with other skeletal diseases of infants and children. *Radiology* 51(1), 1–10.

Broodbank, C., 2000. *An Island Archaeology of the Early Cyclades*. Cambridge: Cambridge University Press.

Broodbank, C., 2015. *The Making of the Middle Sea: A History of the Mediterranean from the Beginning to the Emergence of the Classical World*. London: Thames & Hudson.

Brothwell, D.R., 1959. Teeth in earlier human populations. *Proceedings of the Nutrition Society* 18(1), 59–65.

Brothwell, D.R., 1981. *Digging Up Bones*. London: British Museum (Natural History).

Broushaki, F., M.G. Thomas, V. Link, S. López, L. van Dorp, *et al*., 2016. Early Neolithic genomes from the eastern Fertile Crescent. *Science* 353(6298), 499–503.

Brown, M. & D.J. Ortner, 2011. Childhood scurvy in a Medieval burial from Macvanska Mitrovica, Serbia. *International Journal of Osteoarchaeology* 21(2), 197–207.

Brukner, P., 1998. Stress fractures of the upper limb. *Sports Medicine* 26(6), 415–24.

Bryant, J.D., P. Koch, P.N. Froelich, W.J. Showers & B.J. Genna, 1996. Oxygen isotope partitioning between phosphate and carbonate in mammalian apatite. *Geochimica et Cosmochimica Acta* 60, 5145–8.

Bucholz, R.W. & A. Jones, 1991. Fractures of the shaft of the femur. *Journal of Bone and Joint Surgery – American Volume* 73(10), 1561.

Buckberry, J., 2015. The (mis)use of adult age estimates in osteology. *Annals of Human Biology* 42(4), 323–31.

Buckley, H.R., R. Kinaston, S.E. Halcrow, A. Foster, M. Spriggs & S. Bedford, 2014. Scurvy in a tropical paradise? Evaluating the possibility of infant and adult vitamin C deficiency in the Lapita skeletal sample of Teouma, Vanuatu, Pacific Islands. *International Journal of Paleopathology* 5, 72–85.

Budai, M., I. Ficzere, K. Gabris & I. Tarjan, 2003. Frequency of transposition and its treatment at the Department

of Orthodontics of Semmelweis University in the last five years. *Fogorvosi Szemle* 96, 21–4.
Buhr, A.J. & A.M. Cooke, 1959. Fracture patterns. *Lancet* 273(7072), 531–6.
Buikstra, J.E., 1987. Health and disease in the prehistoric Southwest. *American Anthropology* 89(1), 209–11.
Buikstra, J.E., & L.A. Beck (eds.), 2006. *Bioarchaeology: The Contextual Analysis of Human Remains*. Amsterdam: Academic Press.
Buikstra, J.E. & D.H. Ubelaker, 1994. *Standards for Data Collection from Human Skeletal Remains*. Fayetteville (NC): Arkansas Archaeological Survey Research Series No. 44.
Burger, J., M. Kirchner, B. Bramanti, W. Haak & M.G. Thomas, 2007. Absence of the lactase-persistence-associated allele in early Neolithic Europeans. *Proceedings of the National Academy of Sciences* 104(10), 3736–41.
Burnett, S.E., 2017. Intentional or not? Characterization and reassessment of proposed intentional dental modification cases in the present-day Southwestern United States, in *A World View of Bioculturally Modified Teeth*, eds. S.E. Burnett & J.D. Irish. Gainesville (FL): University Press of Florida, 250–69.
Burnett, S.E. & J.D. Irish, 2017a. *A World View of Bioculturally Modified Teeth*. Gainesville (FL): University Press of Florida.
Burnett, S.E. & J.D. Irish, 2017b. Introduction, in *A World View of Bioculturally Modified Teeth*, eds. S.E. Burnett & J.D. Irish. Gainesville (FL): University Press of Florida, 1–16.
Bury, M., 1995. Ageing, gender and sociological theory, in *Connecting Gender and Ageing: A Sociological Approach*, eds. S. Arber & J. Ginn. Buckingham: Open University Press, 15–29.
Busuttil, G. (ed.), 1969. *Missione Archeologica Italiana a Malta. Rapporto Preliminare della Campagna 1968.* Rome: Consiglio Nazionale delle Ricerche.
Buzzell, R.A., 1996. Carcinogenesis of cutaneous malignancies. *Dermatologic Surgery* 22(3), 209–15.
Byrnes, J.F. & J.L. Muller (eds.), 2017. *Bioarchaeology of Impairment and Disability*. Cham: Springer.
Caffell, A. & M. Holst, 2012. *Osteological Analysis: 3 and 6 Driffield Terrace, York, North Yorkshire*. (Report 0212). York: York Osteoarchaeology.
Caffell, A., C.A. Roberts, R.C. Janaway & A.S Wilson, 2001. Pressures on osteological collections: The importance of damage limitation, in *Human Remains: Conservation, Retrieval and Analysis (Proceedings of a Conference Held in Williamsburg, VA, Nov. 7–11th 1999)*, ed. E. Williams. Oxford: Archaeopress, 187–97.
Caffey, J., 1946. Multiple fractures in the long bones of infants suffering from chronic subdural hematoma. *American Journal of Roentgenology* 56(2), 163–73.
Caffey, J., 1974. The whiplash shaken infant syndrome: Manual shaking by the extremities with whiplash-induced intracranial and intraocular bleedings, linked with residual permanent brain damage and Mental Retardation. *Pediatrics* 54(4), 396–403.
Cagiano de Azevedo, M., 1969a. Lo scavo, in *San Pawl Milqi: Missione Archeologica Italiana a Malta: Rapporto Preliminare Della Campagna 1968,* ed. M. Cagiano de Azevado. Rome: Consiglio Nazionale delle Ricerche, Centro di Studio per la civilta fenicia e punica, Presso l'Istituto di studi Vicino Oriente dell'Universita di Roma, 93–5.
Cagiano de Azevedo, M. (ed.), 1969b. *San Pawl Milqi: Missione Archeologica Italiana a Malta: Rapporto Preliminare della Campagna 1968,* Rome: Consiglio Nazionale delle Ricerche, Centro di Studio per la civilta fenicia e punica, Presso l'Istituto di studi Vicino Oriente dell'Universita di Roma.
Cagiano de Azevado, M., C. Caprino, A. Ciasca, E. Coleiro, A. Davico, *et al*., 1964–73. *Missione Archeologica Italiana a Malta. Rapporti preliminari delle Campagne 1963–1970*. Rome: Istituto di Studi del Vicino Oriente, Università di Roma.
Cai, X.Z., S.G. Yan & G. Giddins, 2013. A systematic review of the non-operative treatment of nightstick fractures of the ulna. *Bone & Joint Journal* 95-B(7), 952–9.
Camilleri, G., 1998. Fluoride and dental caries. *Maltese Medical Journal* 10(1), 6–7.
Campbell, T.D., 1925. *The Dentition and Palate of the Australian Aboriginal.* Adelaide: Hassell Press.
Campbell, T.D., 1944. The dental condition of a skull from the Sikyatki site, Arizona. *Journal of the Washington Academy of Sciences* 34(10), 321–2.
Canci, A., S. Minozzi & S. Borgognini, 1996. New evidence of tuberculosis spondylitis from Neolithic Liguria (Italy). *International Journal of Osteoarchaeology* 6(5), 498–502.
Carancini, G. & R. Guerzoni, 1987. Gli scavi nella Grotta Pavolella presso Cassano allo Jonio (CS), in *Atti della XXVI Riunione Scientifica*. Florence: Istituto Italiano di Preistoria e Protostoria, 783–92.
Cares Henriquez, A. & M.F. Oxenham, 2020. A new comprehensive quantitative approach for the objective identification and analysis of linear enamel hypoplasia (LEH) in worn archaeological dental assemblages. *Journal of Archaeological Science* 113, 105064.
Carr, G. & C.J. Knüsel, 1997. The ritual framework of excarnation by exposure as the mortuary practice of the early and middle Iron Ages of central southern Britain, in *Reconstructing Iron Age Societies*, eds. A. Gwilt & C. Haselgrove. Oxford: Oxbow Books, 167–73.
Carroll, F.A., C.O. Hunt, P.J. Schembri & A. Bonanno, 2012. Holocene climate change, vegetation history and human impact in the Central Mediterranean: evidence from the Maltese Islands. *Quaternary Science Reviews* 52, 24–40.
Caruana, A.A., 1903. Discovery of antiquities at Tarxien, in *The Daily Malta Chronicle*, 8 January 1903. Malta.
Caruso, S., 2016. *La Lavorazione della Pietra nel Complessi Megalitici Neolitici Maltesi: Technologia, Funzione e Cultura*. Unpublished Ph.D. thesis, Università degli Studi di Roma 'La Sapienza'.
Caselitz, P., 1998. Caries – Ancient plague of humankind, in *Dental Anthropology: Fundamentals, Limits and Prospects*, eds. K.W. Alt, F.W. Rösing & M. Teschler-Nicola. Vienna: Springer-Verlag, 203–26.
Cassar, J., 2000. Conservation studies at the Ħal Saflieni Hypogeum, in *The Ħal Saflieni Hypogeum 4000 BC–2000 AD*, ed. A. Pace. Malta: National Museum of Archaeology, 45–52.

Castellana, G., 1995. *La Necropoli Protoeneolitica di Piano Vento nel Territorio di Palma di Montechiaro.* Palermo: Regione Siciliana.

Castro, J.C., W.R. Poi, T.M. Manfrin & L.G. Zina, 2005. Analysis of the crown fractures and crown-root fractures due to dental trauma assisted by the Integrated Clinic from 1992 to 2002. *Dental Traumatology* 21(3), 121–6.

Cataroche, J. & R. Gowland, 2015. Flesh, fire, and funerary remains from the Neolithic site of La Varde, Guernsey: Investigations past and present, in *The Archaeology of Cremation: Burned Human Remains in Funerary Studies*, ed. T. Thompson. Oxford: Oxbow Books, 19–42.

Cave, C. & M. Oxenham, 2016. Identification of the archaeological 'invisible elderly': An approach illustrated with an Anglo-Saxon example. *International Journal of Osteoarchaeology* 26(1), 163–75.

Cazzella, A., 1994. Dating the 'Copper Age' in the Italian Peninsula and Adjacent Islands. *Journal of European Archaeology* 2(1), 1–19.

Cazzella, A., 2000. Due tradizioni alle origini dell' ipogeismo in Italia e a Malta?, in *L'Ipogeismo nel Mediterraneo: Origini, Sviluppo, Quadri Culturali: Atti del Congresso Internazionale.* Sassari-Oristano: Università degli studi di Sassari, 511–18.

Cazzella, A. & M. Moscoloni, 2012. L'Italia centrale tirrenica e adriatica durante l'Eneolitico e l'età del bronzo a confronto, in *Atti del Decimo Incontro di Studi: L'Etruria dal Paleolitico al Primo Ferro – Lo Stato Delle Ricerche*, ed. N. Negroni Catacchio. Milan: Centro Studi di Preistoria e Archeologia, 445–66.

Cazzella, A. & G. Recchia, 2012. Tas-Silġ: the Late Neolithic megalithic sanctuary and its re-use during the Bronze Age and the Early Iron Age. *Scienze dell'antichità* 18, 15–38.

Cazzella, A. & G. Recchia, 2015. Chiefdom societies in prehistoric Malta? *Origini* 38(2), 87–110.

Cereatti, A., F. Margheritini, M. Donati & A. Cappozzo, 2010. Is the human acetabulofemoral joint spherical? *Journal of Bone and Joint Surgery – British Volume* 92–B(2), 311–14.

Ceschi, C., 1939. *Architettura dei Templi Megalitici di Malta*. Rome: Palombi.

Ceschi, C., 1970. Architettura dei Templi Megalitici di Malta, in *Atti del XV Congresso di Storia dell' Architettura, Malta, 11–16 Settembre 1967*, eds. V. Bonello, C. Ceschi, G. Lillu, E. Coleiro, R. La Ferla, *et al*. Rome: Centro di Studi per la Storia dell' Architettura, 31–98.

Chaljub, G., R.F. Johnson III, R.F. Johnson Jr. & C.W. Sitton, 1999. Unusually exuberant hyperostosis frontalis interna: MRI. *Neuroradiology* 41(1), 44–5.

Chalmers, A. & S. Stoddart, 1996. Photorealistic graphics for visualising archaeological site reconstructions, in *Imaging the Past: Electronic Imaging and Computer Graphics in Museums and Archaeology*, eds. A. Higgins, P. Main & J. Lang. London: British Museum, 85–93.

Chalmers, A., S. Stoddart, J. Tidmus & R. Miles, 1995. INSITE: An interactive visualisation system for archaeological sites, in *Computer Applications and Quantitative Methods in Archaeology 1994*, eds. J. Huggett & N. Ryan. Oxford: Tempus Reparatum, 225–8.

Chang, C.C., C.C. Chow, L. Tellier, S. Vattikuti, S. Purcell & J. Lee, 2015. Second-generation PLINK: Rising to the challenge of larger and richer datasets. *Gigascience* 4(1): s13742-015-0047-8. https://doi.org/10.1186/s13742-015-0047-8.

Charabidze, D., T. Colard, B. Vincent, T. Pasquerault & V. Hedouin, 2014. Involvement of larder beetles (Coleoptera: Dermestidae) on human cadavers: A review of 81 forensic cases. *International Journal of Legal Medicine* 128(6), 1021–30.

Charlton, S., A. Ramsøe, M. Collins, O.E. Craig, R. Fischer, M. Alexander & C.F. Speller, 2019. New insights into Neolithic milk consumption through proteomic analysis of dental calculus. *Archaeological and Anthropological Sciences* 11, 6183–96.

Chatzimpaloglou, P., C. French, M. Pedley & S. Stoddart, 2020. Connecting chert sources of Sicily with Neolithic chert artefacts of Malta. *Journal of Archaeological Science: Reports* 29, 1–14.

Chegini-Farahini, S., J. Fuss & G. Townsend, 2000. Intra- and inter-population variability in mamelon expression on incisor teeth. *Dental Anthropology* 14(3), 1–6.

Chenery, C.A., G. Muldner, J.A. Evans, H. Eckardt & M. Lewis, 2010. Strontium and stable isotope evidence for diet and mobility in Roman Gloucester, UK. *Journal of Archaeological Science* 37, 150–63.

Chenery, C.A., V. Pashley, A.L. Lamb, H.J. Sloane & J.A. Evans, 2012. The oxygen isotope relationship between the phosphate and structural carbonate fractions of human bioapatite. *Rapid Communications in Mass Spectrometry* 26 (3), 309–19.

Cherry, J.F., 1981. Pattern and process in the earliest colonization of the Mediterranean islands. *Proceedings of the Prehistoric Society* 47, 41–68.

Cheung, E., R. Mutahar, F. Assefa, M.-T. Ververs, S.M. Nasiri, *et al*., 2003. An epidemic of scurvy in Afghanistan: Assessment and response. *Food and Nutrition Bulletin* 24(3), 247–55.

Childe, V.G., 1925. *The Dawn of European Civilization*. London: K. Paul, Trench, Trubner & Co. Ltd.

Choukas, C. & P. Toto, 1960. Etiology of static bone defects of the mandible. *Journal of Oral Surgery, Anesthesia and Hospital Dental Service* 18, 16–20.

Chrisler, J.C., J.A. Gorman, J. Manion, M. Murgo, A. Barney, *et al*., 2016. Queer periods: Attitudes toward and experiences with menstruation in the masculine of centre and transgender community. *Culture, Health and Sexuality* 18(11), 1238–50.

Clark, D., 2004. Building logistics, in *Malta Before History, the World's Oldest Free-Standing Architecture*, ed. D. Cilia. Malta: Miranda Publishers, 367–77.

Clark, P.U., A.S. Dyke, J.D. Shakun, A.E. Carlson, J. Clark, *et al*., 2009. The Last Glacial Maximum. *Science* 325(5939), 710–14.

Clokie, C.M.L., D.M. Yau & L. Chano, 2001. Autogenous tooth transplantation: An alternative to dental implant placement? *Journal of the Canadian Dental Association* 67(2), 92–6.

Cocchi Genick, D., 2009. *Preistoria*. Verona: QuiEdit.

Coe, W.R., 1959. *Piedras Negras Archaeology: Artifacts, Caches, and Burials*. Philadelphia (PA): University of Pennsylvania Museum.

Cohen, M.N., 2009. Introduction: Rethinking the origins of agriculture. *Current Anthropology* 50(5), 91–5.
Cohen, M.N. & G.J. Armelagos, 1984. *Paleopathology at the Origins of Agriculture*. New York (NY): Academic Press.
Cohen, M.N. & G.M.M. Crane-Kramer, 2007. *Ancient health: Skeletal indicators of Agricultural and Economic Intensification*. Gainesville (FL): University Press of Florida.
Cole, M.G. & N. Dendukuri, 2003. Risk factors for depression among elderly community subjects: A systematic review and meta-analysis. *American Journal of Psychiatry* 160(6), 1146–56.
Colini, G.A., 1898. Il sepolcreto di Remedello Sotto nel Bresciano e il periodo eneolitico in Italia. *Bullettino di Paletnologia Italiana* 24, 1–110.
Constandse-Westermann, T.S. & R.R. Newell, 1989. Limb lateralisation and social stratification in Western European Mesolithic societies, in *People and Culture in Change, Part ii,* ed. I. Hershkovitz. Oxford: British Archaeological Reports International Series 508(i), 405–33.
Conti, A.M., C. Persiani & P. Petitti, 1997. I riti della morte nella necropoli eneolitica della Selvicciola (Ischia di Castro-Viterbo). *Origini* 21, 169–85.
Cook, D.C., 1981. Koniag Eskimo tooth ablation: Was Hrdlička right after all? *Current Anthropology* 22(2), 159–63.
Cook, D.C., 1984. Subsistence and health in the Lower Illinois Valley: Osteological evidence, in *Paleopathology at the Origins of Agriculture*, eds. M.N. Cohen & G.J. Armelagos. New York (NY): Academic Press, 235–69.
Coplen, T., 1995. New IUPAC Guidelines for the Reporting of Stable Hydrogen, Carbon and Oxygen. *Journal of Research National Institute of Standards and Technology* 100(3), 285. doi: 10.6028/jres.100.021.
Coppa, A., L. Bondioli, A. Cucina, D.W. Frayer, C. Jarrige, *et al*., 2006. Early Neolithic tradition of dentistry. *Nature,* Brief Communications 440(7085), 755–6.
Corbett, E. & W.J. Moore, 1976. Distribution of dental caries in ancient British populations IV: The 19th century. *Caries Research* 10(5), 401–14.
Corrucini, R.S., A.C. Aufderheide & J.S. Handler, 1987. Patterning of skeletal lead content in Barbados slaves. *Archaeometry* 29(2), 233–9.
Court-Brown, C.M. & B. Caesar, 2006. Epidemiology of adult fractures: A review. *Injury* 37(8), 691–7.
Couture, C.J. & K.A. Karlson, 2002. Tibial stress injuries: Decisive diagnosis and treatment of 'shin splints'. *The Physician and Sportsmedicine* 30(6), 29–36.
Covani, U., M. Ricci, G. Bozzolo, F. Mangano, A. Zini & A. Barone, 2011. Analysis of the pattern of the alveolar ridge remodelling following single tooth extraction. *Clinical Oral Implants Research* 22(8), 820–5.
Cox, J., 2001. The orientations of prehistoric temples in Malta and Gozo. *Archaeoastronomy* 16, 24–37.
Cox, J., 2008. Moonrise over Malta. *Astronomy & Geophysics* 49(1), 1.7–1.8.
Cox, J. & T. Lomsdalen, 2010. Prehistoric cosmology: Observations of moonrise and sunrise from ancient temples in Malta and Gozo. *Journal of Cosmology* 9, 2217–31.
Cox, M., 2000. Ageing adults from the skeleton, in *Human Osteology in Archaeology and Forensic Science,* eds. M. Cox & S. Mays. London: Greenwich Medical Media, 61–81.
Cox, S., C.B. Ruff, R.M Maier, & I. Mathieson, 2019. Genetic contributions to variation in human stature in prehistoric Europe. *Proceedings of the National Academy of Sciences of the United States of America* 116(43), 21484–92.
Crawford-Adams, J., 1983. *Outline of Fractures* (8th edition). Edinburgh: Churchill Livingstone.
Creech, C.B., D.N. Al-Zubeidi & S.A. Fritz, 2015. Prevention of recurrent Staphylococcal skin infections. *Infectious Disease Clinics of North America* 29(3), 429–64.
Creese, J.L., 2015. Northern Iroquoian deathways and the re-imagination of community, in *Death Rituals, Social Order and the Archaeology of Immortality in the Ancient World*, eds. C. Renfrew, M. Boyd & I. Morley. Cambridge: Cambridge University Press, 351–70.
Cristiani, E., A. Radini, D. Borić, H.K. Robson, I. Caricola, *et al*., 2018. Dental calculus and isotopes provide direct evidence of fish and plant consumption in Mesolithic Mediterranean. *Scientific Reports* 8, 8147.
Crognier, E. & M. Dupouy-Madre, 1974. Les Natoufiens du Nahal Oren (Ouadi Fallah): Etude anthropologique. *Paléorient* 2(1), 103–21.
Cross, M., 1999. Accessing the inaccessible: Disability and archaeology. *Archaeological Review from Cambridge* 15(2), 7–30.
Crozier, R., 2016. Fragments of death. A taphonomic study of human remains from Neolithic Orkney. *Journal of Archaeological Science: Reports* 10, 725–34.
Crozier, R., 2018. *A Taphonomic Approach to the Re-analysis of the Human Remains from the Neolithic Chamber Tomb of Quanterness, Orkney*. Oxford: BAR British Series 635.
Crubézy, E., P. Murail, L. Girad & J.-P. Bernardou, 1988. False teeth of the Roman world. *Nature* 391, 29.
Cumming, E. & W.F. Henry, 1961. *Growing Old: The Process of Disengagement*. New York (NY): Basic Books.
Cunliffe, B.W., 2015. *By Steppe, Desert, and Ocean: The Birth of Eurasia*. Oxford: Oxford University Press.
Cutajar, N., 2000. The archaeological dimension of the Ħal Saflieni project: Excavations in the Hypogeum Upper Level 1990–1992, in *The Ħal Saflieni Hypogeum 4000 BC–2000 AD*, ed. A. Pace. Malta: National Museum of Malta, Museums Department, 23–35.
Cutajar, N., R. Grima, A. Pace, S. Stoddart & H. Hardisty, 2009. Spatial and stratigraphic analysis of Tarxien Cemetery levels, in *Mortuary Customs in Prehistoric Malta: Excavations at the Brochtorff Circle at Xagħra (1987–94)*, eds. C. Malone, S. Stoddart, A. Bonanno & D.H. Trump. Cambridge: McDonald Institute for Archaeological Research, 207–18.
Cvetković, D., S. Nikolić, V. Brkovic & V. Živković, 2018. Hyperostosis frontalis interna as an age-related phenomenon – Differences between males and females and possible use in identification. *Science & Justice* 59(2), 172–6.
Cybulski, J., 1974. Tooth wear and material culture: Precontact patterns in the Tsimshian Area, British Columbia. *Syesis* 7, 31–5.
Cybulski, J.S., 2014. Conflict on the Northern Northwest coast: 2,000 years plus of bioarchaeological evidence, in *The Routledge Handbook of the Bioarchaeology of Human Conflict*, eds. C. Knüsel & M.J. Smith. Oxford: Routledge, 415–51.

Dahlberg, A.A., 1971. *Dental Morphology and Evolution*. Chicago (IL): The University of Chicago Press.

Dalli, K., 2016. 'Migrants may be using toxic twigs to brush teeth', *Times of Malta*, 24 April. [https://timesofmalta.com/articles/view/migrants-may-be-using-toxic-twigs-to-brush-teeth.609812]

Daly, K.G., P.M. Delser, V.E. Mullin, A. Scheu, V. Mattiangeli, *et al*., 2018. Ancient goat genomes reveal mosaic domestication in the Fertile Crescent. *Science* 361(6397), 85–8.

D'Angela, D. & A. Longinelli, 1990. Oxygen isotopes in living mammal's bone phosphate: Further results. *Chemical Geology (Isotope Geoscience Section)* 86, 75–82.

Dann, S., 1951. Metabolic craniopathy: A review of the literature with report of a case with diabetes mellitus. *Annals of Internal Medicine* 34(1), 163–202.

Daramola, J.O., I. Samuel, H.A. Ajagbe & S. Kahn, 1978. Traumatic cyst of the mandible. *Journal of Oral Surgery* 36(4), 282–4.

Daux, V., C. Lécuyer, M.-A. Héran, R. Amiot, L. Simon, *et al*., 2008. Oxygen isotope fractionation between human phosphate and water revisited. *Journal of Human Evolution* 55, 1138–47.

Davies, D.P. & B. O'Hare, 2004. Weaning: A worry as old as time. *Current Paediatrics* 14(2), 83–96.

Davies, T.G., C.N. Shaw & J.T. Stock, 2012. A test of a new method and software for the rapid estimation of cross-sectional geometric properties of long bone diaphyses from 3D laser surface scans. *Archaeological and Anthropological Sciences* 4(4), 277–90.

Davis, L., 2013. Introduction: Disability, normality, and power, in *The Disability Studies Reader* (4th edition), ed. L. Davis. New York (NY): Routledge, 263–77.

Dawson, H., 2014. *Mediterranean voyages: the Archaeology of Island Colonisation and Abandonment*. (Publications of the Institute of Archaeology, University College London 62). Walnut Creek, CA: Left Coast Press, Inc.

Day, M.H. & T.I. Molleson, 1976. The puzzle from JK2—A femur and a tibial fragment (O.H.34) from Olduvai Gorge, Tanzania. *Journal of Human Evolution* 5(5), 455–65.

Debono Spiteri, C., R.E. Gillis, M. Roffet-Salque, L. Castells Navarro, *et al*., 2016. Regional asynchronicity in dairy production and processing in early farming communities of the northern Mediterranean. *Proceedings of the National Academy of Sciences* 113(48), 13594.

de Courten, A., R. Küffer, J. Samson & T. Lombardi, 2002. Anterior lingual mandibular salivary gland defect (Stafne defect) presenting as a residual cyst. *Oral Surgery, Oral Medicine, Oral Pathology, Oral Radiology, and Endodontology* 94(4), 460–4.

Deedler, A.M., R.L. Miller, N. De Jonge & F.W. Krijger, 1990. Detection of schistosome antigen in mummies. *Lancet* 335(8691), 724–5.

De Groote, I. & L.T. Humphrey, 2016. Characterizing evulsion in the Later Stone Age Maghreb: Age, sex and effects on mastication. *Quaternary International* 413(Part A), 50–61.

De Groote, I. & L.T. Humphrey, 2017. The chronology and significance of ablation in the Later Stone Age Maghreb, in *A World View of Bioculturally Modified Teeth*, eds. S.E. Burnett & J.D. Irish. Gainesville (FL): University Press of Florida, 19–32.

de Marinis, R.C., 2013. La necropolis di Remedello Sotto e l'età del Rame nella pianura padana a nord del Po, in *L'età del Rame: La Pianura Padana e Le Alpi al Tempo di Ötzi*., ed. R.C. de Marinis. Brescia: Massetti Rodella Editori, 301–52.

Dembo, A., O. Paulotti & A. Binninghurst, 1949. Criterios para la diagnosis de las mutilaciones dentarias intencionales. *Runa* 2, 139–47.

Dequeker, J., D.J. Ortner, A.I. Stix, X. Cheng, P. Brys & S. Boonen, 1997. Hip fracture and osteoporosis in a XIIth Dynasty female skeleton from Lisht, Upper Egypt. *Journal of Bone and Mineral Research* 12(6), 881–8.

Despott, G., 1918. Excavations conducted at Għar Dalam (Malta) in the summer of 1917. *Journal of the Royal Anthropological Institute* 48, 214–21.

Despott, G., 1923. Excavations at Ghar Dalam (Dalam Cave), Malta. *Journal of the Royal Anthropological Institute* 53, 18–35.

de Vito, C. & S.R. Saunders, 1990. A discriminant function analysis of deciduous teeth to determine sex. *Journal of Forensic Science* 35(4), 845–58.

Devriendt, W., M.D. Piercecchi-Marti, Y. Ardagna, E. Mahieu, I. Hershkovitz, *et al*., 2004. Two Neolithic cases of Hyperostosis frontalis interna. *International Journal of Osteoarchaeology* 14(5), 414–8.

Dhawan, A., S. Gupta & R. Mittal, 2014. Vertical root fractures: An update review. *Journal of Restorative Dentistry* 2(3), 107–13.

Diamond, J., 2004. The astonishing micropygmies. *Science* 306(5704), 2047–48.

Di Bennardo, R. & J.V. Taylor, 1979. Sex assessment of the femur: A test of a new method. *American Journal of Physical Anthropology* 50(4), 635–8.

Dicke-Toupin, C.R., 2012. 'Population Continuity or Replacement at Ancient Lachish? A Dental Affinity Analysis in the Levant.' Unpublished M.A., University of Alaska.

Dittrick, J., 1979. 'Sexual Dimorphism of the Femur and Humerus in Prehistoric Central California Skeletal Samples.' Unpublished M.A., California State University.

Dittrick, J. & J.M. Suchey, 1986. Sex determination of prehistoric central California skeletal remains using discriminant analysis of the femur and humerus. *American Journal of Physical Anthropology* 70(1), 3–9.

Dixon, J., R. Leighton, C. Malone & D.H. Trump 2009. Ground and polished stone, in *Mortuary ritual in prehistoric Malta. The Brochtorff Circle Excavations (1987–1994)*, eds. C. Malone, S. Stoddart, A. Bonanno & D. Trump, Cambridge: McDonald Institute for Archaeological Research, 253–60.

Dobney, K. & D.R. Brothwell, 1986. Dental calculus: Its relevance to ancient diet and oral ecology, in *Teeth and Anthropology*, eds. E. Cruwys & R.A. Foley. Oxford: British Archaeological Reports International Series 291, 55–82.

Dobney, K. & D.R. Brothwell, 1987. A method for evaluating the amount of dental calculus on teeth from archaeological sites. *Journal of Archaeological Science* 14(4), 343–51.

Dobney, K. & D.R. Brothwell, 1988. A scanning electron microscope study of archaeological dental calculus, in *Scanning Electron Microscopy in Archaeology*, ed.

S.L. Olsen. Oxford: British Archaeological Reports International Series 452, 372–85.

Dodson, P. & D. Wexlar, 1979. Taphonomic investigations of owl pellets. *Palaeobiology* 5(3), 279–84.

Dolfini, A., 2006a. Embodied inequalities: Burial and social differentiation in Copper Age central Italy. *Archaeological Review from Cambridge* 2(21), 58–77.

Dolfini, A., 2006b. La Necropoli di Rinaldone e il problema delle sepolture primarie in Italia centrale tra IV e III millennio a.C., in *Atti del Settimo Incontro di Studi: Pastori e guerrieri nell'Etruria del IV e III millennio a.C. La Civiltà di Rinaldone a 100 Anni dalle Prime Scoperte (Viterbo, 21 Novembre 2003 e Valentano 17–18 Settembre 2004)*. Milan: Centro Studi di Preistoria e Archeologia, 77–96.

Dolfini, A., 2010. The origins of metallurgy in central Italy: New radiometric evidence. *Antiquity* 84(325), 707–23.

Dolfini, A., 2015. Neolithic and Copper Age mortuary practices in the Italian Peninsula: Changing of meaning or change of medium?, in *Death and Changing Rituals. Function and Meaning in Ancient Funerary Practices*, eds. J.R. Brandt, H. Ingvaldsen & M. Prusac. Oxford: Oxbow Books, 17–44.

Douglas, M., 1966. *Purity and Danger: An Analysis of the Concepts of Pollution and Taboo*. London: Routledge.

Dreizin, D., A.J. Nam, N. Tirada, M.D. Levin, D.M. Stein, *et al*., 2016. Multidetector CT of mandibular fractures, reductions, and complications: A clinically relevant primer for the radiologist. *RadioGraphics* 36(5), 1539–64.

Drinnan, A.J., 1974. Idiopathic mandibular bone cavity. *Archives of Otolaryngology* 99(4), 264–7.

Duday, H., 2006. L'archéothanatologie ou l'archeologie de la mort, in *The Social Archaeology of Funerary Remains*, eds. R. Gowland & C. Knüsel. Oxford: Oxbow Books, 30–56.

Duday, H., 2009. *The Archaeology of the Dead: Lectures in Archaeothanatology*. Oxford: Oxbow Books.

Duday, H. & Guillon, M., 2006. Understanding the circumstances of decomposition when the body is skeletonized, in *Forensic Anthropology and Medicine: Complementary Sciences From Recovery to Cause of Death*, eds. A. Schmitt & E. Cunha. New Jersey (NJ): Humana Press, 117–57.

Duhig, C., 1996. Burial practices in a Neolithic Maltese Hypogeum – the human remains from the Brochtorff Circle, Gozo, in *Ritual Treatment of Human and Animal Remains. Proceedings of the 1st meeting of the Osteoarchaeology Research Group*, eds. S. Anderson & K. Boyle. Oxford: Oxbow Books, 63–72.

Dukinfield Astley, H.J., 1914. Notes on the Hypogeum at Ħal Saflieni, Malta. *Journal of the Royal Anthropological Institute of Great Britain and Ireland* 44, 394–96.

Dundar, Y., B. Cannon, M.M. Monroe, L.O. Buchmann & J.P. Hunt, 2017. Skull base invasion patterns and survival outcomes of nonmelanoma skin cancers. *Journal of Neurological Surgery Part B: Skull Base* 78(2), 164–72.

Dupras, T.L. & J.J. Schultz, 2014. Taphonomic bone staining and color changes in forensic contexts, in *Manual of Forensic Taphonomy*, eds. J.T. Pokines & S.A. Symes. Boca Raton (FL): CRC Press, 315–40.

Du Toit, F.P. & R.P. Gräbe, 1979. Isolated fractures of the shaft of the ulna. *South African Medical Journal* 56(1), 21–5.

Dwight, T., 1905. The size of the articular surfaces of the long bones as characteristics of sex as an anthropological study. *American Journal of Anatomy* 4(1), 19–32.

Eastridge, B.J., J.B. Holcomb & S. Shackelford, 2019. Outcomes of traumatic hemorrhagic shock and the epidemiology of preventable death from injury. *Transfusion* 59(52), 1423–28.

Eckardt, H., C. Chenery, P. Booth, J.A. Evans, A. Lamb & G. Muldner, 2009. Oxygen and strontium isotope evidence for mobility in Roman Winchester. *Journal of Archaeological Science* 36, 2816–25.

Ehler, E., J. Novotný, A. Juras, M. Chylenski, O. Moravcík & J. Paces, 2019. AmtDB: a database of ancient human mitochondrial genomes. *Nucleic Acids Research* 47(D1), D29–D32.

Elderfield, H., 1986. Strontium isotope stratigraphy. *Palaeogeography, Palaeoclimatology, Palaeoecology* 57, 71–90.

Ellis, R.G. & K.W. Davey, 1970. *The Classification and Treatment of Injuries to the Teeth of Children* (5th edition). Chicago (IL): Year Book Medical Publishers.

Erlandsson, A.E. & B. Bäckman, 1999. A case of dental mutilation. *ASDC Journal of Dentistry for Children* 66(4), 278–9.

Ersts, P.J., 2014. Geographic Distance Matrix Generator (Version 1.2.3). *American Museum of Natural History, Center for Biodiversity and Conservation*. Available at: http://biodiversityinfonratics.armh.org/open_source/gdrrg.

Eshed, V., A. Gopher & I. Hershkovitz, 2006. Tooth wear and dental pathology at the advent of agriculture: New evidence from the Levant. *American Journal of Physical Anthropology* 130(2), 145–59.

Evans, J.A., J. Montgomery & G. Wildman, 2009. Isotope domain mapping of 87Sr/86Sr biosphere variation on the Isle of Skye Scotland. *Journal of Geological Society* 166, 617–31.

Evans, J.A., J. Montgomery, G. Wildman & N. Boulton, 2010. Spatial variations in biosphere 87Sr/86Sr in Britain. *Journal of the Geological Society* 167, 1–4.

Evans, J., M. Parker Pearson, R. Madgwick, H. Sloane & U. Albarella, 2019. Strontium and oxygen isotope evidence for the origin and movement of cattle at Late Neolithic Durrington Walls, UK. *Archaeological and Anthropological Sciences* 11, 5181–97.

Evans, J.D., 1959. *Ancient Peoples and Places: Malta*. London: Thames & Hudson.

Evans, J.D., 1971. *The Prehistoric Antiquities of the Maltese Islands: A Survey.* London: Athlone Press.

Evans, J.D., 1977. Island archaeology in the Mediterranean: Problems and opportunities. *World Archaeology* 9(1), 12–26.

Fahlander, F., 2013. Intersecting generations: Burying the old in a Neolithic hunter-fisher community. *Cambridge Archaeological Journal* 23(2), 227–39.

Fain, O., 2005. Musculoskeletal manifestations of scurvy. *Joint Bone Spine* 72(2), 124–8.

Farikullah, J., S. Ehtisham, S. Nappo, L. Patel & S. Hennayake, 2012. Persistent Müllerian duct syndrome: Lessons learned from managing a series of eight patients over a 10-year period and review of literature regarding malignant risk from the Müllerian remnants. *BJU International* 110(11 Pt C): E1084–9.

Farmer, T.W. & G.R. Wise, 1973. Subdural empyema in infants, children and adults. *Neurology* 23(3), 254–61.

Farrell, M., 2013. Intentional dental modification: Assessment of a historical museum specimen from the Democratic Republic of the Congo. *Faculty Dental Journal* 4(4), 186–91.

Farrugia, C., 2016. Bur Megheż u Tan-Naxxari. *Festa tal-Madonna tal-Gilju 2016*, 163–7.

Fastlicht, S., 1948. Tooth mutilations in Pre-Columbian Mexico. *Journal of the American Dental Association* 36(3), 315–23.

Fastlicht, S., 1976. *Tooth Mutilations and Dentistry in Pre-Columbian Mexico*. Chicago (IL): Quintessence Books.

Faure, G., 1986. *Principles of Isotope Geology*. New York: John Wiley and Sons.

Fazekas, G.I. & F. Kosa, 1978. *Forensic Fetal Osteology*. Budapest: Akademiai Kiado.

Fédération Dentaire Internationale (FDI), 1971. Two digit system of designating teeth. *International Dental Journal* 21, 104–6.

Fehrs, L.J., K. Flanagan, S. Kline, R.R. Facklam, K. Quackenbush & L.R. Foster, 1987. Group A beta-hemolytic streptococcal skin infections in a US meat-packing plant. *Journal of the American Medical Association* 258(21), 3131–4.

Feichtinger, C., B. Rossiwal & H. Wunderer, 1977. Canine transposition as autosomal recessive trait in an inbred. *Journal of Dental Research* 56(12), 1449–52.

Fenech, K., C.O. Hunt, N.C. Vella & P.J. Schembri, 2020. Molluscan remains from the valley cores, in *Temple Landscapes. Fragility, Change and Resilience of Holocene Environments in the Maltese Islands*, eds. C. French, C.O. Hunt, R. Grima, R. McLaughlin, S. Stoddart & C. Malone. Cambridge: McDonald Institute for Archaeological Research, 115–60

Fennell, K.J. & E. Trinkaus, 1997. Bilateral femoral and tibial periostitis in the La Ferrassie 1 Neanderthal. *Journal of Archaeological Science* 24(11), 985–95.

Fennis, W.M., R.H. Kuijs, C.M. Kreulen, F.J. Roeters, N.H. Creugers & R.C. Burgersdijk, 2002. A survey of cusp fractures in a population of general dental practices. *International Journal of Prosthodontics* 15(6), 559–63

Fergusson, J., 1872. *Rude Stone Monuments in All Countries: Their Ages and Uses.* London: John Murray.

Fernandes, R., A.R. Millard, M. Brabec, M.-J. Nadeau & P. Grootes, 2014. Food reconstruction using isotopic transferred signals (FRUITS): A Bayesian Model for diet reconstruction. *PLoS ONE* 9(2), e87436.

Fernández-Jalvo, Y. & P. Andrews, 2016. *Atlas of Taphonomic Identifications: 1001+ Images of Fossil and Recent Mammal Bone Modification*. New York (NY): Springer.

Ferrieri P., A.S. Dajani, L.W. Wannamaker & S.S. Chapman, 1972. Natural history of impetigo. I. Site sequence of acquisition and familial patterns of spread of cutaneous streptococci. *Journal of Clinical Investigation* 51(11), 2851–62.

Finlay, N., 1997. Kid knapping: The missing children in lithic analysis, in *Invisible People and Processes: Writing Gender and Childhood into European Archaeology*, eds. J. Moore & E. Scott. London & New York: Leicester University Press, 203–12.

Finnegan, M. & A. Marcsik, 1980. Anomaly or pathology: The Stafne defect as seen in archaeological material and modern clinical practice. *Journal of Human Evolution* 9(1), 19–20, IN7, 21–31.

Finnegan, M. & A. Marcsik, 1981. The description and incidence of the Stafne idiopathic bone defect in six Avar period populations. *Acta Biologica Szeged* 27(1–4), 215–21.

Finucane, B.C., K. Manning & M. Touré, 2008. Prehistoric dental modification in West Africa: Early evidence from Karkarichinkat Nord, Mali. *International Journal of Osteoarchaeology* 18(6), 632–40.

Flohr, S. & C. Witzel, 2011. Hyperostosis frontalis interna – A marker of social status? Evidence from the Bronze-Age 'high society' of Qatna, Syria. *HOMO* 62(1), 30–43.

Florêncio, T., H. Ferreira, A. França, J. Cavalcante & A. Sawaya, 2001. Obesity and undernutrition in a very-low-income population in the city of Maceió, northeastern Brazil. *British Journal of Nutrition* 86 (2), 277–83.

Foldes, A.J., A. Moscovici, M.M. Popovtzer, P. Mogle, D. Urman & J. Zias, 1995. Extreme osteoporosis in a sixth century skeleton from the Negev desert. *International Journal of Osteoarchaeology* 5(2), 157–62.

Fontaine, J.N., D. Forest & M. Labelle, 1966. Cavité statique mandibrulaire. *Journal of the Canadian Dental Association* 32, 141–5.

Fontenot, E.A., F.H. Arthur & K.L. Hartzer, 2015. Effect of diet and refugia on development of *Dermestes maculatus* DeGeer reared in a laboratory. *Journal of Pest Science* 88, 113–19.

Fordyce, G.L., 1956. Probable nature of a so-called latent hemorrhagic cysts of the mandible. *British Dental Journal* 101, 40–2.

Formicola, V., 1987. Neolithic transition and dental changes: The case of an Italian site. *Journal of Human Evolution* 16(2), 231–9.

Formicola, V. & B.M. Holt, 2007. Resource availability and stature decrease in upper palaeolithic Europe. *Journal of Anthropological Sciences* 85, 147–55.

Formicola, V., Q. Milanesi & C. Scarsini, 1987. Evidence of spinal tuberculosis at the beginning of the 4th millennium BC from Arene Candide cave (Liguria, Italy). *American Journal of Physical Anthropology* 72(1), 1–6.

Forrest, W.R., 1974. Ectopic salivary gland. *Oral Surgery, Oral Medicine, Oral Pathology*, *Oral Radiology* 37(4), 653–4.

Forshaw, R.J., 2009. Dental health and disease in ancient Egypt. *British Dental Journal* 206(8), 421–4.

Foster, J.B., 1964. Evolution of mammals on islands. *Nature* 202(4929), 234–35.

Fowler, C., 2004. *The Archaeology of Personhood: An Anthropological Approach*. London: Routledge.

France, D.L., 1983. 'Sexual Dimorphism in the Human Humerus.' Unpublished PhD, University of Colorado.

Frayer, D.W., 1991. On the etiology of interproximal grooves. *American Journal of Physical Anthropology* 85(3), 299–304.

Frayer, D.W., 2004. The dental remains from Krškany (Slovakia) and Vedrovice (Czech Republic). *Anthropologie* 42(1), 71–103.

Frayer, D.W. & M.D. Russell, 1987. Artifical grooves on the Krapina Neanderthal teeth. *American Journal of Physical Anthropology* 74, 393–405.

Friedman, J., 1964. Ectopic sublingual gland: Report of a case. *Oral Surgery, Oral Medicine, Oral Pathology* 18(2), 219–22.

Friedling, L.J., 2017. Dental modification in modern-day Cape Town, South Africa: A link to the past, in *A World View of Bioculturally Modified Teeth*, eds. S.E. Burnett & J.D. Irish. Gainesville (FL): University Press of Florida, 62–75.

Friedling, L.J. & A.G. Morris, 2005. The frequency of culturally derived dental modification practices on the Cape Flats in the Western Cape. *Journal of the South African Dental Association* 60(3), 97, 99–102.

Friedling, L.J. & A.M. Morris, 2007. Pulling teeth for fashion: Dental modification in modern day Cape Town, South Africa. *Journal of the South African Dental Association* 62(3), 106, 108–13.

Frigo, P. & C. Lang, 1995. Osteoporosis in a woman of the Early Bronze Age. *New England Journal of Medicine* 333, 1468.

Fu, J.-H., C.-C. Hwang & T.-H. Chao, 2003. Tibiofibular synostosis in a military soldier. *Journal of Medical Sciences* 23(2), 135–8.

Fu, Q., C. Posth, M. Hajdinjak, M. Petr, S. Mallick, *et al*., 2016. The genetic history of Ice Age Europe. *Nature* 534, 200–5.

Gaeta, M., F. Minutoli, S. Mazziotti, C. Visalli, S. Vinci, *et al*., 2008. Diagnostic imaging in athletes with chronic lower leg pain. *American Journal of Roentgenology* 191(5), 1412–19.

Galea, H., 1971. The dental health of seven-year-old children in Malta state-run schools. *St. Luke's Hospital Gazette* 6(2), 126–33.

Galea, H., 1997. A strategy for children at high risk of developing dental caries. *Smile for Health*, 3–10.

Galton, F., 1853. *Narrative of an Explorer in Tropical South Africa: Being an Account of a Visit to Damaraland in 1851*. London: Murray.

Garib, D.G., B.M. Alencar, F.V. Ferreira & T.O. Ozawa, 2010. Associated dental anomalies: The orthodontist decoding the genetics which regulates the dental development disturbances. *Dental Press Journal of Orthodontics* 15(2), 138–57.

Garn, S.M., P.E. Cole & W.L. Van Alstine, 1979. Sex discriminatory effectiveness using combinations of root lengths and crown diameters. *American Journal of Physical Anthropology* 50(1), 115–18.

Garn, S.M., A.B. Lewis & R.S. Kerewsky, 1964. Sex differences in tooth size. *Journal of Dental Research* 43, 306.

Garn, S.M., A.B. Lewis & R.S. Kerewsky, 1965. Genetic, nutritional, and maturational correlates of dental development. *Journal of Dental Research* 44, 228–42.

Garn, S.M., A.B. Lewis & R.S. Kerewsky, 1966. Sexual dimorphism in bucco-lingual tooth diameter. *Journal of Dental Research* 45(6), 1819.

Garn, S.M., A.B. Lewis & R.S. Kerewsky, 1967. Sex differences in tooth size. *Journal of Dental Research* 46, 1470.

Garn, S.M., C.G. Rohman & T. Blumenthal, 1966. Ossification sequence polymorphism and sexual dimorphism in skeletal development. *American Journal of Physical Anthropology* 24(1), 101–16.

Garralda, M.D., B. Maureille & B. Vandermeersch, 2014. Hyperostosis frontalis interna in a Neandertal from Marillac (Charente, France). *Journal of Human Evolution* 67(1), 76–84.

Garve, R., M. Garve, K. Link, J.C. Turp & C.G. Meyer, 2016. Infant oral mutilation in East Africa – therapeutic and ritual grounds. *Tropical Medicine and International Health* 21(9), 1099–105.

Geber, J., R. Hensey, P. Meehan, S. Moore & T. Kador, 2017. Facilitating transitions: Postmortem processing of the dead at the Carrowkeel Passage tomb complex, Ireland (3500–3000 cal. BC). *Bioarchaeology International* 1(1–2), 35–51.

Geber, J. & E. Murphy, 2012. Scurvy in the great Irish famine: Evidence of vitamin C deficiency from a mid-19th century skeletal population. *American Journal of Physical Anthropology* 148(4), 512–24.

Geiling, J.M. & A.B. Marín-Arroyo, 2015. Spatial distribution analysis of the Lower Magdalenian human burial in El Mirón Cave (Cantabria, Spain). *Journal of Archaeological Science* 60, 47–56.

Geller, P.L., 2004. 'Transforming Bodies, Transforming Identities: A Consideration of Pre-Columbian Maya Corporeal Beliefs and Practices.' Unpublished PhD, University of Pennsylvania.

Geller, P.L., 2006. Altering identities: Body modifications and the pre-Columbian Maya, in *Social Archaeology of Funerary Remains*, eds. R. Gowland & C. Knüsel. Oxford: Oxbow Books, 279–91.

Gensburg, R.S., A. Kawashima & C.M. Sandler, 1988. Scintigraphic demonstration of lower extremity periostitis secondary to venous insufficiency. *Journal of Nuclear Medicine* 29(7), 1279–82.

Gero, J.M., 1991. Genderlithics: Women's roles in stone tool production, in *Engendering Archaeology*, eds. J.M. Gero & M.W. Conkey. Oxford: Blackwell Publishing Ltd., 163–93.

Gershon-Cohen, J., H. Schraer, & N. Blumberg, 1955. Hyperostosis frontalis interna among the aged. *American Journal of Roentgenology* 73(3), 396–7.

Ghalioungui, P., 1973. *Magic and Medical Science in Ancient Egypt* (2nd edition). Amsterdam: B.M. Israël.

Ghalioungui, P., 1987. *The Ebers Papyrus*. Cairo: Academy of Scientific Research and Technology.

Gilbert, M.T.P., A.S. Wilson, M. Bunce, A.J. Hansen, E. Willerslev, *et al*., 2004. Ancient mitochondrial DNA from hair. *Current Biology* 14(12), R463–4.

Gill, G.W., 1985. Cultural implications of artificially modified human remains from Northwestern Mexico, in *The Archaeology of West and Northwest Mesoamerica*, eds. M.S. Foster & P.C. Weigand. Boulder (CO): Westview Press, 193–215.

Gimbutas, M., 1974. *The Gods and Goddesses of Old Europe, 7000–3500 BC.* Berkeley (CA): University of California Press.

Gimbutas, M., 1989. *The language of the Goddess.* New York (NY): HarperCollins Publishers.

Gimbutas, M., 1991. *The Civilization of the Goddess: The World of Old Europe.* New York (NY): HarperCollins Publishers.

Ginn, J. & S. Arber, 1995. 'Only connect': Gender relations and ageing, in *Connecting Gender and Ageing. A*

Sociological Approach, eds. S. Arber & J. Ginn. Buckingham: Open University Press, 1–14.

Giusti, F., G. Manganelli & P.J. Schembri,1995. *The Non-Marine Molluscs of the Maltese Islands*. Turin: Museo Regionale die Scienze Naturali.

Glab, H., K. Szostek & K. Kaczanowski, 2006. Hyperostosis frontalis interna, a genetic disease? Two medieval cases from Southern Poland. *HOMO* 57(1), 19–27.

Glahn, M. & J. Rud, 1962. Statische knochenkavitäten im unter-kiefer. *Quintessenz* 9, 15–16.

Glencross, B. & B. Boz, 2014. Representing violence in Anatolia and the Near East during the transition to agriculture, in *The Routledge Handbook of the Bioarchaeology of Human Conflict*, eds. C. Knüsel & M.J. Smith. Oxford: Routledge, 90–108.

Gluckman, P.D. & M.A. Hanson, 2006. The developmental origins of health and disease, in *Early Life Origins of Health and Disease (Advances in Experimental Medicine and Biology)* (Vol. 573), eds. E.M. Wintour-Coghlan & J.A. Owens. New York (NY): Springer, 1–7.

Gomez, C.K., S.R. Schiffman & A.A. Bhatt, 2018. Radiological review of skull lesions. *Insights into Imaging* 9(5), 857–82.

González, E.L., B.P. Pérez, J.S. Sánchez & M.M.R. Acinas, 2010. Dental aesthetics as an expression of culture and ritual. *British Dental Journal* 208(2), 77–80.

González-Fortes, G., E.R. Jones, E. Lightfoot, C. Bonsall, C. Lazar, *et al*., 2017. Paleogenomic evidence for multi-generational mixing between Neolithic farmers and Mesolithic hunter-gatherers in the Lower Danube Basin. *Current Biology* 27(12), 1801–1810.e10.

González-Reimers, E., A. Trujillo-Mederos, M. Machado-Calvo, M. Castañeyra-Ruiz, A.C. Ordóñez & M. Arnay-de-la-Rosa, 2015. A skeletal case of hypertrophic osteoarthropathy from the Canary Islands dating from 1000 BP. *International Journal of Paleopathology* 11, 1–6.

Goodman, A.H., 1984. Indications of stress from bones and teeth, in *Paleopathology at the Origins of Agriculture*, eds. M.N. Cohen & G.J. Armelagos. Gainesville (FL): University Press of Florida, 13–49.

Goodman, A.H., 1991. Stress, adaptation and enamel developmental defects, in *Human Palaeopathology: Current Syntheses and Future Options*, eds. D. Ortner & A. Aufderheide. Washington (DC): Smithsonian Institution Press, 280–7.

Goodman, A.H. & G.J. Armelagos, 1989. Infant and childhood morbidity and mortality risks in archaeological populations. *World Archaeology* 21(2), 225–43.

Goodman, A.H., G.J Armelagos & J.C. Rose, 1980. Enamel hypoplasias as indicators of stress in three prehistoric populations from Illinois. *Human Biology* 52(3), 515–28.

Goodman, A.H., G.J. Armelagos & J.C. Rose, 1984a. The chronological distribution of enamel hypoplasias from prehistoric Dickson Mounds populations. *American Journal of Physical Anthropology* 65(3), 259–66.

Goodman, A.H., R. Brooke Thomas, A.C. Swedlund & G.J. Armelagos, 1988. Biocultural perspectives on stress in prehistoric, historical, and contemporary population research. *American Journal of Physical Anthropology* 31(S9), 169–202.

Goodman, A.H. & L. Capasso (eds.), 1992. *Recent Contributions to the Study of Enamel Developmental Defects*. Teramo: Edigrafital.

Goodman, A.H., J. Jones, J. Reid, M.E. Mack, M.L. Blakey, *et al*., 2009. Isotopic and elemental chemistry of teeth: Implications for places of birth, forced migration patterns, nutritional status, and pollution, in *The New York African Burial Ground: Skeletal Biology Report*, eds. M.L. Blakey & L.M. Rakin-Hill. Washington (DC): Howard University Press, 95–118.

Goodman, A.H., J. Lallo, G.J. Armelagos & J.C. Rose, 1984b. Health changes at Dickson Mounds, Illinois (AD 950–1300), in *Palaeopathology at the Origins of Agriculture*, eds. M.N. Cohen & G.J. Armelagos. New York (NY): Academic Press: 271–306.

Goodman, A.H. & J.C Rose, 1990. Assessment of systemic physiological perturbations from dental enamel hypoplasias and associated histological structures. *Yearbook of Physical Anthropology* 33(S11), 59–110.

Goodman, A.H. & J.C. Rose, 1991. Dental enamel hypoplasias as indicators of nutritional status, in *Advances in Dental Anthropology*, eds. M.A. Kelley & C.S. Larsen. New York (NY): Wiley-Liss, 279–93.

Goody, J., 1976. Aging in nonindustrial societies, in *Handbook of Aging and the Social Sciences*, eds. R.H. Binstock & E. Shanas. New York (NY): Van Nostrand Reinhold, 117–29.

Goose, D.H., 1971. The inheritance of tooth size in British families, in *Dental Morphology and Evolution*, ed. A.A. Dahlberg. Chicago (IL): University of Chicago Press, 144–9.

Gould, A.R., A.G. Farman & D. Corbitt, 1984. Mutilations of the dentition in Africa: A review with personal observations. *Quintessence International* 15(1), 89–94.

Gowland, R.L., 2002. 'Age as an Aspect of Social Identity in Fourth-to-Sixth-Century A.D. England: The Archaeological Funerary Evidence.' Unpublished PhD, University of Durham.

Gowland, R.L., 2007. Age, ageism and osteological bias: The evidence from late Roman Britain. *Journal of Roman Archaeology; Supplementary Series* 65, 153–69.

Gowland, R.L., 2015. Elder abuse: Evaluating the potentials and problems of diagnosis in the archaeological record. *International Journal of Osteoarchaeology* 26(3), 514–23.

Gowland, R.L., 2016. Growing old: Biographies of disability and care in later life, in *New Developments in the Bioarchaeology of Care: Further Case Studies and Expanded Theory*, eds. L. Tilley & A.A. Schrenk. New York (NY): Springer International, 237–51.

Gracia-Godoy, F.A., 1981. A classification for traumatic injuries to primary and permanent teeth. *The Journal of Pedodontics* 5(4), 295–7.

Graham, E.E., 1980. A probable submandibular gland defect in a prehistoric mandible. *Oral Surgery, Oral Medicine, Oral Pathology* 50(2), 187–9.

Graustein, W.C. 1989. 87Sr/86Sr ratios measure the sources and flow of strontium in terrestrial ecosystems, in *Stable Isotopes in Ecological Research*, eds. P.W. Rundel, J.R. Ehleringer & K.A. Nagy. New York (NY): Springer-Verlag, 491–512

Green, R. & J. Suchey, 1976. The use of inverse sine transformation in the analysis of nonmetrical data. *American Journal of Physical Anthropology* 45(1), 61–8.

Greenfield, H.J., 2006. Slicing cut marks on animal bones: Diagnostics for identifying stone tool type and raw material. *Journal of Field Archaeology* 31(2), 147–63.

Grewar, D., 1965. Infantile scurvy. *Clinical Pediatrics* 4, 82–9.

Grima, R., 2000. Managing a World Heritage resource, in *The Ħal Saflieni Hypogeum 4000 BC–2000 AD*, ed. A. Pace. Malta: National Museum of Archaeology, 37–44

Grima, R., 2001. An iconography of insularity: A cosmological interpretation of some images and spaces in the late Neolithic temples of Malta. *Papers from the Institute of Archaeology* 12, 48–65.

Grima, R., 2003. Image, Order and Place in Late Neolithic Malta, in *Inhabiting Symbols: Symbol and Image in the Ancient Mediterranean,* eds. J. Wilkins & E. Herring. London: Accordia Research Institute, 29–41.

Grima, R., 2004a. The landscape context of Megalithic architecture, in *Malta Before History, the World's Oldest Free-Standing Architetcure,* ed. D. Cilia. Malta: Miranda Publishers, 327–45.

Grima, R., 2004b. *The Archaeological Drawings of Charles Fredrick de Brocktorff*. Malta: Midsea Books Ltd and Heritage Malta.

Grima, R., 2008. Landscape, territories, and the life-histories of monuments in Temple Period Malta. *Journal of Mediterranean Archaeology* 21(1), 35–56.

Grima, R., C. Malone & S. Stoddart, 2009. The ritual landscape, in *Mortuary Customs in Prehistoric Malta: Excavations at the Brochtorff Circle at Xaghra (1987–94)*, eds. C. Malone, S. Stoddart, A. Bonanno & D.H. Trump. Cambridge: McDonald Institute for Archaeological Research, 57–62.

Grine, F.E., P. Gunz, L. Betti-Nash, S. Neubauer & A.G. Morris, 2010. Reconstruction of the late Pleistocene human skull from Hofmeyr, South Africa. *Journal of Human Evolution* 59(1), 1–15.

Grine, F.E., A.J. Gwinnett & J.H. Oaks, 1990. Early hominid dental pathology: Interproximal caries in 1.5 million-year-old Paranthropus robustus from Swartkrans. *Archives of Oral Biology* 35(5), 381–86.

Grossfeld, S.L., A. Van Heest, E. Arendt & J. House, 1998. Pitcher's periostitis: A case report. *The American Journal of Sports Medicine* 26(2), 303–7.

Guilaine, J., 2016. *L'Emite du Paradis*. Mirebeau-sur-Bèze: Editions Association Totem.

Gullì, D., 2014. *Storie Sepolte. Riti, Culti e Vita Quotidiana all'Alba del IV Millennio a.C. La Necropoli di Contrada Scintilia di Favara, Agrigento*. Palermo: Dipartimento dei Beni Culturali e dell'Identità Siciliana.

Gunz, P., P. Mitteroecker, S. Neubauer, G.W. Weber & F.L Bookstein, 2009. Principles for the virtual reconstruction of hominin crania. *Journal of Human Evolution* 57(1), 48–62.

Gupta, M.K. & M. Singh, 2007. Primary tuberculosis of mandible. *Indian Pediatrics* 44(1), 53–4.

Gurven, M. & H. Kaplan, 2007. Longevity among hunter-gatherers: A cross-cultural examination. *Population and Development Review* 33(2), 321–65.

Guthe, C.E., 1934. Gold-decorated teeth from the Philippine Islands. *Papers of the Michigan Academy of Science, Arts and Letters* 20, 7–22.

Haak, W., I. Lazaridis, N. Patterson, N. Rohland, S. Mallick, *et al*., 2015. Massive migration from the steppe was a source for Indo-European languages in Europe. *Nature* 522, 207–11.

Haapasalo H., H. Sievanen, P. Kannus, A. Heinonen, P. Oja & I. Vuori, 1996. Dimensions and estimated mechanical characteristics of the humerus after long-term tennis loading. *Journal of Bone and Mineral Research* 11(3), 864–72.

Haeussler, A.M., J.D. Irish, D.H. Morris & C.G. Turner, 1989. Morphological and metrical comparison of San and Central Sotho dentitions from southern Africa. *American Journal of Physical Anthropology* 78(1), 115–22.

Haeusler, M. & H.M. McHenry, 2004. Body proportions of Homo habilis reviewed. *Journal of Human Evolution* 46(4), 433–65.

Hagelberg, E., B. Sykes & R. Hedges, 1989. Ancient bone DNA amplified. *Nature* 342, 485.

Haglund, W.D., 1997a. Rodents and human remains, in *Forensic Taphonomy: The Postmortem Fate of Human Remains*, eds. W.D. Haglund & M. Sorg. Boca Raton (FL): CRC Press, 405–14.

Haglund, W.D., 1997b. Dogs and coyotes: Postmortem involvement with human remains, in *Forensic Taphonomy: The Postmortem Fate of Human Remains*, eds. W.D. Haglund & M. Sorg. Boca Raton (FL): CRC Press, 367–82.

Hajdu, T., E. Fóthi, Z. Bernert, E. Molnár, G. Lovász, *et al*., 2009. Appearance of hyperostosis frontalis interna in some osteoarcheological series from Hungary. *HOMO* 60(3), 185–205.

Hammond, A.S., J.M. Plavcan & C.V. Ward, 2013. Precision and accuracy of acetabular size measures in fragmentary hominin pelves obtained using sphere-fitting techniques. *American Journal of Physical Anthropology* 150(4), 565–78.

Hammond, B.T. & J. Charnley, 1967. The sphericity of the femoral head. *Medical & Biological Engineering* 5(5), 445–53.

Hamy, E.T., 1882. Les mutilations dentaires au Mexique et dans le Yucatan. *Bulletins et Mémoires de la Société d'Anthropologie de Paris* 3(5), 879–87.

Handler, J.S., 1994. Determining African birth from skeletal remains: A note on tooth mutilation. *Historical Archaeology* 28(3), 113–19.

Handler, J.S., R.S. Corruccini & R.J. Mutaw, 1982. Tooth mutilation in the Caribbean: Evidence from a slave burial population in Barbados. *Journal of Human Evolution* 11(4), 297–313.

Hanihara, K., 1963. Crown characters of the deciduous dentition of the Japanese-American hybrids, in *Dental Anthropology*, ed. D.R. Brothwell. New York (NY): Pergamon Press, 105–24.

Haour, A. & J.A. Pearson, 2005. An instance of dental modification on a human skeleton from Niger, West Africa. *Oxford Journal of Archaeology* 24(4), 427–33.

Hardaway, R.M., 2006. Traumatic shock. *Military Medicine* 171(4), 278–9.

Hardwick, J.L., 1960. The incidence and distribution of caries throughout the ages in relation to the Englishman's diet. *British Dental Journal* 108, 9–17.
Harris, E.C., 1979. *Principles of archaeological stratigraphy.* New York: Academic Press.
Harris, E.F. & H.L. Bailit, 1980. The metaconule: A morphologic and familial analysis of a molar cusp in humans. *American Journal of Physical Anthropology* 53(3), 349–58.
Harris, E.F. & T. Sjøvold, 2004. Calculation of Smith's mean measure of divergence for intergroup comparisons using nonmetric data. *Dental Anthropology* 17(3), 83–93.
Harris, J.E, Z. Iskander & S. Farid, 1975. Restorative dentistry in ancient Egypt: An archaeological fact! *Journal of the Michigan Dental Association* 57(12), 401–4.
Harris, O.J.T. & J. Robb, 2012. Multiple ontologies and the problem of the body in history. *American Anthropologist* 114(4), 668–79.
Harvey, W. & H.W. Noble, 1968. Defects on the lingual surface of the mandible near the angle. *British Journal of Oral and Maxillofacial Surgery* 6(2), 75–83.
Hasegawa, T., H. Ito, S. Yamamoto, K. Haba & H. Murata, 1983. Unilateral hyperostosis frontalis interna: Case report. *Journal of Neurosurgery* 59(4), 710–13.
Háva, J., 2003. World catalogue of the Dermestidae (Coleoptera). *Studie a zprávy Oblastního Muzea Praha-východ v Brandýse nad Labem a Staré Boleslavi*, Supplement, 1–196.
Háva, J. & D. Mifsud, 2006. The dermestid beetles (Coleoptera: Dermestidae) of the Maltese Archipelago (Central Mediterranean). *Studies and Reports of District Museum Prague-East. Taxonomical Series* 2(1–2), 51–63.
Havill, L.M., D.M. Warren, K.P. Jacobi, K.D. Gettelman, D.C. Cook & K.A. Pyburn, 1997. Late postclassic tooth filing at Chau Hiix and Tipu, Belize, in *Bones of the Maya: Studies of Ancient Skeletons*, eds. S.L. Whittington & D.M. Reed. Washington (DC): Smithsonian Institution Press, 89–104.
Hayden, C., 2006. Simultaneous inventions: The dispersed origins of rock-cut tombs in the central Mediterranean. *Accordia Papers* 11, 71–86.
Hayes, H., 1961. Aberrant submaxillary gland tissue presenting as a cyst of the jaw. Report of a case. *Oral Surgery, Oral Medicine, Oral Pathology* 14(3), 313–16.
Hazan, H., 1994. *Old Age: Constructions and Deconstructions*. Cambridge: Cambridge University Press.
Headland, T.N., 1977. Teeth mutilation among the Casiguran Dumagat. *Philippine Quarterly of Culture and Society* 5(1-2), 54–64.
Hedman, K.M., J.A Bukowski, D.E Cobb & A.R. Thompson, 2017. Modified teeth, cultural diversity and community building at Cahokia (AD 900–1400), in *A World View of Bioculturally Modified Teeth*, eds. S.E. Burnett & J.D. Irish. Gainesville (FL): University Press of Florida, 229–49.
Heithersay, G.S., 1975. Replantation of avulsed teeth. A review. *Australian Dental Journal* 20(2), 63–72.
Hellman, M., 1928. Racial characters in human dentition. *Proceedings of the American Philosophical Society* 67(2), 157–74.
Hemilä, H. & P. Louhiala, 2007. Vitamin C may affect lung infections. *Journal of the Royal Society of Medicine* 100(11), 495–8.
Hendy, J., C. Warinner, A. Bouwman, M.J. Collins, S. Fiddyment, *et al*., 2018. Proteomic evidence of dietary sources in ancient dental calculus. *Proceedings of the Royal Society B* 285, 20180977.
Henschen, F., 1961. Cribra cranii, a skull condition said to be of racial or geographical nature. *Pathological Microbiology* 24, 724–9.
Herrmann, N., 2002. GIS applied to bioarchaeology: an example from the Rio Talgua caves in Northeast Honduras. *Journal of Cave and Karst Studies* 64 (1), 17–22.
Herrmann, N.P., J.L. Devlin & J.C. Stanton, 2014. Bioarchaeological spatial analysis of the Walker-Noe Crematory (15GD56), Commingled and Disarticulated, in *Commingled and Disarticulated Human Remains*, eds. A. Osterholtz, K. Baustian & D. Martin, New York, NY: Springer, 51–66.
Hershkovitz, I., L. Bedford, L.M. Jellema & B. Latimer, 1996. Injuries to the skeleton due to prolonged activity in hand-to-hand combat. *International Journal of Osteoarchaeology* 6(2), 167–78.
Hershkovitz, I., C.M. Greenwald, B. Latimer, L.M. Jellema, S. Wish-Baratz, *et al*., 2002. Serpens endocrania symmetrica (SES): A new term and a possible clue for identifying intrathoracic disease in skeletal populations. *American Journal of Physical Anthropology* 118(3), 201–16.
Hershkovitz, I., C. Greenwald, B.M. Rothschild, B. Latimer, O. Dutour, *et al*., 1999. Hyperostosis frontalis interna: An anthropological perspective. *American Journal of Physical Anthropology* 109(3), 303–25.
Hewlett, B.S., 1991. Demography and childcare in pre-industrial societies. *Journal of Anthropological Research* 47(1), 1–37.
Hicks, R.M., 1983. The canopic worm: Role of bilharziasis in the aetiology of human bladder cancer. *Journal of the Royal Society of Medicine* 76(1), 16–22.
Higuchi, R., B. Bowman, M. Freiberger, O.A. Ryder & A.C. Wilson, 1984. DNA sequences from the quagga, an extinct member of the horse family. *Nature* 312, 282–84.
Hillson, S., 1986. *Teeth.* Cambridge: Cambridge University Press.
Hillson, S., 2000. Dental pathology, in *Biological Anthropology of the Human Skeleton*, eds. M.A. Katzenberg & S.R. Saunders. New York (NY): Wiley-Liss, 249–86.
Hillson, S. 2002. *Dental Anthropology* (3rd Edition). Cambridge: Cambridge University Press.
Hillson, S., 2005. *Teeth* (2nd edition). Cambridge: Cambridge University Press.
Hillson, S., 2008. The current state of dental decay, in *Technique and Application in Dental Anthropology*, eds. J.D. Irish & G.C. Nelson. Cambridge: Cambridge University Press, 111–35.
Hinton, R.J., 1981. Form and patterning of anterior tooth wear among aboriginal human groups. *American Journal of Physical Anthropology* 54(4), 555–64.
Hinton, R.J., 1982. Differences in interproximal and occlusal tooth wear among prehistoric Tennessee Indians: implications for masticatory function. *American Journal of Physical Anthropology* 57, 103–15.
Hirschmann, J.V. & G.J. Raugi, 1999. Adult scurvy. *Journal of the American Academy of Dermatology* 41(6), 895–906.

Hlusko, L.J., 2003. The oldest hominid habit? Experimental evidence for toothpicking with grass stalks. *Current Anthropology* 44(5), 738–41.

Hodges, R.E., J. Hood, J.E. Canham, H.E. Sauberlich & E.M. Baker, 1971. Clinical manifestations of ascorbic acid deficiency in man. *American Journal of Clinical Nutrition* 24(4), 432–43.

Hoefs, J., 1997. *Stable Isotope Geochemistry*. Berlin: Springer.

Hoffman, D.J., R.M. Reynolds & D.B. Hardy, 2017. Developmental origins of health and disease: Current knowledge and potential mechanisms. *Nutrition Reviews* 75(12), 951–70.

Hofmanová, Z., S. Kreutzer, G. Hellenthal, C. Sell, Y. Diekmann, *et al*., 2016. Early farmers from across Europe directly descended from Neolithic Aegeans. *Proceedings of the National Academy of Sciences of the United States of America* 113(25), 6886–91.

Hofrichter, R. (ed.), 2003. *Health and Social Justice: Politics, Ideology and Inequity in the Distribution of Disease*. San Francisco (CA): Wiley.

Holick, M.F., 2003. Vitamin D: A millenium perspective. *Journal of Cellular Biochemistry 88*(2), 296–307.

Holland, T.D., 1991. Sex assessment using the proximal tibia. *American Journal of Physical Anthropology* 85(2), 221–7.

Hooper, G., 1974. Isolated fractures of the shaft of the ulna. *Injury* 6(2), 180–4.

Hoppa, R.D., 2002. Paleodemography: Looking back and thinking ahead, in *Palaeodemography: Age Distributions from Skeletal Samples*, eds. R.D. Hoppa & J.W. Vaupel. Cambridge: Cambridge University Press, 9–28.

Hoppa, R.D. & J.W. Vaupel (eds.), 2002. *Palaeodemography: Age Distributions from Skeletal Samples*. Cambridge: Cambridge University Press.

Hoppe, K.A., P.L. Koch & T.T. Furutani, 2003. Assessing the preservation of biogenic strontium in fossil bones and tooth enamel. *International Journal of Osteoarchaeology* 13, 20–8.

Horden, P. & N. Purcell, 2000. *The Corrupting Sea: A Study of Mediterranean History*. Oxford: Blackwell Publishing Ltd.

Howells, W.W., 1973. *Cranial Variation in Man: A Study by Multivariate Analysis of Patterns of Difference among Recent Human Populations*. Cambridge (MA): Harvard University Peabody Museum of Archaeology and Ethnology.

Hrdlička, A., 1920. Shovel-shaped teeth. *American Journal of Physical Anthropology* 3(4), 429–65.

Hrdlička, A., 1940. *Ritual Ablation of Front Teeth in Siberia and America*. Washington (DC): Smithsonian Institution.

Huang, W.-J. & C.J. Creath, 1995. The midline diastema: A review of its etiology and treatment. *Pediatric Dentistry* 17(3), 171–9.

Huchet, J.-B., F. Le Mort, R. Rabinovich, S. Blau, H. Coqueugniot & B. Arensburg, 2013. Identification of dermestid pupal chambers on Southern Levant human bones: Inference for reconstruction of Middle Bronze Age mortuary practices. *Journal of Archaeological Science* 40(10), 3793–803.

Hughes, S.S., A.R. Millard, S.J. Lucy, C. Chenery, J.A. Evans, *et al*., 2014. Anglo-Saxon origins investigated by isotopic analysis of burials from Berinsfield, Oxfordshire, UK. *Journal of Archaeological Science* 42, 81–92.

Huiskes, R., 1982. On the modelling of long bones in structural analysis. *Journal of Biomechanics* 1(15), 65–9.

Humphrey, L.T. & E. Bocaege, 2008. Tooth evulsion in the Maghreb: Chronological and geographical patterns. *African Archaeological Review* 25(1-2), 109–23.

Hunt, C.O. & A. Bonnano 2015. Palynology of some archaeological deposits from Tas-Silg, in *Tas-Silg, Marsaxlokk (Malta) I: Archaeological Excavations conducted by the University of Malta, 1996–2005*, ed. N.C. Vella. Leuven: Peeters, 437-50.

Huntington, R. & P. Metcalf, 1979. *Celebrations of Death: The Anthropological Analysis of Mortuary Rituals*. Cambridge: Cambridge University Press.

Hwang, K., S.J. Ki & S.H. Ko, 2017. Etiology of nasal bone fractures. *Journal of Craniofacial Surgery* 28(3), 785–8.

Iacumin, P., H. Bocherens, A. Mariotti & A. Longinelli, 1996. Oxygen isotope analyses of co-existing carbonate and phosphate in biogenic apatite: a way to monitor diagenetic alteration of bone phosphate? *Earth and Planetary Science Letters* 142, 1–6.

Iannotti, L. & C. Lesorogol, 2014. Dietary intakes and micronutrient adequacy related to the changing livelihoods of two pastoralist communities in Samburu, Kenya. *Current Anthropology* 55(4), 475–82.

Ibáñez-Gimeno, P., S. De Esteban-Trivigno, X. Jordana, J. Manyosa, A. Malgosa & I. Galtés, 2013. Functional plasticity of the human humerus: Shape, rigidity, and muscular entheses. *American Journal of Physical Anthropology* 150(4), 609–17.

Ikehara-Quebral, R., E.M. Ryan, N. Parr, C. Walth, J. Liston, *et al*., 2017. Intentional dental modification and oral-dental health in Western Micronesia, in *A World View of Bioculturally Modified Teeth*, eds. S.E. Burnett & J.D. Irish. Gainesville (FL): University Press of Florida, 193–210.

Imamura, M., T. Kakihara, K. Yamamoto, C. Imai, A. Tanaka & M. Uchiyama, 2004. Primary tuberculous osteomyelitis of the mandible. *Pediatrics International* 46(6), 736–9.

Insoll, T., 2015. Constructing ancestors in Sub-Saharan Africa, in *Death Rituals, Social Order and the Archaeology of Immortality in the Ancient World*, eds. C. Renfrew, M. Boyd & I. Morley. Cambridge: Cambridge University Press, 153–67.

International Organization for Standardization (ISO), 1984. ISO 3950. *Dentistry – Designation System for Teeth and Areas of the Oral Cavity* (2nd edition).

International Organization for Standardization (ISO), 1995. ISO 3950. *Dentistry – Designation System for Teeth and Areas of the Oral Cavity* (2nd edition). Corrected and Reprinted.

Irish, J.D., 1993. 'Biological Affinities of Late Pleistocene through Modern African Aboriginal Populations: The Dental Evidence.' Unpublished PhD, Arizona State University. Ann Arbor (MI): University Microfilms.

Irish, J.D., 1998a. Dental morphological affinities of late Pleistocene through recent sub-Saharan and North African peoples. *Bulletins et Mémoires de la Société d›Anthropologie de Paris* 10(3), 237–72.

Irish, J.D., 1998b. Diachronic and synchronic dental trait affinities of late and post- Pleistocene peoples from North Africa. *Homo* 49(2), 138–55.

Irish, J.D., 2000. The Iberomaurusian enigma: North African progenitor or dead end? *Journal of Human Evolution* 39(4), 393–410.

Irish, J.D., 2006. Who were the ancient Egyptians? Dental affinities among Neolithic through post-dynastic peoples. *American Journal of Physical Anthropology* 129(4), 529–43.

Irish, J.D., 2010. The mean measure of divergence (MMD): Its utility in model-free and model-bound analyses relative to the Mahalanobis D2 distance for nonmetric traits. *American Journal of Human Biology* 22(3), 378–95.

Irish, J.D., 2016. Who were they really? Model-free and model-bound dental nonmetric analyses to affirm documented population affiliations of seven South African 'Bantu' samples. *American Journal of Physical Anthropology* 159(4), 655–70.

Irish, J.D., 2017. Knocking, filing, and chipping. Dental Modification in Sub-Saharan Africans, in *A World View of Bioculturally Modified Teeth*, eds. S.E. Burnett & J.D. Irish. Gainesville (FL): University Press of Florida, 33–47.

Irish, J.D. & D. Guatelli-Steinberg, 2003. Ancient teeth and modern human origins: An expanded comparison of African Plio-Pleistocene and recent world dental samples. *Journal of Human Evolution* 45(2), 113–44.

Irish, J.D., K.T. Lillios, A.J. Waterman & A.M. Silva, 2017. 'Other' possibilities? Assessing regional and extra-regional dental affinities of populations in the Portuguese Estremadura to explore the roots of Iberia's Late Neolithic-Copper Age. *Journal of Archaeological Science: Reports* 11, 224–36.

Irish, J.D., A. Morez, L. Girdland Flink, E.L.W. Phillips & G.R. Scott, 2020. Do dental nonmetric traits actually work as proxies for neutral genomic data? Some answers from continental- and global-level analyses. *American Journal of Physical Anthropology* 172(3), 347–75.

Irvine, B., J.-L. Thomas & U. Dietrich-Schoop, 2014. A macroscopic analysis of human dentition at Late Chalcolithic Çamlıbel Tarlası, North Central Anatolia, with special reference to dietary and non-masticatory habits. *Interdisciplinaria Archaeologica* 5(1), 19–30.

Işcan, M.Y. & P. Miller-Shaivitz, 1984a. Determination of sex from the tibia. *American Journal of Physical Anthropology* 64(1), 53–7.

Işcan, M.Y. & P. Miller-Shaivitz, 1984b. Discriminant function sexing of the tibia. *Journal of Forensic Sciences* 29(4), 1087–93.

Işcan, M.Y. & P. Miller-Shaivitz, 1986. Sexual dimorphism in the femur and tibia, in *Forensic Osteology: Advances in the Identification of Human Remains*, ed. K.J. Reichs. Springfield (IL): Charles C. Thomas, 101–11.

Işcan, M.Y., M. Yoshin & S. Kato, 1994. Sex determination from the tibia: Standards for contemporary Japan. *Journal of Forensic Sciences* 39(3), 785–92.

Isogg, C., 2019. ISOGG 2019 Y-DNA Haplogroup Tree. Available at: http://www.isogg.org/tree

Ito, T., H. Soya, T. Imai & Y. Matsuse, 1974. Localized bone defect or cavity of the mandible: Clinical and etiological investigation. *Japanese Journal of the Stomatological Society* 23(3), 441–51.

Ivy, R.H. & L. Curtis, 1937. Hemorrhagic or traumatic cysts of mandible. *Surgery, Gynecology and Obstetrics* 65, 640–3.

Iwanaga, J., T.L. Wong, S. Kikuta & R.S. Tubbs, 2019. Stafne bone cavity: A rare cadaveric case report. *Anatomy & Cell Biology* 52(3), 354–6.

Jackson, J.W., 1915. Dental mutilations in Neolithic human remains. *Journal of Anatomy and Physiology* 49(Pt 1), 72–9.

Jacob, R.A. & G. Sotoudeh, 2002. Vitamin C function and status in chronic disease. *Nutrition in Clinical Care* 5(2), 66–74.

Jacobs, K., 1992. Estimating femur and tibia length from fragmentary bones: An evaluation of Steele's (1970) method using a prehistoric European sample. *American Journal of Physical Anthropology* 89(3), 333–45.

Jacobs, M.H., 1955. Traumatic bone cyst. *Oral Surgery, Oral Medicine, Oral Pathology* 8(9), 940–9.

Jaffe, H.L., 1972. *Metabolic, Degenerative, and Inflammatory Diseases of Bones and Joints*. Philadelphia (PA): Lea and Febiger.

Jaffe, H.L. & L. Lichtenstein, 1942. Solitary unicameral bone cyst, with emphasis on roentgen picture, pathologic appearance and pathogenesis. *American Medical Association Archives of Surgery* 44(6), 1004–25.

Janovic, A., P. Milovanovic, J. Sopta, Z. Rakocevic, V. Filipovic, *et al*., 2015. Intracranial arteriovenous malformations as a possible cause of endocranial bone lesions and associated neurological disorder. *International Journal of Osteoarchaeology* 25(1), 88–97.

Jay, M., B.T. Fuller, M.P. Richards, C.J. Knusel & S.S. King, 2008. Iron Age breastfeeding practices in Britain: isotopic evidence from Wetwang Slack, East Yorkshire. *American Journal of Physical Anthropology* 136, 327–37.

Johnson, J.S., 1994. Consolidation of archaeological bone: A conservation perspective. *Journal of Field Archaeology* 21(2), 221–33.

Johnson, K., 1969. A study of the dimensional changes occurring in the maxilla following tooth extraction. *Australian Dental Journal* 8(5), 241–4.

Jones, A., 1992. Tooth mutilation in Angola. *British Dental Journal* 173(5), 177–9.

Jones, A., 2001. Dental transfigurements in Borneo. *British Dental Journal* 191, 98–102.

Jones, E.R., G. Gonzalez-Fortes, S. Connell, V. Siska, A. Eriksson, *et al*., 2015. Upper Palaeolithic genomes reveal deep roots of modern Eurasians. *Nature Communications* 6, 8912.

Jones, E.R., G. Zarina, V. Moiseyev, E. Lightfoot, P. Nigst, *et al*., 2017. The Neolithic transition in the Baltic was not driven by admixture with early European farmers. *Current Biology* 27(4), 576–82.

Jónsson, H., A. Ginolhac, M. Schubert, P.L.F. Johnson & L. Orlando, 2013. mapDamage2.0: fast approximate Bayesian estimates of ancient DNA damage parameters. *Bioinformatics* 29(13), 1682–4.

Jordana, X., C. García Sívoli, I. Galtés, M. Palacios, M. Cos & A. Malgosa, 2007. Report on a Stafne defect in a man from Medieval age. *Journal of Oral and Maxillofacial Surgery* 65(3), 556–9.

Jørgensen, N.O., J. Morthorst & P.M. Holm, 1999. Strontium isotope studies of 'brown water' (organic-rich groundwater) from Denmark. *Hydrogeology Journal* 7, 533–9.

Judd, M., 2000. 'Trauma and Interpersonal Violence in Ancient Nubia During the Kerma Period (*ca*.2055–1500 BC).' Unpublished PhD, University of Alberta.

Judd, M., 2002a. Comparison of long bone trauma recording methods. *Journal of Archaeological Science* 29(11), 1255–65.

Judd, M., 2002b. Ancient injury recidivism: An example from the Kerma period of ancient Nubia. *International Journal of Osteoarchaeology* 12(2), 86–106.

Judd, M., 2008. The parry problem. *Journal of Archaeological Science* 35(6), 1658–66.

Junker, H., 1929. *Giza I: Die Mastabas Der IV. Dynastie Auf Dem Westfriedhof*. Wien: Hölder-Pichler-Tempsky.

Jurmain, R.D., 1999. *Stories from the Skeleton: Behavioural Reconstruction in Human Osteology*. London: Routledge.

Jurmain, R.D, F.A. Cardoso, C. Henderson & S. Villotte, 2012. Bioarchaeology's holy grail: the reconstruction of activity, in *A Companion to Paleopathology*, ed. A.L. Grauer. New York: Blackwell Publishing, 531–52.

Kahl, J.E., R.Y. Calvo, M.J. Sise, C.B. Sise, J.F. Thorndike & S.R. Shackford, 2013. The changing nature of death on the trauma service. *Journal of Trauma and Acute Care Surgery* 75(2), 195–201.

Kanner, L., 1928. *Folklore of the Teeth*. New York (NY): Macmillan.

Kaplan, S.L., A. Forbes, W.A. Hammerman, L. Lamberth, K.G. Hulten, *et al*., 2014. Randomized trial of 'bleach baths' plus routine hygienic measures vs. routine hygienic measures alone for prevention of recurrent infections. *Clinical Infectious Diseases* 58(5), 679–82.

Karell, M.A., H.K. Langstaff, D.J. Halazonetis, C. Minghetti, M. Frelat & E.F. Kranioti, 2016. A novel method for pair-matching using three-dimensional digital models of bone: Mesh-to-mesh value comparison. *International Journal of Legal Medicine* 130, 1315–22.

Karmiol, M. & R.F. Walsh, 1968. Incidence of static bone defect of the mandible. *Oral Surgery, Oral Medicine, Oral Pathology* 26(2), 225–8.

Katsianis, M., S. Tsipidis & I. Kalisperakis 2014. Enhancing excavation archives using 3D spatial technologies, in *Archaeological Research in the Digital Age. Proceedings of the 1st Conference on Computer Applications and Quantitative Methods in Archaeology. Rethymno, Crete, 6–8 March 2014*, eds. C. Papadopoulos, E. Paliou, A. Chrysanthi, E. Kotoula & A. Sarris. Rethymno, Crete: Computer Applications and Quantitative Methods in Archaeology – Greek Chapter, 46–54.

Kavadia, S., S. Papadiochou, I. Papadiochou & L. Zafiriadis, 2011. Agenesis of maxillary lateral incisors: A global overview of the clinical problem. *Orthodontics* 12(4), 296–317.

Kawano, S., T. Tsukamoto, H. Ohtaguro, H. Tustsumi, T. Takahashi, *et al*., 1995. Sex determination from dental calculus by polymerase chain reaction (PCR). *Nippon Hoigaku Zasshi* 49(3), 19–38.

Keene, H.J., 1963. Distribution of diastemas in the dentition of man. *American Journal of Physical Anthropology* 21(4), 437–41.

Keith, A. 1924. Neanderthal Man in Malta. With an account of the survey of Dalam cave (Għar Dalam), by George Sinclair, A.M.I.C.E. *Journal of the Royal Anthropological Institute* 54, 251–74.

Keith, A., 1932. The late Palaeolithic inhabitants of Palestine. *Nature* 130, 284–5.

Keith, K.D., 1973. The paleostomatology at the Moore site (34LF31), LeFlore County, Oklahoma. *Bulletin of the Oklahoma Anthropological Society* 22, 149–57.

Kellehear, A., 2007. *A Social History of Dying*. Cambridge: Cambridge University Press.

Keller, A., A. Graefen, M. Ball, M. Matzas, V. Boisguerin, *et al*., 2012. New insights into the Tyrolean Iceman's origin and phenotype as inferred by whole-genome sequencing. *Nature Communications* 3, 698.

Kelley, M.A., D.R. Levesque & E. Weidl. 1991. Contrasting patterns of dental disease in five early North Chilean groups, in *Advances in Dental Anthropology*, eds. M.A. Kelley & C.S. Larsen. New York (NY): Wiley-Liss, 203–14.

Kelley, M.A. & K. Lytle, 1995. A possible case of melorheostosis from antiquity. *American Journal of Physical Anthropology* 98(3), 369–74.

Kemkes-Grottenthaler, A., 2002. Aging through the ages: Historical perspectives on age indicator methods, in *Paleodemography: Age Distributions from Skeletal Samples*, eds. R.D. Hoppa & J.W. Vaupel. Cambridge: Cambridge University Press, 48–72.

Keyes, P., 1968. Research in dental caries. *Journal of the American Dental Association* 76(6), 1357–73.

Khasnis, S.A., K.H. Kidiyoor, A.B. Patil & S.B. Kenganal, 2014. Vertical root fractures and their management. *Journal of Conservative Dentistry* 17(2), 103–10.

Kieser, J.A., J. Moggi-Cecchi & H.T. Groeneveld, 1992. Sex allocation of skeletal material by analysis of the proximal tibia. *Forensic Science International* 56(1), 29–36.

Killey, H.C. & L.W. Kay, 1972. *Benign Cystic Lesions of the Jaws, Their Diagnosis and Treatment* (2nd edition). London: Churchill Livingstone.

Killgrove, K. & J. Montgomery 2016. All Roads Lead to Rome: Exploring Human Migration to the Eternal City through Biochemistry of Skeletons from Two Imperial-Era Cemeteries (1st–3rd c AD). *PLoS ONE* 11 (2), e0147585.

Kim, Y., 1989. Relationship between the sphericity of femoral head-acetabulum and the low incidence of primary osteoarthritis of the hip joint in Koreans. *Yonsei Medical Journal* 30(3), 280–7.

King, R.E., J.M. Scianna & G.J. Petruzzelli, 2004. Mandible fracture patterns: A suburban trauma center experience. *American Journal of Otolaryngology – Head and Neck Medicine and Surgery* 25(5), 301–7.

Kini, U. & B.N. Nandeesh, 2012. Physiology of bone formation, remodelling and metabolism, in *Radionuclide and Hybrid Bone Imaging*, eds. I. Fogelman, G. Gnanasegaran & H. Van der Wall. London: Springer, 29–57.

Kiratli, B.J., 2003. Immobilization osteoporosis, in *Atlas of Osteoporosis*, ed. E.S. Orwoll. London: Current Medicine Group, 149–64.

Kirk, M., 2006. Researchers discover earliest signs of dental modification at Mexican burial site. *University of*

Connecticut Advance. Available at: http://advance.uconn.edu/2006/060619/06061906.htm

Kirveskari, P., 1974. Morphological traits in the permanent dentition of living skolt lapps. *Proceedings of the Finnish Dental Society. Suomen Hammaslaakariseuran Toimituksia* 70(Suppl 1–3), 3–90.

Kılınç, G.M., A. Omrak, F. Özer, T. Günther, A.M. Büyükkarakaya, *et al*., 2016. The demographic development of the first farmers in Anatolia. *Current Biology* 26(19), 2659–66.

Kjellström, A., 2014. Spatial and temporal trends in new cases of men with modified teeth from Sweden (AD 750–110). *European Journal of Archaeology* 17(1), 45–9.

Klaus, H., 2014. A history of violence in the Lambayeque Valley, in *The Routledge Handbook of the Bioarchaeology of Human Conflict*, eds. C. Knüsel & M.J. Smith. Oxford: Routledge, 389–414.

Klepinger, L.L., J.K. Kuhn & J. Thomas Jr., 1977. Prehistoric dental calculus gives evidence for coca in early coastal Ecuador. *Nature* 269, 506–7.

Kloos, H. & R. David, 2002. The palaeoepidemiology of schistosomiasis in ancient Egypt. *Human Ecology Review* 9(1), 14–25.

Knipper, C., A. Mittnik, K. Massy, C. Kociumaka, I. Kucukkalipci, *et al*., 2017. Female exogamy and gene pool diversification at the transition from the Final Neolithic to the Early Bronze Age in central Europe. *Proceedings of the National Academy of Sciences* 114(38), 10083–8.

Knörich, A.C. 2005. 'Investigations on the importance of early diagenetic processes for the mineralogical stabilisation and lithification of heterozoan carbonate assemblages: (Oligo-Miocene, Maltese Islands and Sicily)'. Unpublished Phd, Universität Potsdam.

Knox, J., A.C. Uhlemann, M. Miller, C. Hafer, G. Vasquez, *et al*., 2012. Environmental contamination as a risk factor for intra-household Staphylococcus aureus transmission. *PLoS ONE* 7(11), e49900.

Knudson, K.J. & T.D. Price 2007. Utility of multiple chemical techniques in archaeological residential mobility studies: Case studies from Tiwanaku- and Chiribaya-affiliated sites in the Andes. *American Journal of Physical Anthropology* 132(1), 25–39.

Knudson, K.J. & C.M. Stojanowski, 2008. New directions in bioarchaeology: Recent contributions to the study of human social identities. *Journal of Archaeological Research* 16(4), 397–432.

Knüsel, C.J., 2014. Crouching in fear: Terms of engagement for funerary remains. *Journal of Social Archaeology* 14(1), 26–58.

Knüsel, C.J. & A.K. Outram, 2004. Fragmentation: The zonation method applied to fragmented human remains from archaeological and forensic contexts. *Environmental Archaeology* 9(1), 85–97.

Knüsel, C.J. & J. Robb, 2016. Funerary taphonomy: An overview of goals and methods. *Journal of Archaeological Science: Reports* 10, 655–73.

Knüsel, C. & M.J. Smith, 2014. Introduction: The bioarchaeology of human conflict, in *The Routledge Handbook of the Bioarchaeology of Human Conflict*, eds. C. Knüsel & M.J. Smith. Oxford: Routledge, 3–24.

Koganei, H., 1912. Cribra cranii und cribra orbitalia. *Mitteilungen aus der Medizinischen Fakultät der Kaiserlichen Universität zu Toyko* 10, 113–54.

Kohn, M.J., M.J. Schoeninger & J.W. Valley, 1996. Herbivore tooth oxygen isotope compositions: Effects of diet and physiology. *Geochimica et Cosmochimica Acta* 60, 3889–96.

Kontulainen, S., H. Sievänen, P. Kannus, M. Pasanen, & I. Vuori, 2002. Effect of long-term impact-loading on mass, size, and estimated strength of humerus and radius of female racquet-sports players: A peripheral quantitative computed tomography study between young and old starters and controls. *Journal of Bone and Mineral Research* 17(12), 2281–9.

Korey, K.A., 1990. Deconstructing reconstruction: The OH 62 humerofemoral index. *American Journal of Physical Anthropology* 83(1), 25–33.

Korneliussen, T.S., A. Albrechtsen & R. Nielsen, 2014. ANGSD: Analysis of next generation sequencing data. *BMC Bioinformatics* 15, 356.

Kovacs, I., 1967. Contribution to the ontogenetic morphology of roots in the human teeth. *Journal of Dental Research* 46(5), 865–74.

Kraus, B.S., 1951. Carabelli's anomaly of the maxillary molar teeth. *American Journal of Human Genetics* 3(4), 348–55.

Kroeber, A.L., 1948. *Anthropology*. New York: Harcourt Brace.

Krogman, W.M., 1962. *The Human Skeleton in Forensic Medicine*. Springfield (IL): Charles C. Thomas.

Kruskal, J.B. & M. Wish, 1978. *Multidimensional Scaling*. Beverly Hills (CA): Sage Publications.

Kuijt, I., 2002. Keeping the peace: Ritual, skull caching, and community integration in the Levantine Neolithic, in *Life in Neolithic Farming Communities: Social Organization, Identity, and Differentiation*, ed. I. Kuijt. London: Kluwer Academic Publishers, 137–64.

Kusaka, S., 2017. Use of stable isotope analysis to reveal relationships between diet and tooth ablation types in Jomon Period Japan, in *A World View of Bioculturally Modified Teeth*, eds. S.E. Burnett & J.D. Irish. Gainesville (FL): University Press of Florida, 41–155.

Kusaka, S., A. Ando, T. Nakano, T. Yumoto, E. Ishimaru, *et al*., 2009. A strontium isotope analysis on the relationship between ritual tooth ablation and migration among the Jomon people in Japan. *Journal of Archaeological Science* 36(10), 2289–97.

Kusaka, S., T. Ikarashi, F. Hyodo T. Yumoto & K. Katayama, 2008. Variability in stable isotope ratios in two Late-Final Jomon communities in the Tokai coastal region and its relationship with sex and ritual tooth ablation. *Anthropological Science* 116(2), 171–81.

Kusaka, S., T. Nakano, T. Yumoto & M. Nakatsukasa, 2011. Strontium isotope evidence of migration and diet in relation to ritual tooth ablation: A case study from the Inariyama Jomon site, Japan. *Journal of Archaeological Science* 38(1), 166–74.

La Fontaine, J.S., 1986. *Sex and Age as Principles of Social Differentiation*. London: Academic Press.

Lahr, M.M., F. Rivera, R.K. Power, A. Mounier, B. Copsey, *et al*., 2016. Inter-group violence among early Holocene hunter-gatherers of West Turkana, Kenya. *Nature* 529 (7586), 394–8.

Lai, L., T.C. O'Connell & R.H. Tykot, 2009. Diet and environment in Maltese prehistory: results and potentials of a stable isotopic perspective on the Circle, in *Mortuary Customs in Prehistoric Malta: Excavations at the Brochtorff Circle at Xaghra (1987–94)*, eds. C. Malone, S. Stoddart, A. Bonanno & D.H. Trump. Cambridge: McDonald Institute for Archaeological Research, 335–40.

Lambert, A., L. Puymerail, K. Chaumoitre & A. Schmitt, 2013. Analyse fonctionnelle des adaptations osseuses du squelette post crânien au Néolithique final en Provence. *BMSAP* 26(1–2), 67–77.

Lamberts, S.W.J., A.W. van den Beld & A.-J. van der Lely, 1997. The endocrinology of aging. *Science* 278(5337), 419–24.

Langsjoen, O., 1998. Diseases of the dentition, in *The Cambridge Encyclopedia of Human Palaeopathology*, eds. A.C. Aufderheide & C. Rodríguez-Martín. Cambridge: Cambridge University Press, 393–412.

Lanyon, L.E. & D.G. Baggott, 1976. Mechanical function as an influence on the structure and form of bone. *Journal of Bone and Joint Surgery* 58–B(4), 436–43.

Laptook, T. & G. Silling, 1983. Canine transposition – Approaches to treatment. *Journal of the American Dental Association* 107(105), 746–8.

Larsen, C.S., 1985. Dental modifications and tool use in the western Great Basin. *American Journal of Physical Anthropology* 67(4), 393–402.

Larsen, C.S., 1995. Biological changes in human populations with agriculture. *Annual Review of Anthropology* 24, 185–213.

Larsen, C.S., 2015. *Bioarchaeology: Interpreting Behavior from the Human Skeleton* (2nd edition). Cambridge: Cambridge University Press.

Larsen, C.S., 2017. Foreword, in *A World View of Bioculturally Modified Teeth*, eds. S.E. Burnett & J.D. Irish. Gainesville (FL): University Press of Florida, xv–xvii.

Larsen, C.S., S.W. Hillson, B. Boz, M.A. Pilloud, J.W. Sadvari, *et al*., 2015. Bioarchaeology of Neolithic Çatalhöyük: Lives and lifestyles of an early farming society. *Journal of World Prehistory* 28: 27–68.

Larsen, C.S. & M.A. Kelley, 1991. Introduction, in *Advances in Dental Anthropology*, eds. M.A. Kelley & C.S. Larsen. New York (NY): Wiley-Liss, 1–5.

Larsen, C.S., C.J. Knüsel, S.D. Haddow, M.A. Pillous, M. Milella, *et al*., 2019. Bioarchaeology of Neolithic Çatalhöyük reveals fundamental transitions in health, mobility, and lifestyle in early farmers. *Proceedings of the National Academy of Sciences* 116(26), 12615–23.

Larsen, C.S., R. Shavit & M.C. Griffin, 1991. Dental caries evidence for dietary change: An archaeological context, in *Advances in Dental Anthropology*, eds. M.A. Kelley & C.S. Larsen. New York (NY): Wiley-Liss, 179–202.

Laslett, P., 1991. *A Fresh Map of Life: The Emergence of the Third Age*. Cambridge (MA): Harvard University Press.

Lau, G.F., 2015. Different kinds of dead: Presencing Andean expired beings, in *Death Rituals, Social Order and the Archaeology of Immortality in the Ancient World*, eds. C. Renfrew, M. Boyd & I. Morley. Cambridge: Cambridge University Press, 168–86.

Lave, J. & E. Wenger, 1991. *Situated Learning: Legitimate Peripheral Participation*. Cambridge: Cambridge University Press.

Lavelle, C.L.B., 1970. The distribution of diastemas in different human population samples. *European Journal of Oral Sciences* 78(1–4), 530–4.

Lazaridis, I., 2018. The evolutionary history of human populations in Europe. *Current Opinion in Genetic Development* 53, 21–7.

Lazaridis, I., D. Nadel, G. Rollefson. D.C. Merrett, N. Rohland, *et al*., 2016. Genomic insights into the origin of farming in the ancient Near East. *Nature* 536, 419–24.

Lazaridis, I., N. Patterson, A. Mittnik, G. Renaud, S. Mallick, *et al*., 2014. Ancient human genomes suggest three ancestral populations for present-day Europeans. *Nature* 513, 409–13.

Lee, C., 2017. The relationship between intentional dental ablation and hereditary agenesis in Late Neolithic to Early Bronze Age China, in *A World View of Bioculturally Modified Teeth*, eds. S.E. Burnett & J.D. Irish. Gainesville (FL): University Press of Florida, 92–101.

Lee, J.Y., K.Y. Nam & K.C. Song, 2010. Distal tibiofibular synostosis after open reduction and internal fixation in a military soldier (A case report). *Journal of Korean Foot and Ankle Society* 14(1), 105–7.

Leek, F.F., 1967. Reputed Early Egyptian dental operation: An appraisal, in *Diseases in Antiquity*, eds. D.R. Brothwell & A.T. Sandison. Springfield: Charles C. Thomas, 702–5.

Leek, F.F., 1972. Did a dental profession exist in ancient Egypt during the 3rd Millennium BC? *Medical History* 16(4), 404–6.

Leemkuil, R.W., 1958. Traumatic bone cysts of the maxilla and mandible. *Iowa Dental Journal* 44, 155–8.

Leigh, R.W., 1937. Dental morphology and pathology of pre-Spanish Peru. *American Journal of Physical Anthropology* 22(2), 267–96.

Leighton, R., 1999. *Sicily Before History: An Archaeological Survey from the Palaeolithic to the Iron Age*. London: Duckworth.

Leonini, V. & L. Sarti 2006. Sepolture e rituali funerari nell'Eneolitico e al passaggio all'età del Bronzo in Italia, in *La Cultura del Morire nelle Società Preistoriche e Protostoriche Italiane. Studio Interdisciplinare dei Dati e Loro Trattamento Informatico: Dal Paleolitico all'Eta del Rame*, ed. F. Martini. Firenze: Istituto Italiano Preistoria e Protostoria, 129–60.

Le Roy, M., 2017. How were infants considered at death during the Neolithic period in France? in *Children, Death and Burial: Archaeological Discourses*, eds. E. Murphy & M. Le Roy. Oxford: Oxbow Books, 19–34.

Lester, C.W., 1967. Melorheostosis in a prehistoric Alaskan skeleton. *Journal of Bone and Joint Surgery* 49(1), 142–3.

Levinson, A.A., B. Luz & Y. Kolodny, 1987. Variations in oxygen isotopic compositions of human teeth and urinary stones. *Applied Geochemistry* 2, 367–71.

Levy, R. & P. Dawson, 2006. Reconstructing a Thule whalebone house using 3D imaging. *IEEE MultiMedia* 13(2), 78–83.

Lewis, M.E., 2004. Endocranial lesions in non-adult skeletons: Understanding their aetiology. *International Journal of Osteoarchaeology* 14(2), 82–97.

Lewis, M.E., 2007. *The Bioarchaeology of Children: Perspectives from Bioarchaeological And Forensic Anthropology*. Cambridge: Cambridge University Press.

Lewis, M.E., 2018. *Paleopathology of Children. Identification of Pathological Conditions in the Human Skeletal Remains of Non-Adults*. London: Academic Press.

Lewis, M.E. & R. Gowland, 2007. Brief and precarious lives: Infant mortality in contrasting sites from Medieval and Post-Medieval England (AD 850–1859). *American Journal of Physical Anthropology* 134(1), 117–29.

Lewis, M.E. & R. Gowland, 2009. Infantile cortical hyperostosis: Cases, causes and contridictions, in *Proceedings of the Ninth Annual Conference of the British Association for Biological Anthropology and Osteoarchaeology*, eds. M. Lewis & M. Clegg. Oxford: Archaeopress BAR International Series 1981, 43–51.

Li, H., 2011 A statistical framework for SNP calling, mutation discovery, association mapping and population genetical parameter estimation from sequencing data. *Bioinformatics* 27(21), 2987–93.

Li, H., B. Handsaker, A. Wysoker, T. Fennell, J. Ruan, *et al*., 2009. The Sequence Alignment/Map format and SAMtools. *Bioinformatics* 25(16), 2078–9.

Li, L., 2000. Ancestor worship: An archaeological investigation of ritual activities in Neolithic North China. *Journal of East Asian Archaeology* 2(1), 129–64.

Lightfoot, E. & T.C. O'Connell, 2016. On the use of biomineral oxygen isotope data to identify human migrants in the archaeological record: intrasample variation, statistical methods and geographical considerations. *PLoS ONE* 11(4), e0153850.

Lignitz, H., 1919–1920. Die künstlichen zahnverstümmlungen in Afrika im lichte der kulturkreisforschung. *Anthropos* 14–15(4–6), 891–943.

Lillehammer, G., 1989. A child is born. The child's world in an archaeological perspective. *Norwegian Archaeological Review* 22(2), 89–105.

Lillehammer, G., 2000. The world of children, in *Children and Material Culture*, ed. J.S. Derevenski. London: Routledge, 17–26.

Lillehammer, G., 2010. Archaeology of children. *Complutum* 21(2), 15–45.

Lillios, K.T., J.A. Artz, A.J. Waterman, J. Mack, J.T. Thomas, *et al*., 2014. The rock-cut tomb of Bolores (Torres Vedras): an interdisciplinary approach to understanding the social landscape of the Late Neolithic/Copper Age of the Iberian Peninsula. *Trabajos de Prehistoria* 71(2), 282–304.

Lind, V., 1972. Short root anomaly. *European Journal of Oral Sciences* 80(2), 85–93.

Linne, S., 1940. Dental decoration in aboriginal America. *Ethnos* 5(1–2), 2–28.

Lipatov, M., K. Sanjeev, R. Patro & K.R. Veeramah, 2015. Maximum likelihood estimation of biological relatedness from low coverage sequencing data. *bioRxiv*, 023374.

Lipschitz, D.A., T.H. Bothwell, H.C. Seftel, A.A. Wapnick & R.W. Charlton, 1971. The role of ascorbic acid in the metabolism of storage iron. *British Journal of Haematology* 20(2), 155–163.

Lipson, M., A. Szécsényi-Nagy, S. Mallick, A. Pósa, B. Stégmár, *et al*., 2017. Parallel palaeogenomic transects reveal complex genetic history of early European farmers. *Nature* 551, 368–72.

Liu, L., B.C. Kang, S.J. Yoon, J.S. Lee & S.A. Hwang, 2018. Radiographic features of lingual mandibular bone depression using dental cone beam computed tomography. *Dentomaxillofacial Radiology* 47(6), 20170383.

Livingstone, D., 1861. *A Popular Account of Missionary Travels and Researches in South Africa.* London: John Murray.

Lock, M., 1993. Cultivating the body: Anthropology and epistemologies of bodily practice and knowledge. *Annual Review of Anthropology* 22, 133–55.

Loison, G., 1998. La nécropole de Pontcharaud en Basse-Auvergne, in *Sépultures d'Occident et Genèses des Mégalithismes (9000–3500 avant notre Ère)*, ed. J. Guilane. Paris: Editions Errance, 189–206.

Longinelli, A. 1984. Oxygen isotopes in mammal bone phosphate: a new tool for paleohydrological and paleoclimatological research? *Geochimica et Cosmochimica Acta* 48, 385–90.

López Olivares, N.M., 1997. Cultural odontology: Dental alterations from Petén, Guatemala, in *Bones of the Maya: Studies of Ancient Skeletons*, eds. S.L. Whittington & D.M. Reed. Washington (DC): Smithsonian Institution Press, 105–16.

Lorentz, K.O., 2016. Challenges for funerary taphonomy viewed through prehistoric Cyprus. *Journal of Archaeological Science: Reports* 10, 757–68.

Lorentz, K.O., S.A.M. Lemmers, C. Chrysostomou, W. Dirks, M.R. Zaruri, *et al*., 2019. Use of dental microstructure to investigate the role of prenatal and early life physiological stress in age at death. *Journal of Archaeological Science* 104, 85–96.

Lorkiewicz, W., 2011. Nonalimentary tooth use in the Neolithic population of the Lengyel culture in Central Poland (4600–4000 BC). *American Journal of Physical Anthropology* 144(4), 538–51.

Lorkiewicz, W., 2012. Skeletal trauma and violence among the early farmers of the North European Plain: Evidence from Neolithic settlements of the Lengyel Culture in Kuyavia, north-central Poland, in *Sticks, Stones, and Broken Bones: Neolithic Violence in a European Perspective*, eds. R.J. Schulting & L. Fibiger. Oxford: Oxford University Press, 51–7.

Lorkiewicz, W., J. Mietlińska, J. Karkus, M. Kurek, P. Borówka, *et al*., 2019. Osteoporotic bone fractures and age-related bone loss in males inhabiting the Kujawy region in north-central Poland from the Neolithic to early modern times. *Journal of Archaeological Science* 103, 16–25.

Lous, I., 1970. The masticatory system used as a tool. *Tandlaegebladet* 74(1), 1–10.

Lovell, N.C., 1997. Trauma analysis in paleopathology. *Yearbook of Physical Anthropology* 40(S25), 139–70.

Lovell, N.C., 2000. Palaeopathological description and diagnosis, in *Biological Anthropology of the Human Skeleton*, eds. M.A. Katzenberg & S.R. Saunders. New York (NY): Wiley-Liss, 217–48.

Lubell, D., M. Jackes, H. Schwarcz, M. Knyf & C. Meiklejohn, 1994. The mesolithic-neolithic transition in Portugal: Isotopic and dental evidence of diet. *Journal of Archaeological Science* 21(2), 201–16.

Lubisich, E.B., T.J. Hilton & J. Ferracane, 2010. Cracked teeth: A review of the literature. *Journal of Esthetic and Restorative Dentistry* 22(3), 158–67.

Luebke, R.G., 1984. Vertical crown-root fractures in posterior teeth. *Dental Clinics of North America* 28(4), 883–94.

Lukacs, J.R., 2007. Dental trauma and antemortem tooth loss in prehistoric Canary Islanders: Prevalence and contributing factors. *International Journal of Osteoarchaeology* 17(2), 157–73.

Lukacs, J.R. & R.F. Pastor, 1988. Activity-induced patterns of dental abrasion in prehistoric Pakistan. *American Journal of Physical Anthropology* 76(3), 377–98.

Lukacs, J.R. & C. Rodríguez Martín, 2002. Lingual cortical mandibular defects (Stafne's defect): An anthropological approach based on Prehistoric skeletons from the Canary Islands. *International Journal of Osteoarchaeology* 12(2), 112–26.

Lukacs, J.R., & S.R. Walimbe, 1984. Deciduous dental morphology and the biological affinities of a late Chalcolithic skeletal series from western India. *American Journal of Physical Anthropology* 65(1), 23–30.

Lulof, P.S., L. Opgenhaffen & M.H. Sepers, 2013. The art of reconstruction: Documenting the process of 3D modeling: Some preliminary results, in *2013 Digital Heritage International Congress (DigitalHeritage)*, 333–6.

Lunt, D.S., 1978. Molar attrition in Medieval Danes, in *Development, Function and Evolution of Teeth*, eds. P.M. Butler & K.A. Joysey. London: Academic Press, 465–82.

Luz, B. & Y. Kolodny 1985. Oxygen isotope variations in phosphate of biogenic apatites, IV. Mammal teeth and bones. *Earth and Planetary Science Letters* 75(1), 29–36.

Lykoudis, S.P. & A.A. Argiriou, 2007. Gridded data set of the stable isotopic composition of precipitation over the eastern and central Mediterranean. *Journal of Geophysical Research: Atmospheres* 112(D18), doi:10.1029/2007JD008472.

Lyman, R.L., 2004. The concept of equifinality in taphonomy. *Journal of Taphonomy* 2(1), 15–26.

MacHugh, D.E., C.J. Edwards, J.F. Bailey, D.R. Bancroft & D.G. Bradley, 2000. The extraction and analysis of ancient DNA from bone and teeth: A survey of current methodologies. *Ancient Biomolecules* 3, 81–102.

Macintosh, A.A., T.G. Davies, T.M. Ryan, C.N. Shaw & J.T. Stock, 2013. Periosteal versus true cross-sectional geometry: A comparison along humeral, femoral, and tibial diaphyses. *American Journal of Physical Anthropology* 150(3), 442–52.

Macintosh, A.A., R. Pinhasi & J.T. Stock, 2014a. Divergence in male and female manipulative behaviors with the intensification of metallurgy in central Europe. *PLoS ONE* 9(11), e112116.

Macintosh, A.A., R. Pinhasi, & J.T. Stock, 2014b. Lower limb skeletal biomechanics track long-term decline in mobility across ~6150 years of agriculture in Central Europe. *Journal of Archaeological Science* 52, 376–90.

Macintosh, A.A., R. Pinhasi & J.T. Stock, 2016. Early life conditions and physiological stress following the transition to farming in central/southeast Europe: skeletal growth impairment and 6000 years of gradual recovery. *PLoS ONE* 11(2), 1–27.

Macintosh, A.A., R. Pinhasi & J.T. Stock, 2017. Prehistoric women's manual labour exceeded that of athletes through the first 5500 years of farming in central Europe. *Science Advances* 3, e3893.

Macintosh, A.A. & J.T. Stock, 2019. Intensive terrestrial or marine locomotor strategies are associated with inter- and intra-limb bone functional adaptation in living female athletes. *American Journal of Physical Anthropology* 168(3), 566–81

Mack, J.E., A.J. Waterman, A.-M. Racila, J.A. Artiz & K.T. Lillios, 2016. Applying zooarchaeological methods to interpret mortuary behaviour and taphonomy in commingled burials: The case study of the Late Neolithic Site of Bolores, Portugal. *International Journal of Osteoarchaeology* 26(3), 524–36.

Mackay, D., L. Wood & A. Rangan, 2000. The treatment of isolated ulnar fractures in adults: A systematic review. *Injury* 31(8), 565–70.

Mackie, M., J. Hendy, A.D. Lowe, A. Sperduti, M. Holst, *et al*., 2017. Preservation of the metaproteome: Variability of protein preservation in ancient dental calculus. *Science & Technology of Archaeological Research* 3(1), 58–70.

Mack, L.M. & H. Woodward, 1969. Static bony defect of the mandible. *Journal of Oral Surgery* 27(4), 262–5.

MacLatchy, L.M. & W.H. Bossert, 1996. An analysis of the articular surface distribution of the femoral head and acetabulum in anthropoids, with implications for hip function in Miocene hominoids. *Journal of Human Evolution* 31(5), 425–53.

Magro Conti, J., 1997. 'The Neolithic hypogeum at Santa Luċija, Valletta.' Unpublished pamphlet.

Mahoney, D.P., 1998. Time travels. *Computer Graphics World* 21(4), 81–4.

Mahoney, P., 2006. Dental microwear from Natufian hunter-gatherers and early Neolithic farmers: Comparisons within and between samples. *American Journal of Physical Anthropology* 130(3), 308–19.

Mallia, F.S., 1965. Prehistoric Finds, in *Missione Archeologica Italiana a Malta. Rapporti preliminari delle Campagne 1963–1970*, eds. M. Cagiano De Azevado, C. Caprino, A. Ciasca, E. Coleiro, A. Davico, *et al*., Rome: Istituto di Studi del Vicino Oriente, Università di Roma, 73–6.

Malone, C., 1997–8. Processes of Colonisation in the central Mediterranean. *Accordia Research Papers* 7, 37–57.

Malone, C., 2003. The Italian Neolithic: A synthesis of research. *Journal of World Prehistory* 17(3), 235–312.

Malone, C. 2007. Structure, art and ritual in a Maltese Temple, in *Cult in Context*, eds. D. Barrowclough & C. Malone. Oxford: Oxbow, 23–34.

Malone, C., 2008. Metaphor and Maltese art: Explorations in the temple period. *Journal of Mediterranean Archaeology* 21(1), 81–108.

Malone, C., 2018. Manipulating the bones: eating and augury in the Maltese temples, in *Ritual, Play and Belief, in Evolution and Early Human Societies*, eds. C. Renfrew, I. Morley & M. Boyd, Cambridge: Cambridge University Press, 187–207.

Malone, C., A. Bonanno, T. Gouder, S. Stoddart & D.H. Trump, 1993. The death cults of prehistoric Malta. *Scientific American* 269(6), 110–17.

Malone, C., A. Bonanno, D.H. Trump, J. Dixon, R. Leighton, *et al*., 2009a. Material culture, in *Mortuary Customs in Prehistoric Malta: Excavations at the Brochtorff Circle at Xagħra (1987–94)*, eds. C. Malone, S. Stoddart, A. Bonnano & D.H. Trump, Cambridge: McDonald Institute for Archaeological Research, 219–313.

Malone, C., N. Cutajar, R. McLaughlin, B. Mercieca, A. Pace, *et al*., 2019. Island questions: The chronology of the Brochtorff Circle at Xagħra, Gozo, and its significance for the Neolithic sequence on Malta. *Archaeological and Anthropological Sciences* 11, 4251–306.

Malone, C., S. Mason & S. Stoddart, 2009b. Methods applied in the analysis of the Circle, in *Mortuary Customs in Prehistoric Malta: Excavations at the Brochtorff Circle at Xagħra (1987–94)*, eds. C. Malone, S. Stoddart, A. Bonanno & D.H. Trump. Cambridge: McDonald Institute for Archaeological Research, 63–78.

Malone, C., R. McLaughlin, B. Mercieca-Spiteri, E. Parkinson, R. Power, *et al*., 2018. The social implications of death in prehistoric Malta, in *Gathered in Death. (Aegis Archéologie du Monde Minoen)*, eds. A. Schmitt, S. Déderix, J. Driessen & I. Crevecoeur. Louvain-la-Neuve: Presses universitaires de Louvain, 128–42.

Malone, C. & S. Stoddart, 1995a. Digging up the future. *Nonesuch*, 40–2.

Malone, C. & S. Stoddart, 1995b. *Malta in the Dawn of Civilisation. (Catalogue of the Exhibition).* Malta: Ministry of Justice and the Arts.

Malone, C. & S. Stoddart, 1995c. The Maltese nation chooses prehistoric ancestors. *Past* 21, 11.

Malone, C. & S. Stoddart, 1995d. Discoveries at the Brochtorff Circle. *Treasures of Malta – Magazine of the Fondazzjoni Patrimonju Malti* 1(2), 15–19.

Malone, C. & S. Stoddart, 1996a. Representations of death – discoveries at the Xaghra stone circle, in *Maltese Prehistoric Art 5000–2500 BC*, ed. A. Pace. Valletta: Fondazzjoni Patrimonju Malti, National Museum of Malta and the Ministry of Culture, 45–51.

Malone, C. & S. Stoddart, 1996b. Excavations on Gozo 1987–94. *Malta Archaeological Review* 1, 1–5.

Malone, C. & S. Stoddart, 1996c. Maltese and Mediterranean megalithism in the light of the Brochtorff Circle, in *The Neolithic in the Near East and Europe. Colloquium XVI. Megalithism*, eds. R. Grifoni Cremonesi, J. Guilaine & J. L'Helgouach. Preprints of the XIII Congress of the UISPP, Forlì, Italy. Forlì: Abaco, 109–14.

Malone, C. & S. Stoddart 2004. Towards an island of mind? in *Explaining social change: studies in honour of Colin Renfrew*, eds. J. Cherry, C. Scarre & S. Shennan. Cambridge: McDonald Institute for Archaeological Research, 93–102.

Malone, C. & S. Stoddart, 2009. Conclusions, in *Mortuary Customs in Prehistoric Malta: Excavations at the Brochtorff Circle at Xagħra (1987–94)*, eds. C. Malone, S. Stoddart, A. Bonanno & D.H. Trump. Cambridge: McDonald Institute for Archaeological Research, 361–84.

Malone, C. & S. Stoddart, 2011. Maltese prehistoric religion, in *The Oxford Handbook of the Archaeology of Ritual and Religion*, ed. T. Insoll. Oxford: Oxford University Press, 758–74.

Malone, C. & S. Stoddart, 2016. Figurines of Malta, in *The Oxford Handbook of Prehistoric Figurines*, ed. T. Insoll. Oxford: Oxford University Press, 729–53.

Malone, C., S. Stoddart, A. Bonanno, T. Gouder, R. Grima & D.H. Trump, 2009c. Introduction: The intellectual and historical context, in *Mortuary Customs in Prehistoric Malta: Excavations at the Brochtorff Circle at Xagħra (1987–94)*, eds. C. Malone, S. Stoddart, A. Bonanno & D.H. Trump. Cambridge: McDonald Institute for Archaeological Research, 1–16.

Malone, C., S. Stoddart, A. Bonanno, T. Gouder & D.H. Trump, 1995. Mortuary ritual of the 4th Millennium BC Malta: The Żebbuġ period chambered tomb from the Brochtorff Circle at Xagħra (Gozo). *Proceedings of the Prehistoric Society* 61, 303–45.

Malone, C., S. Stoddart, A. Bonanno & D.H. Trump (eds.), 2009d. *Mortuary Customs in Prehistoric Malta: Excavations at the Brochtorff Circle at Xagħra (1987–94)*. Cambridge: McDonald Institute for Archaeological Research.

Malone, C., S. Stoddart & G. Cook, 2009e. Dating Maltese prehistory, in *Mortuary Customs in Prehistoric Malta: Excavations at the Brochtorff Circle at Xagħra (1987–94)*, eds. C. Malone, S. Stoddart, A. Bonanno & D.H. Trump. Cambridge: McDonald Institute for Archaeological Research, 341–6.

Malone, C., S. Stoddart & A. Townsend, 1995. The landscape of the island goddess? A Maltese perspective of the central Mediterranean. *Caeculus (Papers on Mediterranean Archaeology, Archaeological Institute, Groningen University)* 2, 1–15.

Malone, C., S. Stoddart & D.H. Trump, 1988. A house for the temple builders. Recent investigations on Gozo, Malta. *Antiquity* 62(235), 297–301.

Malone, C., S. Stoddart, D.H. Trump & C. Duhig, 2009f. Żebbuġ phase levels: Spatial and stratigraphic analysis, in *Mortuary Customs in Prehistoric Malta: Excavations at the Brochtorff Circle at Xagħra (1987–94)*, eds. C. Malone, S. Stoddart, A. Bonanno & D.H. Trump. Cambridge: McDonald Institute for Archaeological Research, 95–108.

Mandy, M. & M. Nyirenda, 2018. Developmental origins of health and disease: The relevance to developing nations. *International Health* 10(2), 66–70.

Manfredini, A., M.A. Fugazzola Delpino, L. Sarti, M. Silvestrini, F. Martini, *et al*., 2009. Adriatico e Tirreno a confronto: Analisi dell'occupazione territoriale tra il Neolitico finale e l'età del Rame in alcune aree campione dell'Italia centrale. *Rivista di Scienze preistoriche* 59(1), 115–79.

Mangion, J.J. & C. Olivieri-Munroe, 1968. Preliminary studies on oral health conditions in Malta. *St. Luke's Hospital Gazette* 3(2), 112–15.

Manhein, M.H., G.A. Listi & M. Leitner 2006. The application of geographic information systems and spatial analysis to assess dumped and subsequently scattered human remains. *Journal of Forensic Sciences* 51(3), 469–74.

Maniscalco, L., 1989. Ocher containers and trade in the Central Mediterranean Copper Age. *American Journal of Archaeolology* 93(4), 537–41.

Mann, R.W., 1990. Incipient lingual cortical mandibular defect in a 10- to 12-year-old American Indian child. *American Journal of Roentgenology* 154(3), 658–9.

Mann, R.W. & D.R. Hunt, 2012. *Photographic Regional Atlas of Bone Disease: A Guide to Pathologic and Normal Variation in the Human Skeleton.* Springfield (IL): Charles C. Thomas.

Mann, R.W. & E.D. Shields, 1992. Cavitation defects on the lingual ramus: A further expression of Stafne's defect. *Journal of Craniofacial Genetics and Developmental Biology* 12(3), 167–73.

Mann, R.W. & P.J. Tsaknis, 1991. Cortical defects in the mandibular sulcus. *Oral Surgery, Oral Medicine, and Oral Pathology* 71(4), 514–16.

Mann, R.W. & P. Tuamsuk, 2016. Stafne's defects in a sample of adult Thai mandibles in the Khon Kaen University Osteology collection, Thailand. *International Journal of Osteoarchaeology* 26(5), 906–11.

Mant, M. & C. Roberts, 2015. Diet and dental caries in post-medieval London. *International Journal of Historical Archaeology* 19(1), 188–207.

Mantini, S., M. Mantini, S. Del Monte, D. Mazza, P. Primicerio, *et al*., 2007. Early dentistry practice in Italian Neolithic site of Gaione (Parma). *Origini* 29, 221–25.

Marchi, D., 2008. Relationships between lower limb cross-sectional geometry and mobility: The case of a Neolithic sample from Italy. *American Journal of Physical Anthropology* 137(2), 188–200.

Marchi, D., V. Sparacello, B.M. Holt & V. Formicola, 2006. Biomechanical approach to the reconstruction of activity patterns in Neolithic Western Liguria, Italy. *American Journal of Physical Anthropology* 131(4), 447–55.

Marchi, D., V. Sparacello & C. Shaw, 2011. Mobility and lower limb robusticity of a pastoralist Neolithic population from north-western Italy, in *Human Bioarchaeology of the Transition to Agriculture*, eds. R. Pinhasi & J.T. Stock. New Jersey (NJ): 317–46.

Marchi, D., C.S. Walker, W. Pianpian, T.W. Holliday, S.E. Churchill, *et al*., 2017. The thigh and leg of Homo naledi. *Journal of Human Evolution* 104, 174–204.

Maresh, M.M., 1970. Measurements from roentgenograms, in *Human Growth and Development*, ed. R.W. McCammon. Springfield (IL): Charles C. Thomas, 157–200.

Márquez-Grant, N., 2015. An overview of age estimation in forensic anthropology: Perspectives and practical considerations. *Annals of Human Biology* 42(4), 308–22.

Martin, D.L., A.H. Goodman & G.J. Armelagos, 1985. Skeletal pathologies as indicators of diet, in *Analysis of Prehistoric Diets*, eds. R.I. Gilbert & J.H. Mielke. London: Academic Press, 227–79.

Martin, D.L., A.L. Magennis & J.C. Rose, 1987. Cortical bone maintenance in a historic Afro-American cemetery sample from Cedar-Grove, Arkansas. *American Journal of Physical Anthropology* 74(2), 255–64.

Martin, L.D. & D.L. West, 1995. The recognition and use of dermestid (Insecta, Coleoptera) pupation chambers in paleoecology. *Palaeogeography, Palaeoclimatology, Palaeoecology* 113(2–4), 303–10.

Martinez-Lavin, M., J. Mansilla, C. Pineda, C. Pijoan & P. Ochoa, 1994. Evidence of hypertrophic osteoarthropathy in human skeletal remains from pre-Hispanic Mesoamerica. *Annals of Internal Medicine* 120(3), 238–41.

Martiniano, R., L.M. Cassidy, R. Ó'Maoldúin, R. McLaughlin, N.M. Silva, *et al*., 2017. The population genomics of archaeological transition in west Iberia: Investigation of ancient substructure using imputation and haplotype-based methods. *PLoS Genetics* 13, e1006852.

Masnicová, S. & R. Beňuš, 2003. Developmental anomalies in skeletal remains from the Great Moravia and Middle ages cemeteries at Devín (Slovakia). *International Journal of Osteoarchaeology* 13(5), 266–74.

Mathieson, I., S. Alpaslan-Roodenberg, C. Posth, A. Szécsényi-Nagy, N. Rohland, *et al*., 2018. The genomic history of southeastern Europe. *Nature* 555, 197–203.

Mathieson, I., I. Lazaridis, N. Rohland, S. Mallick, N. Patterson, *et al*., 2015. Genome-wide patterns of selection in 230 ancient Eurasians. *Nature* 528, 499–503

Maureille, B. & P. Sellier, 1996. Dislocation en ordre paradoxal, momification et décomposition: Observations et hypothèses. *Bulletins et Mémoires de la Société d'Anthropologie de Paris* 8(3–4), 313–27.

May, H., N. Peled, G. Dar, J. Abbas, B. Medlej, *et al*., 2010. Hyperostosis frontalis interna and androgen suppression. *Anatomical Record* 293(8), 1333–6.

May, H., N. Peled, G. Dar, J. Abbas & I. Hershkovitz, 2011a. Hyperostosis frontalis interna: What does it tell us about our health? *American Journal of Human Biology* 23(3), 392–7.

May, H., N. Peled, G. Dar, H. Cohen, J. Abbas, *et al*., 2011b. Hyperostosis frontalis interna: Criteria for sexing and aging a skeleton. *International Journal of Legal Medicine* 125(5), 669–73.

Mayes, A.T., S.B. Barber & A.A. Joyce, 2017. Social complexity and intraregional and interregional variation in dental modification. A test case from the Lower Río Verde Valley, Oaxaca, in *A World View of Bioculturally Modified Teeth*, eds. S.E. Burnett & J.D. Irish. Gainesville (FL): University Press of Florida, 285–97.

Mayhall, J.T., 1992. Techniques for the study of dental morphology, in *Skeletal Biology of Past Peoples: Research Methods*, eds. S.R. Saunders & M.A. Katzenberg. New York (NY): Wiley-Liss, 59–78.

Mayr, A., 1901. Die vorgeschichtlichen denkmäler von Malta. *Abhandlungen der Bayerischen Akademie der Wissenschaften* I XXI(III), 643–726.

Mayr, A., 1908. *The Prehistoric Remains of Malta,* translated from German. Private Circulation.

Mays, S., 1996. Age-dependent cortical bone loss in a medieval population. *International Journal of Osteoarchaeology* 6(2), 144–54.

Mays, S., 1999. Osteoporosis in earlier populations. *Journal of Clinical Densitometry* 2(1), 71–8.

Mays, S., 2015. The effect of factors other than age upon skeletal age indicators in the adult. *Annals of Human Biology* 42(4), 332–41.

Mays, S., 2016. Bone-formers and bone-losers in an archaeological population. *American Journal of Physical Anthropology* 159(4), 577–84.

Mays, S., G. Turner-Walker & U. Syversen, 2006. Osteoporosis in a population from medieval Norway. *American Journal of Physical Anthropology* 131(3), 343–51.

McCown, T., 1939. 'The Natufian Crania from Mount Carmel (Palestine) and Their Interrelationship.' Unpublished PhD, University of California.

McFadden, C. & M. Oxenham, 2020. A palaeoepidemiological approach to the osteological paradox: Investigating stress, frailty and resilience through cribra orbitalia. *American Journal of Physical Anthropology* (Early View), 1–13.

McFarlane, D.A., J. Lundberg & W. Roberts 2010. A geographic information systems approach to the 19th century excavation of Brixham cavern, Devon, England. *Studies in Speleology* 17, 1–11.

McKinley, J.I., 2004a. Compiling a skeletal inventory: Disarticulated and co-mingled remains, in *Guidelines to the Standards for Recording Human Remains (IFA Paper No. 7)*, eds. M. Brickley & J.I. McKinley. BABAO/ IFA, 14–17.

McKinley, J.I., 2004b. Compiling a skeletal inventory: Cremated human bone, in *Guidelines to the Standards for Recording Human Remains (IFA Paper No. 7)*, eds. M. Brickley & J.I. McKinley. BABAO/ IFA, 9–13.

McLaughlin, T. R., 2018. On applications of space-time modelling with open-source 14C age calibration. *Journal of Archaeological Method and Theory* 26, 479–501.

McLaughlin, T.R., S. Stoddart & C. Malone, 2018. Island risks and the resilience of a prehistoric civilization. *World Archaeology* 50(4), 570–600.

McManus, I.C., 2009. The history and geography of human handedness, in *Language Lateralization and Psychosis*, eds. I.E. Sommer & R. Kahn. Cambridge: Cambridge University Press, 37–57.

McMullin, J., 1995. Theorizing age and gender relations, in *Connecting Gender and Ageing: A Sociological Approach*, eds. S. Arber & J. Ginn. Buckingham: Open University Press, 30–41.

Meese, M. & W. Sebastianelli, 1996. Periostitis of the upper extremity: A report of 2 cases and literature review. *Clinical Orthopaedics and Related Research* (324), 222–6.

Meegan, E. 2017. 'Agency and Social Dynamism in Late Neolithic and Early Bronze Age Ireland and Malta.' Unpublished PhD, University College Dublin.

Meier, R., M. Sahnouni, M. Medig & A. Derradji, 2003. Human skull from the Taza locality, Jijel, Algeria. *Anthropologischer Anzeiger* 61(2), 129–40.

Meijer, K.A., M.S. Fury, H. Ennis, L. Grau, M. Baraga, *et al*., 2017. Radial shaft stress fracture in a major league pitcher. *American Journal of Orthopedics* 46(5), E326–9.

Meister, F. Jr., T.J. Lommel & H. Gerstein, 1980. Diagnosis and possible causes of vertical root fractures. *Oral Surgery, Oral Medicine, Oral Pathology* 49(3), 243–53.

Mendenhall, W.M., R.J. Amdur, R.W. Hinerman, J.W. Werning, R.S. Malyapa, *et al*., 2007. Skin cancer of the head and neck with perineural invasion. *American Journal of Clinical Oncology* 30(1), 93–6.

Meng, C.M. & Y.K. Wu, 1942. Tuberculosis of the flat bones of the vault of the skull. *Journal of Bone and Joint Surgery* 24(2), 341–53.

Mensforth, R.P., C.O. Lovejoy, J.W. Lallo & G.J. Armelagos, 1978. Part two: The role of constitutional factors, diet, and infectious disease in the etiology of porotic hyperostosis and periosteal reactions in prehistoric infants and children. *Medical Anthropology* 2(1), 1–59.

Menzel, H.J., 1968. Einige uberlegungen zur atiologie der statischen knochenholen. *Deutsche Zahnaerrtliche Zietschrift* 23, 58–64.

Merbs, C.F., 1968. Anterior tooth loss in Arctic populations. *Southwestern Journal of Anthropology* 24(1), 20–32.

Merbs, C.F., 1983. *Patterns of Activity Induced Pathology in a Candian Inuit Population.* (Archaeological Survey of Canada Paper No. 119). Ottawa: University of Ottawa Press.

Mercieca-Spiteri, B., 2016. Re-examining the prehistoric human remains from the Xaghra Circle. *Tesserae* 3, 58–67.

Mercieca-Spiteri, B., 2020. Burial practices and human remains: a study of the Maltese Islands. *Tesserae* 10, 12-9.

Meyer, C., C. Knipper, N. Nicklisch, A. Münster, O. Kürbis, *et al*., 2018. Early Neolithic executions indicated by clustered cranial trauma in the mass grave of Halberstadt. *Nature Communications* 9(1), 1–11.

Meyer, C., C. Lohr, D. Gronenborn & K.W. Alt, 2015. The massacre mass grave of Schöneck-Kilianstädten reveals new insights into collective violence in Early Neolithic Central Europe. *Proceedings of the National Academy of Sciences of the United States of America* 112(36), 11217–22.

Meyer, C., N. Nicklisch, P. Held, B. Fritsch & K.W. Alt, 2011. Tracing patterns of activity in the human skeleton: An overview of methods, problems, and limits of interpretation. *HOMO* 62(3), 202–17.

Mickleburgh, H.L. & D.J. Wescott, 2018. Controlled experimental observations on joint disarticulation and bone displacement of a human body in an open pit: Implications for funerary archaeology. *Journal of Archaeological Science: Reports* 20, 158–67.

Mifsud, A. & S. Mifsud, 1999. The subterranean sanctuary at Ħal-Saflieni, in *Facets of Maltese Prehistory*, eds. A. Mifsud & C. Savona Ventura. Malta: Prehistoric Society of Malta, 149–68.

Miller, J., 2008. Dental health and disease in ancient Egypt, in *Egyptian Mummies and Modern Science*, ed. A.R. David. Cambridge: Cambridge University Press, 52–70.

Miller, L.G., S.J. Eells, M.Z. David, N. Ortiz, A.R. Taylor, *et al*., 2015. Staphylococcus aureus skin infection recurrences among household members: An examination of host, behavioral, and pathogen-level predictors. *Clinical Infectious Diseases* 60(5), 753–63.

Miller, R.L., N. De Jonge, F.W. Krijger & A.M. Deelder, 1993. Predynastic schistosomiasis, in *Biological Anthropology and the Study of Ancient Egypt*, eds. W.V. Davies & R. Walker. London: British Museum Press, 55–60.

Milner, G.R., 2017. Out of regard to custom: Tooth modification in the ancient and modern worlds, in *A World View of BioCulturally Modified Teeth*, eds. S.E. Burnett & J.D. Irish. Gainesville (FL): University Press Florida, 317–30.

Milner, G.R., E. Anderson & V.G. Smith, 1991. Warfare in late prehistoric west-central Illinois. *American Antiquity* 56(4), 581–603.

Milner, G.R., D.A. Humpf & H.C. Harpending, 1989. Pattern matching of age-at-death distributions in paleodemographic analysis. *American Journal of Physical Anthropology* 80(1), 49–58.

Milner, G.R. & C.S. Larsen, 1991. Teeth as artifacts of human behaviour: Intentional mutilation and accidental modification, in *Advances in Dental Anthropology*, eds. M.A. Kelley & C.S. Larsen. New York (NY): Wiley-Liss, 357–78.

Minozzi, S., G. Manzi, F. Ricci, S. di Lernia & S.M. Borgognini Tarli, 2003. Nonalimentary tooth use in prehistory: An example from early Holocene in Central Sahara (Uan Muhaggiag, Tadrart Acacus, Libya). *American Journal of Physical Anthropology* 120(3), 225–32.

Mitchell, P. & M. Brickley, 2018. *Updated Guidelines to the Standards for Recording Human Remains.* Chartered Institute for Archaeologists and British Association for Biological Anthropology and Osteoarchaeology.

Mitchell, P.D. & A.R. Millard 2009. Migration to the Medieval Middle East with the Crusades. *American Journal of Physical Anthropology* 140(3), 518–25.

Møller-Christensen, V., 1961. *Bone Changes in Leprosy*. Copenhagen: Munksgaard.

Molleson, T.I., 1993. The human remains, in *Excavations at Poundbury 1966–1980. Volume II: The Cemeteries*, eds. D.E. Farwell & T.I. Molleson. Dorchester: Dorset Natural History & Archaeology Society Monograph Series 11, 142–214.

Molleson, T.I., 1994. The eloquent bones of Abu Hureyra. *Scientific American* 271(2), 70–5.

Molleson, T.I., 2006. The third hand: Neolithic basket makers of Abu Hureyra, in *Current Trends in Dental Morphology Research. Proceedings of the 13th International Symposium on Dental Morphology*, ed. E. Żadińska. Łódź: University of Łódź Press, 233–43.

Molleson, T.I., M. Cox, A. Waldron & D. Whittaker, 1993. *The Spitalfields Project. Volume 2: The Anthropology – The Middling Sort*. York: Council for British Archaeology Research Report No. 86.

Molnar, P., 2008, Dental wear and oral pathology: Possible evidence and consequences of habitual use of teeth in a Swedish Neolithic sample. *American Journal of Physical Anthropology* 136(4), 423–31.

Molnar, P., 2011. Extramasticatory dental wear reflecting habitual behavior and health in past populations. *Clinical Oral Investigations* 15(5), 681–9.

Molnar, S., 1971. Human tooth wear, tooth function and cultural variability. *American Journal of Physical Anthropology* 34(2), 175–90.

Molnar, S., 1972. Tooth wear and culture: A survey of tooth functions among some prehistoric populations. *Current Anthropology* 13(5), 511–26.

Montandon, G., 1934. *L'Ologénèse Culturelle: Traité d'Ethnologie Cyclo-Culturelle et d'Ergologie Systématique*. Paris: Payot.

Montgomery, J. 2002. 'Lead and strontium isotope compositions of human dental tissues as an indicator of ancient exposure and population dynamics.' Unpublished Phd, University of Bradford.

Moore, J. & E. Scott, 1997. *Invisible People and Processes: Writing Gender and Childhood into European Archaeology*. London: Leicester University Press.

Moore, S., 1953. The Troell-Junet syndrome. *Acta Radiologica* 39(6), 485–93.

Moore, S., 1955. *Hyperostosis Cranii*. Springfield (IL): Charles C. Thomas.

Moorrees, C.F.A., 1957. *The Aleut Dentition.* Cambridge (MA): Harvard University Press.

Morel, A., J. Hamon, A. Lim, D. Brézulier, V. Fau & O. Sorel, 2018. Tooth autotransplantation: A neglected approach*? Journal of Dentofacial Anomalies and Orthodontics* 21(2), 209–19.

Morel, F., 1929. *L'hyperostose Frontale Interne*. Geneva: Chapalay and Mottier.

Morgagni, B.G., 1719. *Adversaria Anatomica Omnia*. Padua: Patavii Cominus.

Morgan, J., 2011. 'Observable Stages and Scheduling for Alveolar Remodelling Following Antemortem Tooth Loss.' Unpublished PhD, Universitätsbibliothek Mainz.

Morita, W., S. Kusaka, W. Yano & M. Nakatsukasa. 2012. Dental metric variability associated with human migration from skeletal remains of two Jomon sites (Yoshigo and Inariyama) in the Atsumi Peninsula area. *Anthropological Science* 120(2), 167–77.

Morris DH., 1965. 'The Anthropological Utility of Dental Morphology.' Unpublished PhD, University of Arizona.

Morris, J.M. & L. Blickenstaff, 1967. *Fatigue Fractures: A Clinical Study*. Springfield (IL): Charles C. Thomas.

Morse, D., 1969. *Ancient Disease in the Midwest*. Chicago (IL): Illinois State Museum.

Morter, J., 2010. *The Chora of Croton 1: The Neolithic Settlement at Capo Alfiere*. Austin (TX): University of Texas Press.

Mosha, T.C.E., H.S. Laswai & I. Tetens, 2000. Nutritional composition and micronutrient status of home made and commercial weaning foods consumed in Tanzania. *Plant Foods for Human Nutrition* 55(3), 185–205.

Moss, M.L. & L. Moss-Salentijn, 1977. Analysis of developmental processes possibly related to human sexual dimorphism in permanent and deciduous canines. *American Journal of Physical Anthropology* 46(3), 407–14.

Moule, A.J. & B. Kahler, 1999. Diagnosis and management of teeth with vertical root fractures. *Australian Dental Journal* 44(2), 75–87.

Moutafi, I. & S. Voutsaki, 2016. Commingled burials and shifting notions of the self at the onset of the Mycenaean era (1700–1500 BCE): The case of the Ayios Vasilios North Cemetery, Laconia. *Journal of Archaeological Science: Reports* 10, 780–90.

Mower, J.P., 1999. Deliberate ante-mortem dental modification and its implications in archaeology, ethnography and anthropology. *Papers from the Institute of Archaeology* 10, 37–53.

Moynihan, P., 2003. Diet and dental caries, in *The Prevention of Oral Disease*, eds. J. J. Murray, J. H. Nunn & J.G. Steele. Oxford: Oxford University Press, 9–34.

Mubarak, S.J., R.N. Gould, Y.U. Fon Lee, D.A. Schmidt & A.R. Hargens, 1982. The medial tibial stress syndrome: A cause of shin splints. *American Journal of Sports Medicine* 10(4), 201–5.

Muldner, G., C. Chenery & H. Eckardt 2011. The 'headless Romans': multi-isotope investigations of an unusual burial ground from Roman Britain. *Journal of Archaeological Science* 38, 280–90.

Munjal, K., S. Kishan & S. Sabharwal, 2004. Post-traumatic pediatric distal tibiofibular synostosis: A case report. *Foot & Ankle International* 25(6), 429–33.

Muntoni, I.M., 2001. Dalla distribuzione spaziale e funzionale delle struttre all'organizzazione sociale del gruppo: Riflessioni sull'abitato e sulla necropolis di Casale del Dolce, in *Atti della XL Riunione Scientifica*. Florence: Istituto Italiano di Preistoria e Protostoria, 397–410.

Murphy, T., 1959a. Gradients of dentine exposure in human molar tooth attrition. *American Journal of Physical Anthropology* 17(3), 179–86.

Murphy, T., 1959b. The changing pattern of dentine exposure in human tooth attrition. *American Journal of Physical Anthropology* 17(3), 167–78.

Murray, C. & J. Frenk, 2002. Summary measures of population health in the context of the WHO framework for health system performance assessment, in *Summary Measures of Population Health: Concepts, Ethics, Measurement and Application,* eds. C.J. Murray, J.A. Salomon, C.D. Mathers & A.D. Lopex. Geneva: World Health Organization, 1–12.

Murray, J.J., A.J. Rugg-Gunn & G.N. Jenkins, 1991. *Fluorides in Caries Prevention*. Oxford: Wright.

Museum Department, 1904. *Museums Annual Report, 1904*. Valletta: Government of Malta.

Museum Department, 1910–11. *Museums Annual Report, 1910–1911*. Valletta: Government of Malta.

Museum Department, 1928–29. *Museums Annual Report, 1928–29*. Valletta: Government of Malta.

Museum Department, 1933–34. *Museums Annual Report, 1933–34.* Valletta: Government of Malta, xxiii–xxiv.

Museum Department, 1934–35. *Museums Annual Report, 1934–35.* Valletta: Government of Malta, xvii–xix.

Museum Department, 1936–37. *Museums Annual Report, 1936–37*. Valletta: Government of Malta, xvii–xxiii.

Museum Department, 1937–38. *Museums Annual Report, 1937–38.* Valletta: Government of Malta, 43–62.

Museum Department, 1949–50. *Museums Annual Report, 1949–50*. Valletta: Government of Malta.

Museum Department, 1973. *Museums Annual Report, 1973–4.* Valletta: Government of Malta.

Museum Department, 1987. *Museums Annual Report, 1987–8.* Valletta: Government of Malta.

Museum Department, 1989. *Museums Annual Report, 1989–90.* Valletta: Government of Malta.

Nafplioti, A., 2008. Mycenaean political domination of Knossos following the LMIB destructions on Crete: negative evidence from strontium isotope ratio analysis (87Sr/86Sr). *Journal of Archaeological Science* 35, 2307–17.

Nafplioti, A., 2009. Mycenae Revisited part 2. Exploring the local vs. non-local origin of the individuals from Grave Circle A at Mycenae: evidence from strontium isotope ratio (87Sr/86Sr) analysis. *Annual of the British School at Athens* 104, 279–91.

Nafplioti, A., 2011. Tracing population mobility in the Aegean using isotope geochemistry: a first map of local biologically available 87Sr/86Sr signatures. *Journal of Archaeological Science* 38, 1560–70.

Nafplioti, A., 2012. Late Minoan IB destructions and cultural upheaval on Crete: A bioarchaeological perspective, in *Population Dynamics in Prehistory and Early History: New Approaches using Stable Isotopes and Genetics*, eds. E. Kaizer, J. Burger & W. Schier, Berlin: De Gruyter, 241–64.

Nafplioti, A., 2021. Moving forward: Strontium isotope mobility research in the Aegean. *Mediterranean Archaeology and Archaeometry* 21(2), 165–79.

Nafplioti, A., 2022. Strontium isotope ratio research on residential mobility and provenance in Aegean Archaeology: A review. In the Proceedings of the 7th Symposium on Archaeometry: Archaeology – Archaeometry: 30 years later, 9–12/10/2019. Hellenic Society for Archaeometry.

Nafplioti, A., J. Driessen, A. Schmitt & I. Crevecoeur, 2021. Mobile (after-)lifeways: People at Pre- and Protopalatial Sissi (Crete). *Journal of Archaeological Science: Reports* 35, https://doi.org/10.1016/j.jasrep.2020.102718.

Natali, E. & V. Forgi, 2018. The beginning of the Neolithic in southern Italy and Sicily. *Quaternary International* 470(Part B), 253–69.

Neugarten, B.L. & G.O. Hagestad, 1977. Age and the life course, in *Handbook of Ageing and the Social Sciences*, eds. R.H. Binstock & E. Shanas. New York (NY): Van Nostrand Reinhold, 35–55.

Neuhauser, E.B.D., 1970. Infantile cortical hyperostosis and skull defects. *Postgraduate Medicine* 48(6), 57–9.

Newton, J. & K. Domett, 2017. The biocultural context of dental modification in prehistoric Southeast Asia, in *A World View of Bioculturally Modified Teeth*, eds. S.E. Burnett & J.D. Irish. Gainesville (FL): University Press of Florida, 159–81.

Nichol, C.R., 1990. 'Dental Genetics and Biological Relationships of the Pima Indians of Arizona.' Unpublished PhD, Arizona State University.

Nicholls, S.C., 2005. Sequelae of untreated venous insufficiency. *Seminars in Interventional Radiology* 22(3), 162–8.

NIH, 2020. Vitamin C – Fact sheet for health professionals. Available at: https://ods.od.nih.gov/factsheets/VitaminC-HealthProfessional/

Niinimäki, S., 2012. The relationship between musculoskeletal stress markers and biomechanical properties of the humeral diaphysis. *American Journal of Physical Anthropology* 147(4), 618–28.

Nimčenko, T., G. Omerca, V. Varinauskas, E. Bramanti & F. Signorino, 2013. Tooth auto-transplantation as an alternative treatment option: A literature review. *Dental Research Journal* 10(1), 1–6.

Nishijima, D., M. Tomosawa & S. Ohashi, 1969. So-called latent bone cyst: A case report. *Japanese Journal of Oral and Maxillofacial Surgery* 15(3), 205–8.

Niskanen, M., C.B. Ruff, C., J.H. Medicine, & B.M. Holt, 2018. Temporal and geographic variation in body size and shape, in *Skeletal Variation and Adaptation in Europeans: Upper Paleolithic to the Twentieth Century,* ed. C.B. Ruff. London: Wiley-Blackwell, 49–89.

Noman, A.V., F. Wong & R. Ramakrishna Pawar, 2015. Canine gouging: A taboo resurfacing in a migrant urban population. *Case Reports in Dentistry*, 727286.

Northway, W.M. & S. Konigsberg, 1980. Autogenic tooth transplantation. The 'state of the art'. *American Journal of Orthodontics* 77(2), 146–62.

Norton, L., R.M. Gibson, T. Gofton, C. Benson, S. Dhanani, *et al*., 2017. Electroencephalographic recordings during withdrawal of life-sustaining therapy until 30 minutes after declaration of death. *Canadian Journal of Neurological Sciences* 44(2), 139–45.

Novak, S.A., 2000. Battle-related trauma, in *Blood Red Roses: The Archaeology of a Mass Grave from Towton, AD 1461*, eds. V. Fiorato, A. Boylston & C. Knüsel. Oxford: Oxbow Books, 90–102.

Novotny, A., 2008. 2008 bioarchaeological analysis, in *The Chan Project: 2008 Season,* ed. C. Robin. Belmopan, Belize Institute of Archaeology, 84–107.

Nunn, J.F., 1996. *Ancient Egyptian Medicine*. London: British Museum Press.

Nystrom, K.C. & L. Tilley, 2019. Mummy studies and the bioarchaeology of care. *International Journal of Paleopathology* 25, 64–71.

O'Dwyer, K.J., 1991. Proximal tibio-fibular synostosis: A rare congenital anomaly. *Acta Orthopaedica Belgica* 57(2), 204–8.

Ogundare, B.O., A. Bonnick & N. Bayley, 2003. Pattern of mandibular fractures in an urban major trauma center. *Journal of Oral and Maxillofacial Surgery* 61(6), 713–18.

Oikarinen, V.J. & M. Julku, 1974. An orthopantomorgraphic study of developmental mandibular bone defects (Stafne's idiopathic bone cavities). *International Journal of Oral Surgery* 3(2), 71–6.

Okonechnikov, K., A. Conesa & F. García-Alcalde, 2016. Qualimap 2: advanced multi-sample quality control for high-throughput sequencing data. *Bioinformatics* 32(2), 292–4.

Olalde, I., M.E. Allentoft, F. Sánchez-Quinto, G. Santpere, C.W.K. Chiang, *et al*., 2014. Derived immune and ancestral pigmentation alleles in a 7,000-year-old Mesolithic European. *Nature* 507, 225–8.

Olalde, I., S. Brace, M.E. Allentoft, I. Armit, K. Kristiansen, *et al*., 2018. The Beaker phenomenon and the genomic transformation of northwest Europe. *Nature* 555, 190–6.

Olalde, I., H. Schroeder, M. Sandoval-Velasco, L. Vinner, I. Lobón, *et al*., 2015. A common genetic origin for early farmers from Mediterranean Cardial and Central European LBK cultures. *Molecular Biology and Evolution* 32(12), 3132–42.

Olech, E. & B.K. Arora, 1961. Lingual mandibular bone cavity. *Oral Surgery, Oral Medicine, Oral Pathology* 14, 1360–6.

Oritz, A., E.C. Torres Pino & E. Orellana González, 2016. First evidence of pre-Hispanic dentistry in South America: Insights from Cusco, Peru. *HOMO* 67(2), 100–9.

Ortner, D.J., 1966. A recent occurrence of an African type tooth mutilation in Florida. *American Journal of Physical Anthropology* 25(2), 177–80.

Ortner D.J., 2003. *Identification of Pathological Conditions in Human Skeletal Remains*. New York (NY): Academic Press.

Ortner, D.J., W. Butler, J. Cafarella & L. Milligan, 2001. Evidence of probable scurvy in subadults from archeological sites in North America. *American Journal of Physical Anthropology* 114(4), 343–51.

Ortner, D.J. & M.F. Ericksen, 1997. Bone changes in the human skull probably resulting from scurvy in infancy and childhood. *International Journal of Osteoarchaeology* 7(3), 212–20.

Ortner, D.J., E.H. Kimmerle & M. Diez, 1999. Probable evidence of scurvy in subadults from archeological sites in Peru. *American Journal of Physical Anthropology* 108(3), 321–31.

Orwoll, E.S., 1991. The effects of dietary protein insufficiency and excess on skeletal health, in *Nutritional Aspects of Osteoporosis*, eds. P. Burkhardt & R.P. Heaney. New York (NY): Raven, 355–70.

Osterholtz, A.J., K.M. Baustian & D. Martin, 2014. *Commingled and Disarticulated Human Remains: Working Toward Improved Theory, Method and Data*. London: Springer.

Osterholtz, A.J., K.M. Baustian, D. Martin & D.T. Potts, 2014. Commingled human skeletal assemblages: Integrative techniques in determination of the MNI/ MNE, in *Commingled and Disarticulated Human Remains: Working Toward Improved Theory, Method and Data*, eds. A.J. Osterholtz, K.M. Baustian, & D.L. Martin. London: Springer, 35–50.

Owsley, D.W. & R.S. Webb, 1983. Misclassification probability of dental discrimination functions for sex determination. *Journal of Forensic Sciences* 28(1), 181–5.

Oxenham, M.F. & I. Cavill, 2010. Porotic hyperostosis and cribra orbitalia: The erythropoietic response to iron-deficiency anaemia. *Anthropological Science* 118(3), 199–200.

Oya, S., S.H. Kim, B. Sade & J.H. Lee, 2011. The natural history of intracranial meningiomas. *Journal of Neurosurgery* 114(5), 1250–6.

Outram, A.K., 2001. A new approach to identifying bone marrow and grease exploitation: Why the 'indeterminate' fragments should not be ignored. *Journal of Archaeological Science* 28, 401–10.

Oxilia, G., F. Fiorillo, F. Boschin, E. Boaretto, S.A. Apicella, *et al*., 2017. The dawn of dentistry in the late Upper Paleolithic: An early case of pathological intervention at Riparo Fredian. *American Journal of Physical Anthropology* 163(3), 446–61.

Oxilia, G., M. Peresani, M. Romandini, C. Matteucci, C. Debono Spiteri, *et al*., 2015. Earliest evidence of dental caries manipulation in the late Upper Palaeolithic. *Scientific Reports* 5, 1–10.

Pääbo, S., 1985. Molecular cloning of Ancient Egyptian mummy DNA. *Nature* 314, 644–5.

Pace, A.,1990. 'Temple Period Mortuary Remains and Their Potential for Indicating Individual Ranking and Group Differentiation.' Unpublished BA dissertation, University of Malta.

Pace, A. 1992. 'The Development of Megalithic Structures, Mortuary Facilities and Site Location Patterning During the Maltese Late Neolithic and Early Bronze Age. Some Reconsiderations.' Unpublished MPhil, University of Cambridge.

Pace, A., 1996a. *Maltese Prehistoric Art, 5000–2500 BC*. Valletta: Fondazzjoni Patrimonju Malti.

Pace, A., 1996b. The artistic legacy of small island communities: The case of the Maltese Islands (5000–2500 BC), in *Maltese Prehistoric Art 5000–2500 BC,* ed. A. Pace. Valletta: Fondazzjoni Patrimonju Malti, 1–12.

Pace, A. 1997. The Archaeology of Collectivity. *Malta Archaeological Review* 2, 14–9

Pace, A., 2000. The prehistoric Hypogeum at Ħal Saflieni, in *The Ħal Saflieni Hypogeum 4000 BC–2000 AD*, ed. A. Pace. Malta: Nation Museum of Archaeology, 5–22.

Pace, A., 2004a. *The Ħal Saflieni Hypogeum, Paola*. Malta: Heritage Books.

Pace, A., 2004b. The sites, in *Malta Before History*, ed. D. Cilia. Malta: Miranda Publishers, 42–200.

Pace, A., 2006. The emergence of Maltese ritual funerary monuments between 4000–2500 BC, in *First International Conference of the SIEF Working Group on The Ritual Year (Proceedings 2005),* ed. G. Mifsud-Chircop. Malta: Malta University & Publishers Enterprises Group, 135–63.

Pace, A., 2010. Malta, in *The Routledge Handbook of Archaeological Human Remains and Legislation. An International Guide to Laws and Practice in the Excavation and Treatment of Archaeological Human Remains*, eds. N. Márquez-Grant & L. Fibiger, New York: Routledge, 275-85.

Pace, J.L., 1972. *The Anatomical Features of Prehistoric Man in Malta.* Malta: University of Malta.

Pace, J.L. & S. Ramaswamy, 1990. Skeletal remains, in *Excavations at Ħal Millieri, Malta. A Report on the 1977 Campaign Conducted on behalf of the National Museum of Malta and the University of Malta*, eds. T.F.C. Blagg, A. Bonanno & A.T. Luttrell. Msida: Malta University Press, 84–95.

Pacey, L., 2012. Mouth used as third hand by cavemen. *British Dental Journal* 213(7), 336.

Padayatty, S.J., & M. Levine, 2016. Vitamin C: the known and the unknown and Goldilocks. *Oral Diseases* 22, 463–93.

Paine, R.R., 1989. Model life table fitting by maximum likelihood estimation: A procedure to reconstruct paleodemographic characteristics from skeletal age distributions. *American Journal of Physical Anthropology* 79(1), 51–61.

Papathanasiou, A., 2012. Evidence of trauma in Neolithic Greece, in *Sticks, Stones, and Broken Bones: Neolithic Violence in a European Perspective*, eds. R.J. Schulting & L. Fibiger. Oxford: Oxford University Press, 249–63.

Papathanasiou, A., C. Spencer Larsen & L. Norr, 2000. Bioarchaeological inferences from a Neolithic ossuary from Alepotrypa Cave, Diros, Greece. *International Journal of Osteoarchaeology* 10(3), 210–28.

Pardoe, C. & A.C. Durband, 2017. Tooth ablation along the Murray River in Southeastern Australia, in *A World View of Bioculturally Modified Teeth*, eds. S.E. Burnett & J.D. Irish. Gainesville (FL): University Press of Florida, 211–25.

Park, S.J., H. Sung Kim, H. Sook Kim & S.W. Kim, 2015. Complete separation of the vertebral body associated with a Schmorl's node accompanying severe osteoporosis. *Journal of Korean Neurosurgical Society* 58(2), 147–9.

Parker Pearson, M. & Ramilisonina, 1998. Stonehenge for the ancestors: The stones pass on the message. *Antiquity* 72(276), 308–26.

Parkin, I., B.M. Logan & M.J. McCarthy, 2007. *Core Anatomy Illustrated*. London: Hodder Arnold.

Parkinson, E., 2014. 'Joint Articulation in Resolving Commingled Human Remains: Osteometric Analysis of the Acetabulo-femoral and Tibio-femoral Articular Surface Areas.' MSc thesis, University of Sheffield.

Parkinson, E., 2019. 'Body size, skeletal biomechanics and habitual behaviour: a bioarchaeological approach to social and economic change in the Neolithic and Copper Age central Mediterranean'. Unpublished Phd, University of Cambridge . https://doi.org/10.17863/CAM.48812

Parkinson, E., R. McLaughlin, C. Malone, S. Stoddart, J. Stock, *et al*., 2015. The Brochtorff-Xagħra Circle digitising project. *BABAO Annual Conference 2015 Poster*.

Parkinson, E., J.T. Stock, S. Stoddart, M. Miari, F. Bertoldi & F. Bestetti, 2018. Mobility in Copper Age northern Italy: Biomechanical analysis of the femora and tibiae from the Copper Age necropolis of Forlì-Celletta. *PAST* 89, 2–5.

Patterson, K.D., 1993. Meningitis, in *The Cambridge World History of Human Disease*, ed. K. Kiple. Cambridge: Cambridge University Press, 875–80.

Patterson, N., P. Moorjani, Y. Luo, S. Mallick, N. Rohland, *et al*., 2012. Ancient admixture in human history. *Genetics* 192(3), 1065–93.

Patterson, N., A.L. Price & D. Reich, 2006. Population structure and eigenanalysis. *PLoS Genetics* 2(12), e190.

Pavone, B.W., 1985. Bruxism and its effect on the natural teeth. *Journal of Prosthetic Dentistry* 53(5), 692–706.

Pearson, K., 1917–1919. *A Study of the Long Bones of the English Skeleton I: The Femur*. London: Cambridge University Press.

Pearson, O.M. & D.E. Lieberman, 2004. The aging of Wolff's 'law': Ontogeny and responses to mechanical loading in cortical bone. *American Journal of Physical Anthropology* 125(S39), 63–99.

Peck, L., S. Peck & Y. Attiya, 1993. Maxillary canine-first premolar transposition, associated dental anomalies and genetic basis. *Angle Orthodontist* 63(2), 99–110.

Peck, S. & L. Peck, 1995. Classification of maxillary tooth transpositions. *American Journal of Orthodontics and Dentofacial Orthopedics* 107(5), 505–17.

Peck, S., L. Peck & M. Kataja, 1998. Mandibular lateral incisor-canine transposition, concomitant dental anomalies, and genetic control. *Angle Orthodontist* 68(5), 455–66.

Pedersen, P.O., 1949. The East Greenland Eskimo dentition. *Meddelelser om Grønland* 142(3), 1–244.

Pedley, M., M. Hughes Clarke & P. Galea 2002. *Limestone isles in a crystal sea: the geology of the Maltese Islands.* Malta: Publishers Enterprises Group.

Perino, G., 1967. Additional discoveries of filed teeth in the Cahokia area. *American Antiquity* 32(4), 538–42.

Pernter, P., P. Gostner, E.E. Vigl & F.J. Rühli, 2007. Radiologic proof for the Iceman's cause of death (ca. 5'300 BP). *Journal of Archaeological Science* 34(11), 1784–6.

Perry, M.A., 2005. Redefining childhood through bioarchaeology: Toward an archaeological and biological understanding of children in antiquity. *Archaeological Papers of the American Anthropological Association* 15(1), 89–111.

Pessina, A. & N. Vella, 1934 (2012). Introduction, in *Malta. Origini della Civiltà Mediterranea. Origins of Mediterranean Civilisation. A Re-edition with a Foreword and an Introduction by Andrea Pessina and Nicholas C. Vella. Translation of the edition of 1934 by Louis J. Scerri*. Valletta: Midsea Books. xi–xxx.

Peter, T., S. Titus, G. Francis, M.M. Alani & A.J. George, 2013. Ornamental dentistry: An overview. *Journal of Evolution of Medical and Dental Sciences* 2(7), 666–76.

Peterson, S.N., E. Snesrud, N.J. Schork & W.A. Bretz, 2011. Dental caries pathogenicity: A genomic and metagenomic perspective. *International Dental Journal* 61(0 1), 11–22.

Pettifor, J.M., 2004. Nutritional rickets: deficiency of vitamin D, calcium, or both? *American Journal of Clinical Nutrition* 80(6), 1725S-1729S.

Pfeiffer, D., 2001. The conceptualization of disability, in *Exploring Theories and Expanding Methodologies: Where We Are and Where We Need to Go* (Vol. 2), eds. S.N. Barnartt & B.M. Altman. Bingley: Emerald Group Publishing Limited, 29–52.

Philipsen, H., T. Takata, P. Reichart, S. Sato & Y. Suei, 2002. Lingual and buccal mandibular bone depressions: A review based on 583 cases from a world-wide literature survey, including 69 new cases from Japan. *Dentomaxillofacial Radiology* 31(5), 281–90.

Pietrokovski, J. & M. Massler, 1967. Alveolar ridge resorption following tooth extraction. *Journal of Prosthetic Dentistry* 17(1), 21–7.

Pietrusewsky, M. & M.T. Douglas, 2001. Intensification of agriculture at Ban Chiang: Is there evidence from the skeletons? *Asian Perspectives* 40(2), 157–78.

Pietrusewsky, M., A. Lauer, C.-H. Tsang, K.-T. Li & M.T. Douglas, 2017. Tooth ablation in early Neolithic skeletons from Taiwan, in *A World View of Bioculturally Modified Teeth,* eds. S.E. Burnett & J.D. Irish. Gainesville (FL): University Press of Florida, 102–24.

Pike, G., 1971. The human bones from the Xemxija tombs, in *The Prehistoric Antiquities of the Maltese Islands: A Survey*, ed. J. Evans. London: Athlone Press, 236–8.

Pinchi, V., P. Barbieri, F. Pradella, M. Focardi, V. Bartolini & G.-A. Norelli, 2015. Dental ritual mutilations and forensic odontologist practice: A review of the literature. *Acta Stomatologica Croatica* 49(1), 3–13.

Pindborg, J.J., 1969. Dental mutilation and associated abnormalities in Uganda. *American Journal of Physical Anthropology* 31(3), 383–90.

Pindborg J., 1970. *Pathology of the Dental Hard Tissues*. Philadelphia (PA): Saunders.

Pineda, C.J., M. Martinez-Lavin., J.E. Goobar, D.J. Sartoris, P. Clopton & D. Resnick, 1987. Periostitis in hypertrophic osteoarthropathy: Relationship to disease duration. *American Journal of Roentgenology* 148(4), 773–8.

Pinhasi, R., V. Eshed & P. Shaw, 2008. Evolutionary changes in the masticatory complex following the transition to farming in the southern Levant. *American Journal of Physical Anthropology* 135(2), 136–48.

Pittman, T.S. & K.R. Zeigler, 2007. Basic human needs, in *Social Psychology: Handbook of Basic Principles*, eds. A.W. Kruglanski & E.T. Higgins. New York (NY): The Guilford Press, 473–89.

Plavcan, J.M., V. Meyer, A.S. Hammond, C. Couture, S. Madelaine, *et al*., 2014a. The Regourdou 1 Neandertal body size. *Comptes Rendus – Palevol* 13(8), 747–54.

Plavcan, J.M., A.S. Hammond & C.V. Ward, 2014b. Brief communication: Calculating hominin and nonhuman anthropoid femoral head diameter from acetabular size. *American Journal of Physical Anthropology* 155(3), 469–75.

Plunket, D.J., P.S. Dysart, T.B. Kardos & G.P. Herbison, 1998. A study of transposed canines in a sample of orthodontic patients. *British Journal of Orthodontics* 25(3), 203–8.

Pol, L.G. & R.K. Thomas, 2001. *The Demography of Health and Health Care* (2nd edition). New York (NY): Kluwer Academic Publishers.

Pollard, A.M., M. Pellegrini & J.A. Lee-Thorp, 2011. Technical Note: Some observations on the conversion of dental enamel $\delta^{18}O_p$ values to $\delta^{18}O_w$ to determine human mobility. *American Journal of Physical Anthropology* 145(3), 499–504.

Pomeroy, E., 2013. Biomechanical insights into activity and long distance trade in the south-central Andes (AD 500–1450). *Journal of Archaeological Science* 40(8), 3129–40.

Pomeroy, E., A.A. Macintosh, J.C.K. Wells, T. Cole & J.T. Stock, 2018. Relationship between body mass, lean mass, fat mass, and limb bone cross-sectional geometry: implications for estimating body mass and physique from the skeleton. *American Journal of Physical Anthropology* 166(1), 56–69.

Popovich, D., A. McAlhany, A.O. Adewumi & M.M. Barnes, 2009. Scurvy: Forgotten but definitely not gone. *Journal of Pediatric Health Care* 23(6), 405–15.

Powell L., W. Southwell-Wright & R. Gowland, 2017. *Care in the Past: Archaeological and Interdisciplinary Perspectives*. Oxford: Oxbow Books.

Power, R.K., 2008. 'Differential Child and Infant Mortality and Morbidity in Late Anglo-Saxon England (10th–12th Centuries AD).' Unpublished M.A., University of Bradford.

Power, R.K., 2012. 'From the Cradle to the Grave: Child, Infant and Foetal Burials in the Egyptian Archaeological Record from the Early Dynastic Period to the Middle Kingdom (ca. 3300–1650 BC).' Unpublished PhD, Macquarie University.

Power, R.K. & Y. Tristant, 2016. From refuse to rebirth: Repositioning the 'pot burial' in the Egyptian archaeological record. *Antiquity* 90(354), 1474–88.

Pozhitkov, A.E., R. Neme, T. Domazet-Lošo, B.G. Leroux, S. Soni, *et al*., 2017. Tracing the dynamics of gene transcripts after organismal death. *Open Biology* 7(1), 160267.

Press, I. & M. McCool. 1972. Social structure and status of the aged. Towards some valid cross-cultural generalizations. *Aging and Human Development* 3(4), 297–306.

Price, T.D., 2009. Europe's first farmers: An introduction, in *Europe's First Farmers,* ed. T.D. Price. Cambridge: Cambridge University Press, 1–18.

Price, T.D., J.H. Burton & R.A. Bentley, 2002. The characterization of biologically available strontium isotope ratios for the study of prehistoric migration. *Archaeometry* 44, 117–35.

Price, T.D., J.H. Burton, A. Cucina, P. Zabala, R. Frei, *et al*., 2012. Isotopic studies of human skeletal remains from a sixteenth to seventeenth century AD churchyard in Campeche, Mexico: Diet, place of origin and age. *Current Anthropology* 53(4), 396–433.

Price, T.D., V. Tiesler & J.H. Burton, 2006. Early African diaspora in colonial Campeche, Mexico: Strontium isotopic evidence. *American Journal of Physical Anthropology* 130(4), 485–90.

Pryor, A.J.E., R.E. Stevens, T.C. O'Connell & J.R. Lister, 2014. Quantification and propagation of errors when converting vertebrate biomineral oxygen isotope data to temperature for palaeoclimate reconstruction. *Palaeogeography Palaeoclimatology Palaeoecology* 412, 99–107.

Pugliesi da Costa Feliciano, K.M. & A. de França Caldas, Jr., 2006. A systematic review of the diagnostic classifications of traumatic dental injuries. *Dental Traumatology* 22(2), 71–6.

Purkait, R., 2001. Measurements of ulna – A new method for determination of sex. *Journal of Forensic Sciences* 46(4), 891–4.

Queiroz, L.M., R.S. Rocha, K.B. de Medeiros, E.J. da Silveira & R.D. Lins, 2004. Anterior bilateral presentation of Stafne defect: An unusual case report. *Journal of Oral and Maxillofacial Surgery* 62(5), 613–15.

Quesada-Gómez, C., E.V. Castellón, L.B. Aytés, & C.G. Escoda, 2006. Stafne bone cavity: A retrospective study of 11 cases. *Medicina Oral, Patología Oral y Cirugía Bucal* 11(3), E277–80.

R Core Team, 2013. R: *A language and environment for statistical computing*.

Radini, A., 2016. 'Particles of Everyday Life: Past Diet and Living Conditions as Evidenced by Micro-debris Entrapped in Human Dental Calculus. A Case Study from Medieval Leicester and Surrounding.' Unpublished PhD, University of York.

Rafferty, K.L. & C.B. Ruff, 1994. Articular structure and function in Hylobates, Colobus, and Papio. *American Journal of Physical Anthropology* 94(3), 395–408.

Ralf, A., D. Montiel González, K. Zhong & M. Kayser, 2018. Yleaf: Software for Human Y-Chromosomal Haplogroup Inference from Next-Generation Sequencing Data. *Molecular Biology and Evolution* 35(5), 1291–4

Raghavan, V. & C. Singh, 2015. Hypercementosis: Review of the literature and report of a case of mammoth, dumbbell-shaped hypercementosis. *Journal of Indian Academy of Oral Medicine & Radiology* 27(1), 160–3.

Raghavan, M., P. Skoglund, K.E. Graf, M. Metspalu, A. Albrechtsen, *et al*., 2014. Upper Palaeolithic Siberian genome reveals dual ancestry of Native Americans. *Nature* 505, 87–91.

Raikos, A., G.K. Paraskevas, F. Yusuf, P. Kordali, S. Meditskou, *et al*., 2011. Etiopathogenesis of hyperostosis frontalis interna: A mystery still. *Annals of Anatomy* 193(5), 453–8.

Ramaswamy, S. & J.L. Pace, 1979. The medieval skeletal remains from St. Gregory's Church at Zejtun (Malta) Part I. Paleopathological studies. *Archivio Italiano di Anatomia e di Embriologia* 84(1), 43–53.

Ramaswamy, S. & J.L. Pace, 1980. The medieval skeletal remains from St. Gregory's Church at Zejtun (Malta) Part II. Anthropological studies. *Archivio Italiano di Anatomia e di Embriologia* 85(1), 55–69.

Ramchandren, S. & D.S. Liebeskind, 2007. Headache in a patient with Klinefelter's syndrome and hyperostosis frontalis interna. *Journal of Headache and Pain* 8(6), 342–4.

Rangel Goulart, D., L. do Amaral Colombo, M. de Moraes & L. Asprino, 2014. What is expected from a facial trauma caused by violence? *Journal of Oral and Maxillofacial Research* 5(4), e4.

Rasmussen, M., X. Guo, Y. Wang, K.E. Lohmueller, S. Rasmussen, *et al*., 2011. An Aboriginal Australian genome reveals separate human dispersals into Asia. *Science* 334(6052), 94–8.

Ratcliff, S., I.M. Becker & L. Quinn, 2001. Type and incidence of cracks in posterior teeth. *Journal of Prosthetic Dentistry* 86(2), 168–72.

Raymond, M. & D. Pontier, 2004. Is there geographical variation in human handedness? *Laterality* 9(1), 35–51.

Redfern, R.C., 2015. Identifying and interpreting domestic violence in archaeological human remains: A critical review of the evidence. *International Journal of Osteoarchaeology* 27(1), 13–34.

Redfern, R.C., D.R. Grocke, A.R. Millard, V. Ridgeway, L. Johnson & J.T. Hefner 2016. Going south of the river: A multidisciplinary analysis of ancestry, mobility and diet in a population from Roman Southwark, London. *Journal of Archeological Science* 74, 11–22.

Regezi, J.A., J.J. Sciubba & M.A. Pogrel, 2000. *Atlas of Oral and Maxillofacial Pathology*. Philadelphia (PA): W.B. Saunders Company.

Reich, D., K. Thangaraj, N. Patterson, A.L. Price & L. Singh, 2009. Reconstructing Indian population history. *Nature* 461, 489–94.

Reichart, P.A., U. Creutz & C. Scheifele, 2008. Dental mutilations and associated alveolar bone pathology in African skulls of the anthropological skull collection, Charité, Berlin. *Journal of Oral Pathological Medicine* 37(1), 50–5.

Reichs, K.J., 1986. *Forensic Osteology: Advances in the Identification of Human Remains*. Springfield (IL): Charles C. Thomas.

Reilly, P. & S. Rahtz, 1992. *Archaeology in the Information Age.* London: Routledge.

Reimer, P., E. Bard, A. Bayliss, J.W. Beck, P.G. Blackwell, *et al*., 2013. IntCal13 and Marine13 radiocarbon age calibration curves 0–50,000 years cal BP. *Radiocarbon* 55(4), 1869–87.

Reimer, P., S. Hooper, J. Mcdonald, R. Reimer, S. Svyatko & M. Thompson, 2015. *Laboratory Protocols Used for AMS Radiocarbon Dating at the 14CHRONO Centre.* Belfast: The Queen's University, Belfast and English Heritage.

Reinberger, K.L., L.J. Reitsema, B. Kyle, S. Vassallo, G. Kamenov & J. Krigbaum, 2021. Isotopic evidence for geographic heterogeneity in Ancient Greek military forces. *PLoS ONE* 16(5), e0248803.

Relethford, J., 2004. Global patterns of isolation by distance based on genetic and morphological data. *Human Biology* 76(4), 499–513.

Renfrew, C., 1973. *Before Civilisation: The Radiocarbon Revolution and Prehistory*. London: Jonathan Cape.

Renfrew, C. & E.V. Level, 1979. Exploring dominance: Predicting polities from centres, in *Transformations:*

Mathematical Approaches to Culture Change, eds. C. Renfrew & K.L. Cooke. New York (NY): Academic Press, 145–68.

Resnick, D. & G. Niwayama, 1988. *Diagnosis of Bone and Joint Disorders* (2nd edition). Philadelphia (PA): W.B. Saunders.

Rhind, A.H., 1856. Memoir on megalithic remains in Malta. *Archaeological Journal* 13, 397–400.

Richard, E.L. & J. Ziskind, 1957. Aberrant salivary gland tissue in mandible. *Oral Surgery, Oral Medicine, Oral Pathology* 10(10): 1086–90.

Richards, M., R. Hedges, I. Walton, S. Stoddart & C. Malone, 2001. Neolithic diet at the Brochtorff Circle, Malta. *European Journal of Archaeology* 4(2), 253–62.

Richards, R.R. & F.G. Corley, 1996. Fractures of the shafts of the radius and ulna, in *Rockwood and Green's Fractures in Adults*, eds. C.A. Rockwood, D.P. Green, R.W. Bucholz, & J.D. Heckman. New York (NY): Lippincott-Raven, 869–928.

Richards, T.A. & D. Nicole Deal, 2014. Distal ulna fractures. *Journal of Hand Surgery* 39(2), 385–91.

Richardson, M., 2001. *Online Musculoskeletal Radiology Book*. Available online: https://rad.washington.edu/about-us/academic-sections/musculoskeletal-radiology/teaching-materials/online-musculoskeletal-radiology-book/

Richerson, P.J., R. Boyd & J. Henrich, 2010. Gene-culture coevolution in the age of genomics. *Proceedings of the National Academy of Sciences of the United States of America* 107(S2), 8985–92.

Riley, M.W., 1984. Foreword, in *Age and Anthropological Theory*, eds. D.I. Kertzer & J. Keith. Ithaca (NY): Cornell University Press, 7–10.

Rivera, F. & M. Lahr, 2017. New evidence suggesting a dissociated etiology for cribra orbitalia and porotic hyperostosis. *American Journal of Physical Anthropology* 164(1), 76–96.

Robb, J., 1994. Burial and social reproduction in the Peninsular Italian Neolithic. *Journal of Mediterranean Archaeology* 7(1), 27–71.

Robb, J. 1997a. Intentional tooth removal in Neolithic Italian women. *Antiquity* 71(273), 659–69.

Robb, J., 1997b. Violence and gender in early Italy, in *Troubled Times: Violence and Warfare in the Past*, eds. D. Martin & D. Frayer. London: Gordon & Breach, 111–44.

Robb, J., 2001. Island identities: Ritual, travel and the creation of difference in Neolithic Malta. *European Journal of Archaeology* 4(2), 175–202.

Robb, J., 2007a. *The Early Mediterranean Village*. Cambridge: Cambridge University Press.

Robb, J., 2007b. Bodily treatment as transformations of bodily ideology, in *Performing Death: Social Analyses of Funerary Traditions in the Ancient Near East and Mediterranean*, ed. N. Laneri. Chicago (IL): The Oriental Institute, 287–97.

Robb, J., 2013. Creating death: An archaeology of dying, in *The Oxford Handbook of the Archaeology of Death and Burial*, eds. S. Tarlow & L. Nilsson Stutz. Oxford: Oxford University Press, 441–57.

Robb, J., 2016. What can we really say about skeletal part representation, MNI and funerary ritual? A simulation approach. *Journal of Archaeological Science: Reports* 10, 684–92.

Robb, J., E.S. Elster, E. Isetti, C. J. Knüsel, M.A. Tafuri & A. Traverso, 2015. Cleaning the dead: Neolithic ritual processing of human bone at Scaloria Cave, Italy. *Antiquity* 89(343), 39–54.

Robb, J. & H. Farr, 2005. Substances in motion: Neolithic Mediterranean 'trade', in *The Archaeology of Mediterranean Prehistory*, eds. E. Blake & B. Knapp. Oxford: Blackwell Publishing Ltd., 24–45.

Robb, J. & O. Harris, 2013. *The Body in History: Europe from the Palaeolithic to the Future.* Cambridge: Cambridge University Press.

Robb, J., F. Mallegni & D. Ronco, 1991. New human remains from the southern Italian Neolithic. *Rivista di Antropologia* 69, 125–44.

Roberts, C., 2000. Infectious disease in biocultural perspective: Past, present and future work in Britain, in *Human Osteology in Archaeology and Forensic Science*, eds. M. Cox & S. Mays. London: Greenwich Medical Media, 145–62.

Roberts, C. & B. Connell, 2004. Guidance on recording palaeopathology, in *Guidelines to the Standards for Recording Human Remains (IFA Paper No.7)*, eds. M. Brickley & J.I. McKinley. BABAO/ IFA, 34–9.

Roberts, C. & K. Manchester, 2005. *The Archaeology of Disease* (3rd edition). Gloucestershire: Sutton Publishing.

Roberts, C. & J. Wakely, 1992. Microscopical findings associated with the diagnosis of osteoporosis in palaeopathology. *International Journal of Osteoarchaeology* 2(1), 23–30.

Rodgers, S., 1971. Note on the dentition of the Xemxija human remains, in *The Prehistoric Antiquities of the Maltese Islands: A Survey*, ed. J. Evans. London: Athlone Press, 238–9.

Rogers, J., 2000. The palaeopathology of joint disease, in *Human Osteology in Archaeology and Forensic Science*, eds. M. Cox & S. Mays. London: Greenwich Medical Media, 163–82.

Rogers, T.L., 1999. A visual method of determining the sex of skeletal remains using the distal humerus. *Journal of Forensic Sciences* 44(1), 57–60.

Rojas, R.V., D.A. Weston, H.L. Mickleburgh, J.E. Laffoon & A. van Duijvenbode, 2011. El Chorro de Maíta: A diverse approach to a context of diversity, in *Communities in Contact: Essays in Archaeology, Ethnohistory and Ethnography of the Amerindian Circum-Caribbean,* eds. C.L. Hofman & A. van Duijvenbode. Leiden: Sidestone Press, 225–51.

Roksandic, M. & S.D. Armstrong, 2011. Using the life history model to set the stage(s) of growth and senescence in bioarchaeology and paleodemography. *American Journal of Physical Anthropology* 145(3), 337–47.

Romero, J., 1952. Los patrones de la mutilación dentaria prehispanica. *Anales del Museo Nacional de México* 4, 177–221.

Romero, J., 1958. *Mutilaciones Dentarias Prehispanicas de Mexico y America en General.* Serie Investigaciones 3. Mexico: Instituto Nacional de Anthropologia e Historia.

Romero, J., 1960. Últimos hallazgos de mutilaciones dentarias en México. *Anales del Instituto Nacional de Antropología e Historia* XII, 151–215.

Romero, J., 1965. Recientes adiciones a la colección de dientes mutilados. *Anales del Instituto Nacional de Antropología e Historia* 17, 199–256.

Romero, J., 1970. Dental mutilation, trephination, and cranial deformation, in *Handbook of Middle American Indians, Volume 9: Physical Anthropology,* ed. T.D. Stewart. Austin (TX): University of Texas Press, 50–67.

Romero, J., 1986. *Catálogo de la Colección de Dientes Mutilados Prehispánicos IV Parte, Colección Fuentes*. Mexico: Instituto Nacional de Antropología e Historia.

Rose, J.C., K.W. Condon & A.H. Goodman, 1985. Diet and dentition: Developmental disturbances, in *The Analysis of Prehistoric Diets*, eds. R.I. Gilbert & J.M. Meilke. Orlando (FL): Academic Press; 281–305.

Rose, J.C. & P.S. Ungar, 1998. Gross dental wear and dental microwear in historical perspective, in *Dental Anthropology. Fundamentals, Limits and Prospects*, eds. K.W. Alt, F.W. Rösing & M. Teschler-Nicola. Vienna: Springer-Verlag, 349–86.

Rosen H., 1982. Cracked tooth syndrome. *Journal of Prosthetic Dentistry* 47(1), 36–43.

Ross, K.W. & M. Oxenham, 2015. To follow in their footsteps: An examination of the burial identity of the elderly from Non Nok Tha, in *The Routledge Handbook of Bioarchaeology in Southeast Asia and the Pacific Islands*, eds. H. Buckley & M. Oxenham. London: Routledge, 187–219.

Rossignani, M.P., 1969. Ceramica e trovamenti vari, in *Missione Archeologica Italiana a Malta*. *Rapporto preliminare della Campagna 1968,* ed. G. Busuttil. Rome: Consiglio Nazionale delle Ricerche, 97–105.

Roth, E.A., 1992. Applications of demography models to palaeodemography, in *Skeletal Biology of Past Peoples: Research Methods,* eds. S.R. Saunders & M.A. Katzenburg. New York (NY): Wiley-Liss, 175–88.

Rountree, K. 2002. Re-inventing Malta's neolithic temples: contemporary interpretations and agendas. *History and Anthropology* 13 (1), 31-51.

Rubín de la Borbolla, D.F., 1940. Types of tooth mutilation found in Mexico. *American Journal of Physical Anthropology* 26(1), 349–65.

Ruff, C.B., 1990. Body mass and hindlimb bone cross-sectional and articular dimensions in anthropoid primates, in *Body Size in Mammalian Paleobiology*, eds. J. Damuth, & B.J. McFadden. Cambridge: Cambridge University Press, 119–49.

Ruff, C.B., 2000. Body size, body shape, and long bone strength in modern humans. *Journal of Human Evolution* 38(2), 269–90.

Ruff, C.B., 2002. Long bone articular and diaphyseal structure in old world monkeys and apes. I: Locomotor effects. *American Journal of Physical Anthropology* 119(4), 305–42.

Ruff, C.B., 2008a. Biomechanical analyses of archaeological human skeletons, in *Biological Anthropology of the Human Skeleton* (2nd edition), eds. M.A. Katzenberg & S.R. Saunders. New York (NY): John Wiley & Sons, 183–206.

Ruff, C.B., 2008b. Femoral/humeral strength in early African Homo erectus. *Journal of Human Evolution* 54(3), 383–90.

Ruff, C.B., 2019. Biomechanical analysis of archaeological human skeletons, in *Biological Anthropology of the Human Skeleton* (3rd edition), eds. M.A. Katzenberg & A.L. Grauer. London: John Wiley & Sons, 189–224.

Ruff, C.B. & W.C. Hayes, 1983a. Cross-sectional geometry of Pecos Pueblo femora and tibiae – A biomechanical investigation: I. Method and general patterns of variation. *American Journal of Physical Anthropology* 60(3), 359–81.

Ruff, C.B. & W.C, Hayes, 1983b. Cross-sectional geometry of Pecos Pueblo femora and tibiae – A biomechanical investigation: II. Sex, age, side differences. *American Journal of Physical Anthropology* 60(3), 383–400.

Ruff, C.B., B.M. Holt, M. Niskanen, V. Sladék, M. Berner, *et al*., 2015. Gradual decline in mobility with the adoption of food production in Europe. *Proceedings of the National Academy of Sciences* 112(23), 2015–932.

Ruff, C.B., B.M. Holt, M. Niskanen, V. Sladék, M. Berner, *et al*., 2012. Stature and body mass estimation from skeletal remains in the European Holocene. *American Journal of Physical Anthropology* 148(4), 601–17.

Ruff, C.B., B.M. Holt, V. Sladék, M. Berner, W.A. Murphy Jr., *et al*., 2006. Body size, body proportions, and mobility in the Tyrolean 'Iceman'. *Journal of Human Evolution* 51(1), 91–101.

Ruff, C.B., B. Holt & E. Trinkaus, 2006. Who's afraid of the big bad Wolff? 'Wolff's law' and bone functional adaptation. *American Journal of Physical Anthropology* 129(4), 484–98.

Ruff, C.B, E. Trinkaus, A. Walker & C.S. Larsen, 1993. Postcranial robusticity in Homo. I: Temporal trends and mechanical interpretation. *American Journal of Physical Anthropology* 91(1), 21–53.

Ruff, C.B., E. Trinkaus & T.W. Holliday, 1997. Body mass and encephalization in Pleistocene Homo. *Nature* 387, 173–6.

Rushton, M.A., 1946. Solitary bone cysts in the mandible. *British Dental Journal* 81(2), 37–49.

Saluja, G., K. Fitzpatrick, M. Bruce & J. Cross, 1986. Schmorl's nodes (intravertebral herniations of intervertebral disc tissue) in two historic British populations. *Journal of Anatomy* 145, 87–96.

Sandison, A.T. & E. Tapp, 1998. Disease in ancient Egypt, in *Mummies, Disease & Ancient Cultures* (2nd edition), eds. A. Cockburn, E. Cockburn & T.A. Reyman. Cambridge: Cambridge University Press, 38–57.

Sandy, J.R. & D.M. Williams, 1981. Anterior salivary gland inclusion in the mandible: Pathological entity or anatomical variant? *British Journal of Oral Surgery* 19(3), 223–9.

Sansilbano-Collilieux, M., D. Bougault, Y. Darlas & J.-P. Sabatier, 1994. Incidence du sexe et de l'âge sur le contenu minéral osseux. *Actes des 6e Journées Anthropologiques Dossier de Documentation Anthropologique* 17, 159–71.

Sanson, M. & P. Cornu, 2000. Biology of meningiomas. *Acta Neurochirurgica (Wien)* 142(5), 493–505.

Saunders, S.R. & L. Barrans, 1999. What can be done about the infant category in skeletal samples?, in *Human Growth in the Past: Studies from Bones and Teeth,* eds. R.D. Hoppa & C.M. Fitzgerald. Cambridge: Cambridge University Press, 183–209.

Saunders, S.R., D.A. Herring & G. Boyce, 1995. Can skeletal samples accurately represent the living populations they come from?, in *Bodies of Evidence: Reconstructing History Through Skeletal Analysis*, ed. A. Grauer. New York: Wiley Liss, 69–89.

Saville, M.H., 1913. Precolumbian decoration of the teeth in Ecuador. *American Anthropologist* 15(3), 377–94.

Schattmann, A., B. Bertrand, S. Vatteoni & M. Brickley, 2016. Approaches to co-occurrence: Scurvy and rickets in infants and young children of 16–18th century Douai, France. *International Journal of Paleopathology* 12, 63–75

Schembri, P.J., C. Hunt, M. Pedley & C. Malone, 2009. The environment of the Maltese Islands, in *Mortuary Customs in Prehistoric Malta: Excavations at the Brochtorff Circle at Xagħra (1987–94)*, eds. C. Malone, S. Stoddart, A. Bonanno & D.H. Trump. Cambridge: McDonald Institute for Archaeological Research, 17–40.

Scherer, A.K., 2018. Head shaping and tooth modification among the Classic Maya of the Usumacinta River Kingdoms, in *Social Skins of the Head: Body Beliefs and Ritual in Ancient Mesoamerica and the Andes*, ed. V. Tiesler. New Mexico (NM): University of New Mexico Press, 59–80.

Scheuer, L. & S. Black, 2000. *Developmental Juvenile Osteology*. London: Elsevier.

Schneeberg, N.G., G. Woolhandler & R. Levine, 1947. The clinical significance of hyperostosis frontalis interna. *Journal of Clinical Endocrinology* 7(9), 624–35.

Schroeder, H., J.B. Haviser & T.D. Price, 2014. The Zoutsteeg three: Three new cases of African types of dental modification from Saint Martin, Dutch Caribbean. *International Journal of Osteoarchaeology* 24(6), 688–96.

Schroeder, H., T.C. O'Connell, J.A. Evans, K.A. Shuler & R.E. Hedges, 2009. Trans-Atlantic slavery: Isotopic evidence for forced migration to Barbados. *American Journal of Physical Anthropology* 139(4), 547–57.

Schropp, L., A. Wenzel, L. Kostopoulos & T. Karring, 2003. Bone healing and soft tissue contour changes following single-tooth extraction: a clinical and radiographic 12-month prospective study. *International Journal Periodontics Restorative Dentistry* 23(4), 313–23.

Schubert, M., A. Ginolhac, S. Lindgreen, J.F. Thompson, K.A. Al-Rasheid, *et al*., 2012. Improving ancient DNA read mapping against modern reference genomes. *BMC Genomics* 13, 178.

Schulting, R.J. & M. Wysocki, 2005. 'In this chambered tumulus were found cleft skulls...': An assessment of the evidence for cranial trauma in the British Neolithic. *Proceedings of the Prehistoric Society* 71, 107–38.

Schultz, M., 1993. *Vestiges of Non-Specific Inflammation in Prehistoric and Historic Skulls: A Contribution to Palaeopathology*. Aesch: Anthropologische Beitrage.

Schultz, M., 2001. Paleohistology of bone: A new approach to the study of ancient diseases. *Yearbook of Physical Anthropology* 44, 106–47.

Schulz, P., 1977. Task activity and anterior tooth grooving in prehistoric California Indians. *American Journal of Physical Anthropology* 46(1), 87–91.

Schulz, M., P. Carli-Thiele, T.H. Schmidt-Schultz, U. Kierdorf, H. Kierdorf, *et al*., 1998. Enamel hypoplasias in archaeological skeletal remains, in *Dental Anthropology. Fundamentals, Limits and Prospects*, eds. K.W. Alt, F.W. Rösing & M. Teschler-Nicola. Vienna: Springer-Verlag, 294–311.

Schutkowski, H. & R.K. Power, 2010. Differential infant and child mortality and morbidity in Late Anglo-Saxon England. *American Journal of Physical Anthropology* 141(S50), 192.

Schwartz, J.H., 1995. *Skeleton Keys: An Introduction to Human Skeletal Morphology, Development and Analysis*. New York (NY): Oxford University Press.

Schwartz, O., P. Bergmann & B. Klausen, 1985. Autotransplantation of human teeth: A life-table analysis of prognostic factors. *International Journal of Oral and Maxillofacial Surgery* 14(3), 245–58.

Schwartzman, H.B., 2006. Materializing children: Challenges for the archaeology of childhood, in *Children in Archaeology: Perspectives on the Archaeology of Childhood*, ed. J.E. Baxter. *Archaeological Papers of the American Anthropological Association* 15(1), 123–31.

Schweinfurth, G.A., 1874. *The Heart of Africa: Three Years' Travels and Adventures in the Unexplored Regions of Central Africa, from 1868 to 1871* (Vol. 1). New York (NY): Harper.

Sciulli, P.W., 1977. A descriptive and comparative study of the deciduous dentition of prehistoric Ohio Valley Amerindians. *American Journal of Physical Anthropology* 47(1), 71–80.

Sciulli, P.W., 1978. Developmental abnormalities of the permanent dentition in prehistoric Ohio Valley Amerindians. *American Journal of Physical Anthropology* 48(2), 193–8.

Scott, E., 1999. *The Archaeology of Infancy and Infant Death*. Oxford: Archaeopress.

Scott, G.R., 1973. 'Dental Morphology: A Genetic Study of American White Families and Variation in Living Southwest Indians.' Unpublished PhD, Arizona State University.

Scott, G.R., 1991. Dental Anthropology, in *Encyclopedia of Human Biology* (Vol. 2), ed. R. Dulbecco. San Diego (CA): Academic Press, 789–804.

Scott, G.R., 1997. Dental anthropology, in *Encyclopedia of Human Biology* (Vol. 3), ed. R. Dulbecco. San Diego (CA): Academic Press, 75–190.

Scott, G.R. & R. Burgett Jolie, 2008. Tooth-tool use and yarn production in Norse Greenland. *Alaska Journal of Anthropology* 6(1–2), 253–64.

Scott, G.R. & J.D. Irish, 2017. *Human Tooth Crown and Root Morphology: The Arizona State University Dental Anthropology System*. Cambridge: Cambridge University Press.

Scott, G.R. & C.G. Turner II, 1988. Dental anthropology. *Annual Review of Anthropology* 17, 99–126.

Scott, G.R. & C.G. Turner II, 1997. *The Anthropology of Modern Human Teeth: Dental Morphology and its Variation in Recent Human Populations*. New York (NY): Cambridge University Press.

Scott, G.R. & C.G. Turner II, 2009. History of dental anthropology, in *Technique and Application in Dental Anthropology*, eds. J.D. Irish & G.C. Nelson. Cambridge: Cambridge University Press, 10–34.

Sealy, J.C., N.J. Van Der Merwe, A. Sillen, F.J. Kruger & W.H. Krueger, 1991. 87Sr/86Sr as a dietary indicator in modern and archaeological bone. *Journal of Archaeological Science* 18, 399–416.

Seeman, E.R., 2011. *The Huron-Wendat Feast of the Dead: Indian-European Encounters in Early North America*. Baltimore (MD): The John Hopkins University Press.

Seguin, G., E. d'Incau, P. Murail & B. Maureille, 2014. The earliest dental prosthesis in Celtic Gaul? The case of an Iron Age burial at Le Chêne, France. *Antiquity* 88(340), 488–500.

Seidel, J.C., R.H. Colten, E.A. Thibodeau & J.G. Aghajanian, 2005. Iatrogenic molar borings in 18th and early 19th century Native American dentitions. *American Journal of Physical Anthropology* 127(1), 7–12.

Senck, S., F.L. Bookstein, S. Benazzi, J. Kastner & G.W. Weber, 2015. Virtual reconstruction of modern and fossil hominoid crania: Consequences of reference sample choice. *Anatomical Record* 298(5), 827–41.

Senno, T., H. Fuji, K. Matsuzawa & T. Sadaoka, 1969. A case of Stafne's idiopathic bone cavity. *Japanese Journal of Oral Surgery* 15(2), 124–7.

Sereno, P.C., E.A.A. Garcea, H. Jousse, C.M. Stojanowski, J.-F. Saliège, *et al*., 2008. Lakeside cemeteries in the Sahara: 5000 years of Holocene population and environmental change. *PLoS ONE* 3, 1–22.

Serio, G., M. Hoskin & F. Ventura, 1992. The orientations of the temples of Malta. *Journal for the History of Astronomy* 23(2), 107–19.

Serpa Pinto, A.A., 1881. *How I Crossed Africa*: *From the Atlantic to the Indian Ocean.* London: Sampson Low & Co.

Sewell, D.A., S.Y. Lai & R.S. Weber, 2003. Non-melanoma skin cancer of the head and neck, in *Cancer of the Head and Neck* (4th edition), eds. J.Y. Suen, J.N. Meyers & E. Hanna. Philadelphia (PA): WB Saunders, 117–21.

Shafer, W.G., M.K. Hine & B.M Levy, 1983. *A Textbook of Oral Pathology*. Philadelphia (PA): W.B. Saunders Company.

Shahin, A.A., S. Alhoseiny & M. Aldali, 2014. Hyperostosis frontalis interna: An Egyptian case referred to the second dynasty (2890–2650 BC) from Tarkhan-Egypt. *Egyptian Rheumatologist* 36(1), 41–5.

Shakespeare, T., 1999. Commentary: Observations on disability and archaeology. *Archaeological Review from Cambridge* 15(2), 99–110.

Shane, E., 1988. Osteoporosis, in *Metabolic Bone and Mineral Disorders*, eds. S.C. Manolagas & J.M. Olefsky. New York (NY): Churchill Livingstone, 151–92.

Shanks, M. & C.Y. Tilley, 1982. Ideology, symbolic power and ritual communication: a reinterpretation of Neolithic mortuary practices, in *Symbolic and Structural archaeology* ed, I. Hodder. Cambridge: Cambridge University Press, 129–54.

Shapira, Y., 1980. Transposition of canines. *Journal of the American Dental Association* 100(5), 710–12.

Shapira, Y. & M.M. Kuftinec, 1989. Tooth transpositions – a review of the literature and treatment considerations. *Angle Orthodontist* 59(4), 271–6.

Shapira, Y. & M.M. Kuftinec, 2001. Maxillary tooth transpositions: Characteristic features and accompanying dental anomalies. *American Journal of Orthodontics and Dentofacial Orthopedics* 119(2), 127–34.

Shaw, C.N. & J.T. Stock, 2009a. Habitual throwing and swimming correspond with upper limb diaphyseal strength and shape in modern human athletes. *American Journal of Physical Anthropology* 140(1), 160–72.

Shaw, C.N. & J.T. Stock, 2009b. Intensity, repetitiveness, and directionality of habitual adolescent mobility patterns influence the tibial diaphysis morphology of athletes. *American Journal of Physical Anthropology* 140(1), 149–59.

Shaw, J.C.M., 1931. *The Teeth, the Bony Palate and the Manidble in the Bantu Races of South Africa*. London: John Bale, Sons and Danielssen, Ltd.

She, R. & J. Szakacs, 2004. Hyperostosis frontalis interna: Case report and review of literature. *Annals of Clinical and Laboratory Science* 34(2), 206–8.

Shennan, S., 1997. *Quantifying Archaeology* (2nd edition). Iowa (IA): University of Iowa Press.

Shepherd, S., M. Shapland, N.X. Pearce & S. Scully, 1990. Pattern, severity and aetiology of injuries in victims of assault. *Journal of the Royal Society of Medicine* 83(2), 75–8.

Shields, E.D., 2000. Technical note: Stafne static mandibular bone defect – further expression on the buccal aspect of the ramus. *American Journal of Physical Anthropology* 111(3), 425–7.

Shoor, H.N. Sujir, S. Mutalik & K.M. Pai, 2014. Hypercementosis: A rare finding in a patient with systemic lupus erythematosus. *BMJ Case Reports*.

Siebers, T., 2008. *Disability Theory.* Ann Arbor (MI): University of Michigan Press.

Siegel, J.H., 1995. The effect of associated injuries, blood loss, and oxygen debt on death and disability in blunt traumatic brain injury: The need for early physiologic predictors of severity. *Journal of Neurotrauma* 12(4), 579–90.

Silva, A.M., R. Boaventura, M.T. Ferreira & R. Marques, 2012. Skeletal evidence for interpersonal violence from Portuguese Late Neolithic collective burials: An overview, in *Sticks, Stones, and Broken Bones: Neolithic Violence in a European Perspective*, eds. R.J. Schulting & L. Fibiger. Oxford: Oxford University Press, 317–41.

Silva, A.M. & R. Marques, 2010. An arrowhead injury in a Neolithic human axis from the natural cave of Lapa do Bugio (Sesimbra, Portugal). *Anthropological Science* 118(3), 185–9.

Silventoinen, K., S. Sammalisto, M. Perola, D.I. Boomsma, B.K. Cornes, *et al*., 2003. Heritability of adult body height: a comparative study of twin cohorts in eight countries. *Twin Research and Human Genetics* 6(5), 399–408.

Silvestrini, M., A. Cazzella, I. Baroni & G. Recchia, 2004. Le necropoli eneolitiche delle Marche e la facies di Rinaldone, in *Atti del Sttimo Incontro di Studi: Pastori e guerrieri nell'Etruria del IV e III millennio a.C. La civiltà di Rinaldone a 100 Anni dalle Prime Scoperte (Viterbo, 21 Novembre 2003 e Valentano 17–18 Settembre 2004,* ed. Negroni Catacchio. Milan: Centro Studi di Preistoria e Archeologia, 193–202.

Simkin, A., I. Leichter, A. Swissa & S. Samueloff, 1989. The effect of swimming activity on bone architecture in growing rats. *Journal of Biomechanics* 22(8–9), 845–51.

Simmons, L.W., 1945. *The Role of the Aged in Primitive Societies*. Newhaven (CT): Yale University Press.

Simmons, T., R.L. Jantz & W.M. Bass, 1990. Stature estimation from fragmentary femora: A revision of the Steele method. *Journal of Forensic Sciences* 35(3), 628–36.

Simpson, W., 1965. A Stafne's mandibular defect containing a pleomorphiadenoma: Report of case. *Journal of Oral Surgery* 23, 553–6.

Singer, R., 1953. Artifical deformation of teeth: A preliminary report. *South African Journal of Science* 50(5), 116–22.

Singh, G., S. Singh & S.P. Singh, 1975. Identification of sex from tibia. *Journal of the Anatomical Society of India* 24(1), 243–9.

Sjøvold, T., 1973. Occurrence of minor non-metrical variants in the skeleton and their quantitative treatment for population comparisons. *HOMO* 24, 204–33.

Sjøvold, T., 1977. Non-metrical divergence between skeletal populations: The theoretical foundation and biological importance of C.A.B. Smith's mean measure of divergence. *Ossa* 4(S1), 1–133.

Skeates, R., 1997. Copper Age settlement and economy in Marche, central Italy: A social perspective. *Journal of Mediterranean Archaeology* 10(1), 49–72.

Skeates, R., 2010. *An Archaeology of the Senses: Prehistoric Malta*. Oxford: Oxford University Press.

Skelton, R., W. Maixner & D. Isaacs, 1992. Sinusitis-induced subdural empyema. *Archives of Disease in Childhood* 67(12), 1478–80.

Skinner, M., 1986. An enigmatic hypoplastic defect of the deciduous canine. *American Journal of Physical Anthropology* 69(1), 59–69.

Skinner, M. & A.H. Goodman, 1992. Anthropological uses of developmental defects of enamel, in *The Skeletal Biology of Past Peoples: Advances in Research Methods*, eds. S.R. Saunders & M.A. Katzenberg. New York (NY): Wiley, 153–73.

Skoglund, P., H. Malmström, A. Omrak, M. Raghavan, C. Valdiosera, *et al*., 2014. Genomic diversity and admixture differs for Stone-Age Scandinavian foragers and farmers. *Science* 344(6185), 747–50.

Skoglund, P., H. Malmström, M. Raghavan, J. Storå, P. Hall, *et al*., 2012. Origins and genetic legacy of Neolithic farmers and hunter-gatherers in Europe. *Science* 336(6080), 466–9.

Skoglund, P., B.N. Northoff, M.V. Shunkov, A.P. Derevianko, S. Pääbo, *et al*., 2014. Separating endogenous ancient DNA from modern day contamination in a Siberian Neandertal. *Proceedings of the National Academy of Sciences* 111(6), 2229–34.

Skoglund, P., J. Storå, A. Götherström & M. Jakobsson, 2013. Accurate sex identification of ancient human remains using DNA shotgun sequencing. *Journal of Archaeological Science* 40(12), 4477–82.

Sládek, V., M. Berner, P. Galeta, L. Friedl & S. Kurdnová, 2010. Technical note: The effect of midshaft location on the error ranges of femoral and tibial cross-sectional parameters. *American Journal of Physical Anthropology* 141(2), 325–32.

Sládek, V., Berner, M., Holt, B. M., Niskanen, M. & Ruff, C. B., 2018. Past human manipulative behaviour in the European Holocene as assessed through humeral asymmetry, in *Skeletal Variation and Adaptation in Europeans: Upper Paleolithic to the Twentieth Century*, ed. C.B. Ruff. New York: Wiley-Blackwell, 163–208.

Sládek, V., M. Berner & R. Sailer, 2006a. Mobility in central European Late Eneolithic and Early Bronze Age: Femoral cross-sectional geometry. *American Journal of Physical Anthropology* 130(3), 320–32.

Sládek, V., M. Berner & R. Sailer, 2006b. Mobility in central european Late Eneolithic and Early Bronze Age: Tibial cross-sectional geometry. *Journal of Archaeological Science* 33(4), 470–82.

Slavin, M.I., 1950. Ectopically placed parotid gland in the mandible: Report of a case. *Oral Surgery, Oral Medicine, Oral Pathology* 3(11), 1372–6.

Smith, A.L., 1972. *Excavations at Altar de Sacrificios: Architecture, Settlement, Burials, and Caches*. Cambridge (MA): Harvard University Peabody Museum of Archaeology and Ethnology.

Smith, M.J., 2006. Bones chewed by canids as evidence for human excarnation: A British case study. *Antiquity* 80(309), 671–85.

Smith, M.J., 2014. The war to begin all wars? Contextualizing violence in Neolithic Britain, in *The Routledge Handbook of the Bioarchaeology of Human Conflict*, eds. C. Knüsel & M.J. Smith. London: Routledge, 109–26.

Smith, M.J., A. Atkin & C. Cutler, 2017. An age old problem? Estimating the impact of dementia on past human populations. *Journal of Aging and Health* 29(1), 68–98.

Smith, M. & M. Brickley, 2009. *People of the Long Barrows*. Stroud: The History Press.

Smith, P., O. Bar-Yosef & A. Sillen, 1984. Archaeological and skeletal evidence for dietary change during the late Pleistocene/early Holocene in the Levant, in *Paleopathology at the Origins of Agriculture*, eds. M.N. Cohen & G.J. Armelagos. New York (NY): Academic Press, 101–36.

Smith, S. & R.E. Hemphill, 1956. Hyperostosis frontalis interna. *Journal of Neurology, Neurosurgery and Psychiatry* 19, 42.

Smyth, W.H., 1829. Notice of some remains at Gozo, near Malta. Communication in a letter from Captain W.H. Smyth, R.N., F.R.S. and S.A. to Thomas Amyot, Esq., F.R.S. Treasurer. 8 May 1828. *Archaeologia* 22, 294–6.

Snoddy, A.M.E., H.R. Buckley, G.E. Elliott, V.G. Standen, B.T. Arriaza & S.E. Halcrow, 2018. Macroscopic features of scurvy in human skeletal remains: A literature synthesis and diagnostic guide. *American Journal of Physical Anthropology* 167(4), 876–95.

Snoddy, A.M.E., S.E. Halcrow, H.R. Buckley, V.G. Standen & B.T. Arriaza, 2017. Scurvy at the agricultural transition in the Atacama desert (ca 3600–3200 BP): Nutritional stress at the maternal-foetal interface? *International Journal of Paleopathology* 18, 108–20.

Soames, J.V. & J.C. Southam, 2005. *Oral Pathology*. Oxford: Oxford University Press.

Sofaer-Derevenski, J., 2000. *Children and Material Culture*. London: Routledge.

Sofaer, J., 2006. *The Body as Material Culture*. Cambridge: Cambridge University Press.

Sofaer, J., 2011. Towards a social bioarchaeology of age, in *Social Bioarchaeology*, eds. S.C. Agarwal & B.A. Glencross. Chichester: Wiley-Blackwell, 285–311.

Sokolovsky, J. (ed.), 1983. *Growing Old in Different Societies: Cross-Cultural Perspectives*. Belmont (CA): Wadsworth Publishing Company.

Sparacello, V. & D. Marchi, 2008. Mobility and subsistence economy: A diachronic comparison between two groups settled in the same geographical area (Liguria, Italy). *American Journal of Physical Anthropology* 136(4), 485–95.

Sparacello, V., O.M. Pearson, A. Coppa & D. Marchi, 2011. Changes in skeletal robusticity in an Iron Age agropastoral group: The samnites from the Alfedena necropolis (Abruzzo, Central Italy). *American Journal of Physical Anthropology* 144(1), 119–30.

Spence, M.W. & G. Pereira, 2007. The human skeletal remains of the Moon Pyramid, Teotihuacan. *Ancient Mesoamerica* 18(1), 147–57.

Spencer, B., & F.J. Gillen, 1927. *The Arunta: A Study in Stone Age People* (Vol. 1). London: Macmillan.

Sperduti, A., M.R. Giuliani, G. Guida, P.P. Petrone, P.F. Rossi, *et al*., 2018. Tooth grooves, occlusal striations, dental calculus, and evidence for fiber processing in an Italian eneolithic/Bronze age cemetery. *American Journal of Physical Anthropology* 167(2), 234–43.

Spinek, A.E., W. Lorkiewicz, J. Mietlińska, E. Sewerynek, A. Kłys, *et al*., 2016. Evaluation of chronological changes in bone fractures and age-related bone loss: A test case from Poland. *Journal of Archaeological Science* 72, 117–27.

Spruiell, R.C., 1984. 'Sexing of the Femur.' Unpublished M.A., University of Tennessee.

Squyres, N. & C.B. Ruff, 2015. Body mass estimation from knee breadth, with application to early hominins. *American Journal of Physical Anthropology* 158(2), 198–208.

Stafne, E.C., 1942. Bone cavities situated near the angle of the mandible. *Journal of the American Dental Association* 29(17), 1969–72.

Stark, R.J., 2014. A proposed framework for the study of paleopathological cases of subadult scurvy. *International Journal of Paleopathology* 5, 18–26.

Starling, A.P. & J.T. Stock, 2007. Dental indicators of health and stress in early Egyptian and Nubian agriculturalists: A difficult transition and gradual recovery. *American Journal of Physical Anthropology* 134(4), 520–8.

Starr, F., 1909. *Ethnographic Notes from the Congo Free State: An African Miscellany*. Davenport (IA): Davenport Academy of Sciences.

Steckel, R.H, 1995. Stature and the standard of living. *Journal of Economic Literature* 33(4), 1903–40.

Steele, D.G., 1970. Estimation of stature from fragments of long limb bones, in *Personal Identification in Mass Disasters*, ed. T. D. Stewart. Washington (DC): National Museum of Natural History, 85–97.

Steele, D.G. & T.W. McKern, 1969. A method for assessment of maximum long bone length and living stature from fragmentary long bones. *American Journal of Physical Anthropology* 31(2), 215–27.

Steele, J., 2000. Skeletal indicators of handedness, in *Human Osteology in Archaeology and Forensic Science*, eds. M. Cox & S. Mays. London: Greenwich Medical Media, 307–23.

Steele, J. & S. Mays, 1995. Handedness and directional asymmetry in the long bones of the human upper limb. *International Journal of Osteoarchaeology* 5(1), 39–49.

Stene, T. & K.M. Pedersen, 1977. Aberrant salivary gland tissue in the anterior mandible. *Oral Surgery, Oral Medicine, and Oral Pathology* 44(1), 72–5.

Stephens, L., D. Fuller, N. Boivin, T. Rick, N. Gauthier, *et al*., 2019. Archaeological assessment reveals Earth's early transformation through land use. *Science* 365(6456), 897–902.

Stevens, D.L. & A.E. Bryant, 2016. Impetigo, erysipelas and cellulitis, in *Streptococcus pyogenes: Basic Biology to Clinical Manifestations*, eds. J.J. Ferretti, D.L. Stevens & V.A. Fischetti. Oklahoma City (OK): University of Oklahoma Health Sciences Center.

Stewart, R.M., 1928. Localized cranial hyperostosis in the insane. *Journal of Neurology and Psychopathology* 8(32), 321–31.

Stewart, T.D., 1979. *Essentials of Forensic Anthropology*. Springfield (IL): Charles C. Thomas.

Stini, W.A., 1990. Osteoporosis: Etiologies, prevention and treatment. *Yearbook of Physical Anthropology* 33(S11), 151–94.

Stini, W.A., 1995. Osteoporosis in biocultural perspective. *Annual Review of Anthropology* 24, 397–421.

Stock, J.T. & A.A. Macintosh, 2016. Lower limb biomechanics and habitual mobility among mid-Holocene populations of the Cis-Baikal. *Quaternary International* 405(2), 200–9.

Stock, J.T. & A.B Migliano, 2009. Stature, mortality and life history among indigenous populations of the Andaman Isles, 1871–1986. *Current Anthropology* 50(5), 713–25.

Stock, J.T., M.C. O'Neill, C.B. Ruff, M. Zabecki, L. Shackelford & J.C. Rose, 2011. Body size, skeletal biomechanics, mobility and habitual activity from the late Paleolithic to the mid-Dynastic Nile Valley, in *Human Bioarchaeology of the Transition to Agriculture*, eds. R. Pinhasi & J.T. Stock. New Jersey (NJ): John Wiley & Sons, 347–67.

Stock, J.T. & S. Pfeiffer, 2001. Linking structural variability in long bone diaphyses to habitual behaviors: Foragers from the southern African Later Stone Age and the Andaman Islands. *American Journal of Physical Anthropology* 115(4), 337–48.

Stock, J.T. & S. Pfeiffer, 2004. Long bone robusticity and subsistence behaviour among Later Stone Age foragers of the forest and fynbos biomes of South Africa. *Journal of Archaeological Science* 31(7), 999–1013.

Stock, J.T. & R. Pinhasi, 2011. Changing paradigms in our understanding of the transition to agriculture: Human bioarchaeology, behaviour and adaptation, in *Human Bioarchaeology of the Transition to Agriculture*, eds. R. Pinhasi & J.T. Stock. Chichester: Wiley-Blackwell, 1–13.

Stock, J.T. & C.N. Shaw, 2007. Which measures of diaphyseal robusticity are robust? A comparison of external methods of quantifying the strength of long bone diaphyses to cross-sectional geometric properties. *American Journal of Physical Anthropology* 134(3), 412–23.

Stock, J.T., M.K. Shirley, L.A. Sarringhaus, T.G. Davies & C.N. Shaw, 2013. Skeletal evidence for variable patterns of handedness in chimpanzees, human hunter-gatherers, and recent British populations. *Annals of the New York Academy of Sciences* 1288, 86–99.

Stock, J.T. & K. Willmore, 2003. Body size, bone mass and biomechanical analyses of the adult post-cranial remains, in *Bones of the Ancestors: The Archaeology and Osteobiography of the Moatfield Ossuary*, eds. R.F. Williamson & S. Pfeiffer. Quebec: Canadian Museum of Civilisation, 309–30.

Stoddart, S., 1997–8. Contrasting political strategies in the islands of the southern central Mediterranean. *Accordia Research Papers* 7, 59–73.

Stoddart, S., 1999. Mortuary customs in prehistoric Malta, in *Facets of Maltese Prehistory*, eds. A. Mifsud & C.S. Ventura. Malta: Prehistoric Society of Malta, 183–90.

Stoddart, S., 2002. The Xaghra Shaman? in *New Approaches to Medical Archaeology and Medical Anthropology: Practitioners, Practices and Patients*, eds. G. Carr & P.A. Baker. Oxford: Oxbow Books, 125–35.

Stoddart, S. 2004. Cycles of Life or eternity: new light on prehistoric Maltese funerary ritual from the Brochtorff Circle at Xaghra. *2003 Conference in Malta (CD-ROM).* Sarasota, Florida: EMPTC.

Stoddart, S., 2007. The Maltese death cult in context, in *Cult in Context*, eds. D. Barrowclough & C. Malone. Oxford, Oxbow Books, 54–60.

Stoddart, S., 2015. Mediating the Dominion of Death in Prehistoric Malta, in *Death Rituals, Social Order and the Archaeology of Immortality in the Ancient World. 'Death Shall Have No Dominion'*, eds. A.C. Renfrew, M. Boyd & I. Morley. Cambridge: Cambridge University Press, 130–7.

Stoddart, S. & A. Chalmers, 1996. La validità scientifica della ricostruzione virtual reality: Esempi da Sud Africa e Malta, in *Prehistoric Research in the Context of Contemporary Society. Colloquium XXXVII Prehistoric Research in Current Society in Relation to the Economic Development and Evaluation of Sites. Preprints of the XIII Congress of the UISPP, Forlì, Italy*, ed. G. Bermond Montanari. Forlì: Abaco, 109–17.

Stoddart, S. & C. Malone, 2008. Changing beliefs in the human body in prehistoric Malta 5000–1500 BC, in *Past Bodies. Body-Centred Research in Archaeology*, eds. D. Boric & J. Robb. Oxford: Oxbow Books, 19–28.

Stoddart, S. & C. Malone, 2010. Hypogea: concealed caves or constructed temples? The hypogea of Malta and their significance, in *Links between Megalithism and Hypogeism in Western Mediterranean Europe*, eds. J.A. Cámara Serrano, J.A. Afonso Marrero & L. Spanedda, Oxford: Archaeopress, 21–7.

Stoddart, S. & C. Malone, 2013. Caves of the Living. Caves of the Dead. Experiences above and below ground in prehistoric Malta, in *Journeys into the Dark Zone: A Cross Cultural Perspective on Caves as Sacred Spaces*, ed. H. Moyes. Boulder: University Press of Colorado, 45–58.

Stoddart, S. & C. Malone, 2015. Prehistoric Maltese death: Democratic theatre or elite democracy?, in *Death Embodied: Archaeological Approaches to the Treatment of the Corpse,* eds. Z.L. Devlin & E.-J. Graham. Oxford: Oxbow Books, 160–74.

Stoddart, S. & C. Malone, 2018. Reflections on sacred hair in the prehistory of Malta, in *The Lure of the Antique. Essays on Malta and Mediterranean Archaeology in Honour of Anthony Bonanno*, eds. N.C. Vella, A.J. Frendo & H.C.R. Vella (Ancient Near Eastern Studies Supplement 54). Leuven: Peeters, 131–42.

Stoddart, S., G. Barber, C. Duhig, G. Mann, T.C. O'Connell, *et al*., 2009a. The human and animal remains, in *Mortuary Customs in Prehistoric Malta: Excavations at the Brochtorff Circle at Xagħra (1987–94),* eds. C. Malone, S. Stoddart, A. Bonanno & D.H. Trump. Cambridge: McDonald Institute for Archaeological Research, 315–40.

Stoddart, S., A. Bonanno, T. Gouder, C. Malone & D.H. Trump, 1993. Cult in an island society: Prehistoric Malta in the Tarxien period. *Cambridge Archaeological Journal* 3(1), 3–19.

Stoddart, S., P. Hardy, C. Malone, S. Mason, M. Pedley & D.H. Trump, 2009b. The archaeological sequence of the Circle, in *Mortuary Customs in Prehistoric Malta: Excavations at the Brochtorff Circle at Xagħra (1987–94)*, eds. C. Malone, S. Stoddart, A. Bonanno & D.H. Trump, Cambridge: McDonald Institute for Archaeological Research, 79–93.

Stoddart, S., C. Malone, M. Anderson & R. Barratt, 2020. Light and Dark in Prehistoric Malta, in *The Oxford Handbook of Light in Archaeology*, eds. C. Papadopoulos & H. Moyes. Oxford: Oxford University Press. DOI: 10.1093/oxfordhb/9780198788218.013.25.

Stoddart, S., C. Malone, S. Mason, D. Trump & D.H. Trump, 2009c. The Tarxien phase levels: spatial and stratigraphic analysis and reconstruction, in *Mortuary Customs in Prehistoric Malta: Excavations at the Brochtorff Circle at Xagħra (1987–94)*, eds. C. Malone, S. Stoddart, A. Bonanno & D.H. Trump. Cambridge: McDonald Institute for Archaeological Research, 109–205.

Stoddart, S., M. Wysocki & G. Burgess with supporting contributions from G. Barber, C. Duhig, C. Malone & G. Mann, 1999. The articulation of disarticulation. Preliminary thoughts on the Brochtorff Circle at Xagħra (Gozo), in *The Loved Body's Corruption: Archaeological Contributions to the Study of Human Mortality*, eds. J. Downes & A. Pollard. Glasgow: Cruithne Press, 94–105.

Stöger, H., 2000. Albert Mayr (1868–1924). *Malta Archaeological Review* 4, 3–9.

Stojanowski, C.M., C.L. Carver & K.A. Miller, 2014. Incisor avulsion, social identity and Saharan population history: New data from the Early Holocene southern Sahara. *Journal of Anthropological Archaeology* 35, 79–91.

Stojanowski, C.M., K.M. Johnson, K.S. Paul & C.L. Carver, 2016. Indicators of idiosynchratic behaviour in the dentition, in *A Companion to Dental Anthropology*, eds. J.D. Irish & G.R. Scott. New York (NY): John Wiley and Sons, 377–95.

Stojanowski, C.M., R.M. Seidemann & G.H. Doran, 2002. Differential skeletal preservation at Windover Pond: Causes and consequences. *American Journal of Physical Anthropology* 119(1), 15–26.

Stoneking, M. & J. Krause, 2011. Learning about human population history from ancient and modern genomes. *Nature Reviews Genetics* 12(9), 603–14.

Storhaug, C.L., S.K. Fosse & L.T. Fadnes, 2017. Country, regional, and global estimates for lactose malabsorption in adults: A systematic review and meta-analysis. *Lancet Gastroenterology & Hepatology* 2(10), 738–46.

Strouhal, E., 1998. Palaeopathological evidence of jaw tumors, in *Dental Anthropology. Fundamentals, Limits and Prospects*, eds. K.W. Alt, F.W. Rösing & M. Teschler-Nicola. Vienna: Springer-Verlag, 277–92.

Stuart-Macadam, P.L., 1991. Anemia in Roman Britain: Poundbury camp, in *Health in Past Societies: Biocultural*

Interpretations of Human Skeletal Remains in Archaeological Contexts., eds. H. Bush & M. Zvelebil. Oxford: British Archaeological Research International Series, 101–13.

Sugawara, T., 1972. Developmental defect of mandible containing salivary gland tissue: Case report. *Journal of the Japanese Stomatological Society* 21, 406–7.

Sun, C., S. Xing, L. Martín-Francés, C. Bae, L. Liu, *et al*., 2014. Interproximal grooves on the Middle Pleistocene hominin teeth from Yiyuan, Shandong Province: New evidence for tooth-picking behavior from eastern China. *Quaternary International* 354(15), 162–8.

Sureka, J., R.K. Jakkani, M. Ahmed, S. Panwar & S. Shanker, 2012. Congenital distal tibiofibular synostosis. *Radiology Case Reports* 7(2), 555.

Swerdloff, B.A., M.B. Ozonoff & M.T. Gyepes, 1970. Late recurrence of infantile cortical hyperostosis (Caffey's disease). *American Journal of Roentgenology* 108(3), 461–7.

Sylvester, A.D., B.C. Merkl & M.R. Mahfouz, 2008. Assessing A.L. 288-1 femur length using computer-aided three-dimensional reconstruction. *Journal of Human Evolution* 55(4), 665–71.

Szeniczey, T., A. Marcsik, Z. Ács, T. Balassa, Z. Bernert, *et al*., 2019. Hyperostosis frontalis interna in ancient populations from the Carpathian Basin – A possible relationship between lifestyle and risk of development. *International Journal of Paleopathology* 24, 108–18.

Tagliaferro, N., 1910. The prehistoric pottery found in the hypogeum at Ħal Saflieni, Casal Paula, Malta. *Annals of Archaeology and Anthropology* 3(1–2), 1–21.

Tagliaferro, N., 1911. Prehistoric burials in a cave at Bur Mghez, near Mkabba, Malta. *Man* 11, 147–50.

Tagliaferro, N., 1912. Prehistoric burial in a cave at Bur Megħeż, near Mqabba, Malta. *Archivum Melitense (Journal of the Malta Historical and Scientific Society)* 1 (1910–1912) (7 (September 1912)), 143–9.

Talarico, E.F., A.D. Prather & K.D. Hardt, 2008. A case of extensive hyperostosis frontalis interna in an 87-year-old female human cadaver. *Clinical Anatomy* 21(3), 259–68.

Tanasi, D., 2014. Uniti e divisi dal mare. Mobilita di uomini e merci tra la Sicilia e l'arcipelago Maltese nel II Millennia a.C., in *Viaggio in Sicilia: Racconti, Segni e Citta Ritrovate*, eds. M. Congiu, C. Micciché & S. Modeo. Caltanissetta, Sciascia, Atti del X Convegno di Studi sulla Sicilia Antica, Caltanissetta 10–11 maggio 2013, 99–116.

Tannenbaum, K.A. & E. Alling, 1963. Anomalous tooth development: Case reports of gemination and twinning. *Oral Surgery, Oral Medicine and Oral Pathology* 16(7), 883–7.

Tayles, N., 1996. Tooth ablation in prehistoric Southeast Asia. *International Journal of Osteoarchaeology* 6(4), 333–45.

Tayles, N., K. Domett & K. Nelsen, 2000. Agriculture and dental caries? The case of rice in prehistoric southeast Asia. *World Archaeology* 32(1), 68–83.

Tayles, N. & S.E. Halcrow, 2015. Age-at-death estimation in a sample of prehistoric Southeast Asian adolescents and adults, in *The Routledge Handbook of Bioarchaeology in Southeast Asia and the Pacific Islands*, eds. M. Oxenham & H. Buckley. Abingdon: Routledge, 220–38.

Taylor, S.E. (ed.), 1995. *Health Psychology* (3rd edition). New York (NY): McGraw-Hill.

Teasdale, M.D., N.L. van Doom, S. Fiddyment, C.C. Webb, T. O'Connor, *et al*., 2015. Paging through history: Parchment as a reservoir of ancient DNA for next generation sequencing. *Philosophical Transactions of the Royal Society B: Biological Sciences* 370, 20130379.

Temple, D.H., 2019. Bioarchaeological evidence for adaptive plasticity and constraint: Exploring life-history trade-offs in the human past. *Evolutionary Anthropology: Issues, News, and Reviews* 28(1), 34–46.

Temple, D.H. & A.H. Goodman, 2014. Bioarcheology has a 'health' problem: Conceptualizing 'stress' and 'health' in bioarcheological research. *American Journal of Physical Anthropology* 155(2), 186–91.

Terwee, P.J., 1922. 'Die Vererbung des Diastemas.' Unpublished dissertation, University of Bonn.

Teschler-Nicola, M., F. Gerold, M. Bujatti-Narbeshuber, T. Prohaska, C. Latkoczy, *et al*., 1999. Evidence of genocide 7000 BP – Neolithic paradigm and geo-climatic reality. *Collegium Antropologicum* 23(2), 437–50.

Thieme, F.P., 1957. Sex in Negro skeletons. *Journal of Forensic Medicine* 4, 72–81.

Thoma, K.H., 1955. Case report of a so-called latent bone cyst. *Oral Surgery, Oral Medicine, Oral Pathology* 8(9), 963–6.

Thompson, J.E., 2020. 'Heads, shoulders, knees and toes: Exploring bodies, body parts and personhood in late Neolithic Malta through funerary taphonomy'. Unpublished PhD, University of Cambridge. https://doi.org/10.17863/CAM.50091

Thompson, J.E., D. Martín-Vega, R.K. Power, S. Stoddart & C. Malone, 2018. Identification of dermestid pupal chambers to Neolithic Maltese human bone: implications for funerary practices at the Xemxija Tombs. *Journal of Archaeological Science Reports* 22, 123–31.

Thompson, J.E., E.W. Parkinson, T.R. McLaughlin, R. Barratt, R.K. Power, *et al*., 2020. Placing and remembering the dead in late Neolithic Malta: Bioarchaeological and spatial analysis of the Xagħra Circle hypogeum, Gozo. *World Archaeology* 52, 71–89.

Thompson, J.E., R.K. Power, B. Mercieca-Spiteri, J.S. Magnussen, M. Pardey, *et al*., 2021. Analysis of periosteal lesions from commingled human remains at the Xagħra Circle hypogeum reveals the first case of probable scurvy from Neolithic Malta. *International Journal of Osteoarchaeology*. https://doi.org/10.1002/oa.3040

Thompson, S., 1990. Metaphors the Chinese age by, in *Anthropology and the Riddle of the Sphinx: Paradoxes of Change in the Life Course*, ed. P. Spencer. London: Routledge, 102–66.

Tiesler, V., 2001. *Decoraciones Dentales Entre los Antiguos Mayas*. Mexico City: Instituto Nacional de Antropologia e Historia.

Tiesler, V., A. Cucina & M. Ramírez-Salomón, 2017. Permanent dental modifications among the ancient Maya. Procedures, health risks and social identities, in *A World View of Bioculturally Modified Teeth*, eds. S.E. Burnett & J.D. Irish. Gainesville (FL): University Press of Florida, 270–84.

Tilley, L., 2013. 'Towards a Bioarchaeology of Care: A Contextualised Approach for Identifying and Interpreting Health-Related Care Provision in Prehistory.' Unpublished PhD, Australian National University.

Tilley, L., 2015. *Theory and Practice in the Bioarchaeology of Care*. Heidelberg: Springer.
Tilley, L., 2017. Showing that they cared: An introduction to thinking, theory and practice in the bioarchaeology of care, in *New Developments in the Bioarchaeology of Care*, eds. L. Tilley & A.A. Shrenk. New York (NY): Springer, 11–43.
Tilley, L., & T. Cameron, 2014. Introducing the Index of Care: A web-based application supporting archaeological research into health-related care. *International Journal of Paleopathology* 6, 5–9.
Tilley, L., & M.F. Oxenham, 2011. Survival against the odds: Modelling the social implications of care provision to seriously disabled individuals. *International Journal of Paleopathology* 1(1), 35–42.
Times of Malta, 2009. '5000 year-old tombs under study in Kerċem', 10 Oct.
Tiné, S., 1960–1. Giacimenti dell'età del rame in Sicilia e la 'Cultura tipo Conca d'Oro'. Relazione preliminare degli scavi eseguiti ne quinquennio 1954–1959. *Bullettino di Paletnologia Italiana* 13, 113–37.
Tiné, S., 1962. Le tombe dell'eneolitico a Tranchina. *Kokalos* 13–14, 227–33.
Tiné, S., 1983. *Passo di Corvo e la civiltà neolitica del Tavoliere*. Genova: Sagep.
Tolman, D.E. & E.C. Stafne, 1967. Developmental bone defects of the mandible. *Oral Surgery, Oral Medicine, Oral Pathology* 24(4), 488–90.
Tommony, M.G., 1997. 'Mortuary Ritual and Temporal Development in Neolithic/Copper Age Malta – Spatial and Ideological Analysis using GIS at a Site Based Level.' Draft First Year PhD Report, University of Cambridge.
Tontisirin, K., G. Nantel & L. Bhattacharjee, 2002. Food-based strategies to meet the challenges of micronutrient malnutrition in the developing world. *Proceedings of the Nutrition Society* 61(2), 243–50.
Torpiano, A., 2004. The construction of the Megalithic temples, in *Malta Before History, the World's Oldest Free-Standing Architecture,* ed. D. Cilia. Malta: Miranda Publishers, 347–64.
Torpiano, A., 2011. The engineering of the prehistoric megalithic temples in Malta. *University of Malta Scholarly Works – FacBenAUD*. Malta, University of Malta.
Torres-Rouff, C. & M.A.C. Junqueira, 2006. Interpersonal violence in prehistoric San Pedro de Atacama, Chile: Behavioral implications of environmental stress. *American Journal of Physical Anthropology* 130(1), 60–70.
Torroni, A., H.-J. Bandelt, L. D'Urbano, P. Lahermo, P. Moral, *et al*., 1998. mtDNA analysis reveals a major late Paleolithic population expansion from Southwestern to Northeastern Europe. *American Journal of Human Genetics* 62(5), 1137–52
Townsend, G.C. & T. Brown, 1978. Inheritance of tooth size in Australian Aboriginals. *American Journal of Physical Anthropology* 48(3), 305–14.
Townsend, G.C., L.C. Richards, T. Brown, V.B. Burgess, G.R. Travan & J.R. Rogers, 1992. Genetic studies of dental morphology in South Australian twins, in *Structure, Function and Evolution of Teeth*, eds. P. Smith & E. Tchernov. London: Freund, 501–18.
Townsend, P., 1981. The structured dependency of the elderly: A creation of social policy in the twentieth century. *Ageing and Society* 1(1), 5–28.
Tozzer, A.M. (ed.), 1941. *Landa's Relacion de las Cosas de Yucatan: A Translation*. Cambridge (MA): Harvard University Press.
Trinkaus, E., S.E. Churchill & C.B. Ruff, 1994. Postcranial robusticity in Homo. II: Humeral bilateral asymmetry and bone plasticity. *American Journal of Physical Anthropology* 93(1), 1–34.
Trinkaus, E. & C.B. Ruff, 1989. Diaphyseal cross-sectional morphology and biomechanics of the Fond-de-Forêt 1 femur and the Spy 2 femur and tibia. *Anthropologie et Préhistoire* 100, 33–42.
Trinkaus, E. & C.B. Ruff, 1996. Early modern human remains from eastern Asia: The Yamashita-cho 1 immature postcrania. *Journal of Human Evolution* 30(4), 299–314.
Trinkaus, E. & C.B. Ruff, 1999. Diaphyseal cross-sectional geometry of Near Eastern middle Palaeolithic humans: The tibia. *Journal of Archaeological Science* 26(10), 1289–300.
Trinkaus, E., C.B. Ruff & S.E. Churchill, 1998. Upper limb versus lower limb loading patterns among Near Eastern Middle Paleolithic hominids, in *Neandertals and Modern Humans in Western Asia*, eds. T. Akazawa, K. Aoki & O. Bar-Yosef. New York (NY): Springer, 391–404.
Tripathi, S., R.D. Singh, S.V. Singh & D. Arya, 2014. Maxillary canine transposition – A literature review with case report. *Journal of Oral Biology and Craniofacial Research* 4(2), 155–8.
Trotter, M., 1934. Septal apertures in the humerus of American whites and Negroes. *American Journal of Physical Anthropology* 19(2), 213–27.
Trump, D.H., 1962. The origin of the Maltese temples. *Antiquity* 36(141), 59–60.
Trump, D.H., 1966. *Skorba.* (Research Reports of the Society of Antiquaries of London 22). Oxford: The Society of Antiquaries & The National Museum of Malta.
Trump, D.H., 1972. *Malta: an archaeological guide.* London: Faber and Faber.
Trump, D.H., 1976. The collapse of the Maltese temples, in *Problems in Economic and Social Archaeology*, eds. G. Sieveking, I.H. Longworth & K.E. Wilson. London: Duckworth, 605–10.
Trump, D.H., 1981. Megalithic architecture in Malta, in *The Megalithic Monuments of Western Europe*, ed. C. Renfrew. London: Thames & Hudson, 64–76.
Trump, D.H., 1983. *La grotta dei Filiestru a Bonu Ighinu, Mara (SS).* Sassari: Dessì.
Trump, D.H., 1990. *Nuraghe Noeddos and the Bonu Ighinu Valley. Excavation and Survey in Sardinia.* Oxford: Oxbow Books.
Trump, D.H., 1991. The nuraghi of Sardinia, territory and power: The evidence from the commune of Mara, Sassari, in *Papers of the Fourth Conference of Italian Archaeology 1. The Archaeology of Power, Part 1*, eds. E. Herring, R. Whitehouse & J.B. Wilkins. London: Accordia, 43–7.
Trump, D.H., 2002. *Malta: Prehistory and Temples*. Malta: Midsea Books.

Tunzi Sisto, A., 1990. Nuova miniera preistorica sul Gargano. *Atti Convegno Nazionale sulla Preistoria, Protostoria e Storia della Daunia* 12, 63–71.

Tunzi Sisto, A., 1999. *Ipogei della Daunia: Preistoria di un Territorio*. Foggia: Claudio Grenzi Editore.

Turner, B.L., G.D. Kamenov, J.D. Kingston & G.J. Armelagos, 2009. Insights into immigration and social class at Machu Picchu, Peru based on oxygen, strontium, and lead isotopic analysis. *Journal of Archaeological Science* 36, 317–32.

Turner II, C.G., 1967. Dental genetics and microevolution in prehistoric and living Koniag Eskimo. *Journal of Dental Research* 46(5), 911–17.

Turner II, C.G., 1985a. Dental evidence for the peopling of the Americas. *National Geographic Research Reports* 19, 573–96.

Turner II, C.G., 1985b. Expression count: A method for calculating morphological dental trait frequencies by using adjustable weighting coefficients. *American Journal of Physical Anthropology* 68(2), 263–8.

Turner II, C.G., 1987. Late Pleistocene and Holocene population history of East Asia based on dental variation. *American Journal of Physical Anthropology* 73(3), 305–22.

Turner II, C.G., 2000. Dental transfigurement and its potential for explaining the evolution of post-archaic Indian culture in the American Southwest. *Dental Anthropology* 14(1), 1–6.

Turner II, C.G., 2004. A second drilled tooth from prehistoric western North America. *American Antiquity* 69(2), 356–60.

Turner II, C.G. & J.D. Cadien, 1969. Dental chipping in Aleuts, Eskimos and Indians. *American Journal of Physical Anthropology* 31(3), 303–10.

Turner II, C.G. & L.M.C. Machado, 1983. A new dental wear pattern and evidence for high carbohydrate consumption in a Brazilian archaic skeletal population. *American Journal of Physical Anthropology* 61(1), 125–30.

Turner II, C.G., C.R. Nichol & G.R. Scott, 1991. Scoring procedures for key morphological traits of the permanent dentition: The Arizona State University dental anthropology system, in *Advances in Dental Anthropology*, eds. M.A. Kelley & C.S. Larsen. New York (NY): Wiley-Liss, 13–32.

Turner-Walker, G. & S. Mays, 2010. The archaeology of osteoporosis. *European Journal of Archaeology* 4(2), 263–9.

Tusa, S., 1999. *La Sicilia Nella Preistoria* (2nd edition). Palermo: Sellerio.

Tykot, R., 1996. Obsidian procurement and distribution in the central and western Mediterranean. *Journal of Mediterranean Archaeology* 9(1), 39–82.

Tykot, R., 2011. Obsidian finds on the fringes of the central Mediterranean: Exotic or eccentric exchange?, in *Exotica in the Prehistoric Mediterranean*, ed. A. Vianello. Oxford: Oxbow Books, 33–44.

Tyrrell, J., S.E. Jones, R. Beaumont, C.M. Astley, R. Lovell, H. Yaghootkar, *et al*., 2016. Height, body mass index, and socioeconomic status: Mendelian randomisation study in UK. *British Medical Journal* 352, e582.

Ubelaker, D.H., 1989. *Human Skeletal Remains: Excavation, Analysis, Interpretation*. Washington (DC): Taraxacum.

Ubelaker, D.H., 1997. Taphonomic applications in forensic Anthropology, in *Forensic Taphonomy: The Postmortem Fate of Human Remains*, eds. W.D. Haglund & M. Sorg. Boca Raton (FL): CRC Press, 77–90.

Ubelaker, D.H., T. Phenice & W. Bass, 1969. Artifical interproximal grooving of the teeth in American Indians. *American Journal of Physical Anthropology* 30(1), 145–50.

Uemura, S., M. Fujishita & H. Fuchihata, 1976. Radiographic interpretation of so-called developmental defect of mandible. *Oral Surgery, Oral Medicine, Oral Pathology, Oral Radiology* 41(1), 120–8.

Ungar, P.S., F.E. Grine, M.F. Teaford & A. Pérez-Pérez, 2001. A review of interproximal wear grooves on fossil hominin teeth with new evidence from Olduvai Gorge. *Archives of Oral Biology* 46(4), 285–92.

Valdiosera, C., T. Günther, J.C. Vera-Rodrígues, I. Ureña, E. Iriarte, *et al*., 2018. Four millennia of Iberian biomolecular prehistory illustrate the impact of prehistoric migrations at the far end of Eurasia. *Proceedings of the National Academy of Sciences* 115(13), 3428–33.

van Beek, G.C., 1983. *Dental Morphology. An Illustrated Guide* (2nd Edition). Cornwall: Wright.

van Reenen, J.F., 1977. Swallowtail form of tooth mutilation amongst early Iron Age people living at Broederstroom, Transvaal, *circa* 500 AD. *Journal of the Dental Association of South Africa* 32(9), 529–33.

van Reenen, J.F., 1978a. Tooth mutilating practices amongst the Ovambo and the West Caprivi Bushmen of South West Africa (Namibia). *Journal of the Dental Association of South Africa* 33, 665–71.

van Reenen, J.F., 1978b. Tooth mutilation amongst the peoples of Kavango and Bushmanland, South West Africa (Namibia). *Journal of the Dental Association of South Africa* 33(4), 205–18.

van Reenen, J.F., 1986. Tooth mutilating and extraction practices amongst the peoples of South West Africa (Namibia), in *Variation, Culture and Evolution in African Populations*, eds. R. Singer & J.K. Lundy. Johannesburg: Witwatersrand University Press, 159–69.

van Reenen, J.F. & S.J. Briedenhann, 1985. Tooth mutilating practices amongst the Damara of South West Africa (Namibia). *Journal of the Dental Association of South Africa* 40(9), 537–9.

van Rippen, B., 1917. Pre-Columbian operative dentistry of the Indians of Middle and South America. *The Dental Cosmos* 59(9), 861–73.

van Rippen, B., 1918a. Practices and customs of the African natives involving dental procedures. *Journal of the Allied Dental Sciences* 23, 1–23.

van Rippen, B., 1918b. Mutilations and decorations of teeth among the Indians of North, Central and South America. *Journal of the Allied Dental Societies* 13, 219–42.

van Rippen, B., 1918c. Dental procedures among the natives of Australia, Melanesia, Polynesia, and Micronesia. *Journal of the Allied Dental Societies* 13, 365–87.

van der Reijden, A.J., 2014. 'A Global Classification System for Cultural Dental Modification: Created and Assessed.' Unpublished M.A., University College London.

Varalli, A., J. Moggi-Cecchi & G. Goude. Evolution of the dietary patterns in Bronze Age Italy through stable isotopes analysis (Abstract). *American Journal of Physical Anthropology* 153 (S58), 260

Vassallo, P., 2010. The impact of changing fluoride concentrations in the water supplies in the Maltese islands on caries prevalence in 12-year-old Maltese schoolchildren. *Oral Health and Dental Management in Black Sea Countries* 9(4), 235–43.

Vegas, J.I., A. Armendariz, F. Etxeberria, M.S. Fernandez & L. Herrasti, 2012. Prehistoric violence in northern Spain: San Juan ante Portam Latinam, in *Sticks, Stones, and Broken Bones: Neolithic Violence in a European Perspective*, eds. R.J. Schulting & L. Fibiger. Oxford: Oxford University Press, 265–302.

Vehmas, S., K. Kristiansen & T. Shakespeare, 2009. *Arguing About Disability: Philosophical Perspectives.* Abingdon & New York (NY): Routledge.

Vella, A.J. & V. Borg, 1989. Changes in fluoride content of Maltese tap waters: Implications for oral health. *Maltese Medical Journal* 1(3), 14–17.

Vella, C., 2009. The lithic toolkit of late Neolithic Ta' Ħaġrat, Malta. *Origini* 31(4), 85–102.

Vella, C., 2016. Manipulated connectivity in island isolation: Maltese prehistoric stone tool technology and procurement strategies across the fourth and third millennia BC. *Journal of Island and Coastal Archaeology* 11, 1–20.

Vella Gregory, I., 2005. *The Human Form in Neolithic Malta*. Malta: Midsea.

Vella Gregory, I., 2016. Immensity and miniaturism: The interplay of scale and sensory experience in the Late Neolithic of the Maltese Islands. *Oxford Journal of Archaeology* 35(4), 329–44.

Ventura, F. & G. Agius, 2017. An investigation of the possible Equinox Alignment at Mnajdra, Malta. *Journal of Skyscape Archaeology* 3(1), 79–92.

Vianello, D., F. Sevini, G. Castellani, L. Lomartire, M. Capri & C. Franceschi, 2013. HAPLOFIND: A new method for high-throughput mtDNA haplogroup assignment. *Human Mutation* 34(9) 1189–94.

Vitale, T.D. & L.M. Fallat, 1990. Distal tibiofibular synostosis and late sequelae of an ankle sprain. *Journal of Foot Surgery* 29(1), 33–6.

Vodanović, M., I. Galić, M. Strujić, K. Peroš, M. Šlaus & H. Brkić, 2012. Orthodontic anomalies and malocclusions in Late Antique and Early Mediaeval period in Croatia. *Archives of Oral Biology* 57(4), 401–12.

Vodanović, M., M. Šlaus, I. Galić, M. Marotti & H. Brkić, 2009. Stafne's defects in two mandibles from archaeological sites in Croatia. *International Journal of Osteoarchaeology* 21(1), 119–26.

Volpato, V., R. Macchiarelli, D. Guatelli-Steinberg, I. Fiore, L. Bondioli & D.W. Frayer, 2012. Hand to mouth in a Neandertal: Right-handedness in Regourdou 1. *PLoS ONE* 7(8), e43949.

von Jhering, H., 1882. Die künstliche Deformierung der Zahne. *Zeitschrift für Ethnologie* 14(2), 213–62.

Wahl, J. & I. Trautmann, 2012. The Neolithic massacre at Talheim: A pivotal find in conflict archaeology, in *Sticks, Stones, and Broken Bones: Neolithic Violence in a European Perspective*, eds. R.J. Schulting & L. Fibiger. Oxford: Oxford University Press, 77–100.

Wajcman, J., 1991. *Feminism Confronts Technology*. Cambridge: Polity Press.

Waldron, T., 1987. The relative survival of the human skeleton: Implications for palaeopathology, in *Death, Decay, and Reconstruction: Approaches to Archaeology and Forensic Scienc*e, eds. A. Boddington, A.N. Garland & R.C. Janaway. Manchester: Manchester University Press, 55–64.

Waldron, T., 2008. *Palaeopathology*. Cambridge: Cambridge University Press.

Walker, A & R. Leakey, 1993. The postcranial bones, in *The Nariokotome Homo Erectus Skeleton*, eds. A. Walker & R. Leakey. Berlin: Springer, 95–160.

Wallace, I.J., J.M. Winchester, A. Su, D.M. Boyer & N. Konow, 2017. Physical activity alters limb bone structure but not entheseal morphology. *Journal of Human Evolution* 107, 14–18.

Wallduck, R. & S.M. Bello, 2016. Cutting decaying bodies: Micro-morphometric analysis of cut-marks on Mesolithic-Neolithic human remains from Lepenski Vir and Vlasac, Serbia. *Journal of Archaeological Science: Reports* 10, 703–14.

Walsh, S., C. Knusel & N. Melton, 2011. A re-appraisal of the Early Neolithic human remains excavated at Sumburgh, Shetland, in 1977. *Proceedings of the Society of Antiquaries of Scotland* 141, 3–17.

Walter, B.S. & S.N. DeWitte, 2017. Urban and rural mortality and survival in Medieval England. *Annals of Human Biology* 44(4), 338–48.

Warriner, A.H., N.M. Patkar, J.R. Curtis, E. Delzell, L. Gary, *et al*., 2011. Which fractures are most attributable to osteoporosis? *Journal of Clinical Epidemiology* 64(1), 46–53.

Warinner, C., J.F.M. Rodrigues, R. Vyas, C. Trachsel, N. Shved, *et al*., 2014. Pathogens and host immunity in the ancient human oral cavity. *Nature Genetics* 46(4), 336–44.

Warinner, C., C. Speller, M.J. Collins, 2015. A new era in palaeomicrobiology: Prospects for ancient dental calculus as a long-term record of the human oral microbiome. *Philosophical Transactions of the Royal Society B* 370(1660), 20130376.

Wasserzug, O., L. Valinsky, E. Klement, Y. Bar-Zeev, N. Davidovitch, *et al*., 2009. A cluster of ecthyma outbreaks caused by a single clone of invasive and highly infective Streptococcus pyogenes. *Clinical Infectious Diseases* 48(9), 1213–19.

Wasterlain, S.N., M.J. Neves & M.T. Ferreira, 2016. Dental modifications in a skeletal sample of enslaved Africans found at Lagos (Portugal). *International Journal of Osteoarchaeology* 26(4), 621–32.

Wasterlain, S.N. & A.M. Silva, 2010. Study of Stafne's defects in late Neolithic, late Roman, Medieval and modern skeletal samples from Portugal. *International Journal of Osteoarchaeology* 22(4), 423–34.

Waterman, A.J. & J.T. Thomas, 2011. When the bough breaks: Childhood mortality and burial practice in late Neolithic Atlantic Europe. *Oxford Journal of Archaeology* 30(2), 165–83.

Waters-Rist, A., V.I. Bazaliiskii, A. Weber, O.I. Goriunova & M.A. Katzenberg, 2010. Activity-induced dental modification in Holocene Siberian hunter-fisher-gatherers. *American Journal of Physical Anthropology* 143(2), 266–78.

Watrous, A.C., S.C. Anton & A.M. Ploudre, 1993. Hyperostosis frontalis interna in ancient Egyptians. *American Journal of Physical Anthropology* (S16), 205.

Watson, J.T. & C. García, 2017. Dental modification and the expansion and manipulation of Mesoamerican Identity into Northwest Mexico, in *A World View of Bioculturally Modified Teeth*, eds. S.E. Burnett & J.D. Irish. Gainesville (FL): University Press of Florida: 298–314.

Weinberger, B.W., 1948. *An Introduction to the History of Dentistry*. St Louis (MO): C.V. Mosby Co.

Weiss, K.M., 1973. Demographic models for anthropology. *Memoirs of the Society for American Archaeology* 27, i–ix, 1–186.

Weller, R.O., M.M. Sharp, M. Christodoulides, R.O. Carare & K. Møllgård, 2018. The meninges as barriers and facilitators for the movement of fluid, cells and pathogens related to the rodent and human CNS. *Acta Neuropathologica* 135(3), 363–85.

Wells, J.C.K. & J.T. Stock, 2011. Re-examining heritability: genetics, life history and plasticity. *Trends in Endocrinology & Metabolism* 22(10), 421–8.

Wells, J.C.K. & J.T. Stock, 2020. Life history transitions at the origins of agriculture: A model for understanding how niche construction impacts human growth, demography and health. *Frontiers in Endocrinology* 11: 325.

Werner, A., 1906. *The Natives of British Central Africa*. London: A. Constable and Company.

Western, A.G. & J.J. Bekvalac, 2017. Hyperostosis frontalis interna in female historic skeletal populations: Age, sex hormones and the impact of industrialization. *American Journal of Physical Anthropology* 162(3), 501–15.

Weston, D.A., 2008. Investigating the specificity of periosteal reactions in pathology museum specimens. *American Journal of Physical Anthropology* 137(1), 48–59.

Weston, D.A., 2009. Brief communication: Paleohistopathological analysis of pathology museum specimens: Can periosteal reaction microstructure explain lesion etiology? *American Journal of Physical Anthropology* 140(1), 186–93.

Weston, D.A., 2012. Nonspecific infection in paleopathology: Interpreting periosteal reactions, in *A Companion to Paleopathology*, ed. A.L. Grauer. Oxford: Wiley-Blackwell, 492–512.

Weyrich, L.S., K. Dobney & A. Cooper, 2015. Ancient DNA analysis of dental calculus. *Journal of Human Evolution* 79, 119–24.

Whaites, E. 2007. *Dental Radiography and Radiology* (4th Edition). Edinburgh: Churchill Livingstone Elsevier.

White, A.A., 2014. Mortality, fertility, and the OY ratio in a model hunter-gatherer system. *American Journal of Physical Anthropology* 154(2), 222–31.

White, C.D., F.J. Longstaffe, M.W. Spence & K.R. Law, 2000. Teotihuacan state representation at Kaminaljuyu: evidence from oxygen isotopes. *Journal of Anthropological Research* 56, 535–58.

White, C.D., M.W. Spence, H.L.Q. Stuart-Williams & H.P. Schwarcz, 1998. Oxygen isotopes and the identification of geographical origins: the Valley of Oaxaca versus the Valley of Teotihuacan. *Journal of Archaeological Science* 25, 643–55.

White, C.D., M.W. Spence, F.J. Longstaffe & K.R. Law, 2004. Demography and ethnic continuity in the Tlailotlacan enclave of Teotihuacan: the evidence from stable oxygen isotopes. *Journal of Anthropological Archaeology* 23, 385–403.

White, T.D., 1992. *Prehistoric Cannibalism at Mancos 5MTUMR-2346*. Princeton (NJ): Princeton University Press.

White, T.D., 2000. *Human Osteology* (2nd edition). San Diego: Academic Press.

White, T.D., M.T. Black & P.A. Folkens, 2012. *Human Osteology* (3rd edition). Burlington (MA): Elsevier

White, T.D., D. Degusta, G.D. Richards & S.G. Baker, 1997. Prehistoric dentistry in the American Southwest: A drilled canine from Sky Aerie, Colorado. *American Journal of Physical Anthropology* 103(3), 409–14.

White, T.D. & P.A. Folkens, 2005. *The Human Bone Manual*. Burlington (VT): Elsevier

Whitehouse, R., 1972. The rock-cut tombs of the central Mediterranean. *Antiquity* 46(184), 275–81.

Whitehouse, R., 1992. *Underground Religion: Cult and Culture in Prehistoric Italy.* London: Accordia Research Institute.

Whitehouse, R. & C. Renfrew, 1974. The Copper Age of Peninsular Italy and the Aegean. *The Annual of the British School at Athens* 69, 343–90.

Whittle, A. & M. Wysocki, 1998. Parc le Breos Cwm transepted long cairn, Gower, West Glamorgan: Date, contents and contexts. *Proceedings of the Prehistoric Society* 64, 139–82.

Whittlesey, H.G., 1935. History and development of dentistry in Mexico. *Journal of the American Dental Association* 22(6), 989–95.

Wickham, H., 2016. *ggplot2: Elegant Graphics for Data Analysis*. New York (NY): Springer.

Wiemels, J., M. Wrensch & E.B. Claus, 2010. Epidemiology and etiology of meningioma. *Journal of Neuro-oncology* 99(3), 307–14.

Williams, J.S. & C.D. White, 2006. Dental modification in the Postclassic population from Lamanai, Belize. *Ancient Mesoamerica* 17(1), 139–51.

Willis, M.S., L.E. Harris & P.J. Hergenrader, 2008. On traditional dental extraction: Case reports from Dinka and Nuer en route to restoration. *British Dental Journal* 204, 121–4.

Willis, A. & M. Oxenham, 2013. The Neolithic demographic transition and oral health: The Southeast Asian experience. *American Journal of Physical Anthropology* 152(2), 197–208.

Wood, J.W., G.G. Milner, H.C. Harpending & K.M. Weiss, 1992. The osteological paradox: Problems of inferring prehistoric health from skeletal samples. *Current Anthropology* 33(4), 343–70.

Wood, N.K. & P.W. Goaz, 1997. *Differential Diagnosis of Oral and Maxillofacial Lesions*. St. Louis (MO): Mosby.

Woolf, A.D. & A. St John Dixon, 1988. *Osteoporosis: A Clinical Guide*. London: Martin Dunitz.

World Health Organisation, 1978. *Application of the International Classification of Diseases to Dentistry and Somatology (ICD-DA)*. Geneva: World Health Organisation.

Wright, L.E., 2005. Identifying immigrants to Tikal, Guatemala: Defining local variability in strontium isotope ratios of human tooth enamel. *Journal of Archaeological Science* 32, 555–66.

Wright, L.E. & H.P. Schwarcz, 1998. Stable carbon and oxygen isotopes in human tooth enamel: identifying breastfeeding and weaning in prehistory. *American Journal of Physical Anthropology* 106, 1–18.

Wright, L.E. & M.A. Vasquez, 2003. Estimating the length of incomplete long bones: Forensic standards from Guatemala. *American Journal of Physical Anthropology* 120(3), 233–51.

Wright, S., 1943. Isolation by distance. *Genetics* 28(2), 114–38.

Wysocki, M. & A. Whittle, 2000. Diversity, lifestyles and rites: New biological and archaeological evidence from British Earlier Neolithic mortuary assemblages. *Antiquity* 74(285), 591–601

Yabe, T., T. Tsuda, S. Hirose & T. Ozawa, 2012. Comparison of pediatric and adult nasal fractures. *Journal of Craniofacial Surgery* 23(5), 1364–6.

Yamakawa, K., K. Mizutani, M. Takahashi, M. Matsui & T. Mezaki, 2006. Hyperostosis frontalis interna associated with hypogonadism in an elderly man. *Age and Ageing* 35(2), 202–3.

Yap, F.Y., M.R. Skalski, D.B. Patel, A.J. Schein, E.A. White, *et al*., 2017. Hypertrophic osteoarthropathy: Clinical and imaging features. *RadioGraphics*, 37(1), 157–95.

Yoshiga, N., R. Tomita, H. Fuyamada & M. Kaway, 1973. A case report of latent bone cyst including lymphatic tissue. *Japanese Journal of Oral and Maxillofacial Surgery* 19, 714–15.

Young, R., 1957. Postnatal growth of the frontal and parietal bones in white males. *American Journal of Physical Anthropology* 15(3), 367–86.

Yuen, D.E., H.H. Draper & G. Trilok, 1984. Effect of dietary protein on calcium metabolism in man. *Nutrition Abstracts and Reviews* 54, 447–59.

Zahra, E.V. & P. Vassallo, 2011. Dental fluorosis among schoolchildren in Gozo, Malta. *Oral Health and Dental Management* 10(2), 93–9.

Zammit, T., 1909–1912. 'Archaeological Field Notebook 3 (1909-1912).' Unpublished manuscript, Valletta, National Museum of Archaeology.

Zammit, T., 1910. *The Ħal-Saflieni Prehistoric Hypogeum at Casal Paula, Malta.* (The Small Objects and the Human Skulls found in the Ħal-Saflieni Prehistoric Hypogeum, etc.) First report. Malta: Government of Malta.

Zammit, T., 1912a. The inhabitants of the Maltese islands. *Archivum Melitense* 1, 235–46.

Zammit, T., 1912b. A Neolithic grave in Malta. *Archivum Melitense* 1(7), 113–14.

Zammit, T., 1916. The Ħal Tarxien Neolithic Temple, Malta. *Archaeologia* 67, 127–44.

Zammit, T., 1917. Second Report on the Ħal Tarxien Excavations, Malta. *Archaeologia* 68, 263–84.

Zammit, T., 1920. Third Report on the Ħal Tarxien Excavations, Malta. *Archaeologia* 70, 179–200.

Zammit, T., 1924–25. Archaeological Field Notebook 8 (1924–25). Unpublished, National Museum of Archaeology, 33–5.

Zammit, T., 1925. *The Ħal Saflieni Hypogeum 'Casal-Paula – Malta'. A Short Description of the Monument with Plan and Illustrations*. Malta: Empire Press.

Zammit, T., 1926a. *The Ħal Saflieni Neolithic Hypogeum – at Casal Paula-Malta. A Short Description of the Monument with Plan and Illustrations.* Valletta, Empire Press.

Zammit, T., 1926b. 'Archaeological Field Notebook 8 (1926).' Unpublished manuscript, Valletta, National Museum of Archaeology.

Zammit, T., 1928. The Maltese rock-tombs. *The Antiquaries Journal* 8 (4), 478–84.

Zammit, T., 1930. *Prehistoric Malta, The Tarxien Temples*. Oxford: Oxford University Press.

Zammit, T., T.E. Peet & R.N. Bradley, 1912. *The Small Objects and the Human Skulls found in the Ħal Saflieni Prehistoric Hypogeum at Casal Paula, Malta.* Second report. Malta: Government of Malta.

Zapletal, J. R.E. Hekster, J.S. Straver & J.T. Wilmink, 1995. Atlanto-odontoid osteoarthritis. Appearance and prevalence at computed tomography. *Spine* 20(1), 49–53.

Zeder, M.A., E. Emshwiller, B.D. Smith & D.G. Bradley, 2006. Documenting domestication: The intersection of genetics and archaeology. *Trends in Genetics* 22(3), 139–55.

Zhou, J., Y.F. Zhao & L. Jiang, 2012. Periodontitis with hypercementosis: Report of a case and discussion of possible aetiologic factors. *Australian Dental Journal* 57(4), 511–14.

Živanović, S., 1982. *Ancient Diseases: The Elements of Palaeopathology*, trans. L.F. Edwards. London: Methuen Publishing Ltd.

Zoubov, A.A. & N. Haldeyeva, 1979. *Ethnic Odontology of the USSR.* Moscow: Nauka.

Zwemer, T.J., 1993. *Boucher's Clinical Dental Terminology*. St Louis (MO): Mosby.

1000 Genomes Project Consortium, A. Auton, L.D. Brooks, R.M. Durbin, E.P. Garrison, H.M. Kang, *et al*., 2015. A global reference for human genetic variation. *Nature* 526, 68–74.

Appendix 1

Archive images from the 1987–94 campaign

Figure A1.1. *The lower field below the Circle in 1987 with a view southeast towards Malta. This was the daily route to the excavation through the gap in the rubble wall to the right.*

Figure A1.2. *View to the southeast towards the excavation of the rock-cut tomb in 1989. The upper levels of 'Area H' are still unexcavated and full importance of the site yet to be realised.*

Figure A1.3. *Rock-cut tomb under excavation, with Bridget Trump in the entrance to the West chamber in 1988.*

Figure A1.4. *Caroline Malone excavating within the West chamber of the rock-cut tomb in 1988, exposing human remains deposited in an ochred matrix.*

Figure A1.5 *(above). Assemblage of human remains and ceramic sherds under excavation in the East chamber of the rock-cut tomb. Traces of pot containing solid lumps of red ochre to the left.*

Figure A1.6 *(left). Large ceramic Żebbuġ sherd surrounded by red ochre and fragmented human remains in the East chamber, 1988.*

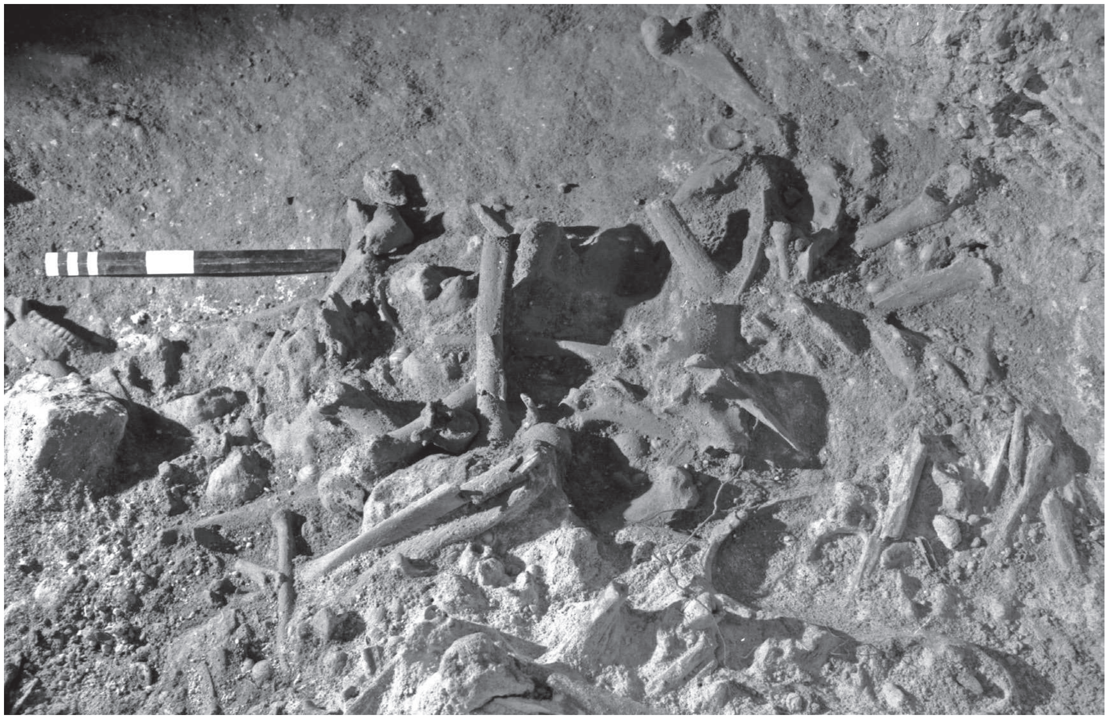

Figure A1.7. *Deposit of commingled human and faunal remains in the rock-cut tomb.*

Figure A1.8. *Group of disarticulated human remains towards the edge of the West chamber, in Context (276), including long bones, crania and os coxae, 1988.*

Figure A1.9. *Group of fragmented human remains in the rock cut tomb West chamber, including at least two mandibles and several cranial fragments.*

Figure A1.10. *Large triton shell against ceramic sherd below the entrance to the rock cut tomb East chamber.*

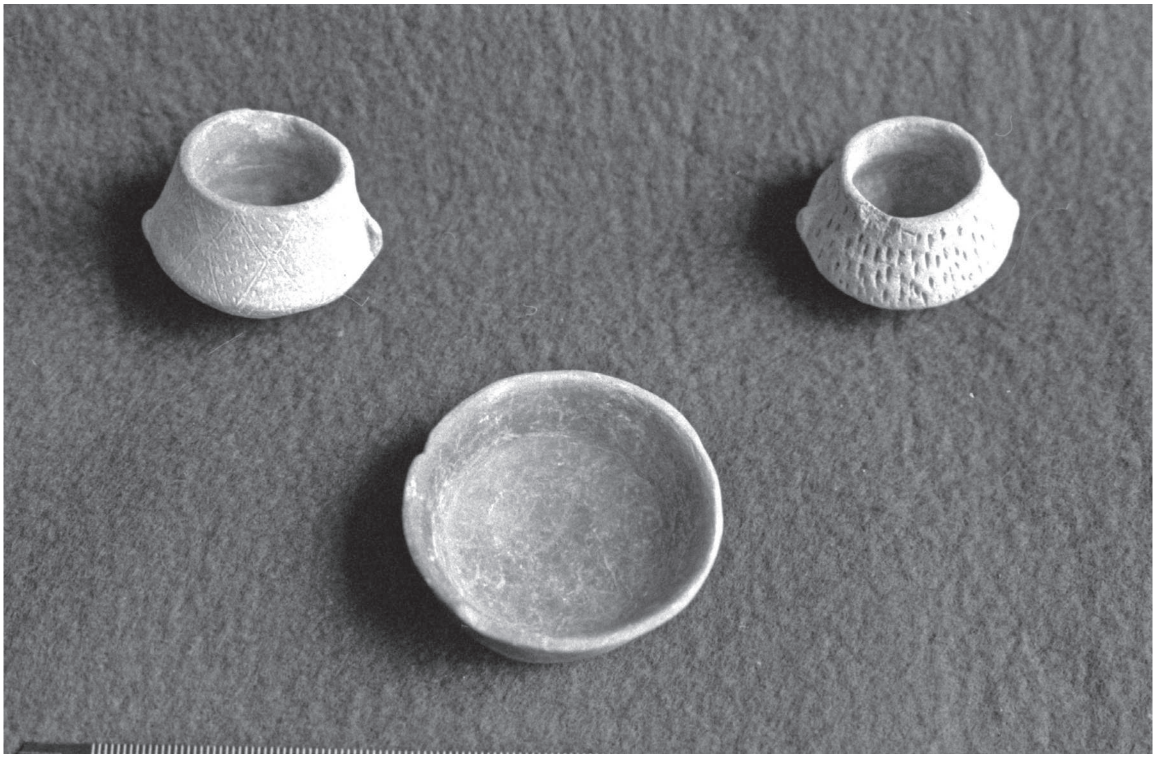

Figure A1.11. *Miniature Saflieni phase ochre pots from the Circle.*

Figure A1.12. *Mikiel Bartolo, the elderly tenant farmer, visiting the Circle during excavation in 1988.*

Figure A1.13. *View to the northeast in 1989, overlooking early excavation of the East Cave and rock-cut tomb.*

Figure A1.14. *Context (354) in the upper level of the North bone pit adjacent to the threshold, comprising a deposit of fragmented and disarticulated human remains.*

Figure A1.15 *(right). Context (622) in the mid-levels of the North bone pit, with some intact articulated regions visible, including most of a right foot above the scale bar.*

Figure A1.16 *(below). Context (622) with disarticulate bone elements and an articulated hand at the centre of the image.*

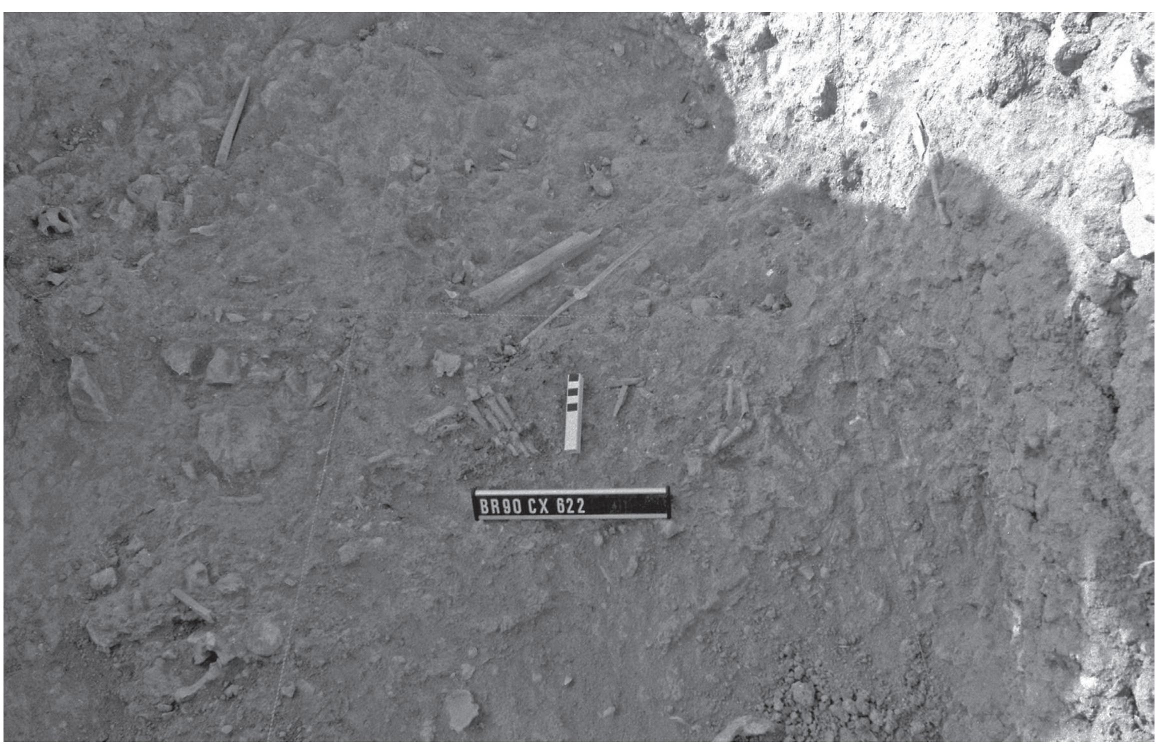

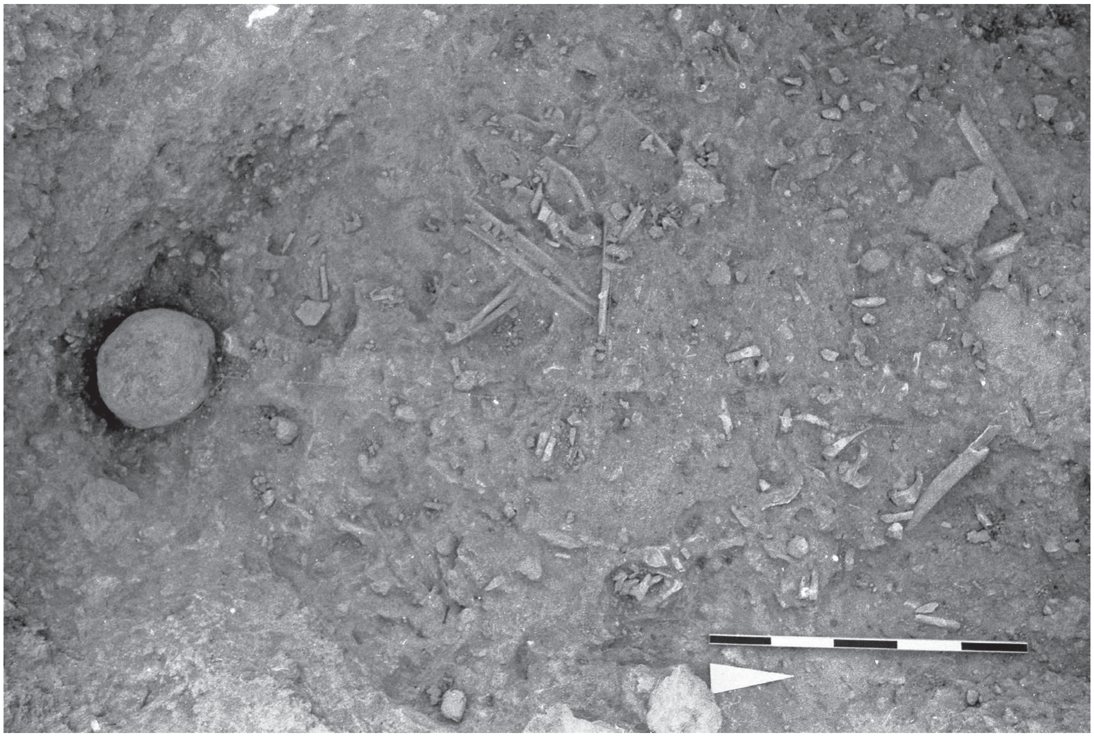

Figure A1.17. *Context (622) or (623) in the mid-levels of the North bone pit. Some articulated elements are visible, such as the paired long bones in the centre and skull set against the cave wall.*

Figure A1.18. *A fragment of right ilium is articulated with a femur and patella in Context (799) in the lower levels of the North bone pit.*

Figure A1.19. *The undisturbed remains of an adult male deposited on his left side in a flexed position are exposed in the base levels of the North bone pit.*

Figure A1.20. *Excavation in 1993 showing upper levels in the 'Shrine' area, exposing the external southern screen and the stone bowl. From the South, the screen effectively shields the bowl from view. The Display area, containing Context (783), is visible to the left.*

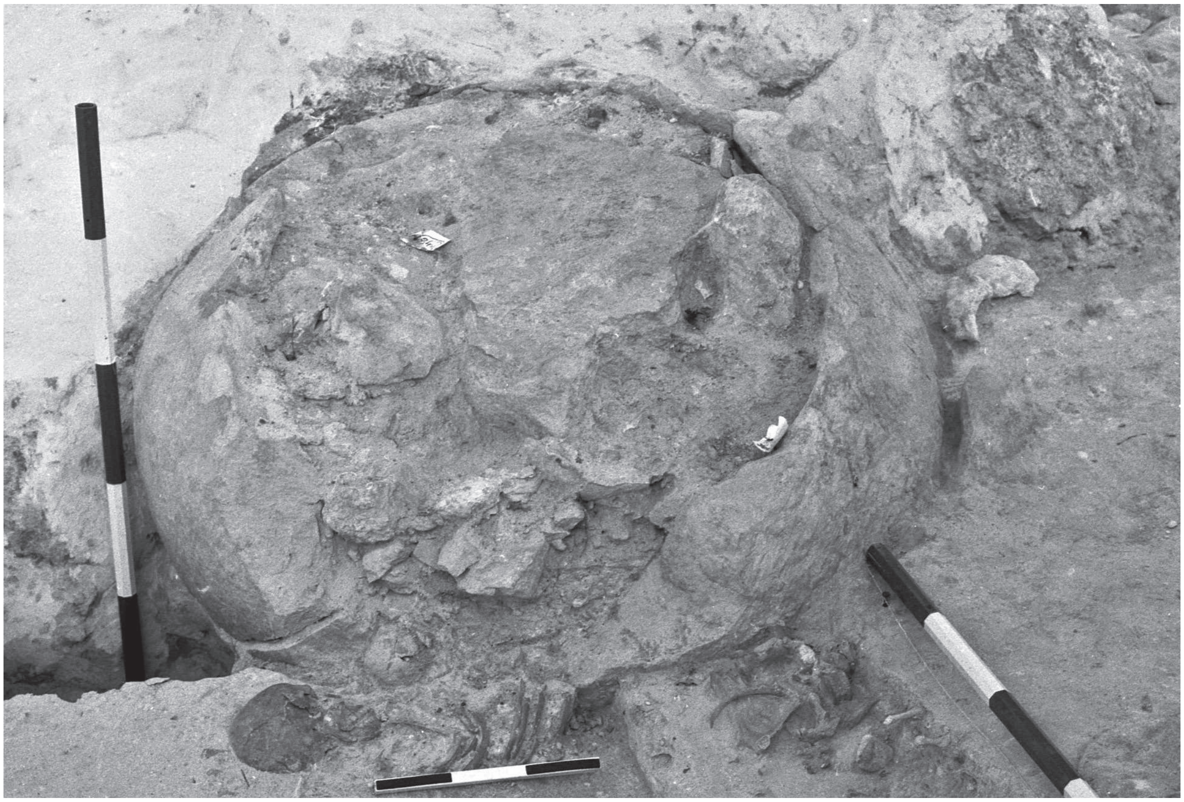

Figure A1.21 *(above). The stone bowl (841) prior to excavation, with some human remains within (Context 842) and surrounding the exposed bowl (Context 1206), and showing the smashed upper level.*

Figure A1.22 *(left). Articulated and nearly complete hand preserved at the base of the stone bowl in Context (842).*

Figure A1.23. *Twin-seated figure (SF743) and ceramic strainer* in situ *in Context (831).*

Figure A1.24. *Figurine cache (SF784) under excavation in Context (831) by conservator Carol Brown, 1991.*

Figure A1.25. *Figurine cache (SF784) fully excavated and* in situ *in Context (831), 1991.*

Figure A1.26. *Context (960) under excavation in the upper levels of the 'Shrine', with the robbed-out trench (1102, 1113) of the East screen visible in the centre.*

Figure A1.27. *Articulated and almost complete infant skeleton in Context (960).*

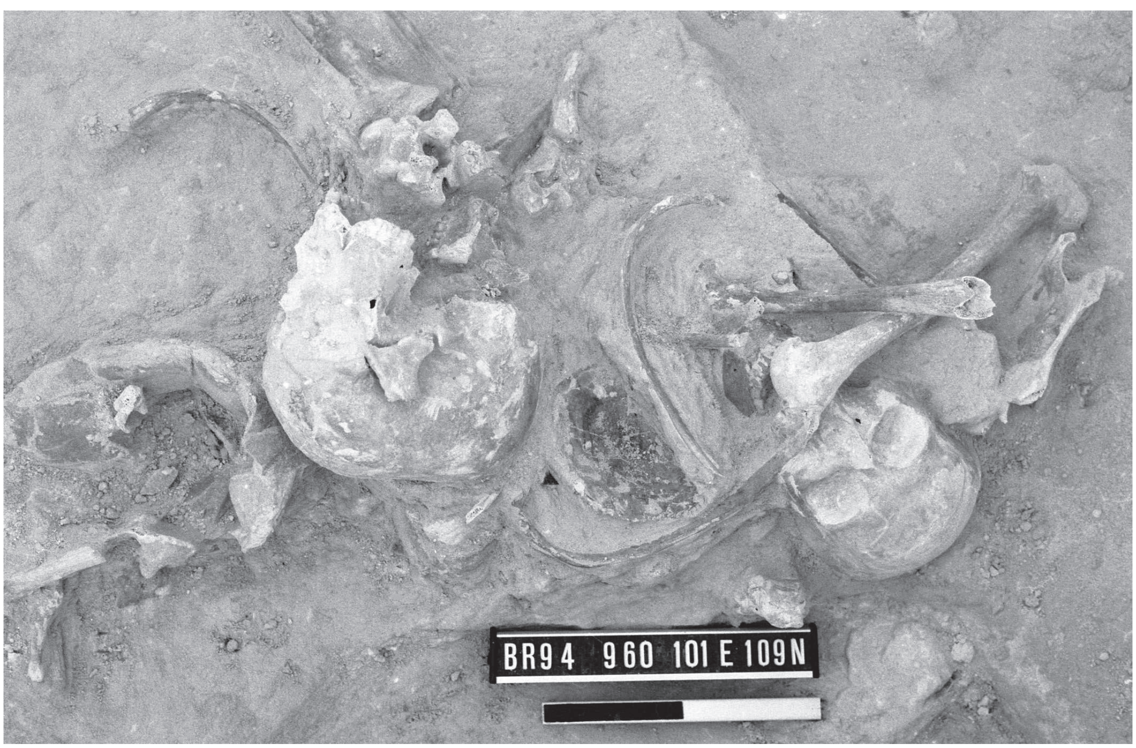

Figure A1.28. *Row of crania and skulls deposited in varying positions in Context (960), alongside long bones, ribs, and vertebrae.*

Figure A1.29. *Pit deposit (Contexts 980/979) in the upper level of the 'Shrine', containing disarticulated elements, principally long bones and a skull arranged east-west along the centre.*

Figure A1.30. *Context (1206) in the mid-level of the 'Shrine', exposing articulated regions of adult skeletons. An articulated and semi-complete pelvic girdle is visible centre-left of the image, with flexed legs leading into the section. In the foreground is a left scapula, articulated ribs and left arm, with a right arm extending toward the right section and overlying a large pot.*

Figure A1.31 *(above). Most of an articulated adolescent skeleton (epiphyses of the proximal femur, proximal tibia and distal tibia are all unfused or fusing) exposed within Context (1206). A further thoracic region is visible to the left of the upper legs.*

Figure A1.32 *(left). Semi-articulated thoracic region, pelvic girdle and upper legs of an adult skeleton with a large pot; the skull and upper limbs are missing.*

Figure A1.33 *(above). Articulated and nearly complete infant skeleton in Context (1206).*

Figure A1.34 *(left). Discrete bone group in Context (1206) containing disarticulated long bones, ribs, vertebrae, a cranium and, in the centre, a mandible surrounding a cluster of loose teeth.*

Figure A1.35 *(left). In the lower levels of the 'Shrine', in Context (1268), an articulated adult skeleton in a flexed position on their right side is exposed, with the upper arms and cephalic extremity extending into the section. Their right femur overlies a large pot. An articulated right humerus and ulna are carefully placed between the leg and the pot. In the foreground are further long bones and an inverted pelvic girdle.*

Figure A1.36 *(below). At the base of the 'Shrine, in Context (1328), were a series of tightly clustered deposits interpreted as 'bundle burials', including this male adult oriented in an east-west direction. The arms are flexed and extend in front of the cranium, but other elements appear disarranged and fragmented.*

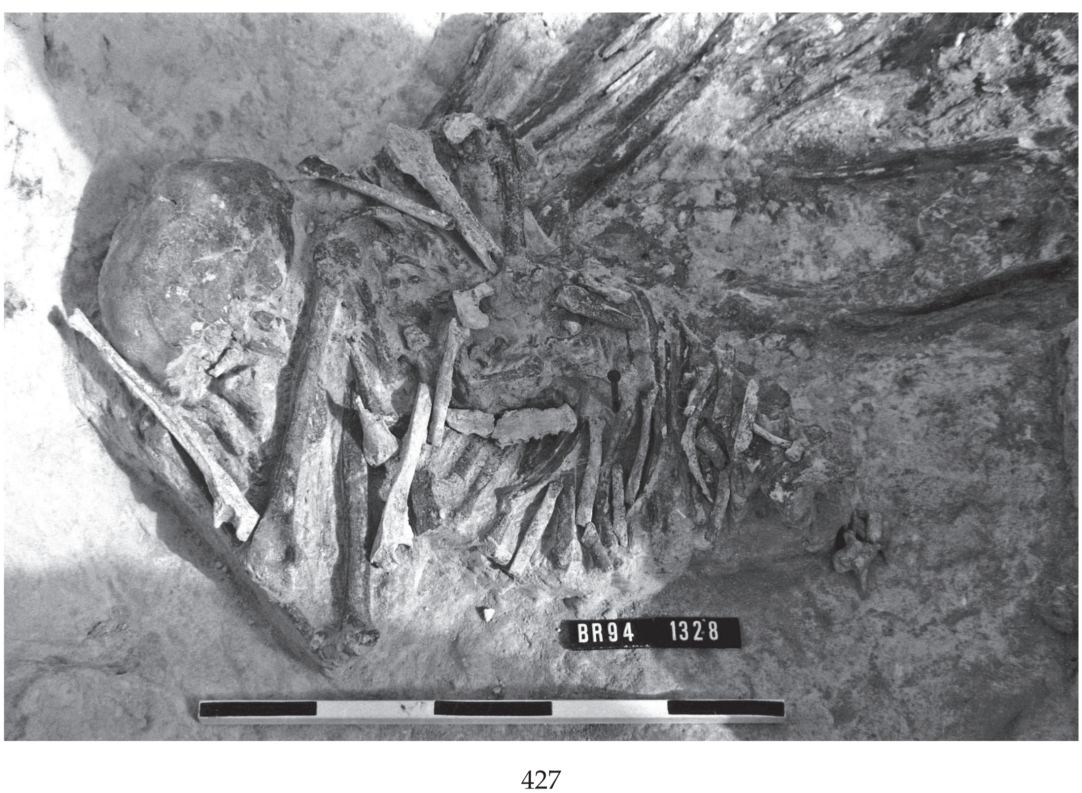

Figure A1.37. *Miniature figurine (SF516) carved into a medial phalanx of Ovis/Capra, from Context (431) in the West Cave (see finger tips for scale).*

Figure A1.38. *North Niche (to the bottom) viewed from the north, with broken Globigerina megalithic slabs (877) separating the area from the Deep Zone.*

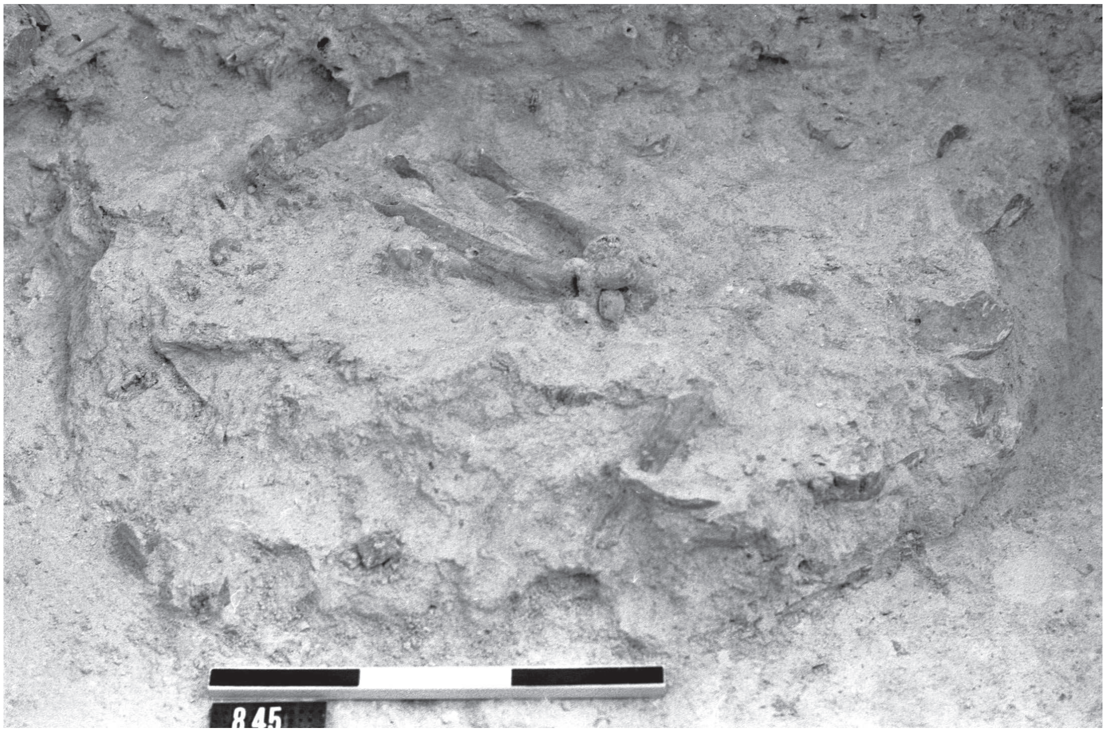

Figure A1.39. *The fragmentary and disarticulated deposit of Context (845) in the North Niche including an almost complete articulated leg was uncovered.*

Figure A1.40. *Deposit (863) with semi-articulated ochred burial resting against megalith (878) in the North Niche.*

Figure A1.41. *19th-century dog burial in Context (920) at the base of the pit excavated by Bayer.*

Figure A1.42. *Dense deposit of mostly disarticulated bones in Context (933) in the upper levels of the Deep Zone.*

Figure A1.43. *Contexts (951) and (1144), the major bone deposits in the Deep Zone, under excavation. Abutting megaliths, to the top of the image, the deposit was densely packed with bone within a solid clay-silt matrix.*

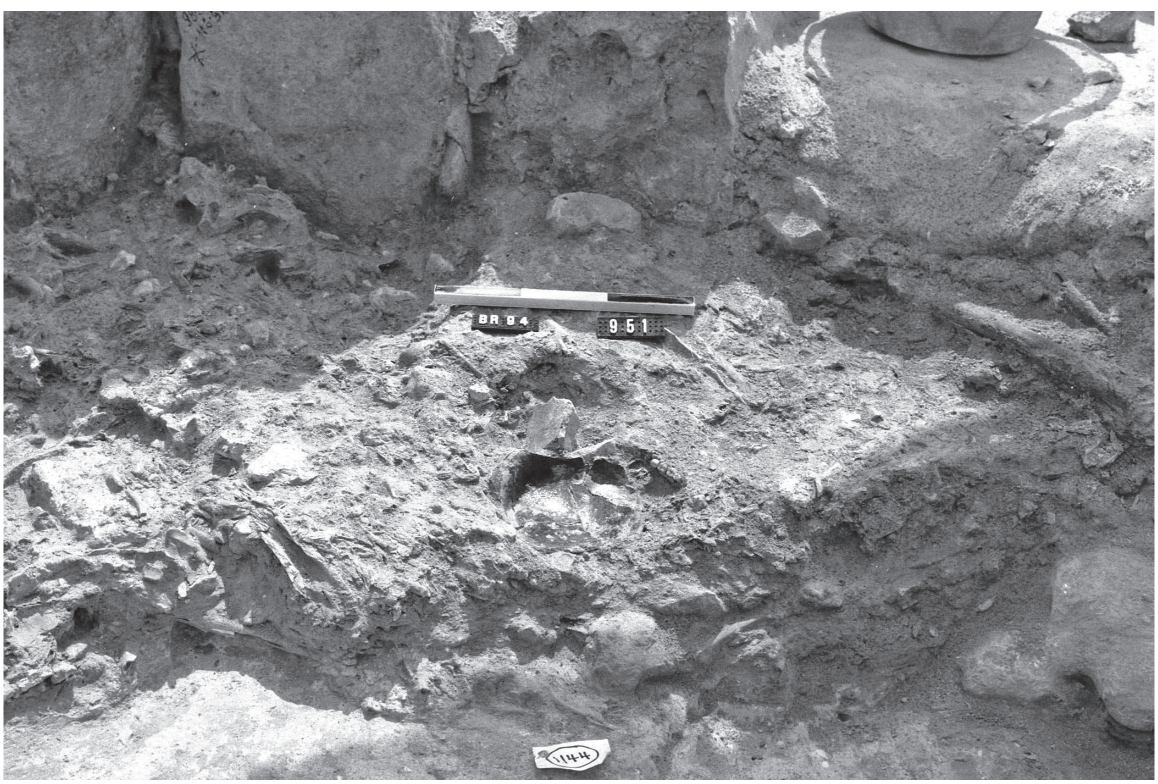

Figure A1.44. *Fragmented deposits of disarticulated bone in Context (951), showing depth of bone dumps.*

Figure A1.45 *(left). Bone group in Context (951) including ribs, fragmented long bones and several articulated vertebrae to the top of the image.*

Figure A1.46 *(below). Group of fragmented crania in Context (951), deposited in varying positions and interspersed with other elements.*

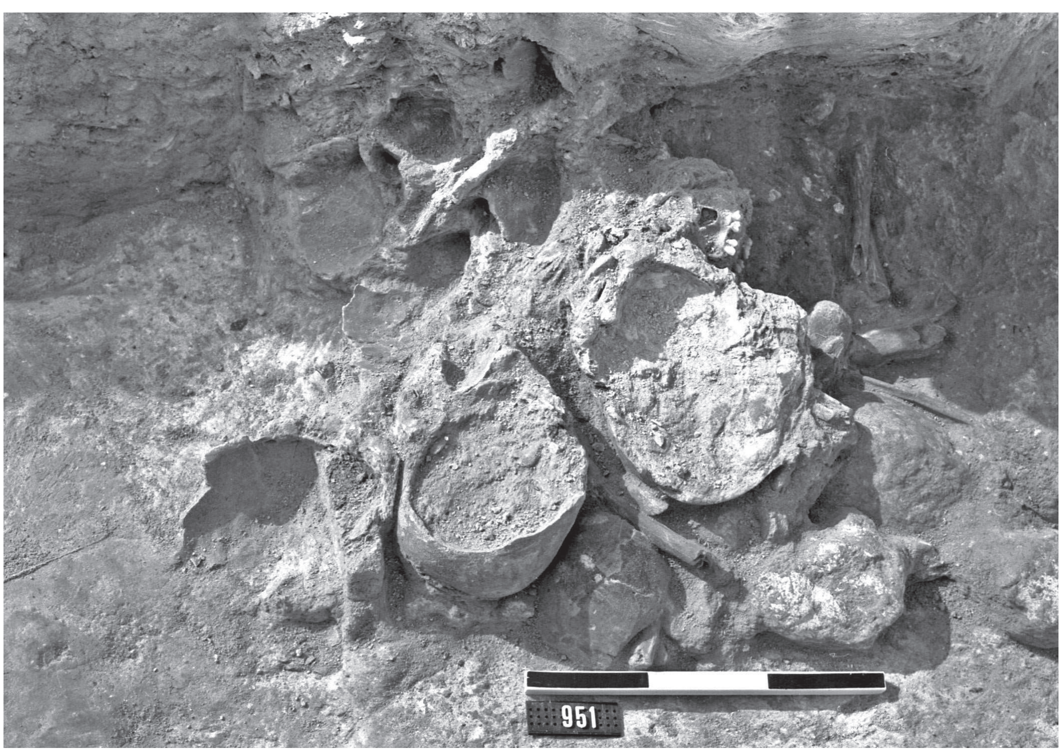

Figure A1.47. *Semi-articulated lower leg and foot in Context (1257) in the lower levels of the Deep Zone, with other elements scattered at the base of the pit and visible in the section.*

Figure A1.48. *Small limestone figurine (SF1184) from Context (474) in the upper level of the Display Zone.*

Figure A1.49. *Figurine SF775* in situ *during excavation of Context (783) in the Display Zone, viewed as found in 95.26E/ 110N.*

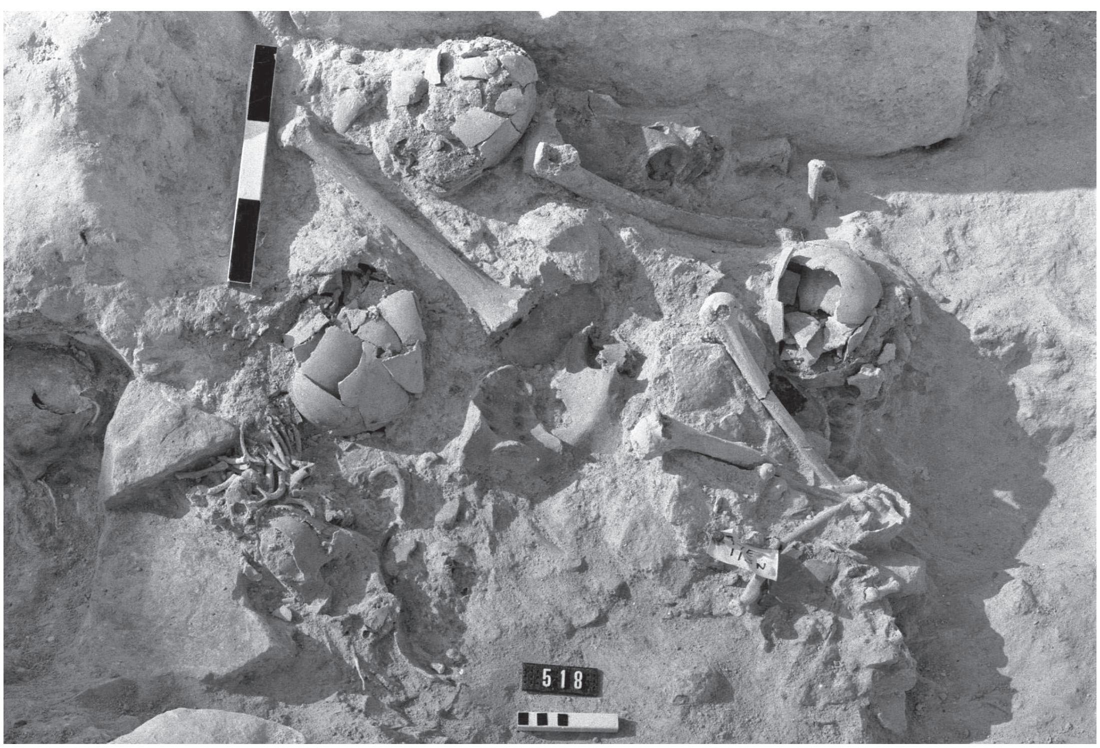

Figure A1.50. *Context (518) in the West niche, adjacent to the Display Zone, exposing a deposit predominantly including long bones and fragmented crania.*

Figure A1.51. *Upper levels of Context (783), in the Display Zone, under excavation in 1991.*

Figure A1.52. *Cranial cluster and various other elements abutting a megalith in Context (518).*

Figure A1.53. *Articulate ribs and column in Context (783).*

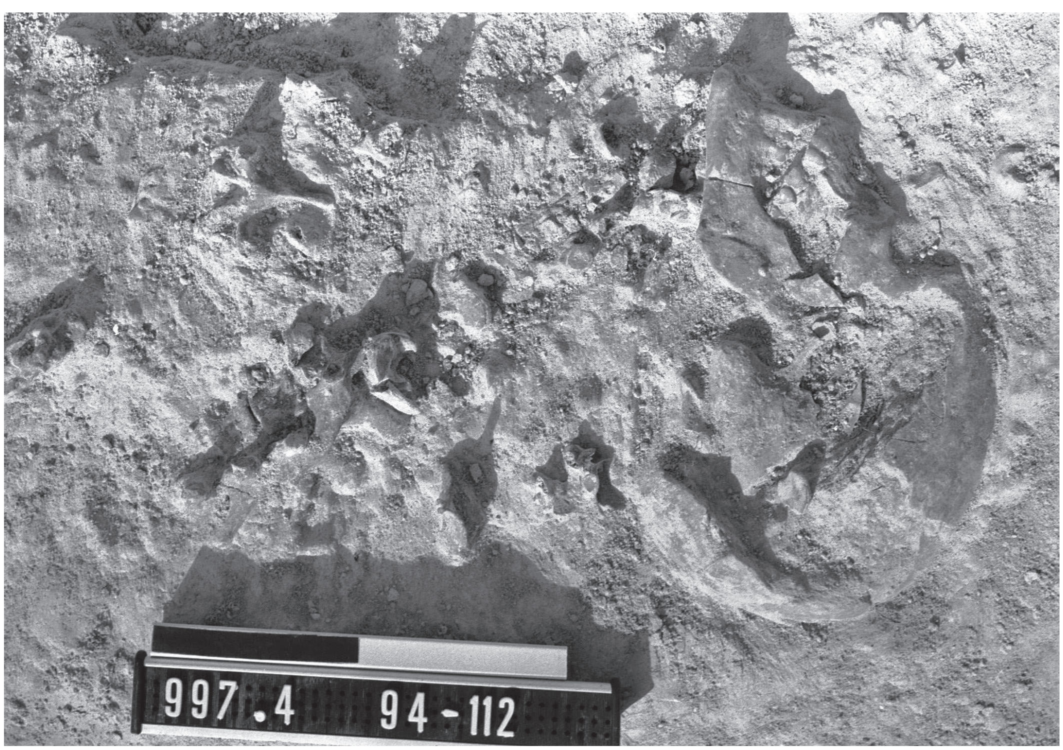

Figure A1.54. *Context (997), spit 4, in the West niche, exposing the skull and articulated cervical vertebrae of an adult individual.*

Figure A1.55: *Semi-articulated skull and torso (possibly consistent with the arm in the foreground) of an adult female in Context (518) in the upper level of the Display area (783)(visible on plan in Fig. 8.60:A, see Stoddart et al. 2009, 159).*

Figure A1.56. *Adult skull adjacent to an articulated infant lower arm and hand in Context (783).*

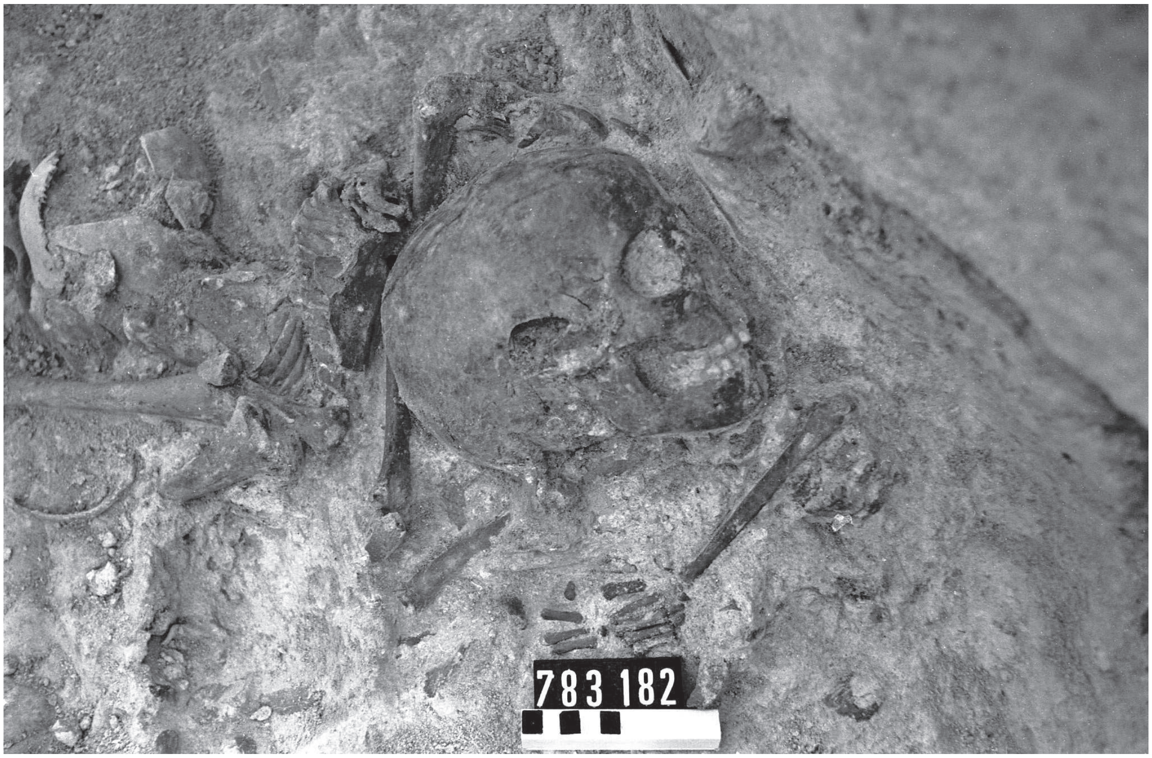

Figure A1.57. *Articulated skull with cervical, thoracic and lumbar vertebrae in Context (783) in the Display Zone.*

Figure A1.58. *Articulated thoracic region in Context (783).*

Figure A1.59. *Articulated right lower leg and foot in Context (783), with further articulated long bones at top of image.*

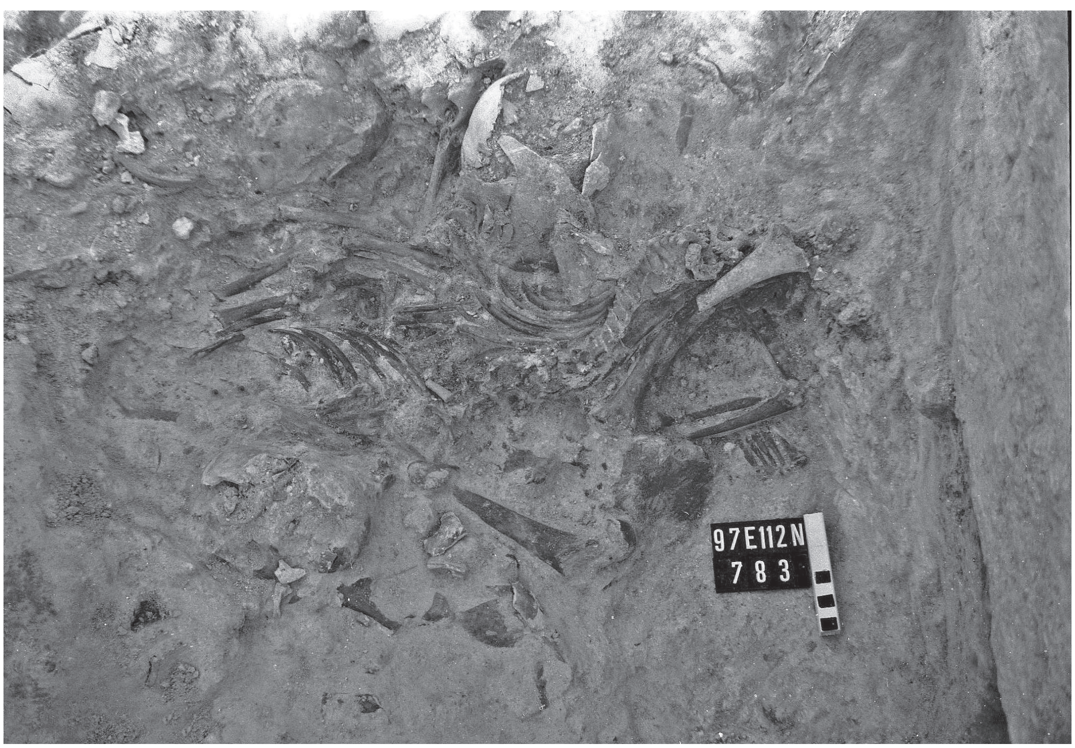

Figure A1.60. *Deposit of disarticulated and semi-articulated remains in Context (783) in the Display Zone, including numerous ribs in anatomical position.*

Figure A1.61. *Semi-articulated adult individual in Context (783), preserved above the pelvis and deposited in a prone position. The right arm is extended laterally and flexed at the elbow with the hand placed beneath the torso, and the left arm is parallel to the torso, flexed at the elbow and extends superiorly.*

Figure A1.62. *Semi-articulated torso with ribs and femurs associated in Context (783).*

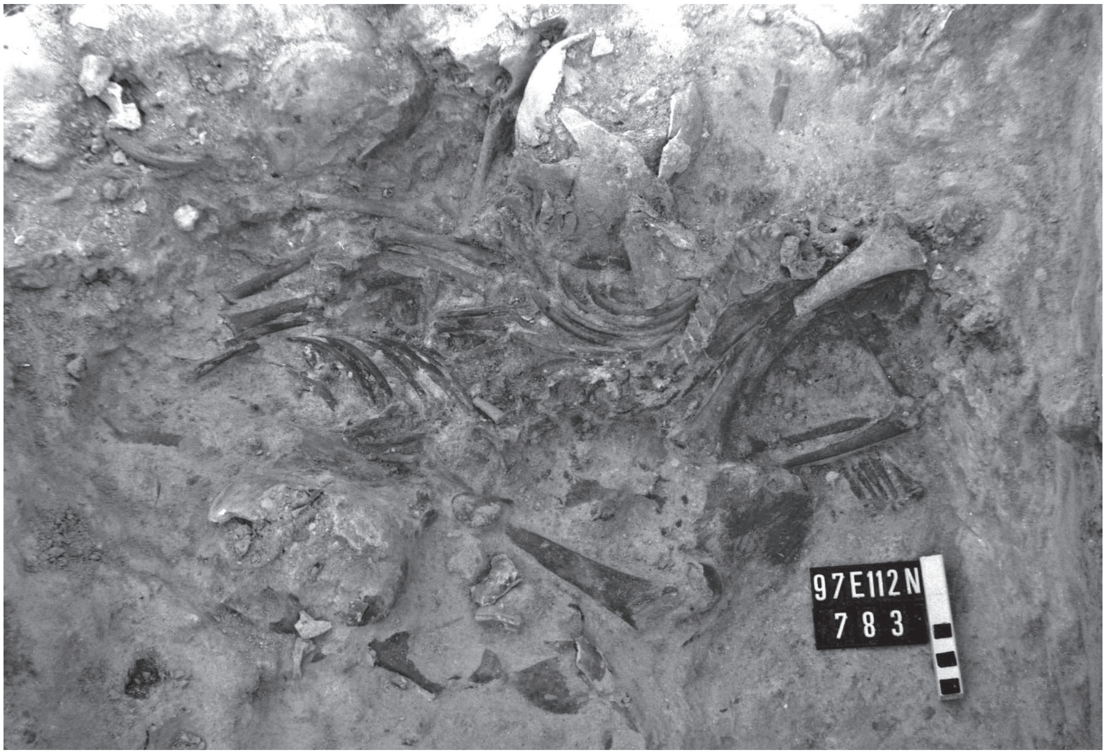

Figure A1.63. *Deposit under excavation in Context (783) 97E/112N, revealing a mixture of semi-articulated skeletal regions and disarticulated bones. Note the articulated segment of vertebrae in the centre, as well as several sets of ribs, paired long bones, and right metatarsals above the placard in the bottom right.*

Figure A1.64. *Figurine SF788* in situ *during excavation of Context (783) in the Display Zone.*

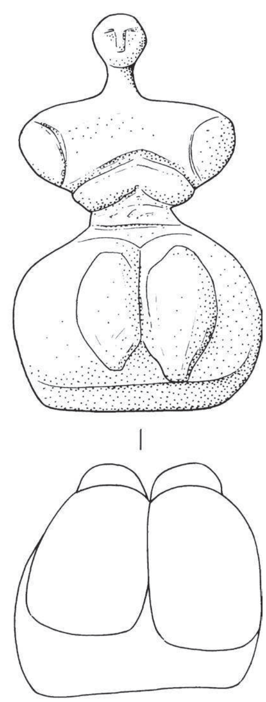

Figure A1.65. *Drawing of restored SF788 (Steven Ashley).*

Figure A1.66. *Head of SF784/5 with the emerging cache stone figures revealed in 1991.*

Figure A1.67. *Group of terracotta figurines. Top row, from left to right: SF946, SF1008, SF693, SF775, SF712, SF773; Middle row: SF736, SF941, SF703, SF781, SF792, SF709, SF758; Bottom row: SF721, SF747, SF760.*

Figure A1.68 *(left). Fragmented skull and cervical vertebrae exposed in Context (704) in the inner niches at the southern extent of the West Cave (visible on plan in Fig 8.74:C, see Stoddart et al. 2009, 178).*

Figure A1.69 *(right). Cranium of an adult male deposited alongside a boar skull in the northern burial niche, Context (897) (visible on Fig. 8.65a:A, see Stoddart et al. 2009, 164).*

Figure A1.70 *(left). Context (1067) in the East Cave contained a partial semi-articulated child skeleton (visible on plan in Fig 8.71:A, see Stoddart et al. 2009, 172).*

Figure A1.71. *Non-adult remains in the Central pit above the East Cave roof collapse, in Context (436).*

Figure A1.72. *Bone group including long bones, ribs and mandible in the Central pit above the East Cave roof collapse, in Context (741), in 1991.*

Figure A1.73. *Articulated ribs and thoracic vertebrae, as well as hand bones, of a non-adult individual in Context (743) in the Central pit, in 1991.*

Figure A1.74. *Betyl Zone bordering the Southeast corner of the East Cave.*

Figure A1.75. *View into the Central Zone of the East Cave from the southwest with remnant cave roof still in position in 1991.*

Figure A1.76. *View of the Central Zone of the East Cave from the South showing remnant cave roof, 1991.*

Figure A1.77. *View of the West Cave and East Cave systems from the southwest, with the external southern screen and 'Shrine' in the centre, the broken megalith between the Deep Zone and North niche at the left, and the betyl zone to the right, toward the end of excavation in 1994.*

Figure A1.78. *Mikiel Bartolo, the tenant of the Circle field, visiting in 1988.*

Figure A1.79. *Caroline Malone, Simon Stoddart and David Trump in 1994 in front of the southern screen in the 'Shrine' area.*

Figure A1.80. *Simon Stoddart and David Trump viewing work in 1991.*

Figure A1.81. *David Trump sorting through ceramic sherds on the balcony of the George Flats, Marsalforn. The ex-military rented Land Rover can be seen in the street below.*

Figure A1.82. *Corinne Duhig refitting a fragmented cranium.*

Appendix 2

Tables

Table A2.1. *Radiocarbon dates. Note: All dates are from samples of human bone unless otherwise stated. The new dates obtained for this project, identified here by the project code, were measured using AMS following the collagen extraction protocols described in Chapter 10.*

Lab ID	^{14}C date	^{14}C s.d.	δ^{13}C	δ^{15}N	C:N	Col. yield	Context	Element	Ref. / project code
UBA-32003	4263	33	-19.5	11	3.26	1.5	21	Mandible L 2 Perm molar	FRAG13.21.37
OxA-3566	4600	65	-20.8				274	Unspecified bone	Malone *et al*. 2009 Table 12.2, 342
OxA-33921	4554	37	-19.77	12	3.2		276	Adult tooth Max M3	Malone *et al*. 2019
OxA-33922	4495	35	-19.52	11.7	3.2		276	Adult tooth Max M3	Malone *et al*. 2019
OxA-X-2676-49	4677	36	-19.2	11.7	3.2		276	Adult tooth Max M3	Malone *et al*. 2019
OxA-27802	4759	27	-19	9.8	3.3		328	Upper thoracic vertebrae	Malone *et al*. 2019
UBA-32005	4727	52	-19.1	9	3.24	4.1	328	Mandible R 2 Perm molar	FRAG110.328.47
OxA-27835	4143	25	-18.6	12.2	3.3		354	Right femur	Malone *et al*. 2019
OxA-33924	4114	37	-19.58	11.7	3.2		354	Adult tooth Max M3	Malone *et al*. 2019
OxA-3569	4250	65	-18.3				354	Unspecified bone	Malone *et al*. 2009 Table 12.2, 342
OxA-3750	3580	75	-17.7				369	Unspecified bone	Malone *et al*. 2009 Table 12.2, 342
UBA-35288	3923	32	-19.2	9.9	3.21	1	433	Mandible L 2 Perm molar	FRAG391.433.37
UBA-35289	4031	32	-19.3	9	3.2	1	436	Maxillary R 2 Perm molar	FRAG395.436.27
UBA-35290	3953	42	-18.7	10	3.21	1.7	436	Maxillary R 2 Perm molar	FRAG396.436.18
SUERC-45316	3948	45	-19.1	10	3.3		518	Rib	Malone *et al*. 2019
OxA-3572	5380	70	-19.6				595	Unspecified bone	Malone *et al*. 2009 Table 12.2, 342
UBA-35266	3995	54	-19.8	10.2	3.21	4.5	595	Mandible L 2 Perm molar	FRAG111.595.37
UBA-35282	4195	28	-19.3	11.8	3.2	9.3	595	Maxillary R 3 Perm molar	FRAG117.595.28
UBA-32006	4102	30	-19	10.7	3.22	3.4	625	Mandible L 2 Perm molar	FRAG22.625.37
UBA-35269	4061	50	-19.4	11.7	3.23	1.6	635	Maxillary R 3 Perm molar	FRAG635.783.18
OxA-3570	4300	65	-17.9				669	Unspecified bone	Malone *et al*. 2009 Table 12.2, 342
UBA-32007	4184	33	-18.9	11.1	3.2	6.7	692	Mandible L 2 Perm molar	FRAG23.692.37
OxA-33923	4194	37	-19.29	11.9	3.2		697	Adult tooth Man M3	Malone *et al*. 2019
UBA-35287	4140	39	-19.4	10.4	3.22	1.4	698	Mandible R 2 Perm molar	FRAG390.698.47
UBA-32008	4136	30	-19.4	11.3	3.21	3.3	704	Maxillary L 2 Perm molar	FRAG24.704.27
OxA-27687	3942	28	-20.6	6.7	3.3		714	Phalanges of a sheep/goat	Malone *et al*. 2019
OxA-3574	4260	60	-18.6				731	Unspecified bone	Malone *et al*. 2009 Table 12.2, 342
UBA-32009	4032	31	-19.8	10.1	3.2	6.7	732	Mandible L 3 Perm molar	FRAG25.732.38
UBA-32010	4147	31	-19.3	11.6	3.25	4.1	735	Maxillary R 3 Perm molar	FRAG26.735.18
UBA-32011	4215	31	-19.3	10.4	3.22	1.2	736	Mandible R 2 Perm molar	FRAG27.736.47
SUERC-45318	3932	45	-18.9	10.6	3.3		743	Left proximal hand phalanges	Malone *et al*. 2019
OxA-3575	4225	70	-18.9				760	Unspecified bone	Malone *et al*. 2009 Table 12.2, 342
UBA-32012	4033	27	-19.7	10.9	3.22	1.2	760	Maxillary L 3 Perm molar	FRAG28.760.28
UBA-32013	4131	29	-19.6	9.5	3.21	2.4	766	Maxillary L 2 Perm molar	FRAG29.766.27
OxA-27839	3990	25	-19.3	10.6	3.3		783	Left femur	Malone *et al*. 2019
OxA-3573	4170	65	-18.3				783	Unspecified bone	Malone *et al*. 2009 Table 12.2, 342
SUERC-45317	3993	45	-18.7	10.1	3.3		783	Proximal phalanges	Malone *et al*. 2019
UBA-32014	3849	26	-19	9.8	3.22	2.5	783	Mandible L 3 Perm molar	FRAG30.783.38
UBA-32015	3903	31	-18.9	8.4	3.21	4.1	783	Mandible L 2 Perm molar	FRAG31.783.37
UBA-32016	4017	31	-19	9.3	3.2	3.5	783	Mandible R 2 Perm molar	FRAG32.783.47
UBA-32017	4009	30	-19.5	9.8	3.22	2.8	783	Mandible R 2 Perm molar	FRAG33.783.47
UBA-32018	3904	30	-19.2	10.5	3.2	4.2	783	Mandible R 2 Perm molar	FRAG34.783.47
UBA-32019	3842	28	-19.3	10.3	3.22	3.4	783	Mandible R 2 Perm molar	FRAG35.783.47

Table A2.1 *(cont.)*.

Lab ID	^{14}C date	^{14}C s.d.	$\delta^{13}C$	$\delta^{15}N$	C:N	Col. yield	Context	Element	Ref. / project code
UBA-32020	3942	28	-18.9	10.7	3.21	3.1	783	Maxillary R 3 Perm molar	FRAG36.783.18
UBA-32021	4069	33	-19.4	10.6	3.2	8.5	783	Mandible L 2 Perm molar	FRAG37.783.37
UBA-32022	3947	32	-19.3	9.5	3.2	3.2	783	Mandible L 2 Perm molar	FRAG38.783.37
UBA-32023	3955	31	-19.5	10.7	3.22	5.4	783	Mandible R 2 Perm molar	FRAG39.783.47
UBA-32024	4043	27	-19.8	11.2	3.21	2.2	783	Mandible R 2 Perm molar	FRAG40.783.47
UBA-32025	4066	27	-19.2	10.5	3.19	7.1	783	Mandible L 2 Perm molar	FRAG41.783.37
UBA-35272	4061	37	Failed	Failed	Failed		783	Mandible L 2 Perm molar	FRAG427.783.37
UBA-35273	3989	38	-19.2	10.8	3.21	3.5	783	Mandible R 2 Perm molar	FRAG43.783.47
OxA-3571	4080	65	-20.2				799	Unspecified bone	Malone *et al*. 2009 Table 12.2, 342
SUERC-45309	3889	45	-18.5	10.7	3.3		799	Skull	Malone *et al*. 2019
UBA-32026	4237	30	-19.2	11.8	3.2	3.8	799	Maxillary R 2 Perm molar	FRAG46.799.18
UBA-32027	3893	28	-18.9	9.2	3.22	3.2	831	Mandible L 3 Perm molar	FRAG47.831.37
UBA-35291	4036	30	-19.7	10.8	3.2	3.2	833	Maxillary R 2 Perm molar	FRAG48.833.27
UBA-35293	4186	65	-19.6	10.1	3.2	3.1	833	Maxillary R 2 Perm molar	FRAG798.833.27
UBA-32028	4118	33	-19.4	11.8	3.22	5.3	842	Mandible R 3 Perm molar	FRAG49.842.48
OxA-27836	4058	26	-18.7	9.9	3.3		845	Right distal end of femur	Malone *et al*. 2019
UBA-32030	4109	34	-19.2	10.3	3.21	2.4	845	Mandible R 2 Perm molar	FRAG51.845.47
UBA-32031	4048	40	-19.4	11	3.21	7.9	856	Maxillary R 2 Perm premolar	FRAG52.856.15
UBA-32032	3983	48	-19.5	10.9	3.24	1.1	863	Maxillary R 2 Perm molar	FRAG53.863.27
UBA-32033	3857	36	-19.4	9.4	3.2	5	866	Mandible L 2 Perm molar	FRAG54.866.37
UBA-32034	3986	34	-19.6	11.3	3.23	2.5	897	Maxillary R 2 Perm molar	FRAG56.897.17
UBA-35281	4034	36	-19.4	9.7	3.22	2	897	Mandible frags	FRAG69
UBA-32035	4129	39	-19.3	11.5	3.21	4.3	908	Mandible R 2 Perm molar	FRAG57.908.47
UBA-32036	3846	33	-19.2	10	3.22	1.6	942	Mandible R 2 Perm molar	FRAG58.942.47
UBA-32037	4031	36	-19.2	10.1	3.22	2.1	951	Maxillary R 2 Perm molar	FRAG59.951.17
UBA-32038	4162	35	-19.4	10.8	3.21	5	951	Mandible R 2 Perm molar	FRAG60.951.47
UBA-32039	4047	39	-19.6	11.3	3.23	2.8	951	Mandible L 2 Perm molar	FRAG61.951.37
UBA-32040	4208	73	-19.6	11.8	3.2	2.7	951	Mandible R 2 Perm molar	FRAG62.951.47
UBA-32041	4150	45	-19.3	11.6	3.21	1.4	951	Mandible R 2 Perm molar	FRAG63.951.47
OxA-27803	4027	26	-19.2	11.6	3.3		960	Right tibia	Malone *et al*. 2019
SUERC-4391	3910	40	-19.7				960	Proximal tibia	Malone *et al*. 2009 Table 12.1, 342
SUERC-45310	3901	45	-18.7	10.7	3.3		960	Skull	Malone *et al*. 2019
UBA-32042	4047	32	-19.5	11.8	3.21	4.2	960	Mandible R 2 Perm molar	FRAG73.960.47
UBA-32043	3877	32	-18.7	9.9	3.21	1.8	960	Mandible R 2 Perm molar	FRAG74.960.47
UBA-35274	4076	42	-19.5	11.7	3.21	2.5	960	Mandible R 2 Perm molar	FRAG698.960.47
UBA-32044	4023	26	-19.7	11.9	3.22	2.8	979	Maxillary R 2 Perm molar	FRAG79.979.17
UBA-32045	3926	28	-19.3	11	3.22	4.3	982	Maxillary L 2 Perm molar	FRAG80.982.27
OxA-27840	3945	27	-19.2	10.1	3.3		997	Bone from left hand	Malone *et al*. 2019
UBA-32046	4351	29	-19.3	11.7	3.23	3.9	1024	Maxillary R 2 Perm molar	FRAG81.1024.17
UBA-32047	4131	25	-19.3	10.8	3.24	2.1	1111	Maxillary R 3 Perm molar	FRAG82.1111.18
UBA-10378	4048	28	-19.6	9.9	3.19		1144	Fibula, sq. 97/113	Malone *et al*. 2009 Table 12.1, 342
UBA-32048	4107	37	-19.5	12.1	3.21	3.1	1174	Maxillary R 3 Perm molar	FRAG83.1174.18
UBA-32049	4065	26	-19.3	10.2	3.22	4.9	1197	Maxillary R 2 Perm molar	FRAG84.1197.17
OxA-27832	4077	33	-18.8	9.9	3.3		1206	Left femur	Malone *et al*. 2019
OxA-33926	4040	35	-20.12	12.3	3.2		1206	Adult tooth	Malone *et al*. 2019
SUERC-4389	4035	35	-19.8				1206	Proximal tibiae	Malone *et al*. 2009 Table 12.1, 342
SUERC-45312	3862	45	-18.9	10.4	3.3		1206	Left tibia	Malone *et al*. 2019
UBA-32050	4130	33	-19.5	11.3	3.24	5.9	1206	Maxillary L 3 Perm molar	FRAG85.1206.28
UBA-32051	3963	32	-19.4	10.7	3.24	3.2	1206	Mandible R 2 Perm molar	FRAG86.1206.47
UBA-32052	3987	27	-19.1	10.7	3.22	4.6	1206	Mandible R 2 Perm molar	FRAG87.1206.47
UBA-32053	3970	25	-19.6	11	3.24	3.6	1206	Mandible R 2 Perm molar	FRAG88.1206.47
UBA-35270	4039	39	-19.4	11	3.21	3.1	1206	Mandible R 2 Perm molar	FRAG97.1206.47
UBA-35284	4286	49	-19.5	13	3.2	3.3	1206	Maxillary R 2 Perm molar	FRAG316.1206.17
UBA-32056	4099	27	-19.4	11.6	3.21	2.6	1215	Maxillary R 3 Perm molar	FRAG98.1215.18
UBA-10383	4054	24	-19.4	9.4	3.15		1220	Radius, sq. 96/117, bone 18	Malone *et al*. 2009 Table 12.1, 342
OxA-27838	3958	24	-19.3	11.2	3.3		1241	Skull	Malone *et al*. 2019
OxA-33927	4050	36	-19.72	10	3.2		1241	Adult tooth Skel 2	Malone *et al*. 2019
OxA-33928	4096	36	-19.69	10.6	3.2		1241	Adult tooth Max M3	Malone *et al*. 2019
SUERC-4390	3920	35					1241	Distal femur/patella	Malone *et al*. 2009 Table 12.1, 342
UBA-32057	4036	27	-19.5	10.1	3.21	4.9	1241	Maxillary R 2 Perm molar	FRAG99.1241.17
UBA-35267	4308	56		11.4	Failed	1.5	1241	Maxillary L 2 Perm molar	FRAG126.1241.27
UBA-35271	3940	36		11.3	Failed	3.7	1241	Mandible R 3 Perm molar	FRAG121.1241.48

Table A2.1 *(cont.).*

Lab ID	^{14}C date	^{14}C s.d.	$\delta^{13}C$	$\delta^{15}N$	C:N	Col. yield	Context	Element	Ref. / project code
UBA-35283	4161	45	-19.8	12.2	3.21	3.2	1241	Maxillary L 3 Perm molar	FRAG123.1241.28
UBA-32059	4128	29	-19.3	11.1	3.23	1.4	1254	Maxillary L 2 Perm molar	FRAG101.1254.28
OxA-27833	4219	26	-19.7	12.3	3.3		1268	Rib	Malone *et al*. 2019
SUERC-45311	3920	45	-19.3	11.1	3.3		1268	Skull	Malone *et al*. 2019
UBA-32060	4039	29	-19.4	12	3.23	3.3	1268	Mandible L 2 Perm molar	FRAG102.1268.47
UBA-32061	4133	41	-19.7	11.4	3.22	2.5	1268	Mandible L 2 Perm molar	FRAG103.1268.37
UBA-32062	3952	55	-19.5	11.2	3.25	1.8	1268	Mandible L 2 Perm molar	FRAG104.1268.37
UBA-35292	4124	64	-19.5	12.7	3.26	3.9	1268	Maxillary R 2 Perm molar	FRAG797.1268.18
OxA-27837	4198	26	-19.6	10.5	3.3		1307	Skull	Malone *et al*. 2019
OxA-X-2676-57	4295	37	-19.7	12.5	3.2		1307	Adult tooth	Malone *et al*. 2019
OxA-27834	4191	25	-19.3	13.3	3.3		1328	Skull	Malone *et al*. 2019
OxA-33925	4234	35	-20.35	13.6	3.2		1328	Adult tooth	Malone *et al*. 2019

Table A2.2. *Strontium and oxygen isotope results. Note: Strontium isotope ratio for sample XEM9130.11.37d was measured on dentine; all others on enamel.*

Fragsus Code	Site	Context	Tooth	Cambridge lab. code (Sr)	Sr ratio	^{14}C cross ref.	Cambridge lab. code (O)	$\delta^{18}O$	$\delta^{13}C_{ap}$	aDNA crossref
FRAG29.766.27	Xagħra	766	27	EP68	0.708751	UBA-32013	G16/1357	-3.074	-14.0698	
XEM8781.17.37	Xemxija	17	37	EP31	0.708787	UBA-35294	M2	-5.3404	-12.9388	
FRAG43.783.47	Xagħra	783	47	EP38	0.708837	UBA-35273	G16 1432	-4.6134	-12.7792	MLT3
FRAG30.783.38	Xagħra	783	38	EP65	0.708861	UBA-32014	G16 1400	-4.877	-14.3888	
FRAG380.715.47	Xagħra	715	47	EP57	0.708862		M25	-6.3362	-13.18	
FRAG38.783.37	Xagħra	783	37	EP70	0.708881	UBA-32022	G16 1429	-6.2226	-14.6058	
FRAG390.698.47	Xagħra	698	47	EP43	0.708889	UBA-35287	M23	-5.1922	-13.8828	
FRAG117.595.28	Xagħra	595	28	EP39	0.708892	UBA-35282	M19	-6.4836	-12.6346	
FRAG698.960.47	Xagħra	960	47	EP37	0.708907	UBA-35274	M8	-5.7802	-15.025	MLT4
FRAG22.625.37	Xagħra	625	37	EP63	0.708919	UBA-32006	G16 1409	-6.3108	-12.935	
FRAG15.276.47	Xagħra	276	47	EP58	0.708936		G16 1321	-4.73842	-12.0372	
XEM9129.11.37	Xemxija	11	37	EP33	0.708942	UBA-35296	M4	-6.4382	-13.1452	
FRAG121.1241.48	Xagħra	1241	48	EP35	0.708962	UBA-35271	M6	-6.7376	-13.9434	MLT1
FRAG427.783.37	Xagħra	783	37	EP36	0.708972	UBA-35272	M7	-6.966	-13.3496	MLT2
FRAG82.1111.18	Xagħra	1111	18	EP60	0.708981	UBA-32047	G16/1351	-4.6162	-13.487	
XEM8783.17.37	Xemxija	17	37	EP30	0.708983	UBA-35295	M1	-5.6642	-14.0622	
FRAG63.951.47	Xagħra	951	47	EP64	0.709003	UBA-32041	G16 1345	-3.73394	-12.661	
FRAG31.783.37	Xagħra	783	37	EP66	0.709024	UBA-32015	G16 1399	-5.414	-12.2976	
FRAG49.842.48	Xagħra	842	48	EP62	0.709028	UBA-32028	G16 1406	-6.6928	-12.2698	
FRAG396.436.18	Xagħra	436	18	EP42	0.709028	UBA-35290	M22	-5.8074	-12.9788	
FRAG60.951.47	Xagħra	951	47	EP61	0.70903	UBA-32038	G16 1349	-3.93006	-10.4864	
XEM9130.11.37	Xemxija	11	37	EP32	0.709034	UBA-35297	M3	-6.5492	-13.8478	
XEM9140.11.37	Xemxija	11	37	EP34	0.709034	UBA-35298	M5	-6.4578	-14.5632	
FRAG798.833.27	Xagħra	833	27	EP41	0.709043	UBA-35293	M21	-6.2264	-13.0632	
FRAG391.433.37	Xagħra	433	37	EP44	0.709069	UBA-35288	M24	-6.6992	-12.959	
FRAG795.1206.37	Xagħra	1206	37	EP59	0.709069					
FRAG85.1206.28	Xagħra	1206	28	EP69	0.709073	UBA-32050	G16 1385	-6.4682	-13.1388	
XEM9130.11.37d	Xemxija	11	37	EP71	0.709098					
FRAG389.738.47	Xagħra	738	47	EP40	0.709099		M20	-6.484	-13.781	
FRAG100.1250.38	Xagħra	1250	38	EP67	0.7092		G16 1419	-6.3466	-13.1234	
FRAG468.783.47	Xagħra	783	47				M38	-8.0950	-13.2310	
FRAG306.1206.47	Xagħra	1206	47				M28	-7.8832	-12.7824	
FRAG316.1206.17	Xagħra	1206	17				M11	-7.136	-14.1388	
FRAG659.783.47	Xagħra	783	47				M35	-7.1236	-13.2980	
FRAG438.783.48	Xagħra	783	48				M37	-7.0680	-13.8774	
FRAG635.783.18	Xagħra	783	18				M15	-7.0314	-12.8314	
FRAG442.783.48	Xagħra	783	48				M46	-6.8470	-13.3554	
FRAG203.951.47	Xagħra	951	47				M76	-6.7158	-13.4080	
FRAG118.595.47	Xagħra	595	47				M51	-6.6278	-13.5624	
FRAG337.1206.48	Xagħra	1206	48				M31	-6.6122	-13.4680	
FRAG288.951.47	Xagħra	951	47				M98	-6.5692	-13.0420	
FRAG211.901.47	Xagħra	901	47				M97	-6.5346	-14.3484	
FRAG50.845.47	Xagħra	845	47				G16/1364	-6.5016	-13.9468	
FRAG229.951.47	Xagħra	951	47				M56	-6.4628	-14.3936	
FRAG106.1268.47	Xagħra	1268	47				G16 1330	-6.43942	-12.4072	
FRAG326.1206.47	Xagħra	1206	47				M30	-6.4328	-13.9352	

Table A2.2 *(cont.)*.

Fragsus Code	Site	Context	Tooth	Cambridge lab. code (Sr)	Sr ratio	^{14}C cross ref.	Cambridge lab. code (O)	$\delta^{18}O$	$\delta^{13}C_{ap}$	aDNA crossref
FRAG456.783.48	Xagħra	783	48				M34	-6.4312	-13.1148	
FRAG360.1206.47	Xagħra	1206	47				M27	-6.4148	-13.3076	
FRAG167.951.47_ BR93	Xagħra	951	47				M69	-6.3398	-13.1618	
FRAG199.951.47	Xagħra	951	47				M71	-6.3246	-12.4652	
FRAG126.1241.27	Xagħra	1241	27				M18	-6.3198	-14.1894	
FRAG668.783.47	Xagħra	783	47				M48	-6.3064	-14.6514	
FRAG28.760.28	Xagħra	760	28			UBA-32012	G16 1412	-6.29	-13.22	
FRAG182.951.47	Xagħra	951	47				M70	-6.2582	-13.4054	
FRAG111.595.37	Xagħra	595	37				M17	-6.2338	-13.5692	
FRAG514.783.47	Xagħra	783	47				M42	-6.2302	-13.6022	
FRAG466.783.47	Xagħra	783	47				M39	-6.2214	-14.6160	
FRAG102.1268.47	Xagħra	1268	47			UBA-32060	G16 1332	-6.22	-14.02	
FRAG327.1206.47	Xagħra	1206	47				M32	-6.1766	-14.9358	
FRAG24.704.27	Xagħra	704	27			UBA-32008	G16/1362	-6.13	-14.25	
FRAG452.783.38	Xagħra	783	38				M50	-6.0534	-13.2784	
FRAG797.1268.18	Xagħra	1268	18				M14	-6.0064	-13.663	
FRAG461.783.47	Xagħra	783	47				M41	-6.0012	-13.8080	
FRAG406.783.47	Xagħra	783	47				M45	-5.9826	-13.8644	
FRAG400.783.48	Xagħra	783	48				M40	-5.9638	-13.6460	
FRAG395.436.27	Xagħra	436	27				M10	-5.9602	-13.4092	
FRAG66.951.47	Xagħra	951	47				G16 1350	-5.93686	-14.1778	
FRAG549.1203.47	Xagħra	1203	47				M29	-5.9058	-12.6698	
FRAG123.1241.28	Xagħra	1241	28				M13	-5.887	-14.6716	
FRAG184.951.47	Xagħra	951	47				M66	-5.8614	-13.5078	
FRAG68.951.47	Xagħra	951	47				G16 1441	-5.636	-13.3592	
FRAG445.783.47	Xagħra	783	47				M33	-5.6080	-14.1252	
FRAG57.908.47	Xagħra	908	47			UBA-32035	G16/1356	-5.59	-13.48	
FRAG250.951.47	Xagħra	951	47				M75	-5.5686	-13.0288	
FRAG89.1206.47	Xagħra	1206	47				G16 1387	-5.5606	-13.063	
FRAG55.866.37	Xagħra	866	37				G16/1352	-5.543	-13.2818	
FRAG56.897.17	Xagħra	897	17			UBA-32034	G16/1361	-5.53	-14.41	
FRAG91.1206.47	Xagħra	1206	47				G16 1394	-5.464	-14.1432	
FRAG103.1268.37	Xagħra	1268	37			UBA-32061	G16 1336	-5.42	-13.95	
FRAG37.783.37	Xagħra	783	37			UBA-32021	G16 1396	-5.41	-13.78	
FRAG292.951.47	Xagħra	951	47				M95	-5.4066	-14.7842	
FRAG80.982.27	Xagħra	982	27			UBA-32045	G16/1353	-5.4	-12.83	
FRAG88.1206.47	Xagħra	1206	47			UBA-32053	G16 1388	-5.4	-13.8	
FRAG40.783.47	Xagħra	783	47			UBA-32024	G16 1434	-5.37	-12.85	
FRAG101.1254.28	Xagħra	1254	28			UBA-32059	G16 1416	-5.35	-13.42	
FRAG75.960.47	Xagħra	960	47				G16 1337	-5.34734	-12.6904	
FRAG39.783.47	Xagħra	783	47			UBA-32023	G16 1433	-5.31	-14.14	
FRAG73.960.47	Xagħra	960	47			UBA-32042	G16 1340	-5.29	-14.23	
FRAG109.1268.37	Xagħra	1268	37				G16 1334	-5.28806	-14.3052	
FRAG32.783.47	Xagħra	783	47			UBA-32016	G16 1436	-5.2856	-13.9546	
FRAG47.831.37	Xagħra	831	37			UBA-32027	G16 1411	-5.27	-12.03	
FRAG363.783.38	Xagħra	783	38				M49	-5.2698	-14.4110	
FRAG105.1268.47	Xagħra	1268	47				G16 1333	-5.20882	-13.6978	
FRAG98.1215.18	Xagħra	1215	18			UBA-32056	G16/1355	-5.1872	-13.6976	
FRAG204.951.47	Xagħra	951	47				M55	-5.1780	-14.2916	
FRAG35.783.47	Xagħra	783	47			UBA-32019	G16 1437	-5.16	-14.18	
FRAG81.1024.17	Xagħra	1024	17			UBA-32046	G16 1418	-5.12	-13.21	
FRAG84.1197.17	Xagħra	1197	17			UBA-32049	G16 1417	-5.12	-12.86	
FRAG93.1206.47	Xagħra	1206	47				G16 1390	-5.055	-12.1838	
FRAG263.951.47	Xagħra	951	47				M79	-5.0254	-13.3394	
FRAG435.783.47	Xagħra	783	47				M47	-5.0224	-15.2194	
FRAG59.951.17	Xagħra	951	17			UBA-32037	G16 1440	-5.01	-13.2	
FRAG158.951.47	Xagħra	951	47				M57	-4.9968	-12.2374	
FRAG87.1206.47	Xagħra	1206	47			UBA-32052	G16 1384	-4.99	-13.86	
FRAG185.951.47	Xagħra	951	47				M64	-4.9774	-13.5176	
FRAG33.783.47	Xagħra	783	47			UBA-32017	G16 1439	-4.96	-13.17	
FRAG58.942.47	Xagħra	942	47			UBA-32036	G16 1420	-4.96	-13.29	

Table A2.2 *(cont.)*.

Fragsus Code	Site	Context	Tooth	Cambridge lab. code (Sr)	Sr ratio	^{14}C cross ref.	Cambridge lab. code (O)	$\delta^{18}O$	$\delta^{13}C_{ap}$	aDNA crossref
FRAG70.951.47	Xagħra	951	47				G16 1346	-4.95358	-13.4714	
FRAG41.783.37	Xagħra	783	37			UBA-32025	G16 1438	-4.94	-13.57	
FRAG401.783.37	Xagħra	783	37				M44	-4.9240	-13.7610	
FRAG74.960.47	Xagħra	960	47			UBA-32043	G16 1381	-4.83	-12.83	
FRAG189.951.47	Xagħra	951	47				M68	-4.8212	-13.8216	
FRAG34.783.47	Xagħra	783	47			UBA-32018	G16 1398	-4.82	-13.3	
FRAG54.866.37	Xagħra	866	37			UBA-32033	G16/1354	-4.81	-12.31	
FRAG46.799.18	Xagħra	799	18			UBA-32026	G16 1413	-4.8	-13.13	
FRAG62.951.47	Xagħra	951	47			UBA-32040	G16 1444	-4.75	-13.19	
FRAG52.856.15	Xagħra	856	15			UBA-32031	G16/1360	-4.71	-13.18	
FRAG61.951.37	Xagħra	951	37			UBA-32039	G16 1443	-4.71	-11.74	
FRAG247.951.47	Xagħra	951	47				M77	-4.7090	-14.0686	
FRAG92.1206.47	Xagħra	1206	47				G16 1392	-4.702	-13.984	
FRAG26.735.18	Xagħra	735	18			UBA-32010	G16/1359	-4.7	-13.6	
FRAG104.1268.37	Xagħra	1268	37			UBA-32062	G16 1329	-4.7	-13.98	
FRAG21.276.47	Xagħra	276	47				G16 1325	-4.6419	-11.754	
FRAG45.783.47	Xagħra	783	47				G16 1431	-4.6262	-13.2206	
FRAG64.951.47	Xagħra	951	47				G16 1424	-4.6034	-14.234	
FRAG14.276.17	Xagħra	276	17				G16 1324	-4.60106	-13.7476	
FRAG86.1206.47	Xagħra	1206	47			UBA-32051	G16 1386	-4.6	-13.95	
FRAG65.951.47	Xagħra	951	47				G16 1442	-4.5698	-13.4272	
FRAG53.863.27	Xagħra	863	27			UBA-32032	G16 1415	-4.54	-13.9	
FRAG67.951.47	Xagħra	951	47				G16 1423	-4.5278	-12.8836	
FRAG83.1174.18	Xagħra	1174	18			UBA-32048	G16 1414	-4.52	-13.93	
FRAG374.715.17	Xagħra	715	17				M16	-4.5168	-13.6602	
FRAG96.1206.47	Xagħra	1206	47				G16 1389	-4.4712	-12.9754	
FRAG107.1268.37	Xagħra	1268	37				G16 1335	-4.46602	-13.6734	
FRAG27.736.47	Xagħra	736	47			UBA-32011	G16 1421	-4.44	-12.68	
FRAG71.951.47	Xagħra	951	47				G16 1347	-4.43034	-12.1702	
FRAG197.951.47	Xagħra	951	47				M63	-4.4208	-13.0610	
FRAG36.783.18	Xagħra	783	18			UBA-32020	G16 1397	-4.37	-13.96	
FRAG282.951.47	Xagħra	951	47				M54	-4.3694	-12.5166	
FRAG95.1206.47	Xagħra	1206	47				G16 1393	-4.3596	-13.9784	
FRAG51.845.47	Xagħra	845	47			UBA-32030	G16 1405	-4.35	-13.55	
FRAG90.1206.17	Xagħra	1206	17				G16 1383	-4.342	-12.9928	
FRAG42.783.47	Xagħra	783	47				G16 1430	-4.3138	-13.387	
FRAG178.951.47	Xagħra	951	47				M58	-4.2876	-14.1010	
FRAG23.692.37	Xagħra	692	37			UBA-32007	G16/1363	-4.28	-12.06	
FRAG78.960.47	Xagħra	960	47				G16 1382	-4.2614	-14.3808	
FRAG171.951.47	Xagħra	951	47				M60	-4.2580	-13.6826	
FRAG268.951.47	Xagħra	951	47				M80	-4.2292	-13.8242	
FRAG94.1206.47	Xagħra	1206	47				G16 1395	-4.1624	-13.563	
FRAG25.732.38	Xagħra	732	38			UBA-32009	G16 1407	-4.12	-13.85	
FRAG19.276.47	Xagħra	276	47				G16 1322	-4.08058	-11.858	
FRAG720.960.38	Xagħra	960	38				M12	-4.0612	-13.7226	
FRAG48.833.27	Xagħra	833	27				M26	-4.0578	-14.034	
FRAG69.951.47	Xagħra	951	47				G16 1422	-4.0466	-12.6662	
FRAG115.595.47	Xagħra	595	47				M52	-4.0356	-13.1474	
FRAG18.276.37	Xagħra	276	37				G16 1323	-4.03114	-12.0858	
FRAG99.1241.17	Xagħra	1241	17			UBA-32057	G16 1410	-4.014	-14.033	
FRAG620.783.37	Xagħra	783	37				M43	-4.0038	-13.9298	
FRAG661.783.47	Xagħra	783	47				M36	-4.0008	-13.3980	
FRAG283.95.47	Xagħra	95	47				M74	-3.9954	-13.5068	
FRAG16.276.37	Xagħra	276	37				G16 1326	-3.92602	-13.2084	
FRAG97.1206.47	Xagħra	1206	47				G16 1391	-3.8542	-9.7526	
FRAG160.951.47	Xagħra	951	47				M62	-3.8332	-12.1226	
FRAG192.951.47	Xagħra	951	47				M59	-3.8218	-13.0554	
FRAG286.951.47	Xagħra	951	47				M94	-3.8094	-13.4944	
FRAG17.276.47	Xagħra	276	47				G16 1327	-3.80462	-11.2394	
FRAG72.951.47	Xagħra	951	47				G16 1348	-3.79866	-13.2208	
FRAG110.328.47	Xagħra	328	47			UBA-32005	G16 1408	-3.7824	-12.8224	
FRAG13.21.37	Xagħra	21	37			UBA-32003	G16 1446	-3.75	-12.95	
FRAG249.951.47	Xagħra	951	47				M78	-3.7392	-13.5150	

Table A2.2 *(cont.).*

Fragsus Code	Site	Context	Tooth	Cambridge lab. code (Sr)	Sr ratio	^{14}C cross ref.	Cambridge lab. code (O)	δ^{18}O	$\delta^{13}C_{ap}$	aDNA crossref
FRAG167.951.47_ BR95	Xagħra	951	47				M65	-3.6514	-14.8576	
FRAG20.276.37	Xagħra	276	37				G16 1328	-3.64138	-13.5906	
FRAG79.979.17	Xagħra	979	17			UBA-32044	G16/1358	-3.62	-14.44	
FRAG76.960.47	Xagħra	960	47				G16 1338	-3.59658	-12.8024	
FRAG44.783.47	Xagħra	783	47				G16 1435	-3.443	-13.5136	
FRAG261.951.47	Xagħra	951	47				M96	-3.3074	-14.2698	
FRAG77.960.47	Xagħra	960	47				G16 1339	-3.23306	-13.5282	
FRAG195.951.47	Xagħra	951	47				M67	-3.0948	-14.5848	
FRAG108.1268.37	Xagħra	1268	37				G16 1331	-2.37266	-8.701	

Table A2.3. *Palaeodietary results from human remains from the Circle. Note: Contexts 272 to 328 are from the rock-cut tomb; all others are from the main hypogeum and associated features. References (1) this study; (2) Stoddart* et al. *2009; (3) Malone* et al. *2009; (4) Malone* et al. *2018.*

ID	Context	Element	$\delta^{13}C_{coll}$	$\delta^{15}N_{coll}$	$\delta^{13}C_{apa}$	Ref.
UBA-32003 G16 1446	21	Tooth 37	-19.5	11	-13.0	(1)
M74	95	Tooth 47			-13.5	(1)
OxA-5038	272	Unspec. bone				(3)
OxA-3566	274	Unspec. bone				(3)
G16 1321	276	Tooth 47			-12.0	(1)
G16 1324	276	Tooth 17			-13.7	(1)
G16 1326	276	Tooth 37			-13.2	(1)
G16 1327	276	Tooth 47			-11.2	(1)
G16 1323	276	Tooth 37			-12.1	(1)
G16 1322	276	Tooth 47			-11.9	(1)
G16 1328	276	Tooth 37			-13.6	(1)
G16 1325	276	Tooth 47			-11.8	(1)
OxA-X-2676-49	276	Tooth 18/28	-19.2	11.7		(3)
OxA-3567	276	Unspec. bone				(3)
OxA-3568	276	Unspec. bone	-19.3	8.3		(3)
OxA-33921	276	Tooth 18/28	-19.77	12		(4)
OxA-33922	276	Tooth 18/28	-19.52	11.7		(4)
OxA-5039	326	Unspec. bone				(3)
UBA-32005 G16 1408	328	Tooth 47	-19.1	9	-12.8	(1)
OxA-27802	328	Vertebrae	-19	9.8		(4)
OxA-3569	354	Unspec. bone	-18.3			(3)
OxA-33924	354	Tooth 18/28	-19.58	11.7		(4)
OxA-27835	354	Femur	-18.6	12.2		(4)
OxA-3750	369	Unspec. bone				(3)
UBA-35288 M24	433	Tooth 37	-19.2	9.9	-13.0	(1)
UBA-35290 M22	436	Tooth 18	-18.7	10	-13.0	(1)
M10	436	Tooth 27			-13.4	(1)
SUERC-45316	518	Rib	-19.1	10		(4)
UBA-35282 M19	595	Tooth 28	-19.3	11.8	-12.6	(1)
M17	595	Tooth 37			-13.6	(1)
M52	595	Tooth 47			-13.1	(1)
M51	595	Tooth 47			-13.6	(1)
OxA-3572	595	Unspec. bone	-19.7	11.1		(3)
UBA-32006 G16 1409	625	Tooth 37	-19	10.7	-12.9	(1)
OxA-3570	669	Unspec. bone	-19.1	9.6		(3)
UBA-32007 G16/1363	692	Tooth 37	-18.9	11.1	-12.1	(1)
OxA-33923	697	Tooth 38/48	-19.29	11.9		(4)
UBA-35287 M23	698	Tooth 47	-19.4	10.4	-13.9	(1)
UBA-32008 G16/1362	704	Tooth 27	-19.4	11.3	-14.3	(1)
UB-10375	714	Humerus	-20.2	7.3		(3)
M25	715	Tooth 47			-13.2	(1)
M16	715	Tooth 17			-13.7	(1)
OxA-3574	731	Unspec. bone	-19.1	10.4		(3)
UBA-32009 G16 1407	732	Tooth 38	-19.8	10.1	-13.9	(1)
UBA-32010 G16/1359	735	Tooth 18	-19.3	11.6	-13.6	(1)
UBA-32011 G16 1421	736	Tooth 47	-19.3	10.4	-12.7	(1)
M20	738	Tooth 47			-13.8	(1)
SUERC-45318	743	Phalanges	-18.9	10.6		(4)

Table A2.3 *(cont.)*.

ID	Context	Element	δ13Ccoll	δ15Ncoll	δ13Capa	Ref.
BR3	760	Unspec. bone	-18.9		-13.9	(2)
UBA-32012 G16 1412	760	Tooth 28	-19.7	10.9	-13.2	(1)
OxA-3575	760	Unspec. bone	-19.4	10		(3)
UBA-32013 G16/1357	766	Tooth 27	-19.6	9.5	-14.1	(1)
UBA-35272 M7	783	Tooth 37			-13.3	(1)
UBA-35273 G16 1432	783	Tooth 47	-19.2	10.8	-12.8	(1)
UBA-32014 G16 1400	783	Tooth 38	-19	9.8	-14.4	(1)
UBA-32015 G16 1399	783	Tooth 37	-18.9	8.4	-12.3	(1)
UBA-32022 G16 1429	783	Tooth 37	-19.3	9.5	-14.6	(1)
UBA-32016 G16 1436	783	Tooth 47	-19	9.3	-14.0	(1)
UBA-32017 G16 1439	783	Tooth 47	-19.5	9.8	-13.2	(1)
UBA-32018 G16 1398	783	Tooth 47	-19.2	10.5	-13.3	(1)
UBA-32019 G16 1437	783	Tooth 47	-19.3	10.3	-14.2	(1)
UBA-32020 G16 1397	783	Tooth 18	-18.9	10.7	-14.0	(1)
M49	783	Tooth 38			-14.4	(1)
UBA-32021 G16 1396	783	Tooth 37	-19.4	10.6	-13.8	(1)
UBA-32023 G16 1433	783	Tooth 47	-19.5	10.7	-14.1	(1)
UBA-32024 G16 1434	783	Tooth 47	-19.8	11.2	-12.9	(1)
M40	783	Tooth 48			-13.6	(1)
M44	783	Tooth 37			-13.8	(1)
M45	783	Tooth 47			-13.9	(1)
UBA-32025 G16 1438	783	Tooth 37	-19.2	10.5	-13.6	(1)
G16 1430	783	Tooth 47			-13.4	(1)
M47	783	Tooth 47			-15.2	(1)
M37	783	Tooth 48			-13.9	(1)
G16 1435	783	Tooth 47			-13.5	(1)
M46	783	Tooth 48			-13.4	(1)
M33	783	Tooth 47			-14.1	(1)
G16 1431	783	Tooth 47			-13.2	(1)
M50	783	Tooth 38			-13.3	(1)
M34	783	Tooth 48			-13.1	(1)
M41	783	Tooth 47			-13.8	(1)
M39	783	Tooth 47			-14.6	(1)
M38	783	Tooth 47			-13.2	(1)
M42	783	Tooth 47			-13.6	(1)
M43	783	Tooth 37			-13.9	(1)
M15	783	Tooth 18			-12.8	(1)
M35	783	Tooth 47			-13.3	(1)
M36	783	Tooth 47			-13.4	(1)
M48	783	Tooth 47			-14.7	(1)
OxA-3573	783	Unspec. bone	-18.7	8.8		(3)
OxA-27839	783	Femur	-19.3	10.6		(4)
SUERC-45317	783	Phalanges	-18.7	10.1		(4)
UBA-32026 G16 1413	799	Tooth 18	-19.2	11.8	-13.1	(1)
OxA-3571	799	Unspec. bone	-19.1	10		(3)
SUERC-45309	799	Skull	-18.5	10.7		(4)
UBA-32027 G16 1411	831	Tooth 37	-18.9	9.2	-12.0	(1)
UBA-35293 M21	833	Tooth 27	-19.6	10.1	-13.1	(1)
M26	833	Tooth 27			-14.0	(1)
UBA-32028 G16 1406	842	Tooth 48	-19.4	11.8	-12.3	(1)
G16/1364	845	Tooth 47			-13.9	(1)
UBA-32030 G16 1405	845	Tooth 47	-19.2	10.3	-13.6	(1)
UB-10380	845	Talus	-20	9.5		(3)
OxA-27836	845	Femur	-18.7	9.9		(4)
UBA-32031 G16/1360	856	Tooth 15	-19.4	11	-13.2	(1)
UBA-32032 G16 1415	863	Tooth 27	-19.5	10.9	-13.9	(1)
UBA-32033 G16/1354	866	Tooth 37	-19.4	9.4	-12.3	(1)
G16/1352	866	Tooth 37			-13.3	(1)
UBA-32034 G16/1361	897	Tooth 17	-19.6	11.3	-14.4	(1)
M97	901	Tooth 47			-14.3	(1)
UBA-32035 G16/1356	908	Tooth 47	-19.3	11.5	-13.5	(1)
UBA-32036 G16 1420	942	Tooth 47	-19.2	10	-13.3	(1)

Table A2.3 *(cont.).*

ID	Context	Element	$\delta^{13}C_{coll}$	$\delta^{15}N_{coll}$	$\delta^{13}C_{apa}$	Ref.
UBA-32038 G16 1349	951	Tooth 47	-19.4	10.8	-10.5	(1)
UBA-32041 G16 1345	951	Tooth 47	-19.3	11.6	-12.7	(1)
M57	951	Tooth 47			-12.2	(1)
M62	951	Tooth 47			-12.1	(1)
M69	951	Tooth 47			-13.2	(1)
M65	951	Tooth 47			-14.9	(1)
M60	951	Tooth 47			-13.7	(1)
M58	951	Tooth 47			-14.1	(1)
M70	951	Tooth 47			-13.4	(1)
M66	951	Tooth 47			-13.5	(1)
M64	951	Tooth 47			-13.5	(1)
M68	951	Tooth 47			-13.8	(1)
M59	951	Tooth 47			-13.1	(1)
M67	951	Tooth 47			-14.6	(1)
M63	951	Tooth 47			-13.1	(1)
M71	951	Tooth 47			-12.5	(1)
M76	951	Tooth 47			-13.4	(1)
M55	951	Tooth 47			-14.3	(1)
M56	951	Tooth 47			-14.4	(1)
M77	951	Tooth 47			-14.1	(1)
M78	951	Tooth 47			-13.5	(1)
M75	951	Tooth 47			-13.0	(1)
M96	951	Tooth 47			-14.3	(1)
M79	951	Tooth 47			-13.3	(1)
M80	951	Tooth 47			-13.8	(1)
M54	951	Tooth 47			-12.5	(1)
M94	951	Tooth 47			-13.5	(1)
M98	951	Tooth 47			-13.0	(1)
M95	951	Tooth 47			-14.8	(1)
UBA-32037 G16 1440	951	Tooth 17	-19.2	10.1	-13.2	(1)
UBA-32039 G16 1443	951	Tooth 37	-19.6	11.3	-11.7	(1)
UBA-32040 G16 1444	951	Tooth 47	-19.6	11.8	-13.2	(1)
G16 1424	951	Tooth 47			-14.2	(1)
G16 1442	951	Tooth 47			-13.4	(1)
G16 1350	951	Tooth 47			-14.2	(1)
G16 1423	951	Tooth 47			-12.9	(1)
G16 1441	951	Tooth 47			-13.4	(1)
G16 1422	951	Tooth 47			-12.7	(1)
G16 1346	951	Tooth 47			-13.5	(1)
G16 1347	951	Tooth 47			-12.2	(1)
G16 1348	951	Tooth 47			-13.2	(1)
UBA-35274 M8	960	Tooth 47	-19.5	11.7	-15.0	(1)
BR4	960	Unspec. bone	-19.8	10.1	-10.0	(2)
M12	960	Tooth 38			-13.7	(1)
UBA-32042 G16 1340	960	Tooth 47	-19.5	11.8	-14.2	(1)
UBA-32043 G16 1381	960	Tooth 47	-18.7	9.9	-12.8	(1)
G16 1337	960	Tooth 47			-12.7	(1)
G16 1338	960	Tooth 47			-12.8	(1)
G16 1339	960	Tooth 47			-13.5	(1)
G16 1382	960	Tooth 47			-14.4	(1)
SUERC-4391	960	Tibia				(3)
SUERC-45310	960	Skull	-18.7	10.7		(4)
OxA-27803	960	Tibia	-19.2	11.6		(4)
UBA-32044 G16/1358	979	Tooth 17	-19.7	11.9	-14.4	(1)
UBA-32045 G16/1353	982	Tooth 27	-19.3	11	-12.8	(1)
OxA-27840	997	Hand	-19.2	10.1		(4)
UBA-32046 G16 1418	1024	Tooth 17	-19.3	11.7	-13.2	(1)
UBA-32047 G16/1351	1111	Tooth 18	-19.3	10.8	-13.5	(1)
UBA-10378	1144	Fibula	-19.6	9.9		(3)
UBA-32048 G16 1414	1174	Tooth 18	-19.5	12.1	-13.9	(1)
UBA-32049 G16 1417	1197	Tooth 17	-19.3	10.2	-12.9	(1)
M29	1203	Tooth 47			-12.7	(1)

Table A2.3 *(cont.)*.

ID	Context	Element	$\delta^{13}C_{coll}$	$\delta^{15}N_{coll}$	$\delta^{13}C_{apa}$	Ref.
UBA-32050 G16 1385	1206	Tooth 28	-19.5	11.3	-13.1	(1)
M28	1206	Tooth 47			-12.8	(1)
M11	1206	Tooth 17			-14.1	(1)
M30	1206	Tooth 47			-13.9	(1)
M32	1206	Tooth 47			-14.9	(1)
M31	1206	Tooth 48			-13.5	(1)
M27	1206	Tooth 47			-13.3	(1)
UBA-32051 G16 1386	1206	Tooth 47	-19.4	10.7	-14.0	(1)
UBA-32052 G16 1384	1206	Tooth 47	-19.1	10.7	-13.9	(1)
UBA-32053 G16 1388	1206	Tooth 47	-19.6	11	-13.8	(1)
G16 1387	1206	Tooth 47			-13.1	(1)
G16 1383	1206	Tooth 17			-13.0	(1)
G16 1394	1206	Tooth 47			-14.1	(1)
G16 1392	1206	Tooth 47			-14.0	(1)
G16 1390	1206	Tooth 47			-12.2	(1)
G16 1395	1206	Tooth 47			-13.6	(1)
G16 1393	1206	Tooth 47			-14.0	(1)
G16 1389	1206	Tooth 47			-13.0	(1)
G16 1391	1206	Tooth 47			-9.8	(1)
SUERC-4389	1206	Tibia				(3)
UB-10377	1206	Humerus	-19.9	9.6		(3)
OxA-33926	1206	Tooth	-20.12	12.3		(4)
SUERC-45312	1206	Tibia	-18.9	10.4		(4)
OxA-27832	1206	Femur	-18.8	9.9		(4)
UBA-32056 G16/1355	1215	Tooth 18	-19.4	11.6	-13.7	(1)
UBA-10383	1220	Radius	-19.4	9.4		(3)
UBA-35271 M6	1241	Tooth 48		11.3	-13.9	(1)
BR1	1241	Unspec. bone	-19.6	10.2	-14.3	(2)
M13	1241	Tooth 28			-14.7	(1)
M18	1241	Tooth 27			-14.2	(1)
UBA-32057 G16 1410	1241	Tooth 17	-19.5	10.1	-14.0	(1)
SUERC-4390	1241	Femur / patella				(3)
OxA-27838	1241	Skull	-19.3	11.2		(4)
OxA-33927	1241	Tooth	-19.72	10		(4)
OxA-33928	1241	Tooth 18/28	-19.69	10.6		(4)
G16 1419	1250	Tooth 38			-13.1	(1)
BR2	1254	Unspec. bone	-19.5	9.9	-9.1	(2)
UBA-32059 G16 1416	1254	Tooth 28	-19.3	11.1	-13.4	(1)
UBA-32060 G16 1332	1268	Tooth 47	-19.4	12	-14.0	(1)
UBA-32061 G16 1336	1268	Tooth 37	-19.7	11.4	-14.0	(1)
UBA-32062 G16 1329	1268	Tooth 37	-19.5	11.2	-14.0	(1)
G16 1333	1268	Tooth 47			-13.7	(1)
G16 1330	1268	Tooth 47			-12.4	(1)
G16 1335	1268	Tooth 37			-13.7	(1)
G16 1331	1268	Tooth 37			-8.7	(1)
G16 1334	1268	Tooth 37			-14.3	(1)
M14	1268	Tooth 18			-13.7	(1)
UB-10376	1268	Humerus	-19.6	10.8		(3)
SUERC-45311	1268	Skull	-19.3	11.1		(4)
OxA-27833	1268	Rib	-19.7	12.3		(4)
OxA-X-2676-57	1307	Tooth	-19.7	12.5		(3)
OxA-27837	1307	Skull	-19.6	10.5		(4)
OxA-33925	1328	Tooth	-20.35	13.6		(4)
OxA-27834	1328	Skull	-19.3	13.3		(4)

Table A2.4. *Palaeodietary results from human remains from Xemxija.*

ID	Box	Element	$\delta^{13}C_{coll}$	$\delta^{15}N_{coll}$	$\delta^{13}C_{apa}$
UBA-35297 M3	11	Tooth 37	-19.6	10.3	-13.85
UBA-35296 M4	11	Tooth 37	-19.3	10.2	-13.15
UBA-35298 M5	11	Tooth 37	-19.1	10.0	-14.56
UBA-35295 M1	17	Tooth 37	-19.5	10.7	-14.06
UBA-35294 M2	17	Tooth 37	-19.1	10.4	-12.94

Table A2.5. *MNE and BRI for all adult skeletal elements from the Xemxija Tombs.*

Element	Left	Axial/unsided	Right	BRI adult	MNI adult
Cranium	-	16	-	20.00	16
Mandible	6	8	12	32.50	26
Clavicle	26	-	27	33.13	26
Hyoid	-	1	-	1.25	1
Cervical vertebrae	-	79	-	14.11	24
Thoracic vertebrae	-	105	-	10.94	9
Lumbar vertebrae	-	23	-	5.75	5
Ribs	132	-	172	15.83	14
Scapula	12	4	12	17.50	12
Manubrium	-	1	-	1.25	1
Sternum	-	8	-	10.00	7
Humerus	30		24	33.75	30
Radius	21	5	31	35.63	31
Ulna	23	13	35	44.38	35
Carpals	29	6	34	6.16	11
Metacarpals	241	93	236	71.25	60
Manual phalanges	-	741	-	33.08	48
Pelvis	5	-	3	5.00	5
Sacrum	-	5	-	6.25	3
Coccyx	-	4	-	5.00	4
Femur	13	8	12	20.63	12
Patella	23	-	31	33.75	31
Tibia	9	13	7	18.13	9
Fibula	17	1	21	24.38	22
Talus	42	-	39	50.63	43
Calcaneus	5	-	9	8.75	9
Tarsals	44	-	37	10.13	45
Metatarsals	315	87	328	91.25	80
Pedal phalanges	-	425	-	18.97	61

Table A2.6. *MNE and BRI for all non-adult skeletal elements from the Xemxija Tombs.*

Element	Left	Axial/unsided	Right	BRI non-adult	MNI non-adult
Cranium	-	9	-	28.13	9
Mandible	7	1	2	31.25	4
Clavicle	12	-	9	32.81	12
Hyoid	-	2	-	6.25	2
Cervicals	-	19	-	8.48	7
Thoracics	-	15	-	3.91	3
Lumbars	-	9	-	5.63	2
Ribs	20	2	16	4.95	3
Scapula	8	-	4	18.75	8
Manubrium	-	1	-	3.13	1
Sternum	-	2	-	6.25	2
Humerus	9	-	10	29.69	10
Radius	6	-	7	20.31	7
Ulna	9	-	5	21.88	9
Carpals	1	-	-	0.22	1
Metacarpals	8	8	6	6.88	3
Manual phalanges	-	23	-	2.68	3
Pelvis	5	-	10	23.44	10
Sacrum	-	3	-	9.38	3
Coccyx	-	0	-	0.00	-
Femur	20	7	16	67.19	20
Patella	3	1	1	7.81	3
Tibia	11	-	9	31.25	11
Fibula	-	2	1	4.69	1
Talus	2	-	0	3.13	1
Calcaneus	2	-	3	7.81	3
Tarsals	1	-	0	0.31	1
Metatarsals	23	28	13	20.00	11
Pedal phalanges	-	19	-	2.12	18

Table A2.7. *MNE, MNI, BRI and FI for (276) in the West chamber of the rock-cut tomb.*

Element	NISP	MNE Left	MNE Axial/unsided	MNE Right	BRI	MNI non-adult	MNI adult	FI
Cranium	215	-	3	-	37.5	-	3	71.7
Mandible	12	3	-	2	31.3	1	2	2.4
Hyoid	0	-	0	-	0.0	-	-	0
Clavicle	10	1	-	2	18.8	-	2	3.3
Cervical vertebrae	11	-	7	-	12.5	-	3	1.6
Thoracic vertebrae	39	-	10	-	10.4	3	-	3.9
Lumbar vertebrae	14	-	5	-	12.5	1	-	2.8
Ribs	91	9	8	9	13.5	1	2	3.4
Scapula	16	1	-	1	12.5	-	1	8
Manubrium	1	-	1	-	12.5	-	1	1
Sternum	2	-	1	-	12.5	-	1	2
Humerus	12	1	-	2	18.8	1	1	4
Radius	6	0	-	2	12.5	-	2	3
Ulna	15	2	-	1	18.8	-	2	5
Carpals	4	4	-	0	3.1	-	1	1
Metacarpals	16	4	3	7	17.5	-	4	1.5
Manual phalanges	24	-	24	-	10.7	1	2	1
Pelvis	13	2	2	1	31.3	2	1	2.6
Sacrum	7	-	2	-	25.0	-	2	3.5
Coccyx	0	-	0	-	0.0	-	-	0
Femur	35	3	-	2	31.3	3	1	7
Patella	0	0	-	0	0.0	-	-	0
Tibia	37	2	-	1	18.8	1	1	12.3
Fibula	4	1	-	1	12.5	-	1	2
Calcaneus	4	1	-	1	12.5	-	1	2
Talus	10	5	-	2	43.8	-	5	1.4
Tarsals	10	6	-	3	11.3	-	2	1.1
Metatarsals	18	6	1	8	18.8	2	2	1.2
Pedal phalanges	17	-	15	-	6.7	1	2	1.1

Table A2.8. *MNE, MNI, BRI and FI for (326) in the East chamber of the rock-cut tomb.*

Element	NISP	MNE Left	MNE Axial/unsided	MNE Right	BRI	MNI non-adult	MNI adult	FI
Cranium	127	-	5	-	71.4	1	4	25.4
Mandible	10	2	2	2	42.9	-	2	1.7
Hyoid	0	-	0	-	0.0	-	-	0
Clavicle	10	2	-	3	35.7	-	3	2
Cervical vertebrae	26	-	7	-	14.3	-	2	3.7
Thoracic vertebrae	37	-	13	-	15.5	1	1	2.8
Lumbar vertebrae	13	-	4	-	11.4	-	1	3.3
Ribs	133	11	1	10	13.1	1	2	6
Scapula	17	1	-	1	14.3	-	1	8.5
Manubrium	0	-	0	-	0.0	-	-	0
Sternum	3	-	2	-	28.6	1	1	1.5
Humerus	15	1	2	1	28.6	2	1	3.75
Radius	22	3	-	2	35.7	1	2	4.4
Ulna	20	2	-	2	28.6	-	2	5
Carpals	14	4	2	7	23.2	1	3	1.1
Metacarpals	28	11	2	13	37.1	2	5	1.1
Manual phalanges	49	-	49	-	25.0	2	3	1
Pelvis	19	1	-	2	21.4	1	1	6.3
Sacrum	9	-	2	-	28.6	-	3	4.5
Coccyx	2	-	1	-	14.3	-	1	2
Femur	22	1	1	1	21.4	1	1	7.3
Patella	9	5	-	3	57.1	-	5	1.1
Tibia	18	1	-	1	14.3	-	1	9
Fibula	17	2	-	1	21.4	1	1	5.7
Calcaneus	8	4	-	2	42.9	-	4	1.3
Talus	8	2	-	4	42.9	-	4	1.3
Tarsals	27	14	-	13	38.6	-	5	1
Metatarsals	40	11	2	19	45.7	-	5	1.25
Pedal phalanges	45	-	44	-	22.4	1	3	1

Table A2.9. *MNE, MNI, BRI and FI for (354) in the North bone pit.*

Element	NISP	MNE Left	MNE Axial/unsided	MNE Right	BRI	MNI non-adult	MNI adult	FI
Cranium	118	-	2	-	66.7	-	2	59
Mandible	0	-	-	-	0.0	-	-	
Hyoid	0	-	-	-	0.0	-	-	
Clavicle	0	-	-	-	0.0	-	-	
Cervical vertebrae	0	-	-	-	0.0	-	-	
Thoracic vertebrae	0	-	-	-	0.0	-	-	
Lumbar vertebrae	0	-	-	-	0.0	-	-	
Ribs	0	-	-	-	0.0	-	-	
Scapula	0	-	-	-	0.0	-	-	
Manubrium	0	-	-	-	0.0	-	-	
Sternum	0	-	-	-	0.0	-	-	
Humerus	0	-	-	-	0.0	-	-	
Radius	0	-	-	-	0.0	-	-	
Ulna	0	-	-	-	0.0	-	-	
Carpals	0	-	-	-	0.0	-	-	
Metacarpals	0	-	-	-	0.0	-	-	
Manual phalanges	0	-	-	-	0.0	-	-	
Pelvis	16	2	-	1	50.0	-	3	5.3
Sacrum	1	-	1	-	33.3	-	1	1
Coccyx	0	-	-	-	0.0	-	-	
Femur	0	-	-	-	0.0	-	-	
Patella	0	-	-	-	0.0	-	-	
Tibia	0	-	-	-	0.0	-	-	
Fibula	1	0	-	1	16.7	-	1	1
Calcaneus	0	-	-	-	0.0	-	-	
Talus	0	-	-	-	0.0	-	-	
Tarsals	0	-	-	-	0.0	-	-	
Metatarsals	0	-	-	-	0.0	-	-	
Pedal phalanges	0	-	-	-	0.0	-	-	

Table A2.10. *MNE, MNI, BRI and FI for (799) in the North bone pit.*

Element	NISP	MNE Left	MNE Axial/unsided	MNE Right	BRI	MNI non-adult	MNI adult	FI
Cranium	176	-	5	-	56	1	4	35.2
Mandible	29	7	1	7	83	3	6	1.9
Clavicle	18	5	-	2	39	2	5	2.6
Hyoid	1	-	1	-	11	-	1	1
Cervical vertebrae	46	-	14	-	22	-	4	3.3
Thoracic vertebrae	127	-	22	-	20	1	1	5.8
Lumbar vertebrae	52	-	12	-	27	2	2	4.3
Ribs	586	15	4	31	23	2	3	11.7
Scapula	45	7	-	3	56	1	6	4.5
Manubrium	2	-	2	-	22	-	1	1
Sternum	4	-	3	-	33	1	2	1.3
Humerus	22	5	-	5	56	1	4	2.2
Radius	31	3	-	4	39	-	4	4.4
Ulna	27	3	-	3	33	1	2	4.5
Carpals	16	8	-	8	22	-	1	1
Metacarpals	40	11	-	20	34	1	6	1.3
Manual phalanges	53	-	49	-	19	-	2	1.1
Pelvis	47	4	3	4	61	2	4	4.3
Sacrum	13	-	5	-	56	-	5	2.6
Coccyx	2	-	1	-	11	-	1	2
Femur	22	5	1	3	50	2	2	2.4
Patella	4	2	-	2	22	-	2	1
Tibia	16	2	1	3	33	-	3	2.7
Fibula	38	5	6	4	83	1	4	2.5
Calcaneus	11	3	-	5	44	-	5	1.375
Talus	6	2	-	4	33	-	4	1
Tarsals	21	10	-	9	42	-	3	1.1
Metatarsals	37	15	2	13	33	1	4	1.2
Pedal phalanges	31	-	31	-	12	-	2	1

Table A2.11. *MNE, MNI, BRI and FI for (783) in the Display Zone.*

Element	NISP	MNE Left	MNE Axial/unsided	MNE Right	BRI	MNI non-adult	MNI adult	FI
Cranium	901	-	12	-	39	11	1	75.1
Mandible	48	-	7	-	25	6	1	6.9
Hyoid	5	-	5	-	18	2	-	1
Clavicle	42	6	1	9	29	8	2	2.625
Cervical vertebrae	164	-	55	-	57	9	1	3
Thoracic vertebrae	342	-	63	-	19	10	1	5.4
Lumbar vertebrae	77	-	34	-	24	8	2	2.3
Ribs	923	69	3	67	21	5	2	6.6
Scapula	45	3	-	10	23	9	1	3.5
Manubrium	2	-	2	-	7	1	1	1
Sternum	39	-	5	-	18	4	1	7.8
Humerus	55	10	-	5	27	9	1	3.7
Radius	51	6	3	7	29	4	1	3.2
Ulna	40	6	2	7	27	7	-	2.7
Carpals	56	17	10	16	12	2	3	5.9
Metacarpals	136	22	4	28	19	9	6	.5
Manual phalanges	251	-	240	-	31	6	5	1
Pelvis	89	8	-	5	23	7	1	6.8
Sacrum	35	-	2	-	7	1	1	17.5
Coccyx	4	-	4	-	14	2	-	1
Femur	78	6	-	5	20	6	1	7.1
Patella	20	8	2	6	29	6	8	1.25
Tibia	58	4	1	6	20	6	1	5.3
Fibula	71	3	4	3	18	4	1	6.5
Calcaneus	14	8	-	5	23	5	3	1.2
Talus	17	7	2	6	27	4	4	1.1
Tarsals	77	27	5	31	23	4	9	1.2
Metatarsals	116	23	36	33	33	3	10	1.3
Pedal phalanges	100	-	97	-	12	4	4	1

Table A2.12. *MNE, MNI, BRI and FI for (951) in the Deep Zone.*

Element	NISP	MNE Left	MNE Axial/unsided	MNE Right	BRI	MNI non-adult	MNI adult	FI
Cranium	652	-	4	-	57	2	2	163
Mandible	10	-	3	-	43	2	1	3.3
Clavicle	6	2	-	1	21	1	1	2
Cervical vertebrae	26	-	7	-	14	-	3	3.7
Thoracic vertebrae	25	-	6	-	7	-	1	4.2
Lumbar vertebrae	17	-	7	-	20	-	2	2.4
Ribs	84	9	-	5	8	-	1	6
Scapula	21	2	-	1	11	1	1	7
Manubrium	0	-	0	-	0	-	-	0
Sternum	2	-	1	-	14	-	1	2
Humerus	15	3	-	3	21	-	3	2.5
Radius	19	1	-	1	7	-	1	9.5
Ulna	24	1	1	1	11	1	1	8
Carpals	0	0	-	0	0	-	-	0
Metacarpals	9	3	-	3	9	-	2	1.5
Manual phalanges	3	-	3	-	1.5	-	1	1
Pelvis	25	2	-	1	11	1	1	8.3
Sacrum	3	-	2	-	29	1	1	1.5
Coccyx	0	-	0	-	0	-	-	0
Femur	42	2	-	6	29	2	4	5.25
Patella	7	3	-	0	11	-	3	2.3
Tibia	28	2	-	1	11	1	1	9.3
Fibula	20	1	-	1	7	-	1	10
Calcaneus	2	2	-	0	7	-	2	1
Talus	5	0	-	4	14	-	4	1.25
Tarsals	2	0	-	1	1	-	1	2
Metatarsals	3	0	1	2	3	1	1	1
Pedal phalanges	3	-	3	-	2	1	1	1

Table A2.13. *MNE, MNI, BRI and FI for (1144) in the Deep Zone.*

Element	NISP	MNE Left	MNE Axial/unsided	MNE Right	BRI	MNI non-adult	MNI adult	FI
Cranium	42	-	2	-	100	1	1	21
Mandible	0	-	0	-	0	-	-	0
Cervical vertebrae	1	-	1	-	7	1	-	1
Thoracic vertebrae	6	-	4	-	17	1	1	1.5
Lumbar vertebrae	2	-	1	-	10	-	1	2
Ribs	29	2	-	3	13	-	1	5.8
Clavicle	0	0	-	0	0	-	-	0
Scapula	2	1	-	0	25	-	1	2
Sternum	0	-	0	-	0	-	-	0
Humerus	0	0	-	0	0	-	-	0
Radius	0	0	-	0	0	-	-	0
Ulna	1	-	1	-	25	1	-	1
Carpals	1	-	1	-	3	-	1	1
Metacarpals	5	0	-	2	5	1	1	2.5
Manual phalanges	8	-	8	-	14	1	1	1
Pelvis	2	1	-	1	50	1	-	1
Sacrum	1	-	1	-	50	1	-	1
Coccyx	2	-	1	-	50	-	1	2
Femur	3	1	-	0	25	1	-	3
Patella	0	0	-	0	0	-	-	0
Tibia	2	1	-	0	25	1	-	2
Fibula	1	0	1	0	25	-	1	1
Calcaneus	1	1	-	0	25	-	1	1
Talus	0	0	-	0	0	-	-	0
Tarsals	2	0	-	2	10	-	1	1
Metatarsals	7	3	1	2	15	1	1	1.2
Pedal phalanges	6	-	6	-	11	1	1	1

Table A2.14. *MNE, MNI, BRI and FI for (1307) in the Deep Zone.*

Element	NISP	MNE Left	MNE Axial/unsided	MNE Right	BRI	MNI non-adult	MNI adult	FI
Cranium	246	-	2	-	100	1	1	123
Mandible	5	-	2	-	100	1	1	2.5
Cervical vertebrae	0	-	-	-	0	-	-	0
Thoracic vertebrae	0	-	-	-	0	-	-	0
Lumbar vertebrae	0	-	-	-	0	-	-	0
Ribs	0	-	-	-	0	-	-	0
Clavicle	0	-	-	-	0	-	-	0
Scapula	0	-	-	-	0	-	-	0
Sternum	0	-	-	-	0	-	-	0
Humerus	0	-	-	-	0	-	-	0
Radius	0	-	-	-	0	-	-	0
Ulna	0	-	-	-	0	-	-	0
Carpals	0	-	-	-	0	-	-	0
Metacarpals	0	-	-	-	0	-	-	0
Manual Phalanges	0	-	-	-	0	-	-	0
Pelvis	0	-	-	-	0	-	-	0
Sacrum	0	-	-	-	0	-	-	0
Coccyx	0	-	-	-	0	-	-	0
Femur	0	-	-	-	0	-	-	0
Patella	0	-	-	-	0	-	-	0
Tibia	0	-	-	-	0	-	-	0
Fibula	0	-	-	-	0	-	-	0
Calcaneus	0	-	-	-	0	-	-	0
Talus	0	-	-	-	0	-	-	0
Tarsals	0	-	-	-	0	-	-	0
Metatarsals	0	-	-	-	0	-	-	0
Pedal phalanges	0	-	-	-	0	-	-	0

Table A2.15. *MNE, MNI, BRI and FI for (960) in the 'Shrine'.*

Element	NISP	MNE Left	MNE Axial/unsided	MNE Right	BRI	MNI non-adult	MNI adult	FI
Cranium	262	-	6	-	24	4	2	43.7
Mandible	14	3	1	4	16	3	1	1.75
Hyoid	2	-	2	-	8	1	1	1
Clavicle	29	9	-	6	30	5	4	1.9
Cervical vertebrae	75	-	45	-	14.3	4	7	1.7
Thoracic vertebrae	93	-	39	-	13	-	4	2.4
Lumbar vertebrae	45	-	19	-	1.5	-	4	2.4
Ribs	436	40	-	37	12.8	-	4	5.7
Scapula	34	5	-	4	18	4	1	3.8
Manubrium	2	-	2	-	8	-	2	1
Sternum	9	-	3	-	12	2	1	3
Humerus	25	5	-	4	18	3	2	2.8
Radius	11	2	1	5	16	4	2	1.375
Ulna	34	6	-	10	32	8	4	2.125
Carpals	58	23	9	25	14.3	1	8	1
Metacarpals	78	26	16	28	28	2	6	1.1
Manual phalanges	145	-	138	-	19.7	3	6	1.1
Pelvis	82	6	-	5	22	4	2	7.5
Sacrum	28	-	5	-	20	3	2	5.6
Coccyx	4	-	3	-	12	-	3	1.3
Femur	46	4	-	9	26	7	2	3.5
Patella	17	10	1	4	30	1	10	1.1
Tibia	37	4	1	6	22	4	2	3.4
Fibula	26	5	1	5	22	5	2	2.4
Calcaneus	11	6	-	2	16	1	5	1.1
Talus	12	6	1	3	20	-	6	1.2
Tarsals	65	28	3	27	23.2	-	8	1.1
Metatarsals	95	31	28	23	32.8	2	9	1.2
Pedal phalanges	113	-	110	-	15.7	1	7	1

Table A2.16. *MNE, MNI, BRI and FI for (1024) in the 'Shrine'.*

Element	NISP	MNE Left	MNE Axial/unsided	MNE Right	BRI	MNI non-adult	MNI adult	FI
Cranium	89	-	2	-	100	1	1	44.5
Mandible	0	-	0	-	0	-	-	0
Clavicle	0	0	-	0	0	-	-	0
Cervical vertebrae	3	-	2	-	14	-	1	1.5
Thoracic vertebrae	11	-	3	-	12.5	-	1	3.7
Lumbar vertebrae	2	-	1	-	10	-	1	2
Rib	65	5	-	1	12.5	1	1	10.8
Scapula	2	1	-	0	25	-	1	2
Manubrium	0	-	0	-	0	-	-	0
Sternum	0	-	0	-	0	-	-	0
Humerus	1	0	1	0	25	-	1	1
Radius	0	0	-	0	0	-	-	0
Ulna	0	0	-	0	0	-	-	0
Carpals	0	0	-	0	0	-	-	0
Metacarpals	0	0	-	0	0	-	-	0
Manual phalanges	1	-	1	-	1.79	-	1	1
Pelvis	1	0	-	1	25	1	-	1
Sacrum	0	-	0	-	0	-	-	0
Coccyx	0	-	0	-	0	-	-	0
Femur	0	0	-	0	0	-	-	0
Patella	0	0	-	0	0	-	-	0
Tibia	0	0	-	0	0	-	-	0
Fibula	0	0	-	0	0	-	-	0
Calcaneus	0	0	-	0	0	-	-	0
Talus	0	0	-	0	0	-	-	0
Tarsals	0	0	-	0	0	-	-	0
Metatarsals	0	0	-	0	0	-	-	0
Pedal phalanges	0	-	0	-	0	-	-	0

Table A2.17. *MNE, MNI, BRI and FI for (1206) in the 'Shrine'.*

Element	NISP	MNE Left	MNE Axial/unsided	MNE Right	BRI	MNI non-adult	MNI adult	FI
Cranium	184	-	6	-	66.7	5	1	30.7
Mandible	8	-	3	-	33.3	3	-	2.7
Hyoid	0	-	0	-	0.0	-	-	0
Clavicle	12	4	-	6	55.6	7	-	1.2
Cervical vertebrae	49	-	33	-	52.4	3	-	1.5
Thoracic vertebrae	101	-	41	-	38.0	3	1	2.5
Lumbar vertebrae	41	-	16	-	35.6	3	1	2.6
Ribs	134	37	1	39	35.6	4	2	1.7
Scapula	9	2	-	5	38.9	4	1	1.3
Manubrium	0	-	0	-	0.0	-	-	0
Sternum	0	-	0	-	0.0	-	-	0
Humerus	5	1	-	2	16.7	1	1	1.7
Radius	6	3	-	3	33.3	3	1	1
Ulna	8	4	-	3	38.9	4	1	1.1
Carpals	16	4	2	10	11.1	-	2	1
Metacarpals	25	5	9	8	24.4	3	2	1.1
Manual phalanges	47	-	43	-	17.1	4	1	1.1
Pelvis	5	2	-	1	16.7	2	-	1.7
Sacrum	12	-	3	-	33.3	3	-	4
Coccyx	1	-	1	-	11.1	1	-	1
Femur	8	2	1	1	22.2	2	1	2
Patella	0	0	-	0	0.0	-	-	0
Tibia	4	1	-	1	11.1	-	1	2
Fibula	6	2	-	1	16.7	2	1	0
Calcaneus	0	0	-	0	0.0	-	-	0
Talus	3	-	3	-	16.7	3	-	1
Tarsals	2	1	1	0	2.2	1	1	1
Metatarsals	8	0	7	0	7.8	1	1	1.1
Pedal phalanges	7	-	7	-	2.8	2	1	1

Table A2.18. *MNE, MNI, BRI and FI for (436) in the Central pit.*

Element	NISP	MNE Left	MNE Axial/unsided	MNE Right	BRI	MNI non-adult	MNI adult	FI
Cranium	6	-	1	-	25	-	1	6
Mandible	4	-	1	-	25	-	1	4
Hyoid	0	-	0	-	0	-	-	0
Clavicle	1	0	-	1	12.5	-	1	1
Cervical vertebrae	3	-	1	-	3.6	-	1	3
Thoracic vertebrae	1	-	1	-	2.1	-	-	1
Lumbar vertebrae	0	-	0	-	0	-	-	0
Ribs	78	4	-	3	7.3	1	3	11.1
Scapula	2	1	-	0	12.5	-	1	2
Manubrium	0	-	0	-	0	-	-	0
Sternum	0	-	0	-	0	-	-	0
Humerus	6	1	-	1	25	-	1	3
Radius	8	1	1	1	37.5	-	2	2.7
Ulna	5	2	-	0	25	-	2	2.5
Carpals	2	0	2	0	3.1	-	1	1
Metacarpals	9	0	6	0	15	-	3	1.5
Manual phalanges	8	-	8	-	7.1	-	1	1
Pelvis	0	0	-	0	0	-	-	0
Sacrum	0	-	0	-	0	-	-	0
Coccyx	0	-	0	-	0	-	-	0
Femur	2	0	1	0	12.5	-	1	2
Patella	0	0	-	0	0	-	-	0
Tibia	0	0	-	0	0	-	-	0
Fibula	1	0	1	0	12.5	-	1	1
Calcaneus	0	0	-	0	0	-	-	0
Talus	0	0	-	0	0	-	-	0
Tarsals	0	0	-	0	0	-	-	0
Metatarsals	0	0	-	0	0	-	-	0
Pedal phalanges	0	-	0	-	0	-	-	0

Table A2.19. *MNE, MNI, BRI and FI for (743) in the Central bone pit.*

Element	NISP	MNE Left	MNE Axial/unsided	MNE Right	BRI	MNI non-adult	MNI adult	FI
Cranium	0	-	0	-	0	-	-	0
Mandible	0	-	0	-	0	-	-	0
Hyoid	2	-	1	-	33.3	1		2
Clavicle	0	0	-	0	0	-	-	0
Cervical vertebrae	0	-	0	-	0	-	-	0
Thoracic vertebrae	8	-	2	-	5.6	-	1	4
Lumbar vertebrae	6	-	1	-	3.3	-	1	6
Ribs	46	4	-	6	13.9	-	2	4.6
Scapula	0	0	-	0	0	-	-	0
Manubrium	0	-	0	-	0	-	-	0
Sternum	0	-	0	-	0	-	-	0
Humerus	2	0	-	1	16.7	-	1	2
Radius	3	1	-	1	33.3	-	1	1.5
Ulna	0	0	-	0	0	-	-	0
Carpals	7	7	-	0	14.6	-	1	1
Metacarpals	11	5	-	2	23.3	-	1	1.6
Manual phalanges	10	0	9	0	10.7	-	1	1.1
Pelvis	3	0	1	0	16.7	-	1	3
Sacrum	0	-	0	-	0	-	-	0
Coccyx	0	-	0	-	0	-	-	0
Femur	0	0	-	0	0	-	-	0
Patella	0	0	-	0	0	-	-	0
Tibia	0	0	-	0	0	-	-	0
Fibula	0	0	-	0	0	-	-	0
Calcaneus	0	0	-	0	0	-	-	0
Talus	0	0	-	0	0	-	-	0
Tarsals	0	0	-	0	0	-	-	0
Metatarsals	0	0	-	0	0	-	-	0
Pedal phalanges	0	-	0	-	0	-	-	0

Table A2.20. *MNE, MNI, BRI and FI for (595) in the Southwest niche.*

Element	NISP	MNE Left	MNE Axial/unsided	MNE Right	BRI	MNI non-adult	MNI adult	FI
Cranium	234	-	6	-	30	5	1	39
Mandible	17	5	2	2	22.5	3	2	1.9
Hyoid	2	-	1	-	5	5	4	2
Clavicle	27	3	2	9	35	6	4	1.9
Cervical vertebrae	98	-	45	-	32.1	5	6	2.2
Thoracic vertebrae	98	-	29	-	12.1	4	1	3.4
Lumbar vertebrae	41	-	16	-	16	3	2	2.6
Ribs	493	27	5	28	12.5	5	1	8.2
Scapula	29	2	-	5	17.5	2	4	4.1
Manubrium	2	-	2	-	10	2	-	1
Sternum	4	-	2	-	10	2	-	2
Humerus	20	3	-	3	15	2	1	3.3
Radius	18	4	1	4	22.5	2	2	2
Ulna	28	5	-	4	22.5	3	2	3.1
Carpals	50	23	5	20	15	1	7	1
Metacarpals	87	21	32	24	38.5	3	8	1.1
Manual phalanges	137	-	133	-	23.8	3	5	1
Pelvis	22	5	2	3	25	5	1	2.2
Sacrum	13	-	5	-	25	3	1	2.6
Coccyx	3	-	1	-	5	-	1	3
Femur	38	4	3	6	32.5	4	4	2.9
Patella	4	1	-	1	5	-	1	2
Tibia	15	1	2	3	15	5	-	2.5
Fibula	40	3	3	2	20	4	1	5
Calcaneus	18	3	1	3	17.5	1	2	2.6
Talus	7	1	1	3	12.5	1	2	1.4
Tarsals	31	14	1	15	15	1	5	1
Metatarsals	93	25	35	20	40	3	7	1.2
Pedal phalanges	92	-	91	-	16.3	3	5	1

Table A2.21. *MNE, MNI, BRI and FI for (656) in the Southwest niche.*

Element	NISP	MNE Left	MNE Axial/unsided	MNE Right	BRI	MNI non-adult	MNI adult	FI
Cranium	2	-	1	-	16.7	1	-	2
Mandible	0	-	0	-	0	-	-	0
Hyoid	0	-	0	-	0	-	-	0
Clavicle	2	0	1	1	16.7	1	1	1
Cervical vertebrae	1	-	1	-	2.4	-	1	1
Thoracic vertebrae	1	-	1	-	1.4	1	-	1
Lumbar vertebrae	4	-	2	-	6.7	-	1	2
Ribs	42	1	1	2	2.8	1	1	10.5
Scapula	17	2	-	1	25	-	2	5.7
Manubrium	0	-	0	-	0	-	-	0
Sternum	0	-	0	-	0	-	-	0
Humerus	5	2	-	1	25	1	1	1.7
Radius	2	0	-	1	8.3	-	1	2
Ulna	8	0	-	1	8.3	-	1	8
Carpals	0	0	-	0	0	-	-	0
Metacarpals	1	0	1	0	1.7	-	1	1
Manual phalanges	7	-	7	-	4.2	1	1	1
Pelvis	1	0	1	0	8.3	-	1	1
Sacrum	0	-	0	-	0	-	-	0
Coccyx	0	-	0	-	0	-	-	0
Femur	18	2	-	4	50	2	2	3
Patella	0	0	-	0	0	-	-	0
Tibia	19	1	1	1	25	-	3	6.3
Fibula	10	1	0	2	25	1	2	3.3
Calcaneus	0	0	-	0	0	-	-	0
Talus	1	1	-	0	8.3	-	1	1
Tarsals	0	0	-	0	0	-	-	0
Metatarsals	2	1	1	0	1.2	-	1	1
Pedal phalanges	0	-	0	-	0	-	-	0

Table A2.22. *MNE, MNI, BRI and FI for (734) in the Southwest niche.*

Element	NISP	MNE Left	MNE Axial/unsided	MNE Right	BRI	MNI non-adult	MNI adult	FI
Cranium	3	-	1	-	33.3	1	-	3
Mandible	1	-	1	-	33.3	1	-	1
Hyoid	0	-	0	-	0	-	-	0
Clavicle	0	0	-	0	0	-	-	0
Cervical vertebrae	0	-	0	-	0	-	-	0
Thoracic vertebrae	2	-	2	-	5.6	1	1	1
Lumbar vertebrae	5	-	2	-	13.3	2	-	2.5
Ribs	5	1	-	1	2.8	1	1	2.5
Scapula	0	0	-	0	0	-	-	0
Manubrium	0	-	0	-	0	-	-	0
Sternum	0	-	0	-	0	-	-	0
Humerus	0	0	-	0	0	-	-	0
Radius	2	0	1	0	16.7	1	-	2
Ulna	1	1	-	0	16.7	-	1	1
Carpals	0	0	-	0	0	-	-	0
Metacarpals	3	1	1	0	6.7	-	1	1.5
Manual phalanges	2	-	2	-	2.4	-	1	1
Pelvis	0	0	-	0	0	-	-	0
Sacrum	0	-	0	-	0	-	-	0
Coccyx	0	-	0	-	0	-	-	0
Femur	10	0	1	0	16.7	-	1	10
Patella	0	0	-	0	0	-	-	0
Tibia	0	0	-	0	0	-	-	0
Fibula	0	0	-	0	0	-	-	0
Calcaneus	0	0	-	0	0	-	-	0
Talus	1	1	-	0	16.7	-	1	1
Tarsals	0	0	-	0	0	-	-	0
Metatarsals	4	2	1	0	10	1	1	1.3
Pedal phalanges	1	-	1	-	1.2	-	1	1

Glossary

We provide brief definitions of some of the technical language with cross-reference to deeper definition within the text. This glossary should be read alongside the index.

Acromegaly – hormonal disorder of the pituitary gland that leads to body growth
Actinomycosis – infectious disease of body tissues
Adenoma – benign tumour of the skin
Aetiology – cause
Ablation – removal
Agenesis – non-development
AIDM – activity-induced dental modification
Alveolar – relating to the tooth socket
Ameloblastic – related to cell responsible for enamel formation
AMTL – ante-mortem tooth loss
Anodic antigen – molecule in the bloodstream
Antimere – opposite side
Arachnoid fovea – protrusions into the outer membrane within the cranium
Ascending ramus – the front part of the rear of the jaw
Autolysis – digestion of cells by the action of their own enzymes
Beta thalassaemia – a blood disorder that reduces the production of haemoglobin
Bioapatite – hydroxylated calcium phosphate, the main biomineral constituent of bone and tooth structures
Buccal – cheek-side (of teeth)
Cancellous – bone tissue with a mesh-like structure typical of the interior of mature bones
CSG – cross-sectional geometry
CVI – chronic venous insufficiency
Calculus – calcified dental plaque
Clivus – a downward sloping surface
Cloaca – chamber with opening
Comminution – a fracture in which bone is splintered
Conchae (**as in nasal**) – shell-shaped networks of bones within the nasal passageways
Coronoid process – eminence projecting forward from the upper and front part of the ulna or mandible
Contralateral – on the opposite side
Cortex/cortices – the dense outer surface of bone
Costochondral – of the joints between the ribs and cartilage
Cribra orbitalia – lesions localized to orbital roof of the cranium
Cricoid – of the cartilage of the wind pipe
Cutaneous – relating to the skin
Dens – projection of second cervical vertebra
Deltoid (**muscle**) – shoulder muscle
Diaphysis(**es**) – central part of long bone
Diastema(**ta**) – space(s) between teeth
Dilaceration – crescent-shaped curvature of tooth root
Diploë – spongy bone between internal and external cranial layers
Diploic – relating to diploë
Dysgnathic – variations of one or both of the jaws and teeth
Dysplasia – variation of development and/or shape of bone tissue
Dystrophy – weakness of muscles
Eburnation – polished appearance of bone surface (like ivory)
Ectocranial – relating to the outside of the cranium
Ectopic – displaced
Endosteal – relating to the interior of bone
Entheseal – relating to attachment sites of muscle, tendon and ligaments to bone
Enthesopathy(**ies**) – changes to the normal surface structure of muscle, tendon and ligament attachments to bone
Epithelium – skin and surface of other organs
Epiphysis(**es**) – cap(s) at the ends of a long bone that fuse when growth is complete
Erythropoietic – pertaining to the production of blood
Ethmoid – perforated cranial bone, allows olfactory nerves into the nose
Eugnathic – free from abnormality of the jaw
Evulsion – forcible extraction
Extravasated – forced out
Falcine – relating to a vein in the cranial cavity
Fibroma – benign tumour
Focal pressure atrophy – local loss of tissue
Fontanelle – membranous gaps between cranial bones of infants
Fractionation, isotopic – the differential partitioning of isotopes between source and product pools because of chemical or physical processes, leading to differences in measured isotope ratio
Germectomy – removal of teeth in a developmental stage
Gingiva – gum (in jaw)
Glabella – part of the forehead above and between the eyebrows
Gonial angle – the angle of the mandible

Gynaecomastia – breast glandular tissue development in males
HCD – hyperostosis calvaria diffusa
HCI – hyperostosis cranii interna
HFI – hyperostosis frontalis interna
Haematuria – blood in the urine
Haematoma(ta) – clotted blood within tissue (bruising)
Haematopoietic – related to blood producing cells in marrow
Haemolytic anaemia – a disorder in which red blood cells are destroyed faster than they can be made
Hydroxylation – oxidation reaction
Hypercementosis – excessive build-up of normal cementum (calcified tissue) in the tooth roots
Hyperostosis – excessive growth of bone
Hypertrophic – relating to enlargement
Hypertrophic osteoarthropathy (HOA) – a syndrome characterized by clubbing of the digits, periostitis of the long (tubular) bones, and arthritis
Hypoplasia – a lack of cells in an organ or tissue
Hypoconid – principal rear outer cusp of a lower molar
Hypodontia – developmental absence of one or more teeth
Iatrogenic – caused by medical treatment
Idiopathic – relating to disease with no identifiable cause
Interradicular septum – plate of bone separating tooth sockets
Involucrum – thick sheath of new bone
Ipsilateral – same side
IPV – inter-personal violence
Jugum – ridge
Keratin – protein that makes up your hair, skin, and nails
Labial – lip side of teeth
Labret – an adornment attached to the lip
Lacrimal – small bone forming the inner part of the eye socket
Lamellation – arrangement in thin layers
Lingual – tongue-side (of teeth)
LSAMAT – lingual surface attrition of the maxillary anterior teeth
Lytic – related to dissolution or resorption
Mastoid process – bone projection on each side of the head just behind the ear
Melorheostosis – abnormal growth of new bone tissue on the surface of existing bones
Mental trigone – protuberance at centre of mandible
Metaphysis(es) – the regions of the bone where growth occurs
Mylohyoid line – a bony ridge on the internal surface of the mandible
Myositis – inflammation in muscles
Neoplasm/neoplasia – mass/masses of tumour
Nuchal crest – ridge on back of cranium
Occlusion – closing of jaw
Occlusal – relating to the grinding or biting surface of a tooth
Olecranon – a bony prominence at the elbow, on the proximal end of the ulna
Osteochondroma – overgrowth of cartilage and bone
Osteoma – new piece of bone usually growing on another piece of bone
Osteomyelitis – inflammation or swelling in the bone
Osteopenia – loss of bone mass
Osteophytosis – bony spurs emanating from vertebral bodies or around the joints
Palatine – relating to the palate
Patent – refers to features which are observable and/or viable
Pectineal – relating to a bony ridge on the thigh bone and pubic bone
Periosteal – relating to the periosteum, a membrane that covers almost all of every bone
Periosteum – a membrane several cell layers thick that covers almost all of every bone
Periostitis – inflammation of the periosteum
Pleomorphic – relating to a group of cells that are very different from each other in either size, shape, or colour
Pleural – relating to the membrane surrounding the lungs
Porotic – porous
Prognathism – bulging out of the maxillae and/or mandible
Pronation – here describes the rotary motion of the forearm that turns the palm from anteriorly facing (thumb lateral) to posteriorly facing (thumb medial)
Pronator ridge – an oblique ridge on the anterior surface of the ulna
Protocone – cusp on the mesiolingual corner of an upper molar tooth
Protoconid – mesiobuccal cusp of a lower molar that corresponds to the protocone
Sagittal plane – a plane that divides the body into symmetrical right and left halves
Schistosomiasis (**bilharzia**) – a disease caused by parasitic worms
Schistosomes – blood flukes
Scoliosis – a sideways curvature of the spine
Scorbutic – relating to scurvy
Sequelae – conditions resulting from injury or illness
Sequestrum – a fragment of dead bone or other tissue that has separated from healthy tissue as a result of injury or disease
SDED – sharply demarcated erosive defects
SES – serpens endocrania symmetrica
Sesamoid – bone embedded in a tendon, principally in the foot
Sigmoid – S-shaped
Splanchnocranium – the facial elements of the cranium
Sphenoid – a bone of irregular form situated at the base of the cranium
Sphenofrontal – relating to a suture on the side of the cranium
Sphenotemporal – relating to a suture on the side of the cranium
Spicule – bony spurs or ledges that occur along the edges or on top of bones
Spondylosis – age-related degeneration of the spine
Squama – a scale, or scale-like part, of bone
Sternal – relating to the sternum, the midline bone of the thorax
Styloid (**process**) – long, cylindrical, cartilaginous bone at base of cranium
Syndesmosis – fibrous joint between two bones
Suture – fibrous joints that connect the bones of the skull
Synostosis – fusion of two or more bones
Trabecula(**e**) – see 'Cancellous'
Trochanter – projection from the proximal femur
Trümmerfeld zone – transverse band of radiolucency
Tubercle – protuberance
Vomer – bone in lower part of nasal cavity
Woven bone – bony tissue in which the collagen fibres of the matrix are arranged irregularly in interlacing networks
Zygoma – cheekbone

Index

Entries in *italic* indicate illustrations.

A

B

I

K

L

M

Temple people

The ERC-funded *FRAGSUS Project* (*Fragility and sustainability in small island environments: adaptation, culture change and collapse in prehistory, 2013–18*) led by Caroline Malone has focused on the unique Temple Culture of Neolithic Malta and its antecedents. This third volume builds on the achievements of *Mortuary customs in prehistoric Malta*, published by the McDonald Institute in 2009. It seeks to answer many questions posed, but left unanswered, of the more than 200,000 fragments of mainly commingled human remains from the Xagħra Brochtorff Circle on Gozo. The focus is on the interpretation of a substantial, representative subsample of the assemblage, exploring dentition, disease, diet and lifestyle, together with detailed understanding of chronology and the affinity of the ancient population associated with the 'Temple Culture' of prehistoric Malta. The first studies of genetic profiling of this population, as well as the results of intra-site GIS and visualization, taphonomy, health and mobility, offer important insights into this complex mortuary site and its ritual.

Remarkable evidence on the bioanthropology of care practised by these populations, together with a relatively low level of interpersonal violence, and examples of longevity, reveal new aspects about the Neolithic Maltese. Detailed case studies employing computerized tomography describe disease such as =scurvy and explore dietary issues, whilst physical activity and body size have been assessed through biomechanical analysis, supported by taphonomic study, isotopic analyses, a review of mortuary practices during prehistory and a robust new chronology. The results form a rich contextualized body of material that advances understanding of cultural change within the context of small island insularity, and provides biological comparisons for the graphic figurative art of early Malta. These data and the original assemblage are conserved in the National Museum of Archaeology in Valletta as a resource for future study.

Editors:
Simon Stoddart is Professor of Prehistory in the Department of Archaeology, University of Cambridge.
Ronika K. Power is Professor of Bioarchaeology in the Department of History and Archaeology at Macquarie University, and the Director of the Centre for Ancient Cultural Heritage and Environment (CACHE).
Jess E. Thompson is a research associate on the 'ANCESTORS' project at the McDonald Institute, Cambridge.
Bernardette Mercieca-Spiteri is the osteological officer of the Superintendence of Cultural Heritage of Malta.
Rowan McLaughlin is a Pathway Fellow at the Hamilton Institute, National University of Ireland, Maynooth, where he is principal investigator of the IRC-funded project 'A deep history of Ireland for the Information Age'.
Eóin W. Parkinson is a Leverhulme Research Fellow at the Department of Classics and Archaeology of the University of Malta.
Anthony Pace was Superintendent of Cultural Heritage on Malta during the course of the *FRAGSUS Project*.
Caroline Malone is Professor in the School of Natural and Built Environment, Queen's University Belfast.

Published by the McDonald Institute for Archaeological Research,
University of Cambridge, Downing Street, Cambridge, CB2 3ER, UK.

Cover design by Dora Kemp and Ben Plumridge.

ISBN: 978-1-913344-08-5

ISBN 978-1-913344-08-5
9 781913 344085

UNIVERSITY OF CAMBRIDGE